Springer Series in Geomechanics and Geoengineering

Peddada Jagadeeswara Rao
Kakani Nageswara Rao · Sumiko Kubo
Editors

Proceedings of International Conference on Remote Sensing for Disaster Management

Issues and Challenges in Disaster Management

Springer

Springer Series in Geomechanics and Geoengineering

Series editor

Wei Wu, Universität für Bodenkultur, Vienna, Austria
e-mail: wei.wu@boku.ac.at

Geomechanics deals with the application of the principle of mechanics to geomaterials including experimental, analytical and numerical investigations into the mechanical, physical, hydraulic and thermal properties of geomaterials as multiphase media. Geoengineering covers a wide range of engineering disciplines related to geomaterials from traditional to emerging areas.

The objective of the book series is to publish monographs, handbooks, workshop proceedings and textbooks. The book series is intended to cover both the state-of-the-art and the recent developments in geomechanics and geoengineering. Besides researchers, the series provides valuable references for engineering practitioners and graduate students.

More information about this series at http://www.springer.com/series/8069

Peddada Jagadeeswara Rao
Kakani Nageswara Rao · Sumiko Kubo
Editors

Proceedings of International Conference on Remote Sensing for Disaster Management

Issues and Challenges in Disaster Management

Springer

Editors
Peddada Jagadeeswara Rao
Department of Geo-Engineering
and Centre for Remote Sensing
College of Engineering,
Andhra University
Visakhapatnam
India

Kakani Nageswara Rao
Department of Geo-Engineering
and Centre for Remote Sensing
College of Engineering,
Andhra University
Visakhapatnam
India

Sumiko Kubo
Department of Geography,
Faculty of Education
Waseda University Geography
Tokyo
Japan

ISSN 1866-8755 ISSN 1866-8763 (electronic)
Springer Series in Geomechanics and Geoengineering
ISBN 978-3-319-77275-2 ISBN 978-3-319-77276-9 (eBook)
https://doi.org/10.1007/978-3-319-77276-9

Library of Congress Control Number: 2018936638

Printed on acid-free paper

This Springer imprint is published by the registered company Springer International Publishing AG
part of Springer Nature
The registered company address is: Gewerbestrasse 11, 6330 Cham, Switzerland

This book is dedicated to Dr. Y. V. N. Krishna Murthy, Director, National Remote Sensing Centre (Indian Space Research Organization), Dr. P. Ravindrababu, IRS and Member of Parliament (Amalapuram Constituency), Prof. G. S. N. Raju, Vice-Chancellor, Centurion University and all Former Vice-chancellors of Andhra University.

Foreword

India is prone to several natural disasters, namely floods, cyclones, agricultural drought, earthquakes, landslides and forest fires. The frequency of occurrence of these disasters is alarming and necessitates suitable disaster management action plan. Today nationwide, with latest technological advances, more particularly, phenomenal growth in space technology, it is believed and accepted by Ministry of Home Affairs, Government of India, that disaster risk reduction must be addressed to minimise the losses while adopting suitable crisis management practices for disaster management. ISRO through its communication and Earth observation satellites facilitates communication needs and silos of geo-spatial data for disaster risk reduction and management. Disaster risk reduction encompasses the pre-paredness, early warning, response and recovery.

Timely, precise and near-real time-information delivery is the key for efficient disaster management. The earth observation, communication, meteorological navigation satellites and aerial surveys are the core observation systems to facilitate the communication during disaster period, early warnings and geo-spatial value-added products/services for preparedness, response, relief and mitigation measures.

Hazard zonation maps for floods and landslides help for preparedness. Early warnings regarding possible occurrence of floods, cyclones, landslides based on meteorological observations are useful for local administration to plan for relief measures. Agricultural drought vulnerability assessment helps to explore alternative cropping practices in addition to insuring the farmer with crop insurance under the PMFBY welfare scheme. Near-real-time monitoring of disaster through satellite data improves the response of administrative machinery for crisis management minimising loss to human life and property.

It is appropriate and the need of the hour that Andhra University College of Engineering (A) and Indian Society of Geomatics—Visakhapatnam Chapter are jointly organising an International Conference on Remote Sensing for Disaster Management (ICRSDM-2017) at Visakhapatnam, Andhra Pradesh, India, to strengthen the disaster management practices by connecting to various research communities for effective implementation.

I wish the conference a grand success.

Hyderabad, India

Dr. Y. V. N. Krishna Murthy
Director, Department of Space, National Remote Sensing Centre, ISRO, Government of India

Preface

Natural Disasters are not new to the Earth. However, the intensity, frequency and extent of damage and devastation due to disasters are increasing year after year in spite of many technological developments. Concerted efforts towards creating public awareness, disaster vulnerability mapping, improved capacity-building and resilience, and technology-driven management is the need of the day to tackle disasters and to reduce the loss of human life and property. Satellite remote sensing with its ability to provide data on Earth's surface features and process-dynamics in near-real time through its multispectral and repetitive capabilities is useful to monitor and thereby mitigate and manage any natural calamity. It is the only technology that can provide data on pre-event, during the event and post-event indicators. Thus, with such authentic information from the remotely sensed data, necessary mitigation measures can be suggested in order to overcome the recurring/episodic occurrence of the hazards. Remote sensing in conjunction with GIS and GPS technologies further enriches the decision-making process in disaster preparedness and mitigation.

The Department of Geo-Engineering, Andhra University, Visakhapatnam has conducted a three-day International Conference on Remote Sensing for Disaster Management during 11–13 October, 2017 with the main objective of providing a platform for exchanging ideas and experiences of scientists and experts in the field of natural and anthropogenic disasters and their management.

Visakhapatnam, the most enchanting city on the east coast of India and a hub of industrial activity, and is vulnerable to cyclones, coastal erosion and industrial disasters has provided a perfect setting for the Conference. More than 100 delegates attended and 78 research papers were presented in the three-day Conference.

The deliberations and scientific discourses during the conference led to several useful suggestions and recommendations. The Conference has resolved that large-scale maps based on geospatial technologies should be prepared high-lighting the erosion prone zones along the sea coast and in the river basins, and landslide prone zones in the mountain terrains. Such maps showing details in local languages should be made available by displaying them in public places and governmental

offices in disaster vulnerable zones. Disaster Management should be a part of the school and college curriculums across all courses.

The governments should set up museums showcasing the disaster management programs in vulnerable areas and also in major urban centres. This helps the citizens to understand the disasters and to get practical training in disaster management processes. Quizzes, mock drills and various other awareness programs should be conducted towards disaster preparedness of the citizens.

Training in first aid methods is essential in rural areas. The Do's and Don'ts, written in local languages are to be displayed in public places. Blood donation centres and mobile clinics shall be established in disaster prone areas. Counselling by psychologists should be arranged to those who lost their family members in disasters. Every office should maintain a disaster management directory. Community education, web portal for helping in search-and-rescue operations, and awareness creation on alternative ways to resources are to be provided.

All the 78 full papers in this Conference Proceedings are segregated into 11 sections representing case studies on the technological advancements and application of remote sensing, geographic information system and global positioning system in mapping and mitigation of various types of disasters. We hope the readers will find this volume a useful reference.

Visakhapatnam, India — Peddada Jagadeeswara Rao
Visakhapatnam, India — Kakani Nageswara Rao
Tokyo, Japan — Sumiko Kubo

Acknowledgements

We are grateful to Prof. G. Nageswara Rao, Vice-Chancellor, Andhra University, Prof. P. S. Avadhani, Principal, Andhra University College of Engineering (Autonomous), and Prof. V. Uma Maheswara Rao, Registrar, Andhra University for their sustained support and encouragement.

We express our heartfelt thanks to the Chief Guest of the inaugural function of the Conference, Dr. P. Ravindra Babu, IRS and Member of Parliament (Amalapuram Constituency) for sparing his valuable time and for his thought-provoking message. We are also grateful to Dr. Y. V. N. Krishna Murthy, Director, NRSC, Hyderabad, and Prof. Chandan Ghosh, Head, Geoscience, NIDM, New Delhi, for their highly informative and inspiring inaugural addresses.

We are thankful to all our colleagues in the Department of Geo-Engineering, Andhra University, Prof. E. Amminedu, Prof. G. Jai Sankar and the former colleagues and non-teaching staff, and to Padmasree Dr. Kutikuppala Surya Rao, a renowned medical expert in Visakhapatnam for their timely help and advice for making every event of the Conference a grand success.

We are thankful to all the members of the Conference Organizing Committee for their support and wise counsel from time to time.

We also thank Dr. T. Venkateswara Rao, Principal, and Dr. N. C. Anil, Vice-Principal of their respective Engineering colleges in Visakhapatnam for organizing the Conference sessions.

We specially thank all the reviewers of the papers included in the Conference Proceedings for sparing their valuable time and selfless efforts in improving the quality of the manuscripts, and the Editor-in-Chief, Springer Series Proceedings of Geomechanical and Geoengineering for publishing this Conference Proceedings.

We appreciate the untiring efforts and timely help of the research scholars in the Department of Geo-Engineering, especially Rajesh Duvvuru, Gudikandula Narasimha Rao, Boyidi Suribabu, B. Sridhar, Ch. Anusha and T. Sridevi, U. Sailaja, and B. Ravikumar during the preparations for not only the Conference, but also several cultural events that were conducted during the three days of the Conference. We are thankful to Dr. Ch. V. Rama Rao, former CE, VUDA,

Dr. N. Victor Babu, Dr. M. Madhuri, Dr. Usha Chirala, Dr. D. Ramprasad Naik and Dr. Chukka Srinivasa Rao, ICRISAT, Hyderabad who has also contributed their might for the successful conduct of the Conference.

We express our sincere thanks to the students of the Department, especially A. Gangabhavani and A. Kavya for their enthusiastic support and dedicated work during the Conference. We also thank K. Dileep, DE, GVMC, for his constant encouragement and timely help in organizing various events of the Conference, in particular the 3K Run, a public awareness program that was organized on the Beach Road in the morning before the commencement of the Conference.

Last but not the least, we gratefully place on record the financial support from the Andhra University College of Engineering under Technical Education Quality Improvement Programme (TEQIP) Phase-III, National Institute of Rural Development & Panchayati Raj (NIRD & PR), Hyderabad, Andhra Pradesh State Disaster Management Authority (APSDMA), Amaravati, Ramky Pvt. Ltd., Visakhapatnam, Andhra Pradesh Council of Science & Technology (APCOST), Vijayawada, Andhra Pradesh Space Applications Centre (APSAC), Vijayawada, National Remote Sensing Centre (NRSC), Hyderabad, Visakhapatnam Port Trust, Visakhapatnam Steel Plant, Council of Scientific and Industrial Research (CSIR), New Delhi, and Indian National Science Academy (INSA), New Delhi, which has immensely helped us in organizing this important international event.

Prof. Peddada Jagadeeswara Rao
Prof. Kakani Nageswara Rao
Prof. Sumiko Kubo

Contents

Chapter 1
GIS Based Management System for Flood Forecast Applications

Sravani Duvvuri

Abstract Water resources of a country constitute mainly surface and ground water, with rainfall being the basic source. Due to non-uniform variation of rainfall in India, one region of India receives floods, and the other region is prone to drought. This situation calls for proper management measures to effective utilization of available water. Recent floods in large river systems called for the urgent need to forecast flood conditions and manage the river environment. The author's study on identification of flood prone areas of Cauvery river basin, generated flood inundation maps of several recurrence intervals by using hydrologic (SWAT) and hydraulic (HEC-RAS) models integrated with GIS. Considering this as preliminary study, a flood forecasting system is planned for Krishna river basin by using GIS and Meteorological data. A display map will be prepared using ArcGIS, which includes flood depth, extent of inundation with display maps and this information will be provided in near real time to concerned authorities for taking necessary action. These tools can be used to identify affected parcels to prioritize for remediation. This will help further to manage the water resources in an effective manner, without letting the water into sea or causing submergence to flood plain areas.

Keywords GIS · SWAT · HEC-RAS · Water surface profile · Flood inundation map

1 Introduction

Flood is one of the most common hydrologic extremes frequently experienced by any country. The rainfall received in India is not uniformly distributed both in time and space. According to government of India flood statistics, about 400,000 km^2 [5] of area is getting inundated due to floods every year. Andhra Pradesh has been

S. Duvvuri (✉)
Rajiv Gandhi University of Knowledge Technologies,
IIIT Nuzvid, Nuzvid, Krishna (Dist) 521202, Andhra Pradesh, India
e-mail: sravanidvr@gmail.com

P. J. Rao et al. (eds.), *Proceedings of International Conference on Remote Sensing for Disaster Management*, Springer Series in Geomechanics and Geoengineering,
https://doi.org/10.1007/978-3-319-77276-9_1

frequently affected by severe floods and has suffered from many flood disasters in terms of the population affected, frequency, extent of inundation and socio-economic costs. The state of Andhra Pradesh has three major river basins; among which Krishna is the second largest perennial river basin. The Krishna River Basin is India's fifth largest river basin covering an area of 258,948 km^2 in Peninsular India, which is nearly 8% of total geographical area of the country [10]. Most of the Krishna catchment area lies in the states of Maharashtra, Karnataka, Telangana and Andhra Pradesh. The river is prone to heavy floods, especially during the South-West monsoon season (June–September) and occasionally due to thunderstorms. Due to rapid land use changes, encroachment and sedimentation, the rivers may not be able to carry the excessive runoff resulting from heavy rains of high intensity. As a result, the river overflows and water enters the flood plain. Flood water surface elevation information is important to know the depth of the flooding. Accurate water surface elevations can be computed using a hydraulic model. Long-term continuous discharge measurements are available only in few locations across the Indian River basins. Since the current study is agricultural watershed, so the flow values at these locations can be simulated using hydrologic model, SWAT [2] based on landuse practices, crop management, irrigation scheduling and reservoir operation.

Flood frequency analysis is carried out for the flow values obtained from SWAT to calculate the flow magnitudes of several recurrence intervals (2, 5, 10, 25, 50 and 100 years) using a statistical technique known as Log-Pearson type-III distribution [9]. In order to map the level of flood inundation at different downstream reaches, water surface profiles are needed at several places along the river reach. But they are available at very limited places along with stream gauges. Hence, to fill this gap, a hydraulic model such as HEC-RAS is often used to compute the flow depth at various locations along the river reach. GIS is used to extract the geometric information from the digital elevation data for input into a hydraulic model, and then used to map the current spatial extent of flood waters using a mapping software. Flood inundation mapping is one of the vital components in developing flood mitigation measures especially nonstructural measures. Flood inundation extent and depth can be found by using a mapping tool called HEC-GeoRAS [8]. Water surface elevations greater than the terrain elevation are included in the inundation depth grid.

2 Study Area

The basin is situated between East longitudes 73° 21′ to 81° 09′ and North latitudes 13° 07′ to 19° 25′ in the Deccan Plateau. There are 13 major tributaries which join the Krishna River along its 1400 km course. About 68% population lives in rural areas and is dependent on agriculture for their livelihoods. There are about 30 major and medium dams and reservoirs constructed in the Krishna River Basin.

The important soil types found in the basin are black soils, red soils, lateritic soils, mixed soils, saline and alkaline soils. Diversified cropping pattern persists in the Krishna River Basin. Principal cultivated crops are: paddy, sorghum, corn, sugarcane, millet, cotton, sunflower, groundnut, turmeric, and a variety of

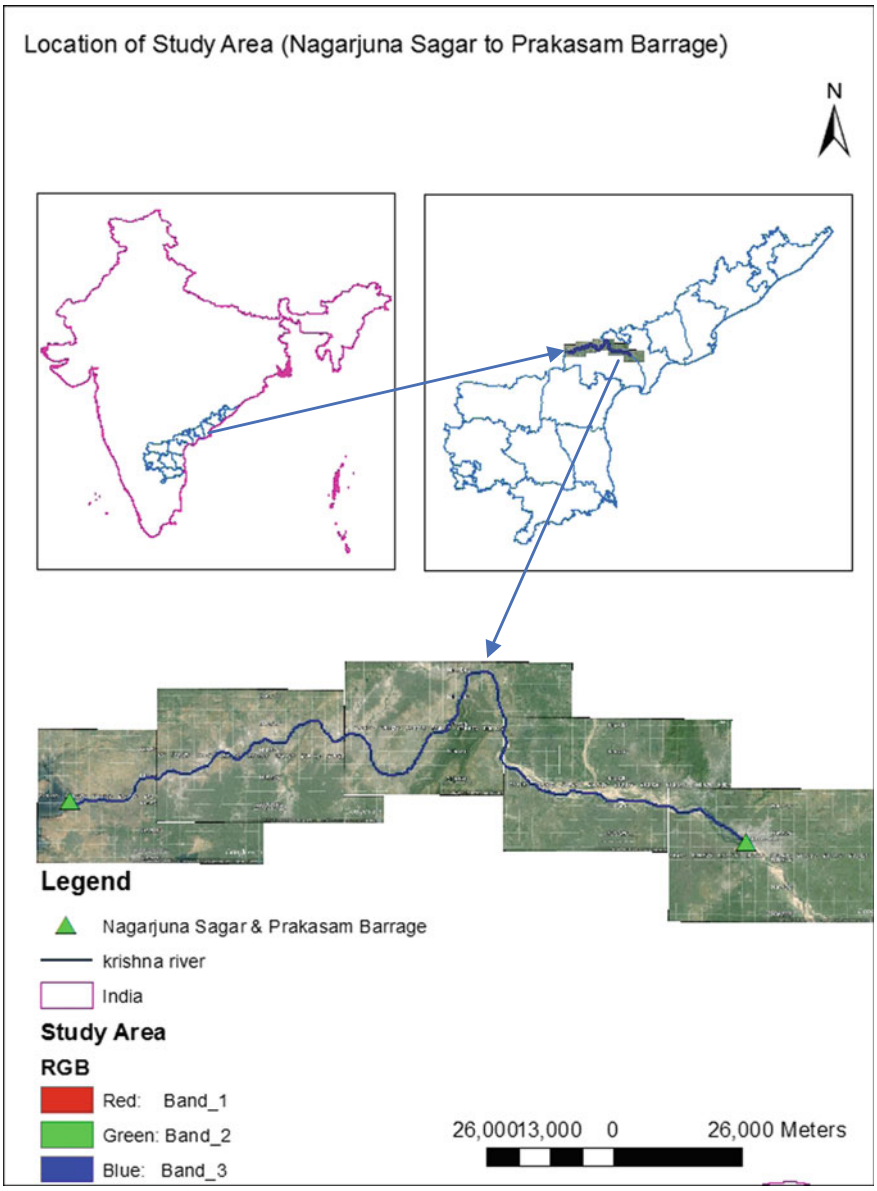

Fig. 1 Location of study area

horticultural crops. The total cultivable area in the basin is about 203,000 km^2, which is equivalent to 78% of the total geographical area of the basin. The current study is identified from Nagarjunasagar to Prakasam Barrage region as shown in Fig. 1. The length of the river reach is 188 km.

3 Methodology

SWAT is a complex physically based distributed parameter hydrologic model developed by the United States Department of Agriculture (USDA), which operates on a daily time step [3]. In SWAT surface runoff is estimated using the SCS curve number procedures [13] from the daily rainfall data. Based on the annual maxima of discharge predicted by SWAT at different reach segments, flood frequency analysis was carried out to predict the flood magnitudes of various recurrence intervals. Log-Pearson Type III distribution is often the preferred statistical technique for flood frequency analysis [12]. The flow values for different recurrence intervals

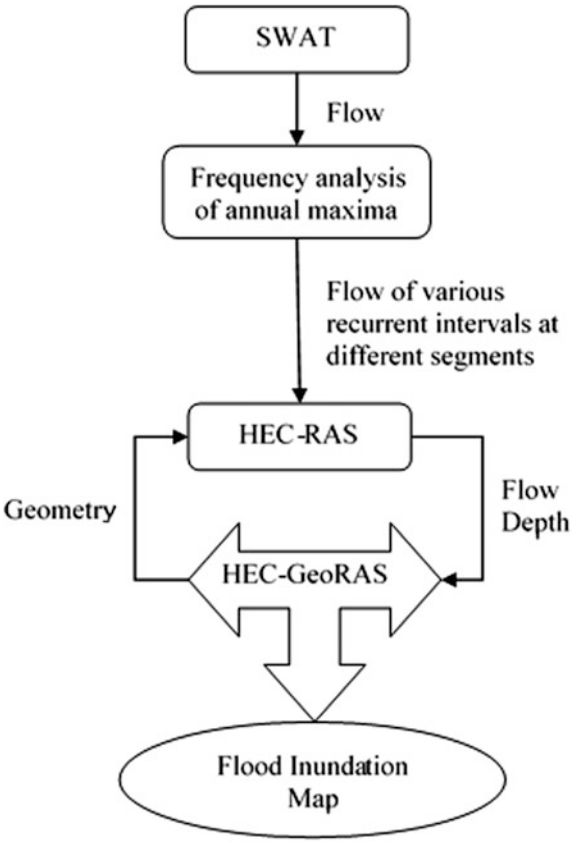

Fig. 2 Overall methodology

from this technique is given as input into a hydraulic model, HEC-RAS to estimate the water surface profiles. Flood inundation map is generated using HEC GeoRAS by comparing water surface TIN (Triangulated Irregular Network) with DEM, to compute the water surface elevation in the channel and flood plain. The overall methodology process is shown in Fig. 2.

3.1 SWAT Model Set-Up

Hydrologic modeling was carried out by using a distributed hydrological model SWAT. The data required to setup SWAT include topography, land use, soil, weather and land management practices. Accordingly, the ArcGIS SWAT model setup involves five major processes: (1) Watershed delineation (2) Landuse and Soil setup (3) Hydrologic Response Unit (HRU) definition (4) Weather data and

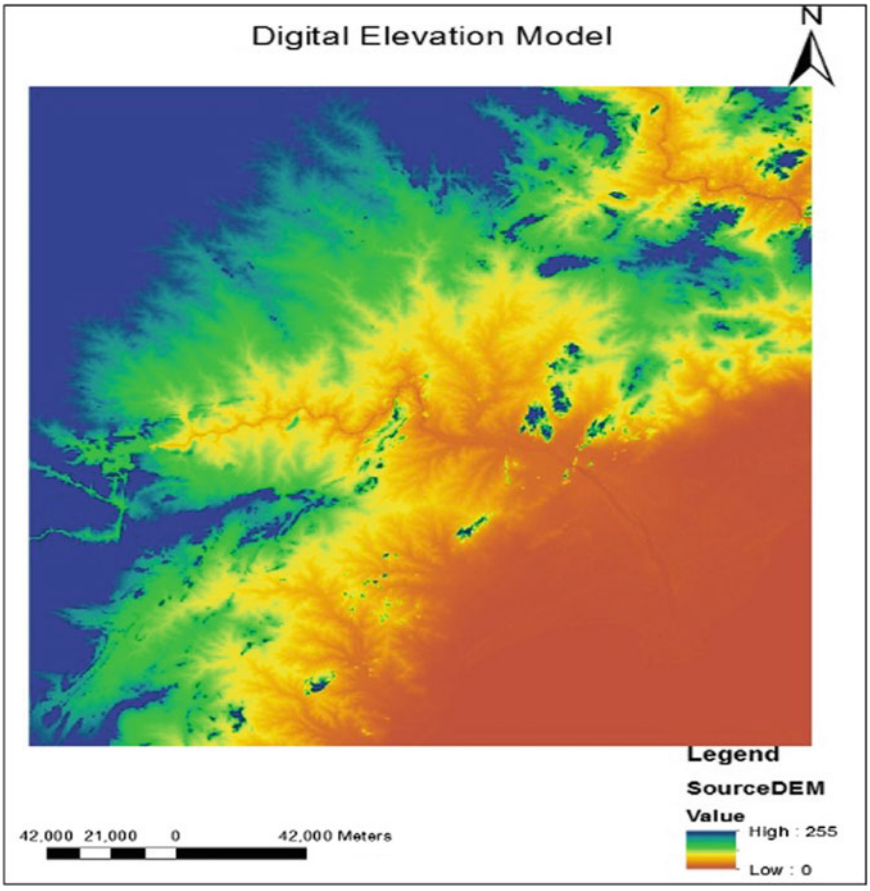

Fig. 3 Digital elevation model

(5) Land management information. ASTER (Advance Space borne Thermal Emission Radiometer) DEM of 30 m resolution was used for watershed delineation as shown in Figs. 3 and 4. Land use/land cover data was obtained from LANDSAT imagery as shown in Fig. 5. Soils data collected from FAO (Food and Agricultural Department), shown in Fig. 6. High resolution (0.5° × 0.5°) daily gridded rainfall data (1971–2005) developed by India Meteorological Department (IMD) [11] and 1° × 1° daily temperature data from IMD (1969–2007) [14] was used as weather data inputs for SWAT modelling. Watershed delineation was performed with a threshold area of 10,000 km^2 and 149 sub basins were obtained as shown in Fig. 4. SWAT performs analysis at HRU level. So, a threshold of 5% is given to land use and soil classifications. 1099 HRUs were obtained after incorporating threshold criteria.

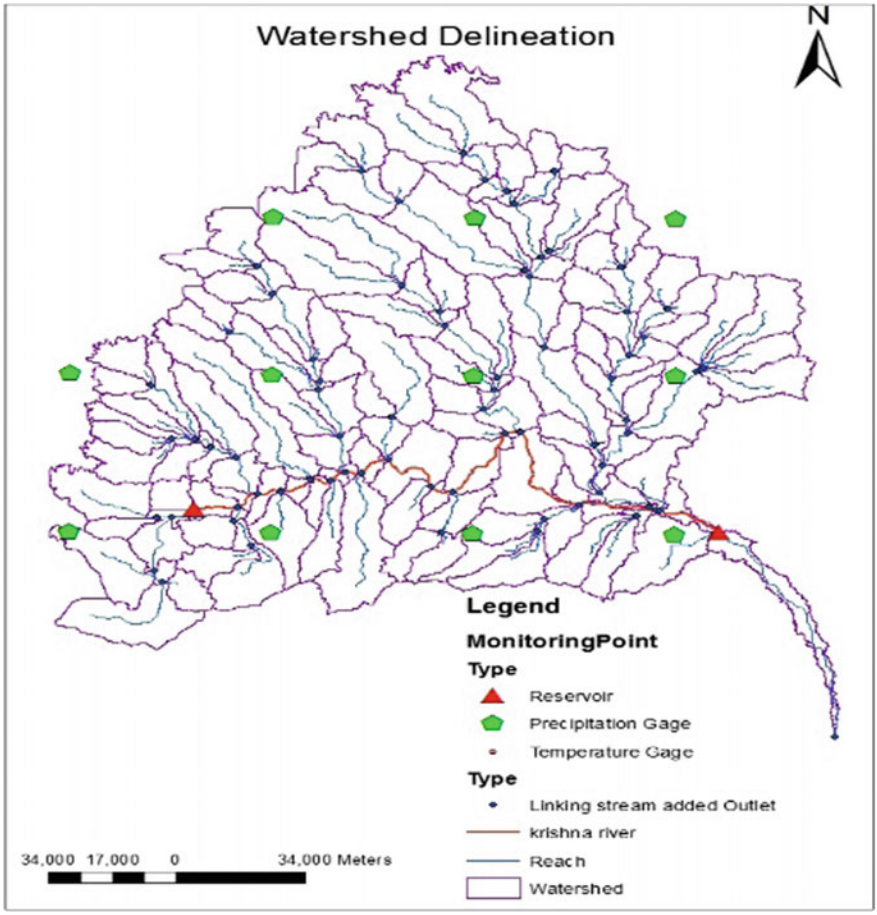

Fig. 4 Watershed delineation

3.2 HEC-RAS Model Set-Up

HEC-RAS is designed to calculate water surface profiles for steady or unsteady Gradually Varied Flow (GVF) in natural and manmade channels. Steady state analysis isperformed in this study to calculate the water surface profiles using the "standard step method". In this method, water surface profiles are computed by solving energy equation using an iterative procedure. HEC-GeoRAS is a geographic river analysis system developed using ArcGIS by U.S Army corps of engineers [7] to function as a pre-processor for preparing the input data for HEC-RAS from GIS and a post-processor to map the extent of flood plain. The data needed to perform these computations are separated into geometric data (elevation, river center-line, hydraulic structures etc.) and steady flow data (flow values of various recurrence intervals). The geometric data required by HEC-RAS were digitized from the Google earth imagery. The network was created on a reach by reach basis, starting from the upstream end and working downstream. Due to the lack of rating curve of flow data, the normal depth condition is assumed as the downstream boundary by assuming the flow below the most downstream section is mostly generally uniform. Many flood plain studies have used normal depth boundary condition at the downstream boundary when the actual water profile or rating curve information is lacking [1, 4]. Water surface profile predicted by HEC-RAS beyond a threshold limit in the river length from the downstream boundary, the effect would be negligible [6].

4 Results and Discussions

The output of the flood modeling is in the form of flood plain map, water surface profiles. The flow values for several return periods at the outlet point of the watershed was obtained by using Log Pearson Type-III distribution was plotted in Fig. 7. It is seen from the results that flood model can simulate the flow profiles for different flow conditions and the flood plain map shows that how much area effected due to flood with different return periods. i.e., 2, 10, 25, 50, 100 years. HEC-RAS provides the user with a large amount of hydraulic information in the form of flood plain maps and water surface profiles for any station or cross section, reach, and profile. sample output of flood plain map and water surface profiles of the region is shown in Fig. 8. The ASTER DEM has a spatial resolution of 30 m, which is a very coarse resolution for flood inundation mapping. So, for many sections along the stream, the active channel portion was not clearly discernable.

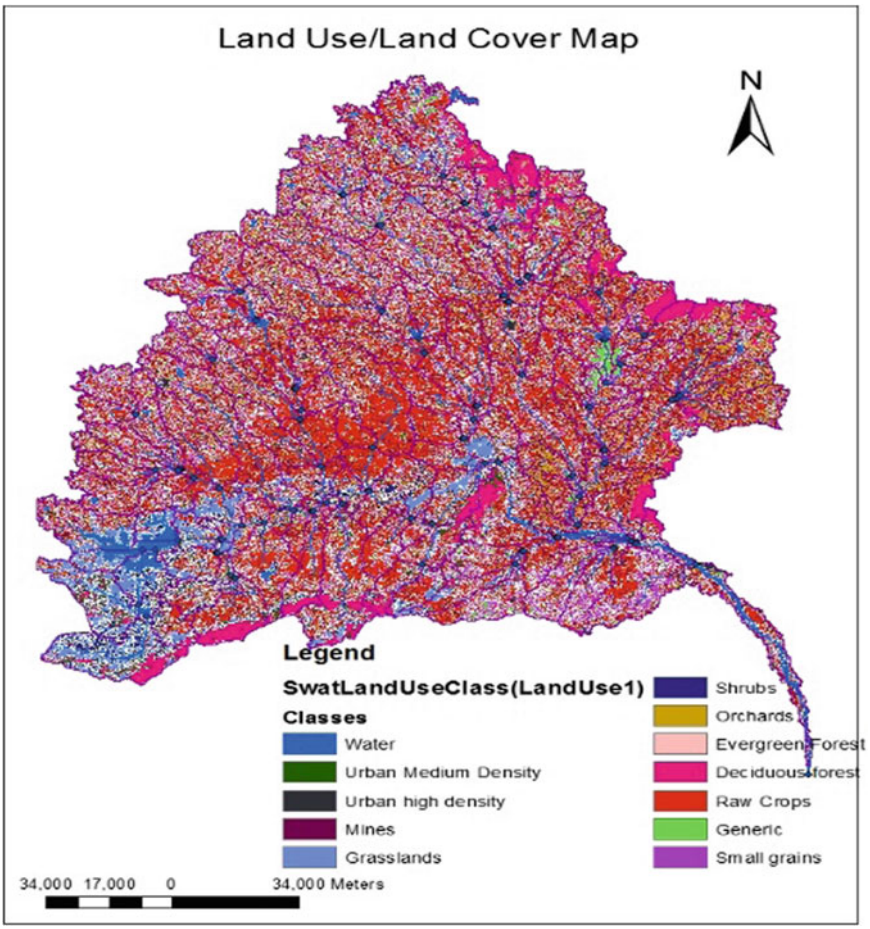

Fig. 5 Land use/land cover

This profile will facilitate to adopt appropriate flood disaster mitigation measures. The flood profiles for different flood intensities with different return periods can be plotted at any given cross section of river. Also, such flood profile can be plotted for entire length of river reach.

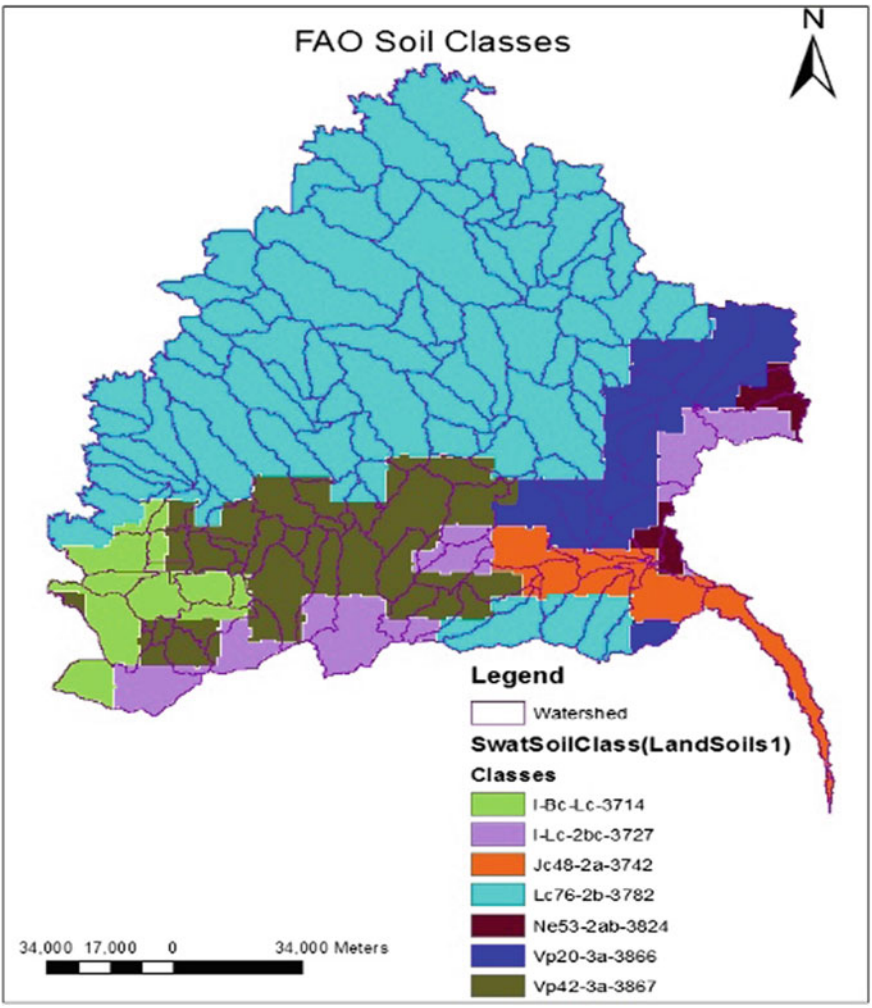

Fig. 6 FAO soils data

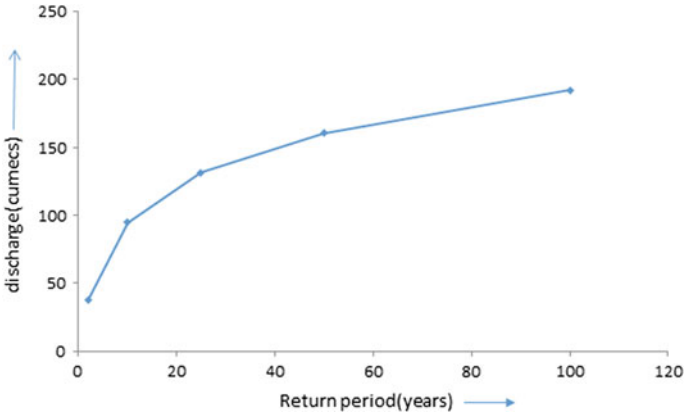

Fig. 7 Frequency analysis

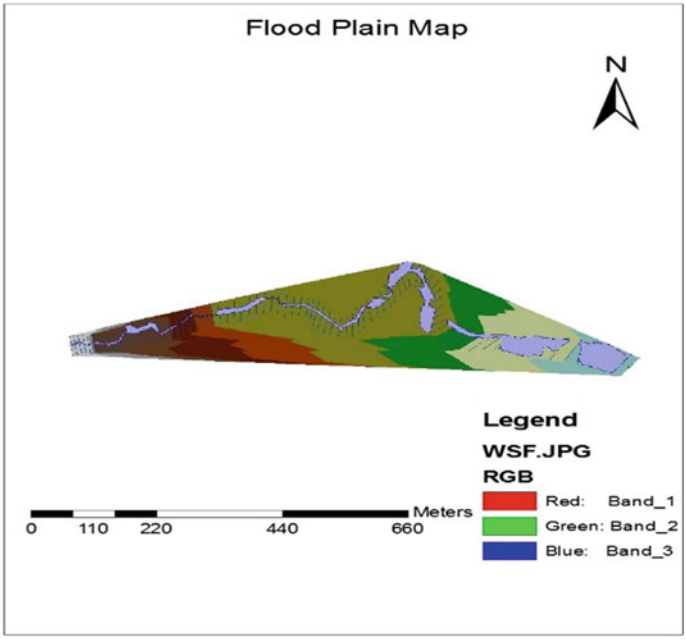

Fig. 8 Flood plain map

5 Conclusions

With the increasing availability of GIS data, the combination of SWAT, HEC-RAS and GIS models provides a method for modelling and visualizing the spatial distribution of the catchment response for a given storm event in terms of flood inundation area. The results of the model could be further improved if dense network of weather stations is available along with a good network of stream gauge data. High resolution digital elevation model or detailed channel cross section is not available for this study. In spite of this, the study demonstrates that ASTER DEM of 30 m resolution could be used for exploratory flood plain study of large watersheds. HEC-RAS being a 1-D model, careful attention should be placed to define the active channel section for modelling the flood depth by placing artificial levees on the channel banks. Flood modeling using HEC-RAS is effective tool for hydraulic study, handling of disaster management measures. These results obtained in this study provide essential information for and administrative to analyze and the manage flood hazards.

References

1. Alho, P., Aaltonen, J.: Comparing a 1D hydraulic model with a 2D hydraulic model for the simulation of extreme glacial outburst floods. Hydrol. Process. **22**, 1537–1547 (2008)
2. Arabi, M., Frankenberger, J.R., Engel, A., Arnold, J.G.: Representation of agricultural conservation practices with SWAT. Hydrol. Process. (2007). https://doi.org/10.1002/hyp.890
3. Arnold, J.G., Fohrer, N.: SWAT2000: current capabilities and research opportunities in applied watershed modeling. Hydrol. Process. **19**(3), 563–572 (2005)
4. Bales, J.D., Wagner, C.R.: Sources of uncertainty in flood inundation maps. J. Flood Risk Manag. **2**, 139–147 (2009)
5. Disaster Management In India: Government of India, Ministry of Home Affairs. National Disaster Management Division/MHA/GOI/28/06/2004 (2004)
6. Haested, Dyhouse G., Hatchett, J., Benn, J.: Floodplain Modeling Using HEC-RAS. Haested Press, USA (2003)
7. Hydrologic Engineering Center (HEC): GIS Tools for Support of HEC-RAS Using ArcGIS: Reference Manual, U.S Army Corps of Engineers, Cameron T. Ackerman, P.E. (2009)
8. Lagason, A.L.: Flood plain visualization using arc view GIS and HEC-RAS: a case study on Kota Marudu flood plain. Thesis, presented to University of Malaysia at Malaysia in Partial Fulfillment of the Requirements for the Degree of Bachelor of Technology (2008)
9. Olofintoye, O.O., Sukle, B.F., Salami, A.W.: Best-fit probability distribution model for peak daily rainfall of selected sites in Nigeria. J. New York Sci. **2**(3) (2009); ISSN 1554-0200
10. Narayane, P.R., Thakare, S.B., Gawande, S.M.: The analysis of physico-chemical characteristics of Water in Krishna River at Bhuinj, Satara. Int. J. Res. Emerg. Sci. Technol. **3**(5) (2016); ISSN 2349-7610
11. Rajeevan, M., Bhate, J.: A high resolution daily gridded rainfall data set (1971–2005) for mesoscale meteorological studies. NCC Research Report No. 9 (2008)

12. Salimi, S., Ghanbarpour, M.R., Solaimani, K., Ahmadi, M.Z.: Flood plain mapping using hydraulic simulation model in GIS. J. Appl. Sci. **8**(5), 660–665 (2008)
13. Soil Conservation Service: Section-4: Hydrology. National Engineering Handbook. SCS, Washington, DC (1972)
14. Srivastava, A.K., Rajeevan, M., Kshirsagar, S.R.: Development of high resolution daily gridded temperature data set (1969–2005) for the Indian Region. NCC Research Report No. 8 (2008)

Chapter 2
Rapid Detection of Regional Level Flood Events Using AMSR-E Satellite Images

Venkata Sai Krishna Vanama, Ch. Praveen Kumar and Y. S. Rao

Abstract Remote sensing plays a prominent role in the rapid detection of the flood event at a regional level. In this paper, the potential of AMSR-E images in regional level flood detection was identified. The study area of the research covers a part of Krishna river basin in the Andhra Pradesh state of India. Spatio-temporal database of daily Land Surface Water Coverage (LSWC) was developed by using Normalized Difference Polarization Index (NDPI). NDPI is calculated using AMSR-E brightness temperature of vertical and horizontal polarizations at 36.5 GHz frequency. The flood anomaly identified from the LSWC database is in strong agreement with actual flood events like Ogni cyclone. To extract the hidden information and similarities in the temporal images, image similarity was calculated by using Bhattacharya distance. Based on the similarity values, all the images in the database are ranked which helps in rapid flood information extraction. Among the various flood events identified by the database, Ogni cyclone is chosen for in-depth analysis. The SAR images acquired during the Ogni cyclone was used to validate the results of AMSR-E outputs.

Keywords AMSR-E · Bhattacharya distance · NDPI · LSWC
Ogni cyclone

V. S. K. Vanama (✉)
Centre for Urban Science and Engineering, Indian Institute of Technology Bombay, Mumbai, India
e-mail: vsaikrishna1990@gmail.com

Ch. Praveen Kumar
Civil Engineering, Indian Institute of Technology Bombay, Mumbai, India
e-mail: ch.praveenkumar786@gmail.com

Y. S. Rao
Centre of Studies in Resources Engineering, Indian Institute of Technology Bombay, Mumbai, India
e-mail: ysrao@csre.iitb.ac.in

P. J. Rao et al. (eds.), *Proceedings of International Conference on Remote Sensing for Disaster Management*, Springer Series in Geomechanics and Geoengineering,
https://doi.org/10.1007/978-3-319-77276-9_2

1 Introduction

Urbanization and climate change have greatly influenced the water cycle which resulted in the growing number of flood disasters globally [1]. The process of flooding is highly dynamic, so a large spatiotemporal database helps in understanding the nature and characteristics of a particular flood event [2]. Hydrologic and hydraulic models play a significant role in regional level flood identification and mapping, but these models are highly data and cost-intensive [3]. The geospatial technologies like Passive Microwave Remote Sensing (MRS) provide continuous spatiotemporal data which is an economical way to understand and identify the regional flood pattern. The main advantage of the MRS is its data acquisition cannot be interrupted by cloud cover. These datasets can be analyzed and processed to gain useful knowledge for formulating the policies and strategies of effective flood management by the government agencies. Passive MRS Sensors such as Advanced Microwave Scanning Radiometer-Earth Observing System (AMSR-E) onboard AQUA satellite has successfully acquired the data over entire globe from June 06, 2002 to Oct 04, 2011. After this Advanced Microwave Scanning Radiometer 2 (AMSR2) onboard GCOM-W satellite was launched by Japan to continue the data acquisition from July 02, 2012.

Many studies show that coarse resolution AMSR-E data was extensively used for identification [4], monitoring [5], analysing [6] the spatiotemporal variability of regional level flood disasters [7] and soil moisture mapping. Active MRS sensors like ENVISAT Advanced Synthetic Aperture Radar (ASAR) acquire images at a high spatial resolution which is very suitable for flood mapping at a local level, i.e. small geographic region. Also, the combined use of both high and coarse resolution MRS data helps in the better analysis of flood events [8]. The objective of this research is to develop a simple and cost-effective approach for regional level flood detection by combining the Land Surface Water Coverage (LSWC) database developed from both active and passive MRS images.

2 Study Area and Datasets

A part of Krishna river basin in coastal Andhra Pradesh (AP) shown in Fig. 1 which was flooded by Ogni cyclone during Oct 28–Nov 04, 2006 [9], is chosen as a study area of the research.

Three coastal districts of AP namely Krishna, Guntur and Prakasam were severely affected by the cyclone. Spatio-temporal datasets of Level-3 AMSR-E Brightness Temperature (BT) acquired with Vertical (V) and Horizontal (H) polarizations at 36.5 GHz from 2003 to 2010 were used for regional level flood event detection, i.e. at a district level. The spatial resolution of Level-3AMSR-E BT is 25 km, and the temporal resolution is 0.5 days, i.e. a day include one ascending

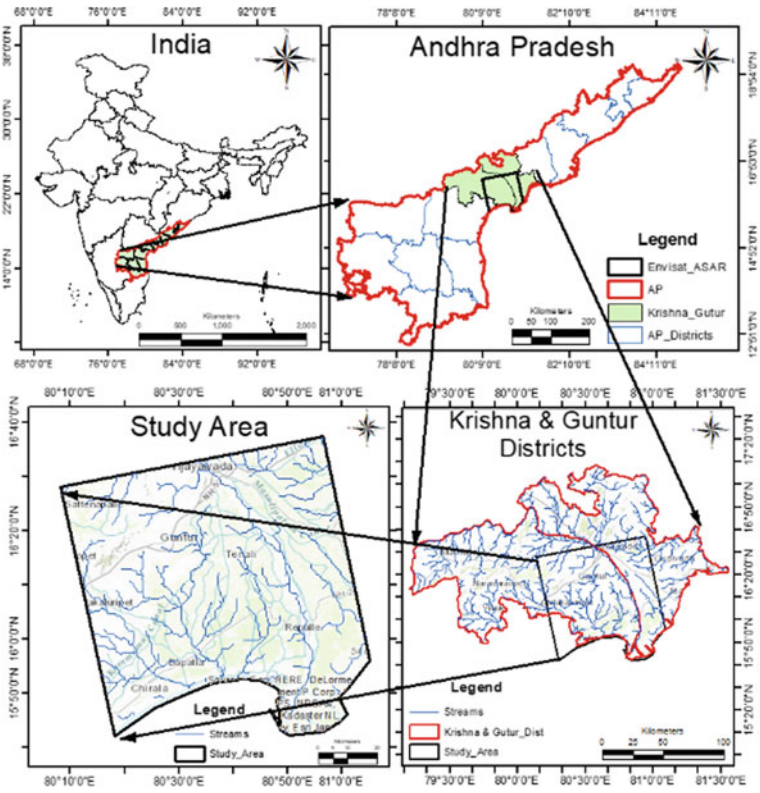

Fig. 1 Study area of the research

and descending passes. ENVISAT ASAR Alternating Polarization Single Look Complex (APS) images acquired before (26/08/2006) and during (04/11/2006) the flood event was used. Both images were acquired in strip map mode during the ascending pass of the sensor with a swath width of 89.35 km, the incident angle ranging from 30.8° to 36.1° and the polarizations include VV and VH.

3 Methodology and Analysis

The methodology of the research is divided into two parts, the first deals with processing and analysis of AMSR-E images, whereas second part deals with ENVISAT ASAR images.

3.1 Spatio-Temporal Analysis of Ogni Flood by AMSR-E Data

Various time series plots are createdfrom AMSR-E images for the entire Andhra Pradesh. Ithelped in quickly identifying the regional level flood events. At this point of analysis, the time and spatial locations of flood events are identified at a grid size of 25 km × 25 km. From the secondary sources, the list of flood events occurred in Andhra Pradesh are identified. Ogni cyclone flood event is selected for detailed analysis due to the availability of high-resolution active MRS data. Therefore, all the AMSR-E images are clipped to the same spatial extent of active SAR images for further analysis.

Level-3 AMSR-E BT images are calibrated by using the calibration factor (0.01) as given in the AMSR-E user manual [10] to obtain the actual BT in Kelvin. After the calibration, ascending and descending pass of AMSR-E images per day are averaged to generate a daily mosaic for both the polarizations. This daily product is further used to generate the normalized difference polarization index (NDPI) [11] by using the formula NDPI = $(BT_{36.5V} - BT_{36.5H})/(BT_{36.5V} + BT_{36.5H})$ where $_{V,H}$ refers to vertical and horizontal polarizations and 36.5 refers to frequencies of the emitted microwave signal to capture the flood. This index can significantly identify the presence of water on the land surface and can segregate the land and water surfaces. A simple normalization technique, the minimum-maximum stretch was applied on the index values to ease the interpretation of data which resulted in the formation of LSWC database from 2003 to 2010. The values of LSWC ranges from 0 to 100 where the higher values represent the flooded areas, and the lower values represent no flooded areas. For any flood-affected region, the fraction of land surface under the water cover is high. Hence, the LSWC computed from AMSR-E also represents a higher range of values. In addition to its applications in flood mapping, LSWC is also one of the most important criteria in crop growth and drought monitoring [12].

3.2 Spatial Analysis of Ogni Flood by ENVISAT Images

The ENVISAT ASAR VV SLC images are chosen for flood detection and mapping because co-polarized images are better than cross-polarized images. VV is more sensitive to water and results in high backscattering values than VH. The pre-processing of both pre and during flood ASAR images include radiometric calibration wherein radar pixel intensity, and the incident angle is used to compute backscattering coefficient (σ_0). The σ_{0vv} images are multi-looked with 8 * 2 (16 looks) to remove the speckle noise. To a certain extent, multi-looking can reduce the speckle noise, but to further reduce it, median speckle filter [13] with a window size of 3 * 3 is used. Slant range to ground range conversion and geocoding is performed to calculate the area of the flooded region. The simple difference method

[14, 15] is used to highlight the flooded regions. In this method, firstly the absolute difference is calculated from the processed σ_0 values of pre and during flood images to obtain the difference image. Secondly, them asking operation is performed on difference image by manually selecting a threshold [16] of Intensity (I) ≥ 10.7 to highlight the flooded regions.

4 Results and Discussions

4.1 Flood Detection from AMSR-E Images

Various time series plots such as daily, monthly and yearly are created from the LSWC database to understand the temporal distribution of flood.

The daily, monthly and yearly variation of LSWC are obtained by day, month and year wise averaging of all the pixels. These averages are calculated on a pixel by pixel basis, and all the computations are done based on the data availability for a particular day and all the missing data are omitted. Figure 2a shows the daily (first level of spatio-temporal aggregation) variation of LSWC for the flooded year (orange colour line) is plotted against all year's average (blue colour line). Figure 2b shows the daily variation of LSWC for all the years continuously that helps in flood trend identification. The flooded pattern is very clear in this figure and the flooded day, i.e. November 04, 2006, is highlighted in green colour vowel shape. The daily LSWC of the flood year is higher than the daily average of all years. Unfortunately, there was no pass of the satellite on some days of cyclone duration, i.e. 30th Oct 2006, 1st Nov 2006. From Fig. 2, it is also seen that some days in the time series are having higher peaks than the flooded regions. The occurrence of high peaks might be because of heavy rainfall during the monsoon season or the presence of large water bodies, diverse land uses and also two pixels in the study area has the part of the ocean. So, the microwave signal emitted from these pixels can also contribute to high LSWC. For in-depth analysis, a special investigation through data mining algorithms [17] and geospatial analysis is needed.

Figure 3a shows the monthly variation of LSWC for the flooded year (orange colour line) is plotted against all year's average (blue colour line). Figure 3b shows a monthly (second level of spatio-temporal aggregation) variation of LSWC for all the years. The flooded month, i.e. October, is highlighted in green colour vowel shape. From Fig. 3, it is also observed that August month is showing the higher LSWC percentage and also the LSWC percentage of the flooded year is lower than the monthly average of all years. This phenomenon can be understandable from Fig. 3b as it is showing the increasing trend of LSWC through the years 2003–2010. Due to low variation in the data and the low intensity of cyclone occurred for few days in October, the monthly LSWC of the flood year is lower than the monthly average of all years in October 2006. Whereas the intensity of cyclone is increased in the November month, the monthly LSWC of the flood year is higher than

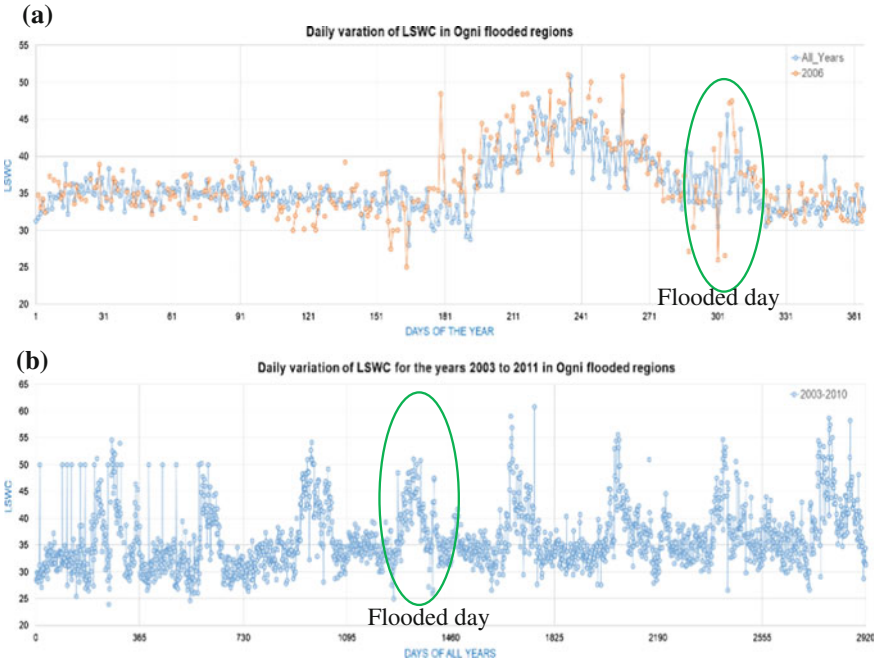

Fig. 2 Daily variation of LSWC in Ogni cyclone flood affected area

the monthly average of all years in November 2006. Figure 4 shows the monthly spatial variation of LSWC in Ogni cyclone flood affected area. A standard deviation stretch with n = 2.5 is applied on the images. The blue colour in the represents 100% LSWC, and red colour represents 0% LSWC. The low spatial variation in the images is attributed to heterogeneous land uses, spatio-temporal aggregation, and coarse resolution of the data.

Figure 5 shows the yearly (third level of spatio-temporal aggregation) variation of LSWC for the years 2002–2010. An exponential regression curve is fitted to the yearly data and obtained an R^2 value of 0.8147. It is seen that there is an increasing trend in LSWC throughout the years. The increasing trend in the LSWC attributes to heavy urbanization in the study area as well as missing data is not accounted in the analysis.

4.2 Image Similarity Calculation

To find out the hidden regularities and to get more information from the LSWC geodatabase, an image with highest LSWC is chosen. Image similarity for all the images is calculated by comparing to highest LSWC image using Bhattacharya

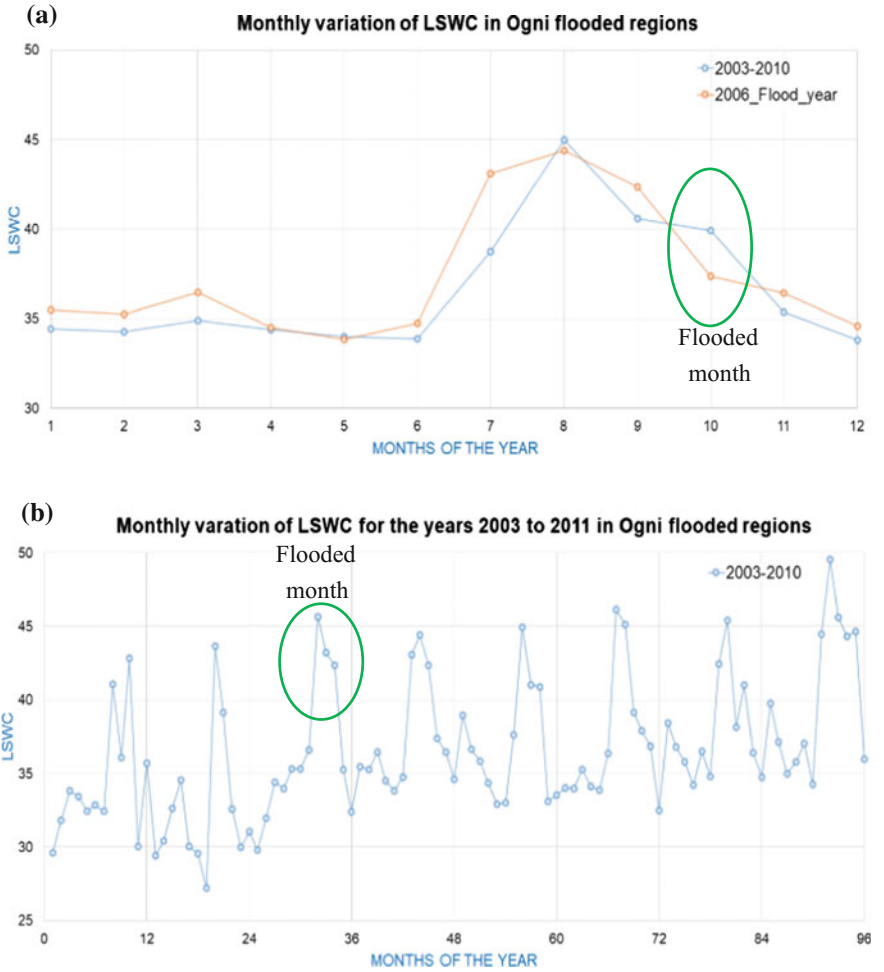

Fig. 3 Monthly variation of LSWC in Ogni cyclone flood affected area

distance. The smaller distance indicates a better match between the two images and vice versa. From the results, it is found that images during the monsoon season have high similarity values. It is mainly due to the heavy rainfall that makes the land surface covered with more water. Based on these similarity values, all the images in the database are ranked which helps in rapid flood information extraction. Out of the eight images from Oct 28 to Nov 04, 2006 when the Ogni flood occurs, Oct 30th image had the highest similarity value with 0.812436 and ranked as a 14th image in the entire database.

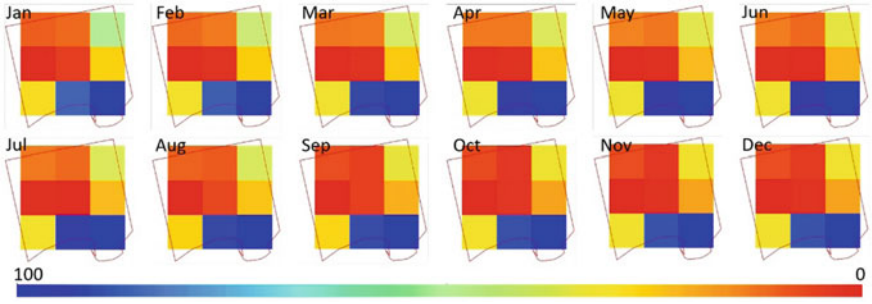

Fig. 4 Monthly spatial variation of LSWC in Ogni cyclone flood affected area

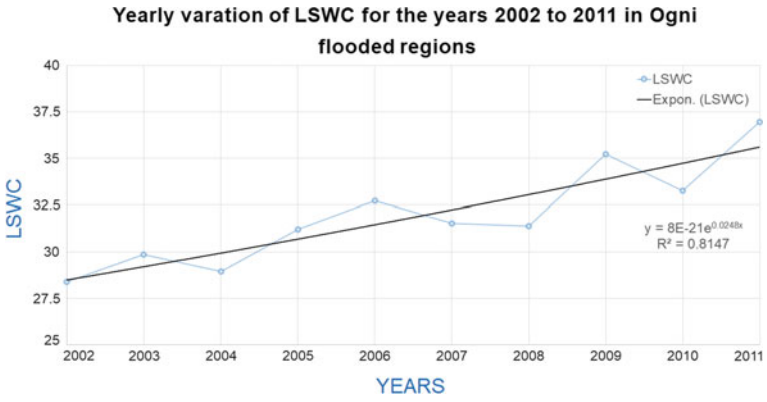

Fig. 5 Yearly variation of LSWC in Ogni cyclone flood affected area

4.3 Flood Detection from ENVISAT Images

The high spatial resolution of ENVISAT ASAR images enables the accurate identification of the flooded regions. From the AMSR-E results, temporal component of the flood is identified but the spatial component, i.e. identification of exact spatial locations of flooded regions can be achieved by ENVISAT ASAR VV pre and during flood images. The spatial extent of flood area identified by difference methods is around 631.402 m^2. A threshold of intensity values greater than 10.1 dB is chosen for flood identification. The SLC images are shown in Fig. 6, and geocoded images are shown in Fig. 7. In Fig. 8, the flooded area is shown in red colour, whereas blue colour showed the permanent water body.

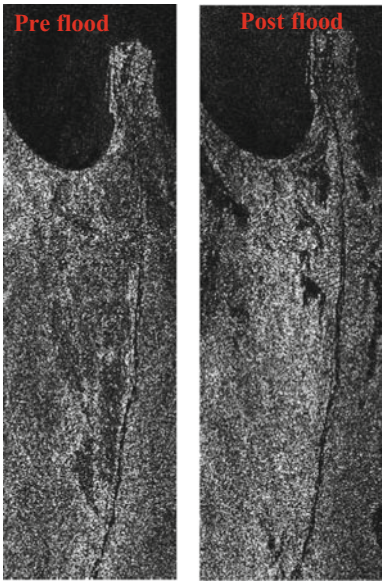

Fig. 6 Pre (left) and during (right) flood ENVISAT ASAR VV SLC images

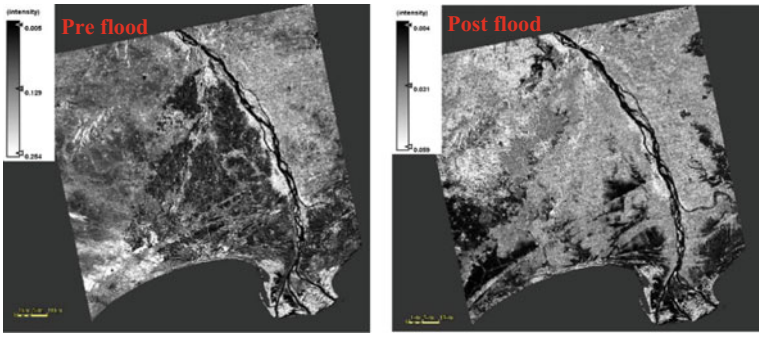

Fig. 7 Pre (left) and during (right) flood geocoded images

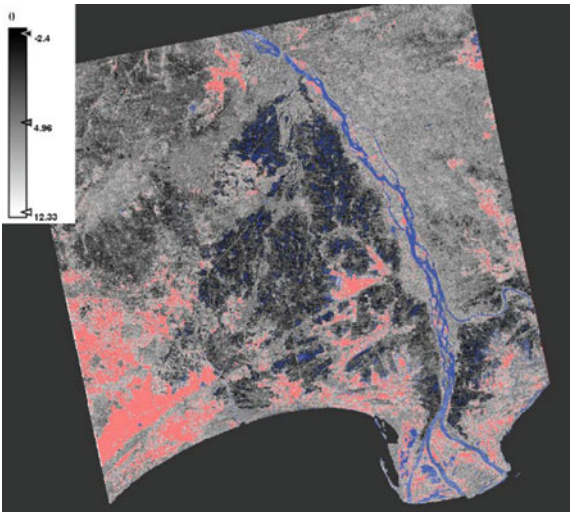

Fig. 8 Flood area (red colour) by difference method

5 Conclusions

In this paper, LSWC is derived from passive coarse resolution AMSR-E BT. The daily LSWC geodatabase in the time series from 2003 to 2010 has been created. This geodatabase has a great potential to quickly identify the spatial and temporal components of various flood events at a regional level. Also, first level of spatio-temporal aggregation of data is more useful for identifying the regional level flood event. Image similarity calculation also plays a major role in getting more information and hidden similarities in the flood pattern. The results of AMSR-E are also in good agreement with the active ENVISAT ASAR images. The limitations of the LSWC geodatabase is the underestimation of the flooded area due to its coarse resolution, and heterogeneous land uses in the study area.

Acknowledgements The first author is thankful to the Ministry of Human Resource Development, GoI for providing necessary computational facilities through the project 14MHRD005 funding. Authors are thankful to ESA for providing ENVISAT SAR data free of cost. We thank Head C-USE, IIT Bombay for his support throughout the research.

References

1. Field, C.B., IPCC, (eds.): Managing the Risks of Extreme Events and Disasters to Advance Climate Change Adaptation: Special Report of the Intergovernmental Panel on Climate Change, 1. publication Cambridge University Press, Cambridge (2012)
2. Kristóf, D., Giachetta, R., Olasz, A., Belényesi, M., Thai, B.N., Harsányi, M.: Using big geospatial data for fast flood detection: developments from the IQmulus project. In: 2015

IEEE International Geoscience and Remote Sensing Symposium (IGARSS), pp. 838–841 (2015)
3. Karmakar, S., Simonovic, S.P., Peck, A., Black, J.: An information system for risk-vulnerability assessment to flood. J. Geogr. Inf. Syst. **02**(03), 129–146 (2010)
4. Singh, Y., Ferrazzoli, P., Rahmoune, R.: Flood monitoring using microwave passive remote sensing (AMSR-E) in part of the Brahmaputra basin, India. Int. J. Remote Sens. **34**(14), 4967–4985 (2013)
5. Arnesen, A.S., et al.: Monitoring flood extent in the lower Amazon River floodplain using ALOS/PALSAR ScanSAR images. Remote Sens. Environ. **130**, 51–61 (2013)
6. Chakraborty, R., Rahmoune, R., Ferrazzoli, P.: Use of passive microwave signatures to detect and monitor flooding events in Sundarban Delta, in , 2011 IEEE International Geoscience and Remote Sensing Symposium (IGARSS), pp. 3066–3069 (2011)
7. Temimi, M., Leconte, R., Brissette, F., Chaouch, N.: Flood and soil wetness monitoring over the Mackenzie River Basin using AMSR-E 37 GHz brightness temperature. J. Hydrol. **333**(2–4), 317–328 (2007)
8. Li, X., Takeuchi, W.: Land Surface Water Coverage Estimation with PALSAR and AMSR-E for Large Scale Flooding Detection. Terr. Atmos. Ocean. Sci. **27**(4), 473 (2016)
9. Roy, S.S., Lakshmanan, V., Roy Bhowmik, S.K., Thampi, S.B.: Doppler weather radar based nowcasting of cyclone Ogni. J. Earth Syst. Sci. **119**(2), 183–199 (2010)
10. Imaoka, K., Kachi, M., Kasahara, M., Ito, N., Nakagawa, K., Oki, T.: Instrument performance and calibration of AMSR-E and AMSR2. Int. Arch. Photogramm. Remote Sens. Spat Inf. Sci. **38**(8), 13–18 (2010)
11. Xi, L., Takeuchi, W.: Development of large scale flooding detection method by integrating historical global record using AMSR-E/AMSR2 with PALSAR. In: 2015 IEEE International Geoscience and Remote Sensing Symposium (IGARSS), pp. 822–825 (2015)
12. Zheng, W., Liu, C., Xin, Z., Wang, Z.: Flood and waterlogging monitoring over Huaihe River Basin by AMSR-E data analysis. Chin. Geogr. Sci. **18**(3), 262–267 (2008)
13. Yulianto, F., Sofan, P., Zubaidah, A., Sukowati, K.A.D., Pasaribu, J.M., Khomarudin, M.R.: Detecting areas affected by flood using multi-temporal ALOS PALSAR remotely sensed data in Karawang, West Java, Indonesia. Nat. Hazards **77**(2), 959–985 (2015)
14. Bormudoi, A., Hazarika, M.K., Samarakoon, L., Phaengsuwan, V., Thanasack, K.: Potential use of ALOS PALSAR in flood hazard mapping, a case study in five districts, LAOPDR, presented at the 8th Annual Mekong Flood Forum, Vientiane (2010)
15. Alexakis, D.D., Agapiou, A., Themistocleous, K., Retalis, A., Hadjimitsis, D.G.: Using ERS-2 and ALOS PALSAR images for soil moisture and inundation mapping in Cyprus, p. 87950Z (2013)
16. Henry, J.-B., Chastanet, P., Fellah, K., Desnos, Y.-L.: Envisat multi-polarized ASAR data for flood mapping. Int. J. Remote Sens. **27**(10), 1921–1929 (2006)
17. Li, X., Takeuchi, W.: Flood analysis and forecasting by spatio-temporal data mining based on historical satellite image database, presented at the Asian Association on Remote Sensing (AARS) (2014)

Chapter 3
GIS Technology for Assessment of Urban Green Cover Area of Madurai Corporation in Tamil Nadu

Nagaraju Thummala, M. Madhuri, E. Srinivas, A. Narsing Rao and V. E. Nethaji Mariappan

Abstract India is one among the developing country that needs attention in the planning and development of urban areas such as smart cities in intention of (urban space index). Remote sensing and geospatial tools includes satellite based systems together with GIS enable a planner to spatially map the urban region in near real time condition, provide management and decision support system for urban planning. An initiative was taken up to map thematic layers Madurai Corporation using high resolution Cartosat-2 satellite data. A visual interpretation technique was employed to delineate spatial features that are individual trees, group of trees, building area, water bodies, parks and temples were derived in GIS environment. Respective thematic are listed as tree cover area 6.0190 km^2, Buildings 29.0749 km^2, Parks 0.1055 km^2, Water bodies 4.0318 km^2 and other area 17.4929 km^2 out of 52.9054 km^2 area coverage of Madurai municipality corporation and total number of trees 2,19,145 trees identified from crown area calculation method. Eventually a methodology is evolved to spatially define applicable green space areas.

Keywords Remote sensing · GIS · Madurai corporation · Crown area Number of trees · Green pace

N. Thummala (✉) · A. Narsing Rao
Department of Geology, Osmania University, Hyderabad 500007, India
e-mail: tnr.2020@gmail.com; tnr.3030@gmail.com

A. Narsing Rao
e-mail: narsing1958@gmail.com

M. Madhuri
MRIT, Maisammaguda, Secunderabad, Hyderabad 500014, India
e-mail: madhurimulpuru@gmail.com

E. Srinivas
Department of Applied Geo Chemistry, Osmania University, Hyderabad 500007, India
e-mail: srinivase4@gmail.com

V. E. Nethaji Mariappan
CRSG, Remote Sensing Department, Sathyabama University, Chennai 600119, India
e-mail: nethajim@gmail.com

P. J. Rao et al. (eds.), *Proceedings of International Conference on Remote Sensing for Disaster Management*, Springer Series in Geomechanics and Geoengineering,
https://doi.org/10.1007/978-3-319-77276-9_3

1 Introduction

Urban green spaces are defined as public and private open spaces in urban areas [1], primarily covered by vegetation, or open spaces which are directly or indirectly available for the user. Green spaces have their own ecological function in the environment. But when we concern with urban environment then we find their social function as well [2]. Urban areas can comprises large variety of green spaces [2, 3], such as gardens green area near government department, private and Industrial green areas [2]. Green crown area plays a major role in urban and industrial areas through their social, economic and environmental benefaction to resident's health and wellbeing [4]. The World Health Organization (WHO) established green space per capita standard values. According to WHO, the minimum amount of green space required per capita for healthy living is 9.5 m^2/person [1]. Remote sensing a new technology that can gather information on a target without coming in direct contact, and usually refers to the acquisition and processing of information on the earth's surface. From this aspect, Crown area and number of trees planning should be an essential part of any urban area development. In this study an integrated approach of GIS and Remote Sensing Technology has been applied to identify and analyze the patterns of spatial information on developments of urban areas. We compare a rather unique dataset from urban trees scrutinize their stem diameter crown width with classified different tree species from Cartosat-2 satellite data. Number of trees calculated from individual trees and group of crown cover area from Cartosat-2 satellite data derived from crown area calculation method.

2 Study Area and Satellite Data

Madurai is one of the industrialized cities referred as Detroit of India The spatial area of Madurai corporation area 53 km^2. Madurai District is located at show location map 9° 56′N 78° 07′E/9.93°N 7.12°E/9.93;78.12 as shown in the Fig. 1. That has an average elevation of 103 m above mean sea level according to the survey of India [5]. Madurai Corporation a tropical climate with average annual temperature of 25.1 °C {min} to 39.8 °C (max). The humidity is generally in the change from 59 to 81% and in the evening time is a blessing to combat the high temperature and humidity during hottest months. The mean annual rainfall of the Madurai Corporation is in the extent of 1283.1 to 1233.2 mm. Madurai Corporation is underlain by various geological formations from the ancient *Archaeans* to the Recent Alluvium.

Data are analysed by using suitable Cartosat-2 satellite data as inputs, new datasets and results for various geo processing tools. This helps to make a reiterate, well—recorded data processing workflow. Utilizer also works with ArcGIS data file

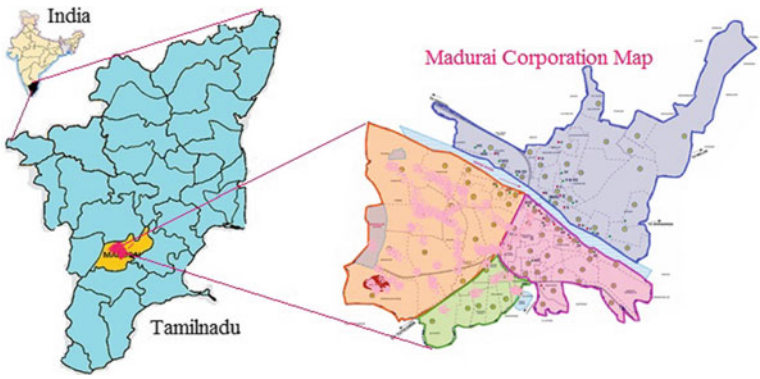

Fig. 1 Location map of the Madurai Corporation study area

to implement spatial analysis. Visual interpretation and different classification plays an important role in describing spatial features of the objects by a geo spatial organization.

3 Methodology

Urban area coverage in Madurai Corporation was mapped using digital image processing software and ArcGIS software for digitization and classification using Cartosat-2 satellite data. The satellite data products were found possess higher resolution and therefore we could able to generate all themes in a precise manner. Thematic features such as trees, buildings, parks, tanks, temples and other areas were derived in Madurai Corporation. Area of each land uses were calculated in square kilometer. Remote sensing is an important source of information for GIS which are then displayed as digital images [6]. Digitizing is the process of making features we can see on the Cartosat-2 image editable and making them. At present, maps are mainly digitized by editing in special sizes of particular earth feature that can be handled by a shape file layer. When preparing the catalogue, consider the characteristics of map data so that it allows convenient access. The basic idea is to express total crown cover area as a relation between the sum of the crown areas of nearby trees at a time and the area of their convex hull [7]. The delineation tree cover was carried out two ways (i) wherever the individual trees are visible at the scale of 1:10,000 such trees are plotted as points within the framework of Madurai corporations [2]. These usually exists as avenues trees or road side trees where the trees are planted linearly thereby enumeration of trees were possible through visual interpretation. (ii) In most of the places, merging of trees happen to be problem, where all the different tree species were grouped together, were individual tree enumeration seems to be practically not possible. In that scenario, boundary of the grouped trees was demarcated spatially and its spatial extent was calculated and

classified areas fulfilling different tree species thresholds. With the expertise available from the individual and the ground truth information the tree diameter is identified. Aggregating the trees diameter to total demarcated area will provide us the number of trees within the spatial extent. Crown area is the actual area of a tree as observed from the space [7]. This study involve only the satellite data component, we used Cartosat-2 data to derive the crown diameter of individual tree for a single tree surrounding group of crown area. In spite of the fact that among the grouping of trees, we devised a novel strategy of deriving the trees area of individual shape file. It is well known fact that there would gaps between the trees, and such gaps will not account for the crown area (i.e.) is to be eliminated from the individual shape file [2]. A separate analysis was taken up on how to deduce the gaps within and between trees to derive the actual crown area. Finally, the potential crown cover area within the study area is determined. The results the sum of classified areas fulfilling different tree species thresholds are compared with field data which area is difficult to identification in satellite data. Water bodies cover with ponds, lakes, rivers, streams and water tanks structures that are spatially sensible on the Cartosat-2 satellite images. These features are dynamic [2] and temporal in nature [8]. It is an illustrious that all the Madurai Corporation possesses large number of concrete shape to accommodate all Government departments, residential and private centres. Such attributes are identified based on reflectance properties of Cartosat-2 satellite that are represented by light tonal differential due to earth surface highest reflectance. Features such as parks and temples usually have a pattern in the form of rectangle or square which will be a minimum requirement for delineation of these boundaries. All these boundaries are identified in shape file format in temples. Areas other than aforementioned features are represented as open area. Usually such are less open area in Madurai corporation and more in all other.

4 Results and Discussion

In Madurai Corporation occupied total area 53 km^2, minimum area occupied in temple area and maximum area occupied building area as well as occupied Tanks, Parks, Trees as shown in the bellow Table 1. In case of sparse distribution, grouping takes place depends on the level of distribution as segments. Sample points were selected to identify centre point of each tree species; radius and diameter of tree crown were also performed for most of the trees. An average tree diameter was arrived, that helped to us to derive circumference of individual tree. The average diameter value was used as an input to derive number of trees from each grouped shape file. Thus tree number and crown area was enumerated for Madurai Corporation. Cartosat-2 data used to derive the crown diameter of individual tree surrounding group of trees. Each tree area calculated (circle area = ΠR^2). Approximately the mean crown area radius modified according to the (http://www.ents-bbs.org/viewtopic) that Equation as follows (1)

Table 1 Madurai corporation different area calculation

Madurai Municipal Corporation area		
S. No	Name	Area (km^2)
1	Total area	52.9054
2	Buildings	29.0749
3	Parks	0.1055
4	Tanks	0.1055
5	Temples	0.1097
6	Trees area	6.0190
7	Others	17.4929

$$Average\ crown\ spread\ radius = (longest\ spread + longest\ cross\ spread)/4 \quad (1)$$

Finally approximately tree circle Radius value was taken as 2 to 5 m as follows in the Eq. (2) and these values applied to classifies group crown area from Cartosat-2 data for estimation of number of trees. Each tree area is occupied 12.56 to 78.5 m^2, finally studied total number of trees from total crown area divided by each tree area [2]. Alternatively the trees crown area can be estimated and crown spread computed from that value Easy Acreage V1.0 (*demo version*) http://www.wildsoft.org/2013 are measurement tool that calculates the area of any tree shape area. The area is arrested as the area of a similar circle. Approximately the mean crown area radius calculates according to the (http://www.ents-bbs.org/viewtopic) that Equation as follows (3). The total number of trees in Madurai Corporation was containing 235,528 trees as shown in the Table 2.

$$Crown\ spread\ radius = (area/\pi)^{1/2} \quad (2)$$

$$Number\ of\ trees = \frac{Total\ crown\ area}{Each\ tree\ crown\ area} \quad (3)$$

$$T_{NT} = \frac{(T_{CRA} - T_{ch})}{\Pi R^2} \quad (4)$$

Table 2 Detail of Madurai Corporation Crown area trees and individual trees from Crtosat-2 data

Crown spread radius(m)	Total tree crown cover area (km^2)	Gaps between tree area (km^2) (convex hull)	Crown area (km^2)	Number of trees
2	1.30	0.08	1.22	97,133
3	2.41	0.06	2.35	83,159
4	2.10	0.18	1.92	38,216
5	0.21	0.16	0.05	637
Total	6.02	0.48	5.54	2,19,145
Individual trees				16,383

where T_{NT} = Total number of trees, T_{CRA} = Total crown cover area, T_{ch} = area of the convex hull.

During the way of the mapping moderns, area of structure as view from satellite data a minimum size of 2 m * 2 m size can be mapped [2].

Larger structures could be spatially arrested in a convenient manner. At all point of time the map scale has been attached to 1:10,000 scales in order to acquire maximum features with exact accuracy. Area calculation was carried out in ArcGIS software to derive total area of the Madurai buildings (29.0749 km^2). A separate work on delineation of tanks was taken up by digitizing boundary of tanks, ponds, lakes, river and streams within the study region. Boundary of water bodies was digitized as area of the water as shown in the Fig. 2. Water level of the water bodies may not be considered as water boundary, as water level of the lakes varies according to the seasonal rainfall [8]. Generally lakes possess different shape as viewed through satellite data. Lake Layer was generated for Madurai region that accounts for (23.73 km^2). These water bodies have a similar pattern as seen through Cartosat-2 satellite data. Parks feature may be represented by the open spaces at the centre of grassland and plantation of trees area as shown in the Fig. 2. A vey minimum concrete shape is available in the grassland for recreation purpose. Such structure are delineated as polygon feature from Cartosat-2 satellite imagery and aggregated to a single layer to derive the park area of Madurai Municipal Corporation that accounted for 3.21 km^2.

Temples are widely dispensed within the Madurai municipal corporation. The older place of warship possesses larger boundary with more open spaces and little tree areas and recent temples are smaller in size having greenery and less open spaces where total area of temples was of 0.85 km^2 of the total area of 52 km^2. Madurai corporations.

The regions that a left other than the aforementioned themes were classified as other regions. Such areas were not extracted from Cartosat-2 satellite data. However, the open spaces left out after delineating all the themes are referred as other regions. These regions include both government parcels and private parcels that are suited for development of greenery within the Madurai Corporation (17.49 km^2).

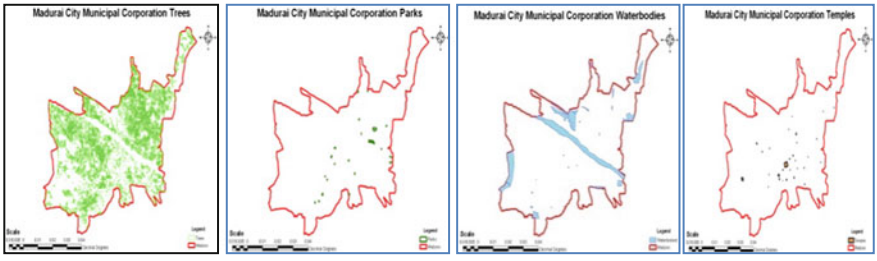

Fig. 2 Madurai City Corporation of tree covers area, parks area, water body and temples

5 Conclusions

A Green cover area evaluation study has been carried out to estimate the existing green cover area in Madurai Corporation of Tamil Nadu calculable. Cartosat-2 data with a pixel resolution of 1 m of gray scale was very efficient in deriving information on large scale objects such as buildings, individual trees, tanks and temples of very smaller size. The methodology adopted in this study can be utilized effectively in other urban centres to calculate the required amount of number of trees, green spaces and to identify the sites to create green spaces, in order to enhance the environmental quality of the city based on WHO standards. It could be effect that a decrease of the tree crown density in urban area leads to an increase of population in urban area. In future studies, the method will be firstly investigated for mixed trees and individual trees; secondly a validation with urban inventory will be performed and evaluation of connected benefits of trees in urban planning processes.

References

1. Kuhelmeister, G.: Urban forestry: present situation and prospects in the Asia and Pacific region, FAO Asia-Pacific forestry sector outlook study. Food and Agriculture Organization of the United Nations, Forestry Policy and Planning Division, Rome (1998)
2. Meera Gandhi, G., Thummala, N., Christy, A.: Urban green cover assessment and site analysis n Chennai, Tamil Nadu—a remote sensing and GIS approach. ARPN J. Eng. Appl. Sci. **10**(5), ISSN 1819–6608 (2015)
3. Heinze, J.: Benefits of green space—recent research. Environmental Health Research Foundation, Chantilly, VA (2011)
4. Faryadi, S., Taheri, S.: Interconnections of urban green spaces and environmental quality of Tehran. Int. J. Environ. Res. 3(2):199–208, ISSN: 1735–6865 (2009)
5. Santhiya, G., Lakshumanan, C., Muthukumar, S.: Applying of landuse/landcover changes of Madurai coast and issues related to coastal environment using remote sensing and GIS. **1**(3), ISSN 0976–4380 (2010)
6. Onur, I., Maktav, D., Sari, M., Sonmez, N.K.: Change detection of land cover and land use using remote sensing and GIS, a case study in Kemer. Turkey. Int. J. Remote Sens. **30**(7), 1749–1757 (2009)
7. Eysn, L., Hollaus, M., Schadauer, K., Roncat, A: Crown coverage calculation based on ALS data. In: SilviLaser 2011, Hobart, Australia, 16–20 Oct 2011
8. Stern, M.J., Powell, R.B., Hill, D.: Environmental education program evaluation in the new millennium: what do we measure and what have we learned?. Education Research, Environ (2013). https://doi.org/10.1080/13504622.2013.838749

Chapter 4
Insight to the Potentials of Sentinel-1 SAR Data for Embankment Breach Assessment

Thota Sivasankar, Ranjit Das, Suranjana B. Borah and P. L. N. Raju

Abstract Embankment breaching is one of the serious issues on the innumerous streams of the Brahmaputra floodplains during the monsoon season, which extends from May to October, leading to major agricultural damages by inundation and sand casting. These floodplains are highly fertile areas supporting a dense population largely dependent on agriculture for livelihood. Therefore, continuous monitoring and management is required so that the annual loss due to embankment breaching can be minimized. Traditional on-site methods are laborious and time consuming. The use of Synthetic Aperture Radar (SAR) data for this application is recommended instead of commonly used optical remote sensing data due to its all-weather capability and high sensitivity towards dielectric constant. This study analyses the potentials of C-band dual polarized (VV + VH) SAR data for embankment monitoring and breach assessment such as identification of breach locations, length of breach and area affected due to inundation after occurrence of breach. For the purpose of study, Solengi river, a north bank tributary of the Brahmaputra in Assam is used as a case study. Temporal Sentinel-1 data are continuously analyzed to monitor critical points of embankments and develop a suitable methodology to operationalize embankment breach monitoring. The initial analysis shows encouraging results. This methodology, if successful, may be helpful to automate the process of monitoring embankment breaches enabling better decision making.

Keywords Sentinel-1 · SAR · Flood · Embankment breach assessment Monitoring

T. Sivasankar (✉) · R. Das · S. B. Borah · P. L. N. Raju
North Eastern Space Applications Centre, Department of Space, Government of India, Umaim 793103, Meghalaya, India
e-mail: siva.iirs@gmail.com

R. Das
e-mail: ranjit1_das@rediffmail.com

S. B. Borah
e-mail: suranjana85@gmail.com

P. L. N.Raju
e-mail: plnraju@gmail.com

P. J. Rao et al. (eds.), *Proceedings of International Conference on Remote Sensing for Disaster Management*, Springer Series in Geomechanics and Geoengineering,
https://doi.org/10.1007/978-3-319-77276-9_4

1 Introduction

Embankments are artificial constructions raised on the banks of rivers that are prone to annual flooding in order to protect the low-lying communities and infra-structure residing next to them. Assam is one of the states of India where huge devastation occurs every year during monsoon due to flood leading to loss of valuable lives and property. Artificial embankments on the innumerous streams of the Brahmaputra valley act as lifelines during the flood season which extends from May to October. But these embankments are highly vulnerable to breaching leading to agricultural damage by inundation and sand casting [1]. Continuous monitoring and management is required so that the annual loss due to embankment breaching can be minimised. Traditional on-site methods are laborious and time consuming. Remote sensing offers the advantage of synoptic and temporal coverage thus reducing the effort and time required for assessment of breached areas. The use of Synthetic Aperture Radar (SAR) data for this application is recommended over the optical remote sensing data owing to its all-weather (clouds, fog, smoke and to some extent rain) capability and high sensitivity towards dielectric constant [2].

Since the successful launch of the first operational space-borne SAR sensor onboard ERS-1, SAR technology has advanced significantly and its potentials for various remote sensing applications has been widely evaluated. Consequently, several space-borne SAR missions have been launched by various countries, providing uninterrupted earth observation data for the remote sensing community. Numerous studies have used SAR data for various disaster monitoring and damage assessment applications [3–5]. On the other hand, there is a trade-off between spatial resolution, swath coverage and temporal resolution of remote sensing data. As far as flood monitoring is concerned, high spatial as well as temporal resolution data covering a larger swath is required for effective planning and decision making. The recent advancement of Terrain Observation by Progressive Scans SAR (TOPSAR), which is an optimized ScanSAR technique, solves the problems of scalloping and azimuth varying ambiguities [6]. Using TOPSAR, the recently launched SAR missions, such as Sentinel-1A/1B, are capable of providing SAR data with spatial resolution (Rz $\times$ Az: 5 $\times$ 20 m) and temporal resolution (12 days) covering a swath of 250 km, which can be particularly useful in flood monitoring and damage assessment [7, 8].

The backscatter thresholding technique, which is a pixel-based operation, has been extensively adopted for flood inundation mapping. If the water fraction is more than 50%, specular reflection is dominant that results in low backscatter [9, 10]. The histogram of SAR backscatter data over water abundant terrain is of bimodal nature. Several techniques have been proposed to automatically determine the threshold value based on bimodal histogram to separate water bodies from other land cover targets [11–13]. However, the bimodal distribution may lose prominence in some of the cases due to increased roughness caused by wind and rain [10, 14]. So, the bi-modal based automatic thresholding approaches may not be a reliable solution for effective monitoring. Unlike the above histogram thresholding

processes, global thresholding approaches have also been extensively applied. In global thresholding technique, a single threshold for all the image pixels is used. Calibrated SAR data (backscatter) is a better representation of the target properties enabling comparison between temporal data as well as SAR data from different sensors [15]. Therefore, this study aims to analyse temporal Sentinel-1 SAR data and identify global threshold values for backscattering coefficients.

Sentinel-1 is providing SAR data in VV/VH polarizations for remote sensing community since 2014. [7, 16] have observed that like-polarization can better delineate open water features rather than cross-polarized data. However, the high soil moisture areas along with flood inundated areas can better help for embankment breach identification and its impact on the surrounding areas.

2 Materials and Methods

Around 40% of the state of Assam is prone to annual flooding which is further aggravated due to severe erosion and embankment breaching. Majority of the embankments in the state is prone to breaching not only due to heavy rainfall and flooding but also due to erosion, encroachment and soil condition. The Solengi river is one of the smaller north bank tributaries of the Brahmaputra river originating from the Arunachal Himalayas and flowing into the Brahmaputra in Biswanath district of Assam. The Solengi river like all other north bank tributaries of the Brahmaputra flows through steep slopes of the Himalayas and suddenly into almost flat terrain of the Brahmaputra plains in Assam. This sudden flattening of slope and heavy sediment in the river results in shallow braided channel in the floodplain region which is tremendously flashy in nature. The Solengi river is protected by embankments on both sides of its entire course through the flood-plain. Heavy rainfall during monsoon leads to sudden swelling of the shallow river which in turn leads to breaching at vulnerable locations during almost every flood season. Therefore this river has been chosen as a case study for demonstrating the capability of SAR data for detection of embankment breach locations and assessing its damage extent.

Sentinel-1 SAR data which operates in C-band (5.407 GHz) has been utilized for carrying out the study. Sentinel-1, part of the European Space Agency's Copernicus programme, consists of two satellites launched on 3 April 2014 and 25 April 2016 which operates in four modes of acquisition viz. Stripmap (SM), Interferometric Wide swath (IW), Extra-Wide swath (EW), and Wave (WV). The procured Sentinel images are dual polarization (VV and VH), with spatial resolution of 5 m $\times$ 20 m (Range $\times$ Azimuth). The observation mode of Sentinel-1 is interferometric wide swath (IW) mode having observation width of 250 km at an off-nadir angle ranging from 29.1° to 46.0°. The details of the eight Sentinel-1 SAR images collected over the study area between 9th April 2016 and 18th October 2016 are listed in Table 1.

Table 1 List of Sentinel-1 scenes used for this study

S. no.	Polarization (s)	Date of acquisition	Mode
1	VV/VH	9th April 2016	IW
2	VV/VH	3rd May 2016	IW
3	VV/VH	27th May 2016	IW
4	VV/VH	14th July 2016	IW
5	VV/VH	7th August 2016	IW
6	VV/VH	31st August 2016	IW
7	VV/VH	24th September 2016	IW
8	VV/VH	18th October 2016	IW

All the 8 scenes have been processed to generate calibrated and terrain corrected Sentinel-1 SAR images using Sentinel's Application Platform (SNAP). In this study, Refined Lee filter of 7 × 7 pixel size was applied to both like-polarized and cross-polarized images. Due to topographical variations of a scene and the tilt of the satellite sensor, distances can be distorted in the SAR images. So, terrain corrections are intended to compensate for these distortions so that the geometric representation of the image will be as close as possible to the real world. The SRTM 1 s HGT data has been used for range doppler terrain correction.

3 Results and Discussions

The eight temporal images downloaded for the entire monsoon season were pre-processed and analysed for identification of embankment breaches. Figure 1 shows all the processed images with cross-polarized VH band in red and like-polarized VV band in green for visualization. Two breach locations are identified and the first breach is identified on image acquired on 14th July, 2016. Another vulnerable area for breaching is observed on image of 7th August, 2016 due to seepage of stream water as high soil moisture area is detected. Embankment breaching in this location is finally observed on the image acquired on 24th September, 2016. If this water leakage condition could be identified in time, the second breach could have been prevented.

Figure 2 shows the histogram of backscatter values for both VH (Red) and VV (Green) polarizations acquired on 14th July 2016. It is observed that the bimodal nature of histogram, which is usually used for backscatter thresholding to separate out land and water bodies, is not prominent in VH whereas it is completely absent in the VV band. Therefore, global thresholding technique was applied and histograms were carefully analysed for selecting the threshold values.

Like-polarization (VV) data is commonly used for detection of open-water features, with low backscatter from open water and increase in backscatter as soil moisture increases [7, 16]. Figure 3 shows the comparison between VH and VV polarized data for 7th August, 2016. It is clearly seen that soil moisture areas are

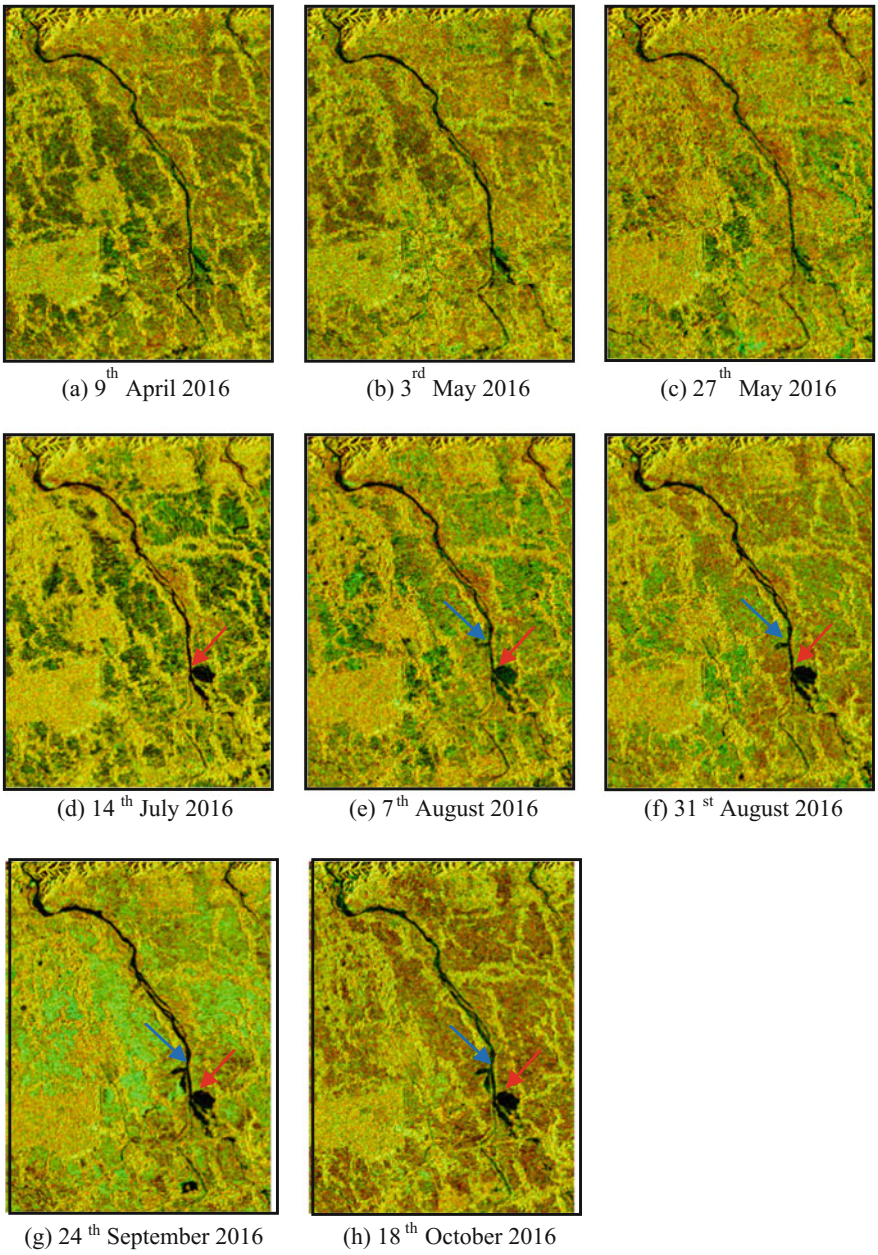

(a) 9th April 2016 (b) 3rd May 2016 (c) 27th May 2016

(d) 14th July 2016 (e) 7th August 2016 (f) 31st August 2016

(g) 24th September 2016 (h) 18th October 2016

Fig. 1 Temporal Sentinel-1 images acquired over study area

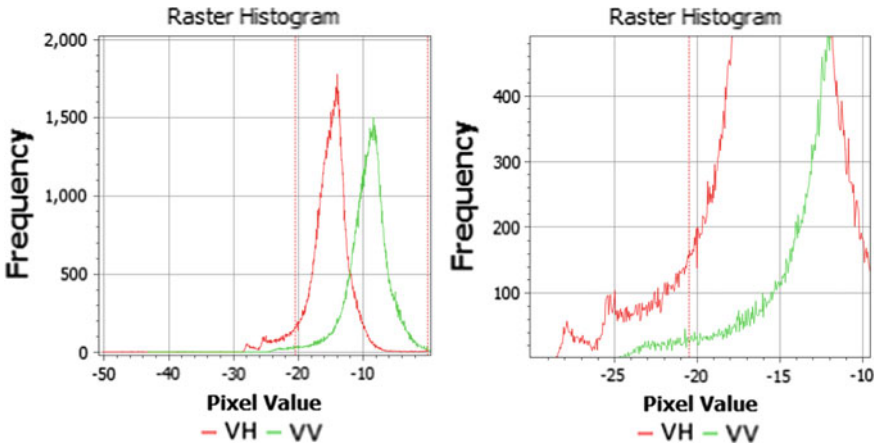

(a) Full view (b) Zoom view

Fig. 2 Histogram of VH and VV backscatter values on 14th July 2016

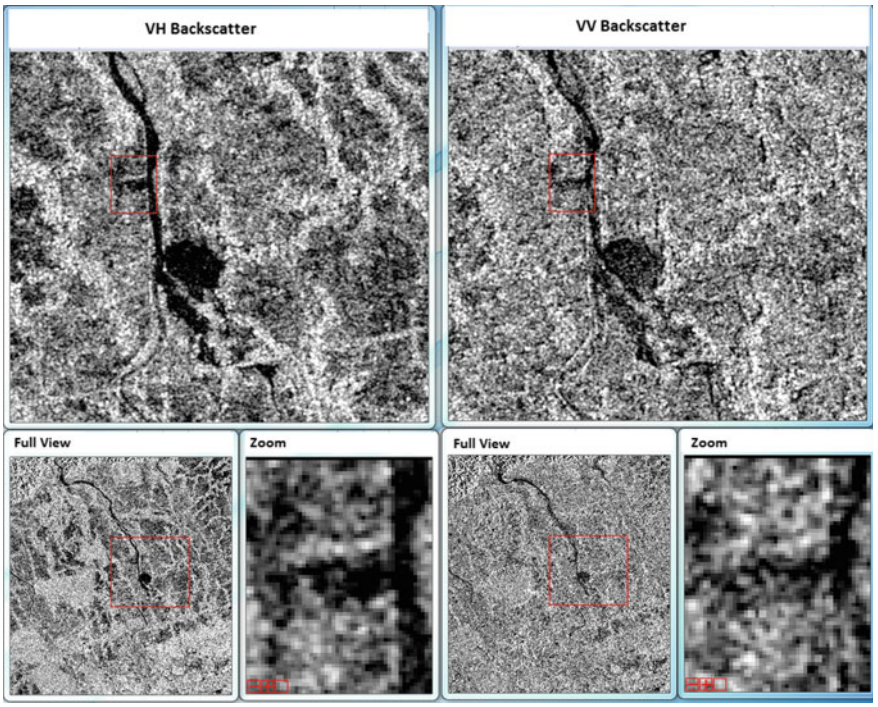

Fig. 3 Backscatter images of VH and VV polarization on 7th August 2016

more prominent in VH polarized data with low backscatter as open water compared to VV polarization with low backscatter from open water and high from soil moisture areas.

This analysis identified VH backscatter is suitable for identification of breaches and to create an inventory of the affected area due to breaching. The global threshold of −22.85 dB for VH backscatter has been defined from the analysis. Figure 4 shows the results of global thresholding technique applied to all the temporal images acquired after the occurrence of the first breach. Inundated areas due to embankment breaching and high soil moisture areas are highlighted. This technique can be effectively used for identifying embankment breaches and areas inundated due to breaching during the flood season as availability of optical data is scarce due to cloud cover during this season. It is observed that the first breach (identified on 14th July image) is of length 78.75 m affecting an area of about 65.89 acres. The second breach (observed on 24th September image) occurred slowly due to water seepage which was observed initially on 7th August 2016 image and reached to an embankment breach of 86.27 m length with affected area of about 30.22 acres on 24th September 2016.

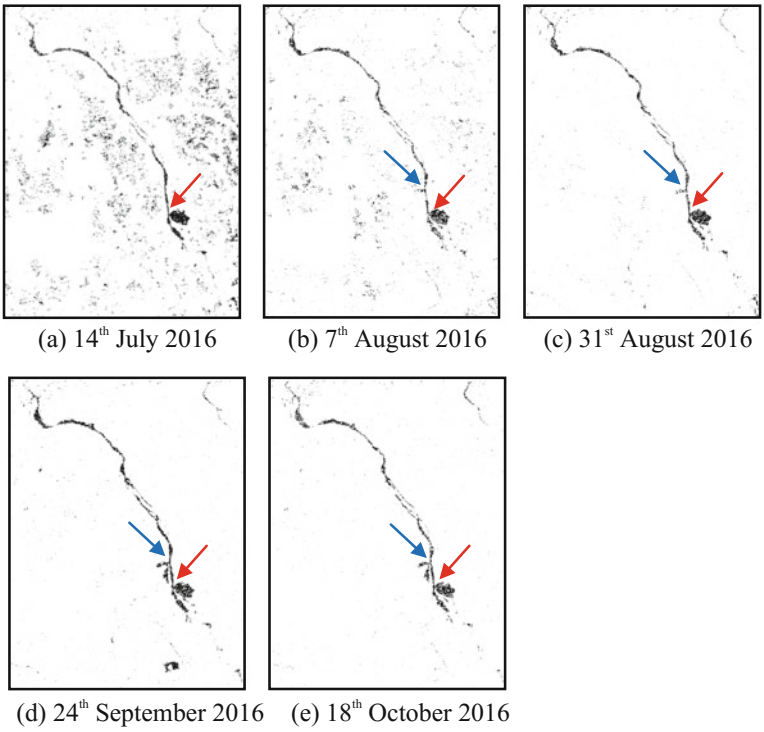

Fig. 4 Temporal inundated areas identified using thresholding technique

4 Conclusions

This study was an attempt to analyse the feasibility and potential of Sentinel-1 SAR data for embankment breach assessment. Eight temporal dual polarized (VV/VH) SAR datasets over Solengi river, Assam has been analysed. The results of the study shows that VH polarized data is more suitable for embankment breach studies. This study also portrays the potential of SAR data in identifying probable locations of embankment breaching if the breaching occurs slowly due to water seepage from weak areas under embankments. Two breaches have been identified in study area, where first breach was observed on 14th July 2016 of length 78.75 m with area affected 65.89 acres and second breach has occurred slowly due to water seepage on 7th August 2016, breaching to a length of 86.27 m with area affected 30.22 acres on 24th September 2016.

The results show that Sentinel-1 SAR data can be effectively used for embankment monitoring and damage assessment due to breaching. The process can also be automated using near real time Sentinel-1 SAR data along with accurate embankment information.

Acknowledgements Authors acknowledge European Space Agency for Sentinel-1 SAR data provision.

References

1. Das, R., Talukdar, B.: Assessment of river bank erosion and vulnerability of embankment to breaching: A RS and GIS based study in Subansiri river in Assam, India. Environ. Ecol. Res. **5**(1), 1–5 (2017). https://doi.org/10.13189/eer.2017.050101
2. Gobeyn, S., Wesemael, A.V., Neal, J., Lievens, H., Eerdenbrugh, K.V., Vleeschouwer, N.D., Vernieuwe, H., Schumann, G.J.-P., Baldassarre, G.D., Baets, B.D., Bates, P.D., Verhoest, N. E.C.: Impact of the timing of a SAR image acquisition on the calibration of a flood inundation model. Adv. Water Resour. **100**, 126–138 (2017)
3. Barra, A., Monserrat, O., Mazzanti, P., Esposito, C., Crosetto, M., Mugnozza, G.S.: First insights on the potential of Sentinel-1 for landslides detection. Geomat. Nat. Hazards Risk **7** (6), 1874–1883 (2016)
4. Shao, Y., Gong, H., Wang, S., Zhang, F., Tian, W.: Multi-source SAR remote sensing data for emergency monitoring to Wenchuan Earthquake damage assessment. In: 2009 Joint Urban Remote Sensing Event, Shanghai, pp. 1–5 (2009). https://doi.org/10.1109/urs.2009.5137745
5. Refice, A., Capolongo, D., Lepera, A., Pasquariello, G., Pietranera, L., Volpec, F., D'Addabbo, A., Bovenga, F.: SAR and InSAR for flood monitoring: examples with COSMO/SkyMed data. In: 2013 IEEE International Geoscience and Remote Sensing Symposium—IGARSS, Melbourne, VIC, pp. 703–706 (2013). https://doi.org/10.1109/igarss.2013.6721254
6. De Zan, F., Guarnieri, A.M.: TOPSAR: Terrain Observation by Progressive Scans. IEEE Trans. Geosci. Remote Sens. **44**(9), 2352–2360 (2006). https://doi.org/10.1109/TGRS.2006.873853
7. Twele, A., Cao, W., Plank, S., Martinis, S.: Sentinel-1-based flood mapping: a fully automated processing chain. Int. J. Remote Sens. **37**(13), 2990–3004 (2016)

8. Pham-Duc, B., Prigent, C., Aires, F.: Surface water monitoring within Cambodia and the Vietnamese Mekong Delta over a year, with Sentinel-1 SAR observations. Water **9**(6), 366 (2017). https://doi.org/10.3390/w9060366
9. Srivastava, H.S., Patel, P., Navalgund, R.R.: How far SAR has fulfilled its expectation for soil moisture retrieval. Proc. SPIE **6410**(641001), 1–12 (2006)
10. Bartsch, A., Trofaier, A.M., Hayman, G., Sabel, D., Schlaffer, S., Clark, D.B., Blyth, E.: Detection of open water dynamics with ENVISAT ASAR in support of land surface modelling at high latitudes. Biogeosciences **9**(2), 703–714 (2012). https://doi.org/10.5194/bg-9-703-2012
11. Sezgin, M., Sankur, B.: Survey over thresholding techniques and quantitative performance evaluation. J. Electron. Imaging **13**(1), 146–165 (2004). https://doi.org/10.1117/1.1631315
12. Fan, J.-L., Lei, B.: A modified valley-emphasis method for automatic thresholding. Pattern Recogn. Lett. **33**(6), 703–708 (2012)
13. Martinis, S., Kersten, J., Twele, A.: A fully automated TerraSAR-X based flood service. ISPRS J. Photogramm. Remote Sens. **104**, 203–212 (2015)
14. Manjusree, P., Kumar, L.P., Bhatt, C.M., Rao, G.S., Bhanumurthy, V.: Optimization of threshold ranges for rapid flood inundation mapping by evaluating backscatter profiles of high incidence angle SAR images. Int. J. Disaster Risk Sci. **3**(2), 113–122 (2012)
15. Mishra, M.D., Patel, P., Srivastava, H.S., Patel, P.R., Shukla, A., Shukla, A.K.: Absolute radiometric calibration of FRS-1 and MRS mode of RISAT-1 synthetic aperture radar (SAR) data using corner reflectors. Int. J. Adv. Eng. Res. Sci. **1**(6), 78–89 (2014)
16. Srivastava, H.S., Patel, P., Sharma, K.P., Krishnamurthy, Y.V.N.: Explored and demonstrated potentials of multiparametric synthetic aperture radar in wetland studies in context of Keoladeo National Park, Bharatpur, India. In: Proceedings of the Second Annual Research Seminar—KNP, Bharatpur, India, pp. 1–30 (2009)

Chapter 5
Security Issues in Geo-Spatial Big Data Analytics with Special Reference to Disaster Management

Rajesh Duvvuru, Gudikandula Narasimha Rao, Ashok Kote, Vijaya Raju Motru, PYLN Swami, Saurabh Singh Thakur, Sunil Kumar Singh, Balakrishna Bangaru, Sudhakar Godi and Peddada Jagadeeswara Rao

Abstract In recent times the usage of Location based services is increasing due to its wide range of applications in the science and engineering. Especially, the Geographic Information Systems (GIS) services and applications are more user friendly to the people. Beside the useful advantages, it has its own limitations like data storage, data organization, data privacy and protection, etc. The specified confronts can be solved using the Geo-Spatial Big Data (GSBD) and its security issues. This paper discusses a few issues like Data Security, Data Privacy, Expenses, Bad Analytics and Bad data. Also work describes threats to the GSBD like Spammy locksmith attack, impersonation attack, Denial-of-Service attack (DOS) and many more and its impact on the GSBD. These security issues will help to researchers and practitioners to design and development, a novel strong security mechanism for GSBD.

R. Duvvuru (✉) · G. N. Rao · B. Bangaru · S. Godi · P. J. Rao
Andhra University, Visakhapatnam, India
e-mail: rajesh.duvvuru@gmail.com

G. N. Rao
e-mail: gudikandhula@gmail.com

B. Bangaru
e-mail: balakrishna.bangaru@gmail.com

S. Godi
e-mail: sudha.godi@gmail.com

P. J. Rao
e-mail: pjr_geoin@rediffmail.com

A. Kote · B. Bangaru · S. Godi
Nova College of Engineering and Technology, Hyderabad, India
e-mail: kote.ashok@gmail.com

P. J. Rao et al. (eds.), *Proceedings of International Conference on Remote Sensing for Disaster Management*, Springer Series in Geomechanics and Geoengineering,
https://doi.org/10.1007/978-3-319-77276-9_5

Keywords Geospatial data · Big data · Security issues · Risks
Survey and GSBD

1 Introduction

Strong and reliable authentication mechanism for the Geo-Spatial Big Data (GSBD). Due to the wide range of applications like scientific research, society administration, commerce, and business Big data got popularity in the recent times [1]. Big data is a broad term for data sets so large or complex that traditional data processing applications are inadequate. Challenges include analysis, capture, data integration, search, sharing, storage, transfer, visualization, organization and information privacy [14]. The term often refers simply to the use of predictive analytics or other certain advanced methods to extract the value of data, and seldom to a particular size of the data set. Accuracy in big data may lead to more confident decision making, which intern results in greater operational efficiency, cost and risk reduction. Analysis of data sets can find new correlations to combat crime, spot business trends, prevent diseases, and many more. Practitioners business executives, Scientists of media and advertising, and governments alike regularly meet difficulties with large data sets in areas including Internet search, finance and business informatics. Scientists encounter limitations in e-Science work, including meteorology, genomics, connectomics, complex physics simulations, and biological and environmental research [3, 18].

This work comprises of: (1) an analysis and requirements of security for geosptail big data; (2) a new survey integrating both security and performance; (3) Various types of security attacks on Big data with geospatial data. The rest of this paper is structured as follows. Section 2 discusses previous works in the area of Geographic Information Systems and its security improvement. Section 3 describes the basic five issues of GSBD. In Sect. 4, it is represented various security attacks on GSBD. Lastly, concluded the paper with future work discussed in Sect. 5.

V. R. Motru · B. Bangaru · S. Godi
Usha Rama College of Engineering and Technology, Telaprolu, India
e-mail: vijayaraju.m@gmail.com

PYLN Swami · B. Bangaru · S. Godi
IIT Bombay, Mumbai, India
e-mail: yogananda.india@gmail.com

S. S. Thakur · B. Bangaru · S. Godi
IIT Kharagpur, Kharagpur, India
e-mail: saurabhjan07@gmail.com

S. K. Singh · B. Bangaru · S. Godi
NIT Patna, Patna, India
e-mail: sksingh.cse@gmail.com

2 Related Works

The geospatial objects can be represented in image (raster) mode or object (vector) mode. In object mode, individual spatial objects can be defined as a polygon or point or a line. In image mode, individual spatial objects can be defined as a set of contiguous cells, which are known as regions. Despite a spatial object and phenomenon can be defined in object mode and image mode. Discrete spatial objects can be more accurately present in object mode and continuous phenomena of spatial objects are more meaningfully presented in image mode. Data sets grow in size in part because they are increasingly being gathered from cheap and numerous information-sensing microphones, mobile devices, Radio-Frequency Identification (RFID) readers, cameras, aerial remote sensing, software logs, and wireless sensor networks. The global technology investment is roughly doubled to store information for the past 25 years with 40 months frequency; Especially in the year 2012, every day 2.5 Hex bytes (2.5 $\times$ 1018) of data were generated; The storage became more challenge for the large scale enterprises in determining who should own big data initiatives that bestride the whole organization [17, 12].

As recently as early March, the Indian communications minister, Sachin Pilot, announced to the media that the China hackers attacked government networks, but the attempts are unsuccessful ". Toronto scientist spoken to the intelligence officials in India on March 24, and said that a spy ring is tracking and also given certain suggestions to the sent restricted and classified documents on the network. That the problem still exists with the Chinese hackers in the rest of the world [15]. Many works previously stated various problems regarding the security issues in various domains with specific solutions [2, 4–7, 16].

3 Issues of Geospatial Big Data

3.1 Data Security

Geospatial data contain sensitive information, which will be useful for the analysis and interpretation of numerous applications. Geo-spatial map focus mainly features like vegetation, water bodies, rural areas, Defense and military structures, Civil constructions, Religious buildings, burial places, Trade, crafts, production places, Natural formations, urban areas, This risk is obvious and often uppermost in our minds when we are considering the logistics of data collection and analysis. Especially in military and defense information is more confidential. Data stealing is a widespread and growing area of transgression—and attacks are getting bigger and more destructive. Previous work refers that, In fact, five of the six most detrimental data steal of all time from giant companies like Ever note, eBay, Chase, JP Morgan, Target, and Adobe were carried out within the last two years. The larger the data,

the massive the target it presents to criminals with the tools to steal and sell it. In the case of Target, the hackers stole credit and debit card information from a bank where 40 million customers, as well as personal identifying information such as email and geographical addresses of up to 110 million people [9].

3.2 Data Privacy

Especially data from the various GIS web site contains a huge volume of data. Geo-spatial Big Data awareness of confidentiality and privacy concerns related to the integration of geo-referenced data from the public health sciences, natural and social. It allows access to resources that analyze these problems and that offer solid techniques, tools, and policies for safeguarding confidential data. Especially military applications contain the bulk amount of geographical information about the sensitive information they are closely related to the issue of security is privacy. But in addition to ensuring that people's personal Identity data are safe from criminals, you need to be sure that the sensitive information you are storing and collecting isn't going to be disclosed through less malicious, but equally damaging mistreatment by ourselves or by people to whom we have entrusted responsibility for analyzing and reporting on it [19].

In Figs. 1 and 2, the high confidential information areas were presented features like borders. If some intruder, changes the borders information on the Google map, it leads to a big disaster internationally. So, the geographical data about the country border representation should be care for processing massive GIS maps.

Fig. 1 Image of landsat, data, SIO, NOAA of India–Pakistan borders and this is the highly confidently area [10]

Fig. 2 Image of landsat, data, SIO, NOAA of India–Tibet–China borders highly confidently area [11]

4 Security Threats to Geospatial Big Data

4.1 Spammy Locksmith Attack

Bryan Seely, explained an attack against Google Maps through which he set up fake Secret Service offices in the company's geo-database, the data are filled with the complete fake phone numbers that rang a switch under his control and then the data sent to real Secret Service offices, allowing him to interrupt and record phone-calls made to the Secret Service. Seely was able to attack Google Maps by adding two ATMs to the database through its Google Places crowd sourcing tool, validating them through a phone verification service, then changing them into Secret Service offices. According to Seely, they put out of action on the phone verification service would not prevent him from conducting this attack again [13].

4.2 Impersonation Attacks

The Impersonation can be bifurcated into many different attacks like address spoofing, device cloning, rogue base station, unauthorized access and replay. The attacks can be detailed description leads to many problems. Instead of one another will take the advantage and do the attack on the Geospatial big data server. This leads to faulty information on the GIS. The Big data need to be more concentrated with this attack [8].

5 Conclusions

Ease of use and security are the two vital parameters for the GSBD analytics with special emphasis on disaster management. The data can be dissimilated to the destination system with proper decision and complete security, this leads to more reliable and accurate. The present study introduces basic five issues about Big data and its security. The usage of Big data analytics is more in the area of Geo spatial industry, but the security is major concern over there. In future the standard and reliable Big data server need to be constructed for the greater access and finer decisions with spatial coordinate system.

References

1. Chen, C.L.P., Zhang, C.-Y.: Data-intensive applications, challenges, techniques and technologies: a survey on big data. Inf. Sci. **275**, 314–347 (2014)
2. Choi, S., Bae, B.: The real-time monitoring system of social big data for disaster management. In: Computer Science and Its Applications, pp. 809–815. Springer, Berlin, Heidelberg (2015)
3. Donovan, S.: Big data: teaching must evolve to keep up with advances. Nature **455**(7212), 461 (2008)
4. Duvvuru, R., Rao, P.J., Singh, S.K.: Improvizing security levels in WLAN via novel BSPS. In: International Conference on Emerging Trends in Communication, Control, Signal Processing & Computing Applications (C2SPCA), 2013 IEEE (2013)
5. Duvvuru, R., Singh, S.K., Rao, G.N., Kote, A., Krishna, B.B., Raju, M.V.: Scheme for Assigning Security Automatically for Real-Time Wireless Nodes via ARSA. InQuality, Reliability, Security and Robustness in Heterogeneous Networks, 1 Jan 2013, pp. 185–196. Springer, Berlin, Heidelberg (2013)
6. Duvvuru, R., Rao, P.J., Singh, S.K., Sinha, A.: Enhanced security levels of BSPS in WLAN. Int. J. Comput. Appl. **84**(2), 33–39 (2013)
7. Duvvuru, R., Rao, P.J., Rao, G.N.: Multi-level chaos based encryption mechanism to enhance security of high security zone areas on Google map satellite images of India. Int. J. Appl. Eng. Res. **10**(3), 8059–8072 (2015)
8. González-Tablas, A.I., et al.: Survey on location authentication protocols and spatial-temporal attestation services. In: Embedded and Ubiquitous Computing–EUC 2005 Workshops, Springer Berlin Heidelberg (2005)
9. http://data-informed.com/the-5-biggest-risks-of-big-data/. Accessed 14 June 2015
10. https://www.google.co.in/maps?source=tldsi&hl=te. Accessed 10 May 2015
11. https://www.google.com/earth/explore/products/desktop.html. Accessed 04 Aug 2015
12. http://bhuvan.nrsc.gov.in/governance/mowr_ganga/. Accessed 18 June 2015
13. http://boingboing.net/2014/03/31/google-maps-spam-problem-pre.html. Accessed 22 Aug 2015
14. Labrinidis, A., Jagadish, H.V.: Challenges and opportunities with big data. Proceedings of the VLDB Endowment **5**(12), 2032–2033 (2012)
15. Markoff, J., Barboza, D.: Researchers trace data theft to Intruders in China. The New York Times (2010)
16. Rachel, S.S., Chittibabu, D.: Article: improvising security of HSZ areas on Google map satellite images of India via COTPCSD mechanism. Int. J. Comput. Appl. **128**(13), 1–7 (2015). October 2015. Published by Foundation of Computer Science (FCS), NY, USA

17. Seelan, S.K., et al.: Remote sensing applications for precision agriculture: a learning community approach. Remote Sens. Environ. **88**(1), 157–169 (2003)
18. Tankard, C.: Big data security. Netw. Secur. **7**, 5–8 (2012)
19. Xu, W., et al.: Channel surfing and spatial retreats: defenses against wireless denial of service. In: Proceedings of the 3rd ACM Workshop on Wireless Security, ACM (2004)

Chapter 6
Monitoring Convective Clouds Over India and Nearby Regions Using Multi-spectral Satellite Observations

Mohammd Rafiq, Anoop Kumar Mishra, Jagabandhu Panda and Som Kumar Sharma

Abstract Convective clouds are the sources of severe weather and extreme precipitation events which often produce flooding, landslides and other disasters. The physical characteristics of convective clouds influence the distribution of radiative heating/cooling in the troposphere. They play a crucial role in atmospheric circulation and the hydrological cycle. Present study deals with the detection of convective clouds using multispectral observations at split window channels (near 11 and 12 μm) and water vapour absorption channels (near 6.7 μm) from EUMETSAT (Meteosat 7) data. Results are compared with the observations (reflectivity-based threshold) from Precipitation Radar (PR) on-board Tropical Rainfall Measuring Mission (TRMM). The Results have also been validated against convective clouds derived from rain gauge based precipitation product from the IMD data. Validation results show a correlation coefficient (cc) of 0.79 and Root Mean Square Error (RMSE) of 2.61 (%) against rain gauge based observations of convective clouds.

Keywords Convective clouds · Flash floods · Remote sensing

M. Rafiq (✉) · A. K. Mishra
Centre for Remote Sensing and Geoinformatics, Sathyabama University, Chennai, India
e-mail: emidamls6@gmail.com

A. K. Mishra
e-mail: daksha112@gmail.com

J. Panda
Department of Earth and Atmospheric Sciences, NIT Rourkela, Rourkela, India
e-mail: pandaj@nitrkl.ac.in

S. K. Sharma
Physical Research Laboratory, Space and Atmospheric Sciences Division, Ahmedabad, India
e-mail: somkumar@prl.res.in

P. J. Rao et al. (eds.), *Proceedings of International Conference on Remote Sensing for Disaster Management*, Springer Series in Geomechanics and Geoengineering,
https://doi.org/10.1007/978-3-319-77276-9_6

1 Introduction

Convective cloud systems in the tropics offer the primary mechanism whereby solar heating of the ocean is moved upward into the free troposphere where it can be transported pole ward and eventually emitted to outer space. In the process, these great engines of the global climate produce precipitation and drive the global-scale circulation. Convective clouds are the source of great energy that drives the atmosphere. These types of clouds are most often isolated clouds with sharp edges. They are usually dense in structure and develop upright in the form of rising hills with base at low level. These clouds are brighter on the upper surface and comparatively darker below with almost horizontal base. These clouds are extremely varying in nature, as they form in an unstable environment, the sections in these clouds can go beyond freezing point to develop ice crystals, ice pellets, snowflakes or super cooled water droplets or combination of all. These clouds often result in convective storms [1] thus posing huge impacts to environment. The result of which has often seen flooding, hail and other storms. 30–40% of signal are from these convective clouds in Intertropical Convergence Zone (ITCZ) and they are very vital in controlling earth's climate by exchanging moisture and heat from earth to atmosphere [2]. Observational networks have very limited record of convective clouds. Active remote sensors like radars have been used to observe these clouds [3, 4]. However their coverage is also very limited. Remote sensing offers an opportunity to monitor these clouds. Indirect technique using remote sensing observations in Thermal Infrared (TIR) and Visible (VIS) frequencies have been utilized to detect these clouds [3, 5, 6]. It difficult to discriminate between deep convective clouds and cirrus clouds if the measurements are being made only by utilizing the IR radiance. As cirrostratus and cirrocumulus clouds are in contact with deep convective clouds having cloud tops below −35 °C [7, 8]. To eliminate the convective and stratiform clouds Anagnostou and Kummerow [9] developed a technique utilizing SSM/I 85 GHz brightness temperature. The technique was improved by Hong et al. [10], however these techniques cannot differentiate the cirrus with deep convective clouds.

The advance in space science provide a better resolution radar systems with the launch of Tropical Rainfall Measuring Mission (TRMM) which can interact with cloud structures. Many researchers documented its usage in detecting convective clouds and storms in tropics [11–14]. TRMM Precipitation Radar (PR) provide more accurate observations as its capability to provide a 3-dimensional structure of deep convective cloud systems [13]. The narrow swath of PR and poor temporal resolution of TRMM limit its usage in identifying most of the convective clouds that last for few days. Convective clouds during South-West Monsoon season over Indian region were identified and net cloud radiative forcing at the top of atmosphere was examined using data from Earth Radiation Budget Experiment (ERBE) [15]. Convective clouds were identified and used for estimating rainfall over India

from Kalpana data at 11 μm observation [16, 17]. Sengupta et al. [18] studied structural evolution of clouds using Multiangle Imaging Spectro Radiometer (MISR)-derived cloud fraction over Indian CTCZ. Multi-spectral observations at 6.7 and 11 μm were used from Meteosat data to identify convective clouds and estimate rainfall over Indian land and oceanic region [19, 20]. Present study focuses on detecting convective clouds using multispectral observations at split window channels (near 11 and 12 μm) and water vapour absorption channels (near 6.7 μm) from Meteosat 7 data over India and adjacent oceanic regions. Results are compared with observations (reflectivity-based threshold) from Precipitation Radar (PR) on-board Tropical Rainfall Measuring Mission (TRMM). We have also validated the results with convective clouds derived from rain gauge based product.

2 Study Area and Data Used

Area of study is illustrated in Fig. 1 which extends from 30°S to 50°N and 50°E to 120°E including the Indian land and nearby oceanic regions (Fig. 1). India is having 29 states and 7 union territories, land surface area is extended over 3,287,590 sq km. With more than seven thousand kilometres of coastline it is surrounded by Arabian Sea, Bay of Bengal and the Indian Ocean.

For the present study, we have used Meteosat 7 data of Meteosat First Generation (MFG). MFG provides images of the full Earth disc, and data for weather forecasts. Meteosat provides observations in Thermal Infra Red (TIR) and Water Vapor (WV) absorption band at half-hourly interval, with a spatial resolution of 4 km. Data has been downloaded from EUMETSAT Portal (https://www.eumetsat.int). We have used Meteosat 7 native data from Meteosat First Generation (MFG) Spacecraft in our study. Meteosat 7 was launched in September 1997, it was seventh and last in the MFG series of satellites. The multispectral observations in Thermal Infrared (TIR) 10.5–12.5 μm and Water vapour (WV) 5.7–7.1 μm are used.

For comparison of our results, we have also used observations from Tropical Rainfall Measuring Mission (TRMM) satellite. TRMM, a joint mission of NASA and the Japan Aerospace Exploration Agency (JAXA), was launched in 1997 to study hydro parameters for weather and climate research. We have used Precipitation Radar (PR) data. Reflectivity factor from level 2 Rain Characteristics Product (TRMM Product 2A23) is used in the study. Description of the instrument can be found at https://gcmd.nasa.gov and data can be downloaded at https://disc.gsfc.nasa.gov/. For validation of our results we have also used rain gauge based precipitation products from India Meteorological Department (IMD) available at 0.25°.

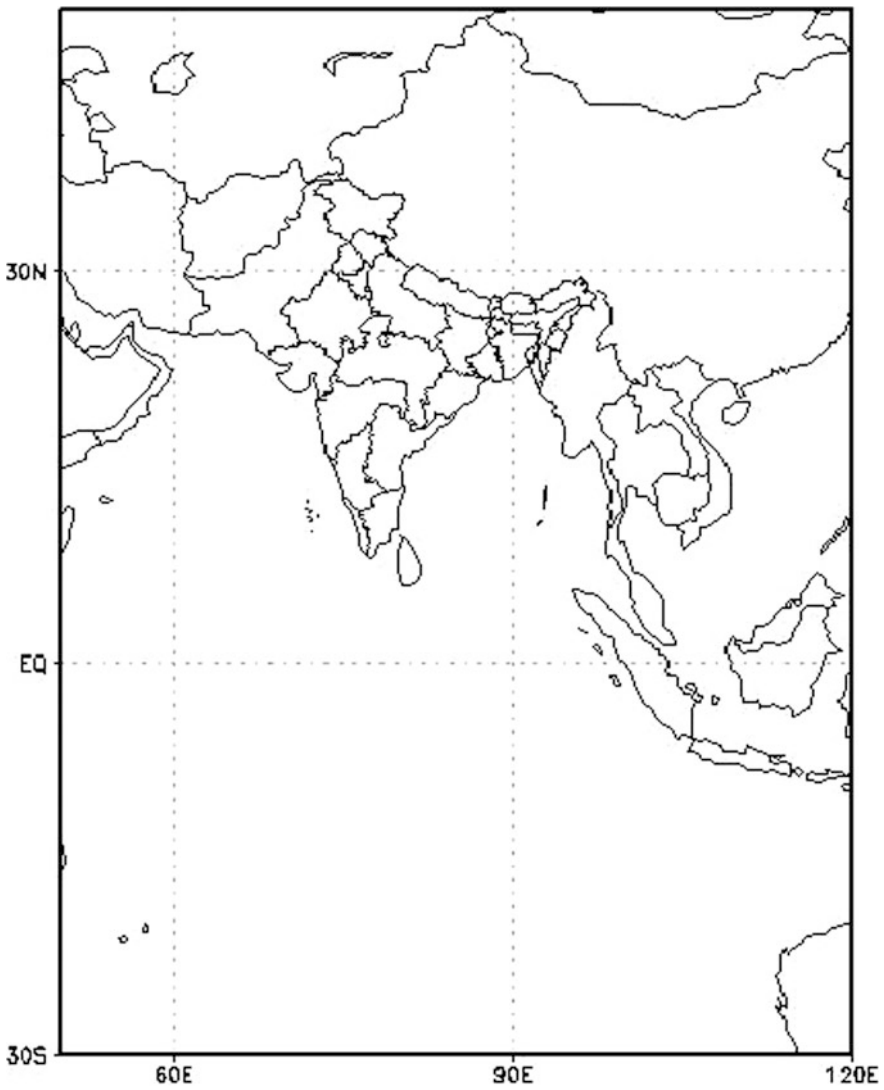

Fig. 1 Study area showing Indian land mass and nearby oceans

3 Methodology

We followed an approach developed by Adler and Negri [21] to remove cirrus clouds for identification of convective clouds. A slope parameter S_P and a temperature gradient T_G was computed for each local temperature minimum. These values are given as:

$$T_G = T_{avg} - T_{min} \quad (1)$$

$$S_P = 0.568\,(T_{min} - 217) \quad (2)$$

where;

T_{min} is the local minimum (derived from TIR channel, 11 μm).

T_{avg} is the mean temperature of the 6 pixels surrounding the current pixel.

A large T_G is associated with convective clouds and a small value indicates a weak gradient and thus detects the cirrus clouds. Convective clouds with overshooting tops were identified using difference of 11 and 6.7 μm channel. Convective clouds with overshooting tops are known to play an important role in the interaction and exchange between troposphere and stratosphere. Simultaneous observations of these clouds in the infrared window region (11 μm) and the water vapour absorption band (6.7 μm), reveal that the equivalent brightness temperature in the latter is larger than in the former. Negative differences (TB_{11}–$TB_{6.7}$) are associated with convective clouds with overshooting tops [22].

Using above approach convective clouds are identified. Occurrence (in %) of convective clouds is calculated by dividing the convective pixels with total pixels. Observations from PR (2A23) is also used to detect the convective clouds for the comparison with present approach of convective cloud detection from Meteosat data. We have used a threshold of 40 dBZ (reflectivity) for detecting convective clouds [23].

There is strong relationship between precipitation extremes and cloud top temperature [19, 24]. Lau and Wu [24] investigated the climatological characteristics of tropical rain and cloud systems over Tropics using brightness temperature (TB) data from Visible and Infrared Scanner (VIRS) and precipitation data from Tropical Rainfall Measuring Mission (TRMM) Microwave Imager (TMI) and Precipitation Radar (PR) onboard TRMM. It is found that Top 10% heavy precipitation may be associated with convective clouds. Precipitation spectrum obtained from IMD rain gauge based product is divided into 10 bins. Top 10% heavy precipitation is used to derive convective clouds.

4 Results and Discussion

Different case studies have been carried out to monitor the convective clouds over Indian region and nearby oceanic regions. A few case studies are presented below for brevity.

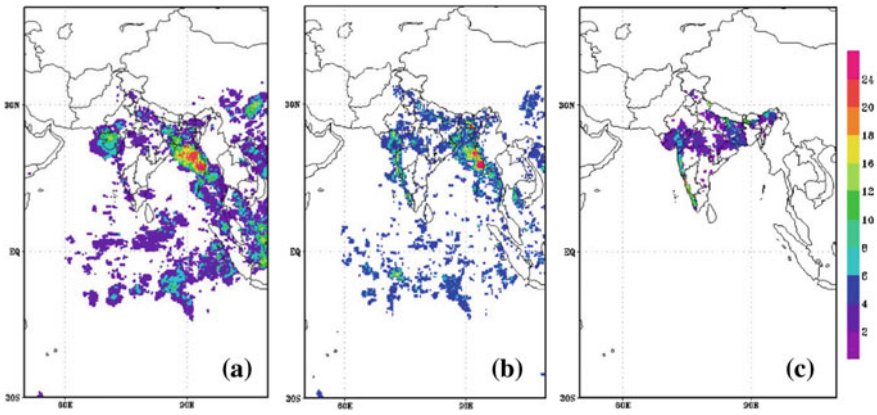

Fig. 2 Fraction of convective clouds (%) from **a** present technique, **b** from PR observations **c** from rain gauge based IMD product during July 2007

4.1 Case Study I

For this case study, we have identified multiple convective events in July 2007 over Bay of Bengal (~90°E, 14°N) and Western part of Indian region (~73°E, 19°N). Figure 2 shows occurrence (%) of convective clouds over study area.

These convective systems brought heavy rainfall over Bay of Bengal and Western Ghats. Few localized convective systems over India Ocean can also be identified. It can be inferred that a maximum of 24% convective clouds (from Fig. 2b) occur over Bay of Bengal which is matching with the observations from present technique (Fig. 2a). Convective systems over Bengal and Bangladesh caused heavy flooding over these regions. Similarly occurrences of convective clouds over Western Ghats are also comparable from present technique and that from Radar observations. Scattered convective systems over Mumbai, Central India and North-eastern parts of Indian region can also be observed from present technique. These observations are consistent with observations derived from ground based rain gauges (Fig. 2c).

4.2 Case Study II

For this case study, we considered the occurrences of convective clouds in July 2008.

Multiple isolated convective clouds were identified over India and nearby oceanic regions. Figure 3 shows the occurrences of these clouds. These convective clouds caused heavy rainfall over these regions. A maximum of 28% coverage of convective clouds were identified over Bay of Bengal and nearby regions (~15°N, 89°E)

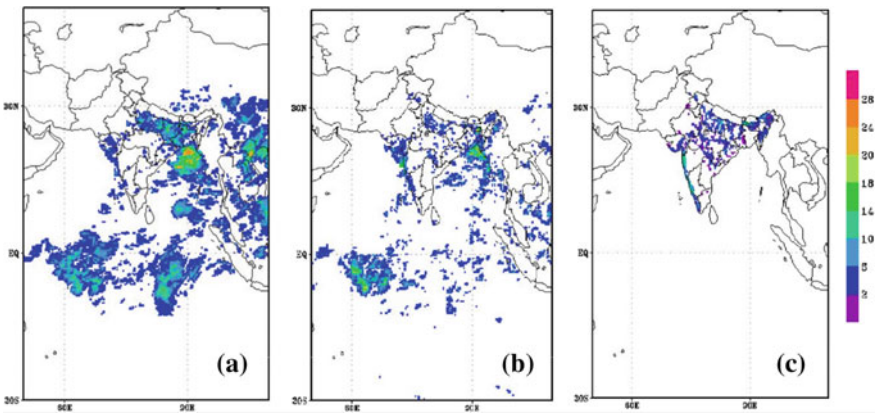

Fig. 3 Fraction of convective clouds (%) from **a** present technique, **b** from PR observations **c** from rain gauge based IMD product during July 2008

from Precipitation Radar observations (Fig. 3b). This observations is matching with observations from present technique. Present technique also shows convective coverage of about 18–20% over Indo-Gangetic Plains. This observation is consistent with PR and ground based observations (Figs. 3b, c). Convective cloud coverage over Equator can also be identified from present technique. This observation is consistent with Radar observation. Similarly convective cloud coverage of about 10–15% can be observed over Western Ghats from the three observations.

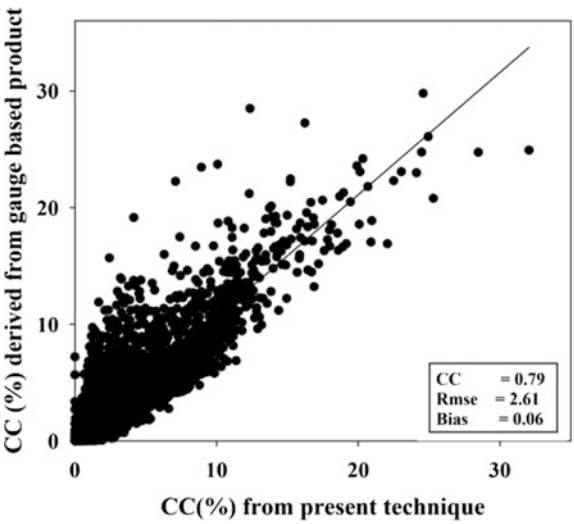

Fig. 4 Scatter plot between convective clouds from present technique and rain gauge based product

4.3 Statistical Validation with Rain Gauge Based Product

Convective clouds obtained from present technique is validated against observations derived from IMD rain gauge based product (Fig. 4).

It can be seen that convective clouds obtained from present technique is matching with the observations derived from rain gauge based product. Validation results show a correlation coefficient (cc) of 0.79 and Root Mean Square Error (RMSE) of 2.61 (%) against rain gauge based observations of convective clouds.

5 Conclusion

Satellite based multispectral observations is used to detect convective clouds over India and nearby Oceanic region. Few cases of convective clouds have been discussed during 2007–2009. Performance of the technique has been evaluated with space based radar observations onboard TRMM and rain gauge based observations from IMD. Results reveal that present technique is able to monitor the coverage of convective clouds efficiently. Approach adopted in the present study to monitor convective clouds is very crucial given the limitation of station and radar data and sampling errors associated with microwave sensors. TRMM data is limited from 1997 to 2015. Moreover, availability of Meteosat data from 1995 onwards presents unique opportunity to maintain a long term data of convective clouds which will be very useful for study focussing on climate change. Which is reported in changing the atmospheric dynamics by changing the variability of precipitation [25–27]. Methodology proposed in the present algorithm finds application in operational contests where MFG, MSG, and MTG data are available in near real time.

Acknowledgements We acknowledge the funding for this work from ISRO under grant No. B. 19012/174/2016-Sec.2. Meteosat data from EUMETSET and TRMM data used in this study is also thankfully acknowledged.

References

1. Stephens, G.L., Vane, D.G., Boain, R.J., Mace, G.G., Sassen, K., Wang, Z., Illingworth, A.J., O'Connor, E.J., Rossow, W.B., Durden, S.L., Miller, S.D.: The CloudSat mission and the a-train: a new dimension of space-based observations of clouds and precipitation. Bull. Am. Meteorl. Soc. **83**(12), 1771–1790 (2002)
2. Hong, G., Heygster, G., Miao, J., Kunzi, K.: Detection of tropical deep convective clouds from AMSU-B water vapor channels measurements. J. Geophys. Res. Atmos. **110**(D5), 2005
3. Liu, G., Curry, J.A., Sheu, R.S.: Classification of clouds over the western equatorial Pacific Ocean using combined infrared and microwave satellite data. J. Geophys. Res. **100**, 13811–13826 (1995)

4. Alcala, C.M., Dessler, A.E.: Observations of deep convection in the tropics using the tropical rainfall measuring mission (TRMM) precipitation radar. J. Geophys. Res. **107**(D24), 4792 (2002). https://doi.org/10.1029/2002JD002457
5. Hall, T.J., Haar, T.H.V.: The diurnal cycle of west Pacific deep convection and its relation to the spatial and temporal variations of tropical MCSs. J. Atmos. Sci. **56**, 3401–3415 (1999)
6. Chou, C., Neelin, J.D.: Cirrus detrainment-temperature feedback. Geophys. Res. Lett. **26**, 1295–1298 (1999)
7. Gettelman, A., Salby, M.L., Sassi F.: The distribution and influence of convection in the tropical tropopause region. J. Geophys. Res. **107**(D10), 4080. https://doi.org/10.1029/2001jd001048
8. Luo, Y., Krueger, S.K., Mace, G.G., Xu, K.M.: Cirrus cloud properties from a cloud-resolving model simulation compared to cloud radar observations. J. Atmos. Sci. **60**, 510–525 (2003)
9. Anagnostou, E.N., Kummerow, C.: Stratiform and convective classification of rainfall using SSM/I 85-GHz brightness temperature observations. J. Atmos. Oceanic Technol. **14**, 570–575 (1997)
10. Hong, Y., Kummerow, C., Olson, W.S.: Separation of convective and stratiform precipitation using microwave brightness temperature. J. Appl. Meteorol. **38**, 1195–1213 (1999)
11. Simpson, J., Halverson, J., Pierce, H., Morales, C., Iguchi, T.: Eyeing the eye: exciting early stage science results from TRMM. Bull. Am. Meteorol. Soc. **79**, 1711 (1998)
12. Nesbitt, S.W., Zipser, E.J., Cecil, D.J.: A census of precipitation features in the tropics using TRMM: radar, ice scattering, and lightning observations. J. Clim. **13**, 4087–4106 (2000)
13. Kelley, O., Stout, J.: Convective towers in eye walls of tropical cyclones observed by the TRMM precipitation radar in 1998–2001. Paper presented at 20th conference on weather analysis and forecasting. American Meteorological Society, Seattle, Wash (2004)
14. Mishra, A.K.: Estimation of heavy rainfall during cyclonic storms from microwave observations using nonlinear approach over Indian Ocean. Nat. Hazards **63**(2), 673–683 (2012)
15. Rajeevan, M., Srinivasan, J.: Net cloud radiative forcing at the top of the atmosphere in the Asian monsoon region. J. Clim **13**(3), 650–657 (2000)
16. Mishra, A., Gairola, R.M., Varma, A.K., Agarwal, V.K.: Study of intense rainfall events over India using KALPANA-IR and TRMM precipitation radar observations. Curr. Sci. **9**(5), 689–695 (2009)
17. Mishra, A., Gairola, R.M., Varma, A.K., Agarwal, V.K.: Improved rainfall estimation over Indian land and oceanic regions using satellite infrared technique. Adv. Space Res. **48**, 49–55 (2011)
18. Sengupta, K., Dey, S., Sarkar, M.: Structural evolution of monsoon clouds in the Indian CTCZ. Geophys. Res. Lett. **40**, 5295–5299 (2013)
19. Mishra, A., Gairola, R.M., Varma, A.K., Agarwal, V.K.: Remote sensing of precipitation over Indian land and oceanic regions by synergistic use of multi-satellite sensors. J. Geophys. Res. **115**(D08106), 1–12 (2010)
20. Mishra, A.: A new technique to estimate precipitation at fine scale using multi-frequency satellite observations over Indian land and oceanic regions. IEEE Trans. Geosci. Remote Sens. **51**(7), 4349–4358 (2013)
21. Adler, R.F., Negri, A.J.: A satellite technique to estimate tropical convective and stratiform rainfall. J. Appl. Meteorl. **27**, 30–51 (1988)
22. Kurino, T.: A satellite infrared technique for estimating 'deep/shallow' precipitation. Adv. Space Res. **19**(3), 511–514 (1997)
23. Steiner, M., Houze Jr., R.A., Yuter, S.E.: Climatological characterization of three-dimensional storm structure from operational radar and rain gauge data. J. Appl. Meteorol. **34**(9), 1978–2007 (1995)
24. Lau, K.M., Wu, H.T.: Climatology and changes in tropical oceanic rainfall characteristics inferred from tropical rainfall measuring mission (TRMM) data (1998–2009). J. Geophys. Res. **116**, D17111 (2011). https://doi.org/10.1029/2011JD015827

25. Rafiq, M., Mishra, A.K.: Investigating changes in Himalayan glacier in warming environment: a case study of Kolahoi glacier. Environ. Earth Sci. **75**(23), 1469 (2016)
26. Mishra, A.K., Rafiq, M.: Analyzing snowfall variability over two locations in Kashmir, India in the context of warming climate. Dyn. Atmos. Oceans **79**, 1–9 (2017)
27. Rafiq, M., Mishra, A.K.: A study of heavy snowfall in Kashmir, India in January 2017. Weather, **73**(1), 15–17 (2018)

Chapter 7
Design and Fabrication of Solar Powered Unmanned Aerial Vehicle for Border Surveillance

R. Vijayanandh, J. Darshan Kumar, M. Senthil Kumar, L. Ahilla Bharathy and G. Raj Kumar

Abstract Unmanned Aerial Vehicles (UAVs) are one of the important types of aircraft, which are controlled by a remote controller or pre-programmed method. Nowadays UAV is being proposed for many critical applications including surveillance, mapping, etc. In general, the surveillance around the international border has been carried out by soldiers. Monitoring the border through soldiers is not perfect surveillance, due to the natural factors of human beings may be the error will occur in the border surveillance. To avoid this problem, the monitoring of the border region is to be covered by UAV. Enemy's activities around the dangerous and large border coverage area are difficult task to handle in border monitoring, so a normal UAV is not suitable for this process. Hence advanced solar UAV is a better solution for this monitoring because it's having unique characters like high operational speed, more stability, long life, etc. This paper proposed to motivate research on aerospace renewable energy sources and primary aims are to make calculations and respective designs to create an e-aircraft model, capable of powering its flight using solar energy, overcoming the challenges by increasing the speed, range, and endurance of the UAV using the solar power in order to provide

R. Vijayanandh (✉) · J. Darshan Kumar · M. Senthil Kumar · L. Ahilla Bharathy
G. Raj Kumar
Department of Aeronautical Engineering, Kumaraguru College of Technology, Coimbatore 641049, Tamil Nadu, India
e-mail: vijayanandh.raja@gmail.com

J. Darshan Kumar
e-mail: darshankumar.j.aeu@kct.ac.in

M. Senthil Kumar
e-mail: senthilkumar.m.aeu@kct.ac.in

L. Ahilla Bharathy
e-mail: sriahillaab@gmail.com

G. Raj Kumar
e-mail: rajkumar.g.aeu@kct.ac.in

P. J. Rao et al. (eds.), *Proceedings of International Conference on Remote Sensing for Disaster Management*, Springer Series in Geomechanics and Geoengineering,
https://doi.org/10.1007/978-3-319-77276-9_7

full-time border surveillance. The overall 3D solar UAV is modeled by CATIA V5 with the inclusion of theoretical design values. The intruders detection in borders through image processing has been completed using MATLAB.

Keywords Border surveillance · Image processing · Renewable energy
Solar cells · UAV

1 Introduction

The modern world needs an innovative solution in the non-renewable energy field, because of its excessive usage. Solar power thus is an interesting option also it is the best alternative, which has needed to be investigating for usage of all aircraft. A solar powered UAV is an aircraft that turns on electric motors rather than internal combustion engines, with electrically coming from solar cells, and batteries. In recent years, the level of interest in the development of fixed-wing UAVs for various missions has risen significantly. A crucial issue concerning these aircraft is their high power consumption compared to their limited energy storage capability. The ability for an aircraft to fly during a much extended period of time has become a key issue and a target of research, both in the domain of civilian aviation and UAVs. The required endurance is in the range of a couple of hours in the case of law enforcement, border surveillance, forest fire fighting or power line inspection. One possibility to increase the up-time is through the use of solar cells [1].

In order to reach the target endurance, the design of the aircraft has to be thought very carefully, as a system composed of many subsystems that are continuously exchanging energy. One of the milestones of this paper is the selection of the general configuration for an UAV and primary objectives are that the design should make efficient use of solar cell converge on the wing with aerodynamic design consideration. The first component considered is the wing, whose basic configuration is determined by area limitations and solar-cell coverage optimization, thereby final consideration in configuration selection is the conventional wing. Note that the rectangular shape of the wing is not very efficient aerodynamically, but allows for maximum coverage of solar cells over the wing area, which is an important parameter to maximizing speed. The shape of the fuselage is keep as small as possible to reduce its contribution to parasite drag also realized that UAV would want a fairly long fuselage to move the airplane's centre of gravity (e.g.) as far forward as required for stability reasons. Figure 1 shows the overall concept of proposed solar flight.

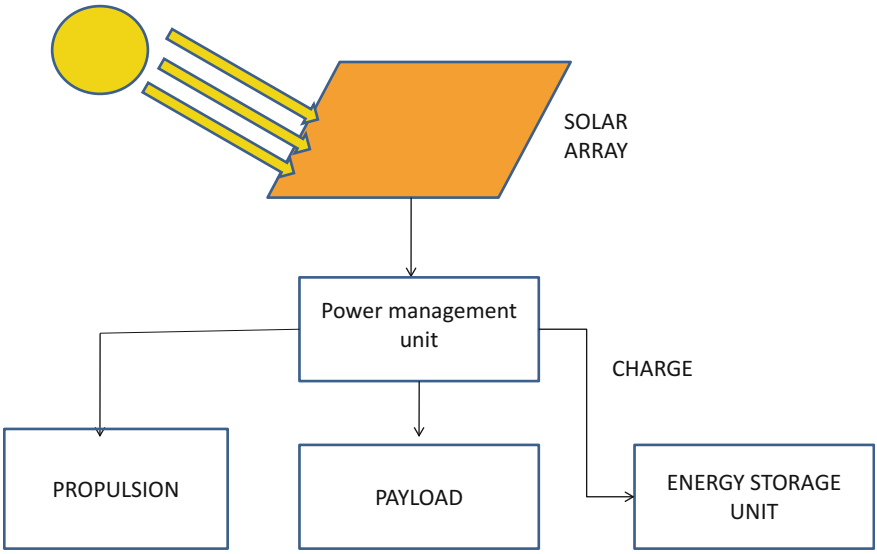

Fig. 1 Concept of proposed solar flight

2 Theoretical Design Approach of a Solar UAV

Theoretical analysis of a solar UAV comprises of Aerodynamics, Structures, Propulsion, Systems and Instrumentations. In general, initial step of theoretical analysis is need to estimate or fix the speed of an UAV before estimating its weight.

The aerodynamics part of a solar UAV is responsible for external configuration layout, component sizing, airfoil selection, stability calculations and control surface sizing, flight testing to resolve to handle quality issues and modifying the test bed to arrive at a final design. For fixed wing UAV, the ratio between span and chord in average model aircraft is between 1:7 and 1:8; thereby the chord is 137/7 = 19.5 cm and the wing surface area determined as 2671.5 cm^2. Aspect ratio as 7.02, Altitude as 0.5–1 km, flight speed as 8–12 m/s. The speed range, at which the airflow will be smooth and laminar, can be estimated using the value of Reynolds number is 170×10^3. The airfoil has been selected for fixed wing of Solar UAV is NACA4418. Optimized speed of the solar UAV is 30 km/hr, which based on account the limited capacity of solar cells and its safety. The mass and life of a solar UAV either determine by top-down approach or bottom-up approach. Choose the top-down approach, since it is easier to make a plane lighter than to increase its lift. The lift and mass have been calculated as 10.3173 N and 1.05 kg respectively through aviation's lift formula. The lift produced by a semi-span of the wing should be proportional to the half of the UAV's weight. From then on each structural member is designed for its specification. The spar design is optimized to withstand the maximum load on the wing while minimizing the overall structural weight. The front spar is placed 20% of the chord leaving space for slat actuators and the rear spar

at 70% of the chord is allowing space for flaps and actuators. Both the front spar and the rear spar can carry bending loads, which are the function of the movement of the centre of pressure. It also becomes necessary to consider the wing thickness (height) available at the spar location i.e. usually rear spars have lower spar height thus requiring a larger spar cap area to provide the required moment of inertia which would take the bending. But in the case of laminar flow airfoil, the maximum thickness occurs at the rear. Hence the rear spar height will be more than the front spar [2].

The propulsion group is assigned two major tasks for this paper, which are selection of the motor and selection of the propeller. Selection of motor for solar UAV concern several parameters. i.e., launching system of solar UAV, types of propellers configuration, solar panels configuration on the aircraft. After surveying the motors available, finally GT2213-09KV1180 motor has been selected for solar UAV. Selection of motor is based on ability to custom the wind power thereby it would operate at the desired current and voltage, the cost of the custom wound motor and the electronic speed controller, the brushless motor controller combination is almost efficient after figuring in losses [3]. For propeller selection, a recommendation has been given to the maximal propeller size, in which the propeller's maximal diameter plays vital role than maximal lead. A propeller with its lead being similar to its diameter is best suited for fast-flying airplanes, whereas a propeller with a small lead and larger diameter is excellent at providing the maximal force. Here the selected specification of the propellers are lead is 17.78 cm, diameter is 25.40 cm and speed of propeller is 34.3 m/s.

2.1 Solar Panel Test

A solar cell is a solid state device, which converts the energy of sunlight directly into electricity by the photovoltaic effect. For critical application, the requirement of the electricity is more so cells are often linked together in groups known as solar modules. Number of solar cells is depends upon the output power requirement [4]. A typical solar cell on the FR 4 sheet has been shown in the Fig. 2.

The placement of solar cells on non-lifting surfaces is ruled out to minimize drag and decrease the sensitivity to side winds. However, if required it is decided to put

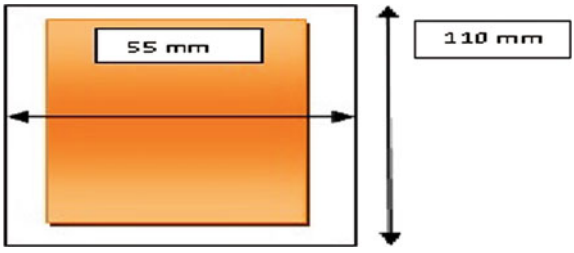

Fig. 2 Fabrication of solar cells on the Fr 4 sheet

solar cells on the rudder and elevator as they would be more effective during dusk and dawn. To integrate the stiff solar cells the following designs are considered (a) the first consists of distorting the airfoil shape by placing the cells on the top cut into pieces (b) the second solution consists of extending the trailing surface of the wing (c) the third involves placing Solar cells inside the wing, enclosed by an anti-reflective coating on top [5]. With the help of solar arrangement possibilities and calculation of wing surface area, we can finalize the arrangement of solar cells in our UAV.

Short circuit current and open circuit voltage of each cell array has been initiated the solar panel test. In which, the arrays are then individually numbered and their electrical characteristics are recorded for health confirmation. Solar testing of a UAV revealed that some cells did not provide the minimum rated short circuit current to be within specification. Several subsequent tests of the solar cells are performed using all 12 cells, which are soldered together and mounted on a sheet of cardboard for overall voltage measurement. Panel test occurred at several different times during the day, but usually, results are taken between 11 AM and 3 PM on relatively sunny days with constant voltage. This variance in testing times gave us an idea how the output from the cells would change in relation to the sun's position in the sky. The current is highly sensitive to the attitude of the cardboard w.r.t the sun so it is shifted from perpendicular to the sun to about 0°, 30° and 45° away from the sun, which demonstrates the cell require direct sunlight throughout the flight and high light intensity. Table 1 shows the solar cells testing output at various angles of incidence.

Solar UAV for forest surveillance is must want a battery as light as possible, yet powerful enough to supply sufficient energy so Ni-Mh Battery is the best option. The renewable energy source is the only way to reduce the weight of an UAV by decrease the components which involves in their propulsion unit [6]. Weight reduction and high-speed achievement is the prime techniques of this solar UAV thereby dimensions of the one solar cell are given here: Length is 25 mm; Breadth is 60 mm; Output voltage is 0.5 V; Output current is 1.5 A; Length of one solar panel as 150 mm; breadth is 135 mm; number of solar cells on wing as 24, which are connected in the series manner. Overall weight estimation and its comparison have been listed in Table 2.

Table 1 Solar cell testing at various angle of incidence

Degree of orientation to the sunlight	Time (hrs)	Voltage (V)
0	12	14.02
	12.5	13.19
	13	12.59
30	12	12.59
	12.5	13.02
	13	12.38
45	12	12.01
	12.5	11.66
	13	11.68

Table 2 Weight estimation

Element	First plan mass (g)	Actual mass (g)
Engine	135	70
Battery	120	50
Servo motors	10	38
ECU	10	35
Receiver	15	12
Propeller	15	10
Solar panels	500	200
Frame	500	500
Payload	50	50
Total weight	1290	965

2.2 *Design and Fabrication of Solar UAV*

Figure 3 shows the different views of a solar UAV, which has been modelled by CATIA. The solar UAV dimensions are has been derived from the standard analytical approaches. The individual components of a solar UAV have been designed with the help of literature survey, existing UAVs design and finally with the inclusion of aerodynamics consideration. Figure 4 shows the final prototype of solar UAV with estimated dimensions.

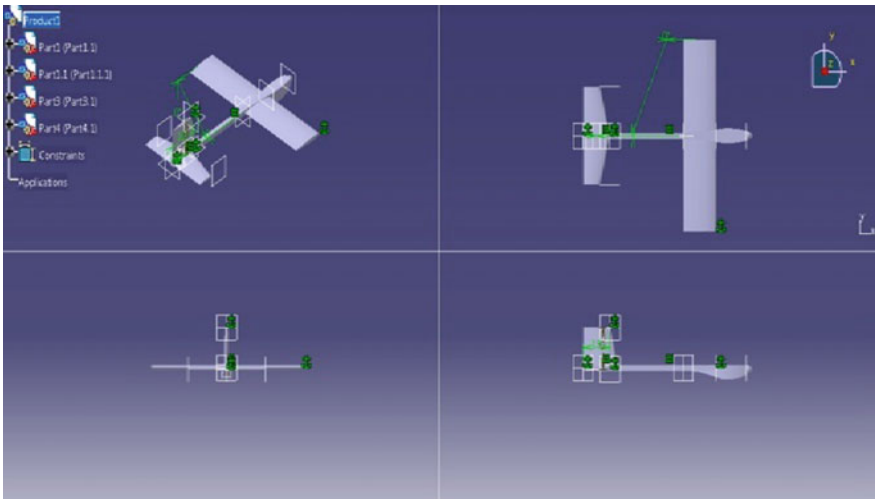

Fig. 3 Different views of solar UAV

Fig. 4 Solar UAV

3 Result and Discussions

The military use of UAVs has emerged because of their ability to operate in dangerous locations while keeping their human operators at a safe distance. Nowadays smaller UAVs are more comfortable than larger UAVs for critical applications. The handling of dangerous applications with smaller UAVs is a challenging task, but this task can be efficiently deals with the help of advanced avionics techniques such as intelligent video surveillance system, moving object detection techniques, feature extraction and template matching. After long survey the most appropriate method is selected and suggested for this paper, in order to recognize the intruder's image and efficiency is measured, which is nothing but the intruder's images are recognized by vision based navigation system. Important component for vision based navigation is localization of perfect intruder's detection algorithms, sensing the intruder's by camera, and finally representations of the border environment. In this work consist of two major steps; first one is creation of the solar UAV prototype and the next one is creation of moving intruder's detection matlab algorithm and its verification. Finally the integration of these two works practically will be carried out in future for the purpose of recognize the intruder's entering in the border region by autonomous solar UAV. Theoretically to know the intruders status in the border region, image processing and signal processing approaches are the methods available in MATLAB. For this work the image processing approach is selected to capture the intruder's images in the border with the help of smaller UAV [7].

3.1 Image Processing

In this paper there is survey of different object detection techniques and for object identification as intruders techniques such as enemy matching, edge based matching, skeleton extraction are studied. In image-processing applications, the brightness of the image and template can vary due to lighting and exposure conditions, so the images can be first normalized. Higher level image processing algorithms have been implemented as finite state machines the high-level control loop cycles through states representing goals. A classification algorithm typically performs better using the statistics extracted using the features instead of using the original data. The intruder's detection algorithms developed for this paper followed the same overall step-by-step with exchangeable sub-components. In this paper, standard vision features such as different intruder's identification, enemies shape, and weapons identification have been used. In addition the analyser also explored the different intruder's features and shapes learning techniques to obtain features that outperformed the standard feature set. The main work of this algorithm is to differentiate the intruder's image from the own country people's image and takes the needful action when an aerial images capture in the camera [8, 9]. In this paper, image processing has been simulated by MATLAB with the help of reference images and aerial images are taken from the internet. The verification of image detection algorithm is vital part in this paper, which may give confidence about intruder's prediction. Figures 5 and 6 show the reference image and UAV captured image, which are taken from the internet. All the images are taken from the internet for the purpose of verify the derived algorithm.

The matching percentage of images are simulated by MATLAB, the result file show in the Fig. 7 is the matching percentage of same images. The matching region in captured image compare with reference image is 100, because both the images are same for the purpose of verification.

Fig. 5 Reference image

Fig. 6 Solar UAV captured image

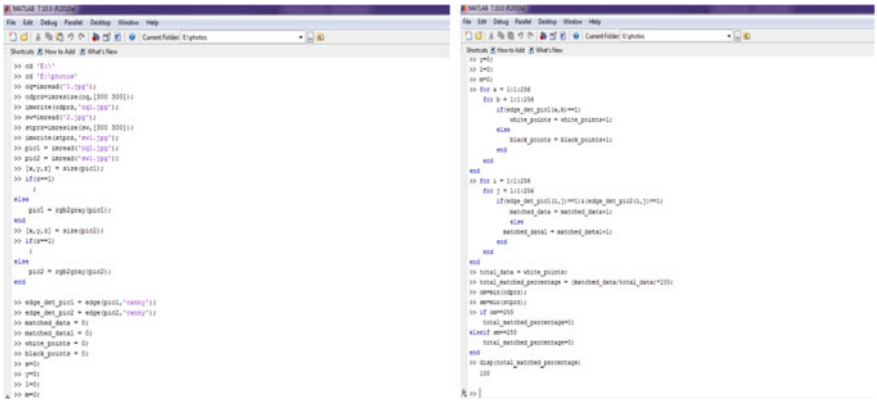

Fig. 7 Enemy detection result

3.2 Vision Based Navigation for Future Surveillance by Autonomous Solar UAV

In future this paper suggest the intruder image capturing techniques to be captured by vision based navigation by video surveillance in order to increase the enemies detection accuracy level in the monitoring area as a reference background for image subtraction. Real time videos will be captured in the border region with the help of rotating camera, which is attached in the autonomous solar UAV. These videos are splits in the form of frames to compare it with reference. Ground control station is the major part of the system, which is used to collect the video captured by the camera. After collecting the images from video, processing of that video in real time is done by the laptop using MATLAB. The error matching percentage of border images will be evaluated with the help of modern techniques and typical kind of intruder's inputs. If the error matching percentage is more than 50% then the alert system will be activate by ground controller and the output will be delivered in the

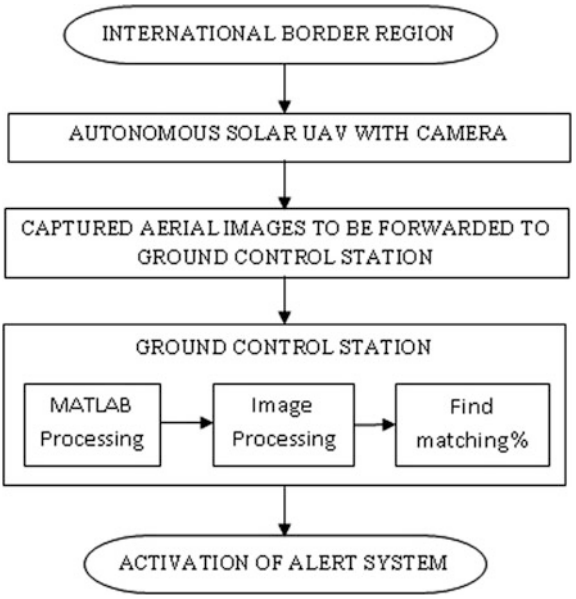

Fig. 8 Working flow chart of autonomous solar UAV

solar UAV. This solar UAV can be used in surveillance, monitoring of border regions that are large distances from the base station and also takes the necessary action with the help of warning system such as create the sound and send the intruder's position images to the ground controllers [9]. The step-by-step procedure of image processing of border region by autonomous solar UAV explained in Fig. 8.

4 Conclusions

Each and every component's specification of a solar UAV has been derived from theoretical calculation. The overall design of a solar UAV has been modelled by CATIA V5. The numerical progression of image processing and matching percentage of an enemy has been completed by MATLAB. Extensive test, numerical progression and respective calculations showed solar UAV is capable of flying, with solar power. Solar UAV has unique characters such as more comfortable flight, high lifespan with low power consume so it can able to reliable and capable to withstand any critical environment for a practical application such as intruders detection, activation of warning system. With the help of solar panels, the UAV can able to track any intruders as well as cover the whole predefined border region with long duration. Hence the proposed solar UAV is a better solution for border surveillance. In future the autonomous solar UAV for border surveillance will be added.

References

1. Raymer, D.P.: Aircraft design a conceptual approach. AIAA educational series (2006). ISBN-13: 978-1563478307
2. Abbot, I.H., Doenhoff, A.E.: Theory of wing sections: including a summary of airfoil data. Dover publications (1959). ISBN-10: 0486605868, ISBN-13: 9780486605869
3. Corke, T.C.: Design of aircraft, 1st edn. (2002). ISBN-13: 978-0130892348, ISBN-10: 0130892343
4. Bruhn, E.F.: Analysis and design of flight vehicle structures. Tri-State Offset Co., 1st edn. (1 Jan 1965). ASIN: B004YLAQC8
5. Bhatt, M.R.: Solar power unmanned aerial vehicle: high altitude long endurance applications. Master project thesis, San Jose State University (May 2012)
6. Tahar, K.N.: Aerial terrain mapping using unmanned aerial vehicle approach. Int. Arch. Photogramm., Remote Sens. Spat. Inf. Sci. **XXXIX**(B7). XXII ISPRS Congress, 25 Oct 2012–1 Sept 2012, Melbourne, Australia, pp. 493–498 (2012)
7. Sri, K.R.B., Aneesh, P., Bhanu, K., Natarajan, M.: Design analysis of solar-powered unmanned aerial vehicle. J. Aerosp. Technol. Manag. **8**(4), 397–407 (2016)
8. Khurana, A. et al.: Design and fabrications of solar-powered unmanned aerial vehicle prepared at innovation cell, IIT Bombay and Birla Institute of Technology and Science, Pilani (July 2014)
9. Rakesh, C. et al.: Design and analysis of solar powered RC aircraft. Int. J. Eng. Sci. (IJES) **4** (12), 29–41 (2015). ISSN (e): 2319–1813, ISSN (p): 2319–1805
10. Vijayanandh, R. et al.: Design, fabrication and simulation of hexacopter for forest surveillance. ARPN J. Eng. Appl. Sci. **12**(12), 3879–3884 (2017). ISSN 1819-6608, June 2017

Chapter 8
Quality Evaluation of CartoDEM in Different Resolutions

E. Venkateswarlu, I. Raghuramulu, T. Sivannarayana, G. P. Swamy and B. Gopala Krishna

Abstract The primary goal of Cartosat-1 mission is to generate, archive and disseminate seamless Digital Elevation Model (DEM) to facilitate the Remote sensing users and cartographers. The production approach identified for generating CartoDEM is through processing based on Ground Control Points (GCPs) using Augmented Stereo Strip Triangulation (ASST) software system. DPGS-NRSC has generated and disseminated 10 m CartoDEM covering India and surrounding countries, part of south- west Asia and in the process of generating DEM covering Australia. 30 m DEM is ported on Indian EO portal Bhuvan for visualization and free download. To explore the improved performance of the DEM, we carried out comparative quality analysis of CartoDEM data with 2.5, 5 and 10 m resolutions generated in operational mode. This study has confirmed the enhanced performance of 2.5 m CartoDEM in terms of hydrological, terrain category and contour analysis. This geospatial input is one of the decision making tools for understanding spatio-temporal variations and better management.

Keywords Digital elevation model · CartoDEM · Slope · Aspect
Terrain relief · Stream network

E. Venkateswarlu (✉) · I. Raghuramulu · T. Sivannarayana · G. P. Swamy
B. Gopala Krishna
Data Processing, Products, Archival and Web Applications Area (DPPA&WAA),
National Remote Sensing Center (NRSC), ISRO, Hyderabad, India
e-mail: venkateswarlu_e@nrsc.gov.in

I. Raghuramulu
e-mail: raghuramulu_i@nrsc.gov.in

T. Sivannarayana
e-mail: sivannarayana_t@nrsc.gov.in

G. P. Swamy
e-mail: swamy_gp@nrsc.gov.in

B. Gopala Krishna
e-mail: bgk@nrsc.gov.in

P. J. Rao et al. (eds.), *Proceedings of International Conference on Remote Sensing for Disaster Management*, Springer Series in Geomechanics and Geoengineering,
https://doi.org/10.1007/978-3-319-77276-9_8

1 Introduction

Digital Elevation Model (DEM) is a digital representation of the Earth's relief that consists of an ordered array of elevations relative to a datum, and referenced to a geographic coordinate system. A DEM can be defined as a regular two-dimensional array of height values describing the varying elevation of an area's terrain [1].

DEMs are useful for many purposes, and are an important precondition for many applications [2]. They are particularly useful in regions that are devoid of detailed topographic maps. DEMs have been found useful in many fields of study such as geo-morphometry, as these are primarily related to surface processes such as landslides which can directly be depicted from a DEM [3], archaeology as subtle changes due to previous human activity in the sub surface can be inferred on detailed DEMs, forestry, e.g. height of trees and relation to preferred tree stem size, hydrology, like deriving drainage network and overland flow areas that contribute to suspended sediment loads and analysis of glaciers and glaciated terrains.

Several techniques and tools are suitable for DEM extraction like digital aerial and terrestrial Photogrammetry, airborne and terrestrial laser scanning, Global Positioning System (GPS) with its different measurement approaches and active and passive remote sensing, with optical satellite imagery systems.

With the launch of the Indian remote sensing satellite Cartosat-1, an along-track stereoscopic imaging mission, possibilities for operational availability of high-resolution stereo-imagery from space for the remote sensing and cartography user communities have emerged [4]. The high-resolution stereo data beamed from twin cameras onboard Cartosat-1 mission facilitates topographic mapping up to 1:25,000 scale. An initiative to generate a database of seamless, homogeneous DEM, named as CartoDEM and associated ortho-image tiles at country level has been undertaken by ISRO. CartoDEM generation system in NRSC has produced the digital surface model covering India and surrounding countries and part of South West Asia using improved software version-3. At present, DEM generation of Australia is under progress.

To explore the improved performance of the CartoDEM, generated data with 2.5, 5 and 10 m resolutions for quality assessment.

2 Quality Assessment

A comparative study is carried out to analyze the CartoDEM data with 2.5, 5 and 10 m resolutions generated in operational mode through indigenously developed software—Augmented Stereo Strip Triangulation (ASST). Sample data sets selected are covering different elevation ranges from 100 to 5700 m. Following

parameters are compared between the data sets with different resolutions—DEM statistics, slope distribution statistics, spatial profiles, terrain categories, contours, stream networks and DEM derivatives (Table 1).

DEMs of the study sites were transformed into the same projection system for quantitative and qualitative assessment. Quality evaluation is done through computation of accuracy measures, visual comparison of derivatives.

Analysis and Results

Elevation range, Mean and Std. dev. of 2.5, 5 and 10 m DEMs are matching (Table 2).

Slope Distribution Statistics

Slopes are derived for all the DEM tiles and slope distribution statistics like maximum slope, average slope and std. dev. are computed. It is observed that maximum and average slopes are matching. Standard deviation of 2.5 m DEM slope is more than 5 and 10 m which shows the presence of subtle details (Table 3).

Surface Spatial Profiles

The spatial horizontal profiles were extracted for the cells that fall along the horizontal cursor line (red) of all three DEM tiles and compared. A graph of elevation profile was produced for comparison. It observed that 2.5 m DEM shows better details in areas of higher elevation range (Fig. 1) and no significant variation in details in plain areas of 2.5 m, 5 m and 10 m DEMs.

Terrain Category Analysis

Terrain analysis employs the digital elevation data in conjunction with other geospatial information like slope, aspect and relief to describe the landscape for

Table 1 Source data for analysis

Tile id.	CartoDEM Tile SW corner co-ordinates
A.	db_33.000N_77.625E
B.	db_31.000N_77.000E
C.	db_30.500N_76.875E
D.	db_28.500N_76.375E

Table 2 DEM statistics

Tile id.	CartoDEM (2.5 m)		CartoDEM (5 m)		CartoDEM (10 m)	
	Min–Max	Mean–Std. dev.	Min–Max	Mean–Std. dev.	Min–Max	Mean–Std. dev.
A.	4275–5768	5108–256	4278–5768	5108–256	4280–5760	5108–256
B.	796–2019	1288–221	796–2018	1288–221	797–2018	1288–221
C.	210–313	265–11	216–318	265–11	216–305	265–11
D.	107–206	165–4	112–191	165–4	113–190	165–4

Table 3 Slope distribution statistics

Tile→	db_33.000N_77.625E			db_31.000N_77.000E			db_30.500N_76.875E			db_28.500N_76.375E		
Slope↓	2.5 m	5 m	10 m	2.5 m	5 m	10 m	2.5 m	5 m	10 m	2.5 m	5 m	10 m
Max. (deg)	87.5	85.6	81.4	85.8	83.4	79.0	82.3	78.9	69.2	84.2	76.9	69.6
Avg. (deg)	34.9	32.8	30.8	29.8	28.0	26.5	6.6	5.8	5.0	5.6	4.9	4.2
Std. dev. (%)	71.9	50.96	37.93	52.3	37.09	27.95	15.03	11.14	8.48	13.89	10.25	7.66

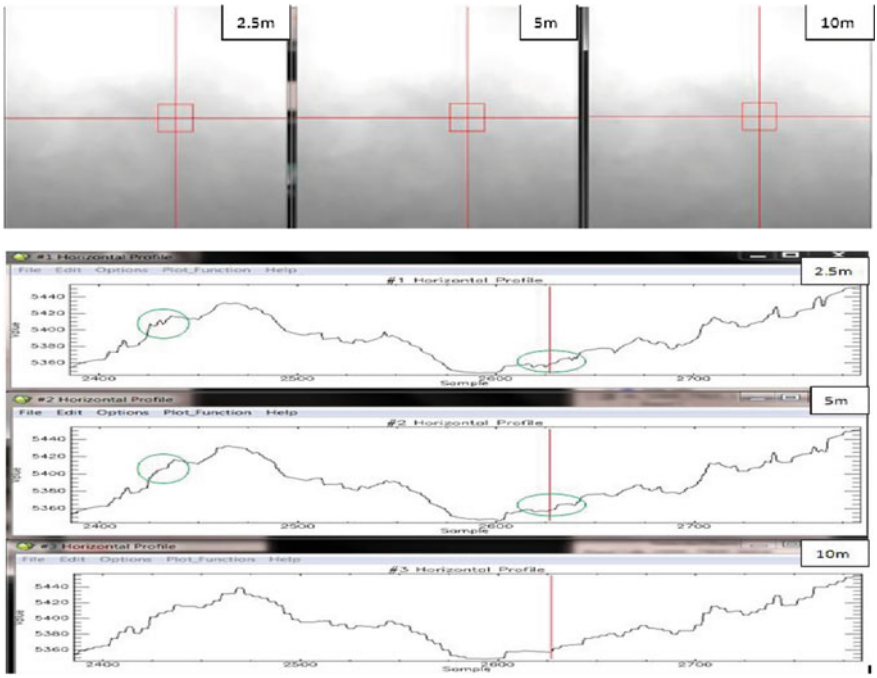

Fig. 1 Profiles of db_33.000N_77.625E data

visualization. It is evident from Fig. 2 that significant details are extracted in 2.5 m DEM than 5 m and 10 m DEMs.

Hydrological Analysis

The hydrologic tools allow to determining the flow direction, calculating flow accumulation, delineating watersheds, and creating stream networks. Stream networks can be delineated from a DEM using the output from the Flow Accumulation function. Flow accumulation in its simplest form is the number of upslope cells that flow into each cell. More lower order streams are delineated in 2.5 m DEM. Visual inspection of delineated streams (Fig. 3) shows that 2.5 m DEM has more details than 5 and 10 m DEMs.

Contour Analysis

Contours are polylines that connect points of equal elevation values and useful for surface representation. They allow simultaneous visualization of flat and steep areas, ridges and valleys. Contours are derived for all the DEM tiles with 10 m

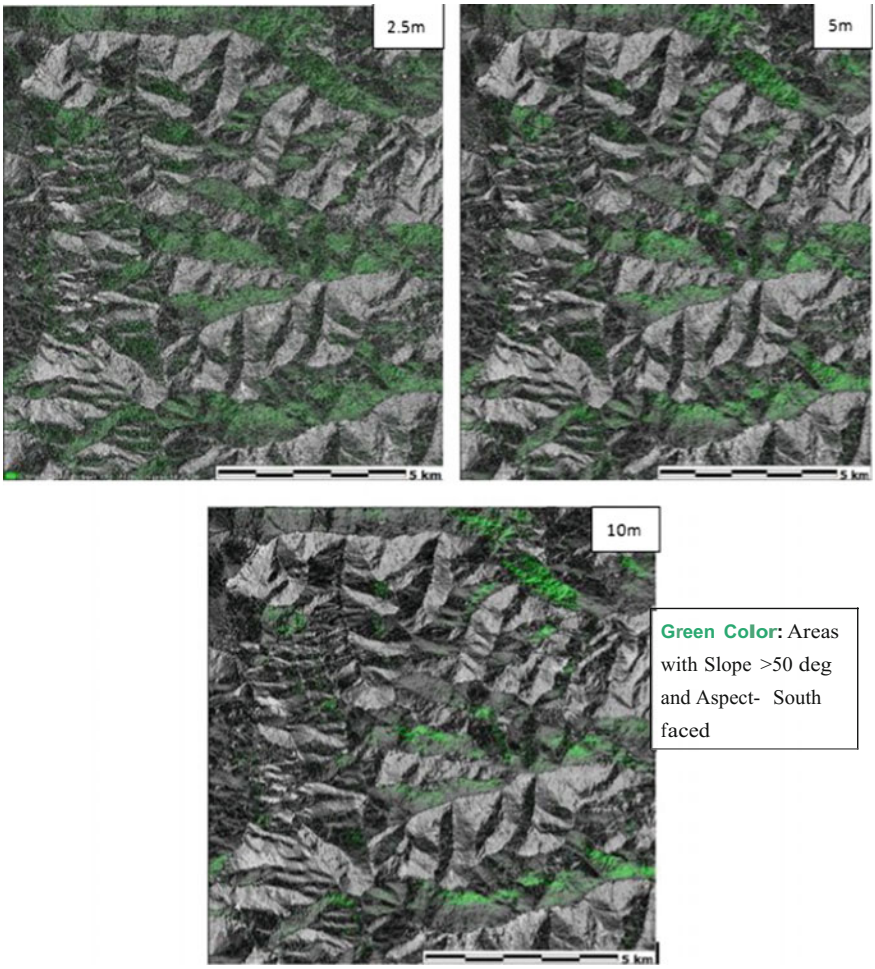

Fig. 2 Terrain category of db_33.000N_77.625E data

interval and overlaid for comparison. The distribution of polylines shows how values change across a surface. The 2.5 m DEM contours appear smooth without any rapid fall (Fig. 4).

Visual Comparison of Derivatives

DEM derivatives like slopes, aspects and terrain relief maps are generated for all data sets and compared.Visual comparison of Figs. 5, 6, 7 confirms that 2.5 m DEM has more details in areas of higher elevation range.

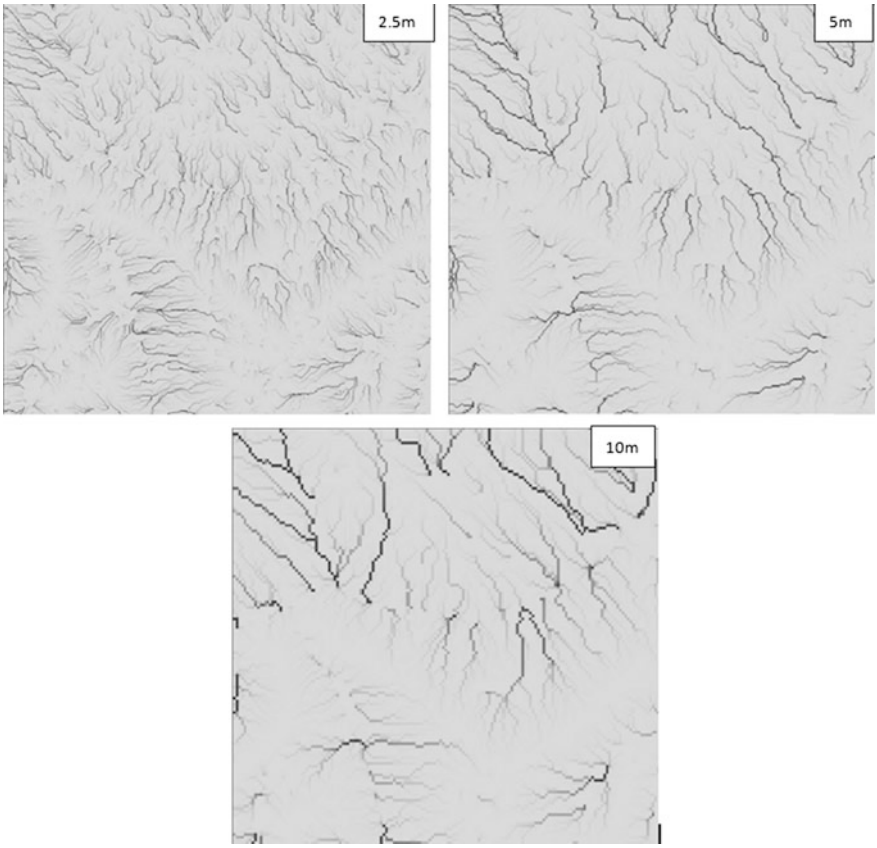

Fig. 3 Stream networks of db_33.000N_77.625E data

3 Discussion and Conclusions

From the spatial profiles, 2.5 m DEMs show better details in areas of higher elevation range. No significant variation in plain areas of 2.5, 5 and 10 m DEMs. From terrain category analysis, significant details of areas with a particular slope and aspect are visible in 2.5 m DEM than 5 and 10 m DEMs. Visual comparison of derivatives like slope, aspect, relief shaded maps confirms that 2.5 m DEM has more details in areas of higher elevation range. Elevation range, mean, std. dev. are matching in three resolution DEMs.

From Slope distribution statistics, Maximum and average slopes are matching. Std. dev. of 2.5 m DEM slope is more than 5 and 10 m which shows the presence of subtle details. From Hydrological analysis, 2.5 m DEM depicts more flow accumulation details than 5 and 10 m DEMs. From Contours analysis, 2.5 m DEM depicts more details than 5 and 10 m DEMs. From the results interpretation, DEMs

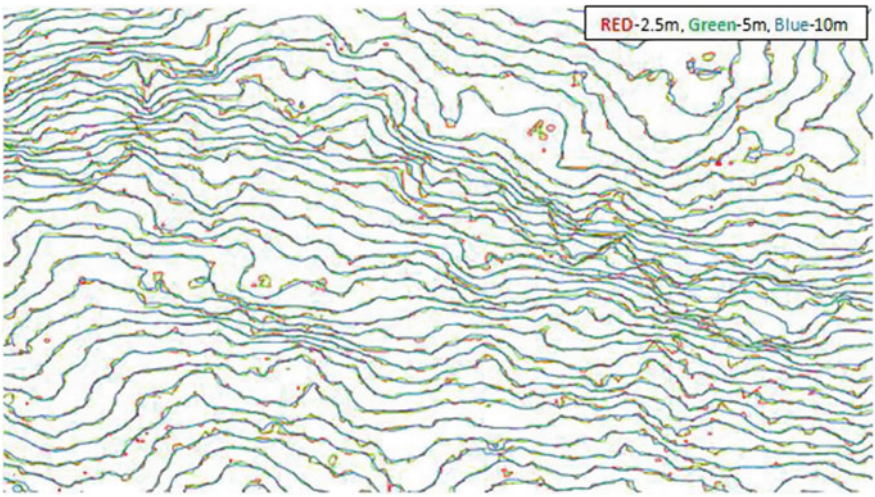

Fig. 4 Contours of db_33.000N_77.625E data

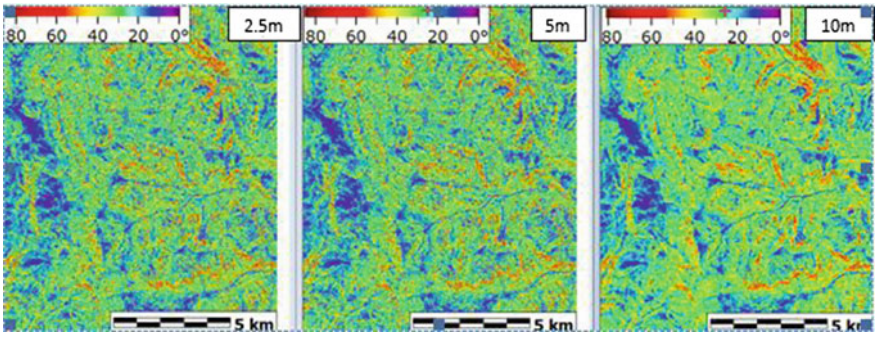

Fig. 5 Slopes of db_33.000N_77.625E data

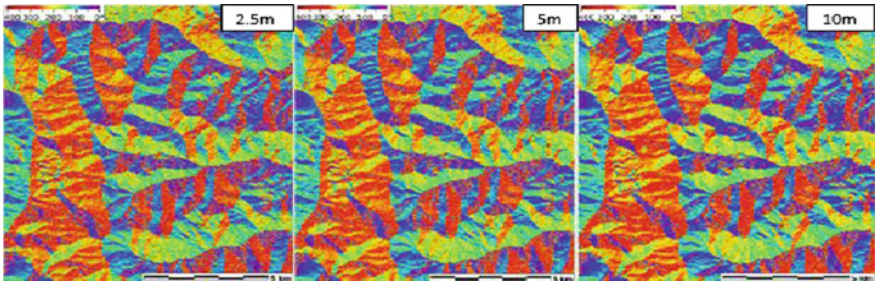

Fig. 6 Aspects of db_33.000N_77.625E data

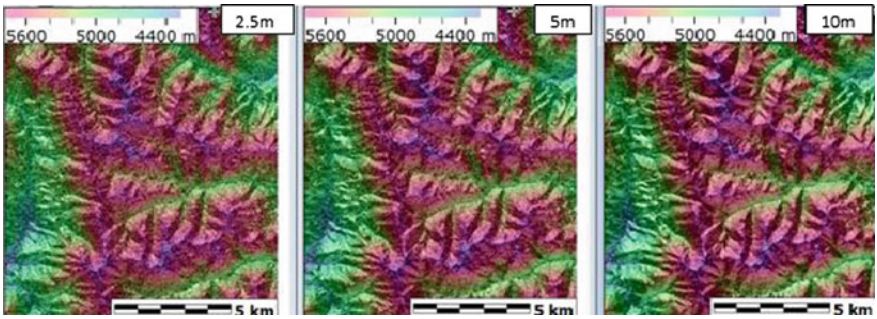

Fig. 7 Terrain relief maps of db_33.000N_77.625E data

generated from coarsely sampled elevation points may have severe limitations in their use for hydrological analysis. The performance of the DEM depends on its spatial resolution and the landscape it represent. This study has confirmed the enhanced performance of 2.5 m CartoDEM in terms of hydrological, terrain category and contour analysis. DEM interpretation based on resolution which contains details about sampled point elevations will be taken up for the future work.

Acknowledgements The authors would like to place on record their deep gratitude for the support provided by Dr. Y. V. N. Krishnamurthy, Director, NRSC for the successful completion of this work. The authors deeply acknowledge the support provided by CartoDEM generation team.

References

1. Burrough, P.A., McDonnell, R.A.: Principles of geographical information systems, pp. 333–335. Oxford University Press, New York (1998)
2. Kim, S., Kang, S.: Automatic generation of a SPOT DEM: Towards coastal disaster monitoring. Korean J Remote Sens. **17**, 121–129 (2001)
3. Pike, R.J., Evans, I.S., Hengl, T.: Geomorphometry: A brief guide
4. Srivastava, P.K., Srinivasan, T.P., Gupta, A., Singh, S., Nain, J.S., Amitabh, Prakash, S., Kartikeyan, B., Krishna, B.G.: Recent advances in Cartosat-1 data processing. ISPRS Hannover Workshop (2007)

Chapter 9
Multi-angle LIDAR for Remote Sensing Smoke Emissions from Wildfires

Y. Meenakshi and Yellapragada Bhavani Kumar

Abstract Wildfires generate plumes of smoke which release toxic pollutants into the atmosphere and affect the surrounding air quality significantly. Smoke contains carbonous particles that influence the regional climate patterns. Wildfires sometimes generate thick smoke layers that cause poor visibility and accidents. Generally smoke tends to disperse in form of layers in the atmosphere. Aircraft measurements are performed to understand the dynamics of smoke plumes. However, these measurements involve cost and enormous amount of exercise. Significant amount of information is required for understanding the dissipation of smoke from wildfires. Occasionally, smoke generated from wildfires cross political boundaries and influence chemical composition of atmosphere. Recently, at a unit of Department of Space (DOS) located near Tirupati, a laser radar system was developed indigenously for remote sensing smoke layers in the atmosphere. The developed laser radar system uses a novel multi-angle method to track the smoke layers in the atmosphere. The LIDAR (Light Detection And Ranging) system uses visible wavelength for probing smoke layers. The system was operated during dry season to remote sense smoke layers produced by wildfires that occurred in the nearby reserve forest. During the observations, the LIDAR system was found suitable for tracking smoke plume boundaries, its top height, dispersion and change of its intensity with time.

Keywords Remote sensing · LIDAR · Smoke

Y. Meenakshi · Y. Bhavani Kumar (✉)
National Atmospheric Research Laboratory, Gadanki,
Pakala Mandal, Chittoor 517112, Andhra Pradesh, India
e-mail: ypbk@narl.gov.in

Y. Meenakshi
e-mail: meena.yellapragada@gmail.com

P. J. Rao et al. (eds.), *Proceedings of International Conference on Remote Sensing for Disaster Management*, Springer Series in Geomechanics and Geoengineering,
https://doi.org/10.1007/978-3-319-77276-9_9

1 Introduction

Wildfires occur by actions of Nature or human and are generally seen in dry season. Strong plumes of flame stem from large forest area produce smoke. Smoke basically originates from incomplete burning of organic material of forest wood. Smoke from forest fires cause devastation, which can spread easily to neighbouring areas due to local winds. Smoke contains minute particles of ash or soot that cause warming and suffocating effect. Remote sensing is an advanced method to locate forest fires. Space-borne (satellite based) instruments equipped with onboard sensors provide information on forest fires over the earth surface. However, smoke sensing is difficult. Active remote sensing instruments provide real-time monitoring of smoke. Radars cannot detect smoke particles due to their limitation in operating frequencies. However, laser radars sensitive to backscattering from airborne particles and detect smoke clouds.

LIDAR utilises the principle of radar for sensing smoke. But, LIDAR uses laser pulses for probing the atmosphere. Each laser pulse of LIDAR produces huge number of photons that interact with basic constituents of the atmosphere. Scattering from atmospheric components constitute signal in LIDAR. Smoke plumes change the composition of atmosphere and hence located easily using LIDAR. The initial applications of laser radar were to monitor smoke generated by local power plants and factories [1]. Over the last thirty years, significant developments have been made in the field of remote sensing particularly in the area of LIDAR technology. Addition of scanning capability to LIDAR helps to identify the position of smoke accurately. The lidars have been employed to understand atmospheric structure, composition and dynamics [2–4]. Several researchers reported the use of LIDAR for detection of smoke from fires [5–12]. The selection of laser wavelength of LIDAR plays a key role in the operational range of LIDAR. Visible wavelengths provide longer range. However, ultraviolet (UV) wavelengths present limited range due to higher molecular extinction [13] and infrared spectrum experience lower target backscattering efficiency [14].

Recently, an elastic backscatter LIDAR was developed at a unit of Department of Space located near Tirupati. The location of LIDAR is a rural site situated in the Chittoor district of Andhra Pradesh. The LIDAR uses green visible laser for probing the atmosphere. The LIDAR was utilized to probe the smoke layers from wildfires that occurred at nearby hills of reserve forest. This paper presents the LIDAR observations of wildfires smoke.

2 Description of LIDAR Site

A map taken from Google that indicated in Fig. 1 shows the topography of LIDAR site of NARL. The LIDAR was developed at the site of National Atmospheric Research Laboratory (NARL), a unit of Department of space that located near a

Fig. 1 Map showing the LIDAR site of NARL that located amid of hills of Panapakam Reserve forest in Chittoor district of Andhra Pradesh. Thick red circle shows the location of LIDAR at NARL site. The right-side of the red circle is the radar antenna

village named Gadanki (13.5°N, 79.2°E, 375 m AMSL) in Chittoor district of Andhra Pradesh. The NARL is a remote sensing centre and it is involved in the development of radars and lidars for atmospheric studies. The NARL operates high power radar and uses a large antenna. One can see the Indian MST radar antenna in Fig. 1. The Gadanki is situated 36 km away from Tirupati, a famous temple town of south India. The NARL site is situated in the tropical part of India and its climate features resemble semi-arid region. The village Gadanki experiences hot tropical climate throughout the year, but months of January and February is cold. The east and southern part of LIDAR site is surrounded by hills, which is a part of Panapakam reserve forest. The Northern and western sides of LIDAR contain agricultural lands and village settlements. During dry season, we see wildfires occurrence around hills that located in the south-eastern side of NARL.

3 Description of LIDAR Instrument

Figure 2 illustrates the LIDAR instrument that used in the study and Table 1 gives the brief specifications of LIDAR instrument employed. Our LIDAR uses a diode pumped Nd:YAG laser that produces a narrow pulse laser at 532 nm wavelength for probing the atmosphere. This wavelength is not eye-safe. Several researchers employed eye-safe wavelength for horizontal LIDAR works such as probing of smoke layers [15, 16]. Our LIDAR collects photon returns from the atmosphere using a custom built telescope of diameter 150 mm. A high gain PMT converts the collected backscattered photons into electrical pulses. A transient recorder unit acts as data acquisition unit and produces LIDAR signal. A dedicated computer with custom built software controls the transient recorder unit and stores the recorded data. The opto-mechanical support of LIDAR allows multi-angle operation of

Fig. 2 LIDAR system used in the study

LIDAR. It permits LIDAR orientation at different elevation and azimuth angles. The LIDAR sensed smoke signal is shown in Fig. 3. The LIDAR signal indicated in Fig. 3 was detected in the near horizontal direction at an elevation of 5°. An intense signal at 1800 m range in Fig. 3 represents the smoke return from wildfires. The LIDAR records temporal variation of signals and presents its strength in milli volts. Our LIDAR supports fast time sampling of smoke signals. The temporal integration of LIDAR signal shown Fig. 3 is around two seconds.

The LIDAR observation of wildfires is shown in Fig. 4. The event took place during dry season. The illustrated figure shows patches of wildfire occurrence at this location. Local winds influence the smoke emanate from these fires. The fire site location is about 1.9 km away from the NARL site, however, sometimes smoke get transported over NARL site due to local winds. One can see thick smoke layers that swirl into the atmosphere from fire points.

The temporal variation of smoke intensity captured by LIDAR is shown in Fig. 5. The signals show that the occurence of wildfire event near NARL site and detection of eminated smoke layers by LIDAR system. Many peaks of layers of

Table 1 LIDAR specifications

Parameter	Specified
Laser	Diode pumped Nd:YAG laser
Wavelength	532 nm
Pulse duration	10 ns
Polarization	>100:1
Transmitter FOV (field of view)	200 µrd
Telescope	150 mm diameter
Field of view	400 µrad
Detector	High gain PMT
Data acquisition	Transient recorder
Range resolution	15 m

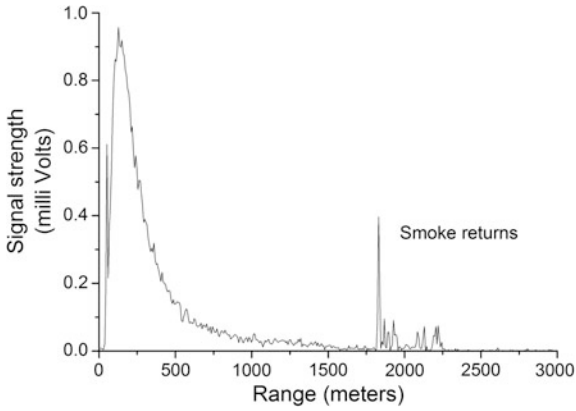

Fig. 3 LIDAR sensed smoke signal trace. The vertical axis indicates strength of the signal and horizontal axis provides range. One can observe the smoke signal as narrow spike at 1800 m range obtained in the near horizontal direction

smoke is seen in the signals that contribute to the whirling nature of smoke while mixing with the atmosphere. Figure 5 illustrates several smoke profiles that integrated over a period of 60 s. Figure 5 provides smoke profiles recorded from 2009 LT to 2017 LT.

4 Conclusions

We developed a LIDAR system that operates on the principle of radar to detect smoke layers in the atmosphere. The LIDAR system uses green wavelength and possible to operate at multi-angles. The multi-angle provision helps to cover the low elevation angle. The LIDAR signals recorded during wildfires event represents the range resolved data and gives exact location of smoke emission in the atmosphere. The system was operated during dry season to remote sense the smoke layers produced by wildfires that occurred at nearby reserve forest range. We utilized the

Fig. 4 Wildfires occurrence on hills near NARL site. One can see the spreading of smoke plumes at fire points. It is a regular event that generally seen during dry season at this location

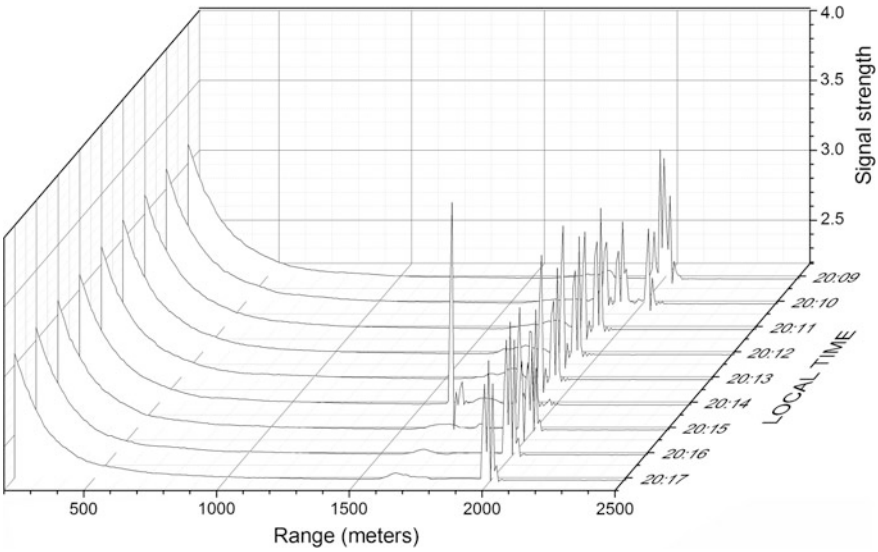

Fig. 5 Temporal variation of smoke intensity that emanate from wildfires

LIDAR to track the smoke layers in the atmosphere. During the observations, the LIDAR system was found suitable for tracking smoke plume boundaries, its top height, dispersion and change of its intensity with time.

References

1. Hamilton, P.M.: The application of a pulsed-light ranger finder (Lidar) to the study of chimney plumes. Phil Trans. Roy. Soc. Lond. A **265**, 153–172 (1969)
2. Kumar, Y.B., Raju, C.N., Krishnaiah, M.: Indo-Japanese Lidar observations of the tropical middle atmosphere during 1998 and 1999. Adv. Atmos. Sci. **23**(5), 711–725 (2006)
3. Kumar, Y.B.: Portable lidar system for atmospheric boundary layer measurements. Optic. Eng. **45**(7), 076201 (2006)
4. Kumar, Y.B., Prasanth, P.V., Rao, D.N., Murthy, M.S., Krishnaiah, M.: The first Lidar observations of the nighttime sodium layer at low latitudes Gadanki (13.5°N, 79.2°E), India. Earth Planets Space **59**(6), 601–611 (2007)
5. Eberhard, W.L.: Eye-safe tracking of oil fog plumes by UV Lidar. Appl. Opt. **22**, 2282–2285 (1983)
6. Bennet, M., Sutton, S., Gardiner, D.R.C.: An analysis of Lidar measurements of buoyant plume rise and dispersion at five power stations. Atmos. Environ. **26A**, 3249–3263 (1992)
7. Andreucci, F., Arbolino, M.V.: A study on forest fire automatic detection systems. 2.-smoke plume detection performance. Nuovo Cimento C **16**, 51–65 (1993)
8. Rauste, Y., Herland, E., Frelander, H., Soini, K., Kuoremaki, T., Ruokari, A.: Satellite-based forest fire detection for fire control in boreal forests. Int. J. Remote Sens. **18**(12), 2641–2656 (1997)
9. Pershin, S., Hao, W.M., Susott, R.A., Babbitt, R.E., Riebau, A.: Estimation of emission from Idaho biomass fires using compact eye-safe diode Lidar. Proc. SPIE **3757**, 60–66 (1999)
10. Vilar, R., Lavrov, A.: Application of Lidar at 1.54 micron for forest fire detection. Proc. SPIE **3868**, 473–477 (1999)
11. Muller, D., Wagner, F., Ansmann, A.: Observations of Boreal Forest fire smoke in the stratosphere by POAM III, SAGE II and Lidar in 1998. Geophys. Res. Lett. **27**, 1403–1414 (2000)
12. Fernandes, A., Utkin, A.B., Vilar, R., Lavrov A.: Recognition of Smoke Signatures in Lidar Signal with a Perceptron. In: Sixth Multi-conference on Systemics, Cybernetics and Informatics, Orlando, Florida, USA, 14–18 July 2002
13. Collis, R.T.H., Russel, P.B.: Lidar measurement of particles and gases by elastic backscattering and differential absorption. In: Hinkley, E.D. (ed.) Laser Monitoring of Atmosphere, pp. 71–152. Springer, Berlin (1976)
14. Srivasta, V., Jarzembski, M.A., Bowdle, D.A.: Comparison of calculated aerosol backscatter at 9.1 and 2.1 μm wavelength. Appl. Opt. **31**(2), 1904–1906 (1996)
15. Utkin, A.B., Lavrov, A.V., Costa, L., Simões, F., Vilar, R.: Detection of small forest fires by Lidar. Appl. Phys. B **74**(1), 77–83 (2002)
16. Vilar, R., Lavrov, A.: Estimation of required parameters for detection of small smoke plumes by Lidar at 1.54 μm. Appl. Phys. B **71**, 225–228 (2000)

Chapter 10
Urbanisation and Tank Systems Adjoining Hyderabad—A Rapid Assessment Using Remote Sensing Techniques

K. Ramesh Reddy, P. Narender Babu and E. Srinivas

Abstract Hyderabad in the Deccan plateau forms a distinct socio-cultural and natural setting and is known for its water bodies such as tanks and reservoirs formed with a long history that still continue to influence the livelihoods of many. Hyderabad's urbanisation with drivers such as rapid industrialisation, surge in IT industry, housing for different classes of population, real estate boom, etc., have exerted tremendous pressure on the tank systems. The present study taken up in Sangareddy district, Telangana, with a prime objective to bring out effects of urbanisation on tank systems and map the spatial and temporal changes of tank catchments, submergence and command area using the Remote sensing techniques. Multi Spectral LANDSAT series and Sentinel 2 data from 2004 to 2016 are used to study the change pattern and understand the changes in terms of plotting, construction and other uncultivated areas. The Satellite data analysed supported by ground truth and relevant secondary data indicates that the tank systems are prone to severe degradation affecting the inflows, storage, irrigation, groundwater recharge and other indirect livelihoods like fisheries. More than 50% of the command area is lost in the last 15 years.

Keywords Tank system · Satellite data · Agricultural land · Urbanisation
Tank ayacut · Irrigation · Change detection

K. Ramesh Reddy (✉)
GIS & Remote Sensing Expert, NABCONS, Hyderabad, India
e-mail: kothamidde6@yahoo.com

P. Narender Babu
Water Resources Expert and Former Associate Professor,
Tata Institute of Social Sciences, Hyderabad, India
e-mail: pallanarendra@gmail.com

E. Srinivas
Research Scholar, Applied Geochemistry, Osmania University, Hyderabad, India
e-mail: srinivase4@gmail.com

P. J. Rao et al. (eds.), *Proceedings of International Conference on Remote Sensing for Disaster Management*, Springer Series in Geomechanics and Geoengineering,
https://doi.org/10.1007/978-3-319-77276-9_10

1 Introduction

Based on the geographic, climatic and topographic back ground, tanks are the back bone of agriculture in Telangana region. Farmers' dependency on tank system has been quite high due to the topography and rainfall pattern in the region. Though the construction of tanks in Deccan region has a long history, since Satavahanas period dated variously from 271 BCE to 30 BCE, Kakatiya reign is known for the technical expertise in the development of tanks system. Similar sprit has been carried by the Muslim rulers of the Telangana region as well.

Hyderabad, having the rich history of 400 years is best known as City of lakes. Nizam's government has taken interest in the tank development in Hyderabad to mitigate droughts. However, with the change in climate, erratic rainfall pattern, improper maintainance of tank system by the community, unplanned growth of urban settlements, surge in the IT industry, housing for different classes of population, real estate boom, etc., gradually affected functioning of tank systems in the region.

The current study focuses on Yenki Cheruvu tank of Sangareddy district, 44 km away from city with a tank command area of 152 acres. The prime objective is to bring out the effects of urbanisation on tank system. Study attempts to map the spatial and temporal changes of tank catchments, submergence and command area using the Remote sensing techniques. Multi Spectral ortho-rectified satellite data of LANDSAT series 5 and 8 for the periods 2004 and 2016 and Sentinel 2 data for the period 2016 are used to bring out the changing pattern of tank system. Trends in land use pattern are mapped to understand the changes in terms of plotting, construction and other uncultivated areas.

2 Materials and Methods

2.1 Study Area

As per the reorganisation of districts taken up in Telangana state during November 2016, selected study tank falls in the newly formed Sangareddy district located in North west direction of Hyderabad city. Yenki Cheruvu in Muthangi village, located 44 km away from Hyderabad city centre lies at latitude 17 32 34N and longitude 78 13 15E. From the secondary data source of Minor Irrigation Department, this tank is selected as it is adversely affected by urbanisation. Yenki cheruvu has a registered ayacut area of 152 acres with a catchment of 3.81 km^2. Total submerged area of tank is 84 acres. Extent of Muthangi village is 8.09 km^2 area with a population of 8777 (Fig. 1).

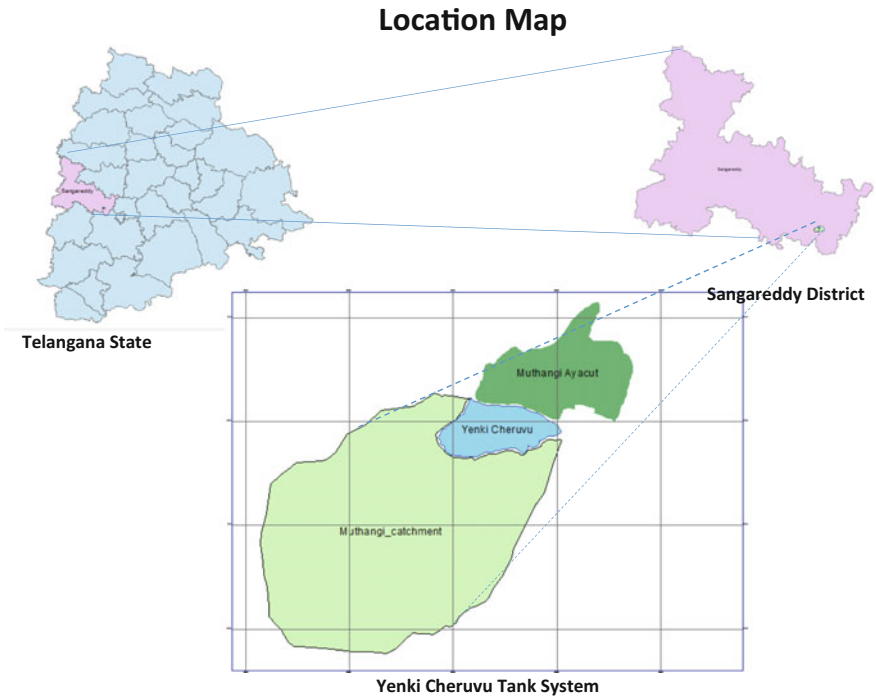

Fig. 1 Location map showing Yenki Tank, ayacut and catchment area

2.2 Datasets

For tracking the spatial and temporal changes in tank catchments, submergence and command area, multi spectral ortho-rectified satellite data of LANDSAT series 5, 7 and 8 for the periods 2004 and 2016 and Sentinel 2 data for the period 2016 were obtained from the public domain service of USGS data centre. Landsat data provide one of the most valuable datasets for mapping and monitoring the earth surface [1].

Cadastral maps from web site http://bhuvan.nrsc.gov.in/governance/twris village Pahanis (land details of farmers) are from http://mabhoomi.telangana.gov.in/GramaPahani_drs.aspx portal.

Landsat-8 has increased capabilities such as new spectral bands in the blue part and cirrus cloud-detection portion of the spectrum, two new thermal bands, improved sensor signal-to noise performance and several developments in radiometric resolution and duty cycle that allows a significant increase in collection of number of images per day [2].

2.3 Methodology

For analysing the effects of urbanisation on tank system, study used GIS softwares such as Arcgis and ERADAS. Cadastral map of the study area is obtained from two different sources, one from the Mandal Revenue office (MRO) and one from Bhuvan web site (http://bhuvan.nrsc.gov.in/governance/twris) to identify the tank ayacut boundary. Village Pahanis were download from http://mabhoomi.telangana.gov.in/GramaPahani_drs.aspx portal for the purpose of identifying the tank ayacutdars (farmers whose land is irrigated by selected tank water). Tank related secondary data has been collected from Command Area Development Authority (CADA) Irrigation department, Telangana and from the stakeholders (farmers) of the tank. Tank ayacut boundary has been marked with the geo-coordinates obtained using GPS instrument with the help of Village revenue officer (VRO)/Neeruganti and overlay of tank ayacut layer on cadastral map was done duly cross checking with the tank ayacutdars survey numbers from village Pahani. Water spread area and catchment area of the tank has been delineated using traverse method along with the GPS and same has been depicted using ArcGIS software.

Remote sensing satellite sensors record digital numbers (DN) of ground features at different wave lengths based on the reflectance capacity of the ground features. All the DN values are stored in the form of bands. The Landsat Thematic Mapper (TM) sensor carried on Landsat 4 and Landsat 5 consists of seven spectral bands with a spatial resolution of 30 m for Bands 1 to 5 and 7. Band 6 was acquired at 120 m resolution, re-sampled to 30-m pixels. Landsat 7 consists of eight spectral bands with a spatial resolution of 30 m for Bands 1 to 7. The resolution for Band 8 (panchromatic) is 15 m.

Sentinel-2 mission is a land monitoring constellation of two satellites (Sentinel-2a and Sentinel-2b) providing global optical imagery with 13 spectral bands using MSI (Multispectral Imager) instrument [3].

As the objective of the study is to bring out the changes in tank ayacut, tank catchment and tank water spread area, unsupervised classification has been used to classify the raster pixels based on the DN value it contains. To perform the unsupervised classification, ISODATA algorithm technique is used that resulted in creation of unlabeled clusters or classes in the satellite image. Using the above method, study area (tank ayacut, tank catchment, tank water spread) is classified into vegetation, settlement and water spread extent. To have image classification accuracy, training samples are created based on the ground truth sample position and create a signature to apply on the images.

Accuracy assessment is an established component of the process of creating and distributing thematic maps [4].

The combined use of Sentinel-2A and Landsat-7/8 poses a number of technical challenges due to the differences in their orbital, spatial, and spectral response functions, and image processing chains. Infact, although the radiometric characteristics of these sensors are similar, they are not identical and can lead to slight differences in surface reflectance and retrieval quantities as confirmed by the

inspection of the data [5]. The study estimate of the encroachment of water spread area of 6.69% was lower than that of the state average of 10% [6], 15.86% in the Kolar district [7] and 20–60% in Tamil Nadu [8].

3 Results and Discussion

The study has facilitated the assessment of effects of urbanisation on tank system resulting in changed land use pattern. Temporal changes in the study area have been brought out using the time series Landsat Thematic Mapper (TM) 2004 and Landsat Enhanced Thematic Mapper (ETM) 2016. Sentinel 2 data of the same period at 20-m resolution is analysed to see the variability of Landsat-8 (30 m) analysed data results. Study focused on vegetation, urban settlements, water spread area in the tank catchment, ayacut and tank areas. Changes in terms of area are assessed separately in the tank system. Study results are presented in Table 1.

3.1 Changes in Ayacut Land Use

The most striking feature observed in ayacut land use change is 149.30% decline of vegetative cover from 2004 to 2016. At the same time, area under urban settlements increased sharply from 4.89 acres in the year 2004 and to 34.92 acres in 2016 which is 6 times of that in 2004. Decline in vegetation during 2016 is a direct result of increase in urbanisation in the ayacut area and indirectly affected by increase of urban settlements in catchment area thus affecting the inflows into the tank (Fig. 2; Table 2).

Catchment area of the tank which is a key land for tank inflows has reduced with increase in urban settlements by 45.12% and there was a decline of 288.27% of vegetation. Even with poor water inflows to the study tank, it is found from the analysis, that there is a slight increase of tank water spread area from 32.04 acres in 2004 to 33.59 acres in 2016. Reasons for the above has found support from the secondary data collected from the irrigation department. Rupees 46.76 lakhs has been spent under Mission Kakatiya Phase I for removal of silt in the tank, improvement of sluices and improvement of channels to the fields etc. (Fig. 3).

As a result of rapid urbanisation, farmers lands in the command area are sold out for real estate plotting with is evident in the satellite image analysis. This can be

Table 1 Percent change in tank system from 2004 to 2016

Tank system	Settlement (%)	Vegetation (%)	Water (%)
Ayacut	85.99	−149.30	–
Catchment	45.12	−288.27	39.76
Tank (water spread)	97.50	−16.36	5.30

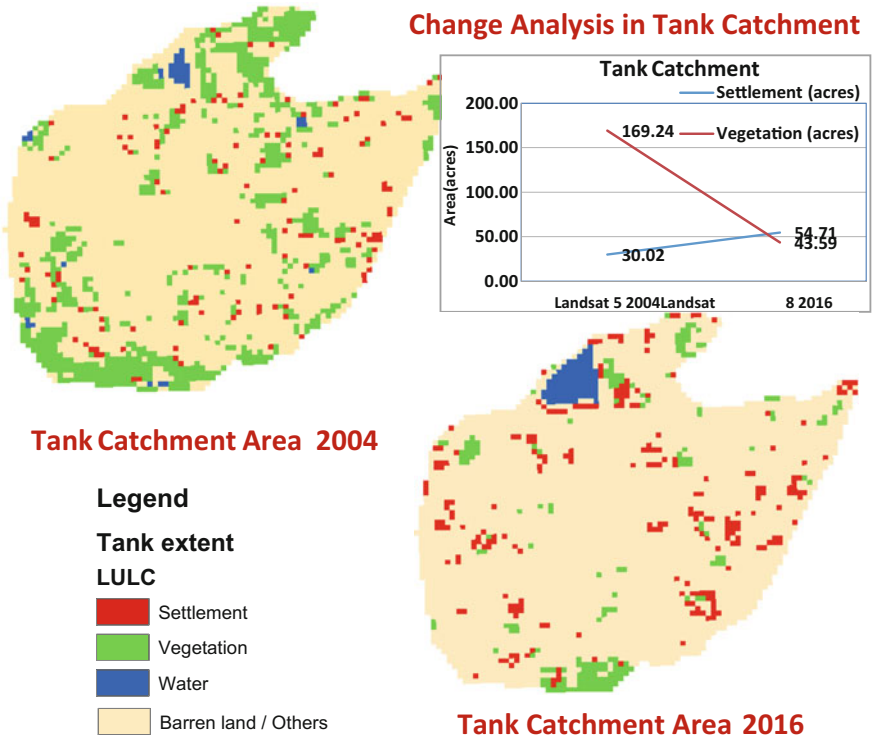

Fig. 2 Change analysis in the tank catchment area

Table 2 Change of landuse pattern with reference to registered tank area, ayacut and catchment

Year	Tank system and Reg. area (acres)	Settlement (acres)	Settlement (%)	Vegetation (acres)	Vegetation (%)	Water (acres)	Water (%)
2016	Ayacut (152)	34.92	22.97	15.79	10.39	_	_
	Catchment (631)	54.71	8.67	43.59	6.91	18.46	2.93[a]
	Tank area (83.9)	8.90	10.60	12.23	14.58	33.58	40.03
2004	Ayacut (152)	4.89	3.22	39.36	25.90	_	
	Catchment (631)	30.02	4.76	169.24	26.82	11.12	1.76
	Tank area(83.9)	0.22	0.27	14.23	16.96	31.80	37.91

[a]Interception by the water bodies in the Catchment

substantiated by the fact that the land values have risen sharply from about Rupees 25 lakhs in 2004 to as high as 70 lakhs to 1 crore per acre in 2016.

From secondary data source, it is observed that around 80 families have been directly or indirectly dependent on fisheries for their livelihood for a period of at least 3 months in a year. Encroachments and change in land use in the catchment, foreshore and water spread area with urban settlements and draining of urban

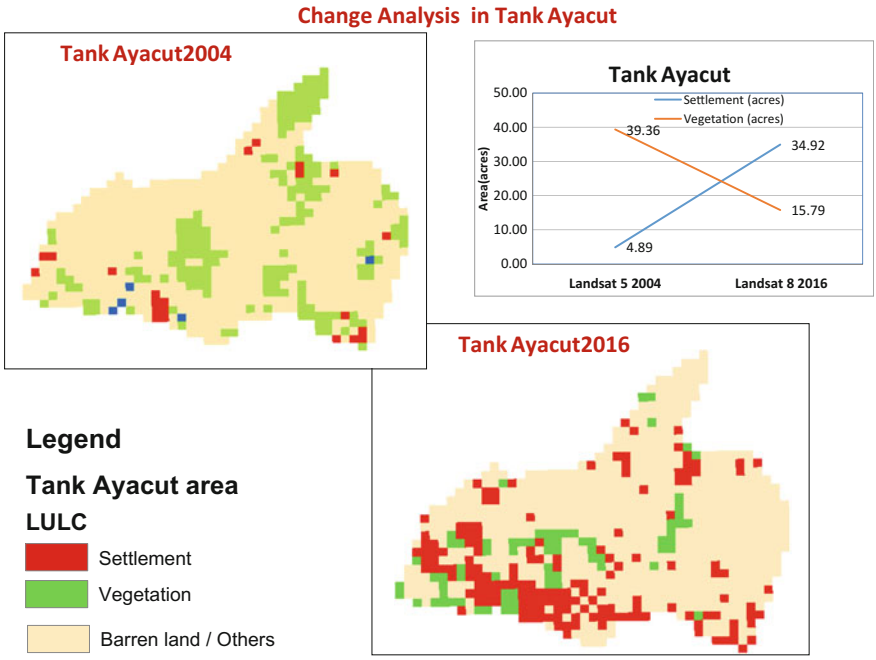

Fig. 3 Change analysis in the tank ayacut area

sewerage to tank area has led to tank water pollution. This adversely affected the livelihood of the families dependent on fisheries directly or indirectly.

As mentioned earlier, Sentinel 2 data for the study area has also been analysed along with the LANDSAT 8 for the period October 2016. Sentinel 2 data analysed at 20 m resolution also shows similar trend as Landsat 8 (Fig. 4).

3.2 Changes in Tank Water Spread Area

It is clear from the analysis that tank encroachment in the year 2016 increased to 97.2% compared to 2004. This is due to the placement of the tank adjoining the busy Hyderabad-Mumbai National highway. Monitoring of the encroachments periodically by the Irrigation Department or by the local body such as Water User Association (WUA) can reduce such activities. Local institution (WUA), which is not active in Telangana may be activated to increase people participation. Tanks are not only the sources of irrigation for the farmers but also serve to protect the local ecosystem through different ecosystem services. In other words, if the land value exceeds significantly downplaying the returns from agriculture, it doesn't necessarily mean the need to do away with the tank systems.

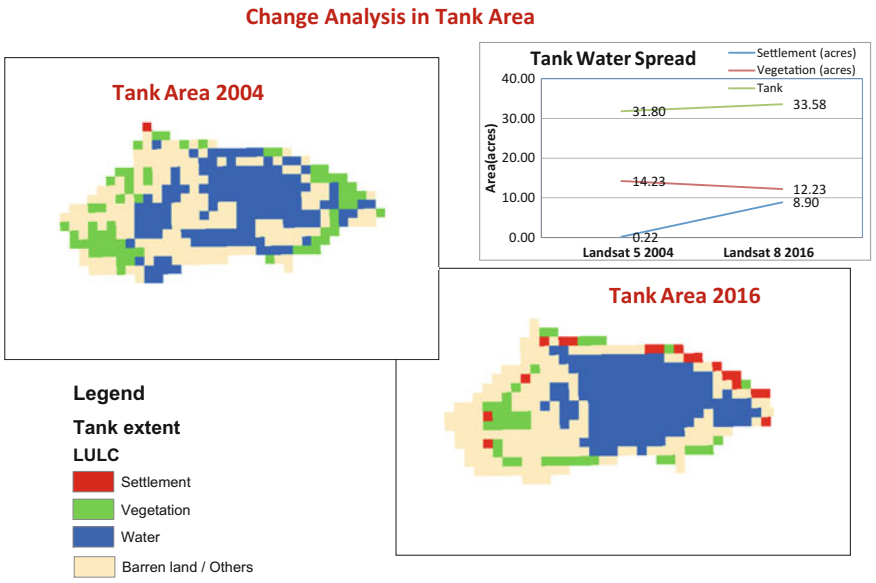

Fig. 4 Change analysis in the tank area

4 Conclusions

Tank systems are traditional means of livelihoods in Telangana that have been ecologically and economically productive since ages. Yenki cheruvu tank system is one such system that has got seriously deteriorated in the last 15 years. Due to the recent developments around Yenki cheruvu such as development of Outer Ring Road (ORR), proximity to the Hyderabad city and tank being adjacent to national highway, there is a huge transformation from agriculture land to urban property along with surge in land values. As tank systems serve much beyond the irrigation needs in the form of ecosystem services including provisioning, supporting, regulating and cultural services, it is important to protect them despite the fall in irrigated area under it. Involvement of institutions such as NGO's, WUA's in the initial phases of tank restoration and encroachments through motivation can give positive results. Government has to use the technology and services of GIS and Remote Sensing experts in mapping the issues around the tanks in the pre-urban and urban areas for sustainable ecosystem management.

Further research can be done using GIS and Remote sensing techniques to map the selected tank systems, which includes catchment, ayacut and tank water spread areas in and around Hyderabad city to bring out the vital statistics about effects of urbanisation on tank system and help in ecological conservation. This kind of study may also contribute to the sharpening of methods and techniques for delineation of

tank system and continuous monitoring. This can be eventually developed into a Decision Support System for the policy makers and administrators. Remote sensing high-resolution satellite data and results can help in framing the regulations for preserving the tank system for future generations.

References

1. Kennedy, R.E., Andréfouët, S., Cohen, W.B., Gómez, C., Griffiths, P., Hais, M., et al.: Bringing an ecological view of change to Landsat-based remote sensing. Front. Ecol. Environ. **12**(6), 339–346 (2014)
2. Roy, D.P., Wulder, M.A., Loveland, T.R., Woodcock, C.E., Allen, R.G., Anderson, M.C., Scambos, T.A.: Landsat-8: Science and product vision for terrestrial global change research. Remote Sens. Environ. **145**, 154–172 (2014)
3. Topaloğlua, R.H., Sertela, E., Musaoğlua, N.I Assessment of classification accuracies of sentinel-2 and landsat-8 data for land cover/use mapping. In: The International Archives of the Photogrammetry, Remote Sensing and Spatial Information Sciences, Volume XLI-B8, 2016 XXIII ISPRS Congress, Prague, Czech Republic. https://doi.org/10.5194/isprsarchives-xli-b8-1055-2016. 12–19 July 2016
4. Stehman, S.V., Wickham, J.D.: Pixels, blocks of pixels, and polygons: choosing a spatial unit for thematic accuracy assessment. Remote Sens. Environ. **115**(12), 3044–3055 (2011)
5. Mandanici, E., Bitelli, G.: Preliminary comparison of Sentinel-2 and Landsat 8 imagery for a combined use. Remote Sens. **1014**, 8 (2016)
6. Abdul Nazir Sab Institute of Rural Development: Management of minor irrigation tanks in Karnataka, In: A Workshop on Tank Irrigation for Southern States, held at Mysore, 13–14 July 1999
7. Thippaiah, P.: Study of causes for the shrinkage of tank irrigated area in Karnataka. Institute for Social and Economic Change (Mimeo), Bangalore (1998)
8. Tushaar, S., Seenivasan, R., Shanmugam, C.R., Vasimalai, M.P.: Sustaining Tamilnadu's Tanks: field notes on Pradhan's work in Madurai and Ramnad, International Development Enterprises and Ford Foundation, New Delhi (1999)
9. URL-1: https://earthexplorer.usgs.gov/. Accessed date 28 May 2017
10. URL-2: http://bhuvan.nrsc.gov.in/governance/twris/. Accessed date 21 Mar 2017
11. URL-3: http://mabhoomi.telangana.gov.in/GramaPahani_drs.aspx. Accessed date 13 Apr 2017

Chapter 11
ACE and HDP of Tropical Cyclones Induced Disasters and Financial Loss Over China Coast During Last Decades (1995–2016)

Venkata Subrahmanyam Mantravadi, Shengyan Yu and Juncheng Zuo

Abstract Northwest Pacific Ocean (NWP) is known to be having higher number of tropical cyclones (TC) than all over the world. About 87% of the typhoons occur in the latitudinal belt between 20°N and 20°S and two third of all typhoons occur in the Northern Hemisphere. China is one of the countries suffering from the devastation caused by typhoons along the coast of the NWP and South China Sea (SCS). The intensity variations have been verified with the TCs landfall at China coast and also due to El Nino. It is found that during El Nino years the number of TCs reduced, however the intensity is higher. TCs which are having higher intensity are going to devastate the coastal area by means of heavy rainfall, strong winds, storm surges, etc. Alternative measures to assess hurricane intensity or damage potential include Accumulated Cyclone Energy (ACE) and Hurricane Destructive Potential (HDP). This work details the relation between the disasters occurred at China coast and ACE and HDP of TC landfall over China coast during 1995–2016. The year 2005 experiences higher finance losses due to marine disasters mainly due to TCs and higher ACE and HDP. TCs generated in the SCS doesn't having much influence on financial losses, however the TCs generated, passing through NWP to SCS are having higher intensity and produce higher losses. The losses due to the passing of TCs over coastal areas of China also found. Further, financial losses over coastal provinces are given separately with respect ACE and HDP.

Keywords Tropical cyclones · Northwest pacific · Accumulated cyclone energy (ACE) and hurricane destructive potential (HDP) · Financial losses

V. S. Mantravadi (✉) · S. Yu · J. Zuo
School of Marine Science and Technology, Zhejiang Ocean University, Zhoushan 316022, Zhejiang, China
e-mail: mvsm.au@gmail.com

S. Yu
e-mail: 1481272763@qq.com

J. Zuo
e-mail: zuo@ouc.edu.cn

P. J. Rao et al. (eds.), *Proceedings of International Conference on Remote Sensing for Disaster Management*, Springer Series in Geomechanics and Geoengineering,
https://doi.org/10.1007/978-3-319-77276-9_11

1 Introduction

Tropical cyclone (TC) intensity defined by maximum wind speed during the storm, thereby create damage through wind, waves, or storm surge over coastal area. Tropical cyclones (TC) classified into four categories as per Saffir-Simpson scale: tropical depression (TD), topical storms (TS), typhoon (TY) and intense typhoon (ITY). The ocean has long been recognized as having a fundamental impact on TC intensity [24, 25] and warm SST of about 27 °C is critical for formation and TC to intensify Chan et al. [7]. The occurrence of strong hurricanes indicating upward trend in worldwide attributing to climate change [33] and the strongest hurricanes are becoming stronger with rising ocean temperature [14].

Atkinson [1] is the first scientist noted that the number of TCs developing in the eastern part of the North Western Pacific (NWP) during the El Nino of 1972 was higher than Neutral years. Several studies have been focused on the total number of TS and genesis location in relation with El Nino [4, 8, 11, 17, 20, 26, 31, 32]. However, there is an interannual variability of typhoon activity, higher intensity, and TS predictability still unknown maybe because of difference in data and methodology, results found are not consistent and also it is important to examine the relation between ENSO (El Nino Southern Oscillation) and the TC activity. Pudov and Petrichenko [28, 29] found an increase in the intensity of TC in El Nino years and the genesis location shifts led by the SST change. The mean cyclogenesis region usually moves toward southeastern of WNP and in La Nina years the location tends to central Pacific region [12, 19, 35]. Though there is no significant linear relation between the number of TC and ENSO, however, a nonlinear relation between ENSO and the number of TC has been found in several studies [3, 5, 9, 10].

The accumulated cyclone energy (ACE), which is otherwise known as TC destruction potential, is associated with the evolution of the character of observed large-scale climate mechanisms including various large scale features. This index is also considered important to analyze the impact of the climate change on TC activity [15, 16]. Trenberth [30] noticed that Atlantic hurricane activity has been significantly enhanced since 1995 in terms of the ACE index. Klotzbzch [22] found ACE is having significant correlation with four fields [Sea level pressure (SLP), 2-m temperature, 850-mb zonal wind (U850), and 200-mb zonal wind (U200)], which have significant impact on Atlantic basin TC activity. However, the May–June-averaged 2-m temperatures over the eastern tropical and subtropical Atlantic has strongly correlation with August–October 2-m temperatures in the main TC development region, while the 200-mb zonal wind flow over the tropical Indian Ocean is shown to strongly correlate with ENSO [23] and also having significant correlation with ACE over Atlantic.

Bell et al. [2] developed the hurricane destructive potential (HDP) index to convey the seasonal magnitude of hurricane activity. HDP is calculated by—summing the squares of the estimated 6-hourly maximum sustained wind speed (V^2 max) for all periods in which the system is a hurricane. The HDP represents the

ACE for the time in which the cyclone is a hurricane or TC. Early work by Gray and Landsea [18] estimated that HDP increased exponentially such that a category 4 or 5 storm produced 100 to 300 times higher than the physical and economic damage as a category 1 hurricane. Pielke et al. [27] estimated the economic costs of hurricanes that made landfall on the Atlantic or Gulf Coasts of the United States from 1900 to 2005 by normalizing the dollar estimates for damage according to changing societal conditions. The economic impacts of hurricanes yielded similar results in that the economic costs of hurricane damage increased exponentially as a function of hurricane category.

The major implication of this study will be the assessment of the trends in strength, duration and intensity of TCs as well as the damage potential and loss due to TCs over the China coastal region. This work details the variation of TCs landfall over China coast (eastern and southern) during 1995–2016. ACE and HDP calculated with respect to wind intensity of TC, and the financial losses occurred due to TC. The relation between ACE and HDP with the financial losses over China coast, east and southern coasts also presented.

2 Data and Methodology

The best-track dataset obtained from JTWC [13] over the period 1995–2016, which includes track, intensity, duration (TC life time). This dataset consists of six hourly center locations, maximum surface wind speeds and minimum central pressure for all TCs. TC tracks landfall over China coast with respect to wind intensity during El Nino (2009), La Nina (1999) and neutral (2013) years are given in the Fig. 1. The number of TCs landfall over China coast, minimum central pressure, duration (or Life time of TC) and maximum surface wind speed for every TC used to calculate ACE and HDP. The monthly sea surface temperature Nino-3.4 indices over the period obtained from National Center for Environmental Prediction (NCEP) National Oceanic and Atmospheric Administration (NOAA). To obtain the anomalies ERSSTv4 data has been used over the Nino regions with the base period 1981–2010. The criteria for the El Nino are positive anomalies higher than 0.4 °C, for La Nina negative anomalies less than −0.4 °C, and in between are neutral years. The data is freely available in the website http://www.cpc.ncep.noaa.gov/data/indices/sstoi.indices. The annual Nino-3.4 SST compared with number of TC to find out the variations of TC formation due to El Nino/La Nina/neutral years.

Previous studies have briefly examined the relationship between typhoon intensity and El Nino events, ACE and HDP been used to measure the destructive power of TC [3, 19, 21]. It is a quantity that combines the number, lifetimes, and intensities of tropical cyclones occurring in a basin over a given period of time, the method of computing ACE is:

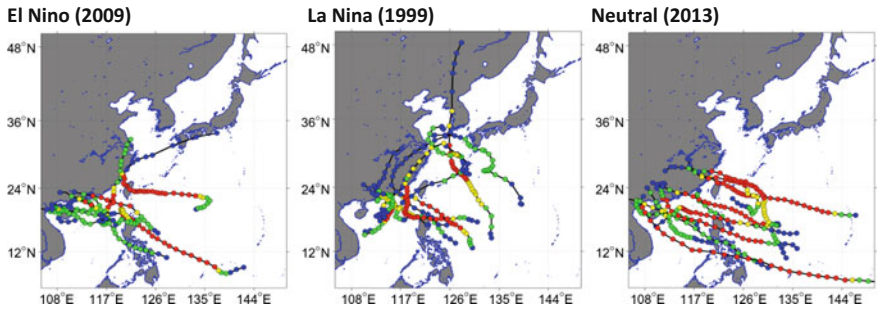

Fig. 1 TC tracks landfall over China coast with respect to wind intensity during El Nino (2009), La Nina (1999) and Neutral (2013) years. (In the track wind speed indicates as follows: Blue circle <35 knots, green 35–45 knots, yellow 46–59 knots, red >60 knots)

$$\mathrm{ACE} = 10^{-4} \sum_{i=1}^{N} \sum_{j=1}^{T} \mathrm{V}_{ij}^{2},$$

N is the total typhoon number in one year, T is the total number of 6-hourly estimate in a typhoon, and V is the 6-hourly maximum sustained wind speed in knots. HDP is same as ACE but for the TC wind is equal and greater than 65 knots.

3 Results and Discussion

3.1 Variation of TC Over NWP and Relation with El Nino

TC formation over NWP during the period 1995–2016 and TCs landfall over China coast are given in the Fig. 2. Over NWP during the study period, mean genesis of 24 TC, wherein 8 TCs are landfall over the China coast (includes both east and south coast). Around 34% of TCs are landfall over China coast with mean duration of 5 days with mean wind speed of 71 knots. During the study period, maximum wind speed of 125 knots attained by a TC in the years 2010 and 2013. Maximum duration of TC is about 14 days in 2003. Maximum number of TC (31) genesis occurred in the year 2013 over NWP, however the TC landfall over China coast are 11 (35%). Lowest formation of TC over NWP in the year 1998 is 16 in which 6 TCs landfall over China coast. Lowest percentage of TC landfall over China coast is 15% in the year 1996 and maximum of 55% in the year 1999.

During the study period, there are 5 El Nino, 5 La Nina and 12 Neutral years and mean variations of TCs during El Nino/La Nina/Neutral years are given in Table 1. Variation of Nino 3.4 SST anomalies and TC generation and TC landfall over China coast are given in Fig. 3. Over the NWP generation of TC are higher during El Nino years and lower during La Nina, however the number of landfall over

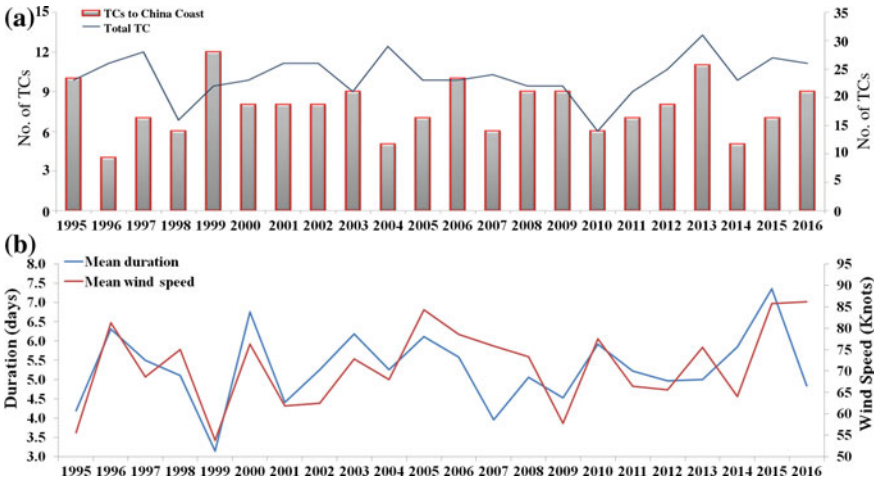

Fig. 2 Time series of **a** TC genesis over NWP and TC landfall over China coast; **b** mean duration (life time of the TC) and mean wind speed during the study period

Table 1 List of El Nino, La Nina and Neutral years with mean number of TCs, duration, wind speed and pressure during the study period

	Years	Mean number of TC genesis	TCs landfall at China Coast	Mean duration (days)	Mean Lowest pressure (hPa)	Mean Max. wind speed (knots)	Max wind speed (knots)	Max duration (days)
El Nino	1997, 2002, 2004, 2009, 2015	26	7	6	963	69	102	12
La Nina	1998, 1999, 2007, 2010, 2011	19	7	5	961	70	105	9
Neutral	1995, 1996, 2000, 2001, 2003, 2005, 2006, 2008, 2012, 2013, 2014, 2016	24	8	5	957	73	100	10

China coast are higher in neutral years. Mean duration of TCs are higher during El Nino years, with higher life time of 12 days when compared with other. During El Nino (La Nina) the mean annual TC generation is higher (lower) over NWP [6]. Mean wind speed is higher in neutral years; however when compared with individual TC, wind speed is higher in La Nina Year.

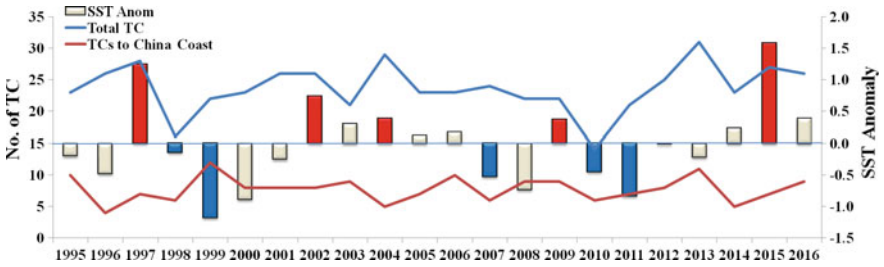

Fig. 3 Time series of Nino 3.4 SST anomalies as bars with genesis of TCs over NWP and TC landfall over China coast (blue and red Line). SST anomalies are indicating as follows: El Nino years (red), La Nina (blue) and rest of them are Neutral years

One can clearly identify that after El Nino year the number of TC generation as well as landfall of TC at China coast reduced rapidly. During 1997, which is an El Nino year 28 TC genesis occurred over NWP, but only 7 TCs landfall over China coast which is 25%. However 1998 is a La Nina year genesis of 16 TC over NWP and 6 TCs landfall over China coast (38%). Similarly, 2009 is an El Nino year, genesis of 22 TC in which 9 TCs landfall over China coast (41%) and 2010 is a La Nina year genesis of 14 TC over NWP and 6 TCs landfall over China coast (41%). This clearly indicates that the formation of TCs is lower in La Nina which immediately flowed by El Nino; however the landfall percentage over China coast is higher. This feature is divergent for neutral year after El Nino, there is no reduction in TC formation in NWP, however TC landfall over China coast increase. Table 1 clearly indicating that maximum TC duration is higher in El Nino than La Nina and neutral years, however maximum wind speed is higher in La Nina year. The mean duration of typhoon tends to increase during strong El Nino events [3]. In El Nino years, genesis location shifts to south-eastern Pacific Ocean [19, 34], the typhoon will experience a longer duration over Ocean before landing, and clearly explains for higher intensity TCs.

In neutral years the genesis of TCs and landfall over China coast has variability including in duration and wind speed. However, the TCs intensities are higher in La Nina year with reduction in genesis of TC over NWP. The percentage of landfall over China coast is lower during El Nino years (27.3%), higher in La Nina years (38.1%) and in neutral years 33.6%. There is a positive relation between Nino 3.4 SST anomalies and the genesis of TCs over NWP (correlation coefficient of 0.40), however the relation between Nino 3.4 SST anomalies and landfall over China coast is indicating an inverse relation (−0.18), which is not significant.

3.2 *Variation of ACE, HDP and Financial Loss Over China Coast*

ACE and HDP calculated by using the wind speed as given formula and presented in Fig. 4 including Financial losses over China coast. ACE is higher on 2000 but HDP is lower, leading to lower financial loss. Higher financial losses (329.8 billion Yuan) observed on 2005 due to higher wind speed of 105 knots with the mean of 84 knots of TCs landfall over China coast leading to higher HDP. From the Fig. 3 it is clearly observed that even though ACE is higher, due to HDP the disasters over the coastal area higher leading to higher financial losses. In the year 1998, the financial losses are at minimum during the study period due to lower ACE and HDP. The year 2014 indicating lower ACE and HDP, however the financial losses over the China coast is 135.78 billion Yuan is mainly due to longer duration of TC and sustained higher wind speeds for longer time, which devastated over the coastal area. Another higher financial loss occurred during 1997, which is an El Nino year having higher intensity of TCs.

From the Table 2, it is clearly observed that during El Nino and neutral conditions financial losses over China coast is higher. This is due to during El Nino, the intensity of TC is higher leading to higher ACE and HDP. However during neutral conditions, the numbers of TCs are higher leading to higher ACE and HDP producing higher financial losses over China coast. The distribution of ACE per year in El Niño (La Niña) years is shifted to larger (smaller) values, and their differences are statistically significant [3]. The correlation between Nino 3.4 SST anomalies and ACE is 0.32, however Nino 3.4 SST anomalies and HDP is 0.37. This reveals the total number of TC is not significantly correlated with El Nino, although for strong El Nino events a relationship can be identified [4, 8]. El Niño years have a large tendency toward more intense TCs. These intense TC dominate HDP and are mainly responsible for the relationship between HDP and El Nino. La Niña years have a lower tendency toward a lower number of TC with their intensity. In neutral

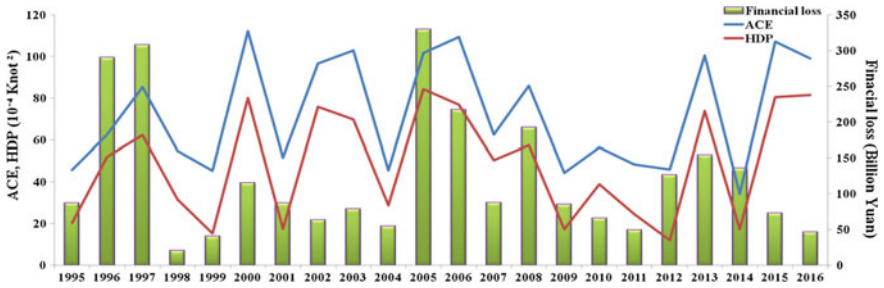

Fig. 4 Time series of ACE (accumulated cyclone energy), HDP (hurricane destructive potential) and financial loss over China coast during the study period

Table 2 ACE, HDP and Financial losses over China coast during El Nino, La Nina and Neutral conditions

	ACE (10^{-4} knot^2)	HDP (10^{-4} knot^2)	Financial loss (billion Yuan)
El Nino	107.215	80.7275	308.0
La Nina	62.5775	50.43	87.2
Neutral	112.3025	84.4825	329.8

years the number of TC landfall over China coast are higher with different intensities of TC, which leading to higher financial losses than El Nino and La Nina which are having lower TC landfall over China coast.

3.3 *ACE, HDP and Financial Losses Over East and South Coast of China*

China coast further divided into east and south coast and compared the difference in ACE, HDP and financial losses over both coasts. ACE, HDP and financial losses over eastern coast are higher than southern coast. The percentage of TCs landfall over southern coast (17.6%) is higher than eastern coast (10.4%) over China coast. Even tough, higher TCs landfall in the southern coast of China; HDP is lower, leading to lower financial loss. From this study, it is observed that the number of TCs generated over SCS is higher, which are having lower wind speeds than the TCs generated over NWP and landfall over southern coast. TCs generated over NWP are having higher ACE and HDP by which disasters are occurring and leading to higher financial loss (Table 3).

There is a clear east–west pattern, with more tropical cyclone activity over east of the Philippines and SCS. Shift in the genesis position in the NWP induced by ENSO [9, 11, 32]. It is observed that in the year 2005, higher ACE and HDP are higher over eastern and southern coasts due to large number of TC and higher intensity leading to higher financial loss. The mean ACE due to TC landfall over

Table 3 Mean distribution of number, ACE, HDP and financial loss over Eastern and Southern Coast of China during the study period

	Mean no. of TC	Mean ACE	Mean HDP	Mean financial loss (billion Yuan)
East coast	2.4	30.8	24.1	76.3
South coast	4.1	22.2	11.2	62.7
Passing TC	1.2	19.7	13.4	[a]

[a]Financial loss due to passing TCs are included in East coast or South coast with respect to passing area

eastern, southern and passing TCs are 30.8, 22.2 and 19.7 respectively. The mean HDP over east coast, south coast and passing TC over eastern and southern coasts of china are 24.1, 11.2 and 19.7 respectively, which clearly indicating that disasters due to passing TC are also higher mainly over eastern coast of China.

4 Conclusion

Following conclusions given from this study:

1. 34% of mean number of TCs landfall over the China coast with standard deviation of 10% which genesis over NWP.
2. Over 23% of TCs are landfall over southern coast when compared with eastern coast of China.
3. When La Nina followed by El Nino generating less number of TCs over NWP and landfall over China coast.
4. TC generated over NWP having higher ACE and HDP, produce higher disasters and financial losses over China southern coast.
5. In the eastern coast of China during El Nino years, higher TC intensity leading to higher ACE and HDP producing higher financial losses.
6. The year 2005 is having higher financial losses over China coast due to higher number and intensity of TC leading to higher ACE, HDP over eastern and southern coast.

Acknowledgements This work was supported by grants from National Basic Research Program (2013CB430302) and The Science and Technology Ministry, China (2016YFC1401905, GASI-IPOVAI-04, GASI-IPOVAI-06, 2017YFA0604900).

References

1. Atkinson, G.: Proposed system for near real time monitoring of global tropical circulation and weather patterns. Pre-prints. In: 11th Technical Conference on Hurricanes and Tropical Meteorology, Miami Beach, FL, Amer. Meteor. Soc., pp. 645–652 (1977)
2. Bell, G.D., Halpert, M.S., Schnell, R.C., Higgins, R.W., Lawrimore, J., Kousky, V.E., Tinker, R., Thiaw, W., Chelliah, M., Artusa, A.: Climate assessment for 1999. Bull. Amer. Meteor. Soc. **81**, S1–S50 (2000)
3. Camargo, S.J., Sobel, A.H.: Western North Pacific tropical cyclone intensity and ENSO. J. Climate **18**, 2996–3006 (2005)
4. Chan, J.C.L.: Tropical cyclone activity in the Northwest Pacific in Relation to the El Niño/Southern Oscillation Phenomenon. Mon. Wea. Rev. **113**(4), 599–606 (1985)
5. Chan, J.C.L., Shi, J.E.: Long-term trends and interannual variability in tropical cyclone activity over the western North Pacific. Geophys. Res. Lett. **23**, 2765–2767 (1996)
6. Chan, J.C.L., Liu, K.S.: Global warming and western North Pacific typhoon activity from an observational perspective. J. Climate **17**, 4590–4602 (2004)

7. Chan, J.C.L., Duan, Y.H., Shay, L.K.: Tropical cyclone intensity change from a simple ocean–atmosphere coupled model. J. Atmos. Sci. **58**, 154–172 (2001)
8. Chan, J.C.L.: Tropical cyclone activity in the northwest Pacific in relation to El Niño/Southern Oscillation phenomenon. Mon. Wea. Rev. **113**, 599–606 (1985)
9. Chan, J.C.L.: Tropical cyclone activity over the western North Pacific associated with El Niño and La Niña events. J. Climate **13**, 2960–2972 (2000)
10. Chen, T.C., Weng, S.P., Yamazaki, N., Kiehne, S.: Interannual variation in the tropical cyclone activity over the western North Pacific. Mon. Wea. Rev. **126**, 1080–1090 (1998)
11. Chia, H.H., Ropelewski, C.F.: The interannual variability in the genesis location of tropical cyclones in the north west Pacific. J. Climate **15**, 2934–2944 (2002)
12. Chu, P.-S.: ENSO and tropical cyclone activity. In: Murnane, R.J., Liu, K.B. (eds.) Hurricane and Typhoons: Past, Present and Potential, pp. 297–332. Columbia University Press, Columbia (2004)
13. Chu, J.H., Sampson, C.R., Levine, A.S., Fukada, E.: The joint typhoon warning center tropical cyclone best-tracks, 1945–2000 (Rep. NRL/MR/7540-02-16). Joint Typhoon Warning Center, Hawaii (2002). Retrieved from http://www.usno.navy.mil/NOOC/nmfc-ph/RSS/jtwc/best_tracks/TC_bt_report.html
14. Elsner, J.B.: Hurricanes and climate change. Bull. Amer. Meteor. Soc. **89**, 677–679 (2008). https://doi.org/10.1175/BAMS-89-5-677
15. Emanuel, K.A.: Emanuel replies. Nature **438**, E13 (2005)
16. Emanuel, K.A.: Increasing destructiveness of tropical cyclones over the past 30 years. Nature **436**, 686–688 (2005)
17. Gray, W.M.: Atlantic seasonal hurricane frequency Part1 El Nino and 30 mb Quasi-biennial oscillation influences. Mon. Wea. Rev. **112**, 1649–1668 (1984)
18. Gray, W.M., Landsea, C.W.: African rainfall as a precursor of hurricane-related destruction on the U.S. East Coast. Bull. Amer. Meteor. Soc. **73**, 1352–1364 (1992)
19. Ha, K.J., Yoon, S.J., Yun, K.S., Kug, J.S., Jang, Ys, Chan, J.C.L.: Dependency of typhoon intensity and genesis locations on El Niño phase and SST shift over the western North Pacific. Theor. Appl. Climatol. **109**, 383–395 (2012). https://doi.org/10.1007/s00704-012-0588-z
20. Hastings, P.A.: 1990: Southern Oscillation influences on tropical cyclone activity in the Australian/South-west Pacific region. Int J. Climat **10**, 291–298 (1990)
21. Hsu, P.C., Ho, C.R., Liang, S.J., Kuo, N.-J.: Impacts of two types of El Niño and La Nina events on typhoon activity. Adv. Meteorol. Article ID 632470, 8p (2013) http://dx.doi.org/10.1155/2013/632470
22. Klotzbach, P.J.: A simplified Atlantic basin seasonal hurricane prediction scheme from 1 August. Geophys. Res. Lett. **38**, L16710 (2011). https://doi.org/10.1029/2011gl048603
23. Klotzbach, P.J.: Prediction of seasonal Atlantic Basin accumulated cyclone energy from 1 July. Wea. Forecast. **29**, 115–121 (2014). https://doi.org/10.1175/WAF-D-13-00073.1
24. Malkus, J.S., Riehl, H.: On the dynamics and energy transformations in steady-state hurricanes. Tellus **12**, 1–20 (1960)
25. Miller, B.I.: On the maximum intensity of hurricanes. J. Meteor. **15**, 184–195 (1958)
26. Pan, Y.H.: The effect of the thermal state of equatorial eastern Pacific on the frequency of typhoon over the western Pacific (in Chinese with English abstract). Acta Meteor. Sin. **40**, 24–34 (1982)
27. Pielke Jr., R.A., Gratz, J., Landsea, C.W., Collins, D.M., Saunders, A., Musulin, R.: Normalized hurricane damage in the United States: 1900–2005. Nat. Hazards Rev. **9**, 29–43 (2008)
28. Pudov, V.D., Petrichenko, S.A.: 1997–1998 El Niño and tropical cyclone genesis in the northwestern Pacific. Izv. Atmos. Oceanic Phys. **37**, 576–583 (2001)
29. Pudov, V.D., Petrichenko, S.A.: Relationship between the evolution of tropical cyclones in the Northwestern Pacific and El Niño. Oceanology **38**, 447–452 (1998)
30. Trenberth, K.: Uncertainty in hurricanes and global warming. Science **308**, 1753–1754 (2005)

31. Wang, S., Zhao Z., Zang H.: Relationship between eastern Equatorial Pacific sea surface temperature and subtropical high in the Western Pacific, Tropical Ocean-atmosphere Newsletter, pp. 13–14 (1984)
32. Wang, B., Chan, J.C.L.: How strong ENSO events affect tropical storm activity over the western North Pacific. J. Climate **15**, 1643–1658 (2002)
33. Webster, P.J., Holland, G.J., Curry, J.A., Chang, H.R.: Changes in tropical cyclone number, duration, and intensity in a warming environment. Science **309**, 1844–1846 (2005)
34. Zhao, H., Wu, L., Wang, R.: Decadal variations of intense tropical cyclones over the Western North Pacific during 1948–2010. Adv. Atmos. Sci. **31**(1), 57–65 (2014)
35. Zhao, H., Wu, L., Zhou, W.: Assessing the influence of the ENSO on tropical cyclone prevailing tracks in the Western North Pacific. Adv. Atmos. Sci. **27**(6), 1361–1371 (2010)

Chapter 12
Disaster Preparedness: Veterinarian Perspective

K. Raja Kishore and K. Vijaya Sri

Abstract Livestock is owned by 70% of the world's poor which is also the group most vulnerable to the impacts of disasters. Animals are impacted by the same disasters and emergencies as humans—natural, manmade, large, and small where veterinarians play a very important role. Disaster management is an expanding speciality within the veterinary profession. Until recently, veterinary relief had consisted of emergency aid or recovery activities, most of which are based on little scientific fact. Veterinarians started to look at how their knowledge on animal health and husbandry, and the relationship between animals and people can be used to protect not only the lives of animals but also the people affected by disaster. It is essential that a veterinary practice should have a written disaster plan comprising of preparedness measures, data on medical record and available manpower i.e. vets, para veterinary staff etc., liaison with local, state, national organizations, co-ordination with non-governmental organizations, insurance and legal issues etc. to combat the occurrence of disasters in advance. The inclusion of animal welfare measures in national and regional disaster management plans strengthens the humanitarian response, builds community resilience and protects food security. Offering training, advice, expertise and guidelines to the veterinarians helps in a big way to protect their animals during disasters. Hence, relief plans and measures should be developed for livestock at all phases of disaster for effective management.

Keywords Disaster · Livestock · Preparedness · Relief plan · Veterinarian role Welfare measures

K. R. Kishore (✉)
Department of Animal Nutrition, NTR College of Veterinary Science,
Sri Venkateswara Veterinary University, Gannavaram, Andhra Pradesh, India
e-mail: rajakishorekonka9@gmail.com; dr_rajakishore@yahoo.co.in

K. V. Sri
Department of Computer Science and Engineering, K L University,
Green Fields, Vaddeswaram, Andhra Pradesh, India
e-mail: kompallivsri@gmail.com; kompalliv@yahoo.com

P. J. Rao et al. (eds.), *Proceedings of International Conference on Remote Sensing for Disaster Management*, Springer Series in Geomechanics and Geoengineering,
https://doi.org/10.1007/978-3-319-77276-9_12

1 Introduction

Disaster is an abrupt, devastating event bringing great damage, loss, destruction and desolation of life and property. This involves both public and private property resulting in psychological, economical, political and cultural devastation [1]. The damage caused by disasters is unpredictable and varies with place of occurrence, climate etc.

The Sendai Framework for Disaster Risk Reduction 2015–2030 gives the outlines to reduce disaster risk, to address existing challenges and prepare for future by focusing on monitoring, assessing, and understanding disaster risk and sharing such information [2]. The Sendai Framework notes that, the disaster action plan requires the strengthening and coordination between various institutions and sectors. Further, it requires investments in research to use the technology to develop multi-hazard Early Warning Systems (EWS), preparedness, response, recovery, rehabilitation, and reconstruction.

During disasters, there is a huge loss to livestock along with the human affecting the food security of the people. This leads to a grave situation if animals are not figured properly in preparedness and mitigation activities of disaster relief plan. Veterinarians have an immense role in combating the loss to livestock during disasters which needs proper training and adoption of a multidisciplinary approach. In India, the Veterinarian aid is not up to the mark and scientific approach for development of nation's disaster relief plan.

2 Disasters and Livestock in India

In India, prevalence of various disasters like drought, earth quakes, floods, cyclones, manmade disasters, fire accidents etc. is more common. These can be categorized into natural or man-made disasters. Whether natural or manmade, disasters will have a negative impact and it will severely cripple society due to improper planning. Disasters affecting livestock will affect the weaker sections in developing countries, especially as their dependence on animals for livelihood is huge. Almost 70% of the livestock owned by 67% is owned by small and marginal farmers and landless labours in India [3]. The loss of animals is not being projected accurately in various disasters which create a large gap for improvement of livestock disaster preparedness activities.

3 Impacts of Disasters on Livestock

The impact of a disaster can be categorized as direct, indirect or tertiary [4]. Human lives, livestock, government and private property will have a direct impact in any disaster. The indirect effects are related to agricultural output, exports, imports, unemployment etc. while health hazards, funds allocation and community migration are categorized under the tertiary impacts. In developing countries, livestock plays an important role in providing milk, meat, eggs etc. which forms the basic source of income to the farmers [5]. In these countries, the poor disaster action plan creates threat to food supply, occurrence of zoonotic diseases leading to loss of both human and animal population and will have a significant impact on public mental health. Therefore, disasters affecting livestock will have a negative impact on the rural infrastructure of a country creating a large gap between the production and distribution of food and goods. The impact of disaster on livestock urges for an effective management plan to study the relationship of animals with disasters. This should include several preparedness activities and managemental strategies for protection of livestock during disasters.

3.1 Focus on an Essential Relationship

The increased frequency of disasters incurs direct and indirect losses to livestock production resulting in great stress to humans in terms of availability of food. Hence, it is essential to have a clear focus on the relation between livestock and human for an effective disaster management plan.

(i) The loss of livestock results in a long-term malnutrition and deficient food supply.
(ii) The national and regional disaster management plans should include animal welfare measures to have effective human response in protection of livestock during disasters.
(iii) There should be a platform for providing knowledge and resources to livestock owners for an effective disaster management plan.

3.2 Phases of Emergency Management of Livestock During Disasters

Disaster management is generally divided into four time bound phases viz. preparedness, rescue, recovery and rehabilitation [6] and the same will apply to livestock during disasters.

Preparedness phase: Every country/state should have its own policy for livestock on prevention and management during disasters. It will help to handle the disaster in first 48 h by its own community. The data about the available resources regarding the staff, hospitals, drugs etc. will help positively to provide the veterinarian aid in time.

Rescue phase: Disasters occur without warning and this phase comes normally between 48 and 72 h of occurrence. During this phase, the animal health component includes heard health, care of pregnant, young and new born animals and prevention of disease risk through vaccination, sanitation etc.

Recovery phase: This phase normally comes after 2–3 days when outside helps start. The carcasses of the dead animals should be safely disposed. Control rooms should be setup for exchange and co-ordination of veterinarian aid. During this time the damage assessment is also done to evaluate claims.

Rehabilitation phase: This is the phase in which the community is back on the normal life. During this time there will be reconstruction of damaged or lost veterinary facilities based on the experience gained from the disaster handling.

3.3 Livestock Managemental Strategies During a Disaster

The following are some of the effective managemental strategies to save livestock during any disaster.

(i) Set up of rescue camps and quick and rapid evacuation of animals is the best measure. This depends on the type of disaster and requires proper identification of animals.
(ii) Adequate feeding and watering of animals should be should be done to meet the nutritional needs. Availability of feeds and fodder during disasters is very critical and utilization of non conventional feed sources such as urea, molasses, feed blocks, silage feeding must be done.
(iii) The animals suffering from illness and injure should be kept separately and provide treatment. Reduce the risk of disease spread by proper sanitation, vector control and mass vaccination against common diseases.
(iv) The carcass of the dead animals should be burned or buried as per the protocol. Avoid throwing them into rivers and streams which will lead to water pollution. The animal waste can be used as manure or fuel after drying.
(v) Strengthen the Veterinary support by deputing the required staff to the needy places. Provide adequate drugs and medicines for effective treatment. Control rooms should be set up to exchange and coordinate veterinary support between public and private agencies.

4 Role of Veterinarians in Disaster

The increased relationship between humans, livestock and climate, the role of veterinarian became more important in improving public health, quality of food and water and reducing the incidence of zoonotic diseases. The achievement of these goals are hugely dependant on the type of disaster-may be natural or manmade affecting the animal and human health [7, 8].

During disasters, the veterinarian support should be of high standard to control the death of animals. This can be achieved by preparing a local pre-disaster plan at village or mandal level. Veterinary aid should be provided in all stages of disasters to increase the chance of survivability of animals [9, 10]. The activity of veterinarians will be efficient and more fruitful if they work in association with the local, national, international people and NGOs dedicated to animal health care. The people involved in disaster management should work by partnering with local and national governments, non-governmental organizations to deliver expert emergency response for animals during disasters. With this background, the importance of building veterinary aid at different levels of society has been highlighted to protect the animals during disasters. This helps in development of policies, planning and programmes, as a pre-requisite for sustained disaster management.

4.1 Disaster Preparedness for Veterinarians

Animals are equally susceptible to disasters like human. Type of disaster and emergency preparedness and response are important issues to the Veterinarians for effective recovery efforts during and after disasters. Veterinarians should be aware of the possible emergencies during disasters which can be abridged by training and participation in the programmes. It is essential to encourage veterinary leadership in local, state and national level to deal with "all hazards/all species" preparedness for disasters. Hence, it is required by Veterinary Councils and Disaster Management Authorities to strengthen the Veterinarian Committees with expertise and guidance in the following roles:

(i) Address the importance of readiness of veterinary and paraveterinary staff to react to the disaster situations.
(ii) The impact of the disasters on livestock and human health should be highlighted.
(iii) Develop proper action plan and guidelines for handling livestock during disasters.

5 Veterinary Services and Disaster Reduction

With the rapid development of resources, prevention measures etc. the high incidence and impact of disease outbreaks is an on-going challenge for the many years. Biological disasters are considered to have greater impact on human and animal health, especially zoonotic diseases [11, 12]. Hence, it is required to integrate the specialized activities, adopting a multidisciplinary approach to combat the spread of zoonotic diseases as it will lead to huge economic losses. The Veterinary Authority should prepare its disaster reduction plan to focus the activities at each stage (preparedness, rescue, recovery and rehabilitation) in the disaster reduction cycle and for each type of disaster, either natural or manmade [13, 14]. Further, veterinary support or aid should be provided based on the time and need during disasters and work in association with the similar bodies. This has to be strengthened by providing proper training to the staff involved so that they can handle any type of disaster involving livestock and human [15, 16]. Despite many efforts to build Veterinary aid, the dynamicity in the occurrence of disasters always keep some gap to react and respond. Hence, the development of strategies to manage disasters should be a continuous process and can be best achieved by identifying weaknesses and adopting the improved preparedness measures.

References

1. Kumar, P.: Community participation in natural disaster management. In: National Conference on Disaster and Technology, Manipal, India. Manipal Institute of Technology, Manipal, pp. 107–109, 25–26 Sept. 1998
2. https://www.unisdr.org/files/43291_sendaiframeworkfordrren.pdf
3. Ganguli, S.K., Urmil, A.C., Somiya, P.A.: Natural disasters: an overview in Indian context. Ind. J. Commun. Med. **18**(3), 110–113 (1993)
4. Gupta, A.: The great Gujarat earthquake 2001—lessons learnt. In: Proceedings of 22nd Asian Conference on Remote Sensing, 5–9 November, Singapore, 1. Centre for Remote Imaging, Sensing and Processing (CRISP) of the National University of Singapore, Singapore Institute of Surveyors and Valuers (SISV), and the Asian Association on Remote Sensing (AARS), Singapore, pp. 306–309 (2001)
5. Rushton, J., Thornton, P.K., Otte, M.J.: Methods of economic impact assessment. In the economics of animal disease control. Rev. Sci. Tech. Off. Int. Epiz. **18**(2), 315–342 (1999)
6. Federal Emergency Management Agency (FEMA): Animals in disaster–module A: awareness and preparedness. Emergency Management Institute (EMI) independent study course. EMI, Emmitsburg, Maryland. www.training.fema.gov/EMIWeb/is10.htm. Accessed on 3 Sept. 2003) (1998)
7. Garland, T., Bailey, E.M.: Toxins of concern to animals and people. In: Biological disasters of animal origin. The role and preparedness of veterinary and public health services. Rev. Sci. Tech. Off. Int. Epiz. **25**(1), 341–351 (2006)
8. Heath, S.E.: The role of veterinarians in disasters. World Veterinary Association Press Release, Washington, DC. http://www.worldvet.org/press73. (2000)

9. Heath, S.E.: Challenges and options for animal and public health services in the next two decades. In: Biological disasters of animal origin. The role and preparedness of veterinary and public health services. Rev. Sci. Tech. Off. Int. Epiz. **25**(1), 403–419 (2006)
10. Rodier, G., Greenspan, A.L., Hughes, J.M., Heymann, D.L.: Global public health security. Emerg. Infect. Dis. **13**(10), 1447–1452. (2007). ww.ncbi.nlm.nih.gov/pmc/articles/PMC2851539/pdf/07-0732_finalPR.pdf
11. Black, P., Nunn, M.: Impact of climate change and environmental change on emerging and re-emerging animal diseases and animal production. In: Compendium of Technical Items Presented to the OIE World Assembly of Delegates or to OIE Regional Commissions. 2009, pp. 1–54 (2009)
12. National Drought Mitigation Center (NDMC).: What is drought? Understanding and defining drought. National Drought Mitigation Center, University of Nebraska, Lincoln (2002)
13. Subbiah, A.R.: Response strategies of local farmers in India. In: Wilhite, D.A. (ed.) Drought: a global assessment, vol. II, pp. 29–34. Routledge, London (2000)
14. International Strategy for Disaster Reduction (ISDR): UNISDR terminology on disaster risk reduction. United Nations International Strategy for Disaster Reduction (UNISDR), United Nations. 39pp (2009)
15. Madigan, J., Dacre, I.: Preparing for veterinary emergencies: disaster management and the incident command system. In: Veterinary education for global animal and public health. Rev. Sci. Tech. Off. Int. Epiz. **28**(2), 627–633 (2009)
16. Vallat, B., Pinto, J., Schudel, A.: International organizations and their role in helping to protect the worldwide community against natural and intentional biological disasters. In: Biological disasters of animal origin. The role and preparedness of veterinary and public health services. Rev. sci. tech. Off. Int. Epiz. **25**(1), 163–172 (2006)

Chapter 13
Delineation of Target Areas for MGNREGA Related NRM Activities Using Web GIS and Multi Thematic Geo Spatial Datasets

Venkumahanti Tejaswini, G. S. Pujar, G. Jai Shankar, K. Mrutyunjaya Reddy and Suribabu Boyidi

Abstract Development of Indian villages is critically dependent on the availability of water and it's judicious use, especially in the context of fast altering climatic trends and land degradation. This paper concentrates on selecting suitable sites for the implementation of natural resource management activities and aims to choose tentative sites for the planning of water conservation activities such as farm ponds, check dams, plantation, horticulture and other drought proof activities. The approach is done by considering the rules and regulations of an Indian labour act called MGNREGA (Mahatma Gandhi National Rural Employment Guarantee Act) designed at improving the rural inadequate and to make resilient resources of mission water conservation. Here, multi thematic geo spatial data sets of Vayalpad mandal of Chittoor district are considered. The inputs used are Land Use Land Cover (LULC), Digital Elevation Model (DEM), Road map, Drainage map, slope map and other topographical features. These layers are tested using allowable thresholds for understanding sensitivity of decisions.

V. Tejaswini (✉) · G. Jai Shankar · S. Boyidi
Department of Geo Engineering, Andhra University College of Engineering, Visakhapatnam, India
e-mail: venkumahantitejaswini9@gmail.com

G. Jai Shankar
e-mail: jaisankar.gummapu@yahoo.com

S. Boyidi
e-mail: suri.sri2008@gmail.com

G. S. Pujar · K. Mrutyunjaya Reddy
Rural Development and Watershed Monitoring Division, NRSC, Balanagar, Hyderabad, India
e-mail: pujar@nrsc.gov.in

K. Mrutyunjaya Reddy
e-mail: reddy_km@nrsc.gov.in

P. J. Rao et al. (eds.), *Proceedings of International Conference on Remote Sensing for Disaster Management*, Springer Series in Geomechanics and Geoengineering,
https://doi.org/10.1007/978-3-319-77276-9_13

Keywords NRM activities · Ridge to valley · Road and drainage network GIS · Weighted overlay

1 Introduction

Remote Sensing and geographic information technology has developed at a remarkable pace over past two decades. This paper concentrates mainly on the planning of suitable sites for mission water conservation activities using GIS. The data analysis in this paper is done using spatial analysis, decision support system, proximity and overlay tools, conversion tools and other advanced geo processing techniques. To perform this, we consider MGNREGA related NRM activities which refer to the management of natural resources such as land, water, soil, plants, and animals with a particular focus on how management affects the quality of life for both present and future landscapes interact. MGNREGA abbreviated as Mahatma Gandhi National Rural Employment Guarantee Act is an Indian labour law and social security measure introduced by the Government of India with main aim of enhancing livelihood security in rural areas by providing not less than one hundred days of unskilled manual works as a guaranteed employment in a financial year to every household in rural areas as per demand resulting in productive assets of prescribed quality and durability [1]. The entire approach is done using the core principle of ridge to valley which means that the ridges are treated first and then progressively approaching the valley. This would help in reducing the velocity of water, prevention of silt deposition in water harvesting structures and soil conservation in the downstream sites. There are three categories in it. Ridge treatment, Drainage treatment and Area treatment. As per MGNREGA, there are 141 NRM works which comes under 17 concentrated areas of improvement. These include development of rural infrastructure, water harvesting, soil and moisture conservation, ground water recharge structures, water management etc. The verification and validation of planning sites is provided by one of the applications of web GIS called BHUVAN. Bhuvan is a software application which allows users to explore a 2D/3D representation of earth. It offers detailed imagery of Indian locations with spatial resolution ranging up to 1 m. The satellite scenes of LISS-IV and Cartosat data is used as the input imagery for the analysis part. IWMP (Integrated Watershed Management Programme) has a focal point at development of rain fed or degraded areas through participatory watershed approach. Accordingly, drought prone area programme (DPAP), desert development programme (DPP) and Integrated watershed development programme (IWDP) of department of land resources have been integrated. This consolidation is for optimum use of resources, sustainable outcomes and integrated planning. The area of consideration is included in IWMP.

2 Study Area

2.1 Description

The study area is an IWMP that comes under Vayalpad mandal of Chittoor district in Andhra Pradesh. It is located 94 km away from district headquarters. The area is located between 13.38N and 78.37S coordinates. The concentrated area comes under one of the watershed management programmes called IWMP-46 implemented in 2011–2012 which is about 720 ha. It is in the elevation of 670 m from the mean sea level and the district receives an annual rainfall of 918.1 mm. which specifically proves it's a rain fed area (Fig. 1).

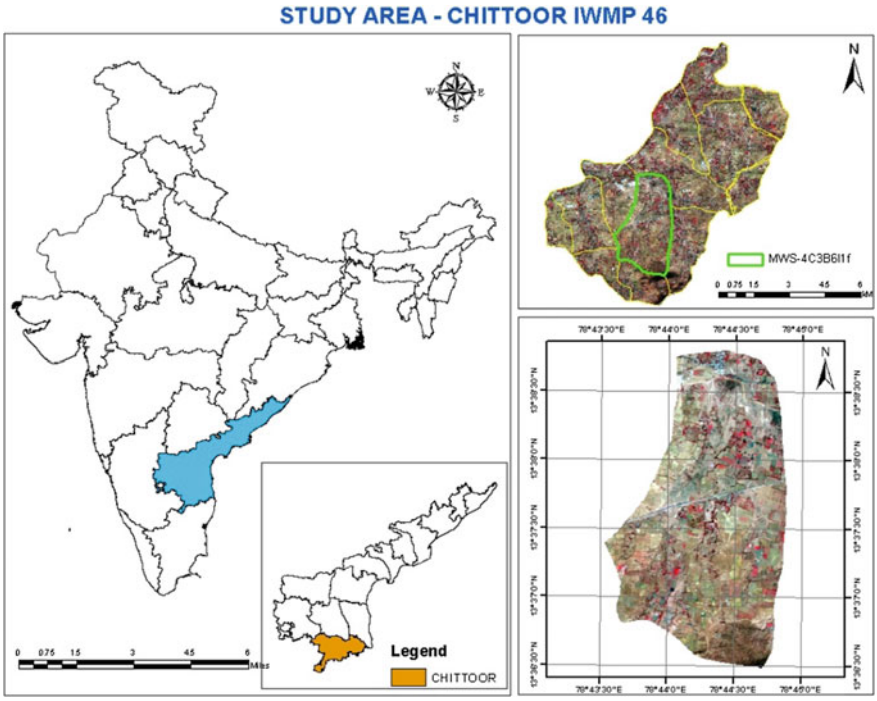

Fig. 1 Study area—Chittoor—IWMP 46 and micro watershed—4c3B611f

3 Methodology

3.1 Work Flow for Planning Suitable Sites

Stage 1: Select an area to implement planning based on ridge to valley principle.
Stage 2: Consider multi thematic dataset of four layers

1. Land use land cover
2. Road network
3. Drainage network
4. Digital elevation model.

Stage 3: Use the DEM map for understanding the relief features of the terrain and classify the area into different zones.
Stage 4: Apply proximity (buffer) to input layers (roads, drainage, settlements) to find the tentative sites considering the future extent.
Stage 5: Make an union of all these above input proximity layers.
Stage 6: Delineate the wastelands which come under these proximity zones. This derived data for acquisition of gap area which are neither undertaken by MGNEGA nor by IWMP [2].
Stage 7: Apart from the above layers, consider the decadal rainfall data for rainfall design and run off estimation which is a key step towards successful analysis.
Stage 8: Extract the suitable sites for suggesting various NRM activities and their accessibility for implementation (Fig. 2).

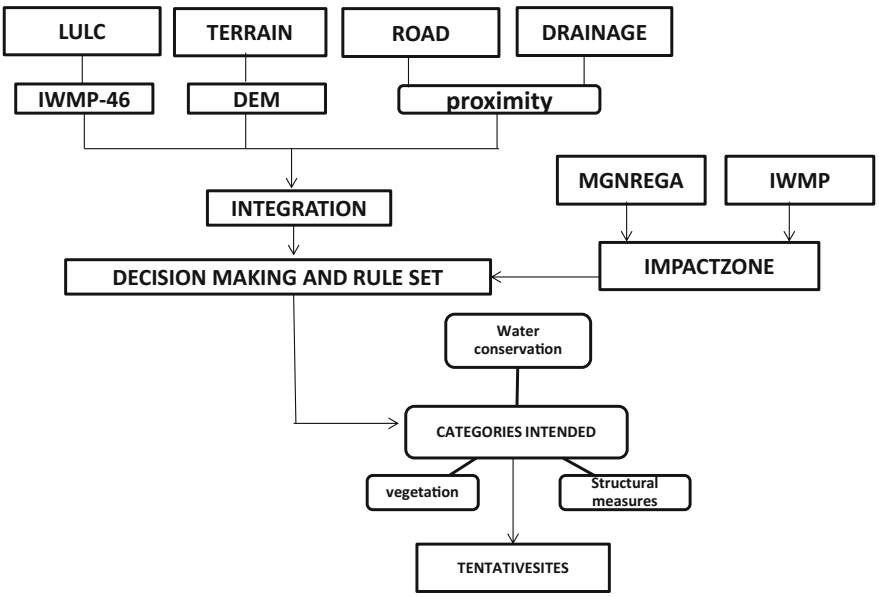

Fig. 2 Methodology to implement planning of activities

4 Satellite Data

1. PAN of 2.5 m resolution—CARTOSAT
2. LISS-IV of 5.8 m resolution and Planet lab data.

5 Software Required

1. Arc GIS
2. ERDAS IMAGINE
3. SHARE X (for image capturing).

6 Input Thematic Layers

6.1 LULC

LULC pertaining to the study area is considered. It includes the five main categories such as agricultural land, forest land, built up, wasteland and water bodies [3]. This theme is tested every time for checking the suitability to plan each NRM activity and to assign the weighted value of site based on suitability criteria to a particular activity (Fig. 3).

6.2 Road Network

Roads play an important role in planning because they serve the purpose of rural connectivity to implement the activities (both labour and machinery). The road map for the study area contains five major categories National High way, Village road, Cart road, and District road and foot path. In the suitability analysis Proximity zones as discussed above are created to evaluate the threshold levels which are helpful for planning. This is shown in Fig. 4a.

6.3 Drainage Network

Drainage network is a key to implement mission water conservation activities [4]. The flow direction estimate is primarily decided by its drainage pattern and number of streams with their respective order. Drainage buffer having a distance of 50 ms is created to allow the extent as shown in Fig. 4b.

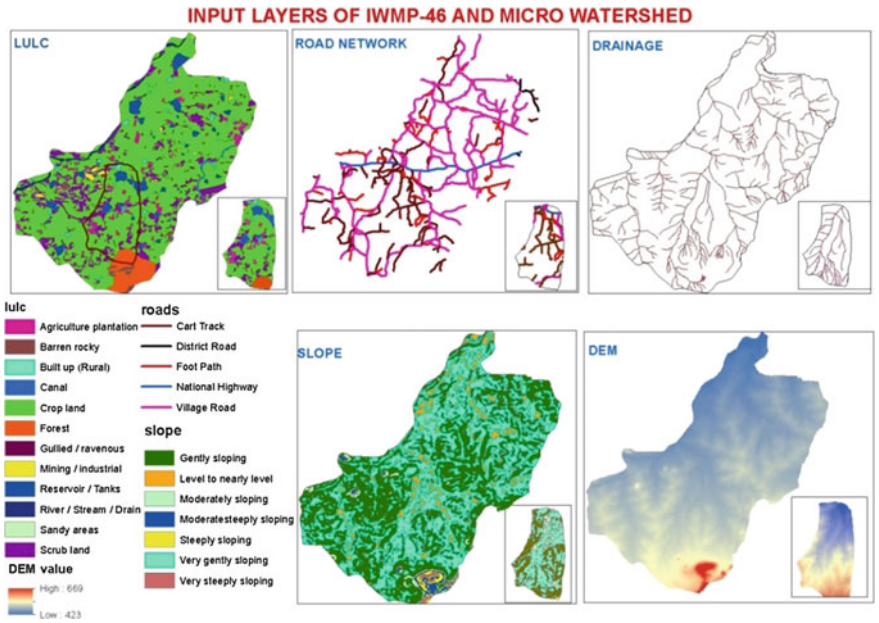

Fig. 3 Input thematic layers (LULC, road map, drainage map, slope and DEM)

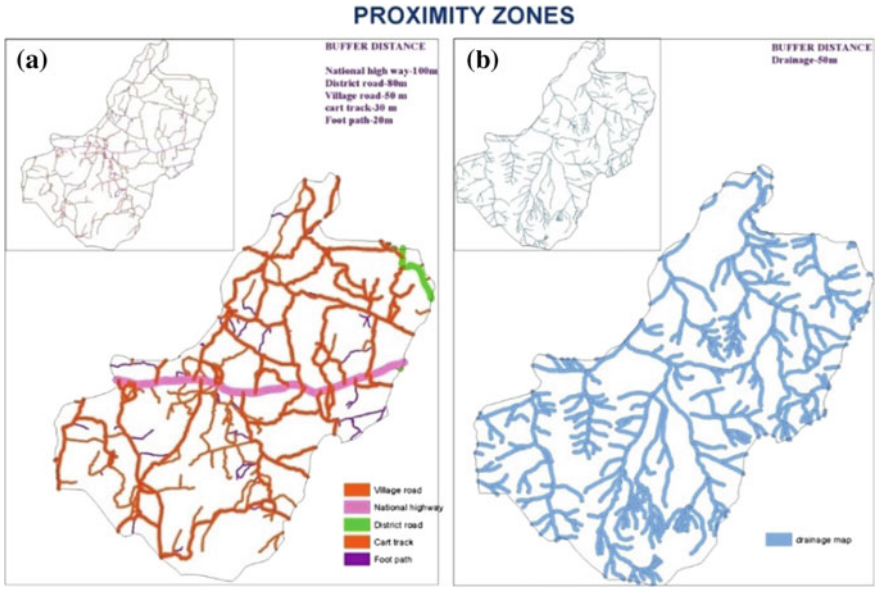

Fig. 4 **a** Proximity road buffer. **b** Drainage buffer- 50 m distance

6.4 Digital Elevation Model

To better understand the elevation of the terrain at each pixel, the DEM points its exact altitude from the mean sea level [5, 6]. The minimum and maximum elevations for the study area are 423 and 669 m from MSL. All the discussed input thematic layers with their specifications are shown in Fig. 3.

7 Proximity Zones

Buffer zones of 50 m for drainage network and 10–100 m by a factor of 20 m each i.e. 20 m to footpath, 40 m to cart track, 60 m to village road, 80 m to district road and 100 m to national highway are created. These buffer zones help for the analysis to check the accessibility to carry out the planning of various activities. Proximity zones can even help for planning in case of further extension of the terrain features (natural or manmade).

8 Rainfall Design

Rainfall design and its estimation of return period plays a crucial role to make a long run planning. It can be analysed by performing rainfall probability analysis of the area i.e. amount of rainfall during a year at or above which the catchment area will provide sufficient runoff. Initially, annual decadal rainfall data is collected and they are arranged in an order giving ranks 1, 2, 3, 4, 5 … (maximum rainfall gets rank 1 and so on).

8.1 Probability of Rainfall and Return Period

The occurrence of probability for each ranked observation is calculated from the Eq. (1) for the last one decade.

$$\text{Probability}\,(\%) = \frac{\mathrm{m} - 0.375}{\mathrm{N} + 0.25} \tag{1}$$

where p is the percentage of rainfall, m is the rank of the observation and N is the total number of observations. Once probability is calculated, the return period T in years can be estimated by using the expression and Table 1.

Table 1 Decadal rainfall data rank wise with % probability

Year	Rainfall (in mm)	Rank	Probability (%)
2005	1543.9	1	5.55
2006	844.6	8	67.77
2007	1092.2	2	14.44
2008	953.3	4	32.22
2009	754.4	10	85.55
2010	1079.5	3	23.33
2011	921	5	41.11
2012	740	11	94.44
2013	856	7	58.88
2014	900	6	50

$$T = \frac{100}{p} \tag{2}$$

where T is the return period and p is the percentage of probability. For example, the return period with 50% probability will be T = 100/50 i.e. two years. Table 1 gives the annual decadal rainfall of the study area. The percentage probability can be computed using Eq. (1).

From Fig. 5, it is clear that there is an expectation of 50% probability to get rainfall of 900 mm. Thus, according to Indian Meteorological Department, this area can be considered as a rain fed region. The finally fitted curve would show the probability of occurrence of rainfall value of a specific magnitude. The yellow line

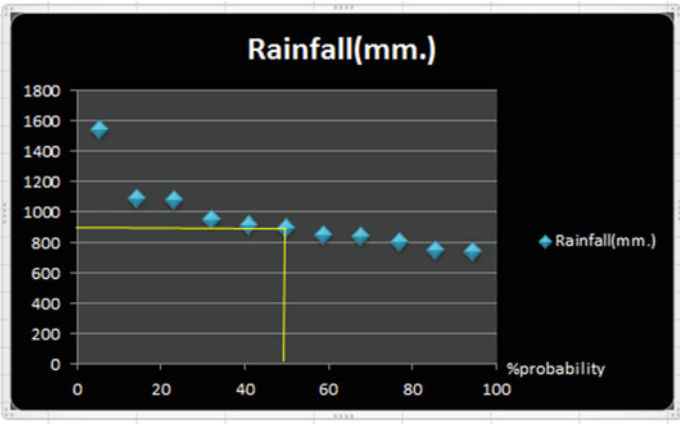

Fig. 5 Graph showing % probability and rainfall

on x axis indicates the 50% probability and the same line on y axis indicates the amount of rainfall at that probability which is 900 mm. This can be computed for every unit and the probability can be estimated.

9 Results and Discussions

9.1 Wasteland Extraction

The total number of wastelands found to be 560 polygons. Of them those which are in the vicinity of the road network are 302 covering an area of 249.32 ha and of drainage network are 318 with an area of 323.22 ha. The waste lands near the settlements are 32. Total wastelands that are neither under the coverage of MGNREGA nor IWMP projects (highly concentrated areas in the planning) are 182. The waste lands are categorized to various classes based on their area and those which are greater than 10 ha are not considered under planning (Table 2).

The number of waste lands in the vicinity of the roads is 302 and in the vicinity of drainage network are 318 which possess the area of less than 10 ha each (Fig. 6a, b). Of them, the waste lands which are neither undertaken by NREGA NRM programme nor by IWMP, are the main targeted areas for suggesting the planning (Fig. 7).

9.2 Integrating Input Data

All the inputs that are taken above are integrated against each layer with respect to their threshold levels so that some common areas can be evolved with the help of which planning can become easier and more helpful so that it can serve multiple purposes. Fig. 8 illustrates the output obtained by performing union to the above input layers and proximity zones.

Table 2 Classification of wastelands in area

Class	Category (ha)	Total area (ha)	No. of wastelands
1	<2	218.42	450
2	>2 to <4	167.71	58
3	>4 to <6	111.40	23
4	>6 to <8	102.81	15
5	>8 to <10	37.88	4
6	>10	(NA)	(NA)

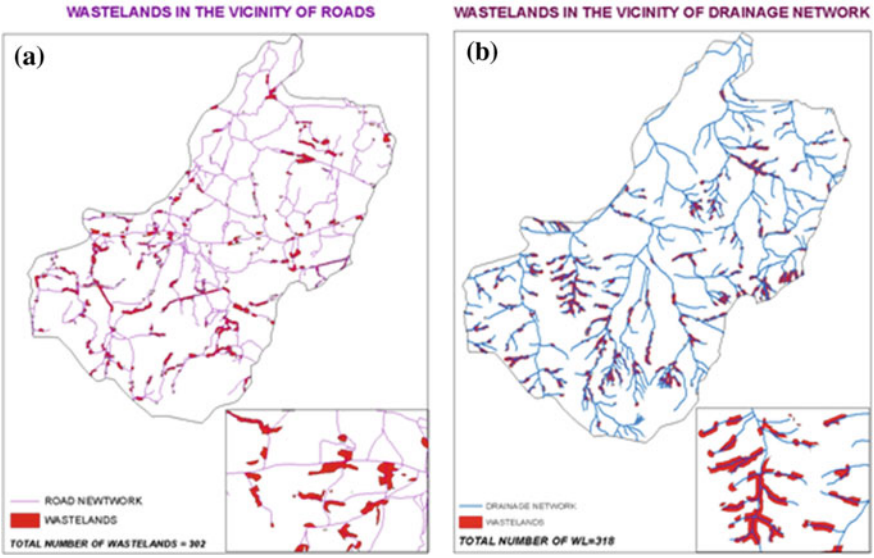

Fig. 6 **a** Waste lands near roads. **b** Waste lands near drainage

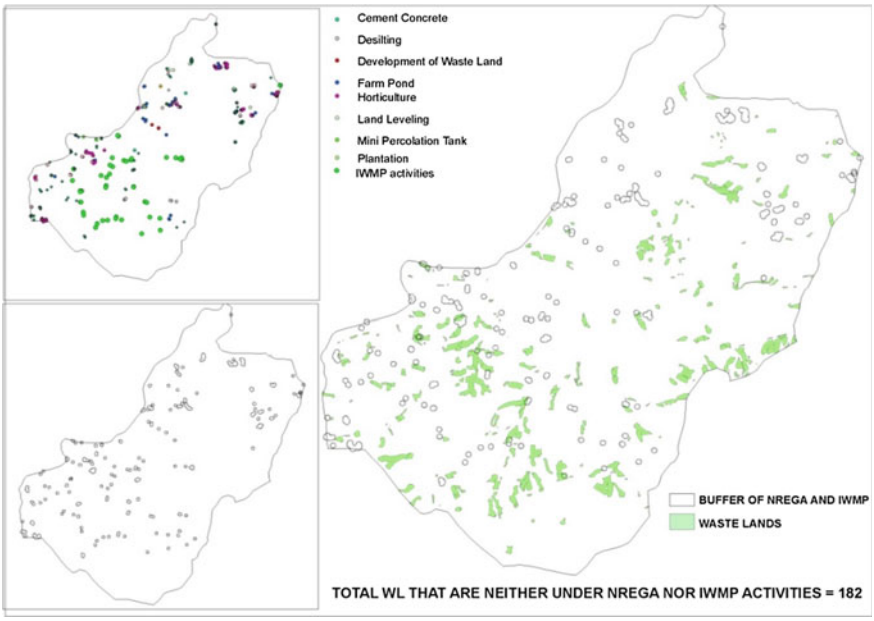

Fig. 7 Total waste lands covered neither by NREGA nor by IWMP activities

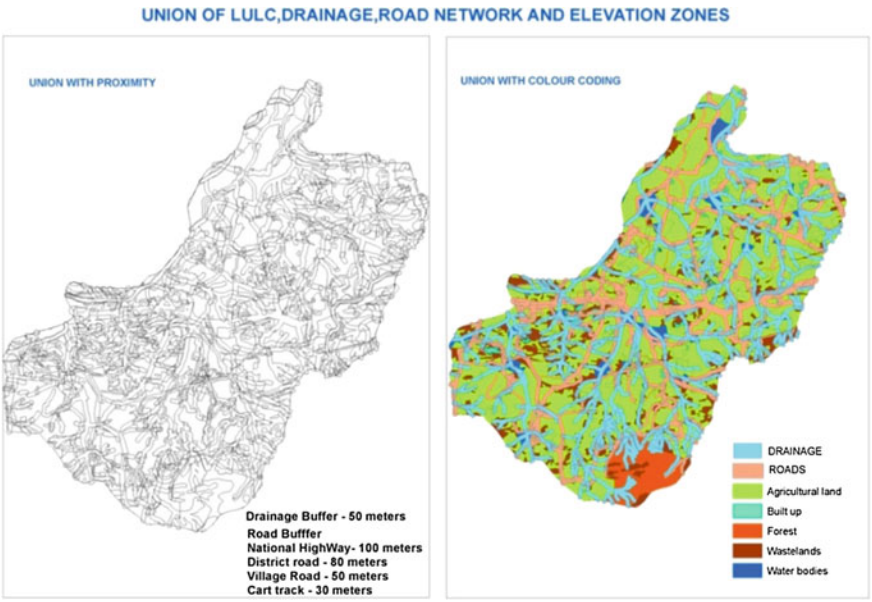

Fig. 8 Union of LULC, buffered roads, buffered drainage, elevation zones

10 NRM Activities—Check Dams

Check dams are to be planned in an area having an annual rainfall less than 1000 mm. and the site should be along the drainage channel (preferably on the second and third order streams). The water way should be on the slope of not more than 30°. Height of the check dam must be in between 2 and 3 ft and its length varies between 6 and 10 m [7]. The spacing between the check dams must be in such a way that toe of the upstream check dam is equal to the elevation of the downstream check dam's crest [8].

10.1 Estimating Peak Rate of Run off

The approximate dimensions of the weir are determined by taking into account the peak run off from the catchment. Peak run off can be estimated by using a rationale formula given below.

$$Q = \frac{CIA}{360} \tag{3}$$

where Q is the peak discharge in m^3/s, c is the run off coefficient taken as 0.5 with respect to available soils, I is the maximum rainfall intensity for the time of concentration taken as 2 mm/h (as per rainfall census of APSDS) and A is the drainage area of the diversion channel, the peak rate of run off can be calculated as 0.05 m^3/s. From this, the length of the weir can be computed suing the below equation.

$$L = \frac{Q}{1.711 \times h^{\frac{3}{2}}} \tag{4}$$

h is the depth of the flow i.e. 0.3 m and by replacing the above values the approximate length of the weir can be 6 m across the drainage channel.

10.2 Input Thematic Maps

After taking the slope, elevation from mean sea level, drainage pattern, rainfall, run off estimation and hydrology into consideration, 7 suitable sites are planned for the construction of check dams for the given micro watershed having an area 720 ha. This output is shown in Fig. 9.

11 Farm Ponds

Farm ponds can be made on any and every crop field (moderately cultivated) in the rain fed regions [9]. It should be made in the farming area so that protective irrigation can easily be given and site should be relatively flat. The main

Fig. 9 Input thematic layers for the construction of check dams and the output tentative sites for planning

requirement is that the farm ponds must be lying on the slopes <3% i.e. along very gently sloping terrain [10]. For regions having mean annual rainfall varying from 500 to 750 mm, farm pond of 500 m^3 capacity can be constructed. Selection of suitable sites for the farm ponds depends on soil type, infiltration rate, slope, topography, drainage pattern, and rainfall distribution. The catchment area of the site should be more than 2 ha. If we want to provide 10 cm of protective irrigation to crop over 1 ha, we need 1000 m^3 of water. Volume of water required is the product of area of the irrigated land and depth of irrigation (1 ha $\times$ 1000 m^3). Farm pond whose dimension is 500 m^2 will yield this amount of water in 1 ha.

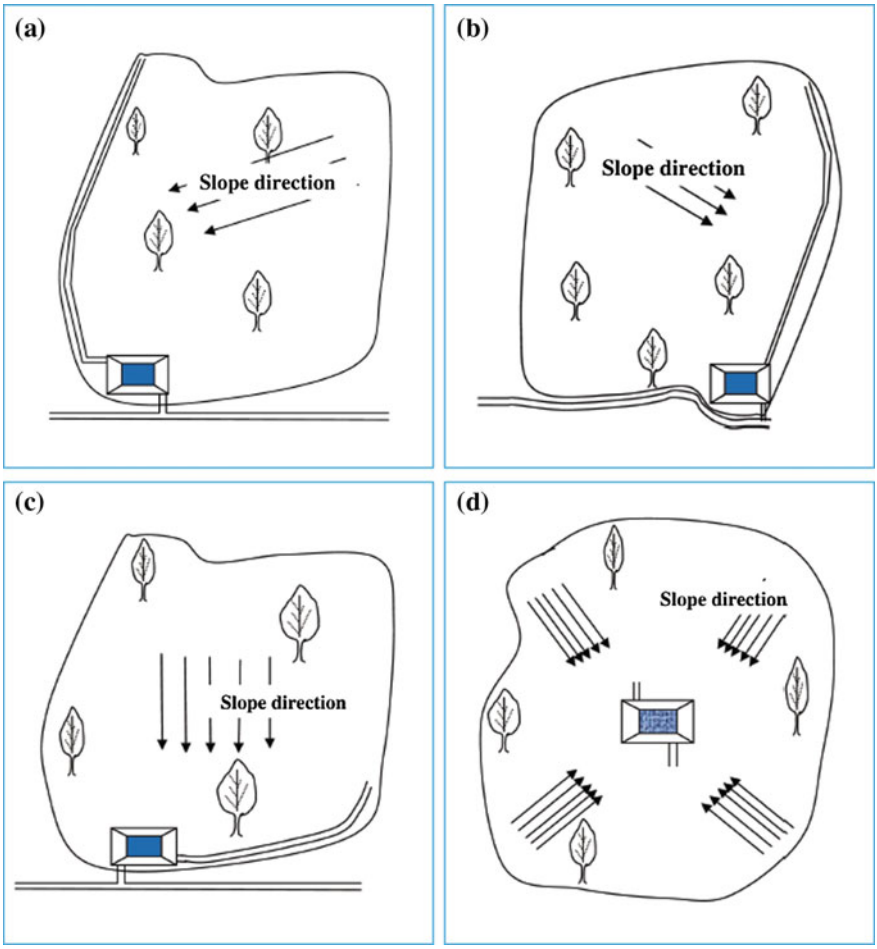

Fig. 10 Slope direction based on elevation

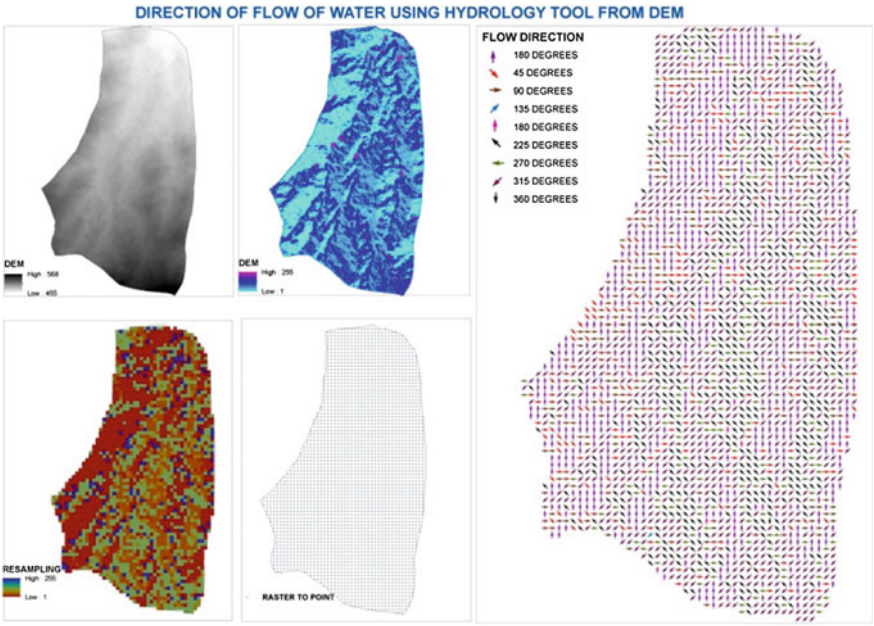

Fig. 11 Hydrology—flow direction and its orientation

11.1 Direction of Water Flow

The direction of the water flow is very important while planning sites for the farm ponds in each field because farm pond must be constructed mostly along the corner which directs the water flow [11]. In order to perform this analysis, we need to

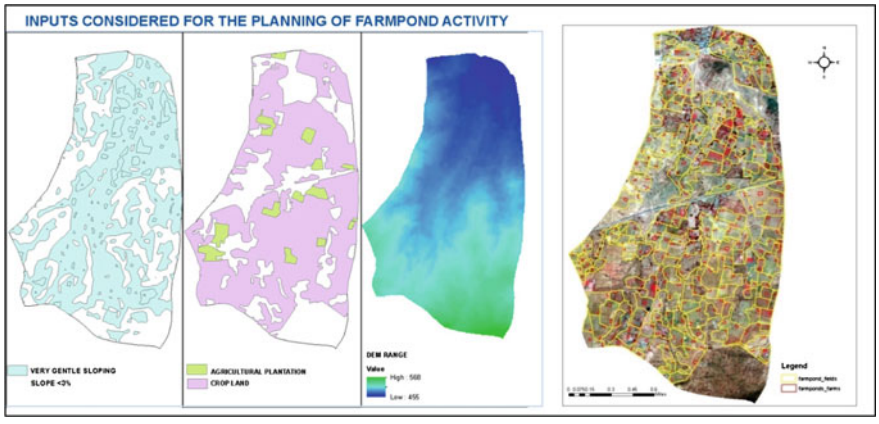

Fig. 12 Input layers considered for planning farm ponds and output site selection for farm ponds

consider the DEM, run the hydrology (flow direction) tool of Arc GIS, perform resampling, covert this raster resampled data into point and display them in terms of directions with respect to particular orientation angles as shown in Figs. 10, 11 and 12.

12 Horticulture

Horticulture is a fruit, vegetable and ornamental agriculture that involves intense care with respect to gardening, agriculture in green house, land scape architecture. Consider LULC map, convert to raster, reclassify it based on category. Consider DEM map, reclassify it into elevation zones. Consider slope map convert to raster, reclassify and save these inputs. Table 3 informs that the layer influencing the planning of the horticulture under land use land cover is 35% with corresponding weighted values of each category are defined. Similarly, the layer influencing the planning under road network is 15%, layer under drainage is 30% and the layer influencing planning of horticulture by DEM is 20%. For example, in Table 3, under LULC, waste lands are given the highest weightage followed by water bodies, built up, agricultural land and forest as shown Table 3.

Table 3 Weighted overlay values to each layer and ranks

Raster	% Influence	Field	Weighted value
LULC	35	Waste lands	6
		Water bodies	5
		Built up	4
		Agricultural land	2
		Forest	3
Road	15	Village road	4
		National highway	3
		Cart track	5
		Foot path	6
Slope	30	Level to nearly level	3
		Moderate sloping	4
		Gentle sloping	5
		Very gentle sloping	1
		Steep slope	1
DEM	20	455–486 m	6
		487–518 m	5
		519–550 m	3
		550–566 m	2

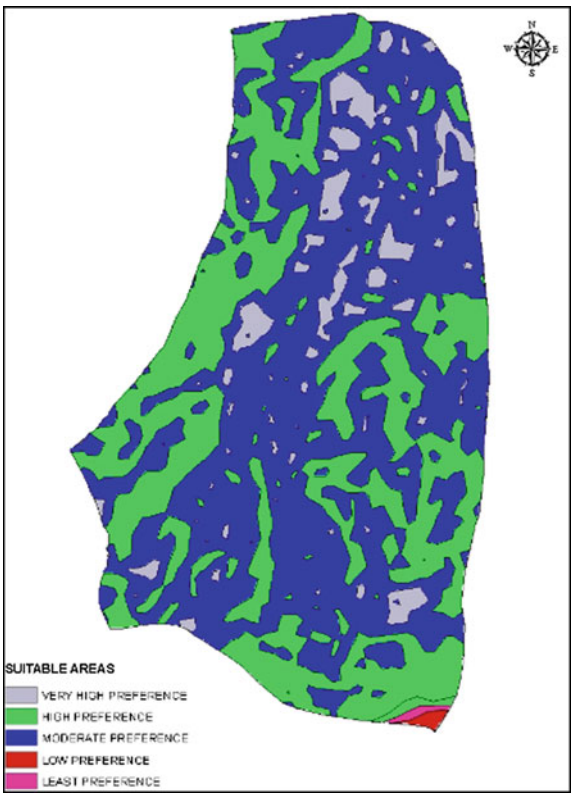

Fig. 13 Tentative sites to plan for horticulture

12.1 Weighted Overlay

From Fig. 13, the suitable sites for the planning of horticulture are obtained by computing percentage influence and weighted values with reference to each layer as shown in Table 3. Grey colour patches are the most important sites which contribute for high suitability and the further suitability is explained colour wise as shown above.

13 Conclusions

The main objective of this project is to suggest some inputs for implementing NRM activities under MGNREGA. The above results show all tentative sites for the implementation of farm ponds, check dams, plantation and horticulture by using some tools of Arc GIS. In this study the input thematic maps that include LULC, Digital elevation maps, terrain, slope map, road map, drainage map are considered. Initially the waste lands where there is a possibility to implement the activities are

delineated. The wastelands concentrated are 182. Of them the total number of sites suitable for check dams are tentatively 7 and 28 most suitable sites are derived for implementing horticulture. The all possible sites for constructing farm ponds are delineated based on the corresponding dimensions of each farm and these are tested for understanding sensitivity of decisions.

Acknowledgements The authors wish to express their sincere thanks to the Director and head Rural development division, National Remote Sensing Centre, Hyderabad for providing the necessary information and complete support during the period of study.

References

1. Sharma, B.R., Paul D.K.: Water resources of India. In: Singh G.B., Sharma B.R. (eds.) 50 of Natural Resource and Management Research. Division of Natural Resource Management, pp. 31–48. Krishi Bhavan, ICAR, New Delhi (1998)
2. ISRO's Geo-Portal Bhuvan: Gateway to Indian Earth Observation, Department of Space, Indian Space Research Organization. Systems and software description, Bhuvan by National Remote Sensing Centre, ISRO-DPPAWA-GWGSG-AUG-205TR-727
3. Watershed Works Manual: Baba Amte Centre for People's Empowerment, Samaj Pragati Sahayog. National Rural Employment Guarantee Act (2006)
4. Sharma G.N.: MGNREGA works field manual. In: Irrigation and Soil Conservation Expert, U.N.D.P., GOI (2005). Burges, S.G.: Trends and directions in hydrology. Water Resour. Res. **22**(9) (1986). Giridhar, M.V.S.S., Viswanath, G.K.: Development of spatial analyst toolbar in ArcGIS. Int. J. Adv. Remote Sens. GIS **1**(1) (2012)
5. Pandey, A., Mall, B.C., Dabral, P.P.: Remote sensing and GIS for the identification of suitable sites for soil and water conservation structures. Land Degrad. Dev. **22**(3), 359–372 (2011)
6. Adham, A., Ritsema, C.: Identification of suitable sites for rainwater harvesting structures in arid and semi-arid regions. Int. Soil Water Conserv. Res. **4**, 108–120 (2016)
7. Samarthya: Technical training manual MGNREGA. Ministry of rural development, Government of India (March, 2015). Jabatan Pengairan Saliran: Guidelines for the design and construction of check dams for prevention and control of peatland fire (2011)
8. Anonymous: Check dam spacing details by department of transportation, Government of Tennessee (1992). Singh, J.P., Singh, D., Litoria, P.K.: Selection of suitable sites for water harvesting structures in Soankhad watershed, Punjab using remote sensing and geographical information system approach. J. Indian Soc. Remote Sens. **37**, 21–35 (2009)
9. Saptasshi, P.G., Raghavendra, R.K.: GIS based evaluation of micro-watershed to ascertain site suitability for water conservation structures. J. Indian Soc. Remote Sens. **37**, 693–704 (2006)
10. Abdullah, N.B.: Land Suitability Mapping for Implementation of Precision Farming. IEEE Published at National Post Graduate Conference, Kaulalampur (2011)
11. Zade, M., Ray, S.S., Dutta, S.: Analysis of run off pattern for all major basins of India derived using remote sensing data. Curr. Sci. **88**(8), 1301–1305 (2005)

Chapter 14
Dynamic Changes of Plantations in the Selected Watershed Project Areas of Andhra Pradesh Using Bhuvan Geo-Information

G. Sravanthi, K. Mruthyunjaya Reddy, G. S. Pujar and Peddada Jagadeeswara Rao

Abstract IWMP aims to enhance the judicious use of natural resources, particularly based on soil and water conservation measures. NRSC/ISRO has designed and developed the required technological interventions (Srishti & Drishti) for monitoring and management of IWMP watersheds through Bhuvan-Integrated Watershed Programme (IWMP). In order to analyze the changes in plantations, IWMP watershed projects corresponding to 6 Agro climatic zones of Andhra Pradesh were selected as they facilitate the specific growth scenario of Plantations in these IWMPs. Dynamic changes in plantations provides us the information of Land cover changes which helps in implementing the sustainable developmental activities in the IWMPs for the growth and for balancing the hydrological cycle properly. The procedure to detect changes in plantations involves a comparison of two or more satellite images acquired at different times that can be used to evaluate the differences in spectral responses. The method of change detection involves analysing the changes in plantations using online Bhuvan geo information and analysing through image processing techniques.

Keywords Bhuvan · IWMP · Change detection · Image processing
NDVI · Per pixel based image analysis · Object based image analysis

G. Sravanthi (✉) · P. J. Rao
Department of Geo-Engineering, Andhra University College of Engineering, Visakhapatnam, India
e-mail: er.g.sravanthi@gmail.com

P. J. Rao
e-mail: pjr_geoin@rediffmail.com

K. M. Reddy
PPEG and RDWMD, Hyderabad, India
e-mail: reddy_km@nrsc.gov.in

G. S. Pujar
RDWMD, NRSC, Hyderabad, India
e-mail: pujar@nrsc.gov.in

P. J. Rao et al. (eds.), *Proceedings of International Conference on Remote Sensing for Disaster Management*, Springer Series in Geomechanics and Geoengineering,
https://doi.org/10.1007/978-3-319-77276-9_14

1 Introduction

Remote sensing technology in combination with geographic information system (GIS) can render reliable information on Plantation cover. Urban growth, in population has been a major factor which has altered natural vegetation cover, due to anthropogenic activities. The results of these have left significant effects on local weather and climate. The use of remote sensing data in recent times has been of immense help in monitoring the changing pattern of Plantations.

The analyzation of the dynamic changes of plantations in the IWMP (Integrated Watershed Management Programme) watershed projects provides us the information of Landover changes which helps in implementing the sustainable developmental activities in the IWMPs for the plantation growth and for balancing the hydrological cycle properly.

The current study focuses on the change detection of plantations and their spatial distribution. Spectral characteristics of features may change over time and these changes can be detected by collecting and comparing multi temporal imagery. Change detection procedures intend to find and where appropriate, to interpret the alterations of objects or phenomenon between the different acquiring times t1, t2, … tn. when using multi temporal remote sensing image data, the value of an image pixel or object at time t1 can be compared with the value of the corresponding image pixel or object at time t2 in order to determine the degree of change. The change analysis includes visual interpretation using Bhuvan geo based information and then confirming the changes using image processing techniques. The image processing methods for change analysis involves both per pixel based image analysis and object based image analysis methods. This is because the coverage changes were affected by the seasonality and the potential usage of high resolution satellite images for the extraction of information from local to national scales.

2 Data and Software Packages

In this study satellite data of Resourcesat-2 LISS-IV data and Planetlab imagery Rapideye and Planetscope are used. For the change detection multi temporal satellite images (T0 & T1) were used. T0 data is acquired from LISS-IV and T1 data is acquired from planet labs satellite imagery. The LISS-IV sensor is a multispectral high resolution camera with a spatial resolution of 5.8 m at nadir. The payload provides multispectral imagery covering a swath of 70 km as compared to 23 km swath of Resourcesat-1. The data is acquired in three spectral bands namely visible and near infrared (B2, B3 and B4). Planet's satellite constellations image the entire world every day. The planetscope analytic data is orthorectified, multispectral data from satellite constellation with four multispectral bands namely blue, green, red and near infrared and having ground sample distance of 3.7 m (at reference altitude of 475 km).

Software packages used were Arc GIS 10.2.1 which is used for discovering geographic information, analysing the information and for creating maps. ERDAS IMAGINE 2016 is aimed primarily at geospatial data processing and for the enhancement of digital images and for the image processing methods that are involved in change detection. eCognition 9.1 used for extracting information from images using a hierarchy of image objects (group of pixels) and is used for image segmentation and classification processes. It solves image analysis tasks through earth science based rule sets and workflows.

2.1 Study Area

For analyzing the changes in Plantations six Agroclimatic Zones of Andhra Pradesh were considered. The Agroclimatic zones facilitates understanding with respect to specific growth scenario in Plantation. Agroclimatic zones refers to soil types, rainfall, temperature and water availability which influences the type of plantations. Therefore to study and analyze the Plantation growth, different IWMPs from each district corresponding to these Agroclimatic zones were selected. They are North Coastal Zone (Vizianagaram), Godavari Zone (West Godavari), Krishna Zone (Prakasam), Southern Zone (Kadapa), Scarce Rainfall Zone (Ananatapur), High Altitude and Tribal Areas Zone (High altitude and tribal areas of Visakhapatnam) (Fig. 1; Table 1).

Fig. 1 Image showing the six selected IWMPs of Andhra Pradesh

Table 1 Represents the study area

Districts	Type of agro climatic zones	IWMPs
Anantapur	Scarce rainfall zone	IWMP-32
Kadapa	Southern zone	IWMP-29
Prakasam	Krishna zone	IWMP-36
Visakhapatnam	High altitude tribal zone	IWMP-11
Vizianagaram	North coastal zone	IWMP-10
West Godavari	Godavari zone	IWMP-01

3 The Hybrid Method

Hybrid method of change detection involves analyzing the changes in plantations using web portal Bhuvan Geo information and through image processing techniques.

3.1 Change Analysis Through Bhuvan Geo Information

The primary analysis of changes in plantations were observed and identified in the six IWMPs of six different agroclimatic zones of Andhra Pradesh using Bhuvan geo information and the changes that are associated with these watersheds were identified as mainly two kinds, they are increase in plantations and felling of plantations. The increase in plantations was further categorized into two types namely large plantation associations and moderate to small plantation associations. The felling of plantations were also categorized into two types namely removal of small patches of plantations and removal of large patch of plantations. These different categories were considered as instances and were identified by visual interpretation using Bhuvan geo information for all six IWMPs that have been selected each for one district of Andhra Pradesh. The total number of instances for each category was given in Table 2.

The large plantation associations were considered as one instance. For illustration from Table 2 the more number of instances of large plantations established that were identified in Southern zone i.e., in Kadapa district IWMP-29 are 25 instances. Figure 2 illustrates the association large plantations (Fig. 3).

3.2 Change Analysis Through Image Processing Techniques

This paper gives an overview of the analysis using both pixel based and object based methods. The object based methods which aim to delineate readily usable objects from imagery while at the same time combining image processing and GIS

Table 2 This table depicts the change analysis of plantations using Bhuvan web based Geo information system

S. no.	Type of change	Vegetation change	Godavari zone	High altitude tribal zone	Krishna zone	North coastal zone	Scarce rainfall zone	Southern zone	Total
1	Planting	Large plantations established	12	10	7	6	5	25	65
		Moderate to small plantation established	56	51	34	16	69	128	354
2	Felling	Removal of small patch of vegetation	9	0	6	2	1	4	22
		Removal of large patch of vegetation	1	0	0	0	0	0	1
		Total	78	61	47	24	75	157	442

Fig. 2 Identifying the association of large plantations on Bhuvan Srishti

The moderate to small plantations that are established are shown in the below image

The removal of large association of plantations are shown by the image below

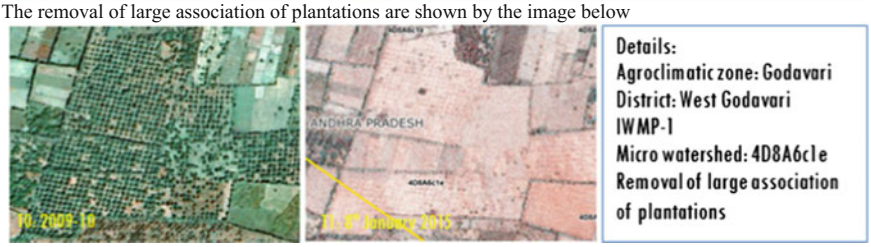

Fig. 3 Identifying the plantation changes in Bhuvan IWMPs

functionalities in order to utilize spectral and contextual information in an integrative way. To avoid salt and pepper effect image can be divided into homogeneous regions prior to classification, instead of classifying the individual pixels. The most common approach used for building objects is image segmentation. High resolution satellite images offer great spectral heterogeneity and spatial variance. Because of spectral heterogeneity and spatial variance in the image, segmentation techniques were used. With this approach, segments not only have spectral properties, but also region based metrics as shape, texture, structure, size and context. Object-based image analysis (OBIA) involves pixels first being grouped into objects based on either spectral similarity or an external variable such as ownership, soil or geological unit. Many variables may be determined, categorized as spectral, shape. Spectral variables are mean value and standard deviation of a specific spectral band; shape variables include size, perimeter and compactness. This can be achieved from ecognition tool which used patented image segmentation and classification processes (Fig. 4).

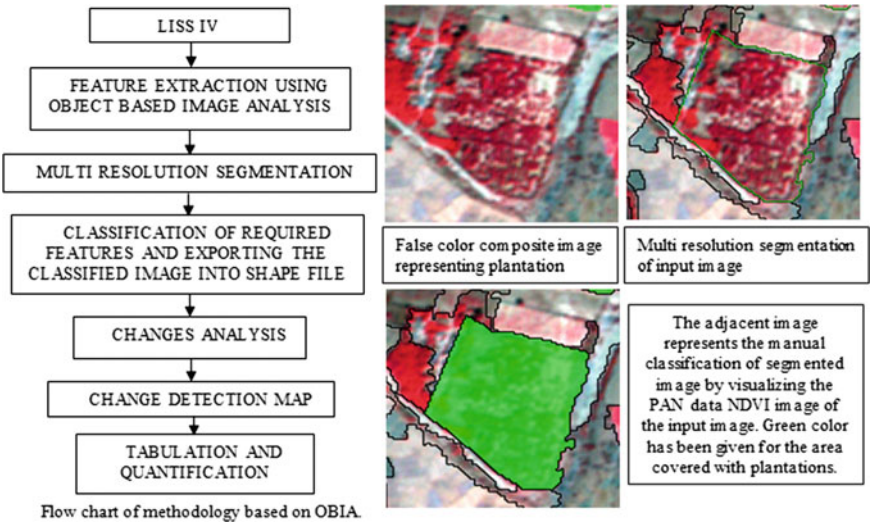

Fig. 4 Change detection using object based image analysis method

A pixel has been the basic unit of image analysis and change detection techniques since the early use of RS data. An image pixel is the atomic analytical unit in these techniques whose spectral characteristics are exploited to detect and measure changes mostly without considering the spatial context. In this paper image differencing method has been applied.

3.3 Image Differencing

Two precisely co-registered multi-temporal images are used to produce a residual image to represent changes. The difference can be measured directly from radiometric values of the pixel or on the extracted/derived/transformed images such as texture or vegetation indices. In this paper we have considered the vegetation indices i.e., NDVI of two multi temporal images for change detection [1].

Mathematically, the difference image is:

$$\mathrm{Id}(x, y) = \mathrm{I1}(x, y) - \mathrm{I2}(x, y)$$

where I1 and I2 are the images obtained from t1 and t2, (x, y) are the coordinates of the pixels. The resulting image, Id, represents the intensity difference of I1 from I2. This technique works only if images are registered. The NDVI image of T0 data and the NDVI image of T1 data were given as inputs to the image differencing tool in change detection tools. The obtained difference image, T0 data (LISS IV) and T1 data (Planetscope) were compared for the confirmation of change detection and

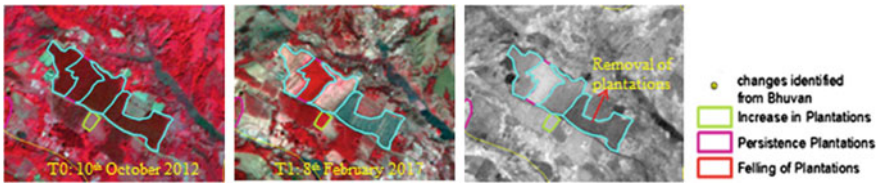

Fig. 5 Change detection using image differencing method [2]

exported to Arc GIS for creating polygon features for the changes obtained and then quantified (Fig. 5).

4 Results and Discussions

In the present study the dynamic changes of plantations in Anantapur district IWMP-32 belonging to scarce rainfall zone of the six agro climatic zones of Andhra Pradesh were detected using the object based image analysis method performed separately on each of the multi temporal data. In this study area along with the plantations, a great change in natural stream vegetation has also been identified. The number of increase in plantations, number of felling of plantations and the number of persistence plantations of periods T0 and T1 were briefly depicted in the Table 3.

The total area under the plantations that are identified in Anantapur IWMP-32 over the time period T0 (3rd March 2012) is 71.48 ha and the total area under the felling of plantations that are detected through object based analysis for the T0 data is 17.03 ha. Similarly the total area of plantations and the area under felling of plantations for the T1 (12th December 2015) are 112.65 and 69.49 ha (Fig. 6).

The changes in plantations were identified in Kadapa district IWMP-29 belonging to the southern zone of the six agro climatic zones of Andhra Pradesh were detected by the method of integration of Bhuvan based analysis with the image differencing methods as shown in Fig. 7.

Table 3 Changes that are identified in T0 and T1 data of Anantapur IWMP-32

Count of object ID	Class name T1		
Class name T0	Natural stream vegetation T1	Plantations established in T1 data	Area without any plantations
Natural stream vegetation T0	227	55	160
Plantations T0	18	36	18
Area without any plantations	217	82	

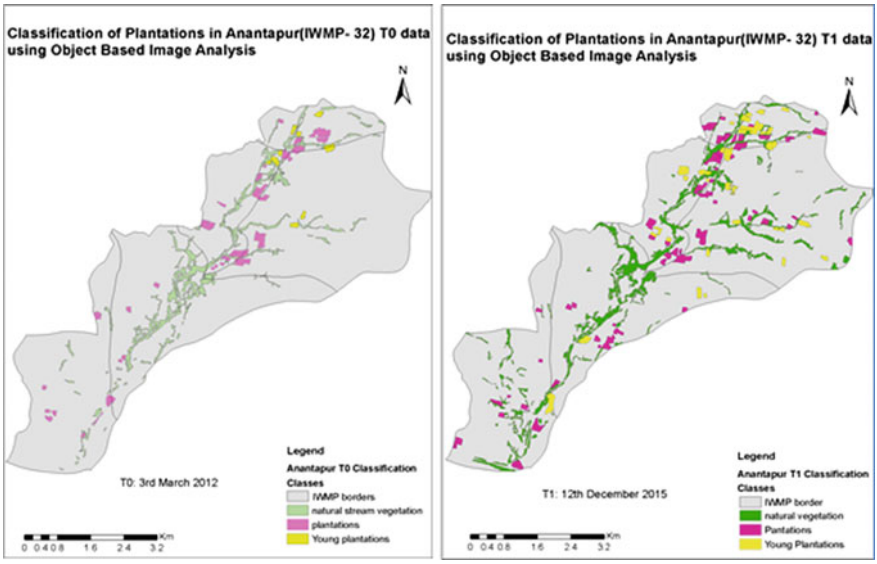

Fig. 6 Change detection in Anantapur IWMP-32 (T0 & T1) using OBIA method [3]

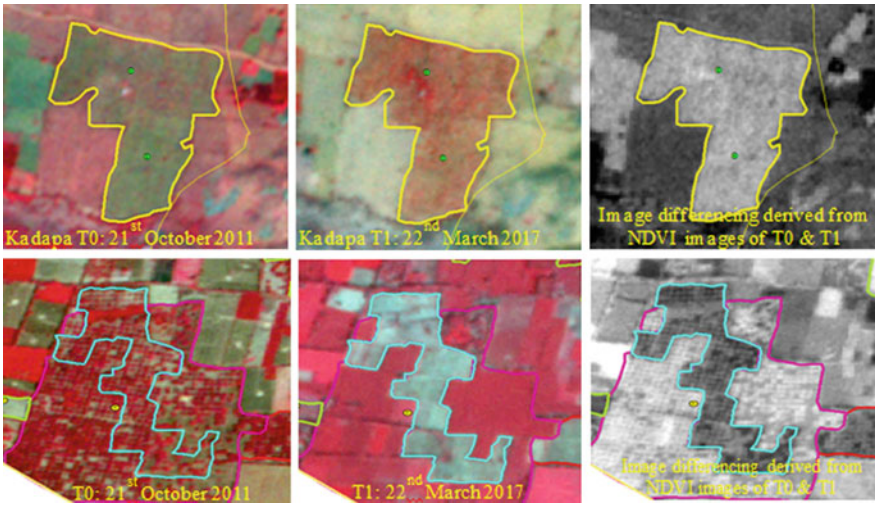

Fig. 7 Image showing the Increase in plantation and felling of plantations

The total increase in the area of the plantations = 370.44 ha and the total area under the felling of the plantations = 2.11 ha (Fig. 8).

Similarly for all the six IWMPs of different agro climatic zones of Andhra Pradesh the dynamic changes of plantations were identified by both the Bhuvan

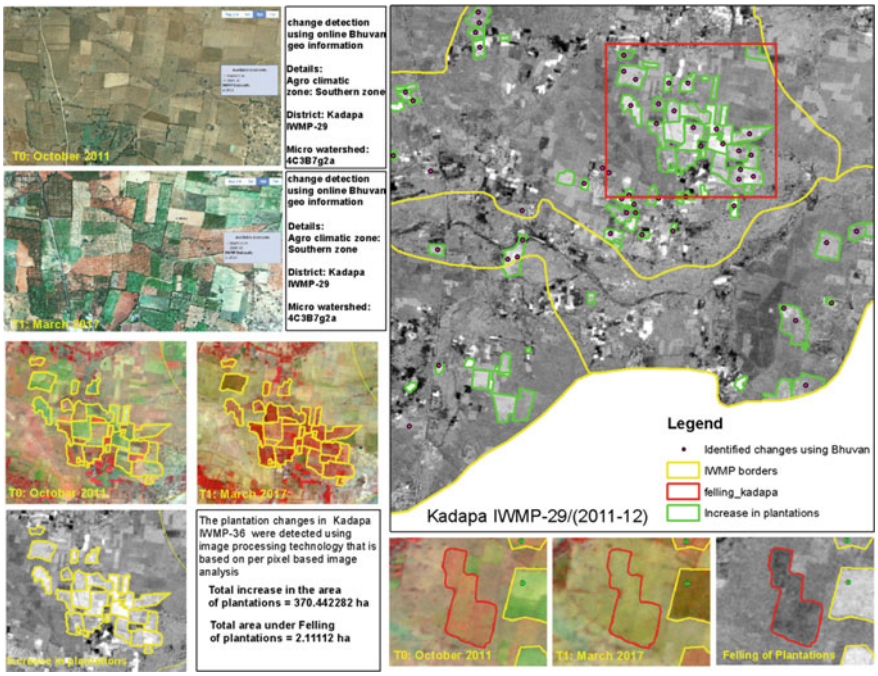

Fig. 8 Change detection through image differencing method in Kadapa IWMP-29

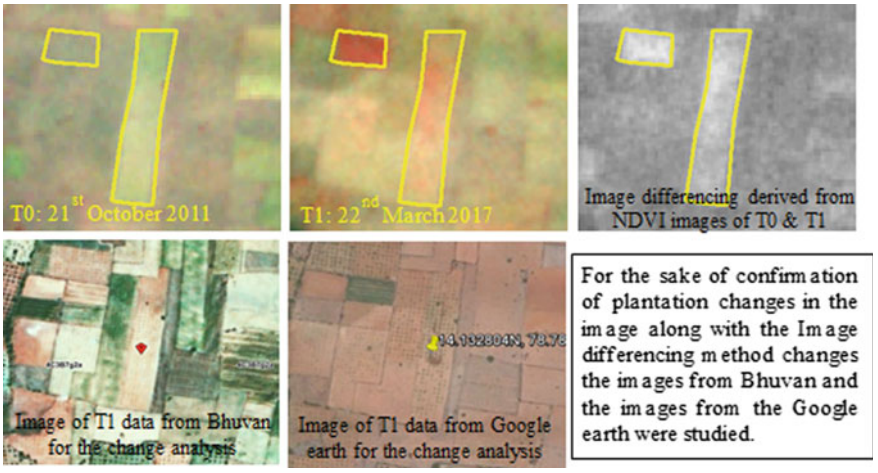

Fig. 9 Image showing the Young plantations through image differencing method

Table 4 Showing the changes in plantations in different IWMPs of Andhra Pradesh

S. no	Type of agro climatic zone	Districts	IWMPs	Total increase in plantations (in ha)	Total area under felling of plantations (in ha)
1	Southern zone	Kadapa	IWMP-29	370.44	2.11
2	Krishna zone	Prakasam	IWMP-36	213.47	41.24
3	High altitude tribal zone	Visakhapatnam	IWMP-11	11.87	5.24
4	North coastal zone	Vizianagaram	IWMP-10	61.34	11.35
5	Godavari zone	West Godavari	IWMP-01	125.62	32.35

based geo analysis and through the image processing techniques involving both the per pixel based image analysis methods and the object based image analysis method (Fig. 9; Table 4) [4].

The total area under the persistence plantations (plantations that were remained unchanged) that are identified in the West Godavari district IWMP-01 is 157.00 ha and that are identified in Vizianagaram IWMP-10 are 500.72 ha.

5 Conclusions

Remote Sensing data of multi spectral spatial and temporal data acquired through space borne remote sensors is of immense help for monitoring requires in watershed project. In the present study multi temporal data sets in conjunction with GIS, pixel based and object based image techniques are used to study the changes in Plantations in the watersheds that helps in implementing the sustainable developmental activities in the IWMPs for the growth and for balancing the hydrological cycle properly. In this study it is observed that by integrating the Bhuvan based analysis with the image processing methods, the dynamic changes in plantations were quantified.

References

1. Chen, G., Hay, G.J., Carvalho, L.M.T., Wulder, M.A.: Object-based change detection. Int. J. Remote Sens. **33**, 4434–4457 (2012)
2. Hussain, M., Chen, D., Cheng, A., Wei, H., Stanley, D.: Change detection from remotely sensed images: from pixel-based to object-based approaches. ISPRS J. Photogram. Remote Sens. **80**, 91–106 (2013)
3. Mag-usara, A.J.T., Japitana, M.V.: Change detection of Forest Areas using Object Based Image Analysis (OBIA): The Csae of Carrascal, Surigao Del Sur, Philippines.
4. Jawak, S.D., Devliyal, P., Luis, A.J.: A comprehensive review on pixel oriented and object oriented methods for information extraction from remotely sensed satellite images with a special emphasis on cryospheric applications. Adv. Remote Sens. **4**, 177–195 (2015)

Chapter 15
Role of Remote Sensing System for Disaster Area Response

G. Anjaneyulu and A. Suseela

Abstract Natural screw ups are excessive events in the earth's machine that bring about death or harm to human beings, and harm or lack of precious items, which include buildings, verbal exchange systems, agricultural land, woodland, natural surroundings and so on. The financial losses because of natural screw ups have proven a growth over the past four decades, resulting from the multiplied vulnerability of the global society, however additionally because of a boom inside the wide variety of weather-associated failures. For the natural disasters, a huge amount of data is required for remote sensing to get the information. Satellite far off sensing is the suitable device for disaster management, since it offers facts over massive regions, and at quick time intervals. Although it can be utilised inside the diverse stages of catastrophe management, which incorporates prevention, preparedness, relief, and reconstruction, in practice up until now it is in maximum cases used for caution and tracking. In olden days, remote sensing as used as a warning system for the natural disasters. The use of faraway sensing facts isn't possible without a proper device to deal with the big amounts of facts and integrate it with facts coming from other assets, inclusive of maps or measurement stations. Therefore, collectively with the boom of the faraway sensing packages, Geographic Information Systems have emerged as increasingly more important for disaster management. This thesis offers a examine of using faraway sensing and GIS for a number of vital catastrophe types.

Keywords Natural screw-up's · Disaster management · Remote sensing

G. Anjaneyulu (✉)
Narasaraopeta Engineering College, Narasaraopet, Andhra Pradesh, India
e-mail: anjig144@gmail.com

A. Suseela
Vasireddy Venkatadri Institute of Technology, Guntur, Andhra Pradesh, India
e-mail: alla.suseela@gmail.com

P. J. Rao et al. (eds.), *Proceedings of International Conference on Remote Sensing for Disaster Management*, Springer Series in Geomechanics and Geoengineering,
https://doi.org/10.1007/978-3-319-77276-9_15

1 Introduction

Natural screw ups are excessive sports within the earth's tool (lithosphere, hydrosphere, biosphere or surroundings) which differs considerably from the propose, resulting in loss of life or harm to humans, and harm or lack of treasured accurate, alongside houses, communiqué systems, agricultural land, wooded location, natural environment. They get the information on the effect of effect of the natural systems upon the socio-monetary system [1]. This effect may fast in earthquakes and slow in droughts and increases gradually. It is crucial to differentiate between disaster and hazard. A potentially unfavourable phenomenon (threat), which consists of an earthquake via itself isn't taken into consideration a catastrophe at the same time as it happens in uninhabited regions. It is known as a catastrophe whilst it occurs in a populated region, and brings damage, loss or destruction. Natural screw ups occur in lots of components of the arena, even though each form of catastrophe is constrained to positive areas. Figure 1 shows the information about the natural disasters like earthquake, floods, droughts and the cyclones in a worldwide.

Are focuses specifically in the world's plate limitations?

Disasters can be categorized in numerous ways. Those may be include:

- Natural screw ups are sports which may be due to in easy terms herbal phenomena and produce harm to human societies (which includes earthquakes, volcanic eruptions, hurricanes);
- Human-made failures are sports which can be because of human sports (which include atmospheric pollutants, commercial enterprise chemical accidents, principal armed conflicts, Nuclear accidents, oil spills;

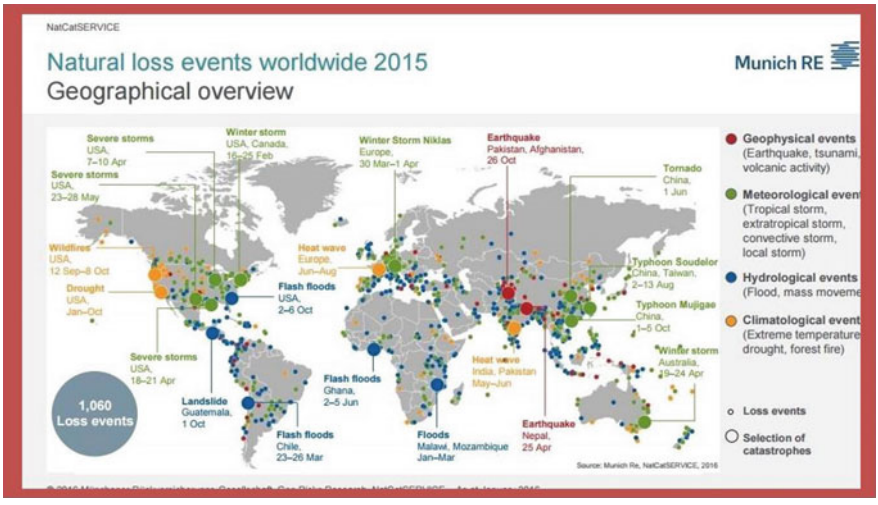

Fig. 1 World map of natural disasters

- Human-delivered on disasters are herbal disasters which may be improved/annoyed by means of manner of human effect.

In desk 1 the numerous disasters are categorised consistent with this kind, the usage of a few intermediate schooling. A landslide, as an example, can be handiest herbal, due to a heavy rainfall or earthquake, but it is able to moreover be human brought on, because of an over steepened road cut. The effect of natural failures to the global environment is becoming increasingly more excessive over the past a long term. The stated wide variety of catastrophe has dramatically multiplied, as well as the rate to the global economy and the amount of humans affected.

2 Disaster Management

One manner of managing natural risks is to disregard them. In many areas, neither the populace nor the government chooses to take the hazard because of herbal risks appreciably, due to many wonderful motives. The final number one terrible event may have happened long term inside the beyond, and is simplest consider as a story from the past. People may additionally moreover have moved in the place these days, even as not having the knowledge on ability risks. Or it can be that the hazard because of natural risks is taken as a right, given the various dangers and problems faced with in people's everyday lives. Cynical government may overlook about risks because the media exposure for their useful resource deliver after the catastrophe has took place has a good deal extra impact on electorate than the give up investment of budget for catastrophe mitigation. To correctly lessen the influences of herbal disasters a whole strategy for disaster manipulate is wanted, which is also known as the catastrophe manage cycle (see Fig. 2).

Disaster manage consists of ranges that take area earlier than a catastrophe takes place, disaster prevention and catastrophe preparedness, and three tiers that take place after the superiority of a disaster, disaster treatment, rehabilitation and reconstruction.

Fig. 2 The disaster management cycle. *Source* National Policy on Disaster Management

Disaster manage is represented right here as a cycle, for the cause that occurrence of a catastrophe event will in the end affect the manner society is making equipped for the Subsequent one.

The records required for catastrophe manages are coming from genuinely considered one of kind clinical disciplines, and must be included. Data integration is one of the strongest factors of GIS. In favoured the subsequent types of information are required:

- Data at the disastrous phenomena (e.g. Landslides, floods, earthquakes), their vicinity, frequency, price etc.
- Data at the environment wherein the disastrous sports activities ought to possibly take region: topography, geology, geomorphology, soils, hydrology, land use, plant life and masses of others.
- Data on the factors that is probably destroyed if the occasion takes place: infrastructure, settlements, populace, socio-monetary statistics and so on.
- Data at the emergency comfort property, which embody hospitals, hearth brigades, police stations, warehouses and loads of others.

The quantity and shape of statistics that must be saved in a GIS for disaster manages relies upon very masses on the level of utility or the size of the control mission. Natural risks data need to be blanketed robotically in improvement planning and investment venture preparation. Development and funding tasks need to embody a price/advantage analysis of making an investment in risk mitigation measures, and weigh them toward the losses which might be probably to arise if those measures are not taken [2] Although the choice of the scale of analysis is commonly decided by means of the supposed software program of the mapping consequences, the selection of a analysis approach stays open. This desire is based upon at the sort of problem, the supply of statistics, the provision of monetary assets, the time available for the research, in addition to the expert experience of the experts involved inside the survey. See additionally Cova [3] for an outline of the usage of GIS in emergency control. In the subsequent sections the use of a ways flung sensing for four forms of herbal disaster is discussed.

3 Remote Sensing and GIS Tools

Mitigation of herbal screw ups may be a hit only at the same time as unique facts is received approximately the predicted frequency, person, and importance of risky events in a place. Many styles of records which can be needed in natural catastrophe manipulate have an crucial spatial element. Spatial facts are data with a geographic thing, including maps, aerial snap shots, satellite TV for pc imagery, GPS information, rainfall records, borehole data and so forth. Many of those data will have a exceptional projection and co-ordinate machine, and need to be brought to a common map-basis, an awesome manner to superimpose them. We now have get

proper of access to records collecting and putting in place generation like some distance off sensing and geographic data structures (GIS), which have examined their usefulness in disaster manipulate.

First of all, far flung sensing and GIS offers a data base from which the evidence left in the back of with the aid of manner of failures that have befell earlier than may be interpreted, and blended with exclusive statistics to arrive at risk maps, indicating which regions are possibly risky. The donation of chance should be the premise for any catastrophe management mission and ought to supply planners and choice-makers with excellent enough and understandable facts. Remote sensing statistics, on the facet of satellite tv for pc tv for laptop images and aerial snap shots allow us to map the variability's of terrain houses, alongside side plant life, water, and geology, every in area and time. Satellite pictures provide a synoptic assessment and provide very beneficial environmental records, for a big variety of scales, from whole continents to information of a few metres. Secondly, many types of failures, which include floods, drought, cyclones, volcanic eruptions, and so on. May have wonderful precursors. The satellites can find out the early tiers of these sports as anomalies in a time series. Images are available at normal brief time durations, and may be used for the prediction of each fast and sluggish failure.

Then, whilst a disaster takes place, the rate of information collection from air and place borne structures and the opportunity of data dissemination with an identical swiftness make it possible to show the incidence of the catastrophe. Many screw ups may also affect large regions and no different device than some distance flung sensing should offer a matching spatial insurance. Remote sensing moreover lets in monitoring the occasion in the course of the time of prevalence whilst the forces are in whole swing. The vantage function of satellites makes it best for us to take into account, plan for and operationally show the event. GIS is used as a tool for the making plans of evacuation routes, for the layout of centres for emergency operations, and for integration of satellite TV for laptop facts with unique relevant statistics in the design of disaster warning structures.

In the disaster remedy phase, GIS is noticeably beneficial in combination with Global Positioning Systems (GPS) in are seeking out and rescue operations in regions which have been devastated and in which it is hard to orientate. The effect and departure of the disaster occasion leaves in the back of a place of big devastation. Remote sensing can help in damage evaluation and aftermath monitoring, imparting a quantitative base for comfort operations.

In the disaster rehabilitation section GIS is used to organise the damage facts and the put up-catastrophe census records, and in the evaluation of web sites for reconstruction. Remote sensing is used to map the ultra-modern state of affairs and update the databases used for the reconstruction of an area, and might help to save you that this type of disaster takes region once more.

The extent of statistics wished for catastrophe control, mainly within the context of incorporated improvement making plans, surely is an excessive amount of to be treated via manual techniques in a timely and effective way. For instance, the post catastrophe damage opinions on homes in an earthquake stricken metropolis, may be masses. Each one will need to be evaluated one at a time as a way to decide if the

building has suffered irreparable harm or now not. After that every one reports must be combined to derive at a reconstruction zoning interior a fairly small period of time.

4 Conclusions

The decade of the 1990s, genuine because of the fact the International Decade for Disaster Reduction, has no longer prompted a discount of the losses because of herbal disasters. On the other, the information show a rapid increase, both associated with an developing vulnerability of massive part of the earth's populace, in addition to to an boom inside the wide variety o f climate associated sports. The decade of the 1990s moreover confirmed a fast boom inside the technological competencies and tools that may be applied in disaster control. Some of those equipment address the gathering and management of spatial facts, consisting of some distance flung sensing and Geographic Information Systems. Although not one of the latest satellites turn out to be specifically designed to be used in catastrophe mitigation, maximum of them moreover have examined their usefulness in disaster prevention, preparedness and remedy.

The operational programs particularly use imagery with low spatial selection, coming from meteorological satellites or NOAA-kind satellite tv for pc tv for computer. The Turn-Around-Time (TAT) is the time required some of the photo is obtained until the solution must take transport of for the caution or monitoring of a selected threat. This differs strongly one shape of catastrophe to a few exceptional. For instance for wildfire the TAT can be very quick (0.5 h), for cyclone's and floods it is 24 h, and for drought it's miles weeks. The TAT depends on many elements, inclusive of the region of the occasion, the satellite constellation, the climate conditions (cloud loose pictures or radar), the records receiving components, records evaluation components (e.g. Visible interpretation or computerized evaluation) and industrial and crook components. In the various climate associated failures, obtaining cloud free pix for harm assessment is usually a immoderate hassle. For some styles of failures, which include floods, debris flows or oil spills, SAR is the solution in that case. For other kinds of screw ups (e.g. Landslides, earthquakes, wildfires) focused optical pictures should be used.

In the section of disaster consolation, satellite tv for pc tv for computer far flung sensing can only play a feature inside the identification of the affected regions, if sufficiently massive. Structural harm to homes can't be placed with the bad decision of the modern structures. Near Real Time harm and the area of viable victims has now end up viable with the availability of the number one civilian optical Very High Resolution (VHR) project, IKONOS-2, even though this could first rate make a difference if appropriate enough temporal selection, swath-coverage and prepared get right of entry to to the records can be completed. The temporal decision provided thru person satellites, mainly considering cloud cover, will now not be enough, and VHR will not turn out to be operational in harm mapping until a couple

of satellites are used. This capability is of excessive issue to consolation companies who require NRT imagery to find feasible victims and structures at risk, and additionally to map any adjustments to get admission to that could have happened. With the predicted availability of VHR information, co-ordination of strive and motivation to gather imagery becomes paramount. Ideally, their desires to be a single co-ordinating body for the ordering, receiving, schooling and dissemination of statistics.

In most times, the availability of GIS databases, containing statistics about elements at hazard, if blended with less centred pictures containing the increase of the area affected, will permit for a quick evaluation of the variety of men and women and homes affected.

References

1. Alexander, D.: Natural Disasters, 632 pp. UCL Press Ltd., University College London (1993)
2. OAS/DRDE.: Disaster, Planning and Development: Managing Natural hazards to reduce Loss. Department of Regional Development and Environment. Organization of American States. Washington, USA, 80 pp. (1990)
3. Cova, T.J.: GIS in Emergency management. In: Longley, P.A., Goodchild, M.F. Maguire, D.J., and Rhind, D.V. Geographical Information Systems, management and Applications (1999)

Chapter 16
Integration of Multiple Technologies in Web Environment for Developing an Efficient Framework for Emergency Management

V. Bhanumurthy and Vinod Kumar Sharma

Abstract Emergency management is a multi-disciplinary endeavor of applying science, technology, planning, and management to deal with extreme events. Effective emergency management demands availability of right data in right format at right time to enable disaster managers for taking efficient decisions at the time of crisis. Technologies and tools including remote sensing, geographical information system (GIS), web services and communication technologies have tremendous potential to support decision making process at the time of emergency. Integration of the available technologies and tool at a common platform for addressing emergency management is a challenge. Different technologies and tools have their own communication protocols and different data standards. To overcome this limitation in integrating all relevant multidisciplinary technologies, a comprehensive framework is proposed with the capabilities of database organization, integration, and decision making tools. This framework is a chain of action for dealing with all phases of emergency management life cycle. It facilitates the necessary components such as preparing for and recovering from a disaster or emergency situation. The integrated system yields as disaster dashboard services, multi-scale geospatial database, decision making tools, set of mobile applications for relief management. To test the capabilities of the framework in real time, it has been translated into a comprehensive emergency information system for National Disaster Response Force (NDRF) as a proof of concept in the form of geo portal. It is an end to end solution fulfilling all the requirements of the NDRF at ground starting from initiating an event to successful completion of the event.

Keywords Emergency management · GIS · Emergency management life cycle NDRF

V. Bhanumurthy · V. K. Sharma (✉)
National Remote Sensing Centre, Hyderabad, India
e-mail: vinod_sharma@nrsc.gov.in

V. Bhanumurthy
e-mail: bhanumurthy_v@nrsc.gov.in

P. J. Rao et al. (eds.), *Proceedings of International Conference on Remote Sensing for Disaster Management*, Springer Series in Geomechanics and Geoengineering,
https://doi.org/10.1007/978-3-319-77276-9_16

1 Introduction

Emergency management is the discipline dealing with risk and risk avoidance [1]. Emergency situation can arise due to a disaster, caused by a technology or natural process. Emergencies or disasters are no respecters of national borders and may not occur at convenient times. It can happen at any time, at any place. Emergency response demands rapid decisions in short time. In emergency conditions, the decision makers may commit mistake due to pressure. To minimize the manual mistake, it is very important to have emergency plans in place. WHO [2] recommends launching of a coordinated response mechanism for comprehensive emergency management. Response to deal with emergency situation relies on execution of one or more response plans. Command and control centre are responsible for proper execution of response plans on ground. The command and control center gives directions to the team on the field based on current situation. A commander on field coordinate and executes the relief activities with the help of support staff on ground, which has been monitored by the control center. New information about the emergency situation have been updated from the ground to the control center which has been analyzed and appropriate decisions have been transferred to on field team for execution. The activities during a disaster or an emergency incident are mostly tiresome and have to be carried out under severe pressure [3]. Selection of emergency plan for execution on the ground depends on the type of emergency or disaster event. Some time it become difficult to execute the emergency plans on ground due to adverse conditions, which includes bad weather, non-accessibility of the site, non-availability of equipments and many more. Hence, a set of optional plans has to be made for implementing most appropriate or suitable one. Real-time monitoring and control of response activities have been considered as integral parts of effective emergency response where the technologies play an important role. The ultimate objective of emergency management is to bring down the extent of disaster impact on the lives or property Therefore, emergency management means to identify challenges and be prepared for possibilities and threats through competence and comprehensive insight in activities and operations [4].

Emergency manager need rapid sharing of the database or information to analyse the situation. It requires the disaster-specific data for data interpretation, analysis and for the rescue and relief operations. Further, detailed spatial information at the larger scale, high resolution satellite data complementing the vector database and detailed spatial attributes with proper linking of secondary information, etc. in addition the above-mentioned database is essential. The most critical and difficult part is to immediately capture the information accurately following a disaster in terms of extent and impact of the event. Such information is important and essential requirement for effective response and decisions making. Unfortunately, the environmental and adverse situations prevailing after a disaster event prevent the timely acquisition of such information through conventional collection methods, such as ground surveys or telephonic reports. During such situations technologies such as Remote Sensing (RS), Global Positioning System (GPS), mobile devices,

communication satellites etc. are of immense use. Image Processing (IP) techniques, Geographic Information Systems (GIS) help in analysing the data received by various means in decision making. The technological advancements in the field of computer science, Information Technology (IT) and Open Geospatial Consortium (OGC) standards have significantly changed the GIS, allowing users to take advantage of new distributed mechanism. Internet GIS has become an important back bone for disseminating spatial database for emergency managers. Therefore, the emergency information systems with robust communication networks with the background of well-structured database, Location Based Services (LBS), decision support tools, etc. need to be integrated into a platform or a portal to assist the people responding to crisis, disasters and calamities.

For enabling the data/information and tools for decision making, an appropriate framework has to be developed with well-defined component for storing static database, ways and means to obtain field data in real/near-real time, integration of data obtained from multiple sources, communication channel/connectivity for exchange of information, dissemination of information to disaster managers and public. Sometimes, appropriate information is required at right time (preferably near-real time) for situation assessment during response. Therefore development of a suitable framework for emergency management has been proposed through integration of multiple technologies for effective management of emergency event.

2 Design Objectives and Multi-disciplinary Technologies for Emergency Management

Emergency management is a key challenge and priority issue for any country. It involves multi-disciplinary fields for real-time decision making. Sometimes, appropriate information is required at right time for situation assessment during response. Various technologies including Remote Sensing, Geographic, Mobile Technology and Global Positioning System and Web Technology have got potential role to play in managing emergency situations. Therefore, it is proposed to develop a suitable framework for emergency management through integration of various multi-disciplinary technologies. This framework results effective exchange of information for decision making, communication among response teams and disaster managers besides information on the situation prevailing at disaster site in real/near real-time.

2.1 Design Objective

The objective of the research is to develop a suitable framework for addressing emergency management through integration of multidisciplinary technologies for effective decision making.

The framework is intended to demonstrate and utilise on pilot basis for National Disaster Response Force (NDRF), a premier organisation of Ministry of Home Affairs, Government of India for carrying out relief and rescue operations.

2.2 *Multi-disciplinary Technologies for Emergency Management*

Today a host of technologies and tools such as Remote Sensing (RS), Geographical Information System (GIS), Global Positioning Systems (GPS), Internet, Web services, Database systems, Information Technology (IT), Communications etc. are widely used in various fields contributing to the geographic mapping and analysis of the Earth and human societies. Availability of these technologies in Free and Open Source Software (FOSS) has open up many new avenues for implementation of emergency management framework. Integration of these diverse technologies into a seamless environment provides an effective and easy to use solution for implementation of geoplatform for decision making process for emergency situations. Some potential technologies are discussed in the following sections.

2.2.1 Remote Sensing

Remote sensing is the acquisition of information about an object or phenomenon without making physical contact with the object. Remote sensing makes it possible to collect data from inaccessible areas. Remote Sensing has a growing relevance in the modern information society. Furthermore, remote sensing exceedingly influences everyday life, ranging from weather forecasts to reports on climate change or natural disasters [5]. The Earth observation satellites covering large areas at various spatial and temporal scales in real-time have become valuable sources of information related to atmosphere and earth surface. Polar orbiting satellites have the advantage of providing much higher resolution imageries, even though at low temporal frequency, which could be used for detailed monitoring, damage assessment and long-term relief management. Geo-stationary satellites provide continuous and synoptic observations over large areas on weather including cyclone monitoring [6].

Satellite images acquired prior and after disaster event show the areas affected thereby assists the disaster managers in assessing the damages.

2.2.2 Geographic Information System

Geographic Information System (GIS) is a computer based information system used to digitally represent and analyse the geographic features present on the earth'

surface and the events that taking place on it. GIS technology plays an important role in the emergency management activities. The important phases of emergency management require variety of database from various sources. This data is typically a spatial data along with attributes and live information as an important input for development of emergency management systems. By utilising the capabilities of GIS, one can share the information through databases on computer generated maps for visualisation. Most of the data requirements for emergency management is of spatial nature and need spatial support for visualisation and decision making. The capabilities of GIS make very large impact on the planning, mitigation, preparedness and response phases through database integration, organisation, and interfacing with high level programming languages for implementation of geoportals [7].

2.2.3 Mobile Technology and Global Positioning System

Use of mobile and GPS technologies in disaster management should be seen as a new era to aid better management of disaster relief operations. The use of mobile applications in disaster management and emergencies has greatly improved due to the leading advances in telecommunication and remote sensing techniques. Mobile technology has its wide application in area of disaster management. The technology is helpful in tracking people in disaster prone areas. Users can be tracked with the help of GPS in mobile phones. As the technology is advancing, the area of mobile usage has greatly expanded due to 3G, social networking, video, android, etc which has led to enormous growth in communication and enhanced channels of communication [8]. Use of smart phones has greatly come over all the technologies due to reduced cost and improved capability. Use of latest technologies enabled in android mobiles help in providing location using GPS, quick internet access and in some mobile devices pre-disaster warning. The users have the capability to receive updates about the disaster events and also pass the messages to others who could be affected.

2.2.4 Web Technologies

The World Wide Web (WWW) is the universe of network-accessible information, an embodiment of human knowledge. Web browsers on the client side for rendering data presentation coded in HTML, a web server program that generates data presentation, an application server program that computes business logic, and a database server program that provides data persistency. The three types of server programs may run on the same or different server machines. Web browsers such as Internet Explorer, Google Chrome etc., can run on most operating systems with limited hardware or software requirement. Adobe Flex is another technology often used in Web 2.0 applications. Compared to JavaScript libraries like jQuery, Flex makes it easier for programmers to populate large data grids, charts, and other heavy user interactions. HTML5 offers many new technologies that allow content to

be delivered to users in a more streamlined and personalized manner. Web 2.0 sites have recently started using Javascript/Ajax framework. There had been a rapid development in field of web. It has its impact in almost every area such as education, research, technology, commerce, marketing etc. So the future of web is almost unpredictable.

All the above mentioned technologies have been integrated together on a platform, resulting in a framework to manage the emergency situations.

3 Methodology

Implementation of proposed framework for addressing emergency management, involves seamless integration of multiple technologies such as Remote Sensing (RS), Geographic Information Systems (GIS), Global Positioning Systems (GPS), Database Management Systems (DBMS), Web GIS, Location Based Services (LBS), Information Technology (IT), Communication Technologies etc.

The multi-disciplinary technologies has been integrated and connected together (Shown in Fig. 1) in the proposed framework to manage emergency situations. The framework have been implemented on a geo-web platform to address the real time emergency situation. The possible emergency phases including Relief Management, Medical services, Contingency plan and Evacuation have been incorporated as a module in a web based spatial decision support system (SDSS). The web based SDSS have been implemented using 3 components:

1. Organisation of database
2. Availability of organized data as an service coupled with web interface
3. Customization of spatial DSS tools, disaster dashboard and communication protocols

The detailed workflow of developed emergency management information system is shown in Fig. 2.

The first major step is to collect and organize the heterogeneous spatial and non-spatial database. Database schema and automatic procedures have developed to arrange and organize the data layers collected from different resources in a seamless way.

The organised data have been coupled with a web based interface developed using open source web technologies to execute data driven web interface. OSGEO open source standards have been followed in development of the web portal. DSS tools have been developed to perform complex GIS operations on to the data for generating the relief and rescue plans. Further the portal is organized, depending on the type of natural disasters. Individual disaster specific modules helps the decision makers to view, analyze and interpret the disaster specific data in an efficient manner. An end to end solution for addressing the emergency situation have been developed to manage the emergency situation. To test the capability of the

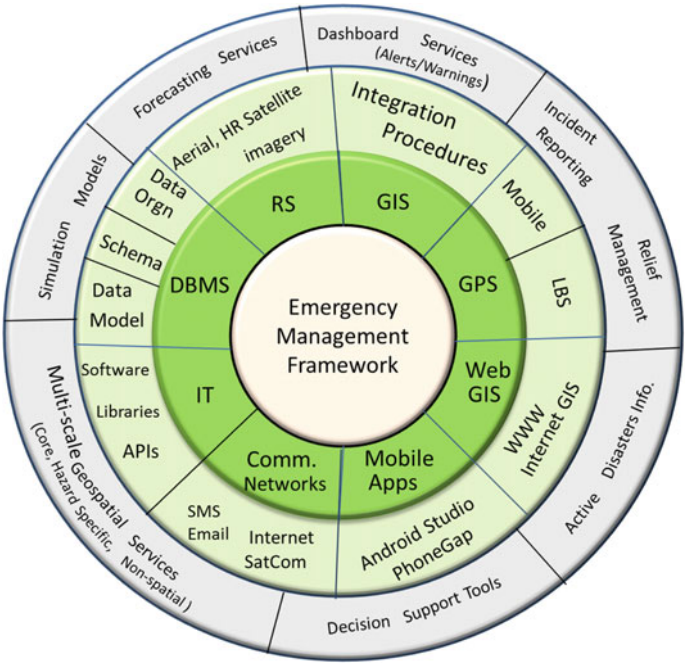

Fig. 1 Multi-disciplinary technologies for emergency management

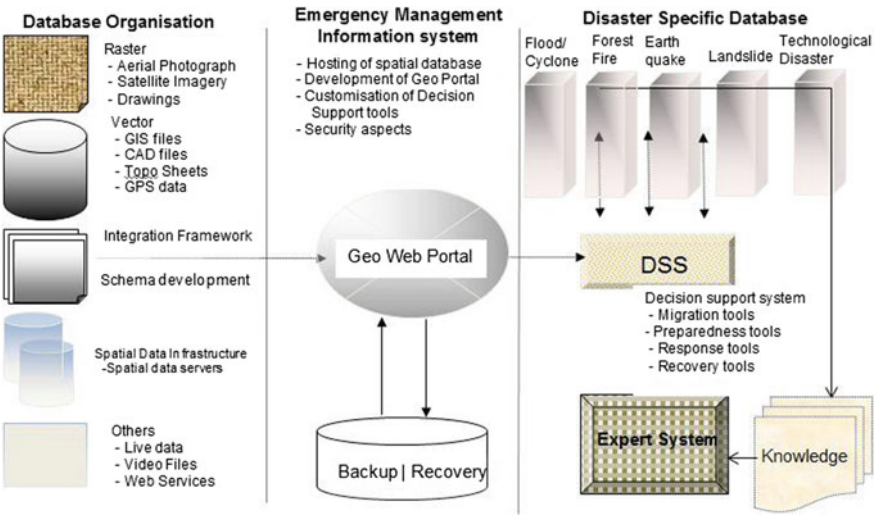

Fig. 2 Workflow for EMIS

developed system in real time, the framework have been customized as per the needs of Natural Disaster Response Force (NDRF) for carrying out relief and rescue operations.

4 Application Case Study

To test the framework capabilities in disaster situation, a dummy disaster situation cum mock drill has been organized by the NDRF officials. The Graduate level officials has been fully trained to use the system developed in web environment, before the mock drills. The framework customized for NDRF has been categorized into 5 modules namely:

1. Situation assessment—Alerts, warnings, live news from disaster dashboard.
2. Map Viewer—Battalion wise/Head Quarter map interface for visualization of multi-scale data services with standard GIS tools.
3. Disaster incident reporting—Incident reporting from the field and subsequent approval from the HQ.
4. Decision support tools—Customized decision support tools for relief and rescue operations.
5. Communication—One to one/many communications means through text messages, live audio video chat, mail etc.

Detailed working of each modules is explained below.

4.1 Situation Assessment Module

A web based disaster dashboard integrating the information about alerts and warning from different nodal departments along with disaster news has developed as shown in Fig. 3.

Live feeds from different nodal departments as an service has been integrated into the dashboards. In addition, heterogeneous data from different resources has been transformed and organized for visualization, analysis and alert generation.

4.2 Spatial Online Map Viewer

An open source spatial web viewer is developed (Fig. 4) facilitating, visualization of multi-scale data services with standard GIS tools to NDRF officials. They can select the datasets to view and analyze, from data driven options provided in spatial web viewer.

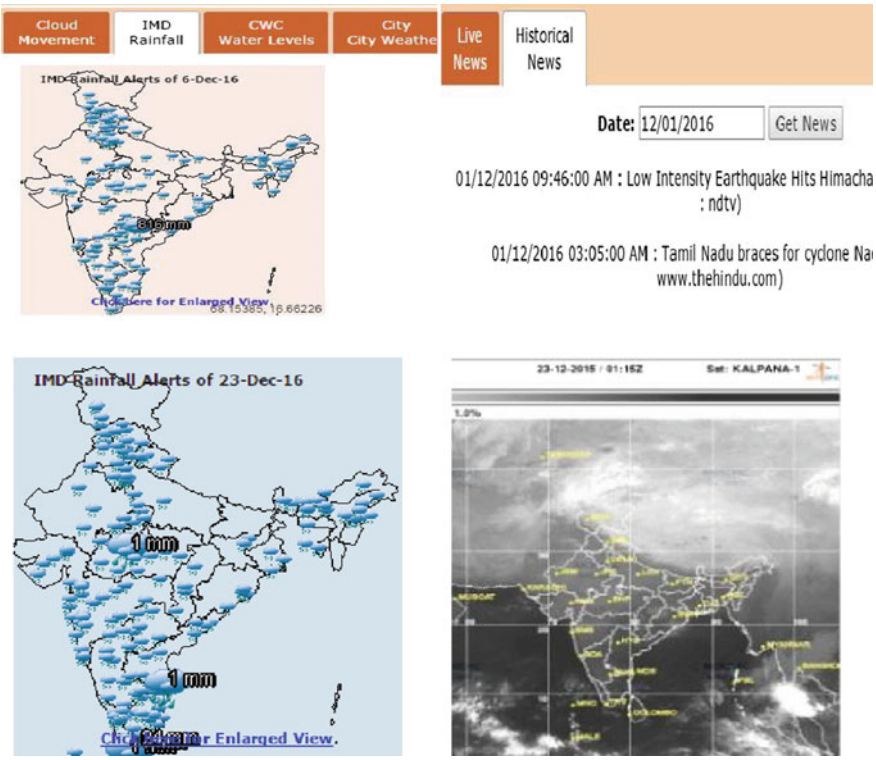

Fig. 3 Live data integrated into disaster dashboard

4.3 Disaster Incident Reporting

Android based mobile application has been developed to report the disaster incidents to the central server from the field in near real time using GPRS. Below mentioned android based mobile applications (Fig. 5) has developed and given to NDRF officials to test the same on ground:

1. Relief management
2. Geo-Spatial data collection
3. Geo-Tagging of emergency facilities

The incident reported using the mobile application from field can be visualized on to the portal and appropriate decisions can be communicated back to the field in near real time. A sample incident reported by the NDRF officials during the mock is shown in Fig. 6.

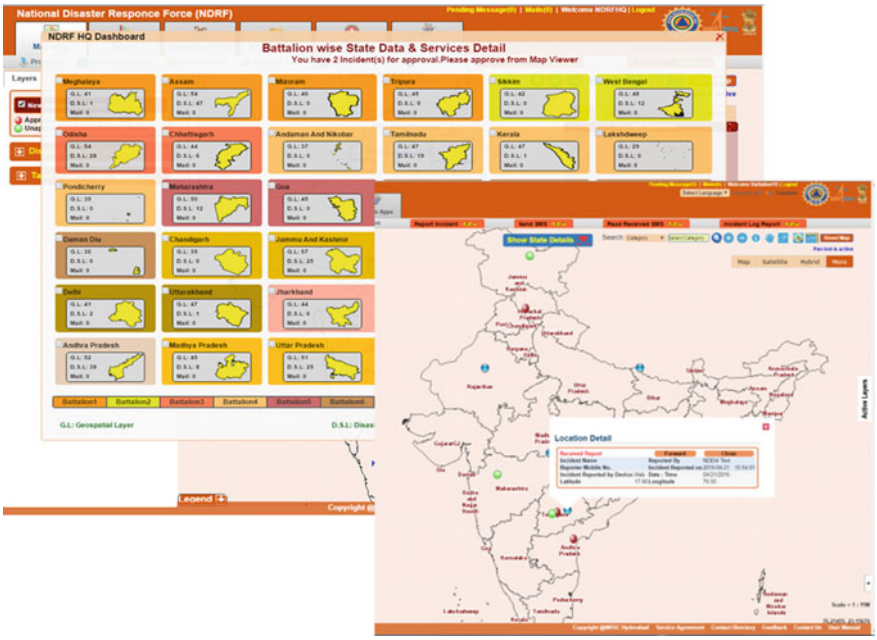

Fig. 4 Spatial web viewer for data visualisation

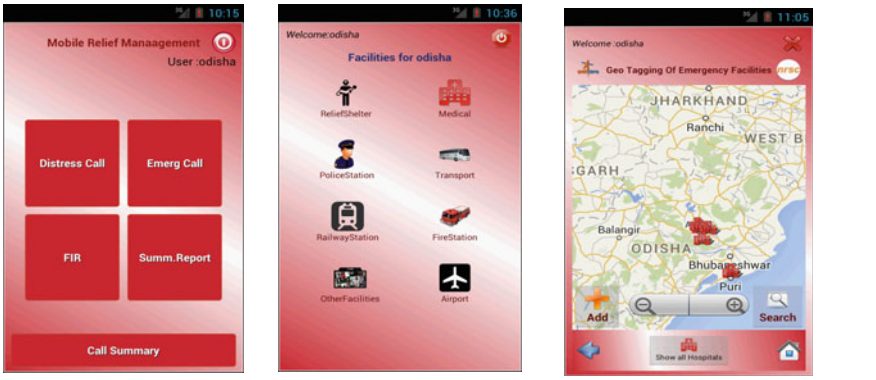

Fig. 5 Android based mobile application

4.4 Decision Support Tools

Decision makers for taking decisions on the reported events needs certain complex tools, which can help them in analyzing the situations. Complex tools like shortest

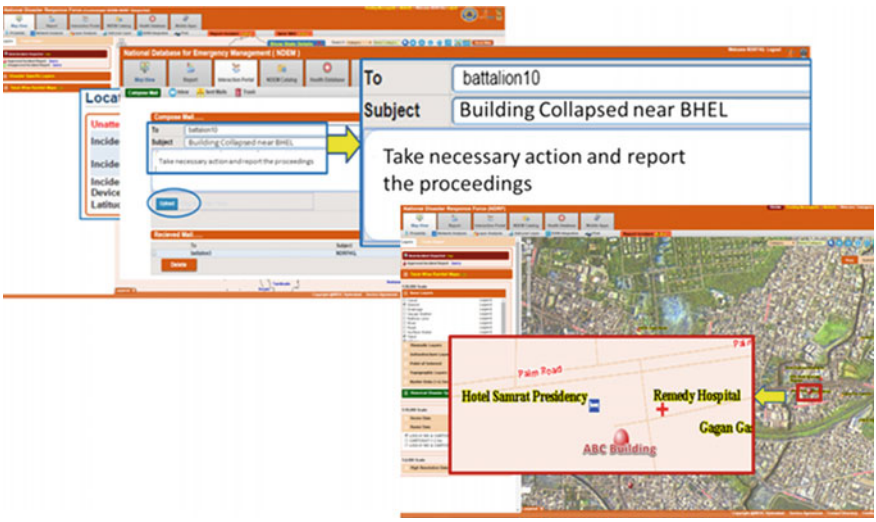

Fig. 6 Disaster incident reporting and decision making

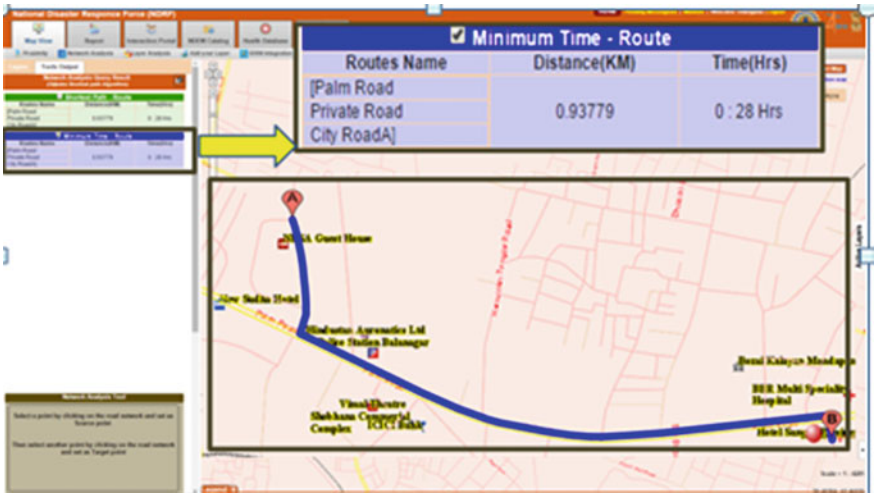

Fig. 7 Executing shortest path

path and proximity analysis can help decision makers to know which are the hospitals near the incident location and which is the shortest path to follow to reach the hospital in less time. To facilitate this, proximity analysis and shortest path tools are integrated and executed on spatial DSS as shown in Figs. 7 and 8.

Fig. 8 Executing proximity analysis

4.5 Communication Module

An audio/video chat with live stream transfer communication shown in Fig. 9 has been implemented in web environment. Using this module more than 2 people can interact with each other by sending text, audio and video. It facilitates live reporting and communicating the decisions from control room to field.

The above explained modules clearly indicated the capability of the framework developed by integrating the multiple technologies to manage the emergency situation. The framework inform of a geo web portal available at http://ndrf.nrsc.gov.in/central/ in internet domain, for NDRF is helping them in managing the emergency situation in real time.

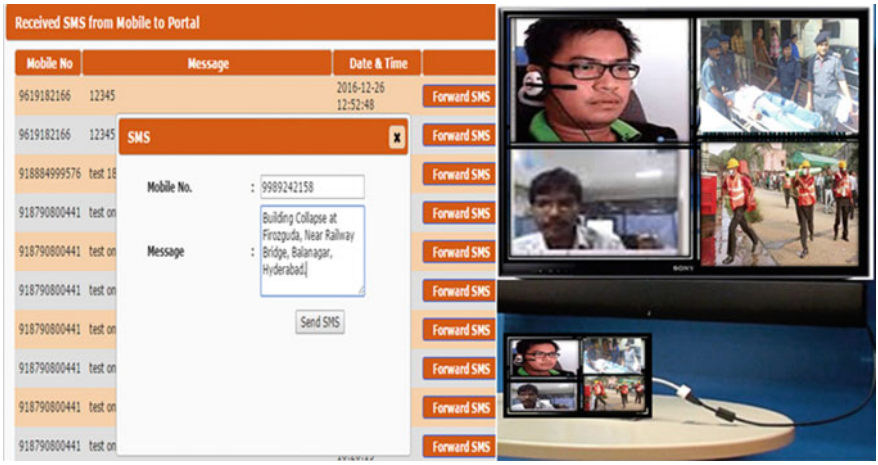

Fig. 9 Communication module showing text/audio/video chat

5 Conclusion

Emergency management involves multi-disciplinary effort, requiring various kinds of data available for emergency managers in right format for effective decision making. No single tool or technology available cannot manage the emergency situation efficiently. There is a need to utilize the services, expertise and availability of different software modules/technologies in an integrated manner, seamlessly. Complexity and nature of available technologies, restricts the direct integration with each other. To overcome this an effective and robust framework is proposed, developed and successfully tested in real time for managing the emergency situation. The developed framework is robust, secure and interoperable in nature. It facilitates relief and rescue organisation with a facility of incident reporting from field using mobile application, which further helps in triggering the response by the responding agencies, in addition of integrating various warning and alerts provided by different nodal agencies. Its ability to organize the multiple, huge heterogeneous data make it an efficient data repository with complex spatial analysis tools, managing important databases like emergency facilities including hospital information. It is an end to end solution for the decision makers by the technological experts.

Acknowledgements We thank Dr. Y. V. N. Krishna Murthy (Director NRSC) for providing the continues guidance throughout the process. We are grateful to colleagues at the National Database for Emergency Management, Disaster Management Support Group & National Disaster Response Force for support and cooperation.

References

1. George, H., Jane, B., Damon, P.C.: Introduction to Emergency Management, 5th edn. Elsevier, Burlington (2013). ISBN 13: 978-1856179591
2. World Health Organization: Risk reduction and emergency preparedness. WHO six-year strategy for the health sector and community capacity development (2007). ISBN 978 92 4 159589 6
3. Mendonça, D., Beroggi, G.E.G., Wallace, W.A.: Decision support for improvisation during emergency response operations. Int. J. Emergency Manage. **1**(1), 30–38 (2001)
4. Karina, A., Torstein, T.: Learning in emergency organisations: trial without error. Int. J. Emergency Manage. **1**(4), 410–421 (2003)
5. Van Westen, C.J., Rengers, N., Terlien, M.T.J., Soeters, R.: Prediction of the occurrence of slope instability phenomenal through GIS-based hazard zonation. Geol. Rundsch. **86**(2), 404–414 (1997)
6. Jayaraman, V., Chandrasekhar, M.G., Rao, U.R.: Managing the natural disasters from space technology inputs. Acta Astronaut. **40**(2–8), 291–325 (1997)
7. Bhanumurthy, V., Jai Shankar, G., Ram Mohan Rao, K., Nagamani, P.V.: Defining a framework for integration of geospatial technologies for emergency management. Geocarto Int. **30**(9), 963–983 (2015). https://doi.org/10.1080/10106049.2015.1004132
8. Lachner, J., Hellwagner, H., Roland Kop, K., Steinberger, C., Günther, C.F.: Information and communication systems for mobile emergency response. In: Information Systems and e-Business Technologies: 2nd International United Information Systems Conference UNISCON 2008 Klagenfurt, Austria, 22–25 Apr 2008 Proceedings. http://dx.doi.org/10.1007/978-3-540-78942 (2008)

Chapter 17
Assessment of Soil Erosion in Upper Tungabhadra Sub basin by Using Universal Soil Loss Equation and Geospatial Techniques

Nekkanti Haripavan, G. V. Ramalingeshwararao, G. Abbaiah and G. Sai krishna

Abstract Soil erosion is an acute problem in India. Soil erosion not only affects the agriculture sector by directly decreasing the crop productivity but also indirectly exacerbates water scarcity by reducing the storage capacity of reservoirs. It is important but very difficult to estimate the precise extent of soil lost in a particular hydrological event of a watershed. Many experimental and theoretical methods were proposed to get the volume of soil lost. Graphical models were also developed for finding the computational and graphical results for soil erosion using different software programmes. Remote Sensing and Geographical Information System Software are emerging as important tools for estimating soil erosion. The main objective of the present study is to find out the quantity of soil lost from Upper Tungabhadra Sub basin by using Universal Soil Loss Equation (USLE), Remote Sensing (RS) and Geographical Information System (GIS). This is accomplished by determining the Soil erodibility (K), Rainfall erosivity (R), Topographic factor (LS), cropping factor (C) and conservation factor (P). The Tungabhadra Upper sub basin constitutes 45 watersheds having different geographical patterns with an average annual rainfall varying from 200 to 2500 mm. The factors affecting the erosion have been obtained by developing Rainfall erosivity, soil erodibility, Digital Elevation Model, Land use Land cover, and Annual rainfall maps.

N. Haripavan (✉) · G. Sai krishna
Gudlavalleru Engineering College, Gudlavalleru, India
e-mail: haripavan77@gmail.com

G. Sai krishna
e-mail: sai.gundapaneni@gmail.com

G. V. Ramalingeshwararao
GPEC, Kurnool, India
e-mail: naga.gajavalli@gmail.com

G. Abbaiah
JNTUK, Kakinada, India
e-mail: abbaiah@yahoo.com

P. J. Rao et al. (eds.), *Proceedings of International Conference on Remote Sensing for Disaster Management*, Springer Series in Geomechanics and Geoengineering,
https://doi.org/10.1007/978-3-319-77276-9_17

Keywords USLE · GIS · RS · DEM

1 Introduction

Soil erosion is a serious problem in today's scenario. Technically, the eroded soil can be calculated by using USLE (Universal Soil Loss Equation) along with an advanced GIS tool. It is difficult to calculate or estimate the soil loss of an area or catchment or a basin through field study in a reasonable time. One could attempt a GIS based assessment which certainly saves much time and could also meet the accuracy expectations for formulating realistic erosion control measures.

Soil erosion

Soil erosion occurs due to heavy rains which erode the top layer of the soil. Soil erodibility can be estimated by the physical properties of the soil. Texture is an important characteristic affecting erodibility, but structure, organic matter and permeability also plays a key role in estimating the erodibility. Generally, soils with faster infiltration rate, higher levels of organic matter and improved soil structure show greater resistance to erosion. Sand, sandy loam and loam-textured soils tend to be less erodible than silt, very fine sand and certain clay-textured soils. Tillage and cropping practices reduce soil organic matter levels, cause poor soil structure, or result in soil compaction, contribute to increases in soil erodibility.

USLE (Universal Soil Loss Equation)

ARS scientists W. Wischmeier and D. Smith, has developed the most widely accepted and utilized soil loss equation to predict average annual soil loss and which can estimate long-term annual soil loss and guide conservationists on proper cropping, management, and conservation practices.

The USLE for estimating average annual soil erosion is

$$\mathbf{A = RKLSCP}$$

A = average annual soil loss in t/ha (tons per hectare)
R = rainfall erosivity index
K = soil erodibility factor
LS = topographic factor—L is for slope length and S is for slope
C = cropping factor
P = conservation practice factor

GIS (Geographical information system)

GIS (Geographical Information System) is a prominent tool used in today's research advancement as it provides facility of create, edit, modify, analyse, store, and retrieve both spatial and non-spatial data. It gives the both graphical and attribute results which can be used for further analysis where needed. With GIS we can generate slope map, rainfall intensity map, soil map, Land Use map which are used to calculate the soil loss.

2 Area of Study

The work has been carried out for Tungabhadra Upper sub-basin of India's second largest Basin Krishna with an extent 74° 48′ to 76° 29′E, 13° 7′ to 15° 44′N covering an area of 28,519.41 km^2. It covers 12 districts of Karnataka state with 45 watersheds (Figs. 1 and 2; Table 1).

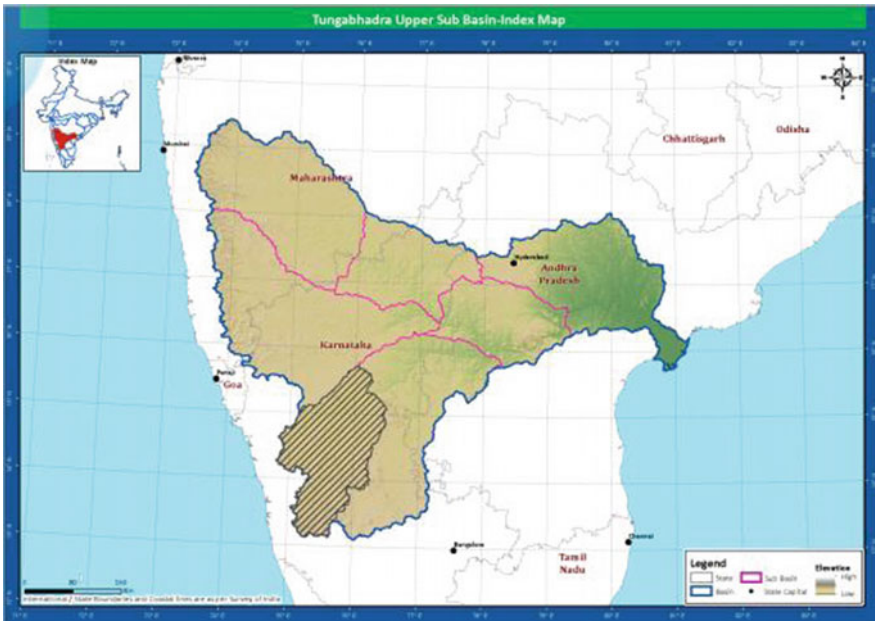

Fig. 1 Study area of Tungabhadra upper sub-basin, Krishna basin

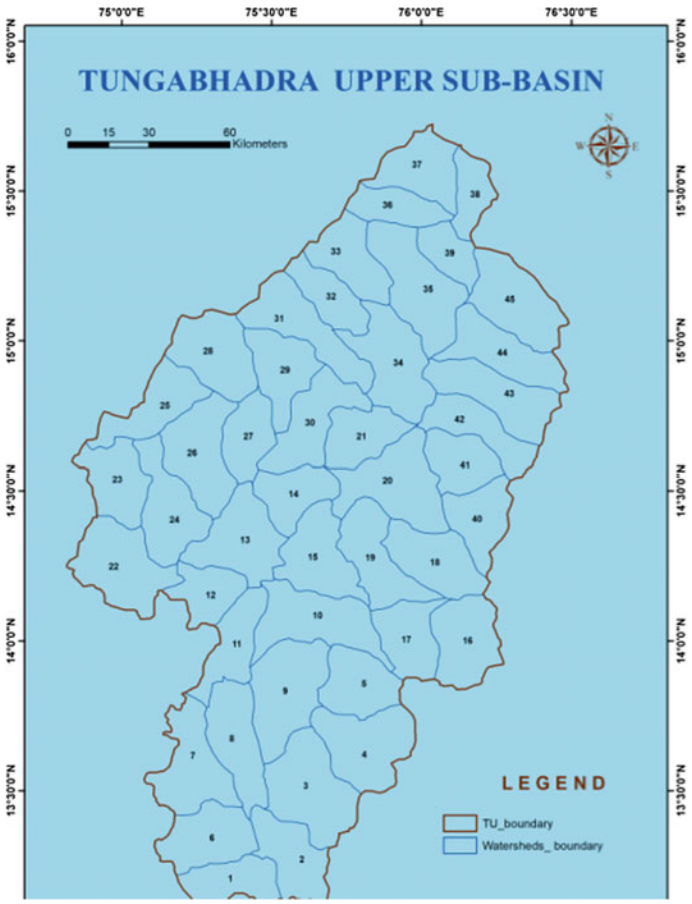

Fig. 2 Tungabhadra upper sub-basin with watershed boundaries

Table 1 Areas of 45 watersheds and their share in the Tungabhadra Upper Sub Basin

Sl. No.	WaterShed code	Area (km^2)	% Area
1	C04TUU01	508.63	1.78
2	C04TUU02	601.89	2.11
3	C04TUU03	923.94	3.24
4	C04TUU04	808.76	2.84
5	C04TUU05	557.26	1.95
6	C04TUU06	636.88	2.23
7	C04TUU07	758.94	2.66
8	C04TUU08	702.33	2.46
9	C04TUU09	853.22	2.99
10	C04TUU10	833.94	2.92

(continued)

Table 1 (continued)

Sl. No.	WaterShed code	Area (km^2)	% Area
11	C04TUU11	520.17	1.82
12	C04TUU12	413.86	1.45
13	C04TUU13	756.15	2.65
14	C04TUU14	478.31	1.68
15	C04TUU15	690.47	2.42
16	C04TUU16	667.22	2.34
17	C04TUU17	551.56	1.93
18	C04TUU18	641.39	2.25
19	C04TUU19	664.11	2.33
20	C04TUU20	876.53	3.07
21	C04TUU21	507.92	1.78
22	C04TUU22	823.27	2.89
23	C04TUU23	562.74	1.97
24	C04TUU24	705.53	2.47
25	C04TUU25	587.19	2.06
26	C04TUU26	761.2	2.67
27	C04TUU27	446.92	1.57
28	C04TUU28	734.83	2.58
29	C04TUU29	557.78	1.96
30	C04TUU30	650.31	2.28
31	C04TUU31	737.82	2.59
32	C04TUU32	425.4	1.49
33	C04TUU33	568.83	1.99
34	C04TUU34	798.76	2.8
35	C04TUU35	921.24	3.23
36	C04TUU36	384.28	1.35
37	C04TUU37	572.05	2.01
38	C04TUU38	347.82	1.22
39	C04TUU39	331.6	1.16
40	C04TUU40	510.57	1.79
41	C04TUU41	479.82	1.68
42	C04TUU42	527.7	1.85
43	C04TUU43	739.34	2.59
44	C04TUU44	646.4	2.27
45	C04TUU45	744.51	2.61

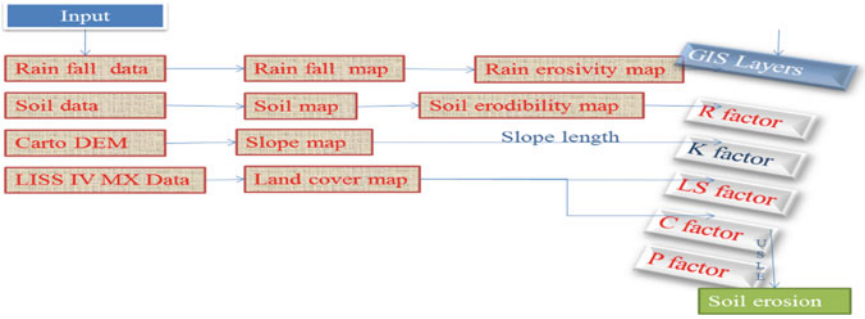

Fig. 3 Work flow of USLE using GIS

3 Methodology

The amount of eroded soil has been calculated by obtaining the parameters R, K, LS, C, P. These parameters are derived by using GIS. The steps involved are, preparing the raster and vector database of annual rainfall map, rainfall erosivity index map, soil map, soil erodibility map, DEM (Digital Elevation Model), slope, aspect and LULC by performing surface analysis (Fig. 3).

4 Experimental Investigations

Digital Elevation Model, slope, slope length maps are obtained from Carto DEM 1 ArcSec from Bhuvan—NRSC, Rain fall map, Rain fall Erosivity maps are composed from the data obtained from Annual rainfall data from IMD, Soil map, Soil Erodibility maps are composed from the data obtained from Geological Survey of India.

Factor values have been adopted depending on the area of study, soil type and cultivation habits. The values for the factors are as follows.

Rainfall erosivity index 'R'

The relationship between erosivity index (R) and annual rainfall has been developed by Singh et al. (1981) after analyzing the data collected from 45 stations distributed in different rainfall zones throughout the country. The relationship can be expressed as

$$\mathrm{R} = 79 + (0.36 * \text{annual rainfall})$$

Soil erodibility factor 'K'

Table 2 Soil erodibility value

Type of soil	K factor
Alluvium	0.17
Red loamy	0.15
Black	0.142
Red and Black	0.16

The factor quantifies the cohesive character of a soil type and its resistance to dislodging and transports due to raindrop impact and overland flow sheer forces (Table 2).

Topographic factor 'LS'—L is for slope length and S is for slope

Steeper slopes produce higher flow velocities. Longer slopes accumulate runoff from larger areas and result in higher flow velocities.

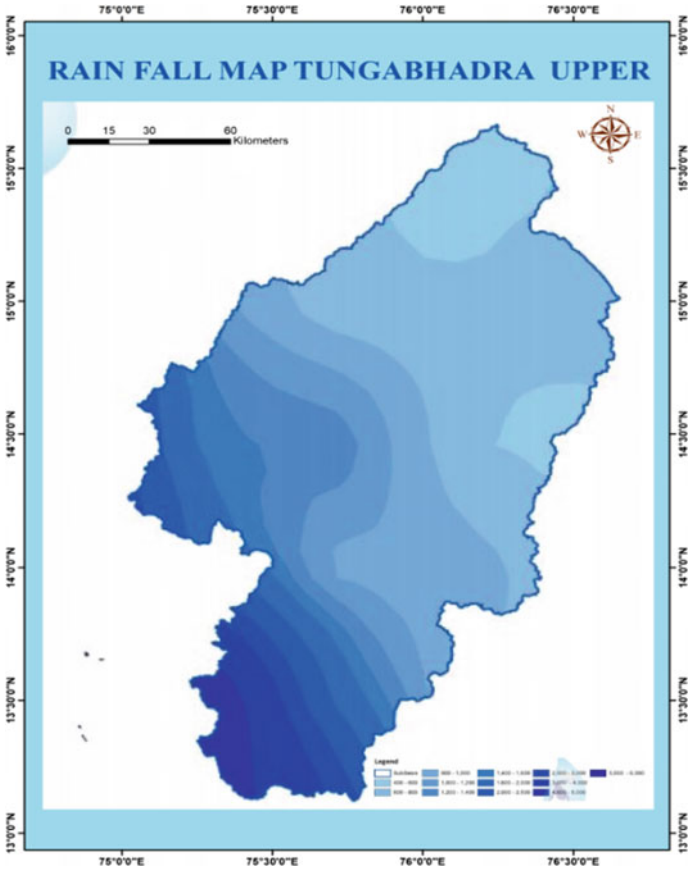

Fig. 4 Rain fall map

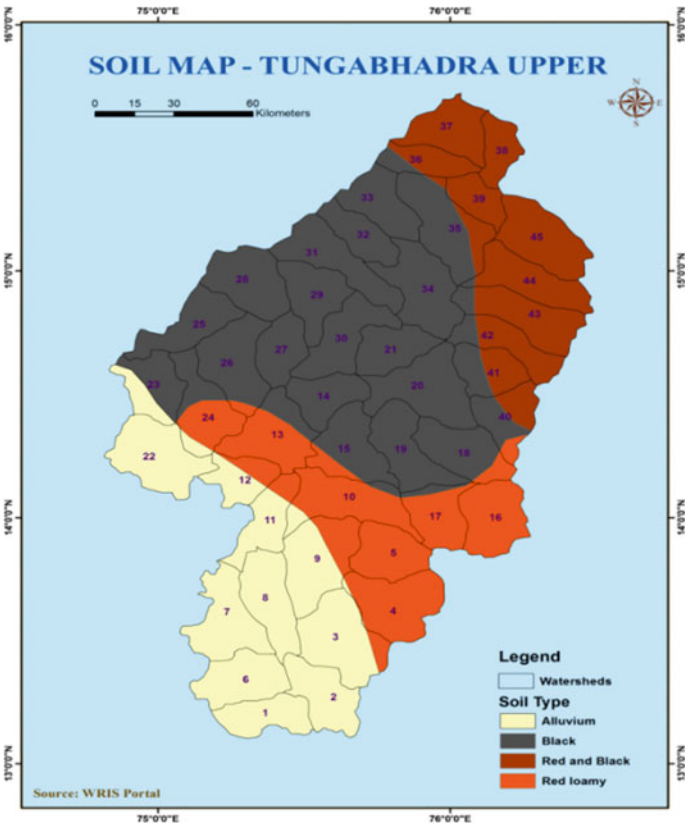

Fig. 5 Soil map

Cropping factor 'C'

The ratio of soil loss from land cropped under specified conditions to corresponding loss under tilled, continuous fallow conditions. It measures the combined effect of vegetation cover and management variables.

Conservation practice factor 'P'

The ratio of soil support practice to the corresponding loss with up and down slope culture. Practices included in this term are contouring, strip cropping and terracing (Figs. 4, 5, 6, 7, 8, 9; Tables 3 and 4).

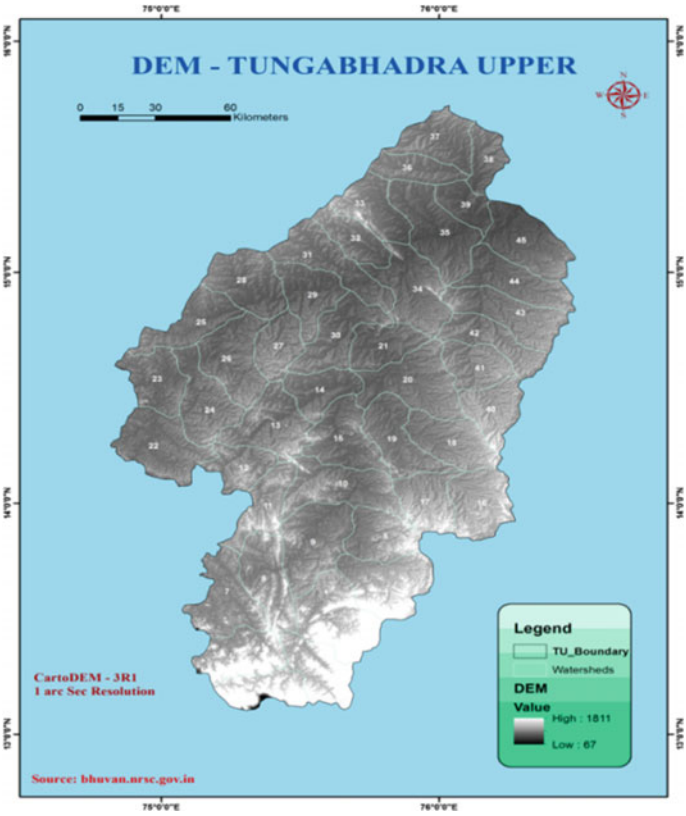

Fig. 6 Digital elevation model

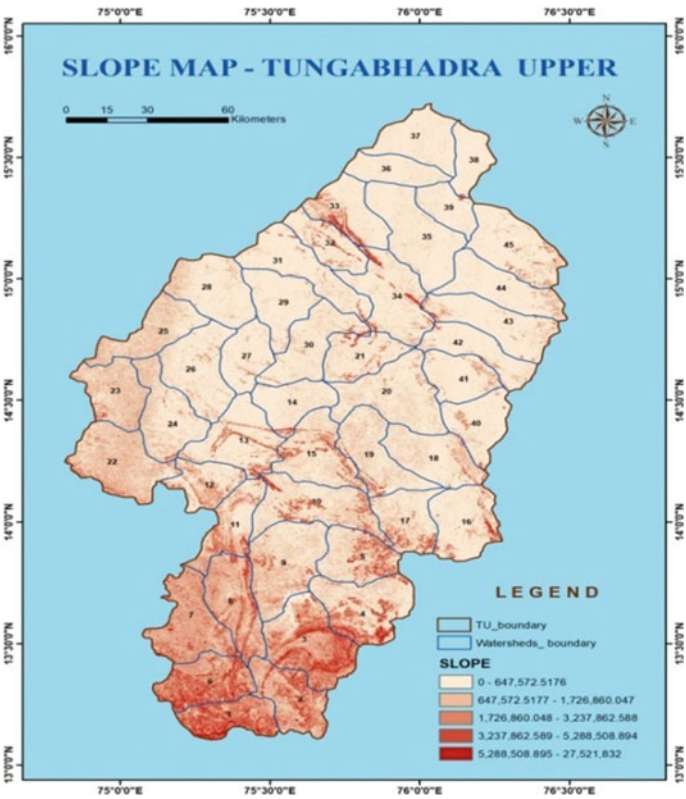

Fig. 7 Slope map

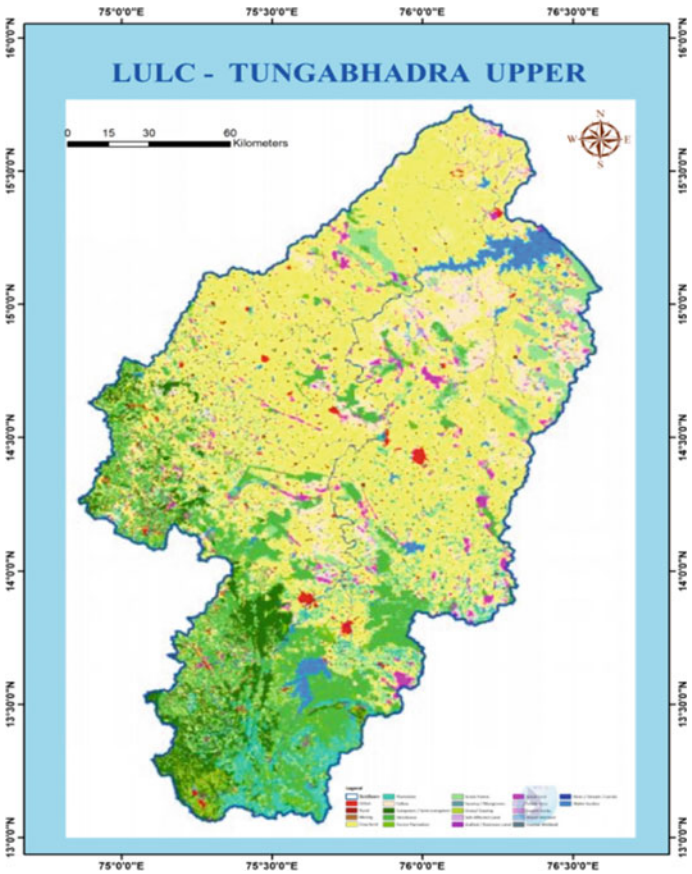

Fig. 8 LULC map

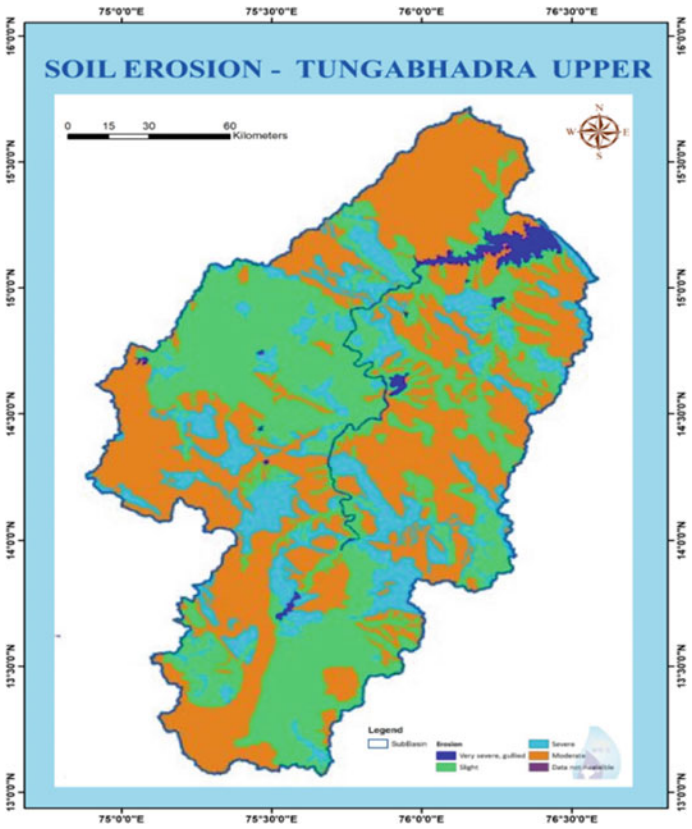

Fig. 9 Soil erosion map

Table 3 Crop management factor

C factor	
Settlement	0.25
Mining	1
Agriculture	0.28
Shrubs	0.15
Forest	0.05
Barren	0.75
Water	0

Table 4 Conservation practice factor

P factor	
Settlement	1
Mining	0.6
Agriculture	0.5
Shrubs	0.23
Forest	0.6
Barren	1
Water	1

5 Results and Discussions

In this analysis, different themes have been developed by using GIS and integrated with USLE concept to estimate the soil erosion. Based on experimental results, the severity of the erosion for watersheds is categorised in to very severe and gullied, moderate and slight. In this, watersheds C04TUU9, 21, 35, 39, 46 fall under very severe and gullied, C04TUU1, 6, 8, 22, 23, 33, 35, 36, 37, 38 under Moderate, C04TUU4, 14, 23, 25, 26, 27, 28, 29, 30 under slight level of erosion respectively (Table 5).

Table 5 WS code and soil loss

WS code	R	K	LS	C	P	Soil loss Ton/ha/year
C04TUU01	1249	0.17	23.24	0.14	0.56	3.94486855
C04TUU02	727	0.17	13.35	0.18	0.55	1.61092968
C04TUU03	619	0.17	11.21	0.11	0.66	0.88494563
C04TUU04	547	0.15	6.21	0.19	0.57	0.56230822
C04TUU05	403	0.15	5.21	0.17	0.61	0.32992496
C04TUU06	1159	0.17	2.31	0.15	0.51	0.34148203
C04TUU07	979	0.17	4.23	0.16	0.55	0.60507833
C04TUU08	727	0.17	4.3	0.15	0.53	0.42360151
C04TUU09	583	0.17	0.8	0.19	0.55	0.08093114
C04TUU10	511	0.15	0.85	0.32	0.64	0.13329489
C04TUU11	475	0.17	0.98	0.15	0.57	0.06925223
C04TUU12	511	0.17	0.96	0.18	0.62	0.09476219
C04TUU13	547	0.15	0.85	0.26	0.59	0.10795459
C04TUU14	547	0.142	0.84	0.25	0.54	0.08838945
C04TUU15	511	0.142	0.96	0.27	0.58	0.11075382
C04TUU16	439	0.15	0.3	0.25	0.54	0.02690634
C04TUU17	439	0.15	0.2	0.24	0.58	0.01835058
C04TUU18	367	0.142	0.35	0.25	0.55	0.0250501

(continued)

Table 5 (continued)

WS code	R	K	LS	C	P	Soil loss Ton/ha/year
C04TUU19	439	0.142	0.6	0.27	0.56	0.05670988
C04TUU20	439	0.142	0.22	0.27	0.58	0.02169966
C04TUU21	439	0.142	0.85	0.26	0.59	0.08239815
C04TUU22	727	0.17	0.99	0.13	0.61	0.1003105
C04TUU23	547	0.17	0.36	0.17	0.59	0.03386567
C04TUU24	547	0.17	0.96	0.25	0.56	0.12484305
C04TUU25	439	0.142	0.7	0.24	0.56	0.05920524
C04TUU26	511	0.142	0.8	0.28	0.56	0.08955421
C04TUU27	511	0.142	0.12	0.27	0.57	0.01318764
C04TUU28	511	0.142	0.68	0.27	0.55	0.07387345
C04TUU29	439	0.142	0.21	0.26	0.55	0.01900207
C04TUU30	475	0.142	0.89	0.26	0.58	0.08977793
C04TUU31	439	0.142	0.76	0.29	0.57	0.07779865
C04TUU32	331	0.142	0.75	0.22	0.55	0.04244961
C04TUU33	259	0.142	0.88	0.29	0.60	0.05636756
C04TUU34	331	0.142	0.98	0.34	0.65	0.10334945
C04TUU35	331	0.142	0.36	0.35	0.70	0.04218809
C04TUU36	259	0.16	0.35	0.28	0.55	0.02236715
C04TUU37	259	0.16	0.32	0.28	0.55	0.02055761
C04TUU38	259	0.16	0.21	0.28	0.54	0.01335112
C04TUU39	331	0.16	0.92	0.24	0.61	0.07241627
C04TUU40	313	0.142	0.95	0.28	0.56	0.06550186
C04TUU41	313	0.142	0.98	0.27	0.56	0.06725594
C04TUU42	331	0.142	0.3	0.32	0.59	0.02658589
C04TUU43	313	0.16	0.2	0.38	0.68	0.02571867
C04TUU44	313	0.16	0.6	0.31	0.63	0.057503
C04TUU45	313	0.16	0.2	0.17	0.70	0.01223023
					A =	10.9288528

Total annual soil loss = 10.92 Ton/ha/year

6 Conclusions

The soil erosion can be controlled if it is predicted accurately and if necessary management strategies and practices are taken. The Universal Soil Loss Equation model has been accepted and used most widely to predict the soil erosion and GIS (Geographical information system) plays an important role in identifying the areas of erosion. So by integrating USLE and GIS we can get better results.

References

1. Modeling Runoff and Soil Erosion in a Catchment Area, using the GIS, in the Himalayan Region, India. Environ. Geol. **51**, 29–37
2. Kothyari, U.C.: Erosion and Sedimentation Problems in India. IAHS publication no. 236 (1996)
3. Jain, M.K., Kothyari, U.C.: Estimation of soil erosion and sediment yield. Hydrol. Sci. J. **45**(4), 771–786 (2000)
4. Jain, M.K., Kothyari, U.C, Ranga K.G.R.: A GIS based distributed rainfall runoff model. J. Hydrol. Elsevier Sci. **299**(1–2), 107–135 (2004)
5. Sedimentations in Reservoirs–CBIP, Technical report-20, vol. I (1997)
6. Tungabhadra reservoir sedimentation studies report (1985). KERS,K.R. Sagar, Mysore
7. Moore, I., Wilson, J.P.: Length Slope factor for the revised universal soil loss equation: simplified method of solution. J. Soil water Conserv. **47**(4), 426–428 (1992)

Chapter 18
Hydrological Viability Analysis for Minor Irrigation Tanks—A Spatial Approach

Y. Raja Rajeswari and N. Bhaskara Rao

Abstract Most of the minor irrigation tanks are interconnected cascades, which allows run-off and return flow of the upstream command area to the downstream tank. This facilitates reuse of water in the command area and increases available water for irrigation. The nature has can use of water transportation to irrigation tanks, into the storage results in of storage capacity which in turn of tank performance. Rehabilitation projects have been undertaken to bring the more agriculture land under from on assured irrigation system. The prediction of water availability in a tank is in important process for sustainable use of water resources in a tank cascade system. The land use/land cover map is prepared using IRS, LISS-III resolution satellite imagery reveals water usage and demand for different development activity. The problems in drainage courses and tank catchment boundaries identified using SOI 1:50,000 scale toposheet and spatial discrepancy have been adjusted with the satellite image. This study identified issues of earthen channel, catchments and head works, area the major problems are to be restored. Remedial measures suggested to improve the tank cascade system.

Keywords Land use and land cover · Tank cascade system · Command area

1 Introduction

To capture monsoon runoff tanks, had been using as a system traditional irrigation in many parts of India. In general tank comprises of catchment area, feeder channels; water spread area, outlet structures (sluices), flood disposal structures (surplus weir)

Y. Raja Rajeswari (✉)
Water Resources Department, Superintending Engineer, CADA, Vijayawada, Andhra Pradesh, India
e-mail: rajarajeswari2003@gmail.com

N. Bhaskara Rao
Water Resources Department, GIS Expert, APIIATP, Vijayawada, Andhra Pradesh, India
e-mail: bhaskar.nird@gmail.com

P. J. Rao et al. (eds.), *Proceedings of International Conference on Remote Sensing for Disaster Management*, Springer Series in Geomechanics and Geoengineering,
https://doi.org/10.1007/978-3-319-77276-9_18

and command area. A study that more than 70–80% of minor irrigation tanks have to be renovated for normal functioning. Tank Rehabilitation/Restoration/Renovation is termed as "the tanks which are dysfunctional are brought to normal functioning by way of undertaking works on breach closing, tank bund strengthening and repairs or reconstruction of sluices and weirs". Many tanks are found in the form of cascades, which is defined as a series of small and medium tanks that are inter connected at suitable locations in one single common water course [4, 8]. These tanks are, interlinked in term of hydro-geologically and socio-economically to ensue of storage, conveying and utilization. If the hydrology of one or few tanks is altered by increasing the storage capacity through rehabilitation programs or command area by developing new paddy lands, the entire cascade hydrology changes Panabokke, C.R (8). In long run, such changes will have a socio-economic impact on the surrounding communities depending on the water availability of the system. Therefore, it is important to take the total tank cascade system rather individual tank into account when planning, development and operations.

Anbumozhi, V (1) analyzed the fundamental reasons to improve the irrigation systems, in which rehabilitation arises because of failures in adequately maintaining irrigation systems. This problem is endemic throughout the world, but especially in the developing countries, due to severe financial constraints. Many works have been done by various researchers for finding out the way and need to improve the performance of the tank system through rehabilitation process. Now a days, the Remote Sensing and Geographic Information System (GIS) best tools for identification and mapping the catchment and command area of minor irrigation tank system. This paper describes briefly the role of Remote Sensing and GIS in the process of rehabilitation of tank cascade system. Toposheets are used for tank position along the drainage courses and catchment boundary. The changes in the linkage of tank cascade and land use due to natural and anthropogenic activities are updated using Remote Sensing and GIS technology.

2 Study Area

The study area covers Tulgam village, Pathapatnam Mandal, Srikakulam district Andhra Pradesh. The catchment boundary is taken from Geo-rectified SOI Map toposheet to study drainage and tanks all along the catchment. The study area covered in 65N 14 SOI topo-sheets of 1:50,000 scale. The study area covers 32.31 km^2. and located 83.8538–83.9218 East Longitude and 18.6516–18.7191 North Latitude (Fig. 1).

In this study, IRS-ID LISS-III satellite data of 2017 have been used. The details act is which are given in Table 1. In addition, SOI 65N/14 toposheet of 1:50,000, hydrographic data and other collateral data used.

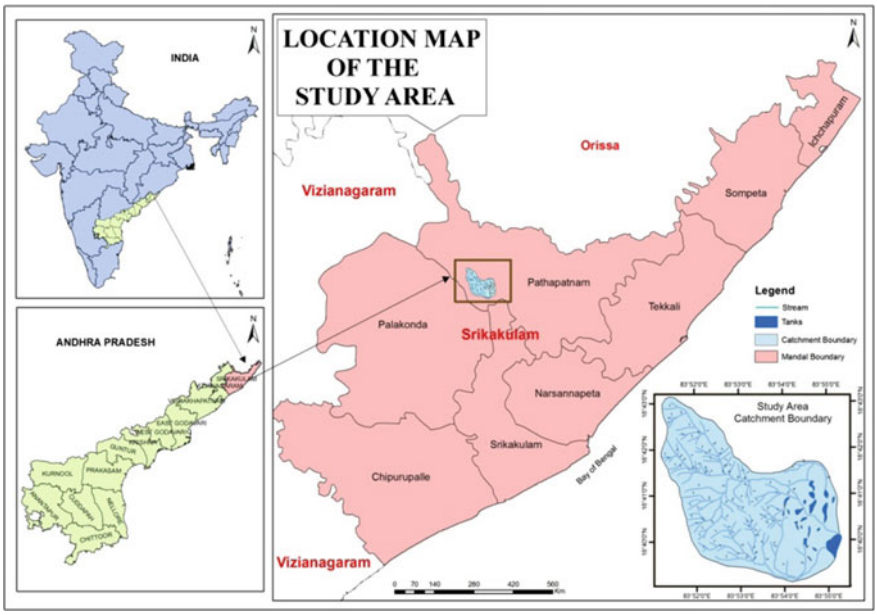

Fig. 1 Location map

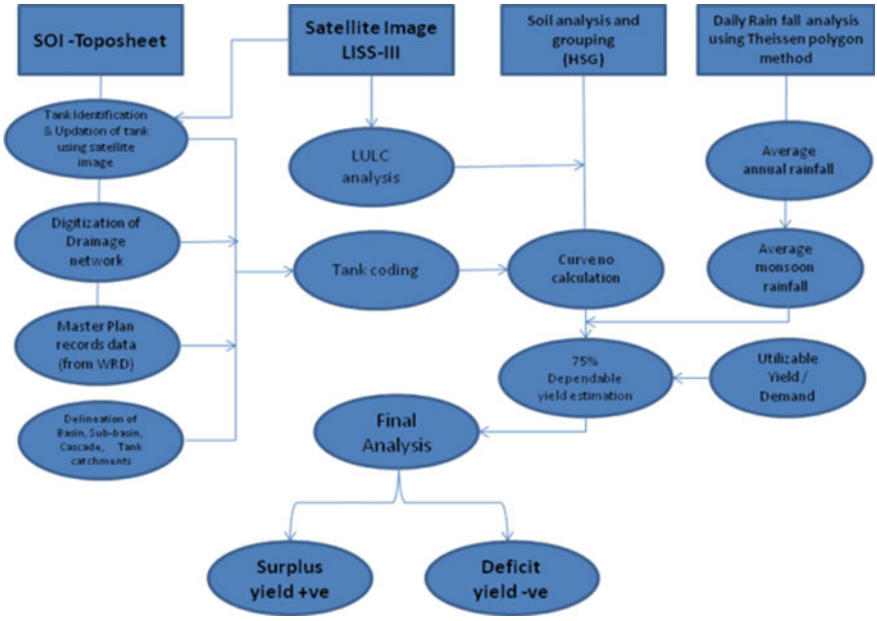

Fig. 2 Methodology

Table 1 Characteristics of IRS Satellite data

Season	Name of the satellite	Sensor resolution	Row	Path	Data of pass
Rabi	IRS-P6	LISS-III—23.5 m	059	105	24th January 2015

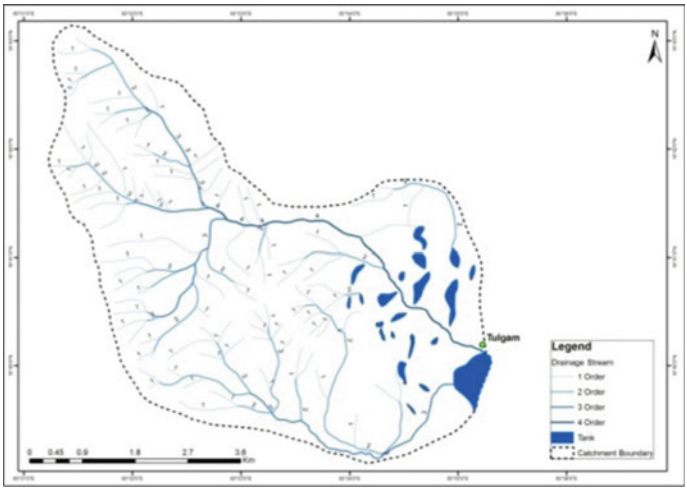

Fig. 3 Stream ordering and catchment of the study area

3 Data and Methodology

The toposheet 65N/14 in collected from the Survey of India and is digitized and then the study area is delineated in QGIS software. Further, the more tanks which are connected in a cascade manner are delineated, its catchment (Fig. 3). The catchment each tank is also delineated besides, water spread area and number of inlet channels (Fig. 2).

4 Drainage

The surface drainage of an area is very methodology of the study important from the point of hydrological regime of the area. Initially, rainfall received is absorbed by the soil and once it gets saturated it goes out as surface runoff. The surface runoff varies with surface conditions namely length and degree of slope, raggedness, soil texture and structure, cover conditions and lithology of the terrain. Every geographical area has a defined drainage system/pattern that determines the ground water potential [2].

Table 2 Stream orders list

S. no.	Stream	Count
1	1st order	99
2	2nd order	53
3	3rd order	24
4	4th order	1

The drainage of the study area is extracted through onscreen digitization from the toposheet 65N/14 of 1:50,000. The drainage which includes streams, canals and tanks are covered in the study. Stream ordering has been followed, because it is universally accepted in this catchment highest stream order is 4th order (Table 2).

5 Land Use/Land Cover

The LU/LC of the area are delineated through on screen digitization on IRS 1D LISS III satellite image in QGIS. For Rabi season IRS-P6 LISS-III satellite data of 24th January 2015 is used. Supervised classification technique has been implemented using the maximum likelihood algorithm and classifications procedure is applied on each scene separately using spectral reflectance and field knowledge. Before classifying the images using supervised classification technique, unsupervised classification was done to attain spectral signature of real land use and land cover. The maximum likelihood algorithm is used for different class segments with separate training data set. The entire study area is broadly divided into eight categories; namely agricultural cropland, scrub land, deciduous forest, plantation, water bodies, scrub forest, built up land, fallow and others (Table 3) and these are shown in Fig. 4.

Table 3 Land use/land cover categories

S. no.	Class name	Km^2	Percentage (%)
1	Agricultural cropland	9.279	28.72
2	Scrub land	2.030	6.28
3	Deciduous forest	16.712	51.72
4	Plantation	1.809	5.59
5	Water bodies	1.479	4.57
6	Scrub forest	0.6	1.85
7	Built-up land	0.104	0.32
8	Fallow	0.295	0.91
	Total	32.308	100

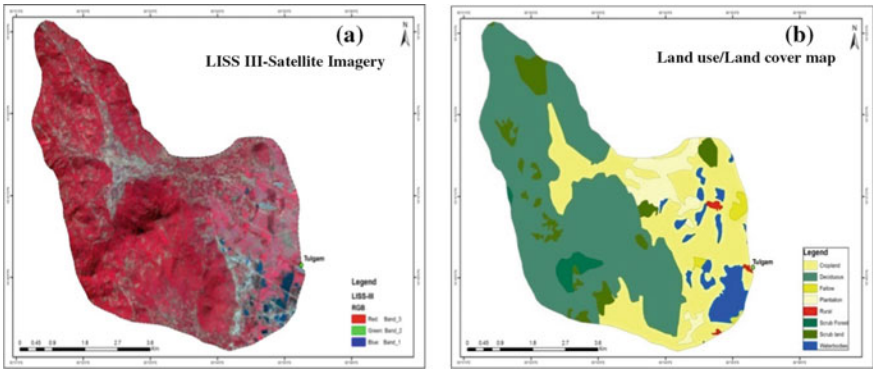

Fig. 4 Map of satellite imagery & LULC

6 Surface Runoff Estimation

Rainfall–Runoff modelling is an essential part in water resources planning and management. The soil conservation service curve number (SCS-CN) is a simulation model that analyzes runoff volumes from the rainfall. It is one of the efficient methods to estimate direct runoff volume in unguaged catchments [3, 9]. It uses the curve number (CN) to determine the runoff volumes. Curve number varies with the terrain conditions. The SCS-CN method uses Land use/Land cover, Soil information and antecedent soil moisture conditions of the catchment [5]. The modifications suggested by the Ministry of Agriculture, Govt. of India, to suit Indian conditions are included in the study. A brief account of inputs and formulae of the SCS method adopted for the present study is given below (Fig. 5).

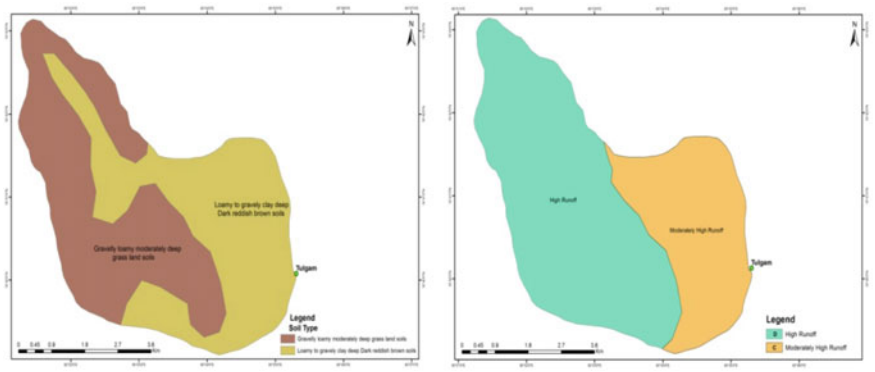

(a) Soil texture (b) Hydrological soil Groups

Fig. 5 Map of soil texture & Hydrological soil

Table 4 Tank—75% dependable yield estimation (Monsoon)

S. no.	Year	Rainfall (mm)	Runoff (mm)	S. no.	Year	Rainfall (mm)	Runoff (mm)
1	2006	1210	312.7	11	1998	966	106.64
2	2014	1043	275.47	12	1999	721	103.11
3	2010	1443	249.71	13	2001	951	96.73
4	2003	1158	234.35	14	1997	1086	63.67
5	2012	1501	229.89	15	1996	643	63.05
6	2005	1119	204.81	16	2002	834	59.89
7	2015	1074	184.95	17	2008	700	58.95
8	2009	894	151.53	18	2011	772	54.86
9	2013	1028	141.95	19	2004	798	54.77
10	2007	883	136.98	20	1995	441	54.55
				21	2000	730	29.34

75% yield in mm—59–89
75% yield in mcft—33.95

(a) Rain gauges in the neighborhood of the tank catchment are taken and weighted average rainfall of catchment arrived using Thiessen polygons [6].
(b) Hydrological soil groups map is prepared based on soil classification map.
(c) Integrating Hydrological soil groups and Land use/Land cover information, a weighted Curve number—CN (II) for each tank catchment is arrived based on cure number table (Table 4).

7 Results and Discussion

The objective of the study is to map the land use/land cover of the study area, to have detailed information on the spatial variation to identify the problems in the drainage course of the tank cascade system through GPS survey and to suggest suitable analysis to measure the base data.

The Minor irrigation tank system components consist of drainage course, catchments, tank bund, sluice and surplus weir locations. The problems identified are excessive weed growth-choaking of sections of canal, thereby reducing the velocity of flow and causing the deposition of sediment, silt accumulation, aquatic weed growth in water submerged areas is a problem because some of this growth eventually reaches the canals,

Total curve number was assigned using the unique land use and hydrological soil group. The ratio of total curve under and its corresponding area gives the weighted curve number (WCN). This generated weighted curve number is a factor for runoff estimation. Demand calculated 10 acres per one mcft of water. 75% dependable yield was estimated for each tank in the cascade using SCS Curve method. The tank wise details are shown in Table 5.

Table 5 Tank analysis results

S. no.	Name of tank	Registered Ayacut in acres	Catchment area (km^2)	Tank capacity (mcft)	75% dependable yield (mcft)	Demand (0.1 mcft per acre)	Balance yield (mcft)	Status
1	Raminaidu tank	160	32.31	22.89	33.95	16.03	17.93	Viable

8 Conclusions

The need to Registered Ayacut area water demand and improve irrigation systems results from deferred maintenance, scarcity of water resources, and a disproportion between the technological state of agricultural production and rising environmental concerns. Changing institutions and management within irrigation systems are now viewed as a catchment area and tank improvement process. This study is conducted towards hydrological viability of minor irrigation tank system. It was found that most of the irrigation tanks do not receive the surplus water from the upstream tanks. Through Rainfall, Runoff and GIS tracking over the drainage course and tank system the problems were identified and suitable remedial measures were suggested for augmenting more water to the tank cascade hydrologic system. For optimum utilization of financial resources it is suggested to receive and restore only those tanks that are hydrologically viable. Hence it is recommended that the rehabilitation of irrigation tank system is very essential, In this study, the and GIS and GPS are proved to be the most effective tools in discerning tank cascade water system.

References

1. Anbumozhi, V., Matsumots, K., Yamaji, E.: Towards improved performance of irrigation tanks in semi-arid regions of India: Modernization opportunities and challenges. Irrig. Drainage Syst. **15**, 293–309 (2001)
2. Gurtz, J., Zappa, M., Jasper, K., Lang, H., Verbunt, M., Badoux, A., Vitvar, T.: A comparative study in modelling runoff and its components in two mountainous catchments. Hydrol. Process **17**, 297–311 (2003). https://doi.org/10.1002/hyp.1125
3. Hawkins, R.H.: Asymptotic determination of runoff curve numbers from data. J. Irrig. Drainage Eng. ASCE **119**(2), 334–345 (1993)
4 Madduma Bandara, C.M.: Catchment eco-systems and village tank in the dry zone of Sri Lanka. In: Lundqvist, J., Lohm, U., Falkernmank, W. (eds.) Strategies for River Basin Management, pp. 265–277. Reidel Publishing Company, Dordrecht
5 Moore, R.J.: The probability-distributed principle and runoff production at point and basin scales. Hydrol. Sci. J. **30**, 273–297 (1985). https://doi.org/10.1080/02626668509490989
6 Paik, K., Kim, J.H., Kim, H.S., Lee, D.R.: A conceptual rainfall-runoff model considering seasonal variation. Hydrol. Process **19**, 3837–3850 (2005). https://doi.org/10.1002/hyp.5984
7 Palmyra Centre for Ecological Land Use: Water Management and Rural Development, Aurovile, rehabilitation of integrated tank management systems. In the Kaliveli watershed, Villupuram district, Tamil Nadu, Final report 1999–2006
8 Panabokke, C.R.: The small tank cascade systems of the Rajarata, their settings, distribution pattern and hydrography. Mahaweli Authority—International Irrigation Water Management Institute, Srilanka (1999)
9 Ponce, V.M., Hawkins, R.H.: Runoff curve number: has it reached maturity? J. Hydrol. Eng. ASCE **1**(1), 11–19 (1996)

Chapter 19
Applications of RS and GIS Techniques for Disaster Studies in East Godavari District, Andhra Pradesh, India

K. Padma Kumari and K. Srinivas

Abstract Natural Disasters are inevitable events. The onset of occurrence is generally short period with prior warning and in many cases without. These disasters cause havoc by loss of life and property in a large scale. From time immemorial, man has been facing the wrath of the nature but could not control it. The only possibility is providing mitigation steps. The present study is an area which has a metaphor—"The rice bowl of Andhra Pradesh"—East Godavari District, Andhra Pradesh, India, encapsulates 81°30, 82°40 East Longitude and 16° 25, 18°00 North Latitude. East Godavari district is vulnerable to 4 hazards, viz. Cyclones, Floods, Landslides and Tsunamis. The climatic condition of the study area is semi humid with an annual rainfall of 1200 mm, temperature range between 23.5 and 45.9 °C. The District is flanked on the North by Visakhapatnam District, South by Krishna district, West by West Godavari District with a part of Telangana State and on the East by Bay of Bengal covering an area of 10,807 km^2. Naturally the study area classified by Uplands, Plains and Delta made up of Gondwana sand stones, Basalt, Ash Beds and rich minerals. The Godavari and its distributaries named Gowthami and Vasistha River provide the surface water. Mapping of Land use/land cover, Geology, Geomorphology, Rainfall, DEM were prepared to generate Flood Zonation Map, Shoreline Change Map, etc. using Landsat-8 data processed over ArcGIS and ERDAS software on 1:50,000 scale. Risk Zone map is developed for better mitigation purpose.

Keywords ArcGIS · ERDAS · Remote sensing · GIS · Disaster management Risk zones

K. Padma Kumari (✉) · K. Srinivas
School of Spatial Information Technology, Institute of Science and Technology, Jawaharlal Nehru Technological University Kakinada, Kakinada 533003, Andhra Pradesh, India
e-mail: geologymadam@gmail.com

K. Srinivas
e-mail: killi.srinivas@gmail.com

P. J. Rao et al. (eds.), *Proceedings of International Conference on Remote Sensing for Disaster Management*, Springer Series in Geomechanics and Geoengineering,
https://doi.org/10.1007/978-3-319-77276-9_19

1 Introduction and Literature

East Godavari District is known as rice bowl of Andhra Pradesh with lush paddy fields and coconut groves. It beckons tourists to have a glimpse of its rich cultural heritage. The entire East Godavari district is broadly classified into 3 natural divisions are Deltas, Upland, and Hill tracts. In East Godavari District there are 5 revenue divisions and consist of 60 revenue mandals with Kakinada being the district head-quarters.

The northern part of the study area covered by 6 mandals, the south-east coastline of the district by 13 mandals, the western boundary of the district is defined by the river bank of Godavari with 11 mandals along the river. The major river is Godavari along with its distributaries Vainateyam and Vasishta. The general elevation of the east Godavari varies from a few meters near to the coast to about 300 m up hills in the agency. Average annual rainfall is 1280 mm. In the past, many Cyclones in the Bay of Bengal have frequently hit the shoreline of the study. A small island named Hope Island is at 11 km from Kakinada coast in the Bay of Bengal, makes a natural harbor at the shoreline. Hope Island is one of the major protruding deltas on the east coast of India bordering the Bay of Bengal and is a densely populated zone of intense economic activity. As a result, the seaward bulge of the delta overlaps the continental shelf across by about 30–35 km when compared to the general trend of the east coast. Several studies on the nature of coastal landforms along the delta front also indicated increased sedimentation rates through the river during the nineteenth century and even over a major part of the twentieth century. Padma Kumari et al., studied on application of Remote Sensing and GIS techniques on Geomorphology [1], Land Use/Land Cover studies [2], Shoreline Morphometrical Analysis [3], Shoreline Erosion and Deposition (2013) and the respective changes [4] of East Godavari district, Andhra Pradesh, India. Nageswara Rao [5] studied on Coastal Morphodyanamics and Asymmetric development of the Godavari Delta, Subsidence of Holocene sediments in the Godavari delta, Coastal erosion and habitat loss along the Godavari delta. Nageswara Rao [6] Impacts of sediment retention by dams on delta shoreline recession: evidence from the Krishna and Godavari deltas India. National Disaster Management Guidelines (2007) prepared by National Disaster Management Authority, Government Authority of India. Thulsi Rao [7] has studied on Coastal and marine nature conservation in EGREE region. Ramasubramanian [8] examined the Mangrove wetlands conservation and management in Andhra Pradesh. Murthy [9] presented the recent changes in the coastal environment along the east coast India-impacts of climatic events.

The major advantage of GIS is that it allows identifying the spatial relationship between features and temporal changes within an area over time. Prasada Rao and Mahadevan [10] based on an analysis of multi-date maps spread over a period of 100 years traced the growth of a 21 km long sand spit at the delta, east of Kakinada that began around AD 1850 and reached more or less the present shape by the 1958 owing to increased sediment supply from the catchment due to deforestation. Sambasiva Rao and Vaidyanadhan (1937) reported overall cumulative accretion of

land due to development of several other sand spits at the distributaries mouths of the Godavari during the period between 1937 and 1977, 1987, based on the study of toposheets. Bhanumurthy and Naidu [11], Sastry et al. [12], in their studies addressed that remote sensing images have been effectively used for monitoring shoreline changes and coastal management in different parts of India. Desai et al. [13], Nayak [14], Singh and Dilip kumar [15], Chen [16], Sreekala et al. [17], applied Remote sensing on various features on the surface. Padma Kumari et al. (2014) identified change and sea-level rise at the Uppada area highly eroded lead to an increase in the cyclone-prone area and loss of life.

2 Study Area

East Godavari district lies in the North-East coast of Andhra Pradesh, India and bounded on the North by Visakhapatnam district and the state of Orissa. On South East part of the study area, Bay of Bengal covers the coastline. The neighbors on the West are Khammam and West Godavari districts. The district headquarters is Kakinada. With the spatial coordinates 16 30, 18 20 North and 18 30, 82 30 East, covers 10,807 km^2 (Fig. 1). The study area is mainly covered by Agriculture land use for Farming, Grassland and other purposes. Annual rainfall is 115 cm. The district flourishes with fertile soils, good rainfall. Climate is mostly hot and humid. The hottest part of the year late May to early June with maximum temp. 38–42. Major rivers are Godavari, Pampa, Thandava and Yeluru rivers. The general elevation of the east Godavari varies from a few meters near to the coast to about 300 m up hills in the agency. Average annual rainfall is 1280 mm. A small island named 'Hope island' located at 5 km from Kakinada coast makes it natural harbor (Table 1).

Being in the coastal region, study area is prone to cyclones and depressions. East Godavari district with a coastline of 177 km covering three revenue divisions is vulnerable to cyclones and storms which are frequent in Bay of Bengal. In the East Godavari district 13 coastal Mandals are highly vulnerable to cyclones and storms and

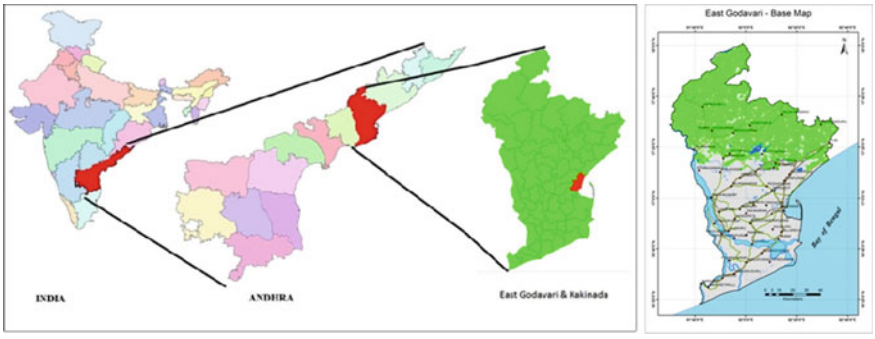

Fig. 1 Study area

have been identified as disaster prone. The villages viz. Chollangi, Chollangipeta, G. Vemavaram, Patavala, Coringa, Polekurru, Neelapalli and P. Mallavaram falling under Tallarevu Mandal and Bhairavapalem and Gokullanka falling under Ipolavaram Mandal are highly cyclone/ storm prone.

3 Objectives

The main objective is to prepare maps of Land use/Land cover, DEM, Watershed map, etc., and to generate Risk Zone Map using Remote Sensing and GIS over the East Godavari district, Andhra Pradesh, India.

4 Data Used and Methodology

Toposheets on 1:50,000 scale were procured from Survey of India which were used to prepare Base Map. Landsat-7 & 8 scenes were downloaded to prepare Landuse/ Landcover Maps and to analyse the pre-post analysis of the disaster. CartoDEM data from bhuvan was used to generate Slope and aspect maps. Thematic maps were also prepared by procuring maps like Geology, Geomorphology from NRSC, Soil map was prepared by using the data from National Bureau of Soils Survey and Land use Planning, Nagpur. Rainfall Data was Procured from India Meteorological

Table 1 History of disasters in study area (1860–2015)

S. no.	Date of occurrence	Disaster type	Description
1	19.12.1869	Earthquake	Magnitude: 3.7
2	12.06.1893	Cyclone	
3	04.09.1895	Cyclone	
4	28.10.1903	Cyclone	
5	25.05.1904	Cyclone	
6	30.09.1915	Cyclone	
7	21.10.1916	Cyclone	
8	13.10.1933	Cyclone	
9	05.05.1955	Cyclone	
10	04.11.1969	Cyclone	
11	31.03.1980	Earthquake	Magnitude: 3.8
12	02.10.1980	Earthquake	Magnitude: 4
13	15.10.1982	Cyclone	
14	30.07.1990	Earthquake	Magnitude: 3.6
15	04.11.1996	Cyclone	
16	26.12.2004	Tsunami	
17	12.10.2014	Cyclone	

Table 2 Landsat specification

LandSat-7 ETM+			LandSat-8 OLI—TIRS		
Bands	Wavelength (μm)	Resolution (m)	Bands	Wavelength (μm)	Resolution (m)
Band 1	0.45–0.52	30	Band 1	0.43–0.45	30
Band 2	0.52–0.60	30	Band 2	0.45–0.51	30
Band 3	0.63–0.69	30	Band 3	0.53–0.59	30
Band 4	0.77–0.90	30	Band 4	0.64–0.67	30
Band 5	1.55–1.75	30	Band 5	0.85–0.88	30
Band 6	10.40–12.50	60	Band 6	1.57–1.65	30
Band 7	2.09–2.35	30	Band 7	2.11-2.29	30
Band 8	0.52–0.90	15	Band 8	0.50–0.68	15
			Band 9	1.36–1.38	30
			Band 10	10.60–11.19	100
			Band 11	11.50–12.51	100
Date of acquisition: 8th December 2000			Date of acquisition: 15th and 24th January, 2015		

Department (IMD), Kakinada. Population and demographic data as per Census-2011 was collected from http://www.censusindia.com web-site, Historical Data was collected from different sources like disaster management websites, IMD, CWC etc., for the occurrences of disaster in the study area (Table 2; Fig. 2).

5 Results and Discussion

Based on the methodology adopted in this study, various maps are generated using Remote Sensing and GIS techniques for Disaster studies in East Godavari District, Andhra Pradesh, India.

5.1 Land Use/Land Cover Classification System

The Land use indicates the usage of land which means man made usage of the earth's surface like built-up lands, agriculture and etc. Land cover is the natural coverage of surface of the earth like forests, water bodies, natural drainage patterns, rivers, oceans, mountains, snow etc. Information on land use/land cover of the area is very important for planning and development activities of agriculture, horticulture, industries and infrastructure and also damage assessment/monitoring by soil erosion, landslides and floods.

Understanding Land use/ Land cover categories, their spatial distribution and the pattern change is very essential for resource mapping, management and

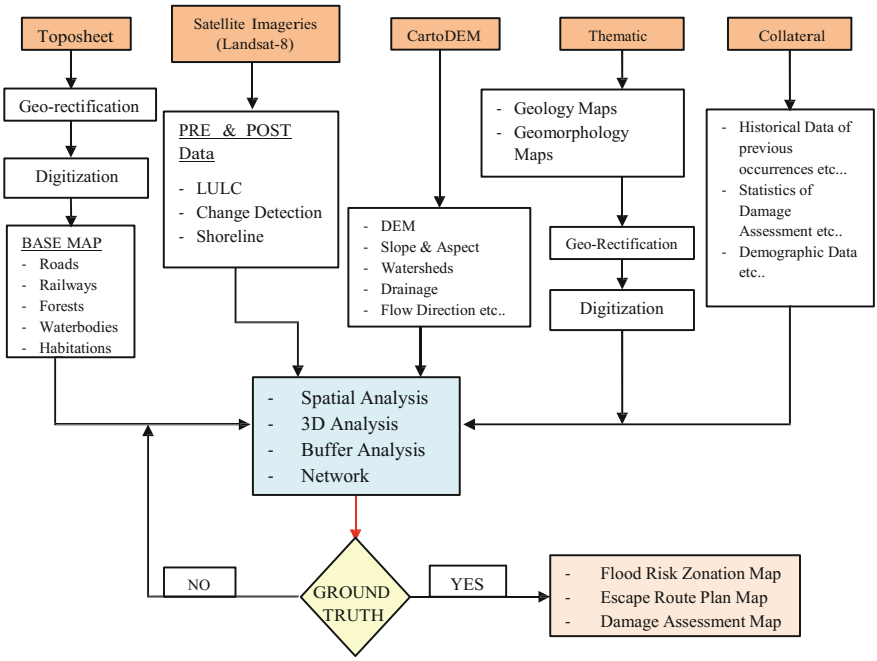

Fig. 2 Flowchart of the methodology

conservation activities [18]. This helps in the analysis of environmental conditions and the associated problems. Several thematic classes such as road network, human habitant, drainage, forest and plantation classes can be classified from the satellite imagery. Land use map of the study area (Fig. 3) was prepared using application software ArcMap-10.1.

The total area of land use/land cover of various crops and other infrastructural facilities of Godavari District is 12,778.53 km^2 and is given in Table 3.

From the current LU/LC studies it is evident that the major land share is owned by CropLands (41.74%). The next major share is followed by land use category Built-up Lands (17.31%), Mangrooves (8.29%), Forests (8.03%) and Saltpan (6.18%) (Fig. 4).

5.2 Geology and Geomorphology

Geomorphology is one of the significant theme information for all the application projects. Hence, the geomorphic maps proposed to be prepared would furnish to the different resource information needs of the country like geo-environment, geo-engineering, geo-hazards, mineral and ground water exploration and interdisciplinary themes like soil, land use/ land cover and forest, etc. This is useful in

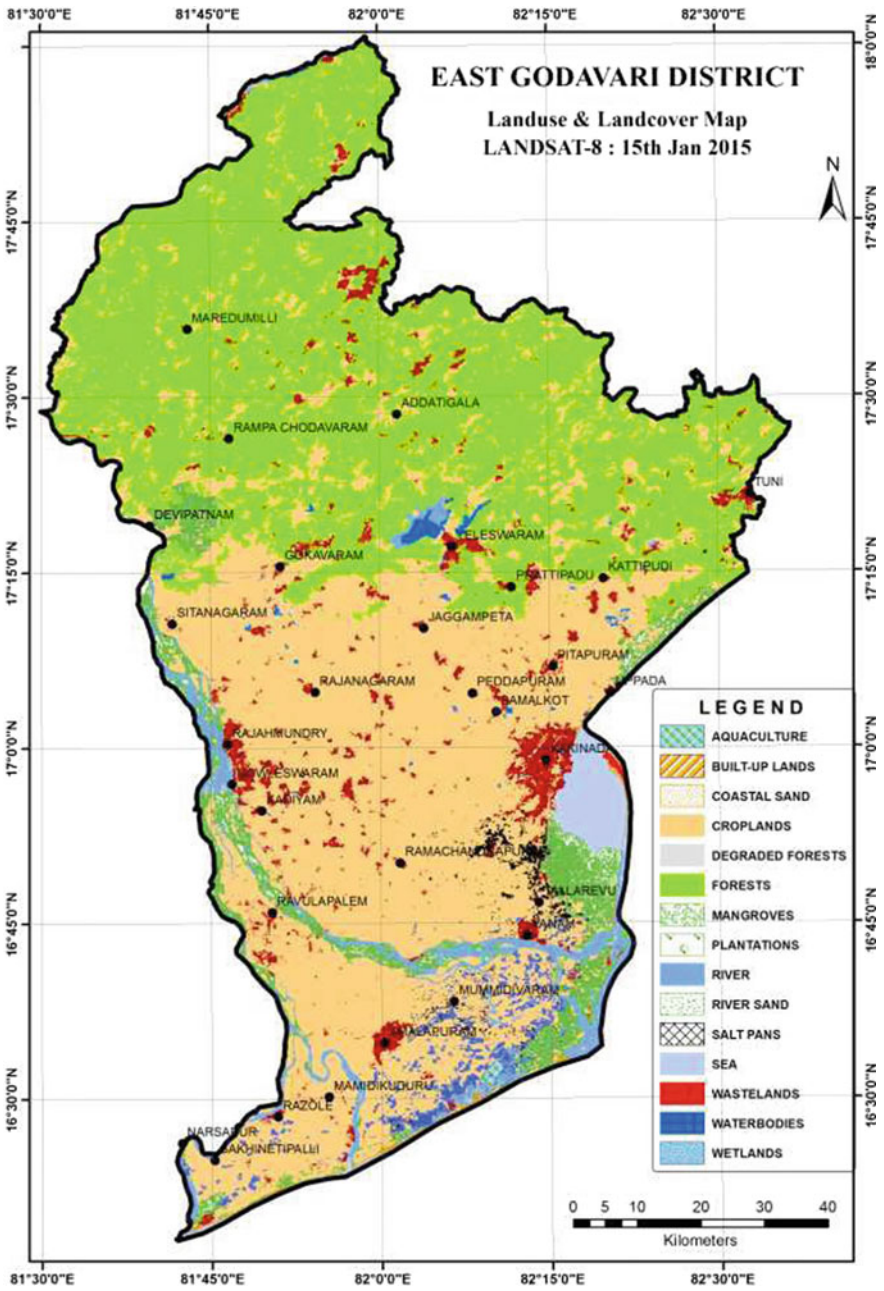

Fig. 3 Land use/land cover classification based on satellite image

Table 3 Landuse/landcover classification

S.no	Category	Area (km^2)	%
1	Built-up lands	2211.55	17.31
2	Croplands	5334.25	41.74
3	Degraded forests	121.23	0.95
4	Forests	1025.72	8.03
5	Mangroves	1059.37	8.29
6	River	213.04	1.67
7	Saltpans	789.93	6.18
8	Sand beds	108.15	0.85
9	Sea	183.26	1.43
10	Waterbodies	1732.03	13.55
	Total	12,778.53	100.00

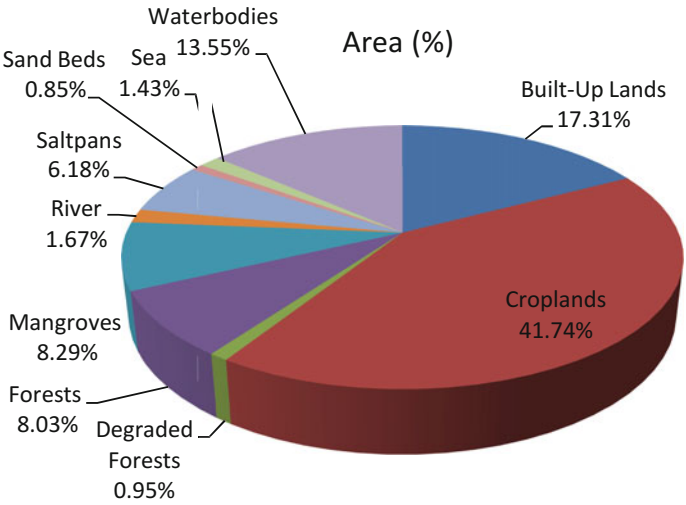

Fig. 4 Pie-chart of East Godavari district land utilization

identification of some of the sample locations, e.g. in the channel/braided/point bars of stream sediments, channel bars and point bars.

In this study, structural hills (34%) are at northern part belongs to Eastern Ghats Mobile Belt, exposing all the characteristic litho units of the Eastern Ghats Super group viz, made up of Khondalite, Charnockite, and Migmatite groups of rocks and rich minerals. Intermotane valley, buried Pediplain, Denudational and Residual hills are 28%, Deltaic plain (18%) is characterized by fluvial to fluvio marine and marine deposits of Quaternary age, Coastal plain (8%) are majority of the landforms. Abundant existence of Mangroves (6%) present at the coastal ecosystem with rich Fauna and Flora. The Deccan Traps occur 2 km North-East of Rajahmundry and extend in ENE-WSW direction. Limestone Intertrappeans, rich in Gastropod and

Lamellibranches fossils, occur near Kotilingala, Korukonda and Kateru. Rajahmundry Formation, named after the type locality, Rajahmundry, is an ensemble of fine-grained, purple to varicoloured Sandstone, Grit and Conglomerate, overlie by current bedded Sandstone with Clay and Shale bands, intermittently exposed between Rajahmundry and Samalkot. It is equivalent to Warkalli Beds of Kerala and Cuddalore Formation Tamil Nadu.

5.3 Shoreline Change Analysis

Identifying the zones of erosion and deposition was done based on the convexity and concavity of the shoreline by using a mathematical model adopted by Li et al. [19]. This is also referred as dynamic method of shore line segmentation. Zones of erosion and deposition were derived by extracting the shoreline information from Landsat-7 dated 8th Dec'2000 and Landsat-8 dated 15th Jan 2015 (Tables 4 and 5). The overlap or cross over points or intersections on these both lines after conversion to polygons has evolved different areas Graphs 1, 2 and Figs. 5, 6.

Table 4 Erosion maxima and minima (2000–2015)

Erosion maxima and minima along Godavari Delta Front (2000–2015)		
Zone of erosion	Erosion_Max (km^2)	Erosion_Min (km^2)
Bhairavapalem		0.6015
Addaripeta	1.0439	
Masanitippa	1.509	
Uppada	2.2500	
SPIT	4.1361	
Total	8.5809	0.6015

Table 5 Deposition maxima and minima (2000–2015)

Deposition maxima and minima along Godavari Delta Front (2000–2015)		
Zone of deposition	Deposition_Max (km^2)	Deposition_Min (km^2)
Nemam		0.2248
Uppulanka		0.3543
Valasapakalu		0.553
Kottapeta		0.6893
SPIT	6.8977	0.0400
Total	6.8977	1.8637

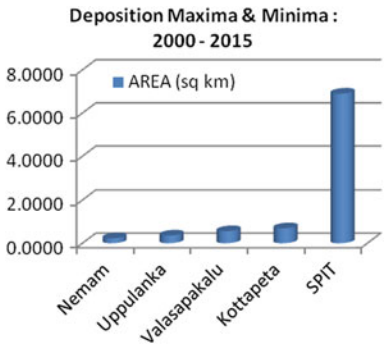

Graph 1 Graph of deposition maxima and minima (2000–2015)

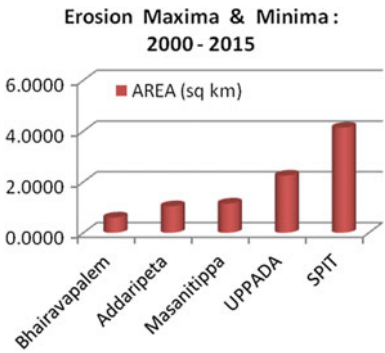

Graph 2 Graph of erosion maxima and minima (2000–2015)

Shoreline change results from coastal erosion, the effect of the breaking waves in the near-shore zone, and near-shore currents. The breaking waves in the near-shore zone and the near-shore currents are responsible for the transportation of beach sediments that results in shoreline change.

The morphometric changes that took place during different periods are mapped and geometry of the shore was arrived at and is mapped in Fig. 7.

5.4 Risk Zone Analysis of Cyclone and Flood

Based upon the selected methodology criteria, the risk zones for the listed disasters are represented in the Fig. 8.

Fig. 5 Zones of erosion and deposition with settlements

6 Conclusions

From the LU/LC studies, it is evident that half of the study area is Crop land. In this scenario, even a little hindrance in the natural conditions shall bear a greater loss in socio-economic conditions.

In the study are the mandals prone to the occurrence of various disasters are as tabulated in Table 6.

With the mitigation of increasing frequency and intensity of disastrous events as a result of climate change, it is more prudent to model these risk zones and low lying areas for both emergency management and development planning.

Fig. 6 Zones of erosion and deposition

The remote sensing and GIS technology has potential use for not only risk mapping it can also be used in the scientific based damage assessment, monitoring, identification of damaged zones, improvement in forecasting and warning models, updating maps, effective and reliable communication etc.

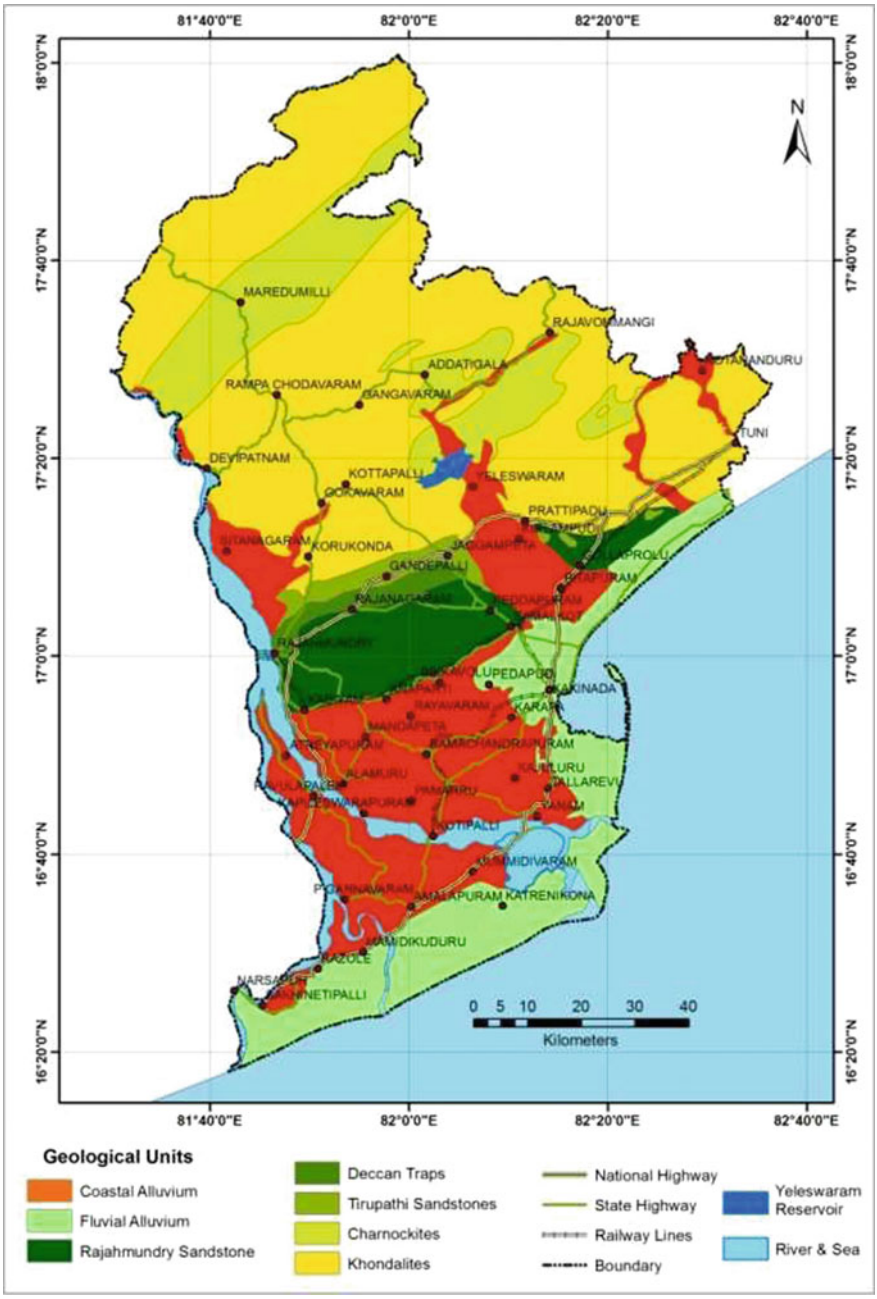

Fig. 7 Geology map

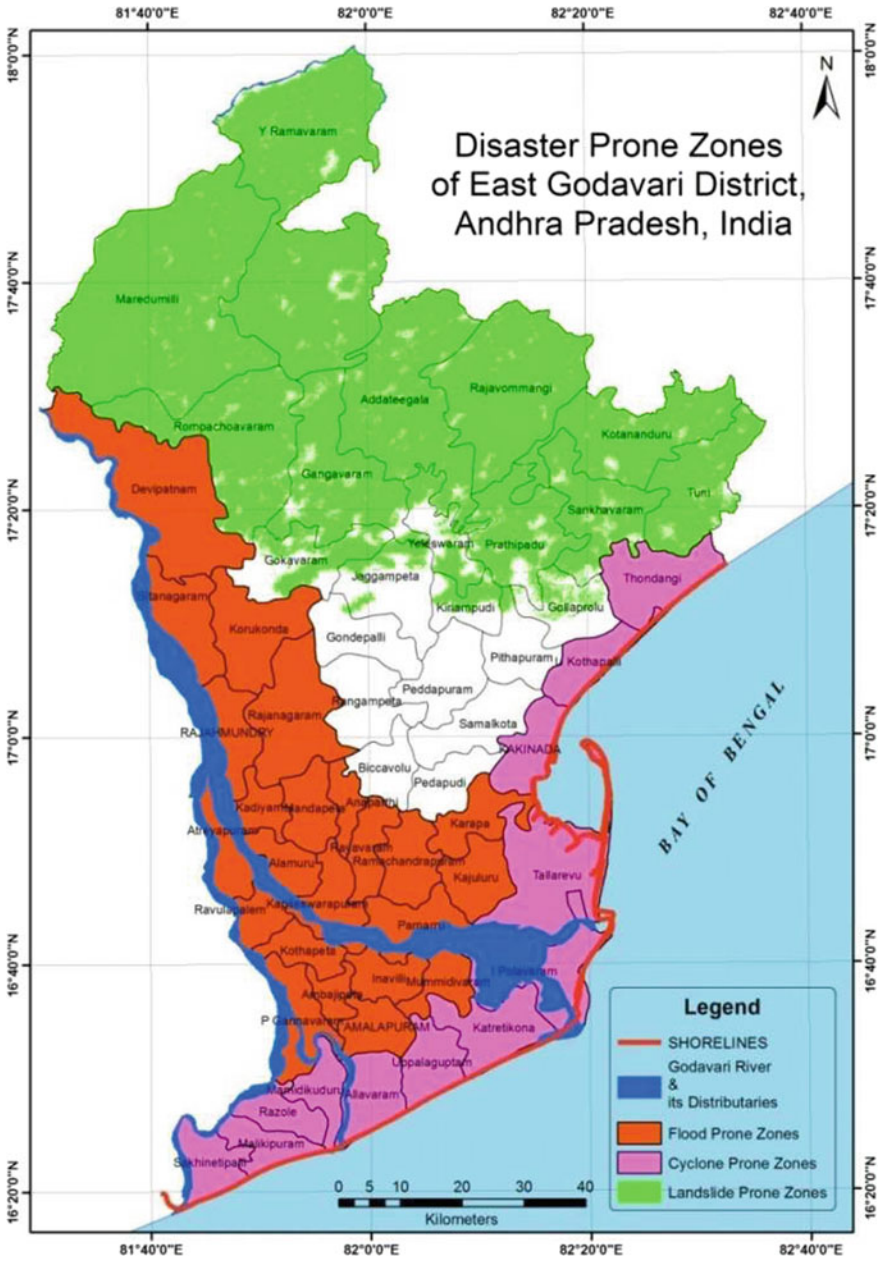

Fig. 8 Disaster prone zones in East Godavari district

Table 6 List of Disaster Prone mandals in the study area

Flood prone mandals (23)	Cyclone prone mandals (12)	Landslide mandals (8)
Devipatnam, Sitanagram, Korukonda, Rajahmundry, Rajanagaram, Kadiyam, Mandapeta, Anaparthi, Alamuru, Rayavaram, Ramachandrapuram, Karapa, Kapileswarapuram, Pamarru, Kajuluru, Atreyapram, Ravulapalem, Kotapeta, Ambajipeta, Amalapuram, Ainavilli, P Gannavaram and Mummidivaram	Sakhinetipalli, Malikipuram, Razole, Mamidikuduru, Allavaram, Uppalaguptam, Katretikona, I Polavaram, Tallarevu, Kakinada, Kothapalli and Thondangi	Y Ramavaram, Maredumilli, Rompachodavaram, Addateegela, Rajavommangi, Kotananduru, Sankhavaram and Gangavaram

Acknowledgements The Author is thankful to USGS/NASA for the download of Landsat-7 & 8 for providing data, and Head of the Spatial Information Technology, IST University college of Engineering Jawaharlal Nehru Technological University Kakinada, Kakinada. And also thanks to faculty and supporting staff of the Department.

References

1. Padma Kumari, K., Jahan, H., Rao, S., Sridhar, P.: Applications of remote sensing and Geographical information system techniques on Geomorphological mapping of coastal part of East Godavari district, Andhra Pradesh, India. Int. J. Eng. Sci. Technol. (IJEST) **4**(10), 4296–4301. ISSN: 0975-5462 (2012)
2. Padma Kumari, K., Jahan, H., Rao, S.: Applications of remote sensing and GIS techniques for land use/land cover, wetland mapping of coastal part of East Godavari District, Andhra Pradesh, India. Int J Earth Sci Eng **6**(4), 908–914 (2012)
3. Padma Kumari, K., Jahan, H., Rao, S., Sridhar, P.: Shoreline morphometric change analysis using remote sensing and GIS in the coastal part of East Godavari District, Andhra Pradesh, India. Int. J. Civil Eng. Appl. Res. (IJCEAR) **03**(02), 129–136 (2012)
4. Padma Kumari, K., Srinivas, K., Gopi Krishna Kasyap, V.: Shoreline change analysis of erosion and deposition using landsat data 2000 & 2015 in the coastal part of East Godavari District, Andhra Pradesh, India. In: Proceeding of CEEC-2015, pp. 111–123 (2015)
5. Nageswara Rao, K.: Coastal morphodynamics and asymetric development of the Godavari Delta: Implications to facies architecture and reservoir heterogeneity. J. Geol. Soc. India **67**, 609–617 (2006)
6. Nageswara Rao, K., Subraelu, P., Naga Kumar, K.C., Demudu, G., Hema Malini, B., Rajawat, A.S., Ajai.: Impact of sediment retention by dams on delta shoreline recession: evidences from the Krishna and Godavari Deltas, India. Earth Surf Process Landforms **35**, 817–827 (2010)
7. Thulsi Rao, K.: Coastal and marine nature conservation in EGREE (East Godavari River Estuarine Ecosystem) region. In: Proceeding of CEEC-2015, pp. 1–22 (2015)
8. Ramasubramanian, R., M.S. Swaminathan Research Foundation: Mangrove wetlands conservation and management in Andhra Pradesh. In: Proceeding of CEEC-2015, pp. 23–64 (2015)

9. Murthy, V.S.N.: Recent changes in the coastal environment along the East Coast of India—impacts of climatic events. In: Proceeding of CEEC-2015, pp. 65–68
10. Prasada Rao, R., Mahadevan, C.: Evolution of Visakhapatnam beach. Andhra University Memoirs in Oceanography. v. 2, pp. 33–47 (1958)
11. Bhanumurthy, P., Naidu.: Modern Delats—A field summer course volume 2003–2004
12. Sastry, J.S., Vethamony, P., Swamy, G.N.: Morphological changes at Godavari Delta region due to waves, currents, and associated physical processes, Mem. Geol. Soc. Ind. **22**: 139–151
13. Desai, P.S., Honne Gowda, H., Kasturirangan, K.: Ocean research in India; Perspective for space [J]. Curr. Sci, **87**(3): 268–278 (2000)
14. Nayak S.R.: Use of satellite data in coastal mapping [J]. Indian Cartographer, **5**: 147–157 (2002)
15. Singh, R.B., Kumar, D.: Monitoring, mapping and mitigation of flood disaster in India using remote sensing and GIS. In: Natural Hazards & Disaster Management Vulnerability and Mitigation, pp. 217–229. ISBN: 978-81-316-0033-7 (2013)
16. Chen L.C.: Detection of shoreline changes for tideland areas using multi-temporal satellite images. Int J Rem Sens. **19**(17): 3383–3397 (1998)
17. Sreekala, S.E., Baba, M., Muralikrishna, M.: "Shoreline changes of Kerala coast using IRS data and aerial photographs", Indian J Mar Sci, **27**, pp. 144–148 (1998)
18. Anderson, J.R., Hardy, E.E., Roach, J.T., Witmer, R.E.: A landuse and land cover classification for use with Remote sensor data, Geological Survey Professional Paper 964, U. S. Department of Interior, U.S. Government Printing Office, Washington, DC, p. 28 (1976)
19. Li, R., Liu, J.-K., Felus, Y.: Spatial modeling and analysis for shoreline change detection and coastal erosion monitoring (2001)

Chapter 20
A Study on the Utility and Geochemistry of Groundwater in Ponneri Taluk of Thiruvallur District, Tamilnadu

S. Sivakumar, K. Srinivasaraju, M. Shanmugam, D. Thirumalaivasan and C. Lakshumanan

Abstract Groundwater, throughout the world it had become important for human survival. Its physical, chemical and bacteriological properties determine the suitability for human consumption. 27 groundwater samples have been collected in south west monsoon season representing the Ponneri Taluk, Thiruvallur district of Tamilnadu. The physicochemical parameters include pH, TDS, cations such as Ca, Mg, Na and K, anions such as Cl, SO_4, HCO_3 and NO_3, PO_4. The samples were classified with sodium absorption ratio, salinity hazard, residual sodium carbonate, sodium percentage (Na%) and permeability index for irrigation, Total hardness and corrosivity index. The classification for drinking water is obtained by drinking water quality index (DWQI). The geochemistry has been studied using piper plot.

Keywords Drinking water quality index · Geochemistry · Remote sensing GIS

S. Sivakumar (✉) · K. Srinivasaraju · M. Shanmugam · D. Thirumalaivasan
C. Lakshumanan
Institute of Remote Sensing, Anna University, Chennai 600025, India
e-mail: geosivakumar@gmail.com

K. Srinivasaraju
e-mail: ksrajuirs@gmail.com

M. Shanmugam
e-mail: shan_mc50@yahoo.com

D. Thirumalaivasan
e-mail: dtvasan@annauniv.edu

C. Lakshumanan
e-mail: drlaks@gmail.com

S. Sivakumar · K. Srinivasaraju · M. Shanmugam · D. Thirumalaivasan · C. Lakshumanan
Centre for Remote Sensing, Bharathidasan University, Trichy 620023, India

P. J. Rao et al. (eds.), *Proceedings of International Conference on Remote Sensing for Disaster Management*, Springer Series in Geomechanics and Geoengineering,
https://doi.org/10.1007/978-3-319-77276-9_20

1 Introduction

Groundwater is a significant and major source of freshwater which is used for drinking and irrigation purpose in worldwide. The quality of groundwater is principally controlled and varied from discharge to recharge regions, nature of host rock and anthropogenic activities. Further, the nature and amounts of dissolved ions in natural water is mainly dependent by their mineralogy and solubility of rock forming minerals [13]. The quality of ground water is function of various chemical constituents which determines its suitability for drinking purposes [1, 6, 17, 19]. The quality of groundwater is now the concern of all experts in countries of the world because 80% of the diseases and deaths in the world are related to water contamination UNESCO (2007), UNDP (1971). Intense agricultural activities and urban development leads to a high demand on groundwater resources and it directly or indirectly plays a significant role in regulating groundwater chemistry (Lowrance et al. 1997; Fakir et al. 2002; Cardona et al. 2004). The input of fertilizers as well as disposal of domestic wastes degrades the groundwater quality in developing countries (Oladeji et al. 2012) and also urbanization, deterioration in groundwater quality occurs (Nkotagu 1996; Stigter et al. 1998; Zilberbrand et al. 2001). The nature of the rock formations, topography, soils, atmospheric precipitation, quality of the recharged water and sub-surface geochemical process are some of the parameters affecting groundwater quality (Todd 1980; Fetter 1994). The information on hydrochemistry is vital to determine the origin of chemical composition of groundwater (Zaporozec 1972). Hence the physiochemical analysis of groundwater is important to evaluate its geochemical process and quality that influences the suitability of water for industrial, domestic and irrigation purposes. The aim of the study is to assess the geochemistry and groundwater quality with special emphasis on drinking water quality index and suitability for irrigation and domestic purposes.

2 Study Area

The study area located in Thiruvallur district, Ponneri Taluk villages as followed as Kolur, Agaram, Uppunelvoyal, Periyaveppathur and Keerapakkam, in Tamilnadu, has the following districts as its neighboring limits. The neighbouring places to the study area include Kancheepuram in the South, Vellore in the West, Bay of Bengal in the East and Andhra Pradesh in the North. The months between April and June are generally very hot with temperature going up to an average of 37.9 °C. During the winter (December–January) the average temperature is 18.5 ºC. The total area extent of about 22.51 km^2 (Fig. 1). The study area is located between north Latitude of 13°24′30″ and 13°29′30″ and East Longitude of 80°12′00″ and 80°15′30″. The coastal areas receive more rains than the inland regions. The average normal rainfall of the district is 1104 mm. Out of the total, 52% of the rainfall

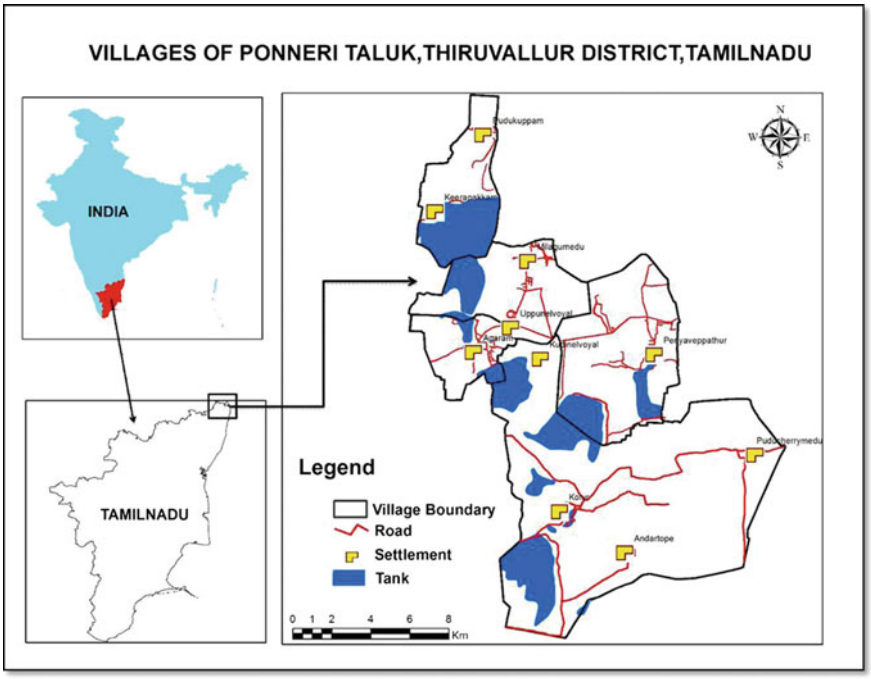

Fig. 1 Study area location map

occurs during the northeast monsoon period and 41% during south west monsoon period. The soil characteristics of the study area includes mostly sandy, mixed with soda or other alkali or stony. The porous formations in the district include sandstones and clays of Jurassic age (Upper Gondwana), marine sediments of Cretaceous age, Sandstones of Tertiary age and Recent alluvial formations. As the Gondwana formations are well-compacted and poorly jointed, the movement of ground water in these formations is mostly restricted to shallow levels. The district underlain predominantly by sedimentary formations, Ground water exists very low phreatic conditions of shallow level of waters [3].

3 Methodology

A total number of 27 water samples were collected from borewells covering the entire study area during the South west monsoon (SWM). Sampling and analysis were carried out using standard procedures [2, 12]. The various parameters of water like pH, Temperature, TDS and conductivity of the water samples were measured in the field using a portable water-analysis kit. Analysis of ions such as Calcium, magnesium, bicarbonate, and chloride were determined by Ti-Trimetric method.

Flame photometry (ELICO CL 378) was used to analyze Sodium and Potassium. Phosphate, and Sulfate were determined by spectrophotometry (ELICO SL 171 minispec). The range of spectrophotometry is 340–1,000 nm with an accuracy of ±2.5 nm.

4 Results and Discussions

The maximum, minimum, and average values of the various surface and groundwater chemical parameters are given in Table 1. The dominating ions in the samples are found in the order,

$$Na > Ca > Mg > K = Cl > NO_3 > HCO_3 > SO_4 > PO_4$$

4.1 Spatial Distribution of Electrical Conductivity

Electrical conductivity is directly associated with the concentration of ions present in water and it creates problems when it is excess in nature. Dissolved solids present in groundwater contains inorganic elements such as carbonate, bicarbonate, chloride, sulphate, phosphate and nitrate of calcium, magnesium, sodium, potassium, iron, and small amount of organic matter and dissolved gases. Higher electrical conductivity is noted as patches in north east, south west and middle regions.

Table 1 Maximum, minimum and average chemical parameters of groundwater

S. no.	Chemical constituents	Statistical parameters		Average
		Maximum	Minimum	
1	pH	8.8	7.7	8.2
2	EC	5090	334	2712
3	TDS	5950	240	3095
4	Cl	1595	124.07	859.53
5	HCO_3	201.3	6.1	103.7
6	CO_3	30	0	15
7	NO_3	256	20.77	138.385
8	PO_4	5.8	0	2.9
9	SO_4	22.57	0	11.285
10	Ca	732	16	374
11	Mg	218.4	0	109.2
12	Na	801.2	36.4	418.8
13	K	94.8	5	49.9

All values are in mg/l except pH and electrical conductivity (EC) in µs/cm

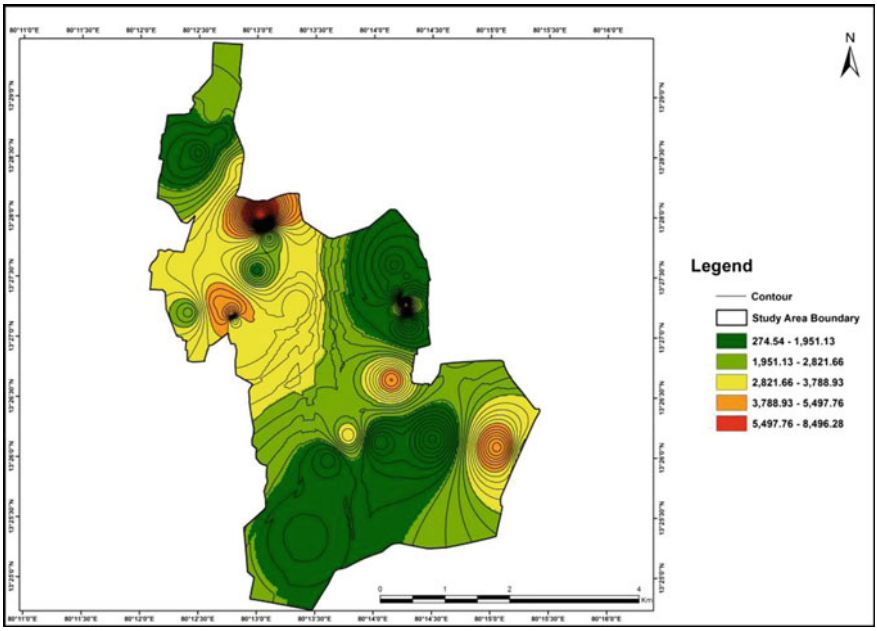

Fig. 2 Spatial distribution of electrical conductivity (µs/cm)

Lower EC is observed in southern and northern regions. The higher EC is observed along the Pulicate lake due to sewage effluents disposal and also due to saline water intrusion (Fig. 2)

4.2 Drinking Water Quality Index

In general assessment of drinking water is comparing the ionic concentration with various Indian and international standards such as BIS, ISI, WHO. This type of evaluation is simple and detailed, but it does not provide a wholistic picture of the region. To overcome this problem, drinking water quality has been used. It is a rating, which reflects the influence of chemical parameters of water. The drinking water quality index (DWQI) is a significant process to assess the suitability of groundwater for drinking purposes. This index was calculated by assigning weights (w) to the water quality parameters (a) based on their threats on human health and also to water quality. The relative weight (Wa) is computed using

$$Wa = \frac{Wa}{\sum_{a=1}^{n} Wa}$$

where Wa = weight of water quality parameter; a and n = number of parameters. Weights (Wa) in a scale of 1–5 based on their importance, were assigned to the parameters as presented in Table 2. Because of their importance in assessment of drinking water quality, weightage of 5 was assigned to pH and TDS. Other parameters were assigned suitable weights between 1 and 4 based on their importance in the water quality evaluation of the region (modified from [11, 16, 18]).

A quality rating scale (q_a) for each parameter and concentration was calculated by dividing its concentration in each water sample by their standards

$$q_a = \frac{C_a}{S_a} \times 100$$

where C_a = concentration of water quality parameter (a) in milligrams per liter and S_a = WHO standard for water quality parameter (a) in milligrams per liter. The sub index (SI) was determined for each parameter, which in turn is used for determining the DWQI as follows:

$$SI_a = W_a \times q_a$$

$$DWQI = \sum SI_a$$

The drinking water quality was classified based on DWQI values of less than 1000, 1000–2000, 2000–3000, 3000–4000, and greater than 4000 as excellent, good, poor, very poor, and unsuitable, respectively (Table 3).

The DWQI maps of the SWM denote majority of the samples in this season are dominated by excellent to good categories. Good category are noted towards form

Table 2 Weights of parameters WHO and ISI Standards (mg/L) for SWM season

DWQI parameters	Weight	Relative weight	WHO standard (2017)
Ca	4	0.13	75
Mg	3	0.10	50
Na	3	0.10	200
K	2	0.06	20
Cl	3	0.10	200
NO_3	4	0.13	50
SO_4	1	0.03	200
HCO_3	1	0.03	350
pH	5	0.16	8.5
TDS	5	0.16	1000
	$\sum$Wa = 31	1.00	

Table 3 Percentage of samples for DWQI

DWQI (WHO-2017)	Category	Samples
<1000	Excellent	2
1000–2000	Good	4
2000–3000	Poor	8
3000–4000	Very poor	7
>4000	Unsuitable	7

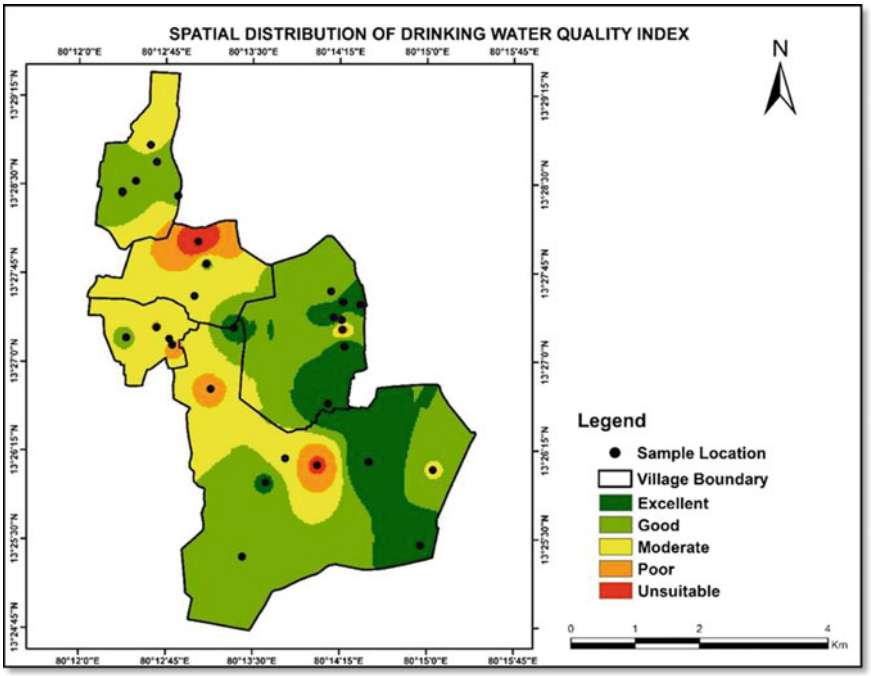

Fig. 3 Spatial distribution of Drinking Water Quality Index for Southwest Monsoon period, with sampling points

northern to southern region. Some patches of poor and unsuitable samples are scattered in southern and north eastern parts. This may be caused due to the leaching of ions, salinity of groundwater, direct connect with nearby coast by the impact of Pulicat lake [7] etc. (Fig. 3).

The samples falling in under moderate category is spatially distributed from mid-south to north and north western regions. The poor water quality may be due to the presence of excess amounts of TDS, Na, HCO_3 and Cl present in the study area.

4.3 Classification for Agriculture Purpose (Irrigation Quality)

4.3.1 Sodium Adsorption Ratio and Sodium Percentage

Sodium adsorption ratio is a measure of the suitability of water for use in agricultural irrigation, as determined by the concentrations of solids dissolved in the water. In order to assess the water quality for irrigation purposes, Na or alkali-hazard expressed in terms of sodium adsorption ratio (SAR) is widely used. If water used for irrigation are high in Na^+ and low in Ca^{2+}, the ion-exchange occurs and Na^+ concentration increases, which destroys the soil structure. The SAR of the water samples in SWM period is computed, using the formula (Hem 1991)

$$\underset{\text{(Sodium Adsorption Ratio)}}{\text{SAR}} = \text{Na}^+ / \sqrt{\left(\text{Ca}^{2+} + \text{Mg}^{2+}\right)/2} \quad \underset{\text{(Sodium Percentage)}}{\text{Na\%}} = [(\text{Na} + \text{K})/(\text{Ca} + \text{Mg} + \text{Na} + \text{K})] \times 100$$

The distribution of SAR based on [14] classification is given in the Fig. 2 by classifying it into excellent, good, poor and unsuitable (Table 4).

From the sodium percentage results, it has been found that excess sodium percentage is the due to the establishment of tight arrangements of dispersed soil particles saturated with sodium. During winter season, sodic soil has poor infiltration and drainage but during summer season, it become quite hard. The distribution of Na% classification after [20] is categorized into excellent, good, permissible, doubtful, and unsuitable categories. Sodium reacts with CO_3 to form alkaline soils whereas with Cl forms saline soil. Both these soil do not help in the growth of plants [8, 9]. Classification of groundwater for irrigation purpose was calculated as, followed as above the formula.

The higher Na% is mainly due to long residence time of water, dissolution of minerals from lithological composition, and the addition of chemical fertilizers by the irrigation waters [10, 15]. According to Eaton (1950), Na percentage is classified into two categories as safe and unsafe (Table 5).

4.3.2 Residual Sodium Carbonate

The RSC equals the sum of the bicarbonate and carbonate ion concentrations minus the sum of the calcium and magnesium ion concentrations, where the ions are

Table 4 Sodium absorption ratio hazard

SAR	Hazard	Samples
<10	No harmful effects from sodium	26
10–18	Appreciable sodium hazard	2
18–26	Harmful effects could be anticipated	1
>26	Unsuitable for irrigation	NIL

Table 5 Sodium percentage hazard

Percentage sodium	Water class	Total no. of samples
<20	Excellent	2
20–40	Good	7
40–60	Permissible	8
60–80	Doubtful	5
>80	Unsuitable	5

expressed in meq/L. A negative RSC indicates that sodium build up is unlikely sufficient since calcium and magnesium are in excess of what can be precipitated as its carbonates. A positive RSC indicates possibility of sodium build up. The excess carbonate in the solution will enhance the precipitation of $CaCO_3$ in soil which in turn will increase sodium in the solution.

Further, during the process of dispersion of ions, Na is likely to be dominated [5]. The dominance of alkaline earth ions influences the suitability of water for irrigation purpose. RSC = $(CO_3 + HCO_3) - (Ca + Mg)$. According to the [14], residual sodium carbonate is classified into four categories, such as High, Medium, Low and None. In southwest monsoon only two samples are affected by Residual Sodium Carbonate parameters (Table 6).

4.3.3 Permeability Index

The soil permeability is affected by long term use of irrigation water. For irrigation, the suitability of water was assessed based on PI of water and can be classified as class I, class II and class III orders (Table 7).

The permeability index (PI) of the water was derived by Doneen [4] by using major cations and HCO_3 concentration using the following expression; $PI = [\{Na + (\sqrt{H}CO_3)\}/(Ca + Mg + Na)] \times 100$ Permeability index is an essential factor to determine the quality of irrigation water in relation to soil for improvement in agriculture (Thilagavathi et al. 2012). When there is a deficient in micronutrients, it will result in the rise of HCO_3 related toxicities.

Table 6 Residual sodium carbonate hazard

RSC	Hazard	Samples
<0	None	25
0–1.25	Low, with some removal of calcium and magnesium from irrigation water	2
1.25–2.5	Medium, with appreciable removal of calcium and magnesium from irrigation water	NIL
>2.5	High, with most calcium and magnesium removed leaving sodium to accumulate	NIL

Table 7 Permeability index

Water class	PI (%)	Samples
Class I	>75	8
Class II	25–75	16
Class III	<25	3

4.4 Hydrogeochemical Processes

Piper (1944) classified hydrogeochemical facies using trilinear plot (Fig. 4). It consists of two lower triangular fields and a central diamond shaped field. The Triangular fields are plotted separately with epm values of cations (Ca, Mg) alkali earth, (Na + K) alkali, (HCO_3) weak acid and (SO_4 and Cl) strong acid. Water facies can be identified by projection of plots in the central diamond shaped field. This plot has been used by several authors to understand the hydrogeochemical facies (Karanth1991; Chidambaram 2000; Subramani et al. 2005; Anandhan 2005; Thivya et al. 2013; Thilagavathi et al. 2012). The geochemical evolution plot has six sub-fields, viz. 1. (Ca–HCO_3 type); 2. (Na–Cl type); 3. (mixed Ca–Na–HCO_3 type); 4. (mixed Ca–Mg–Cl type); 5. (Ca–Cl type) and 6. (Na–HCO_3 type). In study area, samples are clustered in the fields of 2, 4 and 5 the majority of the samples are concentrated in the Ca–Cl type which shows that predominance of anthropogenic impact such as industries. Na–Cl type generally indicates a strong saline nature in groundwater and also due to anthropogenic activities (Pulido-Leboeuf 2004;

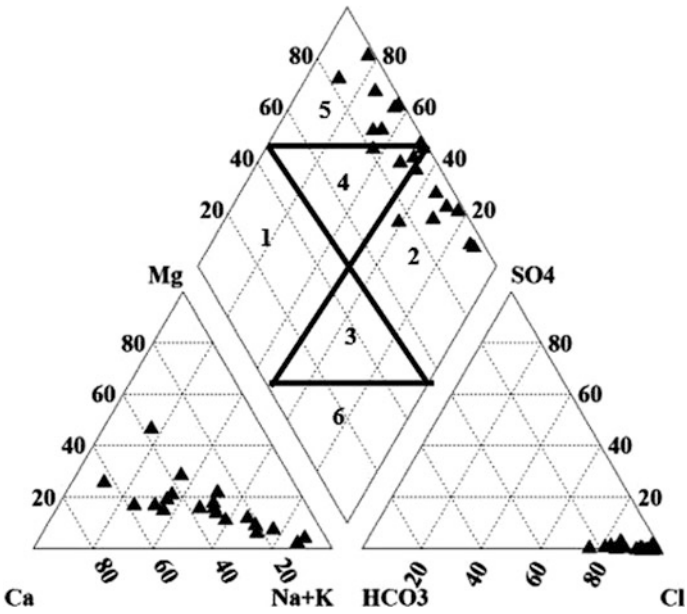

Fig. 4 Piper plot to understand the geochemical processes

Prasanna et al. 2010; Thilagavathi et al. 2012) (Fig. 4). The samples have been collected in south west monsoon, hence some representations are observed in zone 4 of Mixed Ca–Mg–Cl type indicates the leaching processes in groundwater (Thivya et al. 2015).

5 Conclusion

The analysis of chemical properties of the groundwater in the study area reveals the dominant ions as Na and Cl. The study brings out the fact that some of the samples are suitable for drinking purpose and some samples fall in poor categories which can be use after the treatment. Classification on irrigation quality based on SAR, RSC, permeability index most of the samples are suitable for agricultural purposes. According to the corrosivity ratio, all samples fall in unsafe category which is unsuitable for domestic purpose. The major reason for the Hydrogeochemistry found is inferred to be caused by saline water intrusion and anthropogenic activities.

References

1. APHA.: Standard methods for the examination of water and waste water, 20th edn. APHA, Washington DC, USASS (1998)
2. APHA: Standard methods for the examination of water and waste water, 19th edn. APHA, Washington DC, USA (1995)
3. Balakrishnan, T.:District ground water brochure Tiruvallur District, Central Ground Water Board South Eastern Coastal Region, Chennai (2007)
4. Doneen, L.D.: Water quality for agriculture. Department of Irrigation, University of California, Davis. 48 (1964)
5. Emerson, W.W., Bakker, A.C.: The comparative effect of exchangeable Ca, Mg and Na on some soil physical properties of red brown earth soils. 2. The spontaneous dispersion of aggregates in water. Aust. J. Soil Res. **11**, 151–152 (1973)
6. ISI.: Central Water Commision, Indian Standard for Drinking Water as per BIS specifications (IS 10500-1991), (1991)
7. Jasmin, I., Mallikarjuna, P.: Delineation of groundwater potential zones in Araniar River basin, Tamil Nadu, India: An integrated remote sensing and geographical information system approach. Environ. Earth. Sci. (2015). https://doi.org/10.1007/s12665-014-3666-y
8. Karmegam, U., Chidambaram, S., Sasidhar, P., Manivannan, R., Manikandan, S., & Anandhan, P.: Geochemical characterization of groundwater's of shallow coastal Aquifer in and Around Kalpakkam,South India. Res. J. Environ. Earth Sci. **2**(4), 170–177 (2010)
9. Manikandan, S., Chidambaram, S., Prasanna, M.V., Thivya, C., Karmegam, U.: Hydrochemical characterstics and Groundwater quality assessment in Krishnagiri district, Tamilnadu, india. Int. J. Earth Sci. Eng. **04**(04), 623–632 (2011)
10. Qiyan, F., Baoping, H.: Hydrogeochemical simulation of waterrock interaction under water flood recovery in Renqiu Oilfield, Hebei Province, China. Chin. J. Geochem. **121**(2), 56–162 (2002)
11. Ramakrishnaiah, C.R., et al.: Assessment of water quality index for the groundwater in Tumkur Taluk, Karnataka State, India. E-J. Chem. **6**(2), 523–530 (2009)

12. Ramesh, R., Anbu, M.: Chemical methods for environmental analysis. Water Sediments 161 (1996)
13. Raymahashay, B.C.: Geochemistry for Hydrologists, Published by Editions Technip,ISBN 10:710806673 ISBN 13: 9782710806677 (1996)
14. Richard, L.A.: Diagnosis and improvement of saline and alkali soils. USDA Handbook **60**, 160 (1954)
15. Subba Rao, N., Srinivasa Rao, K.V., John Devadas, D., Deva Varma, D., Thirupathi Rao, B., Subrahmanyam, A., Arjunudu, K., Ratnakantababu, K., Venkatakrishna, T.: Quality of groundwater in the coastal area of Visakhapatnam, Bhimunipatnam, Andhra Pradesh. Ind. J. Geochem. **22** (2002)
16. Thivya, C., Chidambaram, S., Thilagavathi, R., Nepolian, M., Adithya, V.S.: Evaluation of drinking water quality index (DWQI) and its seasonal variations in hard rock aquifers of Madurai district, Tamilnadu. Int. J. Adv. Geosci. **2**(2), 48–52 (2014)
17. Trivedy, R.K., Goel, P.K.: Chemical and biological method for water pollution studies. Environ. Publ. (Karad, India), **6**, 10–12 (1986)
18. Vasanthavigar, M., Srinivasamoorthy, K., Vijayaragavan, K., Ganthi, R.R., Chidambaram, S., Anandhan, P.: Application of water quality index for ground water quality assessment: Thirumanimuttarm sub-basin, Tamilnadu India. Environ. Monit. Assess. **171**(1–4), 595–609 (2010)
19. WHO (World Health Organization).: Guidelines for drinking water quality recommendations, vol. 1 (p. 515). Geneva, WHO (1984)
20. Wilcox, L.V.: Classification and use of irrigation water. U.S. Geological Department Agriculture, vol. 969, 19p (1955)

Chapter 21
Assessing the Spatial Patterns of Geotagged MGNREGA Assets on Bhuvan Using GIS Based Analysis

Kaja Divya, K. Mruthyujaya Reddy, G. S. Pujar and Peddada Jagadeeswara Rao

Abstract Mahatma Gandhi National Rural Employment Guarantee Act (MGNREGA) of 2005 which aims at enhancing livelihood security in rural areas of the country by providing at least 100 days of guaranteed wage employment. As per MGNREGA, creation of durable assets and strengthening of livelihood is an important objective of the scheme. In this regard, the Ministry has adapted GeoMGNREGA, to create a Geographical Information System (GIS) solution to visualize, analyze and explore the data of assets created under the MGNREGA. NRSC/ISRO supports MoRD for geotagging of assets. Spatial analysis helps in defining new forms of representation for better understanding the assets and identifies the spatial patterns of it. This option was explored by showing the procedural method of (a) Categorization and quality assessment of asset information (b) Consider the consisted assets of 23,498 (neglecting all inconsistent assets), calculate spatial density by means of Hotspot mapping using Kernel Density Estimation, Hotspot analysis and Grid based analysis using ArcGIS (c) finding the desktop position with respect to and Land Use and Land cover. Study proves that GIS gives us a better synoptic perspective to MGNREGA asset mapping, analysis and sets perspectives in data quality as well.

Keywords MGNREGA · Hotspot mapping · Grid analysis · KDE

K. Divya (✉) · P. J. Rao
Department of Geo-Engineering, Andhra University, Visakhapatnam, India
e-mail: divyakaja2015@gmail.com

P. J. Rao
e-mail: pjr_geoin@rediffmail.com

K. M. Reddy
PPEG and RDWMD, National Remote Sensing Centre, Hyderabad, India
e-mail: reddy_km@nrsc.gov.in

G. S. Pujar
RDWMD, National Remote Sensing Centre, Hyderabad, India
e-mail: pujar@nrsc.gov.in

P. J. Rao et al. (eds.), *Proceedings of International Conference on Remote Sensing for Disaster Management*, Springer Series in Geomechanics and Geoengineering,
https://doi.org/10.1007/978-3-319-77276-9_21

1 Introduction

Rural Employment Creation is the vital process in mitigating economic delinquency of rural poor and should be tackled using best of the technological paradigm available. So, the Central Government formulated the Mahatma Gandhi National Rural Employment Guarantee Act (NREGA) [1]. The MGNREGA notified on September 7, 2005, aims at enhancing livelihood security of households in rural areas of the country by providing at least 100 days of guaranteed wage employment in a financial year to every household whose adult member's volunteers to do unskilled manual work [2]. As per the MGNREGA, creation of durable assets and strengthening of livelihood is an important objective of the scheme. As per the information available with NREGA, around 30 lakh assets are created annually across the country under the rural job scheme, which involves activities like Irrigation Facility, Water Harvesting, Rural Sanitation, Road connectivity, Drought Protection and Land Development [3]. The Ministry of Rural Development has adapted Bhuvan based GIS solutions to visualize, analyze and explore NREGA asset related data and also to manage them efficiently. The creation, availability and effective communication of geo-spatial information and services are very big challenges. In this regard, Ministry has decided to implement Geo tagging of assets under Mahatma Gandhi NREGA using ISRO Bhuvan webGIS portal. Desk based moderation of geo-tagged images available in the Bhuvan portal will be done at the Bhuvan Geo-platform to ensure quality adherence. The existing database is used for analyzing and applying spatial statistical analysis.

2 Study Area

The study was set to West Godavari in Andhra Pradesh. It occupies an area of approximately 7742 m^2 and Eluru is the headquarters of it. The district was situated between 80º 50′ and 81º 55′E, of the eastern longitudes and 16º 15′ and 17º 30′N, of northern latitudes. Khammam District lies to the north, East Godavari District to the east, the Bay of Bengal to the south, and Krishna District to the west. The district is located in delta region of the Krishna and Godavari rivers. The district has population of 3,934,782 as per the 2011 census. The study has selected West Godavari district for two reasons, one is it is the district where the scheme seems to have been implemented successfully compared to other districts, with highest amount of expenditure and with the participation of poor and NGO's, and the second reason is that the west Godavari represents all the typical features of the state, like chronic drought areas, agency (tribal) areas, and settled irrigation areas (Fig. 1).

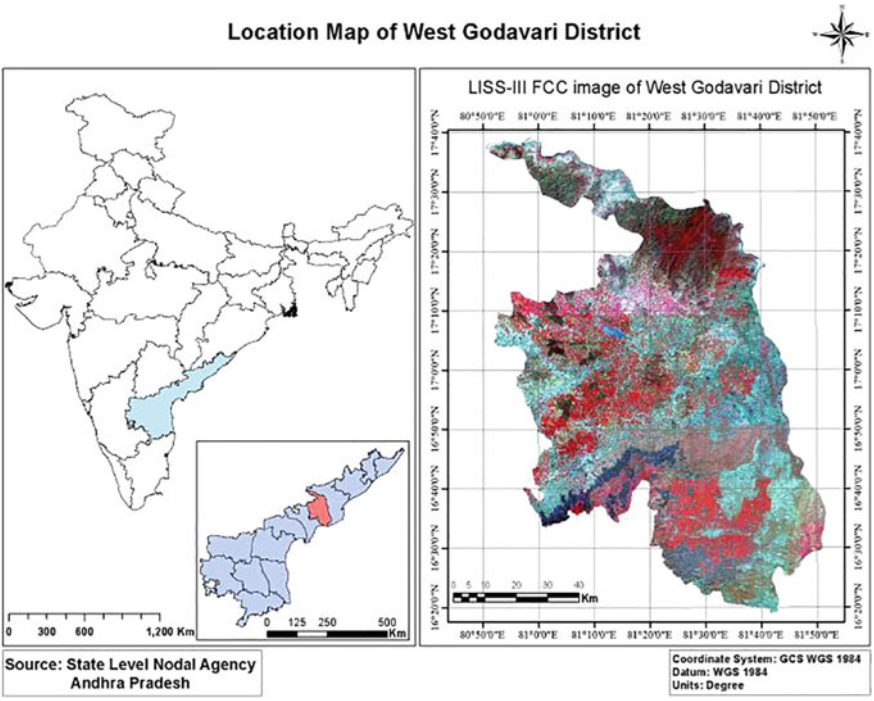

Fig. 1 Location map of the study area

3 Methodology

The overall methodology of this research is given in Fig. 2. In order to find the spatial patterns of geotagged MGNREGA assets in West Godavari district, various vector data layers of the district were collected from Bhuvan-Geoportal and state level nodal agency. These vectors were constructed by digitizing various maps with scale of 1:50,000. The research consists of the following distinct stages.

1. The first step is the categorisation of MGNREGA assets based on the type of activity that takes place in the study area and checking for data consistency.
2. Applying Spatial Statistics to the consisted assets like hotspot mapping techniques by means of Grid analysis, hotspot analysis and kernel density estimation (KDE) using ArcGIS.
3. Finally, we use proximity analysis to know the distribution of assets with maximum vicinity of Land class features.

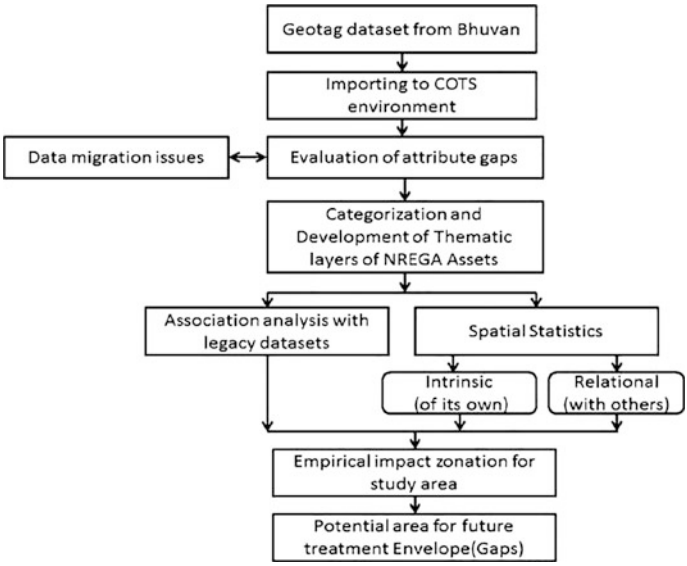

Fig. 2 Flow chart of the study

4 Results

4.1 Sectorwise Assets Created and Geotagged in West Godavari

The total assets in West Godavari district are categorised into different fields based on the type of activity taken place. The Major activities that are covered in West Godavari district are: Micro Irrigation works (24,057), Rural Sanitation (10,072) and Drought Proofing (3961) (Fig. 3).

4.2 Grid Based Analysis of Understanding the Spread of Completed Assets Geotagged in West Godavari District

In order to combat the problems associated with different sizes and shapes of geographical regions, uniform grids (or quadrats) can be drawn in a GIS as a layer over the study area and thematically shaded. Therefore, all areas used for thematic shading are of consistent dimensions and are comparable, assisting the quick and

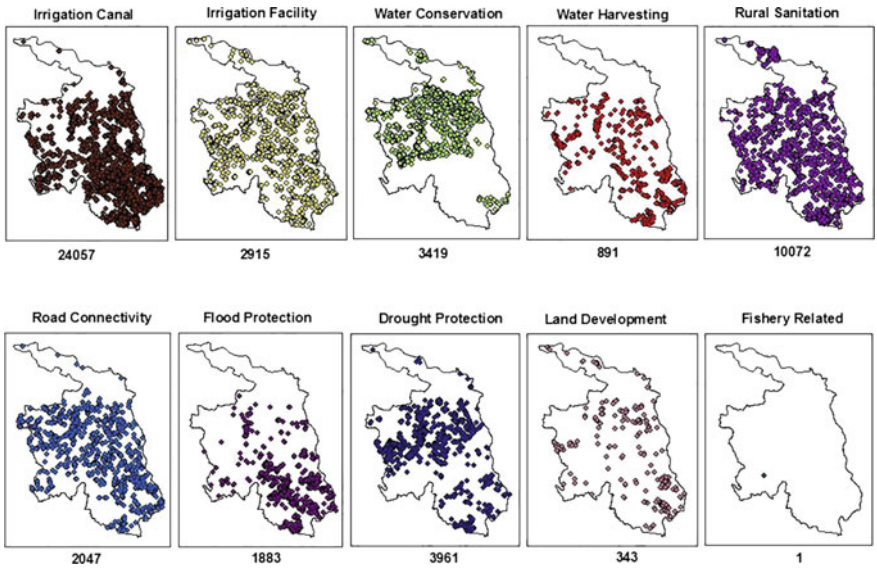

Fig. 3 Sectorwise assets created and geotagged in West Godavari

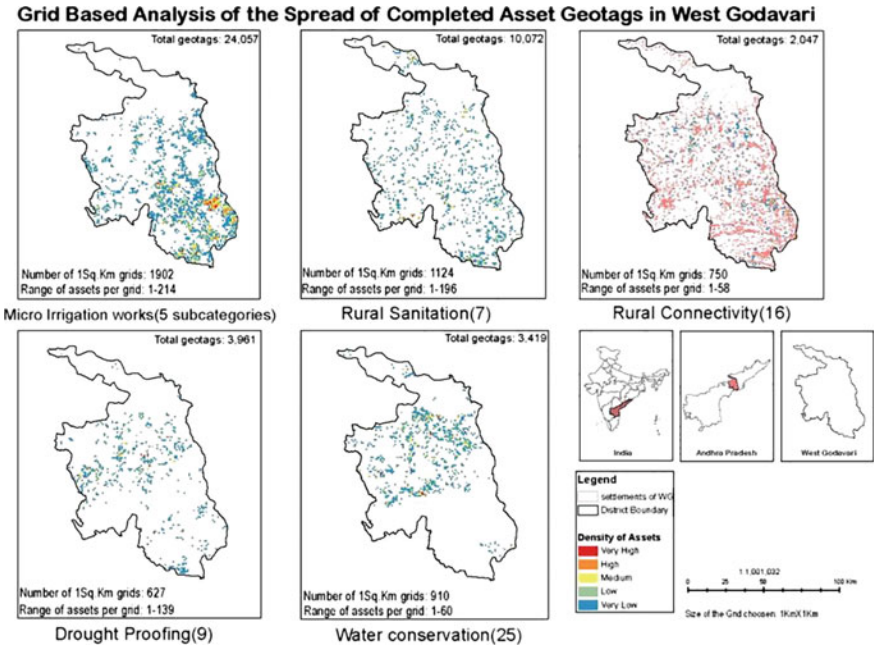

Fig. 4 Grid based analysis for the spread of completed asset geotagged in West Godavari

easy identification of density of assets. Here, the grid size choosen is of 1 m^2. The range of assets in each grid varies. For Micro Irrigation works(IC), the range is 1-214 (Fig. 4).

4.3 Analysis of Internal Match of Work Code Contents to Asset Identity

The MGNREGA assets are categorized into 17 major categories and 153 sub categories [4]. A test analysis is carried out to understand the identity of Completed Assets for their precise categorization and visualization. As an example consider a single MGNREGA asset that is extracted from Bhuvan-Geoportal which contains the following information.

From Table 1, Desilting comes under the category of Water Harvesting structures (WH) but, in the database it is under Micro Irrigation works (IC). Thus, the Category identity in work code does not match with category identity for a subcategory name. So, the mismatch arises. While verifying the internal consistency for the overall data in the district, there is some inconsistency present in the data which can be verified by considering the category short names depicted from the workcode of each asset is compared with subcategory and its corresponding codes. The total number of completed assets which have correctly aligned subcategories are 23,498 (out of 54,254 completed assets) considering all the aspects such as subcategory names, category codes and subcategory code including work code. Thus, the efficiency of completed assets which have understandable identities is **43.3**% (Table 2).

While analysing the data, we identified there are 1865 assets in the database which do not have either subcategory name, category and sub-category code except work code information i.e., assets without any identities are 1865. Likewise the number of assets without having category/sub-category identities is 6990 assets as shown in Table 3.

4.4 Hotspot Mapping Techniques

Three Hotspot mapping techniques were chosen and used for generating hotspot maps [5]. These techniques were Hotspot analysis, grid thematic mapping and Kernel Density Estimation. These techniques were chosen as they are the most common techniques used for generating hotspot maps of consisted MGNREGA assets. Each of these techniques also requires certain parameters to be set for them to operate for them to generate a visual map output [6] (Figs. 5, 6 and 7).

Table 1 Asset data from Bhuvan-Geoportal

Asset ID	State	District name	Block name	Workcode	Work name	Subcategory code	Subcategory name	Derived category short name
02002706771	Andhra Pradesh	West Godavari	Ganapavaram	0205026020/IC/020170086	Desilting of existing field channel	0105	Desilting	IC

Table 2 Verification of inconsistency for the assets in West Godavari

FROM WORK CODE

FROM ACTUAL DATA

CATEGORY CODE	CATEGORY SHORT NAME	1 WH		2 WC		4 RS		5 RC		8 LD		9 IF		11 FR		12 FP		14 DW		15 DP	
		YES	NO	YES	NO	YES	NO	YES	NO	YES	NO	YES	NO	YES	NO	YES	NO	YES	NO	YES	NO
1	WH	708	20735																		
2	WC			2809	1044																
4	RS					10516	5														
5	RC							1904	0												
8	LD									303	42										
9	IF											2937	1812								
11	FR													13	0						
12	FP															86	3				
14	DW																	0	1		
15	DP																			4222	4

Table 3 Completed assets with and without any information except workcode

Subcode	Sub categories	Missing of category and sub-category identities							Total
Missing of category and sub-category identities		DP	FP	IC	LD	RC	RS	WH	
	No identity	31	1129	128		292	16	269	1865
	Afforestation			1					1
	Feeder Channel		34	4162					4196
	Food grain	1							1
	Horticulture	50							50
	Land development				17				17
	Land leveling		429						429
	Others		10						10
	Renovation		421						421
	Grand total	82	2023	4291	17	292	16	269	6990

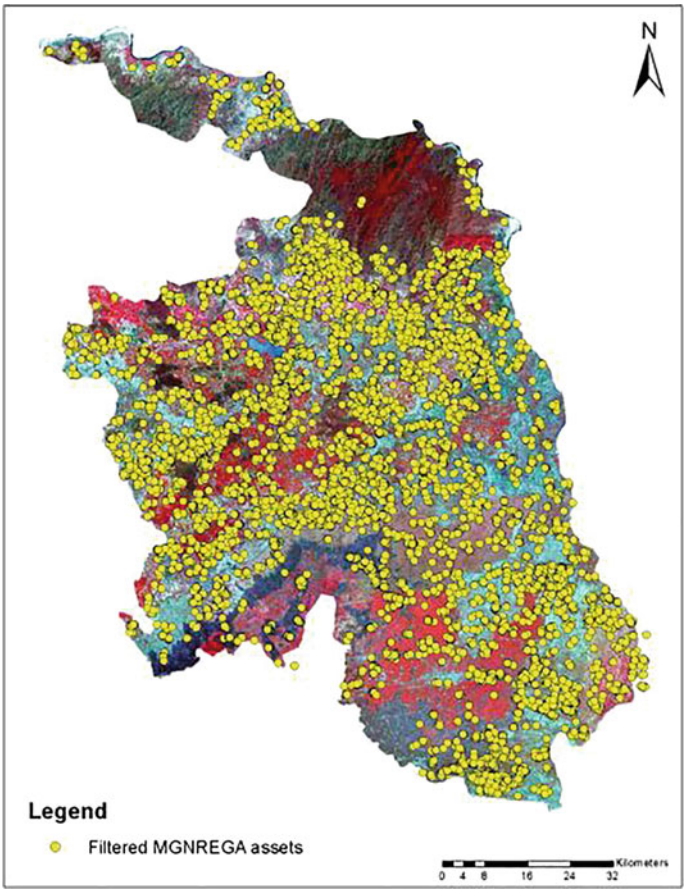

Fig. 5 Point map

4.4.1 Hotspot Analysis

This technique requires Incident point data to be aggregated to polygonal census output areas to generate a count of assets for each output area. This was performed using the standard routines in ArcMap. The selection of the thematic range method and values for determining the Hotspot threshold are explained below as they also apply to grid thematic mapping and KDE.

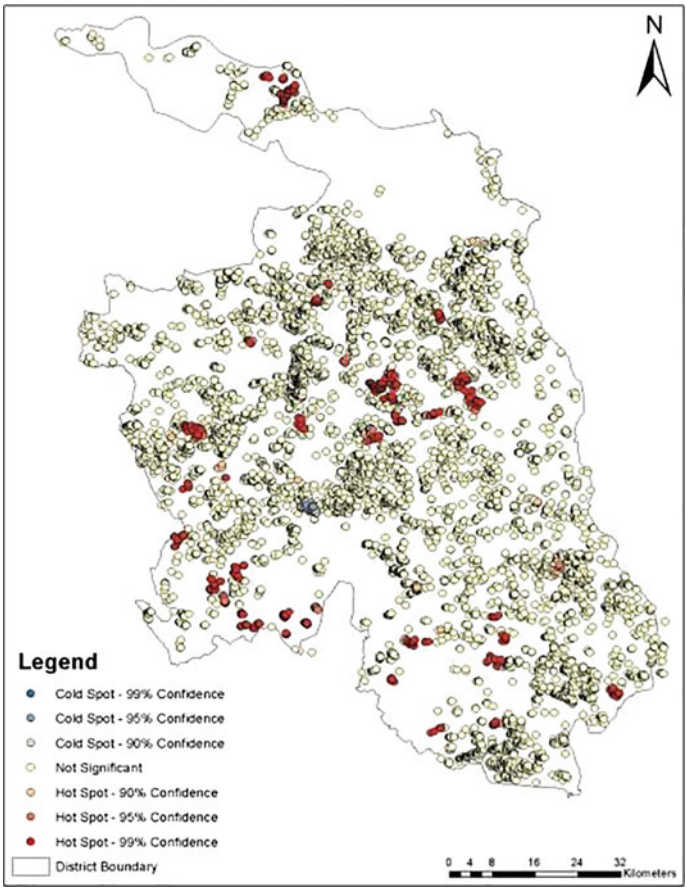

Fig. 6 Hotspot analysis

4.4.2 Grid Thematic Mapping

ArcGIS software enables analysts to specify a grid lattice that can be positioned across the study area. The parameter the user must decide is the size of each square grid cell. There is little guidance on which cell size to select; if the cells are too large, the resulting hotspot map will only show coarse geographic patterns of Assets, and if too small it can be difficult to discern any spatial patterns from the hotspot map. For this research, a grid cell size of 1 m^2 was chosen. Once the grid had been calibrated, functions in ArcMap were used to calculate a count of the number of asset points within each grid cell.

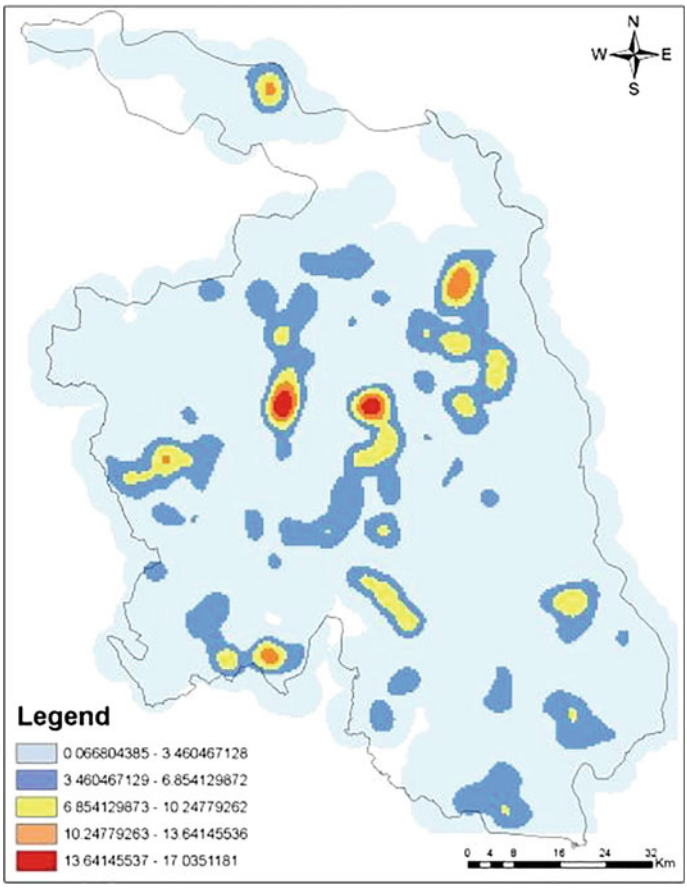

Fig. 7 Kernel density estimation

4.4.3 Kernel Density Estimation (KDE)

KDE hotspot maps were generated using Hotspot Detective. This technique requires two parameters to be entered by the user—the cell size and the bandwidth (also commonly referred to as the search radius). Hotspot Detective determines default settings for these parameters after performing an analysis of the input data.

4.5 Proximity Analysis

Roads, Drainage, Settlements, Wastelands, and Waterbodies are the important landscape features which will facilitate huge and access.

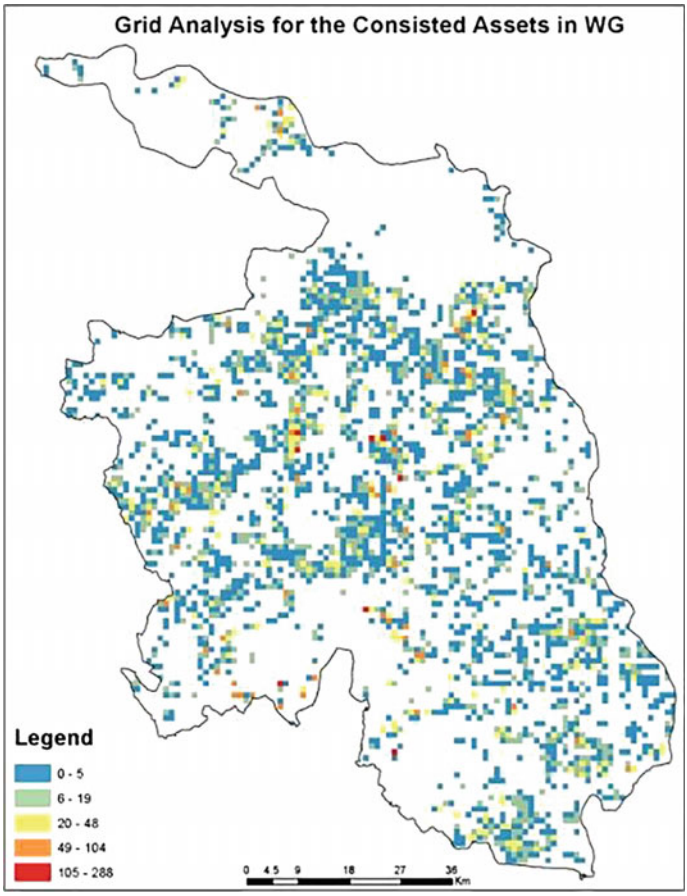

Fig. 8 Grid based analysis

4.5.1 Distribution of Assets with Maximum Vicinity from LULC

Considered the consisted NREGA assets and calculated the distribution of assets with Maximum vicinity from LULC by means of calculating the minimum distance of each asset corresponding to individual landscape feature and plotted in the histogram.

4.5.2 Distribution of Assets Within 50 m from LULC

Considered the consisted NREGA assets and calculated the distribution of assets based on distance from various land class features by means of categorising the classes based on the distance of each asset from individual landscape feature. Thus,

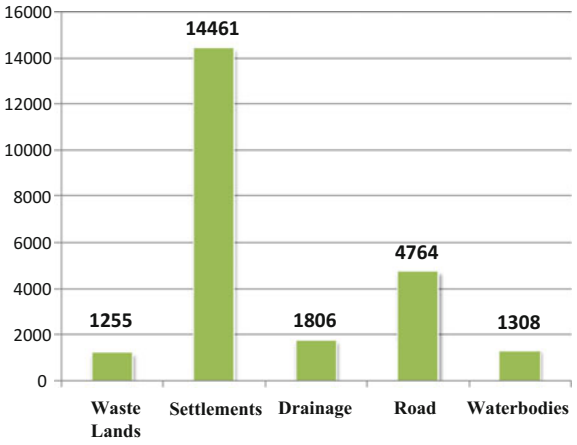

Fig. 9 Distribution of assets with max. vicinity from LULC

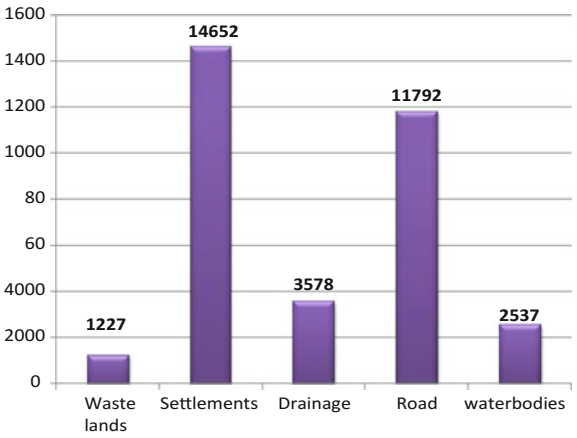

Fig. 10 Distribution of assets within 50 m from LULC

count of assets within 50 m range is being plotted as shown in Fig. 8. This analysis reveals that a high amount of MGNREGA assets are located near to the settlements (Figs. 9 and 10).

4.5.3 Distribution of Assets from Landcover Categories

As MGNREGA is a rural employment scheme, but there are some assets that are being covered in the forest, urban areas and industrial areas. The analysis shows that 120 activities are done in the urban areas in the name of Rural development act (Fig. 11).

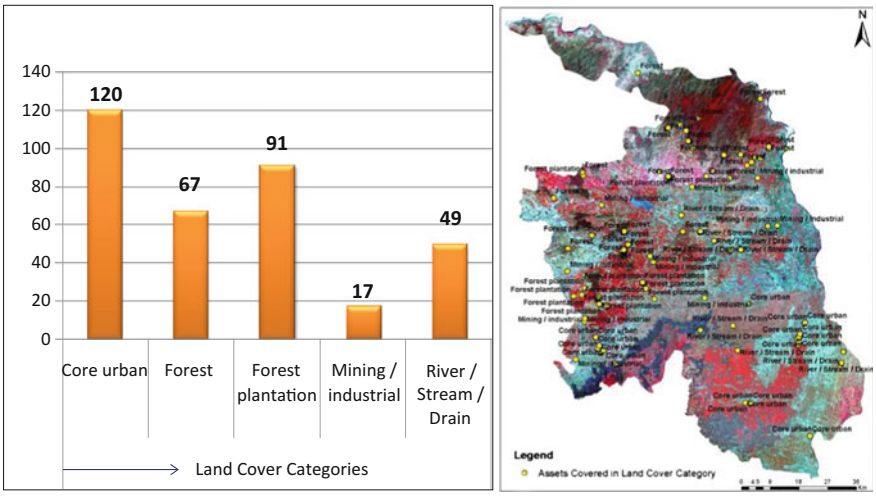

Fig. 11 Distribution of assets from land cover categories along with LISS-III FCC image of West Godavari district

5 Conclusion

The results show that the above three Hotspot techniques not only have similarity in size (in m^2) for each suitability class, but they also have similarity in spatial distribution of each class in whole study area. Their spatial comparison had 75% similarity in the distribution of assets in the study area.

References

1. Ravindar, M.: Empowerment of women through MGNREGS: A study in warangal district of Telangana state. Int. J. Multi. Res. Mod. Educ (IJMRME). **2**(1), (2016). ISSN (Online): 2454 - 6119 (https://www.rdmodernresearch.org)
2. Chandra, G.: A study on mahatma gandhi national rural employment guarantee act opportunity and the corruption (MGNREGA). Int. J. Manag. Res. Soc. Sci (IJMRSS). **2**(1), (2015)
3. MGNREGA Sameeksha An Anthology of Research Studies on the Mahatma Gandhi National Rural Employment Guarantee Act (2005)
4. Samarthya technical training manual MGNREGA. Ministry of rural development, Government of India (2015)
5. Chainey, S., Tompson, L., Uhlig, S.: The utility of hotspot mapping for predicting spatial patterns of crime. Secur. J. **21**, 4–28 (2008)
6. Ansari, S.M., Kale, K.V.: Mapping and analysis of crime in Aurangabad City using GIS. IOSR J. Comput. Eng (IOSR-JCE)
7. http://bhuvan.nrsc.gov.in/governance/mgnrega_phase2.php

Chapter 22
Detection of Landslide Using High Resolution Satellite Data and Analysis Using Entropy

Ibrahim Shaik, S. V. C. Kameswara Rao and Balakrishna Penta

Abstract High Resolution Remote Sensing satellite images offer rich contextual information, including spatial, spectral, and contextual information. In order to detecting the Landslides using high resolution remote sensing data effectively various methods have been suggested. Pixel based approaches are applied to extract information from such remote sensed data, only spectral information is used. Object based classification approaches give good results not only for spectrally same but also compositionally different features. In this study, object oriented classification based on image segmentation is used to detecting Landslides from high resolution remote sensing data, validation and analysis using Entropy. Entropy is the measure of uncertainty in any data and is adopted for maximisation of mutual information in many remote sensing applications. The popular available versions like Shannon's, Tsalli's and Renyi's entropies were analysed and comparative suitability of the various available entropy versions in context of validation and analysis of landslides.

Keywords Classification · High resolution satellite image · Entropy
eCognition

I. Shaik (✉) · S. V. C. Kameswara Rao
Regional Remote Sensing Centre, Nagpur, India
e-mail: ibrahimshaik.1985@gmail.com

S. V. C. Kameswara Rao
e-mail: svc2112@gmail.com

B. Penta
Department of Geo-Engineering, Andhra University, Visakhapatnam, India
e-mail: balakrishna.penta@gmail.com

P. J. Rao et al. (eds.), *Proceedings of International Conference on Remote Sensing for Disaster Management*, Springer Series in Geomechanics and Geoengineering,
https://doi.org/10.1007/978-3-319-77276-9_22

1 Introduction

High resolution satellite images have many applications in various commercial and civil areas in recent years like meteorology, forestry, agriculture geology and landscape. High resolution satellite images have rich contextual information [1]. The information includes shape, texture and spatial characteristics. In order to deal such rich information content for information extraction, pixel-based approaches have faced substantial difficulties. In order to estimate more accurate results object based feature extraction is a newly and widely used method recently used in many study areas. Object based image analysis is implemented in order to extract relevant surface information, combining spectral and spatial information [2]. There by, with the object based approach not only the spectral information in the image will be used as classification information, the texture and context information in the image will be combined into classification as well. The concept of object based information extraction is that to interpret an image, the relevant semantic information is represented by meaningful image objects and their mutual relationship rather than individual pixels. Entropy as a measure of uncertainty associated with information was introduced by Claude E. Shannon being inspired from the common entropy concept in physics [3]. The principle of entropy is to use uncertainty as a measure to describe the information contained in a source. Different versions of entropies have been applied for the effective automation of various remote sensing analysis. The entropy is related to the concept of Kolmogorov complexity of an object is a measure of the computational resources needed to specify the object.

2 Study Area and Data Sets

Landslides are the one of the most important types of natural hazards. Landslides triggered by the heavy rainfall are the most common in hilly regions. The factors which influence landslides are slope angle, climate, weathering, water content, vegetation, geology and slope stability. Landslides occur when the slope changes from a stable to unstable condition. The study area, in Jammu Kashmir had considerable landslide damage following heavy rains in 2014. The following data sets are used to detection of Landslides using eCognition software (Fig. 1).

3 Methodology

First of all both pre and post monsoon images are orthorectified using autosync function in ERDAS. In this study the concept of the object oriented information extraction has been used for the accurate identification of landslides [4]. For high

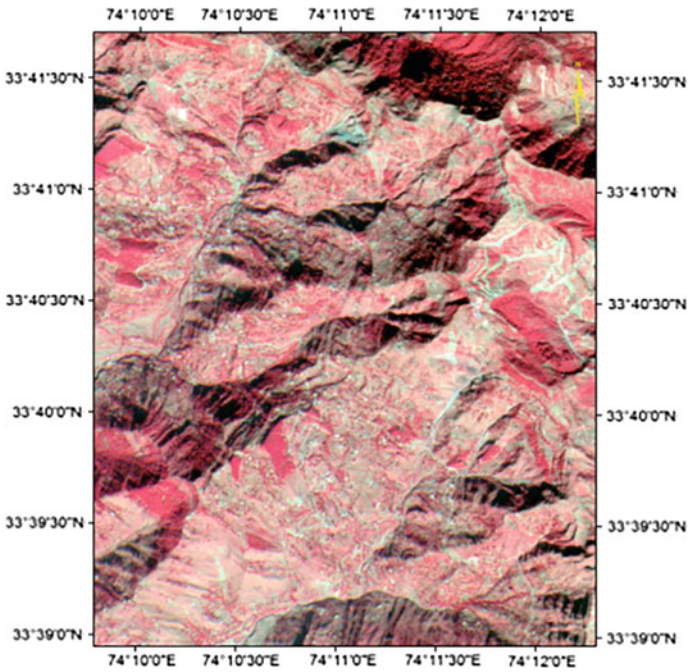

Fig. 1 Study area

resolution satellite imagery, beginning with the initial pre-processing, object-oriented image analysis is performed using the software eCognition. This process has been carried out into three steps: Multiresolution Segmentation, creation of General Classes, and Classification rules (Rule Base). Thereby an initial image segmentation step groups the pixels that are similar in spectral context to get meaningful image objects on an arbitrary number of scale levels. Parameters are set for different object features such as shape, scale and spectral features. These image segments have to be calculated on different scale on hierarchical levels on the basis of trial and error process for achieving proper segmentations of objects of interest (Fig. 2) [5, 6].

4 Rule Set for Landslide Detection (eCognition)

Accurate segmentation is an important issue in the context of object-oriented classification. During the segmentation process meaningful image objects are created on the basis of several adjustable factors of homogeneity and heterogeneity in colour and shape. In this process algorithm select as multiresolution segmentation. In segmentation settings, the layers using for the segmentation (Post image) is made

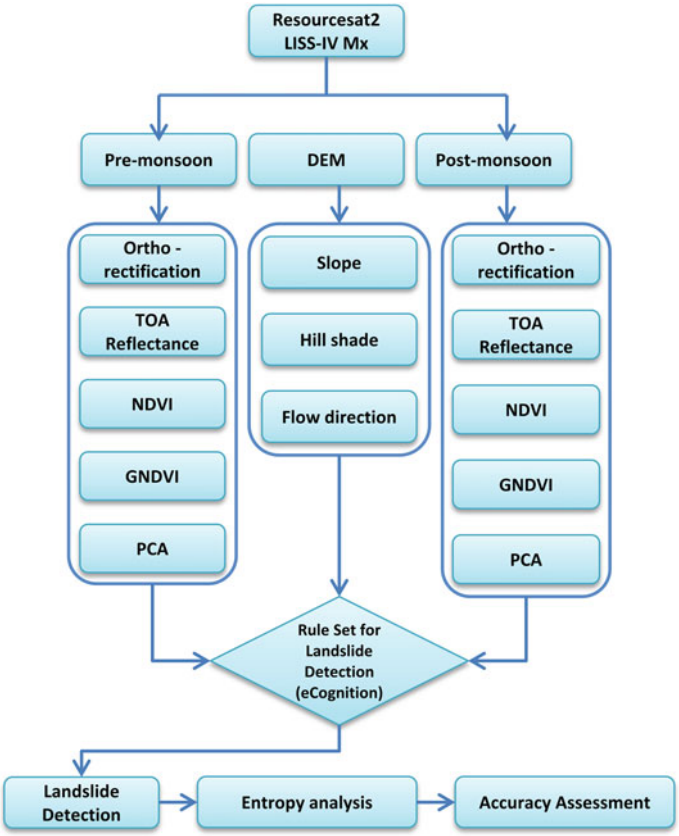

Fig. 2 Flow chart

as 1 and layers not used for segmentation (pre layers and other layers) is made zero and scale parameter is 20. The value of the scale parameters influences the average object size. This parameter influences the maximal allowed heterogeneity of the objects. The larger the scale parameter the larger the objects become. Size of the segments/objects obtained from segmentation technique (a pre-requisite for object-based classification) is determined objectively through a newly created plateau objective function (POF) [7]. POF is a statistical function, created using intrasegment variance and spatial autocorrelation (Moran's I). To remove the background in edit process algorithm made as "assign class" and in threshold condition is created. Process tree (Rule Set) for detecting the landslides is shown in Figs. 3 and 4.

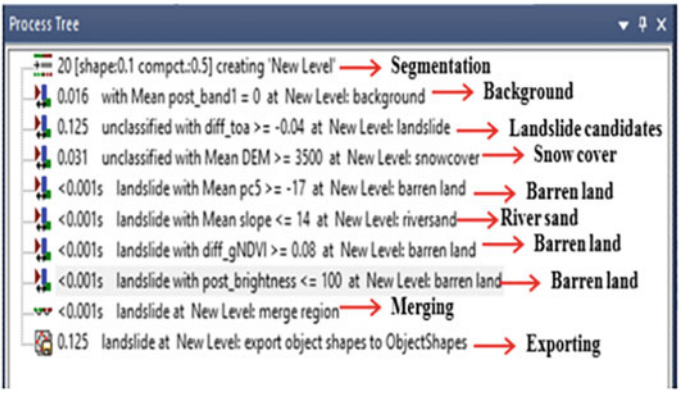

Fig. 3 Process tree

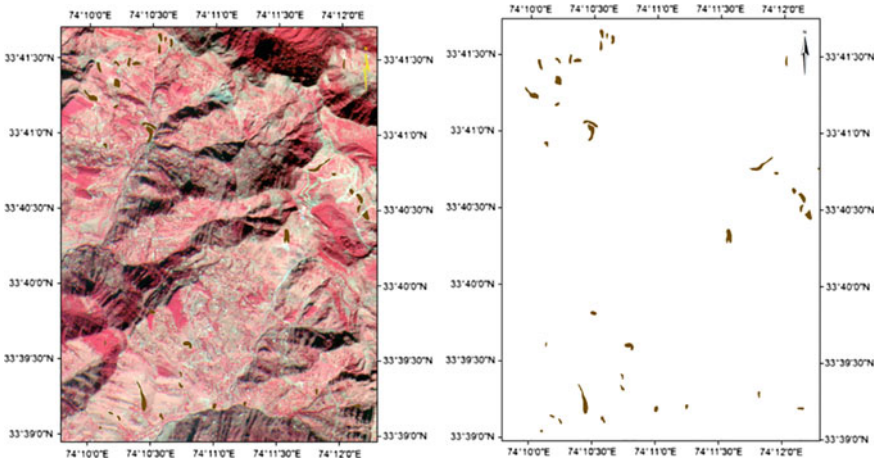

Fig. 4 Landslide map

5 Entropy Analysis and Accuracy Assessment

Entropy is the measure of uncertainty associated with information in many remote sensing applications. The uncertainty affects the quality of information extracted in remote sensing and propagates in processing, transmitting and classification process. In this study we used various types of entropy as a special criterion for visualizing and evaluating the uncertainty of the results. Classification performance is evaluated by criteria such as accuracy and reliability. These criteria do not show the exact quality and certainty of the classification.

5.1 Shannon's Entropy

Claude Shannon defined a formal measure of entropy, called Shannon entropy.

$$S = -\sum_{i=1}^{n} p_i \log_2 p_i \tag{1}$$

where p_i is the probability of occurrence of an event

Shannon entropy is used globally, for the whole data or locally to evaluate entropy of probability density distributions around some points. In this study we determine the entropy of landslide areas using Shannon entropy.

5.2 Renyi's Entropy

Renyi entropy is defined as follows. It has similar properties as Shannon entropy but it contain additional parameter α which can be used to make it more less sensitive to the shape of the probability distributions.

$$I_\alpha = \frac{1}{1-\alpha} \log\left(\sum_{i=1}^{n} p_i^\alpha\right) \tag{2}$$

I has maximum = $\ln(n)$ for $p_i = 1/n$.

5.3 Tsallis Entropy

Tsallis entropy is defined as follows. we determine the entropy of landslide areas using Tsallis entropy. The results of entropy value of each landslide event using above three equations given in Tables 1 and 2.

Table 1 Entropy of each landslide

Landslide event	S	S_α	I_α
1	0.042	0.021	0.034
2	0.038	0.023	0.038
3	0.039	0.022	0.039
4	0.038	0.023	0.040
5	0.036	0.022	0.037

Table 2 Accuracy comparison

S. no	Entropy	Kappa statistics	Overall accuracy (%)
1	Tsallis (S_α)	0.96	95.40
2	Shannon (S)	0.92	92.00
3	Renyi's (I_α)	0.91	91.00

$$S_\alpha = \frac{1}{\alpha - 1}\left(1 - \sum_{i=1}^{n} p_i^\alpha\right) \tag{3}$$

The comparative analysis of the different entropies in context of landslide detection were analyzed and various statistical parameters namely Kappa statistics as over all accuracy were computed for accuracy analysis. The investigation of entropy shows that Tsallis entropy is gave better accuracy.

6 Results and Discussion

Application of remote sensing for landslide detection and assessment have undergone an impressive development in recent years. From the experiment, it can be seen that the classification accuracy has been improved greatly by the newly arisen object-oriented approach. Besides, the whole procedure proves efficient and feasible because of the following reasons: firstly, use of objects multi-feature including spectrum, shape, texture, shadow, context, spatial location. Secondly, the object oriented approach of information extraction guarantee the classification accuracy by making full use of high resolution images information. Thirdly, with manually adjustment of different parameters, multi scale makes image object resolution adaptive for specific requirements, data and tasks.

The uncertainty between urban area and landslides is overcome by using concept of entropy. Results shows that using post and pre monsoon images, the landslides have been detected accurately. The entropy value ranging between (0.036–0.042) for Shannon entropy, (0.021–0.022) for Tsalli entropy and (0.034–0.040) for Renyis entropy. The entropy values for urban and landslide areas are clearly discriminate using Tsallis entropy. By using Tsallis entropy we can reduce the uncertainty between urban and landslide areas. In this study importance of object based classification method for detection of landslides has been studied. The entropy analysis is shows hat using temporal data one class of interest was better identified compare to using one date image. This study provides importance of entropy for landslide studies.

References

1. Nagarajan, R., Mukherjee, A., Roy, A., Khire, M.: Technical note temporal remote sensing data and GIS application in landslide hazard zonation of part of Western Ghat. India. Int. J. Remote Sens. **19**, 573–585 (1998)
2. Moosavi, V., Talebi, A., Shirmohammadi, B.: Producing a landslide inventory map using pixel-based and object-oriented approaches optimized by Taguchi method. Geomorphology **204**, 646–656 (2014)
3. Long Y., Xin, W.H.: Maximum image entropy resconstruction alogorithms based on neural optimization. J. Zhejiang Univ.: Nat. Sci. **50**, 120–130 (2000)
4. Lu, P., Stumpf, A., Kerle, N., Casagli, N.: Object-oriented change detection for landslide rapid mapping. IEEE Geosci. Remote Sens. Lett. **8**, 701–705 (2011)
5. Behling, R., Roessner, S., Kaufmann, H., Kleinschmit, B.: Automated spatiotemporal landslide mapping over large areas using rapideye time series data. Remote Sens. **6**, 8026–8055 (2014)
6. Behling, R., Roessner, S., Golovko, D., Kleinschmit, B.: Derivation of long-term spatiotemporal landslide activity—a multi-sensor time series approach. Remote Sens. Environ. **186**, 88–104 (2016)
7. Martha, T.R., Kerle, N., van Westen, C.J., Jetten, V., Kumar, K.V.: Segment optimization and data-driven thresholding for knowledge-based landslide detection by object-based image analysis. IEEE Trans. Geosci. Remote Sens. **49**, 4928–4943 (2011)
8. Keefer, J.: Landslide risks rise up agenda. Nature **511**, 272–273 (2014)
9. Cheng, G., Guo, L., Zhao, T., Han, J., Li, H., Fang, J.: Automatic landslide detection from remote-sensing imagery using a scene classification method based on BoVW and pLSA. Int. J. Remote Sens. **34**, 45–59 (2013)
10. Blaschke, T.: Object based image analysis for remote sensing. ISPRS-J. Photogramm. Remote Sens. **65**, 2–16 (2010)
11. Pradhan, B., Jebur, M.N., Shafri, H.Z.M., Tehrany, M.S.: Data fusion technique using wavelet transform and Taguchi methods for automatic landslide detection from airborne laser scanning data and QuickBird satellite imagery. IEEE Trans. Geosci. Remote Sens. **54**, 1610–1622 (2016)

Chapter 23
Determination of Surface Water Infiltration on Newly Developed Pervious Concrete Surface on Sandy Loamy Soil of Visakhapatnam and Surrounding Areas by Using Remote Sensing and GIS Technology

Bodasingu Ravi Kumar, Gummapu Jai Sankar, Pendyala Stephen, S. Ganesh, M. Neeraj Kumar and A. Shravan Kumar

Abstract This exploration work includes in deciding the invasion rate through pervious solid segments. While compressive quality was done on the solidified pervious solid 3D squares, invasion rate of water through the segments were resolved. Pervious cement enables fine activity of water to penetrate at high rates, ordinarily 100–200 in. 60 min, while the hidden soils will invade water a much lower rate, more often than not by 1–2 requests of extent. Pervious cement is a permeable structure which permits free entry of water through the solid surface and into the dirt without trading off the toughness or honesty of the solid. This kind of solid surface can be utilized as an invasion media for Tempest water administration. Tempest water administration has turned into an issue for some urban areas and districts because of increment in urbanization of private and business advancement. Pervious cement with Concrete + Flyash is most financially savvy and an ecologically amicable

B. Ravi Kumar (✉) · G. J. Sankar · P. Stephen · S. Ganesh · M. Neeraj Kumar
A. Shravan Kumar
Department of Geo Engineering, Andhra University College of Engineering, Visakhapatnam, India
e-mail: bravikumar.rkb@gmail.com

G. J. Sankar
e-mail: jaisankar.gummapu@yahoo.com

P. Stephen
e-mail: stephenabhi@gmail.com

S. Ganesh
e-mail: ganesh.siyyadri47@gmail.com

M. Neeraj Kumar
e-mail: neerajkumarmdg@gmail.com

A. Shravan Kumar
e-mail: shravan_7676@yahoo.co.in

P. J. Rao et al. (eds.), *Proceedings of International Conference on Remote Sensing for Disaster Management*, Springer Series in Geomechanics and Geoengineering,
https://doi.org/10.1007/978-3-319-77276-9_23

arrangement, which is accessible as porous asphalt keeping in mind the end goal to deal with the uncontrolled run-off, decreases contamination and increment ground-water table. Having less fines, this material has more voids proportion and invades Tempest water. Pervious cement has been utilized as a part of many places, for example, parking areas, Pathways, shoulders, walkways, avenues, neighborhood streets and for Arranging at Open utility Spots. As a part of this study the infiltration test was conducted on Different soils in Visakhapatnam city, Andhra Pradesh, India. The main objective behind the selection of sub soil which were predominate in Visakhapatnam and its surrounding areas with coverage of 90% of the villages of the district. These Soils are poor textured and easily drained. These soils are mapped by using the Remote Sensing imageries and GIS Techniques.

Keywords Capillary action of water · Storm water management parking lots Foot paths · Pervious concrete · GIS

1 Introduction

Pervious solid which is otherwise called permeable concrete and penetrable cement. It has been observed to be a dependable tempest water administration thought for the most concretized ranges. Pervious cement is a blend of rock, bond, compound admixture and water. Pervious cement is utilized as open cell a structure which permits storm water to channel through the asphalt and into the sub review soils. At the end of the day, pervious solid aides in securing the surface of the asphalt and its condition. It can permit the entry of 0.014–0.023 m^3 of water for every moment through its open cells for each square foot 0.0929 m^2 of surface range which is far more prominent than most rain events. Pervious cement is harsh finished, and has a honeycombed surface. Little measure of water and synthetic admixture are utilized as glue. The glue at that point frames a thick covering around total particles, to keep the streaming off the glue amid blending and setting. This glue keeps up bond between the total to have interconnected voids which enable water and air to go through it. It likewise brings about high penetrable solid that channel rapidly. Pervious cement can be utilized as a part of an extensive variety of utilizations, in spite of the fact that it's essential use in asphalts which are lingering streets, low volume asphalts, parking garages, Trails, shoulders, walkways, avenues, neighborhood streets and for Arranging at Open utility Spots.

2 Study Area

The study area is situated in and around the Visakhapatnam city in Visakhapatnam area of Andhra Pradesh. Visakhapatnam is an exceptionally conspicuous city on the east bank of the nation. The aggregate region of the Visakhapatnam city constitutes

around 550 km^2, which including the uninhabited slopes and boggy territories. The number of inhabitants in the city is more than 2.8 million. Quick industrialization in the territory, with subsequent increment in populace caused major issues in water supply administration in the Visakhapatnam city and its encompassing zones. Another significant disadvantage in the territory is that there are no major or minor streams streaming in the region of the city and it has increased the steadfastness on groundwater sources. Then again, the concretization of the surface region in the city is genuinely influencing the groundwater energize as the greater part of the water is running off into the ocean. Furthermore, the urban and modern contaminations alongside seawater interruption are having an unfriendly effect on the nature of ground water. In this foundation, there is each need to comprehend the condition and nature of ground water in the city, with a specific end goal to get ready for better administration of water supply in this urban setting, which is an essential concern (Fig. 1).

An integrated approach of Remote Sensing and GIS for evaluation of land use, land cover, Hydrogeomorphology, Geology and slope followed by determination of surface water infiltration on newly developed pervious concrete surface in different soil types of Visakhapatnam and surrounding areas.

Methods followed in the study comprise field-work, laboratory work, remote sensing and GIS work following the standard scientific procedures.

- Selection of an area to determination of surface water infiltration on newly developed pervious concrete surface in different soil types of Visakhapatnam.
- Creating thematic maps from Satellite data
  - Preparation of Geology map from existing Geology Map
  - Land use land cover M from Satellite data
  - Geomorphology map from Map Satellite data
  - Slope map from contour of survey of India topo sheets

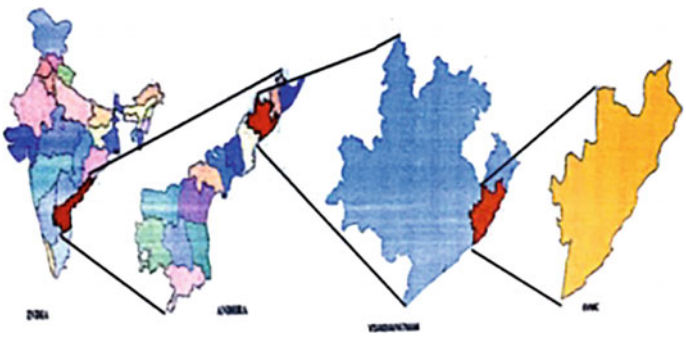

Fig. 1 Study area—location map GVMC, Visakhapatnam

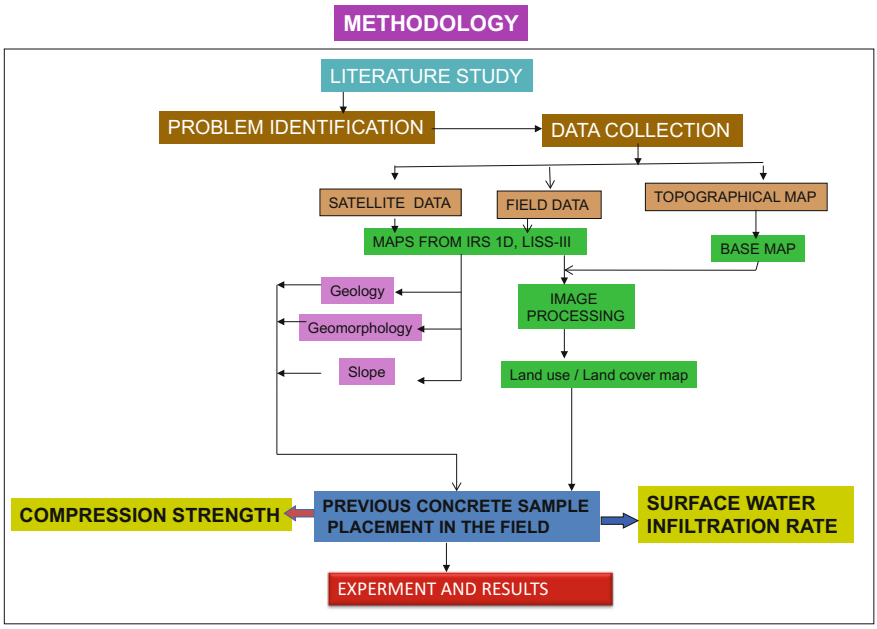

Fig. 2 Methodology and procedure for planning suitable locations to find the infiltration rate

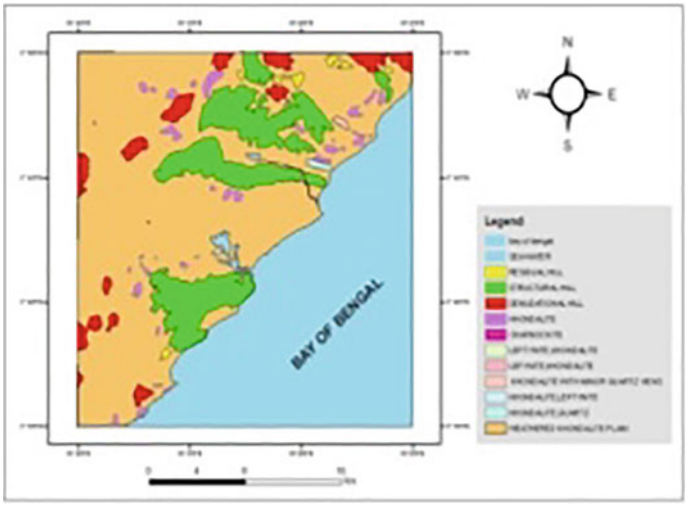

Fig. 3 Geology map

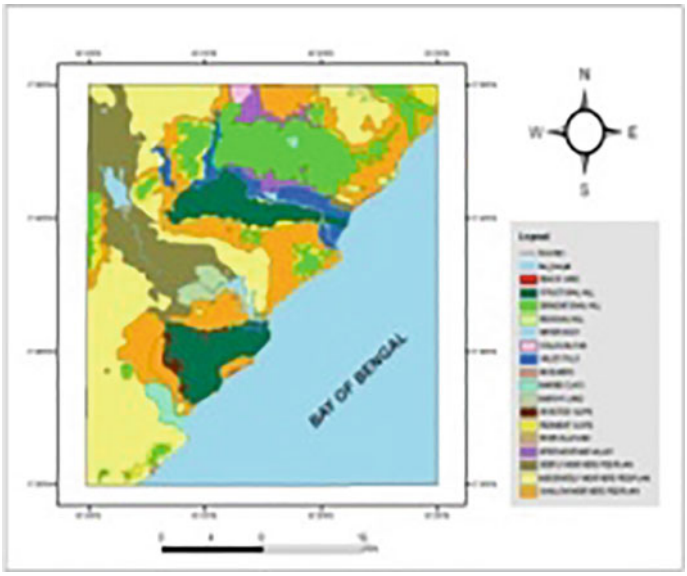

Fig. 4 Geomorphology

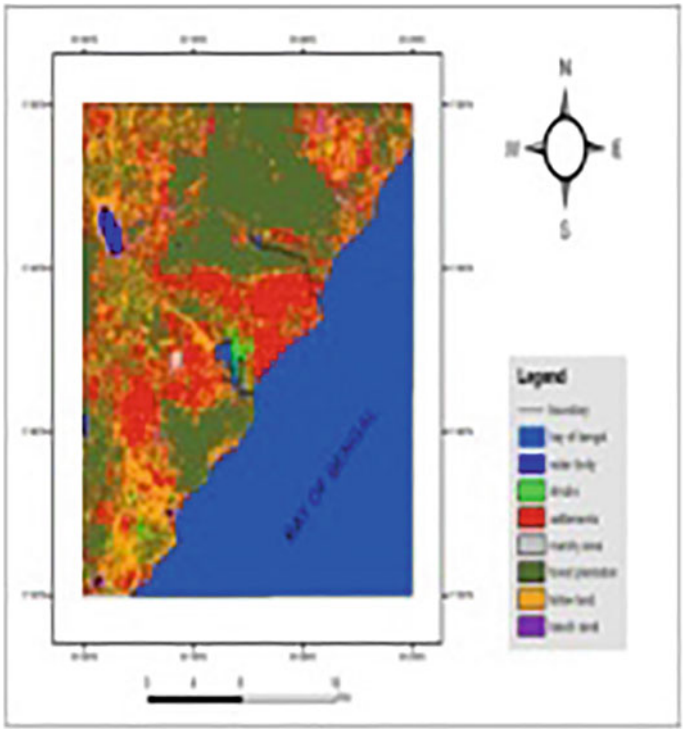

Fig. 5 Land use land cover

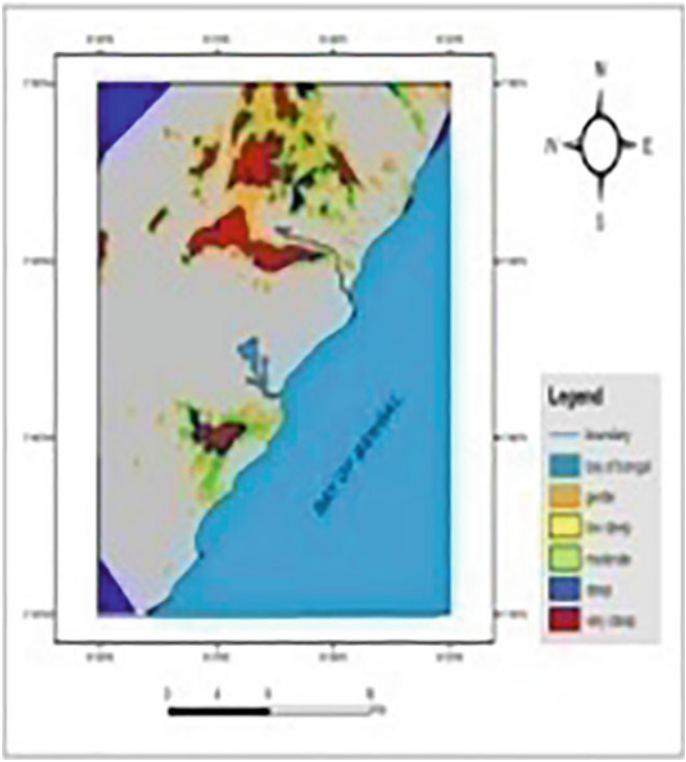

Fig. 6 Slope map

- Preparation of Pervious concrete without fine aggregate.
- Lab and field experimental approach for testing the pervious concrete on sandy soil.
- Placing the pervious concrete on the sandy loamy soil and calculating the infiltration rate.

Apart from the above steps, consider the run off estimation which is a key step for determination (Figs. 2, 3, 4, 5 and 6).

2.1 Data Used

The details of the different data used in this study is given below

- IRS 1C-LISS III and IRS 1D-LISS III data
- Survey of India toposheets—65 0/1, 65 0/2 & 0/3, 65 0/5, 65 0/6, scale 1:250,000.

- Code books of Civil Engineering: ISO 17785-1:2016, IS 456-2000
- Reference maps of various data
- Field data

Software Used

- ARC GIS
- ERDAS IMAGINE.

2.2 Experimental Approach

ASTM C 1701 [1] is the standard infiltration test for pervious concrete. The technique comprises of 4 principle parts: Introducing the infiltration ring, pre-wetting the solid, testing the solid and computing the outcomes.

In the first place we need to clean the internal and external surface of infiltration ring. The infiltration ring must have certain sizes and to be set apart with two lines inside to play out the test accurately. The ring is put on the pervious solid surface and secured with plumber's putty around it. Presently pre-wet the solid surface and infiltration ring with 3.6 kg of water keeping up the head of water between the two stamps on the inside of the ring. Start stop-watch timing when the water hits the pervious solid surface. At the point when water is never again introduce at first glance, record the slipped by time of the pre-wetting. The time taken determines the amount of water to be used in the actual test. We take 18 kg of water which is utilized for the test and record the weight. Include the correct measure of water to the ring. Similarly as with the pre-wetting stage, we will start stop watch timing when the water impacts the pervious solid surface and keep up the water head between the two lines which are set apart on the penetration ring. Once more, when water is never again present of the surface, record the last time of the test. With the information gathered, we can play out the invasion computation by utilizing the mass of the water, the distance across of the penetration ring and time of the test. With that data we have our last invasion rate comes about.

Geology of the area, Geomorphology features, Land use and Land cover features and slope studies were also important factors to understand the infiltration rate of surface water on various soils of the study area.

Infiltration Calculation:

$$I = KM/D^2(T)$$

I Infiltration rate in Mt/h
M Mass of infiltrated water in kg
D Inside diameter of infiltration ring in mm
T Time required for measured amount of water to infiltrate the concrete in h
K 4,583,666,000 (constant)

Similar studies were carried out by Scientists world wise referred and recommended that ASTM C 1701 for Assessing surface Invasion of Penetrable Interlocking Solid Asphalts. ASTM C 1701 is a reasonable and fast test strategy for measuring sub-surface penetration by recreating a little water driven head at first glance test region like those created by extraordinary rain storms and contributing spillover. Conshohocken [3] Stormwater administration strategies look to diminish the negative impacts of land utilize changes by decreasing and weakening surface spillover and by advancing invasion rate. Pervious cement is a sort of permeable asphalt that can be utilized as a penetration rehearse for stormwater administration. It has an open-evaluated structure and comprises of painstakingly controlled segments of coarse total, concrete, water, and admixtures. Mangala et al. [7] have contemplated the invasion rates of various soils and they reasoned that dirt testing empowers a fruitful and powerful tempest water administration plan that joins an appropriate penetration rate for outline counts. Obla [8] has compressed that Pervious concrete is a critical application for maintainable development. He likewise decided the void proportion and invasion rate of pervious solid surfaces. The void substance can go from 18 to 35% with compressive qualities of 27–28 MPa. The penetration rate of pervious solid will fall into the scope of 80–720 l for every moment per square meter. Gâștescu and William [5] has suggested the properties of Water resources and wetlands. Dagadu and Nimbalkar [4] have condensed the Invasion Investigations Of Various Soils Under Various Soil Conditions And Examination Of Penetration Models With Field Information. Single-ring and double fold rings are utilized to evaluate the invasion rate of various soils. Wanielista et al. [10] have considered the performance of pervious concrete at sites and examined infiltration rates for pervious concrete parking lots and their subsoils and improved maintenance techniques. They likewise clarified the distinctive elements which will impact the dirt penetration attributes. GIS considers additionally done by, King [6] has analyzed the status of GIS activities in water assets administration in South Africa to decide if the way and setting of the execution procedure have obstructed or advanced improvement of choice help usefulness in GIS. He inferred that there are a few issue regions adding to absence of understanding the ability and restrictions of GIS. From the study of Solomon and Quiel [9] Groundwater ponder utilizing remote detecting and geographic data frameworks (GIS) technique is developed. This model was proposed as an adjustment in light of the Exceptional list, has been created with the goal of accomplishing more prominent exactness in the estimation of particular defenselessness to nitrate

Fig. 7 Double ring test, one dimensional flow at soil-concrete interface, single-ring infiltrometer, laboratory core test

Fig. 8 Laboratory test and field test with and without soil surface through pervious concrete

Table 1 Concrete 28 days compressive strength results (all values in N/mm^2)

S. no	Cubes with pure cement		Cubes with cement + flyash		Cubes with cement + GGBS	
	Trail 1	Trail 2	Trail 1	Trail 2	Trail 1	Trail 2
1	23.12	22.75	22.47	21.81	23.79	22.37
2	Avg. = 22.94		Avg. = 22.14		Avg. = 23.08	

contamination. It depends on a multiplicative model that coordinates the danger of groundwater contamination by nitrate identified with various land uses and considers both the negative effects, after some time, of some of these utilizations on aquifer media and further more the defensive impacts of others. Chopra et al. [2], gave a thought on Morphometric examination of two sub-watersheds was conveyed utilizing remote detecting and GIS methods (Figs. 7 and 8; Table 1).

3 Results

Compressive strength results of all the combinations of Pervious Concrete samples have achieved moreover same results 22–23 N/mm^2.

INFILTRATION RATE: Lab Test

From ASTM D 1557 code book, a formula is used to find the infiltration rate of water passing through the pervious concrete to sub grade soils (Figs. 9 and 10).

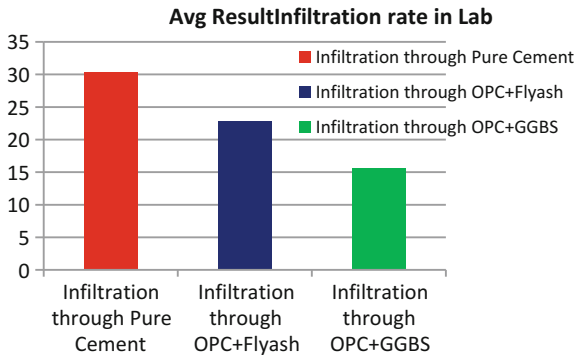

Fig. 9 Average infiltration rate in lab

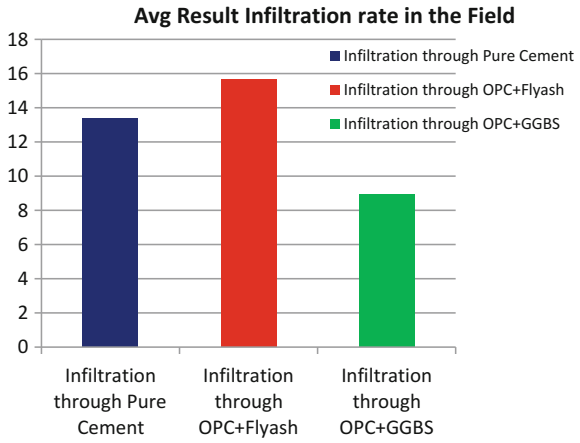

Fig. 10 Average infiltration rate in the field

$I=KM/D^2*t$

I-Infiltration Rate

K-Constant Value (4583666000)

M- Mass of the Water in Kg

D- Diameter of the Ring in mm and T- Time in Sec

Values with Pure Cement:

Trail-1

$I=KM/D^2*t$

$4583666000*18/(300)^2*(32)=28.6$ Mts/hrs

Trail-2

$I=KM/D^2*t$

$4583666000*18/(300)^2*(29)=31.61$ Mts/hrs

Trail-3

$I=KM/D^2*t$

$4583666000*18/(300)^2*(30)=30.55$ Mts/hrs

Average Value I= (28.6+31.61+30.55)/3 = **30.25 Mts/hrs**

Values with Cement + Flyash:

Trail-1

$I=KM/D^2 *t$

$4583666000*18/(300)^2*(38)= 24.12$ Mts/hrs

Trail-2

$I=KM/D^2 *t$

$4583666000*18/(300)^2*(41)=22.36$ Mts/hrs

Trail-3

$I=KM/D^2 *t$

$4583666000*18/(300)^2*(42)=21.82$ Mts/hrs

Average Value I= (24.12+22.36+21.82)/3 = **22.77 Mts/hrs**

Values with Cement + GGBS:

Trail-1

$I=KM/D^2 *t$

$4583666000*18/(300)^2*(60)=15.27$ Mts/hrs

Trail-2

$I=KM/D^2 *t$

$4583666000*18/(300)^2*(58)=15.80$ Mts/hrs

Trail-3

$I=KM/D^2 *t$

$4583666000*18/(300)^2*(59)=15.53$ Mts/hrs

Average Value I= (15.27+15.80+15.53)/3 = **15.53 Mts/hrs**

INFILTRATION RATE: Field Test

Values with Pure Cement:

Trail-1

$I=KM/D^2 *t$

$4583666000*18/(300)^2*(63)=14.55$ Mts/hrs

Trail-2

$I=KM/D^2 *t$

$4583666000*18/(300)^2*(75)=12.22$ Mts/hrs

Average Value I= (14.55+12.22)/2 = **13.38 Mts/hrs**

Values with Cement + Flyash:

Trail-1

$I=KM/D^2 *t$

$4583666000*18/(300)^2*(57)=16.08$ Mts/hrs

Trail-2

$I=KM/D^2 *t$

$4583666000*18/(300)^2*(60)=15.27$ Mts/hrs

Average ValueI=(16.08+15.27)/2 = **15.675 Mts/hrs**

Values with Cement + GGBS:

Trail-1

$I=KM/D^2 *t$

$4583666000*18/(300)^2 *(96) = 9.5$ Mts/hrs

Trail-2

$I=KM/D^2 *t$

$4583666000*18/(300)^2*(110)= 8.3$ Mts/hrs

AverageValueI= (9.5+8.3)/2=**8.9 Mts/hrs**

4 Conclusions

The population of the Visakhapatnam city is more than 2.8 million. Fast industrialization in the region, with ensuing increment in population caused major issues in water supply administration in the city and its surrounding zones. The concretization of the surface range in the city is genuinely influencing the groundwater energize as the vast majority of the water is running off into the ocean. The pervious concrete and subsoil system displays infiltration rates of nearly the same magnitude as the subsoil in the locations where the pervious concrete infiltration rate is higher than that of the subsoil. Proper mix design and placement techniques will be presented in detailed specifications at the completion of this project. This field test may also be applied to soils with lower infiltration rates as seen in the case of Site. Different types of materials like Cement, Fly ash, and GGBS are used in pervious concrete to find the infiltration rate of water through these samples. From the Results of experimental approach: Cement and Cement + Flyash pervious concrete has more infiltration rate in both sub-grade and non-sub-grade soils. The pure OPC and OPC + Flyash can be recommended for the use of pervious concrete over the subgrade soil. As both the cement and Flyash are of fineness materials and more fines are in Flyash passing through 45 micron. Also in commercials point of view, the combination of OPC + Flyash gives us more saving than choosing the pure Ordinary Portland cement (OPC). We can adopt the usage of pervious concrete with the combination of OPC + Flyash, as this is an Environmental Eco-friendly product by minimizing the CO_2 emission into Environment and also the compressive strength results of all the combinations of Pervious Concrete samples has achieved moreover same results 22–23 N/mm^2. The simple test set-up's used in this study are suitable to determine the water permeability and infiltration rates for pervious concrete in the Visakhapatnam area.

References

1. ASTM C 1701/C 1701 M-09 (2012) Standard Test Strategy for Penetration Rate of water into Soils Utilizing Twofold Ring Infiltrometer. American Society for Testing and Materials, China
2. Chopra, R., Dhiman, R.D., Sharma, P.K.: Morphometric investigation of sub-watersheds utilizing remote detecting and GIS methods in Gurdaspur locale, Punjab, India (2005)
3. Conshohocken, P.A., Bean, E.Z., Chase, W.F., Bidelspach, D.A.: Concentrate At first glance Invasion of Penetrable Asphalts (2007)
4. Dagadu, J.S., Nimbalkar, P.T.: Infiltration investigations of various soils under various soil conditions and examination of penetration models with field information. Int. J. Trend Res. Dev. **3**(2), (2012); ISSN: 2394-9333
5. Gâştescu, P., William, L.: Water resources and wetlands. In: Petre Gâştescu, William Lewis Jr., Petre Breţcan Conference Proceedings, Tulcea–Romania; ISBN: 978-606-605-038-8 (2012)
6. King, N.: (1996) Achieving decision support with GIS: learning from water management applications in South Africa

7. Mangala, O.S., Toppo, P., Ghoshal, S.: Study of infiltration capacity of different soils civil engineering department **3**(2); ISSN: 2394-9333. www.ijtrd.com, IJTRD, Bhilai, Chhattisgarh, India (2016)
8. Obla K.H., Pervious concrete for sustainable improvement, exploration and materials building USA. Indian Concrete J. 9–18 (2007); August 2010
9. Solomon, S., Quiel, F.: Groundwater ponder utilizing remote detecting and geographic data frameworks (GIS) in the focal good countries of Eritrea June 2006 **14**(5), 729–741 (2006)
10. Wanielista M., Chopra M., Spence J., Ballock, C.: Stormwater Administration Institute College of Focal Florida Orlando, FL 32816. In: Hydraulic Execution Evaluation of Pervious Solid Asphalts for Stormwater Administration Credit (2007)

Chapter 24
Integrated Approach for Local Level Drought Assessment and Risk Reduction

M. Kavitha, Gajanan Ramteke, A. Kamalakar Reddy and N. Narender

Abstract Timely information about the onset of drought, extent, intensity, duration and impacts can limit drought related losses of life, human suffering and decrease damage to economy and environment. Drought assessment and monitoring is essential for the agricultural sector to take appropriate mitigation measures. Drought indices derived from satellite data play a major role in assessing the health and condition of crops. The study emphasize upon the use of RS and GIS techniques for drought monitoring in Telangana state, which is one of the drought prone state of India. Agricultural drought risk areas were identified based on classifying the deviation of the Normalized Difference Vegetation Index (NDVI) and Normalized Difference Wetness Index (NDWI) from the mean values by using surface reflectance from MODIS satellite data during 2002–2015. Areas facing a combined agricultural and meteorological drought were assessed using an integrated approach involving different indicators viz. mandal wise NDVI and NDWI deviation, rainfall deviation and dry spells. Integrating all indicators, mandals were categorised as "Normal" agricultural situation in 235, "Mild" in 169, "Moderate" in 33 and "Severe" in 06 mandals of the state. The study revealed that, western (South-West and North-West) part of Telangana state is more prone to drought. Alternate contingency plans were prepared based on the results of this study for entire state.

Keywords Drought monitoring · NDVI · NDWI · SPI · Rainfall deviation Dry spell

M. Kavitha (✉) · G. Ramteke · A. Kamalakar Reddy · N. Narender
Telangana State Remote Sensing Applications Centre, Hyderabad, India
e-mail: mkavitha.trac@gmail.com

G. Ramteke
e-mail: gkramteke@gmail.com

A. Kamalakar Reddy
e-mail: kamalreddyisms@gmail.com

N. Narender
e-mail: narenj3@gmail.com

P. J. Rao et al. (eds.), *Proceedings of International Conference on Remote Sensing for Disaster Management*, Springer Series in Geomechanics and Geoengineering,
https://doi.org/10.1007/978-3-319-77276-9_24

1 Introduction

Rising water demand for agricultural sector is to be found to exist in many parts of the world and further challenged by the impact of droughts [1]. Drought is related to the timing and the effectiveness of the rainfall. All types of drought originate from a deficiency of precipitation [2–4]. Below normal precipitation induced meteorological extremes communicate the drought [1, 5]. Deficit rainfall triggers meteorological and subsequently agricultural drought, further transmitted into hydrological drought [6].

A wide range of drought identification and assessment indices are introduced over the globe for meteorological, agricultural and hydrological droughts viz., Palmer drought severity index (PDSI); Rainfall anomaly index (RAI); Normalized difference vegetation index (NDVI); Surface water supply index (SWSI); Standardized precipitation index (SPI); Soil moisture drought index (SMDI), Normalized difference wetness index (NDWI); Vegetation condition index (VCI), Reconnaissance drought index (RDI). These indices have been used in different set of facts or circumstances that surround a situation or event [7].

Rainfall is the main source to derive the meteorological drought indicators. The spatial extent of drought cannot be properly identified unless there is a good distribution of meteorological stations throughout the area [8]. Even then requirement of time and cost for data preparation and chances of error may hinder the procedures of drought mitigation [9]. Also, drought indices calculated at one location is only valid for single location. A key limitation of meteorological based drought indicators is their lack of spatial detail as well as they are dependent on data collected at weather stations [10].

The prediction and monitoring of drought requires rapid and continuous data, and information generation or gathering is not possible using conventional methods [11]. Satellite remote sensing based indices are diverse and accepted for its low cost, synoptic view, repetition of data acquisition and reliability [12]. Thus, drought monitoring through satellite based information has been popularly accepted in recent years [13]. Normalized difference vegetation index, normalized difference wetness index and vegetation condition index are some of the satellite remote sensing derived and extensively used indices in different ecological regions with varying conditions.

Satellite-based observations have proven very useful for detecting vegetation condition anomalies. However, the specific cause(s) for the vegetation stress may not always be determined solely from the remotely sensed data. The anomalies in vegetation condition may be triggered from various natural (e.g. flooding, fire, pest infestation and hail damage) and anthropogenic consequences (e.g. landuse land cover, agricultural management practices). Though, remote sensing data provides a means to monitor detailed spatial patterns of vegetation conditions, however, it is difficult to distinguish drought related vegetation stress from vegetation changes caused by these other drivers without additional information [14]. Accordingly, the

integration of meteorological and satellite remote sensing data provides substantial approach to better spatiotemporal assessment of drought at local level.

The semi-arid rainfed area of Telangana state is characterized by high variability in rainfall and runoff over space and time. The rainfall is seasonal in character with short rainy season of 3–4 months and the state experiences dry conditions for 8–9 months in various parts and more so in southern parts [15]. Agriculture is the major occupation for two-thirds of the population in the state. The impact of drought is quickly felt in the parts of state due to non-availability of irrigation facilities, erratic distribution of rainfall, changes in the monsoon pattern, presence of hard rock aquifer in large areas which limits scope of groundwater exploitation [16]. During most of the years, some parts of the state experience drought which do not have access to water resources other than rainfall. Therefore, there is need to develop strategies for drought monitoring and mitigation as a protection from drought in the state. In this context, Telangana State Remote Sensing Applications Centre (TRAC), a nodal agency for remote sensing and geographical information system applications in the state, has established an integrated seasonal condition monitoring system. An integrated seasonal condition monitoring system mainly focuses on:

- Concurrent monitoring of seasonal conditions using remote sensing, weather network data and continuous ground truth.
- Develop an early warning (monitoring and forecasting) using suite of indicators to identify drought prone areas, which help to preparedness and implement appropriate disaster risk reduction measures.
- Early warning to the districts and mandals.[1]

The specific focus of this study is to assess the impact of meteorological and agricultural drought with an integrated approach using satellite remote sensing and climatic information at mandal level.

2 Study Area

Telangana state of India is the twelfth largest state in terms of both area and the size of population in the country with a geographical area of 114,840 km^2 and having a population of 35.194 million [17]. Telangana is strategically located in the Deccan plateau in a semi-arid region. The climate is predominantly hot and dry. The state experiences seasonally dry conditions during winters and summers. The extreme temperature vary from a maximum of even 50 °C during summer and minimum of 8 °C during winter in some parts. The thermal regime permits arable crop production round the year subject to availability of water. The average annual rainfall

[1]Mandal is an administrative division of India denoting a sub-district comprised several villages or village clusters.

in the state is about 906 mm, 80% of which is received from the South-West monsoon (June–September). There has been an acute deficiency of rainfall in 2014 and 2015 recording a deficit of −31 and −14% consecutively. The actual rainfall received during South-West monsoon of 2014 and 2015 was 494.7 mm and 611.2 mm against the normal rainfall of 713.6 mm, respectively [15]. The rainfall in the state is erratic and uncertain with uneven distribution in various mandals, thus, making agriculture a proverbial gamble in monsoon. The state is divided into three Agro climatic zones: North Telangana zone, Central Telangana zone and South Telangana zone. There are varied soil types including sandy loam, red sandy, deep red loamy and shallow to very deep black soils. Cotton, Rice, Soybean and Maize are the major crops cultivated in both rainfed and irrigated agriculture.

3 Data Used

3.1 Satellite Data

The MODIS Terra 16-day vegetation index (VI) product (https://e4ftl01.cr.usgs.gov/MOLT/MOD13Q1.005) starting from first fortnight of June to the second fortnight of September for the years 2002–2015 was used in the analysis. The data were processed through appropriate image processing software to derive the NDVI and the reflectance of near-infrared and shortwave infrared.

3.2 Rainfall and Dry Spell Data

Mandal wise rainfall and dry spell data provided by Directorate of Economics and Statistics (DE&S), Government of Telangana for the South-West Monsoon season is used for the present study. This data is used for computation of meteorological drought indices.

4 Materials and Methods

4.1 Standardized Precipitation Index (SPI)

McKee et al. proposed SPI, awidely used meteorological drought index [18]. SPI compares precipitation with its multi-year average based on the long-term precipitation record for a desired period. The classification scheme of SPI values for meteorological drought risks are placed at Table 1. Values above zero indicate wet

Table 1 SPI values classification

SPI value	Category
>2.0	Extremely wet
1.5–1.99	Very wet
1.0–1.49	Moderately wet
−0.99 to 0.99	Near normal
−1.0 to −1.49	Moderately dry
−1.5 to −1.99	Very dry
< −2.0	Extremely dry

periods and values below zero indicate dry periods. For any given drought, SPI represents how many standard deviations its cumulative precipitation deficit deviates from the average [12].

4.2 Rainfall Anomaly Index (RAI)

Rainfall Anomaly Index is effective and simple meteorological drought index [19]. RAI uses the average precipitation over weekly, monthly or annual time periods to characterize relative drought. Rainfall anomaly of each year was calculated using long term average rainfall of the study area. Average annual rainfall for a period of 28 years (1988–2015) is used in the RAI analysis. The years with low RAI values indicate negative departure from mean seasonal rainfall which boosts drought years.

4.3 Vegetation Index

The crop/vegetation reflects high energy in the near infrared band due its canopy geometry and health of the standing crops/vegetation and absorbs high in the red band due to its biomass and photosynthesis. Uses of these contrast characteristics of vegetation in near infrared and red bands indicate both the health and condition of the crops/vegetation. Normalised Difference Vegetation Index (NDVI) is widely used for operational drought assessment because of its simplicity in calculation, easy to interpret and its ability to partially compensate for the effects of atmosphere, illumination geometry etc. [20–23]. NDVI is derived by the difference of these measurements and divided by their sum. The vegetation index is generated from each of the available satellite data irrespective of the cloud cover present. To minimize the cloud, monthly time composite vegetation index is generated.

4.4 Surface Wetness Index

Shortwave Infrared (SWIR) band is sensitive to moisture available in soil as well as in crop canopy. In the beginning of the cropping season, soil back ground is dominant hence SWIR is sensitive to soil moisture in the top 1–2 cm. As the crop progresses, SWIR becomes sensitive to leaf moisture content. SWIR band provides only surface wetness information. When the crop is grown-up, SWIR response is only from canopy and not from the underlying soil [24]. NDWI using SWIR can complement NDVI for drought assessment particularly in the beginning of the cropping season. Higher values of NDWI signify more surface wetness.

4.5 Vegetation and Wetness Indices Deviation

The deviation of NDVI and NDWI from normal is calculated using the mean value of the total period from 2002 to 2014. The following equation is used to calculate the deviation.

$$NDVI_{Dev} = \left(\frac{NDVI_i - NDVI_{mean}}{NDVI_{mean}}\right) \times 100$$

where, $NDVI_{Dev}$ is NDVI deviation in ith year, $NDVI_i$ is NDVI for ith period, $NDVI_{mean}$ is the long term average of NDVI.

Above mathematical expression is also used to calculate the deviation of NDWI, similarly. NDVI and NDWI threshold values of deviation are used to classify agricultural drought area in the study region (Table 2).

Proper identification of drought risk areas is needed for formulating and implementing contingency plans. Therefore, a comprehensive and integrated approach is established using both agricultural and meteorological indicators to identify the drought prone risk areas in Telangana state.

Pre-processing of satellite data involved conversion of HDF format to IMG format, re-projection, subset, NDVI and NDWI computed from model maker, and time composite data is derived for the season [10]. NDVI maximum value is composited for the period of one month. In order to remove interference of forest area NDVI with agriculture area, the forest and other non-agricultural areas of the state were masked by using the landuse land cover layer [25]. Based on deviation of

Table 2 Agricultural drought risk classification using NDVI and NDWI deviations

Deviation (%)	Class
≥ 0	No drought/normal
0 to −10	Mild drought
−10 to −20	Moderate drought
< -20	Severe drought

these indices with respect to normal year (2013), mandal wise statistics are derived. The relative deviation of NDVI/NDWI from that of normal and the rate of progression of NDVI/NDWI from month to month gives the indication about the agricultural situation in the district which is then complemented by ground situation as evident from rainfall and sown area. Drought assessment and reporting of information is carried out on fortnightly basis. Seasonal NDVI and NDWI progression, i.e. transformation of NDVI and NDWI from the beginning of the season, comparison of NDVI and NDWI profile with previous normal years—relative deviation, weekly rainfall status compared to normal, dry spells, weekly progression of sowings and historical drought prone border line areas are integrated and taken into consideration for assessing agricultural drought situation in the state/district/mandal.

5 Results and Discussion

5.1 Meteorological Drought Analysis

Monsoon period i.e. June to September is considered for *Kharif* season rainfall analysis as well as dry spell analysis. Rainfall deficiency in current year (2015) continued to persist as experienced in previous year. The state received an average rainfall of 611.2 mm during the South-West Monsoon (June–September), as against the normal rainfall of 713.6 mm which resulted in a deficiency of 14% (Fig. 1). Status of rainfall is categorised into four categories based on the departure from the long-term average of the rainfall viz., excess (+19% or more), normal (−19 to +19%), deficit (−59 to −20%), scanty rainfall (−99 to −60%) and no rain (more than −99%). It is revealed from the analysis that mandals located in western part of state shows deficit rainfall status. However, normal rainfall in northern mandals is more than state average during monsoon period. Deficit rainfall status in 36 mandals of Mahaboobnagar district is witnessed. This may be attributed to the less actual rainfall received during monsoon period compared to remaining districts in the state.

Monthly rainfall of Monsoon season (June–September) for a period of 28 years (1988–2015) is considered to analyse SPI. Figure 2 shows monthly SPI for the state. It is evident from figure that SPI considerably coincide with the drought years. Further, low SPI for the months of July and August triggered meteorological drought over the years. Annual rainfall anomaly index for the Monsoon period (Fig. 3) shows that 16 years experienced below-normal rainfall. Rainfall anomaly directly measures the shortage of rainfall, and is the difference between the observation and the long-term mean. It is clearly illustrates from the figure that below normal rainfall continuously extended from 1991 to 1997.

A wide gap of 21 days or more between two consecutive rainy days in season is called dry spell. Mandals located in South-Western and central part of the state has

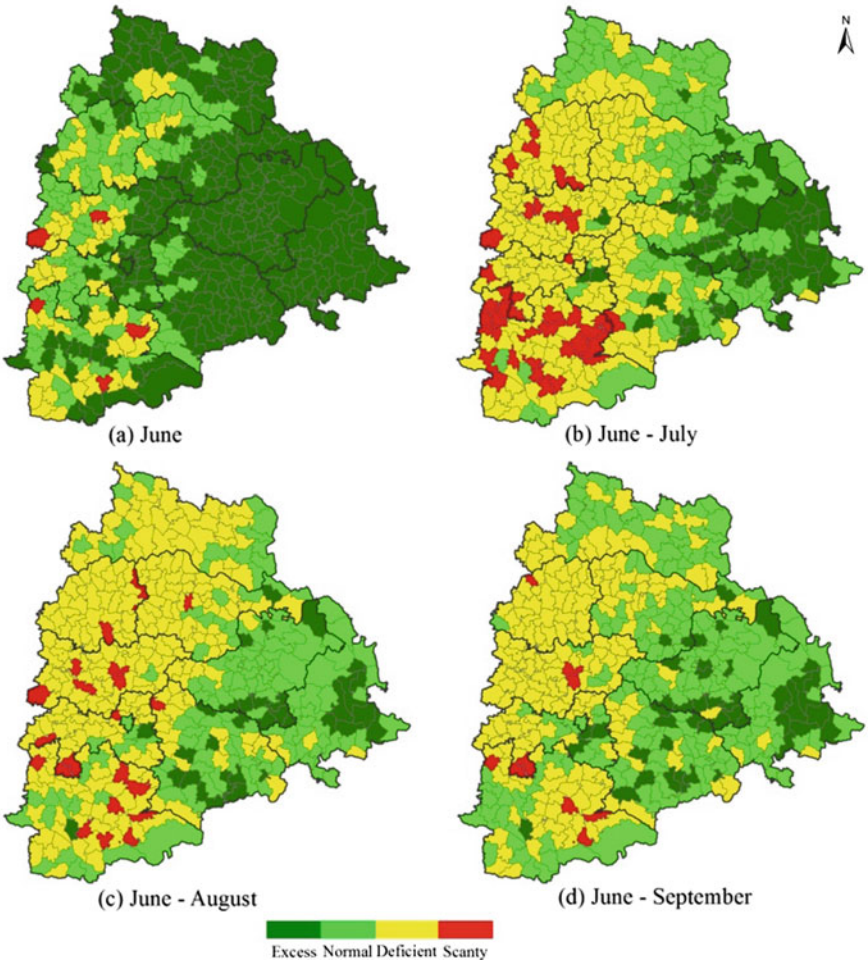

Fig. 1 Spatial distribution of cumulative monthly rainfall deviation for South-West Monsoon 2015

experienced at least one dry spell in Monsoon season. Total 42 mandals of Mahaboobnagar district shows dry spells followed by Ranganreddy and Nalgonda district. There is no evidence of 3, 4 and ≥ 5 dry spells in any mandal of the state. Figure 4 presents the combined criteria meteorological drought using rainfall deficiency, dry spell, SPI and RAI. It is clear from the figure that 98 mandals are under meteorological drought situation.

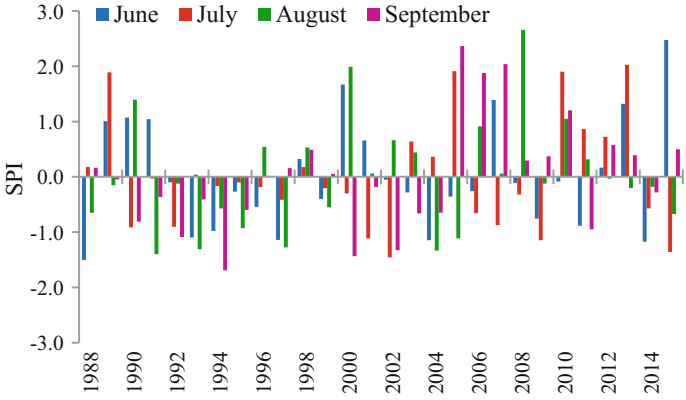

Fig. 2 Standardized precipitation index for South-West Monsoon period

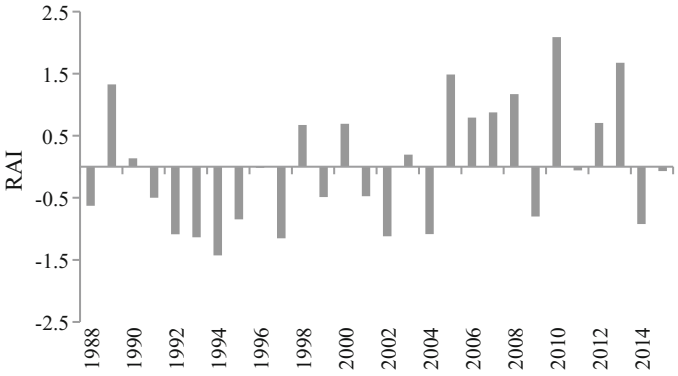

Fig. 3 Rainfall anomaly index for South-West Monsoon period

5.2 Agricultural Drought Analysis

The cropping season starts in the month of June with onset of monsoon. The above normal distribution of rainfall has increased the progression of sowings in the month of June. The excess rainfall in the month of June, all over the state has helped achieving more than normal crop sowings. From the NDVI analysis, it is evident that the crop condition is normal till the first fortnight of July and due to subsequent dry spell situation, the condition degraded and crops suffered vegetation stress (Figure of temporal variation of NDVI is not shown here). NDVI showed negative deviation in the month of September and this may be accounted for the reduced chlorophyll content and leaf water content of severely affected crops.

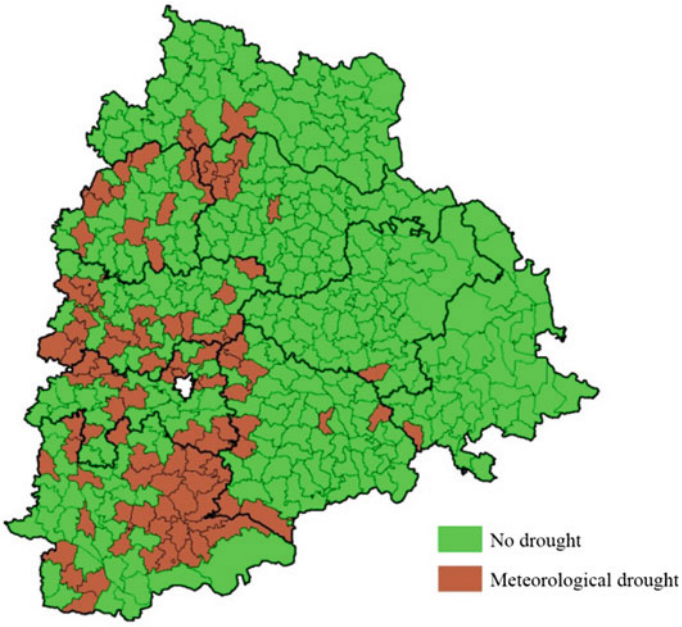

Fig. 4 Meteorological drought map for South-West Monsoon 2015

Maize, soybean and cotton crops experienced severe vegetation and moisture stress during critical stages. NDWI is higher during August unlike NDVI, since NDWI is water sensitive index, the residual soil moisture could sustain the crop during July, however extended dry spells have increased moisture stress in crops during the month of August. In the districts of Mahabubnagar, Nalgonda, Rangareddy, Medak and Karimnagar cotton crop is affected in flowering and boll formation stages which drastically affected the crop yield later on. In spite of good rainfall in the month of September the crops were not recovered from the stress caused due to the dry spell conditions prevailed during the months of July and August. Agricultural drought risk areas are identified by generating anomaly of NDVI and NDWI. Temporal and spatial variability of NDVI (Fig. 5) and NDWI (Fig. 6) are observed which attributed to the uneven and erratic distribution of monsoon rainfall. The onset and extent of vegetation and wetness stress can be clearly observed from the maps of consecutive months. The South-Western and central parts of the state showed significantly more NDVI and NDWI deviation indicating vegetation and moisture stress during season. The deviation above zero indicates the normal vegetation condition.

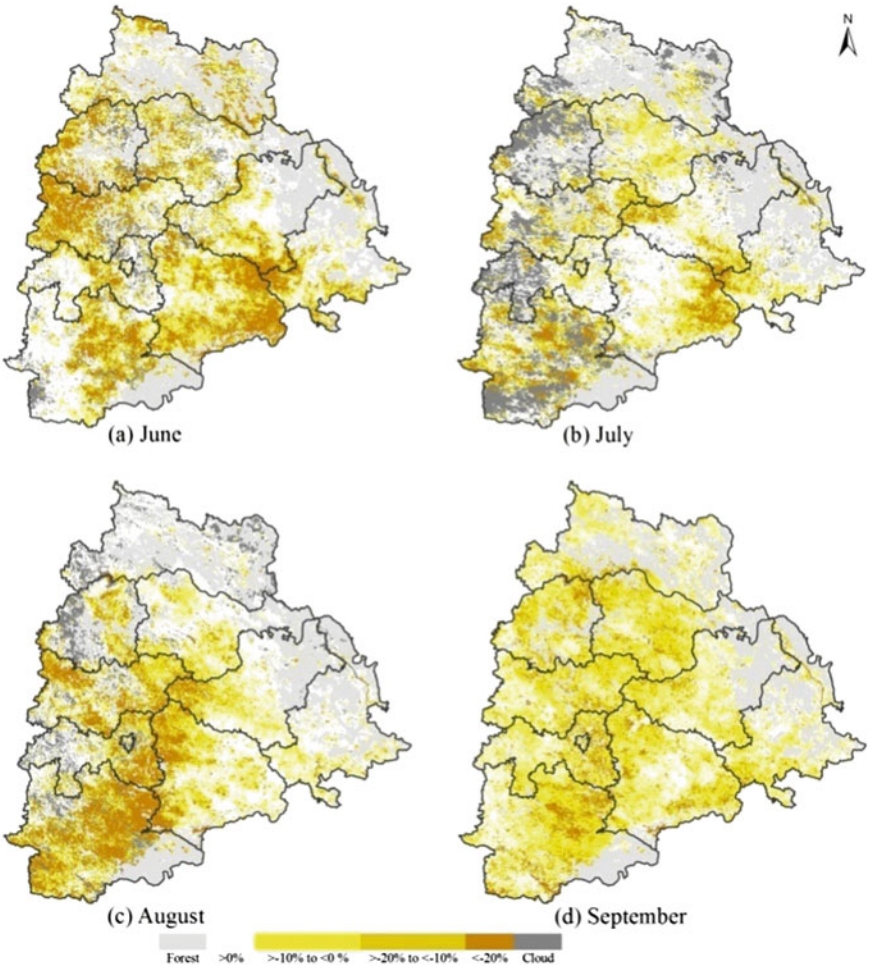

Fig. 5 NDVI deviation for South-West Monsoon period 2015

5.3 Integrated Criteria for Drought Assessment

Integrated meteorological and agricultural drought monitoring plays an important role in order to track the drought severity. The drought situation in the state is assessed using meteorological as well as satellite remote sensing derived agricultural drought indicators. Rainfall deviation, dry spells, SPI, RAI, NDVI and NDWI deviation are used in the integrated drought assessment criteria. Integrated seasonal condition of drought provides prediction information and assesses the risk associated with drought impacts. Early warning resulted from integrated drought

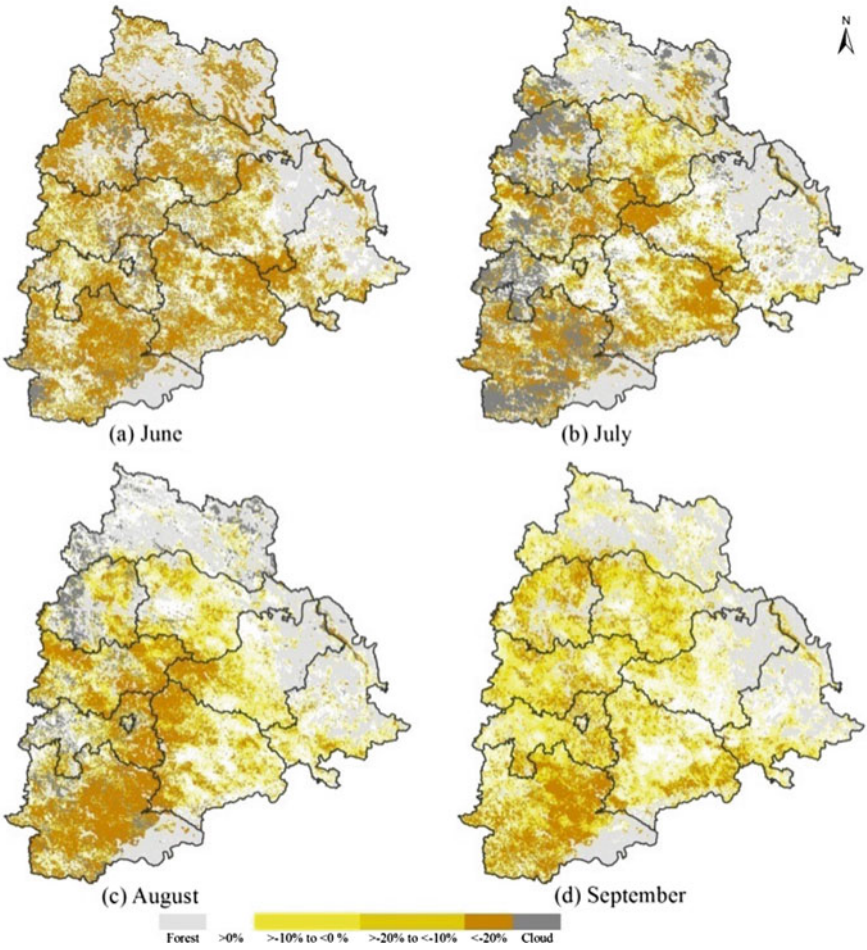

Fig. 6 NDWI deviation for South-West Monsoon period 2015

monitoring plays an important role in coping with drought and its impacts. Integrated seasonal condition of drought for monsoon period of 2015 has been prepared for entire state (Fig. 7). It demonstrated normal situation in 235, mild in 169, moderate in 33 and severe in 06 mandals of Telangana state.

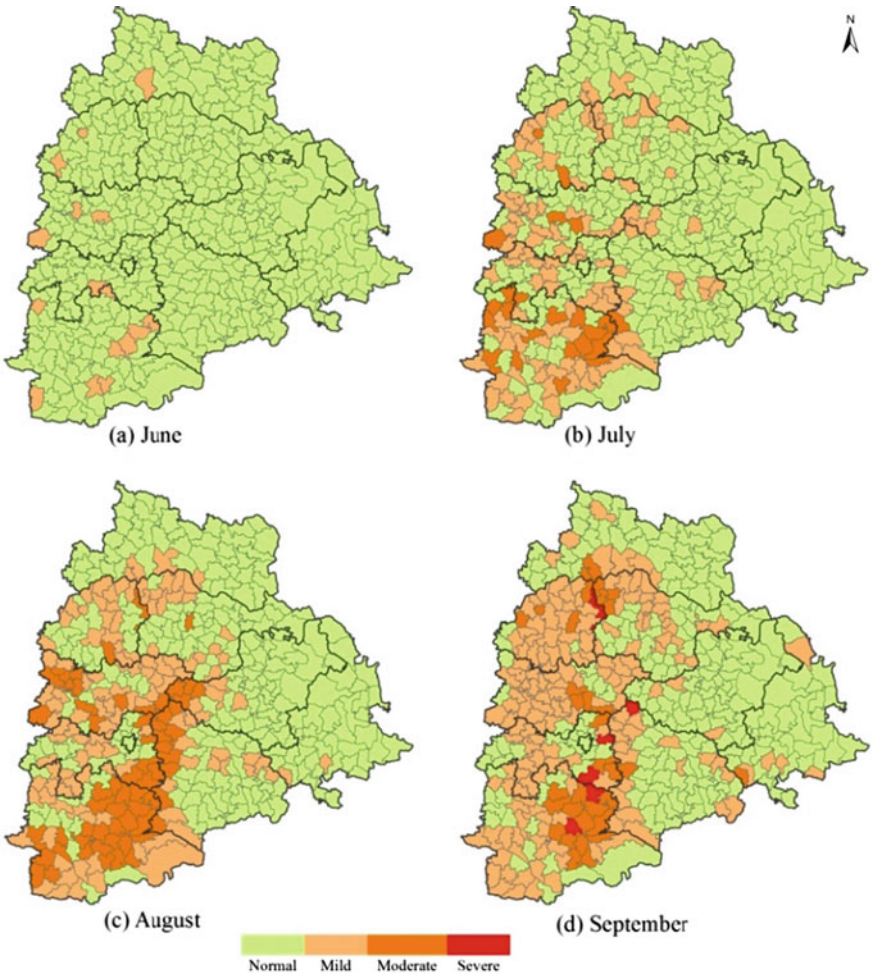

Fig. 7 Integrated assessment of seasonal condition for drought monitoring for South-West Monsoon 2015

6 Conclusions

Telangana State Remote Sensing Applications Centre (TRAC), a nodal agency for remote sensing and geographical information system applications in the state, has established an integrated seasonal condition monitoring system. Concurrent monitoring of seasonal conditions using remote sensing, weather network data and continuous ground truth has been involved in an integrated seasonal condition monitoring system. An early warning system is developed using a suite of indicators to identify drought prone areas in the state. Satellite remote sensing derived

drought indices and meteorological indices, in support with ground data has adequately recognized and illustrated the onset and severity of drought situation. Though, an integrated approach can satisfactorily recognize the severity of drought situation in the state, frequency and interval of consecutive rainfall events carry an important role than total seasonal rainfall, particularly at the critical stages of the agricultural crops. Government of Telangana has prepared alternate contingency plans based on the results of this study for entire state to cope with the disastrous effects of drought. Policy makers found that alternate contingency plans were helpful to reduce the agricultural crop failure risk and ameliorate impact of drought.

References

1. Mishra, A.K., Singh, V.P.: A review of drought concepts. J. Hydrol. **391**(1–2), 202–216 (2010)
2. Wilhite, D.A., Glantz, M.H.: Understanding the drought phenomenon: the role of definitions. Water Int. **10**, 111–120 (1985)
3. Heim Jr., R.R.: A review of twentieth-century drought indices used in the United States. Bull. Am. Meteorol. Soc. **83**(8), 1149–1165 (2002)
4. Wilhite, D.A., Sivakumar, M.V., Pulwarty, R.: Managing drought risk in a changing climate: the role of national drought policy. Weather Climate Extremes **3**, 4–13 (2014)
5. Wanders, N., Wada, Y.: Human and climate impacts on the 21st century hydrological drought. J. Hydrol. **526**, 208–220 (2015)
6. van Loon, A.F., Tijdeman, E., Wanders, N., van Lanen, H.A., Teuling, A.J. Uijlenhoet, R.: How climate seasonality modifies drought duration and deficit. J. Geophys. Res.: Atmos. 119 (8), 4640–4656 (2014)
7. Zarch, M.A.A., Sivakumar, B., Sharma, A.: Droughts in a warming climate: a global assessment of Standardized precipitation index (SPI) and Reconnaissance drought index (RDI). J. Hydrol. **526**, 183–195 (2015)
8. Brown, J.F., Reed, B.C., Hayes, M.J., Wilhite, D.A. Hubbard, K.: A prototype drought monitoring system integrating climate and satellite data. In: PECORA 15/Land Satellite Information IV/ISPRS Commission I/FIE0S 2002 Conference Proceedings (2002)
9. Khosravi, H., Haydari, E., Shekoohizadegan, S., Zareie, S.: Assessment the effect of drought on vegetation in desert area using landsat data. The Egypt. J. Remote Sens. Space Sci. **20**, S3–S12 (2017)
10. Murad, H. and Islam, A. S.: Drought assessment using remote sensing and GIS in north-west region of Bangladesh. 3rd Int. Conf. Water and Flood Manag. **3**, 797–804 (2011)
11. Muthumanickam, D., Kannan, P., Kumaraperumal, R., Natarajan, S., Sivasamy, R., Poongodi, C.: Drought assessment and monitoring through remote sensing and GIS in western tracts of Tamil Nadu, India. Int. J. Remote Sens. **32**(18), 5157–5176 (2011)
12. Zargar, A., Sadiq, R., Naser, B., Khan, F.I.: A review of drought indices. Environ. Rev. **19**, 333–349 (2011)
13. Dutta, D., Kundu, A., Patel, N.R., Saha, S.K. Siddiqui, A.R.: Assessment of agricultural drought in Rajasthan (India) using remote sensing derived vegetation condition index (VCI) and standardized precipitation index (SPI). The Egypt. J. Remote Sens. Space Sci. **18** (1), 53–63 (2015)
14. Brown, J.F., Wardlow, B.D., Tadesse, T., Hayes, M.J., Reed, B.C.: The vegetation drought response index (VegDRI): a new integrated approach for monitoring drought stress in vegetation. GIScience and Remote Sens. **45**(1), 16–46 (2008)

15. Anonymous: Reinventing Telangana, The First Steps, Socio Economic Outlook 2015. Planning Department, Government of Telangana, India (2015)
16. Commissioner Disaster Management: Drought Management Manual for Telangana State. Department of Disaster Management, Revenue Department, Government of Telangana (2016)
17. Registrar General and Census Commissioner: Census of India 2011, Ministry of Home Affairs, Government of India. http://www.censusindia.gov.in/pca/Searchdata.aspx (2011)
18. McKee, T.B., Doesken, N.J. Kleist, J.: The relationship of drought frequency and duration to time scales. In: Eighth Conference on Applied Climatology. American Meteorological Society, Anaheim, CA, pp. 179–186 (1993)
19. van Rooy, M.P.: A rainfall anomaly index independent of time and space. Notos **14**, 43–48 (1965)
20. Malingreau, J.P.: Global vegetation dynamics: satellite observations over Asia. Int. J. Remote Sens. **7**(9), 1121–1146 (1986)
21. Tucker, C.J., Choudhury, B.J.: Satellite remote sensing of drought conditions. Remote Sens. Environ. **23**(2), 243–251 (1987)
22. Johnson, G.E., Achutuni, V.R., Thiruvengadachari, S., Kogan, F.: The role of NOAA satellite data in drought early warning and monitoring: selected case studies. In: Drought Assessment, Management, and Planning: Theory and Case Studies, pp. 31–49 (1993)
23. Kogan, F.N.: Droughts of the late 1980s in the United States as derived from NOAA polar-orbiting satellite data. Bull. Am. Meteorol. Soc. **76**(5), 655–668 (1995)
24. Murthy, C.S., Sesha Sai M.V.R.: Agricultural drought monitoring and assessment. In: Roy P. S., Dwivedi, R.S., Vijayan, D. (eds.) Remote Sensing Applications, National Remote Sensing Centre, Indian Space Research Organization, Department of Space, Government of India, pp. 303–330 (2010)
25. Chandrasekar, K., Sai, M.S.: Monitoring of late-season agricultural drought in cotton-growing districts of Andhra Pradesh state, India, using vegetation, water and soil moisture indices. Nat. Hazards **75**(2), 1023–1046 (2015)

Chapter 25
Temperature and Vegetation Indices Based Surface Soil Moisture Estimation: A Remote Sensing Data Approach

V. Vani, K. Pavan Kumar and Mandla Venkata Ravibabu

Abstract In environmental and agricultural modelling soil moisture condition is one of the main parameter. To estimate surface soil moisture using an operational algorithm at fine spatial and temporal resolutions (thermal and optical sensors) with the help of Ts(Land Surface Temperature)/VI(Vegetation Index) space based triangle method. Theoretical solutions of dry and wet edges were derived from this method. Based on this method we calculated Soil Moisture Index using more than 8 images for year from 2007 to may 2011 for a part of Murrumbidgee catchment in southern new south wales, Australia. Insitu Soil moisture data for 20 agricultural stations were used for validating the satellite observed Soil Moisture Index. The Results indicated that the general pattern of the SMI variation follows the trend of field soil moisture measurement. Different soil backgrounds influenced the SMI computing using optical satellite image. Estimation of regional soil moisture in areas with less ground information (insitu observations) is achieved with the help of SMI model.

Keywords Soil moisture index · Vegetation indices · Land surface temperature and optical remote sensing · ICRSDM

V. Vani (✉)
Centre for Disaster Mitigation and Management (CDMM), Chennai, India
e-mail: vani.volite@gmail.com

K. Pavan Kumar
Department of Environmental and Water Resource Engineering,
School of Civil and Chemical Engineering, VIT University,
Vellore 632014, TN, India
e-mail: pavankumar@vit.ac.in

M. V. Ravibabu
CGARD, School of Science, Technology and Knowledge Systems,
National Institute of Rural Development & Panchayati Raj (NIRD&PR),
Hyderabad, TS, India
e-mail: ravi.mandla@gmail.com; mvravibabu.nird@gov.in

P. J. Rao et al. (eds.), *Proceedings of International Conference on Remote Sensing for Disaster Management*, Springer Series in Geomechanics and Geoengineering,
https://doi.org/10.1007/978-3-319-77276-9_25

1 Introduction

Surface soil moisture is an important parameter in land surface processes, energy and water which segregate the plant, soil and atmosphere. It gives the quantity of water in soil. Knowledge of soil water content play a significant role in many agricultural applications, like the requirement of water for crop growth and irrigation support for productivity [1]. Soil moisture data, collected from different depths below surface over the period are valuable to analyse the condition of various parameters of land resources and response between the climate system and earth. The rate of evaporation from the soil is a result due to exchange of the energy between atmosphere and land surface. Groundwater linked with surface water in vertical migration of the soil moisture supports vegetation to grow. Measuring the accurate in situ soil moisture for long-term in large scale area is too expensive to maintain, because of which insitu soil moisture stations are limited. Local surface soil water condition shows high variability in the surface soil moisture due to spatial variation of terrain, vegetation cover and soil properties [2].

Soil moisture is used for planning irrigation, crop yield estimation and to monitor drought condition [3]. It is very useful to study subsequent precipitation patterns, water quality and temperature change [4]. Satellite images provide information of an area with timely intervals repeatedly, which provides instantaneous measurement of soil moisture in short time. The recent development in the satellite sensors provides detailed study with high spatial image resolution perspective. Many researches established different methods to retrieve the soil moisture by establishing a relationship between vegetation and surface temperature using optical and thermal bands of satellite data. The Normalized Difference Vegetation Index (NDVI) is used to estimate the vegetation cover and Land Surface Temperature (LST) is used to calculate the surface Temperature. The soil moisture index is calculated from LST/VI space [5]. The space is a scatter plot between NDVI and LST is shown in a triangular shape which is known as triangle method. The temperature is sensitive to vegetation cover and the surface soil moisture content. The sensitivity of LST to soil moisture and vegetation cover can be clearly seen in the scatter plot [6]. The LST/VI feature space is limited with the dry and wet edge. Wet edge indicates maximum evapotranspiration and sufficient soil moisture and dry edge represents where the evapotranspiration is minimum with water stress vegetation [7]. The dry edge or driest point of vegetation depends on the type of vegetation and coverage. The wet edge LST was taken as minimized surface temperature and dry edge as maximized surface temperature. Based on the view of surface temperature with fully vegetated area the triangular and trapezoidal methods are developed [8].

In present study surface soil moisture Index (SMI) is calculated from Landsat images of January and March months from 2007 to 2011 to estimate soil moisture. Lambin and Ehrich [9] described the feature space of the LST and NDVI in trapezoidal shape, which is an empirical parameter to estimate SMI. Validation of index is carried using in situ soil moisture measurements from observation centres located in southern New South Wales, Australia. OzNET is one of the soil moisture network centre located in the study area.

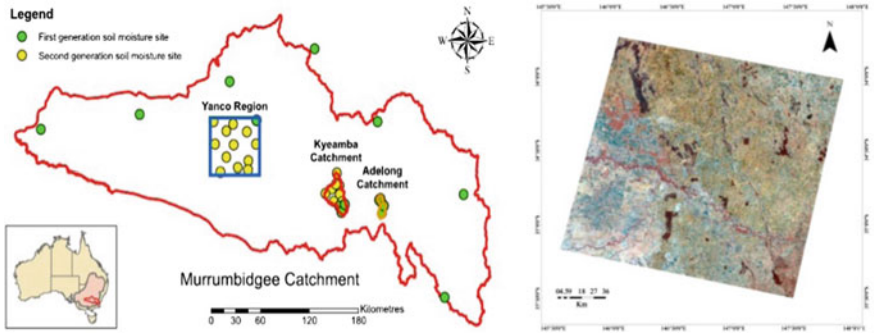

Fig. 1 Location of the study area in Murrumbidgee river catchment

2 Study Area and Data Source

The study area (Fig. 1) is located at the 144° 4′ 16″E, 33° 43′ 50″S to 147° 28′ 26″E, 35° 30′ 32″S is a part of Murrumbidgee catchment in southern New South Wales, Australia. The study area is approximately 29,500 km^2. The Murrumbidgee Soil Moisture Monitoring Network (MSMMN) has thirty eight insitu soil moisture monitoring stations distributed across the Murrumbidgee River basin. The MSMMN consists the data of soil moisture up to root zone (up to 90 cm depth) and monitor at 38 sites at Murrumbidgee River Catchment. The soils vary from sandy clayey, where western plains being dominated by the finer-textured soils and the eastern half of catchment being occupied by medium to coarse textured soils. The average annual precipitation is 300 mm. Major land use land cover is agriculture with sufficient irrigation and steeper parts are occupied with Eucalypts forests [10].

Landsat 5 TM images were downloaded from the USGS web site. The Landsat-5 images of January and March data for 2007, 2008, 2009, 2010 and 2011 is used to study the SMI with reference data. The data available in the study area is cloud free. Reference data from in situ soil moisture stations information data acquired from the OzNET centre website. The 20 stations of OzNET centre with their land use and elevation is used in present study [11].

3 Methodology

Normalized Difference Vegetation Index and Land Surface Temperature were calculated for different Landsat images. The NDVI and LST images were used to construct NDVI-LST feature space and to calculate the Soil Moisture Index values.

3.1 Normalized Difference Vegetation Index (NDVI)

NDVI is the most commonly used vegetation index to study the vegetation. It is proposed by Rouse et al. [12]. The vegetation phenology gives less reflectance in visible light and more in NIR for green vegetation, where as sparse vegetation reflects a great portion of visible light and less portion in NIR. NDVI calculation uses reflectance characteristics of vegetation in visible and NIR regions as a ratio.

NDVI is derived as:

$$\mathrm{NDVI} = \frac{\mathrm{NIR} - \mathrm{RED}}{\mathrm{NIR} + \mathrm{RED}} \tag{1}$$

where, NIR—reflectance in Near Infra-Red band, R—Reflectance in Red band.

The NDVI values are between −1 and +1. Positive values increases with green vegetation and negative values indicate the non-vegetated surface features like water, ice, snow or clouds.

3.2 Land Surface Temperature (LST)

To calculate the LST from thermal band of the satellite data is used, that the temperature at the interface between the earth's surface and its atmosphere. The thermal band for Landsat-5 is TIR band 6 is used to derive surface temperature of the area brightness temperature can be derived in Kelvin's converted into Celsius. This method follow 3 steps:

Step 1: The digital number (DN) was first converted into spectral radiance (L).

$$L = LMIN + (LMAX - LMIN) \times \frac{DN}{255} \tag{2}$$

where, L = Spectral radiance, DN = Digital Number, LMIN = 1.238 (Spectral radiance of DN value1) and LMAX = 15.600 (Spectral radiance of DN value 255).

Step 2: The Spectral radiance was converted to temperature in Kelvin

$$T_B = \frac{K_2}{\ln(K_1 + 1)} \tag{3}$$

where, K_1 = Calibration Constant 1 (607.76), K_2 = Calibration Constant 2 (1260.56), T_B = Surface Temperature.

Step 3: Convert from Kelvin to Celsius

$$T_B(celsius) = T_B - 273 \tag{4}$$

3.3 Soil Moisture Index

The SMI is computed based on the LST-NDVI feature space of Landsat images, where NDVI and LST are used as input parameter for model and the empirical coefficients are used to estimate warm edge and cold edge from linear regression equation of LST-NDVI resulting in trapezoidal shape (Fig. 2).

All types of land cover fell within the trapezoid of the LST-NDVI space. The upper envelope of the trapezoid, A-C, represents the dry condition, is called as dry edge (warm edge). This warm edge gives the upper limit of the LST for vegetation cover. The lower limit of the trapezoid, B-D, corresponds to the well-watered condition, is called as wet edge (cold edge). The SMI values were validated using in situ soil moisture data.

SMI defined as

$$SMI = \frac{LSTmax - LST}{LSTmax - LSTmin} \tag{5}$$

where, LSTmax—maximum surface temperature for NDVI

LSTmin—minimum surface temperature for NDVI

LST—land surface temperature

The empirical parameters are calculated from Eqs. 6 and 7

$$LSTmax = a_1 NDVI + b_1 \tag{6}$$

$$LSTmin = a_2 NDVI + b_2 \tag{7}$$

where, a_1, a_2, b_1, b_2 are empirical parameters.

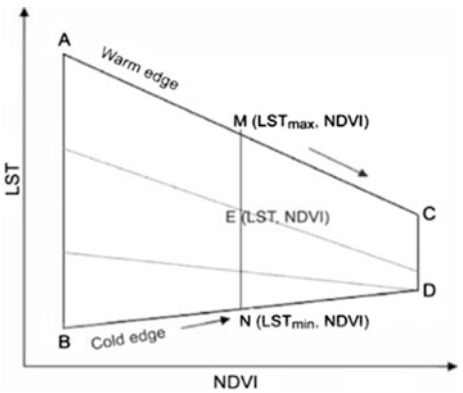

Fig. 2 Scatter plot of LST-NDVI feature space

4 Results and Discussion

In the current study to compare Soil Moisture Index with in situ soil moisture observations, the data was considered for the months of January and March from 2007 to 2011. For every unique NDVI value the minimum and maximum LST was acquired with 0.01 interval and determined dry and wet edge. The linear regression equation values are shown in Table 1.

The cluster of pixels with uniform NDVI values were considered to eliminate extreme values for building a true relationship between LST and NDVI. In all the images it has observed that the slope is negative for dry edge and positive for wet edge. The linear regression equations are applied in the model and calculated SMI. The obtained SMI values are between 0 and 1. It is observed that the SMI value '0' belongs to dry soil or absence of soil moisture and the value '1' represents wet soil area. Some of the SMI images are presented in Fig. 3. The observed soil moisture from the insitu stations were compared with the Satellite image derived Soil moisture index values. Of all the computed images, there is a close relationship between March 2008 SMI values and observed values.

The observed soil moisture and SMI graphs are shown in Fig. 4.

From the above plots it is clear that general pattern of the SMI variation followed the normal trend of field soil moisture except k11 and y11 sites. For the 2010 April and Jan 2011 most of the SMI values are gave similar values to the observed Insitu parameters with difference ±0.02 and the RMSE values are between −0.12 and 0.19. In all the years of study, the average deviation of the SMI with observed values were ±0.05. The relation between LST and NDVI shows the reflection of the observed soil moisture. The time series revealed the estimated soil moisture match the trend line of field surface soil moisture, the seasonal variations show low in rainy season [2]. The method has evolved no mathematical rules to identify the

Table 1 Dry and wet edges in NDVI/LST space estimated by linear regression

Date	Dry edge	R^2	Wet edge	R^2
26-01-2007	y = −10.19x + 37.29	0.973	y = 5.19x + 17.29	0.941
16-04-2007	y = −16.78x + 56.06	0.982	y = 5.799x + 17.21	0.962
13-01-2008	y = −18.04x + 33.42	0.927	y = 14.15x + 24.25	0.978
17-03-2008	y = −20.05x + 40.53	0.984	y = 7.326x + 19.56	0.952
31-01-2009	y = −24.21x + 51.08	0.989	y = 3.368x + 31.21	0.819
05-04-2009	y = −16.91x + 30.21	0.955	y = 5.992x + 12.43	0.899
18-01-2010	y = −26.62x + 43.97	0.988	y = 9.714x + 23.60	0.903
24-04-2010	y = −6.983x + 21.92	0.693	y = 22.72x + 3.677	0.969
05-01-2011	y = −21.13x + 44.61	0.96	y = −1.734x + 24.26	0.804
27-04-2011	y = −10.04x + 26.51	0.966	y = 3.077x + 12.12	0.554

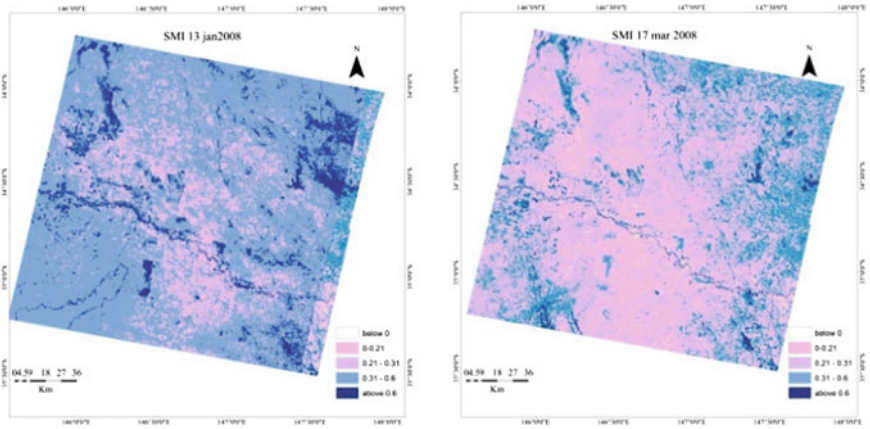

Fig. 3 Soil moisture index image of 13th January 2008 and 17th March 2008

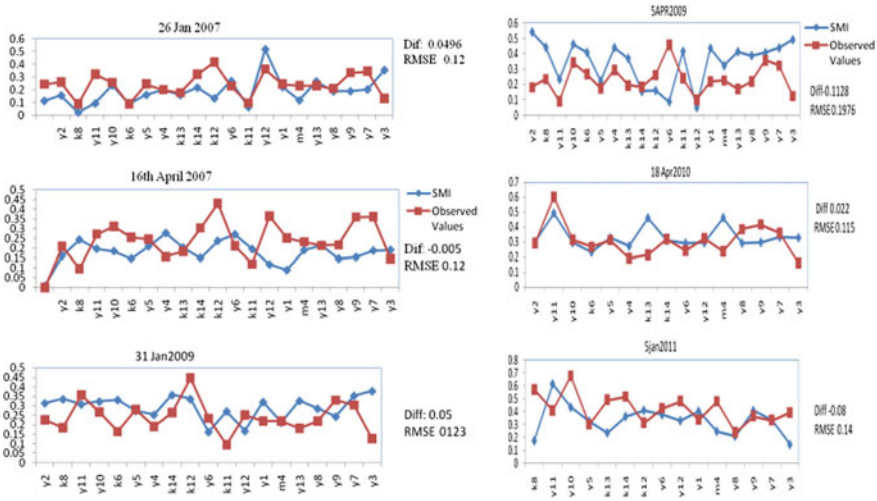

Fig. 4 Trend of the soil moisture from observed sites and SMI values

pixels in the dry and the wet edges. It is purely subjectivity depends on the proposed algorithm that identifies the wet edge and the dry edge. From the results it has been concluded that the SMI can be measured by using satellite data to estimate soil moisture where there is a lag of availability of ground information.

5 Conclusion

The Surface Soil Moisture is retrieved based on the visible, NIR and thermal infrared remotely sensed data acquired from Landsat images using the trapezoidal LST/NDVI feature space. The dry edge and wet edge were derived from visual interpretation of the LST/NDVI feature space. The wet edges shows the positive correlation between NDVI and LST where the dry edges always show the negative correlation. The LST/NDVI space estimate surface SMI for each pixel once the spatial distribution is well defined. This method can improves the ability of retrieve the soil moisture condition for a large spatial area with in high temporal frequency.

The SMI values for the images showing the difference from ± 0.003 to ± 0.14 and the RMSE values are between -0.12 and 0.19, the average deviation from the observed values is ± 0.005. The study made a bold attempt to estimate surface soil moisture index under different temporal conditions. The advantage of soil moisture condition acquiring through remotely sensed data, can give the large spatial scale, which helps significantly in the understanding and monitoring the environment conditions.

References

1. Petropoulos, G., Carlson, T.N., Wooster, M.J., Islam, S.: A review of Ts/VI remote sensing based methods for the retrieval of land surface energy fluxes and soil surface moisture. Prog. Phys. Geogr. **33**(2), 224–250 (2009)
2. Han, Y., Wang, Y., Zhao, Y.: Estimating soil moisture conditions of the greater Changbai mountains by land surface temperature and NDVI. IEEE Trans. Geosci. Remote Sens. **48**(6), 2509–2515 (2010)
3. Bolten, J.D., Crow, W.T., Zhan, X., Jackson, T.J., Reynolds C.A.: Evaluating the utility of remotely sensed soil moisture retrievals for operational agricultural drought monitoring. IEEE J. Sel. Top. Appl. Earth Obs. Remote Sens. **3**(1), 57–66 (2010)
4. Houser, P.R., Shuttleworth, W.J., Famiglietti, J.S., Gupta, H.V., Syed, K.H., Goodrich, D.C.: Integration of soil moisture remote sensing and hydrologic modeling using data assimilation. Water Resour. Res. **34**(12), 3405–3420 (1998)
5. Carlson, T.N., Gillies, R.R., Perry, E.M.: A method to make use of thermal infrared temperature and NDVI measurements to infer surface soil water content and fractional vegetation cover. Remote Sens. Rev. **9**(1–2), 161–173 (1994)
6. Sandholt, I., Rasmussen, K., Andersen, J.: A simple interpretation of the surface temperature/ vegetation index space for assessment of surface moisture status. Remote Sens. Environ. **79** (2), 213–224 (2002)
7. Wang, W., Huang, D., Wang, X.G., Liu, Y.R., Zhou, F.: Estimation of soil moisture using trapezoidal relationship between remotely sensed land surface temperature and vegetation index. Hydrol. Earth Syst. Sci. **15**(5), 1699–1712 (2011)
8. Zhang, D., Zhou, G.: Estimation of soil moisture from optical and thermal remote sensing: a review. Sensors **16**(8), 1308 (2016)
9. Lambin, E.F., Ehrlich, D.: The surface temperature-vegetation index space for land cover and land-cover change analysis. Int. J. Remote Sens. **17**(3), 463–487 (1996)

10. Smith, A.B., Walker, J.P., Western, A.W., Young, R.I., Ellett, K.M., Pipunic, R.C., Grayson, R.B., Siriwardena, L., Chiew, F.H., Richter, H.: The Murrumbidgee soil moisture monitoring network data set. Water Resour. Res. **48**(7), 1–6 (2012)
11. Young, R., Walker, J., Yeoh, N., Smith, A., Ellett, K., Merlin, O., Western, A.: Soil moisture and meteorological observations from the Murrumbidgee catchment. Department of Civil and Environmental Engineering, The University of Melbourne (2008)
12. Rouse, J.W., Haas, R.H., Deering, D.W., Sehell, J.A.: Monitoring the vernal advancement and metrogradation (Green wave effect) of natural vegetation. Final Report, RSC, 1978–4 (1974)

Chapter 26
Runoff Estimation by Using Optimized Hydrological Parameters with Special Reference to Semi-arid Agriculture Watershed

Nagaveni Chokkavarapu, Pavan Kumar Kummamuru and Venkata Ravibabu Mandla

Abstract GIS technology is used to estimate the spatial heterogeneity of the hydrological parameters of a watershed. Hydrological models help to overcome the spatial variability and parameter uncertainties. Runoff is important parameter of hydrological cycle. Soil and Water Assessment Tool (SWAT) which is a physical distributed model developed to forecast runoff, sediment, erosion and nutrient transport from agricultural watershed helps to understand the hydrology of a watershed with rainfall, temperature, solar radiation, wind speed and relative humidity. SWAT simulates better results in both gauged and ungauged watersheds. In the present paper, Krishna river catchment area known as Jurala watershed in Mahabubnagar district, Telangana state of South India is taken to study surface runoff from agricultural areas as this area receives less annual rainfall and agriculture is mostly dependent on seasonal rainfall. Soil has less water infiltration capacity and bottom layer calcium carbonate deposits make soil alkaline due to bore well irrigation. To suggest proper water conservation methods, understanding hydrology of this watershed is important. To simulate runoff from this agriculture watershed SWAT model is used for 11 years from 2000 to 2010. The results are calibrated with observed values.

N. Chokkavarapu (✉)
Centre for Disaster Mitigation and Management (CDMM), VIT University, Vellore, India
e-mail: nagaveni.ch@gmail.com

P. K. Kummamuru
Department of Environmental and Water Resource Engineering,
School of Civil and Chemical Engineering, VIT University,
Vellore 632014, Tamil Nadu, India
e-mail: pavankumar@vit.ac.in

V. R. Mandla
CGARD, School of Science, Technology and Knowledge Systems,
National Institute of Rural Development and Panchayati Raj (NIRD&PR),
Hyderabad, Telangana, India
e-mail: ravi.mandla@gmail.com; mvravibabu.nird@gov.in

P. J. Rao et al. (eds.), *Proceedings of International Conference on Remote Sensing for Disaster Management*, Springer Series in Geomechanics and Geoengineering,
https://doi.org/10.1007/978-3-319-77276-9_26

Keywords Hydrological modeling · Agriculture watershed · Runoff
SWAT

1 Introduction

Sustainable development mainly depends on proper management of natural resources. Water resources management assures improvement in quality of ecosystems and human life standards. Watershed is defined as an area draining into a single water body or river. Spatial modelling of hydrology in a watershed helps to assess the total water yield within the basin [1]. Different hydrological models are available to study the processes running in a watershed. Watershed management is important as it serves as hydrological unit [2] which is closely associated with economical, agriculture, social security and life supporting processes for human life [3]. Data availability and accuracy plays major role in the final output. In remote and inaccessible areas hydrological parameter reliable data availability is uncertain. In many areas in India water stress is caused due to low or lack of rainfall, unpredictable rainfall pattern and also caused due to improper methods to conserve and manage in a sustainable method. This difficulty can be overcome by using mathematical models to calculate hydrological parameters of a watershed using remote sensing and GIS techniques to extract and evaluate different hydrological parameters. Increasing complexity of real world scenarios is becoming challenging for planning and decision making process. For planning and execution of projects, surface runoff estimation based on rainfall is necessary. In arid and semi arid regions rainwater harvesting plays important role for sustainable practice of agriculture. Modelling runoff is important for sustainable growth, where selection of suitable methods to quantify the hydrological parameters of watershed is essential [4]. SWAT model estimates runoff [5], sediment [6] and agricultural chemical quantities in watersheds with varying land use practices [7]. Hydrology parameters of SWAT are precipitation, evapotranspiration, infiltration, percolation and runoff. From recent past computer based hydrological modelling made it easy to estimate runoff in gauged and ungauged watersheds. Runoff is strongly influenced by vegetation cover and land use [8] as these two influence infiltration [9], erosion and evapotranspiration. Existing hydrological models require input parameters for the identification of similar areas with same hydrologic response [10]. SWAT is a continuous time model developed by United States Department of Agriculture's Agricultural Research Service (USDA-ARS) and Texas A&M university, to study the impact of land management/use practices on agricultural and forest watersheds with different soils, land use and slope [11]. Surface runoff directly influences the erosion process.

Better management practices in high runoff areas and steep slope areas are important for sustainable development [12]. Runoff production in a watershed depends upon process of infiltration, rainfall intensities and internal storage capacities. Rate of infiltration also influence by type of land use practice, slope,

vegetation cover and soil properties. Different researchers have been evaluated SWAT model across globe in gauged and ungauged watersheds [13]. Their findings reveal that SWAT model is capable of simulating hydrological processes with maximum accuracy. The SWAT model requires many hydrological parameters related to land use land cover, soil, and climate. These parameters need to be calibrated and validated before using in the model for more realistic values [14]. Calibration and validation of SWAT model is necessary for reducing uncertainties arising due to spatial variability of soil, land use land cover and slope parameters for more realistic and proficient examination [15, 16]. It can be better applied to ungauged basins. In this paper we attempted to test SWAT model capabilities to simulate runoff of the watershed.

2 Study Area and Significance

The Jurala watershed is part of Krishna basin in southern India. The watershed covering an area of 1857 km^2 lying in between Matkal, Narva, Kothakota, Atmakur, Gadwal, Dharur taluk of Mahboobnagar district in Telangana. This study area is drought-prone with a mean annual rainfall of 604 mm. Agriculture largely depends on rainfall and tank/well irrigation. Geographically the area extends between 77° 36′ 3″E to 77° 55′ 46″ longitude and 16° 09′ 43″N to 16° 40′ 54″N latitude (Fig. 1). Major part is undulating plains with a gentle slope cover. Dominant soils are red sandy soils, black soils. Heavy black soils with rain fed conditions are cultivated with cotton, sunflower, chillies, maize, redgram, green gram (kharif season), jower, bengal gram, sunflower (rabi) season. Light soils (sandy red and sandy loamy soils) under rain fed conditions are cultivated with castor and maize (kharif), jower, cotton, ground nut, red gram, green gram (rabi). Another category of soils in this area are saline or alkaline soils (problematic soils). In present study area saline soils have canal water access and grown only paddy. Forty eight percent of the total area belongs to agricultural land. Sixty eight percent of the agriculture land belongs to kharif season that entirely depends on rainfall, wells/tanks. Southwest monsoon variability leads to failure in the crops. Agriculture area is mostly in low rainfall and less fertile soils. Current fallow land reflects low fertility of soils and non availability of farming. Nutrients in soils are nitrogen (low), phosphorous (medium), potash (high) amounts. Red sandy soils occupy largest part and are permeable and well drained. Major irrigation is of three types i.e. canals from Jurala project, tank irrigation, tube or bore well irrigation. Ground water plays major role in agriculture. Cropping pattern depends on local climatic conditions, soil type and type of irrigation. Paddy is mainly grown under canal, tanks and well irrigation. Rain fed area is cultivated with jower, bajra and grams. Commercial crops like chillies, cotton and ground nut are grown under canal irrigation.

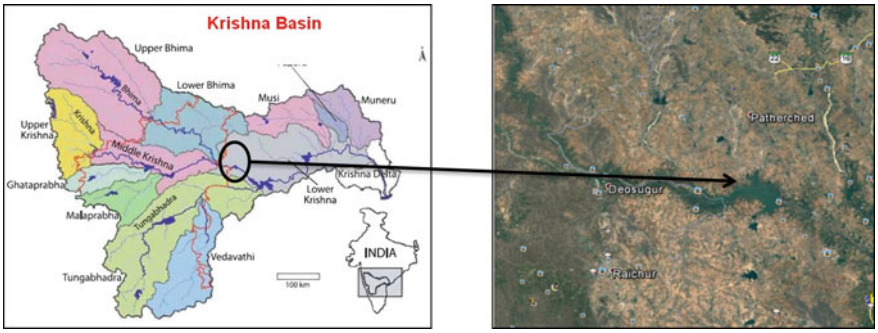

Fig. 1 Location of the study area

3 Data Used

3.1 Digital Elevation Model (DEM)

SRTM (Shuttle Radar Topography Mission) DEM of 90 m spatial resolution is used for watershed delineation. Information acquired and calculated from DEM are slope length, slope classes and elevation. Total 25 sub basins and streams are delineated from SRTM DEM using SWAT delineation process Fig. 2 and Table 1.

Fig. 2 Schematic diagram of Jurala watershed (Sub watershed and streams are delineated from SRTM DEM)

Table 1 Percentage of slope and area distribution of the Jurala watershed

Slope (%)	Area (km^2)	% of Total
0–10	1817.18	97.85
10–20	20.58	1.11
Above 20	19.34	1.01

3.2 Land Use Map

Land use map was obtained from National Remote Sensing Application Centre (NRSA), Hyderabad. Dominant type of land use is agriculture including kharif crop and Rabi crop. Kharif and Rabi crop accounting for 48.94%. Current fallow land occupies 32%, unused waste land 8.24%, forest 5.37% Figs. 3 and 4.

3.3 Soil Map and Database

Soil map is obtained from NBSS&LUP, Nagpur on 1:50000 scale. In case of lack of soil survey, soil information can be taken from, the FAO soil map of the world or ISRIC world soil information. Soil attributes for each soil type related to soil map should be added to user soil database in SWAT. Soil database includes different physiochemical and soil textural properties like water content, saturated hydraulic conductivity, bulk density, soil organic carbon content for each soil and different layers. Using SPAW which is a pedotransfer function soil properties like water content, and saturated hydraulic conductivity are calculated using soil physical properties like soil particle size (sand, silt, clay) and bulk density. Major soils found

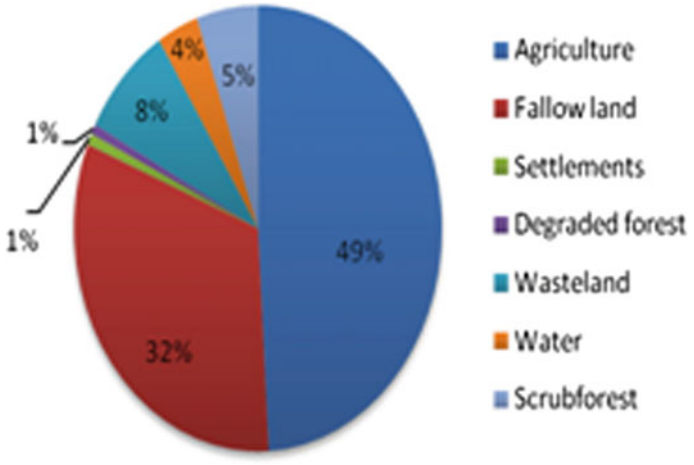

Fig. 3 Land use class distribution in the study area

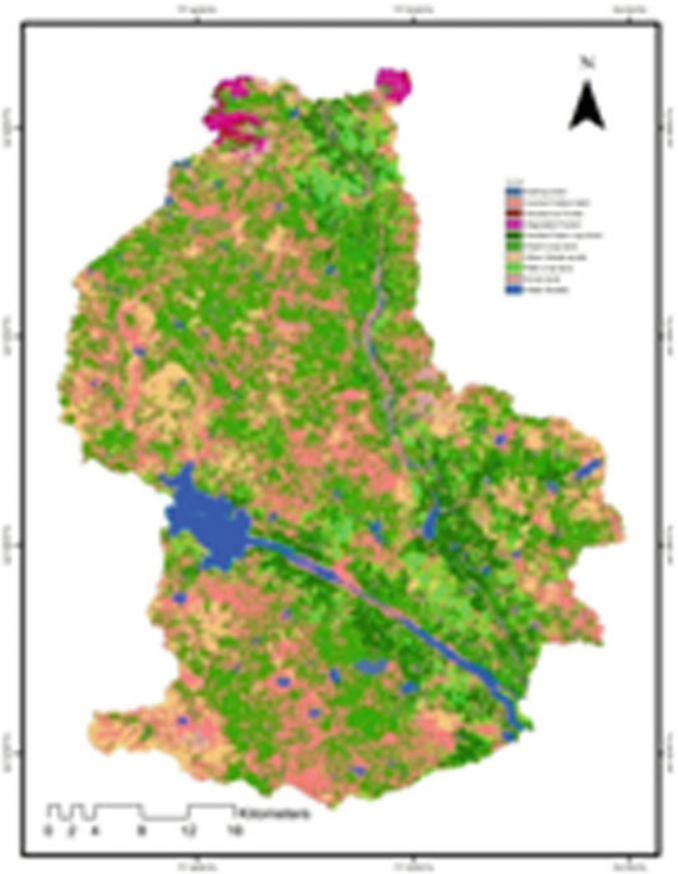

Fig. 4 LULC classes of Jurala watershed

in present study area are clay loam and sandy clay loam [17]. Depending on rate of infiltration soils are further classified into hydrological groups A, B, C, D Table 2.

The rate of transmission of water, nature of texture, structure and degree of swelling when saturated, yield similar runoff amounts. In our study area most of soils belong to group C and D with more runoff rate [18]. According to USDA soil classification these soils belongs to Vertisols. These are swelling and shrinking

Table 2 Classification of hydrological soil group based on soil texture

HSG	Infiltration	(mm/h)	Soil texture
A	High	>25	Sandy loam
B	Moderate	>12.5–25	Silt loam or loam
C	Low	2.5–12.5	Sandy clay loam
D	Very low	<2.5	Clay loam

heavy soils mostly found in river basins, lake bottoms and black swamps. $CaCo_3$ is present in calcic zone in diffuse form or discontinuous amounts. Often it occurs in surface horizon.

3.4 Weather Database

Rainfall data is obtained from CWC (Central Water Commission), Krishna Basin from automatic meteorological stations or rain gauges. Precipitation daily data is used for this area to calculate runoff. Temperature (minimum, maximum), solar radiation, relative humidity and wind speed data is used in weather input files. Using WXGEN stochastic weather generator model gaps in observed weather data were filled.

4 Model Description

SWAT was developed to study the impact of different land use practices on water, sediment and agricultural yields in watershed with various types of land use management practices and different soils, slopes. Land use change impact on runoff generation was analyzed by [19] in three different regions to demonstrate the long term impacts on runoff with varying soils, slope and vegetation cover. To simulate hydrological parameters in SWAT input data is required like weather data, land use map, soil map, topography, vegetation occurring in the watershed. In SWAT, watershed processes calculation is based on land phase and water phase. Processes that occur on land phase are calculated based on water balance Eq. (1).

$$SWt = SWo + \sum_{i=1}^{t}(PREC - SURQ - ET - PERCO - BF) \tag{1}$$

where:

SW_t = soil water content (mm), SW_o = soil water content available for plant uptake, t = time (days), PERC = amount of precipitation, SURQ = amount of surface runoff (mm), ET = amount of evaporation (mm), PERCO = amount of percolation (mm), BF = amount of base flow (mm).

Surface runoff parameter is estimated by using modified Soil Conservation Service (SCS) curve number method. The SCS curve number is calculated using land use, soil permeability, and preceding moisture conditions. It calculates surface runoff as per the following Eq. (2).

$$Q_{surf} = \frac{\left(R_{day} - I_a\right)^2}{\left(R_{day} - I_a + S\right)} \tag{2}$$

Q_{surf} is the surface runoff (mm), R_{day} is the rainfall for the day (mm), I_a is the initial abstractions.

SWAT is a spatially distributed hydrological model developed to calculate water, sediment, pesticide and nutrient transport from agricultural and forest watershed scale. SRTM DEM is used for watershed delineation as a first step in which watershed has been divided into different sub basins which allows assessing hydrologic processes in different sub basins within a watershed and analyzing localized land use management practice impacts on total yield. After giving soil map, land use land cover map as input HRU (Hydrological Response Units) are created which describe spatial variability in terms of slope class, soil type and land use cover within a watershed. Each HRU is a homogeneous unit area of land use and soil properties to quantify the relative impact of vegetation, soil and climate changes. SWAT uses a modified Soil Conservation Service-Curve Number (SCS CN) technique to calculate runoff.

5 Sensitivity Analysis

In present study watershed was divided into 25 sub-basins, number of HRU's 105 based on land use land cover, slope and soil type. The model was calibrated on monthly basis by comparing simulated runoff and measured runoff values. Initially the model was simulated for 2000–2003 period. Prior to model calibration, identifying and quantifying sensitivity parameters is an important step to address the quantity and quality of model output data to given parameter sensitivity.

Sensitivity analysis was performed to assess the parameter sensitivity to hydrological response. Selected parameters were given ranking based on relative sensitive values to calibrate and validate model based on SWAT user's manual [7] parameter range. The most sensitive parameters are ALPHA BF, CN2, SOL K, EPCO, SOL AWC, GW DELAY and ESCO which are important to simulate runoff in a semi arid basin. Selection of these parameters is dependent on field data which change spatially across the watershed. Optimized parameter values belong to site specific in terms of local soils, land use land cover and climate. If any change occur in these field conditions, the values of sensitive parameters also need to be changed otherwise it affects the best model results. The present sensitive parameter values are taken based on local soils, land use land cover and semi arid climate conditions (Table 3).

Curve Number (CN): Curve number gives the runoff potential in an area considering soil group, soil condition and type of land use. CN values range from 1 to 100. As CN number increases the runoff also increases. Below table shows

Table 3 List of sensitive parameters, ranking based on relative sensitivity and optimal values for SWAT calibration

Number	Parameter	Default value	Description	Optimal value
1	ALPHA BF	0.048	Base floe alpha factor (days)	0.524
2	CN2	68–89	SCS runoff curve number for moisture condition	Table 4
3	SOL K	14.2	Saturated hydraulic conductivity	1.22
4	EPKO	0.95	Plant uptake compensation factor	0.885
5	SOL AWC	0.12	Available water capacity of the soil layer	1.25
6	GW DELAY	31	Ground water delay time (days)	2
7	ESCO	0	Soil evaporation compensation factor	0.01

Table 4 Curve numbers for landuse land cover classess in Jurala watershed

S. no	Land use	Hydrological soil group			
		A	B	C	D
1	Cropland	72	81	88	91
2	Double crop	62	71	88	91
3	Scrub land	36	60	73	79
4	Fallow land	74	83	88	90
5	Waste land	96	96	96	96
6	Degraded forest	45	66	77	83
7	Water	100	100	100	100
8	Deciduous forest	36	60	73	79
9	Settlements	89	92	94	95

different curve numbers used for land uses according to Indian conditions like conservative tillage practices and land cover conditions of the watershed [20] Table 4.

6 Model Performance

Watershed models are defined as powerful tools for simulating different hydrological processes and their effect on watershed processes and management like water and soil conservation. The accuracy of simulated data compared to observed values and constituent values can be established by quantitative statistics [21]. Nash-Sutcliffe Efficiency (NSE) and Percent Bias (PBIAS). The simulated values using SWAT and observed values for Jurala watershed were compared monthly to analyze temporal distribution for the 2000–2010. The goodness of fit is evaluated

by statistical measures using co-efficient of determination (R^2) and Nash and Sutcliffe [21] between simulated values and observed values. Generally model efficiency of simulated values is judged satisfactory if NSE > 0.50, RSR $\leq$ 0.70, PBIAS $\pm$ 25%. For calibration process identification of key parameters and parameter precision is needed. The range of NSE values is from 1 to negative 1. If value is zero, then the model result is no better than average annual runoff and between zero and one indicates model predictive ability as nearly true. If NSE value is one then it is said to be model is perfectly predicted simulated values with observed values.

7 Results and Discussion

The simulated runoff values for the year 2000–2003 were compared with measured runoff values for validation Fig. 5. Relationship between measured and simulated values is shown by the coefficient of determination R^2 as 0.72 and NSE as 0.84. According to the results SWAT simulated more realistic values (Fig. 6).

Results of the simulations shows that peak rate of runoff values are observed from August to October of each year. Annual rainfall of this area is 604 mm during monsoon season. Present study area has salt affected land of 34.22 km^2 of total area during 2005–2006 which is irrigated with canal water and grown only paddy. Area under not cultivation was 10.33 km^2 which is under barren area for the year 2005–2006. Makthal, Dharur, Dhanwada, and Ghatt talukas are affected with soil erosion. Most of the soils belong to hydrological group D in this area which is characterized with high runoff potential. They have very low infiltration rates during wet conditions and mainly constitute clay with high swelling potential. June and July months show low rates of runoff due to complete dry conditions of the top layers of

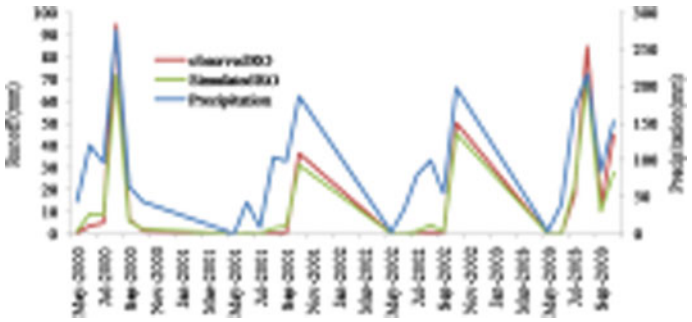

Fig. 5 Observed and simulated runoff values at Jurala watershed from 2000 to 2003

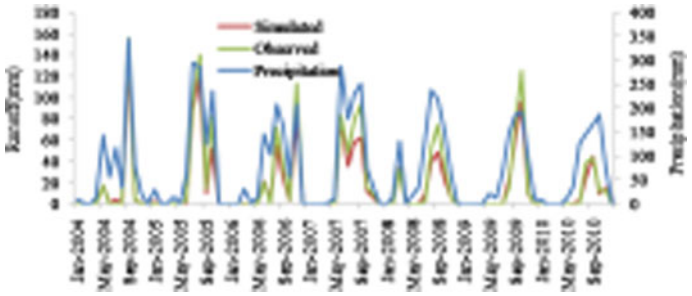

Fig. 6 Observed and simulated runoff values at Jurala watershed from 2004 to 2010

soil. Upon the saturation with water in the top layers from the month of August to October runoff volumes are high. This area is mainly under agriculture use. Dominant types of soils are shallow gravelly red soils next to calcareous moist clayey soils. Rate of runoff volume depends on type of land use and soil characteristics. Red sandy soils in Atmakur, Gadwal, Kothakota mandals are irrigated under Jurala project Table 5.

As irrigation from jurala project is assured paddy is main crop. Groundnut and sunflower are also grown under canal irrigation in some areas as commercial crops. Devarakadra, Dharur, Maldalkal mandals are majorly irrigated with tanks and rice is cultivated during kharif season and Bengal gram during rabi season. Red soils are dominant type with tank irrigation in present study area with rice grown in kharif and maize in rabi season. Black soils with tank irrigation spread in atmakur, devarakadra, dharur, ghatt, matkal, maldalkal mandals. Rice is grown in both Rabi and kharif season. Rain fed area constitutes 63% of total cropped area. These higher values reflect poor soil conservation practices. Agriculture and fallow land occupy highest percentage of land use may cause significant soil erosion. Soil erosion causes loss of soil nutrients making soil low fertile. Eroded sediment can absorb and transport pesticides, heavy metals, nitrogen, phosphates from agricultural runoff into downstream causing serious threat to aquatic life. Sub watershed wise land use land cover classes are shown in Table 6.

The temperatures are high during summer season which increases the rate of evapotranspiration. As major crop is rice which require more irrigation supply also adds increasing rate of evaporation. High rate of evapotranspiration is observed when compared with rate of runoff. Major area is under tube well irrigation which shows pre monsoon ground water levels are low during summer season. Sub watershed W04 shows low runoff and high infiltration volumes when compared with other sub watersheds. Agriculture is dominant land use and sandy loam soils that increases rate of infiltration thus reduces runoff. In watershed W05 deciduous

Table 5 Percentage area of soil classes of each sub watershed of Jurala watershed

WS	1	2	3	4	5	6	7	8	9	10
W01	0.00	0.00	0.00	2.40	0.00	61.46	0.00	13.12	0.00	23.02
W02	62.65	0.00	0.00	0.00	0.00	0.00	0.00	0.00	0.00	37.35
W03	18.53	0.00	0.00	0.00	0.00	4.66	0.00	33.57	0.00	43.25
W04	0.00	0.00	18.09	4.17	0.00	11.11	16.96	31.77	0.00	7.90
W05	0.11	0.00	0.00	2.61	0.00	0.00	20.20	77.07	0.00	0.00
W06	0.00	0.00	0.00	0.00	0.00	2.96	0.00	65.10	0.00	31.94
W07	31.90	7.55	0.00	6.83	0.00	0.00	0.00	11.40	0.00	42.32
W08	0.00	0.00	65.20	0.00	0.00	0.00	34.80	0.00	0.00	0.00
W09	0.33	45.00	0.00	0.00	0.00	20.17	0.00	0.00	0.00	34.49
W10	0.00	0.00	0.00	0.00	0.00	55.78	0.00	0.00	0.00	44.22
W11	0.00	0.00	20.29	0.00	0.00	0.00	35.28	44.43	0.00	0.00
W12	0.00	20.54	0.00	8.17	0.00	7.63	0.00	9.68	0.51	53.48
W13	0.00	0.00	0.00	0.56	0.00	0.31	0.00	59.47	0.00	39.66
W14	73.43	0.00	0.00	0.00	0.00	0.00	0.14	0.00	0.00	26.42
W15	0.00	0.00	0.00	10.93	0.00	59.62	0.00	0.00	0.00	29.46
W16	0.00	0.00	0.00	1.09	0.00	0.00	39.68	57.37	0.00	1.85
W17	0.00	0.00	0.00	0.00	0.00	22.26	0.00	37.92	0.00	39.92
W18	0.00	0.00	54.45	3.34	0.00	0.00	21.20	3.09	0.00	17.92
W19	46.02	4.57	0.00	0.00	0.00	0.00	0.00	0.00	0.00	49.41
W20	0.00	0.00	0.00	0.00	0.00	0.00	20.20	79.80	0.00	0.00
W21	0.00	0.00	0.00	0.00	0.00	19.20	0.00	49.48	0.00	31.31
W22	61.48	0.00	0.00	0.00	0.00	0.00	0.00	0.00	0.00	38.52
W23	0.46	0.00	0.00	0.66	0.91	7.92	56.22	0.00	0.00	33.84
W24	34.42	0.00	0.00	20.86	0.00	4.36	0.00	8.07	0.00	32.29
W25	0.00	62.84	0.00	0.00	0.00	10.52	0.00	0.00	0.00	26.64

Name of the soils: *1* loamy to clayey skeletal deep reddish brown soils; *2* moderately deep black clayey soils; *3* clayey to gravelly clayey moderately deep dark brown soils; *4* waterbodies; *5* moderately deep calcareous black soils; *6* loamy to gravelly clay deep dark reddish brown soils; *7* deep black clayey soils; *8* shallow gravelly red soils; *9* Settlements; *10* moderately deep calcareous moist clayey soils

forest, scrub forest and agriculture are major land uses that reduces amount of runoff. Soil infiltration rate is high in vegetated area. Sub watershed W12 also shows less runoff values as it receives low amount of rainfall. This watershed is irrigated with canal water and cultivated throughout year. Major crop in this area is rice. The sub watershed with clay soils results in high volumes of runoff water. Spatial variability of rainfall and runoff for each watershed is shown in Table 7, Fig. 7 for the period 2005–2009.

Table 6 Percentage area of LULC classes of sub watersheds of Jurala watershed (km^2)

Subwatershed	Kharif	Rabi	Kharif + rabi	Fallowland	Deciduous forest	Degraded forest	Wasteland	Water	Scrubland	Builtupland
W01	34.73	4.99	2.05	32.68	0.00	0.00	17.28	3.95	3.81	0.51
W02	16.12	0.28	0.21	39.1	0.00	0.00	38.31	0.85	4.76	0.38
W03	45.71	4.12	1.29	36.74	0.00	0.00	6.75	0.75	4.01	1.25
W04	34.99	8.18	13.47	26.93	0.00	0.00	6.24	2.19	6.75	1.25
W05	21.06	14.09	16.34	19.08	3.11	10.79	4.75	0.96	9.35	0.47
W06	45.51	1.01	0.79	44.64	0.00	0.00	8.18	0.05	0	0.39
W07	37.1	6.79	13.31	33.4	0.00	0.00	2.53	2.57	0.07	0.74
W08	39.55	6.65	6.08	31.17	0.00	0.00	11.23	0.82	3.51	0.98
W09	32.82	5.55	4.38	51.72	0.00	0.00	0.68	1.02	3.56	0.28
W10	14.17	9.42	23.25	37.07	0.00	0.00	5.91	4.81	3.92	1.44
W11	29.24	9.04	7.00	33.15	0.00	0.00	15.48	1.68	3.74	0.67
W12	35.47	11.76	18.12	16.95	0.00	0.00	1.15	6.02	7.09	3.45
W13	61.12	1.6	0.87	27.22	0.00	0.00	4.5	0.85	3.02	0.82
W14	40.91	0.18	0.23	37.29	0.00	0.00	16.99	0	4.11	0.29
W15	23.29	11.71	17.33	24.15	0.00	0.00	6.95	8.83	7.5	0.24
W16	40.31	3.36	1.18	37.18	0.98	0.45	5.95	0.86	8.89	0.84
W17	36.8	2.01	0.96	34.57	0.00	0.00	20.37	0.36	4.41	0.52
W18	32.01	5.97	12.55	36.29	0.00	0.00	2.18	1.81	8.44	0.75
W19	41.36	0.89	0.91	46.25	0.00	0.00	5.1	2.14	2.71	0.64
W20	38.91	12.47	11.14	27.14	0.00	0.23	2.28	0.61	6.17	0.93
W21	38.13	5.47	1.49	47.63	0.00	0.00	3.87	0.5	2.21	0.7
W22	39.12	3.04	5.33	39.5	0.00	0.00	8.88	1.06	2.62	0.46
W23	34.39	2.97	0.74	37.23	0.00	0.00	18.99	1.77	3.59	0.13

(continued)

Table 6 (continued)

Subwatershed	Kharif	Rabi	Kharif + rabi	Fallowland	Deciduous forest	Degraded forest	Wasteland	Water	Scrubland	Builtupland
W24	18.77	8.69	9.54	31.51	0.00	0.00	7.22	21.12	2.89	0.26
W25	51.29	3.53	12.8	23.27	0.00	0.00	0.73	3.06	5.04	0.36

Table 7 Runoff values of Jurala sub watersheds from 2005 to 2009

SW	RF2005	RO2005	RF2006	RO2006	RF2007	RO2007	RF2008	RO2008	RF2009	RO2009	Area (km^2)
W01	1045	299	942	210	1105	294	1012	181	730	198	31.88
W02	1020	338	804	238	904	278	934	210	710	253	40.04
W03	1203	285	1162	249	1206	262	1097	137	867	209	48.75
W04	1045	310	942	222	1105	307	1012	191	730	207	403.27
W05	1045	195	942	109	1105	161	1012	69	730	136	119.38
W06	1045	308	942	219	1105	305	1012	191	730	204	34.5
W07	1045	244	942	167	1105	226	1012	124	730	166	47.08
W08	1045	295	942	208	1105	290	1012	181	730	196	44.36
W09	1020	282	804	169	904	207	934	179	710	200	61.42
W10	1020	340	804	214	904	261	934	219	710	239	12.36
W11	1045	328	942	236	1105	329	1012	212	730	216	38
W12	1020	103	804	42	904	39	934	31	710	88	90.78
W13	1045	243	942	159	1105	224	1012	128	730	164	35.14
W14	1020	228	804	153	904	172	934	126	710	180	47.41
W15	1020	265	804	158	904	189	934	164	710	190	32.539
W16	1045	316	942	225	1105	314	1012	199	730	209	119.7
W17	1045	302	942	214	1105	299	1012	184	730	201	63.99
W18	1045	312	942	223	1105	310	1012	202	730	204	35.1
W19	1020	237	804	154	904	176	934	135	710	181	75.73
W20	1045	309	942	217	1105	303	1012	187	730	206	69.61
W21	1045	313	942	224	1105	311	1012	197	730	207	30.33
W22	1045	256	942	178	1105	239	1012	131	730	174	40.24
W23	1203	336	1162	296	1206	318	1097	179	867	240	135.16
W24	1045	387	942	294	1105	402	1012	244	730	261	167.4
W25	1020	213	804	120	904	142	934	121	710	159	32.75

RF Rainfall; *RO* Runoff

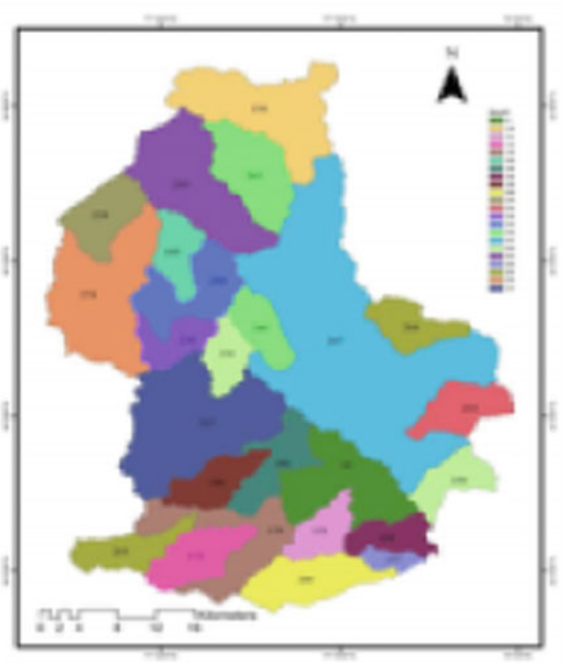

Fig. 7 Annual mean runoff values for each watershed from 2005 to 2009 of Jurala watershed

8 Conclusions

The Jurala watershed with an aggregated area of 1857 km^2 is simulated for runoff volumes. Results indicated that model could adequately anticipate the runoff volumes with NSE of 0.95. Temporal changes in runoff volumes at 25 sub watersheds were adequately simulated by model. For sustainable development appropriate land management practices need to be developed to control runoff volumes. Results showed that runoff values are more from agriculture and fallow land uses. This results in low infiltration rates of rainwater and decreased levels of ground water during pre monsoon and post monsoon (NRSA-WRIS). This area is mainly dependent on rainfall hence suitable soil conservation practices must be adapted. Furthermore bore well irrigation is more than canal and tank/well irrigation for agriculture. Lower annual rainfall and increasing rate of ground water with drawl further result in low fertility of soil and loss of water through evaporation process. Such conditions may aggravate soil erosion lowering soil nutrients and sedimentation of reservoirs in the downstream area. Efforts should be made to increase ground water levels by artificial recharging wells/tanks. Identifying key parameters to improve soil fertility and water holding capacity using organic manure, drip irrigation, sprinklers to conserve water and nutrients in soil is important. Treating

saline soils with suitable chemicals to decrease salt content can improve soil conditions. Wasteland and barren land reclamation policies are recommended to address this problem. The present study proves that the SWAT model can better predict hydrological parameters.

References

1. Abeysingha, N.S., Singh, M., Sehgal, V.K., Khann, M., Pathak, H., Jayakody, P., Srinivasan, R.: Assessment of water yield and evapotranspiration over 1985 to 2010 in the Gomti River basin in India using the SWAT model. Curr. Sci. **108**(12), 2202–2212 (2015)
2. Singh, P., Gupta, A., Singh, M.: Hydrological inferences from watershed analysis for water resource management using remote sensing and GIS techniques. Egypt. J. Remote Sens. Space Sci. **17**(2), 111–121 (2014)
3. Wani, S.P., Sreedevi, T.K., Reddy, T.V., Venkateswarlu, B., Prasad, C.S.: Community watersheds for improved livelihoods through consortium approach in drought prone rain-fed areas. J. Hydrol. Res. Dev. **23**, 55–77 (2008)
4. Shivhare, V., Goel, M.K., Singh, C.K.: Simulation of surface runoff for upper tapi sub catchment area (Burhanpur watershed) using swat. In: International Archives of the Photogrammetry, Remote Sensing and Spatial Information Sciences—ISPRS Archives, pp. 391–397 (2014)
5. Baker, T.J., Miller, S.N.: Using the Soil and Water Assessment Tool (SWAT) to assess land use impact on water resources in an East African watershed. J. Hydrol. **486**, 100–111 (2013)
6. Mishra, A., Froebrich, J., Gassman, P.W.: Evaluation of the SWAT model for assessing sediment control structures in a small watershed in India. Am. Soc. Agric. Biol. Eng. **50**(2), 469–478 (2007)
7. Neitsch, S., Arnold, J.: Overview of soil and water assessment tool (SWAT) model (2009)
8. Kumar, P., Joshi, V.: Applications of hydrological model SWAT on the upper watershed of river Subarnarekha with special reference to model performance and its evaluation. J. Basic Appl. Eng. Res. **2**(13), 1128–1134 (2003)
9. Malunjkar, V.S., Shinde, M.G., Ghotekar, S.S., Atre, A.A.: Estimation of surface runoff using SWAT model. Int. J. Invent. Eng. Sci. **3**(4), 12–15 (2015)
10. Melesse, A.M., Shih, S.F.: Spatially distributed storm runoff depth estimation using Landsat images and GIS. Comput. Electron. Agric. **37**(1–3), 173–183 (2003)
11. Srinivasan, R.S., Ramanarayanan, T.S., Arnold, J.G., Bednarz, S.T.: Large area hydrologic modeling and assessment part I: model development. J. Am. Water Resourc. Assoc. **34**(1), 73–89 (1998)
12. Karlberg, L., Garg, K.K., Barron, J., Wani, P.: Impacts of agricultural water interventions on farm income: an example from the Kothapally watershed India. Agric. Syst. **136**, 30–38 (2015)
13. Aouissi, J., Benabdallah, S., LiliChaba, Z., Cudennec, C.: Evaluation of potential evapotranspiration assessment methods for hydrological modelling with SWAT—Application in data-scarce rural Tunisia. Agric. Water Manage. **174**, 39–51 (2016)
14. Pechlivanidis, I.G., Jackson, B.M., Mcintyre, N.R., Wheater, H.S.: Catchment scale hydrological modelling: a review of model types, calibration approaches and uncertainty analysis methods in the context of recent developments in technology and applications. Global Nest J. **13**(3), 193–214 (2011)
15. White, K.L., Chaubey, I.: Sensitivity analysis, calibration, and validation for a multisite and multivariable SWAT model. J. Am. Water Resour. Assoc. **41**, 1077–1089 (2005)
16. Jha, M.K.: Evaluating hydrologic response of an agricultural watershed for watershed analysis. Water Resour. **3**, 604–617 (2011)

17. Sehgal, J.L., Sohan, L.P.: Sandy soils of India. Agropedology **2**, 1–14 (1992)
18. Satyavathi, P.L., Reddy, M.S.: Characteristics and classification of soils in Southern Telangana Zone of Andhra Pradesh. J. Res. ANGRAU **33**(2), 18–26 (2005)
19. Wang, G., Yang, H., Wang, L., Xu, Z., Xue, B.: Using the SWAT model to assess impacts of land use changes on runoff generation in headwaters. Hydrol. Process. **28**(3), 1032–1042 (2014)
20. Rao, B.S.P., Amminedu, E., Rao, J., Srinivas, N., Rao, N.B.: Run-off and flood estimation in Krishna River Delta using remote sensing and GIS. J. Ind. Geophys. Union **15**(2), 101–112 (2011)
21. Nash, J.E., Sutcliffe, J.V.: River flow forecasting through conceptual models part I—a discussion of principles. J. Hydrol. **10**(3), 282–290 (1970)

Chapter 27
Automatic Landing Site Detection for UAV Using Supervised Classification

Sudheer Kumar Nagothu and G. Anitha

Abstract UAVs plays an important role in day today life. They are used in a variety of applications like search and rescue, power line management etc. During operation of the UAV, sometimes it gets in operated and it has to be landed in the immediate neighborhood. The landing should occur in a proper location because improper landing or landing on the undesirable platform will cause UAV loss. Here a supervised classification is implemented for finding the landing site. In a populated area to land on rooftops a rule set is formed, such as length width, area etc. to locate the rooftop. Similarly train set of buildings, roads and lakes are composed to segregate the area, and an appropriate landing site for a UAV is determined. The results are compared with K nearest neighbor and Support Vector Machine algorithm.

Keywords Supervised classification · Landing · UAV

1 Introduction

Unmanned Aerial Vehicles plays an important role I a day to day life. They are used in many applications like monitoring power lines, wreckage search operations, smart farming etc. During UAV operation, it may be required to land the UAV in emergency situations. Proper landing site has to be determined instantly in order to avoid the loss of UAV. INS-GPS integrated system is also used to determine the precise landing location [1–11]. The normal landing sites in an emergency are roads, rooftops etc. In this paper in order to find the landing sites a set of rules are

S. K. Nagothu (✉) · G. Anitha
Division of Avionics, Department of Aerospace Engineering,
Anna University MIT campus, Chennai 600044, Tamilnadu, India
e-mail: sudheernagothu@gmail.com

G. Anitha
e-mail: anitha_g@annauniv.edu

P. J. Rao et al. (eds.), *Proceedings of International Conference on Remote Sensing for Disaster Management*, Springer Series in Geomechanics and Geoengineering,
https://doi.org/10.1007/978-3-319-77276-9_27

formed, or a supervised learning algorithm such as Support vector machine or a K nearest neighbor is implemented.

2 System Working

Various classification algorithms such as k means clustering, SVM is discussed here. Classifying an image using rules is also discussed. The image to be classified is given in Fig. 1. Here ENVI software is used to process the image [1].

2.1 Rule Based Classification

Here a set of rules is formulated in order to find a feature available in the image. The rules are formulated using various attributes such as spectral, spatial and texture etc. The rules to classify the image include band ratio, area, length, average pixel value etc. the rules to identify the buildings in an image are given in Fig. 2. With these rules it is possible to identify the building in an image.

Fig. 1 Image to be classified

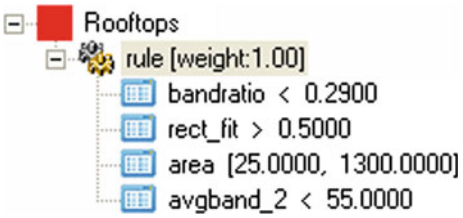

Fig. 2 Rules for building classification

2.2 Support Vector Machines

SVM is an algorithm motivated theoretically. It is developed from Statistical learning theory. It is applicable in many fields (text, bioinformatics, image recognition …) [12].

2.3 K Nearest Neighbor Classifier

The characteristics of each training set are considered as a different dimension in some space, and the characteristic observation value is coordinated in that dimension, so getting a set of points in space. The distance between the training set and entire range is measured. K closest data points to the new observation is picked.

The training set of buildings, road, trees and grass field is shown in Fig. 3a and b.

3 Results

3.1 Rule Based Classification Results

By using the rules defined for rooftop as shown in Fig. 1 the buildings available in the image can be identified as shown in Figs. 4 and 5.

The Fig. 5 shows the rooftops with boundaries. We can further modify the rules in order to get the accurate result.

3.2 Supervised Learning Classification Results

It is a Process of using training data to assign objects of unknown identity to one or more known features. Here we select various training sets such as roads, buildings, and trees etc. as shown in the figure which are assigned to a particular color.

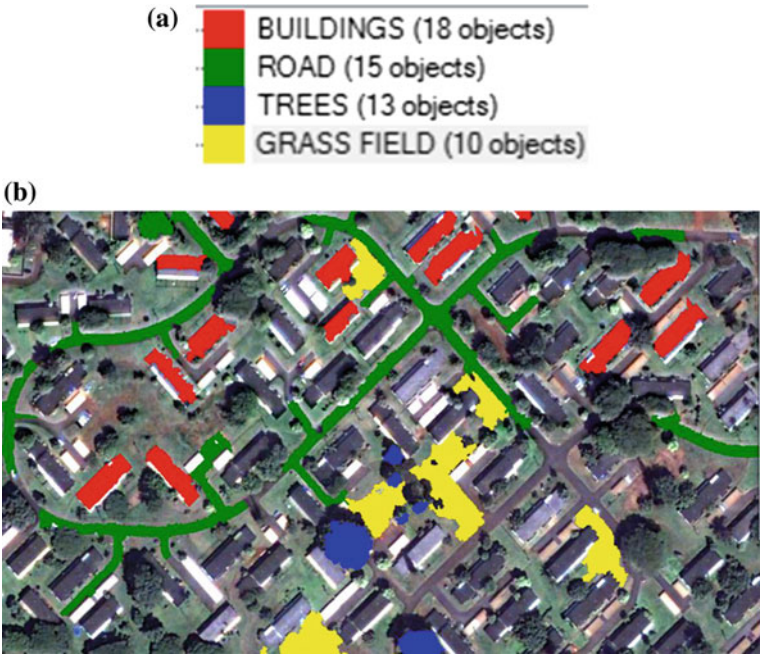

Fig. 3 **a** Number of objects of each feature for training set. **b** Training set for buildings, roads, trees

Fig. 4 Rule based classification result

Fig. 5 Rule based classification result with boundaries

After performing the supervised classification it is possible to get all the features available in the image corresponding to the training set given as shown in Fig. 6 and all the features are assigned with the indicated color as shown in Fig. 7.

Here we are assigning the buildings as known feature which are located with red color and all other features are unknown which is located with yellow color.

Fig. 6 Training set for buildings, roads, trees

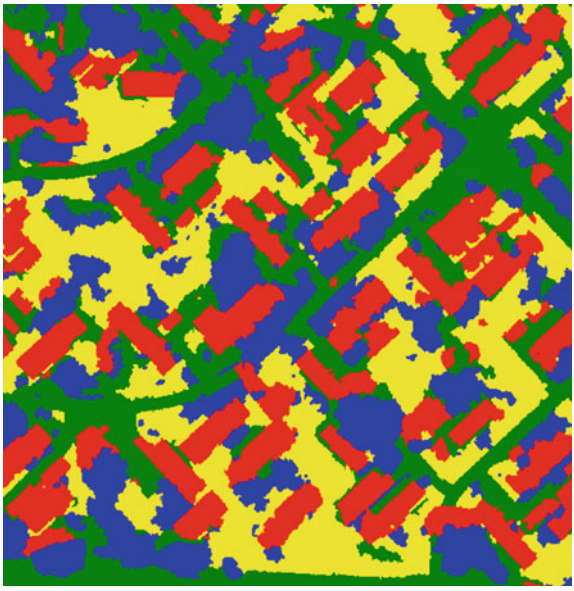

Fig. 7 Support vector machine result

Fig. 8 Training set of buildings (red)

As shown in Fig. 8 the known features (buildings) are compared with all other features using SVM and K nearest neighbor algorithms and the results were shown in Figs. 9 and 10.

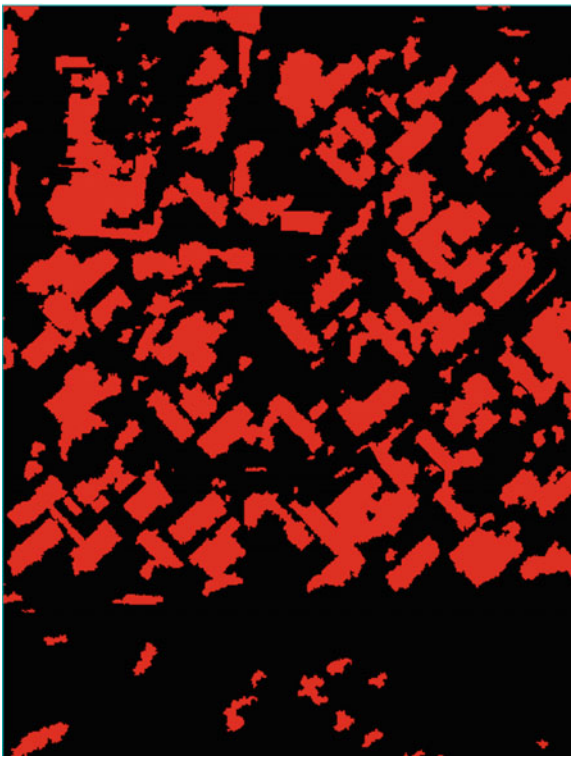

Fig. 9 K nearest neighbor result

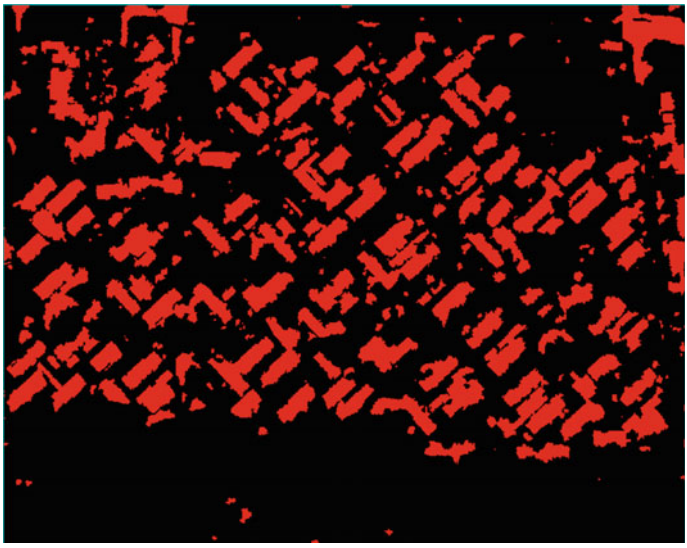

Fig. 10 Support vector machine result

4 Conclusion

Detecting an emergency landing site for a UAV using supervised learning is implemented. The determination of the landing site, such as buildings, roads is also done by defining the rules. The training set of buildings and roads is used to classify the images using SVM and k means clustering, and a proper landing site is found in emergency situations.

References

1. Nagothu, S.K., Kumar, O.P., Anitha, G.: Autonomous monitoring and attendance system using inertial navigation system and GPRS in predefined locations. In: 2014 3rd International Conference on Eco-friendly Computing and Communication Systems, Mangalore, pp. 261–265 (2014). https://doi.org/10.1109/eco-friendly.2014.60
2. Nagothu, S.K., Anitha, G., Annapantula, S.: Navigation aid for people (joggers and runners) in the unfamiliar urban environment using inertial navigation. In: 2014 Sixth International Conference on Advanced Computing (ICoAC), Chennai, pp. 216–219 (2014). https://doi.org/10.1109/icoac.2014.7229713
3. Nagothu, S.K., Kumar, O.P., Anitha, G.: GPS aided autonomous monitoring and attendance system. Procedia Comput. Sci. **87**, 99–104, ISSN 1877–0509 (2016). http://dx.doi.org/10.1016/j.procs.2016.05.133
4. Nagothu, S.K.: Weather based smart watering system using soil sensor and GSM. In: 2016 World Conference on Futuristic Trends in Research and Innovation for Social Welfare (Startup Conclave), Coimbatore, pp. 1–3 (2016). https://doi.org/10.1109/startup.2016.7583991
5. Rengarajan, M., Anitha, G.: Algorithm development and testing of low cost way point navigation system. Eng. Sci. Technol. Int. J. **3**(2), 411–414 (2013)
6. Nagothu, S.K.: Automated toll collection system using GPS and GPRS. In: 2016 International Conference on Communication and Signal Processing (ICCSP), Melmaruvathur, Tamilnadu, India, pp. 0651–0653 (2016). https://doi.org/10.1109/iccsp.2016.7754222
7. Rajaduraimanickam, K., Shanmugam, J., Anitha, G.: ADDR-GPS data fusion using Kalman filter algorithm. In: 24th Digital Avionics Systems Conference 2, vol. 2, 7pp. https://doi.org/10.1109/dasc.2005.1563447
8. Ramalingam, R., Anitha, G., Shanmugam, J.: Microelectromechnical systems inertial measurement unit error modelling and error analysis for low-cost strapdown inertial navigation system. Def. Sci. J. **59**(6), 650–658 (2009)
9. Nagothu, S.K., Anitha, G.: INS—GPS integrated aid to partially vision impaired people using Doppler sensor. In: 2016 3rd International Conference on Advanced Computing and Communication Systems (ICACCS), Coimbatore, pp. 1–4 (2016). https://doi.org/10.1109/icaccs.2016.7586386
10. Nagothu, S.K., Anitha, G.: Low-cost smart watering system in multi-soil and multi-crop environment using GPS and GPRS. In: Proceedings of the First International Conference on Computational Intelligence and Informatics Volume 507 of the series Advances in Intelligent Systems and Computing, pp 637–643, https://doi.org/10.1007/978-981-10-2471-9_61
11. Nagothu, S.K. Anitha, G.: INS-GPS enabled driving aid using Doppler sensor. In:2015 International Conference on Smart Sensors and Systems (IC-SSS), Bangalore, pp. 1–4 (2015). https://doi.org/10.1109/smartsens.2015.7873619
12. http://www.cs.columbia.edu/ ~ kathy/cs4701/documents/jason_svm_tutorial.pdf
13. www.math.le.ac.uk/people/ag153/homepage/KNN/OliverKNN_Talk.pdf
14. http://www.harrisgeospatial.com/portals/0/pdfs/envi/FXRuleBasedTutorial.pdf

Chapter 28
Evaluation of Risk Potential of Industries and Natural Hazards in the Wards of Hyderabad, India–AHP Multi-criteria Modeling Perspective Using Remote Sensing and GIS

Murali Krishna Gurram and Nooka Ratnam Kinthada

Abstract The study aimed at evaluating the combined risk potential of various industrial and natural factors at micro level in the municipal wards of Hyderabad (include 150 wards and 3 other administrative areas), which is the capital of the state of Telangana, India. High resolution imagery was used to precisely map the locations of different categories of industries (chemical, manufacturing and mining) and influence of natural factors (earth quakes, cyclones, floods, landslides and fire) across the Hyderabad city, whereas the GIS technology was used for the integrated assessment of all the spatial information layers thus extracted. Analytical Hierarchy Processing (AHP) multi-criteria modeling technique was used for the overall assessment and mapping of the risk potential comprehensively at the municipal ward level. The results indicate that majority of the wards (82 and 51 no's respectively) covering an area of 676.23 km^2 are susceptible to industrial risk, therefore categorized as 'Poor' and 'Very Poor'. In terms of the natural risk, 'flood' is found to be the most disastrous event which has high influence. Evaluation of combined risk due to natural factors indicate that out of total 153 ward areas 108 wards covering 620.08 km^2 are found with very low risk and rated as 'Excellent'. Only 17 wards are found with high risk potential, therefore rated as 'Very Poor' and 10 wards as 'Poor', which are mostly confined to the eastern and northern fringe parts of the city of Hyderabad.

Keywords Industrial · And natural risk · Risk potential evaluation
GIS and AHP multi-criteria modeling · GHMC

M. K. Gurram (✉)
GIS Technology and Applications, Xinthe Technologies Pvt. Ltd., Visakhapatnam, India
e-mail: murali.krishna.gurram@gmail.com

N. R. Kinthada
Department of Geology, School of Earth and Atmospheric Sciences, Adikavi Nannaya University, Rajamahendravaram, East Godavari (D.T.) 533105, Andhra Pradesh, India
e-mail: ratna_k12@yahoo.com

P. J. Rao et al. (eds.), *Proceedings of International Conference on Remote Sensing for Disaster Management*, Springer Series in Geomechanics and Geoengineering,
https://doi.org/10.1007/978-3-319-77276-9_28

1 Introduction

Rapid aggregation of population for better living opportunities coupled with industrialisation phenomenon are becoming complex and unmanageable scenarios as they increasingly pose a major risk to the socio-economic as well as environmental sustenance of the urban areas. Intensive anthropogenic activities are gradually transforming the overall structure of the society from predominantly rural to urban. This indeed resulting in major irreversible changes in production and consumption of natural resource and the way people interact with nature. The growing needs are certainly creating unwarranted pressure on the finite natural resource. Larry [9] states that while the urbanization creates new opportunities, the economic, social and demographic trends also lead to urban differences or issues. Alberti and Waddell [1] analysed the impact of urban development patterns on ecosystem dynamics and how they alter the ecological conditions (e.g. species composition). Lambin et al. [8] explained the environmental problems associated with urban sprawl. David [4] analysed the implications of population growth and urbanization on climate change due to greenhouse gas (GHG) emissions.

As urban areas strive to become the hubs of socio-economic growth centres, they also become hotspots for industrial development which are associated with various risk factors either in the form of pollution or industrial disastrous. The risk potential of the location depends on the type, scale and nature of the industry existed. At large, the risk impact would be gradual and is directly proportional to the distance from which the population located from the industry. On the other hand, as the process of urban growth continues in the form of a sprawl, it tends to ignore or alter the natural geographical setting or equilibrium of the location which in circumstantial occasions may turn to be a threat to the population manifested over there. Also the population of an urban area may susceptible to certain natural risks which are purely borne out of the locational disadvantage. Various researchers like Robinson and Herbert [14], Ali et al. [2], Condon [3], UNDP [19], TERI [18] studied the dynamics of urban environmental change in the context of sustainable development. In similar studies elsewhere, Jamal et al. [7] studied the urban environmental change in relation to the urban development.

Evaluation and mapping of risk potential due to both man made (i.e. different types of industries) and natural (floods, cyclones, earth quakes etc.) phenomena is essential for designing adequate mitigation and management strategies in urban areas as the consequences may prove to be highly disastrous. As per the guidelines documented by European Commission [6] specifies that the risk analysis is the process to comprehend the nature of risk to determine its impact.

In this backdrop this study was conducted on the municipal wards of Hyderabad city, which is a major metropolitan city in India facing challenges in its path to land-water, environmental and economic resource development. The study employs the Remote Sensing and GIS techniques for decision support coupled with a widely accepted Analytical Hierarchy Model (AHP) multi-criteria evaluation model

to assess the risk potential of the municipal wards due to industry and natural hazards. EPTRI [5], Sarath and Ramani [17] and Murali Krishna et al. [11, 12] studied the pollution scenario and their impact on Hyderabad.

2 About the Study Area

Hyderabad officially called as Greater Hyderabad Municipal Corporation (GHMC) comprises of 150 municipal wards and 3 administrative areas (BHEL, Osmania University and Cantonment) is geographically situated between 17° 19′ to 17° 30′ Northern latitudes and 78° 23′ to 78° 30′ eastern longitudes. Hyderabad is an urban district and capital of the State of Telangana in southern India, comprises twin cities of Hyderabad and Secunderabad. While GHMC extends in 625 km^2 of area Hyderabad metropolitan is extended in 1905 km^2 and is 5th largest metropolis in India. According to the estimates derived for 2015 based on Census 2011 data (68,09,970), GHMC has a population of 79,03,714 with an average density of 10,230 persons/km^2. The city extended on a hilly rugged undulated terrain lies on Deccan plateau with various lakes (Himayatsagar, Hussainsagar etc.) and small rivers (Musi, Esa etc.) and rivulets traversing through it. Floods and cyclones are the prominent natural hazards by which city get affected occasionally. As the city continued to expand in size and population, most of the lakes and river drainage courses have been encroached and now being subjected to heavy flooding during rain seasons. The city is only 500 km away from the coastline and is also subject to cyclonic storms originated in the Bay of Bengal. It also exposed to man-made hazards stemmed from heavy industries located across the city. The various types of risks to which the city is susceptible are euphemistically termed as ‘complex hazards’, which include a wide spectrum of risks [10]. Most of the urban problems emanates due to the catastrophes caused by these ‘complex hazards’ which eventually results in the breakdown of the socio-economic equilibrium.

3 Methodology for Evaluating and Mapping the Risk Potential

The methodology derived and implemented for the evaluation of industrial and natural hazard risk potential in the municipal wards of Greater Hyderabad Municipal Corporation (GHMC) can be applied elsewhere for evaluation and strategy development as applicable for similar urban scenarios.

In order to study the dynamics of urban phenomena in detail, high resolution satellite imagery, other thematic map and attribute data is used as inputs so that the trends can be identified and depicted at micro level. The results would then be taken

as a basis for deriving an efficient strategy plan for the effective mitigation of the risk. The methodology used for the study is mentioned below.

- Administrative units and high resolution satellite image are geo-referenced to use them as the base maps for generating input thematic maps. These geo-referenced inputs are assigned with the real world coordinate system (WGS84 projection) to make them ready for vector data extraction.
- Digital Elevation Model (DEM) is generated using IRS-P5 CartoSAT-1 data and used for analyzing the elevation and slope aspects especially for mapping the low lying zones of the study area.
- Population distribution was mapped to see the influence of industries and natural hazard risk in each location being considered.
- As the study requires an in-depth understanding of physical and natural aspects of the urban area with regard to risk potential, it seeks to probe the combined influence of these parameters at ward level. Risk potential due to industries on the municipal wards of Hyderabad is assessed based on the proximity of the population to certain types of industries located.
- Since the study necessitates a multi-criteria approach which evaluates the scenarios effectively, the analysis was carried out within the framework of AHP and GIS. A structure for parameterization and integration of AHP and GIS framework is conceived using the themes generated. Exceptional vigilance is drawn into the model and analytics employed.
- The combination is also used as decision support tool to calculate the weights of each factor based on several alternatives. A weighted average criterion is engaged and the composite weights computed are integrated to produce map themes representing sustainability scores of wards.

The model draws its inputs from the risk vulnerability assessment for integration and finally arriving at a theme which rates the wards according to their vulnerability to various types of risks. The diversified risk indices taken into account along with their AHP integration weights are Industrial Risk (0.575) and Natural Hazard Risk (0.425). Final risk index map output thus generated can be used to propose a solution with recommendations.

4 Results

The results derived from the study suggest that the stake holders, government and non-government agencies should adopt the best practices for the mitigation and sustainable development of GHMC. The research work utilizes the power of GIS and Remote Sensing technology for its fullest potential by mapping and modelling various environmental, industrial, demographic and topographical parameters to arrive at logical conclusions for the risk assessment at micro level in GHMC.

4.1 GIS-AHP Multi-criteria Analysis

The Analytic Hierarchy Process (AHP) is a multi-criteria decision support tool which can be employed to solve complex decision problems related to the real-world. Initially developed by Satty [15, 16], AHP integrates the real-world phenomena by decomposing it into multiple hierarchical structures of objectives, criteria, subcriteria etc. and alternatives. Murali Krishna et al. [13] successfully implemented AHP multi-criteria evaluation using GIS especially for environmental sustainability mapping of Hyderabad. The pertinent outcomes are derived using a set of comparisons and the process is called pairwise comparison. The pairwise comparison helps obtaining the weights required to indicate the importance of decision criteria. Simultaneously, the relative performance measures the alternatives with regard to each individual decision criterion. Consistency Index (C.I.) which is one of the components of AHP provides a mechanism for improving consistency of comparison.

Pairwise comparison method is used to determine the relative importance of each parameter used in the study. Assigning appropriate weights to all parameters, indices, sub-criteria and criteria (Table 1) ensures relative importance of factors which compensates to arrive at a decision. This helps in simulating different real-world scenarios where adjustments are to be made to accommodate tough choices to make an informed decision to use a right alternative among the choices existed.

4.2 Industrial Risk

It is noticed that, industries are the main source of pollution in Hyderabad which contribute for the major part of air, water, noise and solid waste pollution and deteriorates the environmental quality and sustainability of urban areas. The risk vulnerability of areas and population mostly depends on the proximity to industry. The risk vulnerability and intensity on the population living nearby industry varies depending on the type of industry. In view of this, the section emphasizes to evaluate the intensities and extent of risk posed by various types of industries located in different parts of Hyderabad. Though there are many types of industries existed, for the sake of analysis convenience all the industries have been grouped into 3 major categories such as, chemical, manufacturing and mining. The following sections analyze the aspects of risk posed by these industries to population

Table 1 AHP hierarchy criteria for risk evaluation

Risk Vulnerability					
Risk due to industries			Risk due to natural hazards		
Chemical	Manufacturing	Mining	Earth quakes	Cyclones	Floods

and map the wards according to their extent and exposure level. The risk vulnerability classes are derived from the inputs taken from greencleanguide.com where the regulations for green belt development around industries in India are mentioned.

4.2.1 Risk Due to Chemical Industries

The results obtained from the analysis to assess the risk vulnerability of wards due to its proximity to industries categorized as chemical is shown in Fig. 1. Various classes mapped based on the proximity or distance radius measured in kilometer are 'Very Poor' (<0.250), 'Poor' (0.251–0.500), 'Moderately Good' (0.501–1.00), 'Good' (1.001–2.00) and 'Excellent' (>=2.001).

It is noted that majority of the wards (112) covering an area of 449 km^2 are found in Excellent category showing very low susceptibility. Only 13 wards with 105.24 km^2 area and 15 wards with 85.30 km^2 area are found in 'Very Poor' and 'Poor' classes respectively. Around 3 wards are found in Good and the remaining 9 wards are in 'Moderately Good' category. The wards found in 'Very Poor' or 'Poor' category are in fact located very close to the chemical industries i.e., within the distance radius of <0.250 km and 0.250–0.500 km. These wards are especially located in the industrial zones like, Jeedimetla, Bollarum etc.

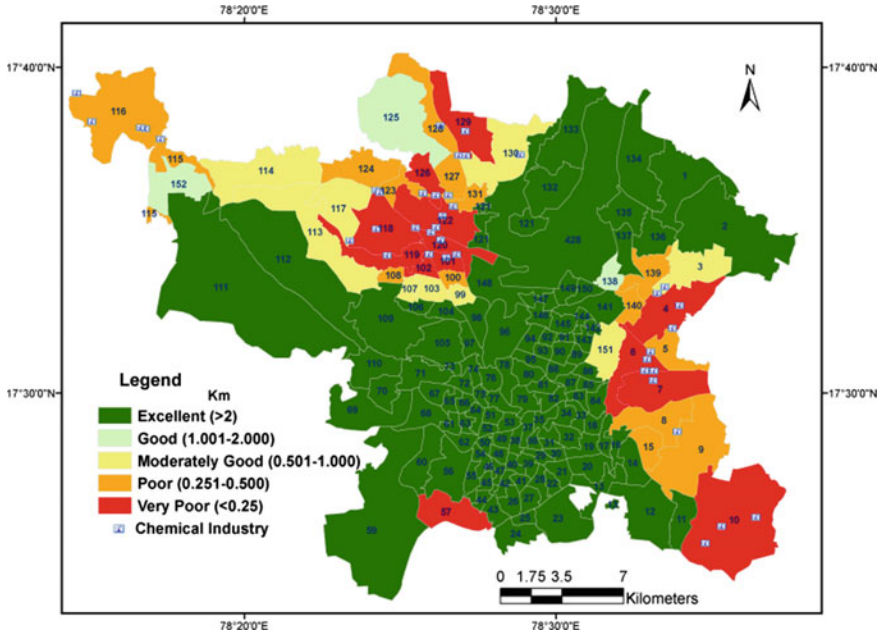

Fig. 1 Risk due to proximity to chemical industry

4.2.2 Risk Due to Manufacturing Industries

Risk vulnerability of wards is assessed due to their proximity to nearest manufacturing industries in kilometer is identified and mapped (Fig. 2). The classes thus mapped are 'Very Poor' (<0.150), 'Poor' (0.151–0.300), 'Moderately Good' (0.301–0.600), 'Good' (0.601–1.00) and 'Excellent' (>=1.001). It is noticed that majority wards (107) covering 478.06 km^2 of area are found in Excellent category indicating very low susceptibility to risk. Around 20 wards covering 108.31 km^2 and 11 wards covering 50.98 km^2 of area are found in 'Good' and 'Moderately Good' categories, respectively. Only 9 wards are found in 'Poor' and 5 wards are in 'Very Poor' category. The results indicate risk due to manufacturing industry is very minimal as compared to chemical industry.

4.2.3 Risk Due to Mining Industry

Risk vulnerability of wards due to its proximity to mining industry is analyzed spatially and mapped (Fig. 3). The classes are derived based on the proximity or distance radius measured in kilometer to the mining industry. The classes are 'Very Poor' (<0.500), 'Poor' (0.501–0.800), 'Moderately Good' (0.801–1.500), 'Good' (1.500–3.000) and 'Excellent' (>=3.001). Majority of the wards (146) having an area of 658.66 km^2 are found in 'Excellent' category indicating very low risk

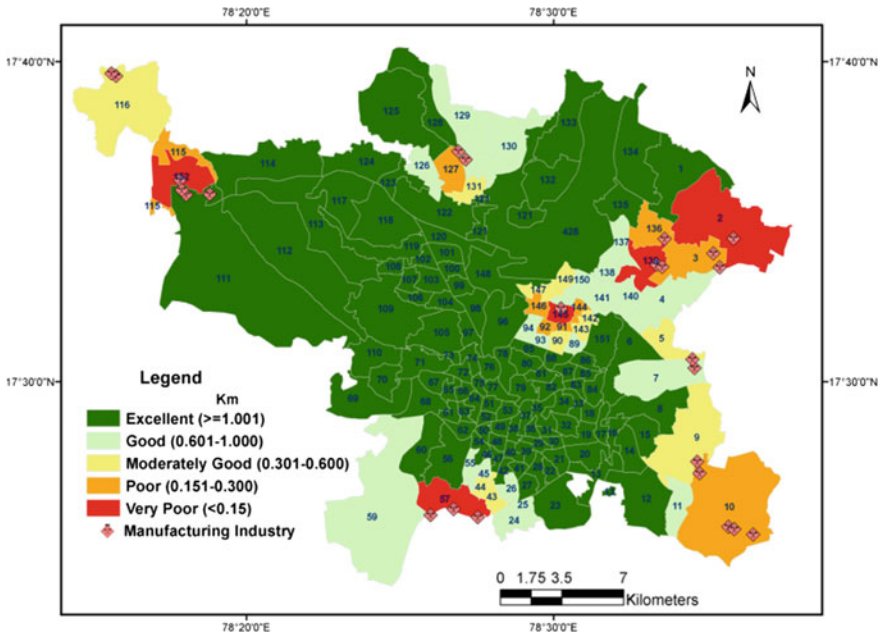

Fig. 2 Risk due to proximity to manufacturing industry

vulnerability. This is also because of the reason that most of the mining activities within GHMC are already completed. Only 2 wards are found in 'Very Poor' category.

4.3 Natural Hazard Risk

Natural hazards are the events which occur due to the severe or extreme climatic disturbances in a region. Natural hazards become natural disasters when they cause damage to lives and livelihood of the people. Depending on the type of topography and climate that they experience natural hazards are common everywhere in the world but they occur in many forms. However, the study consideration only some of those eventual risks like earthquakes, cyclones, floods etc. to which the people of Hyderabad may susceptible to. The following sections in detail analyses the risks due to natural hazards.

4.3.1 Risk Due to Earthquakes

The various seismological studies and geological reports confirm that Hyderabad region lies on the Deccan Plateau of India is less prone to earthquakes. The seismic

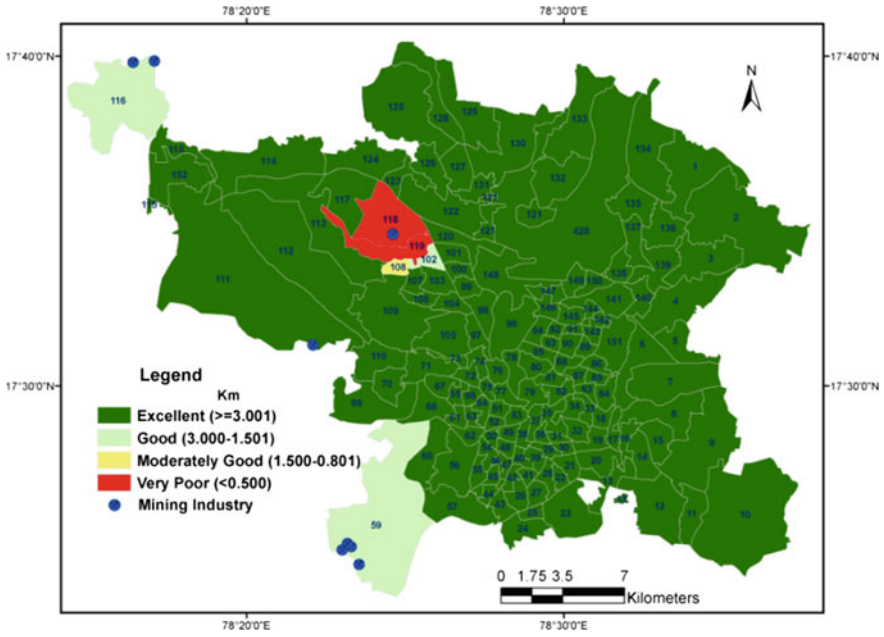

Fig. 3 Risk due to proximity to mining industry

map published by National Geophysical Research Institute (NGRI) is taken as a reference. The map shows Hyderabad under Zone—II which is classified as 'Least Active' and is prone to very less intensive earthquakes of magnitude only <4.5 on Richter scale. Hence, for integrated risk evaluation, the study classifies all the wards of Hyderabad in 'Good' category.

4.3.2 Risk Due to Cyclones

Being situated 500 km away from the coastline, Hyderabad is likely to susceptible to cyclonic storms which may arise in the Bay of Bengal from time to time. According to the map published by India Metrological Department, (IMD), Govt. of India, Hyderabad region comes under the High Damage Risk Zone.

4.3.3 Risk Due to Floods

Hyderabad experiences heavy rains during south-west monsoon season (June–October) and most of the low lying areas get affected by floods. Population, especially living in slums where there is no proper storm water drainage system is vulnerable to flood risk. Based on the percent area vulnerable to floods the wards have been classified into 5 classes, where 'Very High Risk' indicates high vulnerability and 'Very Low Risk' indicates very low vulnerability. Figure 4 shows the wards classified according to their vulnerability to flood risk. Most of the wards are classified into 'Very Low Risk'. Four wards (w.no. 13, 17, 18, 73) near old city are identified with 'Very High Risk', while 13 wards are found with 'High Risk'.

5 Discussion

The risk potential evaluation in the municipal wards of Hyderabad indicates varying trend across the wards. The wards characterised with high risk potential requires immediate attention from the administrative authorities to mitigate the risk by implementing necessary measures as mandatory. The risk index maps generated highlights the levels of risk potential in wards and helps as decision tools for taking adaptive measures. The thematic information can also be used by the rescue teams to precisely identify those locations for intervention on priority basis and plan their actions effectively during any event.

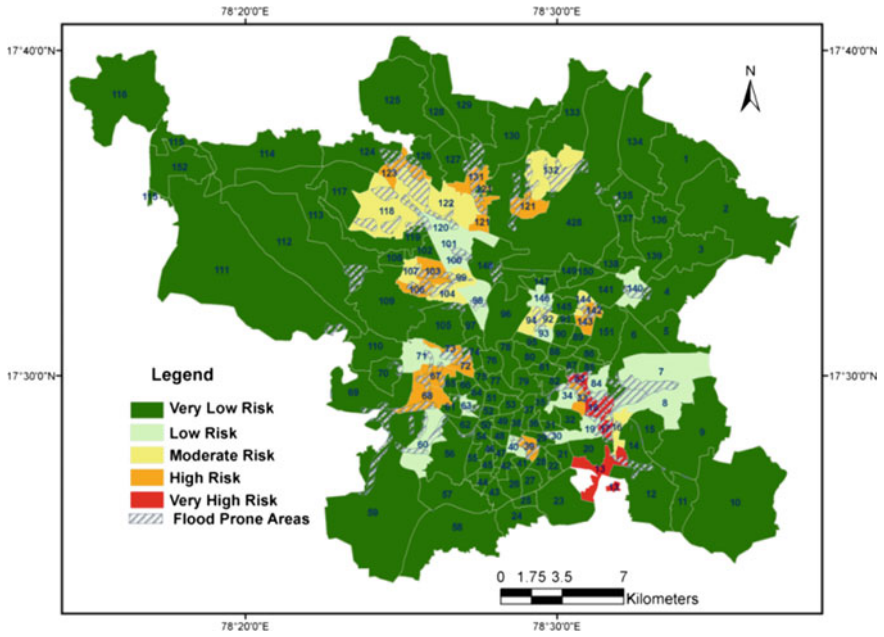

Fig. 4 Wards classified according to their vulnerability to flood risk

5.1 Industrial Risk Index

The industrial risk index includes the risk sub-indices that are grouped based on the nature of the industry. This includes Chemical Industries (0.633), Mining Industry (0.260) and Manufacturing Industries (0.106). Figure 5 shows majority of wards (82 and 51 respectively) covering an area of 676.23 km^2 are found in 'Poor' and 'Very Poor' industrial risk category. Only 17 wards are found in 'Moderately Good' category, while 1 ward (w.no. 46) is found in 'Good' class. The overall risk scenario indicates very alarming picture of the wards in GHMC, which needs immediate attention.

5.2 Natural Hazard Risk Index

This index takes the various natural hazards into account such as landslides (0.043), Fire (0.064), Cyclone (0.184), Floods (0.278) and Earth quakes (0.429). Flood is the major risk found to be active among all. The integrated analysis resulted in overall natural hazard risk map (Fig. 6), which indicates 108 wards covering 620.08 km^2 in 'Excellent' category with very low risk. The remaining 17 and 10

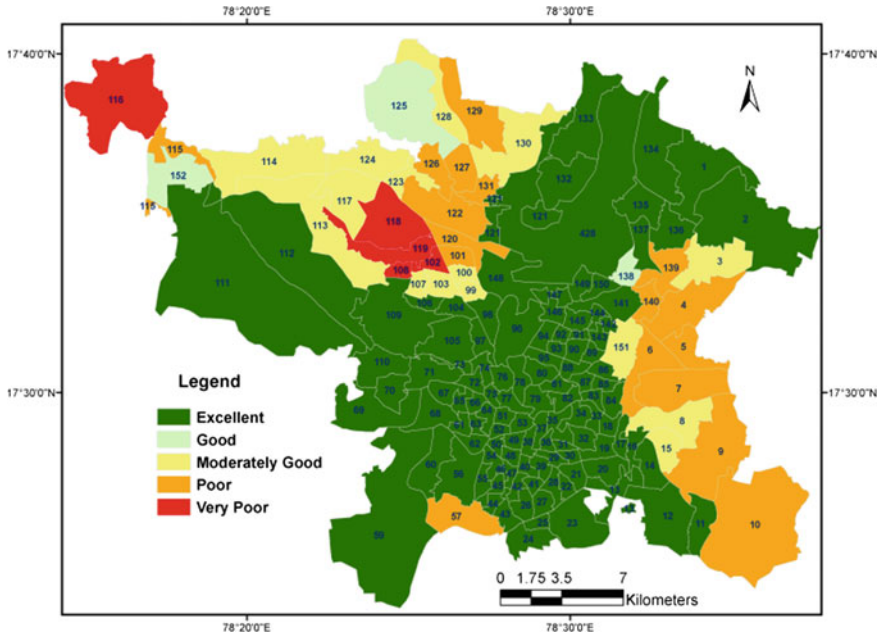

Fig. 5 Industrial risk map

each in 'Very Poor' and 'Poor' category which are mostly confined to the eastern and northern fringe parts of the city.

The integrated risk map (Fig. 7) shows overall risk vulnerability scenario across the wards of GHMC which takes into account the diversified risk emanating due to various industrial and natural aspects. The composite risk vulnerability map (Fig. 7) shows majority wards (95) covering 441.19 $km^2$of area with 45,40,750 of population comes under 'Excellent' category indicating very low risk vulnerability. Around 29 wards having 15,77,568 population with 111.35 km^2 are found under 'Good' category with relatively low or no risk. Around 16 wards are found under 'Moderately Good' category indicating low susceptibility to risk. These wards are mostly located in the eastern and northern fringe areas of the city having a population of 10,35,939 and extended in 138.42 km^2 of area. A total of 6 wards (w.no. 7, 8, 100, 101, 120 and 140) are found in 'Poor' category indicating high susceptibility to risk. These wards are having 3,34,457 of population and extended in an area of 26.64 km^2. The remaining 7 wards (w.no. 99, 103, 107, 118, 122, 123, and 131) especially wards surrounding Jeedimetla, Bollaram etc. industrial areas are found in 'Very Poor' category with high vulnerability to both industrial and natural hazard risk. These wards are having a population of 3,93,487 population and covering an area of 28.87 km^2.

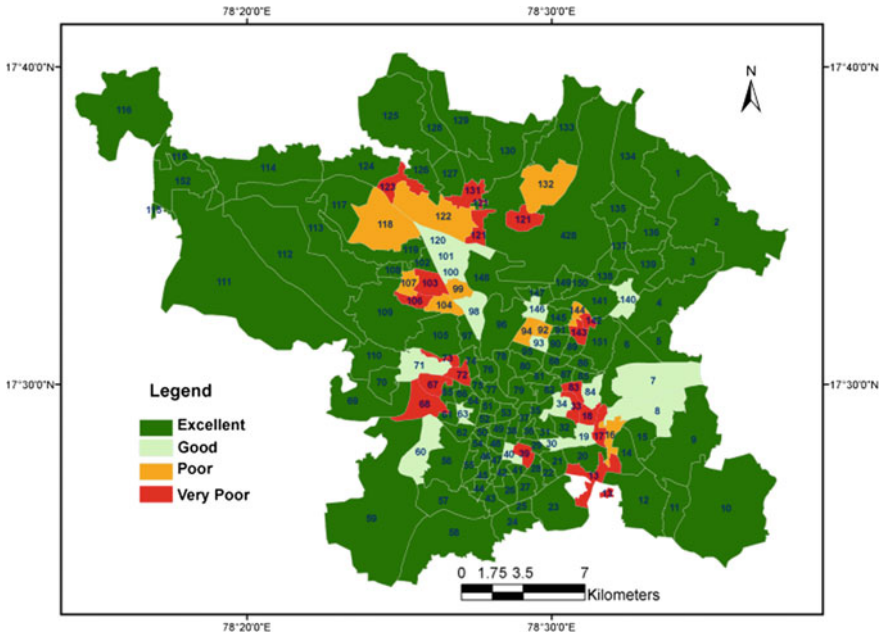

Fig. 6 Natural hazard risk map

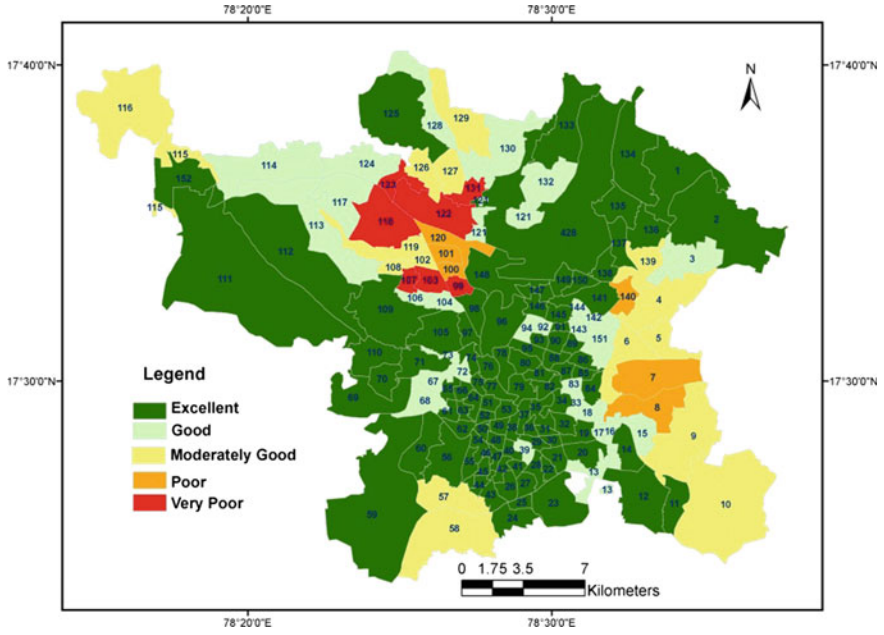

Fig. 7 Overall risk vulnerability map of the wards of GHMC

6 Conclusions

The integrated risk vulnerability rating is the result of diversified risk aspects considered of type industrial and natural. Increase in air pollution levels is mainly due to rapid growth in industrial activity and vehicular population. The results show majority wards in either 'Excellent (95 wards) or 'Good' (29 wards) with a total population of 61,18,318 and area 552.54 km^2 with no or low risk. At the same time the analysis also identified wards (13 no's) susceptible to high or very high risk and categorised them as 'Good' and 'Excellent' respectively. These wards cover a total area of 55.51 km^2 and have a population of 7,27,944. These wards are mostly found around the industrial pockets of GHMC, where environmental risk is most imminent. The methodology employed helps analyzing the characteristics of various risk parameters at micro level and identifies the level and extent of risk potential in the municipal wards of Hyderabad. The diversified risk indices take into account the various heterogeneous risk parameters of different forms and sources. The map outcomes essentially help in formulating strategies to mitigate the risk with a short and long term perspectives. The multi-criteria evaluation method developed for the study is flexible to include any other relevant parameters for further analysis which have direct or indirect influence on the urban environment at micro or macro level.

References

1. Alberti, M., Waddell, P.: An integrated urban development and ecological simulation model. Integr. Assess **1**, 215–227 (2000)
2. Ali, M., Emch, M., Donnay, J.P., Yunus, M., Sack, R.B.: The spatial epidemiology of Cholera in an endemic area of Bangladesh. Soc. Sci. Med. **55**(6), 1015–1024 (2002)
3. Condon, P.M.: Design Charrettes for Sustainable Communities. Island Press, Washington, DC (2007)
4. David, S.: The implications of population growth and urbanization for climate change. Envi. Urbanization **21**(2), 545–567 (2009)
5. EPTRI: Integrated environmental strategies (IES) study for city of Hyderabad, India, pp. 1–380 (2005). Source: http://www.jnias.in/cpipweb/4.IES%20Study%20for%20Hyd%20City.pdf
6. European Commission: Staff Working Paper on Risk Assessment and Mapping Guidelines for Disaster Management. European Commission, Brussels (2010)
7. Jamal, M., Asghar, Z., Omid, M.: Urban sprawl pattern and effective factors on them: the case of urmia city, Iran. J. Urban Reg. Anal. **4**(1), 77–89 (2012)
8. Lambin, E.F., Rounsevell, M.D.A., Geist, H.J.: Are agricultural land use models able to predict changes in land use intensity? Agric. Ecosyst. Envi. **82**, 321–331 (2000)
9. Larry, S.B.: How economic, social and demographic trends are creating new sources of urban difference in canada, new urban divide. Centre Urban Commun. Stud. Res. Bul. **33**, 4 (2007)
10. Mancebo, F.: Natural hazards and urban policies in Mexico City. J. Alpine Res. **95**(2), 108–118 (2007)
11. Murali Krishna, G., Deekshatulu, B.L., Nooka Ratnam, K.: Assessment of water quality scenario in parts of Hyderabad urban agglomeration, India—AHP-GIS modelling perspective. Int. J. Civil Environ. Eng. **35**(2), 1147–1157 (2013)

12. Murali Krishna, G.M., Deekshatulu, B.L., Ratnam, K.N.: Air quality scenario evaluation in the municipal wards of Hyderabad, A.P., India—AHP Based GIS multi-criteria modelling perspective. Int. J. Urban Plan. Trans. **27**(2), 1116–1125 (2013)
13. Murali Krishna, G., Deekshatulu, B.L., Nooka Ratnam, K.: Urban environmental quality assessment at ward level using AHP based GIS multi-criteria modeling—a study on Hyderabad City, India. Asian J. Geoinf. **15**(3), 16–29 (2015)
14. Robinson, J., Herbert, D.: Integrating climate change and sustainable development. Int. J. of Global Envi Issues **1**(2), 130–148 (2001)
15. Saaty, T.L.: The analytic hierarchy process. Polytechnic University of Hochiminh city, Vietnam McGraw-Hill, New York (1980)
16. Saaty, T.L.: Time dependent decision-making; dynamic priorities in AHP/ANP: generalizing from points to functions and real to complex variables. Math. Comp. Model. **46**, 860–891 (2007)
17. Sarath, G.K., Ramani, V.: Source emissions and health impacts of urban air pollution in Hyderabad. India Air Qual. Atmos. Health **1**(1) (2013)
18. TERI: An exploration of sustainability in the provision of basic urban services in Indian cities (2009)
19. UNDP: Proposed environment. In: Sustainability Enhancements to UNDP's Programme and Project Management Policies and Procedures (POPP), Draft (2009)

Chapter 29
A Review on Role of Telemedicine in Disaster Management: A Pharmacist Perspective

Anusha Nutakki, Vijay Kotra, Sathish Kumar Konidala and Nagarjuna Babu Etukuri

Abstract Telemedicine is the use of electronic means of telecommunication like teleconference, phone or email consultation to transfer the medical data from one place to other place. In India nearly 75% of people live in rural villages. More than 600 million people in rural India lack access to basic health care facilities. Because of poor facilities in health care centers and also people travel to speciality hospitals in cities for their treatment very few doctors are available in the rural areas. More over if any disaster occurs in such regions there is an urgent need for the medicines and specialists. In such cases this telemedicine plays an important tool for diagnosis and treatment of patients who are badly affected and not possible to transfer them. This also helps to create awareness for the people affected by disasters. This helps in reducing the consultation time of specialists. Thus this review focuses on the importance of telemedicine especially in the rural areas as a valuable source for diagnosis and treatment during disasters.

Keywords Telemedicine · Disasters · Rural areas

A. Nutakki (✉) · V. Kotra · S. K. Konidala · N. B. Etukuri
University College of Pharmaceutical Sciences, Acharya Nagarjuna University, Nagarjuna Nagar, Guntur 522510, India
e-mail: nuth.anu@gmail.com

V. Kotra
e-mail: vijai.kotra@gmail.com

S. K. Konidala
e-mail: sathishkonidala@gmail.com

N. B. Etukuri
e-mail: etukurinagarjuna@gmail.com

P. J. Rao et al. (eds.), *Proceedings of International Conference on Remote Sensing for Disaster Management*, Springer Series in Geomechanics and Geoengineering,
https://doi.org/10.1007/978-3-319-77276-9_29

1 Introduction

Disaster is a serious disruption which causes injuries or some critical health impact in a relatively short period of time. In such cases one effective approach for diagnosis and treatment with in short period of time is telemedicine. Telemedicine is the transfer of medical information through the phone or the Internet or other networks for consulting, diagnosis, treatment and prevention of diseases or injuries. It also helps for educating health providers about advancements in health and research. This telemedicine can be simple like two doctors discussing a health issue over the telephone. It seems to be also complex involving the use of satellite technology and some other equipment for consultation between specialists of medicine in two different regions. It is helpful in reducing the consultation time of a specialist especially in the rural areas and in the regions where the transfer of patients is impossible. In India about 68.8% of the people live in rural areas and more than six hundred million people in these areas do not have least health facilities also. Most of the patients in these rural areas need to travel distances to have access to quality medical care and for medical specialist consultation. In this view telemedicine provides very fast patient data transmission regarding consultation by a specialist, diagnosis and treatment of a disease or illness, imparting information to the patients for rehabilitation and to improve their health status. So this can reduce the time of travel, patient expenses, effective use of resources, increased quality in diagnosis and therapy, easy consultation of emergency and critical cases and improved patient awareness and education or training purpose. Therefore telemedicine is the promising tool for delivering safe and quality medicine very efficiently.

2 The Telemedicine

Telemedicine unit mainly consists of four systems

- The bio-signal acquisition system
- For capturing of image a digital camera
- Personal computer
- A communication system like telephone or satellite system.

The bio-signals from the biosignal acquisition system are collected from the patient and are transmitted to the Base unit, and biosignals includes:

- Electrocardiogram (ECG)
- Oxygen Saturation
- Heart Rate (HR)
- Blood Pressure (BP)
- Temperature
- Respiration.

The choice of personal computer is dependent on the application of telemedicine. This telemedicine unit can also be used to collect and transfer patient images to the base unit. The telemedicine user need to connect the patient and bio signal monitor and the personal computer is to be switched on. As the telemedicine unit is automatic the personal computer connects to the base unit [1].

2.1 Base Unit

The base unit is nothing but the doctors unit. The incoming signals are displayed in the personal computer of the base unit. A portable personal computer with global system or telephone service for communication is used if the base unit of a doctor is out of the hospital area. The personal computer within the hospital area can be connected to the hospital information network with telephone system.

2.2 Telemedicine Services

The telemedicine system services can be categorized into two types:

- Audio
- Video

Audio service can be by using telephone either offline. E.g. the doctor sends the heart beat of a patient and records by the device analyze and thus gives the report, or online. E.g. the voice of the patient is directly sent to the doctor for the result.

3 Importance of Telemedicine in Disasters

Initially telemedicine system is used in clinical care for diagnosis, treatment, and training, but gradually this has played an important role in disaster management. This can be used before the disaster, at the time of disaster and rehabilitation. In these three steps the telemedicine can be used for effective treatment [1].

Before the disaster: It mainly emphasizes on the prevention of disasters.
After the disaster: With in short span of time after the disaster.
Rehabilitation: The induced effects of disaster after some period of time.

By this telemedicine it is possible to share the medical knowledge which is very much essential in some critical cases and during disaster emergencies where the specialists are unavailable in many rural and remote areas.

The first application of this telemedicine was in 1985, during Mexico City earthquake by the National Air and Space (NASA) that had destroyed all terrestrial telecommunications infrastructure. It became possible to transfer audio to international rescue organizations through Advanced Communications Satellite (ATS-3).

In India telemedicine started at Apollo Arragonda Hospital in Andhra Pradesh in 2000 [4]. By today more than 500 telemedicine centers were linked with about 50 specialist hospitals. Department of Information Technology (DIT), Ministry of communication and IT (MCIT), Government of India providing Telemedicine and Tele-health Education facilities in Kerala; 3 mobile telemedicine units to cater rural population of Kerala and TN focusing on early detection and preventive medicine. Government of India is aiming to implement e health. The steering committee of planning commission for the 12th plan also suggested that all district hospitals and primary health centers and sub-centers are to be connected with telemedicine or similar audiovisual media to encourage M-health (to reach the remote corners of the country [3]. Several projects of telemedicine have been introduced by different organizations like The Department of Information Technology-Government of India (DIT), Indian Space Research Organization (ISRO), Ministry of Health and Family welfare-Government of India, state governments, medical institutes in both the public and the private sector. Thus in India this telemedicine system is growing faster opening new hope for the implementation of this system in disaster management. By employing this tool an unexpected incident which causes heavy loss to public health can be managed.

Advantages of telemedicine:

- Improved quality of health
- Reduction of health care costs and consultation time
- Prevention of medical errors
- Increased administrative efficiencies and
- Decreased paperwork
- Early detection of outbreak of infectious diseases in and around the country
- Improved chronic disease management.

Applications of telemedicine:

- Consultation through various means like telephone, E-mail, or video conferencing.
- Tele-education for development of research, science and technology.
- During Medical emergency in critical situations and in disasters access to medical care within a short period of time.
- Tele-surgery which can reduce costs, waiting time, travelling, etc.
- Telemedicine has applications in different medical specialties as telecardiology, telepathology, telegenetics, teleoncology, teleradiology etc.
- For exchange of Health information, Teletraining, Telemonitoring and Telesupport.

4 Issues and Challenges

Though this telemedicine system is advantageous yet there are some challenges. This includes some difficulties in the introduction of new technologies [2], technical considerations regarding software's etc., unknown handling of equipment and computers by untrained personnel, high initial investment, acceptance by the public because of lack of awareness, some unresolved legal and ethical concerns. Hence all these factors hinder the introduction of this telemedicine system, which can be slowly rectified by implementing some awareness programmes, allocation of some funds, training for the technicians etc.

5 Conclusions

Telemedicine system can be certainly a boon in disaster management. Telemedicine may not prevent the disasters, but it will surely be a significant tool in responding for the public good. Especially in the areas badly affected by disasters and where there is no transportation facilities and in the cases where immediate medical care is required and also in cases where we cannot transfer the patients this telemedicine tool can be very supporting for diagnosis as well as treatment. Also at present the country became super power in the field of science and technology making positive approach towards this system. Thus it offers ample opportunities for accessing safe and quality medical services especially in the rural and remote areas. Finally various studies and reports also shows that one of the best solution to help victims in disasters and to access health facilities for the people of rural areas where the specialists are unavailable is the telemedicine. So it is worth if efforts are taken to encourage this telemedicine for effective and quality medical care.

References

1. Ajami, S., Lamoochi, P.: Use of telemedicine in disaster and remote places. J, Educ. Health Promot. **3** (2014)
2. Bagchi, S.: Telemedicine in rural India. PLoS Med. **3**(3), e82 (2006)
3. Nair, P.: ICT based health governance practices: The Indian experience. J. Health Manage. **16**, 25–40 (2014)
4. Sinha, V.D., Tiwari, R.N., Kataria, R.: Telemedicine in neurosurgical emergency: Indian perspective. Asian J. Neurosurgery **7**(2), 75 (2012)

Chapter 30
Geospatial Flood Risk Mapping and Analysis Tool

S. Johny Samuael, J. Sahaya Arul and Jeni Chandar Padua

Abstract Floods are an important concern in the world, calling for improved intervention strategies like rapid flood mapping using remote sensing and GIS. The central focus of this work is to mark the flood zones of any desired location and prepare flood hazard maps. Flood mapping as presented in this paper uses sophisticated multi-objective optimisation algorithms to identify and assess flood risk. This android application can be used as a Geo-spatial Tool for analysing the probability of floods in any desired location and checking the safety level of the user's location/property and alert the inhabitants thereby helping to evacuate or relocate them to safer zones. This application shows a clear demarcation of risk zones which have maximum flooding and also the safe zones. The two scanning options provided would give results for analysing an individual property or a whole city and provide the possible risk zones in the measured radius. The Algorithm which uses the principle of Artificial Intelligence is highly efficient in sensing the topography of the location regardless of whether it is a mountain or a plain and provides results with great efficacy.

Keywords Flood mapping · Disaster management · ICRSDM

S. J. Samuael (✉)
Corpus Christi School, Peruvilai, Nagercoil, Kanyakumari District, Tamil Nadu, India
e-mail: johnnysamuael@gmail.com

J. S. Arul
University VOC College of Engineering, Thoothukudi, Tamil Nadu, India
e-mail: jsarul2k7@gmail.com

J. C. Padua
Department of Zoology, Holy Cross College, Nagercoil, Kanyakumari District, Tamil Nadu, India
e-mail: jenipadua19@gmail.com

P. J. Rao et al. (eds.), *Proceedings of International Conference on Remote Sensing for Disaster Management*, Springer Series in Geomechanics and Geoengineering,
https://doi.org/10.1007/978-3-319-77276-9_30

1 Introduction

Flood is one of the main factors causing loss of human life, damage to property, leakage in nuclear plants, destruction of vegetation and loss of animal diversity. Populations affected by floods were found to be influenced by post traumatic stress disorder symptoms [7]. In the case of flash floods which occurs rapidly, the damage is high accompanied by landslides, mud flows, bridge collapse, damage to buildings, and fatalities [9]. Flood mapping is one of the powerful tools to identify high risk flood zones. Hence, studies on mapping floods has been done in countries like United States [13], China [11], Egypt [6], Saudi Arabia [5, 15], India [3] and Ghana [8]. These studies are found to help in infrastructure planning, risk management and disaster response services during floods.

Identification of flood risk areas help in planning effective emergency responses leading to creation of flood hazard maps which promote greater awareness on the risk of flooding and be prepared during the onset of floods [18]. Though there have been various flood risk mapping and studies done, it is seen that many of them have major problems which lead to them not being accessible to the general public and also not efficient enough to give accurate details regarding the occurrence of floods. Also, old flood hazard maps seem to be contradictory showing certain areas which are actually on elevated areas, as being located in flood hazard areas. Due to such wrong manual mapping, there have been problems in identifying flood prone areas at the global level. This was mainly because the analysis was based on the sea level and could not map the continental areas which could be affected by river flooding [16, 17].

Another major problem associated with flood mapping is that, surveying and analysing a particular area and executing the algorithms manually has been found to be difficult especially for a larger area. Hence, studies on flood mapping is limited to smaller areas, thereby making the process of mapping or surveying the global flood prone areas a difficult mission. Though several global mapping efforts such as Aqueduct and near-real-time early warning such as the Global Flood Awareness System (GloFAS) exist, scales are often too coarse to be applied locally and empirical validation remains a challenge. In general, community level information is difficult to obtain [14]. There is no proper way by which individual or private property can be analyzed and it is highly difficult for the common man to find out if the land/house in which he resides or is planning to buy, is located in a flood free area.

This android based Geospatial flood risk analysis tool, mentioned in this paper might be a global solution to this problem of flood mapping which prevails all over the world. Here, the idea of remote sensing has been integrated to the algorithms and also, formulas were used to generate user-friendly flood maps automatically, for any desired location thereby helping to analyse flood risk zones of the whole world.

2 Materials and Methods

Smart phones are the most widely used technologies in the field of telecommunication [2] and android operating system has been found to lead the smart phone evolution [1]. Hence, this highly efficient Geospatial flood risk analysis tool was developed in a Smartphone platform running android OS. The major principle of this tool is remote sensing, which can identify the flood zones in any part of the earth from any place. For geospatial analysis, this application uses Shuttle Radar Topography Mission (SRTM) data which is downloaded for the desired location. This is because, SRTM data delivers a digital terrain model of better spatial resolution and accuracy than traditional free global DEM datasets at near-global coverage [12]. The algorithm uses artificial intelligence to sense the topography of the location and shifts the formula accordingly thereby giving accurate results even in mountains and plains. This tool was developed in a laptop having the following specifications: Model Name: Hewlett-Packard Probook 441s; Processor: Intel Core i7; Ram: 4 GB; OS: Windows 7 (32 bit).

The software used to develop this tool was Basic4Android V5.80 which was the latest version during the time of development. This android based Geospatial flood risk analysis tool was tested in different smart phones and in different places around the world. In order to check the accuracy of the tool, historic flood maps prepared for various locations have been compared with the results of this analytical tool. The debugging was done using B4A Bridge using the following smart phone with the following specifications: Model Name: Samsung Galaxy J7 Prime; Model Number: SM-G610F; Android Version: 6.0.1; RAM: 3 GB; Internal Storage: 32 GB.

The tool is user-friendly and the location to be mapped for flood risk, is selected either by Global Positioning System (GPS) or by selecting a point on the Google Map using a custom marker. Though the other flood mapping tools found online have used Google overlay tiles to portray the flood zones, this Geospatial flood risk mapping tool is equipped with markers to make it user friendly. The use of markers help in comparing the location of study with the surrounding location, thereby making the analysis equivalent to a manual survey. Using markers, a quadrilateral area is formed around a given location of study with desired length and breadth so as to show the flood analysis related to that area. The user can check the altitude of the place under study and the area surrounding them. The data is then fed into the sophisticated multi-objective optimisation algorithms, which in return plots the points in different shades according to their level of flood risk, the legends of which are presented with the limit values. Two different scanning options have been provided—property level and area level scanning, which use different algorithms and provide results accordingly. The tool was tested on various mobile phones and tablets in a controlled environment and the fairness of the tests were maintained. Various locations around the globe were analyzed to confirm that the tool works globally, in order to make the experiment fair. Also, no human or animal was harmed or disturbed during the development, testing, redesigning, debugging or finalizing the project. The working principle of the flood mapping tool is given in Fig. 1.

3 Result

The Geospatial Flood Risk Analysis Tool was found to perform well in all the android mobile phones and tabs running android version 4.4 and above, in any location giving accurately scanned results. The location to be studied is chosen by the user in three options—entering the details in the address bar, dropping a pin manually or using GPS to pin point the location. The tool scans the location and the surrounding areas and provides the results in the form of a visual format consisting of a screen with coloured markers which demarcates the various zones. Legends are displayed neatly to understand the meaning of the coloured markers. The app was found to work well in android mobiles of various brands. The results were accurate giving the possible flow of water in any area which is analysed. The safety level of the study area is also identified. The tool gives a clear demarcation showing the risk zones where the flooding would be maximum and the safe zones where the flooding would be minimum. The scanning options namely—Area Level Scanning and Property Level Scanning gives accurate results. Area Level Scanning displays results of a whole village or city that could be acquired according to custom requirements, whereas Property Level Scanning gives results for a private/individual property and the area around it. In order to validate the accuracy of the results, certain locations were chosen which were already studied by researchers

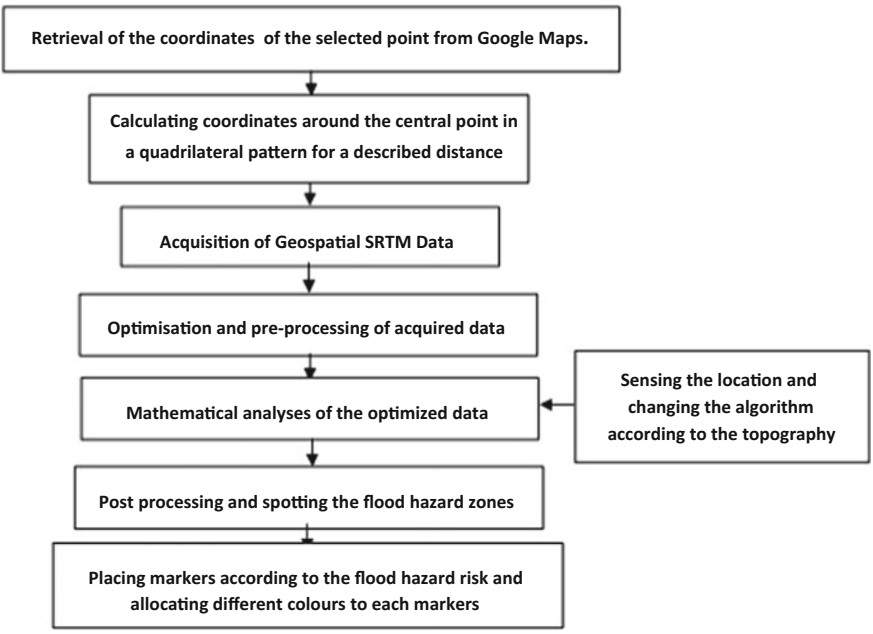

Fig. 1 Working principle

using manual means and their results were compared with the results of the analysis done by this analytical tool.

The results in Fig. 2a, b show that the map generated by this tool correlates accurately with the HECRAS simulation of the Coliseum Area. The legends for the result is given in Fig. 3. In the map, the places which are blue in color denote the flooding areas and those that are green are safe for people to move to, before a flood or to live in during a flood. The user can zoom into the location and view the study areas under:(1) Normal mode, (2) Terrain mode and (3) Satellite mode. The results were accurate when cross-checked with the history of flooding in various areas. The results of the testing showed increased accuracy as regards the flood-mapping-data.

The results of the Property Level Scanning shows shades of blue areas which denote accumulation of water in these areas at various intensities which is probable to flow into the user's location, from this area. Whereas red, pink, and such colors show the barrier regions which might stop the flooding water.

Figure 4a shows the photo of coliseum area during the 1979 floods taken by NOAA (National Oceanic and Atmospheric Administration). Figure 4b is the zoomed flood map showing the centre reference point (Coliseum Area). Figure 4c shows the scanned result of the same area using this tool.

Figure 5a–c depicts a point 3109 m above the sea level. This analysis proves that this tool can be used to find the flood risk even in mountains. The blue area shown in the map is likely to be flooded. The place was heavily flooded and 5000 were killed and 19,000 were stranded during the 2013 North India Floods [10].

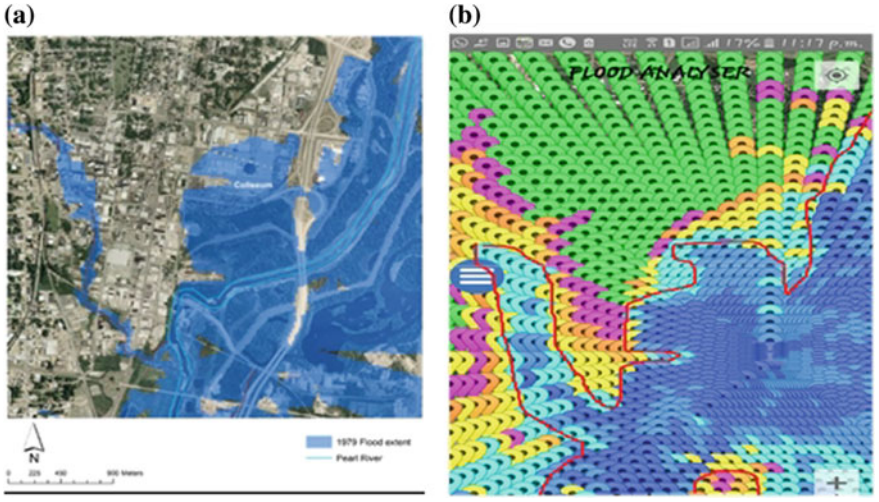

Fig. 2 **a**, **b** HECRAS simulation of the 1979 flood extend in the coliseum Area [19] compared to the flood map generated by the Geospatial Flood risk analysis tool

Fig. 3 The Legends for area level analysis of 1979 flood generated automatically by the geospatial flood risk analysis tool

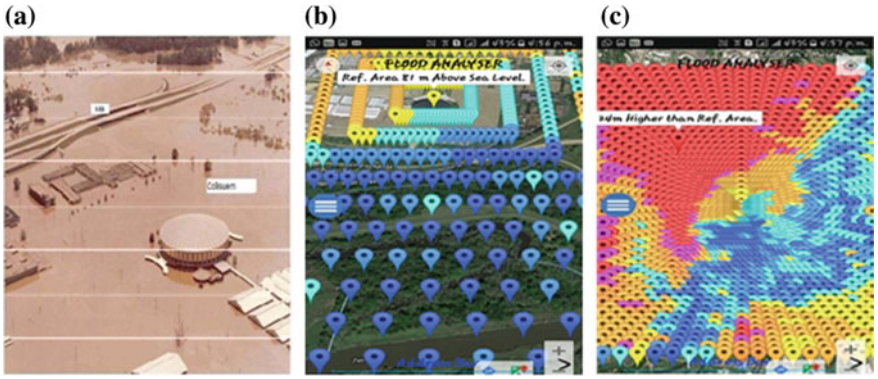

Fig. 4 **a–c** Floods as depicted by American Journal of Geographic Information System 2012 compared to the property level analysis flood map generated by the Geospatial Flood risk analysis tool

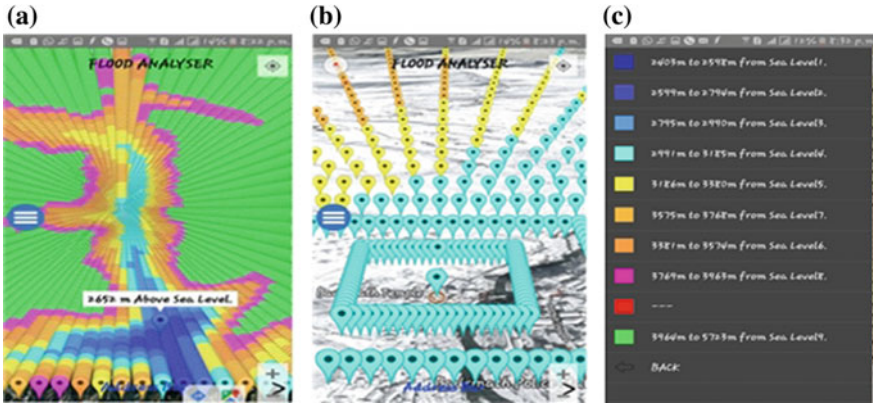

Fig. 5 **a** Area level analysis of Badrinath, Uttarakhand. **b** The centermarker shows the Badrinath temple. **c** The legends for the analysis of Badrinath

4 Conclusions

Floods can happen anywhere at any time. And in most of the areas around the world, floods happen due to heavy rains flooding the rivers or due to accumulation of surface water due to insufficient or ineffective drainage facilities, in thickly populated areas. Floods affect more people globally than any other type of natural hazard.

It is seen that most of the 'flood mapping data' and 'risk analysis data' using elevation models are found to be outdated, inaccurate and hence not reliable.

Hence, great potential exists for new technologies to support flood disaster risk reduction. In addition to existing expert-based data collection and analysis, direct input from communities and citizens across the globe may also be used to monitor, validate, and reduce flood risk.

New technologies offer great potential for rectifying problems associated with existing flood risk analytical tools, thereby serving in effective humanitarian response and recovery.

Lidar based data, in which airplanes map local terrain, by firing laser pulses on the ground, were found to provide much more accurate data than the old methods. But as Lidar technology is highly expensive and inaccessible to researchers who have limited funding [4].

Hence, researchers concentrated on updating and digitizing maps for the populated areas using old and existing flood maps. But, flaws were seen to exist in this system. Because, when old maps were digitized, the new imagery was not seen to line up correctly with the old maps, leading to a "warping" effect which gave a wrong analysis which showed areas that are actually safe, as being in the flood hazard area. Due to this, there were problems in identifying flood prone areas.

It was seen that there had been dozens of home owners filing complaints to governmental organisations that the flood maps used for charging insurance on their property were wrong.

Hence, at the global level, most of the countries which face heavy flooding are in need of an efficient, cost effective and reliable flood mapping tool to satisfy their needs like finding the exact areas which are flood prone and charging flood insurance on people residing in such flood prone areas [16].

In countries which lack proper drainage facilities, and have no proper flood mapping data available, having a flood mapping tool is the need of the hour.

As individual/private property cannot be analysed without support from organisations, it is extremely difficult for the common man to find out if the land/house which he resides or is planning to buy, is located in the flood free area.

Hence, this geospatial analytical tool might be a global solution to the problem of flood mapping which prevails all over the world and can be used as a "flood probability analysis tool/risk mapping tool" during floods or by the general public to analyse their location for insuring a specific property against floods.

References

1. Ahmad Dar, M., Parvez, J.: Evaluating Smartphone Application Security: A Case Study on Android. Global Journals Inc., New York (2013). ISSN: 0975-4172 & Print ISSN: 0975-4350. https://globaljournals.org/GJCST_Volume13/2-Evaluating-Smartphone-Application.pdf
2. Ahmad, N., Boota, M., Masoom, A.: Comparative analysis of operating system of different smart phones. J. Software Eng. Appl. **8**, 114–126 (2015). https://doi.org/10.4236/jsea.2015.83012
3. Bhatt, C.M., Rao, G.S., Manjushree, P., Bhanumurthy, V.: Space based disaster management of 2008 Kosi floods, North Bihar, India. J. Ind. Soc. Rem. Sens. **38**(1), 99–108 (2010)
4. Costabile, P., Macchione, F., Natale, L., Petaccia, G.: Flood mapping using LIDAR DEM. Limitations of the 1-D modeling highlighted by the 2-D approach. Nat. Hazards **77**(1), 181–204 (2015)
5. Dawod, G.M., Mirza, M.N., Al-Ghamdi, K.A.: GIS-based spatial mapping of flash flood hazard in Makkah city, Saudi Arabia. J. Geogr. Inf. Syst. **11**(3), 225–231 (2011). http://dx.doi.org/10.4236/jgis.2011.33019 (URL http://www.SciRP.org/journal/jgis)
6. El Bastawesy, M.: Influence of DEM source and resolution on the hydrographical simulation of WadiKeed catchment, southern Sinai, Egypt. Egypt. J. Rem. Sens. Space Sci. **9**, 68–79 (2007)
7. Fontalba, N., Lucas Borja, M.E., Gil Aguilar, V., Arrebolla, J.P., Pena Andreu, J.M., Perez, J.: Incidence and risk factors for post traumatic stress disorder in a population affected by a severe flood (2016). http://doi.org/10.1016/j.puhe.2016.12.015
8. Forkuo, E.K.: Flood hazard mapping using Aster Image data with GIS. Int. J. Geomat. Geosci. 1(4) (2011)
9. Hapuarachchi, H.A.P., Wang, Q.J., Pagano, T.C.: A review of advances in flash flood forecasting. Hydrol. Process. **25**, 2771–2784 (2011). https://doi.org/10.1002/hyp.8040
10. http://timesofindia.indiatimes.com/india/Uttarakhand-5000-feared-killed-19000-still-stranded/articleshow/20731541.cms

11. Liang, W., Yongli, C., Hongquan, C., Daler, D., Jingmin, Z., Juan, Y.: Flood disaster in Taihu basin, china: causal chain and policy option analyses. Environ. Earth Sci. **63**(5), 1119–1124 (2011)
12. Ling, F., Zhang, Q.W., Wang, C.: Comparison of SRTM data with other dem sources in hydrological researches. In: Proceedings 31st International Symposium on Remote Sensing of Environment, pp. 20–24 (2005)
13. Mastin, M.: Watershed Models for Decision Support for Inflows to Potholes Reservoir, Washington (2009)
14. McCallum, I., Liu, W., See, L., Mechler, R., Keating, A., Hochrainer-Stigler, S., Mochizuki, J., Fritz, S., Dugar, S., Arestegui, M., Szoenyi, M., Laso Bayas, J.-C., Burek, P., French, A., Moorthy, I.: Technologies to support community flood disaster risk reduction. Int. J. Disaster Risk Sci. **7**(2), 198– 204 (2016). https://link.springer.com/article/10.1007/s13753-016-0086-5
15. Saud, M.: Assessment of flood hazard of Jeddah area 2009, Saudi Arabia. J. Water Res. Protect. **2**(9), 839–847 (2010). https://doi.org/10.4236/jwarp.2010.29099
16. www.juneauempire.com/local/2011-06-21/residents-say-fema-draft-flood-maps-are-inaccurate
17. www.sej.org/publications/tipsheet/feds-find-big-flaws-in-current-flood-maps
18. www.climatetechwiki.org/content/flood-hazard-mapping
19. Yeramilli, S.: Am. J. Geogr. Inf. Syst. **1**(1), 7–16 (2012). https://doi.org/10.5923/j.ajgis.20120101.02

Chapter 31
Soil Erosion Assessment of Hilly Terrain of Paderu Using USLE and GIS

Ramprasad Naik Desavathu and Peddada Jagadeeswara Rao

Abstract To assess and predict soil erosion of the Paderu Mandal, is a part of Eastern Ghats of India, was found out with the assistance of Universal Soil Loss Equation (USLE) coordinated with Geospatial technologies. Discoveries from this study, the average value of rainfall erosivity factor (R) was observed to be 535.722 MJ mm ha^{-1} h^{-1} $year^{-1}$ and soil erodibility factor (K) varies in between 0.21 and 0.27 t h MJ^{-1} mm^{-1}. Slope steepness and flow accumulation were to calculate topographic factor (LS) and it is dimensionless. The land use map was derived from IRS P6 imagery of LISS III data (2011) and utilized for examining the crop management factor (C), where support the practice factor (P) value is 1, these is no major conservation practices in the study area. All erosion factors are incorporated and analyzed in GIS environment. Finally, annual soil loss evaluated and furthermore the rate of erosion classes was contemplated. The average annual soil loss of entire study area is 113 t ha^{-1} $year^{-1}$. Around 70.80% of the area is under moderate class (5–10%), 22.06% of the area under slight (0–5%) and rest of classes are high, high and extreme erosion respectively.

Keywords Soil erosion · Universal soil loss equation · GIS · Land use

1 Introduction

Soil erosion in hilly/mountainous region removes the valuable fertile topsoil, further reduce the soil productivity for agriculture development [5, 23]. Livelihood of the people in this region is mainly dependent on farming system and especially on sustainable agriculture [12]. Landslide, mudslides, collapse of man-made

R. N. Desavathu (✉) · P. J. Rao
Department of Geo-Engineering, Andhra University,
Visakhapatnam 530 003, India
e-mail: desnaik@gmail.com

P. J. Rao
e-mail: pjr_geoin@rediffmail.com

P. J. Rao et al. (eds.), *Proceedings of International Conference on Remote Sensing for Disaster Management*, Springer Series in Geomechanics and Geoengineering,
https://doi.org/10.1007/978-3-319-77276-9_31

terraces, soil loss from steep slopes and decline of forest/pasture areas are the main reasons for degradation of soil resources, which is limited in the region [13, 20, 29]. It has been observed that surface and gully erosion, is a common phenomenon and agriculture land has expanded to areas having marginal soil cover. Thus, natural resources in mountainous terrain are significantly afflicting from land degradation as a result of intensive deforestation, overgrazing and subsistence agriculture due to population pressure, vast-scale road development and mining etc. along with anthropogenic activities [14]. As a consequence of deforestation combined with the impact of the high rainfall, the fragile terrains with steep slope have become affected to severe soil erosion [25]. Consequently, it is essential to assess soil erosion affected areas for soil conservation practices. Further, forecast of soil erosion rates are needed to evaluate soil losses and to determine the adequacy of control measures for designing and implementation on a regional scale [27, 32].

Researchers have created many predictive models that estimate soil loss and identify areas where conservation measures will have the greatest impact on reducing soil loss for soil erosion assessments in different region of world [2, 3, 8, 11, 16, 17, 30, 31]. However, owing to its simplicity, the universal soil loss equation continues to be the most widely utilized model for soil loss estimation, which makes them applicable regardless a limited measure of input data, is accessible. For this study Universal Soil Loss Equation (USLE) used to estimate annual soil loss, its spatial distribution and status with the aid of Remote Sensing (RS) and Geographic Information System (GIS) [1, 4, 7, 9, 10, 18, 28, 33, 35] for preparing sustainable soil erosion management strategies with reasonable costs and better accuracy, particularly in the fragile and heterogeneous erosion-susceptible hilly ecosystems [26].

2 Materials and Methods

Paderu Mandal is situated in between the latitudes of 18° 18′ to 17° 56′ and the longitudes of 82° 32′ to 82° 53′ covered by Survey of India (SOI) toposheets no. 65K9, 65K13, 65J12 and 65J16 on 1: 50,000 scale. The total area is 435 km^2, which is surrounded by Pedabayalu Mandal on north, Hukumpeta Mandal on north-east, on south-east by Cheedikada Mandal, on south is Madugula Mandal and G. Madugula on north-west (Fig. 1). Rainfall data of last twenty years (1991–2011) is gathered from six rain gauge stations surrounding Paderu Mandal and District Statistic Abstracts of Visakhapatnam. Soil maps have been taken from Department of Agriculture (Government of Andhra Pradesh). Digital Elevation Model (DEM) of the study area was taken from Shuttle Radar Topographic Mission data downloaded from the United States Geological Survey website. Land use/cover map was prepared by using LISS-III data (23.5 m of spatial resolution) of IRS P6 dated March 2011.

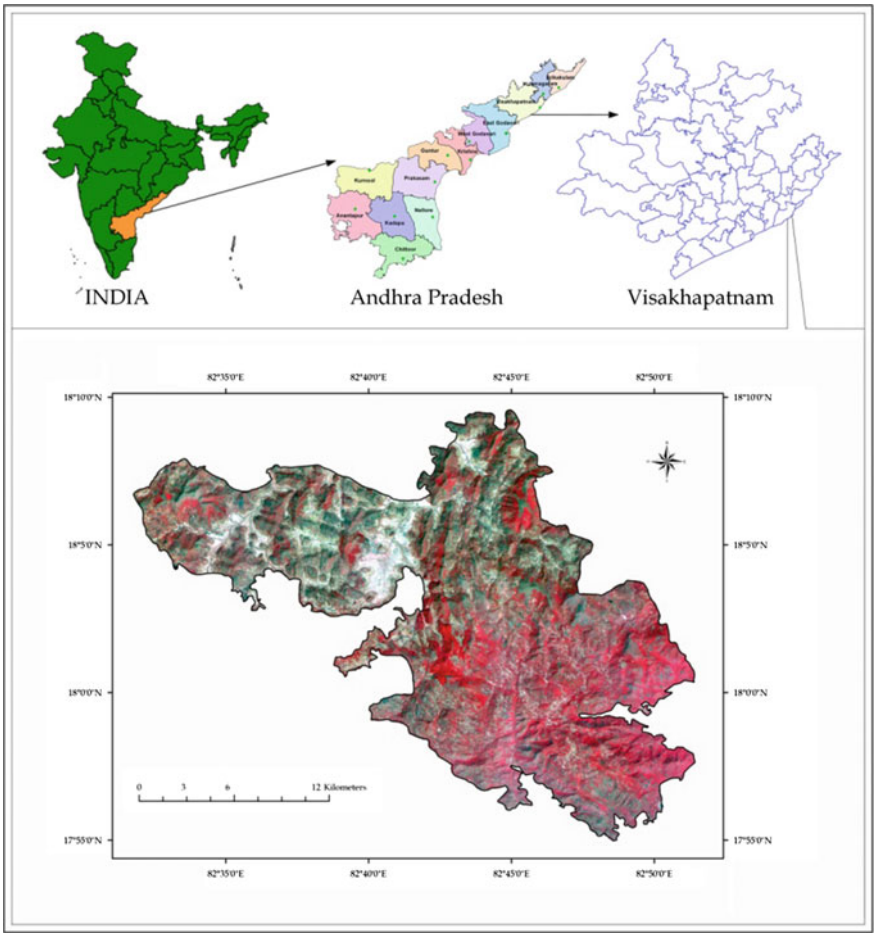

Fig. 1 Location map showing imagery of IRS P6 of the study area

2.1 Estimation of Annual Soil Loss (A)

To compute average annual soil loss (A) by soil erosion factors like rainfall, soils, land use/cover, topography, and soil conservation practices. These factors are involved for the estimation of soil erosion, mapping the spatial distribution and its status with help of GIS in the study area as follows (Eq. 1):

$$\mathbf{A} = \mathbf{R} * \mathbf{K} * \mathbf{LS} * \mathbf{C} * \mathbf{P} \tag{1}$$

where A is computed Soil loss (t ha^{-1} $year^{-1}$), R is the Rainfall-Runoff Erosivity factor (MJ mm ha^{-1} h^{-1} $year^{-1}$), K is the soil erodibility factor (t h MJ^{-1} mm^{-1}),

LS is the slope length factor and slope factor (dimensionless). C is the crop management factor (dimensionless) and P is the supporting conservation practice factor (dimension less).

2.1.1 Rainfall-Runoff Erosivity Factor

Rainfall-Runoff Erosivity (R) is the potential ability of rainfall to cause soil erosion [19]. It is the product of rainfall kinetic energy and the maximum of thirty minutes intensity of rainfall [34] and measured in MJ mm ha^{-1} h^{-1} $year^{-1}$. Non-availability of these two (intensity and kinetic energy of rainfall), average annual rainfall (R_n) has been used to estimate R-factor, which is derived from Eq. (2).

$$\mathbf{R = 79 + 0.363\,R_n} \tag{2}$$

where: R_n is Average Rainfall in mm.

R is the Rainfall Runoff Erosivity Factor.

2.1.2 Soil Erodibility Factor (K)

Soil Erodibility Factor (K) is the combined effect of rainfall, the rate of runoff and infiltration on soil loss; it is a quantitative estimation of erodibility of a specific soil type. Soil texture is the main factor affecting the ability of the soil to erode, however, the other factors affecting K factor are soil structure, permeability, and organic matter content. Soil Erodibility Factor (K) is calculated using the relationship between soil texture class and organic matter [24].

2.1.3 Topographic Factor (LS)

Topographic factor (LS) is the combination of both slope length factor (L) and slope steepness factor (S) where slope length factor is the ratio of soil loss to the field slope length and slope steepness factor is the ratio of soil loss to the field slope gradient. It can be evaluated from a digital elevation model (DEM) using unit stream power hypothesis. In this study, slope steepness and flow accumulation are prepared from ASTER DEM (30 m of resolution) to estimate topographic factor (LS) by using raster calculation in GIS environment as follows Eq. 3 [6, 15].

$$\mathbf{LS} = (([\mathbf{flow\ accumulation}]\ \mathbf{resolution}/\mathbf{22.13})^{\mathbf{0.6}} \times (\mathbf{Sin}([\mathbf{Slope\ of\ DEM}] \times \mathbf{0.0175}/\mathbf{0.0896})^{\mathbf{1.3}}) \tag{3}$$

2.1.4 Crop Management Factor

C factor is fundamentally the vegetation cover percentage and is defined as the ratio of soil loss to specific crops to the equivalent loss from tilled, bare test-plots. The value of C relies on vegetation type, the phase of development and cover percentage. The C factors are related to the land-use and are the reduction factor to soil erosion vulnerability. Accordingly, it is very important to have great information regarding land-use pattern in the study to generate reliable C factor values. Crop and Management factor (C) is calculated from Land use/Land cover generated the map.

2.1.5 Supporting Conservation Practice Factor (P)

In order to prevent exposure of the land to be cultivated to erosive rain the natural protection offered by grass or close-growing crops in the system needs to be supported by practices that will slow down the runoff thereby reducing the amount of soil erosion. Such essential supporting practices are contour cultivation; strip cropping, terrace system and waterways for the disposal of excess rainfall. Conservation practice factor (P) in the Universal Soil Loss Equation is the ratio of soil loss with a specific supporting practice to the corresponding soil loss with up and down cultivation [21].

3 Results and Discussions

Annual soil loss of the study area was studied with the help of USLE incorporated with GIS studies. All the USLE parameters (Rainfall Erosivity, Soil Erodibility, Topographic factor, Crop management and Conservation Practice factors) are determined either in spatial format (or) in numerical format, used to evaluate the annual soil loss of the Paderu Mandal.

For this review, average annual rainfall of last 20 years of six surrounding rain gauge stations was utilized to get the spatial distribution of rainfall, which varied from 945 to 1490 mm. The Rainfall Erosivity factor (R) was calculated from average annual rainfall presented in Table 1 and its spatial distribution is shown in Fig. 2. The resultant annual rainfall erosivity factor is varied from 447.690–594.581 MJ mm ha^{-1} h^{-1} $year^{-1}$. This shows the value of R-factor also varies according to rainfall distribution. The average value of entire R-factor for the study was found to be 535.722 MJ mm ha^{-1} h^{-1} $year^{-1}$. The value of Soil erodibility (K) of the study area can be evaluated using the relationship between soil texture class and organic matter where both of them are derived from the soil map of the study area, prepared by National Bureau of Soil and Land Use Planning [22]. The study area has 2 types of soil viz., sandy loam and sandy clay loam. The values which were assigned to the K factor by considering soil types are shown in Table 2.

Table 1 Rainfall stations in and around Paderu Mandal and Spatial distribution of annual rain fall from 1991 to 2011

Stations	Name	Longitude	Latitude	Annual rainfall (mm)	R-factor
1	Paderu	82.661	18.078	1239	529
2	Pedabayalu	82.594	18.286	1379	580
3	Hukumpeta	82.698	18.150	1154	498
4	G. Madugula	82.538	18.011	1490	620
5	Madugula	82.819	17.914	1304	566
6	Cheedikada	82.894	17.927	945	422

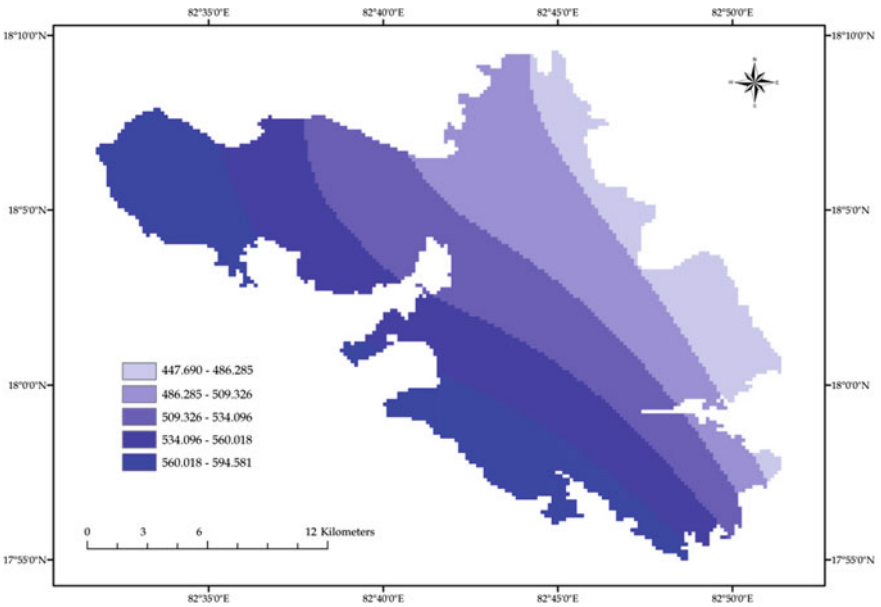

Fig. 2 Rainfall erosivity factor (R) map of the study area

Based on soil map and soil erodibility texture the K factor is varied between 0.19 and 0.27 t h MJ^{-1} mm^{-1} as shown in Fig. 3.

LS factor is calculated by using flow accumulation, a slope of the study area and cell size of used DEM. (all cells with flow accumulation greater than and equal to 6 were assigned as value 6. as DEM has a resolution of 30 m. Hence the flow accumulation cannot exceed 6 grid cells). The topographic factor is dimensionless and ranges in between 0 and 118.

In this study, on-screen visual interpretation was made to arrange the land use/land cover using IRS P6 imagery of LISS III data (2011) and identified features are agricultural land, built-up land, forest, scrubland and water bodies appeared in Fig. 4. The land use map was used for analyzing the C value. After changing the

Table 2 Soil erodibility factor (K)

Textural class	Organic matter		
	<0.5	2	4
Sandy loam	0.27	0.24	0.19
Sandy clay loam	0.27	0.25	0.21

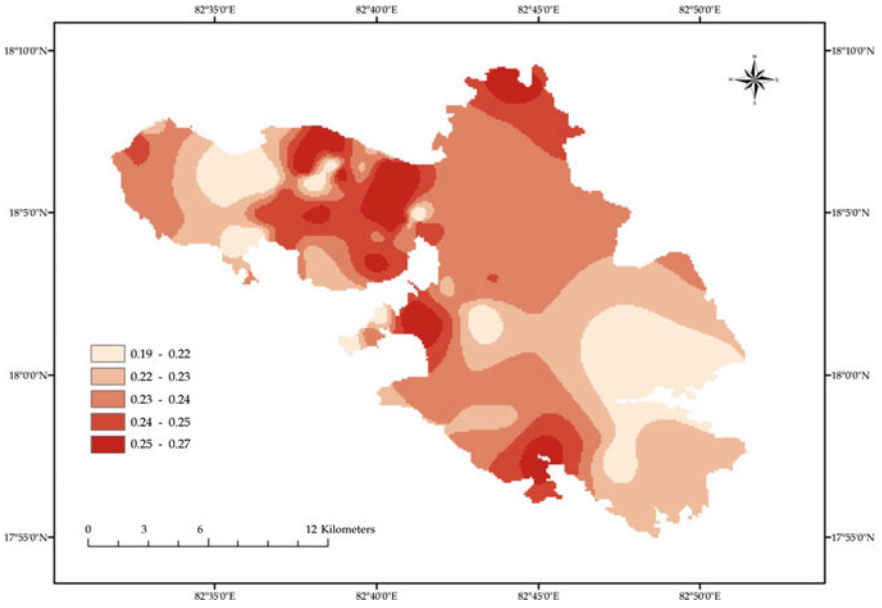

Fig. 3 Soil erodibility factor (K) map

coverage to a grid, a corresponding C value was assigned to each land use classes using re-class method in GIS (Fig. 5). The C factor value and their evaluated spatial distribution according to land use/cover and crop management factor are shown in Table 3. Further P-factor is also derived from same land uses of the study area and its value range is 0–1. Where the lowest value 0 represents very good erosion resistance area like manmade erosion resistance facility and maximum value 1 represents no erosion resistance facility like forest area. In the study area, no significant conservation practices are followed. Hence, all the land uses were assigned P factor of 1.

Their impacting parameters were incorporated and analyzed using Raster calculator in GIS environment. The annual soil loss map of study was obtained and reclassified in the following scales of priority: Slight (0–5 ton/ha/year), Moderate (5–10 ton/ha/year), High (10–20 ton/ha/year), Very High (20–40 ton/ha/year) and Severe (>40 ton/ha/h) annual erosion classes as per Indian conditions. The details of an aerial extent and spatial distribution of soil loss with their rate of erosion classes shown in Table 4 and map in Fig. 6. The annual soil loss evaluated for the entire

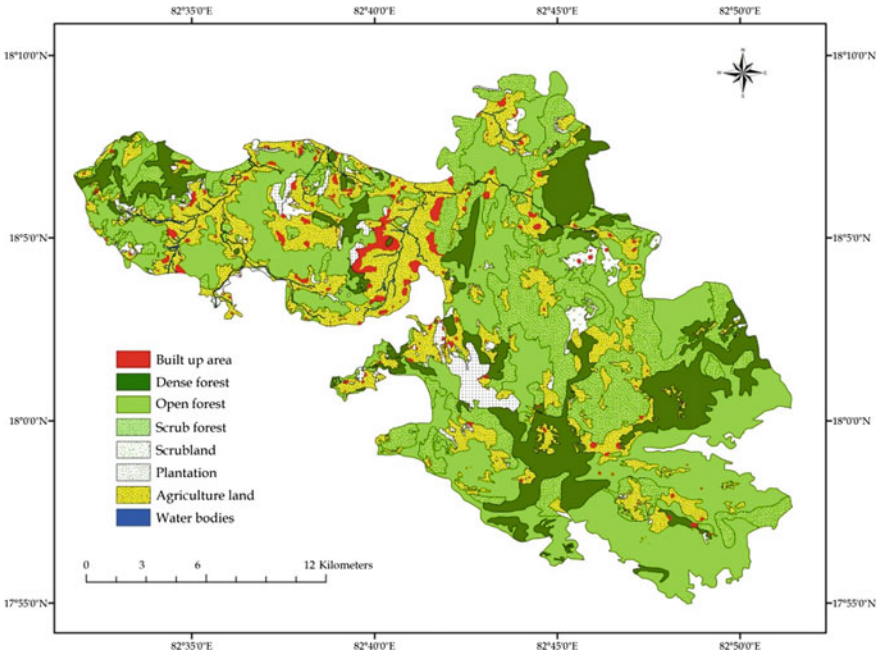

Fig. 4 Land use/cover features derived from IRS P6 imagery of LISS III data (2011)

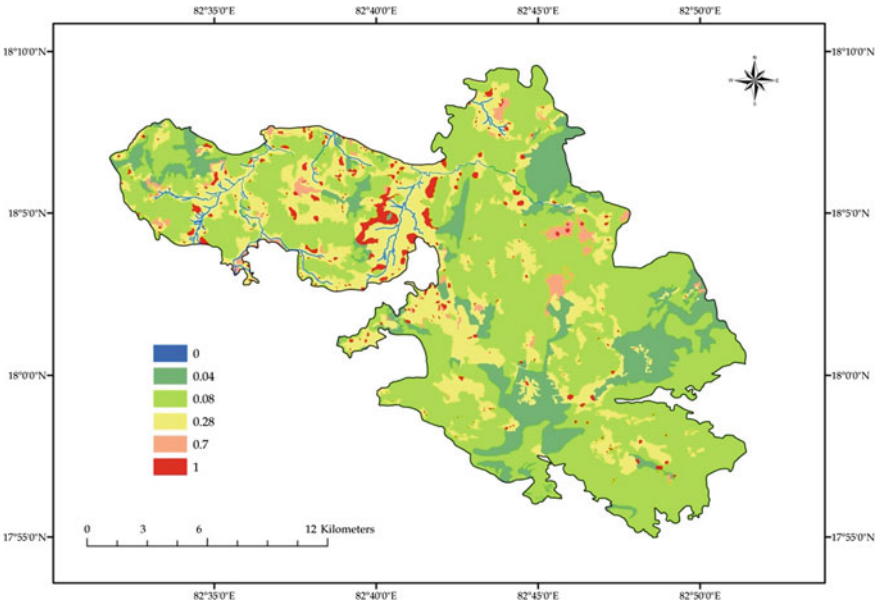

Fig. 5 Crop management factor map (C) of Study area

Table 3 Distribution of land use/cover, C-factor and P-factor of study area

Land use/cover class	Area ($km^{2)}$	Percentage of area (%)	C-factor	P-factor
Built up land	9.13	2.10	1	1
Dense forest	70.3	16.16	0.004	
Open forest	152.4	35.03	0.008	
Scrub forest	93.62	21.52	0.008	
Scrub land	9.2	2.11	0.7	
Plantation	10.8	2.48	0.28	
Agriculture	87.73	20.17	0.28	
Water bodies	1.82	0.42	0	
Total	435	100		

Table 4 Aerial extent and spatial distribution of soil loss with their rate of erosion classes

Erosion class	Rate of erosion	Annual soil loss (ton/ha/year)	Area (km^2)	Percentage (%)
Slight	0–5	25	96	22.06
Moderate	5–10	80	308	70.80
High	10–20	5.2	20	4.60
Very high	20–40	2.2	8.4	1.94
Severe	>40	0.6	2.6	0.60
		113	435	100

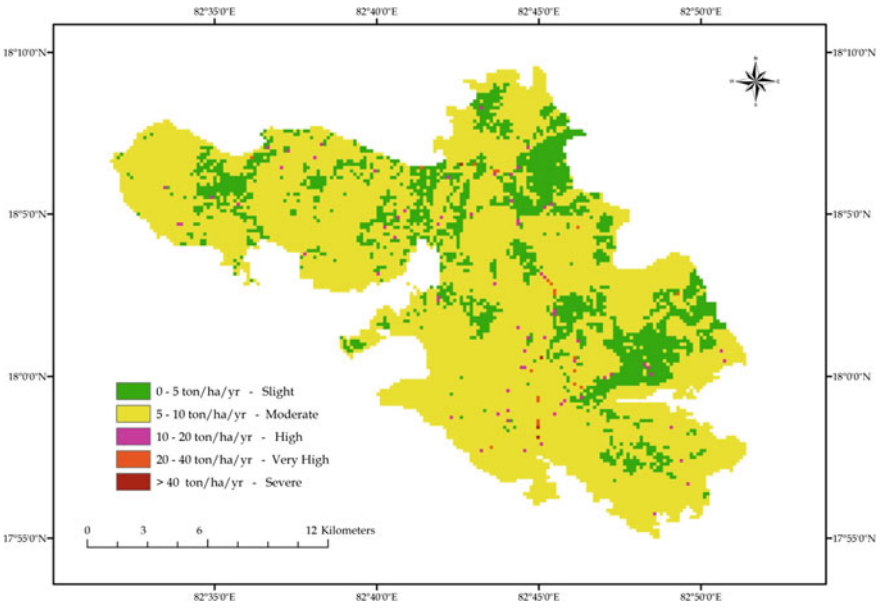

Fig. 6 Annual soil loss (A) of study area

study is 113 t ha^{-1} $year^{-1}$. Most of the area i.e. about 308 km^2 of the study area is found to be moderate erosion class (5–10%), which constitutes 80 t ha^{-1} $year^{-1}$ of annual soil loss (70.80%) of the total geographical area (435 km^2), while rest of areas covered by slight, high, very high and severe erosion classes are 22.06, 4.60, 1.94 and 0.6% respectively. Thus created soil loss maps helps in checking the erosion losses implementation of soil conservations structures effectively.

4 Conclusion

This research study demonstrated that the integration of USLE with geo spatial technologies (Remote Sensing, Geographical Information System and Global Positional System) to model soil erosion assessment is cost effective, timely and reliable information in spatial as well as temporal domain, particularly out of reach areas like hilly terrain, where ground based perceptions are difficult. The procedure and methodology developed in the study has immense potential for adoption at micro level to delineate and prioritize the erosion risk areas for efficient planning strategies for conservation measure without any negative impact on environmentally sensitive hilly region.

References

1. Adediji, A., Tukur, A.M., Adepoju, K.A.: Assessment of Revised Universal Soil Loss Equation (RUSLE) in Katsina area, Katsina state of Nigeria using remote sensing (RS) and Geographic Information System (GIS). Iranica J. Energy Environ. **1**(3), 255–264 (2010)
2. Adinarayana, J., Rao, K.G., Krishna, N.R., Venkatachalam, P., Suri, J.K.: A rule-based soil erosion model for a hilly catchment. CATENA **37**, 309–318 (1999)
3. Al-Quraishi, A.M.F.: Soil erosion risk prediction with RS and GIS for the northwestern part of Hebei Province, China. Pak. J. Appl. Sci. **3**(10–12), 659–666 (2003)
4. Bonilla, C.A., Reyes, J.L., Magri, A.: Water erosion prediction using the revised universal soil loss equation (RUSLE) in a GIS frame work, central Chile. Chil. J. Agric. Res. **70**(1), 159–169 (2010)
5. Dabral, P.P., Baithuri, N., Pandey, A.: Soil erosion assessment ina hilly catchment of North Eastern India using USLE, GIS and remote sensing. Water Resour. Manage **22**, 1783–1798 (2008)
6. Desmet, P.J., Govers, G.: A GIS procedure for automatically calculating the USLE LS on topographically complex landscape units. J. Soil Water Conserv. **51**, 427–433 (1996)
7. Erdogan, E.H., Erpul, G., Bayramin, I.: Use of USLE/GIS methodology for predicting soil loss in a semiarid agricultural environment. Environ. Monit. Assess. **131**, 153–161 (2007)
8. Hoyos, N.: Spatial modeling of soil erosion potential in a tropical watershed of the Colombian Andes. Catena **63**(1), 85–108. IEEE Xplore. **3**, 47–50 (2005)
9. Jose, S.K.: Varghese, A., Kumar, S., Madhu, G., Rakhi, C., Sreekala, T.K.: Soil erosion modeling using GIS and remote sensing. A case study of Shendurney Wildlife sanctuary Southern Western Ghats, Kerala. Ecol. Environ. Conserv. **4** (2011)

10. Lee, S.: Soil erosion assessment and its verification using the universal soil loss equation and geographic information system: a case study at Boun, Korea. Environ. Geol. **45**, 457–465 (2004)
11. Lin, C.Y., Lin, W.T., Chou, W.C.: Soil erosion prediction and sediment yield estimation: the Taiwan experience. Soil Tillage Res. **68**, 143–152 (2002)
12. MacDonald, D., Crabtree, J.R., Wiesinger, G., Dax, T., Stamou, N., Fleury, P., Gutierrez Lazpita, J., Gibon, A.: Agricultural abandonment in mountain areas of Europe: environmental consequences and policy response. J. Environ. Manag. **59**, 47–69 (2000)
13. Mati, B.M.: Assessment of erosion hazard with USLE and GIS—a case study of the upper Ewaso Ng'iro basin of Kenya. Int. J. Appl. Earth Obs. Geoinf. **2**, 78–86 (2000)
14. Merritt, W.S., Letcher, R.A., Jakeman, A.J.: A review of erosion and sediment transport models. Environ. Model. Softw. **18**, 761–799 (2013)
15. Mitasova, H., Mitas, L.: Modeling Soil Detachment with RUSLE 3d Using GIS. University of Illinois at Urbana-Champaign (1999)
16. Morgani, R.P.C., Quintoni, J.N., Smith, R.E., Govers, G., Poesen, J.W.A., Auerswald, K., Chisci, G., Torri, D., Styczen, M.E.: The European soil erosion model (EUROSEM): a dynamic approach for predicting sediment transport from fields and small catchments. Earth Surf. Process Landf. **23**, 527–544 (1998)
17. Nearing, M.A., Foster, G.R., Lane, L.J., Finkner, S.C.: A process-based soil erosion model for USDA-water erosion prediction project technology. Trans. ASAE **32**, 1587–1593 (1989)
18. Pandey, A., Chowdary, V.M., Mai, B.C.: Identification of critical erosion prone areas in the small agricultural watershed using USLE, GIS and remote sensing. Water Resour. Manag. **21**, 729–746 (2007)
19. Paul, E., Glover, E.T., Yeboah, S., Adjei-Kyereme, Y., Yawo, I.N.D., Nyarku, M., Asumadu-Sakyi, G.S., Gbeddy, G.K., Agyiri, Y.A., Ameho, E.M., Aberikae, E.A.: Rainfall Erosivity Index for the Ghana Atomic Energy Commission site. Springer Plus vol. 5, p. 465. https://doi.org/10.1186/s40064-016-2100-1 (2016)
20. Pradhan, B., Chaudhary, A., Adinarayana, J., Buchroithner, M.F.: Soil erosion assessment and its correlation with landslide events using remote sensing data and GIS: a case study at Penang Island, Malaysia. Environ. Monit. Assess. **184**, 715–727 (2012)
21. Prasannakumar, V., Vijith, H., Abinod, S., Geetha, N.: Estimation of soil erosion risk within a small mountainous sub-watershed in Kerala, India, using Revised Universal Soil Loss Equation (RUSLE) and geo-information technology. Geosci. Front. **3**(2), 209–215 (2012)
22. Reddy, R.S., Nalatwadmath, S.K., Krishnan, P.: Soil erosion Andhra Pradesh NBSS Publ. No. 114, NBSS&LUP, Nagpur, 76pp (2005)
23. Parveen, Reshma, Kumar, Uday: Integrated approach of universal soil loss equation (USLE) and geographical information system (GIS) for soil loss risk assessment in Upper South Koel Basin, Jharkhand. J. Geogr. Inf. Syst. **4**, 588–596 (2012)
24. Schwab, G.O., Frevert, R.K., Edminster, T.W., Barnes, K.K.: Soil Water Conservation Engineering, 3rd edn. Wiley, New York (1981)
25. Sezgin, H.: Determination of soil erosion in a steep hill slope with different land-use types: a case study in Mertesdorf (Ruwertal/Germany). J. Environ. Biol. **28**(2), 433–438 (2007)
26. Sharama, J.C., Sharma, K.R.: Land use planning RS&GIS-a case study in Kawal Khad watershed in Himachal Pradesh. Indian J. Soil Conserv. **31**(2) (2002)
27. Sharda, V.N., Mandal, D.: Priority classes for erosion risk areas in different states and regions of India. Bulletin no. T-58/-37. Central Soil and Water Conservation Research and Training Institute, Dehradun, p. 172 (2011)
28. Singh, R., Phadke, V.S.: Assessing soil loss by water erosion in Jamni river basin, Bundelkhand region, India, adopting universal soil loss equation using GIS. Curr. Sci. **90**, 1431–1435 (2006)
29. Temesgen, B., Mohammed, M.U., Korme, T.: Natural hazard assessment using GIS and remote sensing methods, with particular reference to the landslides in the Wondogenetarea, Ethiopia. Phys. Chem. Earth Part C Solar Terr. Planet. Sci. **26**, 665–675 (2001)

30. Veihe, A., Rey, J., Quinton, J.N., Strauss, P., Sancho, F.M., Somarriba, M.: Modelling of event-based soil erosion in Costa Rica, Nicaragua and Mexico: evaluation of the EUROSEM model. CATENA **44**, 187–203 (2001)
31. Wischmeier, W.H., Smith, D.D.: Predicting rainfall erosion losses—a guide to conservation planning. Agriculture Handbook No. 537. US Department of Agriculture Science and Education Administration, Washington, DC, USA, p. 163 (1978)
32. Yada, R.K., Yadav, D.S., Rai, N., Sanwal, S.K.: Soil and water conservation through horticultural intervension in hilly areas. ENVIS Bull. Himalayan Ecol. **14**(1), 4–13 (2006)
33. Yahya, F., Dalal, Z., Ibrahim, F.: Spatial estimation of soil erosion risk using USLE approach, RS, and GIS techniques: a case study of Kufranja Watershed, Northern Jordan. J. Water Resour. Prot. **5**, 1247–1261 (2013)
34. Yuan, J., Liang, Y., Cao, L.: Preliminary study on mechanics-based rainfall kinetic energy. Int. Soil Water Conserv. Res. **2**(3), 67–73 (2014)
35. Yue-qing, X., Jian, P., Xiao-mei, S.: Assessment of soil erosion using RUSLE and GIS: a case study of the Maotiao River watershed, Guizhou Province, China. Environ. Geol. **56**, 1643–1652 (2009)

Chapter 32
Impact of Climate Change on Tropical Cyclones Frequency and Intensity on Indian Coasts

Sushil Gupta, Indu Jain, Pushpendra Johari and Murari Lal

Abstract Climate change is projected to exacerbate intensity of tropical cyclonic storms in selected ocean basins with the rise in sea surface temperatures. Almost all of the tropical cyclonic storms are concentrated in the East Asia, North America, and the Central American regions. The North Indian Ocean—the Bay of Bengal and the Arabian Sea, generates only 7% of the world's cyclones. However, their impact is comparatively high and devastating, especially when they strike the East Indian and Bangladesh coasts bordering the North Bay of Bengal due to high population density clustered around low lying areas along these coastlines. The tropical storms typically do not reach a high intensity in the Arabian Sea due to the unfavorable wind shear; dry air feed from Thar Desert and relatively lower sea surface temperatures. However, the Arabian Sea basin has also produced a few strong tropical cyclones particularly as seen in the recent years. In general, cyclones in North Indian Ocean tend to peak during May, October and November. This paper presents comprehensive analyses of the cyclonic disturbances data of the North Indian Ocean of 140 years (1877–2016) and investigates the likely impacts of climate change on tropical cyclones frequency and intensity on Indian coasts based on historical cyclone data and recent model based findings on plausible changes in Indian Ocean SSTs and circulation systems.

Keywords North Indian Ocean · Climate models · Tropical cyclone
Sea surface temperature · Cyclonic storm · Severe cyclonic storm

S. Gupta (✉) · I. Jain · P. Johari · M. Lal
RMSI, Noida, India
e-mail: sushil.Gupta@rmsi.com

I. Jain
e-mail: indu.jain@rmsi.com

P. Johari
e-mail: pushpendra.johari@rmsi.com

M. Lal
e-mail: murari.lal@rmsi.com

P. J. Rao et al. (eds.), *Proceedings of International Conference on Remote Sensing for Disaster Management*, Springer Series in Geomechanics and Geoengineering,
https://doi.org/10.1007/978-3-319-77276-9_32

1 Introduction

Tropical cyclones are among the most damaging natural hazards of the world. The North Indian Ocean (NIO) accounts for about 7% of global Tropical Cyclones (TCs). Out of these 7% of the cyclones, most forms in the Bay of Bengal (BoB) than the Arabian Sea (AS), which is about 4 times higher [1, 2]. In NIO, there are two cyclone seasons: pre-monsoon (March to May, MAM) and post-monsoon (October to December, OND). Some of the cyclonic disturbances also form in transitional monsoon season (June to September, JJAS). However, during the peak summer monsoon season, the depressions and deep depressions in BoB generally do not intensify to cyclonic storm category due to moderate vertical wind shear. On an average about 5–6 TCs form in the BoB and the AS every year, of which 2–3 reach severe stage. Most of the severe cyclones of the BoB form during the post-monsoon season in the months of October and November. A few severe cyclones form during May also but the post-monsoon cyclones are severest due to which this season is also known as storm season in south Asia [3].

Tropical disturbances have resulted in colossal socio-economic losses to life and property, especially along the east coast of India, Bangladesh and Myanmar every year due to cyclones in the BoB. Due to the high population density and rapid increase in infrastructure projects in the coastal regions of India, the economic losses are increasing leaps and bound. However, loss of life has reduced in recent years to a greater extent due to the advancement in science and technology of cyclone warning facilities and evacuation of a large number of human populations and animals prior to its landfall. The recent October 2013 Cyclone Phailin and the October 2014 Cyclone Hudhud are the two examples on the east coast of India that made landfall near Gopalpur on October 11 at about 2130 IST and at Visakhapatnam on October 12 at about 1330 IST, respectively. For both of these cyclones, the loss of lives have been reduced considerably, thanks to leanings from 1999 Odisha Super Cyclone in which more than 10,000 people perished; however, economic losses of buildings and infrastructure have increased enormously. For example, industrial losses in 2014 Cyclone Hudhud at Visakhapatnam city alone surpassed over INR 4000 Crores, while total losses from this cyclone were estimated over INR 36,000 Crores. Therefore, any change in the TCs frequency and intensity in the BoB and AS would have far reaching socio-economic consequences for India and neighbouring countries.

There have been a few studies on the long-term trends and TCs frequency and intensity over the BoB [3–11]. The TCs data was analysed for a period of 122 years during 1877–1998 [8, 9], and for a period of 129 years during 1877–2005 [3] (Table 1).

Most of these studies have emphasized a marginal decrease in the annual frequency of cyclones; however, there is an increasing trend in the frequency of Severe Cyclonic Storms (SCS) over NIO. Trend analysis reveal that the SCS frequency over the BoB has registered significant increasing trends in past 129 years during the intense cyclonic months, though this does not necessarily imply that SCS

Table 1 Frequency of TCs in the BoB during 1877–2005

Type of tropical disturbance	Month				
	May	Jun.	Sept.	Oct.	Nov.
Cyclonic storm (CS)	59	35	92	41	116
Severe cyclonic storm (SCS)	44	5	40	16	65
SCS/CS	0.75	0.14	0.43	0.39	0.56

Modified after Singh [3]

frequency has increased continuously decade after decade [3]. In fact there has been a slight decrease in SCS frequency after peaking during 1966–1970, although this does not alter the long term trend much. Moreover, the intensification rate (*denoted hereafter by SCS/CS*) during November, which accounts for highest number of intense cyclones in the NIO, has registered a steep rise of 26% per hundred years, implying that a tropical depression forming in the BoB during November has a high probability to reach to severe cyclone stage [3].

This paper presents comprehensive analyses of the long-term cyclonic disturbance data of the NIO of the past 140 years (1877–2016) and investigates the likely impacts of climate change on TCs frequency and intensity on Indian coasts (BoB, AS) based on historical cyclonic disturbances and recent model based findings on plausible changes in Indian Ocean SSTs and circulation systems.

2 Decadal Frequency Analysis of Tropical Disturbances

The long-term decadal frequency analysis of tropical disturbances in the BoB and AS for a duration of 140 years (1877–2016) has been presented in Figs. 1 and 2, respectively. The sources of tropical storms data are India Meteorological Department publication (IMD) and International Best-Track Archive for Climate Stewardship (IBTrACS).

It can be seen from Fig. 1, that there is a general decreasing trend in the decadal frequency of cyclonic disturbances in monsoon, pre-monsoon, and post-monsoon seasons from 1970s onwards in BoB. Similar observations can also be made in the decadal frequency of cyclonic disturbances in monsoon, pre-monsoon, and post-monsoon seasons from Fig. 2, over AS. Both these analyses also corroborate the earlier studies (for example [3, 12, 13]).

3 Intensity Analysis of CS and SCS

As mentioned earlier, we have analysed 140 years of tropical cyclonic disturbances data during 1877–2016. While, Singh [3] and other authors analysed this data as total numbers of CS or SCS numbers (Table 1), we not only analysed it as CS or

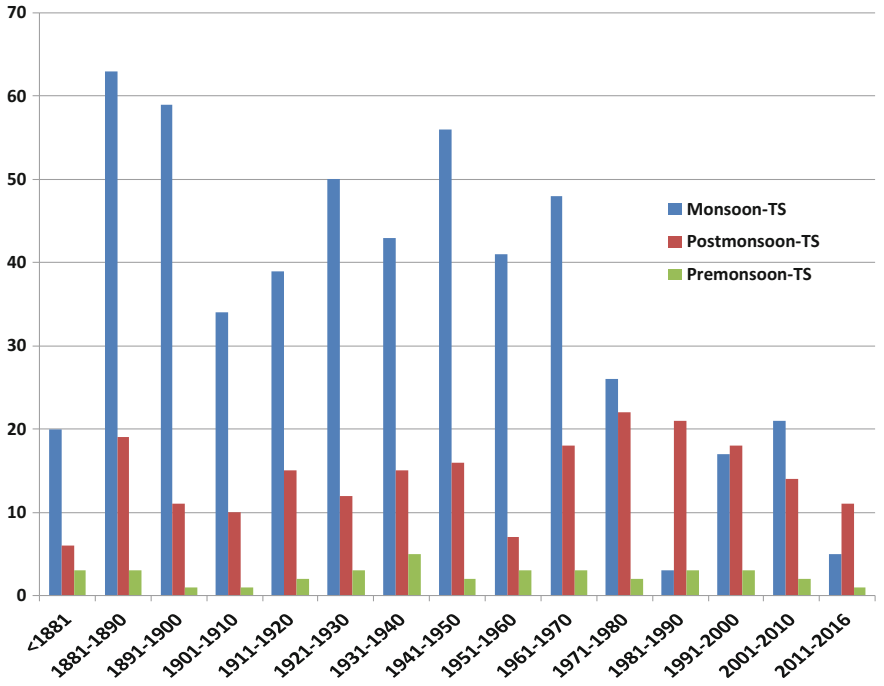

Fig. 1 Decadal frequency analysis of tropical disturbances (1877–2016) over BoB

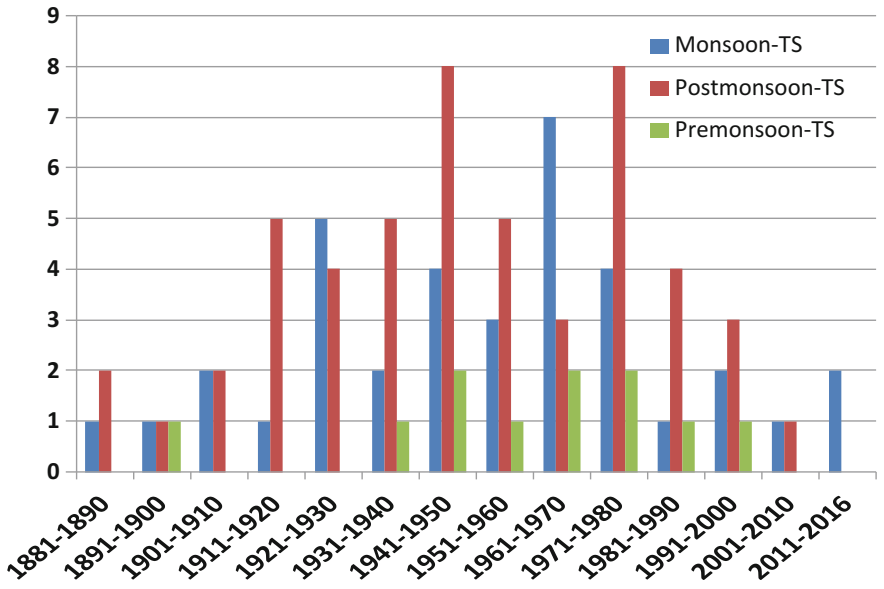

Fig. 2 Decadal frequency analysis of tropical storms (1877–2016) over Arabian Sea

Table 2 Pre- and post-1980, intensity analysis of CS and SCS over Bay of Bengal

Type of tropical cyclone	Pre-1980					Post-1980				
	May	Jun.	Sept.	Oct.	Nov.	May	Jun.	Sept.	Oct.	Nov.
CS	7	26	29	34	11	0	1	1	6	4
SCS	14	2	14	18	30	5	0	0	12	15
SCS/CS	2.00	0.08	0.48	0.53	2.73	INF	–	–	2.00	3.75

Table 3 Pre- and post-1980, intensity analysis of CS and SCS over Arabian Sea

Type of tropical cyclone	Pre-1980					Post-1980				
	May	Jun.	Sept.	Oct.	Nov.	May	Jun.	Sept.	Oct.	Nov.
CS	2	3	2	7	4	0	1	0	1	1
SCS	3	2	2	7	16	2	2	0	1	3
SCS/CS	1.50	0.67	1.00	1.00	4.00	INF	2	–	1.00	3.00

Table 4 Pre- and post-1970, intensity analysis of CS and SCS over Bay of Bengal

Type of tropical cyclone	Pre-1970					Post-1970				
	May	Jun.	Sept.	Oct.	Nov.	May	Jun.	Sept.	Oct.	Nov.
CS	6	25	27	30	10	1	2	3	10	5
SCS	13	2	11	17	22	6	0	3	13	23
SCS/CS	2.17	0.08	0.41	0.57	2.20	6.00	–	1.00	1.30	4.60

Table 5 Pre- and post-1980, intensity analysis of CS and SCS over Arabian Sea

Type of tropical cyclone	Pre-1970					Post-1970				
	May	Jun.	Sept.	Oct.	Nov.	May	Jun.	Sept.	Oct.	Nov.
CS	1	3	2	6	4	1	1	0	2	1
SCS	3	2	1	6	12	2	2	1	2	7
SCS/CS	3.00	0.67	0.50	1.00	3.00	2.00	2.00	INF	1.00	7.00

SCS but also divided in two segments, i.e., pre- and post-1970, and 1980 and rate of intensification (SCS/CS), so that we could analyse the impact of climate change on TCs intensity for both BoB and AS (Tables 2, 3, 4 and 5).

Table 2 clearly shows that rate of intensification of tropical storm in the BoB has increased significantly in the months of May, Oct and Nov post 1980s. In general, similar, observations could also be made for AS (Table 3), however, in the month of October, it has not changed.

If we take it pre- and post-1970s, then the rate of intensification is much more evident in the months of May, Oct and Nov in the BoB than pre- and post-1980s (Table 4). Similarly, for AS, rate of intensification is now much more evident in

pre- and post-1970s than pre- and post-1980s for the month of May, Oct and Nov (Table 4) and this change could be attributed to the recent warming as a consequence of impacts of ongoing climate change.

4 The Influence of Climate Change on Tropical Cyclones

In a study [14], the behavior of Indian summer monsoon in a high resolution climate model and reported that under double CO_2 conditions, fewer cyclonic depressions formed in the month of June. The historical cyclonic disturbances data studied in this paper also corroborate this finding.

Another study published in Nature Geosciences [15] reported that future projections based on theory and high-resolution dynamical models consistently indicate that greenhouse warming will cause the globally averaged intensity of TCs to shift towards stronger storms, with intensity increases of 2–11% by 2100. Existing modeling studies also consistently project decreases in the globally averaged frequency of TCs, by 6–34%. Balanced against this, higher resolution modeling studies typically project substantial increases in the frequency of the most intense cyclones, and increases of the order of 20% in the precipitation rate within 100 km of the storm centre.

Recent global climate models continue to project future decreases in global TC numbers. However, increases in the intensities of the strongest storms and increased rainfall rates are projected. Some studies suggest that, by the end of the century, the number of category 4 and 5 cyclones is expected to double, with heavier rainfall [16]. Globally, the consensus projection is for decreases in TC numbers by about 5–30%, increases in the frequency of categories 4 and 5 storms by 0–25%, an increase of 0–5% in typical lifetime maximum intensity, and increases in TC rainfall rate by 5–20% [16]. Recent high-resolution modeling studies suggest that the frequency of the most intense storms, which are associated with particularly extensive physical effects, will more likely than not increase substantially in some basins under projected 21st century warming and there is medium confidence that TC rainfall rates will increase in every affected region [16]. We obtain similar results for both BoB and AS basins from our analysis of the downscaled high resolution global model data sets produced under CMIP5 experiments. Detailed data analysis is still in progress to strengthen our findings which would be published elsewhere.

5 Conclusions

Our analysis of long-term 140 years of cyclonic disturbances demonstrates that there is a general decreasing trend in the decadal frequency of cyclonic disturbances in monsoon, pre-monsoon, and post-monsoon seasons from 1970s onwards in both BoB and Arabian Sea. Moreover, there is a general increasing trend in the Intensity

of TCs pre- and post-1970s and 1980s in the months of May, Oct and Nov. This change could be attributed to the recent rising trends of BoB and AS as a consequence of impacts of ongoing climate change. The high resolution climate model analysis also suggests that the frequency of the most intense storms in Bay of Bengal and Arabian Sea will likely to increase under projected warming during the 21st century while the total number of cyclonic disturbances should decrease. The analysis also suggests an increase of 10–15% in the rainfall associated with these disturbances within the area under influence of the storm winds.

References

1. Dube, S.K., Rao, A.D., Sinha, P.C., Murty, T.S., Bahuleyan, N.: Storm surge in Bay of Bengal and Arabian Sea: the problem and its prediction. Mausam **48**, 288–304 (1997)
2. Mohanty, U.C., Niyogi, D., Tripathy, S., Marks, F.D., Gopalakrishnan, S.G., Tallapragada, V.: Predicting landfalls, tropical cyclones, eye on the storm. IUSSTF Connect **4**(2) (2012)
3. Singh, O.P.: Long-term trends in the frequency of severe cyclones of Bay of Bengal: observations and simulations. Mausam **58**, 59–66 (2007)
4. Mooley, D.A.: Severe cyclonic storms in the Bay of Bengal, 1877–1977. Monsoon Weather Rev. **108**, 1647–1655 (1980)
5. Mooley, D.A.: Increase in the frequency of the severe cyclonic storms of the Bay after 1964—possible causes. Mausam **32**, 35–40 (1981)
6. Ali, A.: Vulnerability of Bangladesh to climate change and sea level rise through tropical cyclones and storm surges. J. Water Air Soil Pollut. **92d**, 171–179 (1996)
7. Joseph, P.V.: Change in the frequency and tracks of tropical cyclones in the Indian Ocean seas. Workshop on global change and tropical cyclone, Dhaka, Bangladesh, 18–21 Dec (1995)
8. Singh, O.P., Khan, T.M.A., Rahman, S.: Changes in the frequency of tropical cyclones over the North Indian Ocean. Meteorol. Atmos. Phys. **75**, 11–20 (2000)
9. Singh, O.P., Khan, T.M.A., Rahman, S.: Has the frequency of intense tropical cyclones increased in the north Indian Ocean? Curr. Sci. **80**, 575–580 (2001)
10. Srivastav, A.K., SinhaRay, K.C., De, U.S.: Trends in the frequency of cyclonic disturbances and their intensification over Indian Seas. Mausam **51**, 113–118 (2000)
11. Sikka, D.R.: Major advances in understanding and prediction of tropical cyclones over the north Indian Ocean: a perspective. Mausam **57**, 165–196 (2006)
12. Mande, K.S., Bhide, U.V.: A study of decreasing storm frequency over Bay of Bengal. J. Ind. Geophys. Union **7**(2), 53–58 (2003)
13. Climate Council: Cranking up the intensity: climate change and extreme weather events. Accessed at https://www.climatecouncil.org.au/cranking-intensity-report (2017)
14. Lal, M., Bengtsson, L., Cubasch, U., Esch., M., Schlese, U..: Synoptic scale disturbances of the Indian summer monsoon as simulated in a high resolution model. Clim Res. **5**, 243–248 (1995)
15. Knutson, T.R. McBride J.L., Emanuel, J.C.K., Holland G., Landsea, C., Held, I., Kossin, J.P., Srivastava, A.K., Sugi, M.: Tropical cyclones and climate change. Nat. Geosci. **3**, 157–163 (2010). https://doi.org/10.1038/ngeo0779
16. Christensen, J.H., Krishna Kumar, K., Aldrian, E., An S.-I., Cavalcanti, I.F.A., DeCastro, M., Dong, W., Goswami, P., Hall, A., Kanyanga, J.K., et al.: Climate phenomena and their relevance for future regional climate change. In: Climate change: the physical science basis. Contribution of Working Group I to the Fifth Assessment Report of the IPCC AR5. Cambridge University Press, Cambridge (2013)

Chapter 33
Study of Loss of Contact for Rectangular Footings Resting on Soil

M. Kondala Rao, N. Gopika, K. S. Vivek and C. Ravi Kumar Reddy

Abstract Urbanization with its advantages has been constantly attracting people towards towns and cities. Land availability for providing facilities for residential and commercial activities has become a major problem. The engineering solution to this crisis has been addressed through the construction of multistoreyed buildings. Conventional structural design methods neglect the Soil-structure interaction (SSI) effects which is the major concern for risks. The differential settlements and underestimation of foundation pressure are the negative effects of SSI which are to be addressed for urban disaster risk management. In this aspect, an attempt is made in this paper to address some of the issues related to SSI. To quantify the parameters influencing the SSI, A Rectangular footing with L/B (Plan dimensions L, B) Ratios varying from 1.2 to 2 is modeled in ANSYS using SHELL63 elements. The SHELL63 element is capable of modeling the soil underneath the footing. The loss of contact of footing with soil is quantified by Relative Rigidity (RR) and Critical Relative Rigidity (CRR). The analysis is carried out by varying the eccentricity of concentrated load, plan dimension ratio and the Poisson's ratio of soil. It is found that, as eccentricity of concentrated load increases the CRR decreases from 77 to 81%, for a particular L/B Ratio and Poisson's ratio of footing. As the poisons ratio μ increases the CRR value decreases from 6 to 8%, for a particular L/B ratio of footing.

Keywords Soil-structure interaction · Relative rigidity · Critical relative rigidity

M. Kondala Rao (✉) · N. Gopika · K. S. Vivek · C. Ravi Kumar Reddy
Civil Engineering Department, Kallam Haranadhareddy Institute of Technology, Guntur, AP, India
e-mail: kondalarao1530@gmail.com

N. Gopika
e-mail: gopikanallapati@gmail.com

K. S. Vivek
e-mail: vivek3393@yahoo.com

C. Ravi Kumar Reddy
e-mail: ravibecnitw@gmail.com

P. J. Rao et al. (eds.), *Proceedings of International Conference on Remote Sensing for Disaster Management*, Springer Series in Geomechanics and Geoengineering,
https://doi.org/10.1007/978-3-319-77276-9_33

1 Introduction

Most of the civil engineering structures involve some type of structural element with direct contact with ground. When the external forces, such as earthquakes, act on these systems, neither the structural displacements nor the ground displacements, are independent of each other. The process in which the response of the soil influences the motion of the structure and the motion of the structure influences the response of the soil is termed as soil-structure interaction (SSI). Conventional structural design methods neglect the SSI effects. Neglecting SSI is reasonable for light structures in relatively stiff soil such as low rise buildings and simple rigid retaining walls. The effect of SSI, however, becomes prominent for heavy structures resting on relatively soft soils for example nuclear power plants, high-rise buildings and elevated- highways on soft soil. Soil-structure interaction (SSI) analysis evaluates the collective response of three linked systems: the structure, the foundation, and the soil underlying and surrounding the foundation. Problems associated with practical application of SSI for building structures are rooted in a poor understanding of fundamental SSI principles. A rigid base refers to soil supports with infinite stiffness (i.e., without soil springs). A rigid foundation refers to foundation elements with infinite stiffness (i.e., not deformable). A fixed base refers to a combination of a rigid foundation elements on rigid base. A flexible base analysis considers the compliance (i.e., deformability) of both the foundation elements and the soil.

1.1 Brief Description of Terms and Parameters Used in the Paper

(1) LOSS OF CONTACT: To have a loss of concept, footing should have lesser rigidity when compared to that of the soil rigidity.
(2) RELATIVE RIGIDITY (RR) (L. Barden)
Relative Rigidity which is a dimensionless quantity has been defined to incorporate both the footing and soil properties in a soil structure interaction problem as (L. Barden) follows

$$\text{Relative Rigidity} = \Pi L^4 E_S / 4EI(1 - \mu^2) \tag{1}$$

where, L = length of the footing, E_S = modulus of elasticity of the soil, E = modulus of elasticity of the footing, I = moment of inertia of the footing about the shorter dimension = $BD^3/12$, μ = Poisson's ratio of the footing.
(3) MODULUS OF ELASTICITY:
Modulus of elasticity and modulus of sub grade reaction are elastic properties, a relation exists between them; the relation is given by (Terzaghi)

$$K_S = E_S/B(1 - \mu_S^2) \quad (2)$$

where, E_S = modulus of elasticity of soil, B = width of the footing, μ_S = Poisson's ratio of soil

(4) Critical Relative Rigidity (CRR)
It is the Relative Rigidity at which the footing just starts losing the contact. If the Relative Rigidity of the footing is less than the CRR, the footing will be in full contact with the soil. If the Relative Rigidity of the footing is greater than the CRR, the footing will experience loss of contact. This term quantifies the factors influencing the footing contact with the soil.

(5) Modulus of Sub grade Reaction (k_s)
It is defined as the ratio of applied stress to the deformation of soil. In other words it is the pressure required for unit deformation of soil. It is found from the plate load test results usually. This parameter is very often used in the analysis of soil structure interaction. The modulus of sub grade reaction is not a constant but a function of size of foundation.

2 Literature Review

Most of the studies on rectangular plates resting on elastic foundation are based on the classical thin plate theory as presented by Timoshenko and Krieger [5]. Khaiat et al. [4] analyzed plates on elastic foundations by the initial value method. However, the assumption that the foundation's reaction is proportional to plate deflection is not practicable in many cases. The solution method required to determine the response of plates on tensionless foundations is complicated because the contact region is not known a priori.

Plates of infinite extent, circular and rectangular shape on tensionless foundation and subjected to rotationally symmetrical load, were studied by Karniya [3], Villaggio [9], Weistrnan [11]. Zekai [12, 13] studied the problem of rectangular plates on tensionless foundations subject to uniformly distributed load, concentrated loads and moments, using the finite element technique. Weistrnan [11], Zekai [12, 13] showed that regions of no contact can develop under beams and plates that are supported on a tensionless foundation, and that the extent of no contact depends on the ratio of loads in combined loading rather than the levels of these loads. Chakrabarti and Tripathi [1] analyzed embedded steel plates with anchors in the reinforced cement concrete base. In all these studies the effects of transverse shear have been neglected. There is a definite need to study the behaviour of the plates resting on tensionless foundations, considering the realistic factors from actual engineering situations.

Plates on elastic foundation occupies a predominant role in the modern engineering mechanics, since the soil exhibits a very complex behaviour, it's response to external loads is studied. Number of investigators has done the work on footings

founded on elastic support. But many of them have not considered loss of contact phenomenon and the partial contact of footing with the soil. The springs can carry only the vertical force. Vlasov and Leont'ev [10] developed a parameter model for plates resting on elastic soil layer, where the parameters are uniquely computed using the material properties and geometry of the soil.

However, they have introduced another arbitrary 'ϒ' to represent the vertical deformation profile in the soil in their equations. But they did not provide any mechanism to determine the value of 'ϒ'. Vallabhan et al. [7, 8] developed an iterative procedure to compute the value of 'ϒ' uniquely for a beam an elastic foundation problem. Recently, Daloglu and Ozgan [2] and Turhan [6] developed a new model using rectangular finite elements to represent the plate, along with a set of consistent stiffness matrices to represent the soil. They have solved the example problems and compared with the results obtained by few other researchers. They have arrived at a conclusion that there is not a unique value for the modulus of sub grade reaction 'K' for a soil. At least two parameters are necessary to represent the effect of soil. The values of the two parameters depend on the material properties of the soil; depend of the soil medium, stiffness of the plate, and distribution of the loading. Coming to lift-off phenomenon, if the edge of plate is not anchored against lifting off, it is possible to have loss of contact. Transmission of forces will be carried out only within the contact region. This was later supported by Zekai [12, 13] who has done work on circular and rectangular footings. He has considered an elastic circular thin plate on a tensionless foundation. The plate as assumed to be loaded transversally by a uniformly distributed load, a concentrated load and an external moment. But no investigation has so far been carried out to obtain the maximum contact pressure incorporating all the factors like Relative Rigidity, eccentricity to footing width ratio, column to footing width ratio and partial contact of footing with the soil and without the assumption that soil can take tension

3 Methodology

A Rectangular Plate of Plan dimensions (3.6 m × 3 m, 4.2 m × 3 m, 4.8 m × 3 m, 5.4 m × 3 m, 6 m × 3 m) L/B Ratios varying from 1.2 to 2 considering the two way distribution is modeled using the suitable element for the analysis that is shell 63 of the footings for different eccentricity to footing width ratio (e/B)ratios, different eccentricity to length of footing ratio (e/L) that is eccentricity up to middle one third ratio. SHELL63 has both bending and membrane capabilities. Both in-plane and normal loads are permitted. The element has six degrees of freedom at each node: translations in the nodal x, y, and z directions and rotations about the nodal x, y, and z-axes. Stress stiffening and large deflection capabilities are included. The geometry, node locations, and the coordinate system for this element are shown in The element is defined by four nodes, four thicknesses, elastic foundation stiffness, and the orthotropic material properties. Orthotropic material directions correspond to the element coordinate directions. The element coordinate system orientation is as

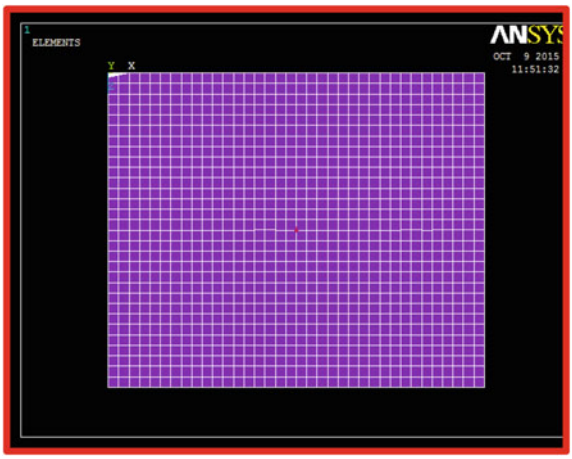

Fig. 1 Modeled rectangular plate using ANSYS

described in The thickness is assumed to vary smoothly over the area of the element, with the thickness input at the four nodes. If the element has a constant thickness, only TK (I) need be input. If the thickness is not constant, all four thicknesses must be input the elastic foundation stiffness (EFS) is defined as the pressure required producing a unit normal deflection of the foundation. The elastic foundation capability is bypassed if EFS is less than, or equal to, zero. For certain no homogeneous or sandwich shell applications, the following real constants are provided: RMI is the ratio of the bending moment of inertia to be used to that calculated from the input thicknesses. RMI defaults to 1.0. CTOP and CBOT are the distances from the middle surface to the extreme fibers to be used for stress evaluations. Both CTOP and CBOT are positive, assuming that the middle surface is between the fibers used for stress evaluation. If not input, stresses are based on the input thicknesses (Fig. 1).

4 Results and Discussions

The results that are obtained from the analysis of a rectangular plate using the ANSYS12.0 software are discussed here. Model calculations are done by taking rectangular Footing of sizes 3.6 m × 3 m (L/B = 1.2), 4.2 m × 3 m (L/B = 1.4), 4.8 m × 3 m (L/B = 1.6), 5.4 m × 3 (L/B = 1.8), 6 m × 3 m (L/B = 2.0) and the poisons ratio is 0.15 and the thickness Of Footing is assumed as 300 mm; RR = 100 And Assume a concentrated load of 500 kN.

Sample Calculations:

$$\frac{RR}{K_s} = \frac{12 \times \Pi \times (3600)^4}{4 \times 22361 \times (300)^3}$$

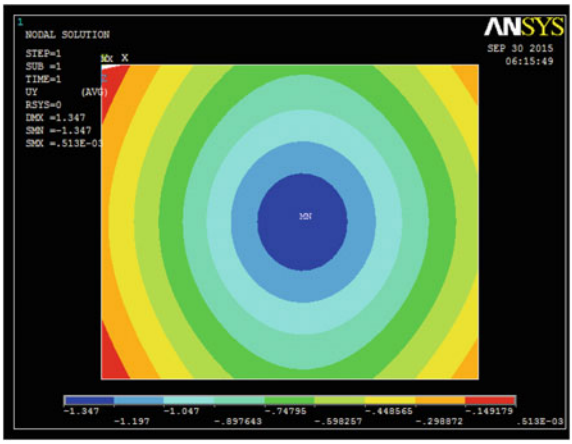

Fig. 2 Vertical displacement of the plate

Poisson's Ratio = 0.15, If RR = 100, modulus of the sub grade reaction is obtained as K_S = 0.0381 (Fig. 2).

The CRR values are obtained for different poisons ratio (0.30–0.40) for the different L/B ratios varying from 1.2 to 2.0 considering the two way distribution and eccentric concentrated load in both the transverse and longitudinal direction up to the middle one third of its shorter and longer span with reference to those values graphs are plotted for the following cases

1. CRR versus e/L Ratios for a particular L/B ratio considering a Poisson's ratio with eccentricity in longitudinal direction.
2. CRR versus e/B Ratios for a particular L/B ratio considering a Poisson's ratio with eccentricity in transverse direction.
3. CRR versus poissons ratio μ for a Particular eccentricity in longitudinal direction.
4. CRR versus poissons ratio μ for a Particular eccentricity in transverse direction.

From the Fig. 3 it is observed that as the eccentricity of concentrated load in the longitudinal direction increases for a poisons ratio, the Critical Relative Rigidity (C.R.R) decreases from 77 to 81%, for a particular L/B Ratio of footing this is because as the L/B Ratio is kept constant, the footing Rigidity is constant, if eccentricity increases there is every chance of loss of contact to bring it in contact with soil, soil rigidity should be reduced, hence Critical Relative rigidity value reduces. From Fig. 4 it is observed that as the eccentricity of concentrated load in the transverse direction increases for a poisons ratio, the Critical Relative Rigidity (C.R.R) decreases from 79 to 85%, for a particular L/B Ratio of footing this is because as the L/B Ratio is kept constant, the footing Rigidity is constant, if eccentricity increases there is every chance of loss of contact to bring it in contact with soil, soil rigidity should be reduced, hence Critical Relative rigidity value reduces.

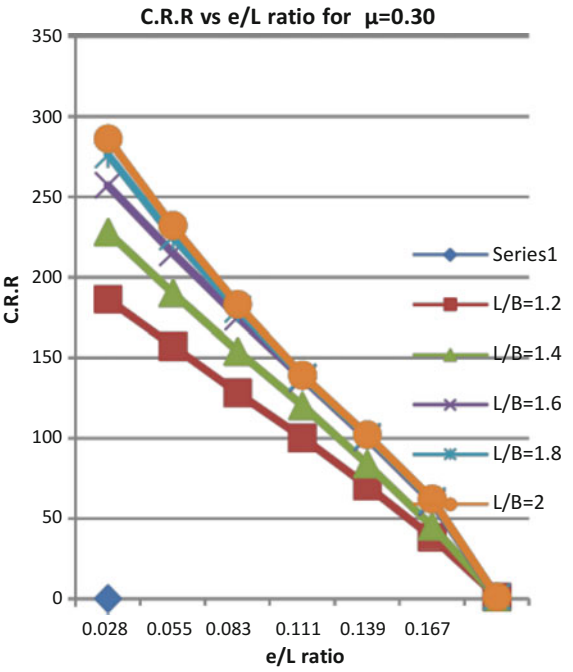

Fig. 3 C.R.R versus e/L ratio for μ = 0.30

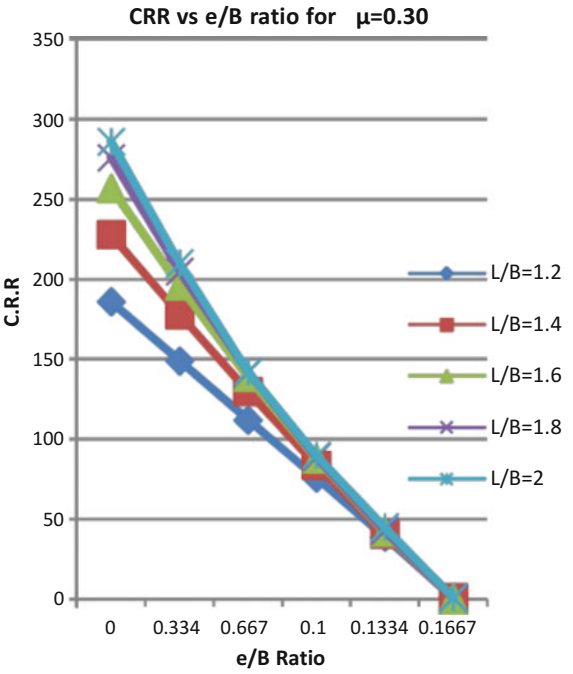

Fig. 4 CRR versus e/B ratio for μ = 0.30

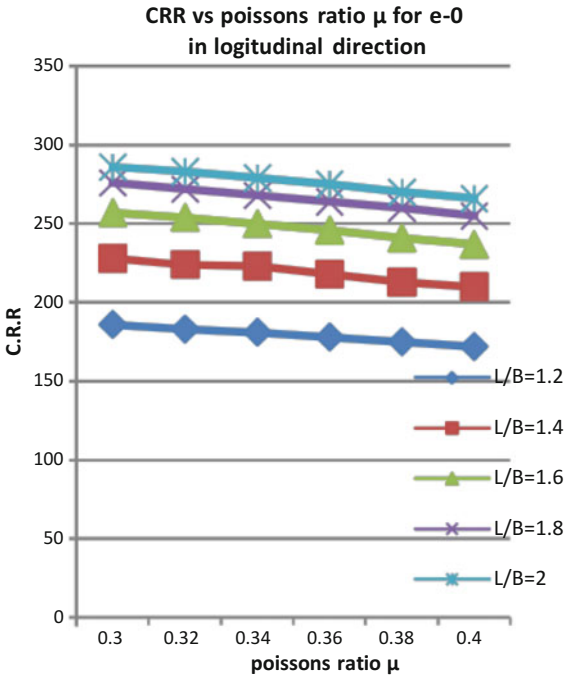

Fig. 5 CRR versus μ for e = 0

From Fig. 5 it is observed that for a particular eccentricity in the longitudinal direction as the poisons ratio μ increases the Critical Relative Rigidity (C.R.R) value decreases from 6 to 8%, for a particular L/B ratio of footing. This is because as the L/B ratio is kept constant, the footing Rigidity is constant if the poissons ratio increases there is every chance of loss of contact hence to bring it to contact with soil, soil Rigidity should be reduced, hence Critical Relative Rigidity (C.R.R) value reduces.

From the Fig. 6 it is observed that for a particular eccentricity in the transverse direction as the poisons ratio μ increases the Critical Relative Rigidity (C.R.R) value decreases from 6 to 8%, for a particular L/B ratio of footing. This is because as t he L/B ratio is kept constant, the footing Rigidity is constant if the poissons ratio increases there is every chance of loss of contact hence to bring it to contact with soil, soil Rigidity should be reduced, hence Critical Relative Rigidity (C.R.R) value reduces.

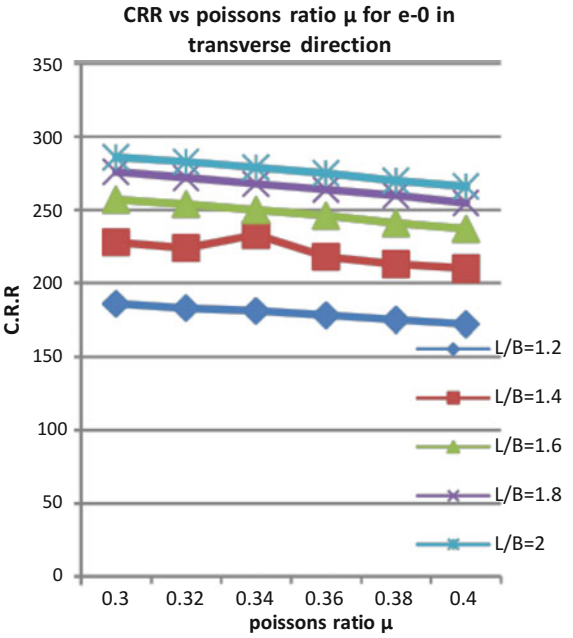

Fig. 6 CRR versus μ for e = 0

5 Conclusions

Following conclusions have been drawn:

1. As eccentricity of concentrated load in the longitudinal direction increases for a poisons ratio, the Critical Relative Rigidity (C.R.R) decreases from 77 to 81%, for a particular L/B Ratio of footing.
2. As the eccentricity of concentrated load in the transverse direction increases for a poisons ratio, the Critical Relative Rigidity (C.R.R) decreases from 79 to 85%, for a particular L/B Ratio of footing.
3. For a particular eccentricity in the longitudinal direction as the poisons ratio μ increases the Critical Relative Rigidity (C.R.R) value decreases from 6 to 8%, for a particular L/B ratio of footing.
4. For a particular eccentricity in the transverse direction as the poisons ratio μ increases the Critical Relative Rigidity (C.R.R) value decreases from 6 to 8%, for a particular L/B ratio of footing.
5. For a L/B ratio as the poissons ratio μ increases for a particular eccentricity in the longitudinal direction the Critical Relative Rigidity (C.R.R) value decreases from 7 to 8%.
6. For a L/B ratio as the poissons ratio μ increases for a particular eccentricity in the transverse direction the Critical Relative Rigidity (C.R.R) value decreases. From 7 to 8%

7. When eccentric concentrated load in the longitudinal direction is applied at the middle one third of its longer span dimension always a loss of contact will occur.

References

1. Chakrabarti, S.K., Tripathi, R.P.: Design of embedded steel plates in reinforced concrete structures. Struct. Eng. Rev. **4**(1) (1992)
2. Daloglu, A.T., Ozgan, K.: the effective depth of soil stratum for plates resting on elastic foundation. Struct. Eng. Mech. **18**, 263–276 (2004)
3. Karniya, N.: A free boundary value problem in plate theory. J. Appl. Mech. Trans. **50**(2) (1977)
4. Khaiat, H.A., et al.:Analysis of plates by the initial-value method. Camp. Struct. **24**(3) (1986)
5. Timoshenko, S.P., Krieger, W.: Theory of Plates and Shells, 2nd edn. McGraw-Hill Book, Co., Inc., New York (1970)
6. Turhan, A.: A consistent Vlasov Model for analysis of plates on elastic foundations using the finite element method. Ph.D. thesis, The Graduate School of Texas Tech University, Lubbock, Texas (1992)
7. Vallabhan, C.V.G., Das, Y.C.: Parametric study of the beams on the elastic foundations. J. Eng. Mech. **144**, 2072–2082 (1988)
8. Vallabhan, C.V.G., Straughan, W.T., Das, Y.C.: Refined model for analysis of plates on elastic foundation. J. Eng. Mech. **117**(12), 2830–2844 (1991)
9. Villaggio, P.: A free boundary value problem in plate theory. J. Appl. Mech. Trans. **50**(2) (1983)
10. Vlasov, V.Z., Leont'ev, N.N.: Beams, Plates and Shells on Elastic Foundations. Translated from Russian. Israel Program for Scientific Translations, Jeruselam (1966)
11. Weistrnan, Y.: On foundations that react in compression only. J. Appl. Mech. Trans. **37**(4) (1970)
12. Zekai, C.: Rectangular plates resting on the tensionless elastic foundation. J. Eng. Mech. **144**, 2083–2092 (1988)
13. Zekai, C.: The circular plate on tensionless Winkler foundation. J. Eng. Mech. **144** (1988)

Chapter 34
Geospatial Technologies as an Aid to Decision Support System for Assessment of Urban Floods in GHMC Areas of Hyderabad

Prathapani Prakash, Aswini Kumar Das, K. Sreenivasulu and G. Sreenivasa Reddy

Abstract Urban flooding is a manmade disaster. Increased surface imperviousness due to urbanization along with encroachments of nalas and waterbodies and inadequate drainage infrastructure system are the chief culprits for urban flooding. Flooding in an urban area brings about severe economic, structural, and environmental damages, and can be associated with casualties too. The current paper illustrates the role of GIS technology in urban drainage mapping and analysis. It identify the pre-disposing factors that lead to urban floods and explains the effect of each factor on urban floods, the trend and relationship to each other. The flooding in some areas of GHMC during September 2016 came as a grim reminder of the unprecedented Musi floods of 1908 and the recent floods in August 2000. There are about 403 different waterbodies like tanks/lakes/reservoirs in GHMC areas as identified from the Survey of India toposheets on 1:25,000 scale. Alarmingly, only a minuscule 169 lakes have a water spread of over 10 ha, an indication of how intertwined political and real estate ambitions have dealt a death blow to many waterbodies. To address city's problems, especially inundation of areas, remodelling of storm water drains (nalas) and identifying the obstructing structures on nalas and lake beds, Remote Sensing & GIS technologies are effective tools. The majority of GHMC area is drained by Musi river catchment. The Digital Elevation Model (DEM) of the entire drainage basin of GHMC is prepared using cartosat data and micro watersheds are also delineated. The daily surface runoff is calculated

P. Prakash (✉) · A. K. Das · K. Sreenivasulu · G. Sreenivasa Reddy
Telangana State Remote Sensing Applications Centre, Hyderabad, India
e-mail: prakashmhbd@gmail.com

A. K. Das
e-mail: aswini.das81@gmail.com

K. Sreenivasulu
e-mail: srinivas.taj@gmail.com

G. Sreenivasa Reddy
e-mail: gantasreddy@gmail.com

P. J. Rao et al. (eds.), *Proceedings of International Conference on Remote Sensing for Disaster Management*, Springer Series in Geomechanics and Geoengineering,
https://doi.org/10.1007/978-3-319-77276-9_34

during the flood days using Automatic Weather Stations (AWS) rainfall data. The natural drainage course is identified from the Survey of India Toposheets on 1:25,000 scale and it is compared with Revenue and Urban parcels data to find out the encroachments and bottle necks in drainage course. The required nala widths are calculated by making use of hydrological parameters. Finally a model storm water plan is developed by making use of existing nala widths to overcome the flood menace in GHMC. Hence Geospatial technology is an effective tool in mapping and analyzing the spatio-temporal data and to inform the stakeholders and decision makers of the locations in controlling flooding and improve decision making.

Keywords Floods · GIS · Nalas · Remote sensing · Urban · Watershed

1 Introduction and Background

India is struggling with disasters for many years. In India about 55% of land area is vulnerable to earthquakes, 12% of area is flood prone and 8% area is with cyclones and about two thirds of India is drought prone area. In Telangana state the major disasters are droughts and floods with occasional cyclones. As compared to other areas the urban areas are more vulnerable to floods as the anthropogenic influences in disturbing the natural water courses like streams/rivers/tanks etc. are more. In Greater Hyderabad area, the improved urbanization combined with decreasing green cover area the major cause of ill effects of floods along Musi river.

Geospatial technologies like Remote Sensing & GIS are cost effective tools to understand and plan the flood menace over a period of time [1]. The legacy map datasets like Survey of India toposheet maps and base maps of municipalities etc. when combined with Remote Sensing data could improve the decision making in and the causes of floods. A study has been taken in GHMC area of Hyderabad to arrest floods and to improve further plan of action.

2 Study Area

The study area i.e. Greater Hyderabad Municipal Corporation (GHMC) covers the entire Hyderabad District and parts of Ranga Reddy, Medchal Malkajgiri and Sangareddy districts Fig. 1, lies in between latitudes 17.19°–17.62°N and longitudes 78.22°–78.70°E and covering the topographic sheet nos. 56 K/2, 3, 6, 7, 8, 10, 11 & 12. The study area covers an area of 1437 km^2 including HMDA area and up to Outer Ring Road of Hyderabad. The population of the city is around 1 crore and the average actual rainfall during 2004–16 years of the study area is 750 mm as against to normal rainfall of 790 mm (Fig. 1).

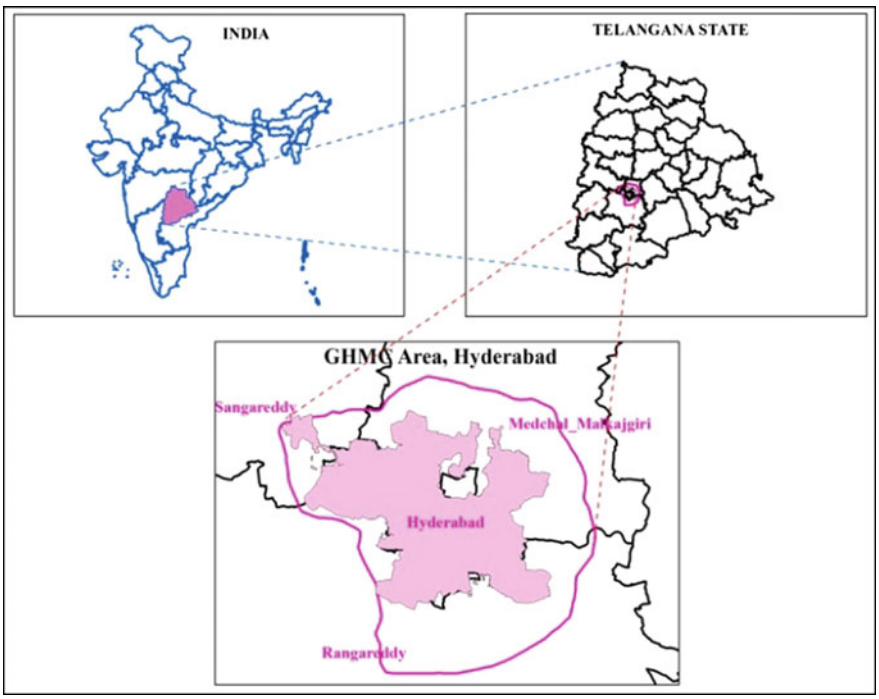

Fig. 1 Location map of study area

3 Aim and Objective

The main aim and objective of the current study is to generate different thematic maps on rainfall intensity, rainfall distribution; Kuntas/Tanks, Nalas, Stream/River network, Drainage system (pre and post periods) and preparation of a model storm water plan [2]. In the process, the following thematic layers/maps are generated:

- Spatial distribution of Rainfall and its intensity
- Micro watersheds to understand quantum of flow water generated with respect to intensity of rainfall in a catchment area
- Municipal ward map and cadastral data depicted over hydrology particulars like nalas/kuntas etc.
- Natural drainage course and present drainage course
- Digital Elevation Model (DEM)
- Waterbodies disappeared/Irregularities in natural drainage course like elimination due to human interference and illegal constructions.

4 Methodology

Overall methodology used for the plan preparation is schematically shown in Fig. 2. Data was collected to capture the background to the problem and also to perform a situation assessment [3].

A brief methodology and list of activities carried out to achieve the specific objectives are as indicated below:

- The Survey of India Toposheets (Parts of 56 K/2, 3, 6, 7, 8, 10, 11 & 12—1999 Year) on 1:25,000 scale of the study area are procured and made co-terminus with high resolution satellite imagery.
- The drainage system including waterbodies are marked and compared with the latest high resolution imagery to know the irregularities in natural courses.
- The Digital Elevation Model (DEM) is generated by using the cartosat data.
- The Micro watersheds are delineated by making use of DEM and Survey of India Toposheets.

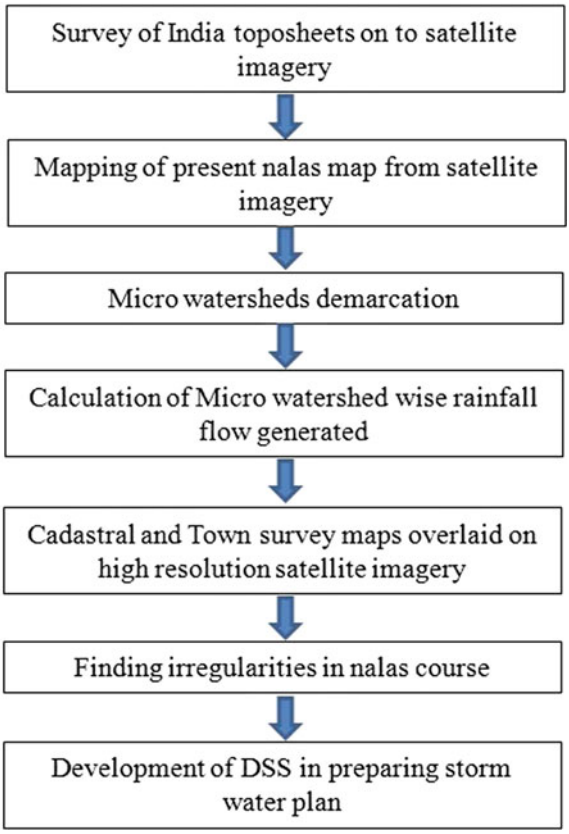

Fig. 2 Methodology for preparation of storm water plan

- The daily rainfall data during September 21–25 is collected from the Directorate of Economics & Statistics (DES) as well as Automatic Weather Data (TSDPS). The daily average rainfall as well as maximum ranfall is calculated.
- The micro watershed wise daily runoff generated during flood days (September 21–25) is calculated in CuSecs with the formula: Runoff water = Area of Micro Watershed X Rainfall.
- The cadastral/town survey maps are geocoded on to high resolution satellite imagery to identify the exact deviations in nalas courses.
- The deviations in nalas courses are identified and used in preparing storm water plans.

5 Remote Sensing and GIS Layers

5.1 Base Map

The Base Map depicting the natural drainage course like stream network, roads, tanks, reservoirs are prepared using Survey of India Toposheets on 1:25,000 scale. These maps are later referenced to high resolution satellite imagery of Cartosat-1 and World View 2 (Fig. 3).

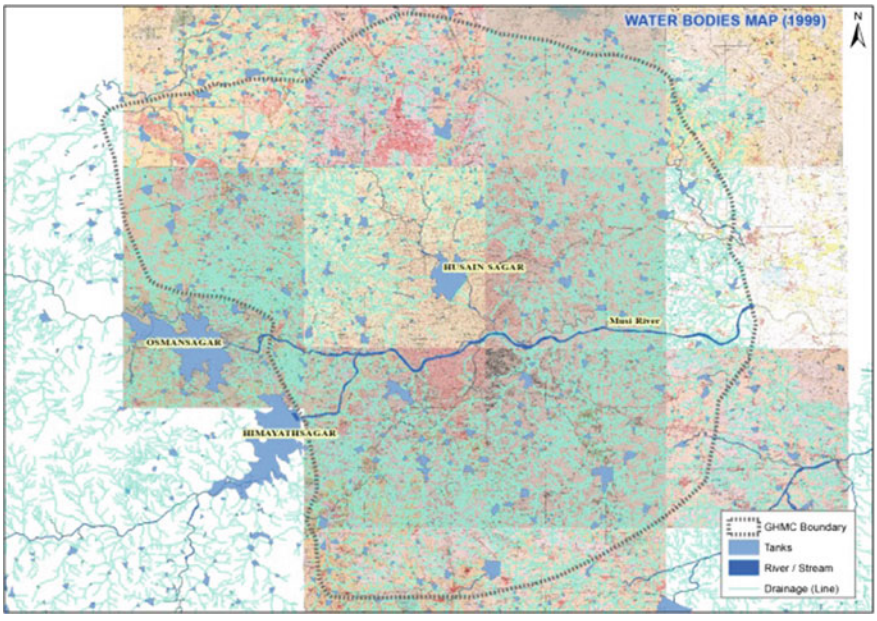

Fig. 3 Base map from survey of India toposheet

5.2 Digital Elevation Model (DEM)

The Digital Elevation Model of Musi catchment around GHMC area is prepared by using the cartosat data which depicts the elevation variations and low lying areas (Fig. 4).

5.3 Micro Watersheds Map

The micro watersheds are delineated in Musi catchment area and the daily volume of rain water generated during flooding days is calculated and as shown in Fig. 5.

5.4 Existing Nalas Map

The existing nalas (173 nos) map with segments is prepared by making use of high resolution satellite data and the blue prints collected from GHMC are made co-terminus (Fig. 6).

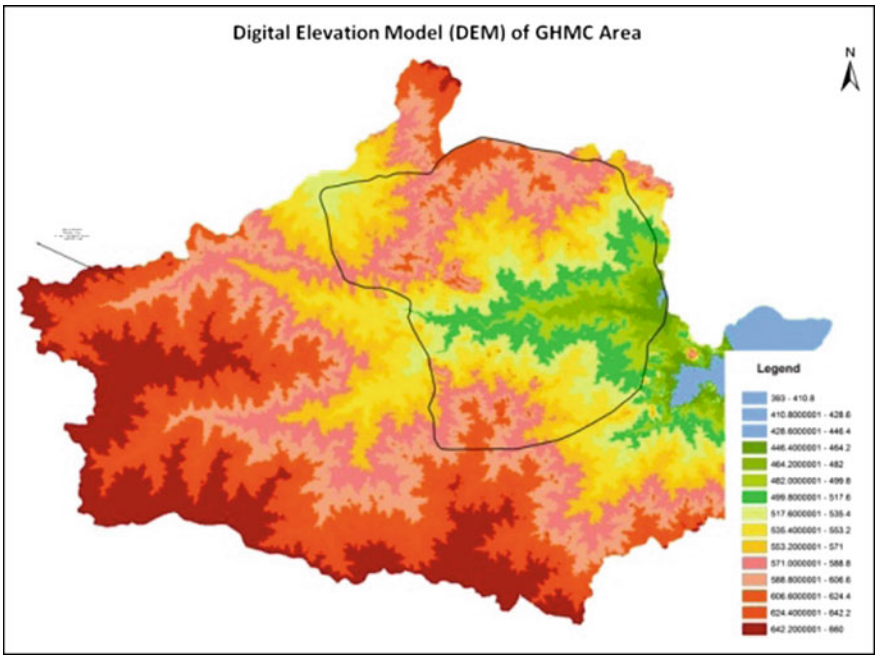

Fig. 4 Digital elevation model (DEM) of the study area

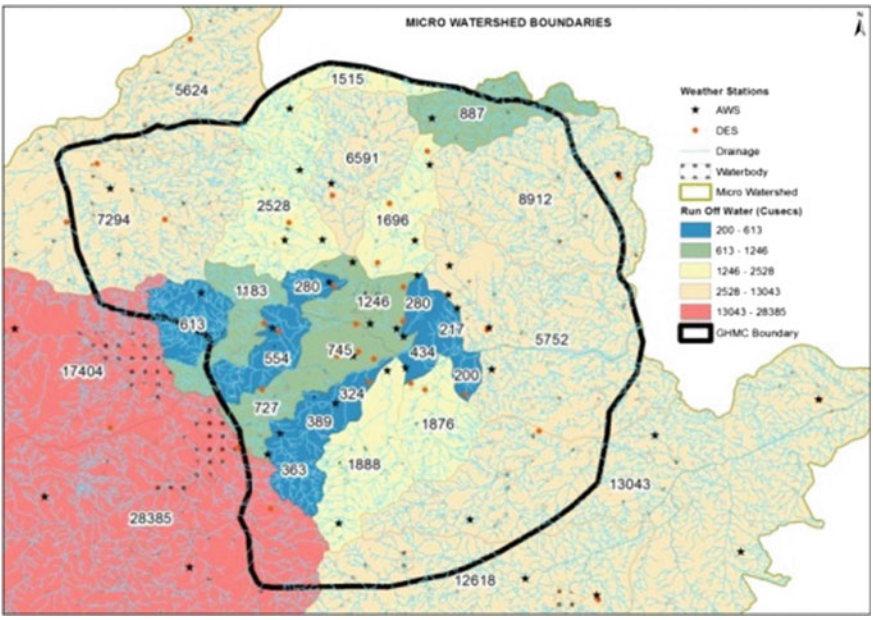

Fig. 5 Micro watersheds of GHMC area

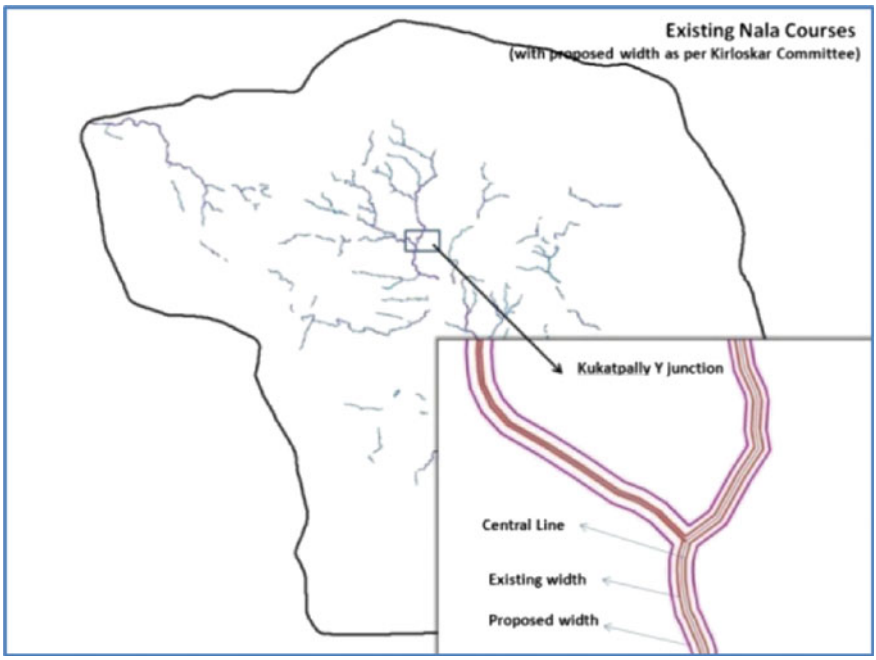

Fig. 6 Existing nalas map

5.5 Cadastral/Town Survey Maps

The non-referenced cadastral maps collected from the Central Survey Office and the Town Survey maps of GHMC area are digitized and geocoded on to high resolution satellite imagery for further studies (Fig. 7).

6 Results and Discussion

There are several causes for causing floods in GHMC area every year. The improved urganization and deforestation, the land becomes obstruction free and water flows with greater speed into water courses and causes flood. Combined to this, the instant heavy rainfall in urban area also causes water to flow its banks, resulting flooding of nearby areas. There are about 500 tanks/waterbodies are either partially or fully affected with built up areas during 1970–2016. This has reduced the water retention capacity of an area and aggravates the floods. Even the widths of Major Streams/Musi River courses are reduced greatly. At some places the steams are either partially diverted with reduced widths.

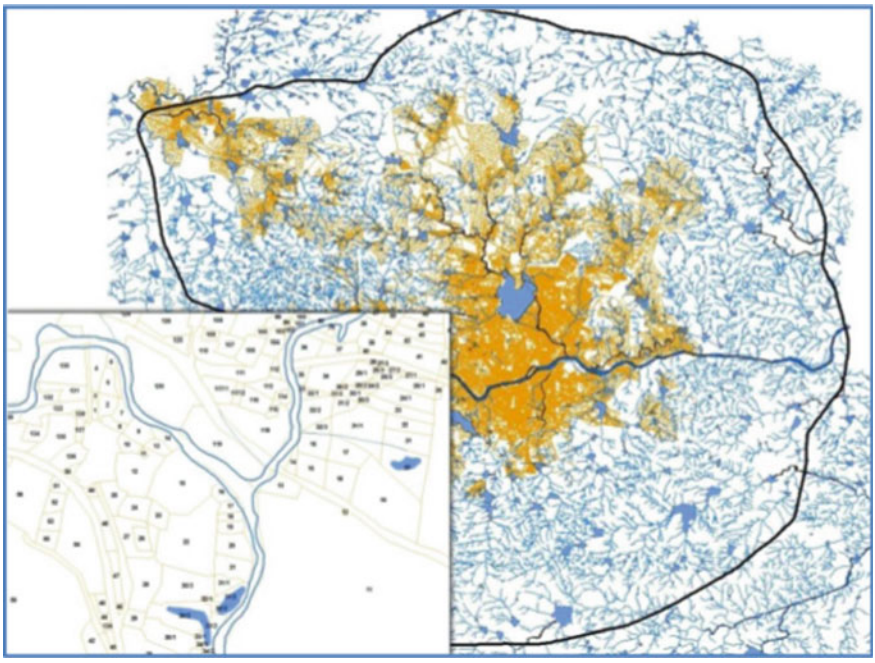

Fig. 7 Cadastral/town survey map

7 Conclusion

The flood in GHMC is a manmade disaster one involving encroachment of natural drainage courses like streams/rivers/tanks etc. The garbage disposal in the natural streams obstructs the already reduced stream widths locally and catalysed with heavy downpour in a short time which leads to flooding in the surrounding areas. The following are the other conclusions as stated below:

- The present study carried out systematic studies using Remote Sensing and GIS techniques and clearly identified the reasons/solutions for rational storm water management.
- The city has only 1500 km of storm water drains against the required length of 5000 km. The GHMC should identify the water logging hot spots using GIS techniques and geotagg the same so that the affected areas can be monitored on the map as and when they are inundated.
- The Nizam's city once flaunted a seamlessly designed network of lakes in a cascading system. The system allowed surplus water from one lake to cascade into the next and eventually flow into the Musi River. But presently the chain of tanks system has been ruptured repeatedly over the past many decades. Waterbodies along these networks have been ruthlessly blocked to make way for real estate projects, which in turn has resulted in frequent inundation of localities. There is a need to fix and restore the Full Tank Levels of all water-bodies and also establish the linking system.
- The storm water drains, constructed during the Nizam's era, were planned for a population of five lakh and needs to be redesigned to suit to the present times.
- The Remote Sensing based GIS data can be used in preparing the storm water plans.

Acknowledgements Authors are thankful to Telangana State Remote Sensing Applications Centre (TRAC), Hyderabad for giving permission to carry out this work at esteemed office.

References

1. Maidment, D. (ed.): Arc Hydro, GIS for Water Resources. Environmental Systems Research Institute, Inc., Redlands, CA (2002). ISBN 1-58948-034-1
2. Lilesand, T.M.: Remote Sensing and Image Interpretation, p. 721. Wiley, USA (1989)
3. Wijesekera, N.T.S., Bandara, K.M.P.S.: Preparation of the stormwater drainage management plan for Matara municipal council. Engineer: J. Inst. Er **44**(3), Sri Lanka (2011)

Chapter 35
Towards Resilient Transportation Systems for Effective Cyclone Management—City of Visakhapatnam

Varsha Akavarapu and Maqbool Ahmed

Abstract Climate change and sea level rise, have been a constant phenomenon affecting millions of people through cyclones and sudden flooding effects the performance of the infrastructure systems. The mobility plays a very crucial role in infrastructure systems, for the prosperity, growth and the movement of communities at all levels. At the local and regional levels, transportation serves a very large crowd working effectively and performing diverse activities all at the same time, which makes people vulnerable to any kind of disruptions. This highlights the requirement of robust transportation systems to, absorb effects from disturbances that are caused due to several reasons and ensure operational continuity. Visakhapatnam, has been a victim of major cyclones over the years. Approximately 448 km of road has been disrupted with a loss of Rs. 1,111 Crore. Since the occurrence of HUD HUD, "Planning for resilience" has been initiated by the governmental agencies and in this context, Visakhapatnam has been cited as one of the first cities undergoing major structural changes for the same. In this regard, this paper would focus mainly on measuring the resilience of the transportation systems by evolving a context specific framework measuring across the four major dimensions of resilience—Robustness, Redundancy, Resourcefulness and Rapidity.

Keywords Resilient infrastructure systems · Planning for resilience
Disaster management · Transportation systems · ICRSDM

V. Akavarapu (✉)
Department of Planning (Former B.Plan Student),
School of Planning and Architecture, Vijayawada, India
e-mail: varshaakavarapuk@gmail.com

M. Ahmed
Department of Planning, School of Planning and Architecture, Vijayawada, India
e-mail: maqbool@spav.ac.in

P. J. Rao et al. (eds.), *Proceedings of International Conference on Remote Sensing for Disaster Management*, Springer Series in Geomechanics and Geoengineering,
https://doi.org/10.1007/978-3-319-77276-9_35

1 Introduction

Advances in the automobile industry have caused considerable increase in global temperatures triggering climate change that further heightens the occurrence of a disaster. A disaster—natural or man-made, is an extreme disruption of the functioning of a society that causes widespread human, material, or environmental losses, that exceed the ability of the affected society to cope with its own resources [1]. The Modernist's view and social understanding of the disasters argues that, the distinction made is artificial, considering the fact that disasters result through the action or inaction of the people and their social, economic and political structures [2]. Further, researchers have claimed that it is often the result of human activities that degrade the environment. While this can form one argument as to what causes the disasters occur, the other argument arises from the background of the people—their socio economic status due to which they live in the areas susceptible to the sudden disruptions. Both the arguments are again compounded by the sudden, seasonal or annual fluctuations besides the unpredictability of the frequency, timing and the magnitude of the disasters, which lead to economic losses. In such scenarios where the quality of life of people is hampered, it has become an imperative for various states to plan for mitigation, essentially involving pre-disaster planning in order to strengthen the social and physical systems of disaster prone areas before the onset of a calamity. Such, planning interventions for effective mitigation of the disasters has taken precedence since the 1980s under the pretext of disaster risk reduction, which was also one of the major agenda's of the Hygogo (2005-2015) and Sendai framework (2015-2030). Both the plan of actions, especially the Sendai framework of action, that has been announced as a continuation to the Hyogo framework has set the agenda for sustainability through which disaster risk reduction and climate change are proposed to be addressed and approached in the years to come.

Disaster Risk Reduction (DRR) as a construct, intends to systematically avoid (prevent) and limit (prepare/mitigate) disaster risks with regard to losses in lives and the social, economic and environmental assets of communities and countries [3] which specifically is defined as an approach that targets multiple hazards, reducing the vulnerability through planned measures and strengthening the capacities and thus enhancing the resilience of the communities and their livelihoods. With such a definition, it becomes important to shift the focus away from merely responding to a disaster after its occurence to initiate risk reduction based strategies well before the disaster actually strikes.

The UNISDR in 2015, after evaluating the progress of HFA (2005–2015), proposed for an agenda for sustainable development—"Transforming our World: 2030"—a transformative plan of action for all countries and all stakeholders. This is an intense plan of action for all the countries, including all the stakeholders to implement 17 Sustainable Development Goals (SDGs) and about 169 targets pertaining to the SDG's, out of which 25 targets relate to disaster risk reduction in 10 of the 17 SDG's—firmly establishing the role of disaster risk reduction and building resilience as a core development strategy re-affirming the urgent need to reduce the

risk of disasters. The 2030 agenda also resonates with the SENDAI framework for Disaster Risk Reduction (formulated in the same year of 2015 up until to 2030)—identifying the need to build resilient infrastructure in order to make cities and its residents resilient [4]. Investing in disaster risk reduction has become a precondition for developing sustainability in an ever changing climatic condition due to the plan of action initiated by the UN.

India, after participating in the SENDAI framework convention has identified the requirement to plan for resilience and has selected tier—1 and 2 cities, justifying that the urban areas are the most susceptible to external shocks and stresses (including climate change). D ue to the fact, that their ecosystems are continuously challenged by various socio-economical factors. These theat impact the urban poor the most - often due to their locational and residential factors or their lower ability to adapt to and respond to calamities. In this repesct certain states in India, such as Gujarat (Surat), Andhra Pradesh (Visakhapatnam) and Assam (Guwahati) have taken commendable strides in planning for climate change by incorporating resilience into their state level disaster plans and further detailing out context specific resilience in the city level disaster plans.

2 Focus of the Study

When a natural disaster is struck, it is the people, infrastructure and the economy that are most adversely hit. Certain types of infrastructure play vital roles in underpinning our economy, security and way of life. These complex and often interconnected systems have become so ubiquitous and essential to workings of day-to-day life that they are easily taken for granted. Often it is only when the important services provided by such infrastructure (Fig. 1) are interrupted such as access to electricity, health care, telecommunications, transportation, access to sanitation, water. For example—that we are conscious of our great dependence on these networks and of the vulnerabilities that stem from such dependence [5].

There is no universal definition of Critical Infrastructure (CI). CIs include a range of engineered systems, assets and facilities which are essential for day-to-day societal functions, as well as continued economic and societal functioning in the aftermath of a disaster event. Critical Infrastructures are divided into physical and socio-economic systems. Physical CI deal with all the basic services, while socio-economic systems encompass organisational and communicational systems. As can be noticed in Fig. 1, all of the CI's are interconnected and inter-dependent systems that fail in the absence or disruption of any other system and it is the transportation system that connects each of the components and hence should be identified as the most critical of the infrastructure systems that require planning for structural resilience.

Transportation systems and networks are critical for the prosperity and growth of communities at all levels, i.e. local, regional, national or international [6]. At the local and regional level, the expansion of large, modern cities due to the increase of

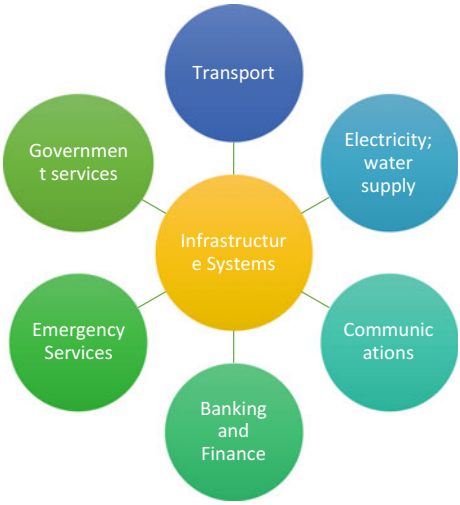

Fig. 1 Critical infrastructure systems (CI's) [5]

population forces the transportation systems to effectively serve a large crowd performing diverse activities all at the same time, increasing its complexity manifold. At the national and international level, globalisation has forced researchers and experts to design and implement complex and large scale systems to integrate all the transportation means in multinational routes for passengers and cargos. Due to this complexity, transportation systems are: (a) multi-modal in terms of passengers and freights transportation, (b) multi-faceted in terms of impact to the society and (c) multi-parametric in terms of design operation and management [7]. In any case, robust transportation systems are required to absorb effects from disturbances that are caused due to several socio-political-environmental reasons and yet ensure operational continuity [7].

- The components of transportation systems can be divided into two categories: the internal (physical) and the external components [5]. While the internal components deal with the structural variables, the external components deal with the organisational and political constructs of the transportation systems. It can be understood from Fig. 2. Here that transportation systems, irrespective of the division are highly dependent on the road networks to function and hence, one of the focus of the study would be to look into how to make the physical structures resilient? The next section - details out the literarture that was studied and anlysed in order to formulate a framework that can measure the current scenario of resilience in an given area and identify its strengths and weaknesses.

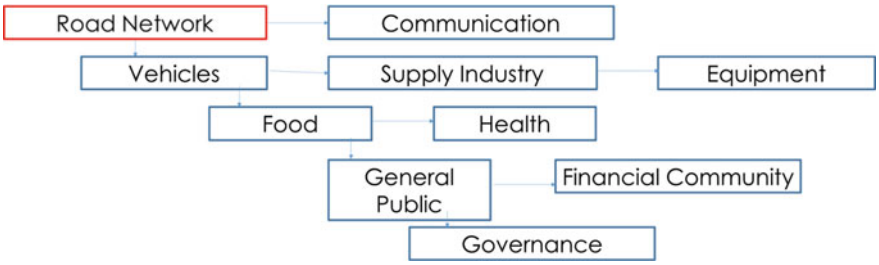

Fig. 2 Interdependency of transportation systems on road network

3 Conceptualising Resilience and its framework of measurment.

Resilience' as a term was first employed by a Scottish engineer to describe the strength and ductility of steel beams in an applied context as a descriptor for robustness of cladding of iron ships (1858) [8]. It was in the early 20th century that 'resilience' as a term evolved to be applied in various schools of thought—medicine, psychology, engineering and textile industry [9]. Late 1950's gave rise to the identification of characteristics of resilience in engineering (robustness and redundancy) and later in psychology (resourcefulness and recovery–addressing vulnerability) [10]. It was in the 1990's when resilience as a concept transitioned from natural ecology [11] to human ecology [12]. In the social sciences, resilience is often considered as a strategy to disaster risk reduction (first mentioned in the Hyogo framework of action) as a means for the socio-ecological systems to bounce back after they have been hit by an uncertainty. Ever since, engineering and the social science disciplines have identified ways to measure resilience both qualitatively and quantitatively. Bruneau et al. [13], conceptualised a quantitative framework to measure and define seismic resilience of communities through identifying 4R's – Robustness (strength or resistance), Redundancy (alternative options during stress), Resourcefulness (ability to identify problems) and Rapid recovery (speed with which losses are overcome and re-stability is achieved) across 4 dimensions: Technical, Organizational, Social and Economic (TOSE) constraints (Fig. 3) [14], while measuring the resilience for transportation systems added 10 variables along the lines of four dimensions mentioned above. While resilience had become quite a prominent concept in the field of engineering, the social sciences, especially the school of spatial planning and geography, began drawing dimensions and formulating frameworks to measure resilience across geographies and communities [8]. Resilience as *stability*, resilience as *recovery* and resilience as *transformation*.

The more advancement humans make, greater is its impact on the society and the more it becomes necessary to build resilience into the communities and infrastructure [15]. Sudden impacts to human life cannot be averted, nor can be the

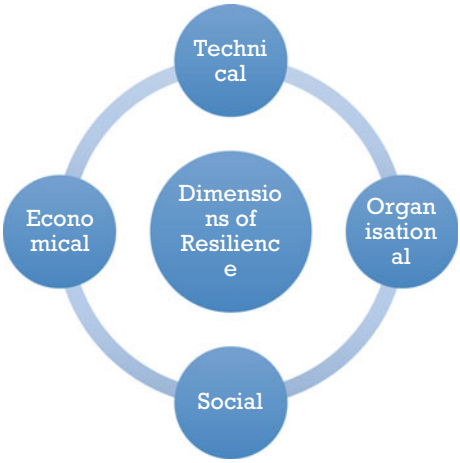

Fig. 3 Dimensions of Resilience [13]

uncertainty that it brings. The society can only be prepared to minimize the impact and return to a normal setting within the shortest possible time, and with the help of as little external resources as possible. Resilience in spatial planning, especially in disaster management is a tool that is extensively utilised in the pre-disaster planning process, to measure the standing of a society/a locality/a city/a region as against to an impending impact—necessarily involving mitigation measures. It can also form a part of the post-disaster planning process, where adaptation measures are concentrated upon, essentially serving as a tool for DRR in both the contexts. Manyena et al. [16] highlight that disasters are accompanied by change, and that instead of resilience involving 'bouncing back' after an event, it should involve 'bouncing forward' and 'moving on'. They argue that 'bouncing back' does not signal change, and may involve returning to the conditions that may have caused the disaster in the first place. They conclude that resilience can be viewed as the 'intrinsic capacity of a system, community or society predisposed to a shock or stress to bounce forward and adapt in order to survive by changing its non-essential attributes and rebuilding itself'. Resilience is considered the ultimate objective of hazard mitigation, that is, "action taken to reduce or eliminate long-term risk to people and property from hazards and their effects" [17]. Levina [18] proposes two key differentiators in resilience definitions, the first being the ability of a system to withstand a disturbance without changing (whether by improvement or deterioration), implying that no damage is done whatsoever, and the second, differentiator is the ability of the system to recover when damage has already occurred. Supplementing to this argument, Maguire and Cartwright (2008) [19] identify three views of resilience: resilience as stability, resilience as recovery and resilience as transformation.

In the context of DRR, it becomes important to understand the various approaches mentioned to measure resilience, not necessarily mean the same as the strategy of building resilience [19]. For example, vulnerability—is a key concept which can be viewed as a component of resilience or could be considered as one

end of a spectrum [18]. In certain scenarios, like in Belize, a vulnerability assessment in terms of aqua culture was taken up to identify the vulnerable species and plan for resilience. Similar studies were taken up in the pacific islands where LiDAR images were used to map hazards as a means to identify key areas vulnerable to climate change [20]. As a contrast, an integration of the social sciences and engineering approach was undertaken in the Republic of Mandova which resulted in changes in Infrastructure design and operations in hospitals [21]. A risk assessment technique could also be adopted as a measure for resilience, like in Madagascar where policies for flood resistant infrastructure and various standards for transport were formulated [22]. In cities like New Orleans, resilience is enhanced through community-led actions, where people unite to build strong neighbourhoods to overcome disasters [23]. Through this, it can be understood that resilience can be measured across the TOSE (Fig. 3) dimensions irrespective of the discipline or school of thought, where understanding vulnerability, hazards and/or risks help in creating a shared learning process among various stakeholders in creating or rather building resilience. Overall, an integrated framework, emphasising on the role of specific systems or system components in formal or informal institutional setups, can help build a case to work towards resilience—measuring first and building next. The next section will detail out the measurement aspects of resilience, in terms of transportation systems, along the simensions mentioned in the above section.

3.1 Transportation Systems and Resilience—The Construction of a Framework

It is understood from the above sections that the idea of resilience when viewed through a critical lens, considers not only natural calamities, but encompasses disaster reduction, more generally, but not limiting to financial shocks, terrorism, chronic stresses and so on. Producing a meaningful index, for something as complex as the resilience of a city—including an all hazards approach is burdened with reputational, conceptual and execution risk [23]. Human wellbeing in the urban context often relies on a complex web of interconnected institutions, infrastructure and information. Cities are also known as growth centres since they are the hubs of economic activity, opportunity and innovation. These very areas are also places where sudden shocks occur that may result in social breakdown, physical collapse or economic deprivation [24]. In such scenarios, risk assessments and certain measures to contain foreseeable hazards will prove to play an important role in urban planning. Several frameworks were developed since after the Hyogo Framework and the recent Sendai Framework to measure the current resilience in urban contexts. However, most of the measuring techniques developed are either hazard specific or dimension (TOSE) specific, measuring the susceptibility to disruption across specific sectors. For example Brueneu et al., [13] developed a

framework to quantitatively assess and enhance the seismic resilience of communities—increasing the vulnerability of the communities involved to various other risks. Similarly, New Zealand developed a National infrastructure policy in 2011 [25], which specifically entails the techniques to measure resilience of transportation systems, where an all hazards approach was chosen, where the framework was proved to be highly subjective dveoid of technicalities. Understanding the qualitative aspect of the study helped in highlighting the importance of quantitative aspects of research and since this study is limited to understanding resilience and/in terms of transportations sytems, it becomes necessary to look into how the concepts of resilience can be linked to transportation systems and if there are any qualitatuve and quantitatvie methods to measure how strong the systems are for future impacts?

As it has been established, the resilience of transport systems to natural hazards has a determining influence on key transport performance indicators, such as reliability, safety, and cost effectiveness. These, and should be specified as a key goal and objective in transport planning. In order to increase the strength of transportation systems or any infrastructure in that matter, hazard mitigation and climate change adaptation should be integrated within transport plans through the greater use of hazard mapping tools and contextually appropriate design approaches. Setting resilience as a key transport objective also goes hand-in-hand with an approach that seeks to understand the role of the asset in the network and its contribution to the economy and community. This entails a greater consideration of the principles of redundancy, safe failure, diversity, and flexibility in the development.

The world bank technical report of 2015 has made a resilience measuring framework involving spatial planning attributes, infrastructural planning attributes linking them with environment and post disaster risk and recovery planning support identifying certain factors effecting the resilience of transportation systems in specific (Fig. 4).

A SMART Transportation Alliance technical Report of 2015 has identified two major or key aspects of transportation resilience—that of Risk Analysis and Risk Mitigation. The proposed adaptation process sets out to be implemented periodically as a part of the local/regional/national transportation network decision-making process. Various technical measurements exist to understand the technicality of the transportation systems. One such method is the Network Robustness Index, which measures the robustness of a network based on certain indicators on TransCAD [26].

A transportation Resilience measuring framework was thus developed, through the literature study, involving both the qualitative and quantitative methods and the principles of resilience—robustness, redundancy, resourcefulness and rapid recovery, which are captured through various methods.

- Robustness—through the application of Network Robustness Index.
- Redundancy through a performance Index—evolved based on the context of the case being investigated.

Fig. 4 Factors effecting resilience of transportation systems

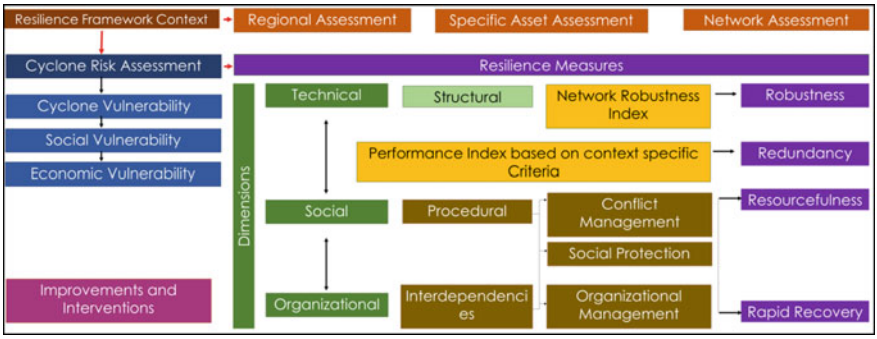

Fig. 5 Transport resilience framework (author)

- Resourcefulness, through context specific indicators evolved for conflict management and social protection.
- Rapid Recovery, through context specific criteria evolved only for the organisational management (Fig. 5).

The context of the framework, on broader terms is divided into three major aspects—Regional Assessment—which deals with the regions as a whole; for example: areas with a specified boundary defined on the basis of administrative terms or prone to disasters or areas high in below poverty line population etc. The second aspect, is the Specific Asset Assessment (SAA), which heavily relies on one

particular asset—be it a building of a particular land use or a structure of cultural importance and the third aspect is the Network Assessment—which is basically the analysis of a particular network—be it the road network or the water supply network or the communication lines. After specifying the context, the first major assessment is to delineate the area of study based on its vulnerability to cyclones and this includes the Cyclone Risk assessment—which also consists of cyclone vulnerability assessment, social vulnerability assessment, economic vulnerability assessment and a physical vulnerability assessment—all of which have underlying and specified attributes which lead to the delineation of the area that is highly prone to cyclonic disruption. The delineated area will then be measured for resilience using varied qualitative and quantitative methods inclusive of the four major dimensions of resilience—robustness, redundancy, resourcefulness and rapid recovery. Robustness is measured through Network Robustness Index which measures the strength of the road network through delay caused in total time of travel, while moving from one place to the other. Redundancy, resourcefulness and rapid Recovery are measured through indicators developed through literature which are then marked on a scale of 1–4 on the basis of how the indicators were dealt in the past when severe cyclonic storms took place in the case study area. The marks achieved in all the indicators are then summed up to understand the present scenario and considering the scores, interventions for the future—"planning for resilience" are considered.

4 Case Study—City of Visakhapatnam

The City of Visakhapatnam, also known as Vizag, is one of the important cities on the east coast of India. It is the industrial capital of the state of Andhra Pradesh. Its health infrastructural facilities and educational opportunities made it as the destiny for the people of the bordering state like Orissa, and Chhattisgarh. Visakhapatnam experiences a variety of natural disasters throughout the year Visakhapatnam has been hit by many cyclones over the years, of which HUD HUD has been the worst. The city then devised a Disaster Management plan for the city. When the transition from the Hyogo Framework of Action to Sendai Framework of Action took place, the world bank sponsored certain projects in the India—Surat, Assam and Andhra Pradesh, to plan for its infrastructure to be resilient and the Greater Municipal Corporation of Visakhapatnam has taken up the project and is presently working towards planning for resilience and incorporating it in the DMP. This research is to identify certain mechanisms, firstly to understand the level of resilience in the city and then to plan for it—hence to understand the mechanism, transportation systems have been selected and the framework developed will be applied for the city of Visakhapatnam.

4.1 Demonstrating the Framework

The context of the framework, on broader terms is divided into 3 major aspects—Regional Assessment—which deals with the regions as a whole; for ex: areas with a specified boundary defined on the basis of administrative terms or prone to disasters or areas high in below poverty line population etc. The second aspect, is the Specific Asset Assessment (SAA), which heavily relies on one particular asset—be it a building of a particular land use or a structure of cultural importance and the third aspect is the Network Assessment—which is basically the analysis of a particular network—be it the road network or the water supply network or the communication lines.

After specifying the context, the first major assessment is to delineate the area of study based on its vulnerability to cyclones and this includes the Cyclone Risk assessment—which also consists of cyclone vulnerability assessment, social vulnerability assessment, economic vulnerability assessment and a physical vulnerability assessment—all of which have underlying and specified attributes (constructed based on the case area-susceptible to change according to the context) which lead to the delineation of the area that is highly prone to cyclonic disruption (Fig. 6).

The delineated area (Fig. 7) will then be measured for resilience using various qualitative and quantitative methods inclusive of the four major dimensions of resilience—robustness, redundancy, resourcefulness and rapid recovery.

Robustness is measured through Network Robustness Index which measures the strength of the road network through delay caused in total time of travel, while moving from one place to the other (Fig. 8).

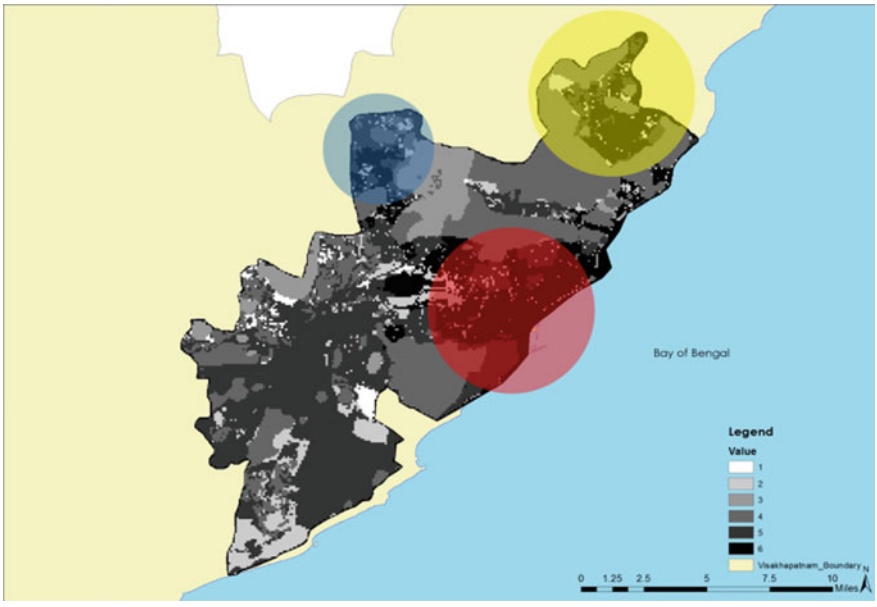

Fig. 6 High cyclone prone area (in red)

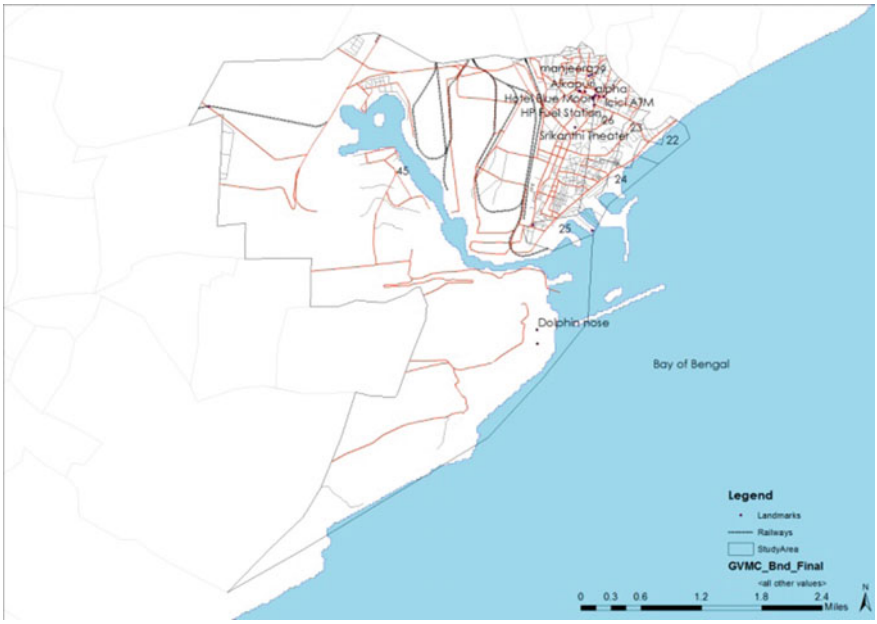

Fig. 7 The delineated area of study

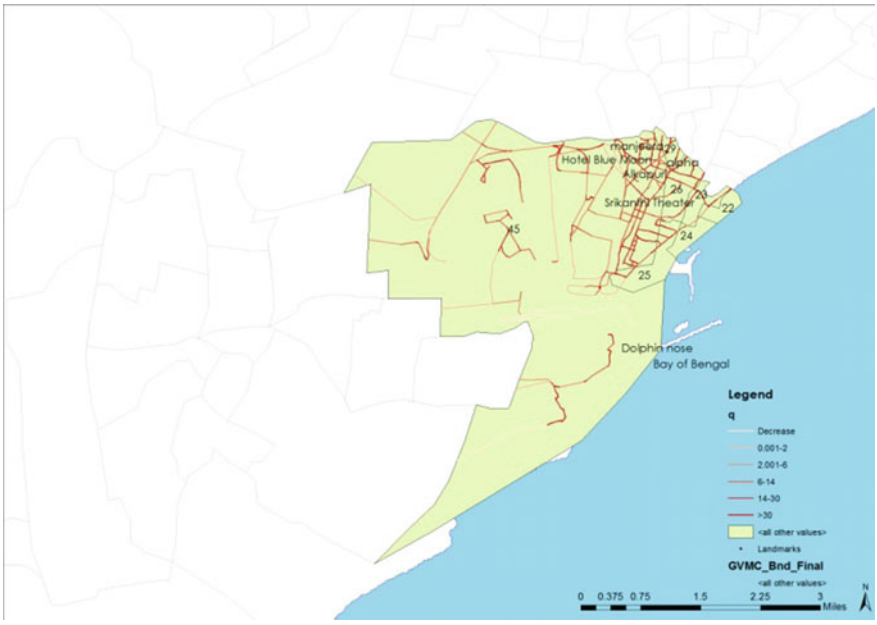

Fig. 8 Increase in travel time—NRI

Redundancy, resourcefulness and rapid Recovery are measured through indicators developed through literature which are then marked on a scale of 1–4 on the basis of how the indicators were dealt in the past when severe cyclonic storms took place in the case study area. The marks achieved in all the indicators are then summed up to understand the present scenario and considering the scores, interventions for the future—"planning for resilience" are considered.

The rest of the dimensions were measured based on certain evolved indicators which were marked again, based on the marking scale specified and a cumulative score for the present resilience as observed in the city was achieved.

Dimension	Aspect of measurement	Measure	Item of measurement	Score
Robustness	Structural	Network robustness index	Road network	2
		Accessibility to evacuation shelters	Road network	3
		Exposure of critical assets to cyclone	Social infrastructure	4
	Design	Design codes for resilience	DDMP, building bye-laws	2
Redundancy	Procedural	Access to lifeline utilities	Road network	3
		Network availability	Road network	2
		Action plans	Plans documents	3
		Access to emergency services	Cyclone reports/ public survey	3
		Access to emergency services for emergency vehicles	Cyclone reports/ public survey	3
Resourcefulness	Procedural	Social protection	Evacuation shelters	3
			Transport mechanisms to evacuation shelters	2
		Conflict management	Mobile technology	4
			Radio communications	4
			Backup equipment	3
Rapid recovery	Interdependency	Organizational capabilities	Roles and responsibilities	4
			Responsiveness	3
			Skills/tool/resources	2
Total				50/ 68

Certain gaps were identified, which are to be considered and addressed while planning for disaster resilience

- Increasing robustness should be a priority—addressing it structurally.
- Design codes for resilience to be developed.
- Redundancy—to be improved based on the past experiences of Phailin and HUD HUD.
- Organizational resilience should be targeted.

5 Conclusion

The Application of the transport resilience framework highlighted certain gaps in all of the four dimensions. When the aspect of robustness is considered, the network robustness Index was again considered, taking 2017 as the base case year. Traffic volumes were projected using the for the years 2030 and 2050 using time-line multiple regression analysis where the constants involved were—the total population and the employed population—projected for 2030 and 2050 respectively and the NRI was built for the same at a + 1 iteration, removing each link for each of the iteration. For the year 2030, the change observed from the base case is 8.7%, indicating that disruption of certain major links, exceeding the capacity can cause re-routing troubles, since the performance i.e., the flexibility is targeted (Fig. 9).

For the year 2030, the change observed from the base case is 24.7%, indicating that disruption of even one major link, exceeding the capacity indicating that the disruption of any link in the case study will lead to the automatic disruption of all the links—owing to a travel time difference of up to 33 min. In such scenarios, certain design codes for resiliency targeting the network should be developed alongside the building bye-laws. Since climate change predicts that future extreme storm events are going to occur, some planned infrastructure changes include:

Fig. 9 Projected NRI—2030 and 2050

- Reconstruct and upgrade streets damaged by cyclones to include resiliency features;
- Integrate a variety of climate resiliency features into future street reconstruction projects;
- Including water management best practices and tools. These features allow water captured on streets to soak into the ground rather than flow into the sewer system, resulting in lower drainage loads on both sewers and wastewater treatment plants;
- Installing bioswales (planted areas in the sidewalk designed to capture storm water from the adjacent roadway) and/or pre-cast permeable concrete gutters, and adding or raising bulkheads top help prevent street flooding;
- Make sure traffic signal electronics are above flood levels and include emergency generators;
- Install floodgates and raise entrances to flood vulnerable traffic tunnels.

References

1. Environment, W.M.: Climate Change Effects and Impacts Assessment—A Guidance Manual for Local Government in New Zealand, 2nd ed. (2008)
2. Beatley, T.: The vision of sustainable communities. In: Burby, R. (ed.) Cooperating with nature. National Academy Press, Joseph Henry Press, Washington, DC (1998)
3. UNISDR: Terminology (2009)
4. Pearson, L., Mark, P.: The UN sendai framework for disaster risk reduction 2015–2030: Negotiation process and prospects for science and practice. J. Extreme Events 2. **1**, 1571001 (2015)
5. Tamvakis, P., Xenidis, Y.: Resilience in Transportation systems. Procedia Soc. Behav. Sci,. 3441–3450 (2012)
6. Brabhaharan, P.: Recent advances in improving the resilience of road networks. In: New Zealand Society of Earthquake Engineering Conference (2006)
7. O'Rourke, T.D.: Critical infrastructure, interdependencies and resilience. Bridge **37**(1), 22 (2007)
8. Alexander, D. E.: Resilience and disaster risk reduction: An etymological journey. Nat. Hazards Earth Syst. Sci. **13**, 2707–2716 (2013)
9. Hoffman, R.: A generalized concept of resilience. Text. Res. J. **18**, 141–148 (1948)
10. Goldstein, S., Brooks, R. B.: Why study resilience?. In Handbook of resilience in children, pp. 3–14. Springer, Boston, MA (2013)
11. Holling, C. S.: Resilience and stability of ecological systems. Annu. Rev. Ecol. Syst. **4**, 1–23 (1973)
12. Batabyal, A. A.: The concept of resilience: Retrospect and prospect. Environ. and Dev. Econ. **3**, 221–262 (1998)
13. Bruneau, M., Chang, S.E., Eguchi, R.T., Lee, G.C., O'Rourke, T.D., Reinhorn, A.M., Shinozuka, M., Tierney, K., Wallace, W.A., Von Winterfeldt, D.: A framework to quantitatively assess and enhance the seismic resilience of communities. EERI Spectra J **19** (4), 733–752 (2003)
14. Murray-Tuite P. M.: A comparison of transportation network resilience under simulated system optimum and user equilibrium conditions. In Proceedings of the 38th conference on Winter simulation, pp. 1398–1405. Winter Simulation Conference, 2006.

15. Madhusudan, C., Ganapathy, G.: Disaster resilience of transportation infrastructure and ports-An overview. Int. J. Geomatics Geosci. **2**, 443 (2011)
16. Manyena, S., O'Brien, G., Rose, P.O.: Disaster resilience: a bounce back or bounce forward reality. Local Environ **16**(5), 417–424 (2011)
17. Godschalk, D.: Urban Hazard Mitigation: Creating Resilienct Cities. Urban Hazards Forum (2002)
18. Levina, E.A.: Adaptation to climate change: key terms. The organisation for Economic Co-Operation and Development and International Energy Agency (2006)
19. Maguire, B., Artwright, S.: Assessing a community's capacity to manage change: A resilience approach to social assessment, Bureau of Rural Sciences Canberra (2008)
20. Kelman, I., Jennifer J. W.: Climate change and small island developing states: A critical review. Eco. Environ. Anthropol 5. **1**, 1–16 (2009)
21. Rockenschaub, G., Harbous, K.: Disaster resilient hospitals: An essential for all-hazards emergency preparedness. Papers from the 38th IHF World Hospital Congress in Oslo, 428 (2013)
22. Folke, C., Carpenter, S., Elmqvist, T., Gunderson, L., Holling, C.S., Walker, B.: Resilience and sustainable development: Building adaptive capacity in a world of transformations. AMBIO. A J. Hum. Environ. **31**, 437–440 (2002)
23. ARUP, Rockefeller Foundation: City Resilience Framework. The Rockefeller Foundation and ARUP (2014)
24. Pyrko, I., Howick, S., Eden, C.: Risk systemicity and city resilience. EURAM (2017)
25. HER MAJESTY'S TREASURY. National infrastructure plan 2011. Infrastructure UK, UK Treasury Department (HM Treasury), http://cdn.hmtreasury.gov.uk/national_infrastructure_plan291111.pdf. (2011)
26. Scott, D. M., Novak, D. C., Aultman-Hall, L., Guo, F.: Network robustness index: A new method for identifying critical links and evaluating the performance of transportation networks. J. Transp. Geogr. **14**(3), 215–227 (2006)

Chapter 36
Application of GIS and Remote Sensing Technique in Drainage Network Analysis: A Case Study of Naina–Gorma Basin of Rewa District, M.P., India

Vimla Singh, L. K. Sinha and Ampa Ganga Bhavani

Abstract The Drainage network analysis of river basin found to be helpful in offering a quantitative description of the existing drainage network, which play a key role in any hydrological analysis such as groundwater potential assessment, watershed planning and environmental management. In the present study Geographical Information System (GIS) and Remote Sensing (RS) techniques are applied for identification of morphological features of the drainage in the Naina–Gorma Basin. The study deals with analysis of linear and areal aspects of the drainage basin. The drainage network was classified according to Strahler's system of classification and it reveals that the basin has mainly sub-dendritic to dendritic type of drainage pattern. It is observed that the drainage density value is low i.e. 1.64 in the basin region which indicates that the basin has highly permeable subsoil and having thick vegetative cover leading to good groundwater potentials in the study region.

Keywords GIS & RS technique · Morphological feature · Drainage network analysis

V. Singh (✉)
Defense Terrain Research Laboratory (DTRL), DRDO, New Delhi, India
e-mail: vs6114@gmail.com

L. K. Sinha
DTRL, DRDO, Metcalfe House, New Delhi, India
e-mail: lksinha@dtrl.drdo.in

A. G. Bhavani
Department of Geo-Engineering, Andhra University College of Engineering, Vishakhapatnam, India
e-mail: bhavani90056@gmail.com

P. J. Rao et al. (eds.), *Proceedings of International Conference on Remote Sensing for Disaster Management*, Springer Series in Geomechanics and Geoengineering,
https://doi.org/10.1007/978-3-319-77276-9_36

1 Introduction

India is a country of diverse having unique geographical features with the mainly monsoon type of climate. The importance of water cannot be underestimated because of its life supporting properties, hence, nowadays greater emphasis being set for its efficient management to achieve optimal and sustainable development. Present paper focuses GIS based analysis of drainage network for the purpose of better understanding of the hydrologic system of the region. Keeping the objective, drainage morphometry has been performed which is the measurement of the shape, characteristics, behavior and drainage pattern of the study region. The morphometric characteristics of various river basins have been calculated earlier by many researchers using conventional method [4, 10, 12], remote sensing and GIS methods [1, 2, 5, 7, 11]. In the present study drainage characteristics of Naina–Gorma basin computed for various linear and areal parameters using GIS and RS technique. The investigation of the drainage network provides significant and valuable key in understanding the Geo-hydrological behavior and expresses the most frequent climate, geology, geomorphology of the study region. Drainage network analysis of the basin using GIS and RS is helpful in watershed management like flood management and ground water potential zone mapping [9].

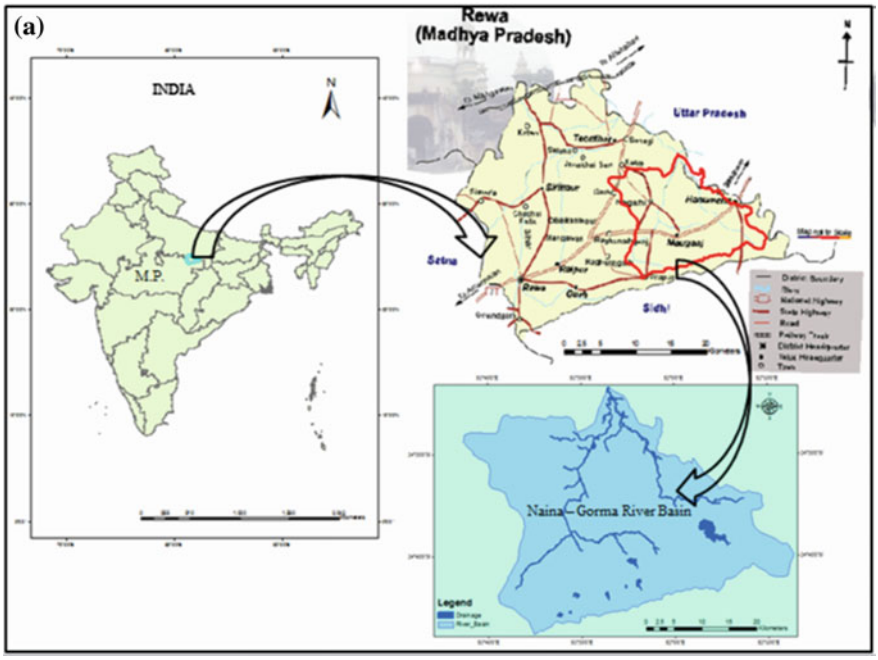

Fig. 1 **a** Location map of the study area. **b** Field picture showing (a) A view of Naina river (b) Vegetation in the region and tributary of Gorma river (c) Topography of the study area (d) Erosion and ravines in the basin

Fig. 1 (continued)

2 Study Area

The concern river, Naina–Gorma is a tributary of the Belan river. The basin area lying between 24° 35′ 00″–24° 57′ 30″N latitudes and 81° 37′30″–82° 15′ 00″E longitudes, acquiring an area of about 1420 km^2 scale (Fig. 1a).

Physical features of the study area are shown in Fig. 1b. The reason behind the selection of this basin is that it is untouched area and till there is no work of that kind is carried out. The Naina–Gorma river flows from south to north (source to mouth), all rivers and its tributaries of basin take their sources over the Rewa plateau and from northern flanks of kaimur range. The study area lying between the Son river in the south and Belan river in the north with various topographic characteristics. The region having slopes gradually northward from Kaimur range to the Rewa Scarps and to plain countries.

It is important to note that the general slope of the region is from south-east to north but height of the Rewa Scarps is gradually decreases northward from Rewa plateau to Vindhyan uplands and plain countries. The southern margins of the study area have been demarcated by Sardaman protected forest i.e. in Damodargarh block and tahsil and beside this forest, Son river flows parallel to the Kaimur Range.

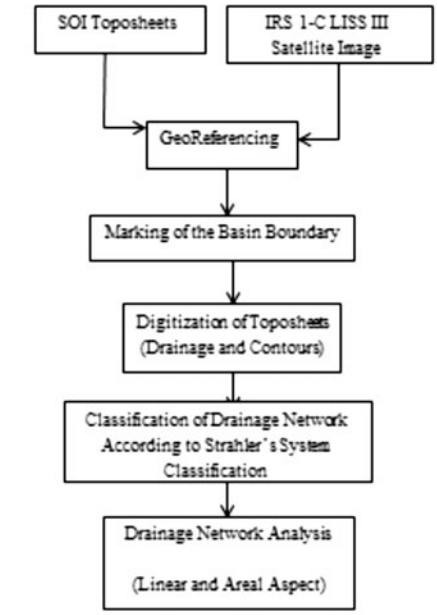

Methodology Flow Chart

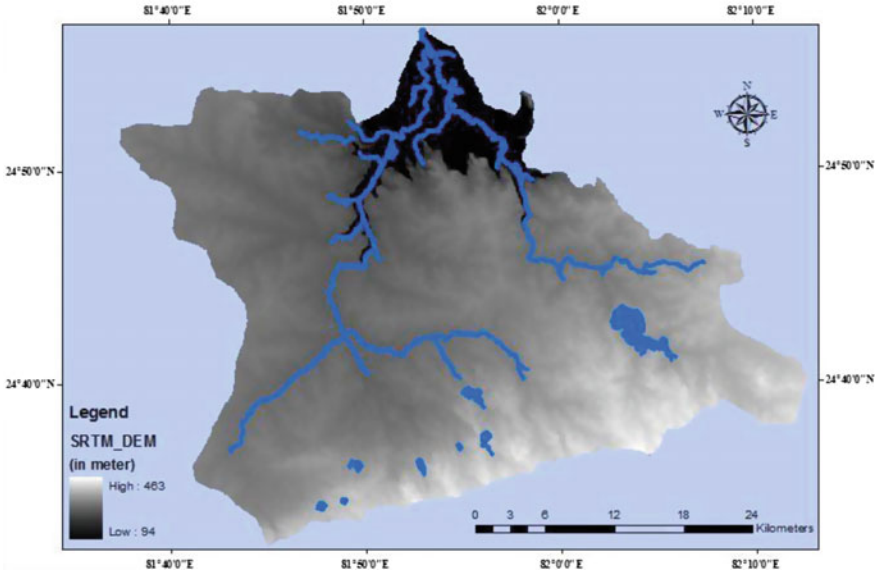

Fig. 2 SRTM DEM of Naina–Gorma Basin

Geologically the Rewa district are comprised of two major geological formations, Upper Vindhyan groups and Lower Vindhyan groups but in the Naina–Gorma basin only Upper Vindhyan groups are covering the major portion of the regions and the Archaeans consist of granites and gneisses besides recent alluvium.

3 Methodology and Data Set

The primary source of the data is the Survey of India (SOI) Toposheets viz. 63H/9, 10, 13, 14 and L/1, 2 on 1:50,000 scale. For recent topographical picture, satellite image of the IRS-1C (LISS III Data, 2008) on the scale 1:50,000, have been used. SRTM DEM of 90 m resolution data has been used for the terrain evaluation in the study basin (Fig. 2). The basin boundary marked on Arc GIS platform after geo-referencing of the toposheets. The drainage pattern (Fig. 3) of the study area has been digitized using toposheets and various other parameters computed with the help of Arc GIS 9.6 software. Method that used in the study is described in the given flow chart.

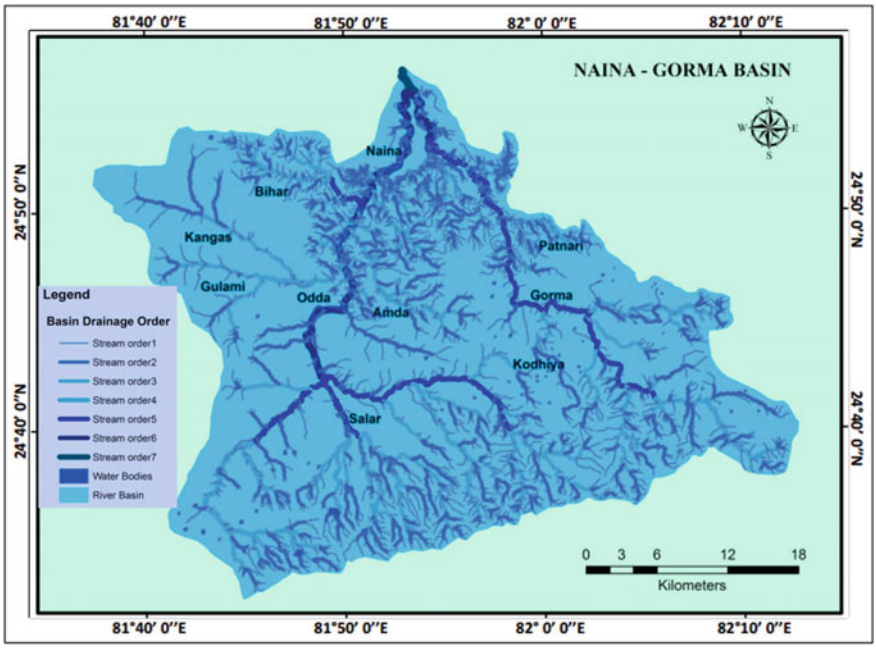

Fig. 3 STRTM DEM Drainage map of the Naina–Gorma Basin

4 Result and Discussion

The morphometric parameters of the Naina–Gorma river basin are categorized as linear and areal aspects. The parameters were calculated using provided equation for each parameter. The result found is tabulated in Tables 1 and 2.

Table 1 Bifurcation ratio and stream length ratio of Naina–Gorma Basin

Stream order (μ)	Number of stream ($N\mu$)	Total length of stream (Km)	Bifurcation ratio (R_b) = $N\mu/N(\mu + 1)$	Stream length ratio $R_l = \bar{L}_{\mu}/\bar{L}_{(\mu-1)}$
1	2376	1296.23	5.30	–
2	448	473.40	4.43	1.95
3	101	270.21	4.59	2.54
4	22	165.21	3.67	2.81
5	6	85.75	3.00	1.90
6	2	42.75	2.00	1.47
7	1	2.58	–	0.13
Total	2956	2259.11	Average R_b = 3.28	

Table 2 Linear and areal morphometric parameter of Naina–Gorma Basin

Morphometric parameters	Symbol/formula	References	Result
Stream order	u	Strahler [13]	7th
Stream number	Nu	Horton [4]	2956
Stream length	Lu	Horton [4]	2259.11
Bifurcation ratio	Rb	Schumn [8]	3.28
Stream length ratio	RL	Horton [4]	(Table 1)
Area (km^2)	A	Arc GIS	1425.85
Perimeter (km)	P	Arc GIS	201.57
Basin length (km) (Lb)	Lb	Arc GIS	140.52
Drainage density (km/km^2) (Dd)	Dd = Lu/A	Schumn [8]	1.64
Stream frequency (Fs)	Fs = Nu/A	Horton [3]	2.08
Texture ratio (T)	T = N1/P	Horton [4]	3.41
Elongation ratio (Re)	$Re = \frac{2\sqrt{A/\pi}}{Lb}$	Schumn [8]	0.30
Circularity ratio (Rc)	$Rc = \frac{4\pi A}{P^2}$	Miller [6]	0.43
Form factor ratio (Rf)	$Rf = A/Lb^2$	Horton [3]	0.072

Where
Lu = Total stream length of all orders
Nu = Total no. of streams of all orders
N1 = Total no. of 1st order streams
Π = 3.14

5 Mapping of Linear Aspects

Linear aspect of drainage network includes number of streams, order of stream, stream length (Lu), Bifurcation ratio (Rb) and stream Length Ratio (RL). The result obtained has been presented in Table 1. The first and foremost parameter computed is Stream Number which is order wise total number of streams of the drainage and it is directly proportional to the size of the river basin and inversely proportional to stream order of the studied basin. Total 2956 stream segments have been found in the study region. Stream ordering of the drainage were perform using Strahler method [12]. for better presentation geometric relationship is graphically shown in form of straight line while the log value of these variables (stream order and stream number) and (stream order and stream length) plotted (Figs. 4 and 5), the analysis suggesting that the area comes under normal basin category.

Stream Length (Lu) is the number of streams of various orders counted and their length is measured in the basin [13].

Figure 5 shows plot of the logarithm of stream order against stream length. It shows linear pattern which point toward the homogeneity in rock feature subject to weathering and erosion characteristics of the basin. The plot (Figs. 4 and 5) shows the normal trend in the basin that indicates the terrain have gentle slope, low relief and homogenous lithology.

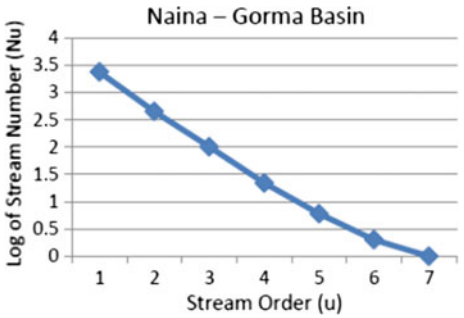

Fig. 4 Regression of logarithm (stream number vs. stream order) of basin

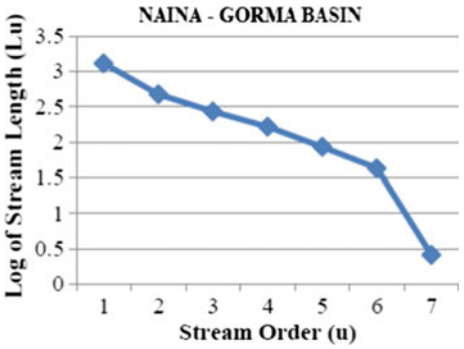

Fig. 5 Regression of logarithm (stream length vs. stream order) of basin

Bifurcation Ratio (Rb) characteristically ranges between 3.0 and 5.0 in studied basin, showing that the geologic structures do not distort the drainage pattern of basin [13]. Rb value 3.28 indicates that the drainage pattern are less disturbed by geological structures of the region. The value of RL indicates their mature geomorphic phase. Stream length ratio (RL) in basin shows an increasing trend as move from lower order to higher order of streams but after 4th order of streams it shows decreasing trend, indicating some early life features. Whereas, basin changes in RL from one order to another is the sign of late youth to established stage of geomorphic development of basin (Table 1).

6 Areal Aspects of the Drainage Basin

Drainage density (Dd), Stream frequency (Fs), Texture ratio (T), Elongation ratio (Re), Circularity ratio (Rc) and Form factor ratio (Rf) were calculated for the aerial aspects of the drainage basin and results have been shown through Table 2.

The Ratio of total streams length per km^2 area in the basin (km/km^2) is representing Drainage density (Dd) of the basin which illustrates the proximity of spacing of streams in the region. Dd of the study area is 1.64 km/km^2 (Table 2), indicates that the region has highly porous subsoil, gentle slope and dense vegetation cover. Texture Ratio (T) is a significant factor in morphometric analysis of river basin, depending on the implicit lithology, permeation capacity and relief aspect of the terrain feature. In the study region the texture ratio of the basin is 3.41 and categorized as moderate in nature. Stream Frequency (Fs) which is the total number of stream segments per unit area in the basin found to is 2.08, value of Fs for the basin show evidence of positive correlation with the Dd value of the area, representing the increase in stream population with increasing value of Dd. Elongation Ratio (Re) is an important indicator of basin shape, it helps to draw an idea regarding the hydrological character of a drainage basin of the study region.

The Re value of the study area contained is 0.30 which implies that study basin comprises low relief and elongated in shape. Circularity Ratio (Rc) value of the basin is 0.43, supports the Miller's range [6] showing basin is elongated in shape, and have highly permeable soil condition. Dimensionless ratio of basin area to the square of basin length is represented by Form Factor Ratio (Rf) (Tables 1 and 2), Rf value of the basin calculated 0.072, showing lower value and hence, represents elongated shape of basin with flatter peak of flow for longer duration.

7 Conclusion

The drainage analysis of drainage network found to be useful in river basin evaluation which ultimately provides a tool in watershed management regarding soil, water, and natural resources management of the study area. The morphometric

parameters of the drainage evaluated using GIS and RS technique, helpful in understand the various terrain features like nature of the bedrock, infiltration capacity, runoff potential, etc. The drainage network analysis shows that the basin encompasses low to high relief terrain and elongated shape. Drainage network of the basin mapped is mainly dendritic type, representing homogeneity in texture of rock which is devoid of structural control of the area. The linear pattern of the graphical representation indicates weathering erosional characteristics of the study area. Similar studies using of high quality satellite data will surely helpful in assessment of landforms and their processes which lead a better planning and management approach like flood management and ground water recharge zone identification of the region in the future.

References

1. Agarwal, C.S.: Study of drainage pattern through aerial data in Naugarh area of Varanasi district, U.P. J. Indian Soc. Remote Sens. **26**, 169–175 (1998)
2. Biswas, S., Sudhakar, S., Desai, V.R.: Prioritisation of subwatersheds based on morphometric analysis of drainage basin a remote sensing and GIS approach. J. Indian Soc. Remote Sens. **27**, 155–166 (1999)
3. Horton, R.E.: Drainage basin characteristics. Trans. Amer. Geophys. Union **13**, 350–361 (1932)
4. Horton, R.E.: Erosional development of streams and their drainage basins: hydrophysical approach to quantitative morphology. Bull. Geol. Soc. Am. **5**, 275–370 (1945)
5. Krishnamurthy, J., Srinivas, G.: Role of geological and geomorphological factors in groundwater exploration: a study using IRS LISS data. Int. J. Remote Sens. **16**, 2595–2618 (1995)
6. Miller, V.C.: A quantitative geomorphic study of drainage basin characteristics in the Clinch Mountain area, Varginia and Tennessee. Project NR 389042 (1953)
7. Narendra, K., Nageswara Rao, K.: Morphometry of the Mehadrigedda watershed, Visakhapatnam district, Andhra Pradesh using GIS and Resources at data. J. Indian Soc. Remote Sens. **34**, 101–110 (2006)
8. Schumn, S.A.: Evaluation of drainage systems and slopes in badlands at Perth Amboy, New Jersy. Bull. Geol. Soc. Am. **67**, 597–646 (1956)
9. Singh, V.: Impact of Terrain morphology on Basin ecosystem: a case study of Naina–Gorma basin of Rewa district, M.P., India. Unpublished D.Phil thesis, Allahabad University (2015)
10. Smith, K.G.: Standards for grading texture of erosional topography. Am. J. Sci. **248**, 655–668 (1950)
11. Srivastava, V.K., Mitra, D.: Study of drainage pattern of Raniganj Coalfield (Burdwan District) as observed on Landsat TM/IRS LISS II imagery. J. Indian Soc. Remote Sens. **23**, 225–235 (1995)
12. Strahler, A.N.: Quantitative analysis of watershed geomorphology. Trans. Am. Geophys. Union **38**, 913–920 (1957)
13. Strahler, A.N.: Quantitative geomorphology of drainage basins and channel networks. In: Handbook of Applied Hydrology, McGraw Hill Book Company, New York (1964)

Chapter 37
Impact of Land Use/Land Cover and Mangrove Degradation on Coastal Erosion in Godavari Delta Region, Andhra Pradesh—A Geospatial Approach

A. Kavya, A. Ganga Bhavani, Peddada Jagadeeswara Rao and V. Bala Chandrudu

Abstract The study focused on spatio-temporal changes in land use/land cover and degradation of mangroves which in turn identification of coastal erosion zones along the 185-km long coast line of Godavari delta region, India. This work analyzed multi-date satellite imagery of Landsat 4, 5, 7 and 8 TM and ETM sensors of 2002, 2011, and 2017 which revealed rapid changes in land use/land cover, mangrove degradation and coastal erosion. From the year 2002 to 2011, a decrease in area of about 36.6 km^2 of mangroves and coastal erosion of 4.535 km^2 is observed whereas from 2011 to February 2017 there is a considerable increase of 19.88 km^2 in mangroves is observed. During 2002 to 2017, severe beach erosion of 0.184 and 0.418 km^2 occurred at Uppada-Konapapapeta coast and Nilarevu river mouth respectively. Similarly, an accretion of 0.526 km^2 is observed in Vakalapudi. This study assessed 16.722 km^2 of mangrove degradation and 4.103 km^2 of coastal erosion because of conversion of mangroves into aquaculture and agriculture. This study suggests construction of sea walls, groins and to prevent conversion of mangroves into aquaculture and agriculture lands are the suitable measures.

Keywords Uppada · Coastal erosion · Accretion · Mangrove degradation

A. Kavya (✉) · A. G. Bhavani · P. J. Rao
Department of Geo-Engineering, Andhra University, Visakhapatnam, India
e-mail: Kavyaalugolu5@gmail.com

A. G. Bhavani
e-mail: bhavani90056@gmail.com

P. J. Rao
e-mail: pjr_geoin@rediffmail.com

V. B. Chandrudu
GSI, Visakhapatnam, India
e-mail: chandrudu66@yahoo.co.in

P. J. Rao et al. (eds.), *Proceedings of International Conference on Remote Sensing for Disaster Management*, Springer Series in Geomechanics and Geoengineering,
https://doi.org/10.1007/978-3-319-77276-9_37

1 Introduction

Natural disasters such as tsunamis, storms, earthquakes, forest fires, coastal erosion, etc. are occurring globally. Coastal erosion is one of the major problems for developing shorelines everywhere in the world. Coastal erosion is the loss of land in the coast into the sea due to natural processes such as tides, waves and currents [1]. About 60% of the world's population lives within 100-km of the coast. As the economic activities in the coastal zones are increasing, pressure is increasing on coastal eco-system. The rate of beach erosion in recent years is increasing due to changes in coastal dynamics and severe anthropogenic activities [2]. This is further intensifying owing to deforestation. Coastal erosion and shoreline management plans are often implemented on an action-reaction and post-disaster basis, resulting in installation of hard engineering structures, such as, groins, seawalls, and breakwaters. These hard stabilization structures usually alter the natural environment of the coast, producing negative impacts [3]. Mangrove and salt marsh vegetation can afford context-dependant protection from erosion, storm surge and potential tsunami waves and conversion of these areas for agriculture, aquaculture and industrial purposes. The major reason for the conversion of mudflats into agriculture lands is, during high tide the sediment is carried into mangroves and during low tide water is moving back into the sea leaving the sediment. Reiteration of this process leads to rise in the elevation of tidal flats over a period of time [4]. The study area, Godavari delta region is enriched with hydrocarbons and extensive paddy agriculture and coconut plantation. Godavari delta coast is being experienced by coastal erosion. Studies revealed more erosion than accretion in Godavari delta region [5]. A study carried by Rao et al. [6] revealed that an area of 20.1 km^2 had been eroded from 1965 to 1990, similarly, 10.4 km^2 from 1990 to 2000 and 7.1 km^2 from 2000 to 2008. It is revealing that erosion is dominating than accretion in Godavari delta coast region [6].

2 Study Area

The study area, Godavari delta region is located between 81° 43′ 25.058″E–82° 19′ 4.687″E lat and 16° 30′ 59.877″N–17° 9′ 17.483″N long (Fig. 1). Taking into consideration of creeks (back waters) and aquaculture in Godavari delta region a 20 km buffer from the sea coast to inland has been considered as study area. The study area is covering 3125 km^2 in East Godavari and West Godavari districts, Andhra Pradesh. The area has significant importance in terms of agriculture, mineral resources, wetland habitats, fish production, oil and natural gas resources and a huge delta with coast line of 185-km [7]. The area is also famous for mangrove forests which are popularly known as Coringa reserved forest, covers 213.03 km^2.

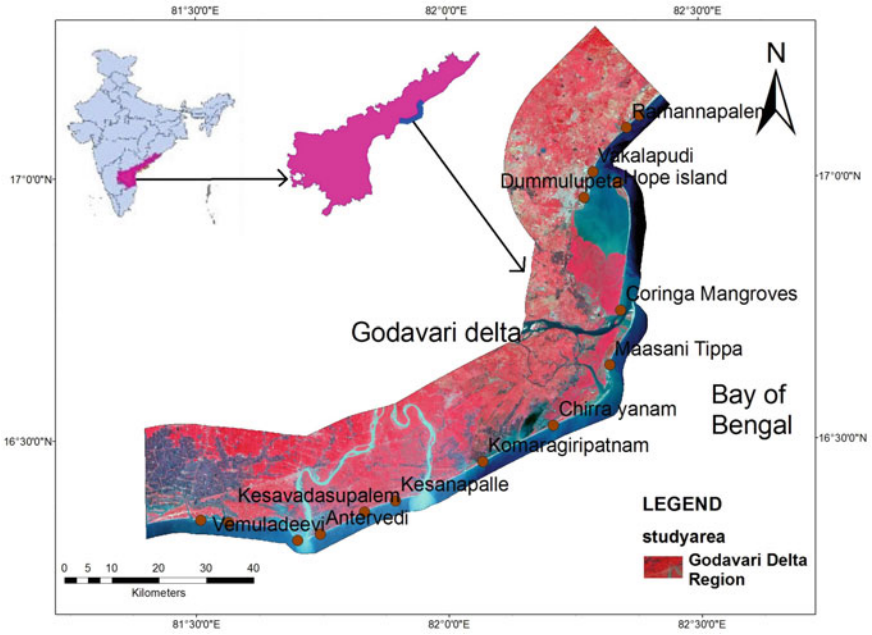

Fig. 1 Location map (Mosaic of Landsat TM image dated October 16 and November 10, 2016)

3 Methodology

The Landsat satellite data have been downloaded from the website www.usgs.gov.in. The data mosaicked in ERDAS Imagine-2014, thereafter, digitization of land use/land cover is carried out in ArcGIS-10.3. Survey of India toposheets 65H/7, 11, 14, 15; 65L/1, 2, 3, 5, 6 and 65K/4 and 8 were performed geometric correction in ERDAS Imagine-2014, a buffer of 20-km from coast line to inland was delineated in ArcGIS-10.3. The study area (AOI) is delineated on mosaicked satellite images. The methodology adopted in this study is shown in Fig. 2.

Landsat 5 (TM, ETM), 7 (ETM+) and 8 (OLI, TIRS) imagery with spatial resolution of 30 m are taken for land use/land cover. Toposheets and other collateral data of the study area are used for correlation. Band combination of 5, 4, 3 are used for Landsat 8 and 4, 3, 2 are used for Landsat 7, 4 and 5 to get false color image and AOI (Area of Interest) of the study area. Land use/land cover is carried out following the standard visual interpretation techniques of guidelines. Digitization of coast, mangroves, built-up area, aquaculture and agriculture (Fig. 2) is done using 2002–2017 satellite imagery in ArcGIS-10.3 and change detection is calculated. The 21-km long spit popularly known as Hope Island is in north eastern side of the Godavari delta region was initiated during 19th century [8]. The bay head delta was characterized by extensive mangrove forest during the early part of 20th century [9].

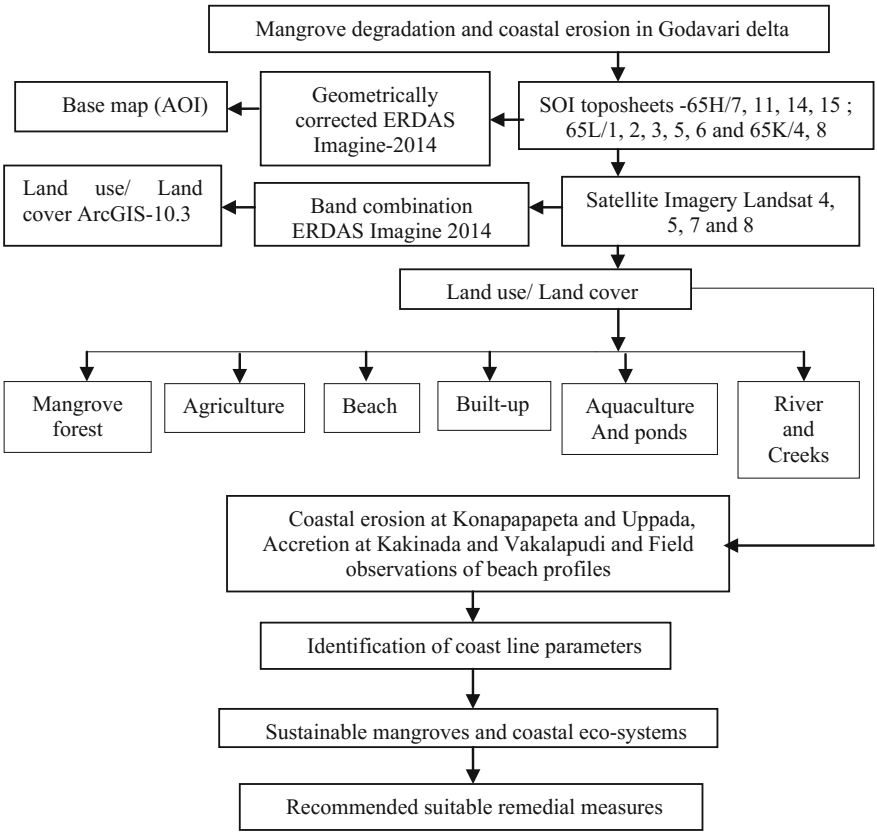

Fig. 2 Conceptual framework of the study area

4 Land Use/Land Cover

Land is the most important natural resource endowment on which all the man's activities are based. The knowledge on the spatial distribution of land use/land cover and its pattern of change, promotes to understand how the land is being utilized. The land use/land cover are delineated through on-screen digitization following the standard visual interpretation techniques in ArcGIS-10.3 is shown in Fig. 3a, b. In this seven land use/land cover categories have been identified namely agriculture and plantation, mangrove forests, beach, river and creeks, built-up, wetlands-saltpans and aquaculture-ponds. Change in land use/land cover from 2002, 2011 and 2017 in Godavari delta region is shown in Table 1.

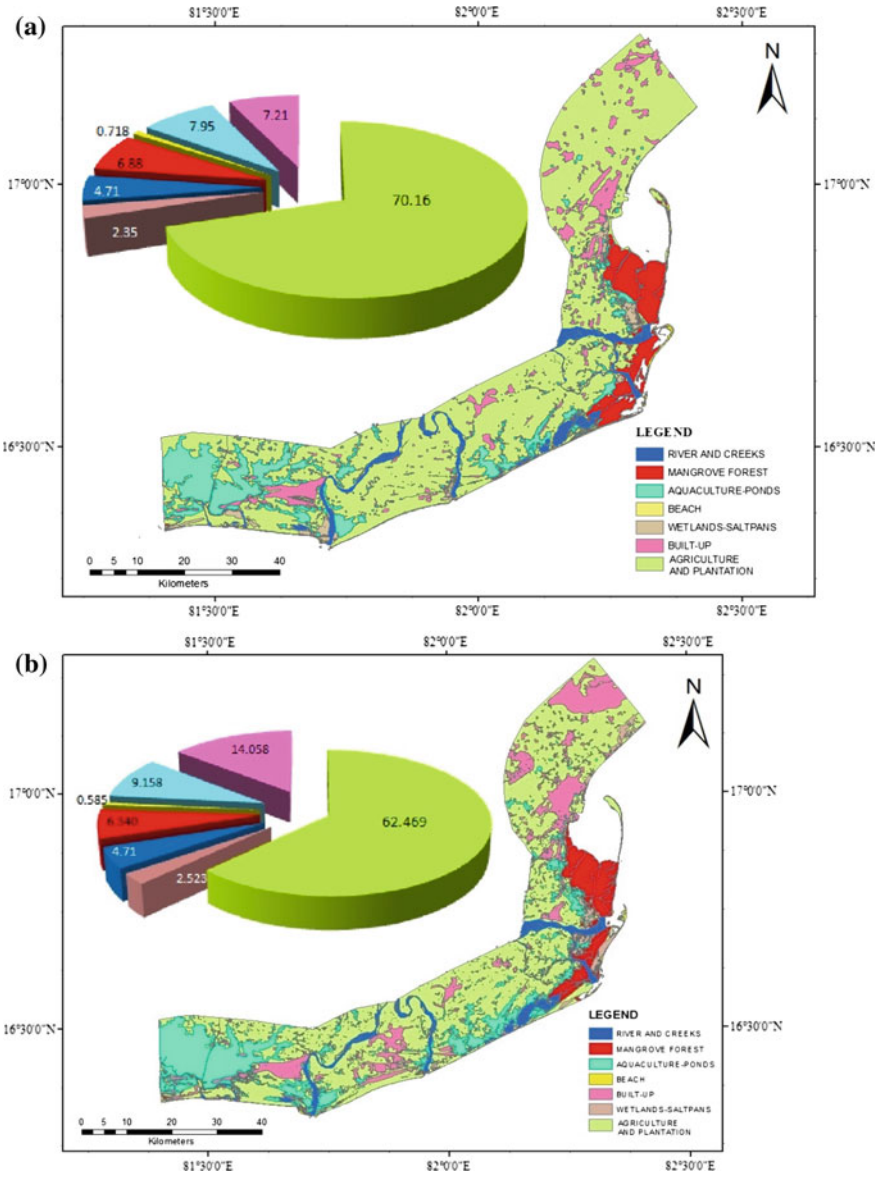

Fig. 3 **a** Land use/Land cover based on Landsat TM-2002. **b** Land use/Land cover based on Landsat OLI and TIRS-2017

Table 1 Areas of land use/land cover

S. no.	Name of feature	Area in 2002 (km^2)	Area in 2011(km^2)	% change in area from 2002 to 2011	Area in 2017(km^2)	% change in area from 2002 to 2017
1	Agriculture and plantation	2172.169	2257.109	3.91	1934.062	(−)14.31
2	Mangrove forest	213.03	176.43	(−)17.18	196.308	11.26
3	Beach	22.243	17.708	(−)20.38	18.14	2.43
4	Aquaculture-ponds	246.27	187.16	(−)24.00	283.53	51.32
5	Built-up	223.425	254.091	13.72	435.25	71.29
6	River and creeks	146	146	0	146	0
7	Wetlands and saltpans	72.87	57.502	(−)21.08	78.139	35.88

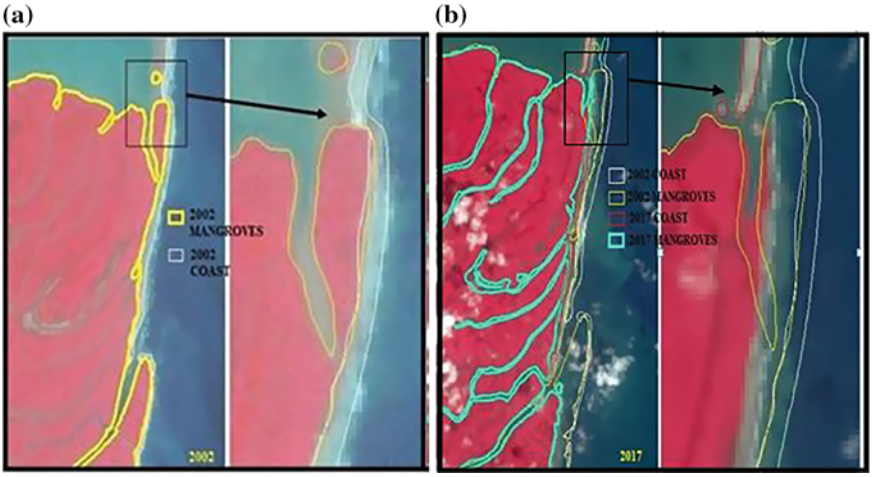

Fig. 4 **a**, **b** Showing temporal variation of mangroves and coast at Hope Island

Table 2 Change detection of mangroves and coast from 2002 to 2017

Area/year	2002	2017	Change in % (%)
Mangroves	213.03	196.308	(−)7.8
Beach	22.243	18.14	(−)18.44

5 Mangrove Forest Role in Coastal Erosion

Mangroves and coast are interdependent to each other. Mangroves and coast help each other in protecting environment from disasters. Destruction of mangrove forests or salt marshes to make way for shrimp farms is directly affecting the delta coast. Figure 4a, b is clearly showing that in 2002 the Hope Island is connected to the land, during that time the mangroves are thick and dense whereas in 2017 the mangroves near the Hope Island are degraded and the tail part of the spit is separated from the land. All over the Godavari delta region from the year 2002–2017 mangroves witnessed degradation by 7.8% and coast eroded about 18.44% (Table 2).

6 Field Observations

Field studies at Konapapapeta and Uppada sea coast revealed erosion and deforestation of Coring mangrove forest. Severe erosion is observed at Uppada and Konapapapeta beach (Fig. 5), where the sea waves removed the existing road and encroached into the agricultural fields. To arrest erosion, a sea wall was constructed. After taking these measures at Uppada coast, the near area Konapapapeta coast has

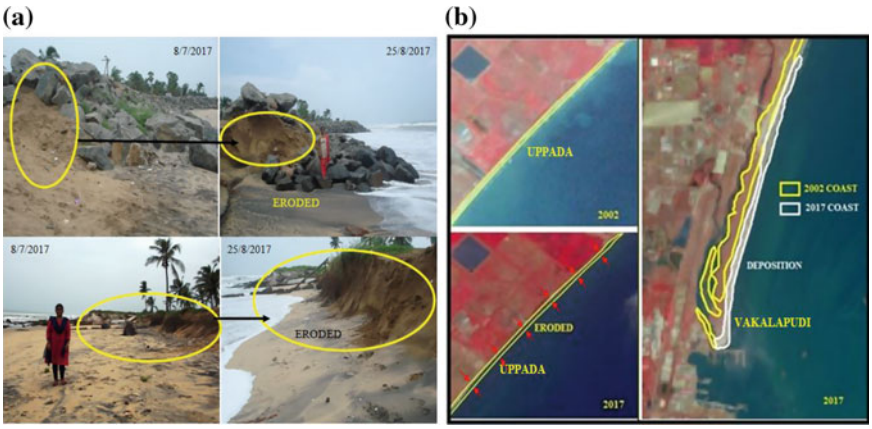

Fig. 5 **a** Showing erosion in Konapapapeta beach near Uppada, Andhra Pradesh within 50 days and **b** showing erosion at Uppada coast and deposition near Kakinada port

been eroded, where similar technique has been used. Near Vakalapudi and Kakinada coast deposition observed. It is assumed and attributed that the Hope Island might be the reason for changing the wave intensity and velocity besides seasonal and global changes.

Temporal change of 15 years shows that there is a deposition at Kakinada port and erosion at Uppada coast which is above the Kakinada port (Fig. 5b).

7 Results and Discussion

Satellite data of 10 years have shown that deforestation of mangroves and coastal erosion is increasing. It is observed, aquaculture which plays an important role in degradation of mangrove forests. The Landsat imagery browsed and downloaded from the Earth Explorer and the areas of mangroves, coastal erosion and aquaculture is calculated in ArcGIS-10.3.

In the year 2002, the coast is about 22.243 km^2 and the total area of mangroves is 213.03 km^2, whereas the area covered by aquaculture is about 246.27 km^2 in Godavari delta region. In the year 2008, the coast is eroded to 14.93 km^2 and the mangroves reduced to 180.91 km^2, whereas the area under aquaculture has decreased to 230.93 km^2. In the year 2011, the coast has gained 2.778 km^2 and total coast area in this year is 17.708 km^2 and the mangroves have again reduced to 176.43 km^2, the area which covered the aquaculture is at 187.16 km^2. In the year 2017, the area under mangroves has increased to 196.308 km^2 and an accretion of around 0.432 km^2 is observed, whereas, area of aquaculture is 283.533 km^2.

Observed in this study, from the past 15 years aquaculture is increased an area of 15.13%, whereas mangrove deforestation and coastal erosion are 7.84 and 18.44%

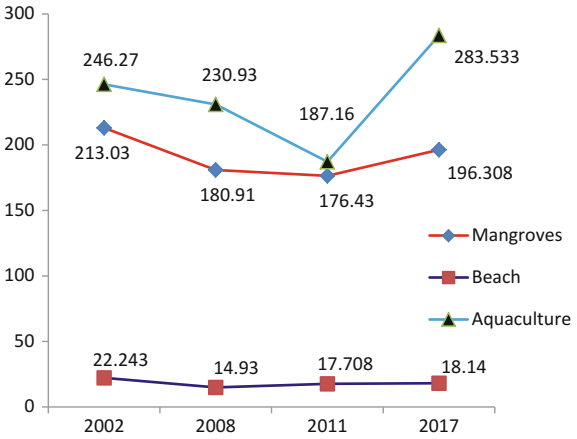

Fig. 6 Change detection of mangroves and coast from 2002 to 2017 along Godavari delta region

respectively. It is clearly showing that aquaculture impact on deforestation of mangroves. If mangroves are degraded it directly influences the coastal erosion (Fig. 6).

References

1. Dobrynin, M., Razumov, S., Brovkin, V., Ilyina, T., Grigoriev, M.: Changes in forcing factors affecting coastal and shallow water erosion in the future Arctic climate change projections. In: EGU General Assembly Conference Abstracts (2016)
2. Space Applications Centre (ISRO), Ahmedabad, India
3. Gracia, C.A., Rangel-Buitrago, N., Oakley, J.A., Williams, A.: Use of ecosystems in coastal erosion management. Ocean Coast. Manag. (2017)
4. Ahmed, N., Cheung, W.W., Thompson, S., Glaser, M.: Solutions to blue carbon emissions: shrimp cultivation, mangrove deforestation and climate change in coastal Bangladesh. Mar. Policy **82**, 6875 (2017)
5. Akbar, A.A., Sartohadi, J., Djohan, T.S., Ritohardoyo, S.: The role of breakwaters on the rehabilitation of coastal and mangrove forests in West Kalimantan, Indonesia. Ocean Coast. Manag. **138**, 50–59 (2017)
6. Rao, K.N., Subraelu, P., Kumar, K.C.V., Demudu, G., Malini, B.H., Rajawat, A.S.: Impacts of sediment retention by dams on delta shoreline recession: evidences from the Krishna and Godavari deltas, India. Earth Surf. Process. Land. **35**(7), 817–827 (2010)
7. Hema, B.M., Rao, K.N.: Coastal erosion and habitat loss along the Godavari delta front—a fallout of dam construction (?). Curr. Sci. **87**(9), 1232–1236 (2004)
8. Pramanik, M.K., Biswas, S.S., Mondal, B., Pal, R.: Coastal vulnerability assessment of the predicted sea level rise in the coastal zone of Krishna-Godavari delta region, Andhra Pradesh, east coast of India. Environ. Dev. Sustain. **18**(6), 1635–1655 (2016)
9. Prasada Rao, R., Mahadevan, C.: Evolution of Visakhapatnam beach. Andhra Univ. Mem. Oceanogr. **2**, 33–47 (1958)

Chapter 38
A Geospatial Approach to Assess the Liquefaction Vulnerability of Kutch District, Gujarat—A Case Study

Kuntal Ganguly, Peddada Jagadeeswara Rao, K. Mruthyunjaya Reddy and Bendalam Sridhar

Abstract The study investigated the influences of earthquake on soil liquefaction utilizing multi-temporal datasets of Landsat ETM+ and ancillary datasets of seismicity, LULC, soil, hydrology, Peak Ground Acceleration (PGA) and Modified Mercalli Intensity (MMI) of the earthquake. The study has identified vulnerable liquefaction zones of Kucth region of Gujarat using Remote Sensing and GIS based multi-criteria analysis technique. The obtained results have categorized the study area into 6 vulnerability zone- very low, low, significant, high, very high and severe. The results shown that the NDMI value was increased significantly from −0.01 to 0.20 after earthquake. It has been observed that most of liquefaction has been predicted for Wetlands land use category. The study has also shown liquefaction probability equally high for those areas having red gravelly and red loamy soils.

Keywords Earthquake · Liquefaction · Multi-criteria analysis · Remote sensing GIS · LULC · PGA · MMI · NDMI

K. Ganguly (✉) · P. J. Rao · B. Sridhar
Department of Geo-Engineering, Andhra University, Visakhapatnam, India
e-mail: gangulykuntal@gmail.com

P. J. Rao
e-mail: pjr_geoin@rediffmail.com

B. Sridhar
e-mail: sridhar.bendalam@gmail.com

K. M. Reddy
National Remote Sensing Centre, ISRO, DOS, Government of India, Hyderabad, India
e-mail: reddy_km@nrsc.gov.in

P. J. Rao et al. (eds.), *Proceedings of International Conference on Remote Sensing for Disaster Management*, Springer Series in Geomechanics and Geoengineering,
https://doi.org/10.1007/978-3-319-77276-9_38

1 Introduction

Soil liquefaction occurs whereby a soil substantially loses strength and stiffness in response to an applied stress, usually earthquake vibration or other rapid loading, causing it to behave like a liquid. Liquefaction is more likely to occur in loose to moderately saturate granular soils with poor drainage, such as silty sands, sandy silts, clayey sands [1] or sands and gravels capped or containing seams of impermeable sediments [2]. Earthquake liquefaction is a major contributor to urban seismic risk [3]. Historically, liquefaction-related ground failures have caused extensive structural and lifeline damage around the world. Recent examples of these effects include the damage produced during the 2001 Bhuj–India, 2010 Haiti, 2010, and 2011 New Zealand earthquakes. It is observed from these earthquakes, that the occurrence of co-seismic liquefaction, and thus the distribution of liquefaction related damage, is generally restricted to areas that contain low-density, saturated, near-surface (<40 feet depth) granular sediments that are found in regions prone to seismic ground motions exceeding a specified threshold level [4]. As the prediction of seismic event is still rudimentary, the developments in science and technology can be effectively used to minimize the devastative effects of an earthquake. The calamities of the recent earthquake made the scientific community in India [5–8] and abroad [9–11] to contribute from different angles converging towards MSZ [12]. One among the important components of MSZ is mapping the liquefaction potential (LP) areas. It is not over emphasized to state that maximum devastation to structures is caused due to liquefaction related ground failures [13, 14]. Though the Kutch area has witnessed several devastative earthquakes in the recent history [15] not much work has been done on liquefaction assessment in particular. The ability of geospatial technologies have proved its effectiveness at decision support level. Thus, the Remote Sensing and GIS can be utilised as a management tool in prior to the occurrence of the event.

2 Study Area

The area is covering the Kutch district of Gujarat state of India having total geographical area of 45,612 km^2. The study area is located between 22° 44′ 08″N to 24° 41′ 30″N latitudes and 68° 7′ 23″E to 71° 04′ 45″E longitude. The great Rann of Kutch is a salty low land and marshy region surrounding Kutch located in the north of the district. The alluvial plain stretches northwards for over 400 km, and joins the Rann of Kutch. Structurally, the Kutch represents a rift basin of Late Triassic-Early Jurassic, manifest the longest evidence of the Mesozoic succession in the western India. The geo-techtonic activities are scattered in the landscape of this area are the proof of palaeo-seismic indicators (Fig. 1).

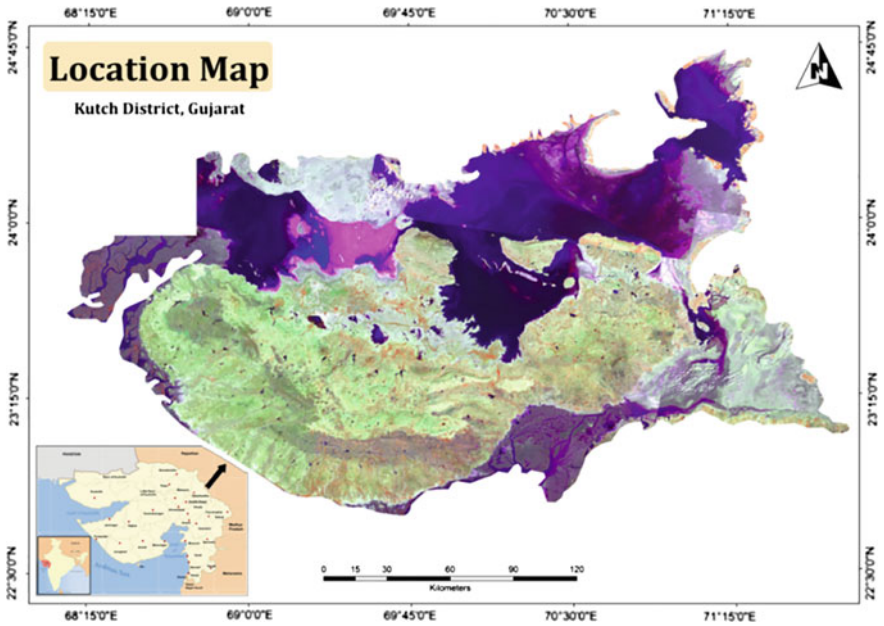

Fig. 1 Location of the study area

3 Data and Softwares Used

In the present study the published data has been utilised from different government and non-government sources and has been analysed and presented for particular applications. The data sources are listed below:

Hydrology and Soil data sources: NATMO, Kolkata
PGA and MMI data sources: USGS

Satellite image specifications are listed in Table 1.

In the present study the Erdas Imagine 2014 has been used for digital analysis of satellite images. Whereas ArcGIS 10.3 has been used for GIS modeling and analysis.

Table 1 Landsat ETM+ image specifications

Sensor	Platform	Path/ row	Band	Spatial resolution (m)
ETM+	Landsat 7	149/43 149/44 150/43 150/44 151/43 151/44	1–5 6–7 PAN	28.5 59.5 14.5

4 Methodology

In the present study a conceptual framework has been developed to analyse the liquefaction probability of the study area. The detailed work flow is given in Fig. 2.

4.1 Normalized Difference Moisture Index (NDMI)

Normalized Difference Moisture Index (NDMI) has been derived from Landsat spectral bands 4 and 5 to assess the surface wetness of the study area before and after the earthquake event. NDMI has been calculated using the following equation:

$$\text{NDMI} = [\text{Band}\,4 - \text{Band}\,5]/[\text{Band}\,4 + \text{Band}\,5]$$

NDMI values ranges from +1 to −1, where, (+1) indicates the high moisture condition and (−1) indicates the low moisture or dryness (Fig. 3).

4.2 Land Use/Land Cover (LULC)

LULC map has been prepared using Landsat ETM+ imageries. The supervised classification approach has been adopted to extract 6 major level 1 LULC classes required for the study. The obtained LULC classes are- Built-up, Cropland, Forest, Wastelands, Wetlands and Rann (Fig. 4).

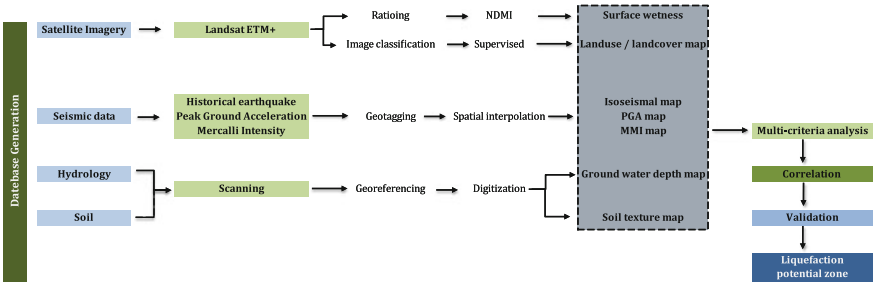

Fig. 2 Conceptual framework of the study

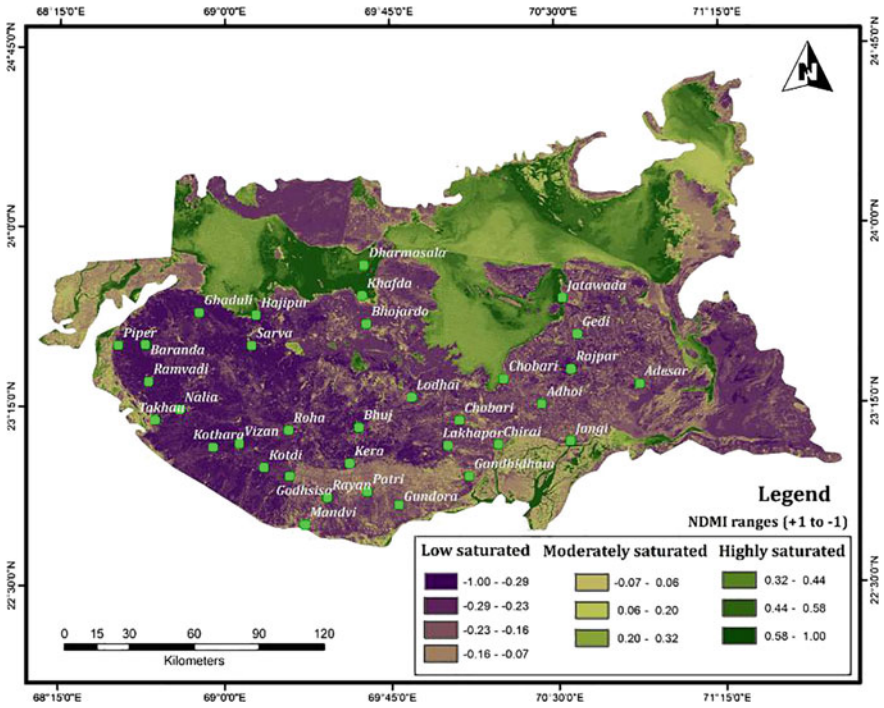

Fig. 3 NDMI map of the study area

4.3 Seismicity Mapping

The seismicity of the study area has been done by utilizing historical earthquake data of 340 years (1668–2008). The data has been further utilized to identify the isoseismic character of the study area (Fig. 5).

4.4 Soil and Hydrology Mapping

Soil and hydrology is the most important factor for liquefaction occurrence for any study area has been mapped from the data published by NATMO. The required classes for the study has been digitized and used for further analysis of the study (Figs. 6 and 7).

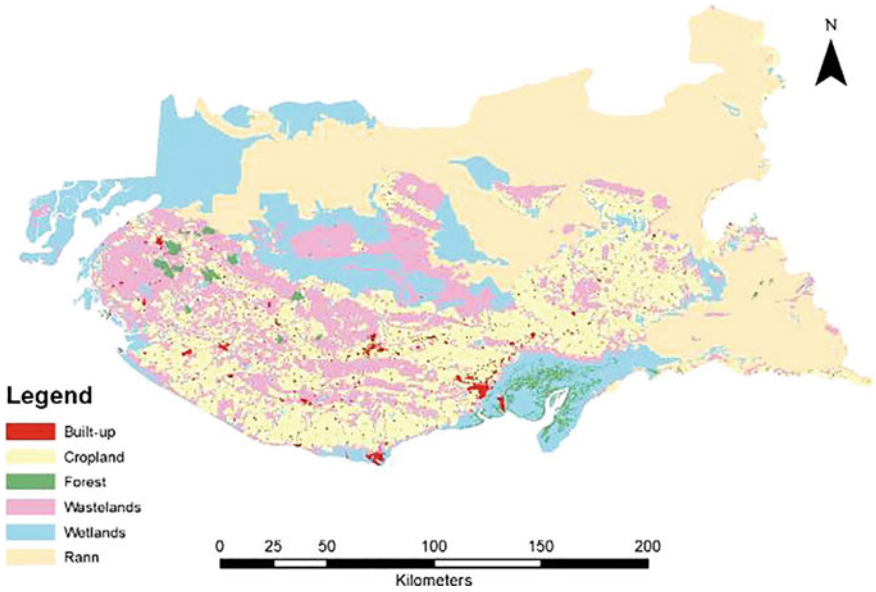

Fig. 4 LULC map of the study area

4.5 Peak Ground Acceleration (PGA) and Modified Mercalli Intensity (MMI)

PGA and MMI data has been obtained to display the extent and variation of ground shaking throughout the affected region immediately after earthquakes. PGA can be exhibited in 'g' (acceleration due to earth's gravity), can be exclaimed as either a decimal or percentage, in m/s^2 (1 g = 9.81 m/s^2) or in Gal, where, 1 Gal = 0.01 m/s^2. So, 1 g = 981 Gal. Whereas, MMI scale was used for measuring the intensity of an earthquake, composed with the scale of 12 increasing level of intensity that range from imperceptible shaking to catastrophic destruction (Figs. 8 and 9).

4.6 Weighted Overlay/Multi-criteria Analysis

Weighted Overlay Analysis (WOA) is a method for a combined analysis of multi-level maps. A weight indicates the relative importance of a parameter with respect to the study objective. WOA method considers the relative importance of the parameters and the classes of each parameter. In the present study, thematic maps were overlaid on each other and ranks and weights were assigned to each

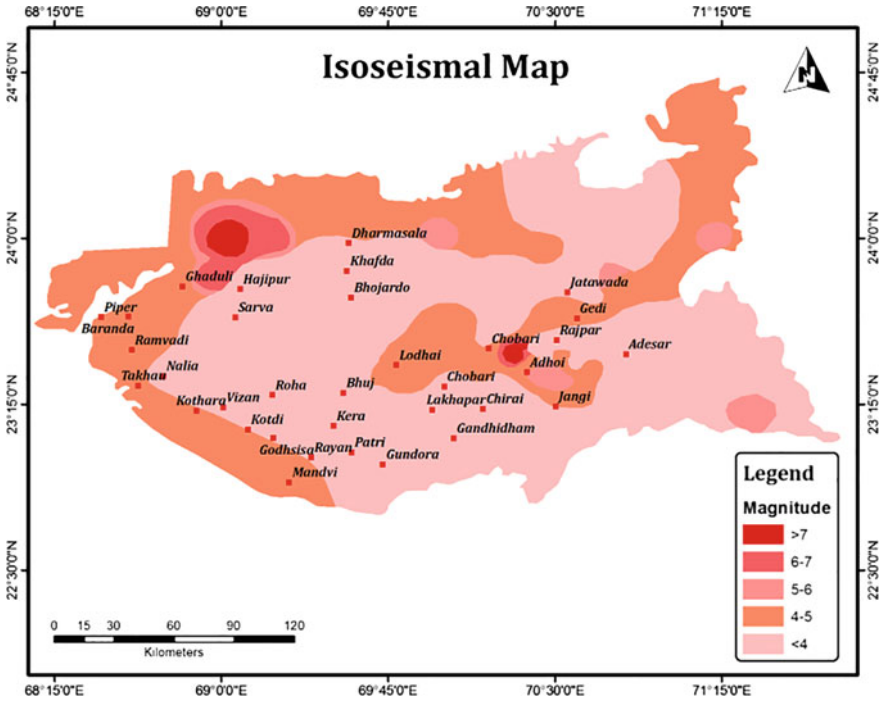

Fig. 5 Isoseismal map of the study area

category in the theme to create a predictive model. Hence, LULC, soil, hydrology, NDMI, seismicity, PGA, MMI layers have been utilized as input to multi-criteria analysis (Table 2).

5 Results and Discussion

In present study a multi-criteria evaluation model was utilized by incorporating the multiple datasets into a standard measuring scale. These layers were further arranged on the basis of its weights and ranks of every factor and its impact on liquefaction vulnerability of Kutch region of Gujarat.

Depending on the seismicity, PGA, MMI, NDMI, LULC, Ground water depth and soil texture the liquefaction vulnerability has been assessed. The seismicity mapping shows higher to lower seismological condition in terms of magnitude (<4 to >7) over the region. As the study focuses on vulnerability assessment, so, highest rank has been given to the highest isoseismic zone (>7 magnitude) and lowest rank to the lowest isoseismic zone (<4 magnitude).

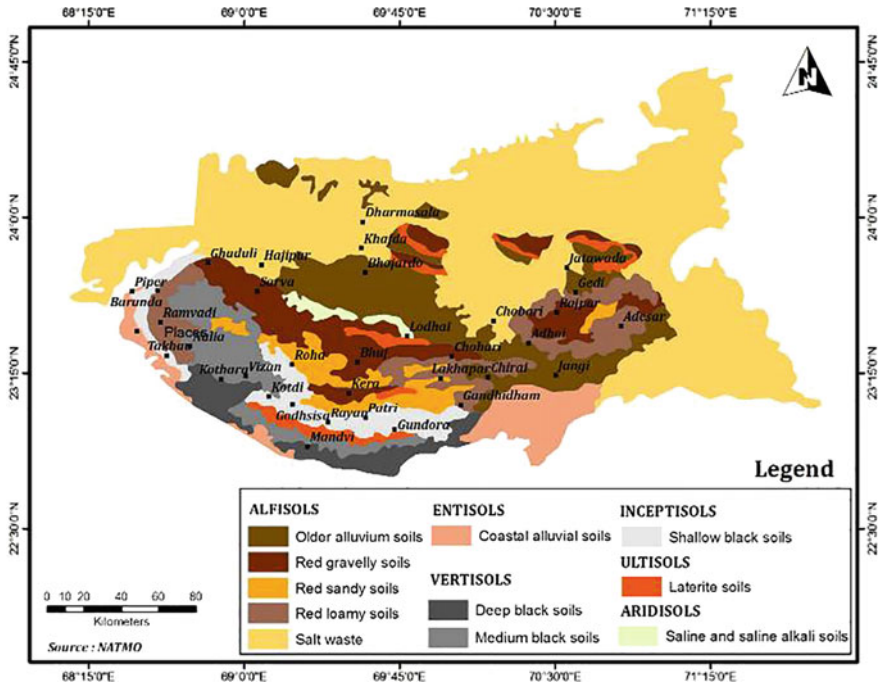

Fig. 6 Soil map of the study area

On the basis of susceptibility to soil liquefaction, the soil classes have been ranked from highest to lowest. Hence, the red gravelly and red sandy soils were assigned highest rank followed by red loamy; coastal and older alluvium; saline and saline alkaline soil and shallow, medium and deep black soil. Hydrological condition also plays an important role as ground water depth is a critical parameter in assessing liquefaction potential. Liquefaction is more prone in areas where ground water level lies within 10 m of the ground surface; although in some cases liquefaction have taken place in areas where ground water deeper than 20 m. Thus, in WOA highest rank has been given to higher water table (less than 10–40 m), whereas, rocky area has been assigned to lowest rank. Similarly, the NDMI derived surface wetness has been ranked by highest to lowest in highly saturated to low saturated respectively. The pre and post-earthquake NDMI has also given significant results as the values have changed from −0.01 to 0.20, indicates rapid response to earthquake event (Fig. 10).

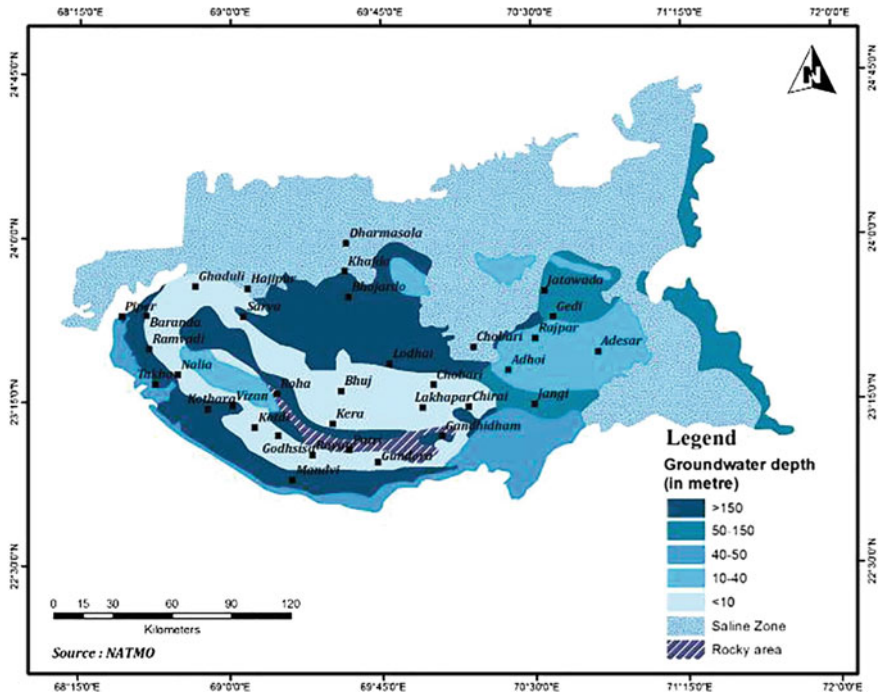

Fig. 7 Soil map of the study area

The study reveals that, mostly red gravelly (25.87%) and loamy soils (20.63%) were characterized by a highly liquefaction probable zone followed by older alluvium soil (15.16%) and sandy soil (12.34%) (Table 3).

The PGA influences the soil and ground water table. PGA values have extreme variability over distances of a few kilometers, particularly with moderate to large earthquakes. The PGA of Bhuj earthquake showing the highest ground motion in the central part of the Kutch district, which was the epicenter of that menace and it is decreasing from the centre towards outside. Thus, on the basis of the severity of PGA and its catastrophic destruction (MMI) ranks have been given to the PGA and MMI. The results show that, the study area has been categorized into six vulnerability zones, namely- severe, very high, high, significant, low and very low zone (Fig. 11).

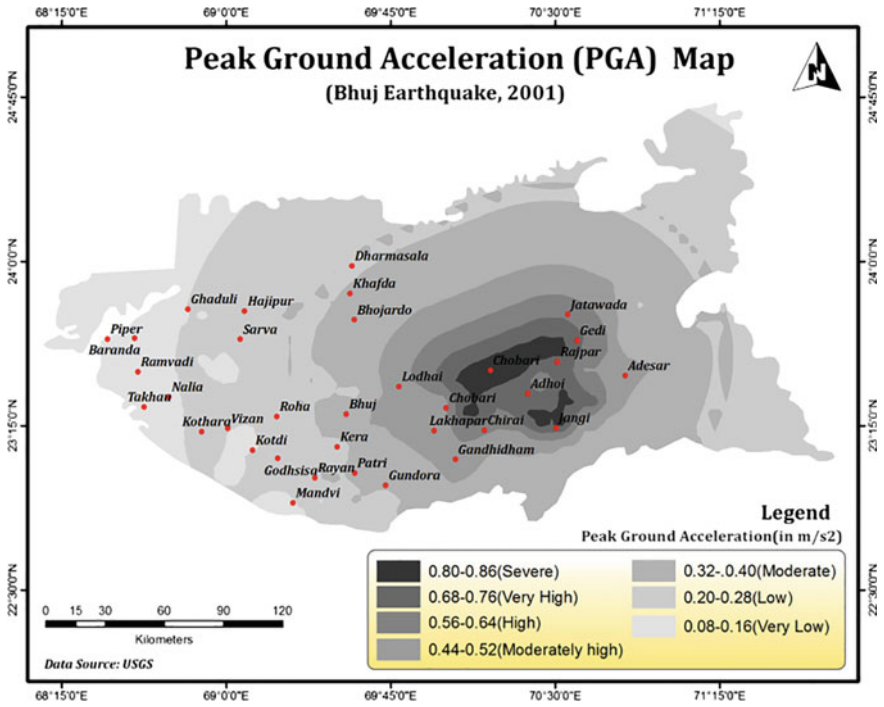

Fig. 8 PGA of the study area during earthquake

It has been observed that, parts of Bhuj, Bhachau and Rapar are more vulnerable to liquefaction. The reason behind the high liquefaction vulnerability is due to sandy and gravelly soil, high ground moisture condition and high ground water depth. It has also been noticed that, 200–415 m^2 area under the moderately high liquefaction zone for Rapar and Bhachau taluk, whereas, 750–850 m^2 area of Abdasa is having the low liquefaction vulnerability. It has also been noticed from the analysis of the relation of LULC with the obtained results that, there is a strong relationship between wetlands and liquefaction. The results show that, the probability of liquefaction is very high in the regions where water table is high (Fig. 12).

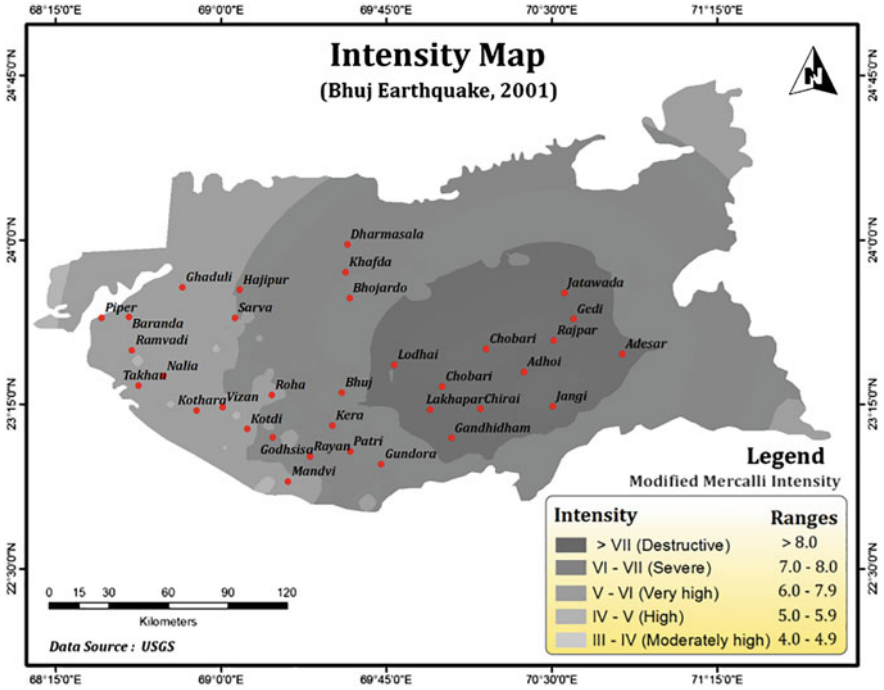

Fig. 9 MMI of the study area during earthquake

Table 2 Ranking thematic layers for multi-criteria analysis

Themes	Weights (%)	Types	Ranks	Remarks
Soil	35	Deep black soil	1	Liquefaction is more likely to occur in loose to moderately saturated granular soils with poor drainage, such as silty sands or sands and gravels capped or containing seams of impermeable sediments
		Medium black and laterite soil	3	
		Salt waste and shallow black soil	5	
		Saline and saline alkaline soil	6	
		Coastal alluvial and older alluvium soil	7	
		Red loamy soil	8	
		Red gravelly and sandy soil	9	
Ground water depth	20	Saline zone and rocky area	1	Generally liquefaction occurs in those areas where ground water is very near to the surface (10–30 m)
		>150 m	3	
		50–150 m	5	
		40–50 m	6	Higher depth, hence, less liquefaction prone
		<10 m	8	Low depth, hence highly liquefaction prone
		10–40 m	9	

(continued)

Table 2 (continued)

Themes	Weights (%)	Types	Ranks	Remarks
NDMI	10	Low saturated	1	Higher moisture condition of the surface, hence liquefaction prone
		Moderately saturated	6	
		Highly saturated	9	
LULC	10	Built-up	8	In any type of LULC liquefaction is more prone to wetlands where the ground water table is high. on the other hand settlement areas are generally cautious about liquefaction as it results in destruction property and lives
		Cropland	6	
		Forest	2	
		Wastelands	3	
		Wetlands	9	
		Rann	1	
PGA	10	Severe	9	Higher PGA condition of the surface, hence liquefaction prone
		Very high	8	
		High	7	
		Moderately high	6	
		Moderate	4	
		Low	2	
		Very low	1	
MMI	15	Destructive	9	Higher MMI condition of the area, hence liquefaction prone
		Severe	8	
		Very high	7	
		High	6	
		Moderately high	5	

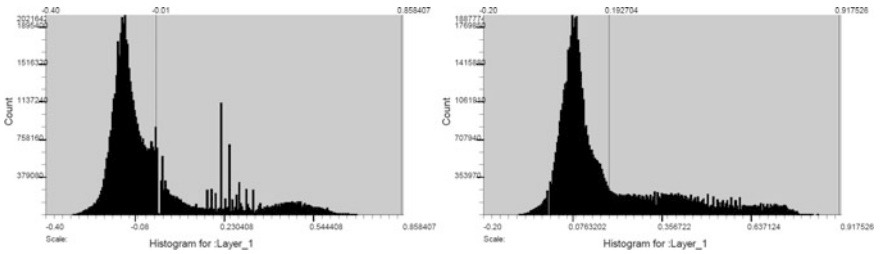

Fig. 10 Pre and Post earthquake NDMI

Table 3 Relation between soil and liquefaction probability

Soil types	High liquefaction (%)
Coastal alluvial soils	15.659
Deep black soils	0.747
Laterite soils	2.314
Medium black soils	0.515
Older alluvium soils	15.162
Red gravelly soils	25.877
Red loamy soils	20.630
Red sandy soils	12.348
Saline and saline alkali soils	0.014
Salt waste	1.633
Shallow black soils	5.101

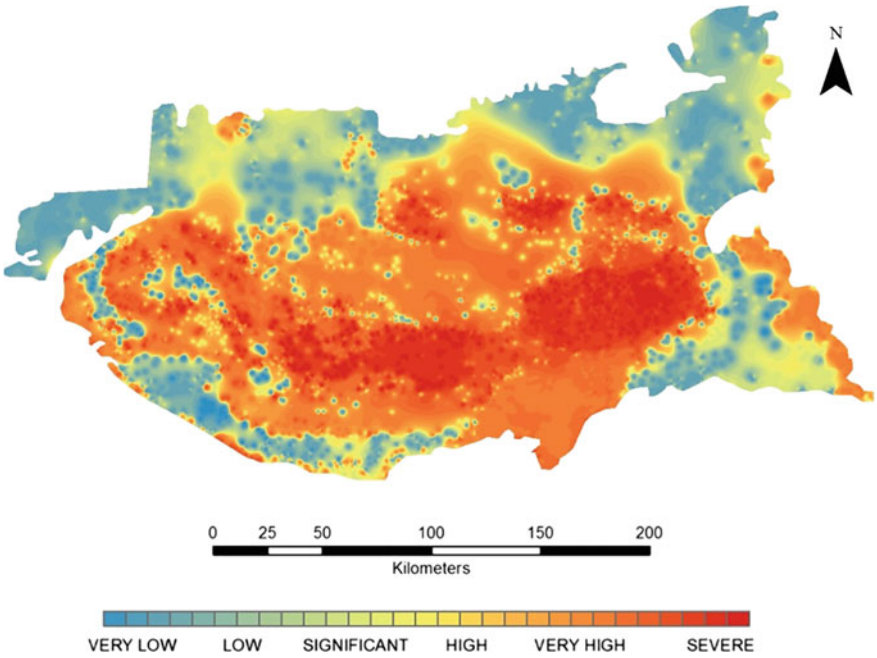

Fig. 11 Liquefaction vulnerability map of the study area

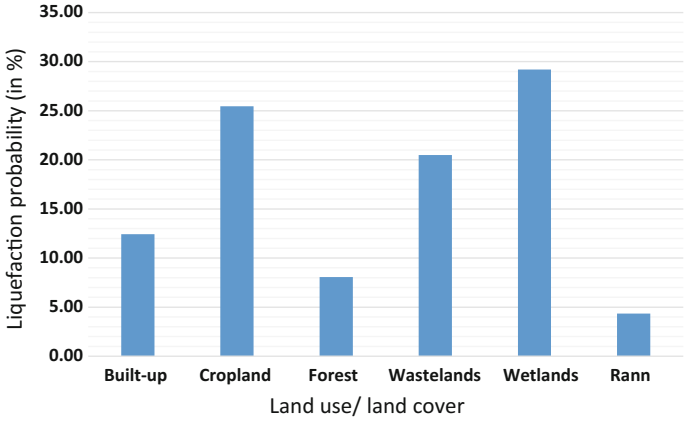

Fig. 12 Relation between LULC and liquefaction

6 Conclusions

The outcome of the current study envisaged the fact that, liquefaction vulnerability can be assessed using geoinformatics. The integrated approach of liquefaction assessment involved, influencing factors like soil type, surface moisture and groundwater depth, ground acceleration, intensity of earthquake, land use pattern to characterize the controls on liquefaction. The study has identified that maximum part of Bhuj is the high seismological liquefaction vulnerable zone, whereas the Mandvi and Bhachau are the next. The analysis also reveals that, the most vulnerable area of Kutch district the isoseismicity is very high during the last 340 years of data analysis. Although many studies have already evaluated the post-earthquake liquefaction and suggested efficient technique to map the post- liquefaction incidents, but the present technique will be helpful to evaluate the liquefaction vulnerability for earthquake prone areas. Thus, the present study will also accredit planners and disaster management groups to execute an action plan for pre and post disaster preparedness and management in a systematic and scientific manner.

References

1. Jefferies, M., Been, K.: Soil Liquefaction: A Critical State Approach. Taylor & Francis, Abingdon (2006)
2. Youd, T.L., Idriss, I.M.: Liquefaction resistance of soils: summary report from the 1996 NCEER and 1998 NCEER/NSF workshops on evaluation of liquefaction resistance of soils. J. Geotech. Geoenviron. **127**(10), 297–313 (2001)
3. Sam, L.D., Poulos, H.G.: Assessment of soil liquefaction incorporating earthquake characteristics. Soil Dyn. Earthq. Eng. **24**(11), 867–875 (2004)

4. Oommen, T., Baise, L.G., Gens, R., Prakash, A., Gupta, R.P.: Application of Satellite Data for Post-liquefaction Reconnaissance, Report. Collaborative Research with Tufts University and University of Alaska Fairbanks, Alaska (2011)
5. Iyengar, R.N., Raghukanth, S.T.G.: Strong ground motion at Bhuj city during the Kutch earthquake. Curr. Sci. **82**(11), 1366–1372 (2002)
6. Karanth, R.V., Sohoni, P.S., Mathew, G., Khadikar, A.S.: Geological observations of the 26 January, 2001 Bhuj earthquake. J. Geol. Soc. India **58**, 193–202 (2001)
7. Rajendran, K., Rajendran, C.P., Thakkar, M., Tuttle, M.P.: The 2001 Kutch (Bhuj) earthquake: coseismic surface features and their significance. Curr. Sci. India **80**(11), 1397–1405 (2001)
8. Jade, S., Mukul, M., Parvez, I.A., Ananda, M.B., Kumar, P.D., Gaur, V.K.: Estimates of coseismic displacement and post seismic deformation using global positioning system geodesy for the Bhuj earthquake of 26 January, 2001. Curr. Sci. **82**(6), 748–752 (2002)
9. Bilham R.: 26th January, 2001 Bhuj earthquake, Gujarat, India. Available at: http://cires1.colorado.edu/~bilham/Gujarat2001.html (2001)
10. Krinitzsky, E.L.: Hynes., M.E.: The Bhuj, India earthquake: lessons learnt forearthquake safety of dams on alluvium. Eng. Geol. **66**(3–4), 163–196 (2002)
11. Tuttle, M.P., Hengesh, J.V., Liquefaction, in Bhuj, India Earthquake of January 26, 2001 reconnaissance report (Jain, S.K., Lettis, W.L., Murty, C.V.R., Barder, J.P. (eds.)). Earthq. Spectra. **18**(Suppl.), 79–100 (2002)
12. Ramakrishnan, D., Mohanty, K.K., Nayak, S.R., Chandran, V.: Mapping the liquefaction induced soil moisture changes using remote sensing technique: an attempt to map the earthquake induced liquefaction around Bhuj, Gujarat, India. Geotech. Geol. Eng. **24**, 1581–1602 (2006)
13. Youd, T.L., Keefer, D.K.: Earthquake Induced Ground Failures, in Facing Geologic and Hydrologic Hazards. U.S. Geological Survey, Washington (1981)
14. Youd, T.L., Perkins, D.M.: Mapping of liquefaction severity index. J. Geotech. Eng.-ASCE **113**(11), 1374–1392 (1987)
15. Malik, J.N., Sohoni, P.S., Karanth, R.V., Merh, S.S.: Modern and historic seismicity of Kutch Peninsula, Western India. J. Geol. Soc. India **54**, 545–550 (1999)

Chapter 39
A Study on Assessment of Pollution in Godavari Estuary East Coast of India by Using Trace Metals Concentration in the Sediments

Hari Prasad, P. Bhanu Murty, M. Sanyasi Rao and Rajesh Duvvuru

Abstract In recent years there has been a rapidly growing interest on the heavy metallic content in estuaries and on the nature and the pathways by which they are introduced into the system. A total of seven sampling stations were fixed along the longitudinal stretch of the estuary, starting from head to mouth of the estuary for the collection of surface and bottom waters and sediments has done seasonally. In which water and sediment samples were collected during pre-monsoon (March), onset of monsoon (June), monsoon (September) and post-monsoon (December) by using Niskin water sampler and Van Veen Grab respectively for a period of one year during 2016. Hydrographic parameters of temperature, pH, and salinity were analyzed for the collected samples with standard methods. Sediment trace metals like cadmium, copper, iron, nickel, lead and zinc were estimated from the collected sediment samples by atomic absorption spectrophotometer after proper acid digestion. The organic carbon content was determined by the method of El-Wakeel and Riley (1957). Temperature, pH and salinity exhibited distinct spatial and seasonal variations in estuarine waters of the Gauthami Godavari. Temperature and pH showed an increasing trend from post-monsoon (winter) to pre-monsoon (summer) in accordance with the variation of atmospheric temperature in the study region. Enrichment factors of the metals were calculated based on the data, cadmium in Stations. 1, 2 are moderately polluted during monsoon season due to the anthropogenic source. Compared to all metals were studied, zinc and cadmium are more

H. Prasad (✉) · P. Bhanu Murty
Department of Geology, Andhra University, Visakhapatnam 530003, India
e-mail: hari003.geo@gmail.com

P. Bhanu Murty
e-mail: pbmauvsp89@yahoo.co.in

M. Sanyasi Rao
National Geophysical Research Institute, Hyderabad 500007, India
e-mail: sunny.geology@gmail.com

R. Duvvuru
Department of Geo-Engineering, Andhra University, Visakhapatnam 530003, India
e-mail: rajesh.duvvuru@gmail.com

P. J. Rao et al. (eds.), *Proceedings of International Conference on Remote Sensing for Disaster Management*, Springer Series in Geomechanics and Geoengineering,
https://doi.org/10.1007/978-3-319-77276-9_39

enriched. All the metals are moderately enriched in the upstream of the estuary due to natural and anthropogenic sources and also higher enrichment was observed during pre and post-monsoon season except cadmium which is in the monsoon season.

Keywords Estuary · Trace metals and pollution

1 Introduction

The estuary can be regarded as a dynamically evolving land form that undergoes a life cycle from valley creation, followed by a drowning phase, and ending with progressive infilling [10]. According to Dionne [7], an estuary could be divided into 3 sectors: (a) a marine or lower estuary in free connection with open sea, (b) a middle estuary, subjected to strong salt and fresh water mixing and (c) an upper or fluvial estuary characterized by fresh water, but subjected to daily tidal action. Chemistry of estuary should be considered in the context of the physical processes of water circulation which occur in them, since the distribution of dissolved and particulate substances are controlled by the circulation and mixing of their waters [2].

The physico-chemical processes which act on rocks and soil of the catchment area normally control the concentration of trace metals in the fluvial and estuarine sediments. Due to anthropogenic input, abnormal concentration of heavy metal are observed in sedimentary phases in several estuaries. The chemical behaviour of a trace metal during its transport within the estuary is determined mainly by its chemical form in which it is transported. It could be either (1) in solution as inorganic ion or (2) adsorbed on to surfaces of solid organic particles, (3) coating on detrital particles after co-precipitation with and sorption on to mainly iron and manganese oxides, (4) in lattice positions of detrital crystalline material, or (5) precipitated as surfaces possibly on detrital particles.

2 Geology of the Godavari Drainage Basin

Godavari River receives its sediments from a variety of geological formations which represent nearly a complete cross-section of the geology of peninsular India. More than half of the drainage basin of the Godavari consists of the Deccan traps of Late Cretaceous-Plaeocene age. They are essentially doleritic or basaltic (Tholeritic) in composition. Upon weathering the Deccan Traps gave rise to laterite, bauxite, and the black cotton (chernozem) soils. The more commonly occurring minerals are augite, diopside, enstatite, magnetite, epidote, biotite, zircon, rutile, apatite, and chlorite. Descending from the Deccan plateau the Godavari river first traverses through a small terrain composed of Archean granites, and unclassified

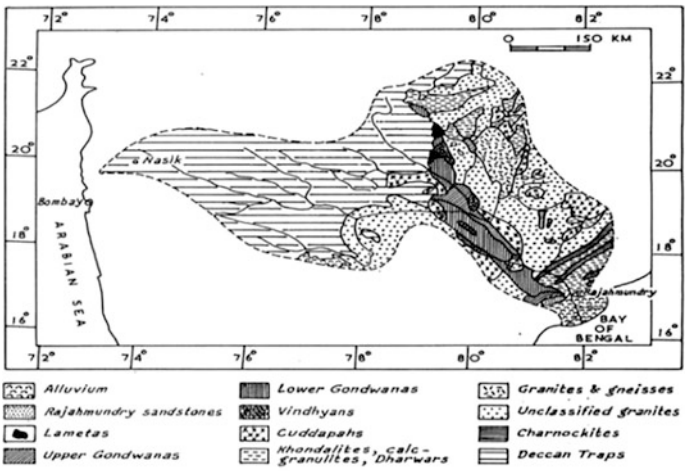

Fig. 1 Geology of the study area

(Dharwars) which are regionally metamorphosed igneous and sedimentary (Pelitic) rocks. These are composed of Phyllites, Quartzites, amphibolites and granites, associated with thick deposits of syngenetic, metasediments manganese ores, and bands of dolomitized marble. Heavy minerals that are likely to be contributed by these reocks are hornblends, biotite, tourmaline, almandine, zircon, epidote, sphene, kyanite and staurolite (Fig. 1).

3 Physiography of the Study Area

The river basin comprising 3,12,812 m^2 which is spread over six states and thirty districts in central India, located between the Latitudes 16° 15′ to 16° 45′N and longitudes 81° 45′ to 82° 25′E. The basin climate is tropical with an average annual rainfall of 1512 mm y^{-1}. About 85% of the total annual rainfall occurs during southwest monsoon (June–September) and the remaining 15% during northeast monsoon (October–January).

4 Geomorphology of Godavari Basin

The various geomorphic features recognized in the depositional environments of the Godavari Delta are Estuary, Mangrove Swamp, Mud flat, Tidal Creek, Lagoon, distributary mouth bar, Shore face, Spit, Point bar and Natural levee. In the lower delta plains of Godavari Delta, and the River channels behave as estuarine channels as they show strong influence of tides.

5 Station Locations and Characteristics

In this present study bottom waters and bottom sediment samples were collected at seven stations in the estuarine waters of Gautami Godavari in which Station 1, is located near the stretch of Gauthami Godavari at Kotipalle, head of the estuary. Station 2, is located at the centre of the river Gauthami Godavari at Dangeru, it is around 8 km down to the Kotipalle. Station 3, is located at the middle of the estuary of Gauthami Godavari near Yanam. Station 4, is located middle of the river at Vrudha Gautami which is a stretch of Gautami Godavari, about 5 km down to Yanam. Station 5, is located at the centre of the river channel at Balusutippa. Station 6, is located at the centre of the creek of the mangrove forest area. Station 7, is located at the centre of the mouth of the estuary, it is connected to the coastal waters of the Bay of Bengal (Fig. 2).

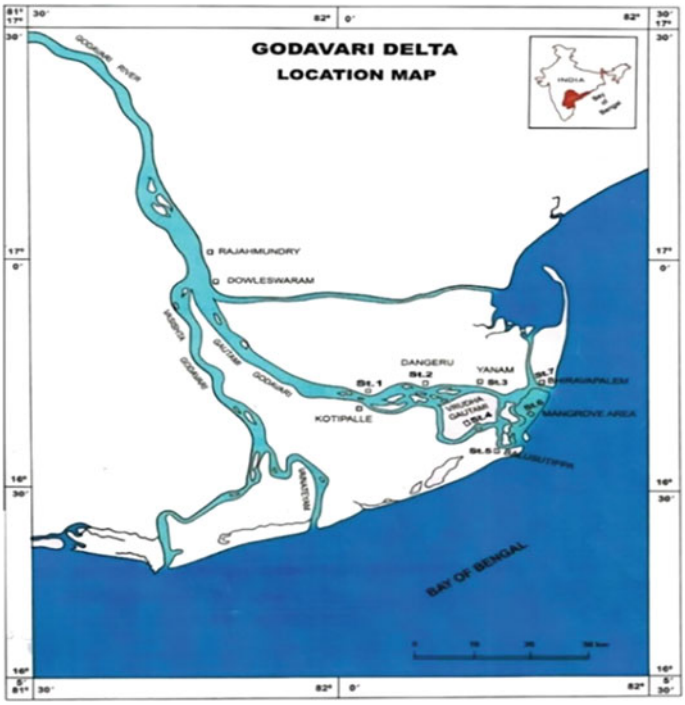

Fig. 2 Map showing sample station locations

6 Sampling Procedure and Materials

Seasonally water and sediment samples were collected for about an equally spread over the mid-point of a pair of consecutive neap and spring tides, suitable dates were selected for the purpose on which, the sampling could be done between 08.00 and 12.30 h in the third week of every season for a period of one year during 2016 in March (pre-monsoon), June (onset of monsoon), September (monsoon) and December (post-monsoon) at all seven stations (St. 1 to St. 7). Surface water samples were collected by using a clean plastic bucket and bottom water samples are with Niskin water sampler (5 l). Sediment samples were collected using a Van Veen Grab. The collected water and sediment samples were transported immediately (within one hour after the collection of the last sample) to the shore laboratory at Yanam, provided by National Institute of Oceanography, Regional Centre, Visakhapatnam.

7 Sediment Analysis

The collected sediment samples were homogenized and air-dried at room temperature, before that all sediments samples were freed from thick granules and shells. A portion of the sample (∼50 g) was taken for grain size (sand, silt & clay %) analyses. For grain size analysis, samples were treated with 35% H_2O_2 and 1 N HCl to remove organic matter and carbonate respectively [19]. After treatment, sediment samples were wet sieved through 230 mesh (0.0625 mm) ASTM sieve for separation of sand samples. Size analysis of very fine particles was carried out by pipette analysis method [11].

Sediment Organic Carbon (C_{org}): The organic carbon content was determined by the method of El-Wakeel and Riley [8]. To a powered sediment sample (0.5 gr), a known quantity of acid dichromate (20 ml 1 N) was added and left for 30 min when all organic matter present in the sample is oxidised. The excess dichromate is back-titrated with ferrous ammonium sulphate using diphenylamine as internal indicator.

7.1 Determination of Metals in the Sediments

For the heavy metal analysis, sediments were dried at 70 °C and finely powdered and sieved through 284 mesh after they were digested (known weigh) in a mixture of HF–$HClO_4$–HNO_3 [12]. Samples were analyzed on a flame AAS (Aanalyst 100 Perkin Elmer) after calibration with suitable E-Merck elemental standards. For cadmium analysis, a Graphite-AAS (ZL 4110 Perkin Elmer) was used.

The precision of the analytical procedure was checked using a triplicate analysis of a certified reference material (NIST) from the Department of commerce, USA.

Enrichment Factor (EF): A number of different enrichment calculation methods and different reference material have been reported [1, 5, 14–16, 18, 20]. The degree of anthropogenic pollution was established by adapting enrichment factor ratios (EF) used by Sutherland et al. [18].

8 Textural Characters of Sediments

Textural characteristic of estuarine sediments are strongly influenced by several factors, including source area composition of adjacent lands, climate, length and energy of sediment transport and redox conditions in the depositional environment [3, 6]. Numerous studies have analyzed grain size properties which can suggest sources and hydrodynamic conditions of marine sediments [4]. Moreover, spatial variations in sand, silt and clay ratio can help to determine present estuarine environment conditions.

Sand: The sand content in the sediments of the Gauthami estuary ranged from 22.35 to 79.25% with an average of 47.45%. Seasonally higher percentages of sand were observed during post-monsoon season, followed by monsoon and onset of monsoon. Lower sand content were observed during pre-monsoon season (Table 1).

Silt. The silt content in the sediments of the Gauthami estuary ranged from 8.35 to 43.45% with an average of 25.54%. The silt content in the sediments of estuarine waters of Gautami Godavari is higher at Balusutippa area and lower at Dangeru area (Table 2).

Clay: The clay content in the sediments of the Gauthami estuary ranged from 12.40 to 45.48% with an average of 27.97%. Higher concentrations clay was observed mangrove area due to higher accumulation of fine grained sediments (Table 3).

Table 1 Station-wise statistical summary of sand (%) in the estuarine sediments of Gautami Godavari

St. no.	Min.	Max.	Average	S.D
Kotipalle	32.35	44.55	38.93	5.23
Dangeru	65.20	72.25	68.63	3.20
Yanam	62.36	79.25	71.05	8.44
V. Gauthami	93.25	71.45	49.61	14.88
Balusutippa	22.35	38.35	31.77	7.18
Mangrove area	26.12	39.34	32.50	5.47
Bhiravapalem	31.78	53.52	39.70	9.93

Table 2 Station-wise statistical summary of silt (%) in the estuarine sediments of Gauthami Godavari

St. no.	Min.	Max.	Average	S.D
Kotipalle	23.25	31.55	28.40	3.65
Dangeru	9.25	12.55	11.03	1.54
Yanam	8.35	19.25	12.99	4.63
V. Gauthami	12.25	33.25	26.00	9.39
Balusutippa	38.00	43.45	41.04	2.43
Mangrove area	28.40	29.25	28.97	0.39
Bhiravapalem	26.12	32.25	30.34	2.90

Table 3 Station-wise summary of clay (%) in the estuarine sediments of Gauthami Godavari during 2016

St. no.	Min.	Max.	Average	S.D
Kotipalle	23.90	39.20	32.68	7.71
Dangeru	15.20	24.50	20.35	3.85
Yanam	12.40	24.40	20.21	5.33
V. Gauthami	16.30	28.62	24.39	5.59
Balusutippa	23.50	34.20	29.70	5.15
Mangrove area	31.40	45.48	38.53	5.81
Bhiravapalem	20.36	37.50	29.97	7.65

9 Sediment Organic Carbon

The organic carbon content of the sediment has a major role in maintaining the fertility of the sediment and thereby flourishing the biological productivity. Knowledge of the nature, origin and transformations of organic matter in sediments provides valuable information on the cycling of trace metals in the aquatic environment (Table 4).

The distribution of organic carbon content in the study area exhibited distinct spatial and seasonal variations and was found to be within the range from 1.16 to 3.41% with a mean value of 2.61%. These values are generally less than the limit for a polluted estuary. Except Kotipalle and Dangeru, all stations recorded higher values during all seasons. Lower organic content at stations 7 associated with the prominent coarse sandy sediment fractions. The high organic carbon in the estuary

Table 4 Station-wise summary of organic carbon (%) in the estuarine sediments of Gauthami Godavari

St. no.	Min.	Max.	Average	S.D
Kotipalle	1.16	3.41	2.52	1.04
Dangeru	1.28	3.30	2.48	0.94
Yanam	2.02	3.16	2.62	0.60
V. Gauthami	2.11	3.16	2.67	0.56
Balusutippa	2.21	3.11	2.69	0.47
Mangrove area	2.20	3.35	2.72	0.50
Bhiravapalem	2.25	3.04	2.58	0.34

can be ascribed to high productivity of the overlying waters, sewage discharges and clayey nature of sediments. Sediment organic carbon exhibited a decreasing trend towards the mouth. This may be due to flushing of organic matter and finer fractions of the sediments by tidal action.

10 Trace Metals in Sediments

Heavy metal contamination in estuarine and coastal sediment has been an increasing eco-toxicological problem, because the estuarine and coastal areas are often receives anthropogenic and industrial wastes from their geographical areas. Estuaries and coastal areas are among the most productive marine ecosystems, it is an important that contamination by trace metals in these sediments should be monitored for effective remedial actions against metal pollution. The contaminants in sediments depend on variety of factors such as basin geology, physiography, chemical reactivity, lithology, mineralogy, hydrology, vegetation, land use pattern and biological productivity.

Cadmium: Cadmium, the least abundant metal in the sediments of Gauthami Godavari estuary ranged from 17.16 to 35.14 μg g^{-1} with an overall mean concentration of 25.10 μg g^{-1}. The lowest (17.16 μg g^{-1}) values of cadmium were observed at the mouth of the estuary (Bhiravapalem) and highest values (35.14 μg g^{-1}) were recorded at head of the estuary (Kotipalle and Dangeru) (Table 5).

Copper: Copper concentrations in the sediments of Gauthami Godavari estuary ranged from 21.25 to 207.50 μg g^{-1} with a mean value of 78.71 μg g^{-1}, and the lowest value is 21.25 μg g^{-1} was observed at the mouth of the estuary (Bhiravapalem) and highest value (207.50 μg g^{-1}) was observed at head of the estuary (Kotipalle). Copper showed significant seasonal variation with higher values during pre-monsoon and post-monsoon season comparatively lower values during monsoon and onset of -monsoon seasons. High saline conditions, which might cause the dissolved copper to precipitate and flocculate, finally settled into the bottom sediments (Table 6).

Table 5 Station-wise statistics of cadmium concentration (μg gr^{-1}) in the estuarine sediments of Gauthami Godavari during 2016

St. no.	Min.	Max.	Average	S.D
Kotipalle	25.20	29.50	27.24	1.76
Dangeru	24.30	35.14	28.37	4.74
Yanam	23.50	33.72	27.28	4.47
V. Gauthami	22.50	31.16	25.64	3.84
Balusutippa	20.15	30.15	23.90	4.35
Mangrove area	18.25	28.17	22.45	4.17
Bhiravapalem	17.16	26.18	20.86	3.87

Table 6 Station-wise summary statistics of copper (μg gr^{-1}) in the estuarine sediments of Gauthami Godavari

St. no.	Min.	Max.	Average	S.D
Kotipalle	38.50	207.50	104.43	79.01
Dangeru	36.30	185.00	95.33	71.17
Yanam	34.20	176.00	89.93	66.98
V. Gauthami	33.10	133.00	75.40	49.34
Balusutippa	32.15	107.50	68.16	40.14
Mangrove area	26.12	102.60	60.56	37.67
Bhiravapalem	21.25	101.50	57.19	38.90

Iron: Iron concentrations in the sediments of Gauthami Godavari, Estuary ranged from 902 to 1472 μg g^{-1} with an overall mean concentration of 1194.50 μg g^{-1}. The lower concentration of iron (902 μg gr^{-1}) were observed at the mouth of the estuary (Bhiravapalem) and higher concentrations of iron (1472 μg gr^{-1}) at the head of the estuary (Kotipalle) with a annual mean concentration of 1194.50 μg gr^{-1}. Iron content was found to be the highest among all the metals at all the stations (Table 7).

Nickel: The Concentration of nickel recorded its minimum of 43.15 μg gr^{-1} at mouth of the estuary (Bhiravapalem) and maximum of 116.48 μg gr^{-1} at head of the estuary (Kotipalle). The annual mean concentration during this study period was 82.07 μg gr^{-1}. The average concentration of total nickel in Godavari estuary was higher than Indian average (37 mg/kg), but it was less than world average as well as average shale concentration (Table 8).

Lead: Lead concentrations in the sediments of Gauthami Godavari, estuary ranged from 30.10 to 62.50 μg g^{-1} with an overall mean concentration of 44.45 μg g^{-1}. The lowest (30.10 μg g^{-1}) values of lead was observed at the mouth of the estuary (Bhiravapalem) and highest value (62.50 μg g^{-1}) was observed at head of the estuary (Kotipalle) (Table 9).

Zinc: The concentration of the zinc in the sediments of Gauthami Godavari estuary ranged from 453 to 1130 μg gr^{-1}. The overall annual mean concentration during the investigation was found to be 831.89 μg gr^{-1}. The lowest (453 μg gr^{-1}) and highest (1130 μg gr^{-1}) concentrations of zinc were recorded respectively at stations Bhiravapalem and Kotipalle. The Bhiravapalem station recorded minimum level of zinc in all seasons due to the sandy nature of sediments (Table 10).

Table 7 Station-wise summary statistics of iron (μg gr^{-1}) in the estuarine sediments of Gauthami Godavari

St. no.	Min.	Max.	Average	S.D
Kotipalle	989	1472	1249.75	208.65
Dangeru	963	1467	1240.00	217.08
Yanam	935	1425	1209.00	2011.63
V. Gauthami	930	1422	1202.50	211.74
Balusutippa	925	1408	1188.00	209.07
Mangrove area	912	1407	1158.75	2011.88
Bhiravapalem	902	1403	1113.50	217.86

Table 8 Station-wise summary statistics of nickel (μg gr^{-1}) in the estuarine sediments of Gauthami Godavari

St. no.	Min.	Max.	Average	S.D
Kotipalle	86.32	116.48	100.64	12.42
Dangeru	73.15	113.94	95.01	17.11
Yanam	70.16	105.16	90.46	14.86
V. Gauthami	63.15	92.70	82.70	13.33
Balusutippa	52.23	84.60	73.35	14.48
Mangrove area	49.20	76.72	67.56	12.45
Bhiravapalem	43.15	74.52	64.76	14.53

Table 9 Station-wise summary statistics of lead (μg gr^{-1}) in the estuarine sediments of Gauthami Godavari

St. no.	Min.	Max.	Average	S.D
Kotipalle	40.10	62.50	52.44	9.39
Dangeru	38.50	58.30	48.86	8.26
Yanam	35.30	55.50	46.14	8.42
V. Gauthami	33.20	51.60	44.16	7.85
Balusutippa	31.40	49.50	41.91	7.61
Mangrove area	31.01	47.20	40.33	6.79
Bhiravapalem	30.10	41.30	37.35	4.96

Table 10 Station-wise summary statistics of zinc (μg gr^{-1}) in the estuarine sediments of Gauthami Godavari

St. no.	Min.	Max.	Average	S.D
Kotipalle	736.00	1130.00	994.25	179.11
Dangeru	713.00	1105.00	970.50	179.07
Yanam	676.00	1008.00	860.00	144.04
V. Gauthami	630.00	1004.00	827.00	154.48
Balusutippa	515.00	985.00	781.50	195.34
Mangrove area	496.00	865.00	710.00	155.84
Bhiravapalem	453.00	823.00	680.00	159.00

11 Metal Enrichment in Sediments

The quantification of trace metal enrichment in the sediments of Gauthami Godavari estuary was attempted by calculating the enrichment factor. In this study Fe was selected as a normalization constituent and enrichment factor calculated using the equation.

$$\text{Enrichment Factor} = (\text{X/Fe})\ \text{Sample}\ (\text{X/Fe})\ \text{Ref},$$

where (X/Fe) sample is the ratio of the concentration of element 'X' to that of iron in the sample sediment, and (X/Fe) Ref, is the same ratio in the sediment from a far upstream station, which is free from industrial pollution. It was found that all the trace metals were enriched in Godavari estuary to varying extents. The enrichment

Table 11 Seasonal variation of Enrichment Factor (EF) for total metals in the surface sediment of Gauthami Godavari Estuary during 2016

Pre-monsoon							Monsoon						Post-monsoon					
Station	Cd	Cu	Fe	Ni	Pb	Zn	Cd	Cu	Fe	Ni	Pb	Zn	Cd	Cu	Fe	Ni	Pb	Zn
1	4.32	3.32	3.25	2.26	2.20	4.55	5.36	3.25	3.15	2.16	2.10	4.35	4.22	3.33	3.23	2.31	2.26	4.85
2	4.35	3.22	3.21	2.24	2.21	4.25	5.32	3.01	3.11	2.1124	2.00	4.05	4.15	3.34	3.25	2.44	2.41	4.65
3	3.36	3.01	3.01	2.22	2.01	4.20	4.45	2.65	2.91	2.102	2.01	3.82	3.65	3.26	3.11	2.32	2.22	4.51
4	3.32	2.62	2.32	2.05	2.00	3.95	4.26	2.55	2.62	2.01	1.67	3.65	3.42	3.22	2.62	2.25	2.11	4.40
5	3.21	2.51	2.22	1.86	1.65	3.65	3.82	2.43	2.52	1.66	1.55	3.41	3.33	2.61	2.42	2.20	1.85	3.81
6	3.02	2.45	2.12	1.65	1.45	3.54	3.65	2.41	2.32	1.45	1.35	3.22	3.22	2.35	2.22	1.75	1.65	3.64
7	2.12	2.31	2.05	1.32	1.20	3.32	2.26	2.16	2.15	1.12	1.10	3.12	2.52	2.21	2.11	1.52	1.25	3.51

factors showed no significant seasonal variation except in the case of lead. Enrichment factors for lead exhibited seasonal variation with higher values during pre-monsoon and post-monsoon seasons.

12 Geochemical Normalization and Enrichment Factors (EF)

In an attempt to compensate for the natural variability of total trace elements in sediments, normalization was done so that any anthropogenic metal contributions could be detected and quantified. Loring [13] indicated that the natural mineralogical and granular variability is the best compensated by the geochemical normalization of major and trace metal data (Table 11).

13 Inter-relationships Among Texture and Trace Metals

Distribution of texture (sand, silt, clay, organic carbon) and trace metals (Cd, Cu, Fe, Ni, Pb, Zn) in sediments in the estuarine waters of Gauthami Godavari is mainly controlled by the inputs of river runoff including weathering materials, domestic sewage, agricultural back runoff, leaching from paints of fishing boats and industrial effluents released into the river (Table 12).

Table 12 Inter-relations between sediment texture and trace metals in the sediments of Gauthami Godavari

Parameter	Sand	Silt	Clay	OC	Cd	Cu	Fe	Ni	Pb
Silt	−0.90								
Clay	−0.84	0.60					N = 28		
OC	−0.21	−0.21	0.33				P = < 0.05		
Cd	0.42	−0.41	−0.51	−0.51					
Cu	0.14	−0.31	0.25	0.88	−0.25				
Fe	0.12	−0.21	0.22	0.89	−0.50	0.88			
Ni	0.33	−0.40	0.12	0.45	−0.31	0.70	0.75		
Pb	0.20	−0.31	0.22	0.56	−0.32	0.87	0.87	0.94	
Zn	0.22	−0.33	0.11	0.62	−0.25	0.77	0.86	0.93	0.97

14 Summary and Conclusion

The temperature values in the surface waters of Gauthami estuary varied from 26.50 to 31.80 (°C) with an average of 29.62 (°C), where as in the bottom waters, the temperature ranged from 25.60 to 31.40 (°C) with an average of 28.84 (°C) during the study period. The values of pH in the surface waters varied in the range of 7.20 to 8.20 with an average of 7.71, where as in the bottom waters, the pH values varied from 7.43 to 8.30 with an average of 7.94. The salinity values ranged from 0.23 to 31.83 psu with an average of 15.43 psu in surface waters and from 4.63 to 34.26 psu with an average of 10.13 psu in the bottom waters.

Temperature and pH showed an increasing trend from post-monsoon (winter) to pre-monsoon (summer) in accordance with the variation of atmospheric temperature in the study region. It also exhibited in general, a decreasing trend from surface to bottom waters in all seasons. The pH and salinity values are lower at head of the estuary and gradually increase towards the mouth of the estuary. Lower pH and salinity values were observed during monsoon season. The vertical pH and salinity distribution (gradient) in this estuary suggests slight stratification in monsoon, partial/well mixed conditions in post/pre-monsoon seasons.

The sand content in the sediments of the Gauthami estuary ranged from 22.35 to 79.25% with an average of 47.45%. Lower sand content were observed during pre-monsoon season. The silt content in the sediments ranged from 8.35 to 43.45% with an average of 25.54%. The clay content in the sediments varies from 12.40 to 45.48% with an average of 27.97%. The organic carbon content in the sediments varied from 1.162 to 3.41% with a mean value of 2.61%. The high organic carbon in the estuary can be ascribed to high productivity of the overlying waters, sewage discharges and clayey nature of sediments. Seasonally higher organic carbon content was observed during pre-monsoon and post-monsoon than that of than that of monsoon season. Cadmium, the least abundant metal in the sediments of Gauthami Godavari estuary ranged from 17.16 to 35.14 $\mu g\ g^{-1}$ with an overall mean concentration of 25.10 $\mu g\ g^{-1}$. The decrease in concentration of cadmium during pre-monsoon and onset of monsoon seasons may be attributed to the formation of chloride complexes, occurring during the mixing of fresh water with seawater and to the desorption of exchangeable metals due to the increasing concentration of major ions.

Copper concentrations in the sediments ranged from 21.25 to 207.50 $\mu g\ g^{-1}$ with a mean concentration of 78.71 $\mu g\ g^{-1}$. The higher content of copper during pre-monsoon season may be due to existing biogeochemical changes in the estuary itself and also to the hydrological and sedimentalogical character, which vary along with reduced river discharge conditions during this season and also coincided with salinity maximum of the ambient water. Iron concentrations in the sediments of Gauthami Godavari estuary ranged from 902 to 1472 $\mu g\ g^{-1}$ with a mean concentration of about 1194.50 $\mu g\ g^{-1}$. Iron recorded higher values in upper reaches which may be due to its proximity to wastewater discharged from the densely populated coastal delta. The Concentration of nickel recorded its minimum of

43.15 μg gr^{-1} to a maximum of 116.48 μg gr^{-1} with annual mean value of 82.07 μg gr^{-1}. Lead concentrations in the sediments of Gauthami Godavari, estuary ranged from 30.10 to 62.50 μg g^{-1} with an overall mean concentration of 44.45 μg g^{-1}. The concentration of the zinc in the sediments of Gauthami Godavari estuary ranged from 453 to 1130 μg gr^{-1}. The overall annual mean concentration during the investigation was found to be 831.89 μg gr^{-1}.

Significant negative correlations are observed between sand and clay indicates that enrichment of silt and clay. Significant positive correlations were observed between organic carbon all metals may be attributed to the enrichment of metals are associated with fine grain sediments. The positive relationship between trace metals and organic carbon in the sediments was due to the simultaneous coagulation and setting of metals along with organic carbon derived from urban sewage or industrial effluents. Nickel, lead and zinc showed high positive correlation with iron indicating the existence of their strong association with oxides and hydroxides of iron. From these observations it was observed that the sediments of Gauthami Godavari is not much polluted.

References

1. Akoto, O., Ephraim, J.H., Darko, G.: Heavy metals pollution in surface soils in the vicinity of abundant railway servicing workshop in Kumasi, Ghana. Int. J. Environ. Res. **2**(4): 359–364 (Autumn, 2008)
2. Aston, S.R.: Nutrients, dissolved gases and general biogeochemistry of esturies. In: Olausson, E., Cato, I. (eds.) Chemistry and biogeochemistry of esturies, pp. 233–257. John Wiley and sons Ltd. (1980)
3. Bhatia, M.R., Cook, K.A.W.: Trace element characteristics of graywackes and tectonic setting discrimination of sedimentary basins. Contrib. Mineral. Petrol. **92**, 181–193 (1986)
4. Carranza-Edwards, A., et al.: Petrography of quartz grains in beach and dune sands of Northland, North Island, New Zealand. N. Z. J. Geo. Geophys. **48**, 649–660 (2005)
5. Charkravarty, M., Patgiri, A.D.: Metal pollution assessment in sediments of the Dikrong River, N.E. India. J. Hum. Ecol. 63–67 (2009)
6. Dickhudt, P.J., Friedrichs, C.T., Sanford, L.P.: Mud matrix solids fraction and bed erodibility in the York River estuary, USA, and other muddy environments, Cont. Shelf Res. **31**(10, Suppl. 1), S3–S13 (2011)
7. Dionne, J.C.: Towards a more adequate definition of the St. Lawrence estuary. Zeitschr. F. Geomorph. **7**(1), 36–44 (1963)
8. El-Wakeel, S., Riley, J.: The determination of organic carbon in marine Mud. Journal du Conseil International pour l'Exploration de la Mer. **22**(2), 180–183 (1957)
9. Emery, K.O., Milliman, J.D.: Suspended matter in surface water: influence of river discharge and upwelling. Sedimentology **25**, 77–80 (1978)
10 Fairbridge, R.W.: (1980) The estuary: Its definition and geodynamic cycle. In: Olausson, E., Cato, I. (eds.) Chemistry and biogeochemistry of estuaries, pp. 1–35. Wiley, New York (1980)
11. Krumbein, W.C., Pettijohn, F.J.: Manual of Sedimentary Petrography, p. 549. Appleton Century Crafts, New York (1938)

12. Loring D.H., Rantala R.T.T.: Manual for the geochemical analyses of marine sediments and suspended particulate matter. Earth-Science Reviews, 32: 2350283, and 1995, Regional Seas, Reference methods for marine pollution studies no. 63, United Nations Environment Programme (1992)
13. Loring, D.H.: Normalization of heavy-metal data from estuarine and coastal sediments. ICES J. Mar. Sci. **48**, 101–115 (1991)
14. Ogunsola, O.J., Oluwole, A.F., Asubiojo, O.I., Durosinmi, M.A., Fatusi, A.O., Ruck, W.: (1994). Environmental impact of vehicular traffic in Nigeria: Health aspects. Sci. Total Environ. **23**, 146–147 (1994)
15. Olubunmi, F.E., Olorunsola, O.E.: Evaluation of the status of heavy metal pollution of sediment of Agbabu bitumen deposit area, Nigeria. Eur. J. Sci. Res. **41**(3), 373–382 (2010)
16. Sekabira, K.: Assessment of heavy metal pollution in the urban stream sediments and its tributaries. Int. J. Environ. Sci. Tech. *7*(3), 435–446 (2010).
17. Sutherland, R.: Environ. Geo. **39**(611), (2000). https://doi.org/10.1007/s002540050473
18. Sutherland, G.D., Harestad, A.S., Price, K., Lertzman, K.: Scaling of natal dispersal distances in terrestrial birds and mammals. Conserv. Ecol. **4**(1), 16 (2000)
19. Van Andel, J.H., Postma, H.: Recent sediments of Gulf of Paria: Reports of Orinco shelf Expedition. North Holland Publishing Co, Amsterdam 245 (1954)
20. Valdes, J., Sifeddine, A., Lallier-Verges, E., Ortlieb, L.: Petrographic and geochemical study of organic matter in surficial laminated sediments from an upwelling system (Mejillones del Sur Bay, Northern Chile). Org.Geochem. **35**, 881–894 (2004)

Chapter 40
Preliminary Analysis of Flood Disaster 2017 in Bihar and Mitigation Measures

Amarjeet Kaur, Tarun Ghawana and Nakul Kumar

Abstract Flooding is a regular disaster in Indian state of Bihar causing major human lives and economic losses. High vulnerability of Bihar towards floods is usually on account of its geo-climatic conditions and other contributing factors. The paper aims to conduct a preliminary analysis of the flood disaster 2017 in Bihar and to suggest sustainable mitigation measures. Satellite imageries based analytical maps from different sources are included showing the spatial rainfall analysis, flooding extent changes, crop damages etc. The paper discusses briefly the previous studies about embankments and floods. Mitigation measures suggested include policy, institutional, innovative physical and community participation measures. Recommendations mention that the transboundary nature of the catchment areas requires enhancing coordination not only between line departments but also on international scale.

Keywords Flood disaster · Mitigation · Bihar

1 Background

Flooding is an annual disaster event for Indian state of Bihar. In recent past several floods have devastated the state with Kosi river being he most common culprit. These floods of 2007, 2008, 2016, as expected, resulted in severe human and infrastructural loss. High vulnerability of Bihar towards floods is usually on account

A. Kaur (✉)
Centre for Disaster Management Studies, Guru Gobind Singh Indraprastha University, New Delhi, India
e-mail: amarjeet_ip@yahoo.com

T. Ghawana · N. Kumar
Visiting Faculty, CDMS, New Delhi, India
e-mail: tarungh@gmail.com

N. Kumar
e-mail: nakultarun.dgcd@gmail.com

P. J. Rao et al. (eds.), *Proceedings of International Conference on Remote Sensing for Disaster Management*, Springer Series in Geomechanics and Geoengineering,
https://doi.org/10.1007/978-3-319-77276-9_40

of its geo-climatic conditions and other contributing factors. South-West Monsoon rain often results in flooding situation in Bihar. Almost all rivers in northern Bihar originate from Nepal or Tibet and have 75% catchment area outside the state boundaries. Total flood prone areas in the state is approximately 68.80 lakh ha, accounting for 73% of its total geographical area and 17% of the total flood prone area in the country [4]. The paper aims to conduct a preliminary analysis of the flood disaster 2017 in Bihar and to suggest sustainable mitigation measures.

2 Methodology

Satellite imageries from National Remote Sensing Centre are used to show the flooding extents in several areas of Bihar on different dates. Loss data during August month is also included Mitigation measures are suggested further.

3 Analysis

In July and early few days of August month of 2017, heavy precipitation was received in north-eastern parts of India along with southern Nepal and Bangladesh. This has caused widespread flood, refer to Fig. 1.

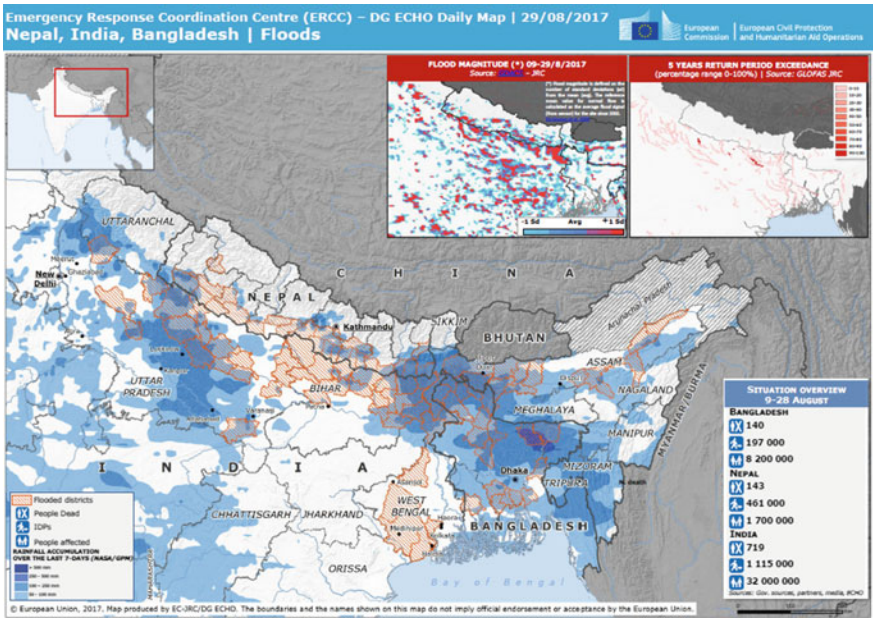

Fig. 1 Flooded regions in Bangladesh, India and Nepal. *Source* [2]

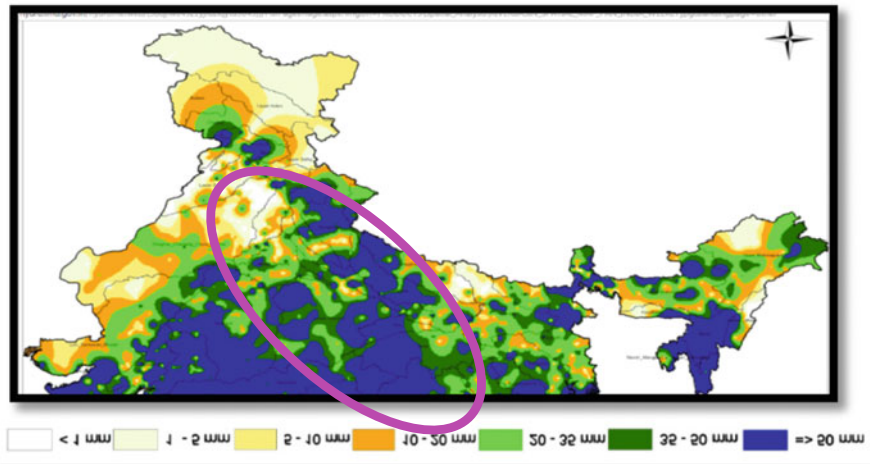

Fig. 2 Weekly spatial rainfall analysis on basin level in India. *Source* [3]

The satellite image analysis can help in decision making based on advanced modeling results overlay. Figure 2 shows the weekly (24–30 August 2017) spatial rainfall analysis in Northern India. In the highlighted area, several basins in the western part and some upper basins in lower eastern part were still having high rainfall (=>50 mm). However, most of the basins in the highlighted area were having weekly rainfall ranging from <1 to 20–35 mm.

Figure 3 shows the flood at initial stages in Bihar state on 4th July, 2017 while Fig. 4 shows the extent flood inundated areas and the orientation of floods in the state on 4th September, 2017. These images show the extent of flooding largely in those areas that are marked 'liable to flood' in the flood zones map of Bihar, refer to Fig. 5.

District wise satellite estimated flood extent in Darbhanga is 582 m^2, in East Champaran 624 m^2, in Madhepura 4 66 m^2, in Samastipur 456 m^2, in Sitamarhi 453 m^2, in Khagaria 501 m^2 and in Muzaffarpur 55 m^2 [12].

Table 1 shows district wise flood impact, around mid-August 2017 in terms of affected population, number of deaths, number of relief camps and number of people in relief camps. The highest number of affected population is in Katihar (0.12 million) and Sitamarhi (0.15 million) districts. Highest number of deaths have occurred in Araia (20) followed by Sitamarhi (11). High number of relief camps are running in Sitamarhi (152) and Araria district (95) and the highest number of evacuated population is in Araria (62,000) followed by Supaul (60,000) and West Champaran (46,000). High numbers of people are sheltered in relief camps in each district with Araria (37,000) top on the list.

Due to Kharif season, rice crops had been sown which are now damaged, refer to Fig. 6a, causing economic loss to the farmers besides loss of livelihoods. For this paper, flooding in Bihar state has been analysed since it is the highest receiver of

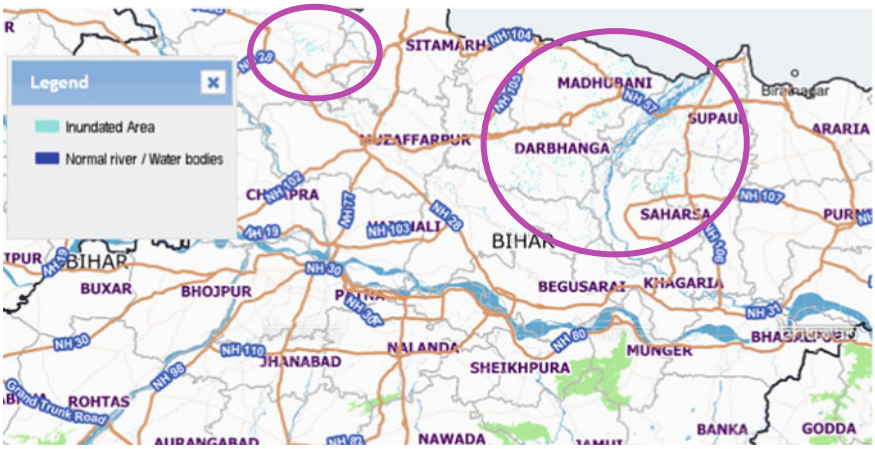

Fig. 3 Flood inundated areas in Bihar, 4 July, 2017 India. *Source* [6]

Fig. 4 Flood inundated areas in Bihar, 4 September, 2017 India. *Source* [6]

flood waters from rivers in upstream Nepal. The large scale flooding has seriously affected the state. Four districts, Kishanganj, Araria, Purnea and Katihar, located along the Indian-Nepal border in Bihar were under high inundation affecting nearly one million people. Flood inundation and damages are also reported in other districts: Darbhanga, Madhubani, Sitamarhi, Madhepura, Saharsa, Supaul as well as East and West Champaran, refer to Fig. 6b [7].

Fig. 5 Flood zones in Bihar. *Source* [12]

4 Embankments and Floods

In Bihar, flooding usually incurs due to rivers overflow because of extreme rainfall in the catchment areas or discharge of large amount of stored water from reservoirs. Flooding of rivers results in breach of embankments or excessive soil erosions [11].

Embankments are a dominant feature of flood management structural measures in Bihar which can be considered as short-term measures. They are popular as cost-effective and time-saving measures. However, the disadvantage of these embankments are that siltation deposit required to make fertile the flood plains are stopped which hinders the process of land formation by rivers, river bed level rises especially in aggrading ones, prevents natural drainage and damages occurring due to breaches.

A study was conducted by Second Bihar State Irrigation Commission (1994) of aggradation of the Kosi rivers bed. The commission findings included that from 1955 to 1962, no silting was found at the river cross-sections between Chatra and Supaul of 102 km reach which was a degrading reach. This period 1955–62 approximately corresponds with the commencement and completion of the embankments [10].

5 Field Visit of CDMS

CDMS officials went on a field study tour to Bihar for several days starting within months of August and September with staff of other relevant organizations. During the visits, the Director also visited several relief camps and learnt first-hand about the flood disaster situation. It was observed that approach to disaster management is still response centric instead of mitigation and prevention. There is a need to check

Table 1 District wise flood impact situation in Bihar around mid-August 2017

Sr. no	Name of flood affected districts	Total flood affected			Total evacuated population	No. of relief camp running	No. of peoples shelters in the relief camp	No. of died persons
		Total affected blocks	Total affected panchayats	Total affected population in lakh				
1	Kishanganj	7	126	10.1	10,200	68	12,800	8
2	Araria	9	145	7.5	62,000	95	37,000	20
3	Purnea	8	94	8.62	30,980	58	22,768	5
4	Katihar	11	118	12.42	37,900	26	7826	
5	East Champaran	7	52	2.0	2620	15	2620	3
6	West Champaran	15	173	6.82	46,000	18	9374	9
7	Darbhanga	6	39	2.4	0	0	0	4
8	Madhubani	15	141	4.24	2213	22	2514	5
9	Sitamarhi	10	150	15.00	8200	152		11
10	Sheohar	4	14	0.48	3000	12	2217	2
11	Supaul	6	56	2.6	60,000	15	12,512	1
12	Madhepura	2	13	0.51	1007	2	1007	4
13	Muzaffarpur	4	19	0.489	9500	16	5500	
14	Gopalganj	6	11	0.27	700	5		
Total		110	1151	73.449	27,4320	504	116,138	72

Source [7]

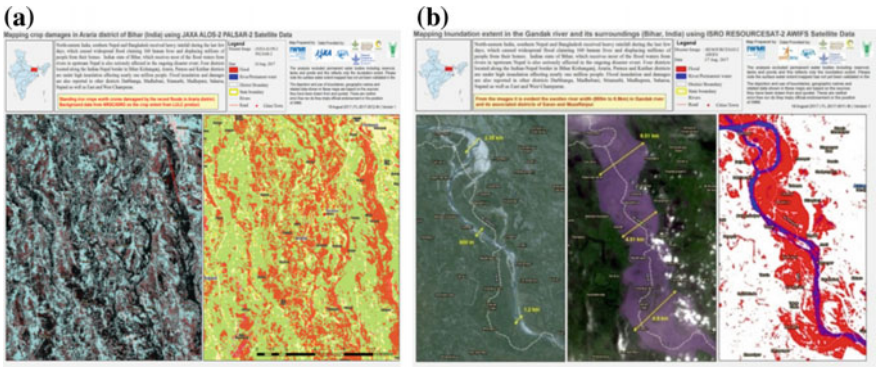

Fig. 6 **a** Mapping crop damages in Araria district of Bihar, India and **b** Mapping inundation extent in the Gandak river and its surroundings (Bihar, India). *Source* [9, 4]

Fig. 7 Interaction with flood victims during visit to flood affected areas in Bihar

the effectiveness of early warning system to avoid or reduce the disaster impacts on human lives & economy. Accountability should be fixed of concerned staff (Fig. 7).

6 Mitigation Measures

Policy Measures

- Zonation development for localized mitigation measures could help in spatial planning on regional and local level to promote area specific development programmes considering flood mitigation. As an example, this can be understood from the fact that the flooding of Gandak shall not affect Saharsa or Supaul areas. Similarly flooding of Kosi shall not affect Gopalganj or Chapra. The idea is to make development river-centered. Thus, the development plan

would include tackling often flooding rivers as an integral part of planning and management process [11].

- Flood management in Bihar is a complex task which requires international cooperation with Nepal. This will result in sustainable long-term flood management. A skilled workforce familiar with advanced technologies and efficient administration should be involved in policy making and implementation process. A participatory approach including all stakeholders at each stage is crucial for the successful interventions [10].

Institutional Measures

- Reviewing and monitoring, considered as best practices, the disaster preparedness activities on the highest level are required including political figures and senior administrators.
- Anticipated positioning of dedicated disaster response forces such as national and state level disaster response forces to minimize the response time and to initiate confidence building measures along with capacity development of local level responders.
- Active use of technology such as active WhatsApp group on disaster management, to facilitate timely decisions and respond. It can help in direct communication with the concerned stakeholders and quick dissemination of information to the incident commander. SMS based Early Warning System involving Indian Meteorological Department and Central Water Commission can also help in early response [8].

Innovative physical Measures

- *To Convert streams/rivulets as reservoirs*:
  Flood water needs to be stored for later use which can be achieved by converting streams/rivulets as reservoirs. Besides this, geospatial based hydroinformatics would be required. For this, the rivulets and tributaries need to be properly structured and meticulously maintained [11].
- *Detention Basins*:
  Detention basins in the form of depressions, locally called 'chaurs', exist in the state. These detentions can absorb a considerable amount of water of the first flood of the season [1].
- Furthering this process, smooth passage to flood water should be provided by desiltating its bed to avoid inundation and by harvesting the inundating waters in reservoirs, ponds and rivulets for productive utilization and to avoid erosion of banks and embankments [11].
- The revival and maintenance of traditional methods of diversion and storage of flood water for multipurpose activities including irrigation etc. [11].
- Roads construction should consider the natural flow pattern on the local and regional levels so as not to obstruct the natural flow of water which could result in flooding.

- Watershed principles based green coverage initiatives so as to regulate the excess runoff causing heavy erosion and thus siltation problem during flood disaster situations.

Community Participation Measures

- Larger involvement of senior citizens from the local areas will be required who have better understanding and knowledge about the traditional practices to deal with floods [11].
- Community consensus should be developed in rural areas to change crop patterns on mass scale to grow water resistant varieties which will reduce the crop damages during flooding events.
- Awareness camapaigns for community, training of officials of line department for capacity building [5].

7 Discussion

Bihar needs a combination of flood measures addressing various needs of early warning to effective international cooperation. As a part of structural measures, embankments creation and maintenance is required as well as creation of multi-purpose dams to create adequate protection from floods. Water detention measures could moderate flooding situations. Under non-structural measures flood plains zoning and management, flood proofing, flood forecasting and warning, disaster preparedness and response planning, etc., may be tried [10].

8 Conclusion

It can be concluded that Bihar floods are caused not only due to geo-climatic conditions but also due to lack of a comprehensive management ineffective to a great extent in its implementation. It predominantly relies on embankment measures which become ineffective during excessive rains causing large inflow of water in the Bihar rivers. The transboundary nature of the catchment areas requires enhancing coordination not only between line departments but also on international scale. There is a need to introduce and adopt innovative mitigation measures giving due space to water storage measures along with advancement of relevant technologies. Community participation is a must for ensuring the sustainability of the flood management measures.

References

1. Agarwal, A.: Bihar floods-causes and preventive measures, Indiawater Portal. http://www.indiawaterportal.org/articles/bihar-floods-causes-and-preventive-measures (2012)
2. European Commission: Nepal, India, Bangladesh Floods, Emergency Response Coordination Centre (ERCC)
3. IMD: Spatial Analysis, Customized Rainfall Information System, Indian Meteorological Department. http://hydro.imd.gov.in/hydrometweb/(S(sz4zyr45m50esu55bmkavsf5))/PdfPageImage.aspx?imgUrl=PRODUCTS\Spatial_Analysis\RIVERBASIN_SPATIAL_MAP_PAN_INDIA_WEEKLY.jpg&landingpage=landing (2017)
4. IWMI: http://www.iwmi.cgiar.org/2017/08/maps-that-matter-when-flooding-strikes/ (2017)
5. NIDM: Bihar Floods: 2007, A Field Report, National Institute of Disaster Management, India (2013)
6. NRSC: Bihar Floods, National Remote Sensing Centre, India (2017)
7. PGVS-Christian Aid: Flood Situation Report (2017)
8. Rai, P.N.: Innovative Measures Taken to Reduce the Impact of Flood, Bihar Flood 2016, Disaster Management Department, Government of Bihar (n.d.)
9. Reliefweb: India: Mapping Inundation extent for Bihar using ESA Sentinel-1 Satellite Data 20 August 2017 (FL-2017-0015-IN | Version 1). Website: https://reliefweb.int/map/india/india-mapping-inundation-extent-bihar-using-esa-sentinel-1-satellite-data-20-August-2017 (2017)
10. Sinha, C.P.: Management of Floods in Bihar, Economic & Political Weekly (2008)
11. State Disaster Management Plan: Section II, Disaster Prevention, Mitigation Preparedness and Capacity Building, Bihar (n.d.)
12. UNDP: Map showing flood zones in Bihar. http://img.static.reliefweb.int/sites/reliefweb.int/files/resources/63B9B1705D18DCC2C12574B700424495-undp_FL_ind080831.gif (n.d.)

Chapter 41
A Spatial Disaster Management Framework for Smart Cities—A Case Study of Amaravati City—Flood Management

Abhishek Arepalli, S. Srinivasa Rao and P. Jagadeeshwara Rao

Abstract A Disaster is an event that causes substantial loses to life, property and environment during a very short time. In this age where urbanization is at its prime, most of the population density is found concentrated in cities. Hence a disaster around such huge population bursts can cause a substantial loss of life and property. The concept of smart cities is a rapidly growing phenomenon for many developing nations. The infrastructure of such cities is being revamped in order to achieve the smart city goals. In this context, many sectors and development indices are taken into consideration for making a city smart. For new cities where everything is built from scratch, this is a more easier task to plan everything from smart city point-of-view. But for existing cities this poses a real challenge as the existing framework has to be replaced or redesigned accordingly. Most cities have little practices for disaster preparedness and put all efforts on disaster response and recovery. An effective Disaster Management plan has to effectively handle all stages of disaster—preparedness, response and recovery. To make this Disaster Management plan more effective, a spatial component is proposed in our study. The spatial component in a disaster management framework helps to better understand the disaster and take necessary steps for its management. In this paper we concentrate on the inclusion of smart city concepts into a spatial disaster management framework to prepare a robust plan in all stages of a Disaster.

Keywords Disaster management · Smart city · Geographic information systems (GIS) · Remote sensing · Smart management · WebGIS

A. Arepalli (✉)
Andhra Pradesh Capital Region Development Authority, Vijayawada, India
e-mail: abhishek.arepalli@gmail.com

A. Arepalli · P. Jagadeeshwara Rao
Department of Geo-Engineering, Andhra University, Visakhapatnam, India
e-mail: pjr_geoin@rediffmail.com

S. Srinivasa Rao
Regional Remote Sensing Centre, NRSC, Jodhpur, India
e-mail: sitiraju@gmail.com

P. J. Rao et al. (eds.), *Proceedings of International Conference on Remote Sensing for Disaster Management*, Springer Series in Geomechanics and Geoengineering,
https://doi.org/10.1007/978-3-319-77276-9_41

1 Introduction

The Information and Communication Technology (ICT) framework sets a paradigm for many other transfer protocols whenever a new technology is to be adopted into an existing framework. Based on those guidelines, we try to design a geospatial framework for the smart cities which tackles many issues in a smart city either an existing city or a newly planned city. The most challenging of these issues is the disaster management of such smart city.

1.1 Disaster Management

The Disaster Management is organization and utilization of resources during the three phases of a Disaster viz., Preparedness, Response and Recovery. Economic losses are high when Disaster strikes in a highly populated area. According to the latest report, 85% losses of Economic resources were due to 4 major disasters viz., flooding, earthquake, cyclones and severe weather in highly populated areas [1]. According to Annual Disaster Statistical Report, flooding and cyclones are cause of major economic losses in India [2].

1.2 Smart City

A definition by the International Telecommunication Union (ITU)'s Focus Group on Smart Sustainable Cities (FG-SSC) reads: "A smart sustainable city is an innovative city that uses ICTs and other means to improve the quality of life, efficiency of urban operation and services, and competitiveness, while ensuring that it meets the needs of present and future generations with respect to economic, social and environmental aspects" [3]. Cities are engines of growth for the economy of every nation, including India. Nearly 31% of India's current population lives in urban areas and contributes 63% of India's GDP a per the Indian Census of year 2011. With increasing urbanization, urban areas are expected to house 40% of India's population and contribute 75% of India's GDP by 2030 [4].

1.3 Integration of Disaster Management into Smart City

Though a disaster cannot be completely avoided, by taking necessary steps to create a effective structure and channel for dissemination and organization of data, most of the damage can be reduced [5]. Smart City databases could help create such effective channel of communication among various functionaries during a crisis.

1.3.1 Integration of Disaster Management Techniques to an Existing City

In a case where Disaster Management needs to be integrated to an existing city, the preparedness activities may have a limited coverage or scope. Hence, in such cases the response activities take high priority.

1.3.2 Integration of Disaster Management Techniques to New City

In case of a new planned city most innovative techniques in Disaster Management can be integrated right from the planning phase. Hence, an integrated Smart Disaster Management system could be envisaged from the stage of its conception.

2 Geographic Information Systems Framework

The quality of life of the urban population in the present age has utmost promise of improvement only through the effective integration of various digital and technological systems into a developmental environment where everyone could be an active or a passive participant. To make this a realization a better understanding of the city through a spatial domain is of primary concern.

2.1 Spatial Data for Disaster Management

All the data collected in reference to a Disaster Management System could be analyzed in terms of spatial relations. The future predictions and modeling can be done using GIS and Remote Sensing data analyzing the past trends. The modeling of the disaster requires various data layers pertaining to factors and effective parameters related to each Disaster that prevails in a certain city [6]. By targeting the frequently occurring disasters in a certain city we can easily optimize the database and thus effectively address the disaster in question.

2.2 Spatial Attributes and Service Layers for a Disaster

Identifying the relevant Spatial Data for Disaster Management is of prime importance. In this paper we attempt to categorize the Disaster management database into 3 Categories viz., Essential Services, Response Services and Disaster Services (Refer Fig. 1).

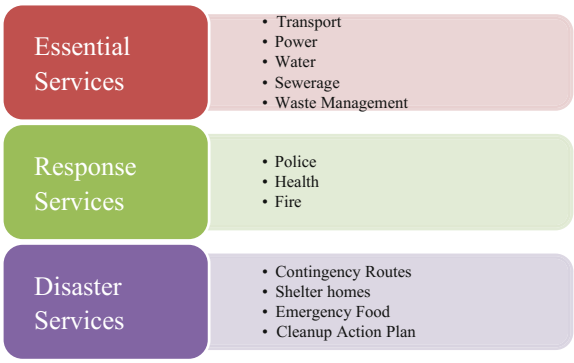

Fig. 1 Various services in disaster management database

3 Disaster Management of Smart City Using Geo-spatial Tools

The Disaster Management of a city consists of planning for disaster, training for response and designing contingencies for recovery. The involvement of Geo-spatial tools to design and plan above procedures effectively could help manage the resources effectively [7]. Many trending technologies like IoT could help better management of disaster in case of smart cities [8]. Combining these technologies could cater needs of greater number of communities in smart cities. The following case discusses a case where Geo-spatial tools were used to create a better Disaster Management Systems for a new planned Smart City.

3.1 Flood Risk Management in Amaravati City

The newly formed Andhra Pradesh Capital Region comprises of rapidly growing Vijayawada, Guntur cities and 9 towns such as Tenali, Mangalgiri, etc., along with the new capital city Amaravati. The Green field area of 217 km^2 on the banks of river Krishna in Guntur District is notified as capital city for Andhra Pradesh State by GoAP. The Capital Region is also prone to floods. Management of the flood waters, especially within the Amaravati Capital city will be one of the key considerations in the planning of city.

3.1.1 Prevent: Reinforce and Realign the Existing the Krishna River Bund

The existing river bund along the Krishna River is approximately 3–5 m above the highest recorded flood level of the Krishna River. The realignment of the Krishna River Bund is proposed for the Seed Development area where the initial start-up

phase will take place. This will protect an additional land area between the Krishna River and the seed area for development.

3.1.2 Control: Detain Storm Water

The location of the detention ponds are determined based on the future landuse. Most of the ponds are sited within the vicinity of green spaces to maximize their use as green spaces. These detention ponds are to detain storm water run-off during heavy rainfall, and then discharge slowly into the reservoirs for water conservation.

3.1.3 Control: Detain Storm Water Externally

In addition to the internal detention ponds within the Capital City, it is recommended that two external detention ponds be constructed outside the Capital City boundary to detain water upstream close to source. This will help to reduce surface runoff into the Capital City planning area.

3.1.4 Conserve: Create Raw Water Storage Using Reservoirs

Three reservoirs have been proposed within the Capital City in order to with hold the in-falling drain and storm water (see Fig. 2). Reservoir R1 is fed by storm water that flows from the south-eastern half of the City, Reservoir R2 is located at an higher altitude which is favorable to be a reservoir due to its natural abutment and Reservoir R3 being a natural low-lying area it has the capacity to act as a detention pond. The three reservoirs will augment water supply to the Capital City by providing raw water storage.

3.1.5 Buffer: Provide an Extensive Green and Blue Drainage Network Using Canals

A minimum buffer of 30 m is proposed to be reserved along all the major canals. In the future, there should be no development of permanent structures within these flood control reserves. As part of the blue network a series of permanent channels is proposed. These channels will retain water permanently in them to form a canal network around the city.

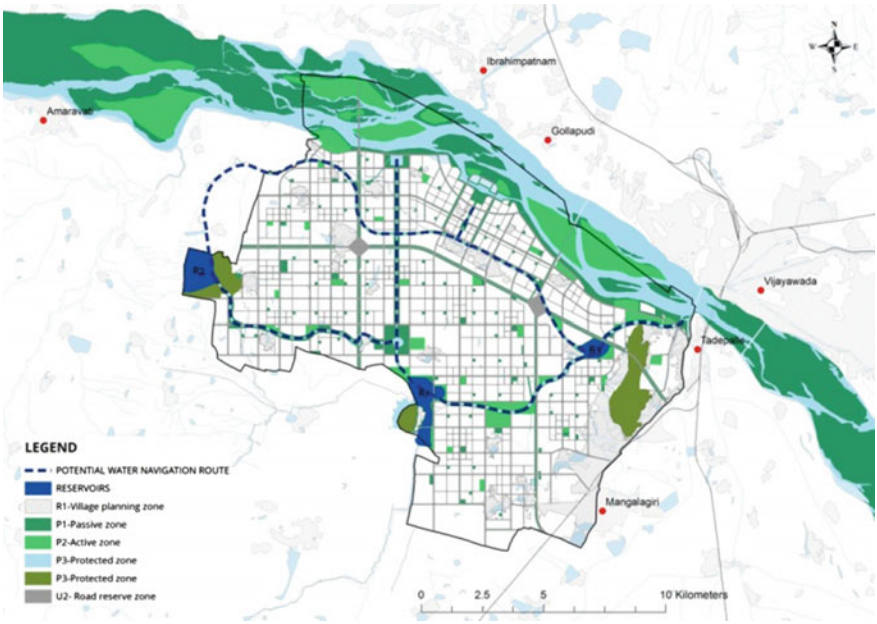

Fig. 2 Potential reservoir sites and blue network

3.1.6 Dispose: Discharge Excess Water into Krishna River

As a final measure of protection, it is recommended that a comprehensive system of sluice gates and pumps are provided at the outfalls of the Capital City boundary where the surface runoff discharges into the Krishna River.

3.1.7 Protect: Raising of Platform Levels

Based on the topographical survey, it is noted that the ground level of the existing villages are at +25 m above mean sea level (AMSL). In addition, it is understood that the historical flood level of the Krishna River is at around +21.7 m AMSL. Hence, the minimum platform level for future developments within the Capital City should be set at +25 m AMSL or at a level higher than the historical flood level in the particular area, subject to further detailed hydrological studies for the Kondaveeti Vagu catchment.

4 Conclusion

The most robust Disaster Management System can be prepared for a smart city using the Geo-spatial Tools. The involvement of such tools from planning stage could definitely help to prepare a more robust responsive system and prevent any loses by planning to avoid the disaster effecting areas or remodeling existing areas to reduce the losses due to disaster. A smart city in all aspects could become a leading example by integrating such geo-spatial planning and preparing ahead for disasters.

Acknowledgements I take this opportunity to thank Commissioner, APCRDA, Director—Planning, APCRDA and other officers at Andhra Pradesh Capital Region Development Authority, Vijayawada who guided and nurtured me to plan and develop the concepts for this project. I also thank the organization for providing me a platform for utilizing data.

References

1. Benfied, A.: 2016 Annual global climate and catastrophe report. Analytics and impact forecasting
2. Guha-Sapir, D., Hoyois, Ph., Below, R.: Annual disaster statistical review 2014: the number and trends, CRED, Brussels (2015)
3. United Nations Conference on housing and sustainable development, Habitat III issue papers 21—smart cities (May, 2015)
4. Ministry of Urban Development, GOI. Smart city mission statement and guidelines (June, 2015)
5. Yusoff, A., Mustafa, I.S., Yussof, S., Din, N.M.: Green cloud platform for flood early detection warning system in smart city. In: Information technology: towards new smart world (NSITNSW), IEEE, pp. 1–6 (Feb, 2015)
6. Shamshiry, E., Nadi, B., Mokhtar, M.B., Komoo, I., Hashim, H.S.: Disaster management base on geoinformatics. In: 2011 IEEE 3rd international conference on communication software and networks, pp. 28–30 (2011)
7. Parsons, R.L., Frost, J.D.: Evaluating site investigation quality using GIS and geostatistics. Geotech. Geoenviron. Eng. 451–461 (2002)
8. Zelenkauskaite, A., Bessis, N., Sotiriadis, S., Asimakopoulou, E.: Interconnectedness of complex systems of internet of things through social network analysis for disaster management. Intell. Netw. Collab. Syst. (INCoS), IEEE, 503–508 (2012)

Chapter 42
Study on Drought Monitoring Based on Spectral Indices in Noyyal River Sub-watershed Using Landsat-8 Imageries

J. Brema, T. S. Rahul and James Jesudasan Julius

Abstract Drought is an extreme condition due to moisture deficiency and has adverse effect on society. Agricultural drought occurs when there is a reduction in soil moisture which produces serious crop stress and affects the crop productivity. The recent advances in the field of earth observation through different satellite based remote sensing systems have provided avenues for researchers to conduct continuous monitoring of soil moisture, land surface temperature and vegetation indices at a global scale. This research study is focused on Noyyal river sub-basin, which comes under a semi-arid region. In this study, Landsat 8 [Operational Land Imager (OLI) and Thermal Infrared Sensor (TIRS)] images of the year 2014, 2015, 2016 and 2017 were used for drought assessment in the summer season. The summer season spans from March to May in Coimbatore. Therefore, in the study the indices are compared corresponding to the months of summer for four consecutive years. The analysis of vegetation cover using NDVI, VCI, TCI, WSVI and VHI indices demonstrates the impact of the drought in the agricultural scenario in the sub-basin.

Keywords Land surface temperature · NDVI · Vegetation · Drought

J. Brema (✉) · T. S. Rahul · J. J. Julius
Department of Civil Engineering, Karunya University, Coimbatore, India
e-mail: brema@karunya.edu

T. S. Rahul
e-mail: rahul.rce@gmail.com

J. J. Julius
e-mail: james2julius1@gmail.com

P. J. Rao et al. (eds.), *Proceedings of International Conference on Remote Sensing for Disaster Management*, Springer Series in Geomechanics and Geoengineering,
https://doi.org/10.1007/978-3-319-77276-9_42

1 Introduction

Drought, which occurs with a frequency involving complex factors, a natural catastrophe that has to be managed by the policy makers in time. It occurs in all climate regions and is one of the prime calamity throughout the earth. Out of all the types of natural calamities, drought has the direct impact on agriculture. As such, a drought survey and identification of drought vulnerable zone physically is a difficult procedure with more time consumption. Remote sensing technology provides coverage throughout the earth in order to facilitate the identification and monitoring of the drought calamity. The implementation of satellite image based drought indicators helps to understand drought impact zone [1, 2]. To monitor drought continuously, Normalized Difference Vegetation Index (NDVI) and Land Surface Temperature (LST) are successfully used. NDVI is a representation of the vegetation condition with the help of spectral characteristics of red light, near infrared band or their simple combination, based on the strong absorbing property of chlorophyll [2]. The following indices can be used to assess the drought condition, Water supplying vegetation index (WSVI), Vegetation Condition Index (VCI), Land Surface Temperature (LST) and Vegetation Temperature Condition Index (VTCI) respectively. The main objective of this research study is to assess the variations in drought in Noyyal river basin using various indices derived from satellite images.

2 Literature Review

Drought is defined as a deficiency of precipitation over an extended period of time resulting in water shortage that causes extensive damage to crops [3]. The remote sensing study shows a drastic change in the builtup land during the period 2000 and 2010 in the Coimbatore corporation limit [1]. A drought is a term relative to normal conditions while water shortage is an absolute term for water demand [4]. In order to have a continuous monitoring of vegetation changes over a long period and spatially, satellite imagery are to be used for deriving various indicators [5]. Variations in vegetation can be assessed by conducting a comparative analysis of derived NDVI indices [6]. NDVI and LST were found to be closely correlated in several land use and land cover categories, especially in vegetated areas. Data from remote sensing is very good for vegetation cover monitoring; it can provide very good information about the vegetation cover [7]. One of the most widely used indicators for vegetation monitoring is NDVI. Satellite derived NDVI is considered as the basis for assessment [8]. The spatial pattern of LST in the study area was arrived at to depict the scenario on urban heat island. The study included a real-time field work performed during the overpass of Landsat-5 satellite on 21/08/2011 over Salt Lake, Turkey. Normalized Difference Vegetation Index (NDVI), Vegetation Condition Index (VCI), and Temperature Vegetation Index (TVI) were used to

evaluate the impact of drought in the region during the period from 1984 to 2011. The results showed that real-time ground and satellite remote sensing data were in good agreement with correlation coefficient value of 0.90. The remotely sensed and treated satellite images and resulting thematic indices maps showed that dramatic land surface temperature changes occurred (about 22 °C) in the Salt Lake Basin area during the 28-year period (1984–2011).

3 Study Area

The Noyyal river basin, sprawls for about 175 km from west to east with an average width of about 25 km. The widest part is located in the central portion with an width of about 32 km. Total extent of the basin is about 3646 km^2. The basin lies between the latitudes 10° 53′ 1.06″N to 11° 21′ 57″N and longitudes 76° 37′ 49″E to 78° 12′ 55.06″E. The sub-watershed considered in this study lies in the head reach of the basin which comes under Coimbatore district, TamilNadu, India as shown in Fig. 1. The total areal extent of the sub-watershed is around 1631.54 km^2.

4 Materials and Methods

Landsat imageries for the study were downloaded from the U.S. Geological Survey website (i.e., landsat.usgs.gov). The months of April and May corresponding to the years 2014–17 were included in the study, as these months reflect the highest vegetation proliferation in a year. Landsat images has a high spatial resolution of 30 m, which is available in a standardized, orthorectified format. Band 5 and Band 4 were considered for NDVI estimation Band 10, Band 11 and thermal infrared bands were considered for estimating land surface temperature in the sub-watershed. From the corresponding bands of the geocoded satellite images, the land surface temperature was calculated from emissivity and NDVI values of

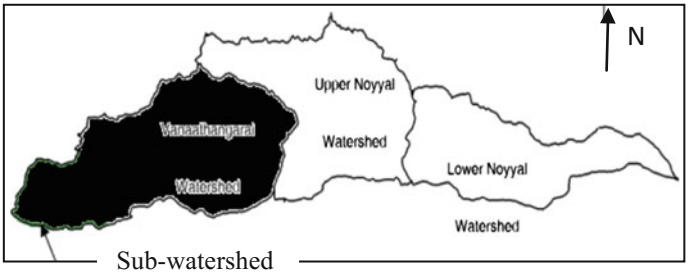

Fig. 1 Study area

the sub-watershed. The NDVI is estimated as a ratio between measured spectral reflectance in the red and near infrared portions of the electromagnetic spectrum. The two spectral bands, Band 4 and Band 5 were chosen as more suitable for the NDVI calculation, as they are affected by the rate of absorption of chlorophyll by the density of green vegetation on the surface. NDVI was calculated as follows:

$$\text{NDVI} = \text{Float}(\text{Band } 5 - \text{Band } 4)/\text{Float}(\text{Band } 5 + \text{Band } 4) \quad (1)$$

where, NDVI values range between −1 and 1.

The Land surface temperature was estimated by using the equation:

$$T_{10} = K_2/\ln(K_1/L_\lambda + 1) - 273 \quad (2)$$

T_{10} = Top of atmosphere brightness temperature, L_λ = Top of atmosphere spectral radiance, K_1 = Band-specific thermal conversion constant, K_2 = Band-specific thermal conversion constant. K_1 and K_2, Rescaling factor values for the above Eqs. 1 and 2 were obtained from Meta data of the satellite images.

$$LST_{10} = T_{10}/(1 + (\lambda T_{10}/\rho)\ln(e) \quad (3)$$

$$\text{Emissivity, } e = 0.004P_v + 0.986 \quad (4)$$

where, Pv is Proportion of vegetation, LST_{10} is land surface temperature (in Kelvin); T_{10} is radiant surface temperature (in °C); λ is the wavelength of emitted radiance (11.5 μm); ρ is h × c/s (1.438×10^{-2} m K); h is Planck's constant (6.26×10^{-34} J s); c is the velocity of light (2.998×10^8 m/s); s is Stefan Boltzmann's constant (1.38×10^{-23} J K).

The Vegetation Condition Index (VCI), the Temperature Condition Index (TCI), and the Vegetation Health Index (VHI) have been calculated using the values of NDVI, LST^{10}, etc. VCI and TCI data were used to calculate VHI, a vegetation drought index which incorporates overall vegetation health and its severity to indicate agricultural drought extent at any time of the year. The VCI, TCI and VHI have been classified and shown in Table 1.

Table 1 Classification of the VCI, TCI and VHI values in terms of drought

Sl. no.	Drought category	Value
1.	Extreme	<10
2.	Severe	<20
3.	Moderate	<30
4.	Mild	<40
5.	No	≥40

5 Results and Discussions

The LST map generated corresponding to Band 10 image acquired on 02.05.2014 is shown in Fig. 2. The temperature is very high nearer to the urbanised locations like Tirupur, Coimbatore corporation etc. In order to assess the impact of landuse changes on meteorological parameters, the daily maximum and minimum temperatures from the meteorological stations were used for correlation. The linear trends computed for the 4 years showed a slight increase in maximum temperature. The standard deviation (S.D.) and the co-efficient of variation (C_v) for both were less for maximum and minimum temperatures indicating only minor variations from year to year.

The maximum NDVI value has decreased from 0.55 to 0.52 showing an indication of decrease in vegetation in the study period. The values of NDVI in the sub-watershed during May 2014 is shown in Fig. 3. The lowest positive and negative NDVI values are observed in the year 2017. Figure 4 shows the relationship between NDVI values with respect to years.

From Fig. 5, it can be seen that there is a decrease in NDVI value during the period of 4 years. The relationship between NDVI and surface radiance temperature was studied for each year through correlation analysis. The Land Surface temperature values tend to correlate negatively with the NDVI values. The highest NDVI was found in the year 2014 as 0.552. However, the lowest negative NDVI value was found in 2017 as −0.025. It can be concluded that a strong negative correlation exists between the land surface radiance temperature and NDVI as higher vegetation content tends to lower the land surface temperature.

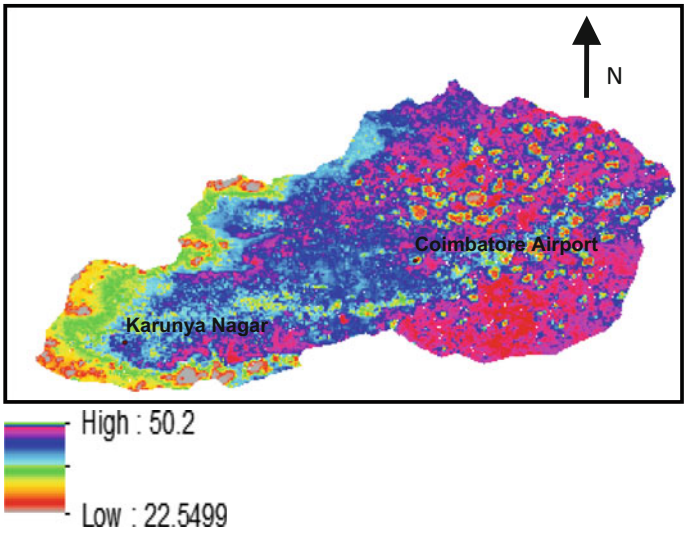

Fig. 2 LST map of the sub-basin

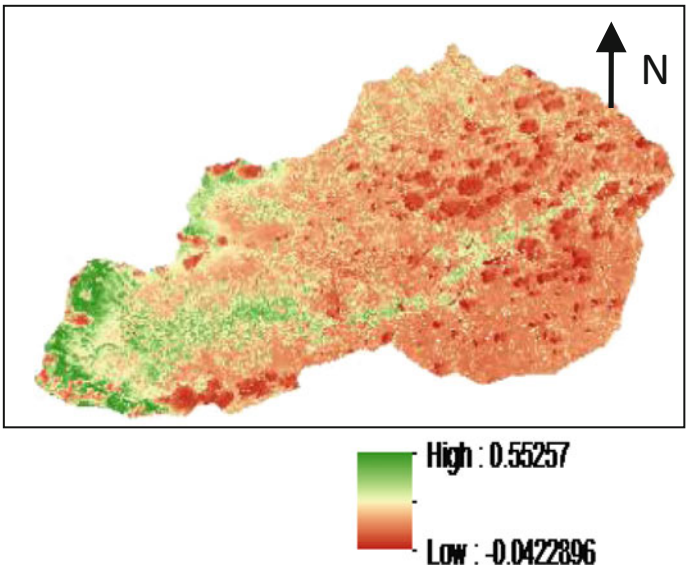

Fig. 3 NDVI Map of the sub-basin

Fig. 4 Estimated extreme NDVI values

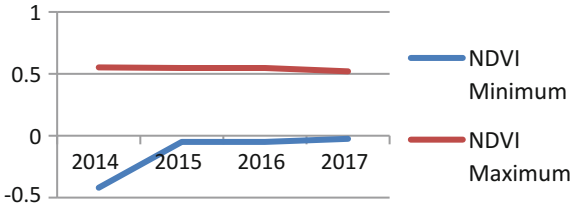

The saturation of soil moisture is directly related to the presence of sufficient precipitation which is highly required for sustained agriculture. Hence, in the study to determine the precipitation status in the study area the Water Supplying Vegetation Index (WSVI) was calculated. The WSVI is an indicator based on the relationship between normalized difference Vegetation Index and surface temperature, which provides effective estimation of surface moisture condition. The WSVI values ranges from −4 for extreme dry (Arid area) to +4 for highly moist condition. The results showed that the WSVI value in the study area ranges from 0.00119 up to 0.0176. It can be inferred that the moisture level in most of the study areas are experiencing more moisture deficit, the moisture levels ranged from moderate to very low moisture levels, which is an indication of less rainfall. The NDVI depicts the variations in vegetation extent, whereas the VCI classifies vegetation variations between 0 and 100 to represent the relative variations in the moisture condition from extremely bad to optimal position. The value of the VCI index was 99.97, 100.01, 100.10 and 100.03 during the May months of 2014, 2015, 2016 and 2017.

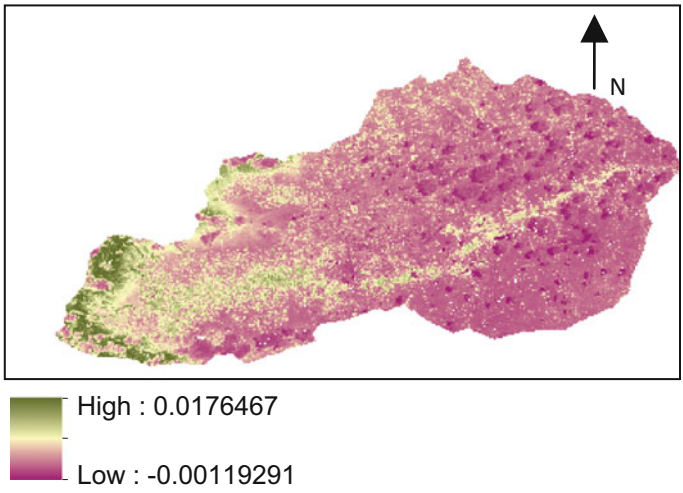

Fig. 5 WSVI during May 2014

The VCI value of the 2014 is lower than the consecutive years, due to less rainfall received in the post monsoon season of 2013. Figure 6 shows the degradation of the health of crop due to insufficient soil moisture present in the soil. The TCI of the study area is shown in Fig. 7. The TCI value is high in and around the Thondamuthur block and very low nearer to the Tirupur and Pongalur blocks.

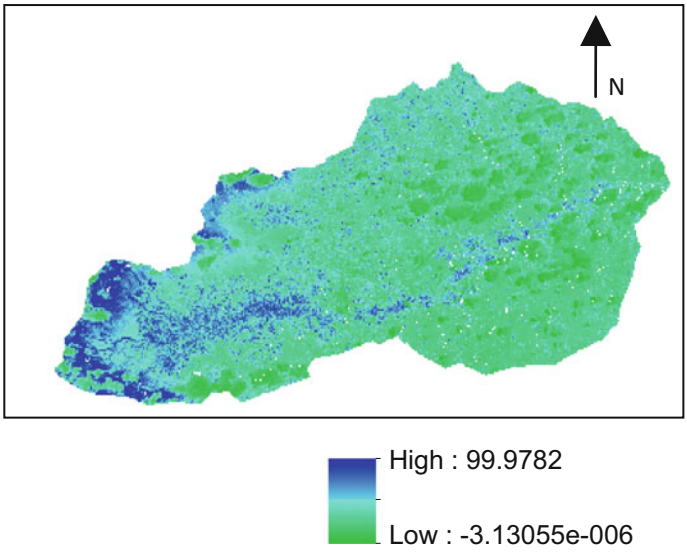

Fig. 6 VCI during May 2014

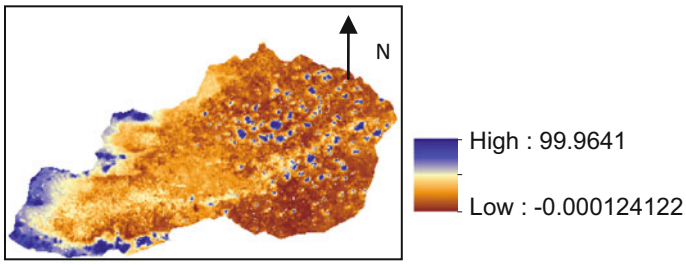

Fig. 7 Temperature condition index during May 2014

Spatial variation of VHI during 2014, 2015, 2016, and 2017 are shown in Figs. 8 and 9. The Figures show that extreme drought was experienced during 2014, 2016 and 2017. There is high vegetation index in the regions of Tirupur, Avinashi and Pongalur due to regional increase in rainfall during the year 2015. The maps show that drought extent in research area has been significant throughout, from mild drought to severe drought.

5.1 Statistical Analysis

The correlation co-efficient values for LST found to be 0.819 and 0.884 for bands 10 and 11 at Karunya university. The correlation co-efficient values were found to be 0.432 and 0.505 for bands 10 and 11 at respectively Coimbatore airport. The results of the LST map also correlated with the drought regions corresponding to VCI and VHI maps. Table 2 shows the estimated values of various indices in the sub-watershed for the years 2014–2017.

From Table 2, it can be seen that the least average WSVI value were observed as 0.01764, 0.02298, 0.0197 and 0.0192. It is observed that vegetation condition is better during the year 2015 compared to the other three years. Due to the disparity in the rainfall region wise the vegetation index is high in certain regions and very low in certain regions of the basin. The greater fluctuation is observed in the Tirupur and Erode region of the basin.

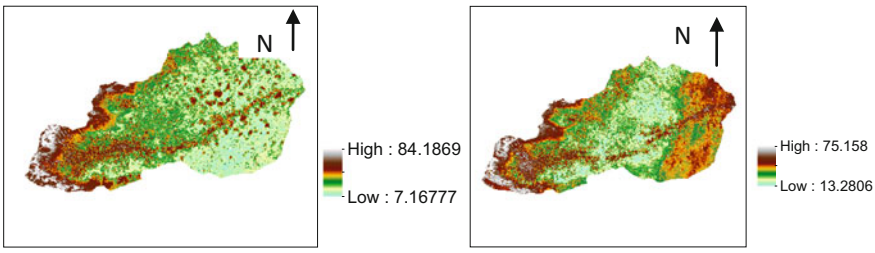

Fig. 8 Vegetation health indices during May 2014 and 2015

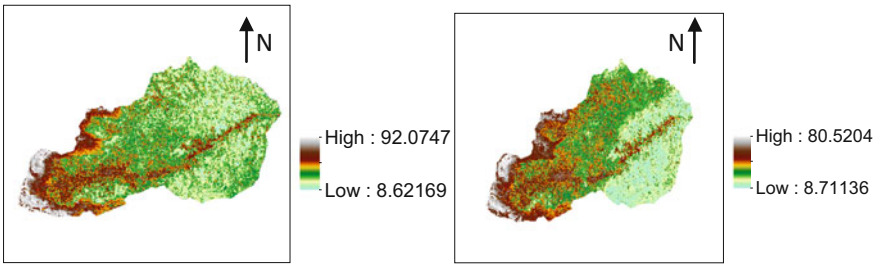

Fig. 9 Vegetation health indices during May 2016 and 2017

Table 2 Estimated NDVI values in the sub-watershed

Indices	Category	2014	2015	2016	2017
NDVI	Minimum	−0.42	−0.05	−0.05	−0.025
	Maximum	0.552	0.547	0.547	0.52
WSVI	Minimum	−0.00119	−0.00186	−0.0017	−0.000804
	Maximum	0.01764	0.02298	0.0197	0.01925
VCI	Minimum	3.13×10^{-6}	−0.0065	−0.0149	−0.000903
	Maximum	99.97	100.001	100.10	100.03
TCI	Minimum	−0.000124	−0.022	−0.0002	−0.0177
	Maximum	99.96	99.997	99.998	99.99
VHI	Minimum	7.16	13.28	8.621	8.7113
	Maximum	84.18	75.158	92.074	80.52

6 Conclusions

In this research, the potential of remote sensing to study the temperature variation and its effect on NDVI in the sub-watershed of Noyyal basin with the help of Landsat 8 has been demonstrated. The result shows that there is a decrease in maximum NDVI values during the study period. The findings of the research highlight the importance of the remote sensing studies in the determination of hydrological drought indices. In this paper, an attempt has been made to derive the Vegetation Health Index (VHI) from the indices of Vegetation Condition, Normalized Difference Vegetation, and the Temperature Condition which were derived from Land Surface Temperature (LST) for a study period from 2014 to 2017. The variation in the drought indices is obviously visible in the lower end of the sub-watershed. The results of VHI estimates can contribute to monitor the onset of agricultural drought as early warning system.

References

1. Brema, J., Arun, S., Rejeesh, Ambadi, M.: Study of rainfall variation with respect to landuse change—Noyyal basin. Int. J. Earth Sci. Eng. **8**(2), 540–543 (April 2015)
2. Chen, S., Tong, Q., Guo, H.: Research of remote sensing information. Beijing Science Press (1998)
3. Keshri, R. et al.: Remote sensing satellite (NOAA AVHRR) based drought assessment and monitoring in Southern Rajasthan (2009)
4. Obi Reddy, B.P., Maji, A.K., Srinivas, C.V., Kamble, K.H., Velayutham, M.: GIS-based basin morphometric information system for terrain and resources analysis. In: Proceedings of first national conference on agro-informatics, Dharwad, India, pp. 37–42 (2001)
5. Hassan, I.M.E.: Desertification monitoring using remote sensing technology. In: Proceeding of the international conference on water resources and arid environment, Saudi Arabia, pp. 1–15 (2004)
6. Malo, A.R., Nicholson, S.E.: A study of rainfall and vegetation dynamics in the African Sahel using normalized difference vegetation index. J. Arid Environ. **19**, 1–24 (1990)
7. Wu, M.L.: Remote sensing applications in water resource protection. In: 22nd Asian conferences on remote sensing, Singapore, vol. 1, pp. 706–711, 5–9 Nov 2001
8. Gibson, D.J.D.: Land degradation in the Limpopo province. South Africa Master of Science Degree (2006)

Chapter 43
Vibration Measurement of a Steel Bridge Using Smart Sensors: Deployment and Evaluation

J. Brema, J. Santhosh Kumar, K. Prathibaa and T. S. Rahul

Abstract Civil infrastructure provides the means for a society to function and include buildings, pedestrian and vehicular bridges, tunnels, factories, conventional and nuclear power plants, etc. Structural health monitoring (SHM) represents one of the primary applications for new sensor technologies. In these cases, structural health monitoring (SHM) can be implemented for damage detection and characterization strategy of engineering structures. The design, fabrication, and construction of smart structures are one of the ultimate challenges to engineers as they form the essence of system intelligence and the cores of smart structures technology centers around innovative sensors and sensor systems. In this study, an attempt has been made to monitor the force and vibration components in a Whipple truss bridge and has been verified it analytically. This paper presents a novel piezoelectric cable vibration sensor prototype for use in a monitoring system that can easily evaluate the vibrations of a steel bridge quantitatively. Results obtained using sensor were compared with results obtained with accelerometers and Abaqus software and it was found that the natural frequencies of vibrations estimated from both procedures are in good agreement. However, additional investigation is required to improve the accuracy and reliability of proposed sensor.

Keywords Vibration · Sensors · Force · Bridges

J. Brema (✉) · J. Santhosh Kumar · K. Prathibaa · T. S. Rahul
Department of Civil Engineering, Karunya University, Coimbatore, India
e-mail: brema@karunya.edu

J. Santhosh Kumar
e-mail: santhoshkumar348@gmail.com

K. Prathibaa
e-mail: prathibaa@karunya.edu

T. S. Rahul
e-mail: rahul.rce@gmail.com

P. J. Rao et al. (eds.), *Proceedings of International Conference on Remote Sensing for Disaster Management*, Springer Series in Geomechanics and Geoengineering,
https://doi.org/10.1007/978-3-319-77276-9_43

1 Introduction

Structural Health Monitoring (SHM) is the process to observe and check the progress or quality of (something) over a period of time; keep under systematic review. It gathers information on routinely basis and used to check a project or a structure as it functions. This method of implementing a damage detection and characterization strategy for engineering structures is referred to as structural health monitoring (SHM). A significant challenge in developing an SHM strategy for civil infrastructure is that except for certain types of public and private housing, every structure is unique. Major drivers in this area have been the oil industry, operators of large dams and highways agencies, whose installations have received the greatest attention and research effort. Residential and commercial structures have received relatively little attention due to potential obligations and consequences of owners knowing about poor structural health. The effectiveness of maintenance and inspection programmes is only as good as their timely ability to reveal problematic performance, hence the move to supplement limited and intermittent inspection procedures by continuous, online, real-time and automated systems.

Truss bridge is a whose load-bearing super structure composed of connected elements usually forming triangular units. The connected elements (typically straight) may be stressed from tension, compression or sometimes both in response to dynamic loads. Truss bridges are one of the oldest types of modern bridges. A truss bridge is economical to construct because it uses materials efficiently. A Whipple truss is named after its inventor Squire Whipple. It is usually considered a subclass of the Pratt truss because the diagonal members are designed to work in tension. The main characteristic of a Whipple truss is that the tension members are elongated, usually thin, and at a shallow angle, and cross two or more bays (rectangular sections defined by the vertical members).

The fundamental objectives of civil infrastructure monitoring are as follows: modifications to an existing structure; monitoring of structures affected by external works; monitoring during demolition; structures subject to long-term movement or degradation of materials; feedback loop to improve future design based on experience; fatigue assessment; novel systems of construction; assessment of post-earthquake structural integrity; decline in construction and growth in maintenance needs and the move towards performance-based design philosophy.

2 Literature Review

Chen et al. [1] have conducted a study to monitor the contents of vibration of a bridge analytically as well as experimentally. The authors have concluded that the purpose of establishing a vibration monitoring system is to obtain the vibration response of the bridge structure in the course of running process, to get the change of the dynamic character which includes natural vibration frequency, damping and

vibration mode, and to provide evidences for the safety evaluation of the bridge structure. Washer et al. [2] have proposed a study to establish vibration remote monitoring system of the bridge structure, a efficient and reasonable sensor layout project needs to be designed in the light of the monitoring propose firstly. According to the theoretical analysis result and the actual condition, the 891-4 type vibration sensors were adopted to monitor the vibration displacement; the MEMS acceleration sensors were adopted to monitor the acceleration. Fabian et al. [3] researched on the acquisition device of vibration signal is the 1601 network data acquisition processor which was autonomously developed. Various analog signals which were transmitted by sensor system were collected, and then the analog to digital conversion was completed by the network data acquisition processor. Chaurasiya [4] have conducted a study using several current vibration sensors which were used widely in basic principles and features. Nagayama et al. [5] have concluded in the study the wireless sensor system installed in a suspension bridge can measure the traffic induced vibrations and this monitoring demonstrates quick and easy installation, measurements, and sensor removal as well as its capability to capture dynamic behavior of the bridge.

3 Methodology

The lifetime of bridge structures nowadays is supposed to be 100 years, without a significant failure during the service life. The failures on bridge structures are by initial inspection visually detectable. The main goal of the research is to investigate conventional defects and failure causes and to prepare recommendations to design new bridges without inherent failures and with higher durability. The automated cracks which cause by heavy moving trucks and also by any other natural calamities to be identified by placing the vibration sensor in the truss bridge which will be connected to a alarming sound signal module. The inspection guide on rectifying crack in the bridge will be the result of the project.

3.1 Proposed System

In proposed method we develop a advanced method of sensing cracks in the joints with the help of vibration sensor. Here vibration, force sensors are placed for monitoring the accurate level of the physical quantities of the moving load and dead load in the structure. force sensor and vibration sensors is placed for measuring the pressure of the structure and also its vibration, if any abnormal data to be found by the sensors it will automatically alert by voice module(APR).

3.2 Sensors

Measurement system comprises of sensors, transducers and signal processing devices. A sensor is a device that detects a change in a physical stimulus and turns it into a signal which can be measured or recorded; a transducer converts a physical quantity to an electrical quantity and hence enables transfer of power from one system to another in the same or in the different form. The types of sensors used in this project are:

a. Force Sensor
b. Vibration sensor

3.2.1 Force Sensor

Force Sensing Resistors (FSRs) are very thin, robust, polymer thick film (PTF) devices that decrease in resistance when increased pressure is applied to the surface of the sensor. FSRs are not a load cell or strain gauge devices though they have many similar properties. They are more appropriate for qualitative rather than precision measurements.

With its paper-thin construction, flexibility and force measurement ability, the Thin Force sensor can measure force between almost any two surfaces, up to 1 kg. To ensure utmost accuracy, a small disc (included) can be placed directly on the sensing pad before applying force to the disc. This will ensure that all the force is applied directly to the sensing pad and not to the surrounding surface (Tables 1, 2 and 3).

3.2.2 Vibration Sensor

Vibrations produced by Heavy load Trucks machinery are vital indicators of machinery health. Vibration analysis is used as a tool to determine the bridge condition and the specific cause and location of problems, expediting repairs and minimizing costs. Monitoring vibration levels over time allows prediction of problems before serious damage can occur. Vibration sensors are sensors for

Table 1 Sensor properties

Sl. no.	Sensor type	Force sensitive resistor
1.	Sensor output type	Ratio-metric
2.	Force min	1 N
3.	Force max	20 N
4.	Maximum measurement error	10%

Table 2 Electrical properties

Sl. no.	Parameters	Value
1.	Current consumption max	1.5 Ma
2.	Output impedance	3.3 Kω
3.	Supply voltage min	4.5 V DC
4.	Supply voltage max	5.3 V DC

Table 3 Physical properties

Sl. no.	Parameters	Value
1.	Sensing area	126.7 mm^2
2.	Operating temperature minimum	−30 °C
3.	Operating temperature maximum	70 °C
4.	Lifespan	10 million actuations

measuring, displaying, and analyzing linear velocity, displacement and proximity, or acceleration. The purpose of establishing a vibration monitoring system is to obtain the vibration response of the bridge structure in the course of running process, to get the change of the dynamic character which includes natural vibration frequency, damping and vibration mode, and to provide evidences for the safety evaluation of the bridge structure. Vibration Frequency can be measured in terms of Hertz. The components in the monitoring system is as follows. The micro controller (PIC16F877A) consists of force sensors, vibration sensors, LCD display and APR module. And the power supply unit includes step down transformer (230–12 V AC), Bridge rectifier, filter circuit and voltage regulator (IC 7805).

4 Results and Discussions

4.1 Ansys

ANSYS is an American computer-aided engineering software developer headquartered south of Pittsburgh in Cecil Township. ANSYS Mechanical is a finite element analysis tool for structural analysis. In civil engineering, it also gives us result of bending moment, shear moment diagram, Equivalent truss, Total deformation, Minimum combined stress and Maximum combined stress. The results are shown in Figs. 1, 2, 3 and 4.

In Fig. 2, it is observed that the stress is maximum at the end and minimum at the edges of the truss and in the total deformation in this truss is maximum at the center and minimum at the both edges.

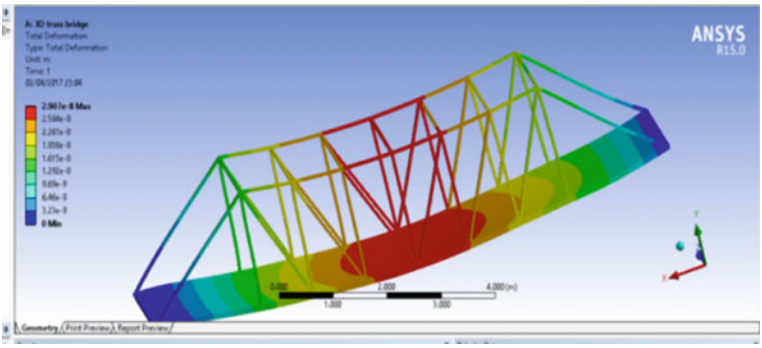

Fig. 1 Deformation results from Ansys

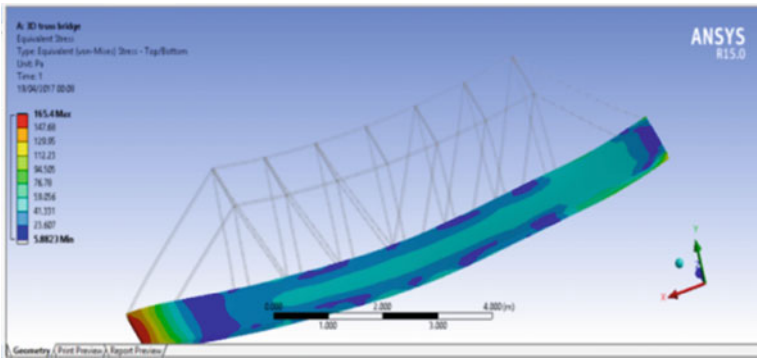

Fig. 2 Equivalent stress results

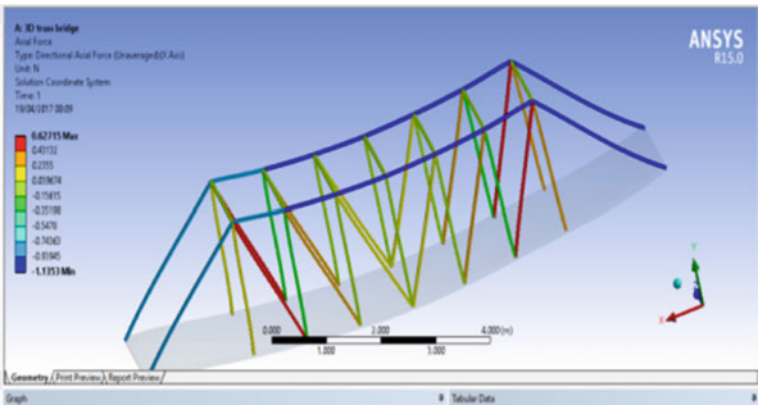

Fig. 3 Axial force in the members

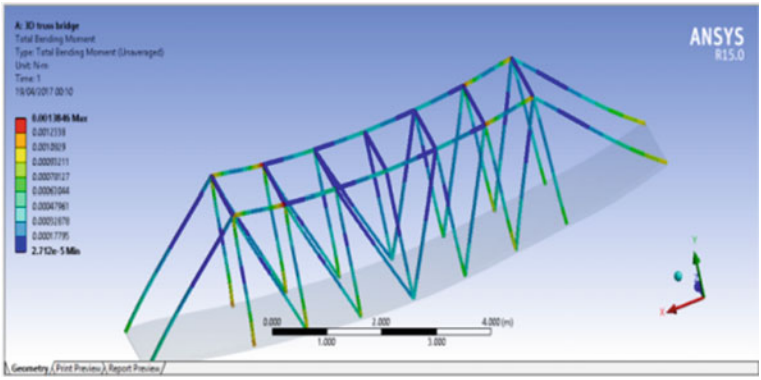

Fig. 4 Bending moment in the members

4.2 Abaqus

Abaqus is a software for finite element analysis and computer-aided engineering, originally released in 1978. It is used in automotive, aerospace, civil and industrial products industries. Here it has been used to find out the frequency of the designed truss (Fig. 5).

According to the result obtained, the frequency (Hz) of the truss is maximum at the center and minimum at the ends for the given load of 7 kN.

The following procedure was used to determine the natural frequency theoretically:

$$k = w/\Delta; \quad \omega = \sqrt{k/m}; \quad f = \omega/2\pi$$

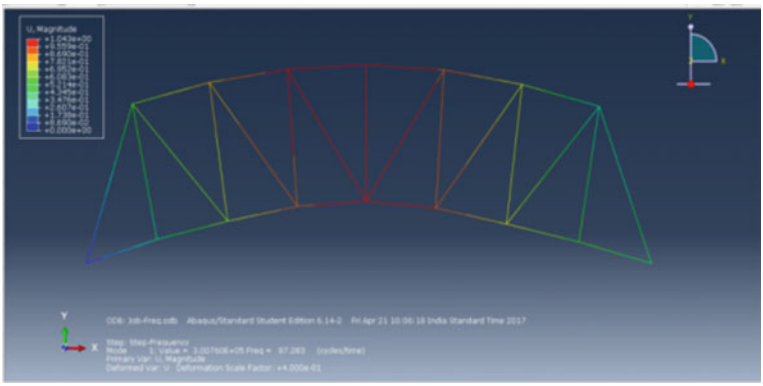

Fig. 5 Frequency results obtained from Abaqus

Table 4 Load versus frequency

Sl. no.	Load (kg)	Frequency (Hz)
1.	0.133	0.0059
2.	0.285	0.0091
3.	0.428	0.013
4.	0.571	0.016
5.	0.714	0.02
6.	0.850	0.024
7.	1.000	0.034

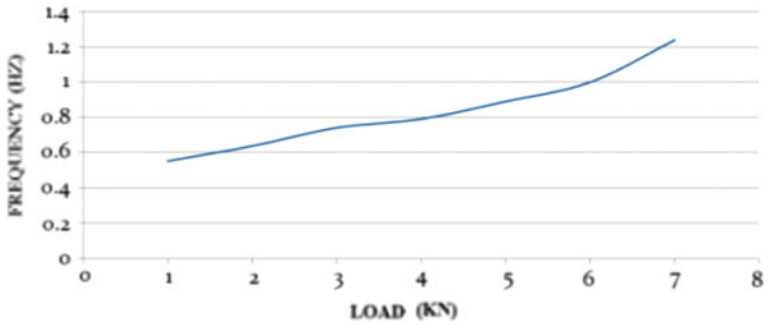

Fig. 6 Load versus frequency curve

k—stiffness of the spring
Δ—deflection
f—frequency.

4.3 Experimental Values

As the force sensor can sense up to maximum of 1 kg only, the values obtained from the experiments were scaled down and the values are given in Table 4.

The experimental values and the observed values correlate well and it have been represented using the graph given in the Fig. 6.

5 Conclusion

The truss was analyzed with the help of the softwares such as Ansys and Abacus to obtain the load carried by the members, to design the truss and to study the frequency in the members respectively. The various parameters of the truss were also

verified experimentally. It is observed that it is possible to obtain the data from truss bridge which will save human life in advance. The real-time monitoring, the real-time displaying, the real-time analyzing and the real-time alarming function are shown in this system. It could provide technical support for discovering the abnormality and damage of the bridge, avoiding the occurrence of bridge collapse accident, ensuring the running safety of bridge structure.

References

1. Chen, S., Su, M., Liu, Y., Wang, Q.: Vibration remote monitoring system of continuous steel truss girder for the Wuhu Yangtze river bridge. In: Proceedings of the 14th World Conference on Earthquake Engineering (2008)
2. Washer, G., Fenwick, R., Nelson, S., Rumbayan, R.: Guidelines for the thermographic inspection of concrete bridge components in shaded conditions. J. Transp. Res. Board. **1**, 13–20 (2013) (Transportation Research Record No. 2360)
3. Fabian, P.R., Washer, G., Dawson, J.: Monitoring vibrations on the jefferson city truss bridge. Final report for Missouri Department of Transportation (2016)
4. Chaurasiya H.: Recent trends of measurement and development of vibration sensors. Int. J. Comput. Sci. **9**(1), 353–358 (2012)
5. Nagayama, T., Ushita, M., Fujino, Y.: Suspension bridge vibration measurement using multihop wireless sensor networks. Proceedia Eng **14**, 761–768 (2011)

Chapter 44
Space Technology Based Disaster Management and Its Societal Implications

Dhruvi Bharwad

Abstract ISRO has been pioneer in embarking the concept of using space technology based societal benefits. It started with vision to utilize space technology for national development. It is also evident that ISRO has actively responded to many developmental spheres of the country. Within last three decades, there has been paradigm shift in the ways of using space technologies for socially relevant fields and disaster management is no exception. Apparently, in present context, when discussing about ISRO and space technology, mostly it is linked with space expeditions, spacecrafts and satellites. Nevertheless, the fact is that these satellites are used to address the developmental need and challenges of the country. ISRO has successfully demonstrated diversified use of satellites benefitting the society directly as well as indirectly. In this context the present study argues that disaster management is an inclusive approach and it addresses disasters from socio-political milieu and ISRO's approach towards disaster management from societal perspective. ISRO's earth observation initiatives coupled with geo spatial technologies and satellite communication and navigation are catering many user driven applications for disaster management, climate and environment. These applications are operationally addressing various natural disasters like floods, cyclone, drought, landslides, earthquakes and forest fires. This approach study further narrates how ISRO is instrumental in building disaster resilient nation through its proactive approach. It is a qualitative attempt to understand societal implications of ISRO's space based disaster management approach and Disaster Management Support (DMS) programme.

Keywords Societal implication · Societal benefits · Satellite · Disaster

D. Bharwad (✉)
Space Applications Centre (SAC), Indian Space Research Organization (ISRO), Ahmedabad, India
e-mail: dhruvi@sac.isro.gov.in

P. J. Rao et al. (eds.), *Proceedings of International Conference on Remote Sensing for Disaster Management*, Springer Series in Geomechanics and Geoengineering,
https://doi.org/10.1007/978-3-319-77276-9_44

1 Introduction

India is one of the most disaster prone countries across the globe and is vulnerable to many disasters such as floods, cyclone, drought, landslides, earthquakes and forest fires. According to National Disaster Management Authority (NDMA) more than 58.6% of the landmass is prone to earthquakes of moderate to very high intensity; over 40 million hectares (12%) of its land is prone to floods and river erosion; close to 5700 km, out of the 7516 km long coastline is prone to cyclones and tsunamis; 68% of its cultivable area is vulnerable to droughts; and, its hilly areas are at risk from landslides and avalanches. Moreover, India is also vulnerable to Chemical, Biological, Radiological and Nuclear (CBRN) emergencies and other man-made disasters. The vulnerability profile as depicted by NDMA further states that disaster risks in India are further compounded by increasing vulnerabilities related to changing demographics and socio-economic conditions, increasing urbanization, development within high-risk zones, environmental degradation, climate change, geological hazards, epidemics and pandemics. Clearly, all these contribute to a situation where disasters seriously threaten India's economy, its population and sustainable development.

The recent disasters and its socio-economic impact on the country at large, has resulted in the need to adopt a multi-dimensional approach involving diverse scientific, engineering, financial and social processes to reduce vulnerability in multi-hazard prone areas. In view of this, the Government of India has brought about a paradigm shift in its approach to disaster management. The change is from "relief and emergency response" to a balanced approach covering all phases of the Disaster Management Cycle. This approach acknowledges disaster management as a part of the development process, and investments in mitigation are perceived to be much more cost effective than relief and rehabilitation expenditure. In this regard, Government of India has taken various initiatives in area of disaster preparedness, mitigation and response through networking of various institutions, institutional capacity building, and policy interventions at all levels. Disaster Management is now being institutionalized into development planning through proactive approach. Various ministries and institutions are in place to cater the efficient disaster management. The role of satellite technology and space based inputs cannot be ignored in ensuring effective disaster management. Various kinds of Satellites, including communications, navigation and remote sensing are useful tools in disaster management.

The Indian Space Programme envisioned the use of space technology for the benefit of common man. There has been paradigm shift in the ways of using space technologies for socially relevant fields and disaster management is no exception. The Indian Space Research Organization (ISRO) has successfully demonstrated diversified use of satellites benefitting the society directly as well as indirectly. The study discusses approach of space technology in managing the disasters and its societal implications. It further discusses the approach of ISRO's disaster management initiatives in light of its societal implications by using secondary data from

open sources. The present study explains that disaster management is an inclusive approach and it addresses disasters from socio-political milieu and ISRO's approach towards disaster management from societal perspective.

2 Space Based Disaster Management: ISRO's Initiatives

As per data available on Press Information Bureau of and India and ISRO portal at present, India has 13 earth observation, 3 meteorological, 13 communication and 7 navigational satellites in operation. The data from earth observation and meteorological satellites in conjunction with ground based information, and services derived from communication & navigation satellites are being used towards Disaster Management Support. The data obtained from meteorological satellites is used for cyclone track, intensity & landfall predictions and forecasting of extreme weather events. The data from earth observation satellites is used for monitoring disaster events and assessing the damages. The communication satellites help to establish emergency communication in remote and inaccessible areas and navigation satellites are used for providing location based services. The fishing sector is being supported through advisories on Potential Fishing Zones and the ocean state forecast generated using satellite data helps the shipping sector. Space Application Centre (SAC) has developed Disaster Management Synthetic Aperture Radar (DMSAR) for flood mapping, landslide, earthquake assessment etc. The dedicated space infrastructure for disaster management includes INSAT 3D and INSAT 3DR.

ISRO has developed very comprehensive space based Disaster Management Support (DMS) programme and been implementing the same through concerned ministries. Under the DMS programme earth observation satellites along with meteorological and communication satellites are used for providing support and services. The programme does monitoring of natural disasters like earth quake, flood, landslide, cyclone, forest fire etc. The programme also supports a National Database for Emergency Management (NDEM). Apart from these, the programme actively responds in many other ways like providing support to International disasters, providing infrastructure for undertaking aerial survey and capacity building initiatives. The programme also contributes in identifying hazard zone of the country and provides near real time information in case of emergencies. The programme also offers near real time mapping of floods, cyclones and forest fires as well as landslide inventory, hazard zone identification and earthquake damage assessment. The major components are shown in Fig. 1.

Specific disaster centric services targeted by the DMS programme are as follows:

Flood and Cyclone (Monitoring and Prediction): Nationwide monitoring of flood and cyclone is carried out and hazard zones are identified. Early warning for flood and cyclone is also disseminated in coordination with Central Water Commission (CWC) and India Meteorological Department (IMD). Through the programme ISRO provides operational services towards delineation of flood affected areas and hence helps in planning critical relief operations. ISRO is supporting the efforts of

Fig. 1 Major components of DMS (*Source* www.sac.gov.in)

India Meteorological Department to predict the tropical cyclone track, intensity and landfall. After the formation of cyclone, its future tracks are regularly monitored and predicted on an experimental basis at Space Application Centre (SAC), ISRO. Real time flood and cyclone prediction helps the disaster management authorities in effective management by taking appropriate measures to reduce the loss of lives and property.

Agricultural Drought: The operational methodology developed by ISRO for prevalence, severity level and persistence of agricultural drought is now institutionalized by setting up Mahalanobis National Crop Forecasting Centre (MNCFC) under the Ministry of Agriculture. Currently, ISRO is concentrating on upgrading the methodology for monitoring the drought and efforts are on to develop early warning systems for agricultural drought.

Forest Fire: Forest fires in India have environmental significance in terms of tropical biomass burning, which produces large amounts of trace gases, aerosol particles, and play a pivotal role in tropospheric chemistry and climate. Active forest fires are detected from the satellite images and the information is uploaded daily to the Indian Forest Fire Response and Assessment System (INFFRAS) website during the forest fire season—February–June.

Earthquakes: Remote Sensing and GIS provide a database from which the evidences left behind by disaster can be combined with other geological and topographical database to arrive at hazard map. These data can be made use to create a very large scale base information of the terrain for carrying out the disaster assessment and for relief measures.

Landslides: Landslides pose a threat of lives and property in mountain areas. Earth observation plays vital role in collecting information on landslides particularly across inaccessible mountains. Under the programme extensive landslide hazard zone mapping in the state of Himachal Pradesh and Uttarakhand has been done. Landslide inventory has also been prepared in case of extreme emergencies like Kashmir earthquake (2005), Sikkim earthquake (2011), Kedarnath disaster (2013) and J&K floods (2014). These maps are very useful for development planning and policy making.

Infrastructure development for Disaster Management: Apart from these initiatives, repository of data to support emergencies a National Database for Emergency Management is also maintained. Further under the programme ISRO has set up a satellite communication based virtual private network. Through the network effective communication support is provided during disasters and it can be accessed from terrestrial network whenever required. Thus the network helps in restoring basic communication in affected areas.

Natural disasters like floods, cyclone, landslides, earthquakes and forest fires damages the natural resources and incurs significant economic losses. But at the same time there are slow and onset disasters like drought, heat wave and cold wave, cloud burst etc. have potential to turn into disaster by incurring economic as well as human life losses. Satellite technology through its forecast and advisories can easily avert the losses arising out of such potential disastrous events. Indian satellites are instrumental in providing advisories, forecasts, alerts and early warnings for weather events on daily basis, which is accessible through its web portals. Meteorological and Oceanographic Satellite Data Archival Centre (MOSDAC), ISRO provides data on heavy rainfall alerts, heat waves, cloudburst, dust storm etc. in near real time. The Indian Geo Platform—Bhuvan also offers information on hailstorms, flood warning, flood vulnerability and other disaster related services. Such information dissemination mechanism helps in minimizing the risk. Some of such products are shown in Figs. 2, 3 and 4.

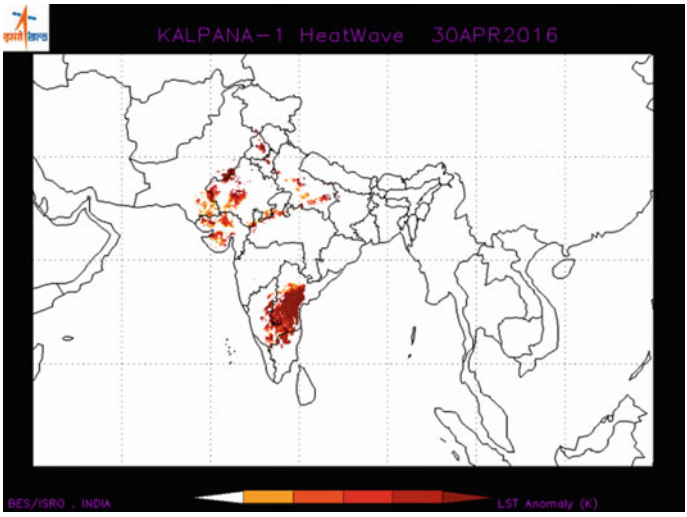

Fig. 2 Heat wave prediction across India, April 2016 (*Source* www.mosdac.gov.in)

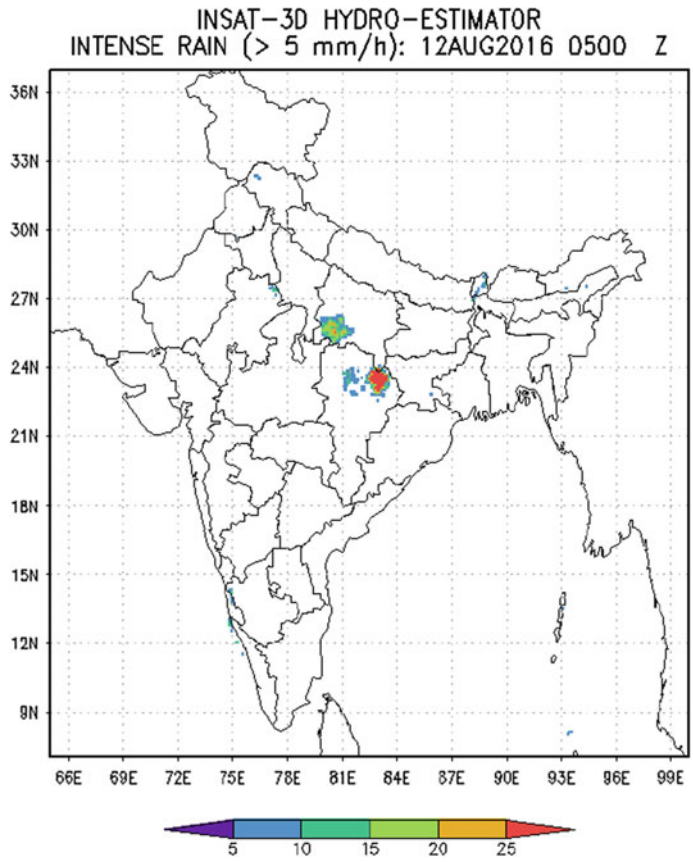

Fig. 3 Heavy rainfall prediction (*Source* www.mosdac.gov.in)

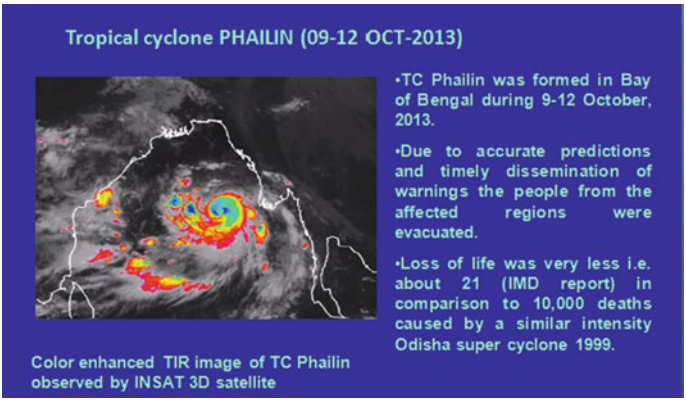

Fig. 4 Cyclone PHAILIN (*Source* www.mosdac.gov.in)

3 Societal Implications of ISRO's Disaster Management Initiatives

Disasters pose serious risk to life, property and infrastructure. Timely information about onset of disasters can help in preventing such losses to a great extent. It also helps in planning response accordingly. Earth observation satellites and communication satellites together can easily ensure effective disaster management. It provides synoptic and unbiased information on disasters that can help in damage assessment, preparedness and mitigation, early warning, impact assessment and emergency communication. Some of the aspects of space technology like Geographical Information System, Global Positioning System, and Earth Observation have been proved very crucial for disaster management. All these aspects are very useful to disaster management authorities and concerned response agencies in planning their response to disaster situation as well as for decision making, policy making.

ISRO's disaster management initiatives ensures timely support and services from aero-space systems, both remote sensing and communications, towards efficient management of disasters in the country. The emergency communication capability of DMS programme is major element for planning relief and rescue operations. It also helps in making emergency response more accurate. It also helps in damage assessment and planning long term mitigation strategy. The database generated through DMS programme helps to a great extent in planning developmental activities as well as for preparing disaster management plans. Hence it is useful in making national, state as well as district level disaster management plans. The programme also addresses many other social dimensions. The initiatives planned under the programme not only aim at reducing damages during disasters but also in planning long term mitigation measures. With the help of earth observation many important activities are done for disaster management. It plays important role in identifying disaster affected area, damage assessment and in monitoring and prediction of disasters. All these factors are inevitable components of socially responsive disaster management.

One of the major areas to build resistance to natural disasters is through capacity building. There are many stakeholders, government and non-government as well as the community (scientists, managers, planners, grassroots, media and general masses). All of them have different level of knowledge capacity hence in order to bring them to single platform; the database generated through space technology can be easily utilized. This type of database provide access to disaster related information like factors responsible for disasters, its repercussions, natural impact as well as human induced impact, prediction etc. The early warning dissemination also helps in planning response and gives time to community for preparedness and hence empowers community to face disasters. Moreover, such space based disaster management enables better disaster response for relief and rescue, timely assessment of damage and mitigation planning reduces economic and human life loss and improves overall disaster response mechanism.

The other societal dimension addressed by space based disaster management is strong remote sensing applications of Indian remote sensing satellites. Some of important initiatives are Groundwater Prospects Mapping under Drinking Water Mission, Forecasting Agricultural output using Space, Agro-meteorology and Land based observations (FASAL), Forest Cover/Type Mapping, Grassland Mapping, Biodiversity Characterization, Snow & Glacier Studies, Land Use/Cover mapping, Coastal Studies, Coral and Mangroves Studies, Wasteland Mapping etc. They play crucial role in reducing vulnerabilities arising out of resource scarcities. The information generated by large number of projects have been used by various departments, industries and others for different purposes like development planning, monitoring and conservation of natural resources. Early warnings, weather forecast and nowcast, advisories, near real time alerts etc. provides information regularly which can be of significant use to administration in decision making. Access to disaster or potential disastrous events is a step towards building disaster resilient nation, as it reduces vulnerabilities.

4 Conclusion

Over the past few decades, there has been an increase in disaster occurrence resulting in human and economic losses. This is because of increasing vulnerability of people to natural disasters. Vulnerability to natural disasters is integrally linked with poverty, resource scarcity, poor coping capacity and lack of disaster resilience. Many a times hazardous situations are common for both rural and urban areas but its adverse impact can be seen more in rural areas, because they are ill equipped with necessary skills, infrastructure, capacities and coping mechanism. Poor socio economic conditions, illiteracy, increasing demographic pressure and poor geo-climatic surroundings further increase their vulnerability. Hence managing disasters skilfully by addressing such social dimension becomes utmost priority. This cannot be achieved without reliance on satellite technologies and space based inputs. It is underlying fact that disasters should be addressed with proactive and holistic approach. The strong remote sensing application front of ISRO coupled with satellite communication and navigation capabilities are addressing emergency communication, damage assessment, prediction, early warning, advisories, alerts etc. Such initiatives eventually reduce vulnerability and enhance coping capacity of masses as well as administration. Hence the Indian Space Based Disaster Management practices have resulted in building disaster resilient nation, by showcasing diversified use of its technologies and applications, benefitting the society. But at the same time there is strong need for capacity building and sensitization of local bodies in order to take maximum advantage ISRO's disaster management initiatives. If local bodies are sensitized towards the effective use of space based disaster management, the it can reach easily reach to the remote and most vulnerable population in true spirit.

Acknowledgements Author is highly indebted to Dr. Parul Patel, Shri Atul Shukla, Shri Vikas Patel and Shri Y. P. Rana, SAC/ISRO for providing their valuable suggestions.

References

1. National Disaster Management Authority. www.ndma.gov.in/en/vulnerability-profile.html
2. Indian Space Research Organization. http://www.isro.gov.in/applications/disaster-management-support-programme
3. Press Information Bureau of India. www.pib.nic.in/newsite/PrintRelease.aspx?relid=160511
4. Space Applications Centre. www.sac.gov.in/vyom/CommNavApplications.jsp
5. Space Applications Centre. www.sac.gov.in/SAC_Industry_Portal/SAC/Radar_Imaging/Disaster_Management_SAR.pdf
6. Meteorological & Oceanographic Satellite Data Archival Centre. www.mosdac.gov.in/data/heatwave_archieval_2016.jsp
7. Meteorological & Oceanographic Satellite Data Archival Centre. www.mosdac.gov.in/data/monsoon.jsp
8. Meteorological & Oceanographic Satellite Data Archival Centre. www.mosdac.gov.in/cyclone-genesis/archieve/archieve-phailin

Chapter 45
Integrated Methodology for Delineation of Salt-Water and Fresh Water Interface Between Kolleru Lake and Bay of Bengal Coast, Andhra Pradesh, India

Harikrishna Karanam, Jaisankar Gummapu and Velaga Venkateswara Rao

Abstract Kolleru Lake is the largest natural fresh water lake located between Krishna and Godavari deltas in Andhra Pradesh in India, is acting as a natural flood balancing reservoir and is fed directly by water from the seasonal rivers Budameru, Ramileru and Tammileru. Land use conversions to aqua-culture and Over-exploitation of groundwater are becoming the sources for salt-water intrusion. Present land use activities has large contribution for the change of water quality. Hydrogeomorphology feature are indicates that paleo beach ridges and buried river courses are potential aquifers around the Kolleru Lake. Though there are number of open wells present in the villages used for potable water earlier, people switched over to imported water as their drinking water source may be due to significant contamination of groundwater resources. Integrated study of remote sensing,, hydrochemistry, hydrogeology and geophysical investigations revealed the extent of salt-water intrusion up to the northern part of the lake which is about 40 km away from the Bay of Bengal coast line. The electrical resistivity of aquifers is less than 1.0 Ωm having salinity of more than 1.2 ppt and the resistivity is around 20 Ωm where the salinity is less than 0.5 ppt, has also served as an excellent criteria for delineating the fresh-water and salt-water interface.

Keywords Saltwater intrusion · Kolleru lake · Hydrogeomorphology Overly techniques · Remote sensing and GIS

H. Karanam (✉)
Professor of Civil Engineering, Dadi Institute of Engineering and Technology, Anakapalle, Andhra Pradesh, India
e-mail: harigis2007@gmail.com; drhkkaranam@gmail.com

J. Gummapu · V. Venkateswara Rao
Department of Geo-Engineering, A.U.College of Engineering, Visakhapatnam, Andhra Pradesh, India
e-mail: jaisankar.gummapu@yahoo.com

V. Venkateswara Rao
e-mail: vrvelagala@gmail.com

P. J. Rao et al. (eds.), *Proceedings of International Conference on Remote Sensing for Disaster Management*, Springer Series in Geomechanics and Geoengineering,
https://doi.org/10.1007/978-3-319-77276-9_45

1 Introduction

Kolleru is one of the biggest shallow fresh water lakes in India which is located between the deltas of Krishna and Godavari River in the state of Andhra Pradesh, India. The lake serves as a natural flood balancing reservoir of these two rivers. The lake receives water from the seasonal Budameru and Tammileru streams and it is connected to the Krishna and Godavari irrigation system by over 66 inflowing drains and channels. The catchment of the lake extends up to 9036.30 km^2. The people in the deltaic region between Kolleru Lake and Bay of Bengal coast mainly depend on agriculture and fishing. Since last two decades aquaculture is developed inside the coastal area encroached into the agricultural lands and into the Kolleru Lake also [1]. Groundwater is the main drinking water source to the population other than the limited surface storage ponds in the study area. Potable groundwater source exists at shallow depth in the limited geomorphic units and people are exploring the source through open wells that are in the range of 3–5 m depth and almost every house having an open well. An attempt is made to understand the problem with multidisciplinary approach to suggest some solution to improve the drinking water situation particularly the area between lake and the coast area.

Saltwater intrusion is contaminated coastal aquifers especially in and around the Kolleru lake region, many farmers to take aquaculture as a more profitable source of income, where salt water is used from the nearby creaks [2]. Saline or brackish groundwater is present below fresh groundwater in coastal and deltaic areas [3]. The coastal aquifers are generally fragile in nature and the shallow aquifers are easily depleted due to overexploitation of groundwater in many parts of India and worldwide [4]. Geophysical, geochemical and remote sensing techniques are used to directly or indirectly supervise saltwater in coastal aquifers, because of the very high chloride concentration in seawater. However, total dissolved-solids concentration or specific conductance of groundwater samples are other indicators of groundwater salinity [5].

Electrical Resistance survey is one of the familiar surface geophysical method to demarcate the sub-surface layers includes aquifers and to certain extent the quality of groundwater [6]. Seawater has a high attention of dissolved ions, its presence in a coastal aquifer can be inferred from measurements of the spatial distribution of electrical conductivity [7].

2 Study Area

The study area is located in two districts namely West Godavari and Krishna, Andhra Pradesh, India. The area covered in this investigation is about 3861.97 km^2 lying in between 80° 50′ to 81° 39′E longitude and 16° 17′ to 16° 59′N latitude. Location map of the study area is shown in Fig. 1. The study area lies in between the delta regions of Krishna and Godavari rivers which include 16 mandals in West Godavari district and 15 mandals in Krishna district.

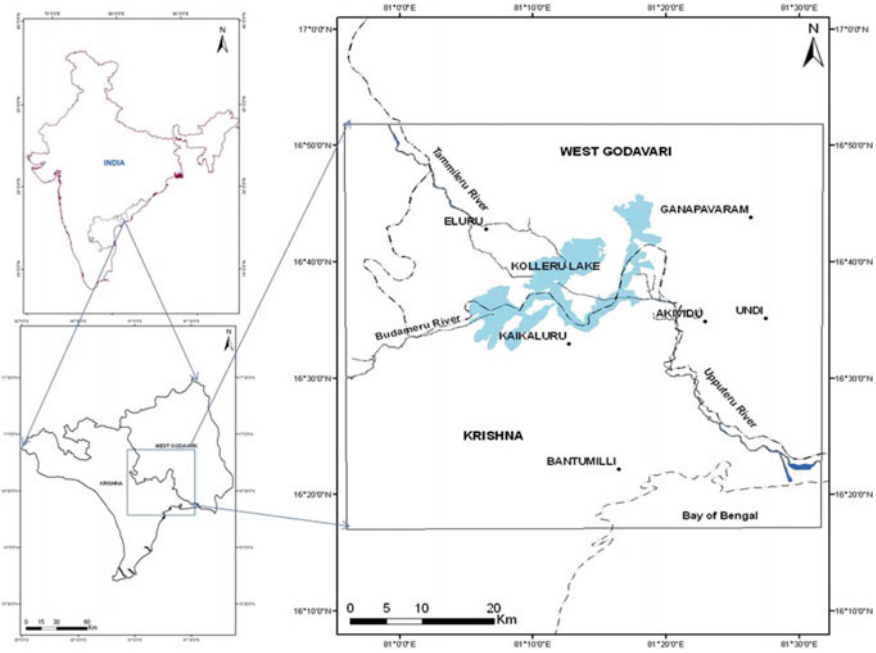

Fig. 1 Location map of the study area

3 Geomorphology

The geomorphological features that are favourable for accumulation of groundwater and possibility of occurrence of fresh water are (i) up land areas with sand stone formations may consists of series of aquifers to deeper depth, (ii) paleo beach ridges that consists of thin sand deposition may have good permeability and forms a good yielding aquifer (iii) flood plains consists of silty sands and silty clays and can hold some quantity of water in top thin layer and (iv) lake bed may consists of silty clay and clay can hold some quantity of water in the form of aquiclude.

4 Hydrogeology

A total number of 194 observation wells in different villages covering the entire study area were inventoried for 4 years to study the behavior of the aquifer and the locations of these wells are presented on the geomorphology map as shown in Fig. 2. All the inventory wells are dug wells and shallow filter points being used for domestic needs. Water levels are measured with automatic water level indicator and coordinates were measured with Global positioning system (GPS).

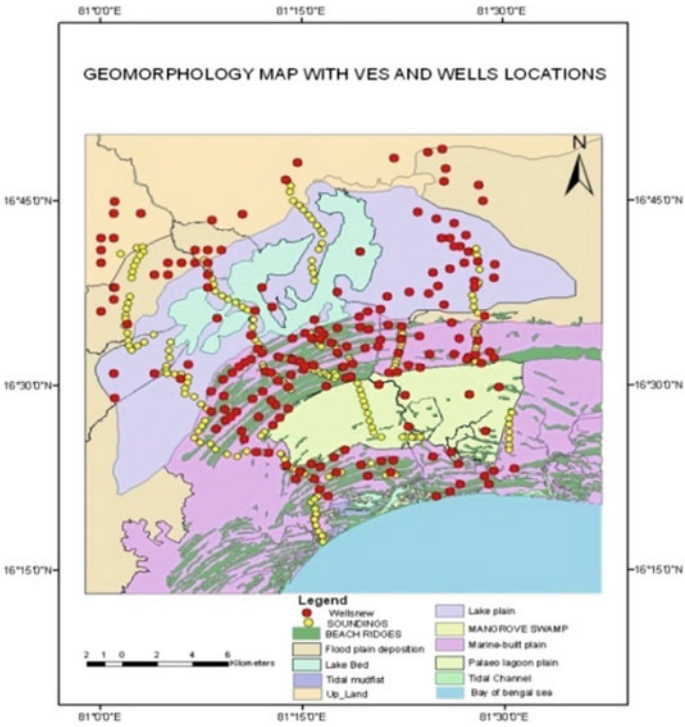

Fig. 2 Wells and VES locations on geomorphology map

Minimum depth of water table is recorded as 0.20 m at Malkapuram during post monsoon period and maximum depth in the same period was 4.12 m at Paturu. Minimum depth of water table was 1.19 m during pre monsoon period at Penumaka lanka and maximum depth was 6.1 m at Paturu village. Nearly 50% of the wells indicated more than 3.0 m depth of water table during pre monsoon period, about 10 wells recorded more than 4 m depth and 2 wells recorded more than 5 m depth during pre monsoon period.

5 Integration of Chemical Data

Chemical parameters of groundwater samples are well explained above comparing the WHO and IS:10500 standards. Broadly the areas of maximum desirable, maximum permissible and beyond permissible limits are demarcated. Here an attempt is made comparing the areas of beyond permissible limit of TDS with all the other parameters. Red boundary line enclosure in Fig. 3 is highest TDS area. Same area with same geographical coordinates superposed over the thematic maps of all over the other 8 parameters. Figure 3a is the areal distribution of TDS and

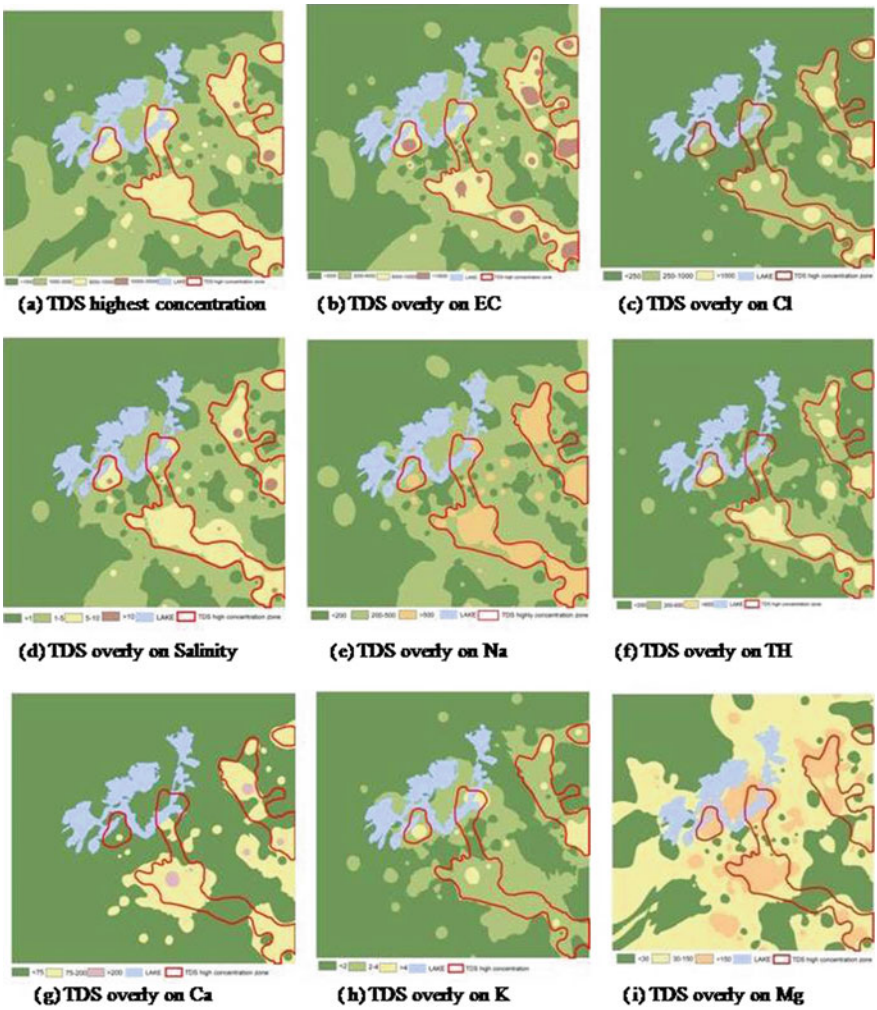

Fig. 3 Comparison of TDS high concentrations with other parameters

Fig. 3b is the aerial distribution of Ca over which the boundary of beyond permissible limit of TDS is super posed. Majority of the beyond permissible area of Ca is coinciding with that of the boundary of TDS. Similarly EC, chlorides, salinity, sodium, potassium and magnesium parameters highest permissible areas matching with TDS beyond permissible limits. Thus integration of the chemical parameters clearly indicates the areas of salinity/polluted groundwater zones.

6 Resistivity Survey

Electrical resistivity method is one of the most commonly used techniques to delineate aquifer composition, groundwater, bedrock, and fresh/salt zones [8]. Many successful attempts in delineating the shallow and deep aquifers using VES measurements with Schlumberger configuration were made in the recent past [9, 10]. In this work Schlumberger resistivity method has been utilized to demarcate saltwater and freshwater. In a general way the resistivity is also controlled by the amount of water present. The more porous or fissured a rock, the lower the

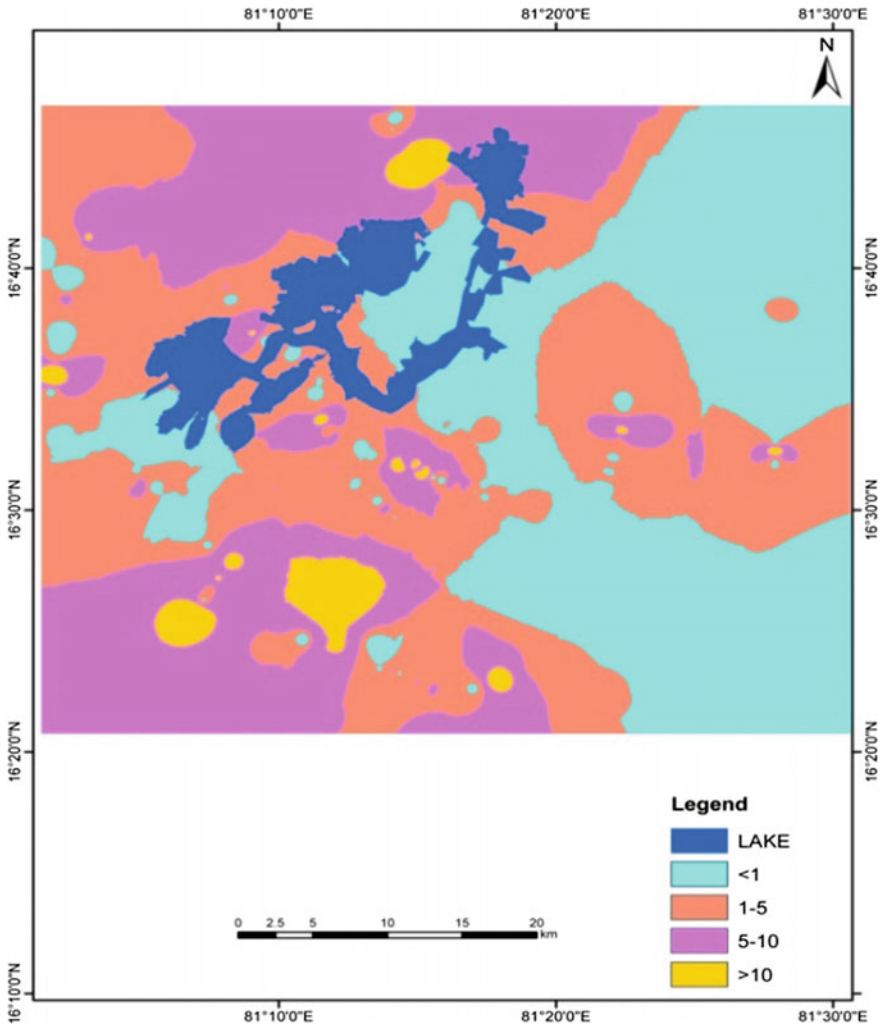

Fig. 4 Spatial distribution of top layer resistivity

resistivity. Higher degree of saturation or greater amount of water presents in pore spaces and fissures also decreases the resistivity [11].

Top soils resistivity in paleo beach ridges, lake plain and uplands are higher and varies between 3 and 68 Ωm. Flood plain deposition, marine built plain and marine lagoon plain having top soil resistivity varies between 2 to 27, 1 to 15 and 0.3 to 15 Ωm respectively. The most dominant geomorphic unit which is favorable for good potable water is paleo beach ridges having top soil resistivity between 8 and 50 Ωm. Spatial distribution of top layer resistivity has shown in Fig. 4.

In the present paper, geophysical resistivity studies and chemical analyses of ground water for TDS, conductivity and salinity of different open wells are compared. Finally, an attempt made to compared analysis of Vertical Electrical Soundings (VES) data and chemical data of observation wells nearby sounding resistivity location which are more related.

7 Integration

The final step of GIS application in this study is to analyze all data layers through the process called "Overlay". Index Overlay is a spatial operation in which superimposed of thematic layers onto another to form a new layer. In this study overlay process was performed under the contributory rule, using arithmetic operation as a key function. This kind of overlay is so called "Arithmetic overlay", which means that values assigned to two or more input themes are combined arithmetically (+, –, *, /) to produce an output grid [12]. Two or more thematic layers may be combined, subtracted, multiplied, etc., to create a new layer with new value for each grid cell [13]. There are a number of applications in the literature where both geoelectrical method and groundwater quality studies have been integrated together [14].

In this case the map classes occurring on each input map are assigned different scores, as well as the maps themselves receiving different weights as before. It is convenient to define the scores in an attribute table for each input map. The averages score is than defined by the equation

$$\bar{S} = \frac{\sum_i^n S_{ij} w_i}{\sum_i^n w_i}$$

where $\bar{S}$ = Weighted score for an area object (polygon, pixels)

S_{ij} = Score for the j-th class of the i-th map

w_i = Weighted score for the i-th map.

There are several methods available to determine inter class dependencies or inter map dependencies such as Binary map analysis, Fuzzy logic and Index Overlay with Multi-class maps. Here an attempt has been made to use multi class maps in Index overlay method [15].

The input layers which are considered for the analysis of groundwater vulnerability zones are Salinity, Total Dissolved Solids (TDS), Resistivity, Electrical Conductivity (EC), Total Hardness (TH), Sodium (Na), Chloride (Cl), Calcium (Ca), Magnesium (Mg), Potassium (K), Nitrate ($N0_3$), Sulphate ($S0_4$), Total Alkalinity (TA) and Hydrogen Ion Concentration (PH). The score values for all individual classes for each map will be assigned along with the map weightages will be entered as an attribute data for the purposes of index overlay analysis purpose to obtain a new spatial vulnerability map.

Map Weights

M1 = Weightage * [class (Salinity)]
M2 = Weightage * [class (TDS)]
M3 = Weightage * [class (Resistivity)]
M4 = Weightage * [class (EC)]
M5 = Weightage * [class (TH)]
M6 = Weightage * [class (Na)]
M7 = Weightage * [class (CI)]
M8 = Weightage * [class (Ca)]
M9 = Weightage * [class (Mg)]
M10 = Weightage * [class (K)]
M11 = Weightage * [class ($N0_3$)]
M12 = Weightage * [class ($S0_4$)]
M13 = Weightage * [class (TA)]
M14 = Weightage * [class (PH)]

Calculate sum of weighted conditions and divided by normalization factor

$$\text{New Vulnerability Map} = \left[\frac{*\text{M1} + *\text{M2} + *\text{M3} + *\text{M4} + *\text{M5} + *\text{M6} + *\text{M7} + *\text{M8} + *\text{M9} + *\text{M10} + *\text{M11} + *\text{M12} + *\text{M13} + *\text{M14}}{\text{SUM}}\right]$$

Depending upon the levels of concentrations of these chemical parameters in the study area these were assigned with a particular weightage number and multiplied to obtain a map which is used for further analysis. In the same way depending upon their levels of concentrations the other chemical parameters were also assigned with a particular weightage and multiplied to obtain maps which as used for overlay analysis of all these chemical parameters along with resistivity of the study area to obtain salt water intrusion areas. Thus each grid cell data is calculated and represented in the form of map showing the saline and non-saline groundwater zones in Fig. 5.

The above figure shows that the groundwater in uplands, flood plains and paleo beach ridge zones are under non saline. The areas of paleo lagoons, marine plains, marine marshy lands shown in the non potable groundwater zones. Saline groundwater zones extend into the lake area and the continuous big brown patch

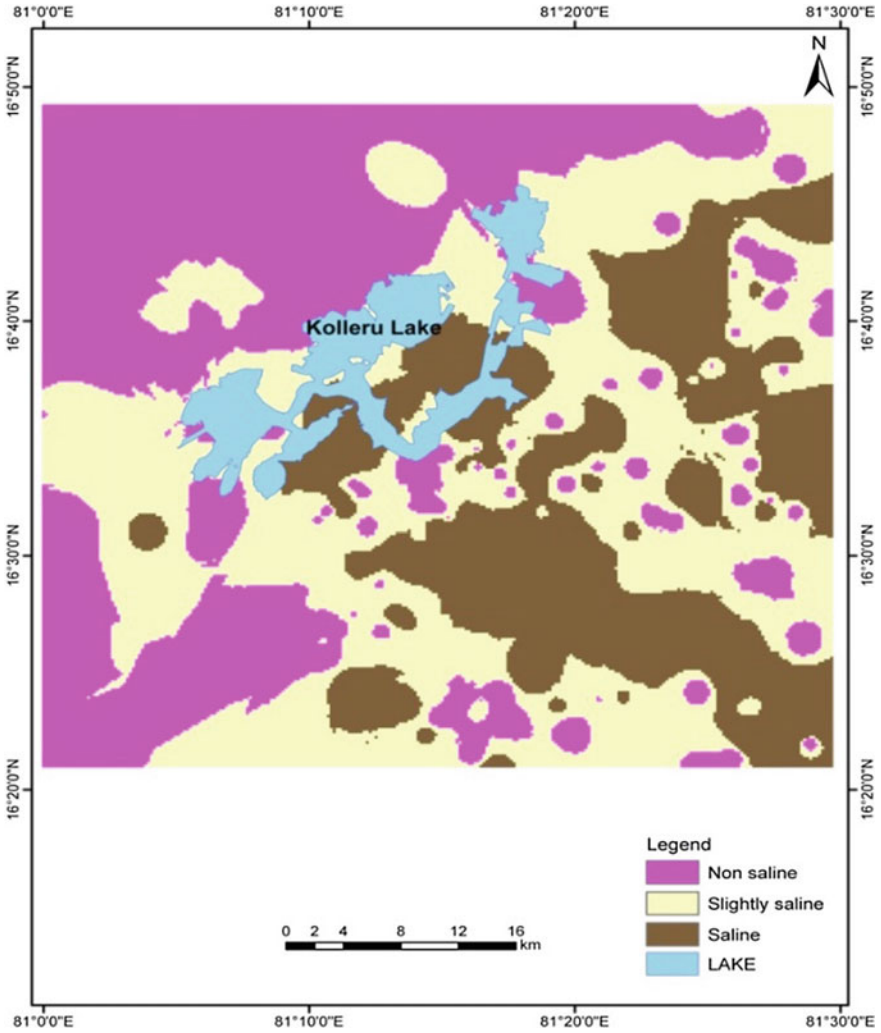

Fig. 5 Broad classification of groundwater as per the integration of hydrochemical data and aquifer resistivity

between lake and the coast may be the main route of salt water intrusion towards the land. There are several potable groundwater patches in pink color shown in Fig. 5 very near to the coast also may be due to presence of sand dunes which hold the fresh water.

8 Conclusion

Physical and geomorphological evidences indicate that the features- uplands and flood plains are not influenced by the marine activity and groundwater in these regions are potable. The other geomorphic features- paleo beach ridges, lake plains, marine plains, paleo lagoon, marine swamps are influenced by marine activity since Holocene period in which paleo beach ridges and some silty sands and silty clays in the lake plains consists of potable water at shallow depth due to their leaching out nature of salts and good rechargeable conditions of groundwater. In the deeper zones of all the marine influenced areas consist of saline water may be due to sea water intrusion and also salts locked up in the clay formations.

Acknowledgements The authors acknowledge DST, New Delhi, for sanctioning the research project "Hydrogeological and Groundwater resource evaluation studies in and around Kolleru Lake". The authors are thanking to Prof. P. Rajendra Prasad and Prof. K. Nageswara Rao for their continuous support to delineate the geomorphological features of the study area.

References

1. Harikrishna, K., Ramprasad Naik, D., Venkateswara Rao, T., Jaisankar, G., Venkateswara Rao, V.: A study on saltwater intrusion around Kolleru lake, Andhra Pradesh, India. Int. J. Eng. Technol. **4**(3), 133–139 (2012)
2. Harikrishna, K., Venkateswara Rao, V., Ramprasad Naik, D., Jaisankar, G., Amminedu, E.: Hydrogeological & geophysical studies for delineation of freshwater source in the paleo beach ridges around Kolleru lake, Andhra Pradesh. IJETT **4**(3), 251–257 (2013)
3. Narayan, K.A., Schleeberger, C., Bristow, C.: Modelling seawater intrusion in the Burdekin Delta irrigation area, North Queensland, Australia. Agric. Water Manage. **89**(3), 217–228 (2007)
4. Mondal, C., Singh, P., Singh, S., Saxena, K.: Determining the interaction between saline water and groundwater through groundwater major ions chemistry. J. Hydrol. **388**(1–2), 100–111 (2010)
5. Choudhury, K., Saha, D.K.: Integrated geophysical and chemical study of saline water intrusion. Ground Water **42**(5), 671–677 (2004)
6. Harikrishna, K., Appala Raju, N., Venkateswara Rao, V., Jaisankar, G., Amminedu, E.: Land use/land cover patterns in and around Kolleru lake, Andhra Pradesh, India using RS and GIS techniques. Int. J. Remote Sens. Geosc. **2**(2), 1–7 (2013)
7. Albouy, Y., Andrieux, P., Rakotondrasoa, G., Ritz, M., Descloitres, M., Join, L., Rasolomanana.: Mapping coastal aquifers by joint inversion of DC and TEM soundings -3 cases histories. Ground Water **39**(1), 87–97 (2001)
8. Griffiths, D.H., Barker, R.D.: Two-dimensional resistivity imaging and modelling in areas of complex geology. J. Appl. Geophys. **29**(3–4), 211–226 (1993)
9. Selvam, S., Sivasubramaniam, P.: Groundwater potential zone identification using geoelectrical survey: a case study from Medak district, Andhra Pradesh, India. Int. J. Geomat. Geosci. **3**(1), 55–62 (2012)
10. Oyedele, K.F., Ogagarue, D.O., Esse, O.: Groundwater potential evaluation using surface geophysics at Oru-Imope, South-Western Nigeria. Eur. J. Sci. Res. **63**(4), 515–522 (2011)

11. Griffiths, E.: Soil structure. In: A system for description and interpretation for permeability assessment. Soil Bureau District Office Report HV14, Department of Scientific and Industrial Research, New Zealand (1986)
12. ESRI.: Getting to know Arc GIS. ESRI Press, Redlands (2001)
13. Bernhardsen, T.: Geographic information systems: an introduction, 2nd edn. Wiley, New York (1999)
14. Zohdy, A.R., Eaton, G.P., Mabey, D.R.: Application of surface geophysics to ground water investigations. In: USGS techniques of water-resources investigations (Book 2. Chap. DI), p. 116 (1974)
15. Bonham Carter, G.F.: Geographic information system for geoscientists: modeling with GIS. Elsevier Science Ltd., The Boulevard, Langford Lane, Kidlington, OX5 1 GB, U.K (2002)

Chapter 46
Identification of Landslide Hazard Zones Along the Bheemili Beach Road, Visakhapatnam District, A.P.

B. Sridhar, Peddada Jagadeeswara Rao, Gudikandhula Narasimha Rao, Rajesh Duvvuru, Ch. Anusha, D. Sanyasi Naidu, E. Srinivas, T. Sridevi, M. Madhuri and Y. Padmini

Abstract Roads and Highways are the index of development of any nation. The study area considered covers the recent road expansion in between MVP colony to Bheemili, is a strategic important road which connects Visakhapatnam and Bheemili. Therefore, the work has been taken up to study the areas liable to collapse along the road expansion. The geological vulnerable zones were located using the spatial technology coupled with civil engineering studies The existing road has been widened removing a small part of Kailasagiri hill at Thenneti Park, is liable to slide as landslide. Soil creep and slump are the major hazards near Rama Naidu Cinema Studios. The road is connecting to bad lands popularly known as ErramattiDibbalu, where soil erosion is more prominent. A huge marine sand dunes

B. Sridhar (✉) · P. J. Rao · G. Narasimha Rao · R. Duvvuru
Ch. Anusha · D. Sanyasi Naidu · E. Srinivas · T. Sridevi
Department of Geo-Engineering, College of Engineering (A),
Andhra University, Visakhapatnam, India
e-mail: sridhar.bendalam@gmail.com

P. J. Rao
e-mail: pjr_geoin@rediffmail.com

G. Narasimha Rao
e-mail: gudikandhula@gmail.com

R. Duvvuru
e-mail: rajesh.duvvuru@gmail.com

Ch. Anusha
e-mail: anu4goal@gmail.com

D. Sanyasi Naidu
e-mail: sndadi@gmail.com

E. Srinivas
e-mail: srinivase4@gmail.com

T. Sridevi
e-mail: srice2001@gmail.com

P. J. Rao et al. (eds.), *Proceedings of International Conference on Remote Sensing for Disaster Management*, Springer Series in Geomechanics and Geoengineering,
https://doi.org/10.1007/978-3-319-77276-9_46

deposited on both sides of the road near INS Kalingas during cyclones. Resorts, educational institutions and fisherman colonies are the major land uses, whereas, thick vegetated hills are the major land cover. The road crosses over small streams where culverts and bridges were constructed. The study has identified landslides vulnerable zones and suggested mitigation measures.

Keywords Landslides · Remote sensing · GIS · Geomorphology
Drainage pattern

1 Introduction

Roads and Highways are the arteries which connects different places is the index of development of any nation. India has the longest Highway road network which connects Kashmir to Kanyakumari. It connects Northern border to Southern tip of India has a length of 2535.74 km. The roads connect different areas of varied types of topography and climate conditions, etc. India has one of the finest road systems in the world. Delhi, Chandigarh and other major metropolitan cities in India have good road network. Recently, Government of India has taken up expansion of the existing roads with a view to accommodate increasing load traffic. Romans had taken up the earliest road contractions. Constructions of major roads have come up during industrial area. America has excellent road network followed by European countries. In Japan, 8 tired road systems have been constructed to divert the heavy traffic to different places. Owing to scarce land, underground roads and railway systems being taken up in most parts of the world.

The present study, recent road expansion in between MVP colony to Bheemili is a strategic important road which connects Visakhapatnam and Bheemili. This road has a length about 23 km and passes along the sea coast of Visakhapatnam and Bheemili. The old Dutch settlement of Bheemili is the second oldest municipality in India. The expansion of existing road has consumed remove hill rock masses which are barely exposed onto the road may likely to collapse as slip landslides, etc. Hence, this topic has been taken up to study the areas liable to collapse along the road. The present topic has been taken up with the following objectives. The study is confined to recent expansion of four lane roads connecting between Visakhapatnam to Bheemili. The road laid adjacent to the sea coast of Bay of Bengal, and it is under the natural vagaries of sea coast on one side and land and its

M. Madhuri
Malla Reddy Institute of Technology, Secunderabad, India
e-mail: madhurimulpuru@gmail.com

Y. Padmini
Dr. B.R. Ambedkar University, Srikakulam, India
e-mail: gbujji.paddu@gmail.com

natural activities on the other side render the road vulnerable. Recently, IT Parks, Rama Naidu Cinema Studio, several resorts and urban built up come into existence. This anthropogenic activities has altered the topography along the road system. The major important places located enroute of this road are Rushikonda, Bojjannakonda, Erramattidibbalu, etc. Apart from natural and historical importances, INS Kalinga as Indian Navy is established adjacent to this road. Traffic load is increasing year after year. In view of the traffic load recent road expansion has been taken up in place of old road network. This activity has led to cutting of hill flanks, foothills, sea sand dunes, culverts, drainages and highly denuded land forms etc. Hence, this topic has been taken up to study the soil creep, rock creep, solifluction, land slips, landslides, tidal action and beach erosion along the Bhimili road. The area is covered with khondalite suite of rocks belonging to Archaean age. Hills are composed of khondalite suite of rock. The isolated hillocks are formed at the foot hill area and are composed of charnockite and quartzite rock types. These rocks are later intrusives into the country rock. The strike of the rocks is NNE-SSW and thus coincides with the general trend of the Eastern Ghats. However, local variations are also identified [1, 2].

2 Study Area

The area of investigation is located in between 17° 73′ and 17° 80′ North latitude and 83° 32′ and 83° 45′ Eastern longitudes. Geographically, the area is covering 236 km^2, out of which approximately half of the area covers under the jurisdiction of GVMC and rest comes under the Bheemili municipality. The study area is a part of Visakhapatnam and Bheemili municipalities of Visakhapatnam district of Andhra Pradesh (Fig. 1).

The study is confined to recent expansion of four lane roads connecting between Visakhapatnam to Bheemili. The road laid adjacent to the sea coast of Bay of Bengal, and it is under the natural vagaries of sea coast on one side and land and its natural activities on the other side render the road vulnerable. Recently, IT Parks, Rama Naidu Cinema Studio, several resorts and urban built up come into existence. This anthropogenic activities has altered the topography along the road system. The major important places located enroute of this road are Rushikonda, Bojjannakonda, Erramattidibbalu, etc. Apart from natural and historical importances, INS Kalinga as Indian Navy is established adjacent to this road. Traffic load is increasing year after year. In view of the traffic load recent road expansion has been taken up in place of old road network. This activity has led to cutting of hill flanks, foothills, sea sand dunes, culverts, drainages and highly denuded land forms etc. Hence, this topic has been taken up to study the soil creep, rock creep, solifluction, land slips, landslides, tidal action and beach erosion along the Bhimili road.

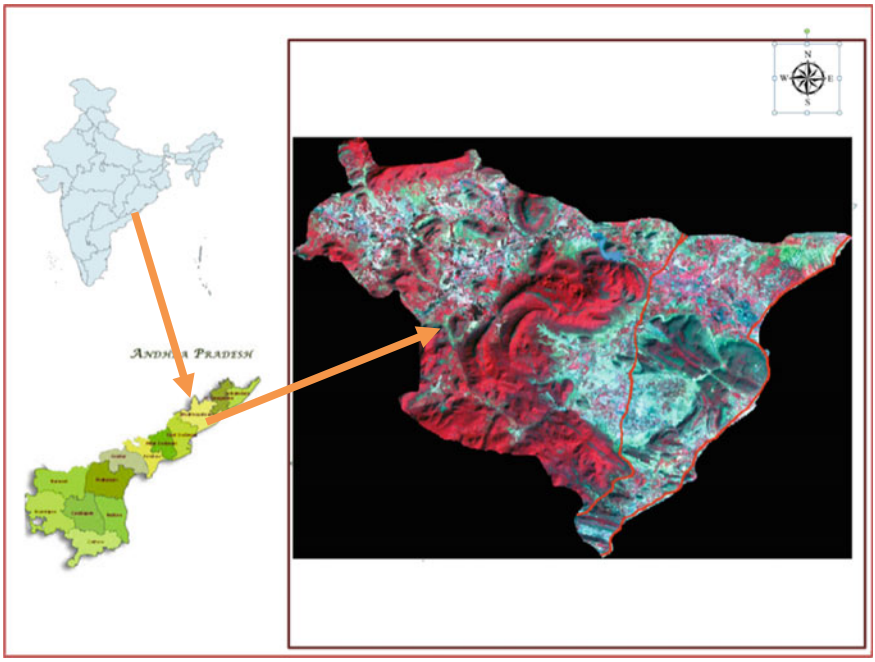

Fig. 1 Location map of the study area

3 Methodology

Maps have been utilized for better organization, income gathering, and so forth for a huge number of years. Be that as it may, it is just inside the most recent couple of decades that the innovation has existed to consolidate maps with PC designs and databases to make Geographic Information Systems or GIS. The subjects in the above realistic are just a little case of the wide exhibit of data that can see or dissect with a GIS. GIS is utilized to show and break down spatial information which are attached to databases. This association is the thing that gives GIS its energy. Maps can be drawn from the database and information can be referenced from the maps. At the point when a database is refreshed, the related guide can be refreshed too. GIS databases incorporate a wide assortment of data including; geographic, social, political, ecological, and statistic. It is evaluated that roughly 80% of all data has a "spatial" or geographic part. So when settling on choices about siting new offices, making climbing trails, ensuring wetlands, coordinating crisis reaction vehicles, assigning memorable neighborhoods or redrawing administrative regions, geology assumes a noteworthy part.

Non-spatial (attribute) data: Attribute data have been generated either at the time of digitization of the polygon/polyline/point feature or after the digitization. All the feature attributes for all the layers have been assigned before the GIS analysis is taken up.

Assignment of weights: Weight values have been assigned depending upon the feature parameter and its importance on assessment of landslide vulnerable zones along the Bhimili road [3]. The output maps generated in the intersection were

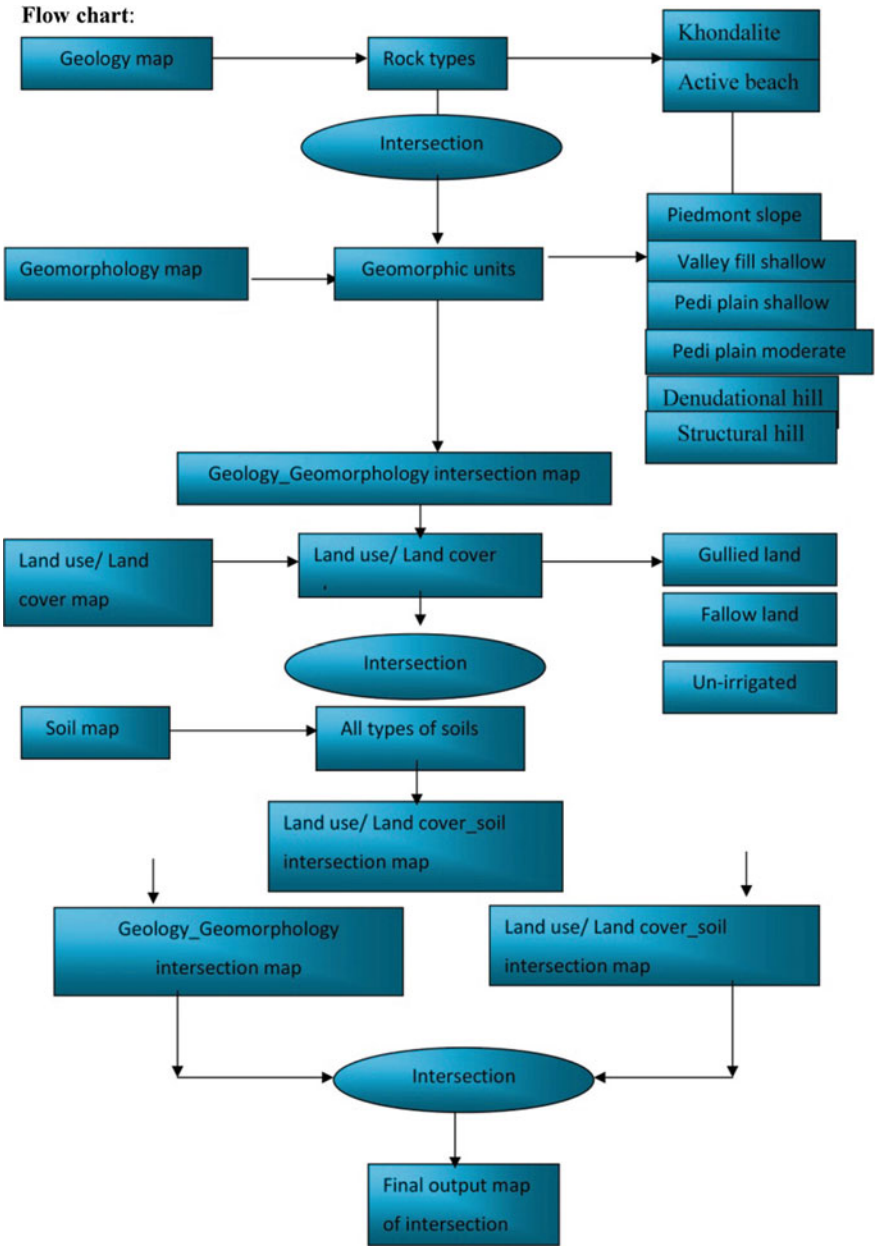

Fig. 2 Methodology adopted for landslides vulnerable zones along the Bhimili road

again intersected with the features to obtain the final output of erosion zones in the study area.

Integration of thematic layers: In this study, geology, soil, geomorphology, land use/land cover and slope thematic layers have been used in GIS analysis. Toposheets have been used for digitization of drainage pattern of the area. Onscreen digitization has been carried out and assigned stream orders (Fig. 2).

4 Results and Discussions

4.1 GIS Analysis

GIS with its capability of map overlaying, reclassification, proximity analysis, and other mathematical operations is used in carrying out criteria based analysis. Thematic layers are overlayed in GIS environment to locate land slide\soil creep zones. Weights have been assigned to geology, geomorphology, land use/land cover and soil. Using Analysis tool in ArcToolbox, intersection was performed to

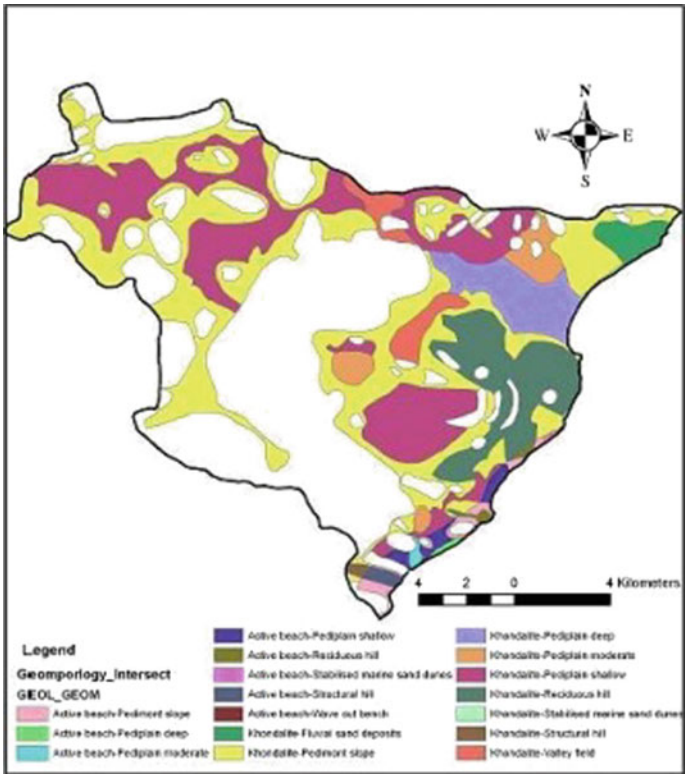

Fig. 3 Intersection map of geology and geomorphology

geology and geomorphology. The combined output is further assigned weightage and intersected with land use/land cover and soil map to locate landslide vulnerable zones along the Bhimili road.

4.2 Integration of Results

Thematic maps of geomorphology, geology, land use/land cover and soil were prepared and overlayed after assigning non-spatial (attribute) data and weightage factors to each theme. The values of weight age factor ranges from 0 to 10 and these have been assigned on the basis of landslide prone characteristics. The GIS analysis was carried out in ArcToolbox (Extension of ArcGIS-10.3) environment. The final output is generated after successful execution shows the landslide zones are about 62 km^2 area (Figs. 3 and 4).

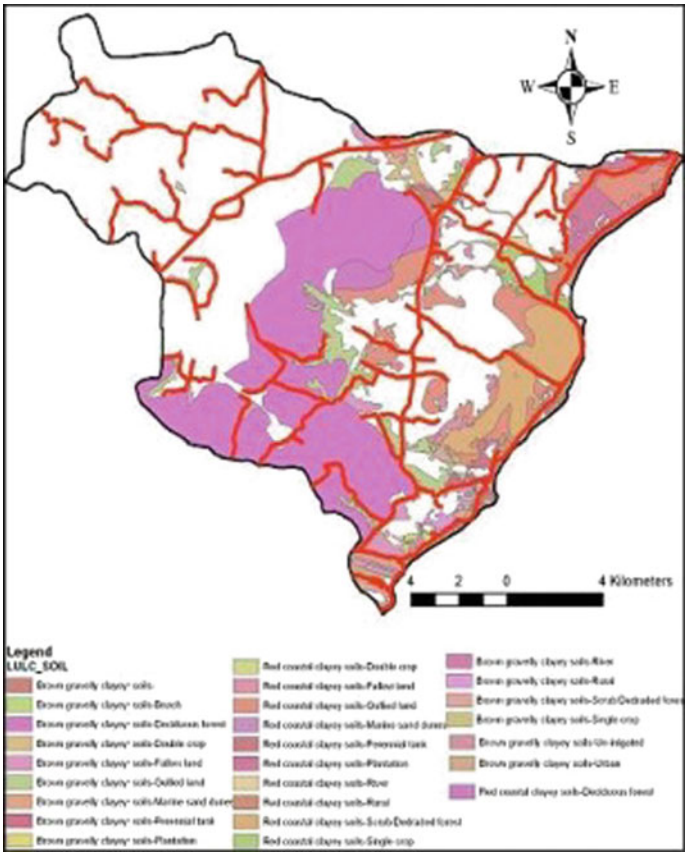

Fig. 4 Intersection map of soil and land use/land cover

5 Conclusions and Future Scope

Thematic layers are overlayed in GIS environment to locate erosion zones. Weights have been assigned to geology, geomorphology, land use/land cover and soil. Using Analysis tool in Arc Toolbox, intersection was performed to geology and geomorphology. The combined output is further assigned weightage and intersected with land use/land cover and soil map to locate soil erosion zones. The values of weightage factor ranges from 0 to 10 and these have been assigned on the basis of erosion characteristics. The GIS analysis was carried out in ArcToolbox (Extension of ArcGIS-10.3) environment. The final output is generated after successful execution shows the landslide zones are about 62 km^2 area. Landslides appear almost associated with developed area around the hill areas. Such as drainage, soil, geology, land use and land cover and slope reveals that the road has been constructed along foothills, marine sand dunes and bad land topography. The existing road has been widened removing a small part of Kailasagiri hill at Thenneti Park, is liable to slide as landslide. Soil creep and slump are the major issues near Rama Naidu Cinema Studios. The road is connecting bad lands popularly known as Erramatti Dibbalu, where soil erosion is more prominent and getting deposited on road leads to skidding of two wheelers. A huge marine sand dune deposited on both sides of the road near INS Kalinga. Resorts, educational institutions and fishermen colonies are the major land use, whereas, thick vegetated hills are the major land cover. The road crosses over small streams where culverts and bridges were constructed. The study has identified landslides vulnerable zones and suggested mitigation measures.

References

1. Sriramadas, A.: Structural geography of the Eastern Ghats in parts of Visakhapatnam and Srikakulam districts, Andhra Pradesh, India. In: Proceedings of XXII International Geological Congress India, Part X, pp. 245–251 (1964)
2. Chetty, M., Buyya, R.: Weaving computational grids: how analogous are they with electrical grids? Comp. Sci. Eng. **4**(4), 61–71 (2002)
3. Jagadeeswara Rao, P., Brinda, V., Suryaprakasa Rao, B., Harikrishna, P.: Determination of landfill destinations for strong waste administration in and around Visakhapatnam City-A GIS approach. Asian J. Geoinf. **7**(3), 35–41 (2007)
4. Singh, I.J., Moharir, S.: Forest management using remote sensing and GIS in Barbatpur range, Betul forest division. J. Indian Soc. Remote Sens. **31**(3), 149–156 (2003)
5. Mani, P., Kumar, R., Chatterjee, C.: Erosion study of a part of Majuli river-Island using remote sensing data. J. Indian Soc. Remote Sens. **31**(1), 12–18 (2003)
6. Shirley, M.D., Landgrebe, D.A., Phillips, T.L., Swain, P.H., Hoffer, R.M., Lindenlaub, J.C., Silva, L.F.: Remote sensing: the quantitative approach, p. 405. McGraw-Hill International Book Co., New York (1978)
7. Swain, P.H., Davis, S.M.: Remote sensing: the quantitative approach. McGraw Hill Book Company, New York, 396p (1978)

Chapter 47
GIS Science for Monitoring of the Health & Emergency Services During Disaster in Tribal Area, East Godavari, Andhra Pradesh, India

Suribabu Boyidi, G. Jaisankar, T. Sridevi, B. Ravi Kumar, K. M. Ganesh, N. C. Anil, U. Sailaja, Rehanaz Sheik, Tulli C. S. Rao and K. Ananda Ratna Kumar

Abstract GIScience for monitoring of the health and emergency services during disaster in tribal area is an important issue in now a days. The habitation in the study area is Monitoring of Disaster, health and all emergency services can be extended to the population in an effective manner for emergency health services in, the during disaster. The road network map along with the locations of habitations and master table information are the main inputs of modules. The input data is fine tuned as per the requirements as Arc GIS 10.3 standards and network analyst module is used to get the final out puts and reports. The output report includes travel time from one destination to another and route length. The calendar for covering the study area is generated by integrating the travel time and health and all emergency services at each Health Habitation.

Keywords Medical GIS · Habitation · Remote sensing · Health monitoring Disaster · Arc GIS · ERDAS

S. Boyidi (✉) · G. Jaisankar · T. Sridevi · B. Ravi Kumar · U. Sailaja
R. Sheik · T. C. S. Rao · K. Ananda Ratna Kumar
Department of Geo-Engineering, Andhra University, Visakhapatnam, India
e-mail: suri.sri2008@gmail.com

G. Jaisankar
e-mail: jaisankar.gummapu@yahoo.com

T. Sridevi
e-mail: srice2001@gmail.com

B. Ravi Kumar
e-mail: bravikumar.rkb@gmail.com

U. Sailaja
e-mail: sailaja.ustala@gmail.com

R. Sheik
e-mail: sk.rehanaz1028@gmail.com

P. J. Rao et al. (eds.), *Proceedings of International Conference on Remote Sensing for Disaster Management*, Springer Series in Geomechanics and Geoengineering,
https://doi.org/10.1007/978-3-319-77276-9_47

1 Introduction

Disasters have proved to be an enormous challenge to most of in the study area of east Godavari tribal continent. The challenges extend also into the fact that modern or current technological trends have not been put to use for an effective management of such disasters. One other factor is the poor management or underutilization of the infra structures roads available. Others, such as unplanned and unregulated land use, urbanization, poor enforcement of building standards, and other development-linked factors increase the vulnerability of the population and infrastructure, making the situation even more disturbing.

2 Study Area

Tribal area of East Godavari district is considered as a pilot area for preparing the module [1]. The study area is a part of Addateegala, Gangavaram, Y. Ramavaram, Rajavommangi, Rampachodavaram, Devipatnam, Maredumilli, Yatapaka, Kunavaram, VRPuram, Chinturu of eleven Mandals including recently added mandals of East Godavari of Andhra Pradesh, which covered by 4 CHNC, 1 AH. It has 18 No's of PHC, 95 sub centers, 9 No's of Ambulances (108), 14 No's of Police Stations, One Fire Station and 829 habitations covering of Total population is 349,919. This area is the border of Telangana, Chuttheesgud and Odisha states and one district of Vishakhapatnam (Fig. 1).

3 Methodology

Introduction to Geographical Information System (GIS) is a "PC framework for catching, overseeing, coordinating, control, breaking down and showing information which is spatially Reference to the Earth". What is recognizes GIS from

T. C. S. Rao
e-mail: gistcs@gmail.com

K. Ananda Ratna Kumar
e-mail: k.anandratnakumar@gmail.com

K. M. Ganesh
SRKR, Bhimavaram, India
e-mail: meharganesh.k6@gmail.com

N. C. Anil
SITAM, Visakhapatnam, India
e-mail: nathianil@gmail.com

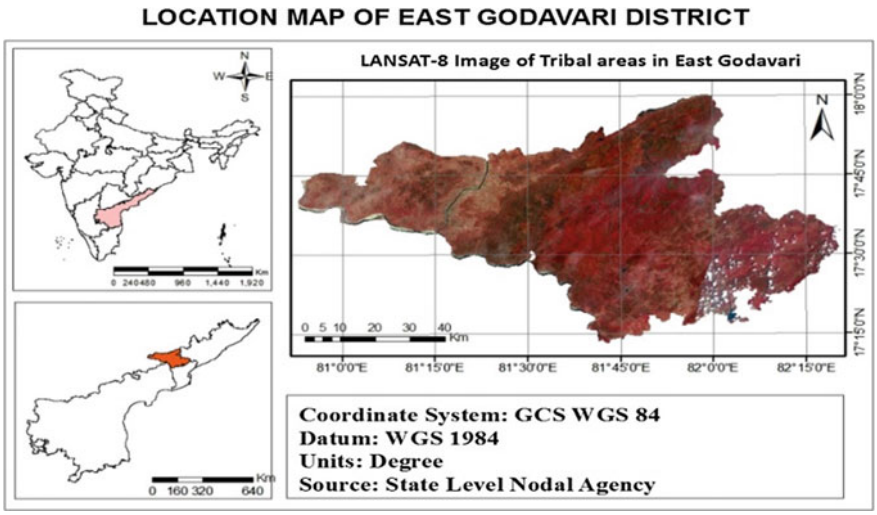

Fig. 1 Location map of the study area

different types of development framework, for example database and spreadsheets is that GIS manages spatial data. GIS has the ability to relate layers of information for a similar point in space joining dissecting lastly, mapping out to the results. In expansive terms, Land Data Framework could be characterized as a PC based device for mapping and breaking down things that exists and occasions that occur on earth. GIS innovation coordinates regular database operations, recognize GIS from other data framework and make it significant to an extensive variety of open and private endeavors. Road network and shape file of study area PHC, CHC, PS, FS, Ambulances and habitations Spatial Database is used to monitor during disaster or any other emergency service in this area.

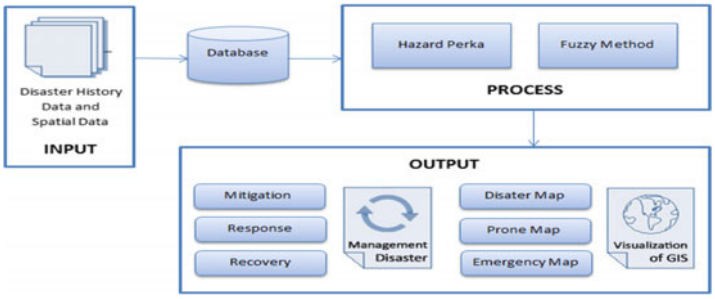

4 Component of GIS

Functional elements that make GIS operations are hardware, software, data, people and a method where hardware is the computer on which GIS operates. Today GIS software runs on a wide range of hardware types, from Administrative central system servers to desktop computers used in stand-alone or network (internet or intranet) configurations. In the above GIS Tribal Area 11 Mandals.xls table PHC Head Quarters are defined. The GIS_Tribal Area 11 Mandals.xls table contains records which are separated and given name as SC. Software of course provides functions and tools necessary to store, analyze and display geographic information.

Natural Disasters: (1) Floods, (2) Cyclones, (3) Forest fires, (4) Landslides, (5) Drought, (6) Spread of epidemics, (7) Earth quakes, (8) Severe wind storms, (9) Snow or ice storms, (10) Severe extreme in temperature.
Data Inputs: The following are the inputs, Shape file of Habitation.
Data base table: GIS Tribal Area of Two Revenue division's xls. CHNC, PHC, SC, Fire station, Police station and Ambulance Data.

Shape file of Road, Tribal Area 11 Mandal Boundary,

The following codes are generated and added to the Master table and Shape File Generate

SC_Code	Sub Center code
PHC_Code	Primary Health Center Code
CHNC_Code	Central Health and Nursing Clustering code
SC_HQ	Sub center Head Quarters
PHC_HQ	Primary Health Center Head quarter
CHNC_HQ	Central Health and Nursing Clustering Head Quarter
PS_HQ	Police Station Head Quarter
FS_HQ	Fire Station Head Quarter
Amb_HQ	Ambulance (108) Location Head Quarter

Creating shape file for Central Health and Nursing Clustering Primary Health Centers, and Sub Centers.

In the above GIS_Study Area 11 Mandals table CHNC head Quarters are defined. Thus GIS 11 Mandals table. These 4 CHNC records are separated and given name_CHNC. It is linked to the GIS_Tribal Area 11 Mandals file, these row tables joined with reference to Habitation codes. After joining the shape (GIS_Tribal Area 11 Mandals_CHNC) file is exported to the same locations. Thus a shape files (GIS_Tribal Area 11 Mandals_CHNC) with rows is created which represent the CHNC (Central Health and nursing clustering) shape file. These 18 PHC records are separated and given name PHC. It is linked to the GIS_Tribal Area 11 Mandals shape file by joining with reference to Habitation code. After joining the shape (11 Mandals_PHC) file it is exported to the same location. Thus a shape files(11 Mandals_PHC) with rows is created which represents the PHC (Primary

Health Center) shape file. In the above GIS Tribal Area 11 Mandals.xls table PHC Head Quarters are defined.

Web GIS: One of the current progress in GIS innovation is online GIS. Well being information is put away in a local server which can be gotten to from different terminals associated with the server through web or intranet. Factual and epidemiological and disaster monitoring techniques should be created to ensure singular privacy while getting to information [2]. Web based GIS innovation dispenses with the customary technique for stream of data and data is in a split second accessible over the globe. Dynamic maps distributed on the web enable patients to find the most advantageous administrations to their home and habitation or work easily. Ref. [3] distance of a CHC, PHC, PS, FS, and area covered by a particular health and disaster program.

Applications of GIS in Health

GIS is being utilized by general wellbeing executives and experts, including strategy creators, analysts, disease transmission specialists, provincial and region medicinal officers [4]. Some of its applications in general wellbeing are said underneath: (1) Analyze spatial and temporal trends. (2) Identify gaps in immunizations. (3) Map populations at risk and stratify risk factors. (4) Document health care needs of a community and assess resource allocations. (5) Plan and target interventions. (6) Manage patient care environments, materials, supplies and human resources. (7) Monitor the utilization of health centers. (8) Route health workers, equipments and supplies to service locations. (9) Publish health information using maps on the Internet. (10) Locate the nearest health facility [5].

5 Analysis

Topology: Create personal geo database (Network) in this data and create the new feature dataset. These feature dataset is imported to the road network arc shape file, right click feature dataset select the new topology and click on all next buttons, tick mark on the road shape file and click next button in this add two rules they are (1) Must not overlap and (2) must be single part. These rules are added then build the topology is built.

Creating the Network Dataset: Start the ARC Catalog and create a personal geodetic base. In this data base create the feature dataset these feature dataset import to the feature class give a file name (road shape file name, these road shape file must be apply to the clean and topology) and give output file name. Select the feature dataset and right click new network dataset then build the network dataset. Select the network dataset properties go to direction and click direction and apply properties to the following [1].

Network Analysis: GIS gives the capacity to rapidly get to the geo statistic flow of an association current administration zone as opposed to the possible interest for administrations at another area [6]. It can distinguish catchment territories of well being focus and further more find appropriate site for another well being office [7]. Effective monitoring administrations conveyed at home can be planned for a more proficient way by investigating transportation components and road designs, and by suggesting the most productive route. GIS Provides convenient data about where well being administrations are found and guidelines and maps on the best way to arrive (Table 1; Fig. 2).

6 Output and Results

The output of the above Monitoring module is as follows

Generation of codes and headquarter names and added to the master table, the final master table i.e., GIS_Tribal Area 11 Mandals contains 4 No's of CHNC, 18 No's of PHC, 95 No's of SC, 14 No's of Police stations, 9 No's of Ambulance (108) Location, One Fire Station and 829 Habitations. A master table generation showing the details of HABCODE, DMVCODE, DNAME, MNAME, VNAME, HNAME, Population, NAME_SC, CODE_SC, SC_DIST_HAB, NAME_PIC, CODE_PHC, PHC_DIST_SC, NAME_CHNCS, CODE_CHNCS, DIST_PHC, CHNC_HQ, PHC_HQ, SC_HQ, PS_HQ,FS_HQ, Amb_HQ and WAIT_TIME. Service time, start time and end time is generated, wait time (field) used Minutes at the time load location then generate the service time. Generation of Road Network layer using SHAPE FILES OF AH, CHNC, PHC, SC and Habitations: Open the network analysis window, Click new route then generate the new layer.

Table 1 Location analytics of emergency services of study area [8]

Name of the mandal	Mandal code	Area Hospital	CHNC	PHC	108 Ambulance	Police Station Total PS	Fire station
Addateegala	4		CHNC ADT	Duppulapalem, Yellavaram 2	Amb Adt (108)	Addatigala, PS Durccharthy 2	
Y.Ramavaram	3		CHNC YRM	Chavitidibbalu, Gurthedu, Mangampadu 3	Amb YRVM	YRamavaram, Donkarai 2	
Maredumilli	1			Maredumilli, Boduluru 2	Amb MRM	Maredumilli 1	
Gangavaram	10			Gangavaram, C Pidathamamidi 2	Location GGRM	Gangavaram 1	
Rampa Chodavarm	11	AH RCVaram		Narsapuram, Geddada, C Vadapa 3	Location RCVaram	RamapaChodavaram 1	Fire Station RCVaram
Devipatnam	2			Devipatnam, Indukurupeta, Konadamodalu 3		Devipatnam 1	
Yatapaka (Nellipaka)	61			Nellipaka, Laxmipuram, Gouridevipeta 3	Location Yatapaka	Yatapaka,	
Kunavaram	63		CHNC Kunavaram	Kuturu 1	Kunavaram	Kunavaram 1	
Chintoor	62		CHNC Chintoor	Tulasipaka, Edugurallapalli 2	Chintoor	PS Chintoor 1	
VeeravaraPuram	64			Rekhapally, Jeeduguppa 2		PS VRPuram 1	
Rajavommangi	5			Rajavommangi, Lagarai, Zaddangi 3	Amb RJVM	Rajavommangi, PSZaddangi2	
Total	–	1	4	18	9	14	1

(continued)

Table 1 (continued)

Name of the mandal	No. of villages	No. of Panchathies	No. of households	Study area (km^2)	Population male	Population female	Total Population
Name of the mandal	No. of villages	No. of Panchathies	No. of households	Study area (km^2)	Population male	Population female	Total Population
Addateegala	99	22	10,811	540	18,686	18,555	37,241
Y.Ramavaram		17	7418	773	13,757	14,857	28,614
Maredumilli	71	12	4801	914	10,166	9341	19,507
Gangavaram	60	17	7550	613	12,393	13,519	25,912
Rampa Chodavarm	77	19	10,554	610	19,185	20,166	39,351
Devipatnam	46	14	8711	517	13,669	14,509	28,178
Yatapaka (Nellipaka)	70	21	100,811	364	19,195	19,766	38,961
Kunavaram	56	16	7726	204	12,351	13,894	26,245
Chintoor	89	15	100,925	955	19,899	20,826	40,725
VeeravaraPuram	62	11	7361	475	12,171	13,426	25,597
Rajavommangi	62	19	11,168	613	19,102	20,480	39,582
Total	829	183	97,836	6431.63	170,574	179,339	349,913

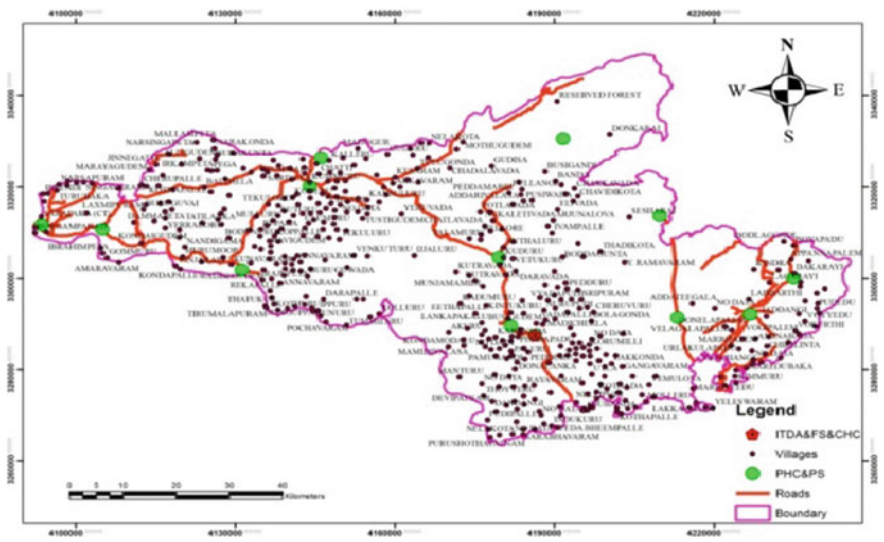

Fig. 2 Locations of emergency services in the study area

7 Conclusion

A."GIScience for Monitoring of the Health & Emergency Services during disaster in tribal area, East Godavari, Andhra Pradesh, India" has been evolved for Rampa Chodavaram Area Hospital(AH) and 4 CHNC of study area using the Network Analyst program in the ARC GIS software. A calendar showing the coverage of population spread over **829** habitations in the above 4 CHNC with **18** PHC's and **95** sub centers. The habitations under the Sub Centers are identified in a rational way keeping in view of the population, treatment time and the distance between the habitations and the respective PHC, SC and CHNC. The total time coverage has come to the Ramp Chadavaram AH. GIS aids in faster and better monitoring of health mapping and analysis than the conventional methods. It gives well being experts fast and simple access to expansive volumes of information. It gives an assortment of Dynamic investigation devices and show systems for observing and administration of calamity. The potential outcomes that can be investigated are boundless, contingent upon the expertise and innovative utilization of the scientists and the readiness of well being division administration to asset its usage. Wellbeing executives, experts and scientists require preparing and client in GIS innovation, information and epidemiological and disaster monitors techniques in order to use GIS properly and effectively.

8 Recommendations

Online Tracking of Vehicle with GPS: GPS (Global Positioning System) is a system of Earth-orbiting satellites, each providing precise time and position information which enables GPS receiving devices to compute position on the earth. Signals must be received from at least satellites in order to establish the receiver's position in latitude (or a national coordinate system provided with the equipment). GPS configuration consists of three parts: (1) Twenty-four HRS Navy satellite orbiting the earth. (2) Portable mobile receiver (aerial plus portable console). (3) Base station receiver positioned at a known geographical position, in order to perform the differential correction of the raw satellite signals.
Information with SMS Facility: The villages in the Habitations can be provided with SMS information about coverage of the sub centers/Habitations along with data and time. Necessary SMS action can also be sent to village centers before starting to the particular village which facilitates the effective organizing of the village camps. Also the information regarding the coverage of the villages can be sent to concerned CHNC, PHC, PS, FS, AMB, SC and authorities.
Travel Routes with Alternative: When road network is affected by problem of Rain Accident, Heavy Traffic then Dynamic new road network can be generated and the updated alternative road network maps can be sent to all sub centers and primary health centers which makes it easy to travel any emergency service [9].
Online access to monitoring system: NET (Network Enable Technology/Network Extended Technology) can be used to make the above module accessible to the implementation officers at CHNC's who can run the network analysis by themselves and can fix the tentative calendars to cover the CHNC's.

References

1. Srivastava, A., Nagpal, B.N.: Mapping malaria. Predictive habitat modelling for forest malaria vector species An. dirus in India–A GIS-based approach. Curr. Sci. **80**(9), 1129–1134 (10 May 2001) Association Stable http://www.jstor.org
2. Richards, T.B., Corner, C.M., Rushton, G., Brown, C.K., Fowler, L.: Geographic information systems and public health mapping the future. Public Health Rep. **114**(359), 373 (1999)
3. Map India 2001 Conference, New Delhi, Feb 2001
4. Weekly Epidemiological Record: Geographical Information Systems (GIS): Mapping for Epidemiological Surveillance. Vol. 74, no. 34, pp. 281–285. WHO, Geneva (1999)
5. Comer, D.E.: Computer Networks and Internet, ISBN-13: 978-0136061274,ISBN-10: 0136066984
6. ESRI White Paper, Enterprise GIS in health and social service agencies (1999)
7. Tanenbaum, A.S.: Computer Network. Prentice-Hall, New Jersey
8. Janmabhoomi directory of habitations and Municipal wards in the state, finance & planning department government of Andhra Pradesh, Hyderabad, July 1998

9. Burrough, P.A.: Principals of Geographic Information System Land Resources Assessments. Clarinda Press, Oxford (1986)
10. Anderson, J.R., Hardy, E.E., Roach, J.T., Witmer, R.E.: A Land use and land cover classification for use with remote sensor data. Geol. Surv. (1976)
11. http://www.cisco.com/public/support/tac/documentation.html
12. http://www.redhat.com/docs
13. http://home.iitk.ac.in/∼navi/sidbinetworkcourse
14. Douglas E.Comer,Computer Networks and Internet,Published in Pearson Prentice Hall

Chapter 48
Inventory and Monitoring of Glacial Lakes in Himalayan Region Using Geo Spatial Technologies

P. Satyanarayana, E. Siva Shankar, E. Amminedu and N. Victor Babu

Abstract The glaciers consist of a huge amount of perpetual snow and ice and are found to create many glacial lakes. Abrupt release of large amounts of stored water in these lakes results in a catastrophic outburst flood. Several such incidents of flash floods were reported all over the world and also in Himalayas region of India causing huge economic losses. To mitigate the impact of these types of events, prior knowledge about the location, the areal extent and the volume of these lakes is very essential. The location of these glacial lakes in rugged and remote terrain makes it difficult to monitor them manually. Remote sensing plays a vital role in creating inventories and monitoring of the glacial lakes quickly and accurately due to wider coverage and repetivity. The satellite images provide greater details for the evaluation of physical conditions of the area. This paper discusses a case study on the inventory and monitoring of glacial lakes or water bodies in Sutlej basin using satellite remote sensing. The study area is Sutlej basin from its origin to Bhakra dam situated in Western Himalayas. This basin is highly rugged terrain with abundant natural water resource in the form of snow pack and glacial lakes. The Inventory of glacial lakes or water bodies was done using Indian Remote Sensing LISS-III data and monitoring using AWiFS data. A total of 197 lakes or water bodies have been identified whose water spread area is greater than 2 ha. 40 lakes with area greater than 10 ha were monitored during June–August 2007. The change in water spread area statistics was observed in 23 lakes with a variation of greater than ±10%.

P. Satyanarayana (✉) · E. Siva Shankar
National Remote Sensing Centre, ISRO, Balanagar, Hyderabad 500 037, India
e-mail: satyanarayana_p@nrsc.gov.in

E. Siva Shankar
e-mail: sivasankar_e@nrsc.gov.in

E. Amminedu · N. Victor Babu
Department of Geo-Engineering, Andhra University College of Engineering, Visakhapatnam, India
e-mail: eamminedu@gmail.com

N. Victor Babu
e-mail: neelavictorbabu@gmail.com

P. J. Rao et al. (eds.), *Proceedings of International Conference on Remote Sensing for Disaster Management*, Springer Series in Geomechanics and Geoengineering,
https://doi.org/10.1007/978-3-319-77276-9_48

Keywords Glaciers · GLOF · IRS · DEM · AWIFS · LISS-III

1 Introduction

Ice in the form of Glaciers is the largest reservoir of fresh water on Earth, and second only to oceans as the largest reservoir of total water. Glaciers cover vast areas of Polar Regions but are restricted to the highest mountains in the tropics. Glaciers are large masses of snow, re-crystallized ice and rock debris that accumulate in great quantities and begin to flow slowly downwards under the pressure of their own weight. Several elements contribute to glacier formation and growth. Figure 1 shows the various zones of a glacier. Accumulation zone is the area, usually the part of the glacier with the highest elevation where snow fall accumulates, adding to the glacier's mass. As the snow slowly accumulates and turns to ice, the glacier increases in weight, forcing glacial movement. Further down the glacier is the ablation area, where most of the melting and evaporation occur. Between these two areas a balance is reached, where snowfall equals snowmelt. Here, the glacier is in equilibrium (firm line). Whenever this equilibrium is disturbed, either by increased snowfall or by excessive melting, the glacier either retreats or advances at more than its normal pace. Glaciers form when yearly snowfall in a region far exceeds the amount of snow and ice that melts in a given summer. In this way, massive quantities of snow accumulate in relatively small periods of geologic time.

A retreating glacier often leaves sections of ice behind which will melt to create glacial lakes. A glacial lake is defined as water mass existing in a sufficient amount and extending with a free surface beside and/or in front of a glacier and originated by glacier activities and/or retreating processes of a glacier. These lakes are often found surrounded by drumlins, along with other evidence of the glacier, such as moraines,

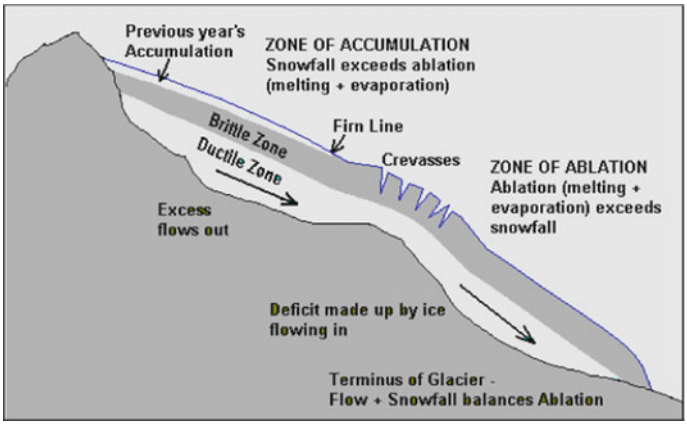

Fig. 1 Different zones of glacier

eskers and erosional features such striations and chatter marks. There are 500 million inhabitants of the Indus, Ganges and Brahmaputra river basins, who rely on the perennial supply of melt-water from the Himalayas [4]. Glacial hazards like glacier ice falls, glacier surges, catastrophic debris flows and glacial lake outburst floods (GLOF) are some of the phenomenon that affects vulnerable settlements downstream the main valleys of this region. Periodic or occasional release of large amounts of stored water in a catastrophic outburst flood is widely referred to as a jokulhlaup (Iceland), or a Glacial Lake Outburst Flood (GLOF) (Himalaya). A jokulhlaup is an outburst, which may be associated with volcanic activity, and a GLOF is a catastrophic discharge of water under pressure from a glacier. A huge displacement wave generated by rockslide or a snow/ice avalanche from the glacier terminus into the lake may cause the water to top the moraines and create a large breach that eventually causes dam failure [3]. Different mechanisms that triggers these events are melting ice cores in the moraines, increasing lake water level and related hydrostatic pressure, groundwater undercurrents and erosion and sudden mass movements into the lakes can lead to a dam burst, discharging millions of cubic meters of water and debris mixture. These GLOFs are highly destructive in nature and lead to long-term environmental degradation and to a high socio-economic loss.

1.1 Remote Sensing and Implication on Glacier Studies

Glaciers and glacial lakes are generally located in remote areas, where access is through tough and difficult terrain. The Inventory of glacial lakes using conventional methods requires extensive time and resources together with undergoing hardship in the field. This is especially true that for most of the high-alpine areas of the Himalayas are inhospitable. Satellite remote sensing due to its synoptic coverage and high repetivity plays a crucial role in creating inventories and monitoring of the glacial lakes quickly and accurately. Successive satellite images over an area constitute time series of satellite imagery leading to a better understanding of glacier retreat and glacial lake formation. Use of these satellite images and aerial photographs for the evaluation of physical conditions of the area provides greater accuracy. Enhanced satellite images draped over Digital Elevation Models (DEM) are highly useful to provide an insight to morphological, glaciological and geomorphological features. For a sound definition of hazard scenarios the interpretation of satellite images and DEMs must always be integrated. Digital image analysis techniques are very useful for the quicker study of glacier, glacial lakes. Presently a constellation of 6 Indian Remote Sensing (IRS) satellites viz. IRS-1C, IRS-1D, IRS-P4, IRS-P6, Cartosat-1 and Cartosat-2 are available for natural resource mapping and monitoring. The Linear Imaging Self Scanning (LISS-III) sensor with a spatial resolution of 23.5 m on IRS-1C, 1D and P6 has a ground swath of 141 km. Advanced Wide Field Sensor (AWIFS) sensor on board IRS-P6 with 56 m resolution and swath of 740 km has a revisit frequency of 5 days. AWiFS sensor is highly suitable for monitoring of glacial lakes due to high

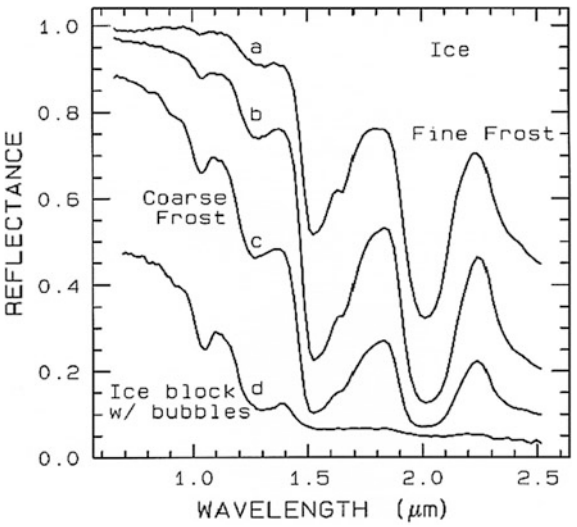

Fig. 2 Spectral reflectance curves of different forms of Ice

receptivity and reasonable spatial resolution. With the availability of more spectral bands it is now possible to differentiate snow and cloud easily in the middle infrared portion of the spectrum, particularly in the 1.55–1.70 μm wavelength band. In this wavelength, the clouds have a very high reflectance and appear white on the image, while the snow has a very low reflectance and appears black on the image. In the visible, infrared bands the spectral discrimination between snow and clouds is not possible, while in the middle infrared it is possible. The reflectance of snow is generally very high in the visible portions and decreases throughout the reflective infrared portions of the spectrum (Fig. 2).

International Centre for Integrated Mountain Development (ICIMOD) developed spatial and attribute database of the glaciers and glacial lakes of whole Nepal in 2001 using remote sensing and geographic information systems techniques. Bajracharya et al. [1] reported that there are altogether 3252 glaciers covering an area of 5322 km^2. Huggel et al. [2] assessed the hazards due to glacial lake outbursts using remote sensing in the Swiss Alps. The observations from an outburst event from a moraine-dammed lake in the Swiss Alps showed the basic applicability of the proposed techniques and they had recommended a systematic application of remote sensing based methods for glacier lake hazard assessment.

2 Case Study

Inventory mapping and monitoring of glacial lakes or water bodies using satellite remote sensing was discussed here with a case study of Satluj Jal Vidyut Nigam Ltd (SJVNL). Monitoring of glacial lakes with lakes of specified size was carried out for 3 months of June, July and August 2007.

2.1 Study Area and Data Used

The study area is Sutlej basin in Western Himalayas. The river Sutlej is one of the main tributaries of Indus and has its origin near Manasarovar and Rakas lakes in Tibetan plateau at an elevation of about 4500 m. It travels about 300 km in Tibetan plateau in North-Westerly direction and changes direction towards South-West and covers another 320 km (approx.) up to Bhakra gorge where 225 m high straight gravity dam has been constructed. This western Himalayan basin is highly rugged terrain with abundant natural water resource in the form of snow pack The Sutlej basin is geographically located between 30° 00′N, 76° 00′E and 33° 00′N, 82° 00′E. Characteristics of the basin and inaccessibility of the major part of it make remote sensing application ideal for hydrologists to monitor the snow cover information of the region and to make inventory of glacial lakes and water bodies in the basin Fig. 3 shows the location of the study area and 4 sub basins of Sutlej study area.

Most of the area in the present study falls in the inaccessible high mountain region of Himalayas. Hence, the Inventory of glacial lakes/water bodies was done using remote sensing methods. IRS LISS-III and AWiFS data sets were used for inventory mapping and monitoring respectively. About 10 LISS-III scenes are required to cover the entire basin. Browsing of satellite data was done to select the suitable cloud free data over the study area. Table 1 shows the data used for inventory mapping. For glacial lakes identification from the satellite images, the image should be with minimum snow cover and cloud free. Hence, the satellite data during the period Jul–Aug–Sep–Oct were considered. The cloud free/partially cloud free LISS-III images from IRS-P6 satellite were procured during the year 2006. In case of non-availability of cloud free IRS-P6 satellite images for the year 2006, additional LISS-III images from IRS-1D during the year 2005 and 2004 were used.

For Monitoring of lakes browsing was done for all possible AWiFS and LISS-III combinations during June to August 2007. Even partly cloud free satellite data sets were used in the study. Table 2 shows the data used for monitoring study.

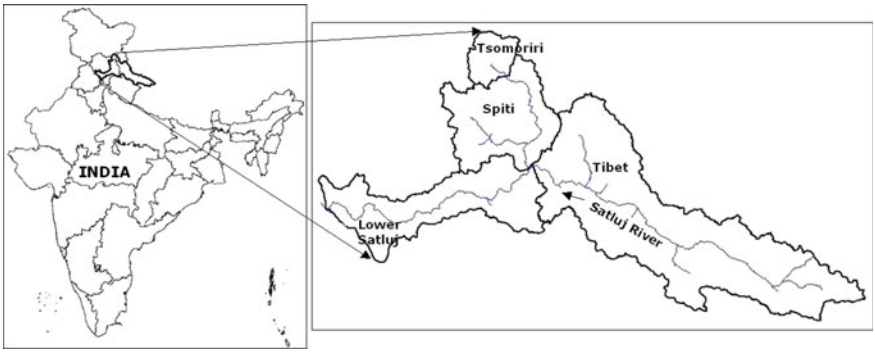

Fig. 3 Location of the study area

Table 1 IRS-P6 satellite data used in the study of inventory mapping

Path–row	Date	Satellite	Sensor
95–48	05 Oct 2006	IRS-P6	LISS-III
95–49	05 Oct 2006	IRS-P6	LISS-III
96–47	10 Oct 2006	IRS-P6	LISS-III
96–48	10 Oct 2006	IRS-P6	LISS-III
96–49	10 Oct 2006	IRS-P6	LISS-III
97–48	02 Sep 2005	IRS-P6	LISS-III
97–49	07 Sep 2004	IRS-P6	LISS-III
98–49	26 Sep 2006	IRS-P6	LISS-III
99–49	01 Oct 2006	IRS-P6	LISS-III
100–49	06 Oct 2006	IRS-P6	LISS-III

Table 2 Satellite data used for monitoring in the study

Date	Path–row	Satellite	Sensor
02 Jun 2007	95–48	IRS-P6	AWiFS
07 Jun 2007	96–48	IRS-P6	AWiFS
12 Jun 2007	97–48	IRS-P6	LISS–III
17 Jun 2007	98–49	IRS-P6	AWiFS
22 Jun 2007	99–49	IRS-P6	AWiFS
27 Jun 2007	100–49	IRS-P6	AWiFS
06 July 2007	97–48	IRS-P6	AWiFS
11 July 2007	98–49	IRS-P6	AWiFS
16 July 2007	99–49	IRS-P6	AWiFS
20 July 2007	95–48	IRS-P6	AWiFS
25 July 2007	96-48	IRS-P6	AWiFS
30 July 2007	97–48	IRS-P6	AWiFS
04 Aug 2007	98–49	IRS-P6	AWiFS
09 Aug 2007	99–49	IRS-P6	AWiFS
14 Aug 2007	100–49	IRS-P6	AWiFS
18 Aug 2007	96–48	IRS-P6	AWiFS
28 Aug 2007	98–49	IRS-P6	AWiFS

2.2 Methodology

Majority of the study area being in Himalayas across international borders, the topographical maps covering the region are not available and the geo-referenced Landsat Thematic Mapper images covering the study area were downloaded from the available Internet resources. The individual image segments are tiled to prepare a reference image covering the whole basin area. With the spatial resolution of LISS-III (23.5 m), the inventory of lakes can be done by identifying lakes of 2 ha or more in area. Each of the LISS-III satellite data sets was individually rectified with the reference image prepared from the downloaded TM data sets. The

geometric rectification was performed using polynomial transformation of third order with resulting Root Mean Square (RMS) error less than one pixel. The rectified IRS LISS-III images were tiled to get a single image covering the entire basin. The Sutlej river basin boundary is superimposed on the satellite image of the basin and the lakes whose areal extent is equal to or greater than 2 ha have been identified and the lake boundaries were digitized using Erdas/Imagine vector module tools. The digitized polygons have been cleaned for open ends and built into a polygon layer. All the polygons have been assigned polygon ID's. The area of the lake was calculated using the digital techniques by counting the number of pixels falling inside the water body polygon. Water spread area is considered to represent the boundary of lake. The geographic latitude and longitude of the center of the lake has been computed using attribute information of the polygon layer. Figure 4 shows the flowchart describing the methodology adopted in this study. The hydro-meteorologically dissimilar regions have been identified and divided into 4 regions namely Spiti, Lower Sutlej, Tibet region and Tsomori regions. The lakes falling in each of the 4 regions of Sutlej basin have been extracted into separate layers. The lakes polygon has been superimposed on Survey of India topo sheet grid of 1:50,000 scale and the lake attributes have been updated with topo sheet reference. The lakes have been numbered based on the region in which they are falling. i.e. All lakes in Spiti region are numbered starting from 1001, Lower Sutlej region starting from 2001, Tibet region starting from 3001 and TsoMori region starting from 4001. Monitoring was carried for glacial lakes with lake area greater than 10 ha in size. With the spatial resolution of AWiFS (56 m) the monitoring of lakes can be done by identifying lakes of 10 ha or more in area. The above mentioned procedure was adopted for the process of procurement of satellite data, geometric rectification and lake area digitization. The lake areas derived using the latest data were compared with the lake area estimated during the inventory study. The comparison was repeated for all the data sets during June to August 2007. There are some lakes which are snow covered and cannot be fully distinguishable in the satellite data. The lakes or waterbodies which are partly snow covered or fully snow covered and could not be distinguishable were not reported (Figs. 5 and 6).

2.3 Results and Discussion

There are 40 glacial lakes/water bodies in Satluj basin whose areal extent is equal to or greater than 10 ha. The areas of these 40 lakes computed from satellite data of June–August 2007, were compared with the areal extent estimated in the inventory study. In the month of June 2007, of the 2 lakes located in spiti region one lake (no. 1017) is under snow cover and a reduction in areal extent is observed in the other lake (no. 1009). Two lakes are located in lower Sutlej region, of which one lake (no. 2007) in snow covered and increase in lake area is observed in other lake (no. 2004). In Tibet region, 34 lakes out of 40 lakes are located. 6 lakes are observed to

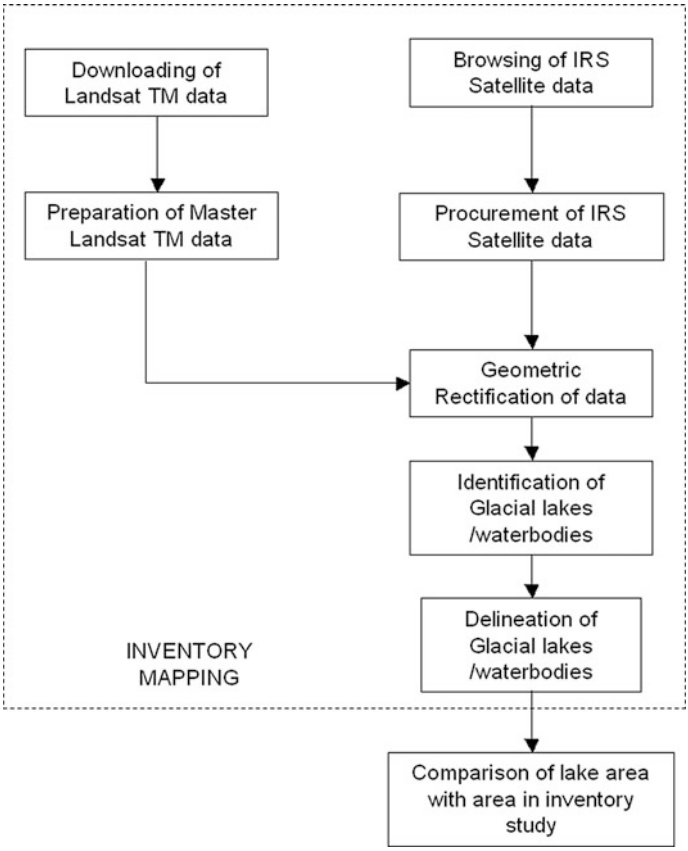

Fig. 4 Flowchart of methodology for inventory mapping and monitoring

be under continuous snow cover. No change is observed in Rakas, Manasarowar and Kongyyu Tsho lakes. Reduction in area is observed in 10 lakes and increase in area is observed in 5 lakes. In 3 lakes no water is observed as these lakes appear to be shallow depressions. 7 lakes are cloud covered and no observation could be made against these lakes. Tsomori region consists of 2 lakes, no change is observed in Tsomori and a reduction in area is observed in another lake (no. 4009). During July 2007, of the two lakes located in Spiti region, increase in areal extent is observed in one lake (no. 1017) and a reduction in areal extent is observed in the other lake (no. 1009). Two lakes are located in lower Sutlej region, of which one lake (no. 2007) in continuously cloud covered and increase in lake area is observed in other lake (no. 2004). In Tibet region, 8 lakes are observed to be under continuous cloud cover and no observation could be made against these lakes. No change is observed in Rakas and Manasarowar lakes. Reduction in area is observed in 10 lakes and increase in area is observed in 12 lakes. In 2 lakes no water spread is observed. In addition to the above 34 lakes in Tibet region, 3 lakes are observed

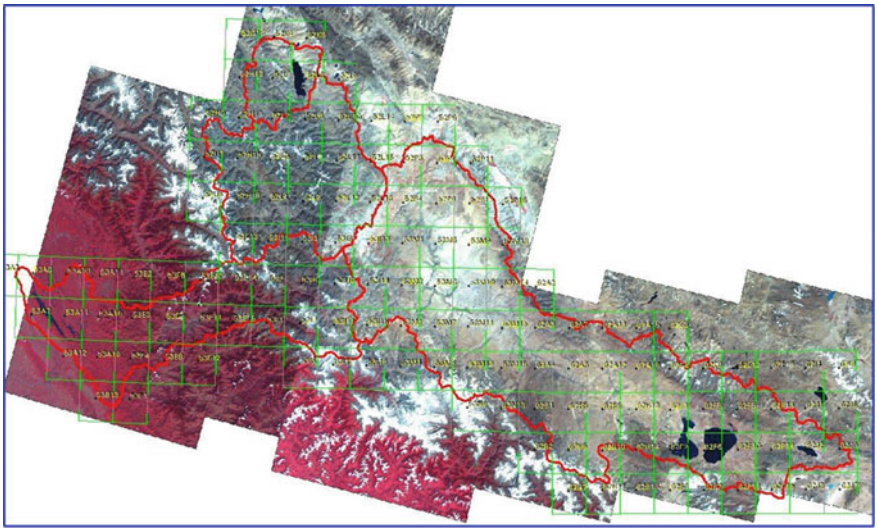

Fig. 5 False colour composite image of Satlej basin

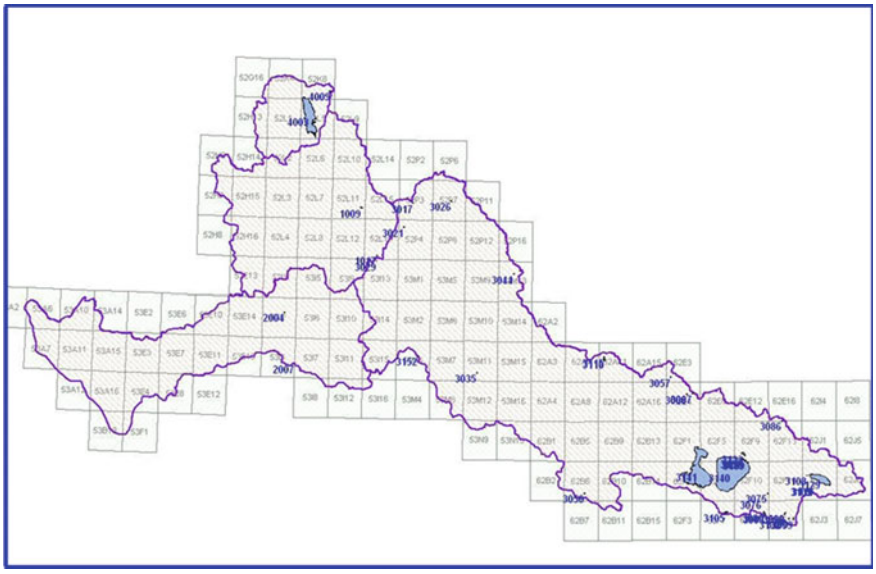

Fig. 6 Glacial lakes/water bodies greater than 10 ha in area in Satlej basin with SOI grid

with lake area greater than 10 ha in the satellite image of 16-July-07. These lakes with lake numbers 3007, 3032 and 3033 have water spread areas 7.73, 4.87 and 7.79 ha respectively in the inventory study report. The water spread area of the lake (no. 3032) again reduced to less than 10 ha in the satellite image of 30-July-07.

Tsomori region consists of 2 lakes, no change is observed in Tsomori and a reduction in area is observed in another lake (no. 4009). In the month of August 2007, of the two lakes located in Spiti region, increase in areal extent was observed in one lake (no. 1017) and a reduction in areal extent was observed in the other lake (no. 1009). Two lakes are located in lower Sutlej region, decrease in areal extent in one lake (no. 2007) was observed and increase in lake area was observed in other lake (no. 2004). In Tibet region, 36 lakes out of 42 lakes are located. 16 lakes are observed to be under continuous cloud cover and no observation could be made against these lakes. Reduction in area was observed in 6 lakes and increase in area was observed in 10 lakes. In 3 lakes no water spread was observed and 1 lake was completely snow covered. Tsomori region consists of 2 lakes, no change was observed in Tsomori and a reduction in area was observed in another lake (no. 4009). Out of total 42 lakes, 16 lakes are cloud covered and no water spread was observed in 3 lakes. The Tsomori lake remain unchanged. The change in area statistics could be observed in 23 lakes. Out of these 23 lakes, in the case of 16 lakes the variation in water spread area was greater than ±10%. Two lakes (no. 3057 and 3083) could not be mapped even once during the period June, July and August due to either snow cover or cloud cover. Lake no. 3033 has increased its size by about 104% (increased from 7.79 to 15.92 ha) whereas lake no. 3116 was completely empty as on 18-Aug-07. Table 3 shows the consolidated statement of status of lakes during June to August 2007.

Table 3 Glaical lakes/waterbodies in Satlej basin

S. No	Lake No	Toposheet No	Area (ha)
1	1001	52H7	4.58
2	1002	52H7	3.71
3	1003	52H7	4.81
4	1004	52H7	11.99
5	1005	52L10	7.63
6	1006	52L10	4.76
7	1007	52L10	2.33
8	1008	52L10	3.69
9	1009	52L11	78.18
10	1010	52L15	6.18
11	1011	52L15	2.17
12	1012	52L16	3.08
13	1013	52L16	2.28
14	1014	52L16	5.39
15	1015	52L16	6.29
16	1016	52L16	3.98
17	1017	52L16	13.60
18	1018	52L16	3.99

(continued)

Table 3 (continued)

S. No	Lake No	Toposheet No	Area (ha)
19	1019	52L3	2.93
20	1020	52L7	2.71
21	1021	52L7	2.60
22	1022	53I5	5.00
23	1023	53I9	3.77
24	2001	53I10	3.18
25	2002	53I10	6.11
26	2003	53I15	2.78
27	2004	53I2	12.20
28	2005	53I7	4.38
29	2006	52L15	4.21
30	2007	52L15	10.04
31	3001	52L15	3.77
32	3002	52L15	5.45
33	3003	52L16	6.18
34	3004	52L16	2.72
35	3005	52L16	2.90
36	3006	52L16	2.75
37	3007	52L16	7.73
38	3008	52L16	8.63
39	3009	52L16	2.57
40	3010	52L16	4.54
41	3011	52L16	4.27
42	3012	52P11	4.11
43	3013	52P12	4.77
44	3014	52P16	2.85
45	3015	52P3	2.43
46	3016	52P3	4.11
47	3017	52P3	11.45
48	3018	52P3	2.92
49	3019	52P3	3.65
50	3020	52P4	6.55
51	3021	52P4	21.47
52	3022	52P4	2.25
53	3023	52P6	2.29
54	3024	52P6	3.81
55	3025	52P7	8.57
56	3026	52P7	20.58
57	3027	52P7	3.25
58	3028	53I10	2.86

(continued)

Table 3 (continued)

S. No	Lake No	Toposheet No	Area (ha)
59	3029	53I13	16.22
60	3030	53I13	3.56
61	3031	53I13	2.79
62	3032	53I13	4.87
63	3033	53I13	7.79
64	3034	53I15	7.36
65	3035	53M11	30.42
66	3036	53M12	3.22
67	3037	53M13	3.19
68	3038	53M13	2.17
69	3039	53M13	8.64
70	3040	53M13	3.77
71	3041	53M13	3.21
72	3042	53M13	4.04
73	3043	53M13	2.35
74	3044	53M13	32.71
75	3045	53M16	2.39
76	3046	53M8	3.41
77	3047	53M8	4.80
78	3048	62B6	2.96
79	3049	62B6	4.66
80	3050	62B6	21.28
81	3051	62E12	7.52
82	3052	62E13	6.30
83	3053	62E13	2.61
84	3054	62E13	3.94
85	3055	62E13	7.53
86	3056	62E3	4.30
87	3057	62E3	11.20
88	3058	62E3	2.71
89	3059	62E3	3.50
90	3060	62E4	6.90
91	3061	62E4	2.96
92	3062	62E4	2.38
93	3063	62E4	3.07
94	3064	62E4	4.11
95	3065	62E4	2.56
96	3066	62E4	7.88
97	3067	62E4	49.55
98	3068	62E4	18.95

(continued)

Table 3 (continued)

S. No	Lake No	Toposheet No	Area (ha)
99	3069	62E4	5.21
100	3070	62E8	7.58
101	3071	62E8	4.94
102	3072	62E8	7.86
103	3073	62E8	3.43
104	3074	62E8	3.58
105	3075	62F10	13.96
106	3076	62F10	13.17
107	3077	62F11	2.26
108	3078	62F11	6.24
109	3079	62F11	6.78
110	3080	62F11	22.78
111	3081	62F11	4.83
112	3082	62F11	2.82
113	3083	62F11	16.20
114	3084	62F11	8.06
115	3085	62F11	3.95
116	3086	62F13	24.04
117	3087	62F13	2.88
118	3088	62F15	2.95
119	3089	62F15	4.06
120	3090	62F15	21.06
121	3091	62F15	3.02
122	3092	62F15	13.57
123	3093	62F15	6.27
124	3094	62F15	6.46
125	3095	62F15	3.51
126	3096	62F15	2.69
127	3097	62F15	8.42
128	3098	62F15	5.40
129	3099	62F15	43.76
130	3100	62F15	10.13
131	3101	62F7	5.35
132	3102	62F7	2.51
133	3103	62F7	7.97
134	3104	62F7	6.95
135	3105	62F7	191.09
136	3106	62F7	9.85
137	3107	62F9	5.61

(continued)

Table 3 (continued)

S. No	Lake No	Toposheet No	Area (ha)
138	3108	62J2	14.79
139	3109	62J2	11.68
140	3110	62J2	13.44
141	3111	52P12	3.22
142	3112	52P16	3.52
143	3113	52P16	2.41
144	3114	52P16	2.24
145	3115	62A11	15.76
146	3116	62A11	85.32
147	3117	62A15	3.68
148	3118	62E4	2.34
149	3119	62E4	2.31
150	3120	62E4	6.34
151	3121	62E8	3.24
152	3122	62E12	4.06
153	3123	62E12	2.16
154	3124	62E12	2.13
155	3125	62F9	2.93
156	3126	62F13	4.31
157	3127	62F13	5.18
158	3128	62J1	2.36
159	3129	62J2	5530.86
160	3130	62J2	3.74
161	3131	62F14	4.14
162	3132	62F15	15.50
163	3133	62F9	342.25
164	3134	62F9	6.42
165	3135	62F9	5.14
166	3136	62F9	7.33
167	3137	62F9	67.55
168	3138	62F9	17.20
169	3139	62F9	46.28
170	3140	62F6	41,225.34
171	3141	62F2	26,268.07
172	3142	62F11	7.97
173	3143	62F11	3.73
174	3144	62F11	3.68
175	3145	62F7	3.43
176	3146	62F7	4.05
177	3147	62B10	3.21

(continued)

Table 3 (continued)

S. No	Lake No	Toposheet No	Area (ha)
178	3148	62B10	5.33
179	3149	62B6	2.41
180	3150	53M12	5.24
181	3151	53M8	3.67
182	3152	53M4	10.84
183	3153	52L15	5.76
184	3154	53M13	4.72
185	3155	53M13	2.58
186	3156	53M13	2.48
187	4001	52K4	2.75
188	4002	52K4	6.01
189	4003	52L5	14,515.26
190	4004	52K8	3.52
191	4005	52K8	6.59
192	4006	52K8	5.83
193	4007	52K8	7.77
194	4008	52K8	9.53
195	4009	52K8	40.18
196	4010	52L5	3.92
197	4011	52L5	2.89

3 Conclusions

The glacial lakes located in Himalaya Mountains pose great dangers to the inhabitants of the Indus, Ganges and Brahmaputra river basins due to glacial hazards. The GLOF is some of the natural phenomenon that affects vulnerable settlements downstream the main valleys of this region. Proper inventory of glacier and glacial lakes and their risk potential is important information to mitigate the losses due to these flash floods. The study shows the importance of remote sensing in creating inventories as well as monitoring of the glacial lakes quickly and accurately. The LISS-III sensor with a spatial resolution of 23.5 m is highly useful in identifying and inventory mapping glacial lakes or waterbodies. The AWiFS sensor due to wider coverage and high repetivity plays crucial role in regular monitoring of lakes.

References

1. Bajracharya, S.R., et al.: Spatial database development of glaciers and glacial lakes in the identification of potentially dangerous glacial lakes of Nepal using remote sensing and geographic information systems. In: Asian Conference on Remote Sensing (2002)
2. Huggel, C., Kääb, A., Haeberli, W., Teysseire, P., Paul, F.: Remote sensing based assessment of hazards from glacier lake outbursts: a case study in the Swiss Alps. Can. Geotech. J. **39**, 316–330 (2002)
3. Ives, J.D.: Glacial lake outburst floods and risk engineering in the Himalaya, p. 42. ICIMOD, Kathmandu (1986)
4. Sharma, S.: The Ganges crisis—government lacks strategic plan. In: Proceedings of Bonn 2001—International Conference on Freshwater, Bonn, Germany, 3–7 Dec 2001 (2001)

Chapter 49
Geospatial Study on Landslide Vulnerability Mapping in the Environs of Araku Valley, Visakhapatnam District, Andhra Pradesh

Ch. Anusha, Peddada Jagadeeswara Rao, Y. Padmini and B. Sridhar

Abstract The study area, the Araku Valley and its environs of Visakhapatnam District, Andhra Pradesh is characterized by hills, belongs to Eastern Ghats Mobile Belt often experiences landslides, hence, this study is taken up to identify potential landslide vulnerable zones. Study area has the highest elevated broad gauge rail, passing through the undulated terrain and roads are passing through hair-pin bends experiences landslides causing disruption of rail and road network. Large number of springs, streams, thick weathered materials and rock masses are exposed to road and rail track are the potential zones for landslides/slips/creep/slump, etc. very often during heavy rains, the area is experiencing debris slides along roads leading to disruption of communication. In this study, thematic maps such as drainage, geology, geomorphology, land use/land cover and slope are extracted from the SOI toposheets, IRS-ID, LISS-III, SRTM satellite data and other ancillary data. The thematic maps are overlayed to select a landslide vulnerable zone map of the area in ArcGIS-9.2. In addition, socio-economic conditions of the area have studied with a view to protect them by adopting suitable remedial measures. Study helps in understanding future landslide zone prediction, land use planning for establishment of different economic activities and to identify the villages whose stability against landslides.

Keywords Landslide · Slump · Creep · Thematic maps

Ch. Anusha (✉) · P. J. Rao · Y. Padmini · B. Sridhar
Department of Geo-Engineering, College of Engineering (A), Andhra University, Visakhapatnam 530 003, India
e-mail: Anu4goal@gmail.com

P. J. Rao
e-mail: pjr_geoin@rediffmail.com

Y. Padmini
e-mail: gbujji.paddu@gmail.com

B. Sridhar
e-mail: sridhar.bendalam@gmail.com

P. J. Rao et al. (eds.), *Proceedings of International Conference on Remote Sensing for Disaster Management*, Springer Series in Geomechanics and Geoengineering,
https://doi.org/10.1007/978-3-319-77276-9_49

1 Introduction

Landslides occur due to a combination of trigger mechanisms and susceptibility factors such as fragile and complex geology, steep slopes, rugged topography, variable climatic and microclimatic conditions, rainfall, earthquake and vegetation degradation [1, 2]. Landslides are triggered by many extrinsic causative factors such as blasting and drilling, cloudburst and flash-floods [3]. Causal factors such as slope inclination, relationship between slope and structural discontinuities, many other tectonic factors often aggravate the instability of slope (Venkatachalam et al. 2006; Tolia et al. 2006; Singh et al. 2011). In India, landslides are one of the major natural disasters which account monetary loss nearly 1000–1500 million per annum. The Himalayas are the major vulnerable landslide prone hills in comparison to other hill ranges in India. There are several episodes of landslides being occurred in Eastern Ghats, as a result, damage has taken place to the life and property and several strategic constructions have been severely affected.

Araku often called as Andhra Ooty and Borra caves are the cynosure. These tourist hill stations are located more than one kilometer above msl. Several landslides/soil creep had been taking place along the ghat sections of Visakhapatnam to Araku state highway and Dandakaranya-Bolangir-Kiriburu (DBK) railway-line. This resulting in disruption of road between Araku with other parts of Visakhapatnam. Fortunately, the events are not very severe, therefore, there is no major loss of property and life. However, railways are being affected and often closes rail transportation. A major landslide occurred in the midnight of 3rd/4th August, 2006 at Kodipunjuvalasa village of Araku mandal, Visakhapatnam district buried 18 people under the debris [4]. Hence, this study has been taken up to identify the landslide vulnerable zones with a view to reduce the loss of life and property.

2 Study Area

The study area comprises of four tribal mandals namely, Araku, Ananthagiri, Hukumpet and Dumbriguda, is characterized by high altitude hilly terrain covering 1938 km^2, located between 18° 11′ 5.715″ North lat 82° 52′ 35.121″ East long in Visakhapatnam district, Andhra Pradesh (Fig. 1). Araku valley and Borra caves are the major tourist centres, attracting tourists from all over the world. Araku is called as “Andhra Ooty” and the area is a cynosure to the tourists. Study area belongs to Eastern Ghats Mobile Belt (EGMB) of Precambrian age [5, 6]. It is covered by metamorphic rocks and igneous intrusives, namely khondalite, charnockite, porphyroblastic granitoid gneiss, leptynite and quartzite. The area has high altitude bauxite, apatite, gemstone, vermiculite and china clay minerals.

Study area is famous for dry deciduous and semi-evergreen forests, altitude ranges from 450 to 1670 m above msl. Hills are covered by hydrophilic soils which

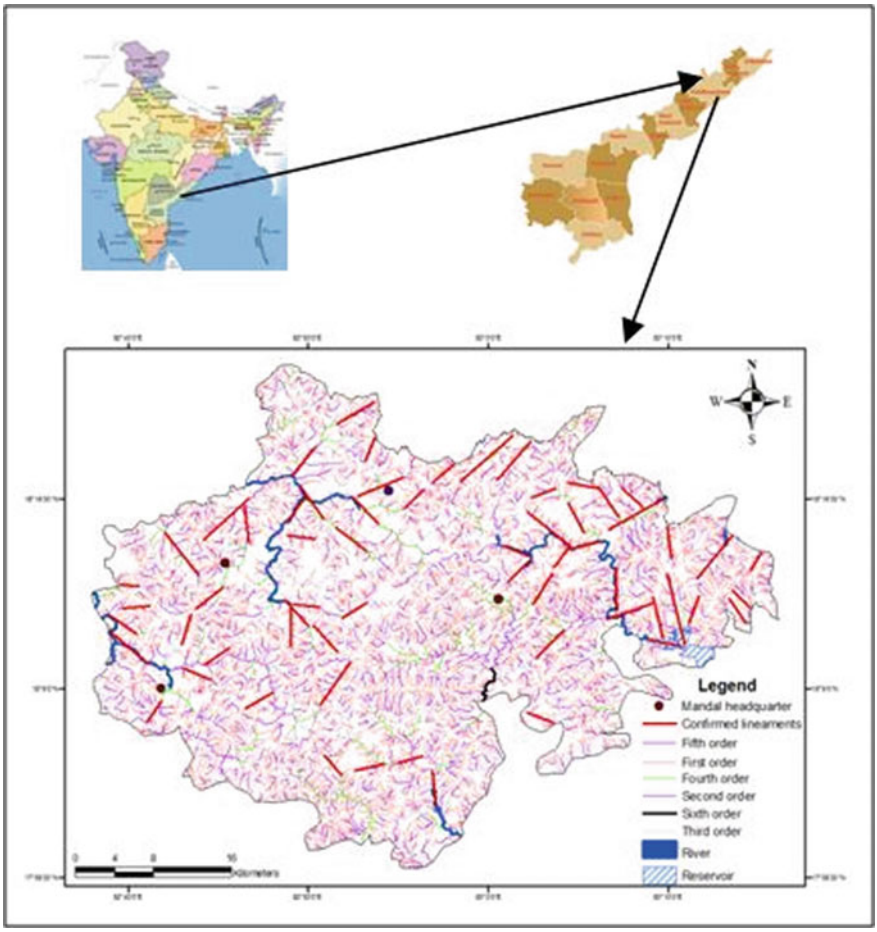

Fig. 1 Location map

supports forests and vegetation. Forest products such as honey, tamarind, pineapple, vegetables, turmeric, coffee, pepper and coco are the major products. The area is a natural habitat for wild flora and fauna. Cheetahs, deers and porcupine are the major animals besides wide variety of plant species. The area is well connected by road and rail. State high-ways and roads are passing through the steep hair pin bends. High elevated broad gauge rail-way line passes through this area, popularly known as DBK rail-way line. Roads and railway lines are being affected by the landslides. In addition, landslides/rock slips/soil creep are very severe in rainy season. Keeping in view of these issues, the present study has been taken up to identify the landslide potential zones using geospatial technologies.

The area is characterized by hills, which are mostly relict hill masses. The average annual rainfall of the Visakhapatnam district is around 1200 mm, however,

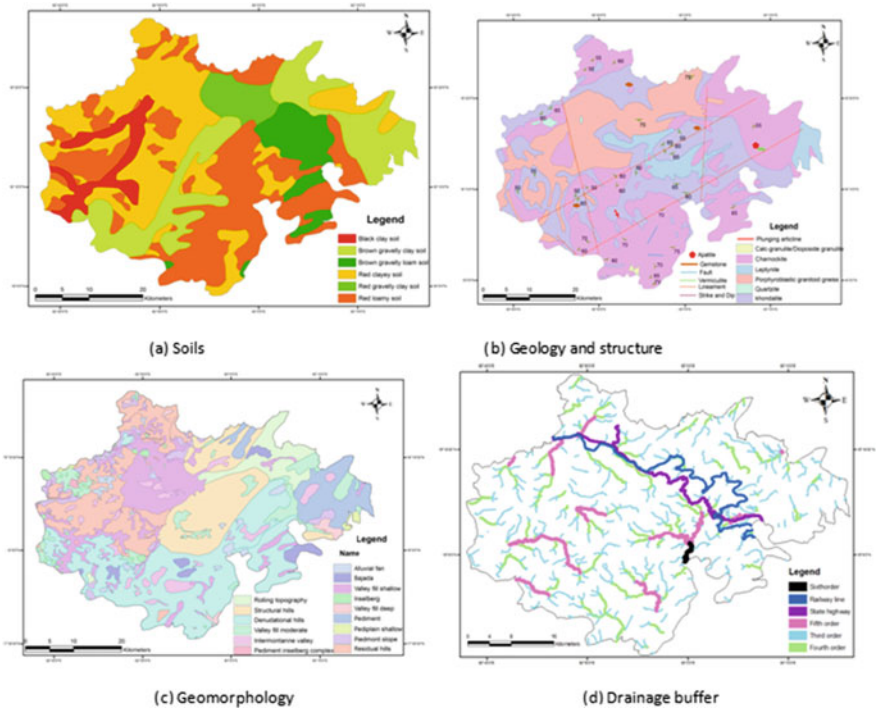

Fig. 2 **a** Soils. **b** Geology and structure. **c** Geomorphology. **d** Drainage buffer

the study area receives excess rainfall than the district average (Fig. 2). Excess rainfall coupled with anthropogenic activities is the major causative parameter for landslide/slips along the road. The landslide occurred at Kodipunjuvalasa village in 2006 is a rainfall induced one which claimed nearly 18 people [4]. In 2016, a major landslide occurred near Borra railway station which disrupted rail traffic.

3 Thematic Layers

3.1 Drainage and Lineaments

The drainage pattern of the area is extracted through visual interpretation from the geometrically rectified toposheets in ArcGIS-9.2. Observed slight shift of major river courses at various places has been adjusted in accordance of satellite image. High drainage density reflects hard rock substratum with steep slopes, thus the area is contributing run-off. Study area is the catchment for Gosthani, Sarada rivers and other non-perennial rivers. Dendritic, sub-dendritic, radial and parallel types of drainages are seen with high drainage density (Fig. 1). The river courses are not

wide as in the case of plains. Narrow and small river courses are perennial, because springs and ground water contributing sustained flow. In this, highest sixth order stream [7] is given ranking to the river Sarada. There are innumerable number of streams, rapids, waterfalls and springs triggering the landslides along the state highway and railway line.

The lineaments are the linear, curvilinear mapable structures which can easily identify on the satellite image [8] (Fig. 1). These could be faults, joints, shear zones, etc. These are structurally controlled may trigger landslides either by rain induced or by small local tremors or by any anthropogenic activities. The lineaments promotes denudation, acts as conduits to store and transmits water. There are innumerable number of springs are being controlled by lineaments. The lineament structures have not been properly understand in laying roads, railway lines and constructions. Observed rock slips, debris slide contributing by the lineaments intersected with railway line and roads are the major potential landslides zones.

3.2 Soils

The study area is covered by different types of soils namely black clay soil, brown gravelly clay soil, brown gravelly loam soil, red clayey soil, red gravelly clay soil and red loamy soil (Fig. 2a). Red soil with clay, gravel and loam are the major categories in the area and these are derived from the parent khondalite rock. Gravel materials derived from the fractured rocks. There are admixed with clay and sand with different proportions. It is porus and permeable, if it is saturated with water liable to slide as slump/creep. Red loamy soils are more dangerous than red gravelly clay soils. Gravel, sand and clay may have more binding property than red loamy soils. In field study observed these two soils are slided as debris slide/slump/creep along the major roads. Black clayey soil and brown gravelly loamy soils are confined to the river valleys.

3.3 Geological Setup

The geology of the study area belongs to Precambrian age, characterized by the occurrence of intrusive meta igneous bodies and meta sediments [9]. The area, comes under the Eastern Ghats Mobile Belt (EGMB) is characterized by hilly terrain which is mainly composed of khondalite suite of rocks. The major rock types are khondalite, charrnockite, porphyroblastic granitoid gneiss are the major rock types which occupy 30% each in the area. However, leptynite, quartzite, calc-granulite are occurring as intrusives. The general strike of the rocks is NNE-SSE, however, local variations observed [5, 6] (Fig. 2b). In tropical and equatorial regions, weathering processes create superficial layer with varying degree of porosity and permeability [10].

The charnockite, leptynite and quartzite rocks are hard and not easy to weather, however, these are fractured/fissured. Steep slopes with fractured rock masses are potential zones, liable to slide as landslides/rockslide. The area is enriched with bauxite, vermiculite, apatite, gemstones and manganese mineral resources.

3.4 Geomorphology

The geomorphic classes of the study area has been delineated on IRS-R2 satellite data following the visual interpretation techniques. In this, fifteen geomorphic classes of fluvial and erosion origin are delineated (Fig. 2c) [11]. Residual and structural hills are stable in terms of rock composition and structure. Because of mound like structure, inselbergs and pediment inselberg complex are not experiencing landslides. The geomorphic processes which are active liable to slide in any form of landslide. The denudational hills covered by porus and permeable soils, saturated with water liable to slide at steep slopes as soil slump.

3.5 Land Use/Land Cover and Slope

The land use/cover of the study area has been carried out on the geometrically rectified IRS-P6, LISS-III satellite data. Delineation of different land use/cover classes were made through onscreen digitization. Remote sensing data have been an attractive source in the determination of land use/cover thematic mapping, providing valuable information for delineating the extent of land cover classes, as well as for performing temporal land use change analysis and risk analysis at various scales [12].

In this study, 29 land use/land cover classes were delineated through onscreen digitization in ArcGIS-9.2 (Fig. 3a). Forest is the major land cover, covers 1307.81 km^2. High density forest is observed in Ananthagiri mandal. Discontinuous and deforestation is more in Dumbriguda and Hukumpet mandals. The forest in this area is a habitat for different wild flora and fauna.

Agriculture is in plains and valleys. Single crop cultivation land use is in Araku and Dumbriguda mandals with an area of 137.24 km^2. Similarly, double crop agriculture is observed in valleys which accounts 26.67 km^2. The area is famous for world famous turmeric, lakka, pineapple and jackfruit, etc.

Gullied lands are identified in valleys and in foothills is covering 36 km^2. Most of the waste land/gullied lands are delineated in Araku and Dumbriguda mandals. Silver Oak in forest areas is supporting coffee, pepper cash crops is covering 19 km^2 in Ananthagiri, Araku and Dumbriguda mandals. Deforestation affects soil erosion, migration of fauna and extinction of native plant species covers 36.78 km^2. Rural built-up is in Araku Valley, sporadic built-up has also been delineated in

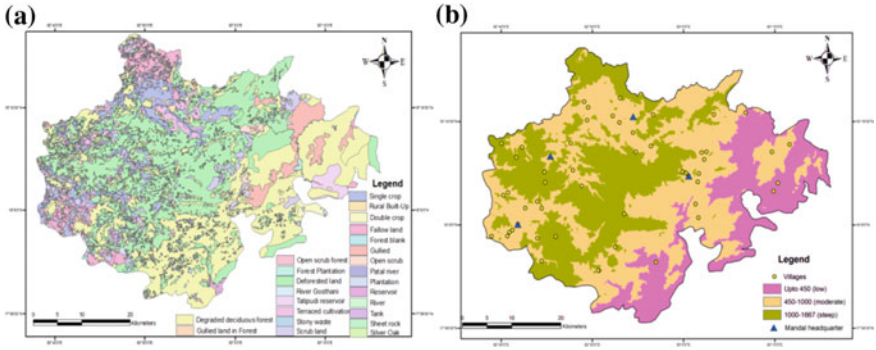

Fig. 3 **a** Land use/land cover. **b** Slope of the study area

other mandals. Mostly, the built-up are residential houses, schools, government offices and tourism cottages, etc. covering 10.60 km^2.

The slope of the area has been divided into steep (>1000), moderate (450–1000 m) and low (<450 m) (Fig. 3b). It is presumed that the steep and moderate slopes with fractures, sparse vegetation and anthropogenic activities further intensifying the landslide activity. In this study, khondalite suite of rocks, porphyroblastic, calc-granulite have been considered to identify landslides. On the basis of slope and rock types, the study area has been divided into three landslide vulnerable zones mostly confined in Araku, Dumbriguda, Hukumpet and Ananthagiri.

4 GIS Analysis

Geographic Information Systems (GIS) analysis has been carried out in ArcGIS-9.2, considering the importance of different classes of thematic layers. In this study, geology, drainage, soils, slope and land use/land cover thematic maps have been used. Multi-criteria weight overlay method was followed to obtain landslide vulnerability index map of the area [murthy].

Several socio-economic parameters have also been considered because the area is famous for tourism, coffee plantation, turmeric and other forest products. This study also focused on vulnerable tribal hamlets in order to reduce life and property. The area is often experiencing blockage of road and railway line which disrupting communication.

Different thematic maps such as roads, drainage were considered for buffer analysis. In this, state high-way road and rail-way line have been assigned 100 and 200 m buffer respectively. Fourth and Fifth order streams were assigned 400–500 m buffer zones with a view to assess landslide activity respectively. The output is overlayed on major tribal hamlets and major tourist resorts which are having close vicinity to moderate to steep slopes are identified as vulnerable to landslides.

The thematic layer classes of drainage, lineaments, geology, geomorphology, road and railway line, soil and land use land cover designated with respective weights [13] are essential to develop database, which provides various categories of landslide vulnerable zones. Least vulnerable is indicated with 1and highest with 10.

5 Landslide Vulnerability Index

Low slopes are the beginning part of hilly terrain of Araku Ghat road, where the area is covered by thick forests. Observed, debris slide and slump along the Visakhapatnam-Araku state-highway. A few landslips also identified in the upper catchment of Thatipudi reservoir. Only khondalite suite of rocks considered, rest of the rocks are hard and stable not easy to experience landslides. Moderate slopes have been experienced landslide/debris slide/soil creep, etc. Thick forest is covered in Ananthagiri mandal, no major landslides reported, except debris slide and slump along the Visakhapatnam-Araku state-highway and DBK railway line.

High vulnerability zones are very few, these are identified on the basis of steep slopes, fractured khondalite rock and structural/denudational hills have chosen to identify the high intensity landslide zones. A discontinuous patches are identified in this analysis (Fig. 4).

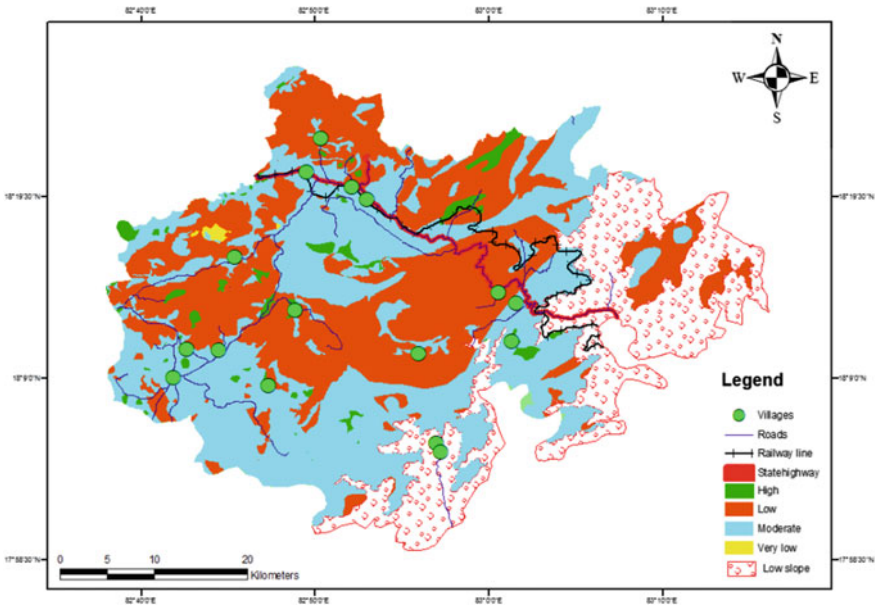

Fig. 4 Landslide vulnerability map

Sl. No	Slope	Road/rail	Mandals	Type of land use/cover	Landslide vulnerability	Remedial measures
1	450–1000 1000–1667	State highway	Araku valley Ananthagiri Dumbriguda	Single crop, Deforested land, Terraced cultivation, Forest, Gullied land	Moderate to high	Afforestation Retaining wall Stability of soils
2	450–1000 1000–1667	Railway line	Araku valley Ananthagiri Dumbriguda	Forest, Gullied land, Deforested land, Scrub land, Single crop, Terraced cultivation	Moderate to high	Afforestation Grouting Riveting and bolting

6 Results

In this study, toposheets, IRS-ID,IRS-P6 and SRTM satellite data have been used to extract thematic maps reveales landslide hotspot zones. The thematic maps are analyzed in ArcGIS-9.2 to identify potential landslide zones. Observed that the khondalite intercepted with later intrusives and these intrusive hill masses are highly fractured are vulnerable areas coupled with structural deformities and drainages. Study identified vulnerable hamlets whose stability against landslides and remedial measures suggested to overcome.

References

1. Gerrard, J.A.: Relationships between landsliding and land use in the Likhu Khola drainage basin, Middle Hills, Nepal. Mt. Res. Dev. **22**, 48–55 (2002)
2. Hasegawa, S., Dahal, R.K., Yamanaka, M., Bhandary, N.P., Yatable, R., Inagaki, H.: Causes of large-scale landslides in the Lesser Himalaya of central Nepal. Environ. Geol. **57**, 1423–1434 (2009)
3. Anbalagan, R.: Landslide hazard evaluation and zonation mapping in mountainous terrain. Eng. Geol. **3**(2), 269–277 (1992)
4. Balaji, P., Pavanaguru, R., Reddy, D.V.: A note on the occurrence of landslides in Araku Valley and its Environs, Visakhapatnam District, Andhra Pradesh, India (2010)
5. Sriramadas, A.: Structural geology of the Eastern Ghats in parts of Visakhapatnam and srikakulam districts, Andhra Pradesh, India. In: 22nd International Geological Congress, India, pp. 245–251 (1964)
6. Chetty, T.R.K., Vijay, P., Suresh, B.V.V., Vijaya Kumar, T.: GIS and the tectonics of the Eastern Ghats, India. GIS Dev. **16**(12), 21–24 (2002)

7. Strahler, A.N.: Statistical analysis in geomorphic research. J. Geol. **62**, 1–25 (1952)
8. O'Leary, D.W., Friedman, T.D., Pohn, H.A.: Lineament, linear, lineation, some proposed new standards for old terms. Bull. Geol. Sci. Am. **87**, 1463–1469 (1976)
9. Narasimha Rao, Ch.: Geology and Petrology of the Kailasa Range. M.Sc. Thesis, Andhra University, Waltair (1945)
10. Mogajia, K.A., Aboyejib, O.S., Omosuyi, G.O.: Mapping of lineaments for groundwater targeting in basement complex area of Ondo state using remotely sensed data. Int. J. Water Resour. Environ. Eng. **3**(7), 150–160 (2012)
11. Jagadeeswara Rao, P., Harikrishna, P., Suryaprakasa Rao, B.: An integrated study on ground water resource of Pedda Gedda watershed. J. Indian Soc. Remote Sens. **32**, 307–311 (2004)
12. Kavzoglu, T., Colkesen, I.: A kernel functions analysis for support vector machines for land cover classification. Int. J. Appl. Earth Obs. Geoinf. **11**, 352–359 (2009)
13. Murthy, K.S.R., Amminedu, E., Venkateswara Rao, V.: Integration of thematic maps through GIS for identification of ground water potential zones. J. Indian Soc. Remote Sens. **31**, 197–210 (2003)

Chapter 50
Assessment of Coastal Erosion Along the Srikakulam District, Andhra Pradesh State Using Satellite Data of 1990–2000 and 2000–2016 Time Frames

Y. Padmini, Peddada Jagadeeswara Rao and Ch. Anusha

Abstract Rising mean sea level (MSL) is one of the major concerns not only for the small islands but also for the mega-cities and the villages in the low elevation coastal zones globally. With recent projections from the IPCC, suggests that sea level may be ~0.6 to 1.5 m higher than present by 2100 AD, and the most direct impact of the sea-level rise is on the coastal zones. Since these narrow zones that fringe the world oceans are low-lying, the sea-level rise would lead to accelerated erosion and shoreline retreat, besides leading to saltwater intrusion into coastal groundwater aquifers, inundation of wetlands and estuaries, and threatening historic and cultural resources as well as infrastructure. The present study will address the shoreline changes along the Srikakulam district through the analysis of multi-date satellite imagery during 1990–2016. The results show that an area of about 288.06 ha, at a rate of 11.07 ha/year was lost due to erosion along the coastal regions of Srikakulam district.

Keywords Sea-level rise · Coastal erosion · Remote Sensing · Geographic Information System (GIS)

Y. Padmini (✉)
Geoscience Department, Dr. B.R. Ambedkar University, Etcherla, AP, India
e-mail: gbujji.paddu@gmail.com

P. J. Rao · Ch. Anusha
Department of Geo-Engineering, Andhra University, Visakhapatnam, AP, India
e-mail: pjr_geoin@rediffmail.com

Ch. Anusha
e-mail: anu4goal@gmail.com

P. J. Rao et al. (eds.), *Proceedings of International Conference on Remote Sensing for Disaster Management*, Springer Series in Geomechanics and Geoengineering,
https://doi.org/10.1007/978-3-319-77276-9_50

1 Introduction

During the last century, concentrations of greenhouse gases have increased significantly in the atmosphere as a result of burning fossil fuels since the industrial revolution leading to increasing global average temperature which is estimated to be 0.8 °C, the rise in temperature in the past three decades alone was 0.6 °C at the rate of 0.2 °C per decade as greenhouse gases became the dominant climate forcing in recent decades [5, 7, 13, 17]. Perhaps the most commonly recognized impact of global warming is the eustatic rise in sea level [1] due to thermal expansion of seawater and in addition to ice-melt water [10]. The analysis of long-term tide-gauge data from various stations along the Indian coastal regions, indicated that sea levels are rising at a rate of about 1.0–1.75 mm per year due to global warming [15, 16]. Shorelines are always subjected to changes due to coastal processes, which are controlled by wave characteristics, sediment characteristics, beach form, etc. [8].

Studies examining long-term and short-term shoreline changes have generally utilized satellite data [3, 9]. Recent studies along the east coast of India, indicated pronounced erosion, more than accretion [2, 4, 6, 11, 12, 14]. In this background, a study is taken up to assess the shoreline changes along the Srikakulam district, Andhra Pradesh state through the analysis of multi-date satellite imagery during 1990–2016.

2 Study Area

Srikakulam district is the northern most district of Andhra Pradesh state with 177 km long coastal region. As per the 2001 census, Srikakulam has the 4th highest concentration of people living in the coastal Andhra Pradesh with Ichchapuram, Sompeta, Tekkali, Narsannapeta, Srikakulam and Chipurupalle taluks bordering the sea coast (Fig. 1). The National Highway No. 5 and the Howrah-Chennai broad gauge railway pass through this region. This entire region is characterized by number of tidal-backwaters, headland-bay configuration rocky structures, beach ridge-swale complexes, mudflats, saltpans, etc.

3 Materials and Methods

The present study is based on the interpretation of remote sensing imagery to assess the changes along the coastal regions of Srikakulam district, Andhra Pradesh state. Shoreline changes along the Srikakulam district have been estimated by comparing three sets of satellite images spread over the past two-and-half decades. Landsat TM image of Path 140/Row 47 dated November 28, 1990; Landsat ETM+ image of Path 140/Row 47 dated November 28, 2000 and Path 141/Row 47 dated December 08, 2000; and Landsat OLI/TIRS image 140/Row 47 dated November 19, 2016 and Path 141/Row 47 dated November 20, 2016 covering the Srikakulam district were

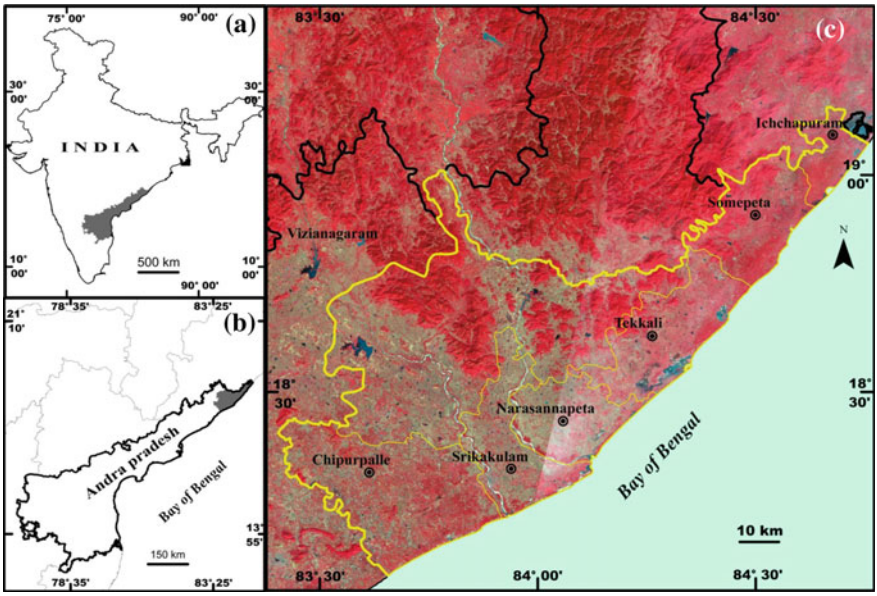

Fig. 1 Mosaic of landsat OLI images dated November 19 and 26, 2016 showing the Srikakulam district and surroundings of Andhra Pradesh state. Thick yellow line is the Srikakulam district and thin yellow line is the Taluk boundary along the coastal region

downloaded from USGS website [http://earthexplorer.usgs.gov] in TIFF format and were digitally processed and were geo-coded. For tracing the shoreline from the Landsat satellite imagery, near infra-red band images were chosen, since the land-water boundary is sharper in that band. The shoreline positions have been traced from all the datasets and then overlaid to find out the changes through overlay analysis. Area lost by erosion and gained by deposition along the entire Srikakulam district during the respective time periods were computed using Union option in the overlay analysis in ArcGIS.

4 Results

Initially, between the 1990 (Landsat TM) and 2000 (Landsat ETM+) the region revealed a net loss of 140.41 ha of area along the entire ~175-km-long coast. Among the 6 taluks, Ichchapuram coastal stretch faced severe erosion with an over loss of about 44.1 ha during this period, followed by Tekkali, Chipurupalle, Sompeta, Srikakulam and Narsannapeta taluks with 32.3, 24.6, 22.3, 15.8 and 1.4 ha respectively (Table 1; Fig. 2). Narsannapeta taluk which is least effected from erosion, showed pronounced deposition along its 22 km long coastal stretch (Table 2). And, most of the deposition is mainly observed along the mouth of the Vamsadhara river (Fig. 2).

Table 1 Area under erosion/deposition along different Taluk of Srikakulam district

Name of Taluk		Ichchapuram (ha)	Sompeta (ha)	Tekkali (ha)	Narsannapeta (ha)	Srikakulam (ha)	Chipurpalle (ha)	Total area (ha)
1990–2000	Erosion	44.1	22.2	32.3	1.4	15.8	24.6	140.4
	Deposition	4.9	6.4	14.6	48.8	34.7	21.1	130.5
2000–2016	Erosion	60.2	40.4	27.3	10.3	9.2	0.25	147.65
	Deposition	21.7	8.3	20.1	28.5	90.1	79.1	247.8

Table 2 Length of coastal region under erosion/deposition/stable along different Taluk of Srikakulam district

Name of Taluk		Ichchapuram (29 km)	Sompeta (27 km)	Tekkali (37 km)	Narsannapeta (22 km)	Srikakulam (29) km	Chipurpalle (33 km)	Total length (km)
Length		km	km	km	km	km	km	
1990–2000	Erosion	16.6	11.2	17.5	1.2	6.8	16.1	69.4
	Deposition	2.9	5.3	6.2	11.8	11.9	8.2	46.3
	Stable	8.5	10.5	14.3	9.1	10.8	7.3	60.5
2000–2016	Erosion	18.8	15	9.8	3.5	1.5	0.2	48.8
	Deposition	4	2.8	5	6.7	13.2	26.9	58.6
	Stable	6.3	9.1	22.2	12	14.1	4.6	68.3

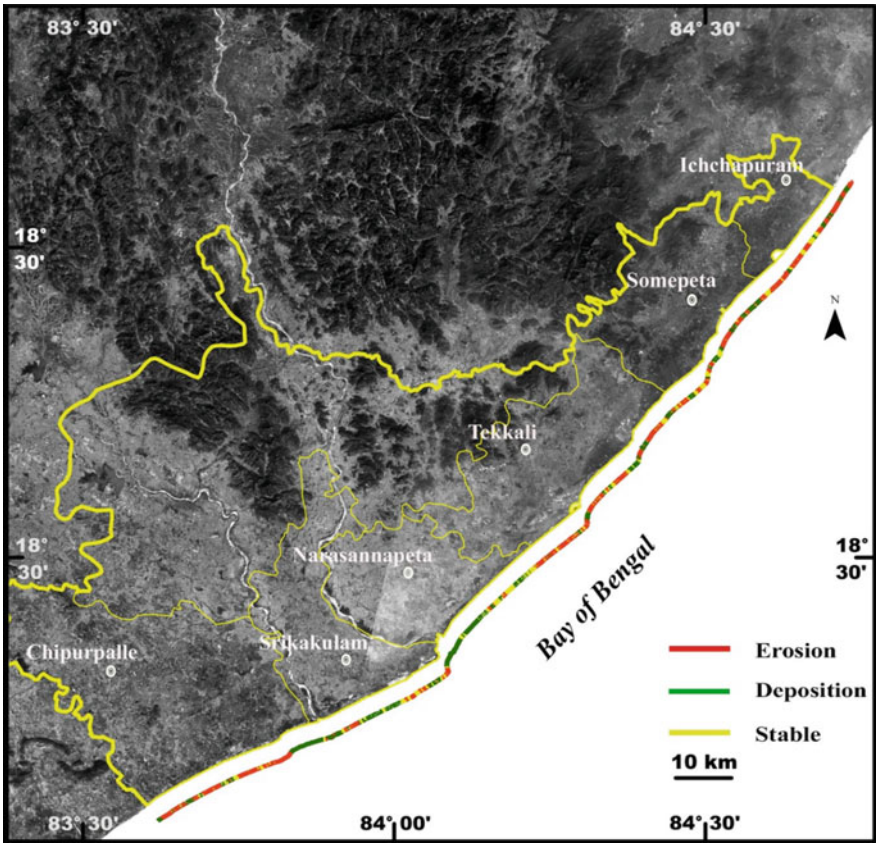

Fig. 2 Landsat ETM+ satellite imagery dated 2000 of Srikakulam district showing the areas of erosion/deposition and stable coast during 1990–2000 time interval

Between 2000 (Landsat ETM+) and 2016 (Landsat OLI/TIRS), there was a net loss of another 147.65 ha area. During this period, northern three taluks i.e. Ichchapuram, Sompeta and Tekkali faced severe erosion when compared with the southern taluks of Srikakulam district (Table 1; Fig. 3). Even during 2000–2016, deposition is observed along the mouth of the rivers. Interestingly, 64% of the Ichchapuram taluk showed erosion along its coastal stretch. On the whole, during the 26-year period between 1990 and 2016, the overall loss of area is about 288.06 ha, at a rate of 11.07 ha/year (Fig. 3).

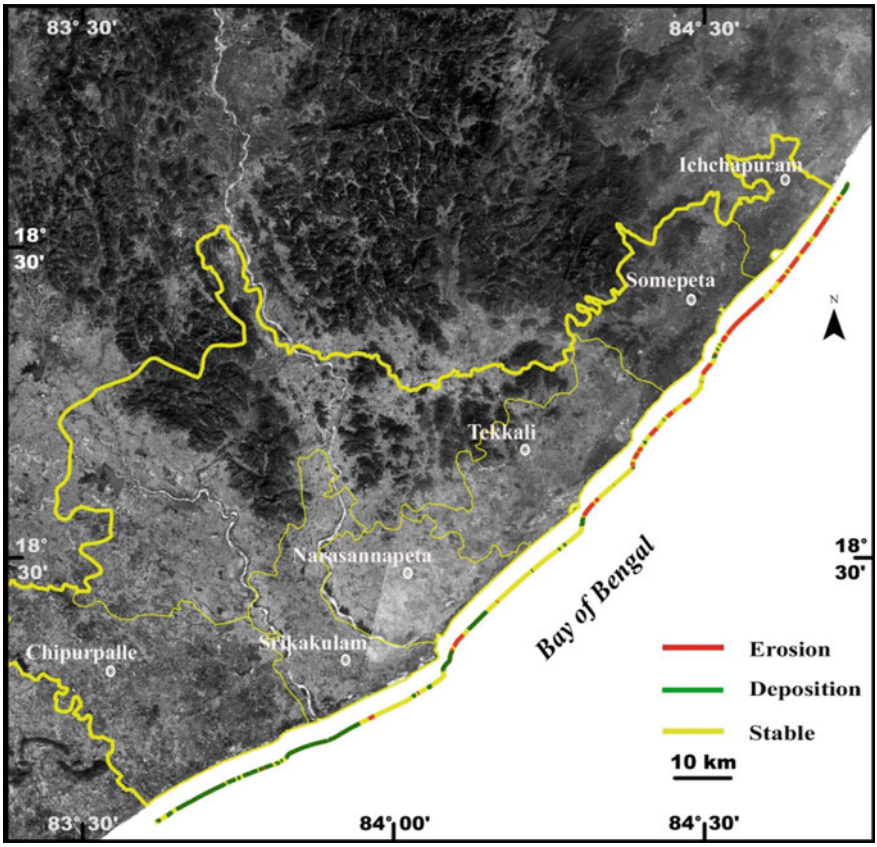

Fig. 3 Landsat OLI_TIRS satellite imagery dated 2016 of Srikakulam district showing the areas of Erosion/deposition and stable coast during 2000–2016 time interval

5 Conclusion

Srikakulam district of Andhra Pradesh state is one of the coastal districts which is severely affected with cyclones, floods, etc. In this background, the present study helped to find out the area/taluks which are under severe erosion to sea level arise. Further detailed studies on Land use/Land cover changes on high resolution satellite imagery coupled with digital elevation models (DEM) will definitely ascertain to demarcate the areas under threat to cyclones, coastal floods, and further helps to build a socio-economic vulnerability index for the Srikakulam district regions, this will help the decision makers to take necessary preparedness measures to reduce the severity of the disasters.

Acknowledgements Authors are thankful to the Vice-Chancellor, B.R. Ambedkar University and Andhra University for giving necessary lab facilities for carrying this work. Thanks to United Nations Geological Survey (USGS) for accessing the satellite imagery of Srikakulam district from their achieve.

References

1. Allen, J.C., Komar, P.D.: Climate controls on US west coast erosion processes. J. Coast Res. **22**, 511–529 (2006). https://doi.org/10.2112/03-0108.1
2. Biggs, T.W., Gaur, A., Scott, C.A., Thenkabail, P., Rao, P.G., Gumma, M.K., Acharya, S., Turrel, H.: Closing of the Krishna Basin: irrigation, stream flow depletion and macroscale hydrology. International Water Management Institute, Colombo, Research Report 111 (2007)
3. Ford, M.: Shoreline changes interpreted from multi-temporal aerial photographs and high resolution satellite images: Wotje Atoll, Marshall Islands. Remote Sens. Environ. **135**, 130–140 (2013)
4. Gamage, N., Smakhtin, V.: Do river deltas in east India retreat? A case study of the Krishna delta. Geomorphology **103**, 533–540 (2009)
5. Hansen, J., Sato, M., Ruedy, R., et al.: Global temperature change. Proc. Natl. Acad. Sci. U S A **103**, 14288–14293 (2006). https://doi.org/10.1073/pnas.0606291103
6. Hema Malini, B., Nageswara Rao, K.: Coastal erosion and habitat loss along the Godavari delta front—a fallout of dam construction (?). Curr. Sci. **87**, 1232–1236 (2004)
7. IPCC Summary for Policymakers: In: Soloman, S.D., Manning, Q.M., Chen, Z., Miller, H.L. (eds.) Climate change 2007: the physical science basis. Contribution of Working Group I to the Fourth Assessment Report of the Intergovernmental Panel on Climate Change Cambridge University Press, Cambridge pp. 1–18 (2007)
8. Kumar, A., Narayana, A.C., Jayappa, K.S.: A Shoreline changes and morphology of spits along southern Karnataka, west coast of India: a remote sensing and statistics-based approach. Geomorphology **120**(3–4), 133–152 (2010)
9. Maiti, S., Bhattacharya, A.K.: Shoreline change analysis and its application to prediction: a remote sensing and statistics based approach. Mar. Geol. **257**(1–4), 11–23 (2009)
10. Meehl, G.A., Washington, W.M., Collins, W.D., et al.: How much more global warming and sea level rise. Science **307**, 1769–1772 (2005). https://doi.org/10.1126/science.1106663
11. Mohanty, P.K., Panda, U.S., Paul, S.R., Mishra, P.: Monitoring and management of environmental changes along the Orissa coast. J. Coast. Res. **24**, 13–27 (2008)
12. Nageswara Rao, K., Subraelu, P., NagaKumar, K.Ch.V., Demudu, G., HemaMalini, B., Rajawat, A.S., Ajai.: Impacts of sediment retention by dams on delta shoreline recession: evidences from the Krishna and Godavari deltas, India. Earth Surf. Process. Landf. **35**, 817–827 (2010)
13. Rosenzweig, C., Koroly, D., Vicarelli, M., et al.: Attributing physical and biological impacts to anthropogenic climate change. Nature **453**, 353–357 (2008). https://doi.org/10.1038/nature06937
14. Sridhar, S.R., Elangovan, K., Suresh, P.K.: Long term shoreline oscillation and changes of Cauvery Delta coastline inferred from satellite imageries. J. Indian Soc. Remote Sens. **37**, 79–88 (2009)
15. Unnikrishnan, A.S., Rup Kumar, K., Fernandes, S.E., et al.: Sea level changes along the Indian coast: observations and projections. Curr. Sci. **90**, 362–368 (2006)
16. Unnikrishnan, A.S., Shankar, D.: Are sea-level-rise trends along the coasts of the north Indian Ocean consistent with global estimates global planet. Change **57**, 301–307 (2007). https://doi.org/10.1016/j.gloplacha.2006.11.02
17. Wood, R.: Natural ups and downs. Nature **453**, 43–45 (2008). https://doi.org/10.1038/453043a

Chapter 51
Landslide Susceptibility Mapping Using GIS-Based Likelihood Frequency Ratio Model: A Case Study of Pakyong—Pacheykhani Area, Sikkim Himalaya

Satyanarayana Prasad Nerella, Simhachalam Alajangi and Dinesh Dhakal

Abstract Himalayan region has highly undulating terrain which is a witness of ongoing orogeny process. The region comes under major seismic zone. These combined geo-environment factors cause numerous occasions of landslides and subsequently major loss of life and property. Landslides in the Himalayan terrain are sometime highly inaccessible. But geospatial technique provides capability of reaching every part of the inaccessible area, identifying all types of landslides and determining landslide prone zone on the basis of major causative factors. The study was carried out to prepare the Land Slide Hazard Zonation mapping using geospatial techniques in the two Gram Panchayat Unit (GPU) namely: Pakyong and Chalamthang-Pacheykhani in East District of Sikkim state. Remote sensing data and Toposheets were used to delineate drainage pattern, lineaments, structural features, lithological features, soil and land/use land/cover type of the study area by applying digital image processing techniques. Apart from the above, Digital elevation model data was used to generate primary topographic attributes namely, slope, aspect, and relative relief. Analyzed the various factors that influence the landslides. Weightage have been given to each and every layer using frequency ration model in geospatial environment. Integrated the weightage layers for the preparation of land slide hazard zonation mapping of the study area.

Keywords Remote sensing · Frequency ratio model · Landslides

S. P. Nerella (✉) · S. Alajangi
NIRDPR, NERC, Guwahati, India
e-mail: prasad.nird@gmail.com

S. Alajangi
e-mail: chalamnird@gmail.com

D. Dhakal
Sikkim State Disaster Management Authority, Gangtok, India
e-mail: dinesh.dilson@gmail.com

P. J. Rao et al. (eds.), *Proceedings of International Conference on Remote Sensing for Disaster Management*, Springer Series in Geomechanics and Geoengineering,
https://doi.org/10.1007/978-3-319-77276-9_51

1 Introduction

A Landslide also referred to as mass movement, slope failures, slope instability and terrain instability, is the mass movement of soil and derbies down a steep slope. Most of the terrain in the mountainous areas has been generally subjected to slope failure under the influence of a variety of causal factors and triggered by events such as earthquake or extreme rainfall. Heavy rainfall and ground water on the hills saturate rocks and soil that decreases shear strength. This phenomenon not only causes loss of life and property, they also pose severe threats to physical infrastructure, lake and disrupt social and economic development [1].

Landslides as one of the most damaging natural hazards in the mountainous terrain like Himalaya as a result the study of landslides has drawn worldwide attention mainly due to increasing awareness of socio economic impacts of landslides [2]. Himalayan region has highly undulating terrain which is a witness of ongoing orogeny process. The region comes under major seismic zone. These combined geo-environment factors cause numerous occasions of landslides and subsequently major loss of life and property. Landslides in the Himalayan terrain are sometime highly inaccessible. But geospatial technique provides capability of reaching every part of the inaccessible area, identifying all types of landslides and determining landslide prone zone on the basis of major causative factors. Since landslide hazard zonation is very much related to spatial information. GIS can be effective in analyzing the various factors at various location of a given area.

2 Aims and Objectives

1. Determine the various factors that will influence the zonation of landslides.
2. Determine the frequency ratio and weight of different layers.
3. Integration of the different layers using GIS to prepare landslide hazard zone.

3 Study Area

The study was carried out in the two Gram Panchayat Unit (GPU) namely: Pakyong and Chalamthang-Pacheykhani covering the total area of 1235.59 ha, located under Pakyong Sub-Division of East District shown in Fig. 1. The study area lies between 88° 34′ 10.67″E–88° 36′ 17.04″E and 27° 11′ 30.21″N–27° 14′ 41.09″N and altitude ranging from 460 to 1940 m. The entire study area is a portion of a hill with

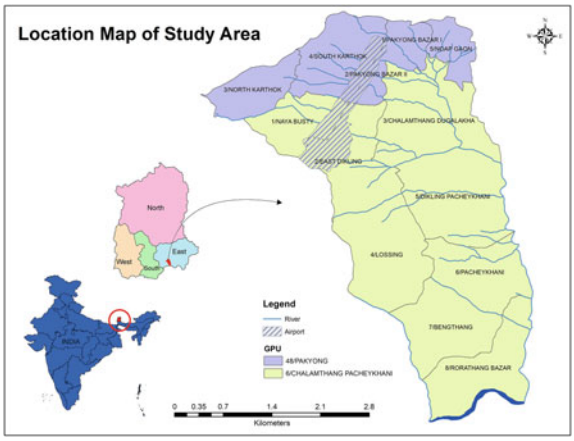

Fig. 1 Study area map

Pakyong town on the northern boundary ridge and Rangpo khola gorge at southern boundary. The climate of the study area is classified as warm temperate with average annual temperature of 18 °C and average annual rainfall of 2550 mm. The greater part of the rainfall is received between May and September. The maximum temperature is usually recorded during July–August and minimum during December–January.

4 Methodology

In this study Remote sensing data was further used to delineate drainage pattern, photo lineaments, structural features, lithological features, soil and land/use land/cover type of the area by applying digital image processing techniques. Geological features were analyzed using criteria such as color, tones, topography and stream drainage pattern from the imageries and toposheets. Apart from the above Digital elevation model data was used to generate primary topographic attributes namely, slope, aspect, and relative relief. Detailed methodology used for preparing landslide hazard zonation mapping is given in Fig. 2.

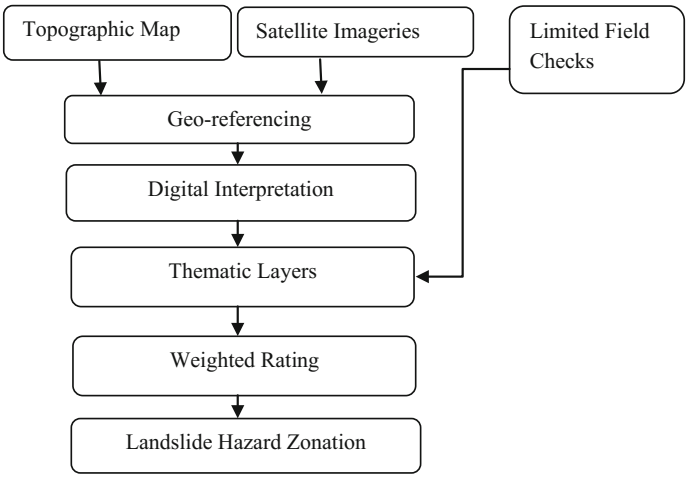

Fig. 2 Methodology used for landslide hazard zonation mapping

5 Data Preparation and Analysis

The digital image processing techniques were used to prepare the land use and land cover. The contours and drainage were extracted from the 1:50,000 scale topo sheets. DEM was prepared from the contours. The soil map is prepared from the NBSS source data is shown in Fig. 3. The lithology prepared based on the Geology and Mineral Resources of Sikkim shown on Fig. 4, consist of Daling Group with Buxa Formation and Gorubathan Formation. The slope, aspect and relative relief are derived from DEM. From the slope map of the study area as on Fig. 5, the slope angles in this region are between 0° and 42°. The aspect of a study are as on Fig. 6, shows the large fluctuation of aspect in the study area due to hilly regions and various ridges. The relative relief map of study area shown in Fig. 8, portrays the real distribution of such variations which has been classified into five groups. The drainage network map as shown in Fig. 7, of study area shows that the overall trend of the drainage basin is from northwest to southeast. Land use and land Cover of study area as on Fig. 9, resulted into eight land/use and land/cover classes such as Water Bodies, Airport construction area, Dry Agriculture Land, Fallow Land, Landslide area, Settlement area, Vegetation and Wet agriculture land. According to Onagh et al. land use is also one of the key factors responsible for the occurrence of landslides, since, barren slopes are more prone to landslides. The overall lineament pattern of study area as on Fig. 10, shows a nearly similar trend as that of drainage pattern. Landslide inventory map is prepared from satellite imageries and field investigations is shown in Fig. 11.

Analysis: Geographical location of the landslide area was prepared and converted into grid for the spatial analysis. To investigate triggering factors, different thematic map were used and relational analysis was carried out. The area of the

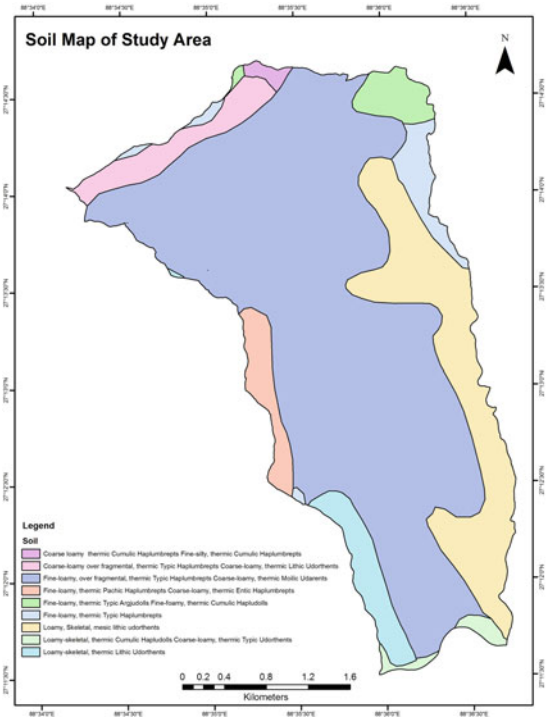

Fig. 3 Soil map

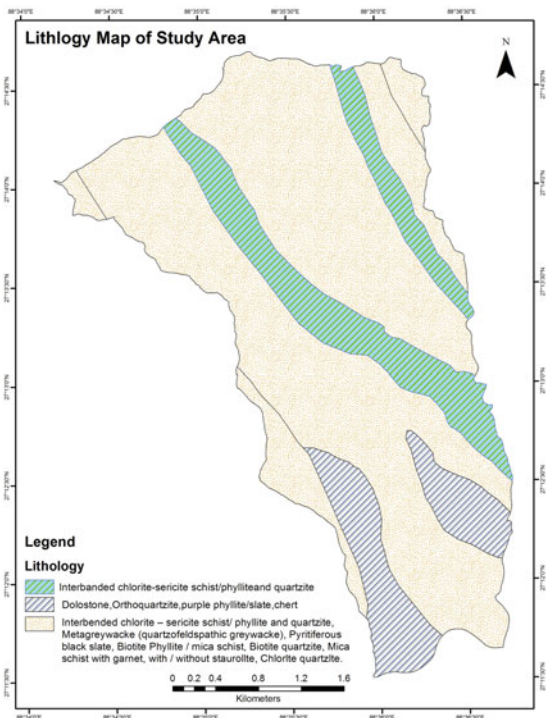

Fig. 4 Lithology map

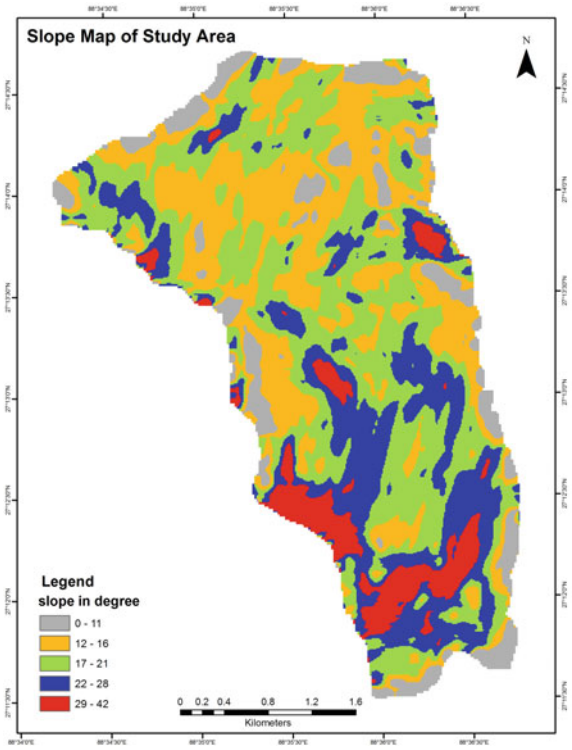

Fig. 5 Slope map

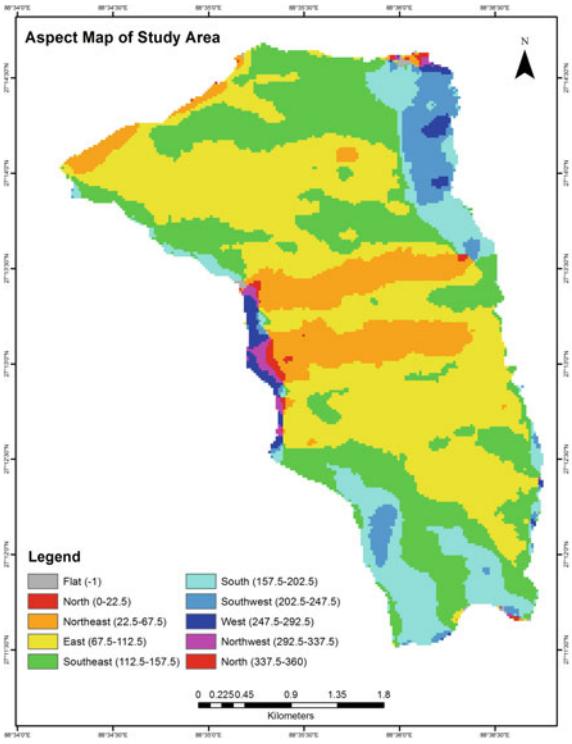

Fig. 6 Aspect map

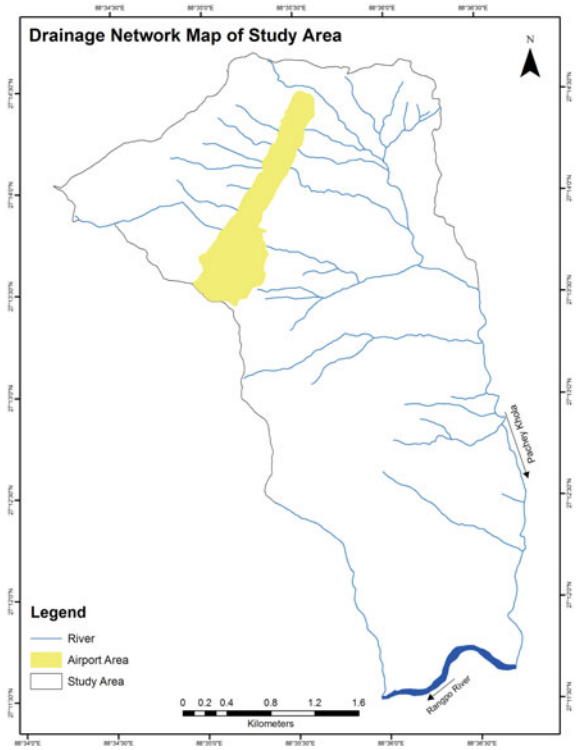

Fig. 7 Drainage map

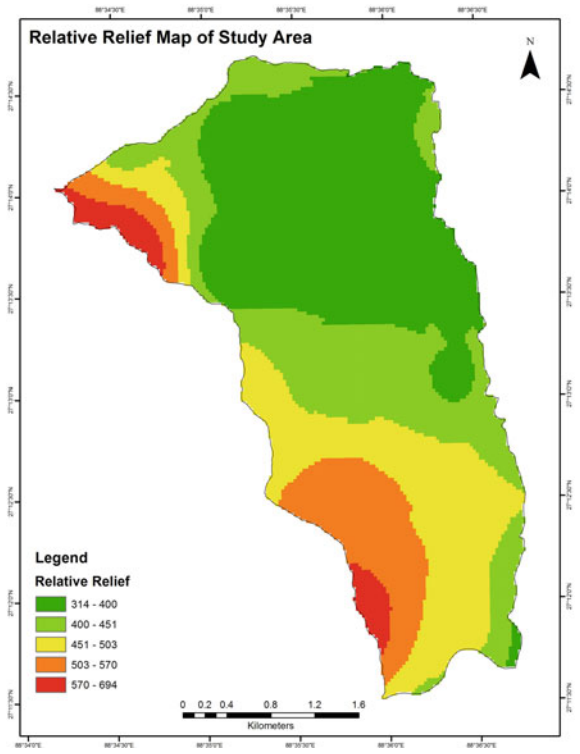

Fig. 8 Relative relief

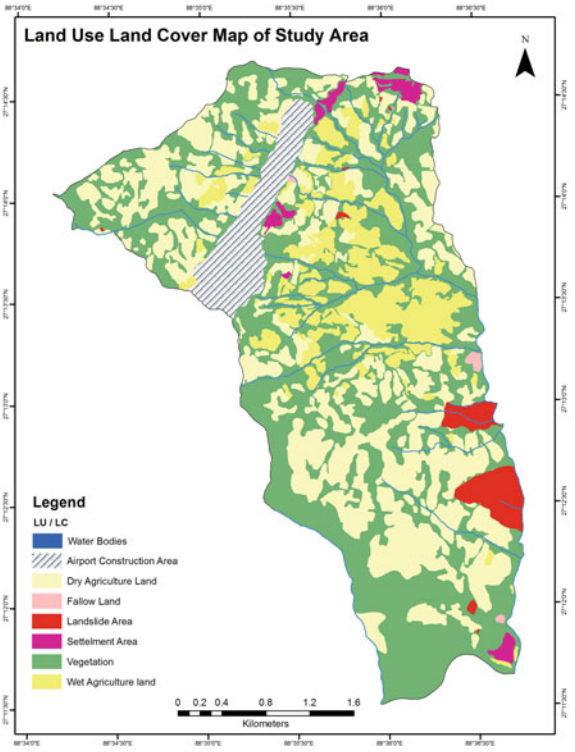

Fig. 9 Land use land cover map

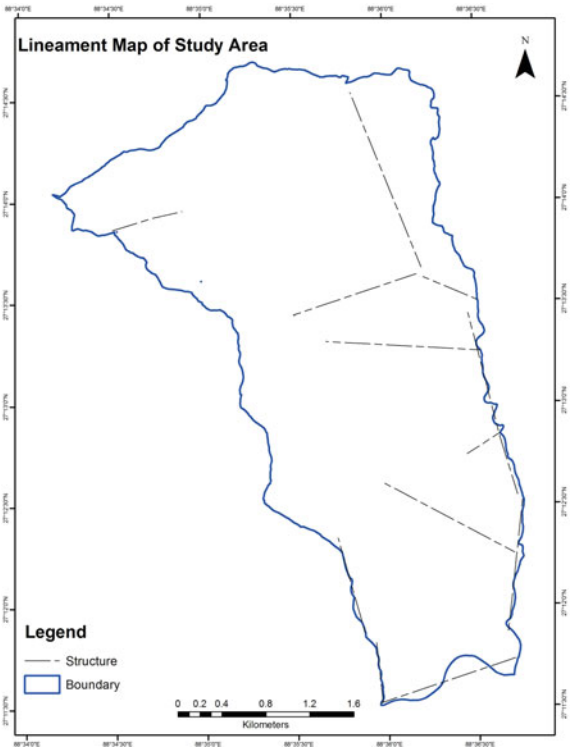

Fig. 10 Lineament map

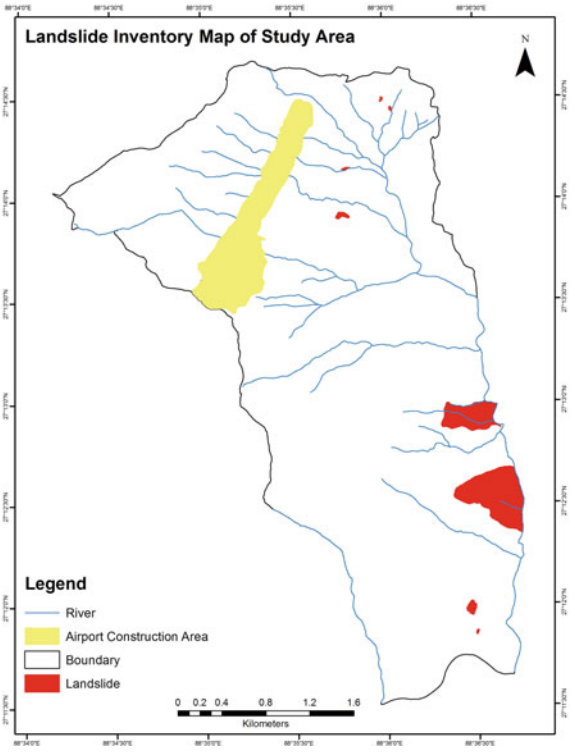

Fig. 11 Landslide inventory map

landslide in a particular class of each of factor maps was determined. Percentage of area covered by landslide for each factor class for different factors was computed by simple mathematical calculation. Frequency ratio method presented by Lee and Talib is one of the new methods used in landslide studies [3]. For every class of data layers, frequency ratio was calculated by the combination of landslide map with criterion map. The following equation is use for calculation of frequency ratio (Fri).

$$Fr_i = \frac{N_{pix}(s_i)/N_{pix}(N_i)}{\sum N_{pix}(s_i)/\sum N_{pix}(N_i)}$$

$N_{pix}(s_i)$ = The number of pixels containing slide in class (i)
$N_{pix}(N_i)$ = Total number of pixels having class (i) in the whole area
$\sum N_{pix}(s_i)$ = Total number of pixels containing landslide
$\sum N_{pix}(N_i)$ = Total number of pixels in the whole area.

Pixel dimensions were 10 m × 10 m in the study area. When the quantity of Fri was larger than one, relationship is positive between landslide occurrence and the

class of a data layer and if this ratio is smaller than one, then relationship is negative. The units' weight of every data layer was calculated using equation given below and the weighted layers was combined together in GIS.

$$w = 1000 \times N_{pix(s_i)}/N_{pix(N_i)} - 1000 \sum N_{pix(s_i)} / \sum N_{pix(N_i)}$$

w = The weight of every unit in a data layer,
$N_{pix(s_i)}/N_{pix(N_i)}$ = Density of landslides in every unit of a data layer
$\sum N_{pix(s_i)} / \sum N_{pix(N_i)}$ = Sum of landslide pixels per sum of total pixels of study area.

The following table shows the Frequency ratio and weighted unit of different Land Use and Land Cover (LULC) in study area (Table 1).

The analysis shows that frequency ratio is highest in Sinking Zones, of LULC class. Therefore, we can infer that this LULC of study area is more prone to landslide. The weighted score for the frequency of occurrence of the landslide is calculated accordingly.

$N_{pix}(s_i)$ = The number of pixels containing slide in class (i)
$N_{pix}(N_i)$ = Total number of pixels having class (i) in the whole area

Similarly the units' weight of every data layer is (From Figs. 12, 13, 14, 15, 16, 17, 18 and 19) calculated and the weighted layers were combined together in GIS environment to make final landslide Susceptibility Map shown at Fig. 20.

Zonation map of landslide was verified using the following equation given below (Gavynav et al. and Ayalew et al.). Landslide inventory map was combined with landslide risk zonation map and for every risk class number of pixels was calculated. Accuracy of the map was checked by using the following formula (Table 2).

$$AF(\%) = \frac{AF_i/A_{sci}}{\sum AF_i/A_{sci}}$$

$AF(\%)$ = Percentage area of every landslide risk class
AF_i = Number of pixels for landslide in every risk class
A_{sci} = Total number of pixels for every risk class.

Table 1 Frequency ratio and weighted unit of different land use and land cover

ID	Grid code	LULC	N pix (Ni)	N pix (si)	N pix (Ni) (%)	N pix (si) (%)	Fri	W
1	1	Dry agriculture	42,236.00	1050.00	34.18	30.87	0.90	−2.66
2	2	Wet agriculture	16,060.00	5.00	13.00	0.15	0.01	−27.21
3	3	Fallow land	301.00	0.00	0.24	0.00	0.00	−27.52
4	4	Settlement	1703.00	0.00	1.38	0.00	0.00	−27.52
5	5	Sinking zones	250.00	239.00	0.20	7.03	34.73	928.48
6	6	Vegetation	56,202.00	2107.00	45.49	61.95	1.36	9.96
7	7	Airport area	6809.00	0.00	5.51	0.00	0.00	−27.52

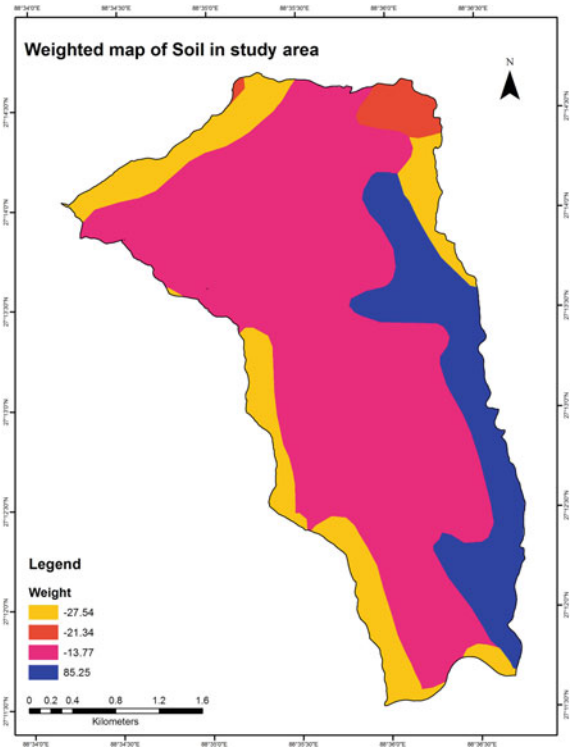

Fig. 12 Weighted map of soil

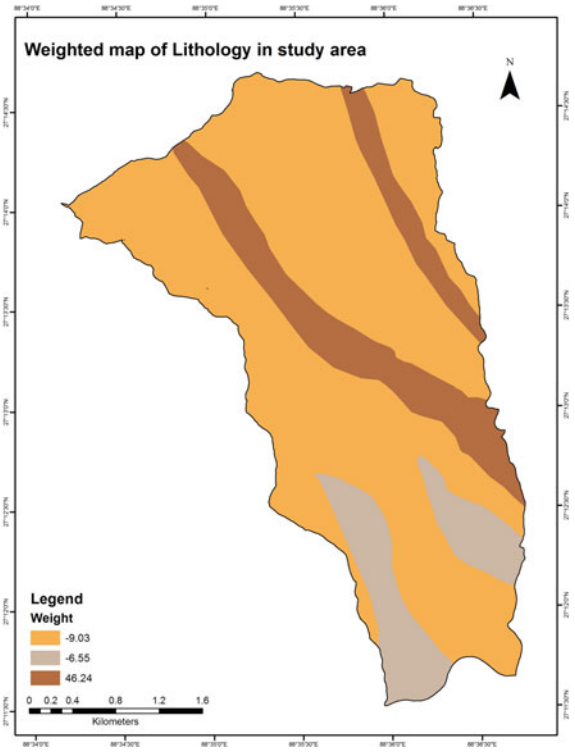

Fig. 13 Weighted map of lithology

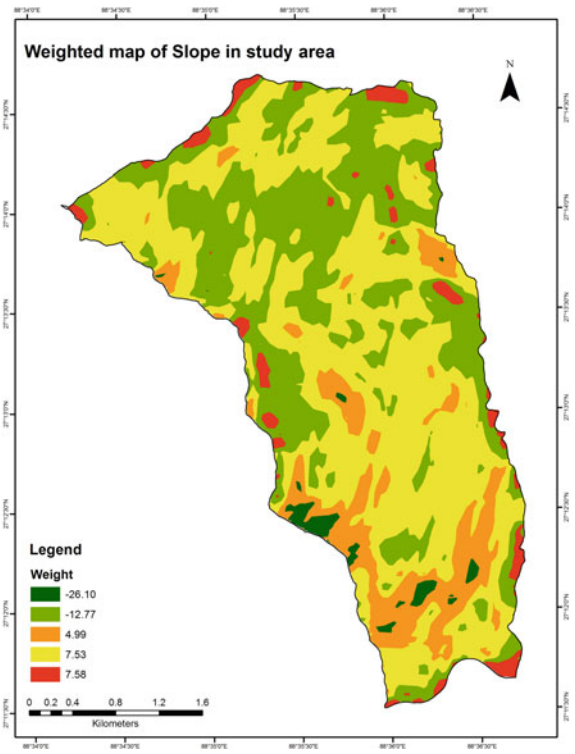

Fig. 14 Weighted map of slope

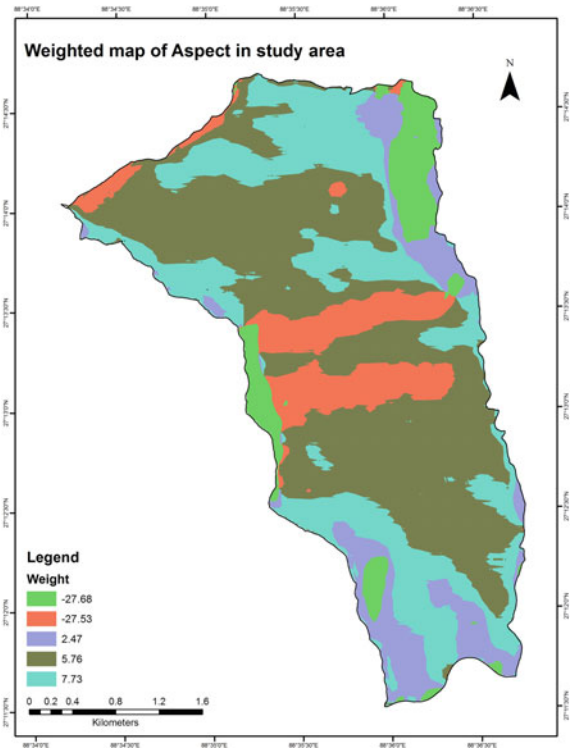

Fig. 15 Weighted map of aspect

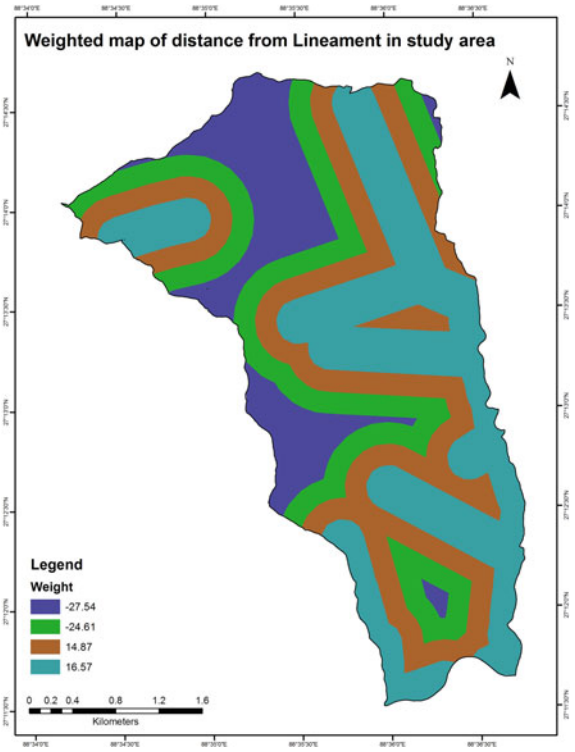

Fig. 16 Weighted map of lithology

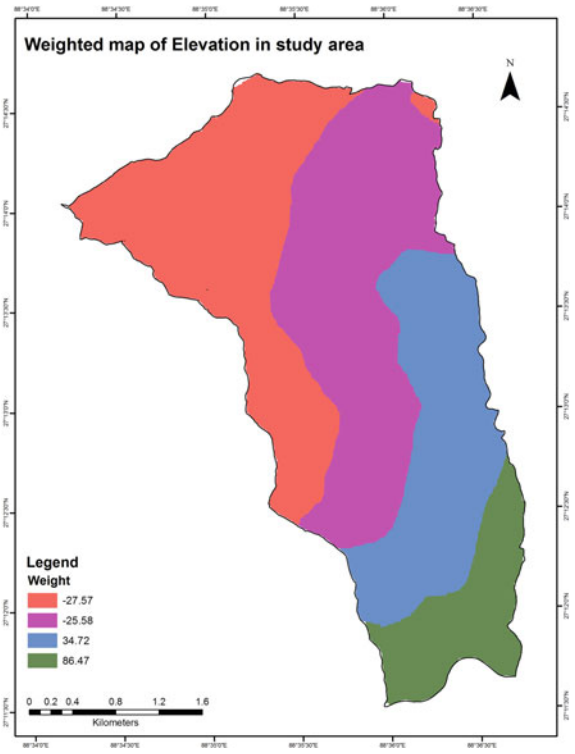

Fig. 17 Weighted map of elevation

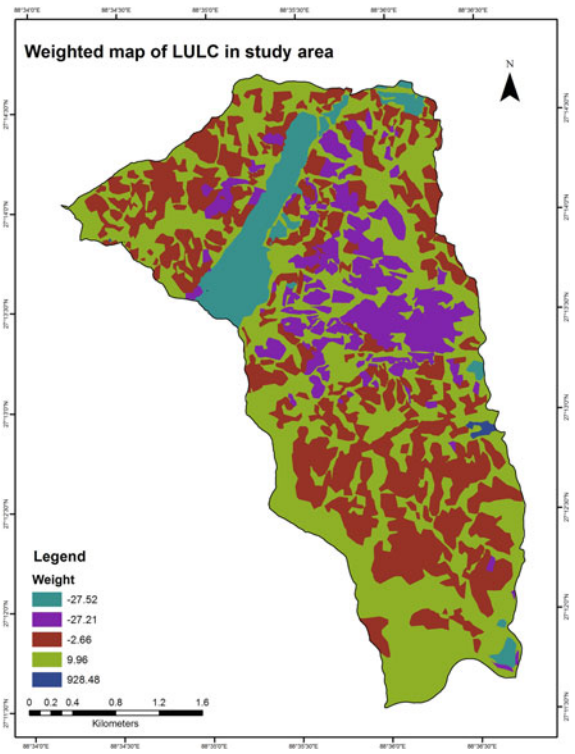

Fig. 18 Weighted map of LULC

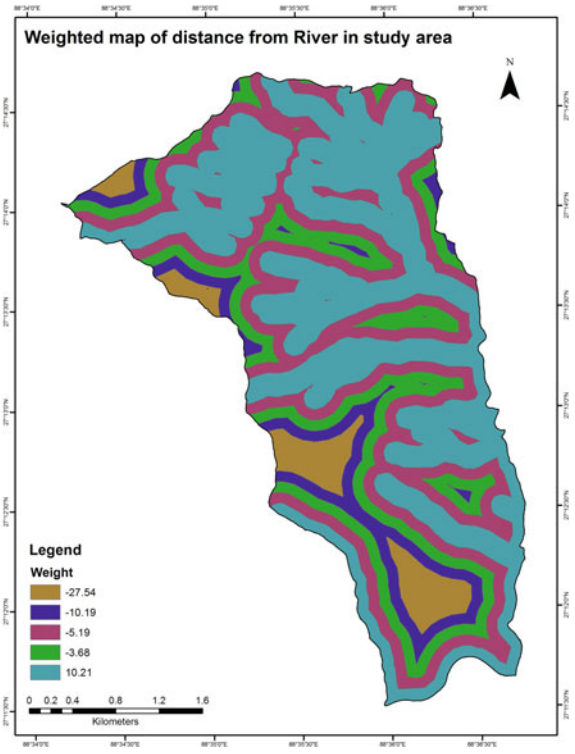

Fig. 19 Weighted map of Dist. From river

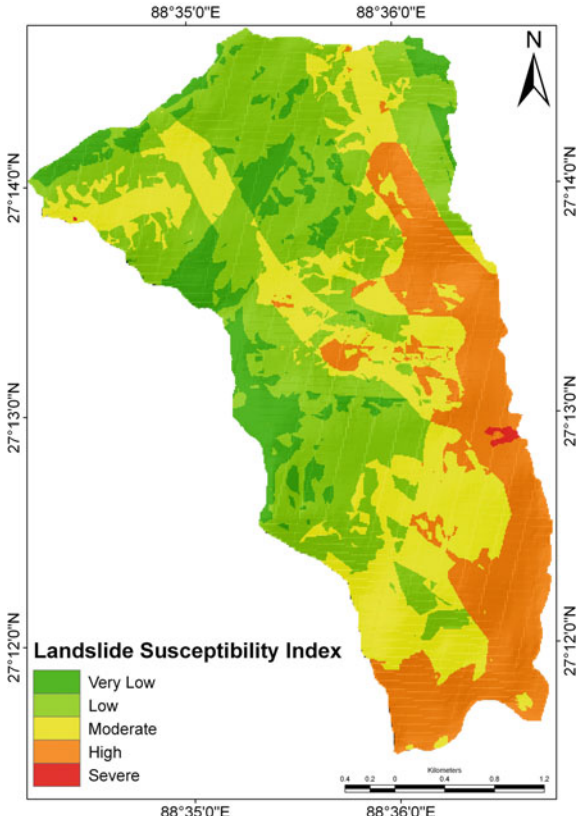

Fig. 20 Landslide susceptibility index

Table 2 Risk categories of zoning landslide map in study area

Susceptibility index	AF_i	AF_i (%)	A_{sci}	A_{sci} (%)	Fri	AF (%)
Very low	2	0.06	13,458	10.98	0.00014861	0.01
Low	66	1.96	47,311	38.58	0.001395024	0.13
Middle	566	16.82	33,852	27.61	0.016719839	1.56
High	2494	74.12	27,753	22.63	0.089864159	8.39
Severe	237	7.04	246	0.20	0.963414634	89.91

6 Results and Conclusion

Layer-wise analysis for the higher frequency ratio can be summarized from Table 3.

AF confirms the accuracy of landslide risk map in the study area. According to data in Table 2 AF is 89.91, 8.39, 1.56, 0.13, and 0.01% respectively in landslide risk classes of Severe, High, Moderate, Low and Very Low. Analysis of the

Table 3 Layer-wise analysis for the higher frequency ratio

Thematic layers	High frequency ratio
Land-use and Land cover	Sinking zone class
Elevation	176–460 ASL
Aspect	Towards south-east
Lithology	Inter banded chlorite-sericite schist/phyllite and quartzite (ptdg1)
Distance from the river	0–100 m Distance
Slope	0°–8.5° and 16.9°–25.3°
Soil	Loamy, skeletal, mesic lithic udorthents
Dist. from the lineaments	0–200 m Distance

land-slide susceptibility shows that 0.20% of the study area falls on severe landslide susceptibility, 22.63% area is under high susceptibility, 27.61 and 10.68% under moderate and low landslide susceptibility respectively. Therefore, more than 50% area in the selected study area falls under moderate to high landslide susceptibility.

The factors responsible for occurrence of the landslide in the study area are inferred as under:

1. Land-use and Land cover: the most vulnerable zone is in the sinking zone class because of high activity of the ground water movement.
2. Elevation of the land: the lower elevations and foothills (174–460 m) are the most susceptible to landslides because of higher probability of occurrence of the ground water and activities of corresponding base-flows.
3. Type and characteristics of the Soil: soil with Loamy, Skeletal, Mesic lithic udorthents class, are another major factor for occurrence of landslide at high and severe risk zone of study area as these soils are characterized sand, silt and small amount of clay. Void ratio of this soil is high resulting in high porosity, as a result movement of ground water in this type of soil is high resulting in occurrence of soil creeping.
4. Lithology: Interbanded chlorite-sericite schist class is also one of the major factors for occurrence of landslide, this is a weak rock which contain smooth surface with low frictional resistance resulting in high probability of occurrence of landslide.
5. Proximity to the Lineaments: the study shows that the area near to the lineament (0–200 m) have the frequency ratio high (1.60) which increases the danger for occurrence of landslide. Similarly area near to the river and streams (0–100 m) has a high frequency ratio (1.37) making this area unstable, because the Himalayan streams and river, during the monsoon have a high potential of carrying the debris and soils which comes in its course, making that area high risk to landslide and debris flow.

7 Conclusion

Landslide hazard zonation helps in identifying strategic points and geographically critical areas prone to landslides and also useful for town planners to plan civil constructions in relatively safe zones in addition to this, environmentally unstable slopes can be given adequate attention by planning suitable control measures.

References

1. Lee, S., Pradhan, B.: Landslide hazard mapping at Selangor, Malaysia using Frequency ratio and logistic regression model. Landslides **4**(1), 33–34 (2007)
2. Rai, P.K., Mohan, K., Kumra, V.K.: Landslide hazard and its mapping using remote sensing and GIS (2014)
3. Avinash, K.G., Ashamanjari, K.G.: A GIS and frequency ratio based landslide susceptibility mapping: Aghnashini river catchment, Uttara Kannada, India. Int. J. Geometrics Geosci. **1**(3), 343–354 (2010)

Chapter 52
Demarcating of Aquifer Zones with Geophysical and Geospatial Approach in South Western parts of Rangareddy District, Telangana State, India

G. Sakram, Sreedhar Kuntamalla, N. Madhusudan, Ratnakar Dhakate and Praveen Raj Saxena

Abstract Aquifer zones are identified by the Geophysical Electrical Resistivity Survey method. This method is useful to delineate the subsurface formations, weathered zone, fracture pattern, etc. An attempt made to identify the subsurface lithology and aquifer zones by geo-electrical resistivity method in parts of Rangareddy District, Telangana State, India. The study area consists of Granites, Basalts of Deccan Traps and Laterites. Electrical soundings have been conducted along 5 profiles across and along the lineaments. In total 148 Vertical Electrical Soundings (VES) were conducted. Integrated studies of interpretation of geomorphologic and geophysical data were used to prepare a groundwater potential map. Geo-electrical parameter and sections have been prepared based on resistivity of the soundings. From the interpretation of results the shallow aquifers is due geomorphologic features and the potential of deeper aquifers is determined by lineaments such as faults and joints.

Keywords Groundwater · Geomorphology · Lineaments and resistivity

G. Sakram (✉) · S. Kuntamalla · N. Madhusudan · P. R. Saxena
Department of Applied Geochemistry, Osmania University, Hyderabad, India
e-mail: drsakramguguloth@gmail.com

S. Kuntamalla
e-mail: sreedhar.kuntamalla@gmail.com

N. Madhusudan
e-mail: madhusudhan.nalla@gmail.com

P. R. Saxena
e-mail: saxenapraveenraj@gmail.com

R. Dhakate
CSIR-National Geophysical Research Institute, Hyderabad, India
e-mail: dhakate.ratnakar@gmail.com

P. J. Rao et al. (eds.), *Proceedings of International Conference on Remote Sensing for Disaster Management*, Springer Series in Geomechanics and Geoengineering,
https://doi.org/10.1007/978-3-319-77276-9_52

1 Introduction

Exploration of groundwater in hard rock terrain is a very challenging and difficult task when the promising groundwater zones are associated with fractured and fissured media. In this environment, the groundwater potentiality depends mainly on the thickness of the weathered/fractured layer overlying the basement. Groundwater is vital for sustaining many streams, lakes, wetlands, and other dependent ecosystems [1]. Global groundwater resources are in a state of crisis [2] because of over abstraction in many semiarid and arid regions and the uncertain consequences of climate change [3] and [4]. Groundwater is an essential part of the hydrological cycle and is a valuable natural resource providing a primary source of water for agriculture, domestic, and industrial uses throughout the world. Nearly half of all drinking water in the world [5] and about 43% of all water effectively consumed in irrigation [6] is sourced from groundwater.

Surface investigations allow us in deciding the information about type, porosity, water content and the density of subsurface creation [1]. Vertical Electrical Sounding (VES) measurements have been carried out using Schlumberger electrode configuration. The Direct Current (DC) electrical resistivity techniques have been widely used to image the geoelectric structure of the shallow subsurface earth [7]. Considerable research work has been carried out by many researchers around the globe on identification of aquifer zones using resistivity method. Lineament analysis followed by resistivity survey is cost effective while studying geomorphologic data [8]. Integrating hydrogeomorphological data with geophysical investigations [9–12] have evolved a simple and rapid approach for demarcation of groundwater potential.

The decrease in precipitation on the area led to the water table lowering. Consequently, many wells, which had been productive, became dry and many trials to drill new producing wells failed. As the recharge became tremendously poor, the water table dropped down and the groundwater flow became almost controlled by the basement structures. Therefore, the present study was suggested to reduce the competitive drilling of dry bore wells, to identify deeper aquifers in the form of fractures, faults, joints, Intertrappean and infra trappean formations by using geoelectrical resistivity method for groundwater exploration and sustainable water supply in the study area.

2 Location of the Study Area

The study area is located in South-Western part of the Rangareddy district at a distance of 90 km from Hyderabad, covering an area of 118,162 ha. Exists between 17.05 to 17.28 North latitudes and 77.76 to 77.99 East longitudes. The average elevation is about 590 m above mean sea level (M.S.L) and falls in the Survey of

India Toposheet no. 56G16 (Fig. 1). Average annual rainfall is about 833 mm. The minimum and maximum temperatures range from 15.1 to 40.9 °C [13].

3 Geological Background

The Prominent geological formations in the study area are Archaean granites, gneisses and the younger Deccan traps. The Archaean crystalline rocks occupy major part of the study area comprising older metamorphic rocks, peninsular gneissic complex (PGC) and younger intrusive rocks. Intrusive of dolerite dyke are visible in the SSW part of the study area. The basaltic flows of the Deccan Traps cover the granitites in the NE and a part in NW part. The geological map of the study area is shown in Fig. 1.

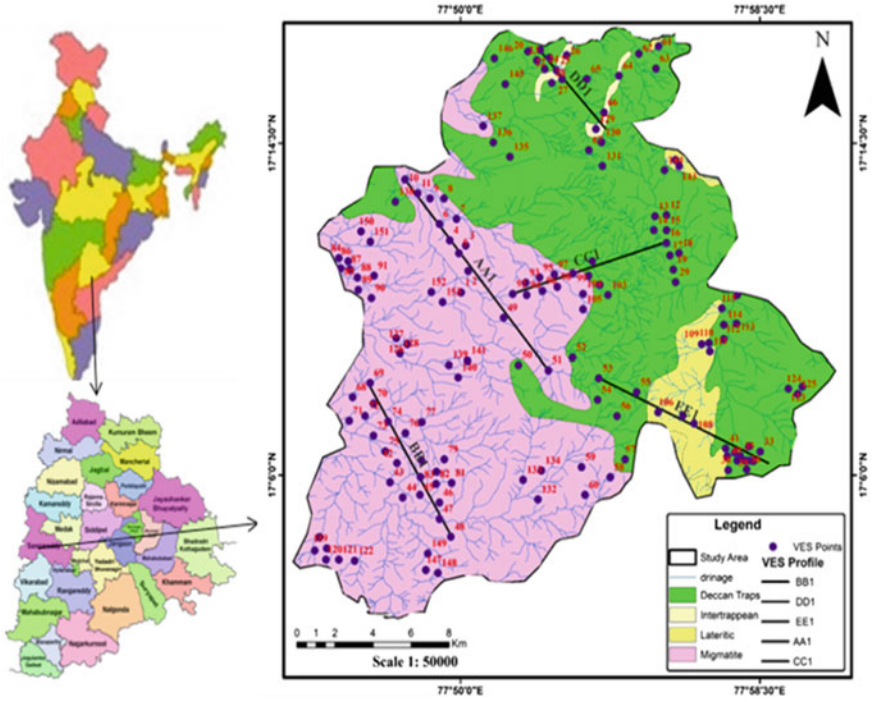

Fig. 1 Location map with drainage and geology

4 Geomorphologic Units

The landforms in the study area are the products of different geomorphic processes such as erosion, deposition, crustal movements coupled with climatic changes operating on the surface. Landforms identified from the satellite images is helpful in identifying favorable zones for groundwater [14]. The specific geomorphologic unit's identified using FCC (False Color Composite) for interpretation are defined and described below. Such studies have been carried out in different parts of India by [8, 15–19]. The various geomorphologic units identified are shown in Fig. 2, and a brief summary of each geomorphologic unit for groundwater prospects is given in Table 1.

4.1 Lineament Density Map

Lineaments are the main features that control the occurrence and movement of groundwater and are the weak zones where accumulation occurs. The lineaments present in the study area have varying dimensions. Based on the concentration and length of lineaments, a lineament density map was prepared. The lineament map as shown in (Fig. 3) was superimposed on a grid map of 1.1 cm by 1.1 cm (2 km by 2 km), and the total length of lineaments passing from each of grid was measured and plotted in the respective grid centers [19]. The values obtained for each grid were interconnected by is lines and based on the concentration and length of lineaments (Table 2).

5 Geophysical Survey

Electrical Resistivity Method is the most widely used method all over the globe because of its efficacy to detect the water bearing layers, besides being simple and inexpensive to carry out the field investigations [20]. The resistivity measurements are normally made by injecting current into the ground through two current electrodes (C1 and C2), and measuring the resulting voltage difference at two potential electrodes (P1 and P2). From the current (I) and voltage (V) values, an apparent resistivity (pa) value is calculated. pa = k V/I; where k is the geometric factor which depends on the arrangement of the four electrodes. The VES data was analyzed with the curve matching using master curves of three, four and five-layer cases for various ratios of absolute resistivity given [21]. The Observed three-layered earth model classified into A, Q, H and K type curves. Similarly four-layer curves as AA, HK, KH, HA, KQ, QH and a five-layer curve HKH identified in the study area.

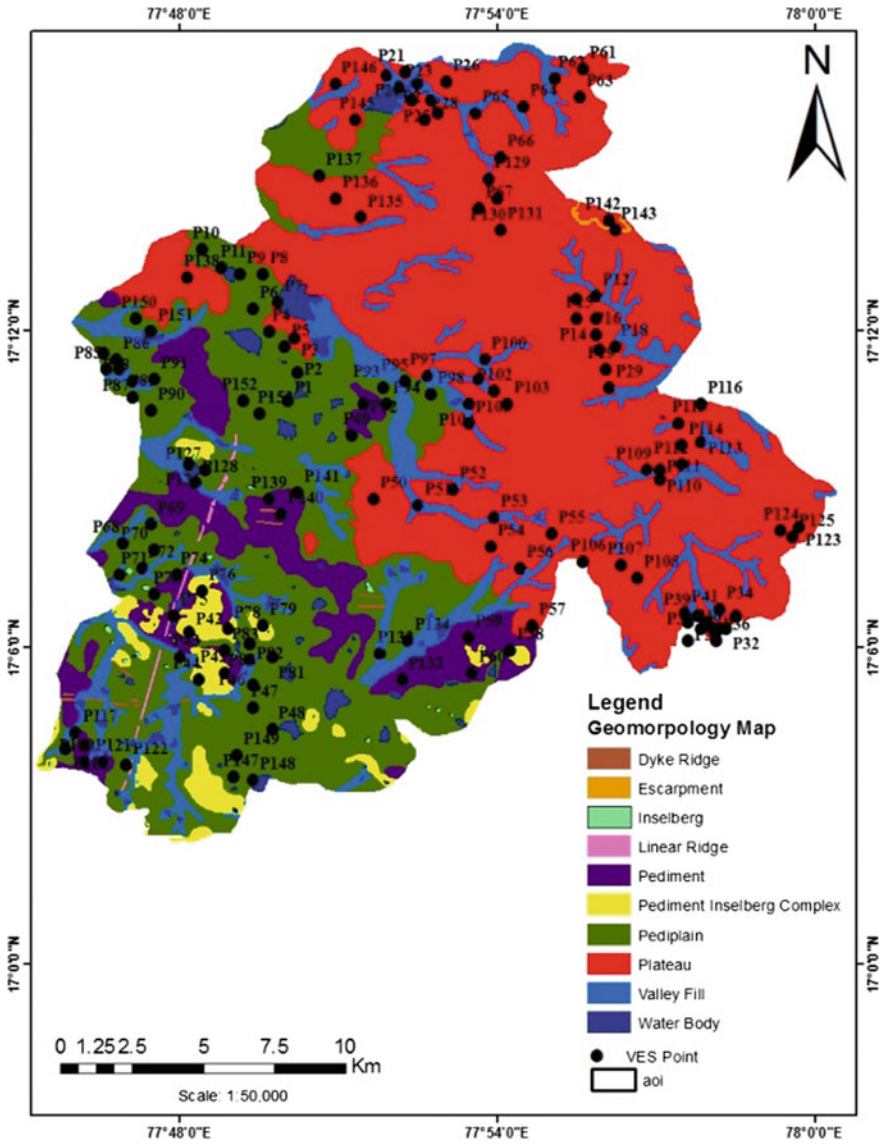

Fig. 2 Geomorphological map with soundings of the study area

6 Results, Discussion and Interpretation

One hundred forty eight vertical electrical soundings (VES) using Schlumberger configuration with 100–150 m half current electrode separation (AB/2) were carried out. The location of these VES is shown along with the geomorphologic map of the

Table 1 Geomorphic units of the study area

Geomorphic units	Area in (ha)	Type of area	Groundwater prospects
Pediplain	44,292	Red brown and black clayey	Good recharge and fracture zone
Plateau (Deccan traps)	47,525	Steep slope and dissected by deep and narrow valleys	Poor recharge zone
Pediment	16,913	Receding hill/mountain slope	Poor recharge zone
PIC (pediment inselberg complex)	1117	Small hills	Poor recharge zone
Inselberg	64.17	Barren, rocky and small hill structure	Very poor groundwater
Valley fills	6004	Unconsolidated material deposited by any weathering agent	Moderate to good recharge zone
Dyke Ridge	55	Isolated flat top hill	Acts as runoff zone/barriers for groundwater movement
Linear Ridge	77	Intrusion of magma into host rocks	Acts as runoff zone/barriers for groundwater movement

area in Fig. 2. The VES data are first interpreted using the curve matching technique [21] and then by Inversion Iteration Method. The interpreted results of VES are given based on resistivity ranges of different sub-surface layers are calculated and given in Table 3. After analyzing the resistivity data interpretation, it is found that the resistivity of the aquifer zone ranges from 10 to 250 Ω m for shallow and deeper aquifer.

Profile line AA1 (Fig. 4) revealed that the line is made up of four layers the first layer is the thin resistive top soil, which is absent at the NE end of the profile line (which is at station 49 and 51), it has resistivity range of 39.2–3975 Ω m and a thickness range of 0.8–10 m. The second layer is interpreted as the weathered rock with lower resistivity value, it has resistivity range of 1.9–95,875 Ω m and a thickness range of 0.2–9.7 m, the thickness is higher at stations P6 and P11 and relatively shallow at station P5. The third layer is interpreted as the fractured rock with low resistivity and massive rock with high resistivity value; it has resistivity range of 31–88,432 Ω m and a thickness range of 2.9–19.9 m. The fourth layer which is infinity also observed a fresh basement rock and has resistivity range of 75.8–4140 Ω m.

The profile BB1 (Fig. 5) revealed that the line is also made up of five layers the first layer is the thin resistive top soil, it has resistivity range of 19.3–2820 Ω m and a thickness range of 0.8–16 m. The second layer is interpreted as the weathered rock with lower resistivity value; it has resistivity range of 3.9–344 Ω m and a thickness range of 0.4–12.3 m. The third layer is interpreted as the fractured rock with low resistivity and massive rock with high resistivity value; it has resistivity range of 30.7.

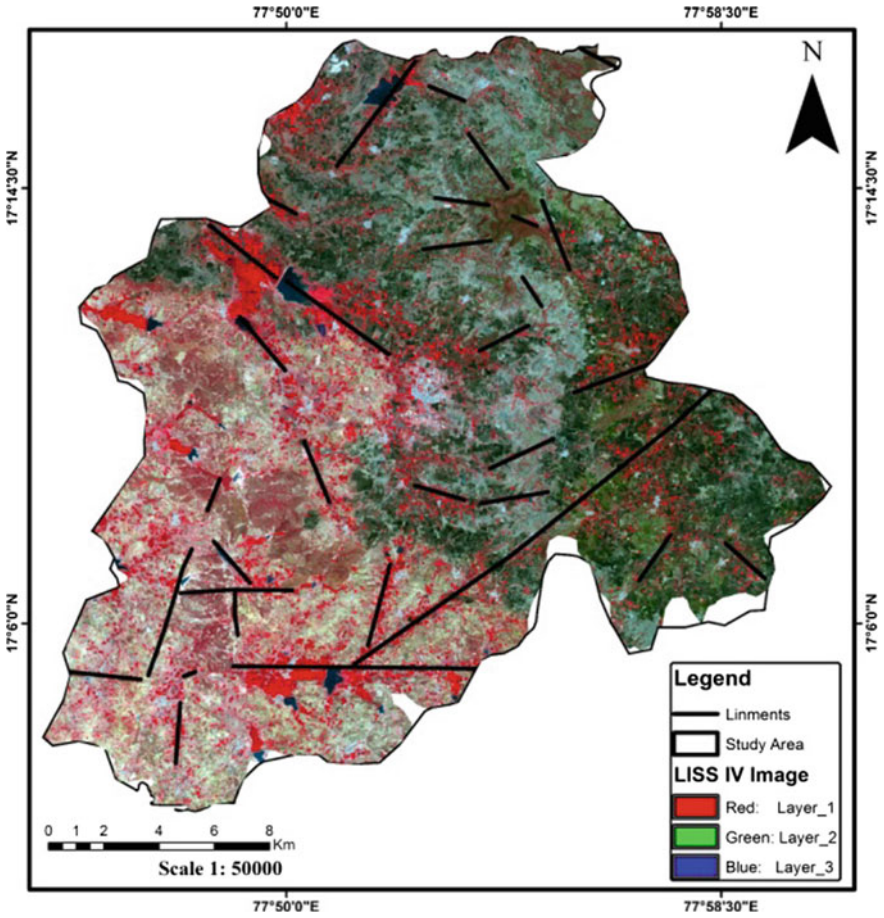

Fig. 3 Lineament map of the study area

Table 2 Criteria for selecting groundwater prospects map using lineament density and shallow and deep aquifer thickness

Sl. no.	Lineament density (m/m^2)	Weathering thickness (m)	Groundwater prospects
1	>1.5	>30	Very good
2	1.0–1.5	20–30	Good
3	0.5–1.0	10–20	Moderate
4	<0.5	<10	Poor

The profile line CC1 (Fig. 6) revealed that the line is made up of four layers the first layer is the thin resistive top soil, it has resistivity range of 234–6865 Ω m and a thickness range of 3.15–17.4 m. The second layer is interpreted as the weathered rock with lower resistivity value; it has resistivity range of 12.3–44,963 Ω m and a

Table 3 Resistivity ranges of different sub-surface formation

Resistivity ranges (Ω m)	Sub-surface/lithology formation
0–20	Clayey layer
20–50	Hard murram
50–120	Semi-weathered to fractured rock
100–250	Fractured rock
>250	Hard rock

Source Ramanuja Chary [22]

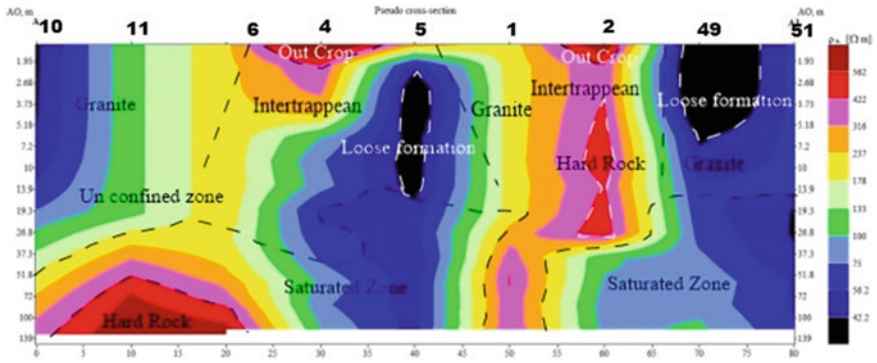

Fig. 4 Profile AA1 in the study area

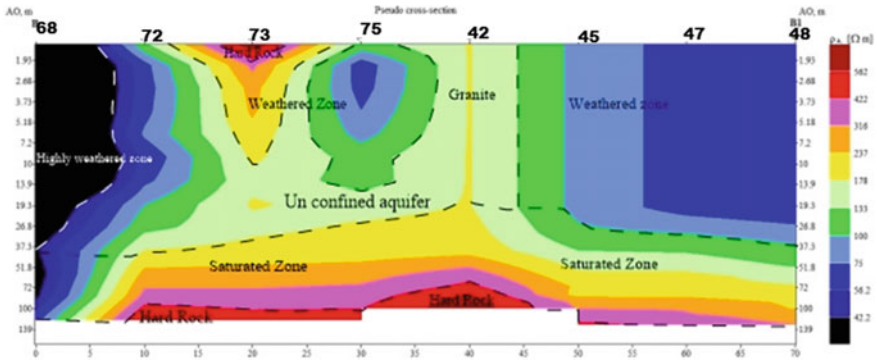

Fig. 5 Profile BB1 in the study area

thickness range of 1.65–48 m. The third layer is interpreted as the fractured rock with low resistivity and massive rock with high resistivity value; it has resistivity range of 6.18–4559 Ω m. The fourth layer which is to infinity also suggests a fresh basement rock and has resistivity range of 21,089 Ω m.

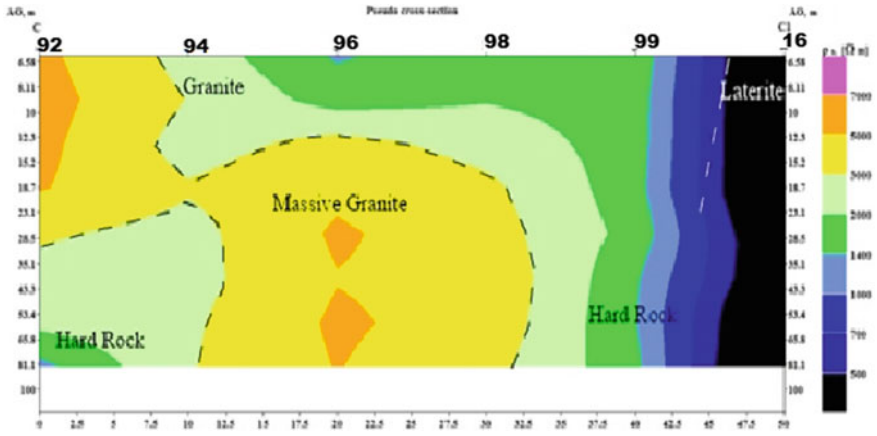

Fig. 6 Profile CC1 in the study area

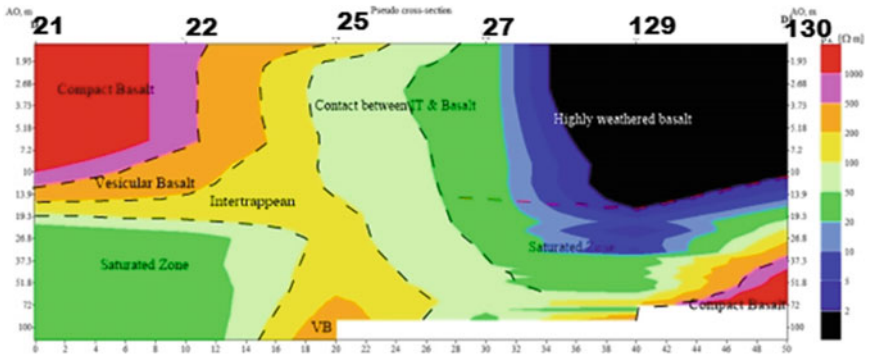

Fig. 7 Profile DD1 in the study area

The profile line DD1 (Fig. 7) revealed that the line is made up of four layers the first layer is the thin resistive top soil, it has resistivity range of 5.75–1505 Ω m and a thickness range of 1.5–56 m. The second layer is interpreted as the weathered rock with lower resistivity value; it has resistivity range of 23.3–10,234 Ω m and a thickness range of 5–218 m. The third layer is interpreted as the fractured rock with low resistivity and massive rock with high resistivity value; it has resistivity range of 19.6–45,867 Ω m. The fourth layer which is to infinity also suggests a fresh basement rock and has resistivity range of 512 Ω m.

The profile line EE1 (Fig. 8) revealed that the line is made up of four layers the first layer is the thin resistive top soil, it has resistivity range of 15.1–305 Ω m and a thickness range of 9.1–29.9 m. The second layer is interpreted as the weathered rock with lower resistivity value, it has resistivity range of 6.82–4153 Ω m and a thickness range of 2.2–48 m. The third layer is interpreted as the fractured rock

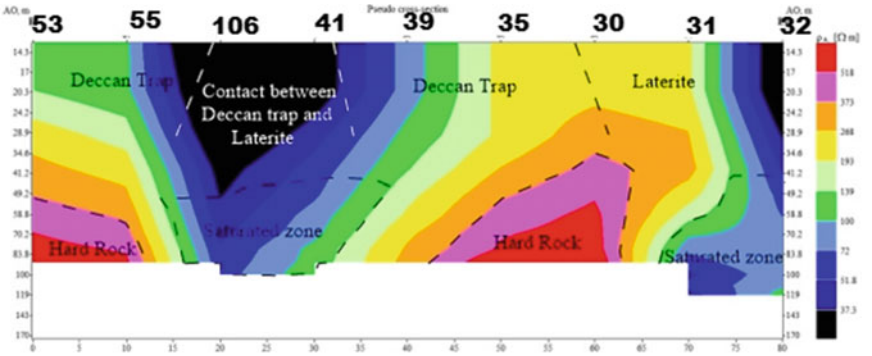

Fig. 8 Profile EE1 in the study area

with low resistivity and massive rock with high resistivity value; it has resistivity range of 22.2–150,000 Ω m and a thickness range of 5–7.5 m. The fourth layer which is to infinity also suggests a fresh basement rock and has resistivity range of 2319–22,732 Ω m.

7 Conclusion

Remote sensing data used to interpret the different geomorphological units including structures like lineaments to identify the zones of groundwater prospects. The various geomorphic units are classified in terms of groundwater prospects, as poor, moderate, good and very good. From VES, it is found that the shallow and deeper aquifer thickness varies spatially and is to some extent controlled by structures. Aquifer thickness is high where the lineament density is high, and such regions possess better groundwater potential. The geomorphic units like valley fills show high degree of weathering. By carrying out comparative study of geomorphic units, lineaments and vertical electrical surveys, one can achieve better results for future groundwater prospects.

8 Ground Water Prospect Map

The groundwater prospects are complicated in the study area where different rock formation present. The deeper aquifers in hard rock terrains are potential only when they are fed by fractures. The top two layers act as an unsaturated zone, allowing the downward passage of water and contaminants to the aquifer. The aquifer zone is primarily unconfined, and hence, the availability of water largely depends on the aerial recharge. Groundwater table is relatively flat, except at the pumping regions.

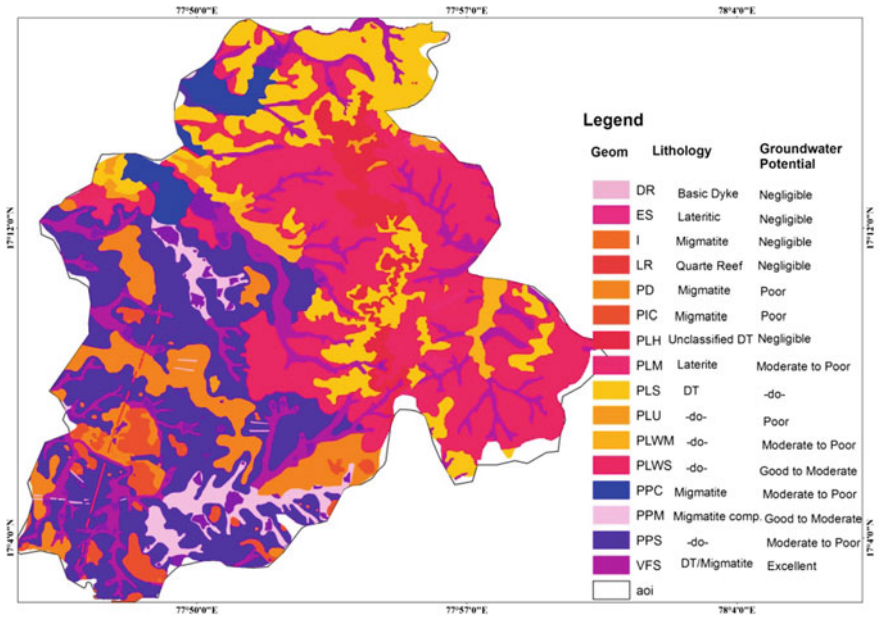

Fig. 9 Groundwater potential map of the study area

The area experience severe drought conditions and shortage for drinking purpose in the dry seasons. Shallow dug wells, which tap weathered zone, with transmissivity, but they are limited in number. The groundwater prospects in the plateau region of the study area are poor to moderate. Based on lineament density and shallow and deeper aquifer thickness, the groundwater potential map has been classified into four major groups [19] (Table 2).

This new groundwater prospect map shown in (Fig. 9) reveals that areas where the lineament density is high possess thick aquifer thickness zones and are good potential regions for prospecting groundwater.

Acknowledgements The authors are thankful to University Grants Commission (BSR) and (UGC-PDF), New Delhi for pursing this program and for providing financial support and also thankful to the Editor of the journal for his kind support and encouragement.

References

1. Kurien E.K., Sheeja P.S., Ritu Prem, Shazna K.: A hydro-geophysical investigation of groundwater potential. Int. J. Eng. Res. Dev. **9**(4), 30–35; e-ISSN: 2278-067X, p-ISSN: 2278-800X, www.ijerd.com, (December 2013) (2003)
2. Famiglietti, J.S.: The global groundwater crisis. Nat. Clim. Change **4**, 945–948 (2014)
3. Climate Change Effects on Groundwater Resources: A Global Synthesis of Findings and Recommendations. CRC Press, Taylor & Francis Group, London (2012)

4. Reddy, M., Sakram, G.: Climate change and water resources: implications and mitigation. Int. J. Recent Sci. **5**(1), 201–204 (2014)
5. World Water Assessment Programme: The United Nations World Water Development Report 3: Water in a Changing World. 349, UNESCO (2009)
6. Siebert, S., et al.: Groundwater use for irrigation—a global inventory. Hydrol. Earth Syst. Sci. **14**, 1863–1880 (2010)
7. Balasubramanian, A., Siddalingamurthy, S., Nagaraju, D.: Studies of groundwater exploration. In: Chamarajanagar Taluk, Using Electrical Resistivity Techniques, Chamarajanagar District, Karnataka, South India, **4**(2) May–August, (2014)
8. Dhakate, R., Singh, V.S., Negi, B.C., Chandra, S., Rao, A.V.: Geomorphological and geophysical approach for locating favorable groundwater zones in granitic terrain, Andhra Pradesh, India. J. Environ. Manag. **88**, 1378–1383 (2008)
9. Srivastava, P.K., Bhattacharya, A.: Groundwater assessment through an integrated approach using remote sensing, GIS and resistivity techniques: a case study from a hard rock terrain. Int. J. Remote Sens. **27**(20/20), 4599–4620 (2006)
10. Sakram, G., Laxman Kumar, D., Sundaraiah, R., Rajitha, S., Ramana Kumar, M., Raj Saxena, P.: Application of remote sensing, GIS and geophysical techniques in groundwater exploration in Karanja Vagu Watershed, Medak District, Andhra Pradesh. Int. J. Earth Sci. Eng. **06**(02), 123–129; ISSN 0974-5904 (2013); (01) April 2013
11. Shahid, S., Nath, S.K.: GIS integration of remote sensing and electrical sounding data for hydrogeological exploration. J. Spat. Hydrol. **2**(1), 1–12 (2002)
12. Teeuw, R.M.: Groundwater exploration using remote sensing and a low-cost geographical information system. Hydrogeol. J. **3**, 21–30 (1999)
13. Ground Water Information of Rangareddy District, Andhra Telangana, CGWB (2013)
14. Thornburry, W.D.: Principles of Geomorphology. Willey, New York (1969)
15. Haridas, V.K., Chandrasekaran, V.A., Kumaraswamy, K., Rajendran, S., Unnikrishnan, K.: Geomorphological and lineament studies of Kanjamalai using IRS-1 data with special reference to groundwater potentiality. Trans. Inst. Indian George **16**(1), 35–41 (1994)
16. Dubey, N., Trivedi, R.K.: Application of LANDSAT TM imagery and aerial photographs for evaluating the hydrogeological conditions around Damoh, M.P. Bhu-Jal New Faridabad **9**(2), 1–4 (1994)
17. Lokesh, K.N., Narayana, S.K.: Geomorphological and hydrogeo-chemical studies of Pangala River basin (D.K), Karnataka. Hydrol. J. **19**(1), 33–43 (1996)
18. Palanivel, S., Ganesh, A., Vasanthakumaran, T.: Geohydrological evaluation of upper Agniar and Vellar basins, Tamilnadu: an integrated approach using remote sensing, geophysical and well inventory data. J. Ind. Soc. Remote Sens. **24**(3), 153–168 (1996)
19. Dhakate Ratnakar, D.K., Chowdhary, V.V.S., Gurunadha Rao, R.K., Tiwary, Sinha, A.: Geophysical and geomorphological approach for locating groundwater potential zones in Sukinda chromite mining area. Environ. Earth Sci. 66, 2311–2325 (2011); (2012)
20. Zohdy, A.A.R., Eaton, G.P., Mabey, D.R.: Application of surface geophysics to groundwater investigation. Techniq. Water Resour. Investig. U.S. Geol. Surv. 116 pp (1974)
21. Orellana, E., Mooney, H.M.: Master tables and curves for vertical electrical sounding over layered structures. Inteciencis, Madrid (1966)
22. Ramanuja Chary, K.R.: Geophysicl Techniques for Groundwater Exploration, p. 85. Professional Book Publisher (2012)

Chapter 53
Estimating Aquifer Characteristics by Conducting Pumping Tests: A GIS and Remote Sensing Approach in South Western Part of Mahbubnagar District, Telangana State, India

Sreedhar Kuntamalla, G. Sakram, N. Madhusudhan and E. Srinivas

Abstract A method to estimate aquifer characteristics has been developed by conducting pumping tests. The method requires long-duration pumping tests on a confined aquifer with significant seasonal water-table fluctuations. The interpretation of pumping tests under initial conditions provides information on the change in hydrodynamic parameters in relation to the initial water-table level. Aquifer characteristics like Transmissivity, permeability and storage coefficient were determined by conducting pumping tests. The transmissivity linearly decreases compared with the initial water level, suggesting a homogeneous distribution of hydraulic conductivity with depth. The hydraulic conductivity is estimated from the slope of this linear relationship. The extrapolation of the relationship between transmissivity and water level provides an estimate of the aquifer thickness. The hydraulically active part of the aquifer is located in both the weathered and the underlying densely fractured zones of the crystalline basement. However, no significant relationship is found between the aquifer storage coefficient and initial water level.

Keywords Aquifer · Groundwater hydraulics · Pumping test · Remote sensing and GIS

S. Kuntamalla (✉) · G. Sakram · N. Madhusudhan · E. Srinivas
Department of Applied Geochemistry, University College of Science, Osmania University, Hyderabad 500007, India
e-mail: sreedhar.kuntamalla@gmail.com

G. Sakram
e-mail: drsakramguguloth@gmail.com

N. Madhusudhan
e-mail: madhusudhan.nalla@gmail.com

E. Srinivas
e-mail: srinivase4@gmail.com

P. J. Rao et al. (eds.), *Proceedings of International Conference on Remote Sensing for Disaster Management*, Springer Series in Geomechanics and Geoengineering,
https://doi.org/10.1007/978-3-319-77276-9_53

1 Introduction

Pumping tests are an important method for studies of hydraulic aquifer properties. Stressing the aquifer, by pumping water, and monitoring resultant water table drawdown in unconfined aquifers or the potentiometric surface in confined aquifers, important hydrogeologic parameters can be obtained at the scale of water usage. These parameters include transmissivity and storage coefficient as well as derived quantities such as permeability in some cases. At smaller scales, Darcy-type tests may be conducted, for example, core analyses [6, 12, 16]. At larger scales, numerical models are frequently constructed to constrain hydrogeologic parameters [1, 2, 7, 9–11, 15].

Considerable research efforts favor interpretation of pumping test data by employing hydraulic tomography and inverse numerical modeling [17], although a discussion of the limitations of these methods has begun [3]. At sites with limited numbers of wells, and/or wells with relatively short well screens, the data required for hydraulic tomography may be impractical to gather and may be beyond the scope of the investigation. Although analytical models that account for unconfined conditions, partial penetration, and so on are available, classic Theis curve matching [13] and, in particular, Jacob distance-drawdown [4, 5] relationships are still widely used for many field applications [14].

The aim and objective of this paper is to estimate the aquifer characteristic from pumping test carried out in the study area.

2 Location of the Study Area

The study area is located in Gangapur Village, South-western part of Mahabubnagar district, Telangana State, 100 km away from Hyderabad city, it lies on latitudes 16.790 and 16.795 North and longitude 78.191 and 78.199 East falling in survey of India toposheet number 56 L/1 (Fig. 1). Remote sensing (RS) and geographic information system (GIS) has proven to be efficient, rapid and cost effective technique producing valuable data on geology, geomorphology, lineaments and slope as well as a systematic integration of these data for exploration and delineation of groundwater potentials zones [8]. The study area boundary is super imposed on the remote sensing data of geo referenced and merged data of IRS-P6 LISS-IV during 2012 (Fig. 1) in the digital mode obtained from the National Remote Sensing Centre (NRSC), Hyderabad. The spatial resolutions of LISS-IV data is 5.8 m.

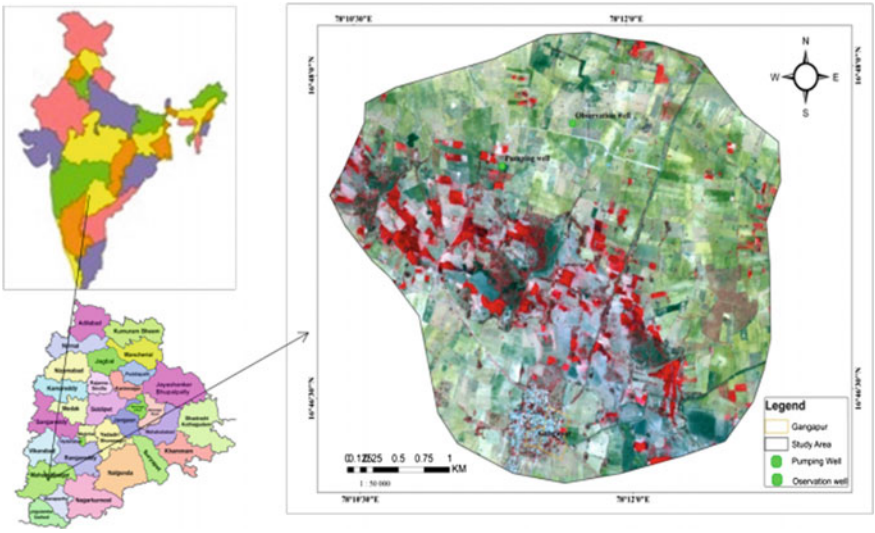

Fig. 1 Location map of study area (LISS-IV Image from NRSC, Hyderabad, during 2012)

3 Geology of the Study Area

Geologically the study area is predominantly covered by peninsular gneissic complex, which is predominant rock type of Archaean, is dominant in Telangana State. It is intruded by Clospet granite and dolerite dykes.

4 Methodology

A Pumping test is conducted mainly; (i) To determine well characteristics and to obtain information about the performance and efficiency of the well being pumped and; (ii) To determine the aquifer characteristics. There are two main types of tests conducted for achieving the above mentioned objectives.

(i) Step Draw down Tests and
(ii) Aquifer performance tests.

The Step draw down test provides information about the well characteristics where as the aquifer performance test helps in determination of hydraulic properties of the aquifer. The procedure of method is to evaluate the properties of the aquifer.

The analysis of pump test data has been made using the Cooper–Jacob straight line method for the determination of aquifer parameters. A semi-logarithmic graph of values of scattered drawdown and residual drawdown data are often interpreted as describing straight lines from different directions. The procedure for determination and finding parameters of confined aquifer outlined as follows:

Plotted the field measurements on semi-logarithmic coordinate paper in which the water levels from ground level (GL) in metres is plotted along the linear y-axis scale and the time (t) in minutes since pumping started is plotted along the logarithmic x-axis scale for step draw down test.

Plotted (S/Q), where "S" is drawdown and "Q" is the discharge along the linear y-axis scale and the discharge (Q) in litre per minute (lpm) is plotted along the logarithmic x-axis scale for the step draw down test, this forms a linear equation in S/Q and Q, so if S/Q is plotted against Q the resultant graph is a straight line with slope C and intercept B. Plotted residual drawdown in (m) on semi-logarithmic coordinate paper along the linear y-axis scale and the time (T/T1) in minutes (min) is plotted along the logarithmic x-axis scale for the step drawdown test. Determine the slope of the straight line per one log cycle each of one drawdown test (Δs) and recovery test ($\Delta s'$).

Plotted the constant discharge measurements for aquifer performance test on semi-logarithmic coordinate paper in which the drawdown (S) is plotted along the linear y-axis scale and the time (t) since pumping started is plotted along the logarithmic x-axis scale.

Plotted residual drawdown in (m) for aquifer performance test on semi- logarithmic coordinate paper along the linear y-axis scale and the time (T/T1) in minutes (min) is plotted along the logarithmic x-axis scale. Determine the slope of the straight line per one log cycle each of one drawdown test (Δs) and recovery test ($\Delta s'$). Extend the straight line of the drawdown test only until it intercepts the time axis where, (s) equal zero and after that read the value of (t_o).

The computation of the aquifer parameters Transmissivity 'T', Storage coefficient 'S' and specific capacity can be performed in the following formulas as follows:

$$T = \frac{2.303Q}{\mathbf{4}\pi\Delta\mathbf{S}} \tag{1}$$

$$S = \frac{\mathbf{2.25Tt_o}}{\mathbf{r^2}} \tag{2}$$

$$C = \frac{Q}{S} \tag{3}$$

$$K = \frac{T}{m} \tag{4}$$

where: Q = pumping rate in m^3/h, T = Coefficient of transmissibility or Transmissivity, Δs = Slope of the curve for one log cycle, S = Coefficient of storage, t_o = time value in days of the intercept of the straight line portion of the drawdown, r = distance in meters from the discharging well, C = specific capacity, S = drawdown in pumping well, K = Hydraulic conductivity or Permeability, m = thickness of the aquifer.

The ultimate draw down in a well measured at the designed rate Q of continuing pumping for a given period is different from theoretical draw down due to well losses.

$Sw = BQ + CQ^n$ (Rorabaugh's Method) where n = 1.5–3.5 depending on the values of Q.

Sw/Q = B + CQ (Jacob's Straight Line Method).

where: B is aquifer loss coefficient and C is well loss coefficient.

The plot of Sw/Q versus Q gives a straight line. The intercept Sw/Q gives formation loss coefficient slope gives the C well loss coefficient. The efficiency of the well is calculated by well loss divided the draw down BQ/Sw.

5 Results and Discussion

The pumping test exercise was carried out for one production well in the study area. The total depth of the bore well was 83 m; static water level measured as 12.36 (GL-m) metres from ground level, 4 inches submersible pump was placed at 60 m below ground level with 3HP was used to perform the test.

5.1 Step Drawdown Test

Four step drawdown tests for two hour each were performed to examine the effect of turbulent and lamina flow of various pumping rates of the production well followed by a recovery test for 2 h was conducted in the study area, Table 1. First step was pumped at 5400 l/h, with a dynamic water level of 36.62 m leaving a drawdown down of 24.26 m and specific capacity of 3.7 (l/min/m). Second step at 7200 l/h, with a dynamic water level of 42.94 m leaving a drawdown down of 6.32 m and specific capacity of 19 (l/min/m). Third step at 9000 l/h, with a dynamic water level

Table 1 Step drawdown data of the production well

Time (min)	1st step		2nd step		3rd step		4th step	
	WL (GL-m)	Draw down m	WL (GL-m)	Draw down m	WL (GL-m)	Draw down m	WL (GL-m)	Draw down m
0	12.36	0.00	36.62	24.26	42.94	30.58	51.20	38.84
0.5	13.78	1.42	36.89	24.53	43.00	30.64	51.22	38.86
1	14.26	1.90	36.97	24.61	43.17	30.81	51.22	38.86
1.5	14.73	2.37	37.14	24.78	43.29	30.93	51.22	38.86
2	15.44	3.08	37.27	24.91	43.40	31.04	51.23	38.87
2.5	15.88	3.52	37.44	25.08	43.50	31.14	51.24	38.88
3	16.36	4.00	37.60	25.24	43.68	31.32	51.24	38.88
4	17.34	4.98	37.94	25.58	43.76	31.40	51.24	38.88
5	18.20	5.84	38.28	25.92	43.89	31.53	51.25	38.89
6	19.03	6.67	38.57	26.21	43.99	31.63	51.25	38.89
8	20.54	8.18	39.08	26.72	44.21	31.85	51.25	38.89
10	22.02	9.66	39.46	27.10	44.47	32.11	51.25	38.89
12	23.49	11.13	39.81	27.45	44.74	32.38	51.25	38.89
14	24.54	12.18	40.09	27.73	45.01	32.65	51.25	38.89
18	26.40	14.04	40.57	28.21	45.72	33.36	51.25	38.89
24	28.52	16.16	40.68	28.32	46.70	34.34	51.25	38.89
30	30.55	18.19	40.89	28.53	47.49	35.13	51.25	38.89
40	33.03	20.67	41.14	28.78	48.75	36.39	51.25	38.89
50	34.17	21.81	41.83	29.47	49.51	37.15	51.25	38.89
60	35.05	22.69	42.13	29.77	50.15	37.79	51.25	38.89
80	35.77	23.41	42.51	30.15	50.80	38.44	51.25	38.89
100	36.24	23.88	42.78	30.42	51.13	38.77	51.25	38.89
120	36.62	24.26	42.94	30.58	51.20	38.84	51.25	38.89

Note WL water level, *GL-m* from ground level in metres

of 51.20 m leaving a drawdown down of 8.26 m and specific capacity of 18.2 (l/min/m) and fourth step at 10,800 l/h, with a dynamic water level of 51.25 m leaving a drawdown down of 0.05 m and specific capacity of 3600 (l/min/m) (Graphs 1, 2, 3 and 4).

Values for B and C in the step drawdown equation are determined from the graph where S/Q plotted against Q.

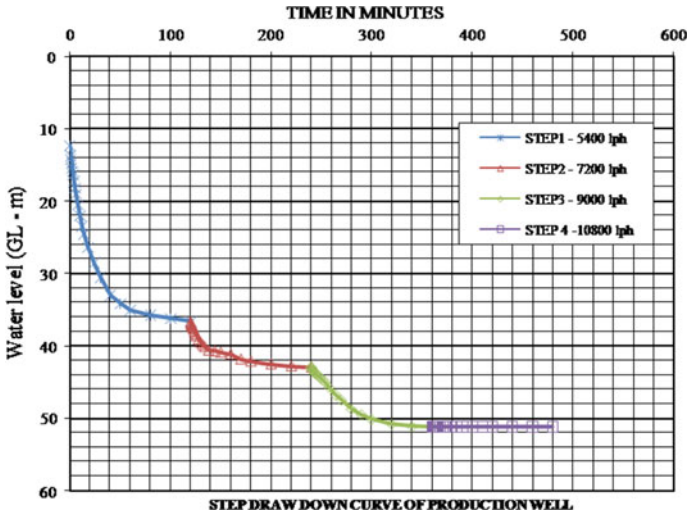

Graph 1 Showing the step drawdown cures

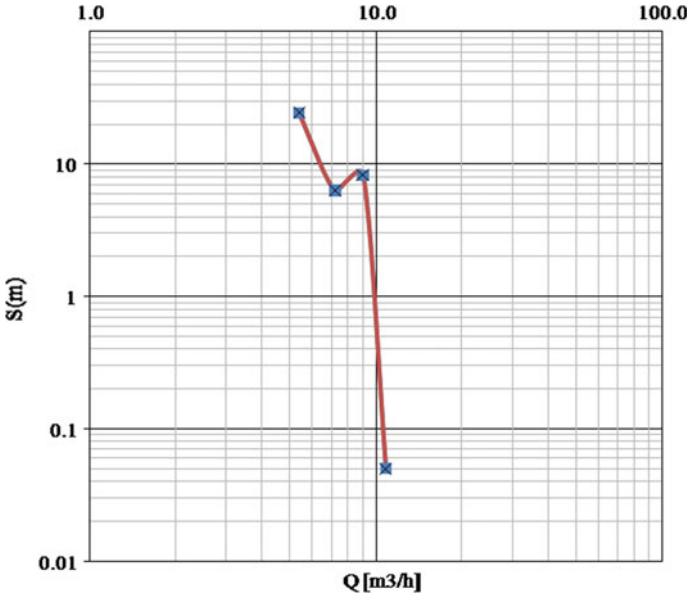

Graph 2 Showing the S-Q curve

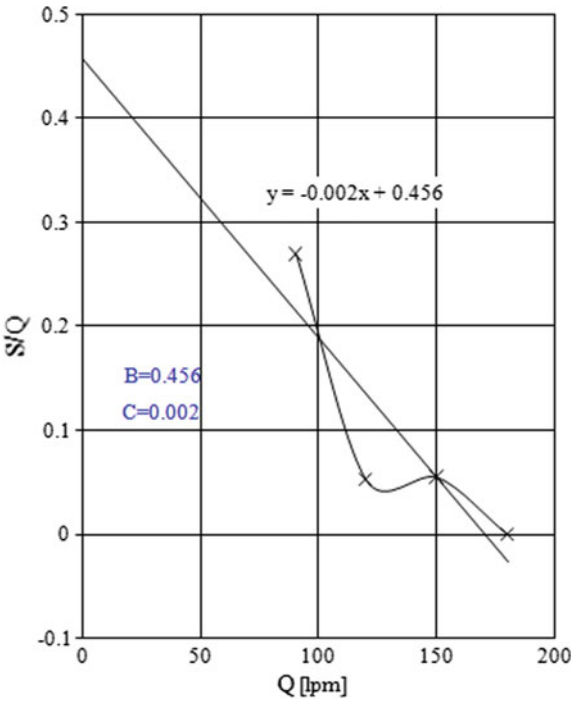

Graph 3 Showing the S/Q curve

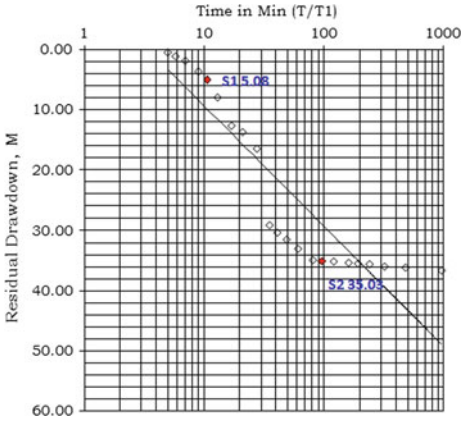

Graph 4 Showing the residual drawdown for step drawdown test

5.2 Residual Drawdown for Step Drawdown Test

See Tables (2 and 3).

.Table 2 Residual data of the production well

Time since pump started in min. (T)	Time since pump stopped (T1)	T/T1	Water level	Residual draw down	Time since pump started in min. (T)	Time since pump stopped (T1)	T/T1	Water level	Residual draw down
480	0		51.25	0	492	12	41	42.69	30.33
480.5	0.5	961	49	36.64	494	14	35.29	41.44	29.08
481	1	481	48.51	36.15	498	18	27.67	28.8	16.44
481.5	1.5	321	48.35	35.99	504	24	21	26.03	13.67
482	2	241	47.95	35.59	510	30	17	24.97	12.61
482.5	2.5	193	47.85	35.49	520	40	13	20.24	7.88
483	3	161	47.71	35.35	530	50	10.6	17.44	5.08
484	4	121	47.5	35.14	540	60	9	15.9	3.54
485	5	97	47.39	35.03	560	80	7	14.14	1.78
486	6	81	47.27	34.91	580	100	5.8	13.39	1.03
488	8	61	45.38	33.02	600	120	5	12.74	0.38
490	10	49	43.85	31.49					

Table 3 Well Loss estimation from step drawdown test

Well losses	
Aquifer loss coefficient (B)	0.456
Well loss coefficient (C)	0.002
Effective drawdown (Se)	32.82 m
(Here 5 m taken as a seasonal variation)	

5.3 Aquifer Performance Test

A large number of analytical methods are available for analyzing aquifer pumping test data such as Cooper–Jacob [4], Theis [13]. These methods are the best agreement to estimate average aquifer parameters. To illustrate the validity of the proposed method, a well penetrated a confined aquifer is pumped at a uniform rate constantly at 10.8 m^3/h for 64 h followed by a recovery test of about 100 min. As shown on the pumping test data, after 3840 h of continuous pumping the maximum drawdown measured was 36.95 m. The evaluated Transmissivity value of the pumping test data on the semi log graph curve shows 3 (l/min/m), whereas the recovery test shows a value of 1.93 (l/min/m). Discharge measurements were observed that after 150 min of pumping the drawdown started to stabilize as illustrated by subsequent measurements.

The initial drawdown of 2.23 m is actually casing storage discharged before the aquifer respond. The measurements of the Recovery data shows the 100% after 80 min of pump stoppage. The Transmissivity values for the pumping test and recovery shows an excellent aquifer respond. Drawdown (s) during the pumping period (t) is measured in an observation well 200 m away (Fig. 1). The water levels in the observation well not sharing the same aquifer of pumped well there is no fluctuation of water, the level remained constant, since it is quite far away from the well. The pump was shut down after 3840 min; thereafter, measurements of residual drawdown (s) and recovery time (t) were taken (Tables 4 and 5; Graphs 5 and 6).

Table 4 Constant discharge data of the production well

Time since pumping started in (minutes)	Water level from GL m	Draw down (m)	Time since pumping started in (minutes)	Water level from GL m	Draw down (m)
0	14.24	0	1320	51.19	36.95
0.5	16.47	2.23	1380	51.19	36.95
1	17.46	3.22	1440	51.19	36.95
1.5	18.41	4.17	1500	51.19	36.95
2	19.32	5.08	1560	51.19	36.95
2.5	20.14	5.9	1620	51.19	36.95
3	21.11	6.87	1680	51.19	36.95
4	23.16	8.92	1740	51.19	36.95

(continued)

Table 4 (continued)

Time since pumping started in (minutes)	Water level from GL m	Draw down (m)	Time since pumping started in (minutes)	Water level from GL m	Draw down (m)
5	24.69	10.45	1800	51.19	36.95
6	26.6	12.36	1860	51.19	36.95
8	29.33	15.09	1920	51.19	36.95
10	33.29	19.05	1980	51.19	36.95
12	36.02	21.78	2040	51.19	36.95
14	38.23	23.99	2100	51.19	36.95
18	40.59	26.35	2160	51.19	36.95
24	43.05	28.81	2220	51.19	36.95
30	44.45	30.21	2280	51.19	36.95
40	46.16	31.92	2340	51.19	36.95
50	48.76	34.52	2400	51.19	36.95
60	50.45	36.21	2460	51.19	36.95
80	51.16	36.92	2520	51.19	36.95
100	51.18	36.94	2580	51.19	36.95
120	51.18	36.94	2640	51.19	36.95
150	51.19	36.95	2700	51.19	36.95
180	51.19	36.95	2760	51.19	36.95
240	51.19	36.95	2820	51.19	36.95
300	51.19	36.95	2940	51.19	36.95
360	51.19	36.95	3000	51.19	36.95
420	51.19	36.95	3060	51.19	36.95
480	51.19	36.95	3120	51.19	36.95
540	51.19	36.95	3180	51.19	36.95
600	51.19	36.95	3240	51.19	36.95
660	51.19	36.95	3300	51.19	36.95
720	51.19	36.95	3360	51.19	36.95
780	51.19	36.95	3420	51.19	36.95
840	51.19	36.95	3480	51.19	36.95
900	51.19	36.95	3540	51.19	36.95
960	51.19	36.95	3600	51.19	36.95
1020	51.19	36.95	3660	51.19	36.95
1080	51.19	36.95	3720	51.19	36.95
1140	51.19	36.95	3780	51.19	36.95
1200	51.19	36.95	3840	51.19	36.95
1260	51.19	36.95			

Table 5 Recovery data for constant pumping of the production well

Time since pump started (T)	Time since pump stopped (T1) in (minutes)	T/T1	Water level	Residual draw down
3840	0	0.00	51.19	0.00
3840.5	0.5	7681.00	49.71	36.95
3841	1	3841.00	49.43	35.47
3841.5	1.5	2561.00	48.75	35.19
3842	2	1921.00	48.26	34.51
3842.5	2.5	1537.00	47.67	34.02
3843	3	1281.00	46.48	33.43
3844	4	961.00	45.75	32.24
3845	5	769.00	45.21	31.51
3846	6	641.00	44.67	30.97
3848	8	481.00	43.40	30.43
3850	10	385.00	41.39	29.16
3852	12	321.00	38.67	27.15
3854	14	275.29	35.56	24.43
3858	18	214.33	28.70	21.32
3864	24	161.00	25.08	14.46
3870	30	129.00	21.84	10.84
3880	40	97.00	18.59	7.60
3890	50	77.80	16.51	4.35
3900	60	65.00	15.43	2.27
3920	80	49.00	14.26	1.19
3940	100	39.40	13.99	0.02

Graph 5 Drawdown curve for constant pumping

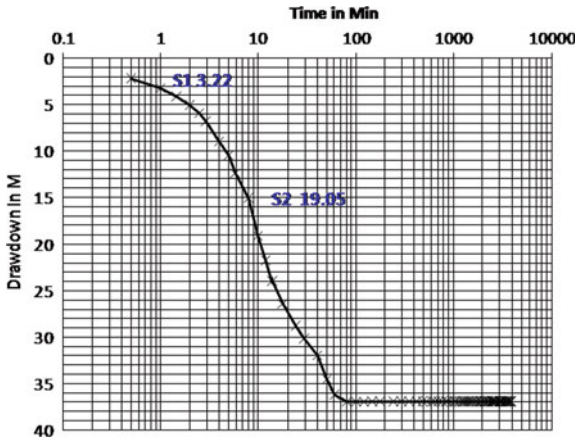

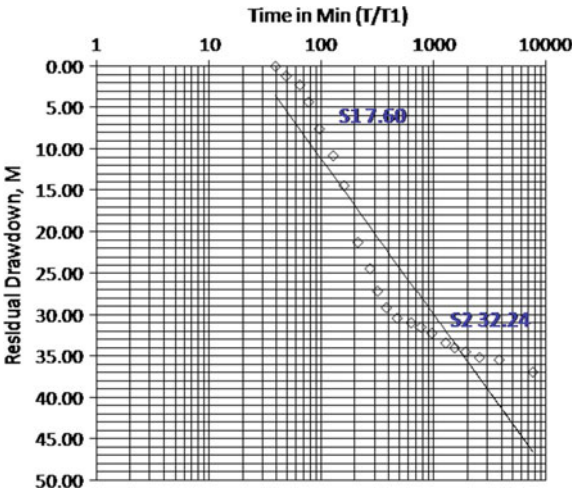

Graph 6 Recovery curve for constant pumping

Table 6 Summary of aquifer characteristics

S. no.	Aquifer characteristics	
1	Pumping method	Continuous pumping rate
2	Pump intake depth	60 m
3	Static water level	14.24 mbgl (meter below ground level)
4	Pumping time	64 h
5	Last pumping water level	51.19 m
6	Transmissivity constant discharge test	3.00 m^2/day
7	Permeability constant discharge test	0.33 m/min
8	Transmissivity recovery test	1.93 m^2/day
9	Permeability recovery test	0.21 m/min
10	Storage coefficient of the well	68
11	Effective drawdown (Se)	32.82 m (here 5 m taken as seasonal variation)
12	Specific capacity of the well	4.87 l/min

6 Conclusion

This paper carried out simple and easy method to determine the aquifer properties from pumping and recovery tests. Data analysis done using the Jacob–Cooper semi-log method which derives aquifer Transmissivity, T, values from plots of the Constant Rate Discharge tests and Recovery tests on the pumped borehole. The data obtained from pumping and recovery tests, from semi- log method suggested, as the maximum drawdown (s) and residual drawdown during recovery (s′) versus log the time since pumping started (t) and time since pumping stopped (t1′). It is concluded

that overall, the draw down and abstraction rate during pumping test reveals good performance of the borehole and moderate yielding aquifer, below is a summary of aquifer parameters derived from the above semi log graphs Table 6.

References

1. Anderson, M.P.: Heat as a ground water tracer. Gr. Water **43**(6), 951–968 (2005)
2. Anderson, M.P., Woessner, W.W.: Applied Groundwater Modeling—Simulation of Flow and Advective Transport, p. 381. Academic Press, New York (1992)
3. Bohling, G.C., Butler Jr., J.J.: Inherent limitations of hydraulic tomography. Gr. Water **48**(6), 809–824 (2010)
4. Cooper Jr., H.H., Jacob, C.E.: A generalized graphical method for evaluating formation constants and summarizing well-field history. Trans. Am. Geophys. Union **27**(4), 526–534 (1946)
5. Cooper Jr., H.H., Rorabaugh, M.J.: Ground-water movements and bank storage due to flood stages in surface streams: U.S. Geological Survey. Water-Supply Paper **1536-J**, 343–366 (1963)
6. Darcy, H.P.G.: Les fountaines publiques de la Ville de Dijon [The public fountains of the city of Dijon]. Paris, France: VictonDalmont. [English translation by P. Bobeck, republished 2004 by Kendall/Hunt, Dubuque, IA] (1856)
7. Forster, C., Smith, L.: Groundwater in systems in mountainous terrain. 1. Numerical modeling technique. Water Resour. Res. **24**(7), 999–1010 (1988)
8. Prasad, R.K., Mondal, N.C., Banerjee, P., Nandakumar, M.V., Singh, V.S.: Deciphering potential groundwater zone in hard rock through the application of GIS. Environ. Geol. **55**, 467–475 (2008)
9. Saar, M.O.: Review: geothermal heat as a tracer of large-scale groundwater flow and as a means to determine permeability fields, special volume on environmental tracers and groundwater flow. Hydrogeol. J. **19**, 31–52 (2011). https://doi.org/10.1007/s10040-010-0657-2
10. Saar, M.O., Manga, M.: Depth dependence of permeability in the oregon cascades inferred from hydrogeological, thermal, seismic, and magmatic modeling constraints. J. Geophys. Res. **109**(B04204), 1–19 (2004). https://doi.org/10.1029/2003JB002855
11. Saar, M.O., Manga, M.: Seismicity induced by seasonal groundwater recharge at Mt. Hood, Oregon. Earth Planet. Sci. Lett. **214**(3–4), 605–618 (2003). https://doi.org/10.1016/S0012-821X(03)00418-7
12. Saar, M.O., Manga, M.: Permeability–porosity relationship in vesicular basalts. Geophys. Res. Lett. **26**(1), 111–114 (1999)
13. Theis, C.V.: The relation between the lowering of the piezometric surface and the rate and duration of discharge of well using ground-water storage. Trans. Am. Geophys. Union **16**, 519–524 (1935)
14. Todd, D.K., Mays, L.W.: Groundwater Hydrol., 3rd edn. Wiley, New York (2005)
15. Walsh, S.D.C., Saar, M.O.: Macroscale lattice-Boltzmann methods for low Pellet-number solute and heat transport in heterogeneous porous media. Water Resour. Res. **46**(W07517), 1–15 (2010). https://doi.org/10.1029/2009WR007895
16. Wenzel, L.K.: Methods for Determining Permeability of Water Bearing Materials with Special Reference to Discharging-Well Methods. U.S. Geological Survey Water Supply Paper 887. Denver, Colorado: U.S. Geological Survey 192p (1942)
17. Yeh, T.-C.J., Lee, C.-H.: Time to change the way we collect and analyze data for aquifer characterization. Gr. Water **45**(2), 116–118 (2007)

Chapter 54
Integrative Spectrum Sensing in Cognitive Radio Using Wireless Networks

Bosubabu Sambana, Linga Srinivasa Reddy, Dharavat Ravi Nayak and K. Chandra Bhushana Rao

Abstract The entire operation of cognitive radio completely depends on the spectrum sensing technology in various areas. The main function of cognitive radio is to detect unused or unchecked spectrum and sharing it to other user without causing harmful interference to the primary user induced by reporting phase. Initially it requires different phases such as detection phase and reporting phase. In detection phase cognitive users detects the presence of primary users (Authenticated user). In reporting phase cognitive user forward their detection report to fusion center on existing system. In this, we proposed to analyze the effect of ROC (Receiver Operating Characteristics) with and without dedicated reporting channel in various specifications.

Keywords Network management · Cooperative spectrum sensing
Cognitive radio · ROC · Spectrum · Network · WLAN · Fusion center

B. Sambana (✉) · L. S. Reddy · D. R. Nayak · K. C. B. Rao
Department of CSE, Avanthi's Research and Technological Academy-Bhogapuram, Jawaharlal Nehru Technological University-Kakinada, Kakinada, Andhra Pradesh, India
e-mail: bosukalam@gmail.com

L. S. Reddy
e-mail: linga.srinu86@gmail.com

D. R. Nayak
e-mail: ravinayak46@gmail.com

K. C. B. Rao
e-mail: cbraokota.ece@jntukucev.ac.in

B. Sambana · L. S. Reddy · D. R. Nayak · K. C. B. Rao
Department of ECE, Avanthi's Research and Technological Academy-Bhogapuram, Jawaharlal Nehru Technological University-Kakinada, Kakinada, Andhra Pradesh, India

B. Sambana · L. S. Reddy · D. R. Nayak · K. C. B. Rao
Department of ECE, University College of Engineering-Vizianagaram, Jawaharlal Nehru Technological University-Kakinada, Kakinada, India

P. J. Rao et al. (eds.), *Proceedings of International Conference on Remote Sensing for Disaster Management*, Springer Series in Geomechanics and Geoengineering,
https://doi.org/10.1007/978-3-319-77276-9_54

1 Introduction

This paper gives us an idea about Cognitive radio detects the unused spectrum and shares it with the other users. The use of cognitive radio improves the Efficiency of wireless spectrum resources. Energy detection, matched filter detection and feature detection: these three are the main categories of signal processing. In order to reduce the fading effect in wireless system, a cooperative spectrum sensing technique is used. In this technique the detection results from various cognitive users are obtained and then combined it at the fusion center together by using various logic rule such as AND fusion rule and OR fusion rule.

The cooperative spectrum sensing process needs two phase: detection phase and reporting phase. For the spectrum sensing process one cannot be designed and optimized these two phases in isolation as they are not independent to each other. In detection phase cognitive users detects the presence of primary users (Licensed user) and cognitive user forward their detection report to the fusion center in reporting phase.

At the fusion center the results are combined by the logic rule. But there is a need to take care of time duration of both the phases as both the phases could affect each other. If the time duration of any phase is more then it will degrade the performance of overall spectrum sensing at the fusion center.

2 Background

Cognitive radio: Cognitive radio may be defined as part of radio systems that perform spectrum sensing in a continuous manner which dentify spectrum holes (unused radio spectrum) dynamically and then perform operation in a time domain when it is not used by primary users. "A cognitive radio may be defined as a radio that is aware of its environment and the internal state and with knowledge of these elements and any stored pre-defined objectives can make and implement decisions about its behavior".

Cognitive radio has four main functions which are:

(1) Spectrum Sharing
(2) Spectrum Management
(3) Spectrum Mobility
(4) Spectrum Sensing

Spectrum Sharing: Spectrum scheduling is done in this method. This method will decide which secondary user of the cognitive radio network can have the access to unused portion of the radio spectrum at some particular time.

Spectrum Management: Spectrum management may be defined as the process of choosing the optimal available spectrum band among the radio spectrum so as to fulfill the requirement of user for proper communication.

Spectrum Mobility: Spectrum mobility is the process in which one secondary user interchanges its frequency of operation with other secondary user present in network.

Spectrum Sensing: Spectrum sensing is the process which is used to detect unused portion of radio spectrum and shares it by estimating the interference level of the primary user.

Advantages of Cognitive Radio:

- Efficiency and utilization of spectrum is improved.
- Reliability of link is enhanced.
- Capable of finding open frequency for accessing the spectrum.
- Helps in improving the performance of SDR (software defined radio) techniques.
- Enhancement in user throughput and system reliability.
- leads to improve the wireless data network performance.
- General and selective spectrum access issues are solved by using Cognitive radio.

Disadvantages of Cognitive Radio:

- Security in a cognitive radio is a major concern and lot of work is to be done to achieve security in cognitive radio.
- Software reliability is not there in cognitive radio.
- It is difficult for cognitive radio to keep up with higher data rates.
- More efforts need to be put forward so that we can implement cognitive radio in real world.

Spectrum Sensing: The most important and crucial task of cognitive radio is to detect the unused portions of the radio spectrum. Cognitive radio has a characteristic that it can sense the spectrum holes and shares it with another secondary users without affecting the work of primary user.

In spectrum sensing, secondary users keep track of primary users to find spectrum holes which are also known as spectrum bands. Spectrum holes can be classified as: temporal spectrum holes and spatial spectrum holes. In temporal spectrum holes, primary user does not use spectrum for the transmission for that particular amount of time so at that time secondary user can use the spectrum for transmission whereas in spatial spectrum holes, primary user activities is bound to a particular area and secondary user can use the spectrum outside that area.

So in cognitive radio, to detect the presence or absence of the primary user various spectrum sensing techniques of cognitive radio such as Matched filter detection, Cyclostationary Feature detection, Energy detection, Higher order statistics, Waveform based sensing, and Eigen value based have been deployed but the performance of every spectrum sensing technique is different in different scenarios (Fig. 1).

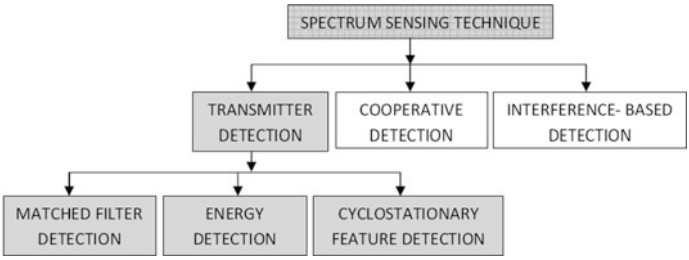

Fig. 1 Different spectrum sensing techniques

3 Related Work

Work proposed by Mohapatra et al. [2] focuses on spectrum sensing techniques, their performance, effectiveness under different transmission conditions. It is based on energy based detection and Cyclostationary detection. Simulation results of different techniques are compared and these techniques detect the presence of primary signal under low SNR condition. In this work, two methods i.e. Energy detection and Cyclostationary based detection are compared and from the simulation results it is observed that if sufficient information about primary user signal is not gathered by receiver, but the power of random Gaussian noise is known to the receiver then Energy detector is optimally suited for this case but this Energy detector doesn't give better performance in case of uncertainty in noise power as well as fading channels.

Work proposed by Kapoor et al. [3] focuses on hybrid model technology in which proper channelization of three techniques i.e. energy detection, matched filter detection, Cyclostationary detection have been presented for detecting unused spectrum bands i.e. underutilized sub bands of radio spectrum for better utilization of spectrum for increasing spectrum efficiency.

Work proposed by Waleed et al. [4] introduced a new local spectrum sensing scheme I3S (Intelligent spectrum sensing scheme) to improve the utilization efficiency of radio spectrum with increasing reliability and decreasing sensing time. In this proposed work, either combined energy detector and Cyclostationary detector is used or match filter detection based on power and band of interest. Then in this proposed I3S is compared with existing detection techniques, and this system gives more reliable results with less mean detection time. Work proposed by Rao et al. [5] discusses the simulation of the energy detection spectrum sensing algorithm for Cognitive Radio under low SNR condition.

The energy detection algorithm is known for its simple implementation but the method to calculate the threshold value lacks in both clarity and defined steps. So in this paper author made an effort to enhance the traditional energy detection technique by fusing it with the statistical Principal Component Analysis (PCA) technique. This methodology is used for different range of SNRs, different values of Pf and frequencies of interest.

4 Proposed Work

We proposed new method for exiting spectrum sensing in Cognitive Radio using Wireless Networks. Those methods are represents strongly evidence of current working stages

System Description: Time duration for detection phase and reporting phases are α and 1-α fractions respectively of one time slots. It is to be assumed that α is same for all cognitive users. CUs forward their detection report to fusion center (FC) over the orthogonal Sub-channel. Sub-channels are equally divided in reporting phase, resulting in multiple time slots. These all CUs will interfere primary user (PU) potentially in the reporting phase so in order to reduce this interference as much as possible we use a concept of selective relay based cooperative sensing scheme where all cognitive users sends their detection report to the fusion center in a selective fashion depending on the presence or absence of primary user. If CU detects that PU is absent in that case it will transmit an indicator signal with encoded cyclic redundancy code (CRC) to the FC else no signal is transmitted.

At the fusion center the signal is decoded and if it is successfully decoded then it means CU detection report says that PU is absent else primary user is present. So the possibility of causing interference is reduced and controlled also as CU will interfere the PU only when it fails to detect the presence of PU.

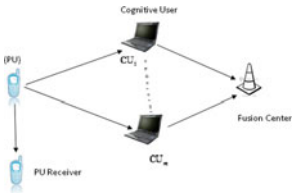

Signal Model: In this model we use a Rayleigh fading and it is constant during one whole time slot. N0 is the power spectral density of the additive white Gaussian noise (AWGN) that is same for the entire receiver. Assume that Pp and Ps are the transmit power of PU and CU. Let Hp = H1 denotes the presence of primary user and Hp = H0 represents absence of it. In the detection phase, the signal received at CUi for the k time slots, can be solve in various methods.

4.1 Spectrum Sensing Techniques

- **Energy Detection**

In this technique primary signal based on sensed energy is detected. This technique is best suited for detecting independent and identically distributed signals in high SNR conditions, but not optimal for detection of correlated signals. This method of spectrum sensing is very simple to implement as in this prior knowledge of primary signal is not required but this method requires proper knowledge of noise power

and hence it is vulnerable to noise uncertainty. Three parameters defined in spectrum sensing for calculating the performance are:

(1) Probability of Detection (Pd).
(2) Probability of Miss Detection (Pm).
(3) Probability of false alarm (Pf).

The probability of detection is defined as a metric in which Secondary user declares the existence of a primary user when the spectrum is occupied by the primary user whereas the probability of false alarm is defined as a metric in which secondary user declares the existence of the primary user when the spectrum is idle. The probability of miss detection is a metric in which secondary user declares the non existence of a primary user when the spectrum is occupied. The probability of miss detection is basically, $Pm = 1 - Pd$. False alarms tends to reduce performance of radio spectrum and probability of miss detection causes hindrances in the work of licensed primary user, So in order to have better performance we should achieve maximum probability of detection with minimum probability of false alarm. Energy Detection method of spectrum sensing requires various components like band-pass filter, an analog to digital converter, square law device and an integrator. First the input signal is passed through a band-pass filter of bandwidth W. Then the filtered signal is squared and integrated over an observation interval T. Finally the output of the integrator is compared with a threshold value to decide whether primary signal is present or not (Fig. 2).

The energy detection technique can be defined by following two equations:

$$\begin{aligned} &X(t) = \{n(t)\} \quad H0 \ (\text{White Space}) \\ &X(t)\{h * s(t) + n(t)\} \quad H1 \ (\text{Occupied}) \end{aligned}$$

where X(t) is the signal received by secondary user, s(t) is the signal transmitted by primary user, n(t) is the additive white Gaussian noise (AWGN) and h is the amplitude gain of the channel.

Advantages:

1. Knowledge of the primary user's signal is not required in prior.
2. Easy to implement.

Disadvantages:

1. Energy detection technique does not perform well in low SNR conditions.
2. This technique of spectrum sensing cannot distinguish between the primary user signal and noise signal.

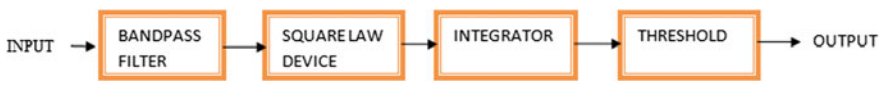

Fig. 2 Energy detector block diagram

3. It is difficult to select a suitable threshold value for Comparing it with the value of the energy signal.

- **Matched filter detection**

The most optimal method for spectrum sensing in cognitive radio is a matched filter detection technique because it maximizes received signal to noise ratio and it takes least time. But it requires the *prior* knowledge of primary users. So every time it requires different signal receivers for each signal type that leads to the implementation complexity. The operation of matched filter detection is expressed as [4]:

$$Y[\quad]=\sum_{k=-\infty}[n-k]\,x\,[k]$$

where "x" is the unknown signal (vector) and is convolved with the "h", the impulse response of matched filter that is matched to the reference signal for maximizing the SNR (Fig. 3).

Advantages:

1. It maximizes the SNR which makes it a optimal detector among all other sensing techniques.
2. Matched filter technique is faster as compared to other techniques.

Disadvantages:

1. These techniques also require the prior knowledge of the primary user signal.
2. Computational complexity is high as compared to other sensing techniques.
3. Power consumption is high.

- **Cyclostationary Feature Detection**

Noise rejection capability makes Cyclostationary a better detection technique as compared to other spectrum sensing techniques. The presence of primary user is detected by using Cyclostationary property of user signal. For checking primary user presence, cyclic correlation function is used instead of power spectral density function.

Cyclostationary feature detection is able to discriminate between primary signal and noise as spectral correlation is applied to the modulated signal. This algorithm gives optimal results for low SNR value. This method basically detects the presence of primary users by using the periodicity in received primary signal. Because of

Fig. 3 Matched filter block diagram

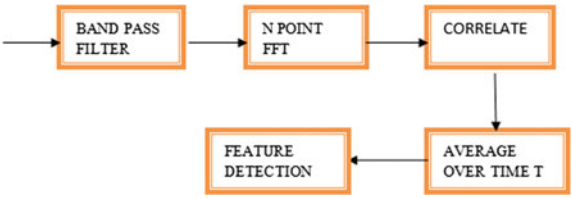

Fig. 4 Cyclostationary detector block diagram

periodicity, periodic statistics and spectral correlation features are exhibited by the Cyclostationary feature detection method (Fig. 4).

Advantages:

1. It gives better performance than energy detection technique and also gives satisfactory results in low SNR regions.
2. Prior knowledge of signal characteristics is not required in the case of Cyclostationary.

Disadvantages:

1. It has more computational complexity as compared to other methods for sensing.
2. It requires more sensing time as compared to the other techniques used for sensing.

5 Conclusions

In this paper we have presented the concept of selective relay based cooperative sensing scheme in cognitive radio network without dedicated reporting channel. We obtained the ROC from proposed method as well as from traditional method and on comparing we found that with this proposed scheme we can save the dedicated channel resources without reducing the ROC performance.

Efficient utilization of radio spectrum is provided by the cognitive radio which uses the method of spectrum sensing to utilize the spectrum holes present in the spectrum. Spectrum sensing is one of the most important task of cognitive radio. In order to sense the spectrum various spectrum sensing techniques are proposed which have their own advantages and disadvantages. And in this paper we have reviewed three main spectrum sensing techniques which are Energy Detection, Matched Filter Detection and Cyclostationary feature Detection. The main advantage of Energy detection is that it is simple to implement and it does not require information about the primary user signal but it does not perform well in low SNR values.

On the other hand Matched filter detection is better than energy detection as it starts working at low SNR of even −30 dB s. Cyclostationary feature detection is better than both the previous detection techniques since it produces better results at

lowest SNR values. The Cyclostationary feature detection spectrum sensing outclasses the other two sensing techniques, but the processing time of Cyclostationary feature detection is greater than the energy detection and matched filter detection techniques and it is more complex as well. As all the techniques are proposed only with limited number of parameters like probability of detection, probability of missed detection, probability of false alarm but in real time various other parameters are to be used with respect to the signal vicinity. This paper can prove a useful means to understand the concept of spectrum sensing in cognitive radio.

References

1. Yadav, N., Rathi, S.: Spectrum sensing techniques: research, challenge and limitations. IJECT **2**(4), (2011)
2. Mohapatra, S.G., Mohapatra, A.G., Lenka, S.K.: Performance evaluation of Cyclostationary based spectrum sensing in cognitive radio network. In: Automation, Computing, Communication, Control and Compressed Sensing (iMac4 s), pp. 90–97 (2013)
3. Kapoor, S., Singh G.: Non-cooperative spectrum sensing: a hybrid model approach. In: International Conference on Devices and Communications (ICDeCom) (2011)
4. Waleed, E., Najam, U.L., Seok, L., Hyung, S.K.: I3S: Intelligent spectrum sensing scheme for cognitive radio networks. In: EURASIP Journal on Wireless Communications and Networking. Springer (2013)
5. Rao, A.M., Karthikeyan, B.R., Mazumdar, D., Kadambi G.R.: Energy detection technique for spectrum sensing in cognitive radio. SAS_TECH J. **9**(1), (2010)
6. Juei, C., Emad, A.: An efficient multiple lags selection method for Cyclostationary feature based spectrum-sensing. IEEE Signal Process. Lett. **20**(2), (2013)
7. Mehta, T., Kumar, N., Saini, S.S.: Comparison of spectrum sensing techniques in cognitive radio networks. IJECT **4**(3), (2013)

Bosubabu Sambana working with Assistant Professor, Department of CSE, Avanthi's Research and Technological Academy, Vizianagaram. He is completed Bachelor of Science from Andhra University. He is completed Master of Computer Applications and Master Degree in Computer Science & Engineering from Jawaharlal Nehru Technological University—Kakinada, Pursing courses on AMIE from Institute of Engineers-Kolkata and Master of Science in Mathematics, Andhra University—Andhra Pradesh, India.

He has 4 years good teaching experience and having a good Knowledge on Space Research, Future Internet Architecture, Cloud Computing, Internet of Things/Services/Data, Data Analytics, Computer Network and Hacking along with Computer Science Subjects. He is Published 18 Research Papers in various reputed International and national Journals, Magazines and conferences.

He filling 3 Patents on Patent Office-Chennai, India and wrote 1 Textbook. He have 4 Copyright and Secured 6 Certifications from NPTEL-Indian Institute of Technology on various specifications like Algorithms for BigData, C++ Programming, Introduction to Research, Wireless Sensor Adhoc Networks, Internet Architecture, Internetwork Security, and Computer Architecture, Cloud computing, Introduction to Cryptography, Design for Internet of Things and Machine Learning etc.

He is participated 4 international and 4 national conferences. He is Participated 5 national Workshop, 2 TEQIP programs and 2 FDP, 1 SDP.

Linga Srinivasa Reddy working with as Assistant Professor, Department of CSE, Avanthi's Research and Technological Academy, Jawaharlal Nehru Technological University-Kakinada.

He is completed Bachelor of Technology in CSE from JNT University Kakinada. He is completed in Master Degree in CSE from Andhra University, Visakhapatnam, Andhra Pradesh, India.

He has 1 year good teaching experience with taught various subjects on good knowledge on DBMS, Mobile computing, Computer Networks, Machine Learning and along with CSE subjects. He is published 3 research papers in reputed International and national level conferences\Journals\Magazines. He is Participated and active member in academic, curriculum and administrative works in various organizations. He is the member of IEEE, IAENG, CSI.

Dharavat Ravi Nayak working with as Assistant Professor, Department of ECE, Avanthi's Research and Technological Academy, Jawaharlal Nehru Technological University-Kakinada.

He is completed Bachelor of Technology in ECE from JNT University Kakinada. He is completed in Master Degree in ECE from Andhra University, Visakhapatnam and Pursing Ph.D. from Jawaharlal Nehru Technological University-Kakinada, Andhra Pradesh, India.

He has 6 years good teaching experience with taught various subjects on good knowledge on EDC, RVSP, SS, ECA, PDC, EMWTL, AC, DC, STLD, DSP, OC, VLSI and along with ECE subjects.

His Qualified GATE-2008 and published 4 research papers in reputed International and national level conferences\Journals \Magazines, 1 book are processing on publishing. He is filling patent application in patent office Chennai. He is Participated and active member in academic, curriculum and administrative works in various organizations. He is the member of IEEE, IAENG.

K. Chandra Bhushana Rao Professor & Head, Department of ECE, Jawaharlal Nehru Technological University-Vizianagaram. He is completed Bachelor of Engineering in ECE and Master Degree in ECE with Specialization of Control System and completed Doctor of Philosophy in Microwave Communication from Andhra University—Andhra Pradesh, India. He has 24 years good teaching experience with taught various subjects on good knowledge on EMI/EMC Antennas, Radar Microwave Communications and EMTL along with ECE subjects. He has 16 years good research experience with published 67 research papers in reputed International and national level conferences \Journals\Magazines, 2 books are processing on publishing and 15 years Administration experience with played vital role in JNTUK, State Government Educational bodies activities and Expert member, RIFD Bureau of AICTE, Evaluator, NBA & NAAC. He filled 2 patents on Patent office, Chennai.

He guided 200 + UG/PG students and 1 Ph.D. student, 3 students are processing. Project evaluator on various platforms under UGC, NBA, AICTE, JNTU Kakinada.

He is the Sr. Member of IEEE, Indian Science Congress, W3C, MECS-PRESS, IAENG, Fellow-IETE, SM-IEEE, LMISTE, SEMCE (I), and LMISSS.

He is the member of IEEE, IAENG, AMIE, CSI, ISC, CSTA, IACSIT, SDIWC, EAI, the IRED, UACEE, Indian Science Congress, W3C, INTERNET SCOCIETY, W3C, NASA (Student), Springer, Elsevier, Science Alert, IEI, Editorial Manager, MECS-PRESS-IJMECS/ IJCSIT, W3C, manuscript-central, TUBITAK-GIRIS, Internet Society, IAENG, IAAET, IJMETMR, IJECSE, IJCST, IJECSE and editorial/review member in ACM, IJMETMR, and Springer-Journal of Big Data.

Chapter 55
A Geospatial Study on Solid Waste Management for the Visakhapatnam Smart City

Neela Victor Babu, Suribabu Boyidi and Sridhar Bendalam

Abstract Municipal solid waste era is among the most noteworthy sources which debilitate the worldwide ecological wellbeing. Site choice is a vital and important issue for waste administration in quickly developing nations like India. Due to the intricacy of waste administration systems, the determination of the proper solid waste landfill site requires thought of various option arrangements. Remote detecting information have been utilized to current states of the land utilize/arrive cover and geomorphology of the investigation range. All components influencing the site condition were considered according to the rules of waste administration and dealing with rules (2008) that incorporate physical condition, manmade system offices. A Geographic Information System (GIS) was utilized for choice of landfill locales. Reasonableness maps were reviewed from 0 (least reasonableness) to 10 (most astounding appropriateness) utilizing spatial information advancements. Reasonable landfill territories speak to ideal destinations. The chosen locales are Kottatalarivanipalem (1.81 km^2), Denduru (1.56 km^2), Yeduruvanipalem (1.07 km^2), Pydivada Agraham (1.03 km^2), Mantripalem (0.97 km^2), Mindivanipalem (0.91 km^2) and Ramayogi Agraharam (0.89 km^2). The landfill site which covers expansive range may last longer period. My work can offer a sitting strategy and gives fundamental help to leaders in the evaluation of waste administration issues in the territory and other quickly creating urban areas in India. The outcomes demonstrates the Greater Visakhapatnam Municipal Corporation (GVMC) dumping site ought to take after the rules and suggestions given by the scientist for additionally overseeing and kill ecological issues in the environ of GVMC.

N. V. Babu (✉)
Baba Institute of Technology and Science, Visakhapatnam, India
e-mail: neelavictorbabu@gmail.com

S. Boyidi · S. Bendalam
Andhra University College of Engineering, Visakhapatnam, India
e-mail: suri.sri2008@gmail.com

S. Bendalam
e-mail: sridhar.bendalam@gmail.com

P. J. Rao et al. (eds.), *Proceedings of International Conference on Remote Sensing for Disaster Management*, Springer Series in Geomechanics and Geoengineering,
https://doi.org/10.1007/978-3-319-77276-9_55

Keywords Solid waste · GIS · Landfill sites · GVMC

1 Introduction

The term smart cities became buzz word in the global arena. In recent times urban development became a key issue globally. Especially India like densely populated countries, the problem is more concern about urbanisation. According to the recent statistics states that, % migrated from rural to urban. This reflected in many sever issues like pollution issues, subject the off by introducing the concept of smart cites it the urbanisation became one of the major issue more challenging and other developing countries. Municipal solid waste is, disposed of/rejected material regularly being forgotten from the diverse open sources. Examinations in think about zone uncovered that, fast development in populace amid the current decades brought about expanding amount of urban solid wastes. Municipal solid waste comprises of everyday devoured and disposed of things, for example, sustenance wastes, holders, item bundling, and different random like private, business, institutional and modern sources. The natural issues existing in the urban territories of creating nations, municipal solid waste administration and its effect on groundwater quality have been the most conspicuous in the current years [1]. The Greater Visakhapatnam Municipal Corporation (GVMC) is the second greatest municipal corporation in the territory of Andhra Pradesh, India. Age of municipal and modern solid wastes expanding quite a long time is posturing ecological difficulties around there. A large portion of the ventures have their own particular component for taking care of mechanical solid waste. There are no significant surface water bodies in the zone and the reliable groundwater assets are being dirtied at a disturbing rate. Directly, groundwater quality is the real concern and in this manner rose as a standout amongst the most vital ecological issues. Water interest for drinking and residential purposes has been expanding because of progress of ways of life of individuals and statistic weights [2]. Consequently, this investigation has been taken up to find out groundwater contamination hotspots in the environs of GVMC region. The modern effluents of the Zinc smelter-Alum production line in Mindi Visakhapatnam, move toward groundwater development and stream towards swamp arrive through local locations because of topographic control [3].

2 Study Area

The examination territory covering around 1143 km2 has all the earmarks of being saucer formed and lies in the middle of 17° 31′ 42″ to 17° 55′ 29″ Northern lat. furthermore, 83° 2′ 5″ to 83° 25′ 17″ Eastern long (Fig. 1). The elevation of

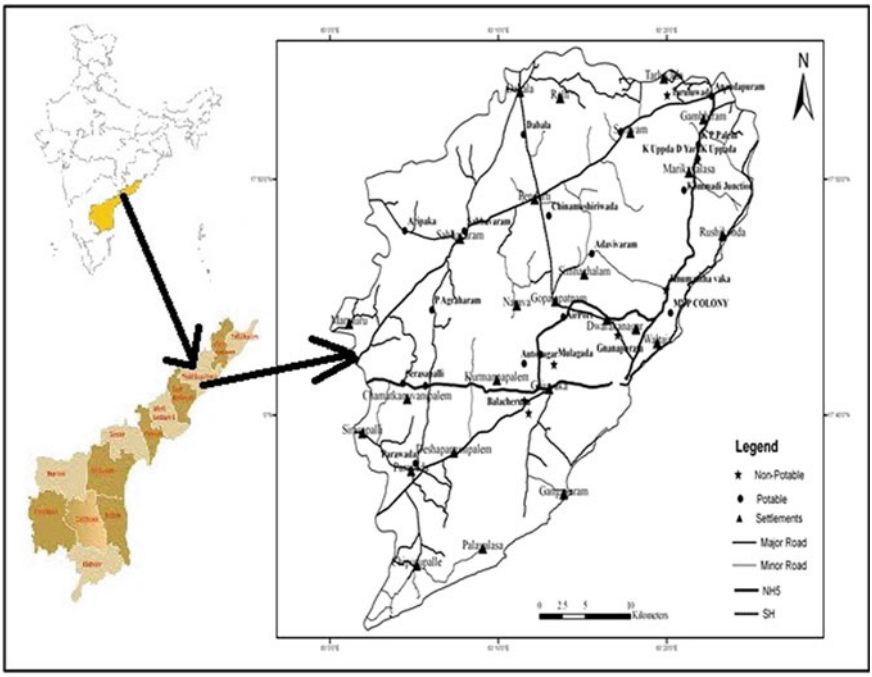

Fig. 1 Proposed landfill sites in GVMC

Kailasagiri and Yarada konda slope runs around 507 and 357 m above msl individually. The eastern side is encompassed by the Bay of Bengal. The region has been secured with deciduous timberland around 33.33 km^2, declining quickly because of urbanization and industrialization [4]. The examination zone is inhabitated with around 2 million populaces other than major and other auxiliary businesses. According to 2001 statistics, the decennial development rate of populace in the territory is around 22.44%. The high thickness of populace is around 3670 km^2 in urban regions though less thickness in provincial regions. Strong waste creating from the urban condition is contaminating water, soil and air, other than unhygienic environment. The city strong waste is being arranged at Kapulauppada, open sterile landfill site throughout the previous two decades. In any case, the household squanders are dumped in unlined sewage wastes (rivulets) bringing about pollution of surface and groundwater. In provincial condition, strong squanders are dumped in unlined sewage depletes and surrendered burrowed wells, prompting groundwater contamination. In GVMC, modern effluents and civil strong waste dump brings about groundwater contamination other than ocean water interruption (contamination) at places along the ocean drift.

3 Methodology

The examination zone covering around 1143 km^2 seems, by all accounts, to be saucer formed and lies in the middle of 17° 31′ 42″ to 17° 55′ 29″ Northern lat. what's more, 83° 2′ 5″ to 83° 25′ 17″ Eastern long (Fig. 1). The elevation of Kailasagiri and Yarada konda slope runs around 507 and 357 m above msl separately. The eastern side is encompassed by the Bay of Bengal. The region has been secured with deciduous timberland around 33.33 km^2, declining quickly because of urbanization and industrialization [5]. The investigation region is inhabitated with around 2 million populaces other than major and other subordinate enterprises. According to 2001 statistics, the decennial development rate of populace in the region is around 22.44%. The high thickness of populace is around 3670 km^2 in urban zones while less thickness in rustic regions. Strong waste producing from the urban condition is contaminating water, soil and air, other than unhygienic environment. The metropolitan strong waste is being arranged at Kapulauppada, open sterile landfill site throughout the previous two decades. In any case, the local squanders are dumped in unlined sewage seepages (rivulets) bringing about pollution of surface and groundwater. In country condition, strong squanders are dumped in unlined sewage depletes and relinquished burrowed wells, prompting groundwater contamination. In GVMC, mechanical effluents and city strong waste dump brings about groundwater contamination other than ocean water interruption (contamination) at places along the ocean drift.

4 Results

The substance parameters acquired in this investigations uncovering that the pH differs from 6.43 to 7.73 of soluble nature inside as far as possible. The electrical conductivity (EC) values are in the middle of 226–4237 µs. The groupings of Ca^+, SO_4^-, F- and Cl-particles are watched nearer to the most extreme reasonable points of confinement in the towns of Sukkavanipalem and Kapulauppada. These towns are in low lying territories of Hindustan Zinc Ltd. also, Kapulauppada sterile landfill site separately. The convergences of TDS and TH and Na^+, Mg^{2+}, and Fe have surpassed greatest admissible points of confinement in Kapulauppada and Sukkavanipalem. The higher substance in these towns could be drainage from the unlined sewage deplete. These components cause cardio vascular maladies which are accounted for in delicate water zones. Up until this point, no case has been accounted for with respect to contaminated groundwater in the zone. The principle hotspot for sodium in groundwater assets is plagioclase feldspars, feldspathoids and earth minerals. Sodium content around 200 mg/l might be destructive to people having heart and renal maladies and in ladies with toxemia related with pregnancy [6]. The centralization of sodium differs from 10 to 540 mg/l. Two examples observed to be overabundance of Na^+ than the most extreme admissible breaking

points in Kapulauppada and Sukkavanipalem. The calcium is a noteworthy constituent of most volcanic, changeable and sedimentary rocks.

The primary wellspring of Ca^{+} in groundwater is individuals from the silicate mineral gatherings like plagioclase, pyroxene and amphibole among molten and changeable rocks and limestone, dolomite and gypsum among sedimentary rocks. Transfer of sewage and mechanical squanders are likewise essential wellspring of calcium. Focuses up to 1800 ppm has been found not to disable any physiological response in man [7]. The calcium extends in the middle of 16–160 mg/l. The magnesium focuses in the investigation zone fluctuates from 5 to 136 mg/l. Kapulauppada and Mulagada tests are having overabundance content than as far as possible in Table 1. Iron is basic to all creatures and is available as hemoglobin, however at more elevated amounts they are poisonous [8]. Iron focuses in the groundwater shift from 0.10 to 1.30 mg/l.

Iron is fundamental to all living beings and is available as hemoglobin, however at larger amounts they are poisonous [8]. Iron fixations in the groundwater shift from 0.10 to 1.30 mg/l. Kapulauppada landfill territory, Kapulauppada town and Mulagada territories are having higher focus. Chloride substance of more than 250 mg/l makes the water salty; nonetheless, exorbitant chloride fixation influences the taste, however there is no known physiological peril in the zone. The chloride levels in common water are an essential thought for the choice out in the open water supplies [9]. Gajuwaka, Sukkavanipalem, Kapulauppada town and Kapulauppada dump yard site tests have higher chloride content. The fluorine is the most plentiful component and is broadly appropriated all through nature [10]. Fluoride assumes a key part in water quality administration because of its unfavorable wellbeing impacts. Fluoride additionally causes respiratory disappointment, hypotension and loss of motion. Loss of weight, anorexia, frailty, squandering and cachexia are among the basic discoveries in ceaseless fluoride harming [11]. The fluoride content in the investigation region runs in the middle of 0.68–1.94 mg/l. The towns which have higher fluoride content and surpassing as far as possible are, Kapulauppada dump yard, Kapulauppada, Autonagar and Sukkavanipalem. Local sewages and mechanical effluents, other than natural oxidation of decreased sulfur species, may add sulfate to water. Water with sulfate fixation up to 500 mg/l or more will be severe taste [12]. The sulfate content in the region ranges from 10 to 298 mg/l. The higher substance of these components in these towns could be leachates from the unlined sewage channels, dumping strong waste in an informal way and furthermore leachates from the strong waste dump yard at Kapulauppada site. Broken up metals in many occurrences are found at unnaturally higher focuses in view of mechanical procedures. In higher measurements, these metals demonstrate deadly to life forms, including people. Follow metals, subsequently, constitute a noteworthy class of components having environmental centrality. At more elevated amounts they are poisonous [13]. A standout amongst the most essential environmental issues today is groundwater sullying [14] and wide decent variety of contaminants influencing groundwater assets. Substantial metals get specific concern considering their solid danger even at low fixations [15]. In the examination territory Al ranges from 3.87 to 30.17 (ppb) in Akkireddipalem, Balachervu, Dabala

Table 1 Physical and chemical parameters concentration in the study area (in ppm)

Parameters	Parawada	Kapula Uppada	Gajuwaka M.R. Office	Sukkavanipalem/Mulagada	Gnanapuram	Autonagar	Sontyam
Physical parameters							
pH	6.420	7.037	7.754	7.543	7.737	6.65	7.104
EC	6.22	2.062	2.192	4.336	814.6	1.577	1.216
TDS	139	1170	1189	2839	461	949	679
TH	87	539	519	861	249	461	371
BOD	BDL	29	0.21	2.5	0.8	2.8	<0.41
COD	BDL	67	0.5	3.6	1.50	4.2	0.8
TA	89	589	579	979	299	581	449
Chemical parameters							
Ca^{+}	15	107	110	159	63	111	83
Mg^{2+}	13	69	73	111	23	45	39
Na^{+}	7.8	71	77	539	25	89	53
K^{+}	0.12	1.29	0.93	3.30	0.20	0.390	0.118
HCO_3	27	359	316	523	161	279	273
Cl^{-}	19	229	261	879	55	167	113
F^{-}	0.690	1.530	1.130	1.930	0.690	1.330	0.950
NO_3	0.880	12.30	3.49	6.80	2.90	7.20	2.50
$SO_4{}^{-}$	9.9	95	103	297	33	103	39
PO_4	0.890	3.40	1.75	2.58	1.44	2.14	0.971
Fe	0.118	2.30	0.440	1.20	0.750	0.110	0.230

(continued)

Table 1 (continued)

Parameters	Airport/ akaninagar	Taruluwada	Anandapuram Junction	Kottaparadesipalem	M.V.P. Colony Sector-11	Hanumanthavaka Juntion	Kapula Uppada
Physical parameters							
pH	7.351	6.507	6.892	7.164	7.72	7.52	7.037
EC	1.441	461.2	500.4	2.064	1.21	841	2.172
TDS	759	219	279	1079	691	491	1179
TH	441	119	151	459	392	241	539
BOD	1.1	BDL	0.49	1.91	0.70	1.20	27
COD	1.79	0.4	1.39	2.83	1.20	2.60	65
TA	479	139	161	501	459	267	591
Chemical parameters							
Ca^{+}	89	39	47	95	77	111	15
Mg^{2+}	53	6	9	51	41	71	13
Na^{+}	63	9	25	69	67	77	7.8
K^{+}	0.264	0.490	0.770	1.290	0.26	0.97	0.11
HCO_3	267	83	97	304	281	316	27
Cl^{-}	159	25	49	145	141	259	17
F^{-}	1.240	0.711	0.750	0.870	0.79	1.110	0.670
NO_3	3.30	1.46	1.39	4.35	2.20	3.49	0.880
$SO_4{}^{-}$	53	17	21	11	47	103	11
PO_4	1.39	0.750	1.33	2.15	1.87	1.77	0.801
Fe	0.085	0.180	0.240	0.850	0.23	0.460	0.118

Table 2 Trace metals concentration in the study area (in ppb)

Element conc. (ppb)	C. Musirivada	Adavivaram	Kommadi Junction	Sabbavaram	Aripaka	Dabala
Li	1.6746	0.7611	2.1592	3.1623	6.0194	22.3094
Be	0.0046	0.0230	0.0114	0.0313	0.0125	0.0118
Al	3.86	7.9242	30.1741	11.0255	5.7687	25.4382
V	17.8497	0.5882	19.3064	6.1375	13.4416	18.0372
Cr	0.1782	0.2937	0.8685	0.1956	0.4075	6.1812
Mn	1.7482	68.5895	3.2524	3.3514	0.9185	2.1773
Fe	4.9407	15.2143	24.0505	50.8324	6.3886	13.6235
Co	0.0318	0.1315	0.0924	0.0651	0.0374	0.0082
Ni	0.6197	1.2617	9197	1.5812	0.6137	0.7387
Cu	0.2393	1.1918	3.0481	0.9206	0.9623	2.7580
Zn	2.9793	12.0117	19.1614	93.2401	2.1704	2.9184
Ga	4.1687	28.7125	10.1392	42.8035	19.0475	18.6542
As	0.192	0.1331	1.2001	0.2741	0.3618	4.1750
Se	0.4175	0.6285	2.3485	2.1017	2.9232	2.9161
Rb	0.1252	0.7914	0.3312	2.6676	2.7926	5.5457
Sr	370.232	398.501	338.077	1121.57	796.542	1043.87
Ag	0.0122	0.0631	0.0842	0.0235	0.012	0.000001
Cd	0.021	0.0155	0.0496	0.1492	0.005	0.0349
Cs	0.002	0.0052	0.0156	0.0103	0.0101	0.0301
Ba	27.6117	177.987	51.2904	266.70	121.312	115.282
Tl	0.0025	0.0082	0.0154	0.0163	0.0160	0.0181
Pb	0.1647	0.3094	1.2171	0.3580	0.0536	0
U	0.2815	0.7862	4.3914	2.6183	1.9142	33.8513

Element conc. (ppb)	Akkireddypalem	Balacheruvu	Lankelapalem	Sirasapalli	P. Agaraharam
Li	4.6864	12.7007	3.2131	2.78298	2.8307
Be	0.0261	0.0243	0.0113	0.0113	0.0085
Al	21.8684	16.5070	12.8503	7.9686	7.2376
V	10.6507	8.6760	4.6124	12.8016	12.7702
Cr	0.6481	0.9927	0.2512	0.8232	0.7795
Mn	3.8085	82.4661	25.632	1.0952	1.0281
Fe	6.6591	3.1844	4.9882	1.1502	1.3165
Co	0.1294	0.6043	0.1193	0.0810	0.0798
Ni	1.1481	1.7875	1.3283	0.3312	0.3922
Cu	4.2340	1.805	9.2659	1.3065	1.2751
Zn	16.0084	5.1180	31.105	0.9822	1.2733
Ga	28.4885	13.2320	22.6401	15.4475	15.3901
As	0.3972	0.7345	0.5023	2.4923	2.4633
Se	2.0141	4.1592	1.0445	3.4922	3.4976

(continued)

Table 2 (continued)

Element conc. (ppb)	Akkireddypalem	Balacheruvu	Lankelapalem	Sirasapalli	P. Agaraharam
Rb	0.6292	4.1634	4.2426	6.5451	6.4875
Sr	1161.71	1691.81	725.261	559.1043	549.407
Ag	0.0205	0.4335	0.094	0.0705	0.0521
Cd	0.031	0.017	0.0237	0.0032	0.0044
Cs	0.0070	0.0150	0.0137	0.0155	0.0166
Ba	170.333	68.8953	138.362	92.4742	93.1877
Tl	0.0424	0.0615	0.0292	0.02302	0.0226
Pb	0.1647	0	0.5348	0	0.0503
U	1.2550	13.264	1.0817	4.2619	4.2601

and Kommadi towns. Mn ranges from 0.91 to 82.46 in Balachervu, Adavivaram territories (Table 2). Cu ranges from 0.23 to 9.26 with a normal of 2.455. Se runs in the middle of 0.41–3.49 with a normal of 2.32 every one of the qualities are inside as far as possible. In our nation, a large portion of the groundwater is constantly contaminated by modern and household squanders. Zinc is one of the fundamental components required for legitimate working of the body framework [16]. Zn ranges from 0.98 to 93.24 with a normal of 17.00 in Akkireddipalem, Sabavaram and Kommadi territories. The Ni can cause unfavorably susceptible responses separated from being cancer-causing [17].

5 Conclusions

Therefore, chemical monitoring of water sources become an essential part of water management. The measurements and characterization of these metals are necessary to understand their distribution and pathways in the ecosystem and to assess the impact of their discharge into environment. The results of physical, chemical parameters and trace metals of groundwater have been compared with the Bureau of Indian standards-10500 (1991) and World Health Organization. The area chosen for study is significant for industries, coastal environment and dense population. So far, no major studies have been carried out on solid waste interaction with groundwater. In this study, it is observed that the groundwater regime is being highly polluted due to improper dumping of solid waste in unlined sewage drains, besides geological causes.

References

1. Badgie, D., Manaf, L.A., Samah, M.A.A.: Municipal solid waste generation and composition in the Kanifing Municipal Council Area (KMC)—The Gambia. J. Solid Waste Technol. Manage. **42**(1) (2016)
2. Madha Suresh, V., Vignesh, K.S., Aaron, A., Kaleel, M.I.M., Fowzul Ameer, M.L.: A study on impact of municipal solid waste on groundwater in and around the dumping yard of Visakhapatnam, AP, India (2016)
3. Devi, K.P., Bindu, C.S., Reddy, T.B., Basavaiah, K., Vani, P.: Accumulation of fluoride from soil by various plant species in the vicinity of fertilizer factory, Visakhapatnam, India (2016)
4. Rao, P.J., Harikrishna, P., Srivastav, S.K., Satyanarayana, P.V.V., Rao, B.B.D.: Selection of groundwater potential zones in andaround Madhurwada Dome, Visakhapatnam District—a GIS approach. J Indian Geophyl Union, **13**(4), pp. 191–200 (2009)
5. Jagadeeswara Rao, P., Satyanarayana, P.V.V., Venkateswara Rao, T., Harikrishna, P.: Influence of land use/land cover on groundwater in the environs of Madhurawada Dome, Visakhapatnam District—a remote sensing approach. J. Eastern Geogr. **XVI**(1), 15–18 (2010)
6. Nas, T.F.: Cost-Benefit Analysis: Theory and Application. Lexington Books, Lanham (2016)
7. Sabah, A., Bancon-Montigny, C., Rodier, C., Marchand, P., Delpoux, S., Ijjaali, M., Tournoud, M.G.: Occurrence and removal of butyltin compounds in a waste stabilisation pond of a domestic waste water treatment plant of a rural French town. Chemosphere **144**, 2497–2506 (2016)
8. Driscoll, J.R., Healy, D.M.: Computing Fourier Transforms and Convolutions on the 2-Sphere. Adv AppL Math **15**(2): 202–250 (1994)
9. Ahmad, S., Iqbal, J.: Transboundary impact assessment of Indian dams: a case study of Chenab River Basin in perspective of Indus Water Treaty. Water Policy **18**(3), 545–564 (2016)
10. Kumar, R.S., Priyadharshini, S.: The hydro-chemical and microbial analysis of ground water samples in two different districts of Madurai and Virudhunagar Districts, Tamil Nadu, India. Asian Pac. J. Health Sci. **1**, 385–394 (2014)
11. Villanueva, C.M., Kogevinas, M., Cordier, S., Templeton, M.R., Vermeulen, R., Nuckols, J. R., Nieuwenhuijsen, M.J., Levallois, P.: Assessing exposure and health consequences of chemicals in drinking water: current state of knowledge and research needs. Environ. Health Perspect. **122**(3), 213 (2014)
12. Gopal, R., Ghosh, P.K.: Fluoride in drinking water-its effects and removal. Defence Sci. J. **35** (1), 71–88 (2014)
13. Bashkin, V.N.: Environmental biogeochemistry. Mod. Biogeochem. 355–430 (2002)
14. Sun, M., Arevalo, E., Strynar, M., Lindstrom, A., Richardson, M., Kearns, B., Pickett, A., Smith, C., Knappe, D.R.: Legacy and emerging perfluoroalkyl substances are important drinking water contaminants in the Cape Fear River Watershed of North Carolina. Environ. Sci. Technol. Lett. **3**(12), 415–419 (2016)
15. Oke, S., Vermeulen, D.: Geochemical modeling and remediation of heavy metals and trace elements from artisanal mines discharge. Soil Sediment Contam. Int. J. **26**(1), 84–95 (2017)
16. Ahmad, H.R., Aziz, T., Zia-ur-Rehman, M., Sabir, M., Khalid, H.: Sources and composition of waste water: threats to plants and soil health. In: Soil Science: Agricultural and Environmental Prospectives, pp. 349–370. Springer International Publishing, Berlin (2016)
17. Bonta, M., Hegedus, B., Limbeck, A.: Application of dried-droplets deposited on pre-cut filter paper disks for quantitative LA-ICP-MS imaging of biologically relevant minor and trace elements in tissue samples. Anal. Chim. Acta **908**, 54–62 (2016)

Chapter 56
Landslide Susceptibility Mapping Using AHP Along Mechuka Valley, Arunachal Pradesh, India

Amitansu Pattanaik, Tarun Kumar Singh, Mrinal Saxena and B. G. Prusty

Abstract An integrated approach based on remote sensing and GIS is described for generating Landslide Hazard Zonation and to identify the weaker zones in Mechuka valley in the West Siang district of Arunachal Pradesh. Remote Sensed images are combined in the GIS environment with other spatial factors which influences the occurrence of Landslides. Important terrain factors having an influence on the Landslide occurrence are identified and corresponding thematic layers are generated. These layers include DEM, Slope angle and direction, Lineaments, Drainage, Geomorphology, Landuse/Landcover, Topographic Wetness index and Stream power index. Analytical Hierarchy Process (AHP) modelling is used to assign weightage to the causative factors. Layers are first divided into classes for assigning the ratings and weighted are assigned to the factors on the basis of their influence on landslide occurrence. LHZ map of the study area is generated after assigning the weightages.

Keywords AHP · GIS · Landslide · Mechuka · West siang · Remote sensing

A. Pattanaik (✉) · B. G. Prusty
Defence Terrain Research Laboratory (DTRL), DRDO, Metcalfe House, Delhi 110054, India
e-mail: amitansu@yahoo.com

B. G. Prusty
e-mail: bgprusty@dtrl.drdo.in

T. K. Singh · M. Saxena
Department of Earth Science, University of Petroleum and Energy Studies (UPES), Dehradun, India
e-mail: kumar.singhtarun14@stu.upes.ac.in

M. Saxena
e-mail: mrinalsaxena99@gmail.com

P. J. Rao et al. (eds.), *Proceedings of International Conference on Remote Sensing for Disaster Management*, Springer Series in Geomechanics and Geoengineering,
https://doi.org/10.1007/978-3-319-77276-9_56

1 Introduction

Landslides, a common natural hazard often results in tremendous loss of lives and economy every year due to unpredictability and ignorance. The losses caused by the impact of the hazard can be minimized by recognizing the locations prone to landslides. To prioritize an area of hazard- mitigation efforts, it is beneficial to have a Landslide-susceptibility zonation [1]. Landslide Hazard Zonation (LHZ) is a very important content of landslide hazard prediction modelling [2]. In general, the LHZ map divides the landslide prone hilly terrain into different zones according to the relative degree of susceptibility to landslides [3]. The process of creating these maps requires several qualitative or quantitative approaches [4–6]. A number of factors determines the stability of the slopes but the main controlling factors are Land cover/Land use, Drainage pattern, Lineaments, Slope angle, aspect and anthropogenic activity [7]. AHP model is used to assign weights to the causative factors. The AHP is a theory of measurement for dealing with quantifiable and intangible criteria has been applied to numerous areas, such as decision theory and conflict resolution [8]. In this method, weight of each layer depends upon the judgment of expert, so that the more precise is the judgment, the more compatible is the produced map with reality [9].

Various qualitative and quantitative methods have been conceived for landslide-susceptibility analyses which are mentioned below. Analytical hierarchy process methodology is adopted for preparing landslide susceptibility maps by NRSA [10]. An integrated approach using remote sensing and geographical information system (GIS) is suggested by Sarkar and Kanungo [11]. Rawat and Joshi [12] demonstrate a landslide-susceptibility zonation using the landslide index method. Gokceoglu and Aksoy [13] adopts image processing techniques and deterministic stability analyses for landslide susceptibility mapping. Pachauri and Pant [14] uses geological attributes for landslide hazard mapping.

The upcoming tourist destination near Indo-China border, the mountainous terrain of Mechuka is hosting a small airport and an old famous monastery. Due to the combined effect of snowfall and rainfall, the area is prone to natural mass movement. Hence it warrants a detailed investigation of slope failure analysis. In the present study an attempt has been made to find out the weaker zones or landslide susceptibility mapping using AHP. Here, landslide hazard map is developed by assigning weights to the causative factors on the basis of their effect on landslide susceptibility. The AHP method is used for assigning weight to the causative factors. The LHZ map is prepared and analyzed by using AHP model and integrating GIS and the data obtained from satellite imagery.

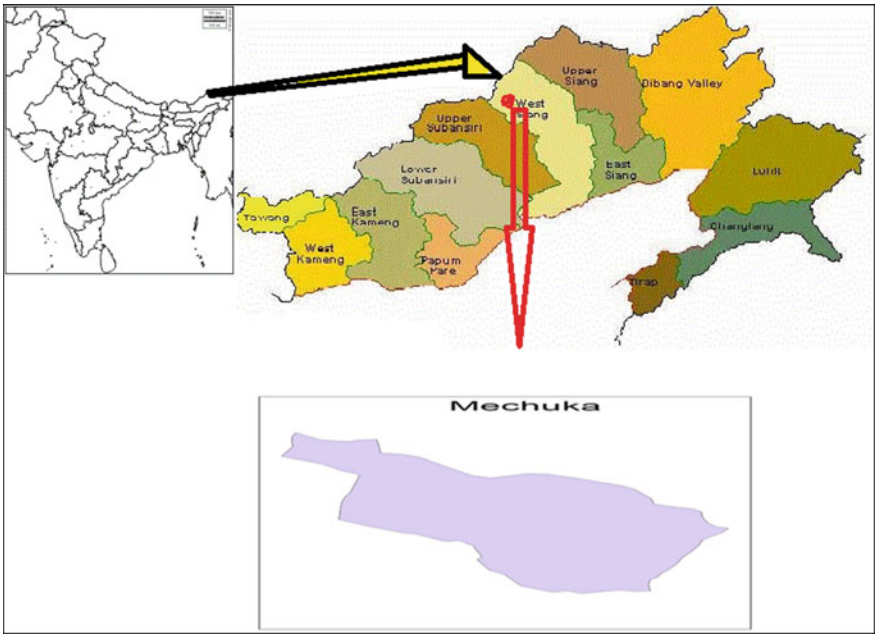

Fig. 1 Study area map

2 Study Area

Mechuka valley in West Siang district of Arunachal Pradesh located about 29 km from Macmohan line at 6000 ft (1829 m) above sea level surrounded by pine trees and thorn bushes is selected for this study, which range from longitude 93.969286 to 94.236334 and latitude 28.434752 to 28.751586. The river Yargyapchu flows in the Mechuka valley from west to east direction. Mechuka is connected to Aalo by a 185 km road which is of strategic importance connecting further to the border village Yarlong from Mechuka. The singing formation is well exposed in the Mechuka quartzite, marble and amphibolites in the lower part and sillimanite schist in the upper part (Fig. 1).

3 Causative Factors Layer Preperation

The key issue in forecasting the landslide or other geological hazards is the identification and collection of the relevant predictors whose nature, character and role vary depending on the types of disaster and geological, geomorphological and climate setting of the region affected by the extreme event [15]. In this paper, a total of 10 layers are created that contributes towards occurrence of landslides. These

layers are: Slope map, Aspect map, Drainage Map. Lineament Map, Road Network, Landuse/Landcover map, Stream power index, Topographic Wetness Index, Soil Erosion Map and Geomorphological Map. A Digital Elevation Model of the study area was used to extract information about slope, aspect, SPI and TWI.

3.1 Digital Elevation Model (DEM)

DEM of the study area is extracted from the ASTER GDEM Ver. 2 satellite data with DEM accuracy (stdev.) of 7–14 m and posting interval of 30 m. A DEM of the study area is shown in Fig. 2.

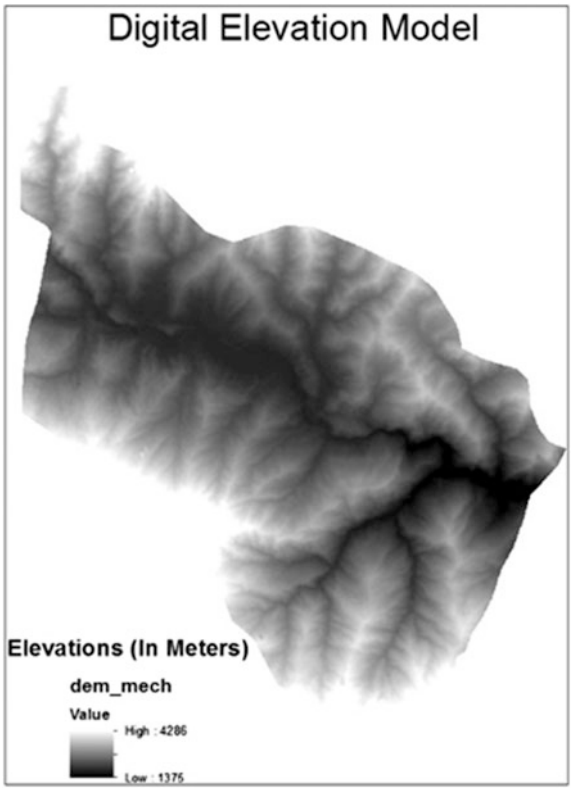

Fig. 2 DEM map of the study area

3.2 Slope

Slope map of the study area is prepared from the digital elevation model of the area. The slope map shows the slope angle of the terrain ranging from 0° to 88°. The slope value are divided into five different ranges and then reclassified into five values from 1 to 5 based on their steepness. Slopes having slope angle between 30° and 45° are more susceptible to landslides (Fig. 3; Table 1).

3.3 Aspect Map

Aspect is also considered an important factor in the preparation of landslides hazard zonation maps. Aspect map shows the direction of the hill slopes ranging from 0° to 360°. The aspect of the area is classified into flat, north, northeast, east, southeast, south, southwest, west and northwest facing classes. It is reclassified to give the slope orientation values ranging from 0 to 6 with 6 contributing highest and 0 contributing lowest to the landslide occurrence (Fig. 4; Table 2).

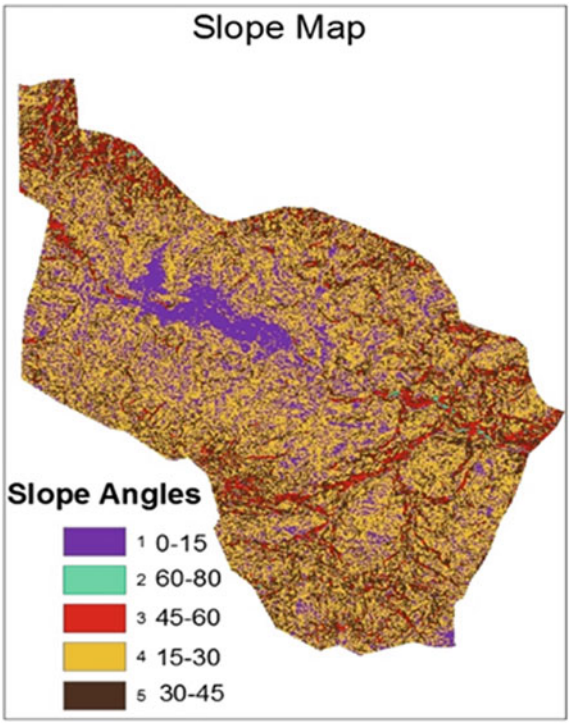

Fig. 3 Slope map of the study area

Table 1 Slope statistics

Slope subclass	Slope	Rating value
A	0–15	1
B	15–30	4
C	30–45	5
D	45–60	3
E	60–80	2

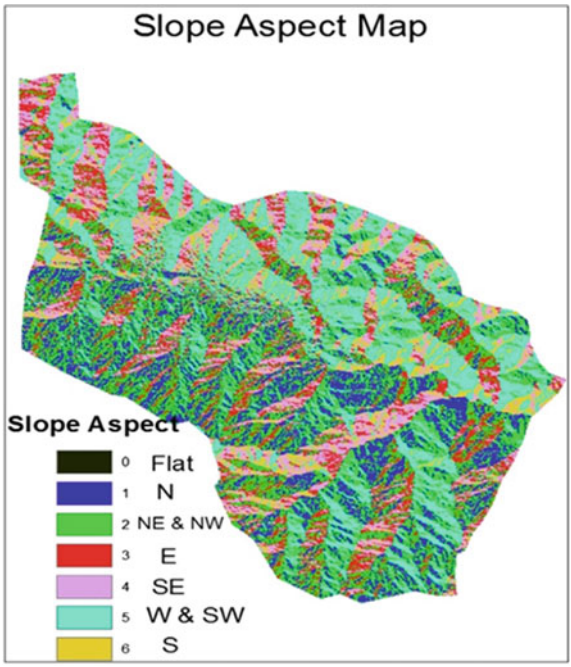

Fig. 4 Aspect map of the study area

Table 2 Aspect statistics

Aspect subclass	Aspect	Rating value
A	Flat	0
B	North	1
C	North east	2
D	East	3
E	South east	4
F	South	6
G	South west	5
H	West	5
I	North west	2

3.4 Lineaments

Lineament map is formed by digitizing the lineament map of scale 1:50,000 of the study area provided by Bhuvan. Thy types of lineaments found in the study area are mainly Geomorphic lineaments, Drainage parallel. As the distance from the lineaments become smaller, the fracture of the rock masses and the degree of weathering increases resulting in greater chances of landslide occurrences [16]. So the ring buffer of the lineament is prepared showing 100, 200 and 400 m distances and the weightage is given based upon the distance from the lineaments (Fig. 5; Table 3).

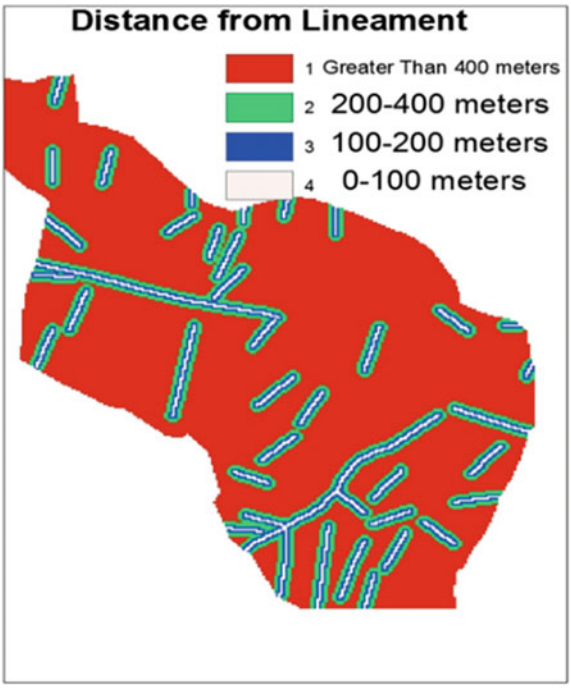

Fig. 5 Reclassified lineament map

Table 3 Lineament rating value

Distance from lineaments (subclass)	Distance from lineament (meters)	Rating value
A	0–100	4
B	100–200	3
C	200–400	2
D	>400 m	1

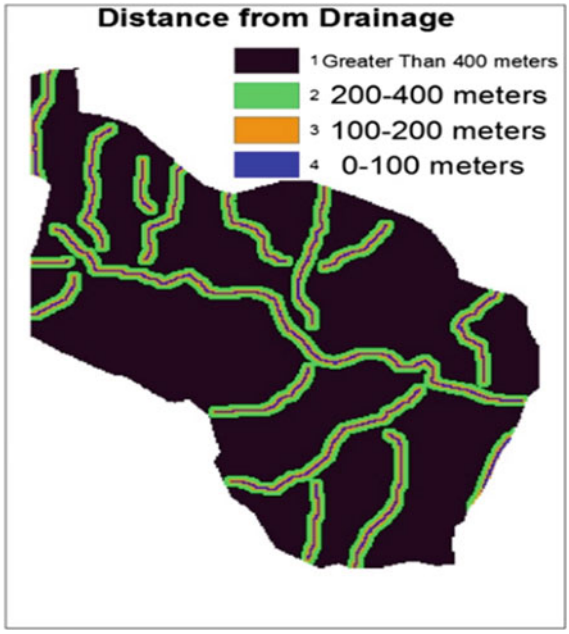

Fig. 6 Drainage map

3.5 Drainage Map

Improper drainage pattern results into increase in fluid pressure and increase in weight due to the addition of water which can lead to the occurrence of the landslides. Drainage map is prepared by digitizing a drainage map provided by GSI. Buffering of drainage pattern is done and value are given on the basis of the distance from the drainage (Fig. 6).

3.6 Land Use/Land Cover

The land use/land cover map is prepared from sentinel satellite imagery data having resolution of 20 m of the study area. Supervised classification is done to divide the study area into five classes: (1) Grass/grazing, (2) Water, (3) Built up, (4) Deciduous forest, (5) Agricultural land. From various investigations, it is learnt that landuse/vegetation cover, especially of a woody type with strong and large root system helps to improve the stability of slopes [17].

Non forest area which are nearer to river and built up are more susceptible to landslides as compared to forest areas. The area covered by different classes are given in Table 4. Based on their effect on the landslide occurrence relative weights are given to the classes. The rating value are given in Table 5 (Fig. 7).

Table 4 Land use/land rating value

Landcover subclass	Landcover	Rating value
A	Evergreen forest	1
B	Water body	3
C	Builtup/agriculture land	4
D	Grass/barren land	5

Table 5 Land use/land cover statistics

Feature of land use/land cover	Area covered (m^2)
Water	4,093,462.25
Built up/agriculture	2,790,991.83
Grass land/barren land	39,427,565.44
Evergreen forest	413,647,840

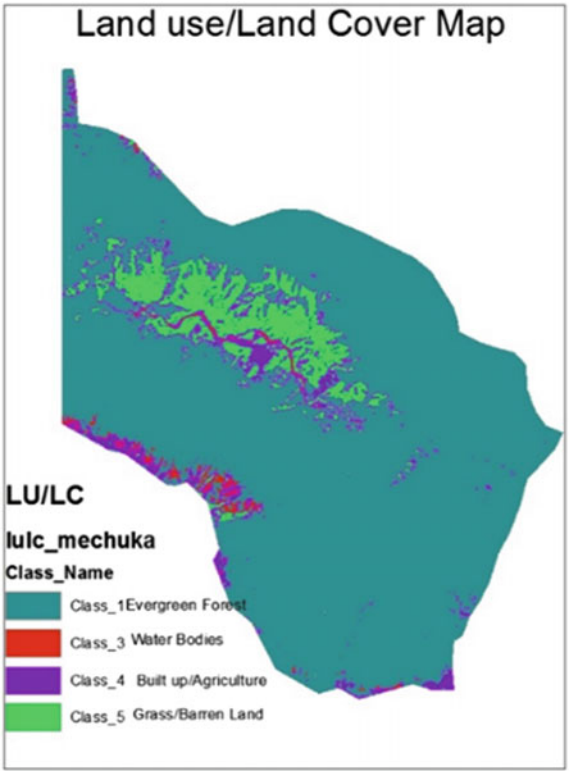

Fig. 7 LU/LC map of the study area

3.7 Soil Erosion Map

The soil erosion map is created by digitizing the erosion map of the study area having scale 1:50,000 provided by BHUVAN. The type of erosion which occurs in the study area is sheet erosion. The area which are affected by sheet erosion are shown in the map (Fig. 8).

3.8 Geomorphology Map

The geomorphology map is created by digitizing the geomorphology map of the study area obtained from the BHUVAN having a scale of 1:50,000. The geomorphology map is divide into three classes: (a) Moderately dissected structural hills, (b) Low dissected structural hills, (c) Wetlands. Relative rating is given to them on the basis of their influence on the occurrence of the landslide. Moderately dissected hills are more prone to landslides than lowly dissected structural hills (Fig. 9; Table 6).

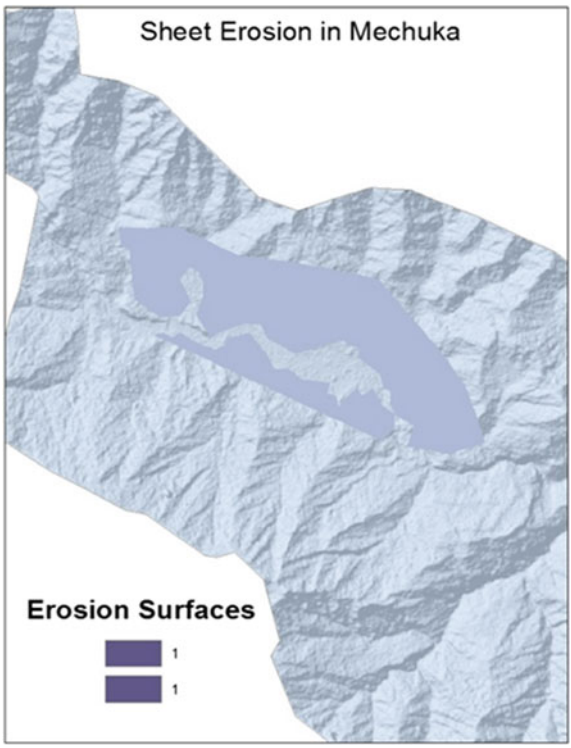

Fig. 8 Soil erosion map of the study area

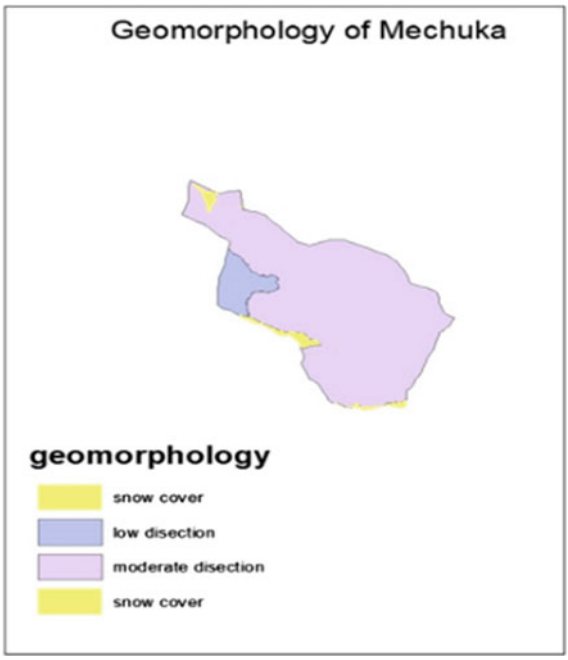

Fig. 9 Geomorphology map

Table 6 Geomorphology rating

Geomorphological feature	Rating value
Snow cover	1
Low dissection	1
Moderate dissection	2

3.9 Road Network Map

A road network map is developed by digitizing the district map of West Siang. A multiple ring buffer is created around the road network dividing the distance around the road in 4 categories. The area closest to the roads are more susceptible to landslide (Fig. 10; Table 7).

3.10 Stream Power Index

Stream Power Index can be used to describe the potential flow erosion at a given point of the topographic surface. Stream Power index is calculated for a given point using the slope and flow accumulation values of that point and putting into the equation:

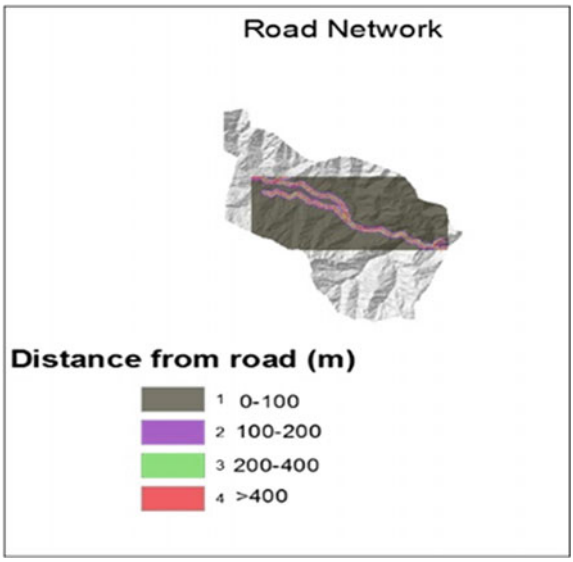

Fig. 10 Road network map

Table 7 Road map rating

Distance from roads (m)	Rating value
0–100	4
100–200	3
200–400	2
>400	1

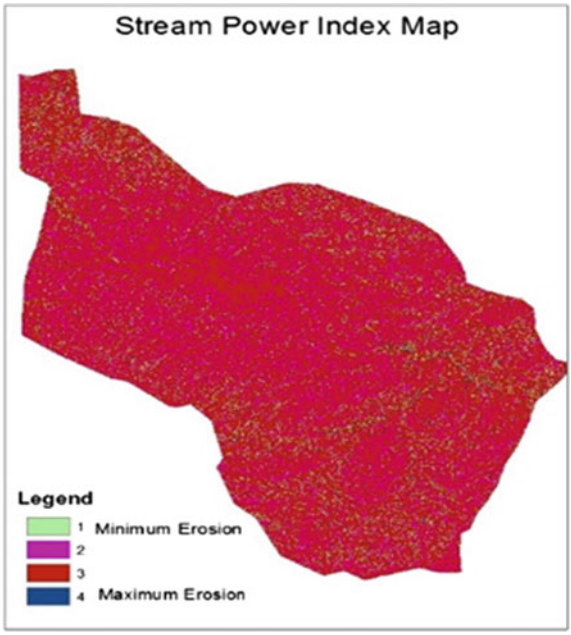

Fig. 11 Stream power index map

$$\mathbf{Ln}\,(\mathbf{FA}+\mathbf{0.001})*((\mathbf{Slope}/\mathbf{100})+\mathbf{0.001})$$

where, FA = Flow Accumulation Values and Slope = Slope Angle (Fig. 11).

3.11 Topographic Wetness Index

Topographic Wetness Index is a steady state Wetness Index. It is commonly used to quantify topographic control on hydrological processes. Topographic Wetness Index can be calculated for a given point by using the flow accumulation and slope values for a given point. Equation for calculating topographic wetness index is:

$$\mathbf{Ln}(\mathbf{FA}+\mathbf{0.001})/((\mathbf{Slope}/\mathbf{100})+\mathbf{0.001})$$

where, FA = Flow Accumulation Values and Slope = Slope Angle.

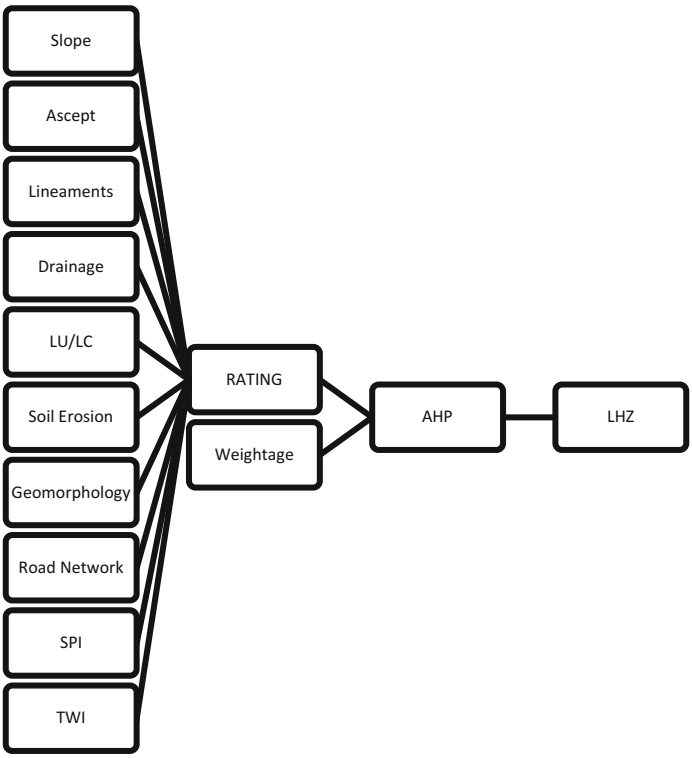

Fig. 12 Methodology chart

4 Methodology

The weighting-rating system is applied to perform LHZ [18]. The various causative factors are rated on the basis of their effect on landslide occurrence. Firstly, each layer is broken into smaller factors, then these factors are weighted based on their importance, and eventually the prepared layers are assembled and the final map is produced. It is based on three principles: decomposition, comparative judgment and synthesis of priorities [19] (Fig. 12).

5 Result

The study area is divided into four classes on the basis of the degree of landslide susceptibility by landslide hazard zonation map. The areas covered under the four classes are shown in Fig. 13. The four classes are: Very Low, Low, Medium and High susceptibility zones. The area covered by each classes is mentioned in Table 8. The weaker zones along the road network are shown in Fig. 14.

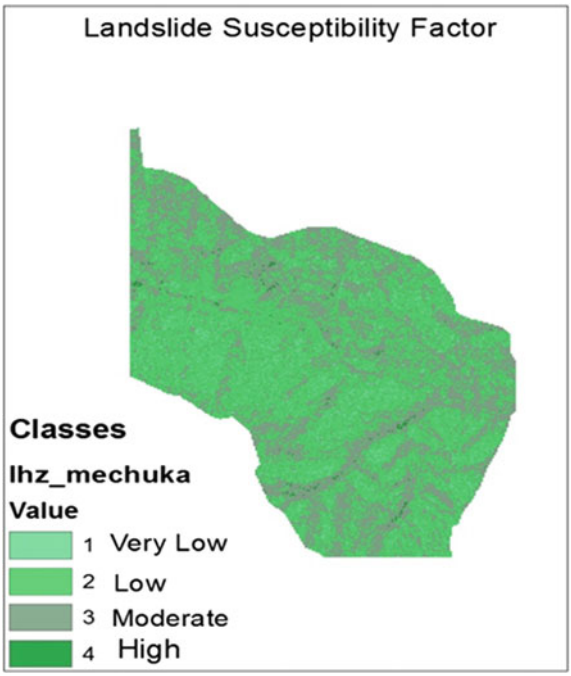

Fig. 13 LHZ map

Table 8 Weightage table

Landslide casual factors	Weighted values
Slope	0.20
Aspect	0.10
Distance from drainage	0.15
Distance from lineament	0.15
Landuse/landcover	0.05
Topographic wetness index	0.10
Stream power index	0.10
Distance from roads	0.05
Soil erosion	0.05
Geomorphology	0.05

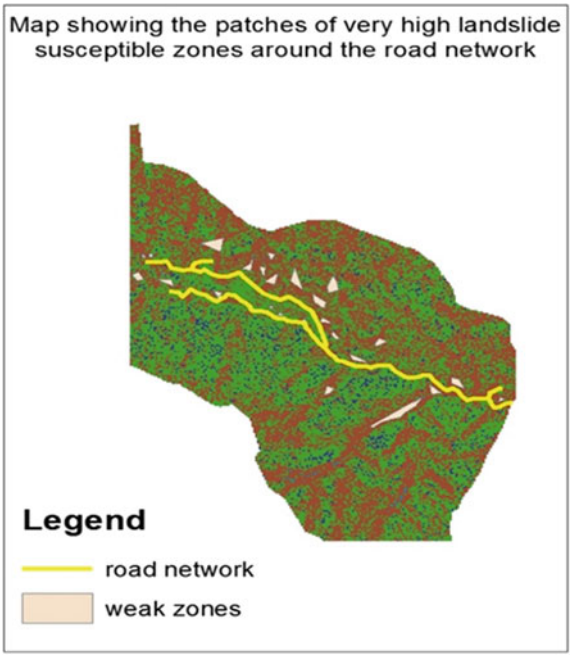

Fig. 14 Patches of weak zones around the road network

6 Conclusion

In this paper the landslide hazard zonation mapping is done by integrating both remote sensing and GIS, the remote sensing based parameters and data are evaluated by the help of GIS techniques to create the LHZ map and to detect the weaker zones in the study area. The LHZ map divides the area into four zones from very low susceptibility risk to high susceptibility risk. The weightage is assigned to causative factors and LHZ map is prepared by the use of analytical hierarchy

process (AHP). This study suggests that the causative factors must be selected with care and the rating scheme must be improved iteratively by evaluating the results. The south facing slope has a greater influence on landslide occurrence which may be because of the direction of the wind flowing and climate in Himalayan region. This method can be very effective for the rapid assessment of the risk of landslide even in inaccessible areas. Afforestation of barren lands, proper drainage arrangement and controlled settlement and infrastructure facilities are very important for reducing and controlling the landslide activities in the study area.

References

1. Anbalagan, R.: Landslide hazard evaluation and zonation mapping in mountainous terrain. J. Eng. Geol. **32**, 269–277 (1992)
2. Wang, J., Peng, X.: GIS-based landslide hazard zonation model and its application. Proc. Earth Planet. Sci. **1**, 1198–1204 (2009)
3. Marrapu, B.M., Jakka, R.S.: Landslide hazard zonation methods: a critical review. Int. J. Civil Eng. Res. **5**(3), 215–220 (2014)
4. Soeters. R., Van Westen, C.J.: Slope instability recoginition, analysis, and zonation. In: Turner, K.A., Schuster, R.L. (eds.) Landslide: Investigation and Mitigation, pp. 129–177. Transport Research Board Specila Report, 247
5. Guzzetti, F., Carrara, A., Cardinalli, M., Reinchenbach, P.: Landslide hazard evaluation: a review of current techniques and their application in multi-scale study Central Italy. Geomorphology **31**(1–4), 181–216 (1999)
6. Onagh, M., Kumra, V.K., Rai, P.K.: Landslide susceptibility mapping in part of Uttarkashi district (India) by multiple linear regression method. Int. J. Geol. Earth Environ. Sci. **2**(2), 102–120 (2012)
7. Mathur, V.K., Sarkar, S.: Recent trends in landslide hazard zonation and risk assessment: an overview. In: Nagarajan, R. (ed.) Landslide Disaster, Assessment and Mointoring, pp. 97–103. Anmol Publication, New Delhi (2004)
8. Vargas, L.G.: An overview of the analytica hierarchy process and its applications. Eur. J. Operational Res. **48**, 2–8 (1990)
9. Moradi, M., Bazyar, M.H., Mohammadi, Z.: Gis-based landslide susceptibilty mapping by Ahp Method, a case study, Dena City, Iran.j. Basic. Appl. Sci. Res. **2**(7), 6715–6723 (2012)
10. NRSA: Landslide hazard zonation mapping along the corridors of the pilgrimage routes in Uttaranchal Himalaya, Technical Document. NRSA, Hyderabad (2001)
11. Sarkar, S., Kanungo, D.P.: An integrated approach for landslide susceptibility mapping using remote sensing and GIS, photogram. Eng. Remote Sensing **23**, 357–369 (2004)
12. Rawat, J., Joshi, R.: Remote-sensing and GIS-based landslide-susceptibility zonation using the landslide index method in Igo River Basin, East. Himalayan, India. Int. J. Remote Sensing **33**(12), 3751–3767 (2012). https://doi.org/10.1080/01431161.2011.633
13. Gokceoglu, C., Aksoy, H.: Landslide susceptibility mapping of the slopes in the residual soils of the Mengen region (Turkey) by deterministic stability analyses and image processing techniques. Eng. Geol. **44**, 147–161 (1996)
14. Pachauri, A.K., Pant, M.: landslide hazard mapping based on geological attributes. Eng. Geol. **32**, 81–100 (1992)
15. Carrara, A., Guzzetti, F., Cardinali, M., Reichenbach, P.: Use of GIS technology in the prediction and monitoring of landslide hazard. Nat. Hazards **20**, 117–135 (1999)
16. Farrokhnia, A., Pirasteh, S., Pradhan, B., Pourkermani, M., Arian, M.: A recent scenario of mass wasting and its impact on the transportation on Albrozmountations, Iran using

geo-information technology. Arab. J. Geosci. (2010). https://doi.org/10.1007/s12517-010-0238-7
17. Gray, D.H., Leiser, A.T.: Biotechnical slope protection and erosion control. Van Nostrand Reinhold, New York (1982)
18. Saha, A.K., Gupta, R.P., Arora, M.K.: GIS-based landslide hazard zonation in the Bhagirathi (Ganga) Valley, Himalayas. J. Remote Sensing. **2**(2002), 357–369 (2002)
19. Malezewski, J.: GIS and multi-criteria decision analysis. Wiley, NewYork (1999)

Chapter 57
Geo Spatial Study on Fire Risk Assessment in Kambalakonda Reserved Forest, Visakhapatnam, India: A Clustering Approach

Gudikandhula Narasimha Rao, Peddada Jagadeeswara Rao, Rajesh Duvvuru, Sridhar Bendalam, Roba Gemechu, Dadi SanyasiNaidu and Kondapalli Beulah

Abstract Wild fire classifications can be demonstrated as a stochastic opinion process wherever actions remain considered through their spatial positions then incidence popular interval. Group examination licences recognition of the planetary/period decoration circulation of wild fires. Such investigates remain valuable to support excitement supervisors in classifying hazard zones, applying precautionary actions and steering policies for an effectual dissemination of the fire fighting possessions. This research objectives to classify burning adverts in wild excitement structures via means of the Space-time Image Statistics Change (SISC) ideal besides a Geographical Information System (GIS) on behalf of statistics plus consequences conception. The image geometric procedure habits a perusing gap, it transfers through universe and interval, identifying native extremes for actions in

G. N. Rao (✉) · P. J. Rao · R. Duvvuru · S. Bendalam · R. Gemechu · D. SanyasiNaidu
Department of Geo-Engineering and Centre for Remote Sensing, Andhra University, Visakhapatnam, India
e-mail: narasimha.geo@cea.auvsp.edu.in; gudikandhula@gmail.com

P. J. Rao
e-mail: pjr_geoin@rediffmail.com

R. Duvvuru
e-mail: rajesh.duvvuru@gmail.com

S. Bendalam
e-mail: sridhar.bendalam@gmail.com

R. Gemechu
e-mail: robageme2009@gmail.com

D. SanyasiNaidu
e-mail: sndadi@gmail.com

K. Beulah
Gayatri Vidya Parishad College of Engineering (A), Visakhapatnam, India
e-mail: kondapalli.beulah@gmail.com

P. J. Rao et al. (eds.), *Proceedings of International Conference on Remote Sensing for Disaster Management*, Springer Series in Geomechanics and Geoengineering,
https://doi.org/10.1007/978-3-319-77276-9_57

exact zones ended a certain period of time. Lastly, geometric consequence of every collection is assessed over proposition analysis. The case revision of wild fires recorded via the forest provision in Kambalakonda Reserved Forest, Visakhapatnam (India) from 2000 to 2016. Such dataset contains of geo referenced solitary actions with position of the burst facts plus other facts.

Keywords Wild fires · Cluster exploration · Point patterns · Space-time image statistics change

1 Introduction

Forests cover around 30% of the whole earth terrestrial part in addition to require a key role in the lifespan on ground. For example, they are important for special guideline of CO_2 and O_2, earth preservation, instruction of the hydrological series, though concurrently provided that habitation aimed at numerous classes and valuable harvests [1]. Plantation delivery plus arrangements remain frequently exaggerated through excitements. That proceedings may benefit woodland bionetworks through adaptable classes arrangement besides inducing herbal growth and imitation; though, excitements can harshly impend the fundamental atmosphere after they remain unrestrained otherwise once the forestry environments stay non fire altered. Wild excitement spectacles display composite and uneven spatio-temporal deliveries, they sort the situation tough on behalf of demonstrating in addition forecasting of that performance [2].

Visakhapatnam remains normally never exposed towards large otherwise mutual plantation excitements; however, roughly 20 excitements yield place each year in its ground, terminating awake to 100 hectares of woodlands those remain prized in the direction of the country's public commercial segments in addition aimed at the shield in contradiction of additional normal dangers. The mainstream of the jungle excitements in this district are located in the built-up region, dry leafs, etc. [3]. Wild fires incidence, strength and dissemination are measured by the concurrence of diverse issues those are occurrence of oil, excitement conductive ecological circumstances in addition explosion vitality [4]. Once excitement occasions remain persistent with reliable in a specific zone ended a definite era of interval, they typically consequence of an exact excitement management [5]. Now a day's fires are mostly the outcome of resolution wars in background corruption as a concern of anthropogenic events.

In this perspective, the main goal of the current revision is to notice spatio-temporal gatherings of plantation excitements, by way of examine with explosion reasons of subsequent collections. That information should additional assistance fire supervisors and native establishments to describe in addition to develop excitement strategy as well as switch actions. Normally, spatial gathering study may define through intimate of procedures pointing by alignment three dimensionally disseminated substances viewing a native over compactness.

Those procedures could be gathered in universal in addition to native approaches. At main cluster pursues towards mathematically describe those proceedings below revision demonstrates an accidental scattering otherwise grouped configuration. That subsequent cluster, native approaches, proposes to classify and find clusters in space [6].

The following section (Sect. 2) describes the study area, the data set collected by the Forest Survey of India, and the scan measurements procedure applied in the expansion of this study. Section 3 describes the consequences found after simulations. Sections 4 present a discussion and conclusions, correspondingly, drawn from the analyses.

2 Materials and Methods

2.1 Study Area

The State of Andhra Pradesh is placed in the middle of eastern half of the Indian Peninsula lying between 12° 41′–19° 54′N latitudes and 76° 46′–84° 45′E longitudes. The Greater Visakhapatnam Municipal Corporation (GVMC) is one of the biggest fire regions in Andhra Pradesh. The study area is Kambalakonda Reserved Forest spread over 7146 hectares located near Visakhapatnam, Andhra Pradesh, India. Although quite often a natural phenomenon, wildfires constitute a very dangerous environmental hazard that causes significant ecological damage and many human casualties every year around the world [7].

The expansion of the wild land urban interface (WUI) areas of our modern cities, the drought caused by the elevation of the mean temperatures, as well as short-sighted human interventions, have created favorable conditions for more frequent forest fire eruptions that are getting increasingly complicated to deal with. A wildfire behavior simulation program capable to estimate accurately the fire's propagation path can be an important tool for effective crisis management [8]. The following Fig. 1. Location map of Kambalakonda Reserved Forest Region, Visakhapatnam, India.

2.2 Forest Fire Geo-Database

General statistics of plantation excitements in Kambalakonda Reserved Forest, Visakhapatnam, India has been gathered by the Forest Survey of India. Beginning since 1985, the statistics consumes remained prepared for interactive geodatabase, which supplies geo-tagged evidence to only excitement measures: Latitude and longitude directs of the explosion facts, day of main apprehension, time of excitement extermination, explosion reason, blackened zone, angle, and elevation.

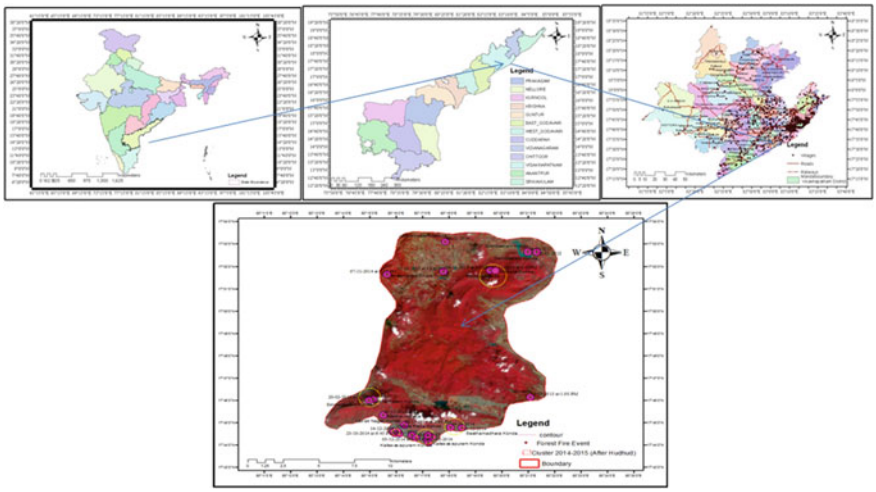

Fig. 1 Location map of Kambalakonda Reserved Forest, Visakhapatnam, India

On behalf of current revision, examined whole plantation excitements documented among January 1st 1985 in addition to November 30th 2016 including number of excitement measures [9]. From this geodatabase, numerous datasets were mined to accomplish dissimilar replications concerning fire-origins with diverse covering eras. Merely the two more important revisions are described in this paper: The first examination by all the occasions permitting a completes examination of all excitements, and the another examination seeing only the actions due to lightning in Simhachalam hills, kappa Rada Konda, Kailasapuram Konda and Seethammadhara konda etc.

Since the technique suggested on that research never differentiate bunches payable to the growth danger of excitement otherwise payable towards the diverse environmental occurrence circulation on dissimilar periods, the main dataset, that contains all excitements, was split into four clusters in order to get further similar fire regime situations as likely for a complete numerical examination. It describes after Hudhud cyclone effect of fire regions in Visakhapatnam from 2014 to 2015 due to the reason of dry leafs, dry plants and trees. Hudhud produced wide destruction to the municipality of Visakhapatnam besides the adjacent regions of Vizianagaram and Srikakulam of Andhra Pradesh in 2014 [10].

The most capable fire-preventative natures measured at examines. The leading excitement groups reformation applied in 1985, an efficient use of helicopters for together conveyance of the excitement battalions in addition terrestrial fire fighting in 2014; an execution of dual defensive permissible performances (1989 and 2015) pointing in elimination boiling events at those exposed places. The sudden excitement dataset remained distinctly examined above whole training time (2014–2016) including an overall of 34 occasions, specified which excitement command is

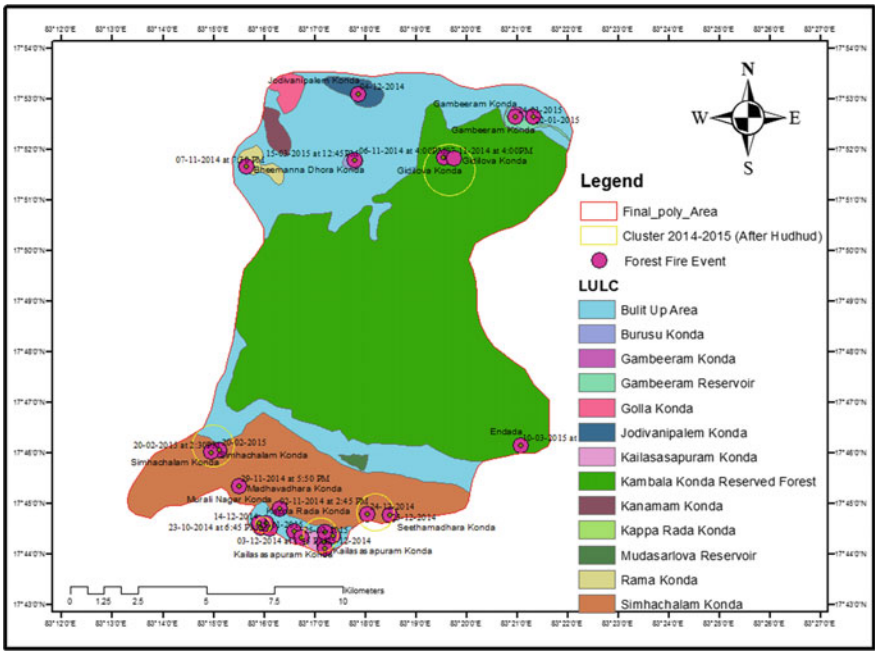

Fig. 2 Land use land cover map of Kambalakonda Reserved Forest, Visakhapatnam

fairly dissimilar after the anthropogenic affected excitements besides the ignition amounts never exaggerated through which procedures stated overhead.

As shown in Fig. 2, the dissemination of the yearly sum of excitements throughout the entire study era is somewhat uneven, with an overall implication in the direction of minor fire incidences (<60 events per year) over 2014 [11]. The yearly burnt parts in Fig. 3 are usually of minor dimensions (<500 ha per year) with a tendency to lesser standards after 1985; nevertheless, fires can get out of switch when fire-prone situations are present through the year.

2.3 Space-Time Image Statistics Change

Image measurement signifies a group of approaches, recycled and improved in various areas, to examine for native extremes of actions (clusters) in together space and/or period. The highest determination is to control whether or not an experiential collection, expected to fit to an arbitrarily dispersed design, is statistically important or has slightly happened by accidental. The technique remained first established in fitness discipline by Naus, and additional recently, on one occasion extra in the fitness area, Kulldorff industrialized three-dimensional and spatio-temporal delays.

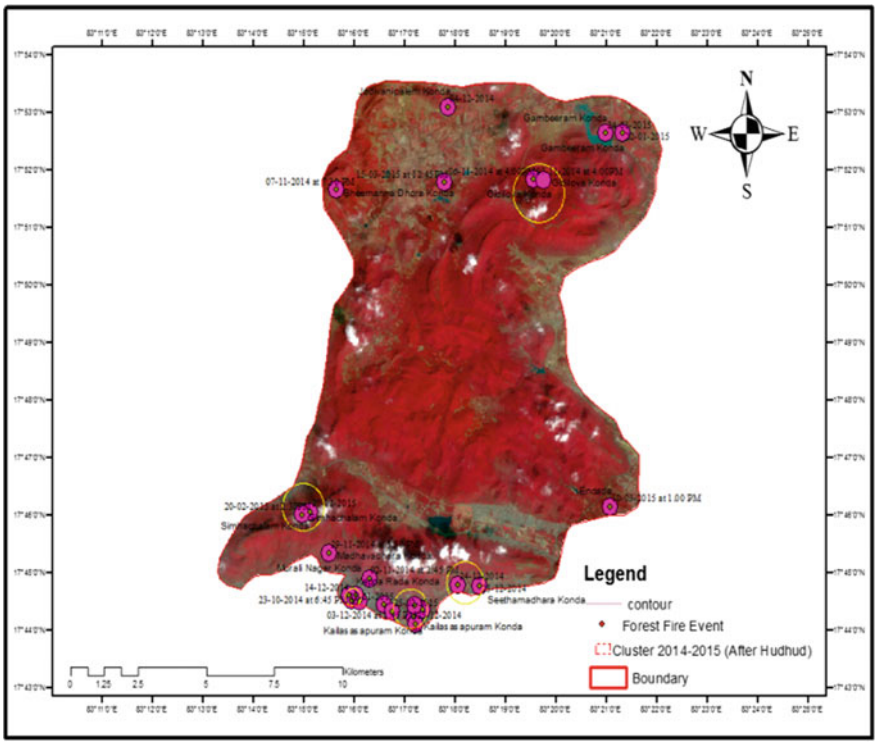

Fig. 3 Satellite image of Kambalakonda Reserved Forest fire clusters

At the present time, these approaches are applied in a big diversity of arenas. For the morally three-dimensional image measurements, the area below learning is look over through rounded gap focused at every occasion. Every space changes diagonally the whole zone, changing its range constantly after zero up to a static higher boundary. Every ring receipts the nearest neighbor events position decreasing confidential and associates them with those lying external. Below the useless theory of three-dimensional chance, these proceedings are incidental to be dispersed rendering with recognized separate formal arbitrary procedure, such restrictions must be assessed. Assumed that supposition, these proceedings remain arbitrarily then autonomously dispersed with an exact part.

The likelihood function, demonstrating the possibility that an exact region comprises a cluster, is calculated for each imaginable perusing gap in addition the single exploiting task signifies maximum probable collection. That numerical consequence to engaged possible collections are assessed in mandate towards examine or not those must happened through accidental [12]. On behalf of such determination, Monte Carlo hypothesis testing stood achieved through a huge amount of accidental duplications database produced below the unimportant assumption.

The abundant of full probability beginning the actual dataset remains associated by the abundant of extreme probability after accidental datasets. Intended for example, any probability relation through greatest probable bunch goes beyond 90% over the ideals in the Monte Carlo imitations. Finally bunch is measured to be important by 5% level (p-value 00.05). That technique, it is likely toward castoff a bunch at what time the equivalent p-value is overhead the static onset price. Grounded at this wanted onset, the amount of Monte Carlo imitations remains recognized.

That computing technique of the space-time image measurements are the version of the morally three-dimensional image number in universe and period. This spherical gap remains substituted through a piston by the circular improper on behalf of physical universe and elevation consistent with interval period at possible collections. Chamber's dimensions may growth since null up to an extreme worth in together interplanetary and period. By way of decently longitudinal image measurements, all chamber calls every occasion physical position then, moreover, the situation calls every likely period era.

Let C be the total number of observed cases and C_{zd} the number of cases observed within a zone z in a day d. The expected number of cases U_A for a space-time cylinder A can be estimated as the sum of U_{zd} (the number of expected cases per day and per zone) belonging to cylinder A:

$$U_A = \sum_{zd€A} U_{zd}, \quad \text{Where } U_{zd} = 1/C\left(\sum_{z} C_{zd}\right)\left(\sum_{d} C_{zd}\right)$$

Let CA be the number of observed cases in a cylinder A. Inferring that this variable follows hyper geometric distribution and that C is large compared to $\sum$z€ACzd and $\sum$d€ACzd, then C_A can be considered to be Poisson-distributed with mean UA. Thus, a Poisson Generalized Likelihood Ratio (GLR) can be computed as follows:

$$\text{GLR} = (C_A/U_A)_A^{(C)}(C - c_A/C - u_A)_A^{(C-C)}$$

This proportion is considered and exploited for each likely chamber and Monte Carlo imitations are made to examine the arithmetical implication of the noticed clusters. SISC technique is a arithmetical tool exact valuable for the study of the supply of ecological information [4].

3 Results

In the current study intentions were achieved with SaTScan software established by Martin Kulldorff. The platform permits the operator to specify all the necessities to achieve the investigation, such as contribution statistics, organizes scheme,

study era, sum of Monte Carlo repetitions, etc. Regarding the participation statistics and the study era, cluster examines were showed for four datasets as labeled in and for each one a SaTScan imitation was achieved [13]. All fire proceedings were stated as separate positions by every opinion demonstrating one fire incidence (case) and the connected date of fire-ignition in the presentation of day-month-year. The outcomes are non-overlapping clusters recognized by the reflective space-time variation ideal [14].

4 Conclusions

The exhaustive fire catalogue from Visakhapatnam permitted the identification of the excitements included in all of the noticed five clusters. The investigation of triggered fires, mutual with the consequences of the SISP examines (groups position and border time), delivers actual valuable evidence regarding the features of the clusters and their physical and sequential works. Likewise, the recognition of sudden excitement groups might be a first opinion for a shallower investigation for excitement inhibition in the hilly areas, in assessment of the dryer and fast fire richer summer times in the prospect. This procedure should be an exact computationally severe, taking up to many days or weeks.

Acknowledgements Authors thank to forest conservative officer, Visakhapatnam, India for their data support from last several years. Special thanks to ABN Andhra Jyothi, Visakhapatnam, India for supply of fire videos to this study.

References

1. ArcGIS Server 9.3 Help: Publishing optimized map services? Release 9.3. Redlands
2. APIeXMLeWunderWiki: http://wiki.wunderground.com/index.php/API-XML. Accessed 04 Feb 12
3. Ortmann, J., Limbu, M., Wang, D., Kauppinen, T.: Crowdsourcing linked open data for disaster management. In: Proceedings of the Terra Cognita Workshop on Foundations, Technologies and Applications of the Geospatial Web. Bonn, Germany (2011)
4. Rao, G.N., Rao, P.J., Duvvuru, R.: A drone remote sensing for virtual reality simulation system for forest fires: semantic neural network approach. In: IOP Conference Series: Materials Science and Engineering. vol. 149. no. 1. IOP Publishing, 2016
5. Rao, G.N., et al.: An enhanced real-time forest fire assessment algorithm based on video by using texture analysis. Perspect. Sci. **8**, 618–620 (2016)
6. Rothermel, R.C.: A mathematical model for predicting fire spread in wildland fuels, USDA FS, Odgen TU, Res. Pap. INT-115 (1972)
7. Williams, D.: On the elements of being. Rev. Metaphys. 7, 3–18 (1953). Reprinted in Metaphysics: The Big Questions (1998)
8. Rao, G.N., et al.: An automated advanced clustering algorithm for text classification. IJCST **3**(2–4), eISSN 0976–8491, pISSN 2229–4333 (2012)

9. Weatherspoon, C.P., Skinner, C.N.: An assessment of factors associated with damage to tree crowns from the 1987 wildfires in Northern California. For. Sci. **41**, 430–451 (1995)
10. Tversky, B., Lee, P.U.: How space structures language. In: Freksa, C., Habel, C., Wender, K.F. (eds.) Spatial Cognition: An Interdisciplinary Approach to Representing and Processing Spatial Knowledge, vol. 1404, pp. 157–175. Springer, Berlin (1998)
11. Vasilakos, C., Kalabokidis, K., Hatzopoulos, J., Kallos, G., Matsinos, Y.: Integrating new methods and tools in fire danger rating. Int. J. Wildland Fire **16**(3), 306–316 (2007)
12. Rao, G.N., Rao, P.J.: A clustering analysis for heart failure alert system using RFID and GPS. In: ICT and Critical Infrastructure: Proceedings of the 48th Annual Convention of Computer Society of India, vol I. Springer, Cham (2014)
13. Rogstadius, J., Teixeira, C., Vukovic, M., Kostakos, V., Karapanos, E., Laredo, J.: CrisisTracker: crowdsourced social media curation for disaster awareness. IBM J. Res. Dev. **57**(5), 4:1–4:13 (2013)
14. Unnikrishnan, P.N.: Silent Valley National Park Management Plan 1990.91–99, 2000, pp. 1–83. Silent Valley National Park Division, Mannarghat (1989)

Chapter 58
Signatures of Last Glacial Cycle and Tectonics Along Gopalpur-Konark Coastal Tract, Odisha

B. M. Faruque

Abstract The signatures of transgression of Last Glacial Cycle (LGC) can be inferred from the continental shelf sediments and onshore landforms. The sea level lowered to 122 m exposed, almost the entire width of the continental shelf, to subaerial condition. The LGC transgressive sea level reached the present sea level about 6–7 ka BP. The rise of the sea level above the psl has given final shape to Mahanadi delta and evolved Lake Tampara as a trace of the palaeoshoreline, now located at 5.90–7.25 m above the present sea level. Two major lakes—Samang Lake and Sar Lake, originally brackish water turned fresh water after the shoreline receded from these water bodies, are the remnants of palaeoshoreline north of Puri. Bhargavi river which meandered southerly till early Holocene took a westerly turn due to the ENE–WSW trending ridge to the north of Puri, and alternating linear depressions. There is an increase in the episodes of beach erosion in some parts of Odisha. It is relevant to mention here that the erosion occurring along the Puri beach, is triggered by strong wave events and lowering of atmospheric pressure. The problem of erosion needs to be handled in a way that does not interfere with the natural systems.

Keywords Last glacial cycle · Palaeobeach ridges · Abandoned channels Closed basin · Dunes

1 Introduction

The rhythm of climatic change was much more complex than the simple idea of climatic alternation, and the studies during the last few decades have revealed that every glacial period was interrupted by minor interglacial phases, during which the ice front receded, and similarly each interglacial stage was punctuated by colder phases during which ice sheets formed afresh or made notable advance in their

B. M. Faruque (✉)
Geological Survey of India, Zahirland, Tinkonia Bagicha, Cuttack, India
e-mail: bmfaruque@gmail.com

P. J. Rao et al. (eds.), *Proceedings of International Conference on Remote Sensing for Disaster Management*, Springer Series in Geomechanics and Geoengineering,
https://doi.org/10.1007/978-3-319-77276-9_58

shrunken conditions. The Quaternary climatic history has been subdivided on the basis of the drift deposits and the four major glaciations have been named in the ascending order as Gunz, Mindel, Riss and Wurm with intervening warmer periods. The most important phenomenon related to these climatic variations, observable all over the globe, was that of the world wide glacio-eustatic sea level changes. A close relationship, however, existed between climatic stages and the eustatic sea levels, glacials lowered the sea levels, while interglacials were periods of high sea levels.

Last Glacial Cycle has left various types of impressions on the continental shelf and along the onshore rocky promontories of east coast of India. Indications of low sea level stands from some offshore geomorphic features were brought to light by the geoscientists [1] of GSI Marine Wing during the cruises on board GSI Research Vessel Samudra Kaustubh. An attempt has been made in this study to collect evidences of low and high sea level stands related to the Last Glacial Cycle, off southern Odisha coast of India. The signatures of regression, transgression and still stands are retained in the continental shelf with or without geomorphic expressions in the sedimentologic, palaeontologic, and chemical character of the seabed sediments.

2 Objective and Area of Study

In this paper an attempt has been made to unravel the impact of Last Glacial Cycle in the sediments and palaeo-geography of the continental shelf and the onshore 140 km long coastal tract from Gopalpur to Konark in southern Odisha. The stretch of coastal tract from Gopalpur to Konark spread over a length of 140 km forms a part of stable coastline with well developed beach, berm and dunes, generally accreting, though in short stretches there are episodes of beach erosion near Gopalpur, Aryapalli, western fringe of Puri and Ramchandi. The study area can be divided into three sectors based on the land forms, coastal processes and fluvial and lagoonal inputs. **(I) Western: Gopalpur to Palur**: The alluvial and coastal plain to aeolian flat monotony is broken by occasional inselbergs and bornhardts in the western part from Gopalpur to Paluru derived from the Eastern Ghats rocks, Traces of palaeo-shoreline as elongated strips of brackish water-turned-fresh water lakes, three generations of dune and the beach on the western sector from Gopalpur to Palur. **(II) Central: Palur to Satpara**: The central area from Palur to Satpara consists of the sand bar spit and deltaic sediments enclosing the Chilka Lagoon from the Bay of Bengal. **(III) Eastern: Satpara to Konark**: The eastern part of the area from Satpara to Konark is made up of deltaic sediments of Mahanadi distributaries—Daya, Bhargavi and Kushabhadra—with the alluvial plain, the mud flats, abandoned channels, channel avulsion, the marshy wetlands of Samang and Sar lakes, the aeolian flats, three generations of dunes and a sandy beach. The deltaic plain is characterized by a number of ENE–WSW trending basement faults which were reactivated during Cenozoic period [2].

3 Last Glacial Cycle, Continental Shelf and Mahanadi Delta

The glacials in the tropics, away from the polar areas, did not have actual glacial ice, but the glacials and interglacials were adequately reflected in the comparable climatic conditions. The late Quaternary glacials and interglacials in the tropical areas are manifested as arid-cold or warm-humid climates and are recorded in the shelf sediments as signatures of regression and transgression respectively. Advancing shoreline writes its story on the sediments of the continental shelf. So the impact of the Last Glacial Cycle (LGC) can be seen in the palaeostrandlines formed during the Last Glacial Maximum. The lowering of the sea level due to LGC began about 35 ka BP. The intensification of cooling lowered the sea level to 122 m (Fig. 1) from the present sea level, during the Last Glacial Maximum (ca. 18 ka BP), which exposed, almost the entire width (about 50 km) of the continental shelf, in this sector, to subaerial condition. By about 14 ka BP deglaciation sets in and sea level begins to rise with the transgression [3]. The process of transgression has given the final shape to the continental shelf and the shoreline present today. Beginning with the Last Glacial Maximum this paper tries to record the imprints of glacial cycle in various landforms, mineral assemblages and sediments (Fig. 1).

The flat continental shelf between Gopalpur and Puri is interrupted by shore parallel, low relief beach ridges at 30, 62, 76 and 122 m water depth [4]. The width of the shelf is about 50 km in this sector and the shelf break occurs at 150 to 180 m depth. The four ridges picked up in the seismic as well as bathymetric records vary in relief from 3 to 6 m in general, and the Ridge I at 122 m depth has a relief of 17 m (Fig. 1). The ridges in the outer shelf are rich in biogenic and chemogenic carbonate sediments where as those in the inner shelf zone are rich in silicate sands which also contain heavy minerals (Fig. 2) in this sector [5]. The ridges have been numbered Ridge I (122 m), Ridge II (76 m), Ridge III (60 m) and Ridge IV (30 m). The Ridge-I at 122 m, was formed during the Last Glacial Maximum has a radiocarbon date of 13,820 years BP [4]. The ridges I and II are made up of grainstones composed

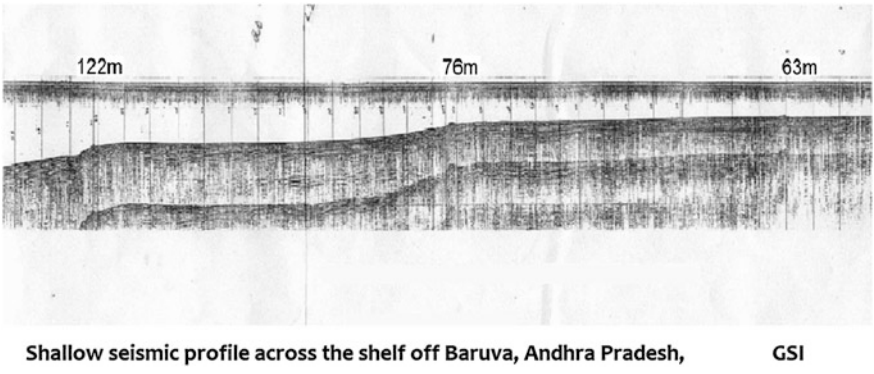

Fig. 1 Shallow seismic record showing profile of the width of the continental shelf between Baruva and Godalpur

of coarse silica and carbonate sand, bioclasts of small bivalves and coralline debris (generally Acropora and Porites) often cemented together with calcareous matrix. Chemogenic precipitates in the form of ooids have been picked up from depths of 90 to 120 m. The concentration of ooids increases to its west in the Andhra Pradesh sector. The ridge is prominent in its uniform morphology in all the transects and from observations by other workers in this area [6]. The swales are composed of silty fine sand to silty clay, fining progressively towards shelf break. The presence of coarse sand (58.32 to 89.7% of +230 fraction) and buried coral colonies, shell fragments point to a high energy environment and their formation can be attributed to nearshore environment of deposition, formed during the low sea level.

The swales, intervening the ridges, are generally flat seafloor for a width of about 11 km between two consecutive ridges, usually composed of silty clay to clayey silt, except near the ridges where the sediment texture changes to coarse sand. There are massive Red sediment ridges buried sometimes under younger sediments, which were formed during the arid climate of LGM (Fig. 3).

Though no dates are available in this sector, it is surmised from data from adjoining areas that the LGC transgressive sea level reached the present sea level about 6 to 7 ka BP. The rise of the sea level above the present level has given final shape to the Mahanadi delta and the shoreline with the beach, fore dune, older dunes, aeolian flat, linear lakes and the mudflat.

Beach ridges in Mahanadi delta are few because of a dominant fluvial action which wiped out most of the beach deposits. The oldest beach ridge is recognised by a small patch of relict sandy ridge at 35 km from the present coast [7].

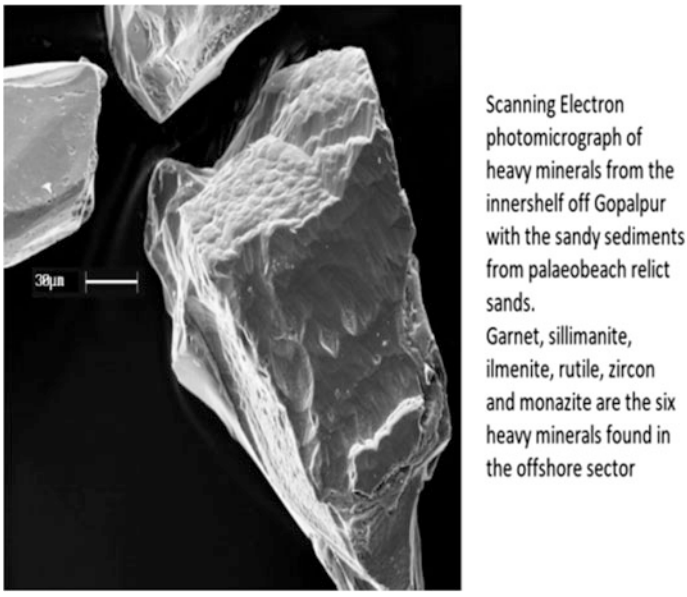

Fig. 2 SEM micrograph of heavy minerals

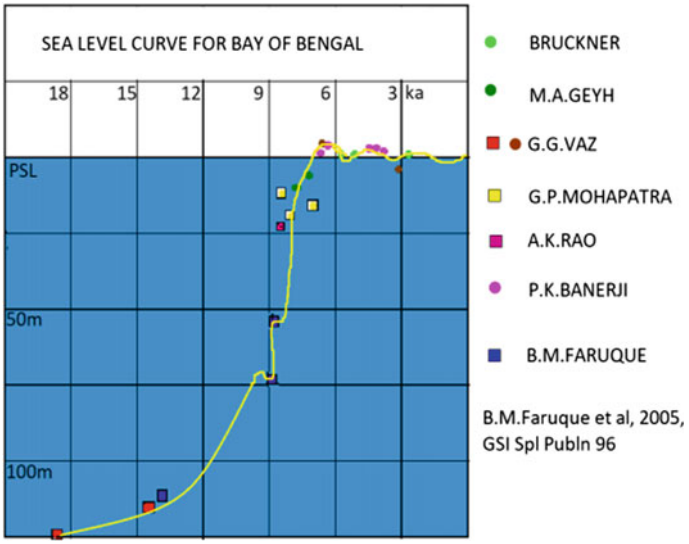

Fig. 3 Sea level curve for Bay of Bengal

Mid-Holocene palaeo-strandline north of Puri passes along the northern shores of Sar and Samang lakes [4]. The northern bank of Chilka Lagoon constitutes the palaeo-shoreline of this area before the onset of Holocene transgression. The sediments dumped by the western distributaries of Mahanadi in the northern part of Chilka embayed Chilka (Fig. 4a) from the open Bay of Bengal. And littoral current from the south carrying sediments from south developed the sand bar from the southern end near Palur to enclose the bay into a lagoon. Some of the coastal geomorphic features are well preserved in western and eastern parts of the study area that expose geomorphic features such as spit, swash zone, active berm, fore dune ridge, back dune series, red sediments from older dunes, older ridge and swale, and a vast expanse of alluvial plain and restricted low level laterite duricrust

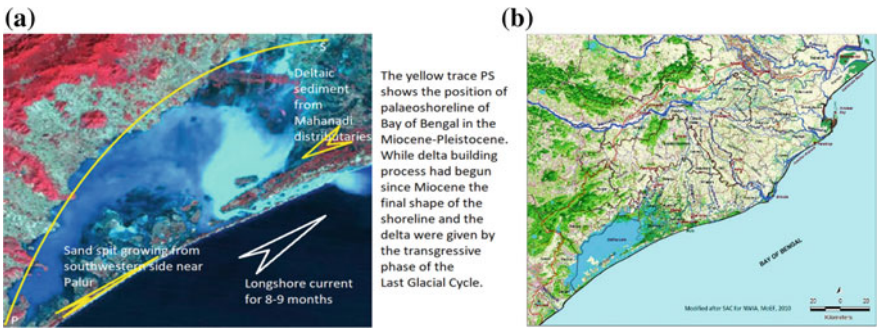

Fig. 4 **a** Sat image of Chilka Lagoon. **b** Map of Mahanadi Delta

near Gopalpur. The coastal stretches under erosional phase exhibit a steep (9°–12°) beach face, a narrow and seaward sloping berm and a fore-dune with scarped toe.

Nageswar Rao and Sadakata [6] have identified four stages of growth for Mahanadi Delta. In the beginning (Stage I to Stage II) the growth of the Mahanadi Delta was rapid in the southern front which was built by sediments being brought by Daya, Bhargavi and Kushabhadra rivers. But later (Stage II to Stage III and IV) the southern front had ceased to grow whereas the north eastern front around Dhamra kept growing steadily. During this phase, two very significant changes had taken place. The rivers Bhargavi and Kushabhadra were debouching into the Bay of Bengal traversing southerly from its ramification off Mahanadi near Cuttack. Both the rivers Bhargavi and Kushabhadra, had become sluggish, resulting in the southern delta front registering no growth during stages III and IV of Nageswar Rao and Sadakata [6]. Sometime in the Holocene period Bhargavi river took a westerly turn (Fig. 4b), and instead of falling into Bay of Bengal it debouched into Chilka Lagoon. Here the author would like to refer to a study by Fuloria et al. [2] of Oil India Limited. According to Fuloria et al. [2] Mahanadi Basin, a peri-cratonic basin was initiated probably during Late Jurassic by rifting and subsidence of the Pre-Cambrian Basement by a number of major faults with a dominant ENE–WSW trend and subordinate NNE–SSW and NNW–SSE trends. Fuloria et al. [2] describe that the major part of delta building process was initiated after a regression of Early Middle Miocene and continued till Recent with minor fluctuations. Of these basement faults those along ENE–WSW trends had the maximum influence on the basin formation and its configuration during Cretaceous period. These faults, parallel/sub-parallel to the present day coast line divided the basin into a number of linear depressions and uplifts like: Cuttack-Chandbali Depression, Bhubaneswar-Kendrapara Uplift, Paradeep Depression, Nimapara-Balikuda Uplift, Puri Depression and Konark Uplift from north to south in the onshore part [2, 8].

The author believes that the ENE–WSW trending ridges (Fig. 5) and alternating linear depressions (inferred by Fuloria et al. [2]) might have got reactivated along their faults and the Nimapara-Balikuda Uplift caused the westerly swerve of Bhargavi river to debouch in Chilka Lagoon. Remote sensing studies followed by ground truthing have revealed three sets of lineaments traversing the Mahanadi delta viz. (1) Northeast–southwest, (2) northwest–southeast and (3) east–west [9].

Various drainage patterns like abandoned channels and closed basins, channel avulsion, ox-bow depressions and swamps characterise the southern front. On the north-eastern front, one comes across zones of meandering belts and braided river system, narrow floodplains of upper deltaic plain, presence of certain geomorphic features such as beach ridges, palaeo-sand dunes and tidal flats demonstrate that the delta today is building in its northeasterly front around Dhamra.

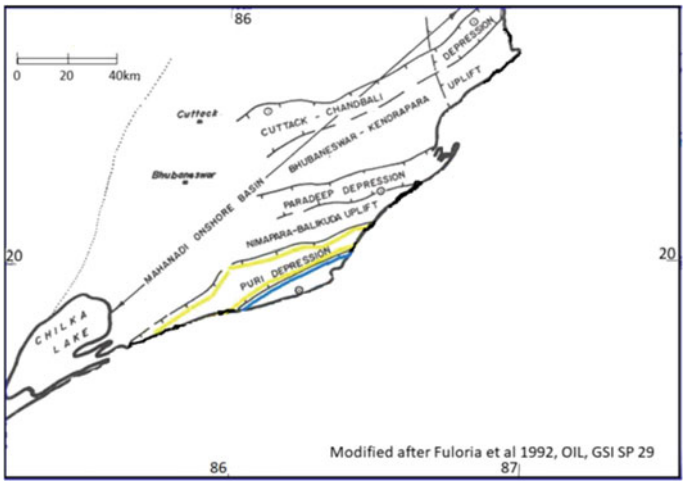

Fig. 5 Ridges and linear depressions in the basement rocks under deltaic sediments (Fuloria et al. [2])

4 High Sea Stands

Lake Tampara, a trace of the palaeoshoreline is now located at 5.90 to 7.25 m above the present sea level. In the eastern sector around Puri town, the alluvial plain has two major natural lakes—Samang Lake in the west and Sar Lake to the east, originally brackish water lakes turned fresh water after the shoreline receded from these water bodies. A small river offshoot of Bhargavi meandering southerly, met the palaeoshoreline at Samang Lake, which is a remnant of brackish water body developed along the palaeoshoreline. Samang Lake is now three kilometres away and 8 m above the present shoreline. When the shoreline receded from the Samang Lake position the branch of Bhargavi had become dormant and remained a closed basin, before losing its fluvial properties. Samang and Sar lakes have degraded into marshy wetlands and swampy mud flats. Older dunes, stabilized and aligned parallel to the present shoreline are seen in the north of Gopalpur to Chhatrapur and in some parts of Satpara, which were formed during high sea stands of late Holocene.

5 Shoreline Changes, Erosion and Accretion in Recent Times

Chilka shoreline: The south-eastern part of Chilka Lake is bordered by a linear barrier spit which is about 42 km long and 150 m wide. Except at two points in the north eastern part where the sea water used to flush into the lake, two-three decades

ago, the channel linking Chilka with Bay of Bengal is practically closed now and makes news when it ever opens, as it did in August 2008.

Kushabhadra-Prachi beach and west of Puri: A study of Marine Wing of GSI carried out in the year 1985–87 reveals that the stretch of 18 km long shoreline between Kushabhadra and Prachi has accreted a minimum of 63 m of land in about 52 years (i.e. from 1928 to 1980). Konark temple was erected in the 12th century AD on the beach and today it is 3 km away from the shoreline. **Puri beach**: The marine drive to the west of Puri town runs parallel to the shoreline for about 2.5 km of which 1.4 km is affected by erosion in July 2007.

6 Factors Contributing to Changes Along the Shoreline

The present day signals of the interglacials are seen in the form of cyclonic storms landing in this sector of Odisha quite often. Coastal areas have varied topography and are generally dynamic environments. Continental and oceanic processes converge along coasts to produce landscape capable of rapid changes. There are five factors which could be contributing to beach erosion.

1. Sediment Budget
2. Longshore Current
3. Sea Level Rise/Episodic sea level rise due to Low pressure
4. Wave energy/Cyclone/Surge
5. Subsidence/Neotectonics.

Along Puri coast three coastal elements appear to have contributed to beach erosion.

Sediment budget: The coastline along Puri-Konark sector is nourished by sand through longshore current which transports sediments from west to east during greater part of the year. The three distributaries Daya, Bhargavi and Kushabhadra ramifying from Mahanadi have gone sluggish and transport no sediments. The Daya and Bhargavi rivers debouch into Chilka Lagoon and the sluggish flow of these rivers have been the reason of Chilka Lagoon getting clogged.

Longshore Current: Longshore current has been shifting sands from west to east in this sector. The sediment brought in by the river Rushikulya is transported to the eastern side of the river by littoral current. Some researchers opine that the opening of Mangalakat on the west of Puri town has disrupted the sand movement along the innershelf zone due to long shore current. And have caused the beach erosion of August 2016. A sediment starved shelf will only get eroded if the littoral current remove its sediment to further east. The author of this paper does not subscribe to the idea that Mangalakat opening is the sole reason for beach erosion.

Wave energy/Cyclonic surges: All the events of beach erosion recorded in this sector are synchronized with rainy season during July–August, is a clear pointer to the low atmospheric pressure giving rise to episodic sea level rise and strong wind surges during the swell causing the beach erosion.

7 Conclusion

Coastal erosion is not necessarily a disastrous phenomenon, however, problems crop up when erosion and cultural activity come into confrontation. Our activities perhaps come in the way of natural processes. This is compounded by the global warming and its consequential rise in sea level and erratic weather pattern, like increase in the frequency of storm surges, irregular monsoon and long dry seasons, unusually hot summers.

It is relevant to mention here that the erosion occurring along the Puri beach, is triggered by strong wave events and lowering of atmospheric pressure which gives rise to swell in the sea level, compounded by south westerly strong winds. The beach along southern part of Puri town has on record two very prominent events which eroded the beach up to a depth of 3 m in July 2007 and August 2016. The author does not subscribe to the reason suggested by some authors that the opening of Mangalakat channel on the western part of the town has caused the beach erosion. Any study on the changes along the shoreline during the Last Glacial Cycle must take into account all the parameters of palaeogeography, like the distribution of landforms, the strength or weakness of fluvial system, the longshore current direction, the condition of hot and humid or cold and arid climate which was a part of Last Glacial Cycle. It is relevant to include older basement structural elements and their possible reactivation during the formation of younger sediments. The problem of erosion needs to be handled in a way that does not interfere with the natural systems. Any interference with the natural processes produces a variety of secondary or tertiary changes, many of which may have adverse consequences. Stabilisation of the coastal zone by the use of engineering structures protects the property of a few at the cost of a larger community. The policy makers must explore the eco-friendly alternatives. The best solution is to keep away from beach, dune and older dunes.

References

1. Banerji, A., Sengupta, R.: Evidence of low sea stands on the continental shelf on the east coast of India. GSI Sp. Publ. 29 (1992)
2. Fuloria, R.C., Pandey, R.N, Bharali, B.R., Mishra, J.K.: Stratigraphy, structure and tectonics of Mahanadi offshore basin. GSI Sp Pub 29 (1992)
3. Faruque, B.M., Vaz, G.G., Mohapatra, G.P.: Continental shelf of Eastern India, In: Chiocci, F. L., Chivas, A.R. (eds.) Continental Shelves of the World, Memoir 41. Geological Society of London (2014)
4. Faruque, B.M.: Geology of the continental shelf. In: Mahalik, N.K. et al (eds.) Geology and Mineral Resources of Orissa. SGAT (2006)
5. Faruque, B.M.: Eustatic and fluvial influence on placer minerals in the shelf off Aryapalli-Kushabhadra, East coast of India, In: IGCP514 Conference Guilin, China (2009)
6. Mohapatra, G.P, Rao, B.R., Biswas, N.R.: Morphology and surface sediments of the Eastern Continental shelf of Peninsular India. GSI Sp Pub 29 (1992)

7. Nageswara Rao, K., Sadakata, N.: Holocene evolution of deltas on the east coast of India. In: Symposium Volume Deltas of the World (1993)
8. Jagannathan, C.R., Ratnam, C., Baishya, N.C., Das Gupta, U.: Geology of offshore Mahanadi Basin. Pet. Asia J. ONGC **6**, 4 (1983)
9. Kumar, K.V., Bhattacharya, A.: Geological evolution of Mahanadi delta, Orissa using high resolution satellite data. Current Sci. **85**, 10 (2003)

Chapter 59
A Geospatial Study on Emergency Response Management System to Combat Fire Accidents—A Case Study of Chennai, Tamil Nadu

T. Sridevi, Peddada Jagadeeswara Rao, Suribabu Boyidi, P. Madhu Chandra, B. Sridhar and M. Madhuri

Abstract Urban fire is one of the most disturbing problems for many cities around the world. Fire risks in urban areas have increased over the years especially in metropolitan cities which are characterized by dense population, frequent traffic jams, congested roads and presence of slums. The effect of major fire breakout is disastrous and the consequent damage will run into heavy loss of lives and property. The objective of this paper is therefore to establish a GIS (Geographic Information System) [1] based emergency response management system where fire services can identify the optimal route from its station to any fire incident. Since access to a fire incident and timely intervention play a crucial role in managing urban fire, the optimal route was modeled based on the distance of travel, time of travel, and the delays in travel times. Besides using this analysis to timely respond to urban fire emergency services, analysis also performed on the spatial distribution of fire accidents to understand the scenario of previously occurred fire accidents.

T. Sridevi (✉) · P. J. Rao · S. Boyidi · P. Madhu Chandra · B. Sridhar
Department of Geo Engineering, Andhra University, Visakhapatnam
Andhra Pradesh, India
e-mail: srice2001@gmail.com

P. J. Rao
e-mail: pjr_geoin@rediffmail.com

S. Boyidi
e-mail: suri.sri2008@gmail.com

P. Madhu Chandra
e-mail: madhuflo@gmail.com

B. Sridhar
e-mail: sridhar.bendalam@gmail.com

M. Madhuri
Department of Civil Engineering, Malla Reddy Institute of Technology,
Secunderabad, India
e-mail: madhurimulpuru@gmail.com

P. J. Rao et al. (eds.), *Proceedings of International Conference on Remote Sensing for Disaster Management*, Springer Series in Geomechanics and Geoengineering,
https://doi.org/10.1007/978-3-319-77276-9_59

Keywords Network analysis · Optimal route · Geo-database · Impedance
Turn table

1 Introduction

Fire incidents in urban areas are frequently destroying and brings about death toll and property. Because of the Rapid increment in population, industrialization, settlements, tall structures, and so forth.

The financial cost to the Nation is extraordinary since flame flare-ups have a tendency to worsen the destitution level in the nation. Crisis reaction benefit, particularly in the zone of urban fires, is in this manner imperative to spare the nation from losing rare assets. TNFS has 25 fire stations all through the city. These stations were outfitted with present day procedures to protect lives, property, and common assets for the economic advancement of the general population of Chennai city. Indeed, even today, regardless of these cutting edge procedures of fire anticipation and concealment, fires keep on damaging properties particularly in the southern area of Chennai because slums and socioeconomic factors.

The objective of this paper is to set up a Geographic Information System (GIS) based emergency response management system for TNFS where time plays important role. In building up fire emergency response database [2], crisis readiness arranging is a critical issue that can affect individual's lives. In the event that arranged legitimately and actualized rapidly, it can spare hundreds or thousands of human lives and moderate a portion of the financial misfortunes in influenced territories.

As indicated by ESRI [3], there are five reflex time grouping for overseeing urban fire: (1) Dispatch time, which is the measure of time that it takes to get and process a fire call; (2) Turnout time, which is the time from when units recognize notice of the fire incident to the starting purpose of reaction time; (3) Response time, which the time that starts when units are in transit to the fire episode and finishes when units land on the scene; (4) Access time, which is the measure of time required for the team to move from where the contraption stops to where the fire exists; and (5) the measure of time required for fire division units to set up, associate hose lines, position stepping stools, and get ready to extinguish the fire.

2 Study Area

The study area chosen is south Chennai. This area was chosen considering the fact that this area majorly contains slums and congested roads and settlements (Fig. 1).

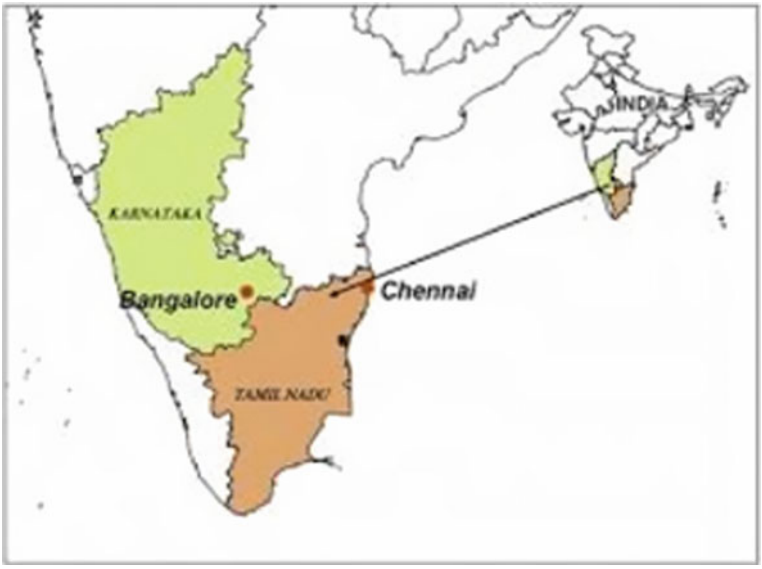

Fig. 1 Study area, Chennai city

The Road network map of the area has been digitized, projected, and geo-referenced in GIS environment at scale of 1:25,000 using SOI toposheets. Satellite images of IRS 1C and IRS 1D has been used to digitize new roads and minor roads (Figs. 2 and 3).

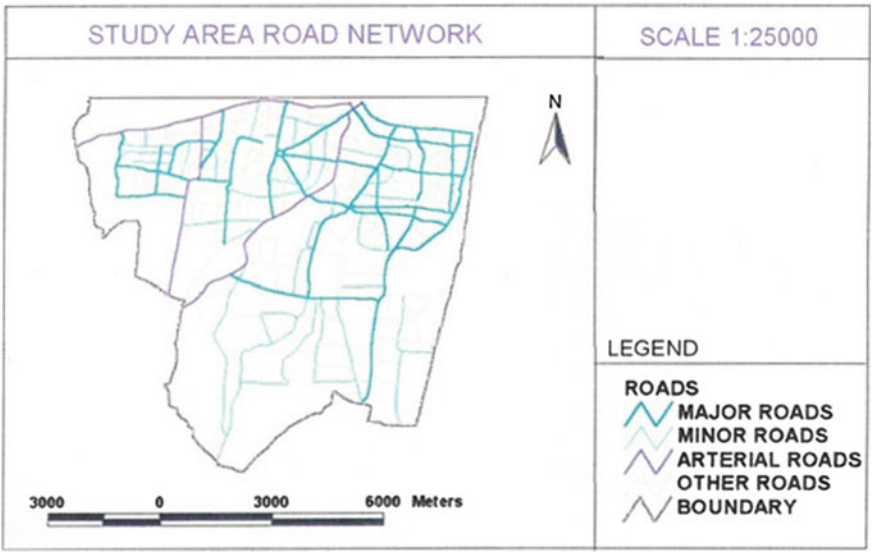

Fig. 2 Study area road network

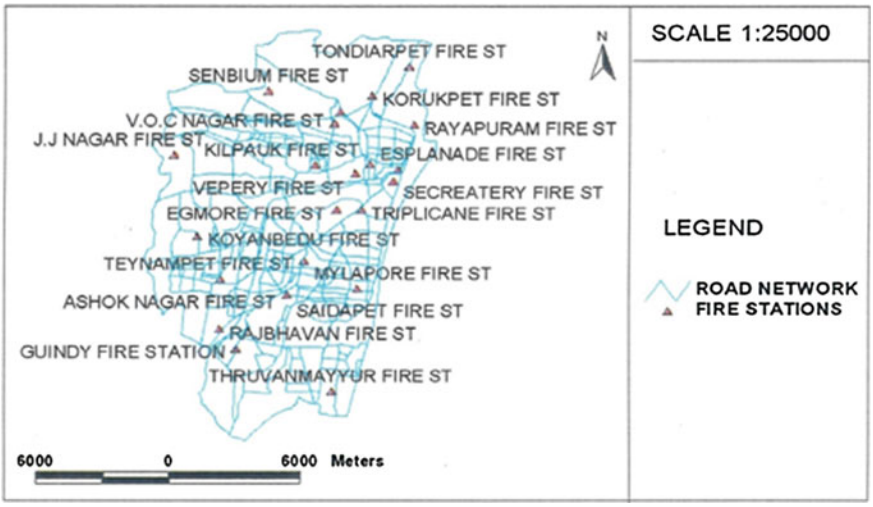

Fig. 3 Fire stations in Chennai city

3 GIS Network Analysis for Optimal Path

As one of the main functions of GIS, network analysis [4] plays an important role in optimal routing, traffic estimation, urban planning, electric power, and closest facility [5]. This network (as implemented in ArcGIS) is used, among other things, to build an immediate, rapid and efficient emergency fire response system for the study area. Given the data of roads and cost attributes, the network analyst can be used to analyze problems such as optimal routing, closest facility and service area.

The TNFS could identify the optimal route from its service station to the fire incident and could also perform analysis to locate the closest fire hydrant. In network analysis, the most fundamental and the most critical problem is the computation of optimal route between different locations on a network. The optimal route (also called the least cost path) in this paper is the path of lowest impedance or the lowest cost. This route takes into consideration all the impedances (which include the distance, travel time, number of signals and turns, intersection delays, volume of traffic and parking).

4 Impedance Factors

An optimal route in a network is the route of lowest impedance, also called the least-cost path. Impedance is a measure of the amount of resistance, or cost, required to traverse a path in a network or to move from one element in the network

to another. Resistance may be a measure of travel distance, time, and speed of travel multiplied by distance. Higher impedance values indicate more resistance to movement, and a value of zero indicates no resistance. With this objective of optimizing travel time, the various impedance factors that play a significant role in deciding the travel time such as volume of traffic, type of road, road width, number of junctions, and turns are analyzed in determining the optimal route having the minimum travel time.

The travel time utilized for the streets in the investigation zone depended on the speed limits of the streets. With as far as possible and the separations known, the travel times for the different streets were then figured. One way confinements were likewise considered in this investigation. A field called one way was added to the database table of the street include class and was demonstrated by the example of digitizing. Crossing point delays at street intersections were additionally utilized as one of the impedances since a few intersections in the investigation range are known to be especially congested constantly.

5 Methodology

A detailed road network map of the study area is prepared using SOI toposheets and IRS-1C and IRS-1D satellite data by using On-Screen Digitization in ARC GIS Desktop platform. Geo database is prepared for fire stations and road network.

For optimal routing, the accident spot was geocoded using locate address function. The link and turn impedance values are assigned using turn table and journey speeds are assigned to all the links of the road network. The time impedance is calculated using the following formula:

$$\text{Time impedance} = (18 * (\text{length of the arc}/5))/\text{journey speeds}$$

Turn impedances are assigned to specific turns using set turn command. Optimal route was found from fire station to the place of fire accident using network analysis.

6 Results

An emergency response management system [6] for fire services has been developed for TNFS to find optimal route from their location to any place of fire accident. This system includes a database of the fire stations, (Table 1), and with this, queries could be made to locate fire incident on the GIS interface within a particular service

Table 1 Fire stations in Chennai city

S. no	Division	Name of the fire station	Total number of fire calls
1	North division	Esplanade	41
2		Washermanpet	124
3		Royapuram	40
4		Tondiarpet	84
5		Senbium	87
6		Vyasarpadi	104
7		VOC Nagar	79
8		Vepery	50
9		Kilpauk	129
10		Ennore	45
11		Secretariat	3
12		Korukkupet	63
13		Manali	46
14		Athipattu	95
			Total = 990
15	South division	Egmore	123
16		Triplicane	71
17		Mylapore	118
18		Teynampet	100
19		Saidapet	48
20		Guindy	127
21		Ashok Nagar	127
22		Koyambedu	109
23		J.J Nagar	84
24		Raj Bhavan	78
25		Thiruvanmiyur	80
			Total = 1065

Source TNFS

area (Fig. 6). As can be seen in Fig. 6, proximity analysis such as spatial buffering tool could be performed to suggest possible locations and allocations of fire hydrants.

As appropriate access to a fire occurrence and time assume a pivotal part in overseeing urban fire, the most limited and speediest courses in light of time of travel are examined and the outcomes exhibited in Fig. 5. The most brief course (as in Fig. 4) between a specific fire station and a fire episode was computed utilizing geometric separations as it were. Essentially, the speediest course (Fig. 4) be that as it may, was discovered considering the travel time, the turns and the crossing point delays. That is, this course joins the impedance factors.

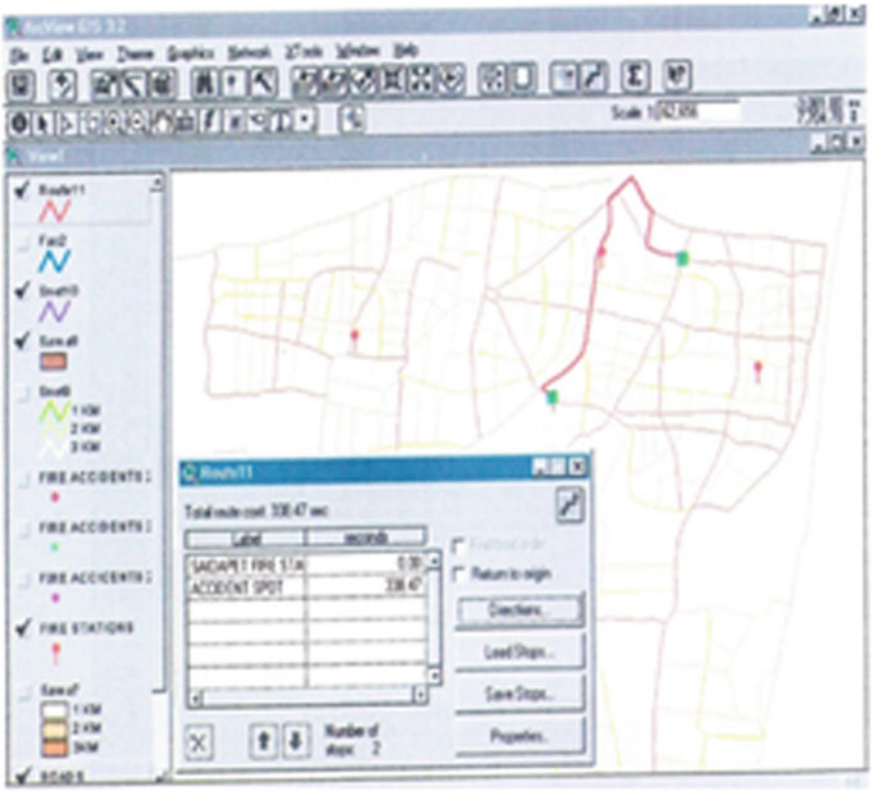

Fig. 4 Optimal route from fire stations to fire incident

The fire department in the wake of accepting a crisis require a fire episode can query the created database to discover the area of that fire occurrence (Fig. 5a) and notwithstanding the show of the area of the fire episode, a content depiction of the route to this area (Fig. 5b) is likewise shown. Coordinating every one of the impedances, the optimal route is shown in Fig. 6a. This demonstrates the minimum cost route from that specific fire station to any fire area. This way is the one with the least impedance inside the street organize in the investigation zone or it is a way that the aggregate sum of its weights is insignificant.

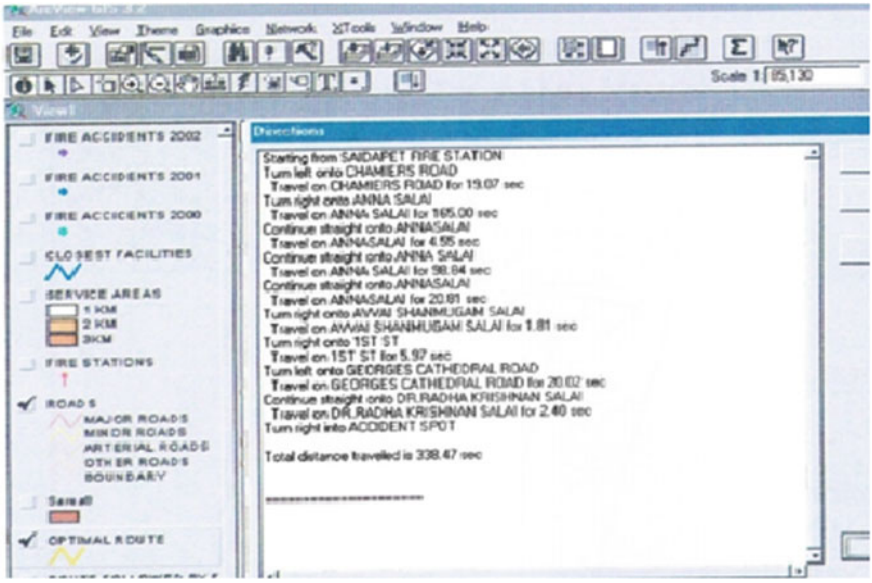

Fig. 5 Directions for optimal routing

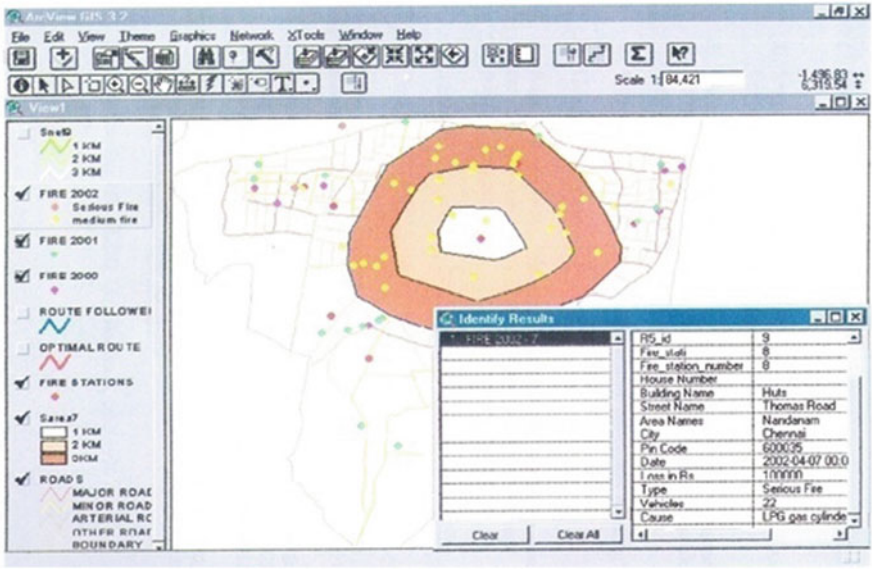

Fig. 6 Service areas for enquiry

Table 2 Attributes of the fire stations

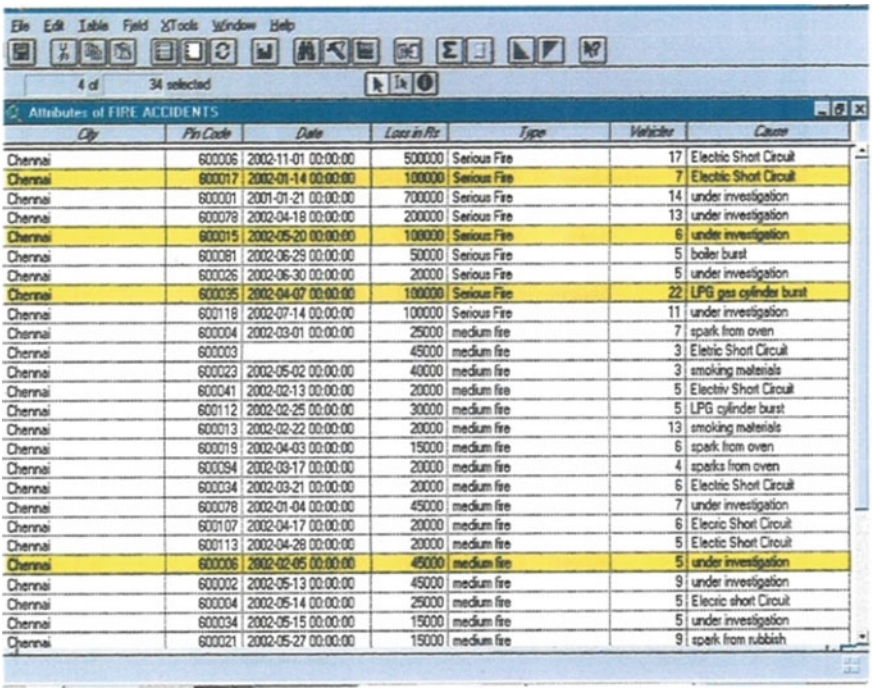

Attributes of FIRE ACCIDENTS

City	Pin Code	Date	Loss in Rs	Type	Vehicles	Cause
Chennai	600006	2002-11-01 00:00:00	500000	Serious Fire	17	Electric Short Circuit
Chennai	600017	2002-01-14 00:00:00	100000	Serious Fire	7	Electric Short Circuit
Chennai	600001	2001-01-21 00:00:00	700000	Serious Fire	14	under investigation
Chennai	600078	2002-04-18 00:00:00	200000	Serious Fire	13	under investigation
Chennai	600015	2002-05-20 00:00:00	100000	Serious Fire	6	under investigation
Chennai	600081	2002-06-29 00:00:00	50000	Serious Fire	5	boiler burst
Chennai	600026	2002-06-30 00:00:00	20000	Serious Fire	5	under investigation
Chennai	600035	2002-04-07 00:00:00	100000	Serious Fire	22	LPG gas cylinder burst
Chennai	600118	2002-07-14 00:00:00	100000	Serious Fire	11	under investigation
Chennai	600004	2002-03-01 00:00:00	25000	medium fire	7	spark from oven
Chennai	600003		45000	medium fire	3	Eletric Short Circuit
Chennai	600023	2002-05-02 00:00:00	40000	medium fire	3	smoking materials
Chennai	600041	2002-02-13 00:00:00	20000	medium fire	5	Electriv Short Circuit
Chennai	600112	2002-02-25 00:00:00	30000	medium fire	5	LPG cylinder burst
Chennai	600013	2002-02-22 00:00:00	20000	medium fire	13	smoking materials
Chennai	600019	2002-04-03 00:00:00	15000	medium fire	6	spark from oven
Chennai	600094	2002-03-17 00:00:00	20000	medium fire	4	sparks from oven
Chennai	600034	2002-03-21 00:00:00	20000	medium fire	6	Electric Short Circuit
Chennai	600078	2002-01-04 00:00:00	45000	medium fire	7	under investigation
Chennai	600107	2002-04-17 00:00:00	20000	medium fire	6	Elecric Short Circuit
Chennai	600113	2002-04-28 00:00:00	20000	medium fire	5	Electic Short Circuit
Chennai	600006	2002-02-05 00:00:00	45000	medium fire	5	under investigation
Chennai	600002	2002-05-13 00:00:00	45000	medium fire	9	under investigation
Chennai	600004	2002-05-14 00:00:00	25000	medium fire	5	Elecric short Circuit
Chennai	600034	2002-05-15 00:00:00	15000	medium fire	5	under investigation
Chennai	600021	2002-05-27 00:00:00	15000	medium fire	9	spark from rubbish

7 Conclusion

When a fire incident is reported, to the fire department, they can query the database to find the location of that fire incident Table 2 and in addition to the display of the location of the fire incident, a text description of the direction to this location (Fig. 5) is also displayed. Integrating all the impedances, the optimal route is displayed in Fig. 4. This indicates the least cost route from that particular fire station to any fire location. This path is the one with the lowest impedance within the road network in the study area or it is a path that the total amount of its weights is minimal.

References

1. Understanding GIS—ESRI, Inc., Redlands, calif. (1990)
2. Sunil, C.B.: Creating spatial database for the Mumbai Fire Service by using GIS/RS techniques: a case study of CBD, Mumbai. In: www.gisdevelopment.net/application/naturalhazards/fire/nhf002.htm. (1999)

3. ESRI (Environmental Systems Research Institute).: Fire Agencies Improve Response with GIS, Arc User Online (2011)
4. Singh, M., Joshpar, K.: Emergency response management system for Hyderabad city. In: www.gisdevelopment.net/application/naturalhazards/fire/nhf0001.htm. (2000)
5. Min, S., Wei-fang, W.: Application of GIS Best Path Algorithm in Harbin Roads. World Rural Observations **4**(1), pp. 86–90 (2012)
6. Miles, M.: Network analysis for emergency planning. In: Geo Asia Pacific vol. 2 (2000)

Chapter 60
Road Network for Disaster Guide in Rural Area, East Godavari District, AP, India—A Case Study of Spatial Approach

Shaik Rehanaz Begum, G. Jaisankar, Suribabu Boyidi, B. Ravi Kumar, K. M. Ganesh, T. Sridevi, N. C. Anil, U. Sailaja and K. Dileep

Abstract This guideline is intended to assist state, local, and tribal area during disaster management for professionals in the initiation of response activities during the first 24 h of an emergency or disaster. It should be used in conjunction with existing emergency operations, plans, procedures, guidelines, resources, assets and incident management systems. It is not a substitute for public emergency preparedness and planning activities. The response to any emergency or disaster must be a coordinated community effort. The guide begins with a brief section on public emergency preparedness assumptions. The next section provides guidance and

S. Rehanaz Begum (✉) · G. Jaisankar · S. Boyidi · B. Ravi Kumar
K. M. Ganesh · T. Sridevi · N. C. Anil · U. Sailaja · K. Dileep
Department of Geo-Engineering, Andhra University, Visakhapatnam, India
e-mail: sk.rehanaz1028@gmail.com

G. Jaisankar
e-mail: jaisankar.gummapu@yahoo.com

S. Boyidi
e-mail: suri.sri2008@gmail.com

B. Ravi Kumar
e-mail: bravikumar.rkb@gmail.com

K. M. Ganesh
e-mail: meharganesh.k6@gmail.com

T. Sridevi
e-mail: srice2001@gmail.com

N. C. Anil
e-mail: nathianil@gmail.com

U. Sailaja
e-mail: sailaja.ustala@gmail.com

K. Dileep
e-mail: dileepkillana@gmail.com

P. J. Rao et al. (eds.), *Proceedings of International Conference on Remote Sensing for Disaster Management*, Springer Series in Geomechanics and Geoengineering,
https://doi.org/10.1007/978-3-319-77276-9_60

information on public health emergency response actions that should be initiated during the first 24 h of an incident. The road network map along with the locations of habitations and master table information module. The report includes the travel time from one destination to another. Master table for covering the study area is generated by integrating the travel time.

Keywords Disaster · Analysis · Roads · Travel time

1 Introduction

Disaster management essentially deals with management of resources and information towards a disastrous event and is measured by how efficiently, effectively and seamlessly one coordinates these resources [1]. The ability to effectively deal with disasters has become a challenge to modern technology. It is apparent that disaster problems cut across various disciplinary lines [2]. One cannot effectively address disaster management difficulties by focusing on the isolated problems of a single type. Effective disaster management is influenced by the activities of a host of independent organizations at national and inter-national level. Disaster management at the individual and organizational level deals with issues of planning, coordination, communication and risk assessment. Communication is one of the key issues during any emergency, pre-planning of communications is critical [3]. Miscommunication can easily result in emergency events escalating unnecessarily. Preparedness measures can take many forms ranging from focusing on individual people, locations or incidents to broader, government-based "all hazard" planning. There are a number of preparedness stages between "all hazard" and individual planning, generally involving some combination of both mitigation and response planning.

2 Study Area

East Godavari district is situated on north east of Andhra Pradesh in the geographical coordination of 16° 30′ and 18° 20′ of the northern latitude and 81° 30′ and 82° 36′ of the eastern longitude. The study area is bounded on the north by Visakhapatnam district and the state of Odisha, on the east by Peddapuram revenue division and west by Godavari River and south by the Chattisgarh state. Study area is the border of 3 states Telangana, Chattisgarh and Odisha. As per 2011 census there are 552 habitual villages.

The total area covered in study area is 4580.67 km^2 and total population is 218,385 in this area. Now total mandals are 7 and 1 revenue division and it had one assembly constituency, revenue division is Rampachodavaram. The study area is only had 45% road network facility from each village of all type of roads are

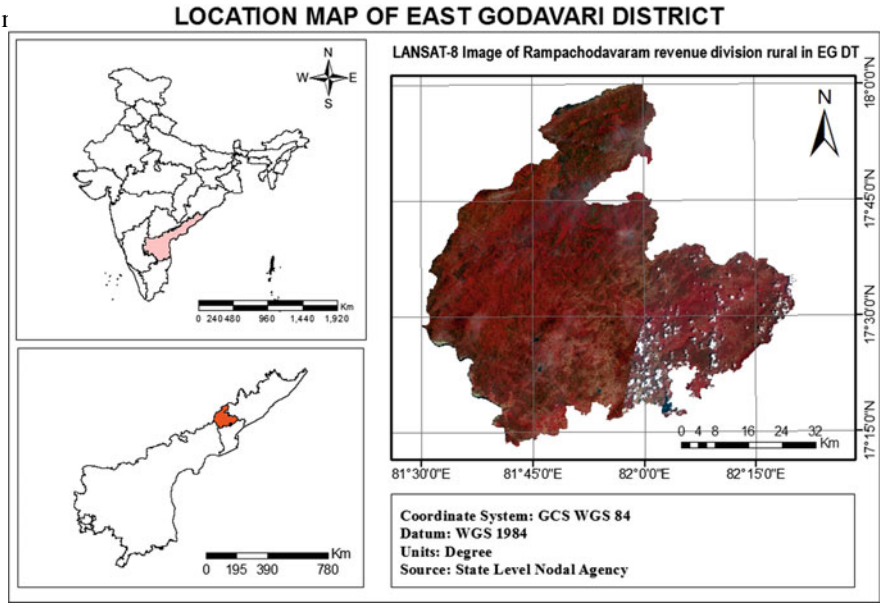

3 Methodology

The Landsat satellite data have been downloaded from the website www.usgs.gov.in. The data mosaicked in ERDAS Imagine-2014, thereafter, digitization of land use/land cover is carried out in ArcGIS-10.3. Survey of India toposheets 65G/10, 11, 12, 13,14, 15; 65K/2, 3, 6,7 were performed geometric correction in ERDAS Imagine-2014, a buffer of 20-km from coast line to inland was delineated in ArcGIS-10.3. The study area (AOI) is delineated on mosaicked satellite images. The methodology adopted in this study is shown in Fig. 1.

Land sat 8 (OLI, TIRS) imagery with spatial resolution of 30 m is taken. Toposheets and other collateral data of the study area are used for correlation. Band combination of 5, 4, 3 are used for Landsat 8 to get false color image and AOI (Area Of Interest) of the study area. The standard visual interpretation techniques of NRSA (1990) guidelines are followed. Digitization is done using 2017 satellite imagery in ArcGIS-10.3. Using the toposheets of AOI we identify the road network and villages. Perform the network analysis.

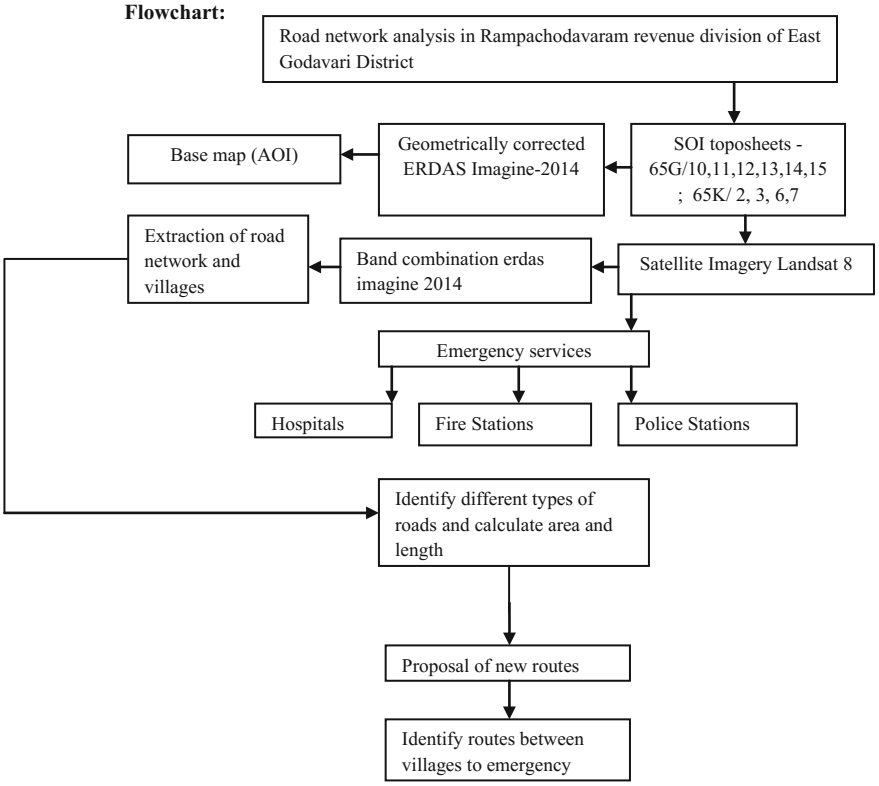

Fig. 1 Conceptual framework of the study area

3.1 How GIS Works

GIS stores data about the world as a gathering of topical layers those can be connected together by topography. This straightforward yet amazingly effective and flexible idea has demonstrated important for tackling some true issues extending from following conveyance vehicles, recording subtle elements of arranging applications and displaying.

3.2 Network Analysis

The network analysis in the GIS based on the following the new route features they are

Stops feature layer: This layer stores the system areas that are utilized as stops in route analysis. The Stops layer is symbolized by default in four types: Located

Stops, Unallocated Stops, Error and Time Violation Stop. You can modify the symbology in the Layer Properties dialog box of Stops. There is a new symbology category, Network Analyst Stops, added for the stops network analysis class. You can modify the symbol, color or text symbol for any type of stop. When a new route analysis layer is created, the Stops layer has no features. It is populated only when network locations are added into it.

3.3 Stop Properties

ObjectiD: The unique ID of the network location is assigned automatically.

Name: The name for a network location is assigned automatically when it is added to the map. You can rename the network location by clicking it, selecting the existing text and replacing it with the new name.

RouteName: This represents the name of the route to which the stop belongs. Using this name property, stops within one route analysis layer can be assigned to multiple routes.

Barriers feature layer: Barriers are used in route analysis to denote points from which a route cannot traverse through. The Barriers layer is classified by default in three types: Located, Unallocated and Error. The symbology of each can be modified in the Layer Properties of the Barriers layer. The Barriers layer functions as any other feature layer in Arc Map. When a new route analysis layer is created, the Barriers layer has no features. It is populated only when network locations are added into it.

Route feature layer: The Route feature layer stores the resultant route of route analysis. As with other feature layers, its symbology can be accessed and altered from the Layer Properties dialog box. The Route layer on the Network Analyst Window is empty until the analysis is complete. Once the best route is found, it is displayed on the Network Analyst Window.

4 Analysis

4.1 Network Analyst Layers

GIS can handle complex network problems, such as road network analysis. A GIS can work out travel times and the shortest path from two points. This facility can be build into more complicated models that might require estimates of travel time, accessibility or impedance along a route system; an example is how a road network can be used to calculate the risk of accidents. There are of courses, other types of network analysis involving stream networks [4]. Network Analyst layers are special group layers used to express and solve network routing problems. Each sub layer in

a Network Analyst layer represents some Aspect of the routing problem (such as Stops, Facilities, Barriers or incidents) and the routing solution (such as shortest route lines or service area polygons). These sub layers reference features that are held in memory, not on disk. A common task in network analyst models is to extract these in-memory features and write them as feature classes on disk. The Select Data tool is used in this task. The model below calculates a shortest route. The first process creates the Network Analyst Route Layer and the second process, add locations, adds the customers to be visited on the route. The third process, solve, calculates the route. After Solve, The layer contains two sub layers: Stops (the customers) and Routes (the shortest Route). Select Date is used to select the Routes from the in-memory layer and the model uses Copy Features to copy the routes to a new feature class on disk.

4.2 Applying

Road networks are vulnerable to natural disasters such as floods, earthquakes and forest fires which can adversely affect the travel on the network that remains intact after an event. However, not all road links equally affect the travel conditions in a given network; typically some links are more critical to the network functioning than the others [5]. Typically after the occurrence of an event some places become less accessible. Studying and analyzing vulnerability of road networks will help in prioritizing the planning, budgeting and maintenance of road sand also will be useful in preparing emergency response plans. Studying and analyzing vulnerability will help in developing the mitigating measures. The analysis of vulnerability has far wider applications such as in planning and maintaining road networks, prioritizing and budgeting, preparing for emergency response. Modeling the performance of a network under degraded conditions is essential in transport planning for developing mitigating measures [6]. It helps the planners understand how the network can absorb disturbances, and also how to deal with and adapt so that the road network retains essentially the same function, structure and identity.

Rural road connectivity, and its sustained availability, is a key component of rural development. Rural roads are connecting areas of production with markets and connecting these with each other or to the state and national highways. The unavailability of database is major constrain to the access of rural roads [7]. This paper envisages consolidation of the existing rural road network to improve its overall efficiency as a provider of transportation services for people, goods and services. This study has undertaken an extended attempt to develop geographic information system (GIS) based rural road database so that planners, decision makers, researchers and other different level authorities in the rural road sector will be benefited from the final output.

Network analysis has been proposed to select shortest path, service area accessibility and closest facility, location allocation of a facility and shows the vehicle routing in terms of travel time, between two locations in the study area. The

interface of the system is user friendly and Inter active. It holds the spatial data layer dynamically linked to the attribute data, organized according to different administrative hierarchies of local authority bodies, ITDA project officer, each and every mandal magistrate (MRO) and other officials etc. Effectiveness of proposed framework will be expanded with the assistance of calamity observing based question framework for recovering non-spatial traits for the entire chain of command.

4.3 Customized GIS Application

An intuitive and user friendly GUI (graphical user interface) with customized disaster based query and search and shortest distance toolbar in addition to built in tools and buttons of OPENLAYERS makes it to perform all required tasks for decision making, monitoring and planning for case as disaster. Customized queries enables the user to generate complex queries for affected area statistics, latitude longitude situation and other real life experiences at the place for disaster management. Queries of this sort are possible in detailed hierarchy at all levels of administrative boundaries like districts, mandals and villages etc.

In cases like disaster, due to dynamic nature of system data regarding road network could be embedded into the system in spatial as well as non spatial form with the help of back end POSTGRESS SQL, data regarding damaged and effected portion of road network in the state could be inserted into the system and viewed with the help of user friendly front end interface for planning and decision making (Fig. 2).

5 Conclusion and Proposals

In the study area of East Godavari tribal area Rampachodavarm revenue division to identify road network from Rampachodavarm to each and every study area 7 mandals and villages for suggest and monitor disaster and emergency services network with respect to all different levels of officials. Customized view interface facilities of the road network with respect to all different levels of administrative units. Customized menu—bar and drop downs enables user to easy access and retrieval of information for selected road information like surface condition, base type, location, shortest distance, village connectivity status, unconnected villages, other possible alternative for damaged part of road and other required information can be obtained. Preparation and printing of thematic maps of desired scale will also possible and set up. Such an application is very beneficial for the situation like disaster for monitoring situation and managing road network in after disaster situation. The identified main road is 20% and including unmetalled roads and cart track roads are 45% of whole area.

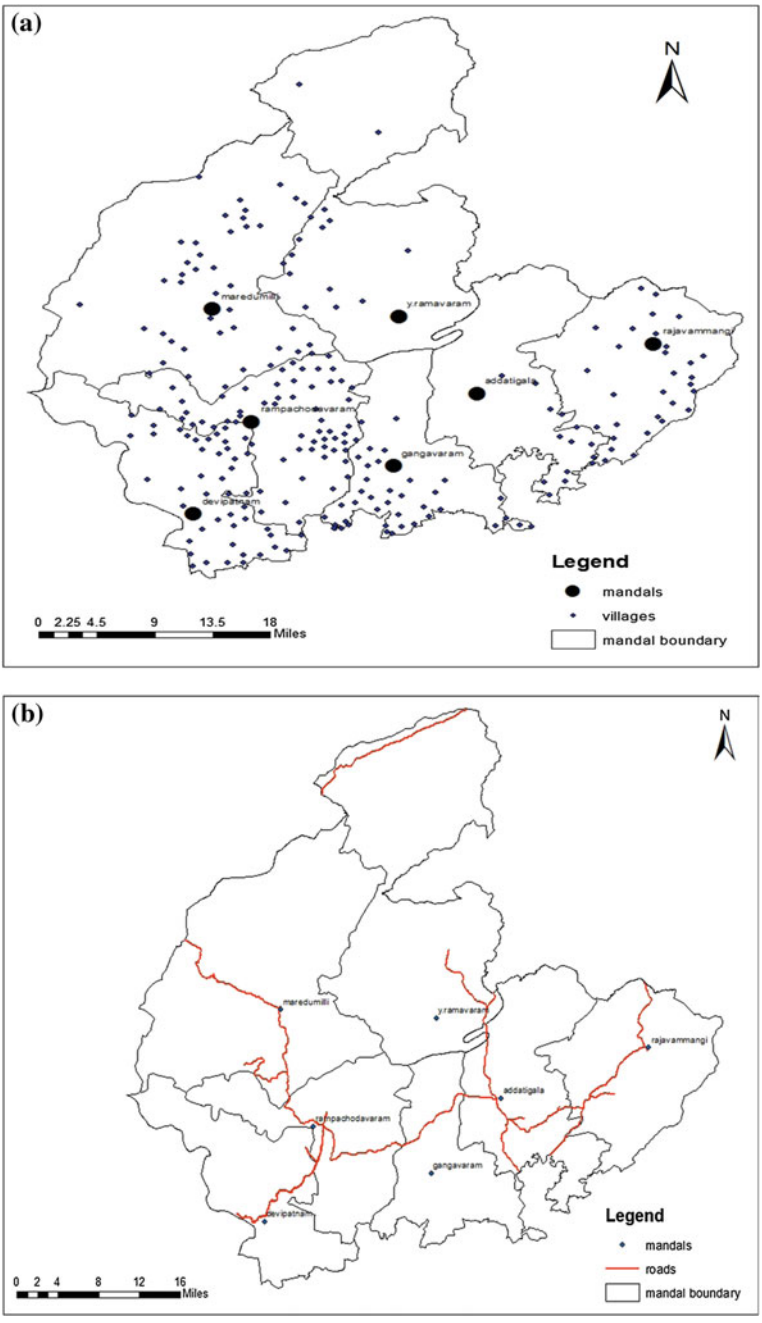

Fig. 2 **a** Villages. **b** Roads generated. **c** Different types of roads in study area

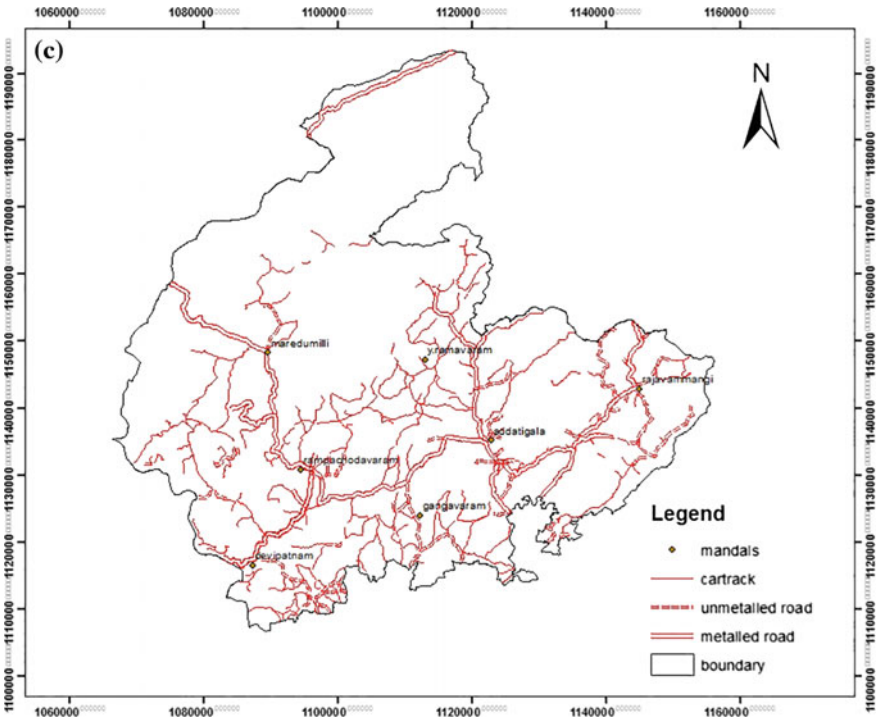

Fig. 2 (continued)

The total study area occupied is 4580.91 km^2. The total length of main roads in AOI is 325.12 km. The total length of unmetaled is 190.15 km and the length of cart tracks road is 732.48 km. The total population of AOI is 2,18,385 and the total villages are 554.

References

1. Burrough, P.A: Principals of Geographic Information System Land Resources. Assements Clarendom Press, Oxford, United Kingdom (1986)
2. Anderson, J.R., Hardy, E.E., Roach, J.T., Witmer, R.E.: A landuse and land cover classification for use with Remote sensor data, Geological survey (1976)
3. Janmabhoomi directory of habitations and Municipal wards in the state, finance and planning department government of Andhra Pradesh Hyderabad July 1998
4. Tanenbaum, A.S.: Computer Network, Prentice-Hall
5. Comer, D.E.: Computer Networks and Internet
6. Hudsal, J.: Fastest path problem in dynamic transportation networks (2000). http://www.husdal.com/mscgis/resear-h.html. Last accessed 22 Nov 2015
7. Cho, H.-J., Chung, C.-W.: An efficient and scalable approach to CNN queries in a road network. In: Proceedings 31st International Conference on Very Large Data Bases, 2005, pp. 865–876

Chapter 61
Public Health Emergencies During Disasters—A Strategic Response

Surya Rao Kutikuppala

Abstract In recent times disaster management has gained momentum in India, in particular due to the rise in vulnerabilities to disasters. However, concerns have been raised about the efficacy of public health emergency response system in the wake of recent floods, cyclones, earthquakes and the threat of epidemics. Successful and workable plans need to be in place to reduce human suffering, loss of life and to contain the spread of epidemics and dangerous diseases in disaster-affected regions. We cannot forget the age old adage—"A stitch in time saves nine". Timely and well thought out response with necessary preparedness shall be instrumental to any successful disaster response efforts. Contagious diseases that pose a health risk to people have always existed. The risk just multiplies during these difficult times of disaster occurrence thereby putting additional stress on the public health system. Hence, strategic planning for immediate care in the form of first-aid for the injured; timely evacuation; prioritizing the medical provisioning to those affected/injured based on the assessment of the available resources; making provision for food and safe drinking water in the temporary shelters; enhancing the health services to protect the affected public from the spread of diseases should be a top priority.

Keywords Disaster management · Hudhud cyclone · Emotional support Public health

1 Introduction

Disaster by definition means any occurrence that causes damage, ecological disruption, loss of human life or deterioration of health and health services on a scale sufficient to warrant an extraordinary response from outside the affected community or area [1]. In part, it suggests that the resources from within the affected community wouldn't be sufficient to deal with the situation. Etymologically speaking,

S. R. Kutikuppala (✉)
IMA College of General Practitioners, Chennai, India
e-mail: kutikuppalasuryarao@gmail.com

P. J. Rao et al. (eds.), *Proceedings of International Conference on Remote Sensing for Disaster Management*, Springer Series in Geomechanics and Geoengineering,
https://doi.org/10.1007/978-3-319-77276-9_61

the term is derived from the Italian word 'Disastro', which is a combination of the word 'dis'—expressing negation and 'astro' meaning star. Thus disaster means 'ill-starred event' [2].

The Asia-pacific is the most disaster-prone region of the world. Over the last two decades, approximately 41% of all reported disasters in the world occurred in this region [3]. In 2015, South Asia, of which India is a part, accounted for a staggering 64% of the total global fatalities Inter-alia, the Bhopal gas tragedy in 1984 has spurred policy measures with new and more effective strategies to scientifically face the challenges posed by disasters and to alleviate the suffering and human loss [4]. These figures and major disasters point towards the pressing need for systematic improvement in disaster preparedness and upgradation of public health emergency response systems in this region. Amongst the recent disasters that created large scale destruction was the Hudhud cyclonic storm that struck Visakhapatnam and adjoining regions of coastal Andhra Pradesh in Nov, 2014. The coastline of India stretching around 7500 km is probably the most cyclone battered region on the planet earth, leading to very severe loss of life and economic damage. While natural disasters cannot be avoided altogether, the scale of its damage can certainly be minimized with appropriate planning and well coordinated policy for disaster prevention, mitigation, preparedness, emergency response, rehabilitation and reconstruction, in order to minimize loss of life, property, including agricultural crops and livestock.

There are various types of disasters such as cyclones, floods, droughts, cloud-burst, storm surge, landslides, earthquakes, volcanic eruptions, industrial chemical and nuclear accidents. While response for some disasters can be planned in advance based on meteorological projections, others occur without warning signs making it very difficult to respond. Hence, the public health emergency response system has to be tuned based on the nature and type of disaster. There cannot be 'one size fits all strategy' to deal with all the disasters as the effects vary from disaster to disaster. On the basis of this understanding, the response network has to focus on the following major aspects:

(a) Immediate first-aid for pain relief.
(b) Dealing with potential spread of contagious diseases.
(c) Protecting the wider elements of public health—Safe drinking water, nutritional needs, sanitation, safe disposal of the dead etc.

As it is well known, there are 3 phases in the disaster management cycle: Pre-disaster phase; disaster phase; Post-disaster phase. Each phase will require its own set of measures that are to be undertaken in a comprehensive and coordinated manner for a successful strategy.

2 Public Health Emergency and Information Dissemination

Disasters often create conditions for public health issues, especially in context of the scarcity of safe drinking water, diseases spreading due to stagnant and contaminated water and lack of sanitation leading to cholera, gastro enteritis Amoebic Dysentery, Bacillary Dysentery, Diarrhea, typhoid, hepatitis A, hepatitis E etc. Epidemic outbreaks are a scenario that we should be vary and ready during a disaster situation. It is of paramount importance to educate the public and keep them informed about public health emergencies and provide the information needed to protect and save lives during epidemics. When unexpected disasters keep happening across the globe, some find it extremely difficult to face them. Yet, preparedness based on scientific approach with focus on creating awareness will certainly help people dealing with disasters much more effectively and efficiently [5].

2.1 Contingency Distribution Network

When disaster strikes, often many will not have access to food, water and electricity for some time. We need to be prepared for providing the required potable water, food supplies, clothing, temporary sanitized shelters and emergency kits, that can provide essential supplies for all the affected till reasonable normalcy is achieved. It may include canned foods and other staples. A normally active person needs to drink at least half gallon of water per day. We have to store at least 3-day food supply and consider storing a two-week supply of water. In such a situation, safety of pets and livestock needs to be factored [6].

2.2 Local Community/Neighborhood Approach

The ability of communities to manage disaster situations can be considerably enhanced with a team approach and being skillfully and effectively trained to face situations in advance.

Periodical mock-drills can boost their confidence and ability to face any unexpected eventualities. In the process, they have to identify warning signals, develop a plan to help the children, elderly and differently abled. Children and youth should be made aware about the possible fallouts of fire, extreme weather conditions and other hazardous situations so as to prepare the ground for collective action [7].

2.3 Immediate Coordinated Response to Disaster Situation

The search and rescue efforts following the impact of a disaster are crucial to reduce loss of life. During this phase, the first-aid acts as a very useful tool in alleviating human suffering. At the same time, healthcare resources have to be redirected towards disaster relief. Emergency services are to be maximized in these hours of need. Additional provision should be made for food and shelter at the healthcare service points itself.

The disasters also put tremendous pressure on the limited healthcare facilities and personnel available. Such situations require drawing upon the philosophy of the great British philosopher and jurist, Jeremy Bentham who elaborated the principle of "Greatest happiness of the greatest number". The medical approach of triage is the process of deciding which patients should be treated first during disasters based on how sick or seriously injured they are rather than the 'first-come-first-serve' basis. The higher priority is to be given to those victims whose chances of survival increase by simple intensive medical intervention. The overall idea is to maximize the number of survivors than focusing on morbid patients, with questionable benefit, who require a great deal of attention [8].

2.4 Relief in Temporary Shelters

Utmost care is to be taken to avoid over-crowding and poor sanitation in temporary relief centers else there are high chances of acute respiratory and Gastro-Intestinial infections. If we fail to follow strict hygienic principles, providing emergency food, water from different sources to the affected in shelters may itself be a source of infectious diseases.

2.5 Dealing with Epidemics in the Aftermath of Floods

Floods and the consequent overflowing of waters, stagnation of water pools could result in epidemics like gastro enteritis, food poisoning, water-borne diseases, cholera, typhoid, jaundice, vector-borne diseases like malaria, dengue etc., so there should be careful, effective planning towards a specific disaster management strategy keeping in view public health as a top agenda [9]. Moreover, large number of dead bodies of human and animals during floods can obstruct the efficiency of the rescue efforts in addition to contaminating the water streams resulting in variety of diseases. Therefore, appropriate disposal is of major importance [10].

2.6 Restoration of Normalcy

The healthcare services are to be recognized and prioritized based on the pattern of health needs. After few weeks of the disaster, ecological health measures like reviving the green cover, securing the integrity of the water supply network, food safety and kitchen sanitation at temporary shelter camps, vector-control to prevent dengue, malaria, leptospirosis, plague etc., become more significant.

2.7 Emotional Support

A healthy mind has got remarkable healing power during stressful situations. The difficult times of disaster tests the resilience and strength of the victims. Emotional support to overcome the anxiety and mental unease of the agony that they have undergone is an important step in reintegrating disaster survivors into the mainstream society. With counseling, Yoga practice and meditation resilience is to be developed through thought process and actions [11]. More importantly, the orphaned and displaced population during disasters have to be provided with suitable institutional support of the government and the NGOs.

3 Conclusions

Disasters make one thing very clear that local, national and transnational capacities are critical. Therefore, we need to build capacities through educational programmers; "Information Education Communication" campaigns through traditional and modern media; organizing mock-drills so as to prevent, prepare, respond and recover from emergencies and disasters. Timely policy blueprint on public health responsiveness to different disasters should be developed and made accessible. Special training and skills should be imparted to the volunteers, civil society and in particular to the public health staff who are supposed to be the front line soldiers in the relief efforts. Further, all the national and international resources are to be mobilized and utilised to the fullest during disasters. The STATE's capacity to respond to disasters is crucial. It cannot do it alone and will definitely require the support from the first-response force i.e. the local non-affected community and Non-governmental organizations. International organizations also have a critical role to play by providing financial and material resources during disasters. Not only this, the international organizations provide key impetus to national governments in developing and adopting the risk reduction frameworks and other policy initiatives. In this regard, WHO recognized the commitment and leadership of Mexico in the field of disaster risk reduction, especially through the Safe Hospitals Initiative [12]. Following the devastating 1985 earthquake in Mexico City, the Ministers of Health

of the Americas were urged to establish strategies on Disaster Risk Reduction in Health. Mexico has gone a step further to apply the Safe Hospitals principles to the protection of other critical infrastructure, including schools, transportation network and hotels, which should be replicated by countries across the world, including India. Effective management of psychological trauma/stress and anxiety levels that would be faced by the affected in the aftermath of the disaster will go a long way in enhancing their ability and resilience to cope with the situation when they are rehabilitated. Hence, innovative ideas have to be coupled with actions to stabilize the situation in a public health emergency scenario.

References

1. Coping with Major Emergencies: WHO Strategy and Approaches to Humanitarian Action. World Health, Organization, Geneva (1995)
2. https://en.oxforddictionaries.com/definition/disaster
3. The sixth Global Environment Outlook (GEO-6) Regional Assessment for Asia and the Pacific, released by UNEP, 2016
4. Disasters in Asia and the Pacific: 2015 Year in Review, UN Economic and Social Commission for Asia and the Pacific (2015)
5. Dizon, N.Z.: Terrorism drill comes to Chicago. Chicago Tribune. 13 May 2003
6. Buchanan, S.: Emergency preparedness. In: Paul, B., Roberta, P. (eds.) Preservation Issues and Planning, pp. 159–165, ISBN 978-0-8389-0776-4. American Library Association, Chicago (2000)
7. Velasquez, III, A.: Regional Administrator FEMA Region V, Family Emergency Planning Guide. 10 Jan 2011
8. PAHO: Natural disasters, Protecting the public health, Scientific Publication No. 575 (2000)
9. Marx, M.A., Rodriguez, C.V., Greenko, J., Das, D., Heffernan, R., Karpati, A.M., et al.: Diarrheal illness detected through syndromic surveillance after a massive power outage: New York City, August 2003. Am. J. Public Health **96**, 547–53 (2006). https://doi.org/10.2105/AJPH.2004.061358
10. Gayer, M., Connolly, M.A.: Communicable diseases control after disasters. In: Noji, E.K. (ed.) Public Health Consequences of Disastwers, 2nd edn. Oxford University Press, Oxford (2005). (in revision)
11. Chiesa, A., Serretti, A.: Mindfulness-based stress reduction for stress management in healthy people: a review and meta-analysis. J. Altern. Complement. Med. **15**(5), 593–600 (2009)
12. DSG UN Mrs Amina Mohammed Gearing up to reduce risks from emergencies and disasters, World Health Organization, Cancun (Mexico), 25 May 2017

Chapter 62
Integrated Assessment of Climate Change Impacts on Maize Crop in North Coastal Region of Andhra Pradesh, India

Chukka Srinivasa Rao and Peddada Jagadeeswara Rao

Abstract Current crop productivity in North Costal Andhra Pradesh of India is low compare to other locations of Andhra Pradesh region and due to projected climate change this may be further worse. The present study investigates the spatial-variability of impacts of climate change on maize crop yields in the north costal districts of Andhra Pradesh of India and examines the adaptation strategy contributions on crop yield. Five future climate models with RCP 8.5 pathways were selected in this study and the projections from these models were integrated with DSSAT crop simulation model to simulate the impact on rainfed maize crop productivity over North Costal Andhra Pradesh region. Influence of amount rainfall and onset of monsoon and rainy days on rainfed maize yield was significant in North Costal Andhra Pradesh region. Rainfed maize productivity is expected to decrease to a maximum of 16% from the present yield level due to change in climate. The climate change impacts could be reduced by early sowing (altering the sowing date) to June last week/July first week against July second/third week. Supplement irrigation during delay monsoon will give yield increase under future climate.

Keywords Climate change · Maize · Climate models · Crop models
Crop yield

C. S. Rao (✉) · P. J. Rao
Andhra University, Visakhapatnam, India
e-mail: chukkasr@gmail.com

P. J. Rao
e-mail: pjr_geoin@rediffmail.com

P. J. Rao et al. (eds.), *Proceedings of International Conference on Remote Sensing for Disaster Management*, Springer Series in Geomechanics and Geoengineering,
https://doi.org/10.1007/978-3-319-77276-9_62

1 Introduction

Climate change is considered as major global level issue in recent and becoming more and more complex than it was before. The climate change issue is part of the greater challenge of sustainable development. According to the latest scientific findings, since the pre-industrial era the earth's climate system has changed on both global and regional scales. North coastal Andhra Pradesh is highly vulnerable to seasonal fluctuations with respect to temperature, rainfall, relative humidity, wind speed and radiation which cause uncertainty in crop production. Characteristically agriculture is very sensitive to climate conditions, this is one of the important sector most susceptible to the impacts and risks of global climate change [1, 2]. Adaptations is the main factor that will influence and shape future severity of impacts of climate change on food production [3]. It is very difficult to understand the impact of the changes in climate on agriculture; a variety of effects are likely to occur at different stages of crop growth.

Coupled with climate models, crop models can simulate to study the effects of climate change on agriculture. Crop simulation models using weather-soil-crop dynamics and integrate crop resources capture principles can assist in the evaluation of the impacts and find adaption options in a wide range of climates, season and soil types. The crop models have been developed with different levels of biological details [4] and run for various environmental conditions and management to simulate crop growth and development processes.

Maize (Zea mays L.) is important cereal crop which has special characteristics that include its carbon pathways (C4), wider adaptability, higher multiplication ratio, desirable architecture, superior transpiration efficiency, high versatile use etc. In North costal Andhra Pradesh region maize crop grown mostly as Kharif crop and productivity under rainfed condition is highly influenced by the climate variations and expected to be vulnerable to adverse climate changes [5]. We need to evaluate the relative potential of adaption options, and to develop effective strategies to cope with climate risk. Main objectives of this study are (a) assess the climate change impact and (b) identify adaption options to minimize the climate change impacts on rainfed maize in North costal Andhra Pradesh.

2 Materials and Methods

Integrated assessments have been done using crop simulation models of DSSAT for Maize crop in North Coastal region of Andhra Pradesh. The study area comprises of North Costal Part of Andhra Pradesh spreading between 17° 15″ and 19° 15″ of the northern latitude and 82° 00″ and 84° 47″ of the eastern longitude. About 60% of its area is cultivated purely under rainfed conditions and even the remaining area is mostly dependent on the rainfall received for water storage or ground water recharge even though which is termed as irrigated area. The climate is characterized

by high humidity throughout the year with high temperature in summer season and good seasonal rainfall. About 96% soils of this region are medium fertility comprises of Sandy loams, Red and Sandy soils. The yields of Maize are many a times were unpredictable due to erratic distribution of rainfall coupled with many other biotic factors. Maize crop under rainfed ecosystem was considered for this study (Fig. 1).

Thirty years (1980–2010) of observed climate data has been obtained from ANGR Agricultural University and these baseline weather datasets have quality controlled for outliers and if found such values were corrected by using AgMERRA data which were prepared based on a combination of daily outputs from retrospective analysers, gridded temperature and precipitation station observations and satellite information for Solar radiation and rainfall. In order to create a representative 30 years weather series for each location, neighbouring sites from the highly spatially resolved WorldClim data. A total of 115 grid points were used for this study. Using the "delta" method the future climate projections were created, in which changes from baseline for Representative Concentration Pathways (RCP) 8.5 for mid-century were applied. Physical and chemical properties of the soil were estimated for each grid based on the available soil profile data and expert knowledge. Crop management details were collected for each location from the farmers. DSSAT crop simulation model coupled with climate data were analysed to

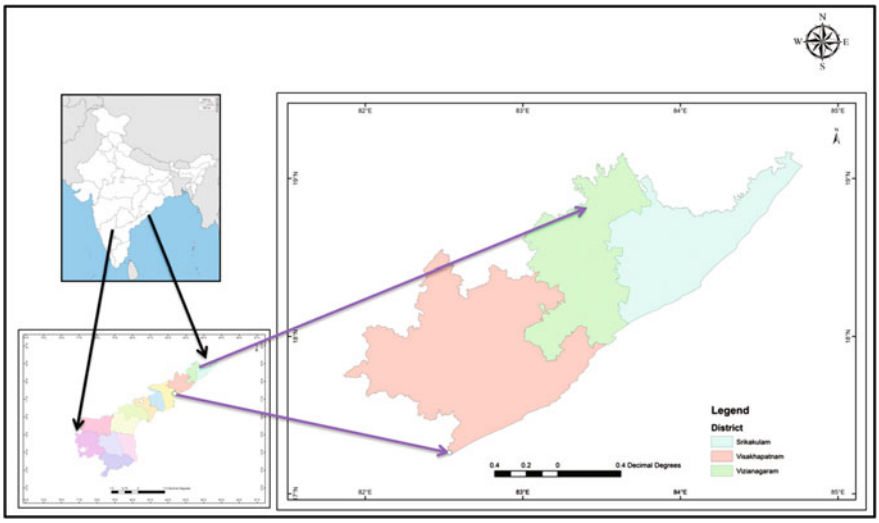

Fig. 1 Study area

understand spatial variability impact in maize productivity. Potential adaptation choices were customized to suit the spatially varying impacts.

3 Results

Observed climate and its variability over the study area were analysed through observed data. The annual maximum temperature was found 31.6 °C and it varies from a minimum of 18.6 °C to a maximum of 46.2 °C with a standard deviation derived for 20 years is 2.9. The annual minimum temperature was found 23.5 °C and it varies from a minimum of 9 °C to a maximum of 34.6 °C with a standard deviation derived for 20 years is 3.6 (Table 1).

Climate projections from the selected GCMs were studied as seasonal and annual averages to know the changes predicted. To represent the possible spatial variations by mid-century, grid to grid comparison was studies to extract the projected changes. The absolute change in maximum temperature and minimum temperature from base period to that of mid-century was calculated. Similarly percent change of rainfall was computed. Spatial variation in rainfed maize productivity simulated using DSSAT model over North costal Andhra Pradesh for the current climate (mean productivity of 1981–2010) is depicted in Table 2. From the analysis, it could be noticed that average productivity of 5246 kg ha^{-1}. Nearly 2/3 grids are falling under the range of 4500–6000 kg ha^{-1}. Spatial response of maize productivity for the future climatic conditions was studied using the future climate date generated by five GCMs depicting Cool/Wet, Cool/Dry, Middle, Hot/Wet and Hot/Dry situations under 8.5 scenarios for mid-century.

Table 1 Climatic normal of weather parameters over north costal Andhra Pradesh

Parameter	Statistics	Annual	SWM	NEM
Maximum temperature	Mean	31.6	32	29.5
	Max	46.2	45.8	38.9
	Min	18.6	19.8	18.6
	SD	2.9	2.4	2
Minimum temperature	Mean	23.5	25.5	20.2
	Max	34.6	34.6	30.8
	Min	9	17	9
	SD	3.6	1.8	3.6
Rainfall	Mean	1003	709	197
	Max	1368	1139	443
	Min	650	389	36
	SD	188	146	108

Table 2 Spatial variability of baseline maize yield (mean of 1981–2010) over north costal Andhra Pradesh

Yield class (kg/ha)	Frequency (no. of grids)	% of grids	Mean yield (kg/ha)	SD (kg/ha)	CV (%)
3501–4000	7	6.1	3796	139.9	3.7
4001–4500	14	12.2	4220	136.9	3.2
4501–5000	23	20.0	4864	111.8	2.3
5001–5500	27	23.5	5304	151.4	2.9
5501–6000	23	20.0	5730	128.0	2.2
6001–6500	18	15.7	6145	95.5	1.6
6501–7000	3	2.6	6660	246.7	3.7
Total	115	100	5246	1010.2	19.6

DSSAT simulation indicated that the magnitude of benefit of early sowing and increased fertilizer adaptations got reduced in future climatic conditions when compared to adaptation applied under current climatic conditions.

DSSAT simulated yield changes under future climatic conditions as a result adaption strategies was estimated by comparing with the future yields simulated without adaptation. In RCP 8.5 scenario early sowing exhibited positive effects in most parts of North costal Andhra Pradesh. Results indicated that delayed sowing under future warmer climate would result in yield decline in rainfed maize and could not be recommended.

4 Discussions

Integration of climate and crop model was considered to assess the spatial variability of climate change impact on productivity of rainfed maize. Annual maximum temperature was projected to increase from 1 to 2.8 °C and annual minimum temperature was projected to increase from 1.1 to 2.8 °C and annual rainfall was projected to change both negatively and positively (a decrease of −18.5% to an increase of +51.5%) by RCP 8.5 by the end of mid-century. Monsoon rainfall projections were studied as it plays vital role in rainfed agriculture of this region. The spatial spread of rainfall projections was analyzed. The spatial variation could also be attributed to the increased temperatures and subsequent increase in evaporation that intensifies the hydrological cycle [6]. Baseline rainfed maize yield simulations varied between the locations and ranged between 6945 and 3647 kg ha^{-1} with an average productivity of 5255 kg ha^{-1} (Table 3).

Impact of change in climatic parameters in the future on rainfed maize yield would dependent on the interplay of the agro-climatic variables, as well as other non-climate variables, but such analyses can help the scientists to identify the most important variables to consider under future climate change. The benefits of adaptation strategies were evaluated by comparing maize productivity with and

Table 3 Projected changes in annual maximum temperature over north costal Andhra Pradesh

Future models	Change in max temperature	Change in min temperature
Hot-dry	2.1	2.0
Middle	1.8	1.6
Hot-wet	1.8	1.9
Cool-dry	1.1	1.3
Cool-wet	1.3	1.7

Table 4 Variation in rainfall change projected over north costal of Andhra Pradesh across seasons and scenarios

Models	Annual		SWM		NEM		Summer	
	Highest	Lowest	Highest	Lowest	Highest	Lowest	Highest	Lowest
Hot-dry	−4.8	−18.5	−12.1	−20.1	15.5	−1.6	−20.3	−43.8
Middle	10.3	−4.9	10.3	−7.8	21.8	7.7	−6.9	−21.8
Hot-wet	51.5	22.1	82.3	43.5	−1.7	−23.3	35.5	−44.5
Cool-dry	−1.1	−4.4	0.9	−5.8	2.2	−9.3	12.2	−9.8
Cool-wet	34.5	7.2	16.7	0	60.9	16.2	122.4	−26

without adaptation in the current as well as future climatic conditions. Under current conditions, rainfed maize productivity was compared with and without adaptation option (Table 4).

Results indicated that advancing the date of sowing by 15 days produced considerably higher yield gains. This might be due to favorable environment prevailed during the critical stages of growth with early planting. Early date of sowing as adaptation option in the present study showed consistent increase in yield with all the five climate models projections compared to future without adaptation. Results of the current study showed that the negative impacts of future climate change could be reduced under early date of sowing, than normal and late planting (Table 5).

Table 5 Per cent variation in maize yield from Baseline yields for different models projected over north costal of Andhra Pradesh

Future models	Dry yield (kg/ha)	% Variation from Baseline yield
Hot-dry	4354	−16
Middle	4933	−5
Hot-wet	5562	7
Cool-dry	5102	−1
Cool-wet	5291	2

5 Conclusions

Advancing the sowing date for 15 days for better maize productivity at macro level under current and future climatic conditions and early maturity varieties with resistance to high temperature was suggested. Irrespective of the scenarios and models studied, the minimum and maximum temperatures are projected to increase. Rainfall influence on yield of rainfed maize was significant. In future due to climate change, it is expected that the rainfed maize productivity will be reduced to a maximum of 16% from the current yield levels. Early sowing (changing the sowing date from July second/third week to July first week/end of June) during Kharif season may reduce the impact of the future climate change. Supplement of irrigation during critical stage will also improve the productivity.

References

1. Reilly, J.: Climate change and global agriculture: recent findings and issues. Am. J. Agric. Econ. **77**, 727–733 (1995)
2. Smit, B., Skinner, M.W.: Adaptation options in agriculture to climate change: a typology. Mitigat. Adapt. Strat. Global Change **7**, 85–114 (2002)
3. Lobell, D.B., Burke, M.B., Tebaldi, C., Mastrandrea, M.D., Falcon, W.P., Naylor, R.L.: Prioritizing climate change adaptation needs for food security in 2030. Science **319**, 607–610 (2008)
4. Thornton, P.K., Bent, J.B., Bacsi, Z.: A frame work for crop growth simulation model applications. Agric. Syst. **37**, 1–330 (1991)
5. Stone, P.J., Sorensen, I.B., Jamieson, P.D.: Effect of soil temperature on phenology, canopy development, biomass and yield of maize in a cool-temperate climate. Field Crops Res. **63**, 169–178 (1999)
6. Ramanathan, V., Crutzen, P.J., Kiehl, J.T., Rosenfeld, D.: Aerosols, climate and the hydrological cycle. Science **294**, 2119–2124 (2001)

Chapter 63
Comparison of Tsunami Arrival Times Using GIS Methods: A Case Study in the Makran Subduction Zone, West Coast of India

Praveen Mupparthi, G. Jai Shankar and Kirti Srivastava

Abstract Western Indian Ocean is not free from tsunami threat. Earthquakes along the Makran Subduction Zone are rare but cannot overlook the seismicity in this region, as the historical tsunamis have not been properly documented due to lack of instrumental data. Documented reports and letters about the historical tsunamis from this subduction zone that caused damage to the surrounding regions like Iran, Oman, Southern Pakistan, India, Maldives and other bordering countries of the Arabian Sea. The earthquake recorded; observed and documented on 27th November 1945 in the Northern Arabian Sea generated a Tsunami caused devastation and destruction in the neighboring countries. This paper presents the estimation of tsunami arrival times computed using GIS methods at different locations along the Western Coast of India and compared with the arrival times computed using the Tunami N2 model. The results obtained are in good agreement with an R^2 value of ~ 0.8. This provides information to assist with the rapid tsunami evacuation operations and further helps to develop a decision support system for local decision makers.

Keywords Tsunami · Makran subduction zone · Tsunami arrival times Tsunami model · GIS

P. Mupparthi (✉) · K. Srivastava
National Geophysical Research Institute (CSIR), Uppal Road, Hyderabad, India
e-mail: praveenm63@gmail.com

K. Srivastava
e-mail: kirti@ngri.res.in

G. Jai Shankar
Department of Geo-Engineering, College of Engineering, Andhra University, Visakhapatnam, India
e-mail: jaisankar.gummapu@yahoo.com

P. J. Rao et al. (eds.), *Proceedings of International Conference on Remote Sensing for Disaster Management*, Springer Series in Geomechanics and Geoengineering,
https://doi.org/10.1007/978-3-319-77276-9_63

1 Introduction

The Makran Subduction zone is located in the southwestern part of Pakistan and southeastern Iran. The length of the Subduction zone is ~1000 km and has resulted due to the convergence between the Arabian plates with the Eurasian plate as shown in Fig. 1 [1]. In this region the Oman oceanic lithosphere slips below the Iranian micro-plate and is characterized by extremely shallow subduction angle [2]. This region is divided into two by the Sistan Suture Zone based on morpho-tectonic features, contrasting seismicity patterns and the varying rupture histories.

In 326 BC Alexander's Navy is known to have been destroyed due to large earthquake near the Indus delta/Kutch region due to massive sea waves in the Arabian Sea [3]. Documented evidence revealed that in 1008 an earthquake had generated a tsunami [4, 5]. Ambraseys and Melville [6] and Byrne et al. [7] have documented the occurrence of 1765 earthquake as a great rupture beneath the easternmost end of the Makran Subduction zone which generated a tsunami. Merewether [8] generated reported that on 19th April 1851 an earthquake occurred and a tsunami got inundating several houses in Gwadar region.

The earthquake which was recorded, observed and documented was the 27th November 1945 Makran earthquake in the northern Arabian Sea which generated a tsunami and caused devastation and destruction. Epicenter of this earthquake is located at 63.48°E, 25.15°N off the Makran coast in the northern Arabian Sea about 100 km south of Karachi and about 87 km south west of Baluchistan, Pakistan. The

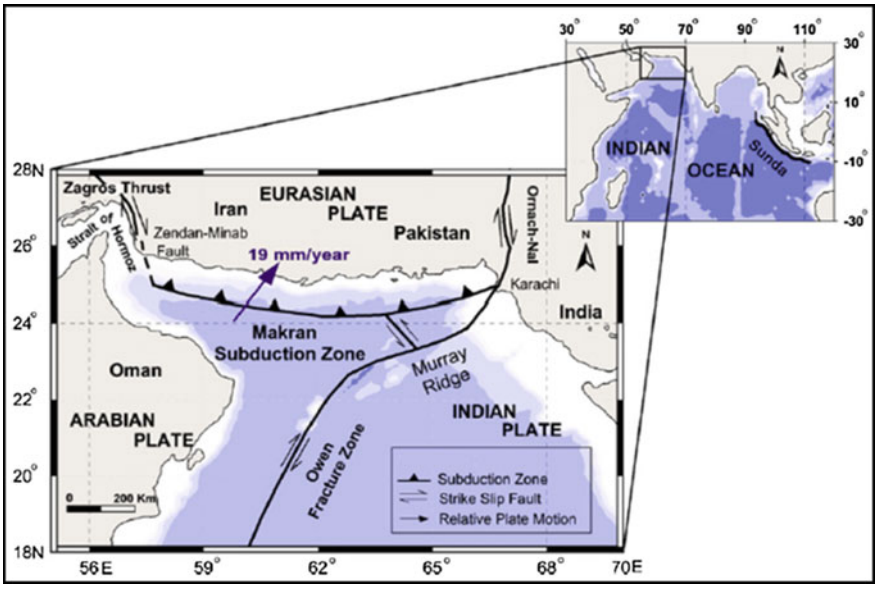

Fig. 1 Tectonic map of Makran subduction zone

magnitude of the earthquake is estimated to be around Mw 8.1 with an estimated focal depth of around 25 km [7, 9, 10]. This earthquake triggered a tsunami with a maximum run-up height of 11 m along the Makran cost and the waves propagated from the epicenter and reached Karachi with a wave height of about 2 m [10, 11]. This earthquake is known to have caused the eruption of a mud volcano a few miles off the Makran coast of Pakistan and ruptured the entire eastern segment of the Makran Subduction zone.

1.1 Application of GIS Technology in Tsunami Evacuation

GIS techniques have been used extensively in tsunami modeling. Romstad et al. [12] studied the effect of rockslide tsunami hazard to several Norwegian lakes where the input data is a raster based digital elevation model. The DEM which is embedded within the GIS has been used by Volker [13], to calculate the land slide volume. Using these GIS techniques several authors have studied the tsunami risk assessment [14, 15] and modeling [16]. Spatial patterns of damage areas through different land characteristics have been studied [17] by Sirikulchayamon et al. [18]. GIS technology has been used in Indian Tsunami early warning system based at INCOIS, Hyderabad that performs 24 X 7 operations right from data reception, display, analysis, modelling, and decision support system for generation of tsunami advisories following a standard operating procedure [19].

In the present study, different GIS methods were used to calculate the tsunami arrival times for a known source in Makran subduction zone for different locations identified along the Indian West coast.

2 Study Area

The West Coast of India from Gujarat to Maldives of the Indian Ocean has been considered as the study region. 11 locations covering Dwaraka, Porbandhar, Mangrol, Diu, Mumbai, Ratnagiri, Goa, Mangalore, Kerala, Karachi, Maldives with a possibility of occurrence of tsunami inundation along the coast were selected to estimate the tsunami arrival times using GIS techniques for comparison. Epicenter of this earthquake is located at 63.48°E, 25.15°N off the Makran coast in the northern Arabian Sea about 100 km south of Karachi and about 87 km south west of Baluchistan, Pakistan as shown in Fig. 2.

Fig. 2 Location of the Tsunamigenic earthquake Epicenter and locations identified for tsunami arrival times estimation

3 Materials and Methods

3.1 Datasets Used for the Study

The ETOPO2 Bathymetry data of Indian Ocean from the National Geophysical Data Centre has been used for tsunami wave propagation with a good coverage of topography information with uniform vertical and horizontal spacing (www.noaa.ngdc.gov.in). The horizontal datum is WGS-84; the vertical datum is Mean Sea Level. ETOPO2 is in the Cylindrical Equidistant Projection (sometimes called Latitude-Longitude, or Geographic). The horizontal grid spacing is 2-minutes of latitude and longitude (1 min of latitude = 1.853 km at the Equator). The vertical precision is 1 m. The grid values represent the elevation at the grid intersections at odd multiples of 2 min of latitude and longitude, averaged over the cell's area. Coverage of ETOPO2 is +90° to −89°58′ in Latitude and −180°W to +179°58′ in Longitude with the number of cells 5400 rows of data (180 × 30), each with 10,800 columns of data (360 × 30). Figure 3 shows the ETOPO2 bathymetry data

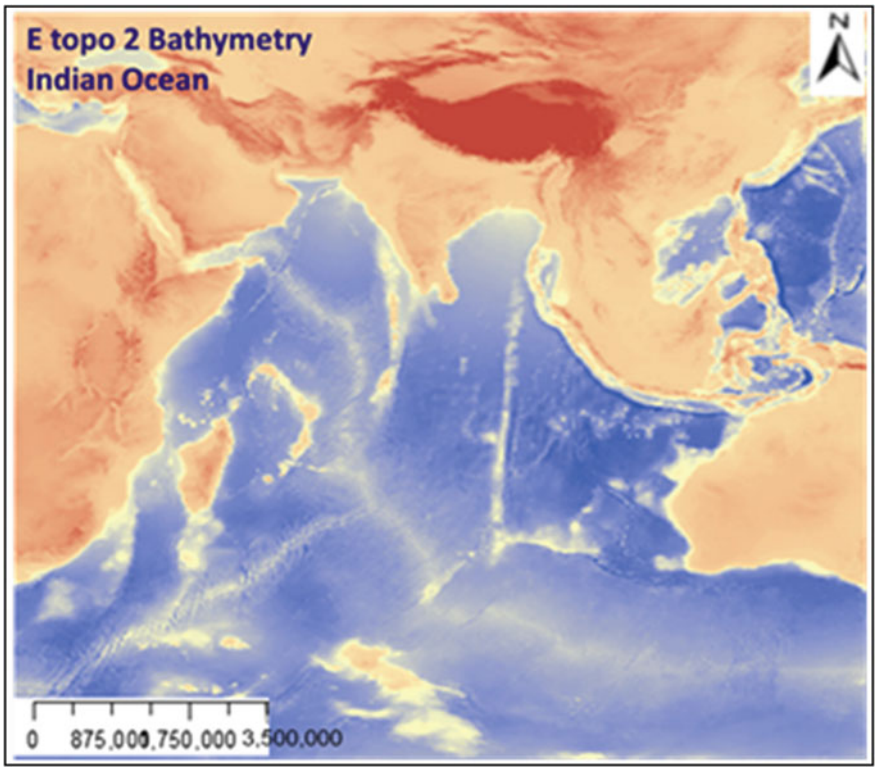

Fig. 3 ETOPO 2 bathymetry data of the Indian Ocean

of the Indian Ocean. ARCGIS v.10.1 software has been used as a tool to estimate the tsunami travel times and the TUNAMI N2 code for the model results on travel times.

3.2 Methodology: GIS Techniques

GIS technology has been used to estimate the tsunami travel times using bathymetry as one of the important parameter for tsunami wave propagation. The key to being able use GIS techniques shows an accurate DEM representing the desired bathymetry of the Indian Ocean. Three GIS techniques were used in the study like Con Tool method, Profile Method and Contour Line method. The epicenter location of the tsunamigenic earthquake is considered as source point as mentioned in Sect. 3. The methodology implemented in the estimation of the tsunami arrival times is shown in Fig. 4.

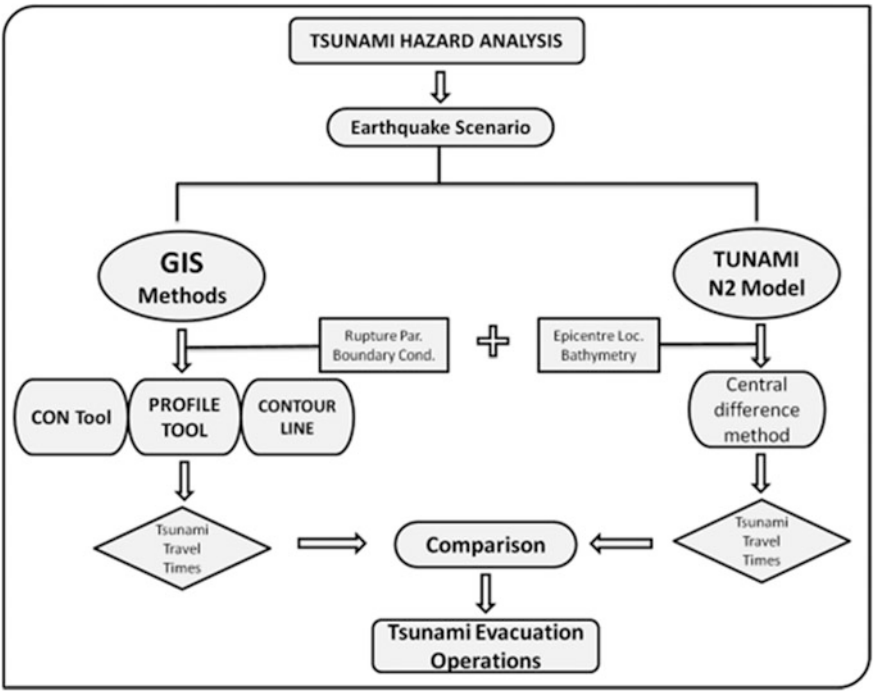

Fig. 4 Methodology on comparison of Tsunami travel times

3.2.1 CON (Conditional Tool Method (Conditional Tool Method)

Using ArcMap, for the bathymetry data of the Indian Ocean the areas below the sea level were isolated into a new raster data by taking the average values of the depth (bathymetry) and elevations (topography) i.e. dividing the land and the sea with their respective constant values using the conditional tool to generate a new raster in order to select the locations of the tsunami affecting areas on the land. The speed of the tsunami is calculated by using the expression shown in Eq. (1) and a new raster image showing the speed pixels will be generated.

$$\text{Speed} = \int \sqrt{(([rasterdata] * -1) * 9.8)} \tag{1}$$

The vector data representing the point and line features of the locations will be overlayed on the raster image representing the speed of a tsunami. The various tsunami speeds that crossed the line features between the epicenter and the city locations will be extracted into new raster images with various tsunami speeds along with their respective lengths. These extracted raster images were converted into polygons by converts each speed pixel into a polygon and intersected with the line features of the locations by creating new vector line features which gives the

length for each speed pixels. The data obtained from the vector line feature is used to calculate time (in sec) travelled by a tsunami by using Eq. (2)

$$\text{Time (in sec)} = \frac{\text{length of each line segment (m)}}{\text{Speed (m/s)}} \tag{2}$$

3.2.2 Profile Method

The profile of the ocean floor elevations from the epicentre to the locations were generated by creating profile graphs using 3D analyst tools. The data from this graph was exported into excel to perform the speed calculations using Eq. (3) which further used to compute the travel times.

$$\text{Speed} = \sqrt{(9.8 * (depth))}\,\text{m/s} \tag{3}$$

3.2.3 Contour Line Method

In this method, contour lines were generated with an interval of 2000 m using spatial analyst tools on the bathymetry data. 2000 m interval is chosen because it generates a manageable amount of contour lines and reasonable final destination travel times. Depth is decided to be the middle number in between the contour lines. So in between shore and 2000 m contour the depth would be 1000 m, and so on. It is to mention that not all of the values where going to be the same but considered that if we took the middle number, it would close to the mean number. Then the lengths were measured from source to the next contour line and from each contour line started a new segment. This is done until the end point is reached. Then taking the depth of the ocean in Eq. (1) the tsunami speed is computed. This gives how fast the tsunami moves at certain depth. Then the length needed to be divided by how fast the wave was traveling in that section of the ocean. All of the lengths where then multiplied by the corresponding speed of the tsunami and then added up to find a total time.

3.3 Tsunami Modeling

Tsunamis are long waves which are mainly generated by the movement of sea bottom due to earthquakes. The generation of tsunami waves has been discussed by several researchers [20–23]. Initial sea bottom deformation is an important parameter in order to obtain the initial surface wave conditions. Mansinha and Smiley [24] have given a complete set of analytical expressions to obtain the internal as well as surface deformation. To obtain this one needs the information

pertaining to the earthquake source parameters such as fault length, width of the fault, focal depth, dip angle, slip angle and displacement. Once the initial wave is generated one of the wave fronts would start moving toward the deep ocean and the local shoreline.

Since the vertical acceleration associated with tsunami waves is small compared with the gravity acceleration, tsunamis waves are usually resolved using 2D hydrostatic models and mathematically it is expressed as

$$\frac{\partial \eta}{\partial t} + \frac{\partial M}{\partial x} + \frac{\partial N}{\partial y} = 0 \tag{4}$$

$$\frac{\partial M}{\partial t} + \frac{\partial}{\partial x}\left(\frac{M^2}{D}\right) + \frac{\partial}{\partial y}\left(\frac{MN}{D}\right) + gD\frac{\partial \eta}{\partial x} + \frac{gn^2}{D^{7/3}} M\sqrt{M^2+N^2} = 0 \tag{5}$$

$$\frac{\partial N}{\partial t} + \frac{\partial}{\partial x}\left(\frac{MN}{D}\right) + \frac{\partial}{\partial y}\left(\frac{N^2}{D}\right) + gD\frac{\partial \eta}{\partial y} + \frac{gn^2}{D^{7/3}} N\sqrt{M^2+N^2} = 0 \tag{6}$$

In the above equation M and N are expresses as

$$M = u(h+\eta) = uD; \quad and \quad N = v(h+\eta) = vD \tag{7}$$

where D is the total water depth given by $h + \eta$, t is time, h(x, y) is unperturbed depth, g is the gravitational acceleration, u and v are components of the horizontal velocities, M and N are the discharge fluxes in the x- and y-directions.

3.3.1 TUNAMI N2 Model

Imamura et al. [20] used a finite difference technique based on Leap-Frog scheme to develop a code to solve the tsunami wave propagation i.e. TUNAMI-N2. The formulation uses the central difference method with a second order truncation error. The associated boundary conditions were taken using Mansinha and Smilye [24] method and open Sea boundary conditions i.e. at the open sea the boundary condition is free transmission and the boundary condition on land is assumed to be a perfect reflector. The frictional coefficient used in this study is 0.025. The code is being used extensively by tsunami modelers to quantify the tsunami propagation, and compute the arrival times at different locations.

3.4 Case Study of 1945 Makran Tsunamigenic Earthquake

In this study we modeled the 27th November 1945 tsunamigenic earthquake of magnitude 8.1 which occurred in the Makran Subduction Zone. The epicentral coordinates of the source are 63.48°E, 25.15°N as shown in Fig. 2 [7]. The rupture

Table 1 Rupture parameters of 1945 Makran tsunmigenic earthquake

Parameter	Lat	Lon	Magnitude	Fault length	Fault width	Slip	Strike	Dip	Rake	Focal depth
Value	63.48°E	25.15°N	8.1	150 km	70 km	7 m	246°	7°	89°	27 km

parameters used in the numerical modeling for the Makran tsunami are given in Table 1. Tsunami arrival times at 11 locations selected along the West Cost of India were obtained from the model results and GIS methods as well are shown in Table 2. In the present study, GIS tools implemented to compute the arrival times of a tsunami wave mainly depends on the depth of the ocean along the path (line) between epicenter and the site locations which varies with the distance and the

Table 2 Rupture parameters of 1945 Makran tsunmigenic earthquake

Location	Latitude	Longitude	Distance (km)	GIS Methods			Model
				Con-tool	Profile	Contour line	TUNAMI N2 code
Dwaraka	68.964	22.325	650	147.4	138.05	150	136.95
Porbandhar	69.586	21.637	745	170.4	148.27	157.8	143.4
Mangrol	70.051	21.083	814.62	175.02	173.04	168	142.6
Diu	70.895	20.704	911.82	208.7	202.39	225.6	206
Mumbai	71.87	18.99	1099.16	203.85	200.95	199.2	191.1
Ratnagiri	72.67	16.94	1305.14	245.4	228.32	268.2	165.45
Goa	73.76	15.408	1505	232.8	218.13	237	207.1
Mangalore	74.256	12.932	1739.83	185.4	183.74	267	194.95
Kerala (Neendakara)	76.535	8.936	2239.21	285.6	263.37	303.6	271.7
Karachi	66.654	24.838	371	49.46	48.76	132.6	69
Maldives	78.825	4.47	2500	218.53	216.49	211.2	214.35

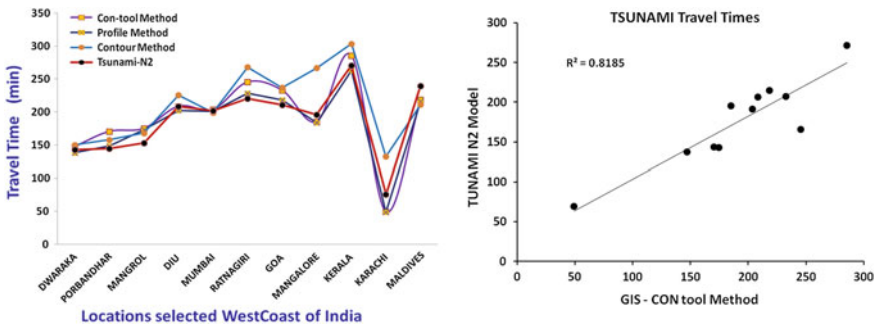

Fig. 5 Comparison of Tsunami travel times computed using GIS methods and TUNAMI N2 model

comparison shows that they are in good agreement with the model output and the among the three GIS method implemented, the CON tool methods shows a good correlation with an R^2 value of ~ 0.8 (Fig. 5).

In Profile method tsunami arrival time depends mainly on the line length between source to the location, whereas in the Contour Line method the line segment length between two contours from source to the location and finally in Con-Toll method the arrival time depends on the line length from source to the location.

4 Conclusions

The Makran subduction zone has generated many significant earthquakes which further caused great tsunamis in the past. This paper showed that the tsunami arrival times at 11 locations along the west coast of India using different GIS techniques and comparison with the results obtained from tsunami mode. Analysis shows that the arrival times obtained are seen to be in agreement at most locations with a few minutes variation. The variation in arrival times is due to the fact that the TUNAMI N2 uses the fault segment as a source where as the GIS techniques uses the epicenter point as a source. In TUNAMI N2 code the boundary conditions such as free transmission at open sea and the boundary condition on land is assumed to be the perfect reflector which is not considered in GIS techniques. GIS based techniques are fast way of obtaining the tsunami arrival times at different locations and provides information to assist with the rapid tsunami evacuation operations and further helps to develop a decision support system for local decision makers.

References

1. Heidarzadeh, M., Pirooz, M.D., Zaker, N.H., Yalciner, A.C., Mokhtari, M., Esmaeily, A.: Historical tsunami in the Makran subduction zone off the southern coasts of Iran and Pakistan and results of numerical modeling. Ocean Eng. **35**(8–9), 774–786 (2008)
2. Koppa, C., Fruehn, J., Flueh, E.R., Reichert, C., Kukowski, N., Bialas, J., Klaeschen, D.: Structure of the Makran subduction zone from wide-angle and reflection seismic data. Tectonophysics **329**, 171–191 (2000)
3. Lisitzin, E.: Sea Level Changes. In: Oceanographic Series New York, Elsevier (1974)
4. Murty, T.S., Bapat, A., Prasad, V.: Tsunamis on the coastlines of India. Sci. Tsunami Hazards **17**(3), 167–172 (1999)
5. Rastogi, B.K., Jaiswal, R.K.: A catalog of tsunamis in the Indian Ocean. Sci. Tsunami Haz. **25** (3), 128–143 (2006)
6. Ambraseys, N.N., Melville, C.P.: A History of Persian Earthquakes, p. 219. Cambridge University Press, London (1982)
7. Byrne, et al.: Great trust earthquakes and aseismic slip along the plate boundary of the Makran subduction zone. J. Geophys. Res. **97**(B1), 449–478 (1992)

8. Merewether, W.: A report of the disastrous consequences of the severe earthquake felt in the provinces of Upper Scinde. J. Bombay Geog. Soc. **10**, 284–286 (1852)
9. Beer, A., Stag, J.M.: Seismic sea wave of November 27th 1945. Nature **158**, 63–64 (1945)
10. Pendse, C.G.: The Makran earthquake of the 28th November 1945. India Meteorol. Dept. Sci. Notes **10**, 141–145 (1948)
11. Carayannis, G.P.: Potential of tsunami generation along the Makran subduction zone in the northern Arabian Sea, case study: the earthquake and tsunami of November 28, 1945. Sci. Tsunami Hazard. **24**, 358–384 (2006)
12. Romstad, B., Harbitz, C.B., Domaas, U.: A GIS method for assessment of rock slide tsunami hazard in all Norwegian lakes and reservoirs. Nat. Hazards Earth Syst. Sci. **9**, 353–364 (2009)
13. Volker, D.J.: A simple and efficient GIS tool for volume calculations of submarine landslides. Geo-Mar. Lett. **30**(5), 541–547 (2010)
14. Sinaga, T.P.T., Adhi, N., Lee, Y.-W., Suh, Y.: GIS mapping of tsunami vulnerability: case study of the Jembrana Regency in Bali, Indonesia. KSCE J. Civ. Eng. **15**(3), 537–543 (2011)
15. Wegscheider, S., Post, J., Zoosseder, K., Muck, M., Strunz, G., Riedlinger, T., Muhari, A., Anwar, H.Z.: Generating tsunami risk knowledge at community level as a base for planning and implementation of risk reduction strategies. Nat. Hazards Earth Syst. Sci. **11**, 249–258 (2011). https://doi.org/10.5194/nhess-11-249-2011
16. Theilen-Willige, B.: Tsunami hazard assessment in the Northern Aegean Sea. Sci. Tsunami Hazards **27**(1), 1–16 (2008)
17. Strunz, G., Post, J., Zosseder, K., Wegscheider, S., Muck, M., Riedlinger, T., Meli, H., Dech, S., Birkman, J., Gebert, N., Harjono, H., Anwar, H.Z., Sumaryono, Khomarudin, R.M., Muhari, A.: Tsunami risk assessment in Indonesia. Nat. Hazards Earth Syst. Sci. **11**, 67–82 (2011)
18. Sirikulchayanon, P., Sun, W., Oyana, T.J.: Assessing the impact of the 2004 tsunami on mangroves using remote sensing and GIS techniques. IJRS **29**(12), 3553–3576 (2008)
19. Kumar, T.S., Kumar, C.P., Nayak, S.: Performance of the Indian tsunami early warning system. Int. Arch. Photogramm. Remote Sens. Spat. Inf. Sci. **38**(Part 8), 271–274 (2010)
20. Imamura, F., Yalciner, A.C., Ozyurt, G.: Tsunami modeling manual. In: UNESCO Tsunami Modeling Course, UNESCO (2006)
21. Imamura, F.: Review of tsunami simulation with a finite difference method. In: Yeh, H., Liu, P., Synolakis, C. (eds.) Long-Wave Run-Up Models, pp. 25–42. World Scientific (1996)
22. Witham, G. B.: Linear and Non Linear Waves. Wiley Inter Science Publications (1974)
23. Yalçiner, A., Pelinovsky, E., Talipova, T., Kurkin, A., Kozelkov, A., Zaitsev, A.; Tsunamis in the Black Sea: comparison of the historical, instrumental, and numerical data. J. Geophys. Res Oceans. **109**(C12), (2004)
24. Mansinha, L., Smilie, D.E.: The displacements fields of inclined faults. Bull. Seismol. Soc. Am. **61**(5), 1433–1440 (1971)

Chapter 64
Study on Sustainable Management of Groundwater Resources in Greater Visakhapatnam Municipal Corporation, Visakhapatnam District, India—A Hydro Informatics Approach

Dadi Sanyasi Naidu and Peddada Jagadeeswara Rao

Abstract The growing urbanization and industrialization are the major sources for polluting water sources. As a result, surface and groundwater resources are unsuitable for domestic and industrial and agricultural purposes. The study area, the Greater Visakhapatnam Municipal Corporation (GVMC) is the largest municipal corporation in the state of Andhra Pradesh, India. It is covering an area of 545 km^2 bounded by Bay of Bengal, Kailasagiri and YaradaKonda. A systematic delineation of groundwater potential zones using modern techniques is essential for proper utilization and management of this precious natural resource. In this study SOI, IRS-1D and SRTM satellite data have been used to delineate thematic maps such as drainage, soil, geomorphology, geology, lineament, land use/land cover, and slope. Besides quantity of groundwater resources has been assessed using GEC Norms-1997 based on Novel the proposed Hydro Spatial Analysis Information System (HAIS) model. A comparative analysis was conducted on various open GIS software's like Spatialite-GIS, QSWAT, OGR2OGR and GDAL.

Keywords Pattern recognition · GIS · Algorithms · Disaster management
Floods · Rescue · Risk

D. S. Naidu (✉) · P. J. Rao
Department of Geo-Engineering and Centre for Remote Sensing,
Andhra University College of Engineering, Visakhapatnam, India
e-mail: sndadi@gmail.com

P. J. Rao
e-mail: pjr_geoin@rediffmail.com

P. J. Rao et al. (eds.), *Proceedings of International Conference on Remote Sensing for Disaster Management*, Springer Series in Geomechanics and Geoengineering,
https://doi.org/10.1007/978-3-319-77276-9_64

1 Introduction

The Geographic Information Systems (GIS) have turned into a helpful and vital tool in hydrology and to hydrogeology in the logical study and administration of water resource [1]. Environmental change and water pollution are the major concern. GIS systems already were for the most part static in their geospatial representation of hydrologic components [2]. Hydroinformatics is a branch of informatics which focuses on the utilization of Information and Communications Technologies (ICTs) in tending to the undeniably major issues of the impartial and effective utilization of water for various purposes [3]. The proposed Hydrospatial Analysis Information System (HAIS) gives a comprehension of groundwater distribution and quantity; weather conditions are improving or more terrible after some time; and how regular components and human exercises influence those conditions. Observing information are coordinated with geographic data on hydrological attributes, arrive utilize, and other landscape includes in models to stretch out water-quantity comprehension to unmonitored regions. With a clear user interface (UI) and an attention on visualizing information sources of info and yields, HAIS recognizes groundwater quantity and spatial distribution conditions and streamlines the way to a rundown appraisal. The gathered information might be put away in a wide range of routes, going from Excel spreadsheets through to complex social databases. Be that as it may, it is frequently hard to get to the required data without the help of a database master.

The rest of this paper is organized as follows. Section 3 discusses HAIS schematic diagrams and algorithmic approach. Section 4 describes the simulations and comparative analysis of various open source GIS software's. Lastly, the paper was concluded with future works in Sect. 5.

2 Related Works

The Open source extends normally are chipped away at by a group of volunteer software engineers. Open source GIS programs depend on various base programming dialects. SpatiaLite is an open source library expected to stretch out the SQLite center to help completely fledged Spatial SQL capacities [4]. Then the QSWAT by running QSWATinstall1.3.exe or a later form. This includes a few documents to the SWATEditor: a task database and a reference database in Databases, SWATGraph in the SWATGraphfolder, and furthermore stores the TauDEM executable in another Catalog [5]. The OGR toolbox is a sub unit of the Frank Warmerdam (FW) Tools Toolkit The Frank Warmerdam (FW) Tools Toolkit is a toolbox accessible in both Linux furthermore, Windows executable frame and also source code shape [6]. GDAL is an interpreter library for raster and vector geospatial information designs that is discharged under an X/MIT style Open Source permit by the Open Source Geospatial Foundation. As a library, it shows a solitary raster conceptual information model and single vector dynamic information model to the calling application for every bolstered design [7]. The HAIS architecture and working procedure discussed in the next section.

3 Hydro Spatial Analysis Information System (HAIS)

3.1 System Design

This section describes various activities and class diagrams for the designation of the HAIS. System design is the process of defining the architecture, components, modules, interfaces, and data for a system to satisfy specified requirements.

The HAIS is classified manly into four classes. All four classes uses the all the packages. In addition DisplayShapeFile method uses additional package called SharpMap for displaying data on the output screen or user interface. Figure 1 shows the level-2 use case diagram of the entire system. Whereas the class diagram. The interconnection between each class was clearly demonstrated in Fig. 2 and Table 1 describes the functionalities of each specific class.

3.2 Algorithms of Modules

3.2.1 Algorithm for Create Database, Tables and Load ShapeFile, Raster Data into SQL Server

Step 1: Use CREATE DATABASE command with name—HydroGeomorphology‖
Step 2: Use ALTER DATABASE command to modify database default values
Step 3: Use CREATE TABLE command to load Shapefile, Raster Data
Step 4: Load the ShapeFile into table created using—Shape2Sql‖ tool

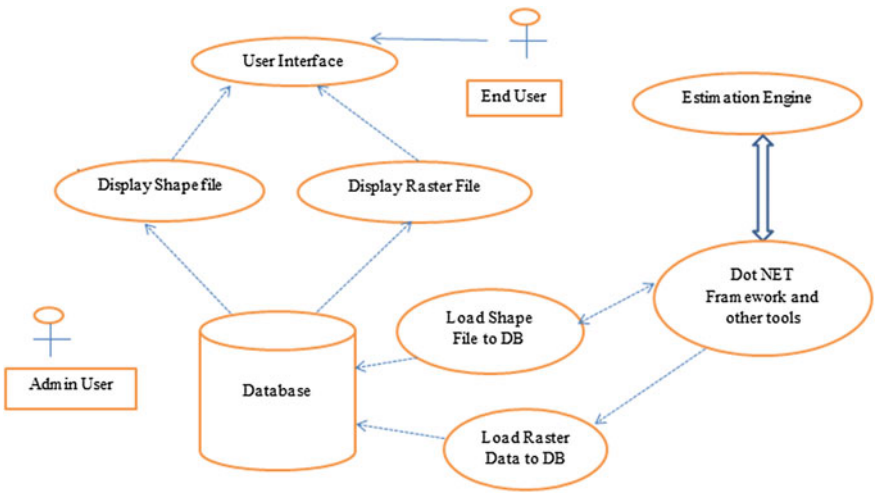

Fig. 1 Level-2 use case diagram of the system

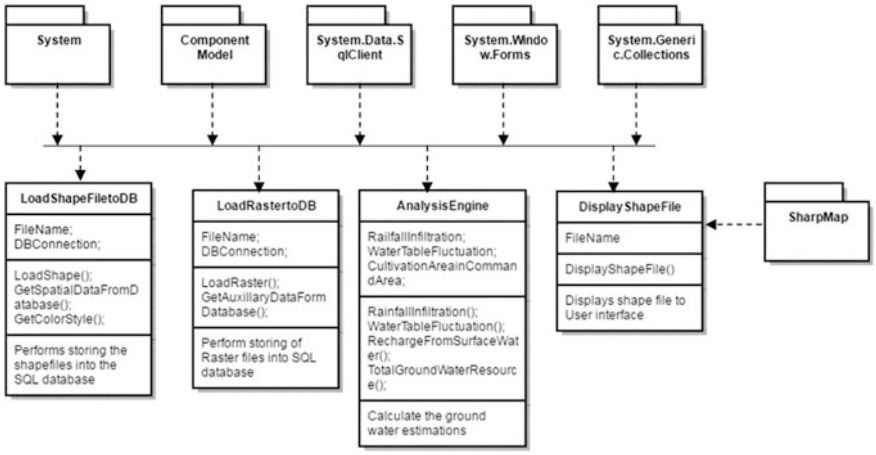

Fig. 2 Class diagram of HAIS

Table 1 Functionalities of the each class of HAIS

S. no	Class name	Functionality
1	LoadShapeFileDB	It stores the shapefiles into the SQL database
2	LoadRastertoDB	It performs storing of Raster files into SQL database
3	AnalysisEngine	It computes all groundwater estimations
4	DisplayShapeFile	It generates user interface window for the end user for the roundwater estimation results

Step 5: Use Update command (SQL) to clean the geom column in above loaded table with MakeValid and STIsValid function
Step 6: Load Raster Data using SQL server Import/Export Wizard.

3.2.2 Algorithm for Display Images and Maps on User Interface Screen

Step 1: Declare an object to connect SQL server.
Step 2: Declare SharpMap.Map object
Step 3: Declare SharpMap.VectorLayer object
Step 4: Set the following properties values to VectorLayer
Database connection string
Database Table Name
Column Name
Step 5: Add the above VectorLayer to Map Declared in the Step 4
Step 6: Declare PictureBox control on User Interface.

Step 7: Set the Map to PictureBox crated in Step 6.
Step 8: Declare DataGrid to display data for Shapefile.
Step 9: Get the Data from Database and set result Dataset to DataGrid Defined in Step 8
Step 10: Declare DataGrid to display data for Raster File.
Step 11: Get the Raster Data from Database and set result Dataset to DataGrid Defined in Step 10.

3.2.3 Algorithm for Groundwater Estimation

Step 1: Provide groundwater estimation Input file
Step 2: Execute the GroundWaterEstimationAnalysisEngine, it will give the following results
Step 2.1: Recharge In Command area Monsoon season
Step 2.2: Recharge from rainfall
Step 2.2.1: Rainfall infiltration method (I)
Step 2.2.2: Water table fluctuation method (W)
Step 2.2.3: PD expressed as percentage (I)
Step 2.2.4: Recharge considered when PD = >(−) 20% and <(+)20% = 32.446 Ha.m
Step 3: Recharge from other sources
Step 3.1: Recharge from surface water
Step 3.1.1: Recharge from tanks
Step 3.1.2: Total groundwater resource
Step 3.1.3: Net annual groundwater available
Step 4: Recharge In Command area Non Monsoon season
Step 4.1: Recharge from rainfall
Step 4.1.1: Rainfall infiltration method (I)
Step 4.1.2: Water table fluctuation method (W)
Step 4.1.3: PD expressed as percentage (I)
Step 4.1.4: Recharge considered when PD = >(−) 20% and <(+)20% = 32.446 Ha.m.

4 Simulation and Results Analysis

The HAIS were divided into three modules in the examination stage that were appeared in the utilization case level-1 diagram. Usage is the most significant stage in accomplishing a framework and giving the client's certainty that the new framework is compelling and helpful. Execution of another application to supplant a current framework assumes essential part. The entire system is developed using WinForms as front end as 199 well as RDBMS- MS-SQL Server 2012 is a back end of the system. Middle tier is developed using C# DOT NET frame work 4.5 for

communicate between front end and back end. It plays a crucial role in detection of groundwater levels in specific zones. Whole program is tried exclusively at the season of improvement utilizing the information base and has checked that this program connected together in the path indicated in the projects determination, the framework and its surroundings is tried as per the general inclination of the client in recognizing of groundwater potential zones. On the off chance that the picture demonstrates blue shading then that is spoken to as water body around there. Something else that shows red shading, then it can treat that is lesswater levels. A basic working methodology is incorporated so that the client can comprehend the diverse capacities obviously and rapidly. At first as an initial step the executable type of the application is to be made and stacked in the normal server machine which is available to the whole clients and the server is to be associated with a system. The last stage is to record the entire framework which gives segments and the working methodology of the shape documents from client necessities. This framework ought to be evaluated quantity and amount of groundwater in chosen region; furthermore it indicates groundwater potential zones (Fig. 3).

Figure 4 shows result window of Monsoon and Non-Monsoon season, but both consists of water sources form rainfall and other sources. Rain fall filtration button- It shows Pre-filtration is the filtration that takes place prior to water entering the tank. These are typically gravity fed filter systems. Prefiltration is typically the only filtration required when using the collected rainwater for irrigation. Post-filtration is the filtration that takes place after the collected rainwater has left the tank. Post-filtration systems are typically a pressurized system that filters to a much lower number of microns than typical pre-filters. Post sediment filtration and disinfection is usually required anytime the water will be used for indoor use such as flushing toilets, washing clothes, or shower usage. Water table fluctuation: The water-level rise DH(tj) is estimated as the difference between the peak of a water-level rise and the value of the extrapolated antecedent recession curve at the time of the peak. The recession curve is the trace that the well hydrograph would have followed had there not been any recharge. Extrapolation of the recession curve is not always straightforward. At least two approaches can be used to estimate DH(tj) in the WTF method: graphical extrapolation and calculation from a master recession curve (MRC). Finally it calculates total groundwater resource and net annual groundwater

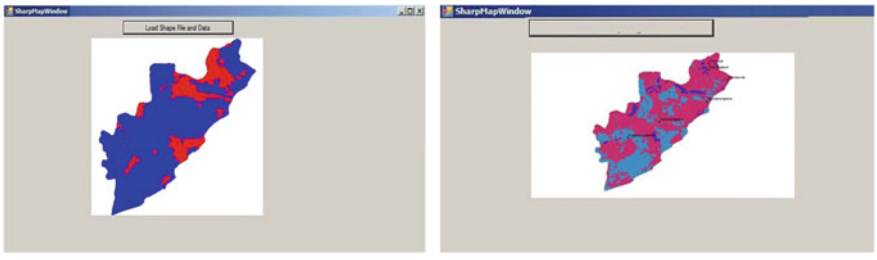

Fig. 3 Shape files loaded from database

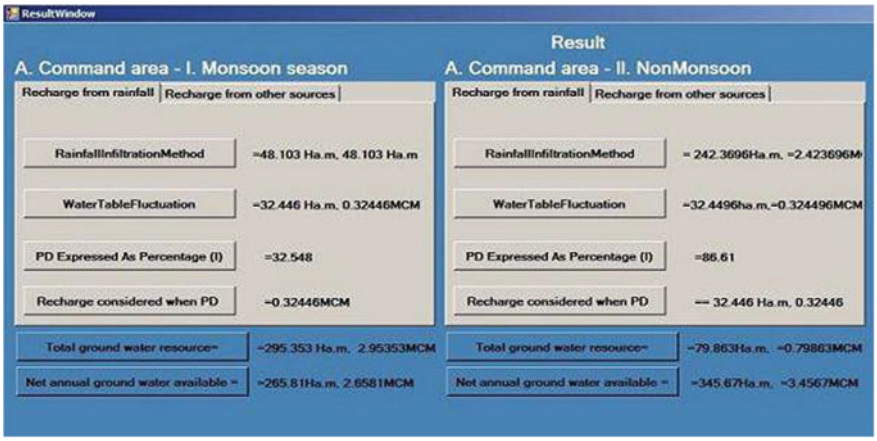

Fig. 4 Screenshot of the command area recharge from rainfall

available in monsoon and non-monsoon seasons. And it calculates total annual recharge in study area as well as calculation of population for 2021 and 2031. That is completely depending upon user requirements and groundwater availability.

4.1 Comparative Study on Groundwater Sources Tools Memory Sizes

Hydro Spatial Analysis Information System (HAIS) is efficient analysis software for spatial distribution and quantity assessment of groundwater. When comparing to remain software tools, it is accurate and fast process time software. HAIS occupies less memory and limited functionalities to compute the water quantity also. But HAIS supports more number of databases without change of source code (Fig. 5).

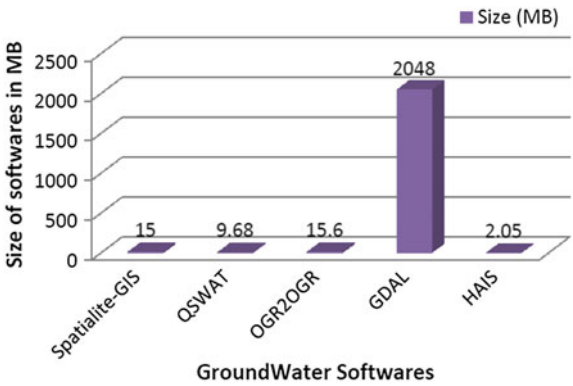

Fig. 5 Various groundwater sources tools memory sizes

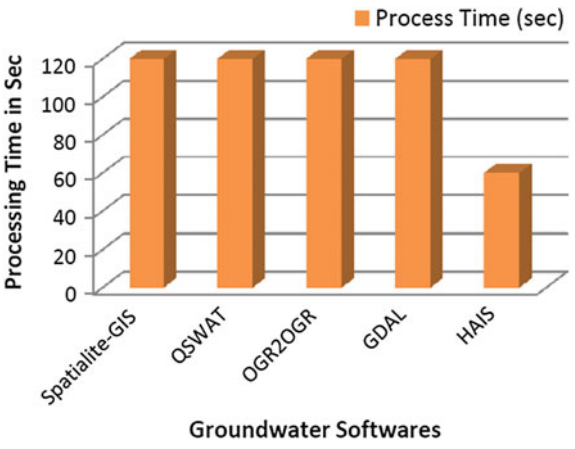

Fig. 6 Various groundwater software process time in seconds

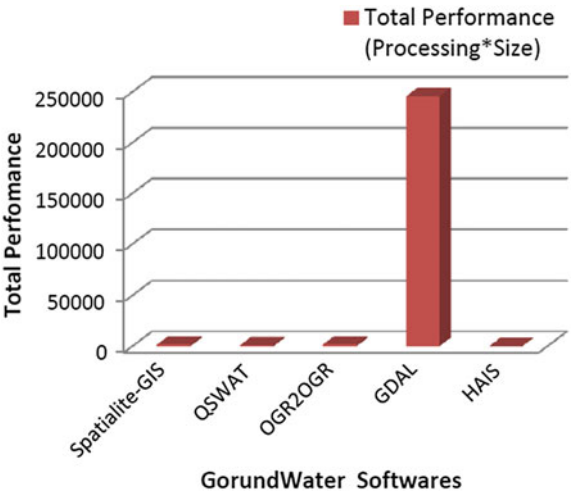

Fig. 7 Various groundwater total performances

Figure 6 describes software process time in seconds in Groundwater software tools. Most probably the above four software tools processing time is same. But HAIS shows outstanding processing time when compared to remaining all software tools. Processing speed of HAIS is less than or equal to 50 s.

Figure 7 refers groundwater total performance level based on processing time and memory occupation. GDAL shows bad performance when comparing to remain software tools. But HAIS describes good performance level in all software tools. Every customer or user should be depending upon performance levels. Therefore HAIS must be fulfilling user desires in short span of time (Table 2).

Table 2 HAIS tool total performance comparison with other tools

Groundwater estimation software name	Process time (s)	Size (MB)	Total performance (processing * size) in units
Spatialite-GIS	120	15	1800
QSWAT	120	9.68	1161.6
OGR2OGR	120	15.6	1872
GDAL	120	2048	245,760
HAIS	60	2.05	123

5 Conclusions and Future Scope

The growing urbanization and industrialization are the major sources for polluting water sources. As a result, surface and groundwater resources are unsuitable for domestic and industrial and agricultural purposes. The study area, the Greater Visakhapatnam Municipal Corporation (GVMC) is the largest municipal corporation in the state of Andhra Pradesh, India. It is covering an area of 545 km^2 bounded by Bay of Bengal, Kailasagiri and YaradaKonda. A systematic delineation of groundwater potential zones using modern techniques is essential for proper utilization and management of this precious natural resource. In this study SOI, IRS-1D and SRTM satellite data have been used to delineate thematic maps such as drainage, soil, geomorphology, geology, lineament, land use/land cover, and slope. Besides quantity of groundwater resources has been assessed using GEC Norms-1997 based on Novel The proposed Hydro Spatial Analysis Information System (HAIS) model 221. The HAIS provides an easy understanding of water-quantity analysis. This software is bifurcated into two modules; they are (i) User Interface and (ii) Processing unit. The User interface displaying the geographical map for the users. The processing unit will perform all background computations that are required for the groundwater estimations. The HAIS application is related to the Hydroinformatics application with respect to the spatial coordinates. HAIS helps in researchers and practitioners in reduction of computation time for the spatial water quantity analysis. The HAIS application was tested successfully and all results are accurate with geographical maps. At present the HAIS is limited to the desktop application.

References

1. Pourtaghi, Z.S., Pourghasemi, H.R.: GIS-based groundwater spring potential assessment and mapping in the Birjand Township, southern Khorasan Province. Iran. Hydrogeol. J. **22**(3), 643 (2014)
2. Crestaz, E., Habashi, N., Ambrosini, P., Schätzl, P., Gibin, M.: Advancements in concurrent native spatial database technology for groundwater monitoring and modeling applications. A case study aimed at PostgreSQL-PostGIS coupling with GIS and Feflow. In: Proceedings of MODFLOW and More 2015 International Conference, 31 May–3 June 2015

3. Lee, Y., Kim, H.S., Chun, G.: Introduction of drought monitoring and forecasting system based on real-time water information using ICT. In: AGU Fall Meeting Abstracts, Feb 2016
4. Egenhofer, M.J.: Spatial SQL: a query and presentation language. IEEE Trans. Knowl. Data Eng. **6**(1), 86–95 (1994)
5. Bansode, S., Patil, K.: Water balance assessment using Q-SWAT. Int. J. Eng. Res. **5**, 515–518 (2016)
6. van den Eijnden, B., Syncera, I.T.: De Open Source GIS wereld
7. Neteler, M., Bowman, M.H., Landa, M., Metz, M.: GRASS GIS: a multi-purpose open source GIS. Environ. Model. Softw. **31**, 124–130 (2012)

Chapter 65
Disaster Management Emergency Responsive Mechanism Using GIS and Networking with Android Technology

Gadi Hari Krishna, Veeturi Sarath Chandra, Suribabu Boyidi, Gummapu Jaisankar, Ch. Anusha, Bendalam Sridhar, Nathi Anil, Ustala Sailaja, K. Mehar Ganesh, B. Ravi Kumar, T. Sridevi, L. V. V. S. Narayana Narayanam and Killana Dileep

Abstract Emergencies, post disasters which are very crucial in times and require quick actions. In cities and towns where the population is very high and the traffic is a day to day issue, We have come across many incidents where the ambulance got stuck in the traffic and ultimately resulted in the death of the victim. So the basic solution for this problem is to reach the victim's basic location and his/her state of condition to the emergency service providers as soon as possible and the emergency

G. Hari Krishna (✉) · V. Sarath Chandra · S. Boyidi · G. Jaisankar
C. Anusha · B. Sridhar · U. Sailaja · B. Ravi Kumar · T. Sridevi
L. V. V. S. Narayana Narayanam · K. Dileep
Department of Geo-Engineering, Andhra University, Visakhapatnam, INDIA
e-mail: gadiharikrishna@gmail.com

V. Sarath Chandra
e-mail: ssarath524@gmail.com

S. Boyidi
e-mail: suri.sri2008@gmail.com

G. Jaisankar
e-mail: jaisankar.gummapu@yahoo.com

C. Anusha
e-mail: anu4goal@gmail.com

B. Sridhar
e-mail: sridhar.bendalam@gmail.com

U. Sailaja
e-mail: sailaja.ustala@gmail.com

B. Ravi Kumar
e-mail: bravikumar.rkb@gmail.com

P. J. Rao et al. (eds.), *Proceedings of International Conference on Remote Sensing for Disaster Management*, Springer Series in Geomechanics and Geoengineering,
https://doi.org/10.1007/978-3-319-77276-9_65

vehicles such as Ambulances or Fire engines has to reach the victim as quickly as possible. So, some kind of new mechanism has to be developed in order to overcome this problem with the help of technology. This technology has to be common and widely used to reach large mass. The basic technology used by every individual these days is a Smartphone and the internet. On this ground truths an android application named "DIGI SURAKSH" has been developed. This app if installed on an android device will be to able to locate the nearest ambulances and can even send a request to the nearest ambulance. The ambulance driver who also has an android device installed with the driver version of this app gets notified on the request of victim or victim's attendee and when the request is accepted by driver, a shortest and fastest route to the requested location by the user is displayed on the map in his android device. So, an android app with GIS technology as backbone and making use of android and computer networking serves us the solution. The pieces of technologies that are to be combined together to get the outcome are ArcGIS runtime SDK version 100.1.0, Android Studio 2.3.3 and the Android build tools 26.0.1 which works on the devices with SDK versions 21 and above which means all the post lollipop devices support this application. The database used is NOSQL database, Firebase by Google.

Keywords Android app · Disaster monitoring · Online GIS · GPS Technology · Base map · Firebase · ArcGIS

1 Introduction

The word 'emergency' originated from Latin word 'emerge' which means 'arise, bring to light'. Oxford dictionary defines emergency as "serious, unexpected, and often dangerous situation requiring immediate action. According to Wikipedia,

T. Sridevi
e-mail: srice2001@gmail.com

L. V. V. S.Narayana Narayanam
e-mail: mimesatish@gmail.com

K. Dileep
e-mail: dileepkillana@gmail.com

N. Anil
Sanketika Institute of Technology, Visakhapatnam, INDIA
e-mail: nathianil@gmail.com

K. Mehar Ganesh
SRKR Engineering College, Bhimavaram, INDIA
e-mail: meharganesh.k6@gmail.com

"**emergency**" is a situation that poses an immediate risk to heath, life, property, or environment: [4, 5] Most emergencies require urgent intervention to prevent a worsening of the situation, although in some situations, mitigation may not be possible and agencies may only be able to offer palliative care for the aftermath. Any situation of emergency arises directly or indirectly through a hazard. Hazards can be dormant or potential which is an agent that has the potential to cause harm to a vulnerable target. An event that is caused by interaction with a hazard is called an incident. The risk associated with an incident depends upon the consequences of the hazard. If there is no possibility of a hazard contributing towards an incident, there is no risk.

2 Different Types of Emergencies Post Disasters

1. Medical Emergencies, 2. Fire Emergencies, 3. Security Emergencies: The purpose of any Emergency Department is to save lives. An emergency is any medical problem that could cause death or permanent injury if not treated quickly. Severe pain in some instances can also be a medical emergency, such as the pain associated with kidney stones or appendicitis and heart strokes [2] (Table 1).

Table 1 Previous database of disaster

Year	No. of accidents		No. of persons		Accidental severity
	Total	Fatal	Killed	Injured	
2007	40,749	73,650	84,647	408,711	20.8
2008	406,726	73,589	85,998	435,122	21.1
2009	429,910	79,357	92,618	464,521	21.5
2010	43,925	83,491	94,968	465,282	21.6
2011	460,920	93,917	105,749	496,481	22.9
2012	479,216	101,161	114,444	513,304	23.9
2013	484,704	106,591	119,860	523,193	24.7
2014	486,384	110,993	125,680	515,458	25.8
2015	499,628	119,558	134,513	527,512	26.9
2016	497,686	121,618	142,854	511,394	28.6

Source Information supplied by states/UTs police department accidental severity: number of persons killed per 100 accidents

3 Methodology

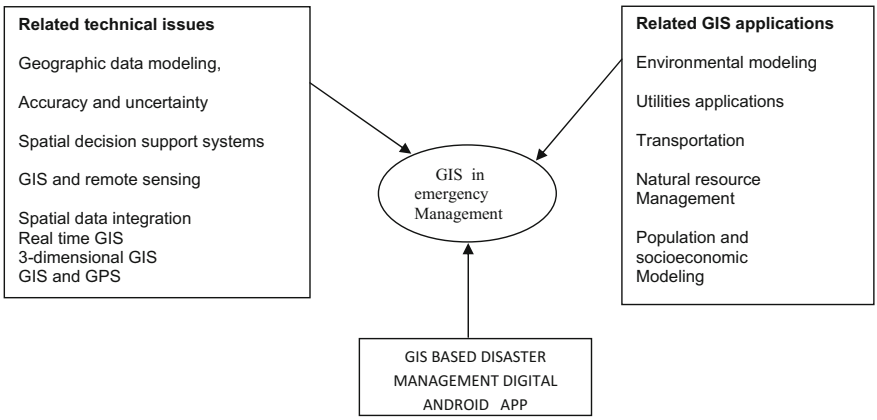

4 Current Emergency Services Trends in India

It is terms like 'The Golden Hour' and the 'Platinum Ten Minutes' that epitomize the significance of Emergency Medical Services (EMS) everywhere throughout the world. A patient who gets fundamental care from prepared experts and is transported to the closest social insurance office inside 15–20 min of a crisis has the best shot of survival. EMS is a fundamental piece of the general human services framework as it spares lives by giving consideration quickly. It's this acknowledgment that has prompted innovative work in EMS [3]. Throughout the years a few headways have been made and examine is in progress to make benefits that give therapeutic help to patients at the most punctual. Be that as it may, the territory of EMS differs radically from created to creating nations like India. Despite the advancement in the human services segment over the previous decade, India is yet to make a solitary, complete EMS that can be gotten to all through the nation as compared to developed countries with proper emergency systems in place, there is no single system which could play a major role in managing emergency medical services in India. There is a fragmented system in place to attend the emergencies in the country. 102 is the emergency telephone number for ambulance in parts of India (5). There are different emergency numbers in India's 29 states and seven Union Territories. Hospitals in the country provide different telephone numbers for ambulance services. Clearly, India is in need for proper emergency medical service that can be accessed from anywhere in the country. The existing fragmented system falls terribly short of meeting the demand.

Trauma continues to be one of the major causes of death in India. To avoid preventable deaths and disabilities, India has planned to have a common effective system that could provide emergency care with equity of access. In a bid to address this problem, The Centralized Accidents and Trauma Services (CATS) was set up by the Delhi Government in the early 1990s. This service was later expanded throughout the country. Unfortunately, it didn't succeed despite having a toll free number (102) that was made available through various media. More recently, NGOs and hospitals have come forward to provide their own EMSs. There have been considerable efforts by states across India to develop emergency services. Organizations like Emergency Management and Research Institute (EMRI) and American Association of Physicians of Indian Origin (AAPI)'s EMS are banned by corporate. EMRI is an exception in the otherwise struggling EMS system.

EMRI was established in 2005. In any case, its operations were restricted to Hyderabad and Andhra Pradesh with a dream of reacting to 30 million crises and sparing 1 million lives per year. EMRI handles medicinal, police and fire crises through its 108 crisis benefit. Satyam is the innovation accomplice of EMRI. EMRI has additionally gone into PPP with Indian Emergency Number Authority, National Emergency Number Association, American Association of Physicians of Indian Origin (AAPI), Shock Trauma Center, Stanford University USA, Singapore Health Services, City of Austin in Texas, USA and Government of AP. EMRI likewise includes an exploration foundation, which does medicinal research, frameworks research and operations examine. Through this, EMRI gives look into papers to aversion and administration of crises. EMRI's different administrations incorporate free therapeutic counsel on telephone on another toll free number 104 with access to more than 200 restorative specialists and a few more paramedics. It has gone into an association with Stanford Hospital, the School of Medicine for preparing 150 paramedics and 30 paramedic educators over a two-year time span in India. In spite of the fact that a positive, this is probably not going to take care of the demand for paramedics in the nation. "So far neither of these two administrations in Mumbai (AAPI) or Hyderabad (EMRI) have the sort of HR and gigantic preparing software engineers required", agrees Dr. N. Bhaskara Rao, Chairman, Center for Media Studies, New Delhi. In 2007, with the expansion of Ambulance Access for All (AAA's) administrations, American Association of Physicians of Indian Origin (AAPI) established Emergency Medical Service (EMS) for Mumbai. AAPI has teamed up with the Confederation of Indian Industries (CII) and marked a MOU to embrace the development of the medicinal services segment in India, particularly in rustic territories. This assertion is to give information and innovation exchange and give EMSs to create human services offices in India. Another such office, Life Support Ambulance Service (LSAS) working in Mumbai for a long time in relationship with London Ambulance Service, UK, has now made advances into Kerala and has 500 ambulances that can be come to on a toll free number 1298. Recently, the Gujarat state government set up the Gujarat Emergency Medical Services Authority (GEMSA). Establishment of Kidney Diseases and Research Center

(IKDRC), U.N. Mehta Institute of Cardiology and Research Center, Gujarat Cancer Research Institute (GCRI), EMRI and Public Health Institute, Gandhinagar have gone into a few other PPP undertakings to enhance the crisis benefits in the state.

5 GIS Application in Emergency Services

An essential advance in looking at the part of GIS in crisis administration is choosing a calculated structure to help sort out existing innovative work exercises. One such system that shows up broadly in crisis administration writing is "thorough crisis administration" (CEM) (Drabek and Hoetmer 1991) [2]. This depends on the fleeting measurement of debacles and recuperation. Moderation includes moves that are made to wipe out or decrease the level of long haul hazard to human life and property from risks. Readiness is worried about moves that are made ahead of time of a crisis to create operational abilities and encourage a successful reaction to and crisis the reaction stage includes moves that are made. Quickly some time recently, amid, or specifically after a crisis happens, to spare lives, limit harm to property, and improve the adequacy of recuperation. The recuperation stage is portrayed by action to return life to ordinary or enhanced levels. In inspecting the GIS writing, maybe it is more fitting to decrease the four periods of complete crisis administration into three stages: moderation, readiness and reaction, and recuperation. This is just in light of the fact that many, GIS created in the readiness stage are used in the reaction stage. As such, frameworks intended to enable crisis directors to react to a real debacle are every now and again used to prepare crisis work force and create readiness designs. From a GIS point of view, this serves to obscure the readiness and reaction stages into a solitary stage. In any case, GIS applications in the periods of alleviation (e.g. chance mapping) and recuperation (e.g. harm evaluation) are obviously unmistakable from the proposed combined readiness and reaction stages [1].

6 Software Approach to Emergency Services

GIS sciences can be used to improvise the existing emergency service providing methods. Along with GIS, Android technology has to be integrated with it to reach every single person. As android is the mostly used mobile operating system through out the world. Arcgis 10.4.1 serves the purpose of creating maps for an area. All the datasets has to be created and the network analysis has to be done.

7 Analysis using Android Technology

Topology: Make individual geo database (Network) in this database and make the new component dataset. These element dataset is foreign made to the street curve shape record, right snap highlight dataset select the new topology and tap on every next catch, tick stamp out and about shape document and snap next catch in this include two guidelines they are (1) Must not cover and (2) must be single part. These guidelines are included at that point fabricate the topology is constructed. Begin the topology and amend all line blunder, hub mistakes at that point end the topology, spare the topology and close ARC GIS before the system is assembled the topology might be erased Right snap include dataset and select new system dataset. Snap to every single next catch at that point construct the system dataset. After the system is manufactured the layer is taken into Mxd.

Creating the Network Data set: Start the ARC Catalog and create a personal geodetic base. In this data base create the feature dataset these feature dataset import to the feature class give a file name (road shape file name, these road shape file must be apply to the clean and topology) and give output file name. Select the feature dataset and right click new network dataset then build the network dataset. Select the network dataset properties go to direction and click direction and apply properties to the following

The Network Attribute: Network attributes are properties of the network elements that control reversibility over the network. Examples of attributes include the time to travel a given length of road, which streets are restricted for which vehicles, the speeds along a given road, and which streets are one-way. Network attributes have five basic properties: name, usage type, units, data type, and use by default. Additionally, they have a set of assignments defining the values for the elements. Network attributes are created either in the New Network Dataset Wizard (when defining a new network) or on the Network Dataset properties dialog box on the attributes tab.

Directions: Directions can be displayed in Arc Map after the generation of a route in route analysis and closest facility analysis to display directions, on the Network Analyst toolbar; click the Directions A Sample from the Arc GIS map showing the route from the victim's current location to the Emergency service provider (Ambulance in this case). The blue marker indicates the current location of the user.

Window button. The Directions Window displays turn-by-turn directions and maps with the impedance. If the impedance was set to time, the Directions window displays the time taken for each segment of the route. Additionally the Directions window can display the length of each segment. If the route supports time windows, the Directions window displays the Attar_[time] and Wait_[time] attributes. However, the violation_[time] and Attar_[length] attributes are not supported (Fig. 1).

Network layer contains 3 properties they are (a) stops (2) barriers (3) route, In the Network Analyst window, right click stops and click load locations click

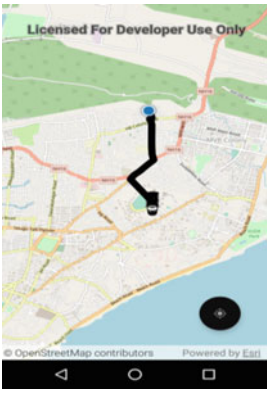

A Sample from the Arc GIS map showing the route from the victim's current location to the Emergency service provider (Ambulance in this case). The blue marker indicates the current location of the user.

Fig. 1 Android app location identification image

browse button and choose a point feature class. In the table of contents, right-click the Route layer and click properties. Click the Analysis Settings tab set the route properties to be used in the analysis if you want to set properties for the directions, click the Directions tab.

Android's Role: The Android studio with the version 2.3.3 and with the build tools 26.1.0 has been utilized in the working model. Application package index (Api) provided ESRI's ArcGIS runtime sdk with version 100.1.0 for the network analysis and the display of baseman and even the location services of the user and the routing services in the runtime. The exchange of spatial data between the victim and the emergency service provider is done through the NOSQL database by Google named Firebase and all the user's data such as phone number and other primary details are stored in the Firebase and can be retrieved anytime. The Android and the Arc GIS provided together facilities in displaying the different emergency provider's current location. The victim or a person in need of emergency service can open this app which is preinstalled and the app lands him to an activity showing him a map with a blue marker indicating his current location. On swiping the left navigation drawer or by clicking on the hamburger at the top left corner displays him a list view showing different Emergency service providers such as ambulance, Fire stations and Police patrolling vehicles. Based on the requirement of the user, selects an option from the list view. On selecting one of the options a layer gets added to the base map showing the nearby corresponding emergency service providers. For example if a user selects an ambulance service from the list view a layer with the nearby ambulances gets added to base map with a marker of an ambulance shape indicating the location of the ambulance. This location of the ambulance is updated in real time. On changing the location of the ambulance the new location gets updated in the database further resulting in the updating of the new location on the user's device as well as shown below (Fig. 2).

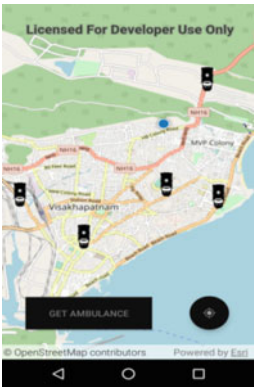

Map showing an ambulance layer added to the base map pointing the current location of the user and the ambulance markers indicating their corresponding real time locations.

Fig. 2 Android app corresponding real time application image

8 Results

Online Tracking of Vehicle with GPS: GPS (Global Positioning System) is a system of Earth-orbiting satellites, each providing precise time and position information which enables GPS receiving devices to compute position on the earth. Signals must be received from at least satellites in order to establish the receiver's position in latitude (or a national coordinate system provided with the equipment). GPS configuration consists of three parts: (1) Twenty-four HRS Navy satellite orbiting the earth. (2) Portable mobile receiver (aerial plus portable console). (3) Base station receiver positioned at a known geographical position, in order to perform the differential correction of the raw satellite signals.

Travel Routes with Alternative: When road network is affected by problem of Rain Accident, Heavy Traffic then Dynamic new road network can be generated and the updated alternative road network maps can be sent to all sub centers and primary health centers which makes it easy to travel any emergency service.

Online access to monitoring system: NET (Network Enable Technology/ Network Extended Technology) can be used to make the above module accessible to the implementation officers at hospitals who can run the network analysis by themselves and can fix the tentative calendars to cover the hospitals.

9 Conclusion

The DIGI SURAKSH for Monitoring of the Health & Emergency Services during disaster and the distance between the habitations and the respective hospitals. GIS aids in faster and better monitoring of health mapping and analysis than the conventional methods. It gives well being experts fast and simple access to expansive volumes of information. It gives an assortment of Dynamic investigation devices

and show systems for observing and administration of calamity. The potential outcomes that can be investigated are boundless, contingent upon the expertise and innovative utilization of the scientists and the readiness of well being division administration to asset its usage. Well being executives, experts and scientists require preparing and client in GIS innovation, information and epidemiological and disaster monitoring techniques in order to use GIS properly and effectively.

10 Proposals

This approach can be more extended in passing on information about the arrival and the travel of the ambulance to the traffic constable who is serving at any point on the route generated between the victim and the Emergency service provider. Another version of this application for the traffic police has to be created connecting the user's application, the emergency service provider's application and the traffic police men's application. There will be the spatial data exchange between these applications. By making use of this mechanism the traffic police man can be pre notified about the ambulance's arrival in that route and he can take necessary actions to take the traffic factor into control assuring the smooth travel of victim to the emergency service center.

In case of medical emergency, the hospitals require the victim's basic information. It is so mandatory that hospitals does not provide the medical services other than first aid to the victim without filling a form containing his basic details called an Out Patient Form (OP Form). There are many cases which lead to patient's death because of the delay in filling the out patient form. We can overcome this with a facility of providing the victim's details through the app that shows a list of nearby hospitals and selecting one among them. All the departments that are providing emergency services has to work on a single platform together for providing better services to the public.

References

1. Burrough, P.A.: Principals of Geographic Information System Land Resources Assements. Clarendom Press, Oxford, United Kingdom (1986)
2. http://www.Geog.Utah.Edu/∼Cova/Cova-Bb2-1999.Pdf
3. https://www.Asianhhm.Com/Healthcare-Management/Emergency-Services-India
4. https://En.Oxforddictionaries.Com/Definiton/Emergency
5. https://En.Wikipedia.Org/Wiki/Emergency

Chapter 66
Impact of Water Conservation Structures on Hydrology of a Watershed for Rural Development

Vinit Lambey, A. D. Prasad, Arpit Chouksey and Indrajeet Sahu

Abstract A watershed is an area of land from which all rain water drains to a common location. In their natural state, streams and their associated floodplains provide a variety of important functions including the movement of water and sediment, storage of flood waters, recharge of groundwater, treatment of pollutants, dynamic stability, and habitat diversity. Disturbances to this system, either natural or human-induced, places stress on the system and has the potential to alter structure and/or impair the ability of the stream to perform ecological functions. Water conservation structures are helpful in maintaining the desired flow requirement and sediment yield within the watershed area. In this study, Jonk River, a tributary of Mahanadi basin has been selected to assess the impact of conservation structures for disaster risk reduction, sustainable agriculture and rural development. The outlet of Jonk River is located near Rampur in Chhattisgarh. Total area of the watershed is computed as 3424 km^2. Soil and Water Assessment Tool (SWAT) has been used to calculate the discharge and sediment flow on daily and monthly basis for the year of 2001 considering two case scenarios i.e. with and without ponds as conservation structure (20 ponds in the villages are considered along the buffer area of the centreline of jonk river). The simulated discharge and sediment flow data has been compared with the observed data and the correlation coefficient is found to be 0.84 & 0.77 respectively. The annual discharge and sediment flow value in "with pond scenario" has been detected to be reduced by 69.27 and 64.10% respectively.

V. Lambey · A. D. Prasad (✉) · I. Sahu
Civil Engineering Department, National Institute of Technology Raipur, Raipur 492001, India
e-mail: adprasadiit@gmail.com

V. Lambey
e-mail: vinitlambey39@gmail.com

I. Sahu
e-mail: iamindraa14@gmail.com

A. Chouksey
Water Resources Department, Indian Institute of Remote Sensing, Dehradun 248001, India
e-mail: arpit@iirs.gov.in

P. J. Rao et al. (eds.), *Proceedings of International Conference on Remote Sensing for Disaster Management*, Springer Series in Geomechanics and Geoengineering,
https://doi.org/10.1007/978-3-319-77276-9_66

The results observed in the present work can be used for site suitability analysis of soil and water conservation structures in the areas those are prone to soil erosion and floods. The study also reveals that the applications of Geographic Information Systems (GIS) and Geospatial Data Management can be used efficiently for watershed management and rural development.

Keywords Watershed · SWAT · Sediment flow · Discharge · Geoinformatics

1 Introduction

Water is an essential element for survival of living things. It is vital for increasing growth of agriculture, industries and leads to rural development, economic development of the region. A watershed is comprised of land areas and channels and may have lakes, ponds or other water bodies. The flow of water on land areas occurs not only over the surface but also below it in the unsaturated zone and further below in the saturated zone [8] which can be enhanced by providing water conservation structures. This results in improvement of ground water level and can significantly contribute in development and management of rural areas. To deal with water management issues especially in rural areas, one must quantify the different elements of hydrologic processes taking place within the area of interests and analyse them. Geographic Information Systems (GIS) is a suitable tool for the efficient management of large and complex database and to provide a digital representation of watershed characteristics used in hydrological modelling. It has improved the efficiency of modelling process and ultimately increased the estimation capabilities of hydrological modelling [1].

Hydrological models coupled with geoinformatics such as MIKE-SHE, TOPMODEL, HEC-GeoHMS, VIC, WATFLOOD and SWAT, are capable of simulating spatio-temporal variations in hydrological processes. Many previous studies have demonstrated the ability of SWAT in detecting the impacts of land use and climate change on hydrological components in different areas [2, 4, 5, 7, 9]. SWAT model is physically based, efficient and capable of continuous simulation for a long period. Therefore, Soil and Water Assessment Tool (SWAT) model has been chosen to simulate or estimate the changes in runoff and sedimentyield over daily, monthly and annual timescales.

In the present study SWAT Model is used to assess the impact of small water conservation structures over discharge and sediment yield which helps in developing the part of rural areas which are affected by soil erosion and floods. Jonk watershed, which is a tributary of Mahanadi basin, has been selected as study area. The model has been run for two case scenarios i.e. watershed with pond as conservation structures and watershed without ponds or any conservation structure. The study has been carried out for the year 2001. However more emphasis was given to the monsoon season.

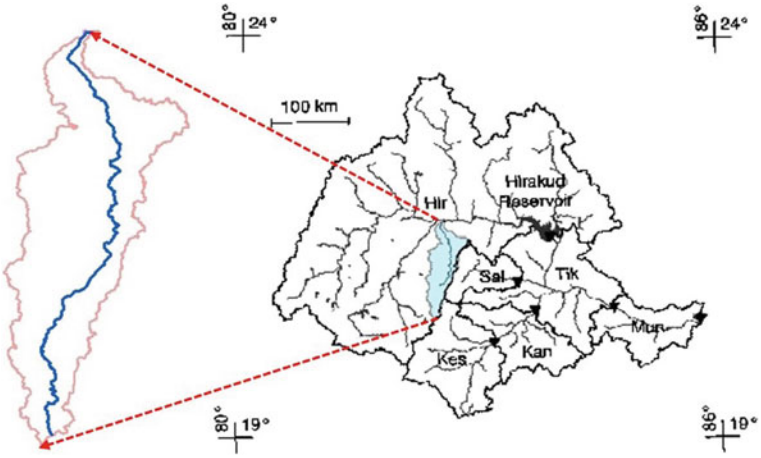

Fig. 1 Jonk watershed

2 Study Area

The Jonk watershed lies between geographic latitude 20° 28′ and 21° 44′N and longitudes 82° 20′ and 83° 00′E (Fig. 1). The river Jonk originates from Nuapada district of Orissa at an elevation of 700 m from MSL. It merges with Seorinarayan, upstream of Hirakud Dam after travelling the distance of 182 km having a drainage area of 3424 km^2.

The climate of the area is characterized by hot summer except during south-western monsoon. The watershed receives about 90% of the rainfall during monsoon which is active from middle of June to the end of September. Normal minimum temperature is 10 °C and maximum temperature is 43 °C (CWC). Geologically, the watershed consists of gneiss rock formation. The sub-basin comprises of alluvial formation of various thickness.

3 Materials and Methods

Soil and Water Assessment Tool (SWAT) is a semi-distributed, partially physically based, data driven model and requires several types of data such as rainfall, temperature, land use, soil, wind velocity, etc. [6]. Data has been collected from various sources and carried out post-processing processes on the datasets. The methodology of the study is presented in Fig. 2.

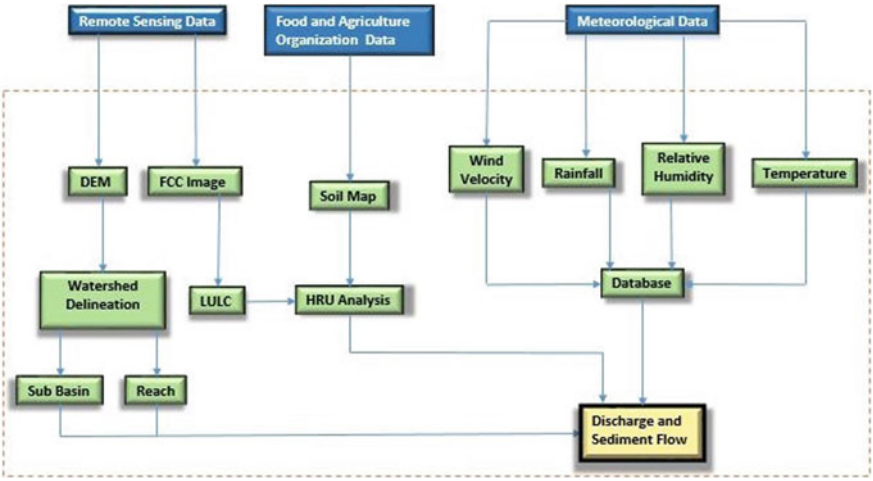

Fig. 2 Methodology for estimating discharge and sediment flow

3.1 Land Use Database

False color composite (FCC) image of Landsat 8 (dated: 9th Nov 2013) has been used for this study. The image was re-projected to UTM 44 N projection using ArcGIS software. The land use map has been derived using maximum likelihood method under supervised classification by using ERDAS Imagine software.

3.2 Soil Database

Soil dataset has been obtained from Food and Agriculture Organisation (FAO) [3]. The necessary input information required by the SWAT model was extracted from the same database for each soil type, namely soil texture, Hydrological Soil Group (HSG).

3.3 Weather Database

SWAT requires daily values for precipitation, maximum and minimum temperature, solar radiation, relative humidity and wind speed for modeling of various physical processes, soil and rainfall being the most important. Daily meteorological data was collected from India Meteorological Department (IMD).

3.4 SWAT Project

Advanced Spaceborne Thermal Emission and Reflection Radiometer (ASTER) Digital Elevation Map (DEM) of 30 m resolution has been used for this study. DEM was converted from geographic coordinate system to projected coordinate system (UTM, datum: WGS84). The processed DEM has been imported to SWAT project to start watershed delineation. After importing to SWAT project, streams are defined based on the drainage area threshold. The outlet for the whole watershed has been defined near Rampur for delineation of watershed boundary. The watershed sub basin parameters are calculated with locating the positions of the reservoirs. For each sub basin land use data and soil data are defined. As the runoff depends on the actual hydrologic conditions of each land cover and soil present in the watershed, therefore impact of each landuse is considered. Hydrologic response unit (HRU) is defined as 20% for landuse, slope and soil class for each sub basin. One of the main sets of input for simulating the watershed in SWAT is climate data. Climate inputs consist of precipitation, maximum and minimum temperature, solar radiation, wind speed and relative humidity. The daily precipitation records of 2001 were used which were analyzed to develop the climate-input files required for the model. After addition of all the above data, the SWAT model is set up and run on the basis of daily and monthly simulation. In this case study, the main emphasis is on the reduction of discharge and sediment flow in the Jonk watershed by addition of ponds as water conservation structures. In SWAT, runoff volume is estimated from daily rainfall using the modified SCS-CN (Curve Number Method) and Green-Ampt methods. The SCS-CN equation is:

$$Q_{surf} = \frac{(R_{day} - I_a)^2}{(R_{day} - I_a + S)} \tag{1}$$

where, Q_{surf} is accumulated runoff, R_{day} is rainfall depth for the day, I_a is the initial abstractions commonly taken as (0.2 * S), S is the retention parameter which is given as

$$S = \left(\frac{25{,}400}{CN}\right) - 245 \tag{2}$$

The discharge is calculated with the help of rational formula which is written as:

$$Q_{peak} = \frac{C * i * A}{3.6} \tag{3}$$

where, Q_{peak} is the peak runoff rate (m^3/s), i is the rainfall intensity (mm/hr), C is the runoff coefficient, A is area of the sub basin (km^2) and 3.6 is the unit conversion factor.

Similarly, the sediment flow is obtained from the Modified Universal Soil Loss Equation (MUSLE) which is given as:

$$\text{Sed} = 11.8 * \left(Q_{\text{surf}} * Q_{\text{peak}} * \text{area}_{\text{hru}}\right) 0.56 * \text{KUSLE} * \text{LSUSLE} * \text{CUSLE} * \text{PUSLE} * \text{CFRG} \quad (4)$$

where, Sed is the sediment yield on given day (metric tons), Q_{surf} is the surface runoff volume (mm/ha), Q_{peak} is the peak runoff rate (m^3/s), $area_{hru}$ is area of HRU (ha), KUSLE is the USLE soil erodibility factor, LSUSLE is the USLE topographic factor, CUSLE is USLE cover and management factor, PUSLE is USLE land practice factor, CFRG is coarse fragmentation factor.

Here, the SWAT model has been run for the total 20 ponds (Table 1) in the villages that fall in the buffered area of 2 km on both sides from the centre line of the river (Fig. 4).

Table 1 Location of ponds in villages

Name	Longitude (°E)	Latitude (°N)
Pond 1	82.65	21.14
Pond 2	82.64	21.43
Pond 3	82.61	21.44
Pond 4	82.57	21.56
Pond 5	82.60	21.51
Pond 6	82.65	21.36
Pond 7	82.66	21.28
Pond 8	82.61	21.24
Pond 9	82.62	21.08
Pond 10	82.61	20.99
Pond 11	82.58	21.00
Pond 12	82.49	20.90
Pond 13	82.46	20.82
Pond 14	82.46	20.81
Pond 15	82.41	20.75
Pond 16	82.43	20.75
Pond 17	82.51	20.90
Pond 18	82.62	21.31
Pond 19	82.67	21.36
Pond 20	82.53	21.59

4 Results and Discussion

A physically based SWAT model has been used for assessment of the impact of small water conservation structures on hydrology of a watershed and the results obtained are quite satisfactory. Figures 3, 4, 5, 6, 7 and 8 shows the maps of River centre line buffer area, LULC, Slope, Drainage network, Hydrologic response unit and Soil respectively. The results obtained are for the period of July to October i.e. from pre-monsoon to post- monsoon period. The annual mean reduction of the discharge due to pond construction is found to be 69.27% while mean reduction in

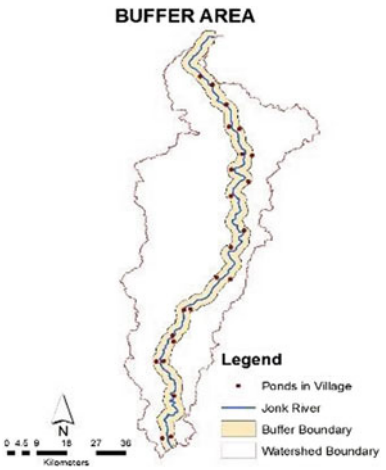

Fig. 3 Jonk river centreline buffer map

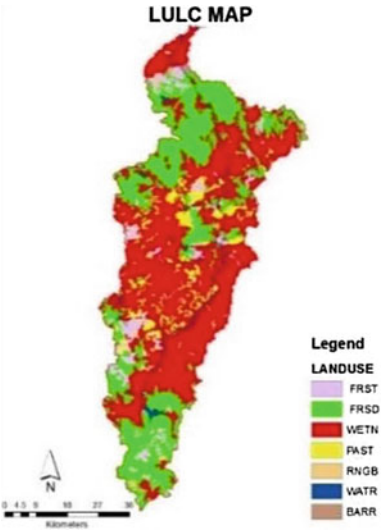

Fig. 4 Land use and land cover map

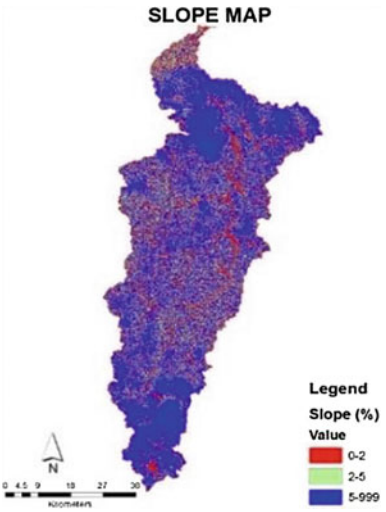

Fig. 5 Slope map

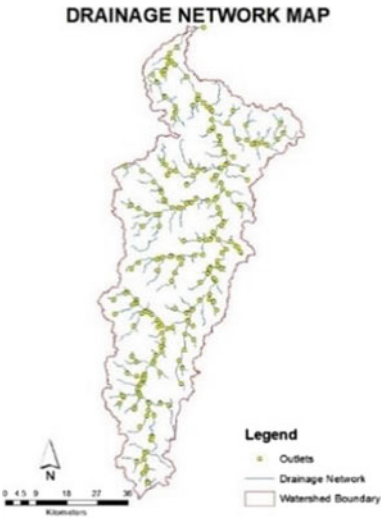

Fig. 6 Drainage network map

sediment flow due to construction of pond is found to be 64.10%. From the above study, it can be concluded that construction of small water conservation structures can be very helpful in controlling the discharge which can cause floods and controlling the sediment flow which causes the sedimentation of the reservoirs. The maximum daily discharge and sediment flow in Jonk watershed is found to be 2.97 cumecs and 1.937×10^5 t/ha/yr respectively for the year 2001 when there was no pond as water conservation structures and the same is reduced to 1.984 cumecs and 0.29×10^5 t/ha/yr due to presence of pond (Figs. 9 and 10). The maximum monthly discharge and sediment flow is also observed to be decreased from 2.13 to

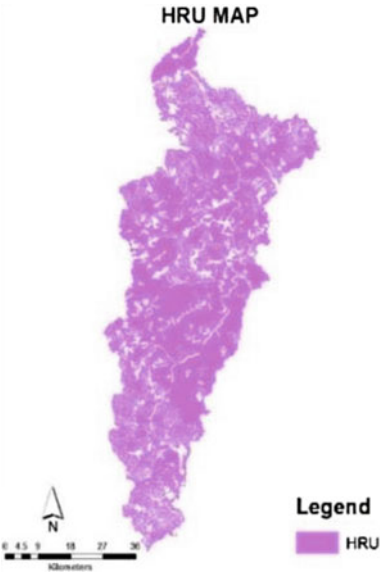

Fig. 7 Hydrologic response unit map

Fig. 8 Soil map

1.25 cumecs and 5.05 $\times$ 10^5 to 1.22 $\times$ 10^5 t/ha/yr respectively due to addition of pond as water conservation structures (Figs. 11 and 12). The comparison of different parameters with the both case scenarios is shown in Table 2. The reduction in monthly discharge due to addition of water pond as water conservation structure is found to be 41–89%. The reduction in monthly sediment flow due to addition of

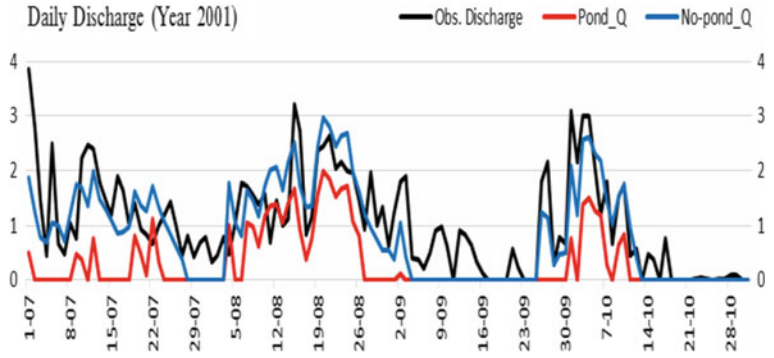

Fig. 9 Plot of observed and simulated daily discharge (cumecs) in two scenarios

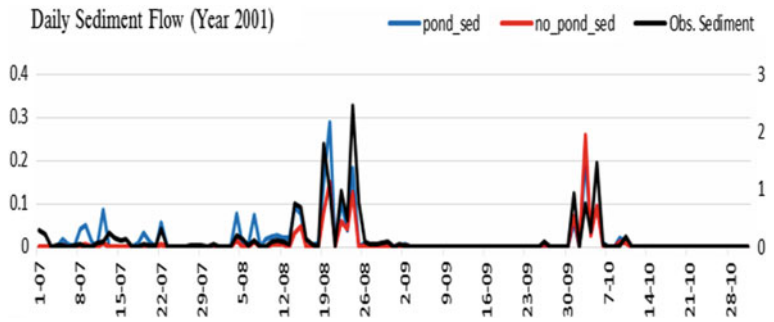

Fig. 10 Plot of observed and simulated daily sediment flow (t/ha/yr) in two scenarios

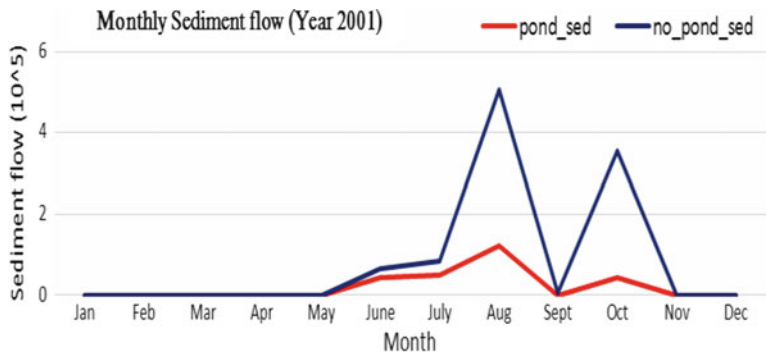

Fig. 11 Plot of simulated monthly sediment flow (t/ha/yr) in two scenarios

water pond as water conservation structure is found to be 32–88%. Due to addition of the water structure, the flow of sediment is reduced which results in less soil erosion also the capacity of reservoir will increase. Deposit of sediments will

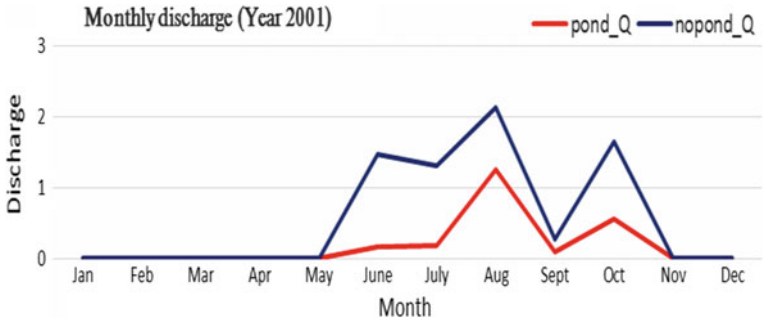

Fig. 12 Plot of simulated monthly discharge (cumecs) in two scenarios

Table 2 SWAT model standard output

Hydrological parameters	Scenario 1 (without pond)	Scenario 2 (with pond)
Precipitation (mm)	768.7	768.7
Lateral soil runoff (mm)	29.00	30.00
Shallow aquifer runoff (mm)	0.00	0.20
Deep aquifer runoff (mm)	0.20	0.90
Deep aquifer recharge (mm)	0.40	1.60
Total aquifer recharge (mm)	7.60	31.30
Total water yield (mm)	106.70	130.40
Percolation out of soil (mm)	7.85	32.35
Total sediment loading (t/ha)	1.50	1.45

increase the percolation of the water in the ground, which results increase in ground water recharge in and around the 20 rural areas. This is a good sign for the population in terms of quality of life and development of the region.

5 Conclusion

The study of Jonk watershed area using the SWAT model is reliable for estimation of monthly discharge and sediment flow. The simulated discharge and sediment flow data has been compared with the observed data and the correlation coefficient is found to be 0.84 & 0.77 respectively. The annual discharge and sediment flow value in "with pond scenario" has been detected to be reduced by 69.27 and 64.10% respectively. The results observed in the present work can be used for site suitability analysis of soil and water conservation structures in the areas those are prone to soil erosion and floods. The study also reveals that the applications of GIS and Geospatial Data Management can be used efficiently for watershed management and rural development.

References

1. Bhuyan, S.J., Koelliker, J.K., Marzen, L.J., Harrington, J.R.: An integrated approach for water quality assessment of Kansas watershed. Environ. Model Softw. **18**, 473–484 (2003)
2. Fan, M., Shibata, H.: Simulation of watershed hydrology and stream water quality under landuse and climate change scenarios in Teshio River watershed, northern Japan. Ecol. Indic. **50**, 79–89 (2015)
3. FAO: United Nations Food and Agriculture Organization, Soil Map of the World, vols. 1–10 (1:5 M scale maps). UNESCO, Paris (1981)
4. Gassman, P.W., Reyes, M.R., Green, C.H., Arnold, J.G.: The soil and water assessment tool: historical development, applications, and future research directions. Trans. ASABE **50**(4), 1211–1250 (2007)
5. Guo, H., Hu, Q., Jiang, T.: Annual and seasonal streamflow responses to climate and land-cover changes in the Poyang Lake basin, China. J. Hydrol. **355**(1), 106–122 (2008)
6. Nasrin, Z., Sayyad, G.A., Hosseini, S.E.: Hydrological and sediment transport modelling in maroon dam catchment using soil and water assessment tool (SWAT). Int. J. Agron. Plant Prod. **4**(10), 2791–2795 (2013)
7. Nie, W., Yuan, Y., Kepner, W., Nash, M.S., Jackson, M., Erickson, C.: Assessing impacts of landuse and landcover changes on hydrology for the upper San Pedro watershed. J. Hydrol. **407**(1), 105–114 (2011)
8. Singh, V.P., Frevert, D.K.: Mathematical modelling of watershed hydrology. Chapter 1, in: Mathematical Models of Small Watershed Hydrology and Applications, Water Resources Publications, Littleton, Colorado, pp. 1–3 (2002)
9. Zhou, F., Xu, Y., Chen, Y., Xu, C.Y., Gao, Y., Du, J.: Hydrological response to urbanization at different spatio-temporal scales simulated by coupling of CLUE-S and the SWAT model in the Yangtze River Delta region. J. Hydrol. **485**, 113–125 (2013)

Chapter 67
A Geospatial Study on Visakhapatnam Smart City Based on Hydrogeochemistry Analysis

Neela Victor Babu, Peddada Jagadeeswara Rao, Suribabu Boyidi and Sridhar Bendalam

Abstract Groundwater tainting because of ocean water interruption is a surely understood issue in Madhurawada panchayat (group of villages). This investigation endeavor to give answers the hydrogeochemistry idea of groundwater synthetic parameters in Madhurawada Panchayat. In the ponder we apply existing field bore well and burrowed well perception which join with research facility water test examination as indicated by WHO and BIS norms and obviously aberrant addressing with the villager. The outcome has demonstrated the sullying level of EC, TDS, TH, Ca^{+}, Na, Cl^{-}, F^{-}, and Fe in the Paradesipalem, Boravanipalem, KommadiJn, Marikavalasa, Thotlakonda, Jodugullapalem and Boddapalem in both bore well and burrowed wells over the farthest point of reasonable farthest point for drinking limit. Calcium and magnesium are the predominant cations display in groundwater beside sodium and chloride in this district. In this manner, order ought to take at the season of groundwater utilization.

Keywords Ground water samples · GIS · GVMC · Hydrogeochemistry

N. V. Babu (✉) · S. Boyidi · S. Bendalam
Baba Institute of Technology and Science, Visakhapatnam, India
e-mail: neelavictorbabu@gmail.com

S. Boyidi
e-mail: suri.sri2008@gmail.com

S. Bendalam
e-mail: sridhar.bendalam@gmail.com

P. J. Rao
Andhra University College of Engineering, Visakhapatnam, India
e-mail: pjr_geoin@rediffmail.com

P. J. Rao et al. (eds.), *Proceedings of International Conference on Remote Sensing for Disaster Management*, Springer Series in Geomechanics and Geoengineering,
https://doi.org/10.1007/978-3-319-77276-9_67

1 Introduction

The term smart urban communities moved toward becoming trendy expression in the worldwide field. Lately urban advancement turned into a key issue internationally. Particularly India like thickly populated nations, the issue is more worry about urbanization. As indicated by the current insights expresses that, % moved from rustic to urban. This reflected in many disjoin issues like contamination issues, subject the off by presenting the idea of smart refers to it the urbanization wound up noticeably one of the significant issue all the more difficult and other creating nations. Metropolitan strong waste is, discarded/rejected material consistently being overlooked from the assorted open sources. Examinations in consider zone revealed that, quick improvement in masses in the midst of the present decades realized growing measure of urban strong squanders.

The natural issues existing in the urban zones of creating nations, squander administration and its effect on groundwater quality have been the most conspicuous in the current years [1]. The Greater Visakhapatnam Municipal Corporation (GVMC) is the second greatest civil partnership in the territory of Andhra Pradesh, India. There are no real surface water bodies in the zone and the trustworthy groundwater assets are being dirtied at a disturbing rate. By and by, groundwater quality is the real concern and hence rose as a standout amongst the most critical ecological issues. Water interest for drinking and local purposes has been expanding because of progress of ways of life of individuals and statistic weights [2]. The modern effluents of the Zinc smelter-Aluminum manufacturing plant in Mindi Visakhapatnam move toward groundwater development and stream towards bog arrive through local locations because of topographic control. Hence, this investigation has been taken up to discover hydrogeochemistry attributes of groundwater in the Madhurawada Panchayat, Visakhapatnam area, Andhra Pradesh.

2 Study Area

The investigation zone is covering roughly 102 km^2. In the year 2004 the Madhurawada is real panchayat in Visakhapatnam region, in the year 2006, 100 km^2 Visakhapatnam Municipal Corporation was stretched out to 545 km^2 zone of Greater Visakhapatnam Municipal Corporation (GVMC). In this complexity the Madhurawada Panchayat was converged in Greater Visakhapatnam Municipal Corporation (GVMC). The GVMC is popular for significant enterprises, regularly called as Industrial City or Visakha Steel City. The region has four noteworthy slope ranges viz., Kailassa, Yarada, Naraka and Kambalkonda. Whatever remains of the zone is portrayed by undulating geography. The waste is for the most part dendritic to sub-dendritic (Fig. 1).

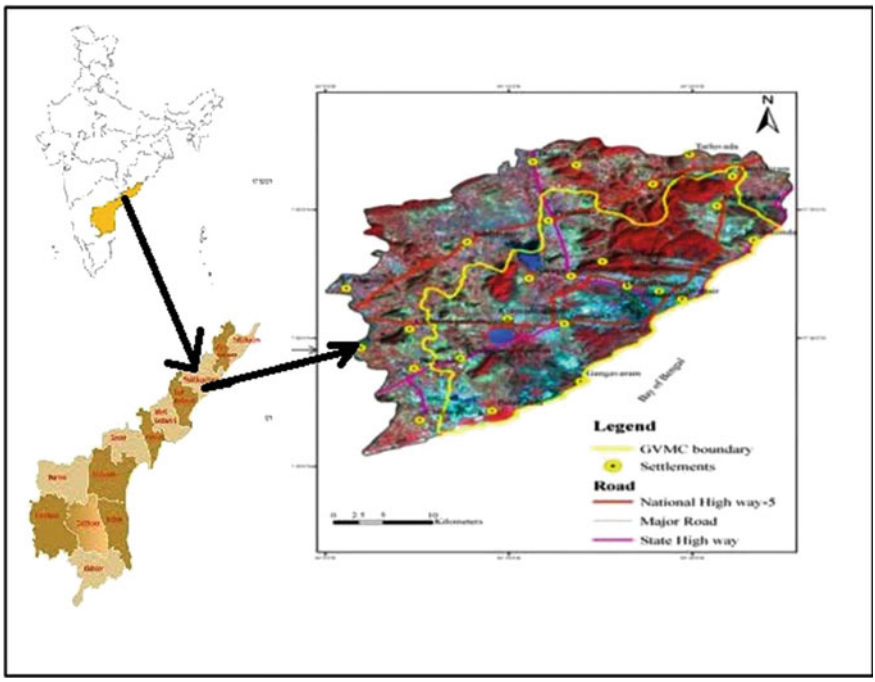

Fig. 1 Greater Visakhapatnam Municipal Corporation Study Area

3 Methodology

In post storm, around 14 groundwater tests were gathered covering the whole Panchayat amid February, 2014. In Monsoon, around 27 water tests were gathered adjoining the unlined sewage channels (gedda) amid August 2014 to recognize the water quality parameters regarding physical and substance on the premise of APHA Standard System [3]. Orderly work has not been done for the collection of higher toxicants in these zones. The convergences of physical, substance parameters in groundwater tests were contrasted and the Bureau of Indian Standards (BIS) and World Health Organization (WHO). The examples were investigated for deciding the groupings of different concoction components, for example, pH, EC, TDS, TH, BOD, COD, TA, Ca^{+}, Mg^{2+}, HCO_3, Cl^{-}, F^{-}, and Fe. Tests were broke down in research facility utilizing Flame Photometer for, Ca^{+} and Mg^{2+} components, they were examined by EDTA Titrimetric technique. $NO_3{}^{-}$, $PO_4{}^{3-}$, Fe were investigated utilizing UV Visible Spectrophotometer strategy, $SO_4{}^{-}$ by Gravimetric technique, F^{-} by Orion Ion specific strategy, Cl^{-} by Argentometric Method. Every one of these strategies are a piece of APHA system for the examination of water quality. The information are introduced by utilizing flute player graph to see the focus level of hydrogeochemical particle.

4 Results

The synthetic parameters acquired in this investigations uncovering that the pH differs from 6.12 to 7.76 of soluble nature inside as far as possible. The electrical conductivity (EC) values are in the middle of 0.99–840 ms. The centralizations of Ca^{+}, Mg^{2+}, F^{-} and Cl^{-} particles are watched nearer to the most extreme reasonable breaking points in the towns of Boyapalem, Paradesipalem, Boravanipalem, Mangamaripeta and Kapulauppada. These towns are in downstream territories of Kapulauppada landfill site. The groupings of TDS and TH and Na^{+} and Fe have surpassed greatest reasonable breaking points in Kapulauppada, Thotlakonda and Mangamaripeta. The higher substance in these towns could be drainage from the unlined sewage deplete. These components cause cardio vascular ailments which are accounted for in delicate water zones. Up until now, no case has been accounted for in regards to contaminated groundwater in the territory. The principle hotspot for sodium in groundwater assets is plagioclase feldspars, feldspathoids and dirt minerals. Sodium content around 200 mg/l might be unsafe to people having cardiovascular and renal sicknesses and in ladies with toxemia related with pregnancy [4]. The grouping of sodium fluctuates from 10 to 540 mg/l. Two examples observed to be abundance of Na^{+} than the most extreme admissible points of confinement in Kapulauppada and Thotlakonda. The calcium is a noteworthy constituent of most volcanic, transformative and sedimentary rocks. The main wellspring of Ca^{+} in groundwater is individuals from the silicate mineral gatherings like plagioclase, pyroxene and amphibole among volcanic also, changeable rocks and limestone, dolomite and gypsum among sedimentary rocks. Transfer of sewage and mechanical squanders are likewise critical wellspring of calcium. Fixations up to 1800 ppm has been found not to impede any physiological response in man [5]. The calcium extends in the middle of 16–160 mg/l. The magnesium focuses in the examination zone shifts from 5 to 136 mg/l. Kapulauppada and Mulagada tests are having abundance content than as far as possible in (Table 1). Calcium and magnesium are the predominant cations introduce in groundwater beside sodium and chlorine in this district. Be that as it may, the development of bicarbonate is nearly at immaterial rate. The motivation behind why the centralization of carbonate increments in this investigation may be because of the accessible carbonates In these stone may have broken up and added to the groundwater framework amid water system, precipitation penetration and groundwater development. Also, if the Ca^{2+} and Mg^{2+} exclusively began from carbonate and silicate weathering, these ought to be adjusted by the alkalinity alone. Nonetheless, the majority of the focuses are put in the Ca^{2+} + Mg^{2+} side, which shows abundance calcium and magnesium got from different process, for example, switch particle trade responses.

Table 1 Physical and chemical parameters concentration in the study area (in ppm)

S. no.	Constituents	Bureau of Indian Standard (IS-10500:1991)	Pre-monsoon (Aug 2012)	Post-monsoon (Mar 2012)
			Range	Range
1	pH	6.5–8.5	6.15–7.73	6.44–7.79
2	EC	700–3000	0.50–2.58	1.26–850
3	TDS	500–2000	572–1148	210–2530
4	TH	300–500	140–907.5	130–830
5	BOD	–	0.50–3.02	0.3–26
6	PO_4^-	–	–	0.5–3.8
7	COD	–	5.8–0.95	0.4–69
8	TA	–	140–865	85–980
7	Fe	1.0	0.19–1.25	0.85–2.3
8	Ca^+	75–200	61–155	76–180
9	Mg^{2+}	30–100	21.69–746.5	7–145
10	SO_4^-	150–400	28–148	10–288
11	Na^+	200–300	–	10–535
12	K^+	10	–	0.1–3.5
13	Cl^-	250–1000	69.58–441.3	18–890
14	HCO_3	500	85.40–379.20	28–526
15	NO_3^-	45	2.20–5.90	1.4–12.56
16	F^-	1.5	0.65–1.95	0.68–1.66

5 Conclusions

This exploration work expected to get reply about hydrogeochemistry of Madhurawada panchayat, Visakhapatnam District, Andhra Pradesh, India. Examinations in think about territory uncovered that, quick development in populace amid the current decades brought about expanding the utilization of groundwater. Amid this examination, it is watched that the higher substance of various components in groundwater is because of effluents, from ventures and leachates from dishonorable treatment of urban strong squanders. Along these lines suitable sewerage for the modern waste is high prescribed.

References

1. Nirmal Rajkumar, A., Barnes, J., Ramesh, R., Purvaja, R., Upstill-Goddard, R.C.: Methane and nitrous oxide fluxes in the polluted Adyar River and estuary, SE India. Mar. Pollut. Bull, **56** (12): 2043–2051 (2008)
2. Swarnalatha, K., Letha, J., Ayoob, S.: An investigation into the heavy metal burden of Akkulam– Veli Lake in south India. Environ Earth Sci, **68**(3): 795–806 (2013a)

3. APHA, Standard Methods for the Examination of Water and Wast Water, American Public Health Association, American Water Workes Association, Water Environment federation, Washigton, DC, USA, (2005)
4. NAS (National Academy of Science).: Drinking water and health. Safe Drinking water committee, US National Research Council. Washington, DC, (1977)
5. Lehr, J.H., Gass, T.E., Pettyjohn, W.A., De Marre, J.: Domestic Water Treatment. Mc Graw-hill Book Co., New Delhi, p. 655, (1980)

Chapter 68
Remote Sensing and GIS Approach for Planning and Analysis of Storm Water Drainage System

Ch. Ramesh Naidu

Abstract Floods are among the most destructive acts of nature. World-wide, flood causes damage to agriculture, houses and public utilities amount to billions of dollars each year in addition to the loss of precious human and cattle lives. India is no exception as far as floods are concerned. Severe floods occur almost every year in one part of the country or the other causing tremendous loss of life, large scale damage to property and untold misery to millions of people. In building sustainable and smart cities Storm water modeling and management is a challenging task in the proposed smart cities in India. Recent floods in urban areas in India and across the world have brought susceptibility and helplessness of Smart Cities to disasters into attention. Geospatial technologies can help cities to prepare and mitigate the impacts of floods—as they design and build the smart systems. While storm water modeling with GIS can help ULB's exercise caution in mitigate the risk, it also offers a huge potential for development of the area. It is now important that Disaster planning, Modeling and Mitigation are closely interrelated with sustainable development of the smart cities. Using RS and GIS technology cities can evaluate potential risks in future. With the use of RS images and GIS technology the required information for flood analysis can be developed in the form of spatial and non-spatial database.

Keywords Storm water drainage network · Geo spatial technology
Rational method · Storm water modeling · Urban local bodies

1 Introduction

Urban catchments are very dynamic in nature due to the lack of pervious surfaces. Because of rapid and un controlled developments, day by day the percentage imperviousness is increasing in urban catchments. In result quick flow of runoff

Ch. R. Naidu (✉)
GVP College of Engineering (A), Madhurawada, Visakhapatnam, Andhra Pradesh, India
e-mail: rameshnaidu@gvpce.ac.in

P. J. Rao et al. (eds.), *Proceedings of International Conference on Remote Sensing for Disaster Management*, Springer Series in Geomechanics and Geoengineering,
https://doi.org/10.1007/978-3-319-77276-9_68

happens and reaches to outlets with in short time from urban micro catchments. Almost all Urban Local Bodies (ULB) are facing the same scenario. Most of these ULBs does not have proper surface and sub surface drainage system. Storm water drainage system is very essential to accommodate and regulates certain percentage of surface run off. Geo Spatial technology helps planners and design engineers to prepare a storm water network conceptual plan by analyzing the existing topography, soil, landuse and climate conditions. Satellite images provide a better spatial and temporal resolution to identify the nature of the topography, drainage system and physiography. GIS provides tools to check the network continuity, determine the flow direction, flow velocity and simulate the flow with reference to hydraulic gradient line. Building a storm water network and components with reference to its micro catchments in GIS platform facilitates a better decision support system for effective planning and maintenance operations by the concerned engineers and managers.

2 Methodology

Before the design, planning of storm water drainage system involves geographical understanding of the study area includes existing transportation system and traffic, existing underground utilities, climate, physiography, terrain slope, landuse and soil. Using Remote Sensing images and Geo Spatial technology these topographical features and physical facilities can be interpreted and developed in the form of thematic layers.

For design considerations, storm water drainage system must have adequate capacity to take and transport the storm runoff for the design frequency. It should be capable to withstand the future developments. To plan and design storm water drainage system, it requires high resolution satellite images to produce large scale GIS database. In addition to planimetric details, elevation and slope often needed in determining the flow characteristics for analysis and hydraulic simulation. To design the network, road levels along the road centre and road edges to be collected using Electronic Total Station and Auto level instruments. The survey observations can be digitally imported and integrated in GIS software. Further using the DEM, flow direction, catchment and sub catchment boundaries and flow accumulation points at micro level can be interpreted from watershed tools available in GIS software. These flow directions and flow accumulation areas helps to determine and locate inlets and outfall locations. Alternatively stereo satellite images can be used to produce topographical contours and subsequently generates slope and 3D terrain.

Rational method is most suitable method for finding discharges of urban catchments when catchment area is less than 200 acres. Sometimes a run off hydrograph is essential when components like detention tanks and pumping stations are a part of storm network. The formula for calculating Runoff volume is,

$$Q = 10CIA$$

where

Q Run-off in Cumec/h
C Coefficient of Runoff
I Intensity of Rainfall in mm/h
A Area of Catchment in hectares.

Catchment run off depends on run off coefficient, rain fall intensity and time of concentration. Run off coefficient directly depends on landuse and soil conditions of the catchment. Rainfall intensity changes with rainfall return period or recurrence frequency. Rainfall intensity can be determined by plotting the Intensity-Duration and Frequency (IDF curves) curves. Most of the urban local bodies are designed the storm water drainage system with 1–10 year return periods. If the return period increases the runoff also increases. The time of concentration varies catchment wise and mostly depends on the average slope. Time of concentration decides the inlet spacing and size of the pipe. The storm drains are usually designed by considering full gravity flow using the design frequency discharge.

After preliminary planning of inlets, pipe network and outfalls of all the catchments can be digitized in the GIS platform in the form of thematic layers.

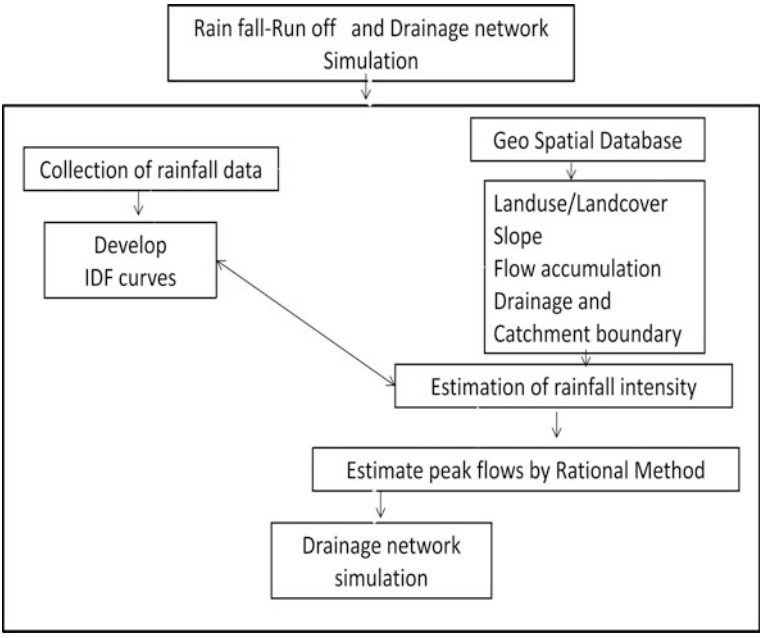

Fig. 1 Rainfall-runoff and drainage network simulation

The network continuity checks can be managed with GIS tools. The runoff calculated from the rational method is used to define the capacity of the storm drain which includes drain size and gradient required to convey the run off discharge. Drain size and gradients can be decided by simulation in Epa SWMM software after importing the network from GIS to Epa SWMM. Figure 1 shows the steps to manage rainfall- runoff and drainage system simulation.

3 Conclusions

The Rational method of estimating storm water discharge is mostly useful for manual design of storm drainage system. Using Epa SWMM, these flows can be used to simulate the drain sizes and velocity. Geo Spatial database can be used effectively to calculate the input parameters required for hydraulic modeling in Epa SWMM. Inputs like landuse, sub catchment boundaries and slope allows the user to run the functions and routines simultaneously to determine the time of concentration, catchment areas, length of the drain, run off coefficient for all the sub catchments within the main catchment. Though there are some limitations in rational method for urban flooding studies, it is simple and justifies the modeling of average intensity of rainfall.

References

1. Drainage manual: Minnesota Department of Transportation. https://www.dot.state.mn.us/bridge/pdf/hydraulics/drainagemanual/chapter%208.pdf
2. Genovese, E.: A methodological approach to land use-based flood damage assessment in urban areas, prague case study (2006)
3. Aksoy, H., Kirca, V.S.O., Burgan, H.I., Kellecioglu, D.: Hydrological and hydraulic models for determination of flood prone and flood inundation area (2016)
4. Manual on Sewerage: The Central Public Health and Environmental Engineering Organization (CPHEEO), Government of India (1993)
5. Supplementary Material on Urban Flooding, Monsoon School, Department of Civil Engineering, IISC, Bangalore, India
6. Quantum GIS. http://www.qgis.org
7. Guidelines on Management of Urban Flooding-National Disaster Management Authority, Government of India
8. Rossman, L.: SWMM 5: a case study of model re-development (2012)
9. EPA's Storm Water Management Model (SWMM). https://www.epa.gov

Chapter 69
Classifications of SAR Images Using Sparse Coding

Battula Balnarsaiah, G. Rajitha and Balakrishna Penta

Abstract In this paper a novel Sparse Coding for Classification of Synthetic Aperture Radar (SAR) Images is proposed. Features utilized in SC (Sparse Coding) are extracted from the multisize patches around each pixel to precisely describe the complex terrains. In these one or two level thresholds techniques are introduced in the sparse coding for classifier of SAR Images to the restrict the range of reconstruction residual, which classifies the consistent classified points, and the rest of the pixels are considered as the indecisive ones in the original SAR image. Compared with habitual SC of SAR image classification and support vector machines (SVM) in a number of fixed-size patches. Later, the performance measure parameters like accuracy, kappa coefficient and time are calculated and compared for all RISAT-1 images sizes. The above mentioned classifications techniques are development and performance parameters are calculated using MATLAB 2014a software.

Keywords We image classifications · Sparse coding (SC) · Synthetic aperture radar (SAR) · Multisize patches

B. Balnarsaiah (✉)
Department of ECE, University College of Engineering,
Osmania University, Hyderabad, TS, India
e-mail: battulabalu@gmail.com

G. Rajitha
Department of Geography, University College of Science,
Osmania University, Hyderabad, TS, India
e-mail: rajithaa68@gmail.com

B. Penta
Department of Geo-Engineering, Andhra University,
Visakhapatnam, AP, India
e-mail: balakrishna.penta@gmail.com

P. J. Rao et al. (eds.), *Proceedings of International Conference on Remote Sensing for Disaster Management*, Springer Series in Geomechanics and Geoengineering,
https://doi.org/10.1007/978-3-319-77276-9_69

1 Introduction

The Synthetic Aperture Radar of raw data image user defined different type's categories. The raw data of remote sensing can be categorized in lot of various customs. The images of pixel based on procedure use statistical models for predict the best parameters that fit to the raw data views. The Bayesian inference for pixel-based information extraction was proposed. The fields of Markov Random parameters were predictable en suite to the image SAR [1]. Presently methods for different categorization of optical images are applied intensively to the remote sensing data that is raw data of SAR image [2, 3]. In the literature, most various classifications have been employed to the remote sensing data, including the K-nearest neighborhood and support vector machine (SVM) [4]. The sparse code representation classification methods [1] have become very popular [5]. Presently, the research of automatic classified based on high-resolution SAR image has obtained rapid development [3]. Different classifiers can be used in classification of image such as support vector machine (SVM) [6], and sparse code-based classification (SC) [7]. Sparse representation has been also applied to remote sensing image processing, such as SAR image compression [8], hyperspectral imagery classification [5].

2 Literature Review

SAR images cannot be segmented successfully by using traditional methods because of the existence of speckle noise in SAR images [7]. For example, simple classification methods based on thresholding techniques of gray levels are generally inefficient to classify the images with speckle noise, due to high degree of overlap between the distributions of the different classes [3]. SAR image Classification is various from classification of normal images, an efficient algorithm for identification of texture of Synthetic Aperture Radar (SAR) images is developed, one of the most important classification is support vector machine (SVM), it is utilized for as a wavelet transform feature extraction of SAR image classifications [8]. A new classification method for detection of ship in TerraSAR-X images, is proposed based on sparse representation in feature space by X. Xing [9]. An application to pattern extraction from noisy signals is described in [10]. Sparse Representation-Based Classification (SRC) with random projections-based features can outperform a number of conventional face recognition schemes [8, 11].

3 Study of Area

In many different classifiers have been employed to the remote sensing data, including the K-nearest neighborhood and support vector machine [4]. In recent years, the sparse representation-based classification methods have become very popular [5]. Sparse coding has been used successfully in several classification scenarios. The advantages of wavelet transform, sparse coding, and dictionary learning were used for classification purposes [8]. Hierarchical sparse representation features were used for SAR data classification in [9]. Zhao et al. [10] proposed to characterize SAR patches using a discriminate feature that is generated in a semi supervised manner and spare ensemble learning procedure. A multi kernel joint sparse graph was proposed to segment SAR images [11]. A supervised method based on sparse representation for PolSAR image classification was proposed in. The classification via sparse representation and multitask learning was presented for target recognition in the SAR image [12]. This letter was motivated by the fact that interferometric SAR (InSAR) data contain phase information, which is usually not used [1].

4 Proposed Method

In this letter, we utilize a gray-level histogram [10, 11] and a gray-level co-occurrence matrix (GLCM) [10] to get the features of a SAR image. Gray-level histogram is stable in the presence of noise and over change in view and can be used to distinguish and characterize the objects. GLCM is also used to represent SAR image texture, and we utilize a range of different size patches to adequately capture both microtextures and macrotextures in the original SAR image(RISAT-1 Image). We add a two level-threshold techniques to SC (Sparse Code), which separates from the initial SAR images of the consistent pixels, and the outstanding ones will be classified in the same way in the later layer until a traditional sparse code classifier outputs the final result Fig. 1. The feature of a fixed-size patch cannot well represent terrains experimental results show that the proposed method outperforms SVM and traditional SC within different fixed-size patches in terms of classification accuracy and enhances the visual effect in several real SAR images.

4.1 Sparse Code (SC)

The A single class that lies in a linear subspace is SC, it can express to the samples. Assume that classes are known, e.g., we can identify a dictionary constructed by

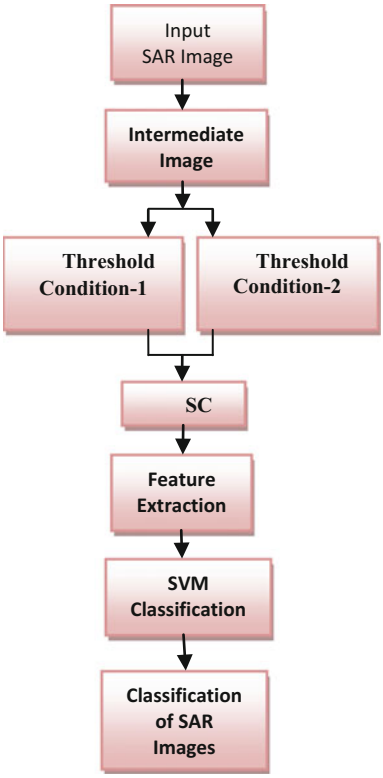

Fig. 1 Classification of SAR image

concatenating feature vectors of those classes. The testing sample can be formulated by a series of training samples as follows:

$$y = D\psi_0 \in R^m \tag{1}$$

where $\psi_0 = \left[0, \ldots 0, \varphi_{i,1}, \varphi_{i,2}, \varphi_{i,n_i}, 0 \ldots, 0\right]^T \in R^n$a coefficient vector is whose entries are zeros except those associated with the ith class. The sparser the coefficient ψ_0 is, the easier it can estimate the identity of the y testing sample. It is necessary to find the sparsest solution to satisfy $y = D\psi_0$. Based on the aforementioned analysis, the problem about SC can be modeled as

$$\psi_0 = \arg\min \|\psi\|_0 \text{ subject to } D\psi = y \tag{2}$$

where $\|\cdot\|_0$ denotes the ℓ^0-norm. Depending on the development in sparse and compressed sensing, it has been proved that if the solution ψ_0 is sparse enough, the solution to ℓ^0 minimization problem equals to the solution to ℓ^1 minimization one, which can be relaxed as

$$\hat{\psi}_1 = \arg\min \|\psi\|_1 \text{subject to } D\psi = y \tag{3}$$

$\hat{\psi}_0$ Let δ_i: $R^n \rightarrow R^n$ be the characteristics function for each class. For $\psi \in R^n$, $\delta_i(\psi)$ is a new coefficient vector in which nonzero entries are the ones in ψ that associated with class i. Using the vector $\delta_i(\psi)$, we can get a linear reconstruction $\hat{y}_i = D\delta_i(\hat{\psi})$ approximate the testing sample y [10].

As follows:

$$\min_i r_i(y) = \left\| y - D\delta_i\left(\hat{\psi}\right) \right\|_2 \tag{4}$$

4.2 Dictionary Training of Multisize Patch Using SC

The framework of our method is shown in Fig. 1. In this section, we will introduce the proposed method in detail. Sparse coding applications are constructing a dictionary is the first step. The dictionary in our method is not constructed directly by pixel values. In this method 16-D and 4-D feature vectors are produced by exploiting statistics properties in the gray-level histogram and utilizing texture statistics distribution in GLCM, respectively. We select n_i vectors of training samples from the ith class in the hth layer as columns to construct a matrix $A_i^h = \left[x_{i,1}^h, x_{i,2,\ldots}^h, x_{i,n_i}^h\right] \in R^{m \times n_i}$ where m denotes the dimension of the feature vector. Then we define the dictionary D^h as the concatenation of the n_i training sample vectors of all K defined classes in the fixed hth layer

$$D^h = \left[A_1^h, A_2^h, \ldots, A_K^h\right] = \left[x_{1,1,}^h x_{1,2}^h, \ldots, x_{K,n_K}^h\right] \tag{5}$$

where D^h denotes a fixed dictionary. Let $h = \{h_1, h_{2,\ldots,}, h_H\}$ enumerate the H latent layers; H also means the total classification number.

Multisize Patch SC (Sparse Coding) using Two Level Thresholding Techniques (TLTT) Algorithm

1. Constructing initial dictionary (h = 1 or 0): Given K classes, select n_i samples from each class randomly, each sample is represented by an m-dimensional vector that constrict the initial dictionary $D^{init} = \left[A_1^{init}, A_2^{init}, .., A_K^{init}\right]$, init = ∓ 1, where the feature vectors are extracted by the patch in the first layer that is zero level layer of given input image.
2. Sparse Coding techniques of classification ($1 \leq h \leq H - 1$): classify all pixels the first layer at the zero level and uncertain points. Determine which category of the testing sample y belongs to.

3. Constructing hth dictionary ($2 \leq h \leq H$): Select n number of points from each class which is labeled as new training samples in the previous layer, and extract the feature vector $x_{i,j}^{h}$ at h-th layer. Arrange these vectors as columns to construct the H dictionary $D^{h} = \left[A_{1,}^{h} A_{2}^{h}, \ldots, A_{k}^{h}\right] \in R^{m \times n}$.
4. Classification at the last layer ($h - H$): Utilize the Hth dictionary D^{H} to classify the uncertain points or pixels in SAR (RISAT-1 image) image by traditional sparse coding of classifier.
   To deal with the challenge, we develop a sparse coding representation classifier with a two level-threshold techniques (TLTT) to improve the classification of the SAR image. We make a judgment on the residual $r_i(y)$ to approximate the reliability of classified pixels. In other words, if $r_i(y)$ lies in a specified range. Here, we explicitly describe SC with the judgment of residual $r_i(y)$ at the $hth(1 \leq h \leq H - 1)$ layer, i.e., two level threshold techniques (TLTT) decision condition. The minimum residual $r_{min}^{h}(y)$ in the hth layer is given by

$$\tau^{h} = r_{min}^{h}(y) = \min_{i=1\ldots K} r_{i}^{h}(y) \tag{6}$$

$$\theta^{h} = \arg\min_{i=1\ldots K} r_{i}^{h}(y) \tag{7}$$

where K and θ denote the number of the class and the label with the minimum residual. The label of each pixel under the residual judgment is determined as follows:

$$\text{Label}(y)^{h} = \begin{cases} \min_{i} r_{i}^{h}(y), \tau^{h} \leq \Delta_{1,} \left| r_{i \neq \theta^{h}}^{h}(y) - \tau^{h} \right| \geq \Delta_{2} \\ \text{uncertain, else} \end{cases} \tag{8}$$

where Δ_1 and Δ_2 represent the threshold techniques parameter. The proposed algorithm is summarized in Table 1.

Table 1 Classification accuracies and kappa coefficients of image

Method	SC 8 × 8	SC 6 × 6	SVM 8 × 8	SVM 6 × 6	Multi patch SVM	SC using TLTT[a]
Accuracy (%)	93.62	93.62	96.60	93.80	90.16	96.82
Kappa	0.8972	0.8922	0.9448	0.8983	0.8686	0.9728
Time (s)	101.02	101.18	47.24	48.06	47.85	216.21

[a]Two Level Threshold Techniques-TLTT

4.3 *Influence of Thresholds*

To test the influence of thresholds on the classification result, a C-band uninhabited airborne vehicle synthetic aperture radar (UAVSAR) sub image (598 × 430 pixels) with 3-m resolution in Tanjavur City in India, is selected, as shown in Fig. 2a. This image consists of three types of land covers: trees, temple, and vehicles. It is difficult to obtain the ground-truth map of the SAR imagery (RISAT-1 Image), so we manually select some representative points to quantitatively evaluate. The training samples are randomly selected in them. The number of land markings are or Points that is identification temple, tree and vehicles are 1026, 842 and 628 respectively. As per according to the terrain in image 1, we represent the patch size 8 × 8. The two level threshold techniques are also very important for connecting classification at different layers.

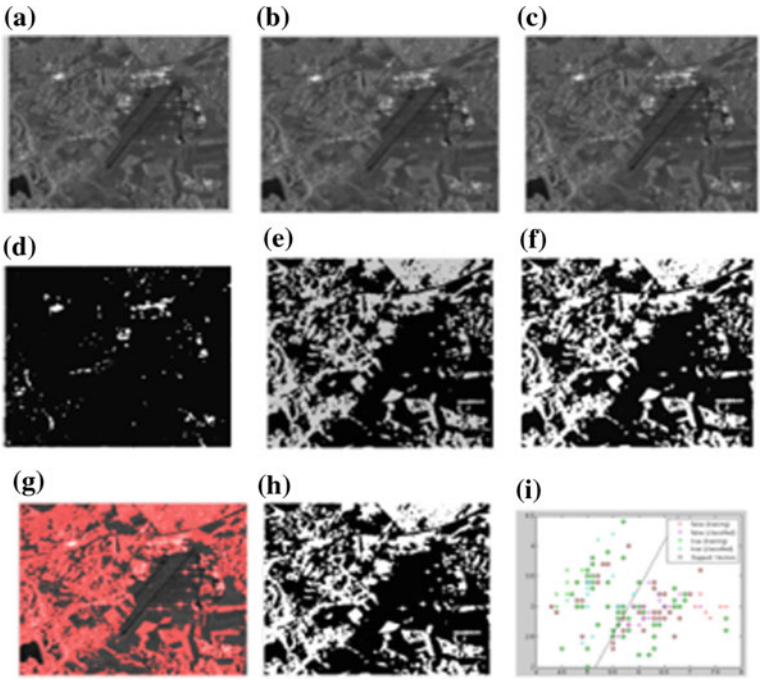

Fig. 2 Three typical structures of classification process for image. **a** Original SAR image (RISAT-1 image). **b** First layer. **c** Fifth layer. **d** Last layer. **e–f** show the classification results, and **g** RGB classifications of SAR Image later containing uncertain points. **h** Final results of SAR Image classification. **i** SVM classifications of SAR Image

5 Results and Discussion

In this section, we investigate the classification performance of our method and compare it with the traditional SC and SVM in several patch sizes. In order to accurately calculate the classification accuracy and kappa coefficient, we carry out our algorithm with $\Delta_1 = 0.14$ and $\Delta_2 = 0.05$ contrast methods repeatedly for 50 times, and then average the results. The quantitative evaluation of different methods for Image1 is shown in Table 1. Multisize patch-SVM is a method that utilizes a long feature vector concatenated by feature vectors of several used patches in SC. Figure 2 shows the classification results of Image1, Fig. 2a is the result of the proposed method, and Fig. 2b shows the result of Multi-Patch-SVM. It also can be seen that the results obtained by the SC and SVM methods at 8×8 size. The accuracies of our method will be greater than 97%. The reason could be that the number of uncertain points varies with two level threshold techniques at each layer, which results in the variation of the final classification result.

6 Conclusion

In this letter, a new classification of SAR image method based on SC is implemented. The two level threshold techniques (TLTT) to usual planned method mainly add judgment condition to new traditional algorithms is SC and Multisize patches its various features of RISAT-1 images. This is investigated by the quantitative evaluation and the visualization results in SAR images classification. Our future work will focus on feature extraction and automatic selection of patches to improve the classification performance of SAR images that is RISAT-1 raw data image.

References

1. Planinšiĉ, P., Gleich, D.: InSAR patch categorization using sparse coding. IEEE Geosci. Remote Sens. Lett. **14**(6), (2017)
2. Feng, J., Jiao, L.C., Zhang, X., Yang, D.: Bag-of-visual-words based on clonal selection algorithm for SAR image classification. IEEE Geosci. Remote Sens. Lett. **8**(4), 691–695 (2011)
3. Cui, S., Dumitru, C.O., Datcu, M.: Ratio-detector-based feature extraction for very high resolution SAR image patch indexing. IEEE Geosci. Remote Sens. Lett. **10**(5), 1175–1179 (2013)
4. Demirhan, M.E., Salor, Ö.: Classification of targets in SAR images using SVM and k-NN techniques. In: Proceedings of 24th Signal Processing Communication Application Conference (SIU), May 2016, pp. 1581–1584 (2016)

5. Jia, S., Hu, J., Xie, Y., Shen, L., Jia, X., Li, Q.: Gabor cube selection based multitask joint sparse representation for hyperspectral image classification. IEEE Trans. Geosci. Remote Sens. **54**(6), 3174–3187 (2016)
6. Zhang, J., Zhu, D., Zhang, G.: Adaptive compressed sensing radar oriented toward cognitive detection in dynamic sparse target scene. IEEE Trans. Signal Process. **60**(4), 1718–1729 (2012)
7. Ophir, B., Lustig, M., Elad, M.: Multi-scale dictionary learning using wavelets. IEEE J. Sel. Topics Signal Process. **5**(5), 1014–1024 (2011)
8. Hou, B., Ren, B., Ju, G., Li, H., Jiao, L., Zhao, J.: SAR image classification via hierarchical sparse representation and multisize patch features. IEEE Geosci. Remote Sens. Lett. **13**(1), 33–37 (2016)
9. Zhao, Z., Jiao, L., Liu, F., Zhao, J., Chen, P.: Semisupervised discriminant feature learning for SAR image category via sparse ensemble. IEEE Trans. Geosci. Remote Sens. **54**(6), 3532–3547 (2016)
10. Gu, J., Jiao, L., Yang, S., Liu, F., Hou, B., Zhao, Z.: A multi-kernel joint sparse graph for SAR image segmentation. IEEE J. Sel. Topics Appl. Earth Observ. Remote Sens. **9**(3), 1265–1285 (2016)
11. Mallat, S.G., Zhang, Z.: Matching pursuits with time-frequency dictionaries. IEEE Trans. Signal Process. **41**(12), 3397–3415 (1993)
12 Xing, X., Ji, K., Zou, H., Chen, W., Sun, J.: Ship classification in TerraSAR-X images with feature space based sparse representation. IEEE. Geosci. Remote Sens. Lett. **10**(6), 1562–1566
13 Xu, S., Fang, T., Li, D., Wang, S.: Object classification of aerial images with bag-of-visual words. IEEE Geosci. Remote Sens. Lett. **7**(2), 366–370 (2010)

Chapter 70
A Case Study on Soil Erosion and Risk Assessment in Thandava Reservoir Catchment, Visakhapatnam District, A.P.—A Geo-spatial Approach

Madhuri Mulpuru, Peddada Jagadeeswara Rao and T. Sridevi

Abstract Soil erosion by water occurs throughout the world, especially more in the humid/sub-humid mountainous region. It is the process of detachment or entrainment, transportation of surface soil particles from original location and accumulation of it to new depositional area. This research paper aim to study the soil erosion risk assessment. Remote sensing has become significant source by providing synoptic real-time and accurate data related to land and soil. It enables homogeneous information over large area with high temporal resolution, and can therefore greatly contribute to assess reliable regional erosion (Siakeu and Oguchi 2000; King and Delpont 1993). A GIS can be used to scale up to regional levels and to quantify the differences in soil loss estimates produced by different scales of soil mapping used as a data layer in the model. The integrated use of remote sensing and GIS could serve to assess quantitative soil loss at several scales and also to identify the potential risk areas for soil erosion (Sahaatel 1992). Several studies showed the potential utility of GIS technique for quantitatively assessing soil erosion hazard based on various models (Sahaatal 1992; Shrestha 1997; Suresh Kumar and Sharma 2005). Bear on our mind the above discussion, the present study aims at characterizing the land resources through remote sensing and other ancillary data and to integrate these information in GIS to compute quantitative soil loss using RUSLE model for sustainable development.

Keywords Toposheet · DEM · GIS · RUSLE calculations

M. Mulpuru (✉)
Department of Civil Engineering, Malla Reddy Institute of Technology, Secunderabad, India
e-mail: madhurimulpuru@gmail.com

P. J. Rao · T. Sridevi
Department of Geo-Engineering, College of Engineering (A), Andhra University, Visakhapatnam, India
e-mail: pjr_geoinfo@rediffmail.com

T. Sridevi
e-mail: srice2001@gmail.com

P. J. Rao et al. (eds.), *Proceedings of International Conference on Remote Sensing for Disaster Management*, Springer Series in Geomechanics and Geoengineering,
https://doi.org/10.1007/978-3-319-77276-9_70

1 Introduction

Soil erosion by water occurs throughout the world, especially more in the humid/sub-humid mountainous region. It is the process of detachment or entrainment, transportation of surface soil particles from original location and accumulation of it to new depositional area. Various human activities disturb the land surface of the earth, and thereby induce the significant alteration of natural erosion rates. Soil erosion by running water has been recognized as the most severe hazard threatening the protection of soil as it reduces soil productivity by removing the most fertile topsoil. In the world map on the status of human-induced soil degradation (UNEP/ISRIC 1990), it is accounted that loss of topsoil and terrain deformation due to soil erosion are the consequence of deforestation, removal of natural vegetation and overgrazing in the mountainous regions (Shrestha 1997). Soil erosion is a global environmental crisis in the world today that threatens natural environment and also the agriculture. The soil erosion risk assessment can be helpful for land evaluation in the region where soil erosion is the main threat for sustained agriculture, as soil is the basis of agricultural production.

2 Study Area

The non-perennial Thandava reservoir catchment area is located in the hilly terrain of the Eastern Ghats region of Visakhapatnam district, Andhra Pradesh. The catchment area of Thandava reservoir is 467 km^2 and constructed with the gross storage capacity of 4960 Mcft. It is a major category non-perennial river with one tributary namely Bodderu (ThandavaNadi). Thandava reservoir is located between 17° 45′ 50″ North latitude and 82° 15′ 20″ East longitude. The study area is covered in the survey of India toposheet 65K/5, 65K/6, 65K/9, 65K/10 on 1:50,000 scale and IRS-1D-LISS-III digital data of 2011 have been used for extraction of thematic information on the drainage pattern, geomorphology, geology, and soils. The reservoir drainage pattern gives the information about the land evaluation in the region where soil erosion effects (Fig. 1).

3 Objectives

Remote sensing provides significant source for real-time and accurate data related to land and soil. It enables homogeneous information over large regions, and can therefore greatly contribute to regional erosion assessment (King and Delpont 1993; Siakeu and Oguchi 2000). A GIS can be used at regional level scales to quantify the deviation in soil loss estimates produced the model by considering soil map data layer at different scales. The integrated use of remote sensing and GIS could help

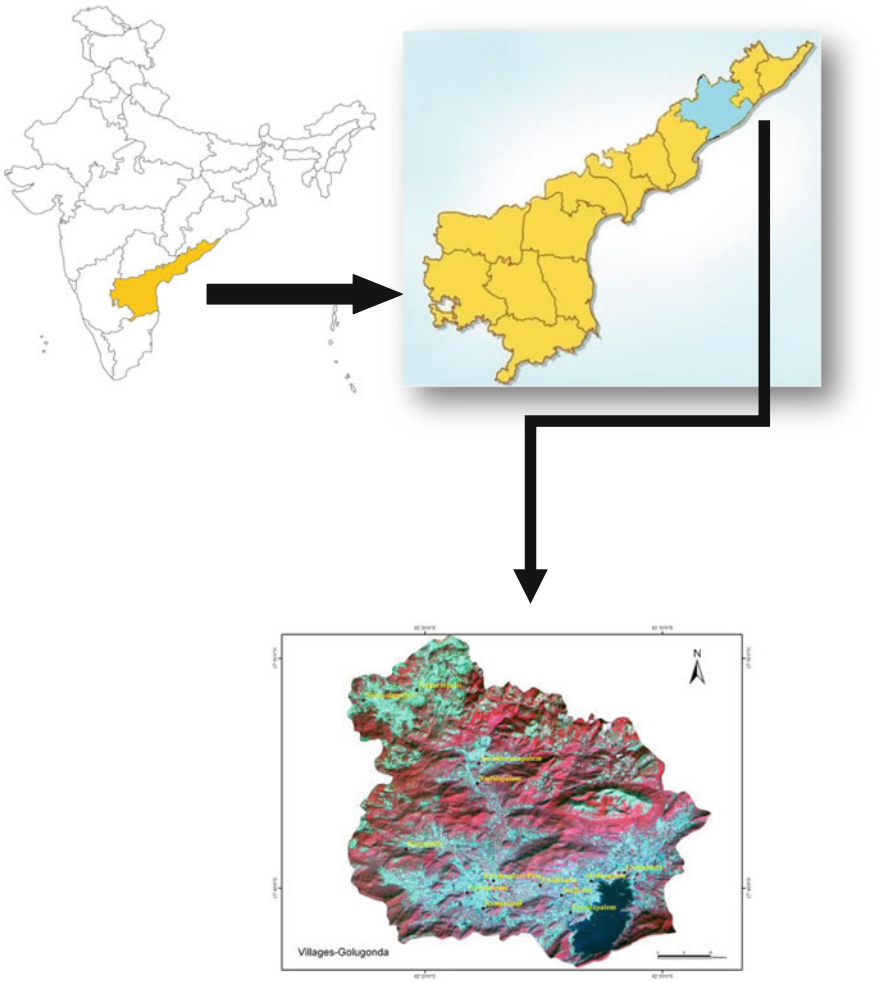

Fig. 1 Base map of Thandava reservoir

to assess quantitative soil loss at various scales and also to identify areas that are at potential risk of soil erosion (Sahaatel 1992). Several studies showed the potential utility of GIS technique for quantitatively assessing soil erosion hazard based on various models (Sahaetal 1992; Shrestha 1997; Suresh Kumar and Sharma 2005). Bear on your mind the above discussion, the present study aims at characterizing the land resources through remote sensing and other ancillary data and to integrate these informations in GIS to compute quantitative soil loss using RUSLE model for sustainable development.

4 Methodology

Using SOI toposheet, the contour lines with vertical elevation intervals of 20-m were traced on tracing sheet based on visual interpretation method. This manually traced contour map have been exported into GIS platform and perform visual based digitization to prepare vector layer. The elevation data were processed followed by graphic simulation was carried out in which an elevation (or Z profile) was recorded at every X, Y location to make topographic data more useful. Surfacing function in "Image Interpreter" was used to generate a DEM, which is a one-band image, to represent as topography where the pixel value indicates the elevation. A gray scale was used to differentiate variations in terrain and in the mean time ASTER 30 m resolution DEM data was draped on the contour based DEM for further clarification. Slope map was generated in ArcGIS 9.3 software by using DEM.

Soil erosion can be estimated using erosion models. Many of the complex interactions that influence rates of erosion have been considered in soil erosion modeling by simulating erosion processes in the watershed. The arbitrary information related with soil type, landuse, landform, climate and topography are required by most of these models to estimate probable soil loss. They are intended for particular set of conditions of specific area. The Universal Soil Loss Equation (USLE) (Wischmer and Smith 1965) was intended to anticipate soil loss from sheet and rill erosion in particular conditions from agriculture fields. The modified version of USLE, Modified Universal Soil Loss Equation (MUSLE) (Williams and Berndt; Meyer 1975), is applicable to different conditions by considering hydrological runoff factor for sediment yield estimation. The process based continuous simulation model, Water Erosion Prediction Project (WEPP) (Lane and Nearing 1989), had developed to replace USLE (Okoth 2003). Areal non-point source watershed environment response simulation (ANSWERS) (Beasley et al. 1980) intended to estimate soil erosion inside a watershed. The European Soil Erosion Model (EUROSEM) (Morgan et al. 1991, 1992) is a solitary process-based model for surveying and hazard forecast of soil disintegration from fields and small catchments. The mean annual soil loss can be derived from Morgan, Morgan and Finney (MMF) model (Morgan et al. 1984), which is an empirical model, based on field-sized areas on hill slopes with strong physical base.

5 Revised Universal Soil Loss Equation (RUSLE) Calculation

The factors causing erosion such as climate, soil properties, vegetation cover and management practices are considered for estimating soil loss. The RUSLE equation is a multiplicative function of five factors controlling the rill and inter-rill erosion [1] and can be expressed as:

Table 1 Soil erosion risk classes and equivalent RUSLE values [19]

Soil erosion risk class	RUSLE value
Very low	(0–5 ton/ha * year)
Low	(5–12 ton/ha * year)
Medium	(12–25 ton/ha * year)
High	(25–60 ton/ha * year)
Very high	More than (60 ton/ha * year)

$$A = R * K * LS * C * P \quad (1)$$

where:

A is the mean annual soil loss expressed in ton\ha * year
R is rainfall and runoff erosivity index (in MJ * mm\ha * year)
K is soil erodibility factor (in ton * ha * h/ha * MJ * mm)
LS is slope Steepness and slope Length factor (dimensionless)
C is the cover factor (dimensionless)
P is the conservation practice factor (dimensionless).

The final quantitative RUSLE values shows the quantity loss of soil in ton/ha per year, ranging from less than 1 to very high soil loss rates (223.6 ton/ha). For a better visual understanding of these quantities, RUSLE values have been grouped in five classes of soil erosion risk following Bergsma classification (Table 1) [5, 19].

The first two classes are considered in the range of soil loss tolerance values. Medium and high classes need conservation applications to maintain a sustainable productivity, while the last class (very high), is very dangerous because it can be destructive in few years if no intervention are done and soil loss level is maintained constant in the future. Not relevant (NR) polygons correspond to villages, urban areas and water bodies, which has not been considered in the evaluation.

Soil erosion risk map (Fig. 2) has been generated by applying the final RUSLE values on the land unit map which had been created in ArcGIS 9.3 through raster calculator. Figure 2 shows the soil erosion risk map for the study area. In order to better understand the results, it is important to analyze them in relation with soil, morphological and topographical characteristics, paying attention even to the land cover.

6 Results and Conclusion

The RUSLE model show that, very low and low classes erosion are scattered in the upper most part of the study area due to the structured topographical nature of the Land Units and represent almost 25.9% of the study area. The Very Low class is occupying 8.47% of the study area in correspondence to deciduous forest coverage, where the low erosion risk class allows the forest to keep reserved and conserved. These types of soils are deeper and have better permeability than in other places

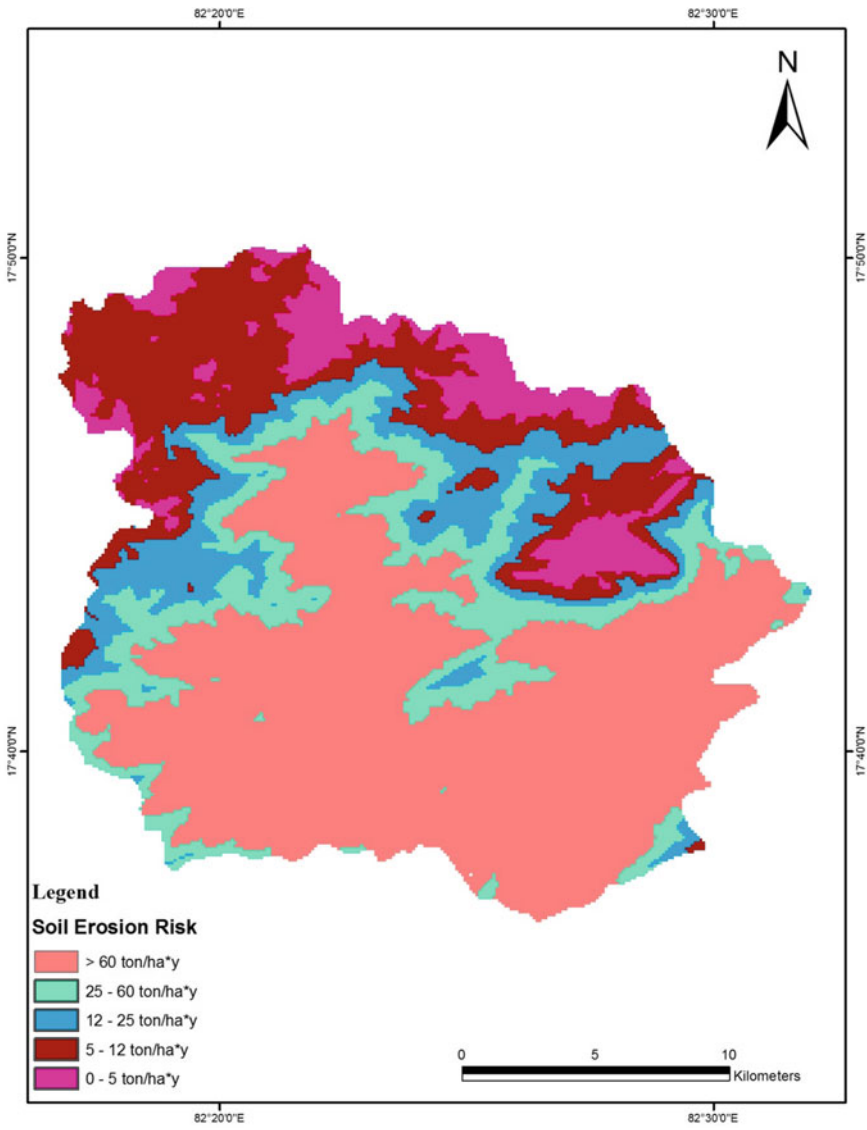

Fig. 2 Erosion risk map

of the study area because of the structured morphology which enables conserving of soil sediments lost by erosion due to runoff. Low class is occupying 17.44% of the study area and has been found in the Jadumulu, Sitarampadu, and Totamamidividi village. The increasing of soil loss amount is mainly due to slightly greater inclinations in comparison with the previous landforms. The Medium class in the study

area is only in KitapParvatam and Somagiri and some pocket areas as 11% of the study area. In this case, the combination of the different factors computing soil loss rates gives an intermediate situation.

The High class is mainly concentrated in the Singadhar, Domalagonda and Gopararam representing 13.88% of the study area. In both places slope length factor is increasing considerably and the absence of stone bunds along the contours allows a significant loss of soil, which is not sufficiently stopped by land cover (scrubs). The most dangerous situation (Very High class), has been found in correspondence to strongest slopes, absence of soil conservation practices and low vegetation cover to face the strong water erosion. Surprisingly this class is occupying 49.19% of the study area that accompanied with valley fill which excessively observed in Sarabhannapalem, Bangarampeta, Krishnadevipeta, Totaluru, nagapuram and Jagampeta. The uncertainties regarding data sources may introduce larger uncertainties in soil erosion estimates. Great attention should be paid to the evaluation and preprocessing of data sources, such as data interpolation, conversion, and registration.

References

1. Renard, K.G., Foster, G.R., Weesies, G.A., McCool, D.K., Yoder, D.C.: Predicting Soil Erosion by Water: A Guide to Conservation Planning with the Revised Universal Soil Loss Equation (RUSLE). U.S. Department of Agriculture, Agriculture Handbook, No. 703, p. 404 (1997)
2. Wischmeier, W.H., Smith, D.D.: Predicting Rainfall Erosion Losses: A Guide to Conservation Planning. Agriculture Handbook No. 537. USDA/Science and Education Administration, US. Govt. Printing Office, Washington, DC, 58pp (1978)
3. Kinnell, P.I.A.: Raindrop impact induced erosion processes and prediction: a review. Hydrol. Process. **19**, 2815–2844 (2005)
4. Giordani, C., Zanchi, C.: Elementi di conservazionedelsuolo. Bologna. p. 260 (1995)
5. Lu, D., Li, G., Valladares, G.S., Batistella, M.: Mapping soil erosion risk In Rondonia, Brazilian Amazonia: using RUSLE, remote sensing and GIS. Land Degrad. Dev. **15**, 499–512 (2004)
6. Arnoldus, H.M.J.: Predicting soil losses due to sheet and rill erosion, pp. 99–124. Land Water Development Division in Guidelines for Watershed Management FAO, Rome (1977)
7. Poesen, J.W., Torri, D., Bunte, K.: Effects of rock fragments on soil erosion by water at different spatial scales: a review. CATENA **23**, 141–166 (1994)
8. Hairsine, P.B., Rose, C.W.: Modeling water erosion due to overland flow using physical principles. 2. Rill flow. Water Resour. Res. **28**(1), 245–250 (1992)
9. Hoyos, N.: Spatial modeling of soil erosion potential in a tropical watershed of the colombian Andes. CATENA **63**, 85–108 (2005)
10. Jha, M.K., Paudel, R.C.: Erosion predictions by empirical models in a mountainous watershed in Nepal. J. Spat. Hydrol. **10**(1), 89–102 (2010)
11. Andrade, O., Kappas, M., Erasmi, S.: Assessment of erosion hazard in torres municipality of LARA State (Venezuela) based on GIS. Interciencia **36**(5), 348–356 (2010)
12. Foster, G.R., Yoder, D.C., Weesies, G.A., Mccool, D.K., Mcgregor, K.C., Bingner, R.L.: User's Guide, Revised Universal Soil Loss Equation, Version 2 RUSLE2, p. 77. USDA Agricultural Research Service Washington, D.C. (2003)

13. Nyssen, J., Gebremichael, D., Vancampenhout, K., Poesen, J., Deckers, J., Yihdego, G., Govers, G., Kiros, H., Haile, M., Moeyerons, J., Naudts, J., Haregeweyn, N.: Interdisciplinary on-site evaluation of stone bunds to control soil erosion on cropland in Northern Ethiopia. Soil Tillage Res. **94**, 151–163 (2007)
14. Milward, A.A., Mersy, J.E.: Adapting RULSE to model soil erosion potential in a mountainous tropical watershed. CATENA **38**, 109–129 (1999)
15. Reusing, M., Schneider, T., Ammer, U.: Modeling soil erosion rates in the Ethiopian Highlands by integration of high resolution MOMS-02/D2-stereo-data in a GIS. Int. J. Remote Sens. **21**, 1885–1896 (2000)
16. Angima, S.D., Stott, D.E., O'neill, M.K., Ong, C.K., Weesies, G.A.: Soil erosion prediction using RUSLE for central Kenyan highland conditions. Agric. Ecosyst. Environ. **97**, 295–308 (2003)
17. Ma, J.W., Xue, Y., Ma, C.F., Wang, Z.G.: A data fusion approach for soil erosion monitoring in the Upper Yangtze River Basin of China based on Universal Soil Loss Equation (USLE) model. Int. J. Remote Sens. **24**, 4777–4789 (2003)
18. Sonneveld, B.G.J.S., Keyzer, M.A., Albersen, P.J.: A non-parametric analysis of qualitative and quantitative data for erosion modeling: a case study for Ethiopia. In: Sustaining the Global Farm. Selected Papers of the ISCO 1999 Conference, pp. 979–993. Purdue University, West Lafayette, Indiana (1999)
19. Bergsma, E.: Aspects of mapping units in the rain erosion hazard catchment survey. In: Siderius, W. (ed.) Wageningen (Netherlands), No. 40. International Workshop on Land Evaluation for Land-Use Planning and Conservation in Sloping Area. Enschede (Netherlands) pp. 17–21, 84–104 (1986)
20. Sadeghi, S.H.R., Moatamednia, M., Behzadfar, M.: Spatial and temporal variations in the rainfall erosivity factor in Iran. J. Agric. Sci. Technol. **13**, 451–464 (2011)
21. Efe, R., Ekinci, D., Curebal, I.: Erosion analysis of Sahin Creek Watershed (NW of Turkey) using GIS based on RUSLE (3d) Method. J. Appl. Sci. **8**(1), 49–58 (2008)
22. Stone, R.P., Hilborn, D.: Universal Soil Loss Equation (USLE), Agricultural and Rural Ministry of Agriculture, Food and Rural Affairs, Ontario, Canada (2000). Available at http://www.gov.on.ca/OMAFRA/english/engineer/facts/00-001.htm. Accessed 5 Feb 2011

Chapter 71
Spatial Distribution of Groundwater Quality Parameters in Amaravathi Region—A GIS and Remote Sensing Approach

J. Netaji, G. N. M. Lavanya, P. Srinivas, K. Govind Sourabh and G. Bhogayya Naidu

Abstract Groundwater is the most important natural resource required for drinking to many people around the world, especially in rural areas. The resource cannot be optimally used and sustained unless the quality of groundwater is assessed. The study described here uses geographic information system (GIS) technology to map groundwater quality for drinking and construction, utilizing data generated from chemical analysis of water samples collected from the area under study. In this work, we are going to study various geographical features of Amaravathi by collecting different types of data related to ground water. All this data is used to interpret a map and digitize it with the help of Q-GIS software. Using GIS contouring methods, spatial distribution maps of pH, TDS, TH, Cl, HCO_3, SO_4, NO_3, Ca, Mg, Na and K, have been created. Form this map one can easily assess the quality of water present at various places of this area and also it helps in taking decision of what are the improvements that are to be made in the water usage and its quality. The physico-chemical results were compared to the standard guideline values as recommended by the World Health Organization (WHO) for drinking and public health in order to have an overview of the present groundwater quality.

J. Netaji (✉) · G. N. M. Lavanya · P. Srinivas · K. Govind Sourabh
Department of Geo-Engineering, Andhra University, Visakhapatnam, India
e-mail: netajigangulian@gmail.com

G. N. M. Lavanya
e-mail: gnmlavanya@gmail.com

P. Srinivas
e-mail: srinivaspatnala1995@gmail.com

K. Govind Sourabh
e-mail: govindsourabh511@gmail.com

G. Bhogayya Naidu
V. R. Siddhartha Engineering College, Vijayawada, India
e-mail: gudivadaaditya2011@gmail.com

P. J. Rao et al. (eds.), *Proceedings of International Conference on Remote Sensing for Disaster Management*, Springer Series in Geomechanics and Geoengineering,
https://doi.org/10.1007/978-3-319-77276-9_71

Keywords Q-GIS · Chemical analysis · Quality maps · pH · Sulphates content Chlorides content · Total hardness · Total dissolved solids · Sodium content Carbonate hardness · Calcium content

1 Introduction

GIS in Water Resource Engineering presents a review of the concepts and applications of GIS in the various sub-fields of water resource engineering. After a summary review of analyses and database functions, the book addresses concepts and applications in the respective areas:

Surface Water Hydrology, Groundwater Hydrology, Water Supply and Irrigation systems, Wastewater and Storm water Systems, Floodplain Management, Water Quality, Water Resource Monitoring and Forecasting, River Basin Planning and Management.

In this work we are going to map the ground water quality parameters of Amaravathi region. This is done using the software QGIS [1] the details of water quality of the region are collected and are plot on a map using the techniques in QGIS by this project we are going to gain knowledge of quality of ground water in this area and what are the measures to be taken in order increase the quality if there any impurities or irregular properties QGIS is free and open source software.

Using GIS contouring methods [2, 3], spatial distribution maps of pH, TDS, TH, Cl, HCO_3, SO_4, NO_3, Ca, Mg, Na and K, have been created. An interpolation technique, ordinary Inverse Distance Weighted (IDW), was used to obtain the spatial distribution of groundwater quality parameters.

2 Materials and Methods

The proposed capital region of Andhra Pradesh is taken as the area of interest in order to perform this water analysis as this is the developing area due to the capital one has very use by knowing the quality of water one requires the quality of water at that area. The area consists of places in and around Thulluru which is central part of our proposed capital city. The area extends from bank of Krishna river and is extends up to Mangalagiri and Vaikuntapuram on other side it is spread in the area of 200 km^2. Dependency on groundwater is currently very high and it is preferred for drinking purpose by large number of the population. Because of the inadequacy and concern over quality of tap water, ground water will continue to be a significant source of domestic water supply for this city (Fig. 1).

Amaravathi is the recent developing city and many changes are going to take place in this region based on various aspects population may increase very rapidly and it is necessary to supplies adequate amount of water to the people who are

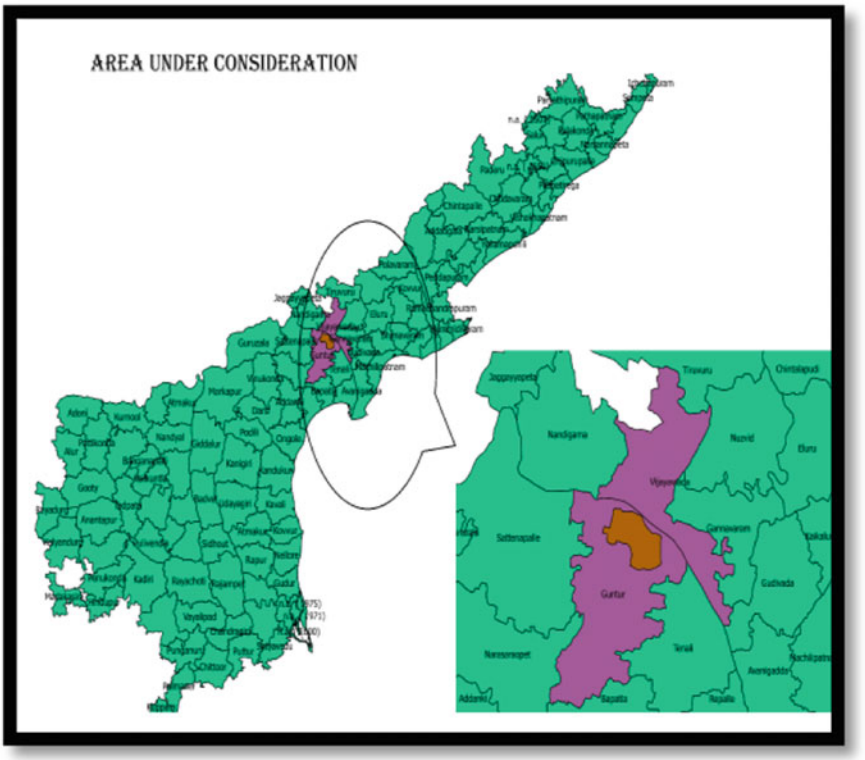

Fig. 1 .

ought to come and many industries and other companies are going to be established in future so it is very important to know about the quality of water at this region as it is the very essential to survive.

2.1 Ground Water Sample Collection and Analysis

As a part of study the ground water samples from various regions of the city are collected for testing [4]. The samples are taken from various villages. The samples taken are analyzed for various physico-chemical parameters. Bottles used for water sample collection are first thoroughly washed with the water being sampled and then were filled. After collection of the samples, the samples are preserved and shifted to the laboratory for analysis (Table 1).

Table 1 Attribute table showing the various chemical properties of ground water

S. No	1	2	3	4	5	6	7	8
Details of sample	Penumaka	Rayapudi	Pedaparimi	Mangalagiri	Amaravathi	Vykuntapuram	Mandadam	Pedamadduru
Type of well	PZ	PZ	PZ	OB	PZ	PZ	OB	OB
T.D.S	751	1176	2273	960	3043	1980	2575	1391
Bicarbonate hardness	140	90	50	110	160	80	50	140
Cl (mg/L)	152	410	520	390	656	560	390	480
SO_4 (mg/L)	51	60	770	167	1225	390	535	115
Na (mg/L)	143	199	422	230	725	284	366	68
Ca (mg/L)	8	24	48	8	48	48	184	160
Mg (mg/L)	58	78	175	44	160	141	160	131
K (mg/L)	3.2	87.5	49.5	2.8	52	188	2.8	45
T.H as $CaCO_3$	260	380	840	200	780	700	1120	940

3 Preparation of Water Quality Maps

The locations of the various points in the city are collected such as the location of each village in the study area is collected by using hand held GPS trackers. The latitude longitudes of these points are noted in a tabular form.

3.1 Coordinate Reference System

It is the reference system of points i.e., any point collected on the ground refers to a certain point the points are calculated as a distance from one fixed point each country has its own coordinate reference system. One need to specify this system in order to locate the points collected in site exactly place at the respective points in maps (Fig. 2).

The points are thus located in the map and then the area of interest is located on map by tracing and joining feature boundaries by using add feature option which is located in toolbar of q-gis and then the area is clipped in order to get only the area that we are opted to study this layer may be saved as different shape file the data now obtained is the vector data.

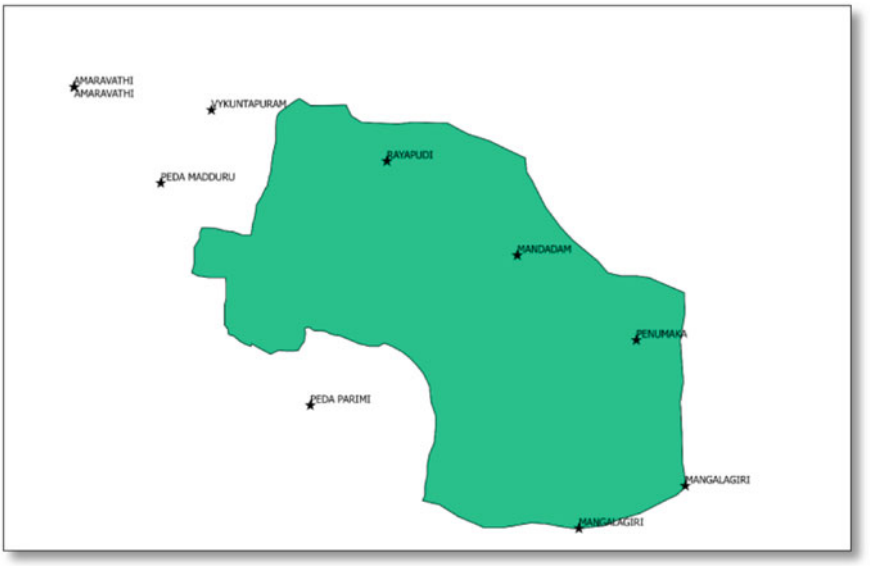

Fig. 2 .

3.2 *Collection of Coordinate Points*

The coordinates of the bore wells present in each village of the amaravathi region are found by using the hand held GPS tracker. The presence of bore wells in the areas are known previously and then their location with latitude and longitude are located just by placing this instrument over that and by just tracing the location these data is noted down in a prescribed manner for future use. The trackers works on the CRS principle i.e., the locations are given corresponding to the CRS of our country.

4 Maps of Various Properties in pH

pH may be defined as the negative logarithm of the hydrogen ion concentration measured in moles per liter. Acidic water has a pH below 7; alkaline water, above 7. The health effects of pH on drinking water depend upon where the pH falls within its range. The U.S. Environmental Protection Agency, which classifies pH as a secondary drinking water standard, recommends a pH between 6.5 and 8.5 for drinking water (Figs. 3 and 4).

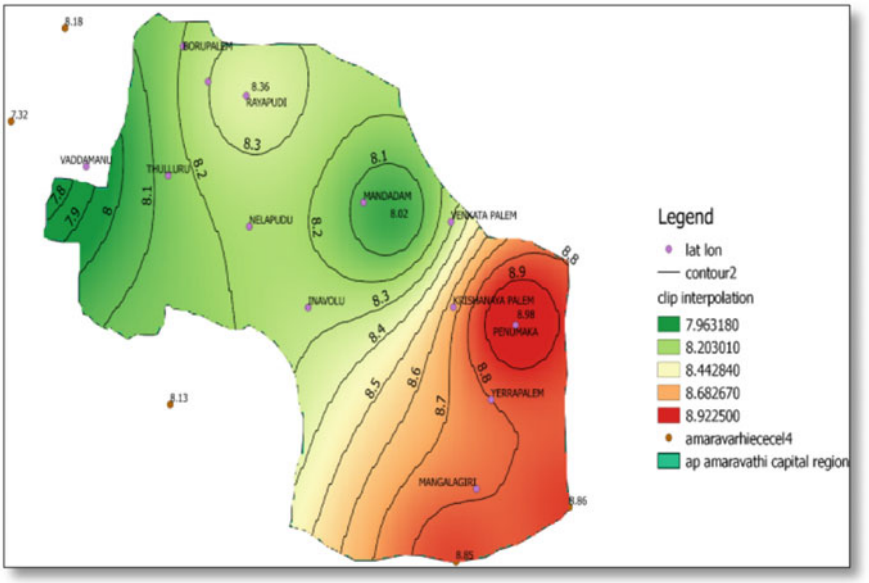

Fig. 3 .

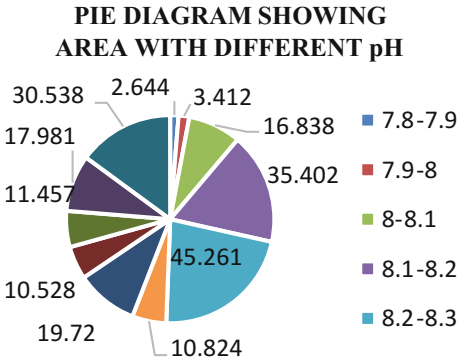

Fig. 4 .

5 Sulphates Content in Considered Area

Sulphate may have a laxative effect that can lead to dehydration and is of special concern for infants. With time, people and young livestock will become acclimated to the sulphate and the symptoms disappear. Sulphur-oxidizing bacteria pose no known human health risk. The Maximum contaminate level is 250 mg/L (Figs. 5 and 6).

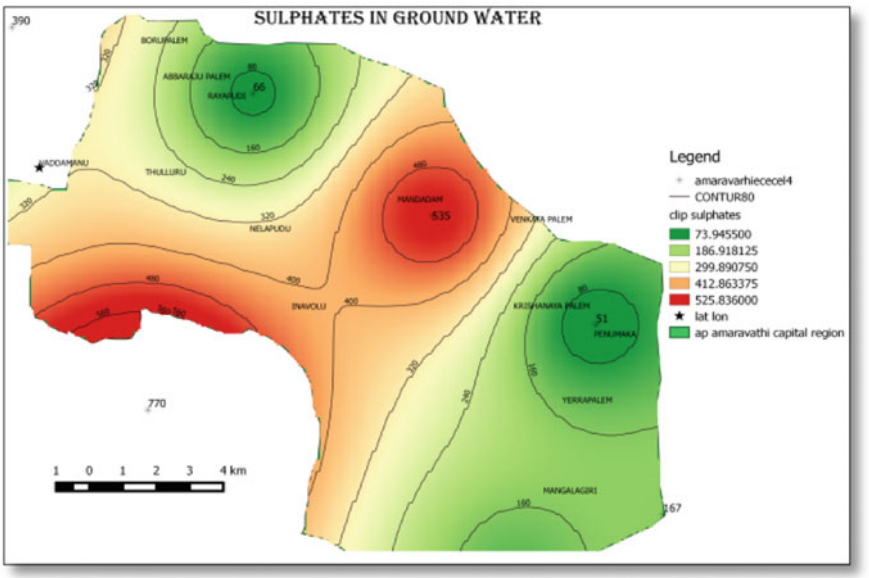

Fig. 5 .

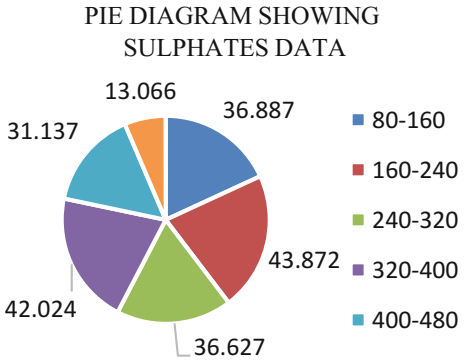

Fig. 6 .

6 Chlorides Content in Considered Area

Chloride is not toxic to human health at low levels but does pose taste and odor issues at concentrations exceeding 250 mg/L. The good news is that chlorides can easily be removed from water with either a reverse osmosis system or a distiller (Figs. 7 and 8).

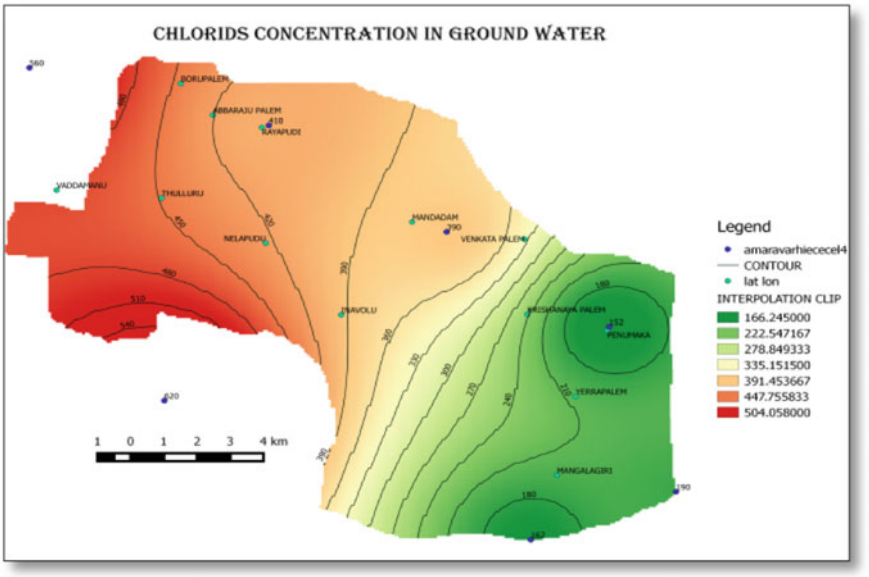

Fig. 7 .

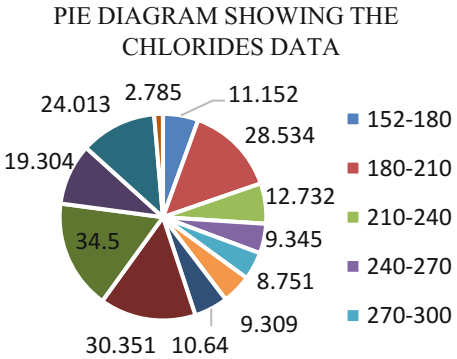

Fig. 8 .

7 Total Hardness Content in Considered Area

Total hardness is the combination of carbonate and bicarbonate hardness. Carbonate hardness caused duo to the presence of carbonates and bicarbonates of calcium and magnesium bicarbonate hardness is caused due to the aluminates and sulphates of calcium and magnesium (Figs. 9 and 10).

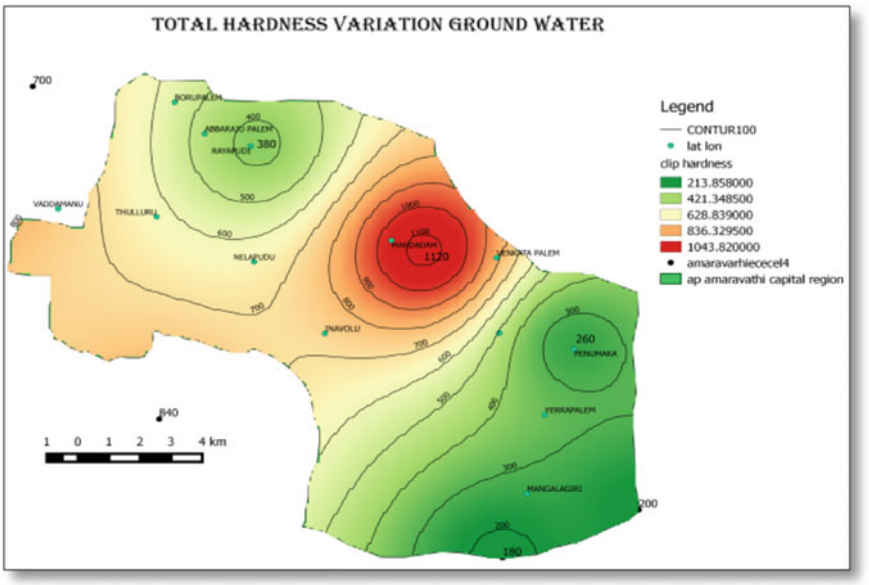

Fig. 9 .

Fig. 10 .

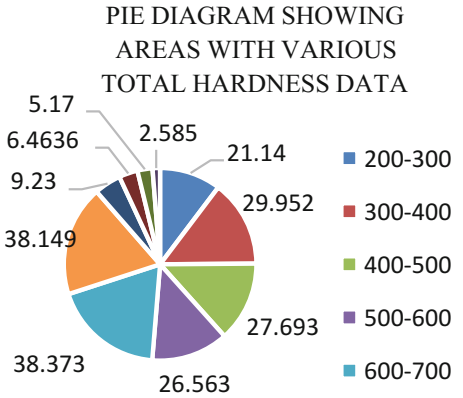

8 Total Dissolved Solids Distribution Map

A total dissolved solid (TDS) is a measure of the combined content of all inorganic and organic substances contained in a liquid in molecular, ionized or micro-granular (colloidal sol) suspended form. Total dissolved solids are differentiated from total suspended solids (TSS), in that the latter cannot pass through a sieve of two micrometers and yet are indefinitely suspended in solution The two principal methods of measuring total dissolved solids are gravimetric analysis and conductivity Total dissolved solids are normally discussed only for freshwater systems, as salinity includes some of the ions constituting the definition of TDS [5] (Figs. 11 and 12).

9 Map Representing the Sodium Content

Sodium is a common element in the natural environment and is often found in food and drinking-water. In drinking water, sodium can occur naturally or be the result of road salt application, water treatment chemicals or ion-exchange softening units. Sodium is not considered to be toxic. The human body needs sodium in order to maintain blood pressure, control fluid levels and for normal nerve and muscle function. Sodium is a mineral commonly found in food and water. Your body needs sodium daily to regulate fluids, maintain blood pressure, and for muscle and nerve functions. If the sodium concentration in your drinking water is 20 mg/L, drinking up to 2 L of water per day will add 40 mg of sodium to your diet, about 2% of a teaspoon of salt. For healthy adults, this sodium level in drinking water does not pose a risk (Figs. 13 and 14).

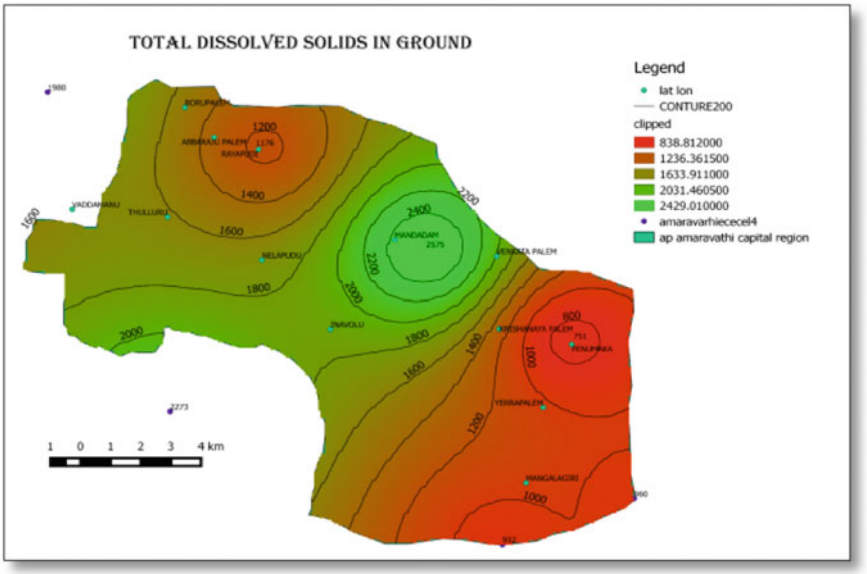

Fig. 11 .

Fig. 12 .

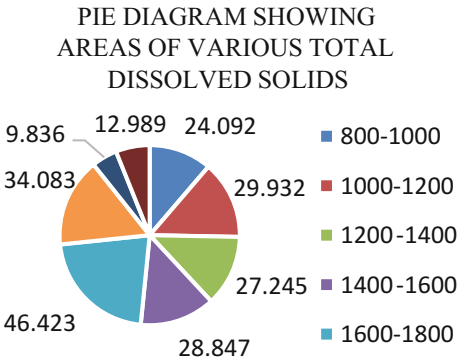

10 Map Representing the Calcium Content in the Area Considered

Calcium is LIKELY SAFE for most people when taken by mouth or when given intravenously (by IV) and appropriately. Calcium can cause some minor side effects such as belching or gas. Calcium is possibly unsafe for both adults and children when taken by mouth in high doses. Avoid taking too much calcium. The Institute

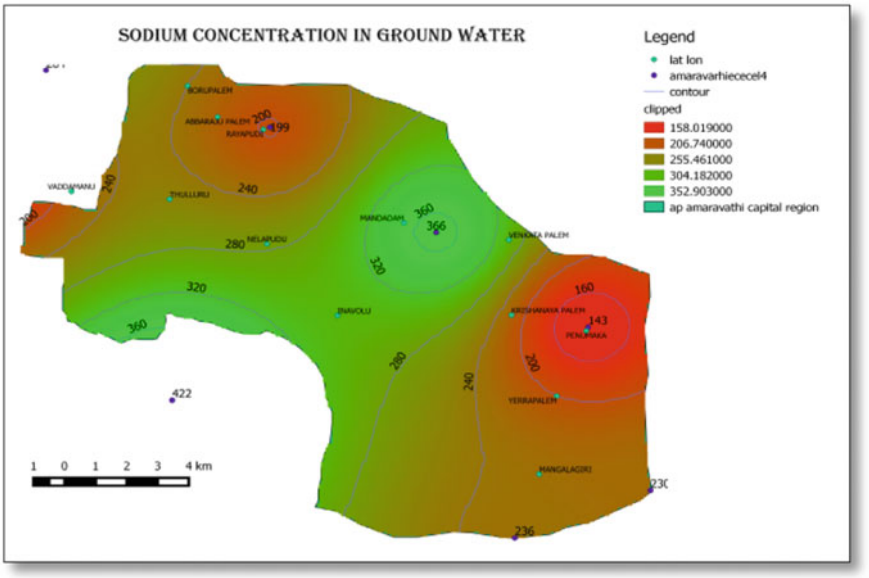

Fig. 13 .

Fig. 14 .

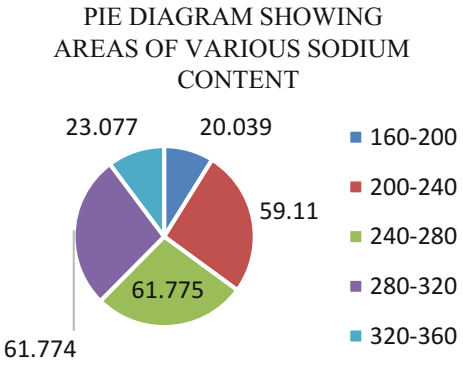

of Medicine sets the daily tolerable upper intake level (UL) for calcium based on age as follows: Age 0–6 months, 1000 mg; 6–12 months, 1500 mg; 1–8 years, 2500 mg; 9–18 years, 3000 mg; 19–50 years, 2500 mg; 51+ years, 2000 mg. Higher doses increase the chance of having serious side effects (Figs. 15 and 16).

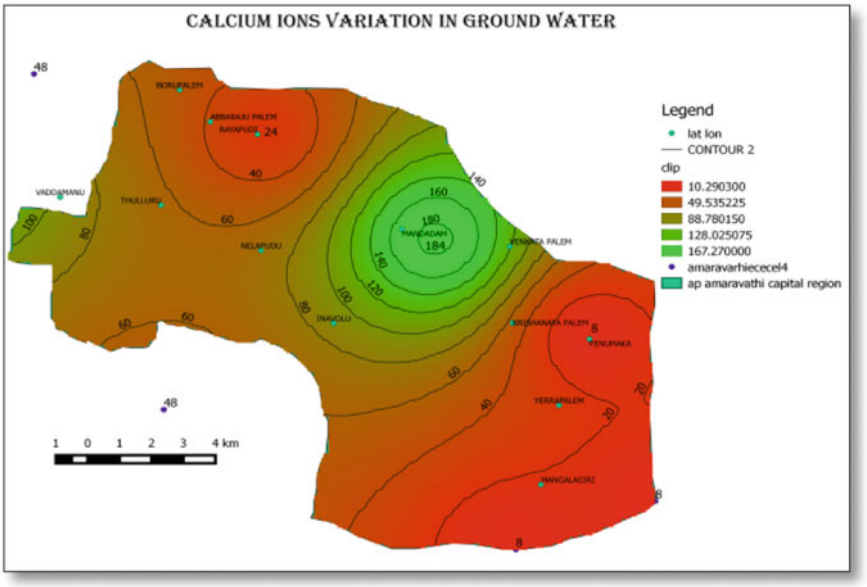

Fig. 15 .

Fig. 16 .

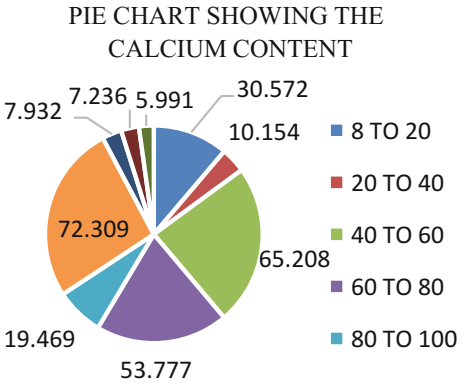

11 Carbonate Hardness Distribution Map

Carbonate hardness, or carbonate alkalinity is a measure of the alkalinity of water caused by the presence of carbonate (CO_3^{2-}) and bicarbonate (HCO_3^-) anions. Carbonate hardness is usually expressed either as *parts per million* (ppm or mg/L), or in degree KH (dKH) (from the German "*Karbonathärte*") (Figs. 17 and 18; Table 2).

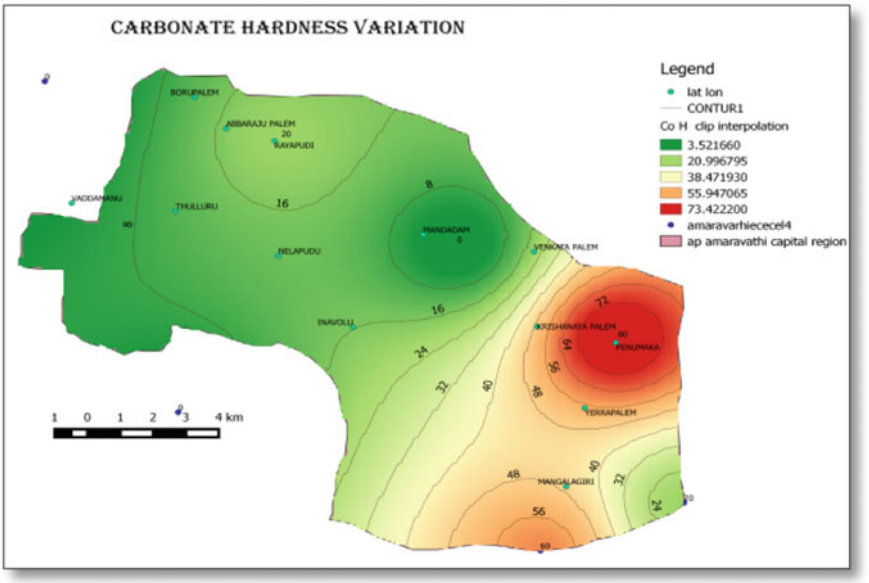

Fig. 17 .

Fig. 18 .

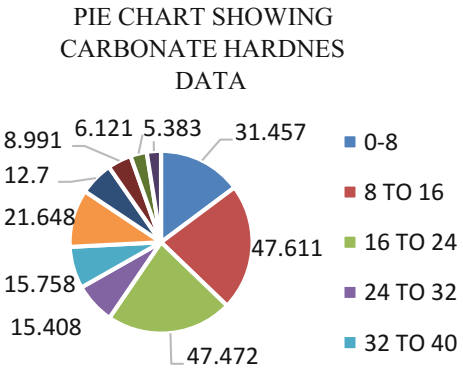

12 Results and Conclusions

In the present investigation an attempt was made to evaluate and to map ground water quality of Amravati region. Spatial distribution of ground water parameters was carried out through GIS. These groundwater quality maps are useful in assessing the usability of the water for different purposes. Moreover the maps are made in easily understood format using the GIS. It is shown that the majority of the samples presented a pH value within the maximum permissible limit, except for one or two samples which reflected a pH value exceeding this limit. The Water Quality

Table 2 Area within and beyond limits of various parameters

Parameter	Area within the limits (km^2)	Area beyond the limits (km^2)	Total area taken (km^2)
pH	139.496	70.504	210
Chlorides	70.33	139.67	210
Sulphates	87.56	122.44	210
Calcium	97.3	112.7	210
Magnesium	93.6	116.4	210
Total dissolved solids	153	56.908	210
Total hardness	110	99.97	210

Index is a very useful and an efficient tool to summarize and to report on the monitoring data to the decision makers after any disasters in order to be able to understand the status of the groundwater quality; and to have the opportunity for better use in future as well. From the above maps it is easily understood the quality scenario of the ground water distribution in our area. One can easily access the properties of water. It is seen that some of parameters are exceed in some of the regions in such regions the remedial measures may be taken in order to reduce the effect of the water. It is seen that from maps the water is somewhat within limits in regions of Thullur, Inavolu, Borupalem, Nelapudi. The water in these regions is within parameters.

References

1. Open Source GIS History—Osgeo Wiki Editors. Retrieved 21 Mar 2009
2. Cowen: 1988 GIS versus CAD versus DBMS: what are the differences? Photogramm. Eng. Remote Sens. **54**(11), 1551–1555 (1988)
3. Anji Reddy, M.: Remote Sensing and GIS. BS Publications, India (2008)
4. Mendham, J., Denney, R.C., Barnes, J.D., Thomas, M.J.K.: Vogel's Text Book of Quantitative Chemical Analysis, 6th edn. Prentice Hall, New York (2000)
5. Methods for Chemical Analysis of Water and Wastes. EPA Publication, March 1979. EPA#600/4-79-02
6. Fu, P., Sun, J.: Web GIS: Principles And Applications. ESRI Press, Redlands (2010). ISBN 1-58948-245-X
7. Foresman, T.: The History of GIS (Geographic Information Systems): Perspectives From The Pioneers (Prentice Hall Series In Geographic Information Science), 1st edn. Prentice Hall PTR; 416P (10 Nov 1997) (1997)
8. The Remarkable History of GIS—Geographical Information Systems: The Remarkable History of GIS. Retrieved 05 May 2015
9. American Public Health Administration (APHA): Standard Methods For The Examination of Water and Waste Water (1992)
10. Huisman, O., De By, R.A.: Principals of Geographic Information System. ITC Press, Enschede (2009)

Chapter 72
An Integrated Study on the Status of Surface Water Bodies in GVMC Area Using Geo-Spatial Technologies

L. Tejaswini, E. Amminedu and V. Venkateswara Rao

Abstract The Visakhapatnam Municipal Corporation (GVMC) area was 120 km^2 till January 2006 and now expanded to 540 km^2 by adding 32 villages and renamed as Greater Visakhapatnam Municipal Corporation. Major activity of the included villages was agriculture and the irrigation is through number of surface water bodies like ponds and tanks. After urbanization these became idle under encroached by public and private organizations for residential and other activities. There is a need for conservation of these water bodies for managing the urban storm water and useful for recharging the aquifers. Change of Land use pattern abruptly from rural to urban environment resulting in more runoff i.e. double to triple than the soil covered area. As per the topographic sheets 1976, the no. of water bodies in GVMC are 401 and the total area of these is 1097.32 ha. Water bodies area range between minimum 0.001618 ha and maximum 128.52 ha. Out of the 401 water bodies, 114 disappeared under major industries like Steel plant, NTPC and other residential areas. The total area of tanks lost due to the encroachment is about 263.96 ha and 84 water bodies are partially occupied or near to occupation in which 50.95 ha occupied by settlements and the remaining 235.65 ha are near to occupation. The remaining water bodies are 203 which are little away from the well developed centers and the area is about 546.72 ha. In future these may also get affected by the intense urbanization. The negative impact of occupancy of water bodies is already well experienced in the major cities like Chennai, Mumbai and Hyderabad. Keeping in view of the lessons learnt from these cities, water bodies are to be protected which are about to occupation. The main advantages of protecting the water bodies are: (i) to conserve the storm water and avoid inundation in the low lying areas, (ii) to recharge the ground water, (iii) to store the transported water from Godavari

L. Tejaswini (✉) · E. Amminedu · V. Venkateswara Rao
Department of Geo-Engineering, Andhra University, Visakhapatnam, India
e-mail: tejuishu93@gmail.com

E. Amminedu
e-mail: eamminedu@gmail.com

V. Venkateswara Rao
e-mail: vrvelagala@gmail.com

P. J. Rao et al. (eds.), *Proceedings of International Conference on Remote Sensing for Disaster Management*, Springer Series in Geomechanics and Geoengineering,
https://doi.org/10.1007/978-3-319-77276-9_72

flood flows by developing the existing water bodies. Some physical measures are suggested to conserve the water bodies.

Keywords GVMC · Disappeared tanks · Tanks under threat · Storm water management · Aquifer recharge

1 Introduction

Throughout history much of the world has witnessed ever-greater demands for reliable, high-quality and inexpensive water supplies for domestic consumption, agriculture and industry [1]. The urban growth has also affected water resources both, qualitatively and quantitatively in the region [2]. The effect of urbanization declines, in relative terms, as flood recurrence intervals increase [3]. Catchment urbanization can alter physical, chemical, and biological attributes of stream ecosystems. In particular, changes in land use may affect the dynamics of organic matter decomposition, a measure of ecosystem function [4]. The mechanisms of interactions between groundwater and surface water (GW–SW) as they affect recharge–discharge processes are comprehensively outlined, and the ecological significance and the human impacts of such interactions are emphasized [5]. The transformation of other land use types into urban area dynamically continued in the North-East and Southern parts of the city. In the North-East direction, the urban growth was mostly due to growth industrial and residential area in Southern part, mostly due to residential growth [6]. The effects of watershed urbanization on streams are well-documented.

2 Study Area

The study area Visakhapatnam Municipal Corporation (VMC) has extended its jurisdiction from 120 km^2 till 2006 to 540 km^2 in 2006 by engulfing 32 adjacent villages in the urban fringe areas in view of better development of the area and renamed as GVMC. The boundary covering the toposheets 65O/1NE, 65O/1NW, 65O/1SE, 65O/1SW, 65O/2NE, 65O/2NW, 65O/2SE, 65O/2SW, 65O/5NE, 65O/5NW, 65O/5SE, 65O/5SW and 65O/6NW on 1:25,000 scale. The area is bounded between 17° 53′ and 17° 86′ Northern Latitudes and 83° 08′ and 83° 40′ Eastern Longitudes. The location map of the study area is shown in Fig. 1.

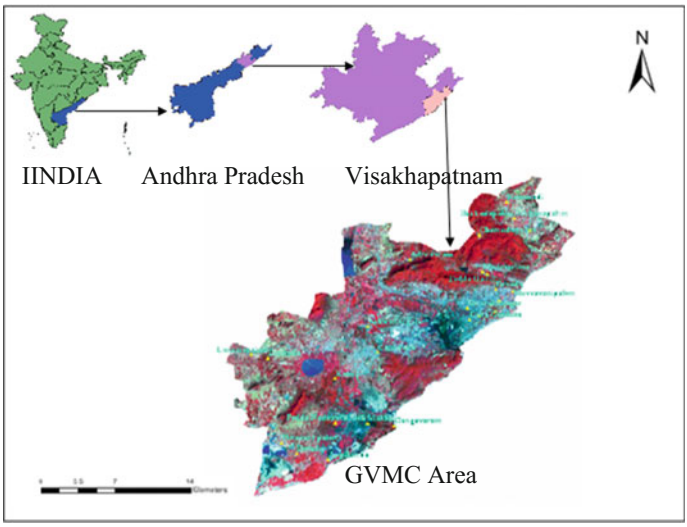

Fig. 1 Location map of the study area

3 Methodology

The Resourcesat-2; LISS-III satellite data of 2013 has been downloaded from the website www.bhuvan.nrsc.gov.in. The data mosaicked in ERDAS Imagine-2014, thereafter, extraction of water bodies is carried out in ArcGIS-10.3. Survey of India topographic sheets 65O/1, 65O/2, 65O/5, 65O/6 were Geo-coded in ERDAS Imagine-2014, finally it is updated using satellite imagery Resourcesat-2: LISS-III. The study area (AOI) is delineated on mosaicked satellite images. The methodology adopted in this study is shown in Fig. 2.

Flow chart:

See Figs. 3 and 4.

4 Categorization of Water Bodies

Surface water bodies mainly the tanks are categorized as per the present condition such as (i) tanks occupied or encroached between the year 1976 and 2014, (ii) tanks encroached partially or about to occupy by the urban development and (iii) tanks unaffected so far.

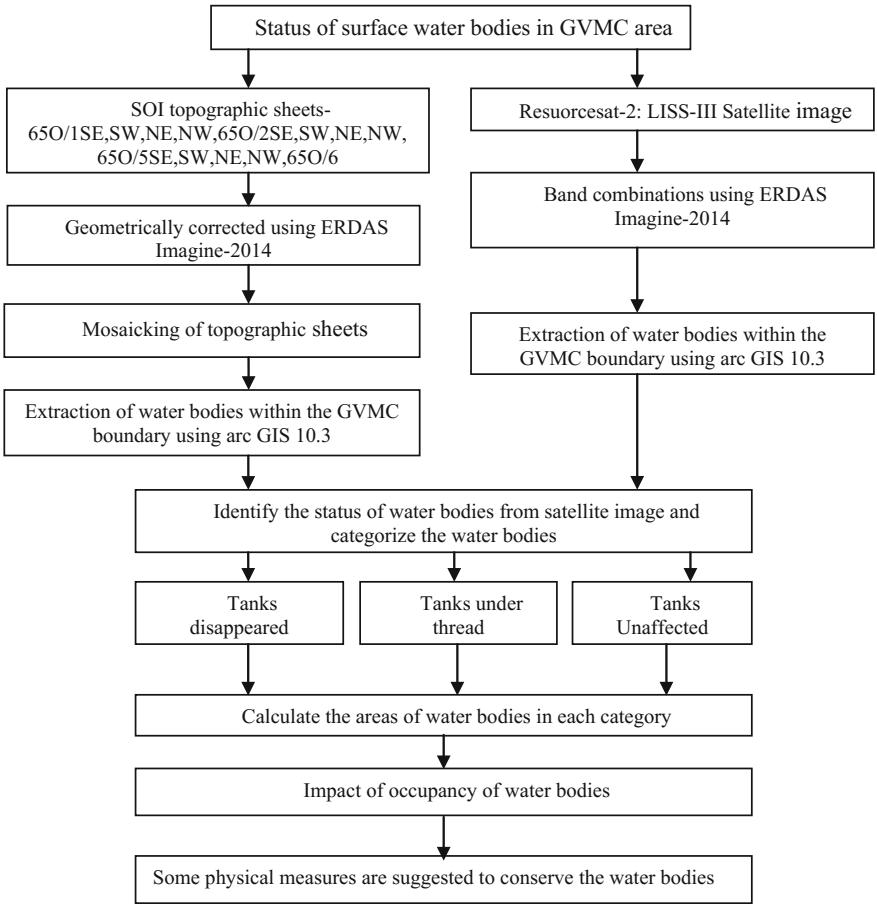

Fig. 2 Conceptual framework of the study area

4.1 Tanks Completely Encroached Between 1976 and 2013

The area of investigation is limited to GVMC area. In assigned areas of Visakhapatnam Steel Plant and NTPC, about 48 number of tanks disappeared and the total area of these tanks is about 134.27 ha and details of each category is listed in Table 1. Going by authentic topographic sheets of 1976 an example is shown in Fig. 5. The cricket stadium came up at Potina Mallayyapalem as shown in Fig. 6 is the place of two tanks of covering an area of 9.85 ha. In the earlier GVMC area, two tanks between Isukathota and Sitammadhara and one at Sivajipalem has completely occupied by the residents. And many tanks are disappeared under steel plant and NTPC. The tanks disappeared are identified in Fig. 5.

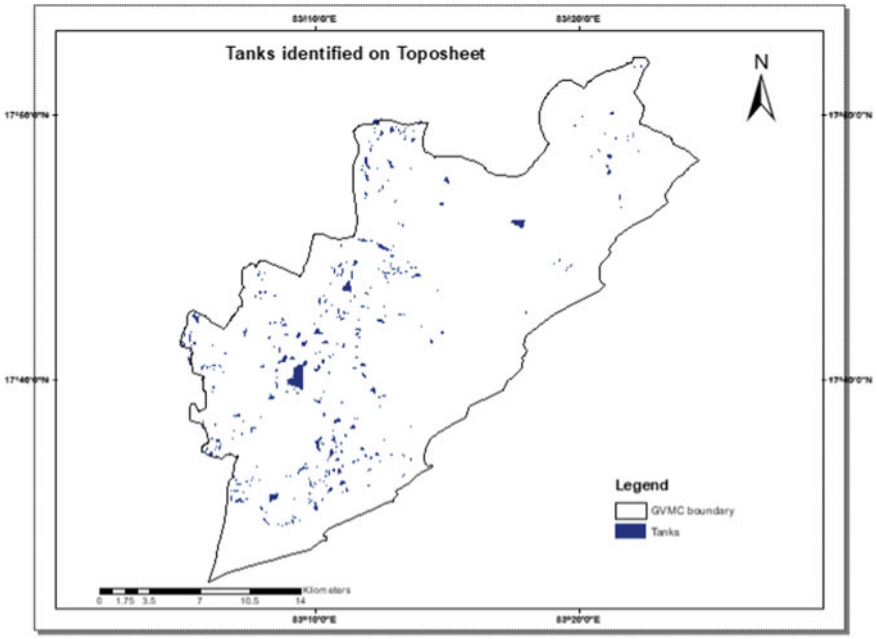

Fig. 3 Tanks extracted from the topographic sheets of SOI 1976

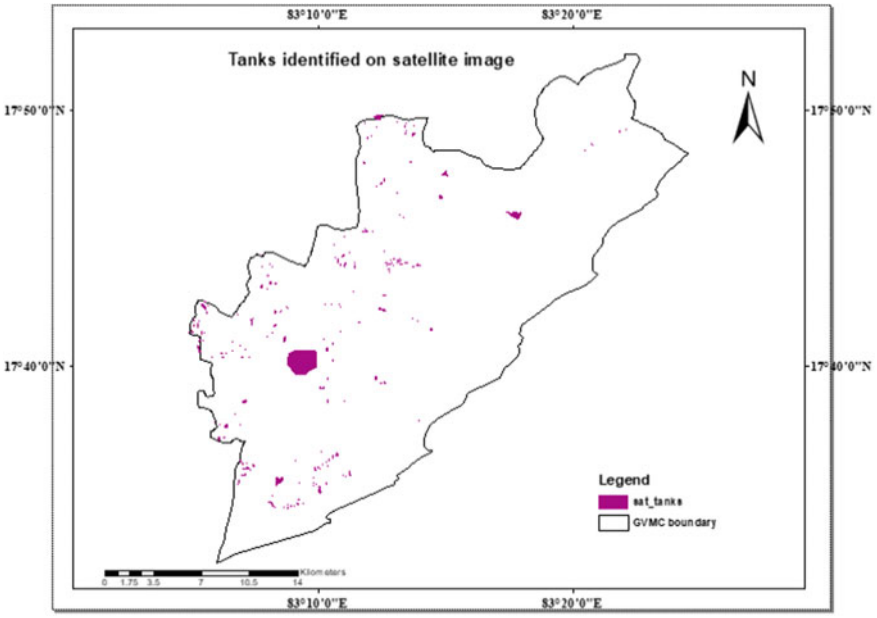

Fig. 4 Tanks identified from the Resourcesat-2: LISS-III sat image dated on 3rd Feb 2013

Table 1 Shows the categorization of water bodies

Category		No. of water bodies	Area in hectors
Disappeared water bodies		114	263.96
Tanks under threat	Occupied area	84	50.95
	Near to occupation		235.65
Tanks unaffected		203	546.72
Total		401	1097.32

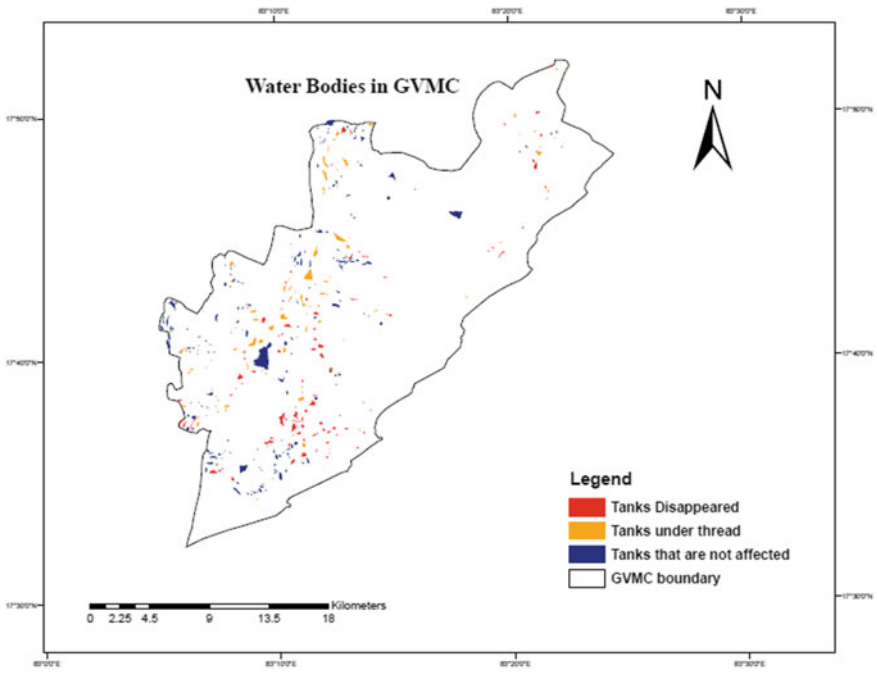

Fig. 5 Map shows the categorization of water bodies in GVMC area

4.2 Tanks Under Threat

The tanks under threat defines that they are in danger state or in a state where they are getting degraded. Examples for such tanks in our study area are Sujatanagar, Airport, Sakopuram area, Kottapalem and Silparamam–Madhrawada. Nearly 50% of Sujatanagar tank occupied between 2010 and 2016 and few satellite images acquired during that period is shown in Fig. 7. The tanks under the threat are identified Shown in Fig. 5.

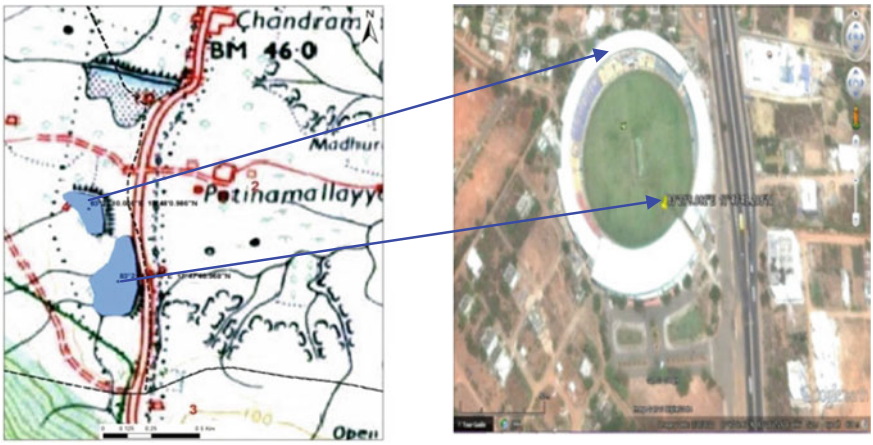

Fig. 6 Shows the tanks being occupied due to urban activity (Potinamallayyapalem stadium)

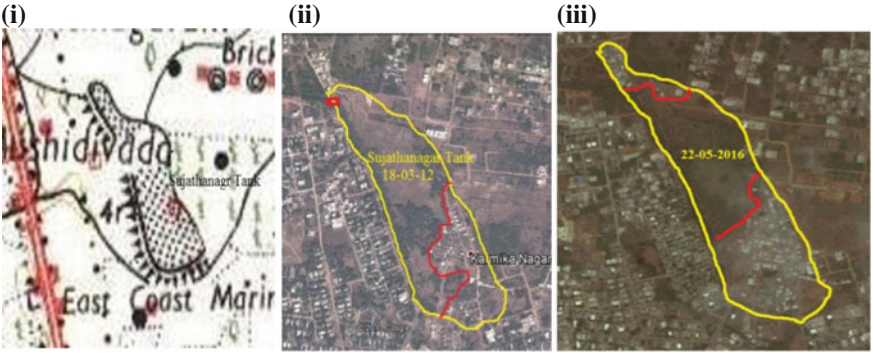

Fig. 7 (**i**) Shows the sujatanagar tank in topographic sheet 1976 (**ii**) & (**iii**) shows the occupation of sujatanagar tank images taken from the Google earth dated on 18-03-2012 & 22-05-2016

4.3 Tanks that Are Unaffected

These tanks are little away from the well developed canters. In future these may also get affected by the intense urbanization. These tanks are to be protected now itself to be available in future for management of urban storm water are shown in Fig. 5.

Table 2 Surface water bodies as per the present land use/land cover derived from Resourcesat 2: LISS-III satellite imagery and comparing with the toposheet 1976

Category	Water bodies extracted from topographic sheets	Water bodies extracted from satellite image	Disappeared water bodies	Occupied area
No. of water bodies	401	287	114	–
Area in hectors	1097.32	782.37	263.96	314.95

5 Results and Conclusions

The GVMC area has about 401 tanks, a majority of them meant for irrigation before the villages are merged with GVMC. Quite shockingly over a period of time 114 of them had disappeared due occupation by private people or by government authorities for other purposes. Another 84 have been badly affected by unbridled and unplanned urbanization. Some of the tanks are affected by sewerage and sullage water accumulation at present GVMC is going for underground drainage system, the affect of sewerage/sullage pollution into the water bodies get reduced. At present the GVMC population depending on groundwater source at least by 50% of their domestic water requirement. Storm water storage in surface water bodies will increase groundwater source and become an augmentation source for GVMC water supply. The tanks are getting gradually less in number when compared to the earlier times. This can be proved by Table 2.

(1) There are 401 tanks as per topographic sheet of given GVMC area. So far 114 tanks are occupied by the residential and various purposes of urban activities. And still 84 tanks are under process of occupation, so there is a threat of losing all water bodies in urban area.
(2) Nearly 50% of water requirement is met from ground water source, and towns of sub urban areas mainly depend on ground water.
(3) The present tanks are acting as ground water recharge sources, so hence it is very essential to protect the tanks for holding the storm and recharging the ground water.

6 Protection Measures to Be Taken up by GVMC

As per the survey of India topographic sheet of the year 1976, there are about 401 tanks in the present boundary of GVMC area. Total area of the tanks bed is about 1097.32 ha or 10.973 km^2 which is about 2.03% of the geographical area of GVMC (540 km^2).

(1) All the tank boundaries should be identified by GVMC in collaboration with the land survey department.
(2) Some trenches are to be made along the boundary of the tank in the fore shore area to avoid encroachment by the neighbors.
(3) The tanks should be de-silted and depth should be increased to accommodate the additional runoff created due to urbanization.
(4) The de-silted material may be used for increasing the width of the bunds as well to improve parks over them. Bigger tanks can be used for aqua sports and making them as tourism spots.
(5) The protection of water bodies is not only useful to improve surface and ground water potential and also can be utilized as flood flow storage tanks when water is transported from outside the area say when Polavaram water comes to Vizag.
(6) The Government of Andhra Pradesh has proposed to transport 24 T.M.C of water to Visakhapatnam through Polavaram left Main Canal. Protected and improved water bodies can be used as storage system for transported water.

References

1. Loucks, D.P., van Beek, E., Stedinger, J.R., Dijkman, J.P.M., Villars, M.T.:The use of system dynamicssimulation in water resources management
2. May, C.W., Horner, R.R., Karr, J.R., Mar, B.W., Welch E.B.: Effects of urbanization on small streams in the puget sound lowland ecoregion, University of Washington, Seattle, Washington
3. Hollis, G.E.: The effect of urbanization on floods of different recurrence interval an Agu Journal
4. Chadwick, M.A., Dobberfuhl, D.R., Benke, A.C., Huryn, A.D., Suberkropp, K., Thiele, J.E.: Urbanization affects stream ecosystem function by altering hydrology, chemistry, and biotic richness
5. Sophocleous, M.: Interactions between groundwater and surface water: the state of the science
6. Analysis of urban growth using Landsat TM/ETM data Hemant Balwant Wakode & Klaus Baier & Ramakar Jha & Raffig Azzam

Chapter 73
Morphometric Analysis and Characterization for Sub-watershed Delineation in Gomukhi River Basin of Villupuram District, Tamilnadu Using GIS

V. Govindaraj and C. Lakshumanan

Abstract In India is developing country and back bone of the India economy is agricultural activities. The most of Indian agricultural practices involved into river irrigation system. Rivers water flow in northern India is perennial system but south India rivers non-perennial system. The most of the district of Tamilnadu are affected by drought in the every year, so that need for the scientific way of watershed planning and management. The water resources are important for the human life, to conserve the water resources for future generation. The drainage basins, catchments and sub catchments are the fundamental units for administrative purposes to conserve natural resources. The catchment management concept recognizes the interrelationships among the linkages between uplands, low lands, land use, geomorphology, slope and soil. The Planning of sub watershed and prioritization is indispensable for sustainable development, particularly in the drought prone areas. The Morphometric characterization is important to recognize hydrological behavior of the basin for carrying out management strategies of the river basin. The Gomukhi river basins located in the Kalvarayan hills of Villupuram district in Tamilnadu state total area covered about 1122.67 km^2. The 69 sub watershed was delineated and each sub-watershed morphometric analysis like, bifurcation ratio, stream length, drainage density, stream frequency, form factor, elongation ratio, circularity ratio, constant of channel maintenance, length of overland flow, drainage texture, relief ratio, total stream length, mean stream length, stream length ratio, basin length, basin parameter, basin area, Compactness constant was calculated, these parameters was computed through geo-statistical techniques for identifying critical and priority sub-watersheds. The Sub-watershed was classified into very high, high, medium, and poor priority zones. There illustrate that 56.15% of sub watersheds are very

V. Govindaraj (✉) · C. Lakshumanan
Centre for Remote Sensing, Bharathidasan University, Tiruchirappalli 620023, India
e-mail: geogovindaraj@gmail.com

C. Lakshumanan
e-mail: drlaks@gmail.com

P. J. Rao et al. (eds.), *Proceedings of International Conference on Remote Sensing for Disaster Management*, Springer Series in Geomechanics and Geoengineering,
https://doi.org/10.1007/978-3-319-77276-9_73

high susceptible zones, which shows potential sub-watershed area for preferential conservation works planning and management.

Keywords Morphometric parameters · Statistical analysis · WSA technique

1 Introduction

The study of watershed is having its crucial role in socio-political-ecological aspects, as various activities involved in watershed program directly/indirectly satisfying the demand of food for survival, as well as providing life support services by social and economic security mainly to rural people. The criteria for selecting watershed size also depend on the objectives of the perspective of development and terrain slope. In hilly areas or where intensive agriculture development is planned, the size of watershed relatively preferred is small. The Majority of population of India depends on agriculture and agro-based activities. To enhance various agricultural practices, Government of India and its respective bodies/departments/organizations implemented and has been implementing suitable and sufficient programs under watershed development schemes. These schemes comprehensively aimed to achieve two things, the first, success of conservation of natural resources with formation and strengthening of the local level institutions in rural areas; the second, its multiplier effects in social mobilization, women empowerment, community development and livelihood improvement as well as good governance at local level, Management of multi-dimensional and voluminous data to the administrative bodies is a challenge and managing temporal changes, related information from respective sources being difficult. The real challenge on planning and management of available natural resources at a micro-level is due to high precision in data requirement. Therefore, micro-level hydrological units are chosen circumspectly for improved planning and management approach by solving the key issues such as soil degradation, soil erosion, droughts, and floods. Natural drainage system characteristics in the forms of morphology, topography, soil properties.

2 Study Area

Gomukhi river basin located in the eastern side of Villupuram District, southern side of Salem district, western side of Dharmapuri district, northern western side of Tiruvannamalai district and south eastern side is Cuddalore district. The area geographically falls between 11° 31′ 40.7″N to 11° 51′ 53.185″N and 78° 36′ 44.894″E to 79° 7′ 45.337″E. The areal extent of the river basin about 1122.67 km^2 and covers SOI toposheets 58I/9, 58I/10, 58I/13 and 58I/14 on 1:50,000 scale. The total population is around 452,443 out of this 228,385 male population and 224,058 female population and population density is 403 for per km^2 in census of India in

2011 data. In the study area almost tropical deciduous forest and reserved forest area covered 130.97 km^2. The maximum temperature is during the summer season is 38 °C and minimum temperature during the winter season recorded is 22 °C and also the basin gets around 75% of rainfall from the North-East monsoon during the winter months and its 25% rainfall receiving the South-West monsoon during the summer month. The average annual rainfall is around 1085. The maximum rainfall receive in the north-western region of the basin is 1260 mm and minimum rainfall receives around 792 mm in the western region of basin. The Gomukhi river flowing from west to east direction and major catchment is in the north western side of the Kalrayan hills. The Kalrayan hills are the major range of hills situated in the Eastern Ghats of Tamil Nadu. The study area falls in the Kalrayan hills is around 369.5 km^2 and highest elevation point observed in the nearby the area of Kallur village (1257 MSL, 1298 MSL) of north western region (Fig. 1).

3 Methodology

The base maps of were prepared using Survey of India (SOI) Topographic maps on a 1:50,000 scale (Fig. 2). The 30 m resolution Digital Elevation Model (IRS-P5 DEM) data was downloaded from the NRSA (Bhuvan) for cartosat-1. Based on these data,

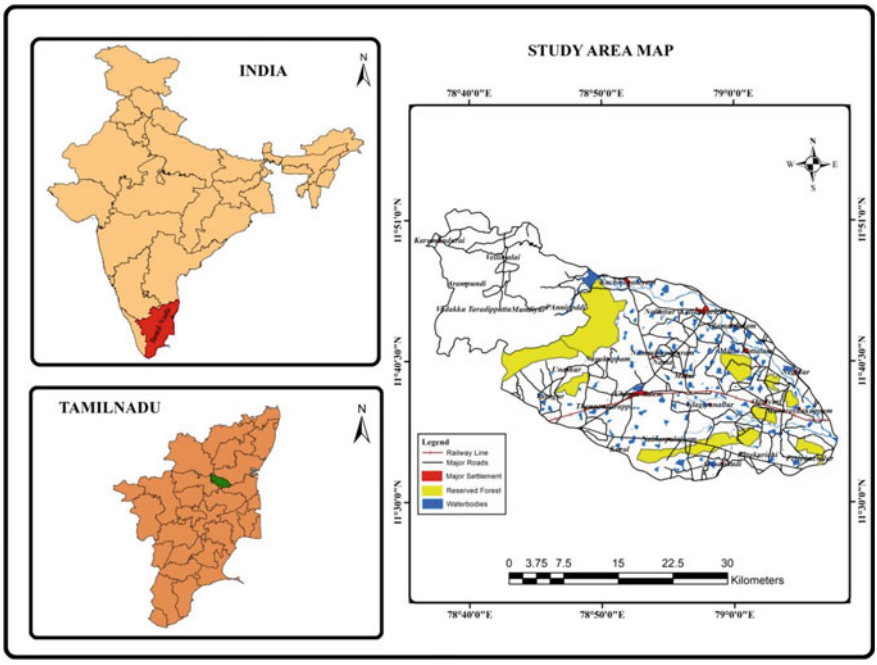

Fig. 1 Location map

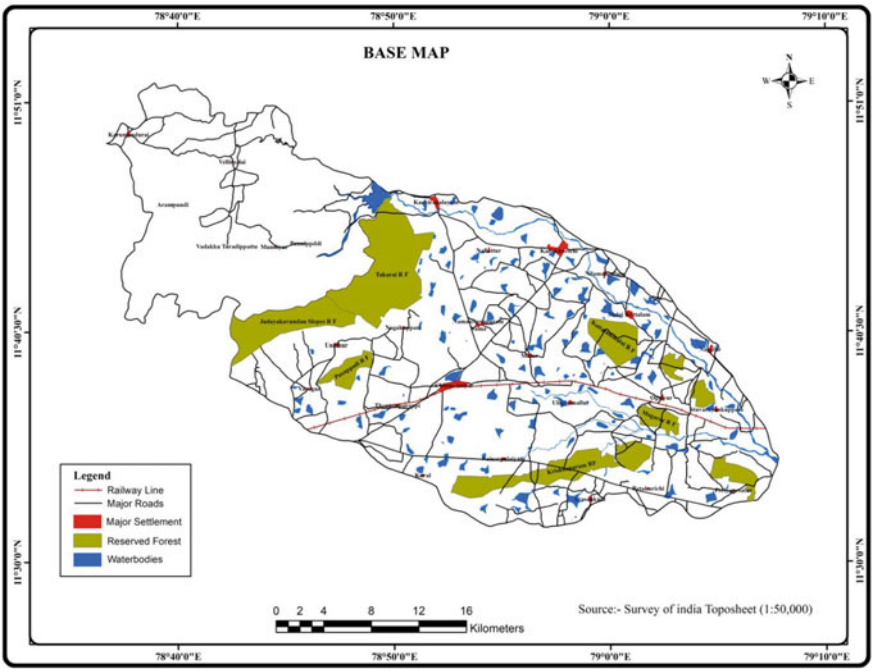

Fig. 2 Base map

the slope, and topographic elevation maps for the watersheds were prepared. The drainage network of the watersheds were SOI Toposheets no. 58I/9, 58I/10, 58I/13 and 58I/14 (1:50,000). It's digitized in ArcGIS 10.1 platform. The stream order was classified according to drainage order following Strahler [9]. The 14 morphometric parameters calculated and used statistical analysis for (SPSS-14) software correlation matrix and rotated component factor score analysis and identify the magnitude controlling, run-off controlling, basin shape is controlling characterization of the sub-watershed [1]. The morphometric, based prioritization given after that correlation frequency and finally used Weighted Sum Analysis techniques.

4 Results and Discussion

The Morphometric analysis was performed through the measurement of linear aspects, areal aspects and relief aspects of the basin. The stream orders are designed by using Strahler [9] (Fig. 3).

Stream length (Lu): According to Horton's second law, total length of stream segments was maximum in first order streams and decreased with the increase in stream order. The sub-watersheds is sw-4, sw-6, sw-8, sw-9, sw-11, to, sw-sw-45

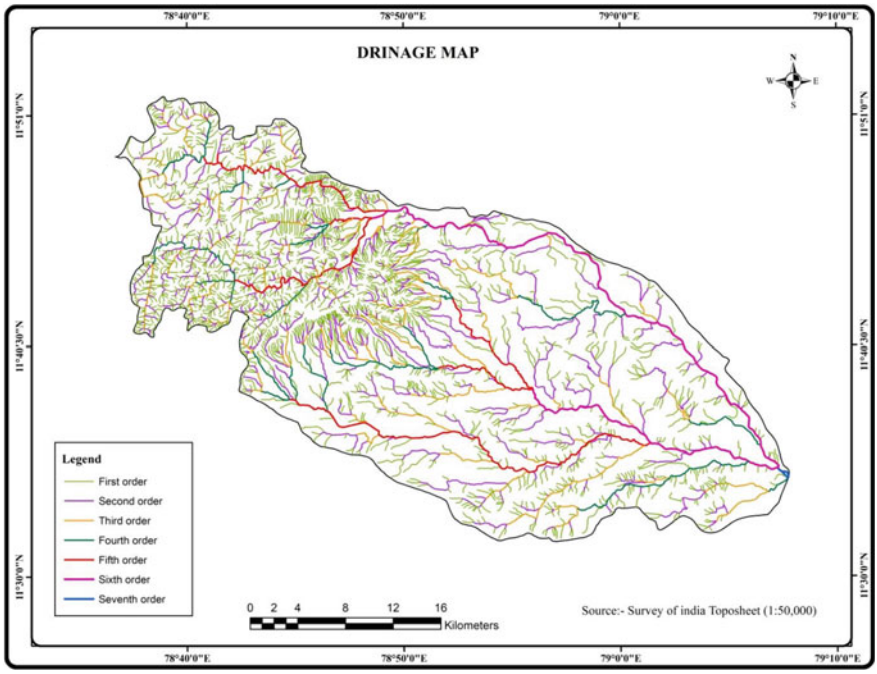

Fig. 3 Drainage map

to sw-49, sw-51, sw-52, sw-54, sw-55 to sw-59, sw-61 to sw-69 were satisfying Horton's general statement that the number of stream segments has an inverse relationship with stream order number.

Stream order (U): The classification of stream order is important to index the size and scale of the basin. According to Strahler's system [8] of stream ordering, the drainage of the watershed has been classified and the main stream is of 5th order stream. The present study area total 2038 (1751.60 km^2) stream order observed respectively first order stream 1560 (1010.71 km^2), second order stream 352 (376.33 km^2), third order stream 103 (259.32 km^2), fourth order stream 20 (88.89 km^2) fifth order stream 3 (16.35 km^2).

Bifurcation ratio (Rb): The considered bifurcation ratio as an index of reliefs and dissections. Strahler [8] demonstrated that bifurcation ratio shows only a small variation for different regions with different environments except where powerful geological control dominates if the bifurcation ration of a stream network is low than there is higher chance of flooding as the water will be concentrated in the channel rather that spread out as a higher bifurcation will be indicate. The bifurcation ratio can also show which parts of a drainage basin are more likely to flood, comparatively, by looking at the separate ratios [3]. The present study area sw-1-3, sw-5, sw-7, sw-9, sw-10, sw-13, sw-17, sw-24, sw-25, sw-29, sw-30, sw-32, sw-34, sw-36, sw-40-41, sw-44, sw-45, sw-48, sw-50, sw-53, sw-57, sw-60, sw-62, sw-64,

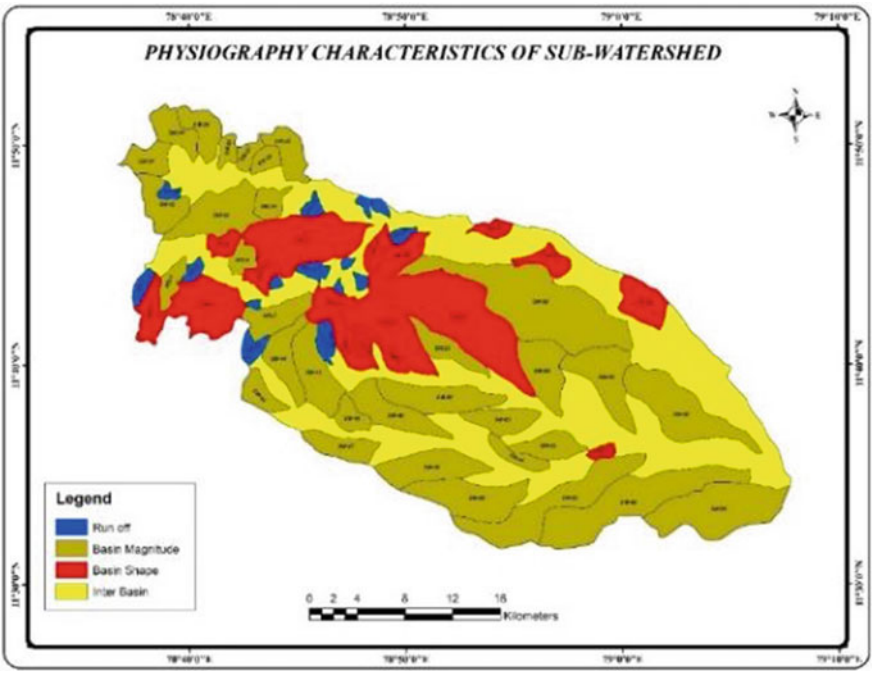

Fig. 4 Physiography characteristics of sub-watershed

sw-68-69 value range 5–11 more geological structurally disturbed sub watershed region.

Stream length ratio (RL): The stream length ratio is the ratio of mean of segments of order (Lu) to mean of segments of next lower order (Lu-1) [4]. Stream length ratio was estimated as the ratio of mean stream length of any given order (u) to the antecedent order of mean stream segment length (u_1). The RL between different sub-watersheds showed an increase in the stream length ratio from lower to higher stream order and shows the developed geomorphic stage of streams, whereas in the sw-53, sw-54, sw-60, sw-61, sw-63 and sw-65 a change was obtained from one to another stream order, suggesting the delayed youth phase of geomorphic development of streams.

Length of overland flow (Lg): Lg refers to that flow of precipitated water, which moves over the land surface and leads to the Stream channels that generally depend on slope length and land cover conditions. The Lg values less than 0.20 is observed in sw-1-24 and sw-29, sw-30, sw-54 to sw-60. This indicates short flow-paths, with steep ground slopes, reflecting the areas associated with more run-offs and less infiltration this is sub watersheds area more soil erosional causes so this area need for the soil conservation activity [10]. The Lg values between 0.20 and 0.30 is observed in sw-28, sw-31-34, sw-64, sw-67, sw-68, indicating the presence of moderate ground slopes, where the run-off and infiltration are moderate. The Lg

value more than 0.30 is observed in sw-37 to sw-40, sw-47, sw-48, sw-49, sw-52, sw-53, sw-65, sw-66, sw-69 indicating the occurrence of long flow-paths, and thus, gentle ground slopes, which reflects areas of less surface run-offs and high infiltration rate its sub watershed best suitability for artificial recharge structures.

Stream frequency (Fs): It is known as the ratio of streams numbers per unit area of the basin. Melton [5] analysed the direct relationship of drainage density and stream frequency with runoff processes. The stream frequency value less found in Sub-watershed is sw-45, sw-46, sw-48, sw-52, sw-64, sw-, sw-60, sw-32, sw-26, sw-35, sw-67 which reflects areas of less surface run-offs and high infiltration rate. The Fs value moderate observed in sw-21, sw-24, sw-23, sw-17, sw-9, sw-8, sw-57, sw-3, sw-29, sw-10, sw-36, sw-19, indicating the presence of moderate ground slopes, where the run-off and infiltration are moderate. The Fs value high to very high observed in sw-2, sw-11, sw-7, sw-1, sw-4, sw-56, sw-55, sw-20, sw-54, sw-5, sw-41 sw-18, sw-14, sw-42, sw-6, sw-15, sw-16, sw-22. This indicates with steep ground slopes, reflecting the areas associated with more run-off and less infiltration rate compares to other sub watershed.

Form factor (Ff): The value of form factor is less than 0.30. Smaller the value of form factor, more elongated will be the sub-watershed is sw-1 to sw-3, sw-7, sw-12, sw-15, sw-17, sw-19, sw-21, sw-25, sw-27, sw-29, sw-30, sw-34, sw-35, sw-66, sw-64, sw-68, sw-69 whereas, elongated sub watershed with low form factors have lower peak flow of longer duration. The sub watershed is sw-5 to sw-11, sw-13, sw-14, sw-16, sw-18, sw-20, sw-22, sw-23, sw-24, sw-26, sw-28, sw-31, sw-32, sw-33, sw-38, sw-41 to sw-46 for high form factors more than 0.30, have high peak flows of shorter duration.

Elongation ratio (Re): The value of Re approaches 1 if basin shape approaches to a circle and generally it varies from 0.6 to 1.0 over different geological and climatological conditions. Typical values are close to 1 for areas of very low relief and are between 0.6 and 0.9 for regions of strong relief and steep ground slope [9]. The sub watersheds is varying from 0.60 to 0.90 signifying the steep slope with high relief of the region. The sub watershed is sw-4, to sw-14, sw-41, 43, sw-46, sw-65, sw-67. The sub watershed in sw-1, sw-44, sw-45, sw-47 to sw-64 and sw-68, sw-69 are oval shape while are less/more elongated in nature. The Regions with low elongation ratio values are susceptible to more erosion whereas regions with high values correspond to high infiltration capacity and low runoff.

Circularity ratio (Rc). As basin shape approaches to a circle, the circulatory ratio approaches to unity [6]. Various hydro-geological parameters like land usages, relief, and drainage patterns signifies the Rc of the watershed. Greater the value is more is the circularity ratio. It is the significant ratio which indicates the stage of dissection in the study region. Its low, medium and high values are correlated with youth, mature and old stage of the cycle of the tributary watershed of the region. The Rc value between 0.30 and 0.50 in sw-39, sw-40, sw-44, sw-48, sw-50, sw-51, sw-53, sw-54, sw-55, sw-56, sw-59, sw-60, sw-61, sw-62, sw-64, sw-66, sw-68. This indicates highly permeable homogenous geologic materials present in the area, the watershed is elongated in shape, low discharge of runoff and highly permeability of the subsoil condition. The Rc values are between 0.50 and 0.80, which is

less than unity, and indicates almost an elongated and circular in shape of the sub watershed is sw-1, sw2, sw-4 to sw-31, sw-33, sw-35, sw-36, sw-38, sw-41, sw-42, sw-63, sw-65, sw-67, sw-69. The highest value of Rc (0.80) for sw-11 is due to delay in topographical development/ maturity stages and assortment of various geological conditions.

Drainage density (Dd): Drainage density is estimated as the ratio of total length of channels of all orders in the basin to the drainage area of the basin [4] and depends on permeability of sub-surface material, vegetation types and relief. Generally, less Dd is usually occurred in highly permeable sub-surface earth conditions where land is covered with dense vegetation and relief is low. High drainage density is the result of weak or impermeable sub-surface material, sparse vegetation and mountainous relief. Low density leads to coarse drainage texture while high drainage density leads to fine drainage texture. The percent study observed in sw-31, 32, sw-37, 40, sw-45 to 50, sw-52, 53, sw-62 to sw-64, sw-68 low value of Dd this region good groundwater potential it sw-26, sw-34, sw-65 to 68, sw-69 sub watershed is moderate groundwater potential, the sub watershed is sw-1, sw-3, sw-4, sw-7, sw-8, sw-9, sw-10, sw-12, sw-13, sw-59, sw-60 observed high value range (2.49–3.73) more runoff less infiltration most topography is high. The drainage density value very high (>4.97) observed in sw-2, sw-5, sw-54 to 57 very high runoff no infiltration rate mostly soil erosional accruing place while soil conservation structure more important.

Drainage texture (T): Drainage texture ratio (Rt) was estimated as the ratio of total number of stream segments (Nu) of all orders to the perimeter (P) [4]. The drainage texture depends upon a number of natural factors such as climate, rainfall, vegetation, rock and soil type, infiltration capacity, relief and stage of development (Smith 1950). According to the T value classification of five category is very coarse (<1), coarse (1–2), moderate (2–3), fine (3–4) and very fine (>4).

Compactness constant (Cc): It derives the relationship between actual hydrologic basins to the exact circular basin having the same area as that of hydrologic basin. It is directly proportional to the erosion risk assessment factors. The present study of Gomukhi river basin classified in three category is the Cc values is less than 1. It is less vulnerability for risk factors, while Cc values between (1 and 2)… it is moderate vulnerability for risk factors while Cc higher values (>2) indicates great vulnerability and represents the need of implementation of conservation measures.

Constant of channel maintenance (C): Constant of channel maintenance depends upon the rock type and permeability, climatic regime, vegetation cover, relief, the duration of erosion and climatic history. The sub watershed value of less than 0.30 is sw-1 to sw-30, sw-33-36, sw-41, sw-42-45, sw-54-59, sw-60, sw-64, sw-67 this values indicate that magnitude of surface area of watershed is needed sustain unit length of stream segment, also close dissection. The higher values is observed in >50 is sw-31, sw-32, sw-37-40, sw-46-53, sw-61, sw-62, sw-63, sw-65, sw-66, sw-68, sw-69 this sub watershed indicate that higher basin area is required to maintain 1 km length of a stream as compared to low C value of sub watershed.

Basin relief (H): The basin relief or total relief is the maximum vertical distance between the lowest and the highest points in the watershed. Schumm [7] measured

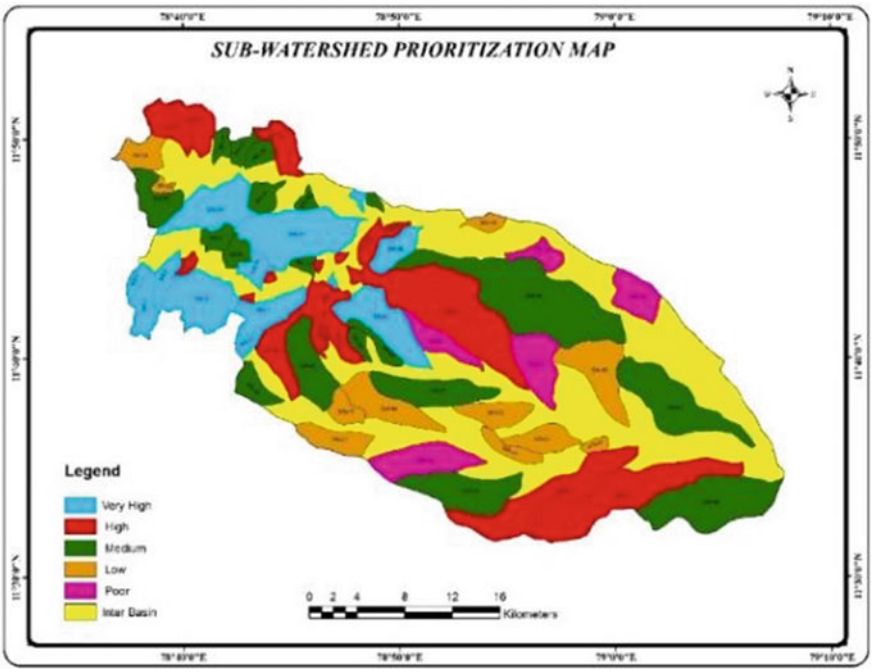

Fig. 5 Sub-watershed prioritization map

it along the longest dimension of the basin parallel to the principle drainage line, and Strahler [8] obtained it by determining the mean heights of the entire watershed divide above the outlet. The maximum relief was observed in sw-2 (1298M) other than above 1000M relief was observed in sw-2-3, sw-5, sw-10, sw-30, sw-34, sw-27-29.

Relief ratio (Rh): Relief ratio is estimated as the ratio of the basin relief and the distance over which the relief was measured [7]. Furthermore, a hydrological characteristic of a drainage basin bears correlation with the relief ratio. The value of Rn in sub watershed of Gomukhi river basin more than 1 (Above 700 m) is sw-2-4, sw-6, sw-10, sw-11-16, sw-18, 19, sw-21-23, sw-41, sw-42, sw-54-57, this sub watershed occurring more erosion process. High value of relief ratio is the characteristics of the hilly region. This sub watershed slop range is very steep slope (>35%) while moderate relief ratio between range (0.03 and 0.09), moderately slope (5–10%) of sub watershed is sw-1, sw-5, sw-7-9, sw-17, sw-20, sw-25, sw-26, sw-28, sw-29-34, sw-36, sw-43-46, sw-48, sw-58, sw-59, sw-60, sw-63, sw-64, sw-65, sw-67, elevation range is 300M–700M. Than very gently sloping (3–5%) of sub watershed is sw-35, sw-37, sw-38, sw-39, sw-40, sw-47, sw-49, sw-50-53, sw-61, sw-62, sw-66, sw-68-69.

Ruggedness number (Rn): The areas of low relief but high drainage density were as ruggedly textured as areas of higher relief having less dissection. Extensively

high value of ruggedness number occurs for a high relief region with high stream density and low value of ruggedness number occurs for a valley and Pedi plan relief region with low stream density. The present study of observed the Rn value range Very high (>2), High (1–2) and low (<1) respectively.

Rotated component Matrix in Sub-watershed Wise: Factor-1 is highly dominated magnitude controlling sub watershed (Fig. 4) is sw-2,3, sw-7, sw-9, sw-24-32, sw-34,35, sw-37-40, sw-43-53, sw-61-63, sw-65, sw-66, sw-68, sw-69. Factor-2 is highly dominated run off controlling sub watershed is sw-1, sw-4, sw-6, sw-11, sw-14-16, sw-18-20, sw-22, 23, sw-36, sw-41, 42, sw-54-57. Factor-3 is highly dominated shape controlling sub watershed is sw-5, sw-8, sw-10, sw-12, 13, sw-17, sw-21, sw-33, sw-58-60, sw-64, sw-67.

Prioritization on the basis of morphometric parameters: In the current study the gomukhi river basin 69 sub-watershed divide based on the topography condition and 3 order base.

Prioritization = Fs + Rb + Dd + Dt − Rc − Ff − Re + Cc + Bs where Fs is the stream frequency; Rb the bifurcation ratio; Dd the drainage density; Dt the drainage texture (Dt); Rc the circularity ratio; Ff the form factor; Re the elongation ratio; Rc the circularity ratio; Cc the compactness constant; and Bs is the basin shape. Finally the compound parameter values of all the 69 sub watersheds were estimated on the basis of weightages of each morphometric component (Fig. 5).

5 Conclusions

In this research, efforts were made to demonstrate the imperative role of remote sensing, GIS and statistical approaches in morphometric characterization as well as assigning priorities to all the sub-watersheds of the study area. Morphological characterization carried out through the measurement of linear, areal, and relief aspects illustrated their correspondence with hydrologic behaviour of the watershed and considered as an accomplished contrivance for prioritization of hydrological units. The Statistical analysis techniques and rotated compounded factor score analysis techniques is very much use full for river management activity and micro level planning purpose. The result shown in the highly susceptible zone fall that sw-1-3, sw-5, sw-7, sw-10, sw-15, sw-17, sw-22, sw-34, sw-36, sw-41, sw-42, sw-60 obtained first ranking on the basis of integrated weightage analysis. This sub watershed area mostly in hill area high run off and low infiltration ratio so need for soil conservation activity and sw-31, sw-35, sw-46, 47, sw-48, sw-51, 52, sw-63, sw-66, 67, sw-37, 38, sw-49, sw-61, sw-65 this sub watershed are more suitable for artificial recharge zones and farmable for the ground water potential zone.

References

1. Anantha Rama, V: Drainage basin analysis for characterization of 3rd order watersheds using geographic information system (GIS) and ASTER data. J. Geomat. **8**(2), 200–210 (2014)
2. Aher, P.D., Adinarayana, J., Gorantiwar, S.D.: Quantification of morphometric characterization and prioritization for management planning in semi-arid tropics of India: a remote sensing and GIS approach. J. Hydrol. 850–860 (2014)
3. Horton, R.E.: Drainage basin characteristics. Trans. Am. Geophys. Union **13**, 350–361 (1932)
4. Horton, R.E.: Erosional development of streams and their drainage basins; hydrological approach to quantitative morphology. Geol. Soc. Am. Bull. **56**, 275–370 (1945)
5. Melton, M.A.: Correlations structure of morphometric properties of drainage systems and their controlling agents. J. Geol. **66**, 442–460 (1958)
6. Miller, V.C.: A quantitative geomorphic study of drainage basin characteristics in the Clinch mountain area. Technical Report-3, Columbia. University Department of Geology, New York (1953)
7. Schumm, S.A.: Evolution of drainage systems and slopes in Bad Lands at Perth Amboy, New Jersey. Geol. Soc. Am. Bull. **67**, 597–646 (1956)
8. Strahler, A.N.: Quantitative analysis of watershed geomorphology. Trans. Am. Geophys. Union **38**, 913–920 (1957)
9. Strahler, A.N.: Quantitative geomorphology of drainage basins and channel networks. In: Chow, V.T. (ed.) Handbook of Applied Hydrology. McGraw Hill Book Company, New York, Section 4-11 (1964)
10. Thakkar, A.K., Dhiman, S.D.: Morphometric analysis and prioritization of miniwatersheds in a Mohr watershed, Gujarat using remote sensing and GIS techniques. J. Ind. Soc. Remote Sens. **35**(4), 313–321 (2007)

Chapter 74
Restoration of Ecological Balance Through Regression Analysis in Kothapally Agricultural Fields

G. Venkata Ramana, R. Suresh Kumar and P. Balakrishna

Abstract The broad objective of the present study is to estimate the daily runoff from the rainfall data using SCS-CN (Soil Conservation Service-Curve Number) method for Kothapally agricultural field. The data of daily, monthly, and yearly rainfall, temperature, relative humidity, wind speed, evaporation data of 11 years data from 2006–2016, was collected from the ARI (Agricultural Research Institute, Rajendra Nagar), Hyderabad. The data collected such as rain fall and also analyzing temperature, and humidity and wind velocity, relative humidity which is collected from the ARI (Agricultural Research Institute), Rajendra Nagar data collected from the International Crops Research Institute for the Semi-Arid Tropics (ICRISAT), and NIRD (National Institute of Rural Development) Hyderabad, and Fifth economic census 2005 issued by the Directorate of Economics & Statistics, Hyderabad. The present study area Kothapally agricultural field involves collection of service data like satellite data, survey of India topo sheets, and prepares various thematic maps like base map, contour map, drainage map, soil map, slope map, land use/land cover map are prepared by using survey of India topo sheets and satellite imageries. The methodology is used for the analysis of data is the Soil Conservation Service-Curve Number (SCS-CN) for computation of runoff, and regression analysis by using rainfall and estimated runoff of daily, monthly, yearly from collecting data and also calculate the correlation coefficient and coefficient of determination.

Keywords Correlation coefficient · Soil conservation service-curve number (SCS-CN) · Regression analysis · Relative humidity

G. V. Ramana · R. Suresh Kumar (✉)
Department of Civil Engineering, Institute of Aeronautical Engineering, Dundigal, Hyderabad 500043, Telangana, India
e-mail: sureshkumar.r17@gmail.com

G. V. Ramana
e-mail: ramanagedela@gmail.com

P. Balakrishna
Department of Geo-Engineering, Andhra University, Visakhapatnam, India
e-mail: balakrishna.penta@gmail.com

P. J. Rao et al. (eds.), *Proceedings of International Conference on Remote Sensing for Disaster Management*, Springer Series in Geomechanics and Geoengineering,
https://doi.org/10.1007/978-3-319-77276-9_74

1 Introduction

Watershed degradation is a phenomenon by which the potentiality of the watershed is getting reduced over time , which can be conformed to the forest loss, and the rate of soil erosion increment: Malleswara Rao [1] Kothapally agriculture field consists of the land that drains water, sediment and other material to a common point. Land evaluation, non political borders, defines Kothapally agriculture field boundaries. Integrated watershed development is the strategy adopted in the country for sustainable development of dry land areas and a recent comprehensive assessment of watershed programs in India undertaken by International Crops Research Institute for the Semi-Arid Tropics (ICRISAT) consortium revealed that integrated watershed can be become the growth engine for sustainable development of dry land areas by improving the performance two third of the country. In the present study, [2] SCS curve number runoff simulation model is used to assess the harvesting potential of a watershed. The model is developed at ICRISAT. Hyderabad. The runoff simulation is helpful for planning of a watershed, to improve the crop productivity and for proper planning of crops. Capece [3] found that the best results for estimating runoff in Florida flatwoods with a modified SCS equation included an antecedent depth to the water table. Water table depth controls the formation of variable source areas, which play a significant role in the production of runoff, especially toward the end of the wet season. Variable source areas are regions that generate runoff before other regions of the catchment as a result of having soil that fills to capacity more quickly than at other locations. The water table depth is the indicator of available soil storage. As the water table rises in the wet season, the soil storage decreases and the total area of saturation increases, causing the source of runoff to increase. Water for human consumption, wildlife industry and recreation are all impacted by activities that occur within kothapally agriculture field. Kothapally agriculture field management planning works protects the water resources by empowering local people to provide for the environmental, social and economic health of the community. Kothapally agriculture field is also useful for soil conservation natural resources available to mankind. Bultot et al. [4] simulated the impact of Land use changes on stream flow by means of lumped parameters models. In their studies, the effects of land use changes were estimated by altering the proportions of existing vegetation types in the catchment, rather than introducing new species which may have given problems in obtaining the hydrological model parameters. It is a driving force for all development activities and development of forests and vegetation. According to U.S Soil conservation Technical Release (TR - 55) [5], presents a numeros methods for estimating the different parameters involved the runoff and peak discharges. Heatwole [6] stated that since the curve number method is storage based, it should be a good model for analyzing the flat woods watersheds in Florida, if an appropriate estimate of the S parameter can be determined. The idea is that the concepts of the SCS method are useful and could be adjusted to suit a different interpretation of the original methodology.

Garg and Sen [7] in their study stated presented a new algorithum to Identify watershed features kike channels ridges and overland flow panteas from a dem location data of discreate points of a watershed. Kothapally agriculture field is an ideal unit and accepted approached for planning, development and management of land water resources. Kothapally agriculture field management requires the understanding of relationship among land use, soil and water. The entire life depends on water and is one of the important and is of great importance to people and environment. Sridhar et al. [8] the use of Geographical Information Systems (GIS) in water resources has a rich heritage. Some of the key contributions include prepartion of base maps of water features of the landscape, digital elevation models delineating watersheds and stream networks, geospatial data preprocessors supporting water resources simulation models, floodplain maps built using automated hydrology and hydraulics and precisely measured land surface elevation. Besides, Pahari [9] suggested that the Remote Sensing and GIS can be successfully used for monitoring land use dynamics and soil erosion in a mountain watershed then for making sustainable land use modeling. Providing water in desired quantity and quality has been a constant Endeavour of all the countries. According to Kachroo [10] proposed a value of Nash coefficient of efficiency R^2 of 90% which indicates fairly good model values of R^2 in the range 60–80% would indicate un satisfactory model fit.

1.1 Identification of Problem of Kothapally Agriculture Field

The success of Kothapally agriculture field management largely depends on the community's participation. In a recent review [11], (Kerr et al. 2000) on the Kothapally agriculture field projects in India, it was observed that most Kothapally agriculture field projects did not address the equity issues of benefits, community participation, scaling-up approaches, monitoring and evaluation. Moreover, most of these projects relied heavily on government investments and were structure-driven (rainwater harvesting and soil conservation structures), and failed to address the issue of the efficient use of natural resources (soil and water). This is mainly due to the lack of technical support to such projects implemented by Non Governmental Organisations (NGOs).

1.2 Objectives of the Study

1. To delineate the Kothapally agriculture field map, to overlay various thematic layers, to prepare drainage map, using ARC GIS environment.
2. To prepare the Triangulated Irregular Network (TIN) map, to develop Digital Elevation Model (DEM) for the study area.

3. To prepare Land Use/Land Cover map of Kothapally agriculture field.
4. To compare the results of rainfall and measured runoff using regression analysis and calculation of correlation coefficient.

2 Study Area

The kothapally agriculture field is located in Kothapally village (longitude 78° 5′ to 78° 8′ E and latitude 17° 20′ to 17° 24′ N), SankarPally Mandal, Ranga Reddy district, Telangana. The village Kothapally is situated 47 km from Hyderabad towards South East direction, the state capital of Telangana. The population of the village is 1492 with 274 households. The total land area is 507 hectares, with an average landholding per household of 1.7 hectares. The Kothapally kothapally agriculture field is characterized by undulating topography and black soil.

3 Methodology

As with correlation, regression is used to analyze the relation between two continuous (scale) variables. However, regression is better suited for studying functional dependencies between factors. The term functional dependency implies that X determines the level of Y. For example, there is function dependency between age and blood pressure since as one age's blood press increases. In contrast, there is no functional dependency between arm length and length since increasing the length of an arm will have no effect on leg length (or vice versa).

Correlation describes the strength of a linear relationship between two variables. Linear means "straight line". Regression tells us how to draw the straight line described by the correlation. As with correlation, regression is used to analyze the relation between two continuous (scale), variables. However, regression is better suited for study functional dependencies between factors. The term functional dependency implies that X (partially) determines the level of Y. In addition regression is better suited then correlation for studying samples in which the investigator fixes the distribution of X Regression analysis is used to predict the value of a dependent variable based on the value of at least one independent variable. Explain the impact of changes in an independent variable on the dependent variable. Dependent variable we wish to explain where as the Independent variable used to explain the dependent variable.

The Regression models are four types:

1. Positive Linear Relationship
2. Relationship NOT Linear
3. Negative Linear Relationship
4. No Relationship.

3.1 Regression Model

Correlation describes the strength of a linear relationship between two variables. Linear means "straight line". Regression tells us how to draw the straight line described by the correlation. As with correlation, regression is used to analyze the relation between two continuous (scale) variables. However, regression is better suited for studying functional dependencies between factors. The term functional dependency implies that X determines the level of Y.

The algebra that a line identified by its slope (the angles of the line describing the change in Y per unit X) and intercept (where the line crosses the Y axis). Regression describes the relation between X and Y with just such a line (Fig. 1).

$$\hat{Y} = a + b\,x$$

$$\bar{x} = \sum x\ /n$$

$$\hat{y} = \sum y/n$$

$\bar{y}$ represent the predicted value of y
a represent the intercept of best fitting line, and
b represent the slope of the line

The goal is to determine a line minimizes the sum of the squared residuals. This line is called the least squares line. The slope (b) of the least squares line is given by:

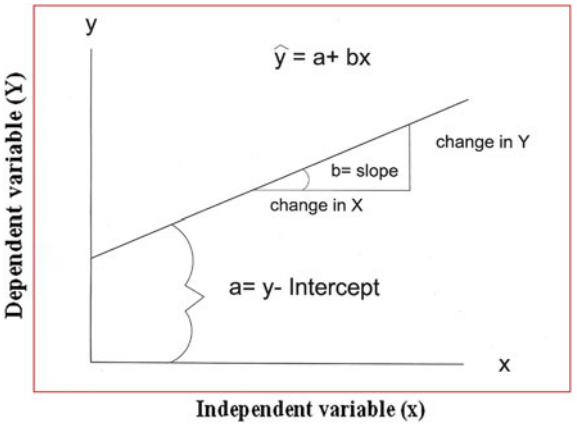

Fig. 1 Graphical representation of Regression analysis model

$$b = \frac{SS_{xy}}{SS_{xx}} \quad a = \bar{y} - b\bar{x}$$

where SS_{xy} is the sum of the cross products and SS_{xx} is the sum of the squares for variable x.

$$SS_{xy} = \sum xy \ \frac{\sum x * \sum y}{n}$$

$$SS_{xx} = \sum x^2 \frac{(\sum x)^2}{n}$$

$$SS_{yy} = \sum y^2 \frac{(\sum y)^2}{n}$$

where SS_{yy} sum of the squares of y

$$R^2 = \frac{b \times SS_{xy}}{SS_{yy}}$$

n = number of items
R^2 is another important measure of linear association between x and y ($0 \leq R^2 \leq 1$)
In the single independent variable case, the coefficient of determination is $R^2 = r^2$
R^2 = Coefficient of determination
r = Simple correlation coefficient

3.2 Coefficient of Determination (R^2)

Correlation is a statistical technique used to determine the degree to which two variables are related. This number services as an evaluation of the closeness of the relationship and represents. The proportion of variation in y "explained" by variation in x, how closely data points cluster around the regression line Necessarily, ($0 < R^2 < 1$). The sign of r denotes the nature of association while the value of r denotes the strength of association. If the sign is positive this means the relation is direct (an increase in one variable is associated with an increase in the other variable and a decrease in one variable is associated with a decrease in the other variable). While if the sign is negative this means an inverse or indirect relationship (which means an increase in one variable is associated with a decrease in the other).

Range between −1 and 1
The closer to −1, the strong negative linear relationship
The closer to 1, the strong positive linear relationship
The closer to 0, the weaker the linear relation.

This number services as an evaluation of the closeness of the relationship and represents the proportion of variation in y "explained" by variation in x. How closely data points cluster around the regression line.

4 Results and Discussions

4.1 Kothapally Agriculture Field Average Slope

Kothapally agriculture field average slope offers information about the kothapally agriculture field influences radically the value of the time of the concentration and, directly the runoff generation by a rainfall series of methods have developed estimated H_a average slope of kothapally agriculture field The method proposed by earlier and Leclerc (1964) consists of calculating the weighted mean of the elementary surfaces the exists between two lines (Musy 2001),

$I_a = D \times L/A$
I_a = Average slope of kothapally agriculture field
D = Equiv distance between two consecutive contour lines = 5 m
A = Area of the kothapally agriculture field in km^2 = 5.07 km^2
L = Total length of Contour lines in km = 2500 km
Average slope of kothapally agriculture field is 2.5.

4.2 Drainage Density

It is the ratio of the total length of all streams of all order in the kothapally agriculture field to the area of kothapally agriculture field. Where,

$D_d = \sum L/A$ (where D_d = Drainage density; Sigma L = Total length of all order in km; A = Ares of kothapally agriculture field in km^2)

$D_d = 12.7/5.07 = 2.5$.

4.3 *Based on the Results the Overall Analysis of Total Rainfall*

The yearly average rainfall of the study area of eleven years from Table 1 is 850.37 mm based on the data collection the highest rainfall was recorded according to the data 1375.65, 1165, 1159 mm, for the years of 2008, 2009, 2010, respectively, based on the results it is observed that the extreme irregularities, 640.70, 486.70, 649.82, 522.3, 899.00, 965.30, 1135.65, 1165.00, 1159.00, 659 mm, from 2006 to 2016 respectively. The highest rainfall was observed from data 1375.65 mm, for the year of 2013, and the lowest rainfall is recorded was 486.70 mm for the year of 2007.

4.3.1 Based on the Overall Analysis of Total Runoff

The yearly average calculated runoff of the study area from Table 1 is 454.98 mm based on data collected in the rainfall of eleven years the calculated rainfall excess using SCS-CN method it is observed that the particular years runoff is high 806.64, 778.16, 759.42 mm, for the years of 2013, 2014, 2015, respectively this is also extreme irregularities changes from 2006 to 2012 and then decreasing trend from 2013 to 2016.

The highest runoff was observed 806.64 mm, for the year 2013, and the lowest runoff was observed was 162.68 mm for the year of 2007. Generally rainfall and runoff goes on first increase sand then decreasing trendy (Fig. 2; Table 2).

Table 1 Rainfall & runoff data from the year 2006–2016

S. No.	Year	Rainfall (mm)	Runoff (mm)
1	2006	640.70	183.79
2	2007	486.70	162.68
3	2008	649.82	345.07
4	2009	522.30	283.88
5	2010	899.00	550.43
6	2011	965.30	284.71
7	2012	831.68	501.18
8	2013	1375.65	806.64
9	2014	1165.00	778.16
10	2015	1159.00	759.42
11	2016	659.00	348.86
	Average	850.37	454.98

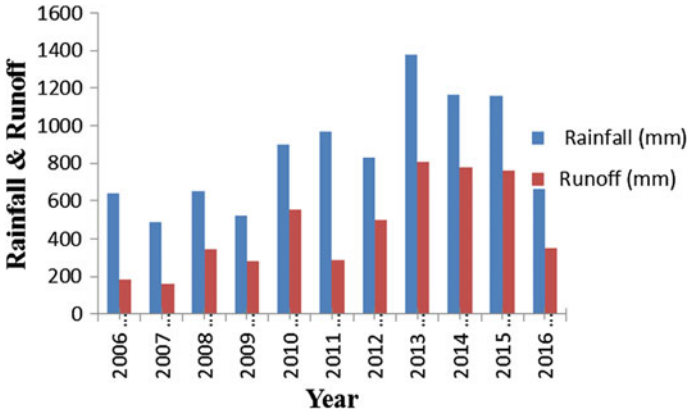

Fig. 2 Graphical comparison of rainfall and runoff for the study area from 2006–2016

4.3.2 Regression Analysis Between Monthly Rainfall and Estimated Monthly Runoff for the Year 2016

The regression analysis between rainfall and runoff of the year 2016, as shown in Table 3. The rainfall and runoff of the year 2016 the highest rainfall recorded 245.10 mm in the month of July whereas calculated runoff was 173.65 mm, for the month of July, and lowest rainfall 45.40 mm, for the month of October and lowest runoff was 23.57 mm, for the month of October, the total rainfall recorded was 628.00 mm and total calculated runoff 348.86 mm, for the year of 2016, the rainfall and runoff 0.00 recorded was no rainfall and runoff The X and Y co-ordinates it is observed that the there is a stronger linear relationship between X and Y, ($0 < R^2 < 1$). The procedure as follows first select the rainfall and runoff in the excel sheet go to insert and select the chart X Y (Scatter) and select the layout select the trend line select the linear trend line, then select the display chart and select the R^2 value chart and close and displayed the trend line chart. The $Y = 0.630x - 3.921$ and the R^2 value was 0.947 shows the strong positive relation between rainfall & estimated runoff for the year 2016. The regression analysis between monthly rainfall and estimated monthly runoff using SCS-CN method for the year 2016 is shown in Fig. 3.

4.3.3 The Overall Regression Analysis of Rainfall and Runoff from the Year 2006–2016

The regression analysis between of yearly rainfall and estimated runoff in x-axis and y-axis respectively, the coefficient of determination of R^2 value which is linear relationship between x & y axis, from Table 4, from the year 2006 to 2009, is 0.906, 0.918, 0.967, 0.989, slowly increasing and from 2010 to 2012 also

Table 2 Estimation of rainfall and runoff coefficeints for calculation of R^2

S. No.	Month	Rainfall (mm) x	Runoff (mm) y	x * y	x^2	y^2
1	Jan	0.00	0.00	0.00	0.00	0.00
2	Feb	0.00	0.00	0.00	0.00	0.00
3	Mar	1.00	0.00	1.00	1.00	0.00
4	Apr	34.60	12.24	423.50	1197.16	149.82
5	May	0.00	0.00	0.00	0.00	0.00
6	Jun	109.00	43.68	4761.12	11,881.00	1907.94
7	Jul	51.80	17.12	886.81	2683.24	293.09
8	Aug	86.60	27.40	2372.84	7499.56	750.76
9	Sep	192.70	50.85	9798.79	37,133.29	2585.72
10	Oct	165.00	32.50	5362.50	27,225.00	1056.25
11	Nov	0.00	0.00	0.00	0.00	0.00
12	Dec	0.00	0.00	0.00	0.00	0.00
	Total	$\sum x = 640.7$	$\sum y = 183.79$	$\sum x * \sum y = 23{,}605.56$	$\sum x^2 = 87{,}620.25$	$\sum y^2 = 6743.58$

Table 3 Regression analysis between monthly rainfall and estimate monthly runoff using SCS-CN method for the year 2016

S. No.	Month	Rainfall (mm)	Runoff (mm)
1	Jan	0.00	0.00
2	Feb	0.00	0.00
3	Mar	0.00	0.00
4	Apr	0.00	0.00
5	May	0.00	0.00
6	Jun	104.40	40.2
7	Jul	245.10	173.65
8	Aug	97.00	46.15
9	Sep	136.10	65.29
10	Oct	45.40	23.57
11	Nov	0.00	0.00
12	Dec	0.00	0.00
	Total	628.00	348.86

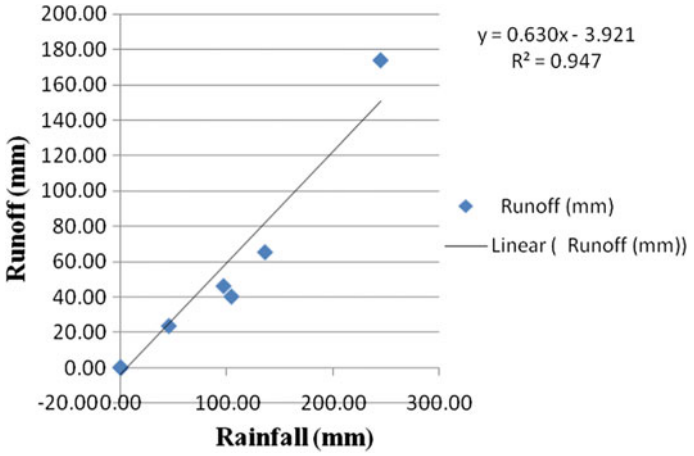

Fig. 3 Regression analysis between monthly rainfall and estimated monthly runoff using SCS-CN method for the year 2016

increasing highest coefficient of determination recorded is 0.98, and changes were observed from 2013 to 2016 slowly goes on decreased. The averages R^2 value can be computed was 0.958. It is concluded that the R^2 value is more than 0.90, means nearer to one the runoff condition of study area is more accurate.

Based on results of regression analysis from the year 2006 to 2016 from the Table 4, the highest rainfall recorded was 1375.65 mm, for the year of (2013) and lowest rainfall was recorded was 486.70 mm, for the year of (2007) and the highest

Table 4 Regression analysis of yearly rainfall and estimated yearly runoff using SCS-CN method from the year 2006–2016

S. No.	Year	Rainfall (mm)	Runoff (mm)
1	2006	640.70	183.79
2	2007	486.70	162.68
3	2008	649.82	345.07
4	2009	522.30	283.88
5	2010	899.00	550.43
6	2011	965.30	284.71
7	2012	831.68	501.18
8	2013	1375.65	806.64
9	2014	1165.00	778.16
10	2015	1159.00	759.42
11	2016	659.00	348.86
	Average	850.37	454.98

calculated runoff recorded was 806.64 mm, and lowest runoff recorded was 162.68 mm, for the year (2007). The X and Y co-ordinates it is observed that the there is a stronger linear relationship between X and Y, ($0 < R^2 < 1$).The procedure as follows first select the rainfall and runoff in the excel sheet go to insert and select the chart X Y (Scatter) and select the layout select the trend line select the linear trend line, then select the display chart and select the R^2 value chart and close and displayed the trend line chart. The runoff data shows a increasing trend line equation, $Y = 0.778x - 184.8$ and the R^2 value was 0.928 from the year 2006–2016. The regression analysis of yearly rainfall and estimated runoff from 2006–2016 is more accurate is shown Fig. 4.

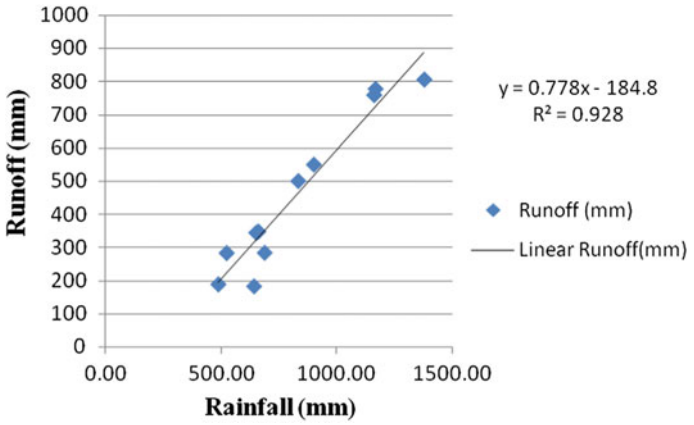

Fig. 4 Regression analysis of yearly rainfall and estimated yearly runoff using SCS-CN method from the year 2006–2016

Table 5 Comparison of coefficient determination values of rainfall and runoff from the year 2006–2016

S. No.	Year	R^2 (Observed)	R^2 (Calculated)
1	2006	0.906	0.899
2	2007	0.918	0.920
3	2008	0.967	0.971
4	2009	0.989	0.980
5	2010	0.956	0.942
6	2011	0.958	0.960
7	2012	0.982	0.973
8	2013	0.972	0.967
9	2014	0.970	0.965
10	2015	0.976	0.970
11	2016	0.947	0.950
	Average	0.958	0.954

4.3.4 Comparison of Correlation Coefficient and Coefficient of Determination Values from the Year 2006–2016

The analysis of Table 5, the correlation coefficient of estimated runoff the coefficient of determination of R^2 value from 2006–2016 the highest R^2 value was 0.989 for the years 2009, and lowest R^2 value was 0.906 for the year 2006. The averages R^2 value can be computed was 0.958, and in the calculated R^2 average value 0.980 for the year 2009 and lowest correlation value was 0.899, the average calculated R^2 value was 0.954, from the results it is concluded that the observed and calculated R^2 value was nearer to one, means, there is strong positive relation between rainfall and estimated runoff, the variation in the trend line of rainfall & runoff has obtained shows the increasing trend for the period of 2006–2016 the runoff condition is more accurate.

5 Conclusions

1. The Runoff measurement using SCS-CN method which is accurate, stability for calculating the runoff and is used for better water management practices.
2. The rainfall and estimated runoff using SCS-CN method the regression analysis is used to calculate the perfect results of coefficient of determination. The analysis of rainfall and runoff from the year 2006–2016 of the eleven years using SCS-CN method.
3. The highest rainfall recorded as 1375.65 mm for the year 2013 whereas calculated runoff was 1062.07 mm, for the year 2013 and lowest rainfall 486.70 mm for the year 2007 and lowest runoff was 289.86 mm for the year 2007, and mean rainfall of the eleven years from 2006–2016 was 850.37 mm and average estimated runoff was 454.98 mm. The runoff data shows a

increasing trend line equation, Y = 0.778x − 184.8. it is concluded that the rainfall and runoff correlation is more accurate.

4. The rainfall and runoff analysis shows that it is necessary to create network of runoff management structures for recharge of ground water and recycling for irrigation & domestic purpose, and reduces runoff and soil loss, improve the land cover (vegetation),
5. Kothapally agriculture field management is used for conservation, up gradation, and optimum utilization of natural resources land, water and vegetation in an integrated manner.
6. Kothapally agriculture field is required to effectively consider the ecological effects of various alternative actions, economic benefits and costs of alternative actions ensuring long term sustainability of the ecosystem and better standard living of people.

References

1. Malleswara Rao, B.N.: GIS based action plan for water resources management, a case study of a central India kothapally agriculture field. In: Proceedings of 3rd international conference on hydrology and kothapally agriculture field management, vol. II, pp. 956–964 (2010)
2. "Use of Satellite Data for Kothapally Agriculture Field Management and Impact assessment", J. Int. Crops Res. Ins. Semi-Arid Tropics (ICRISAT), Patancheru, Andhra Pradesh, India, 149–157, (2008)
3. Capece, J.C.: Estimating runoff peak rates and volumes from flat, high-water-table kothapally agriculture fields. Master's Degree thesis, University of Florida, Gainesville, Florida (1984)
4. Bultot, F., Dupries, G.L., Gellens, D.: Simulation of land use changes and impact on the water balance-a case study for Gelgium. J. Hydrol. **114**, 327–348 (1990)
5. U.S. Soil Conservation Service Technical Release 55: Urban Hydrology For Small Kothapally Agriculture Fields. USDA (U.S. Department of Agricultural), June 1986, (1986)
6. Heatwole, C.D.: Field and basin scale water quality models for evaluating agricultural nonpoint pollution abatement programs in a South Florida flatwoods kothapally agriculture field. Ph.D. dissertation, University of Florida, Gainesville, Florida (1986)
7. Garg, N.K., Sen, D.J.: Determination of kothapally agriculture field features for surface runoff models. ASCE, J. Hydrol. Eng. **18**(4), 427–447 (1994)
8. Sridhar, P.S.N., Jowhar, T., Garg, A., Kedareswarudu, U.: "A Framework of Information Technology for Water Resources Management", Int. J. Comp. Appl, Vol. 30, No. 5, September 2011, (2011)
9. Pahari, K., Delsol, T., Murai, S.: Remote sensing and GIS for sustainable kothapally agriculture field management a study from Nepal. Paper presented at the 4th symposium on high mountain remote sensing cartography, Karlstad- krishna- Thoma, 19–29 Aug 1996
10. Kachroo, R.K.: Homs work shop on river flow forecasting Nanjing China. Unpublished international report, Department of Engineering Hydro, University college Galway Ireland (1986)
11. Joshi., Pangare., Shiferaw, B., Wani, S., Bouma, J., Scott.: "Watershed development in India: Synthesis of past experiences and needs for future research", Indian J. Agri. Eco, July 2004, (2000)

Chapter 75
Intelligent Object Tracking in River Floods, Andhra Pradesh, India Using MOTSC Approach

Rajesh Duvvuru, Peddada Jagadeeswara Rao, Gudikandhula Narasimha Rao, Sridhar Bendalam and Suribabu Boyidi

Abstract Disaster management (DM) and aerial remote sensing plays an extensive environmental and economic disruptive role in human life. It goes beyond the capability of the affected society or community to deal with using its own resources. Floods are the recurring major disaster which resulting in huge loss of life and property year after year, though the world is being equipped with modern technology. Floods are the most common and widespread major natural disasters in India. In the past two decades, Information and communication Technology (ICT) has taken a giant leap in the development of various applications related to Internet-of-Things (IoT) especially in Geographical Information Systems (GIS) and DM applications. Still automatic recognition or identification of motion objects such as humans and animals float in the flood water and its spatial coordinates is a big challenge in the area of DM. This paper introduces a novel Motion Objects Tracking with Spatial Coordinates Algorithm (MOTSC) to focus light on flood related disasters. MOTSC analyze and recognize motion objects and also finds it spatial coordinates. The results obtained in this study reveal that the MOTSC is proved to be an innovative approach for the Dynamic Flood rescue operation.

R. Duvvuru (✉) · P. J. Rao · G. N. Rao · S. Bendalam · S. Boyidi
Department of Geo-Engineering, Centre for Remote Sensing,
Andhra University College of Engineering, Visakhapatnam, India
e-mail: rajesh.duvvuru@gmail.com

P. J. Rao
e-mail: pjr_geoin@rediffmail.com

G. N. Rao
e-mail: gudikandhula@gmail.com

S. Bendalam
e-mail: sridhar.bendalam@gmail.com

S. Boyidi
e-mail: suri.sri2008@gmail.com

P. J. Rao et al. (eds.), *Proceedings of International Conference on Remote Sensing for Disaster Management*, Springer Series in Geomechanics and Geoengineering,
https://doi.org/10.1007/978-3-319-77276-9_75

Keywords Pattern recognition · GIS · Algorithms · Disaster management
Floods · Rescue · Risk

1 Introduction

In recent times the applicability and usage of ICT became more popular because of its wide range of utilization in GIS. Many GIS applications like Geographic information storage, Disaster management, Hydrology, Historical geographic information systems, waste management, spatial, crime mapping, wastewater systems, storm water systems, pattern identification, Public Participation GIS, visual presentation of spatial relationships, Road Networking, Traditional knowledge GIS, Spatial Data mining, remote sensing etc [1]. Among the specified applications Disaster management is one of the key issues where GIS, ICT and IoT has to concentrate more in saving valuable human life's and their assets. Disaster management majorly classified as accidental or man made and Natural DM's [2]. Earthquakes, cyclones, Droughts, Floods, volcanic eruptions, Landslides, Avalanches are designated under the Natural Disaster (ND), Whereas Fire accidents, major rail and road accidents etc. are categorized as Accidental Disaster (AD). Presently, various applications are available for warning and perdition of AD and ND according to their needs like Disaster Alert, Disaster Radar, Disaster Warning System and more, but these applications provide information about pre or post Natural disasters. For instance ND like major Flood Disaster time to time updated information is unable to collect and retrieve the data from real-time scenario [3, 4]. Due to flaw specified, National Disaster Response Force (NDRF) is unable to take right decision at right moment in rescuing the valuable lives [5]. If the data is available in the form of Satellite data and aerial data about floods but its analysis were made manually. Manual analysis and Time-to-time updates are two key factors in saving time in taking right decision. These two parameters reflects in saving the life's those who are about to sink and in dangerous situation.

As it was stated earlier Indian Subcontinent are more prone to Floods. According to the recent report by Geological Survey of India (GSI) 2012, more than 50% of lands were identified as flood affected areas. It covers 11 states of India that includes Uttarpradesh, Bihar, Punjab, Rajasthan, Assam, West Bengal, Haryana, Orissa, Andhra Pradesh, Gujarat and Kerala. Also reports states that the major flood prone areas of India cover almost 12.5% area of the country. Uttarakhand floods in 2013 and Jammu and Kashmir floods in 2014 few among the major floods, where 4021 and 150 lost their lives respectively. In the literature of DM, floods can be predicted and alert systems are available, but still Dynamic Flood Rescue System (DFRS) is not available yet [6–9].

This paper discusses mainly about DFRS and Floods and its management through Pattern Recognition (PR). Flood can identified and mapping by using satellite data. But, identifying the objects automatically in the motion flood water is still a major challenge for the researchers and practitioners. For instance Identifying

the humans objects in the flood water is bit tough task. If the recognition were made, there is a possibility of rescuing those sorts of people from running flood. The pattern recognition is applicable on two different types of data; first one is static and next dynamic. Normally, motion flood water is in dynamic in nature, but the data can be obtained through two different modes; they are static Image and dynamic videography. Flood data can be obtained through satellite image, if clouds were not present; else data can be acquired through aerial photography and videography [10–12]. Static data object distortion and identification is easier than dynamic data. But the acquiring of the static data is a typical task, because of cloud presence. In dynamic flood data object tracking and identification are two functions are needed to perform, whereas in static image only identification function is sufficient. In the literature of artificial interalliance, there are many pattern recognition and object tracking ageratums are available like Kanade-Lucas-Tomasi (KLT), Continuously Adaptive Mean Shift (CAMShift), Hungarian algorithm, Kalman filtering and much more [13–16].

The rest of this paper is organized as follows. Section 2 discusses literature works in the area of Flood mapping, satellite data, Object Tracking algorithm, and Pattern recognition algorithms. Section 3 explains the Dynamic Flood Rescue System (DFRS) and Motion Objects Tracking with Spatial Coordinates Algorithm (MOTSC). In Sect. 4, we present the simulation and results analysis of the proposed algorithm. Lastly, the paper was concluded with future works in Sect. 5.

2 Related Works

The As it was specified in an earlier section, disaster management plays a vital role in serving and saving people. To a certain extent disaster warning systems are helping people by forecasting the alerting and dissemination of the information to the concerned group of organizers. Tseng and Chen designed and developed a probabilistic model for calculating the loss of earthquakes and how to manage the disaster [17]. Yap illustrated the role of ICT in disaster management in developed countries with respect to climate change [18]. Chanuka Wattegama explained in detail about application of ICT for Disaster management. ICT is used for Disaster Prevention, mitigation, preparedness, response and recovery [19]. Especially this work was limited to the flood and its Emergency management. Bedient et al., addressed the Flood warning systems through the radar-based rainfall estimation using next generation radar (NEXRAD), their model exemplifies the design, implementation, and results in the advanced flood warning system, developed for the Texas Medical Center, which make use of the NEXRAD radar for hydrologic forecast in the Brays Bayou watershed of Houston, Texas [20]. The later NEXRAD model was adopted by many researchers to model various such incidents. Vieux and team developed a model on the basis of NEXRAD for the Distributed hydrologic prediction through sensitivity to accuracy of initial radar rainfall input and soil moisture conditions [21]. In continuation Vieux once again proposed a new

model for the flood forecast to assess distributed flash flood forecasting accuracy, using radar and rain gauge input for a physics-based distributed hydrologic model [22]. Whereas Mason et al., introduced a vital technique for the flood detection in the urban areas. With the help of TerraSAR-X synthetic aperture radar data the flood detection was taking place. The observed results were TerraSAR-X, 76% right was made detection, with 25% associated false positive rate. The urban water pixels were considered, and also shadow and layover regions, these results fell to 58 and 19%, correspondingly [23]. Schumann extended TerraSAR-X and proposed a sequential aerial photography and SAR data for observing urban flood dynamics [23]. Developing country like India, have rich expertise in handling the disasters. The Govt. of India organization National Disaster Management (NDM) works intelligently in saving the people from disaster [24]. For instance the recent National Disaster Response Force (NDRF) teams were sent to the Nepal's Earthquake for rescuing the people of Nepal [25].

Even NDM has good experiences in facing the disaster; it need more help through ICT, especially in handling the floods in India and other parts of the world. Till now floods can be detected through various satellite data, but identification of people and rescuing them is still a critical task for NDRF teams and other country teams in the world.

3 Motion Object Tracking with Spatial Coordinates Algorithm (MOTSC)

This section further classified into three subsections, they are Assumptions and Notations, Object tracking KLF Algorithm, Object Spatial Coordinate Identification Algorithm and MOISC algorithm. Random probability distribution function time is assumed to perform the whole rescue operation manually. Slow moving flooded river is chosen for experimentation because this experimentation is the first of its kind. It is also assumed that, they obtained data will be useful to NDRF to take the right step.

3.1 The Object Tracking KLF Algorithm

Step 1 An array of tracks is initialized using initialize Tracks function creates, where each track is a moving object.
Step 2 Fetch the next frame from the video file.
Step 3 Binary Mask, Boundary boxes and Centroid of objects are identified using detect Objects function.
Step 4 Kalman filter is applied to each track to predict the centroid to update bounding box.

Step 5 Cost effective object, assigning and detections are as follows:

- Step 5.1 Object detection cost is calculated using the Euclidean distance method. However the experimental output is displayed by M × N matrix. Where M is the number of tracks, and N is the number of detections.
- Step 5.2 Track assignment and unassignment problem represented by the cost matrix using the assign Detections to Tracks function.

Step 6 Next the update Assigned Tracks function updates, current assigned track with respect to the detection.

Step 7 Identify every unassigned track as invisible, and increase its age by 1. Delete Lost Tracks.

Step 8 The delete Lost Tracks function deletes tracks that have been invisible for too many consecutive frames.

Step 9 New tracks are created from unassigned detections. Where, unassigned detection is represented with a new track.

Step 10 Lastly the display Tracking Results function is called for bounding box and label ID display for each.

3.2 Object Spatial Coordinate Identification (OSCI) Algorithm

The algorithm identifies the object and its initial spatial coordinates. Also tracks its intermediary coordinators' and final coordinates for the contiguous spatial coordinates. Each frame is subjected to identification of the object for its spatial coordinates. OSCI combines object identification and Georeference in a static frame.

Step 1 Goto to Google earth and identify the area where flood is flowing and record the approximate latitude and longitude.

Step 2 Initialize the El-shayalSmart software, download the shape by providing the initial coordinates.

Step 3 Load the shape file into Matlab MapViewer software. So that coordinates are identified along with the object.

Step 4 Repeat Step 1 until all frames are processed ELSEGOTO next step.

Step 5 Stop.

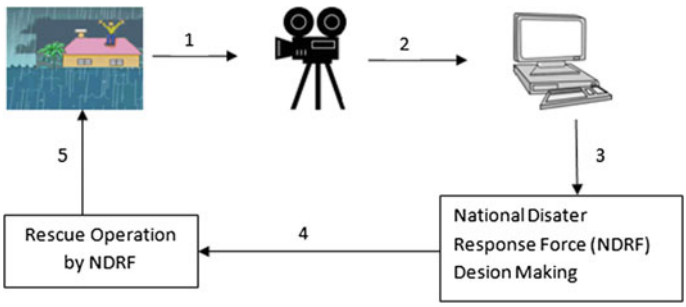

Fig. 1 Architecture of dynamic flood rescue system (DFRS)

3.3 The MOTSC Algorithm

MOTSC algorithm combines KLF algorithm and OSCI algorithm. Figure 1 shows the proposed architecture of the Dynamic Flood Rescue System (DFRS). Step-by-step representation of MOTSC algorithm is as follows:

Step 1 Initially acquire the video of the flood of the river through Camera Sensor.
Step 2 Forward and store the flood data from Camera Sensor to the Workstation or Personal Computer for video processing and analysis.
Step 3.1 Apply KLF procedure on the video for the detection of object and its tracks.
Step 3.2 Then apply OSCI mechanism for contagious spatial coordinates. These coordinates are sent to the NDRF team.
Step 4 According to the computed spatial coordinates the NDRF team will take decision and perform the Rescue Operation.
Step 5 GOTO Step 1 IF object is not rescued ELSE Step 6.
Step 6 Stop.

4 Simulations and Results

4.1 Simulation of Object Tracks Through KLF Algorithm

Flood data on Gostani River are acquired through a Sony video camera with a resolution of 576 × 720 dpi. Gostani River geographically located in Andhra Pradesh, India with 17° 56′ 18.03″N and 83° 25′ 17.10″E as spatial coordinates. The river originated in Ananthagiri Hills of the Eastern Ghats and flows via the Borra Caves. Before joining the Bay of Bengal it flows for 120 km through an estuary near Bheemunipatnam. The river basin drains the two coastal districts of

Visakhapatnam and Vizianagaram. The Gosthani's river covers a total drainage area of 2000 km^2 and it is a minor river. The present flood video is collected on 23rd June 2015 at Thagarapuvalasain Gostani River. Data is acquired on a cloudy day and there is no rain. In this experiment air filled car tube is used to float on the river water instead of human beings. Car tubes are assumed as human heads with black hair. At the time of collection of field data the Gostani river water runoff is 256 most c/s. In general, the flood estimations were made based on the inflow and outflow of the nearby reservoir. The Thatipudi reservoir is situated on the Gostani River. For the past 15 years data collected from the Irrigation Department, Government of Andhra Pradesh, India. The data contains the following attributes for the flood estimation in the Gostani River (Fig. 2).

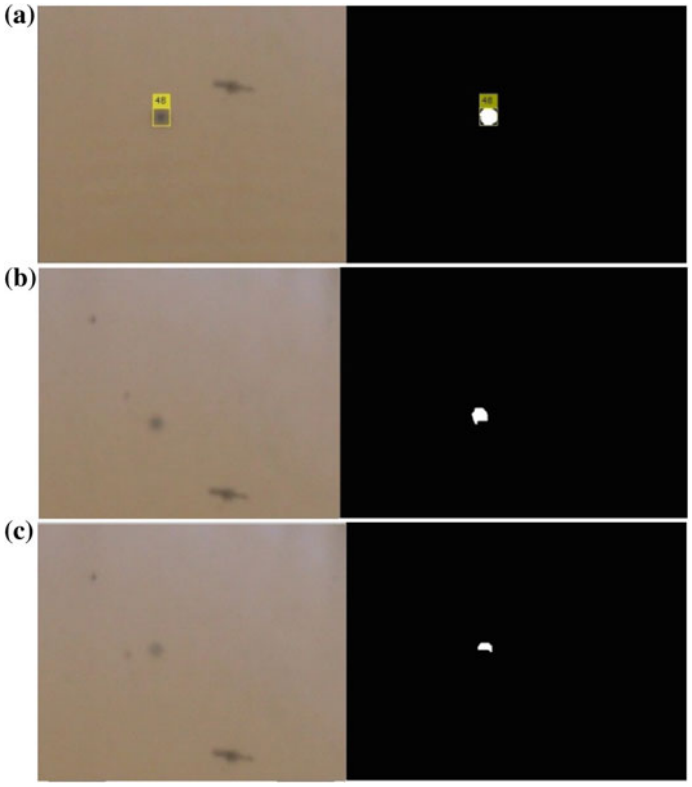

Fig. 2 Screenshot of the tracking of objects in the Gostani River flood water video frames experimentation results at frame numbers 475 (**a**), 870 (**b**) and 1107 (**c**)

4.2 Simulation of the OSCI Algorithm

4.2.1 Simulation of the Shape File Acquisition Using El-ShayalSmart

The shape files acquired using Google and all El-shayalSmart. Initial coordinates are given in the Elshayal Smart and connected to the Google earth through an interface. Shape file is downloaded in Grayscale. Once again after saving the file in Google earth we obtained the original color image.

4.2.2 Simulation of the Geo-Referencing Using Maltab's Mapviewer

After obtaining the Gostani River shape file the data is loaded to the Mapviewer tool and spatial coordinates obtained. The map scale is set to 1:0 ratio and Map units in Meters.

4.2.3 Results of MOTSC Algorithm

The object detection and tracking was done using KLF simulations, Matlab and Elshayamal used for Georeferencing. With the tracking object and obtained coordinates the data are provided to the NDRF to perform the rescue operation. Few estimated coordinates according to the track of the objects are shown in Table 1, taking video frames into consideration. This model is first of its kind. The present manual method may consume more time to identify objects and to compute its spatial coordinates.

The Overall Performance of MOTSC (OPMOTSC) can be calculated in Eq. 1.

$$\text{OPMOSTSC} = \text{AKFk} + \sum_{\text{K}=0}^{\text{n}} \text{GT}_{\text{k}} \tag{1}$$

Where Xk is the Kalman filter function to estimate the object track and GT summation of total time taken for Georeference of the required area.

Table 1 Information to the NDRF to go rescue operation

Frame no.	Spatial coordinates (appox.)		Time of the event (in sec)
	Latitude (N)	Longitude (E)	
475	17° 56′ 20.42″	83° 25′ 19.39″	19
870	17° 56′ 21.10″	83° 25′ 20.10″	67
1107	17° 56′ 21.33″	83° 25′ 21.17″	126

5 Conclusions and Future Scope

Reducing the loss of human life from natural disasters has been a billion dollar question yet to be answered. Especially managing disaster like floods is more complex. Current manual methods estimations are limited to pre and post flood events. To rescue the people from the flood, NDRF team needs instant information to go for the rescue operation. MOTSC approach addresses this issue through object tracking and also finding approximate coordinates of the object. MOTSC comprises of KLF and OSCI algorithm. The obtained object detection and spatial data will be helpful to NDRF team. Manual methods will consume more time to rescue the people from floods. The proposed method is partially automated. If the spatial coordinate time is reduced, the rescue operation will be faster; this results in saving more human lives from the flood disasters.

References

1. Wolf, P.R., Dewitt, B.A.: Elements of Photogrammetry: With Applications in GIS, vol. 3. McGraw-Hill, New York (2000)
2. Albala-Bertrand, J-M.: Political economy of large natural disasters: with special reference to developing countries. OUP Catalogue (1993)
3. Carpenter, T.M., et al.: National threshold runoff estimation utilizing GIS in support of operational flash flood warning systems. J. Hydrol. **224**(1), 21–44 (1999)
4. Price, M.J., Wurman, G.: Earthquake warning system. U.S. Patent Application 13/993,394
5. http://nidm.gov.in/PDF/pubs/ukd-p1.pdf
6. http://ndrfandcd.gov.in/cms/Ndrf.aspx. Accessed 05 April 2015
7. http://nidm.gov.in/PDF/pubs/India%20Disaster%20Report%202012.pdf. Accessed 16 April 2015
8. http://www.ndma.gov.in/images/pdf/DG%20Presentation%2001%20Oct%202013.pdf. Accessed 05 May 2015
9. http://jkfcr.nic.in/pdf/Master_Plan_Version_IV.pdf. Accessed 05 May 2015
10. Chen, C.-H., Pau, L.-F., Wang, P. S. (eds.): Handbook of Pattern Recognition and Computer Vision, vol. 27. Imperial College Press (2010)
11. Neale, C.M.U., Crowther, B.G.: An airborne multispectral video/radiometer remote sensing system: development and calibration. Remote Sens. Environ. **49**(3), 187–194 (1994)
12. Schumann, G.J.-P., et al.: The accuracy of sequential aerial photography and SAR data for observing urban flood dynamics, a case study of the UK summer 2007 floods. Remote Sens. Environ. **115**(10), 2536–2546 (2011)
13. Yu, Q., Medioni, G.: Motion pattern interpretation and detection for tracking moving vehicles in airborne video. In: IEEE Conference on IEEE, Computer Vision and Pattern Recognition 2009, CVPR 2009 (2009)
14. Suhr, J.K.: Kanade-Lucas-Tomasi (KLT) feature tracker. In: Computer Vision (EEE6503), pp. 9–18 (2009)
15. Wang, Z., et al.: CamShift guided particle filter for visual tracking. Pattern Recognit. Lett. **30** (4), 407–413 (2009)
16. Chan, Y.T., Hu, A.G.C., Plant, J.B.: A Kalman filter based tracking scheme with input estimation. IEEE Trans. Aerosp. Electr. Syst. **2**, 237–244 (1979)

17. Tseng, C.-P., Chen, C.-W.: Natural disaster management mechanisms for probabilistic earthquake loss. Nat. Hazards **60**(3), 1055–1063 (2012)
18. Yap, N.T.: Disaster management, developing country communities & climate change: The role of ICTs. Manchester: Report, Heeks, R., Ospina, A. (eds.) for IDRC, Centre for Development Informatics, Institute for Development Policy and Management, University of Manchester (2011)
19. Sriramesh, K., Wattegama, C., Abo, F.J.: The role of ICTs in risk communication in Asia Pacific (2007)
20. Bedient, P.B., et al.: NEXRAD radar for flood prediction in Houston. J. Hydrol. Eng. **5**(3), 269–277 (2000)
21. Vieux, B.E.: Distributed Hydrologic Modeling Using GIS. Springer, Netherlands (2001)
22. Looper, J.P., Vieux, B.E.: An assessment of distributed flash flood forecasting accuracy using radar and rain gauge input for a physics-based distributed hydrologic model. J. Hydrol. **412**, 114–132 (2012)
23. Mason, D.C., et al.: Flood detection in urban areas using TerraSAR-X. IEEE Trans. Geosci. Remote Sens. **48**(2), 882–894 (2010)
24. http://ndma.gov.in/en/. Accessed 26 July 2015
25. http://zeenews.india.com/tags/national-disaster-response-force.html. Accessed 28 July 2015
26. Brivio, P.A., et al.: Integration of remote sensing data and GIS for accurate mapping of flooded areas. Int. J. Remote Sens. **23**(3), 429–441 (2002)

Chapter 76
Identification of Landslide Hazard Zones in Greater Visakhapatnam Municipal Corporation, Andhra Pradesh, India—A Geospatial Approach

Peddada Jagadeeswara Rao, P. V. V. Satyanarayana, Ch. V. Rama Rao, Rajesh Duvvuru, G. Narasimha Rao, Dadi Sanyasi Naidu, Ch. Anusha and G. V. Vidya Sagar

Abstract The study area, Greater Visakhapatnam Municipal Corporation (GVMC) is the largest one which occupies an area of 545 km^2 is also a gateway to industries and tourism in Andhra Pradesh. The area is characterised by hilly terrain with moderate valleys and coastal plains comes under the Eastern Ghats. The area has been covered by reserved forests, within the jurisdiction of GVMC. Owing to industrialisation, urbanisation and migration of rural people encroaching into the Kailasagiri and Yaradakonda thick vegetated hill ranges leading to deforestation.

P. J. Rao (✉) · R. Duvvuru · G. N. Rao · D. S. Naidu · Ch. Anusha
Department of Geo-Engineering, College of Engineering, Andhra University, Visakhapatnam, India
e-mail: pjr_geoin@rediffmail.com

R. Duvvuru
e-mail: rajesh.duvvuru@gmail.com

G. N. Rao
e-mail: gudikandhula@gmail.com

D. S. Naidu
e-mail: sndadi@gmail.com

Ch. Anusha
e-mail: anu4goal@gmail.com

P. V. V. Satyanarayana
Department of Civil Engineering, College of Engineering (a), Andhra University, Visakhapatnam, India
e-mail: pasalapudisat@yahoo.com

Ch. V. Rama Rao
Guest Faculty, Andhra University, VUDA, Visakhapatnam, India
e-mail: chappa.rama@gmail.com

G. V. Vidya Sagar
Deputy Director General, Geological Survey of India, Visakhapatnam, India
e-mail: gvvsagar1@gmail.com

P. J. Rao et al. (eds.), *Proceedings of International Conference on Remote Sensing for Disaster Management*, Springer Series in Geomechanics and Geoengineering,
https://doi.org/10.1007/978-3-319-77276-9_76

Thatched and asbestos roof houses, single to multi-storied buildings are being constructed in the foothills of these two hill ranges without following the building norms and topographic conditions. Rainfall induced landslides/slips are more common claiming innocent lives. In this study, SOI toposheets, IRS-P6-LISS-III satellite imagery and SRTM-30 data used to generate drainage, geology, geomorphology, land use/land cover, slope revealing fractured and jointed khondalite rocks, altered drainage, erosion, fluvial and marine landforms. Jointed khondalite hillocks, porous and permeable, weathered zones and erosion by different agencies are the potential landslide zones. The Soil Bearing Capacity (SBC) ranges from 28 to 40 t/m^2 in the foothill areas. Study suggests, terrain characteristics are to be taken into account besides SBC before taking up of constructions in hilly terrain. Terraced or split level foundation with adequate retaining wall support is a suitable technique which can withstand to the hill slope conditions.

Keywords Eastern ghats · Khondalite · Landslides · Landforms
Split level foundation

1 Introduction-Landslides

The landslide is a result of a wide variety of geoenvironmental processes, which include geological, meteorological and human factors. The important factors that influence landslides are lithostratigraphic units which include structure, degree and depth of weathering, geomorphology, slope and aspect. The upper layer of soil porosity, permeability and structure, land use and land cover, particularly anthropogenic activities in hilly terrains and cloudburst are the induced factors [1, 2]. The Himalayan mountains experiences about 10% world landslide/soil creep, etc., which disrupt communication, loss of life and property. The South India is having oldest hills which are partially stable to landslides. However, the number of major landslides being occurred in different places leading to ecological imbalance. The study area, the GVMC comes under the South India, where the hills are covered by dry deciduous and semi-evergreen forests. A major landslide occurred in the midnight of 3rd/4th August, 2006 at Kodipunjuvalasa, Araku Mandal, Visakhapatnam district, buried 18 people under the debris [3].

2 Study Area

The study area, Greater Visakhapatnam Municipal Corporation (GVMC) is located between 17° 56′16.26″ to 17° 59′25″ North lat and 83° 40′31″ to 83° 53′50″ East long. The city appears as a saucer shape bounded by the Bay of Bengal on eastern side covers 545 km^2 (Fig. 1). The area comes under Eastern Ghats comprising khondalite suite of rocks. Hills are covered by hydrophilic soils which supports dry

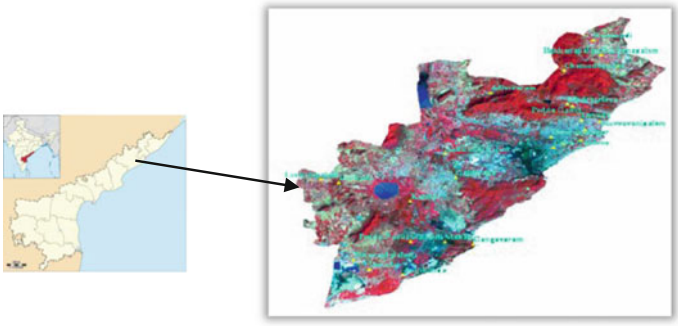

Fig. 1 Location map (Study area as viewed on IRS P6-LISS-III, January, 2011)

deciduous forests. Later intrusives of charnockite and quartzite hillocks are highly fractured and huge rock blocks are exposed in places. A marine creek has a length of about 1 km which extends up to the Visakhapatnam Airport.

The altitude of the area varies from 0 to 350 m above MSL with an average annual rainfall of 1201 mm.

According to 2011 censes, the total population in GVMC is around 1.73 million [4]. It is one of the fastest developing cities in India often it is called as "industrial city". The natural topography has been altered due to various constructions. Foothill soils removed for laying roads and other major constructions besides encroachments leading to deforestation. A historical pilgrim centre Lord Narasimha Swamy temple and Kailasagiri park with a sea view is developed over the hill ranges. Similarly, several military establishments have come up in recent years in Yarada Konda hill range. Huge number of urban slums are in the hills which are vulnerable to landslides. There is rainfall induced landslides in hilly areas in GVMC (Table 1). Hence, this study is taken up to identify the Landslide Hazard Zones (LHZ) using geospatial technologies.

Table 1 Landslides occurred in recent years in GVMC area

Year of landslide	Area	Loss of life	Injured
2011	Krishna Nagar, Gajuwaka	2	5
2012	Bojjanna Konda	1	–
2013	Pentayya Nagar	3	–
2015	Simhagiri Colony, Gajuwaka	2	–
2015	Sanjeevayya Nagar	4	3

Source Saakshi Telugu daily news paper, Dt. 13-10-2015, Eenadu, 21-12-2015

Table 2 Particulars of data used

Data type		Sensor & resolution (m)	Scale	Data derivatives
Satellite data	IRS-P6	LISS-III-23.5	1:50,000	Land use/cover & geomorphology, lineaments
	IRS-P6	LISS-III-23.5	1:50,000	
	SRTM	C-band and X-band 30	1:50,000	DEM
Toposheet	65 O/1, 2, 3, 4, 5, 6	–	1:50,000	Drainage & lineaments

3 Data Used

In this study, IRS P6-LISS-III satellite data of 2011 and 2016 have been used (Table 2). The SRTM-30 m data, rainfall and temperature data collected from IMD, Visakhapatnam district, Visakhapatnam Geology and Mineral map (GSI, 2001), soils map is derived from the District Soil map (Assistant Director of Agriculture, Visakhapatnam) and Survey of India toposheets 65 O/1, 2, 3, 4, 5 and 6 on 1:50,000.

4 Results

4.1 Drainage and Lineament Density

Drainage density reflects the signature of climate on the topography which dictates the boundary conditions for surface hydrology [5]. The less permeable rock is, the less infiltration of rainfall, which conversely tends to be concentrated in surface runoff. As shown in Fig. 2a, the study area has fifth higher order streams [6]. The drainage in the study area has been severely altered due to urban built-up. Several constructions have been constructed on hills which are altering drainage courses resulted in landslides/soil creep, etc.

Lineament map generated following the standard visual interpretation techniques on satellite imagery with major controlling features of drainage on toposheet map (Fig. 2). Lineaments provide important information on sub-surface fractures that may control the movement and storage of groundwater [7] and use of satellite data defines the spatial zones based on the geomorphology and its associated structures [8]. Landmass denudation coupled with anthropogenic activities transformed the lineaments as potential landslide/landslip zones.

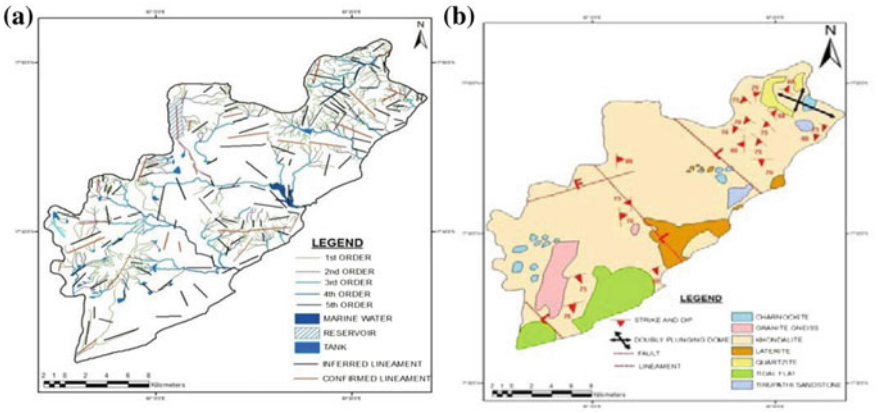

Fig. 2 **a** Drainage and lineaments of the study area. **b** Geology of the study area

4.2 Geology

The geology of the study area belongs to Precambrian age, characterized by the occurrence of intrusive meta igneous bodies and meta sediments [9]. It is composed of high-grade metamorphic rocks and igneous rocks. The different rock types and structural trends were digitized in ArcGIS-9.2 (Fig. 2b). Spatial discrepancy of different rocks has been adjusted considering terrain elements on the satellite image. The strike of the rocks is NNE-SSW, however, local variations are identified at places [10–12].

Majority unscientific constructions are made in the foothill areas of Yarada and Kailasa hills. Areas such as Kancherapalem and Thatichetlapalem hills consists of khondalite and granite gneiss which are highly fractured. Hills are covered by thick hydrophilic soils, admixed kankar. Removal of materials in small areas for constructions in hill slopes are liable to slide as landslides/soil creep, etc. during heavy rains on human habitations, causing monetary and human loss.

4.3 Geomorphology

Geomorphology involves study of landforms, reconstruction of process responsible for their origin and study of the influence of tectonics in time and space. In this, 17 geomorphic classes of erosion, fluvial and marine origin were delineated following of visual interpretation techniques (Fig. 3). In tropical and equatorial regions, weathering processes create a superficial layer with varying degree of porosity and permeability [13]. Geomorphology and lineament, it is well known fact that the geomorphological characteristics of an area affect its response to a considerable extent of landslide/soil creep occurrence. Thus, linking of geomorphological

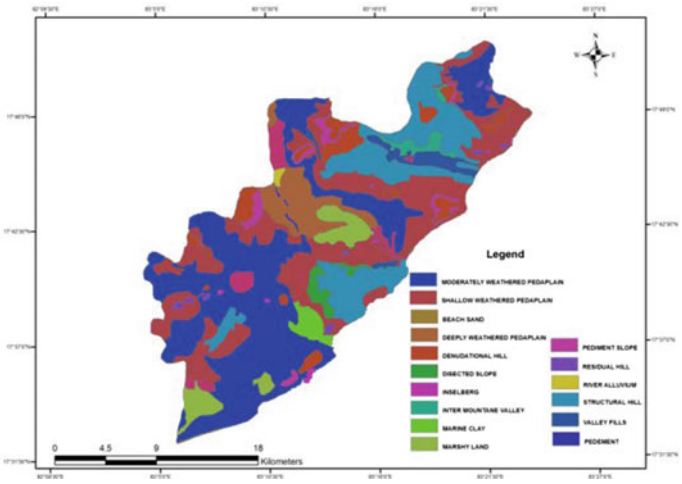

Fig. 3 Geomorphology of the study area

parameters with hydrological characteristics of an area provides a simple way to understand their hydrological behaviour. The piedmont slopes, alluvial fans and cones are being occupied by urban built-up. Industries along the seashore occupied mudflats. Part of the HPCL storage tanks and the Visakhapatnam airport are on mudflats.

4.4 Land Use/Land Cover

Land use/land cover mapping serves as a basic inventory of land resources for all levels of government, environmental agencies, and private industries throughout the country. Visual interpretation and classification of IRS-P6 LISS-III November 2009 and January, 2011 satellite data resulted into 23 land use/cover classes carried out following the standard visual interpretation techniques [14]. In this analysis, 12 land use and 1 1 land cover categories demarcated, out of which urban built-up area covering 139.22 km^2 is the major land use, whereas forest with 104.11 km^2 is the major land cover (Fig. 4a). Economic development and population growth have triggered rapid changes to Earth's land cover throughout the year, and there is every indication that the pace of these changes will accelerate in the future.

Cities grow and spread which consumes agricultural area. The urban sprawl often infringes upon viable agricultural or productive forest land, neither of which can resist nor deflect the overwhelming momentum of urbanization. All land use planning processes in most of the countries are based on geomorphological units [15]. The study area has been expanded from a small fishermen colony to the largest municipal corporation. The study area has unique saucer shape topography, major

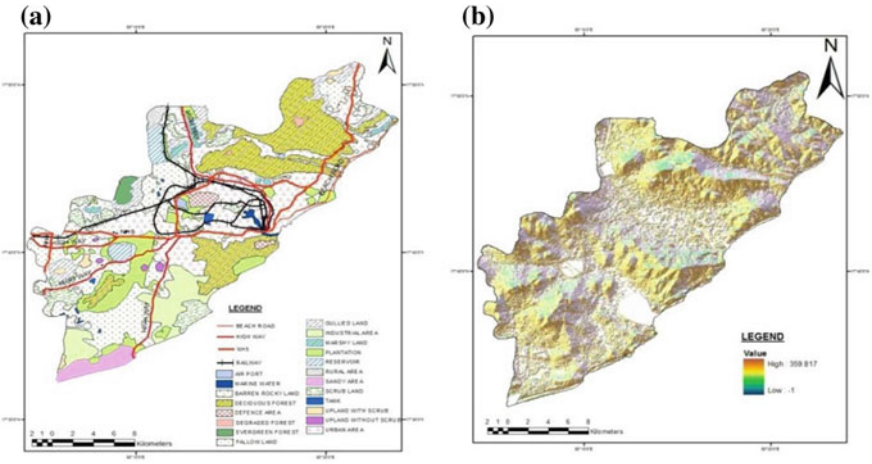

Fig. 4 **a** Land use/land cover. **b** Digital elevation model map (DEM)

hills are covered by thick reserved forests. Greenery is reducing year after year, due to developmental activities. The forests in the GVMC are the natural habitats for the wild flora and fauna which are under threat due to encroachment. The urbanisation is moving towards Madhurawada–Ananadapuram, Pendurthy–Sabbavaram and industrial corridor towards the southern side has emerged as one of the fastest growing cities in India. Urbanisation is in plains, encroachments, IT Park and Naval establishments are in hilly terrain. The encroachment areas are often experiencing landslides/landslips resulting in loss of life and property.

4.5 Digital Elevation Model

A Digital Elevation Model (DEM) can be represented as a raster is referred to as a secondary (computed) DEM [16]. SRTM-30 satellite data used to generate DEM map (Fig. 4b) of the area. The DEM of the study area varies from 0 to 350 m above the msl. Plains and valleys are under urban built-up, whereas, the hills are covered by thick forests. Hills near the Thatichetlapalem, Kancherapalem, Hanumanthavaka, Arilova, Krishna Nagar and Gajuwaka are fractured/fissured. The encroachments in these hilly areas, altered the natural topography, became potential landslide zones.

4.6 Landslide Hazard Zones

The study area has dominated by hills, majority constructions unauthorized. These are mostly in Kancherapalem, Arilova areas, where most of these constructions

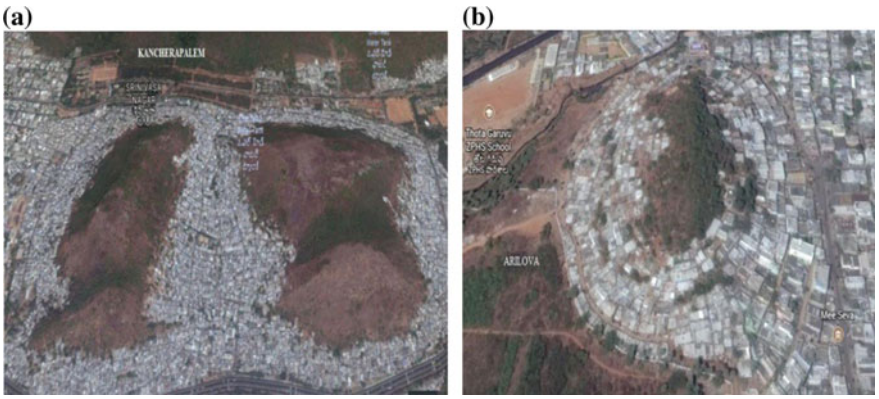

Fig. 5 **a**, **b**. Kancherapalem and Arilova areas as viewed on Google Earth (19th February, 2017)

were not followed any building norms and experiencing landslides during rainy season (Fig. 5a, b).

4.7 Remedial Measures

Observed during the field study, there are few single story buildings constructed in the hill slopes had been experienced settlements and foundation failure in Dayal Nagar, Gajuwaka, Visakhapatnam. It reflects that these constructions have not been

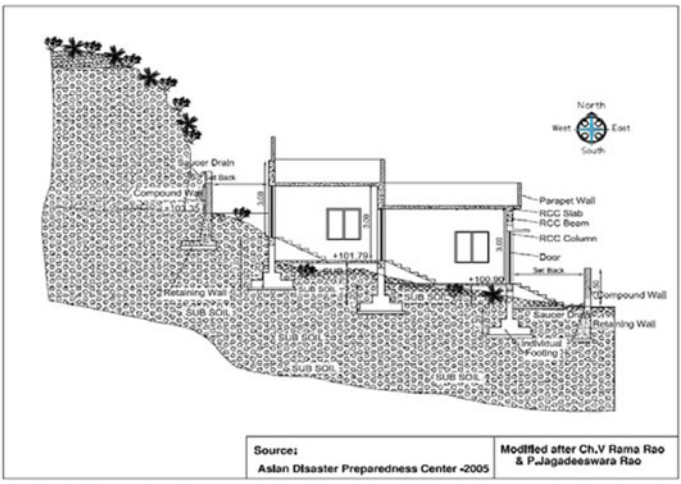

Fig. 6 Terraced foundation

followed any scientific measures. Keeping in view of this, a terraced foundation with adequate retaining wall support has been suggested. To let out drainage, sufficient provision is to be provided (Fig. 6).

5 Conclusions and Discussion

Low altitude hills in GVMC are covered by urban settlements. The natural drainages have been altered due to urban built-up. Because of the constructions, the topography has been altered, which triggers into landslides, soil creep, rock slip, etc. This has been resulted in deforestation, removal of soil and earth materials at the foothills. During rainy season, landslides are taking place only in the constructed part in hilly areas. Urban area (139.22 km^2) is the major land use and forest (104.11 km^2) is the major land cover.

Construction areas ranging from 30 to 200 km^2 are made up of load bearing and a few are RCC. These are constructed on uneven hill slopes without understanding the surrounding geologic set-up. Safe RCC structure with proper foundation design is suggested to overcome the landslide problem. In general, the physical characteristics of soils in hilly areas are gravel 5%, sand 45%, and fines 50% with SBC values ranges from 3.00 to 35 t/m^2. The physical characteristics of hilly areas are 54% gravel 21% sand and 25% fines with SBC ranging from 28 to 40 t/m^2. Road expansion of the existing Bheemili beach road, the hills en-route were partially removed. These hill masses are highly vulnerable to landslides.

References

1. Varnes, D.J.: Landslide hazard zonation: a review of principles and practice, UNESCO. Nat. Hazards **3**, 61 (1984)
2. Anbalagan, R.: Landslide Hazard evaluation and zonation mapping in mountainous terrain. Eng. Geol. **3**(2), 269–277 (1992)
3. Balaji, P., Pavanaguru, R., Reddy, D.V.: A Note on the Occurrence of Landslides in Araku Valley and its Environs, Visakhapatnam District, Andhra Pradesh, India (2010)
4. httpjnnurm.nic.inwp-contentuploads20140329-Vishakapatnam-Draft-Report.pdf
5. Ashnafi Tolessa, G., Jagadeeswara Rao, P.: A geospatial based study on mapping of flood inundation zones in Tandava River Basin, Andhra Pradesh. Int. Jour of Remote Sens. Geosci. **2**(2), 34–37 (2013)
6. Strahler, A.N.: Statistical analysis in geomorphic research. J. Geol. **62**, 1–25 (1952)
7. Raghu, V., Mruthyunjaya Reddy, K.: Hydrogeomorphological Mapping at Village Level Using High Resolution Satellite Data and Impact Analysis of Check Dams in Part of AkuleduVanka Watershed, Anantapur District, Andhra Pradesh. The J. Indian Geophys. Union **15**(1), 1–8 (2011)
8. Rao, P.J., Harikrishna, P., Srivastav, S.K., Satyanarayana, P.V.V., Vasu Deva Rao, B.: Selection of groundwater potential zones in and around Madhurawada Dome, Visakhapatnam District—a GIS approach. J. Indian Soc. Remote Sens. **13**(4), 191–200 (2009)

9. Narasimha Rao, C.H.: Geology and petrology of the Kailasa range. M.Sc. thesis, Andhra University, Waltair (1945)
10. Sriramadas, A.: Structural geology of the Eastern Ghats in parts of Visakhapatnand Srikakulam districts, Andhra Pradesh, India. In: 22nd International Geological Congress, India, pp. 245–251 (1964)
11. Chetty, T.R.K., Vijay, P., Suresh, B.V.V.Vijaya, Kumar, T.: GIS and the tectonics of the Eastern Ghats, India. GIS Dev. **16**(12), 21–24 (2002)
12. Rao, P.J., Suryaprakasa Rao, B., Jagannadha Rao, M., Harikrishna, P.: Geo-electrical data analysis to demarcate ground water pockets and recharge zones in Champavathi River Basin, Vizianagaram District. Andhra Pradesh. J. Ind Geophys. Union **7**(2), 105–113 (2003)
13. Mogajia, K.A., Aboyejib, O.S., Omosuyi, G.O.: Mapping of lineaments for groundwater targeting in basement complex area of Ondo state using remotely sensed data. Int. J. Water Resour. Environ. Eng. **3**(7), 150–160 (2012)
14. NRSA: Mannual of Nationwide Land Use/Land Cover Mapping Using Satellite Imagery (Part I). National Remote Sensing Agency (NRSA), Hyderabad (1989)
15. Dragut, L., Blaschke, T.: Automated classification of landform elements using object-based image analysis. Geomorphol. **81**(3), 330–344 (2006)
16. Ronald, T.: Terrain models-a tool for natural hazard mapping. Avalanche formation, movement and effects. In: Proceedings of the Davos Symposium, September 1986, International Association of Hydrological Sciences. No. 162 (1987)

Chapter 77
Flood Inundation Simulation of Mahanadi River, Odisha During September 2008 by Using HEC-RAS 2D Model

Tushar Surwase, G. SrinivasaRao, P. Manjusree, Asiya Begum, P. V. Nagamani and G. JaiSankar

Abstract Odisha state witnessed severe flooding in the years 2003, 2008, 2009 and 2011 which affected major districts like Cuttack, Khurdha, Jagatsinghpur, Puri and Kendrapada. HEC-RAS 2D is a hydraulic model which is used to simulate water flowing through rivers and open channels. In addition, the model also provides the depth of water, velocity and water surface elevation with respect to time. Using this model, part of Mahanadi River stretch from Tikarpara to Mundali was taken as the study area for simulating floods during September 2008. Inputs to the model like CARTO DEM at 10 m posting, discharge data, roughness co-efficient were provided and flood inundation was simulated. The flood extent from the model was validated with the satellite derived flood extent obtained from RADARSAT satellite. Model performance was evaluated based on the parameters F1 and F2 where, F1 and F2 are measures of fit which range from 0 to 1 and −1 to 1 respectively. If the fit value is closer to 1, it indicates that the model performance is better. Sensitivity analysis is carried out to investigate the model performance for

T. Surwase (✉) · G. SrinivasaRao · P. Manjusree · A. Begum
Disaster Management Support Group, RSAA, NRSC, Hyderabad 500037, India
e-mail: tusharsurwase@ymail.com

G. SrinivasaRao
e-mail: rao_goru@yahoo.com

P. Manjusree
e-mail: pmanjusree69@gmail.com

A. Begum
e-mail: asiya.nrsc@gmail.com

P. V. Nagamani
Earth and Climate Science Area, NRSC, Hyderabad 500037, India
e-mail: pvnagamani@gmail.com

G. JaiSankar
Department of Geo-Engineering, Andhra University,
Visakhapatnam, Andhra Pradesh 530003, India
e-mail: jaisankar.gummapu@yahoo.com

P. J. Rao et al. (eds.), *Proceedings of International Conference on Remote Sensing for Disaster Management*, Springer Series in Geomechanics and Geoengineering,
https://doi.org/10.1007/978-3-319-77276-9_77

different roughness coefficients of the flood plain. From the study, it is observed that the model performed well for roughness coefficient 0.020 and the measures of fit F1 and F2 were found to be 0.85 and 0.74 respectively. A flood hazard map was prepared based on the flood depth for the study area.

Keywords Flood simulation · HEC-RAS 2D · Mahanadi river
Satellite · Flood hazard

1 Introduction

Riverine floods are the floods caused by the water overflowing from the river banks into the flood plains. Flood is the most prominent natural hazard in India and its frequency is higher than any other natural calamities, in India, 8 million hectares is the average area which is affected by floods annually and 40 million hectares is the total area which are liable to floods in which 4.18% is contributed by Odisha which is 1.672 million hectares [10]. Odisha state witnessed severe floods in the year 2003, 2008, 2009 and 2011 which affected major districts like Cuttack, Khurdha, Jagatsinghpur, Puri and Kendrapada. Though some control measures like Hirakud Dam, Barrages, Embankments and are constructed across the Mahanadi River but due to High rainfall in the upper as well as in lower catchment these control measures were not able to control the flood for the year 2008. Several cattle's and cultivated paddy fields were swamped by the flood. The death count of Human lives was about 90 and about 4, 30,856 people were affected and there was immediate response from Rescue and Relief team, they evacuate the people to safer places and provided them with temporary shelters [4]. The satellite remote sensing data is used in order to analyze and evaluate the flood extent, so this analysis is only limit to the specific discharges at the time of flood events [7]. So in order to look for future events, the use of HECRAS 2D model allows flood inundation simulation for different flood events and Discharges. HEC-RAS is Hydrologic Engineering Center-River Analysis System is a freely available and popular Hydraulic model developed by United States Army Corps of Engineers (USACE). The flood inundation can be simulated by using 1D one dimensional or 2D two dimensional model. HEC-RAS earlier version was limit to 1D model which can be used to analyze the flow in open channel (natural or artificial). 1D model is congenial for the study of water flowing below danger level in the channel which can be considered model to be 1 dimensional behavior because the water is constraints by its banks but when water levels exceeds danger level and water comes to the flood plain there is possibility of water to move in two directions. So taken this into account USACE has developed 2D model version 5.0.1 in Feb 2016. The study uses HEC-RAS 2D Model Version 5.0.1 February 2016 release for simulating the floods for September 2008 Mahanadi river flood. The simulations performed by inputting daily river discharge values at the time of flood event which was obtained from Central Water Commission. The model shows the simulation results in the

form of flood extent with depth and velocity which helps to developed flood hazard map based on depth. The results were further validated with RADARSAT satellite image which shows better resemblance in terms of view as well as in terms evaluated values. From present study it has been notice that the model is more sensitive to manning's roughness coefficient 'n'. The sensitivity analysis has been carried out for different manning's 'n' assigned for flood plains.

2 Study Area

The study area is a part of Mahanadi river in Odisha also falls in Mahanadi Graben [1] stretching from Tikarpara to Mundali as shown in Fig. 1, the floodplains lies between the latitudes 20° 12′00″N and 20° 36′30″ and longitudes 84° 46′00″ and

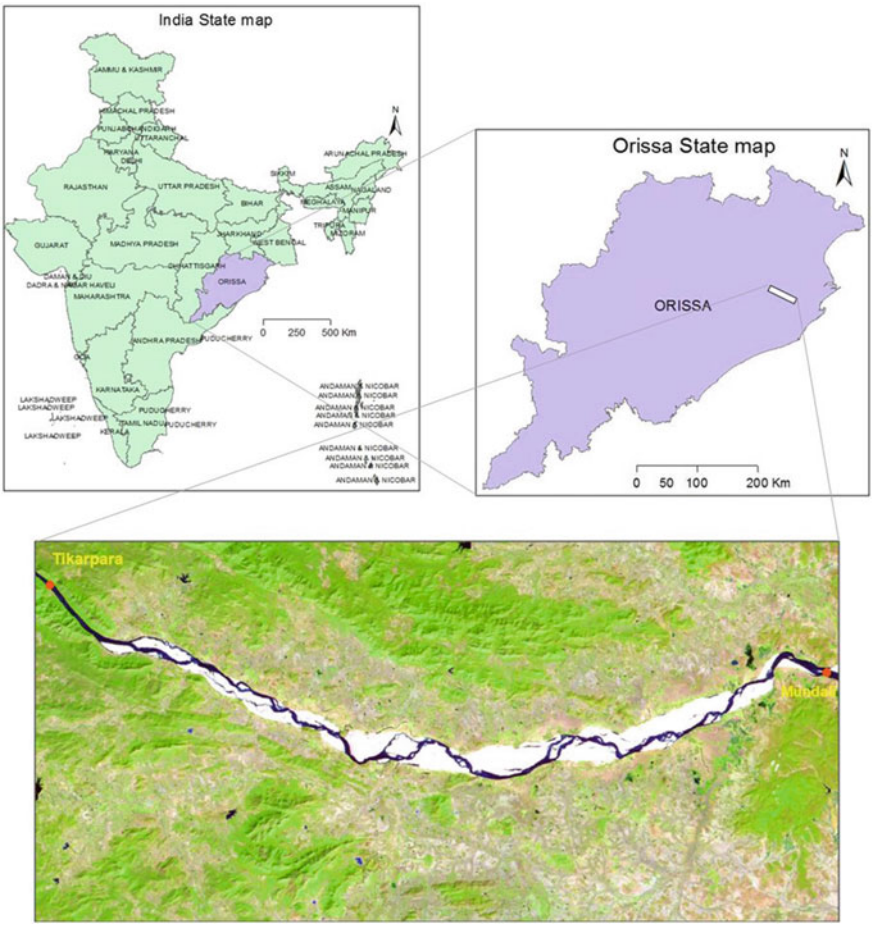

Fig. 1 Study area.

85° 40′00″. The topographic condition of Odisha state comprises of fertile land mainly paddy lands along East Coast and forested highlands in interior. The average elevation is 45 m above mean sea level and having mild slope of 4 cm/km. The soil type observed for the study area is Laterite soil which occupies 0.7 MHa of lands in Khurda, Cuttack, Puri, Dhenkanal, Keonjhar, Mayurbhanja and Sambalpur districts [4]. As laterite soil contains impermeable clay it favors the inundation. The area downstream of Hirakud dam to Mundali intercepts a catchment of 48,700 km^2 which is responsible of floods in Mahanadi deltaic area [8].

The September 2008 flood event was reported as unprecedented flood situation by Ministry of Home Affairs Government of India, because its severity and Magnitude has crossed the Disaster for 1982 and 2001 flood which was observed to be greatest flood event [4]. There was immediate response from ODRAF, NDRF, and NAVY (INS Chilika) with boats for rescue operation. On the other hand Indian Air force was immediately flies into service for Airdropping food packets in the Marooned areas for rescued people.

3 Data Used

Data used for simulation were mainly two types geographic data and river discharge data of Mahanadi River in Odisha. Geographic data deals with Digital Elevation Model (DEM) from CartoDEM 10 m resolution data which is a product of CartoSAT 1 satellite designed and maintained by Indian Space Research Organization (ISRO) Government of India—Department of Space. The study area starts from Tikarpara gauging station which is located at downstream side of Hirakud Dam. The discharge data at Tikarpara gauging site on Mahanadi River recorded and maintained by Center Water Commission (CWC), Ministry of Water Resource Government of India. For study area, the daily discharge data at Tikarpara gauge site was obtained from CWC. The study simulated the flood event in between September 02, 2008 and September 30, 2008. This time was selected because it was severely affected by flood event. Land use Land Cover (LULC) was also considered for the study area to separately give the manning's roughness coefficient for river channel and floodplains. For floodplains a unique value of roughness coefficient was given as study is carried out by sensitivity analysis.

4 Methodology

HEC-RAS Version 5.0.1 model was used to simulate the September 2008 flood event. This version of HEC-RAS has capabilities to solve 2D Full momentum equation (Saint Venant equation) or 2D Diffusion wave equation. The methodology chart as shown in Fig. 2 shows a brief outline of the model.

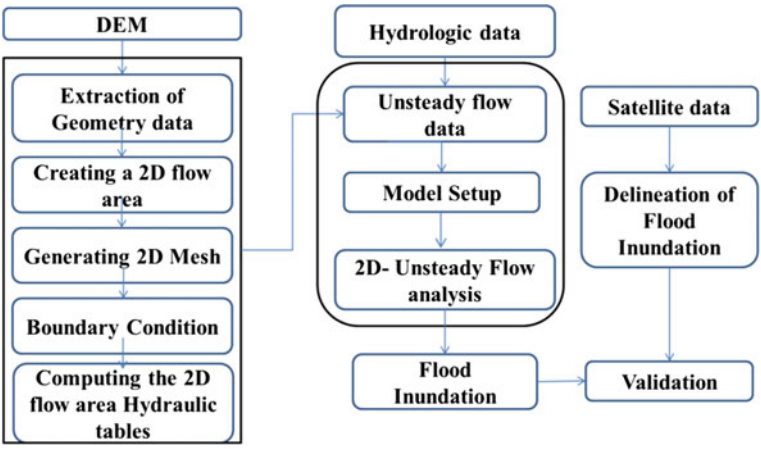

Fig. 2 Methodology flow chart

The study area was defined by a 2D closed polygon. The 2D polygon area is the area within which inundation is about to occur. The 2D polygon is defined by two methods for optimization of 2D cells. One is to define polygon which will cover the inundated area previously observed by satellite in severe condition for study area. Second method is adopted when satellite data is not available for the study area. The polygon is defined by connecting higher elevation like mountain where inundation will not extend beyond the features. After defining the polygon the computational cells are generated, the cells are in rectangular grid called staggered grid and at the boundary of 2d polygon the cells may be non staggered grid which is composed by polygons having 3 to maximum 8 sides. The spacing of rectangular cell was kept to be 10 m × 10 m so as to have closer towards the DEM used 10 m × 10 m resolution. Further, Two boundary condition has been assigned to study area one Hydrograph Boundary condition Representing observed discharge at Tikarpara upstream side. The width of river at Tikarpara is 760 m covered by 76 cells. The inflow hydrograph as shown in Fig. 3 was assigned to these 76 cells. Second boundary condition normal depth was assigned at Mundali downstream side.

Considering topographic conditions and DEM values, slope value of 0.001 was used. Before starting for simulations hydraulic property tables are computed. The properties like hydraulic wetted perimeter and cross sectional area are computed for every 2D computational cell. Manning's Roughness coefficient 0.032 for river channel (n_r) used, study by prabeerkumarparhietal [8] for the same study area. Manning's roughness coefficient for flood plains (n_f) was selected based on the sensitivity analysis [7] in which three roughness coefficient for flood plains was considered 0.020, 0.030, 0.040 for three different simulations as shown in Table 1.

This version of HEC-RAS has capabilities to solve 2D Full momentum equation (Saint Venant equation) or 2D Diffusion wave equation. Full momentum equation includes all parameters such as Gravity, Pressure, Friction, Corollis effect,

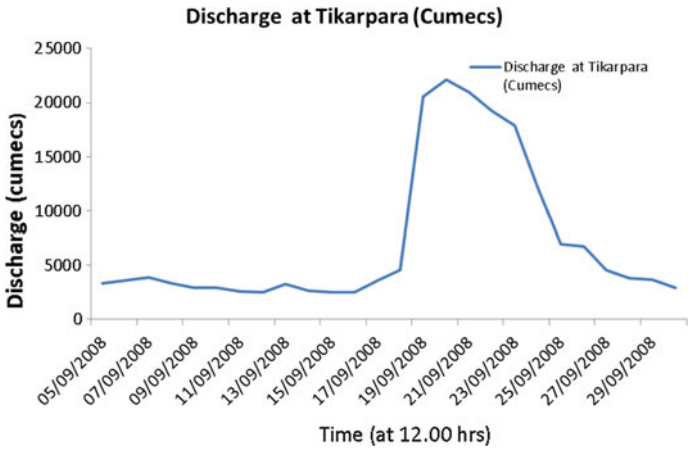

Fig. 3 Flow hydrograph at Tikarpara gauge station (CWC)

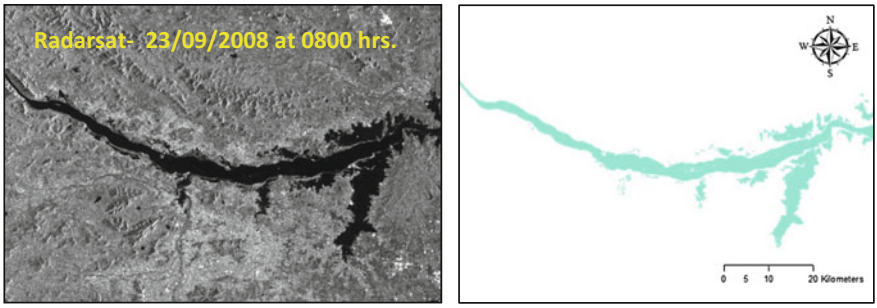

Fig. 4 Flood inundation observed by RADARSAT satellite image and its delineation

Table 1 Simulation for different roughness coefficient

Simulation	Roughness coefficient for channel (n_c)	Roughness coefficient for floodplains (n_p)
1	0.032	0.020
2	0.032	0.030
3	0.032	0.040

Acceleration, Turbulent eddy viscosity. Diffusion wave equation only includes Gravity, Pressure, and Friction parameters. For present study Full momentum equation (as shown below) was used as it takes all parameters in account.

$$\frac{\partial p}{\partial t}+\frac{\partial}{\partial x}\frac{(p^2)}{(h)}+\frac{\partial}{\partial y}\frac{(pq)}{(h)}=-n^2pg\frac{\sqrt{(p^2+q^2)}}{h^2} - gh\frac{\partial s}{\partial x}+pf+\frac{\partial}{\rho\partial x}(h\tau_{xx})+\frac{\partial}{\rho\partial y}(h\tau_{xy}) \quad (1)$$

$$\frac{\partial p}{\partial t}+\frac{\partial}{\partial x}\frac{(q^2)}{(h)}+\frac{\partial}{\partial y}\frac{(pq)}{(h)}=-n^2qg\frac{\sqrt{(p^2+q^2)}}{h^2} - gh\frac{\partial s}{\partial x}+qf+\frac{\partial}{\rho\partial y}(h\tau_{yy})+\frac{\partial}{\rho\partial x}(h\tau_{xy}) \quad (2)$$

where, h is the water depth (meters), p and q are the specific flow in the x and y directions (m^2/sec), s is the surface elevation in (meters), g is gravitational acceleration m/sec^2, n is the manning's resistance, ρ is the density of water (kg/m^3), τ_{xx}, τ_{yy}, τ_{xy} are the components of effective shear stress and f is the Corollis (/sec). Computational time step was calculated based on the courant friedrich lewy condition

$$cr=\frac{C\Delta t}{\Delta x} \quad (3)$$

where, cr is courant number, c is celerity (m/sec), Δt is computational time step (sec), Δx is grid cellsize (m). The celerity 'c' calculated considering the maximum water depth observed at Tikarpara station. Thus Eq. 3 can be return as

$$\frac{\sqrt{gh}}{\Delta x}\frac{\Delta t}{1}=\leq 1 \quad (4)$$

$$\text{Since } c=\sqrt{gh}$$

g is gravitational acceleration (m/sec^2), h is the maximum depth of water observed at Tikarpara station. The evaluation of model performance was done based on measures of fit F1 and F2 [3, 7, 2]

$$F_1=\frac{A}{A+B+C}$$

$$F_2=\frac{A-B}{A+B+C}$$

where, A is correctly predicted flood cell by model, B is over predicted flood cells and c is under predicted flood cells, F_1 is the value ranges from 0 to 1, F_2 is the value ranges from −1 to 1. The value F_1 and F2 found closer to 1 means model performance is better. The flood hazard map was prepared according to flood water depths which are categorized into flood hazard by Japan ministry of land infrastructure and transport [6] (Table 2).

Table 2 Flood hazard classification according to [6]

Flood hazard	Depth (meters)	Hazard
H_1	<0.5	Very low
H_2	0.5–1	Low
H_3	1–2	Medium
H_4	2–5	High
H_5	>5	Extreme

The flood hazard has been classified in 5 categories H_1,H_2, H_3, H_4 and H_5. H_1 Flood hazard (depth less than 0.5 m) or also titled very low hazard zone. Where people do not exposed to any hazard and people can evacuate on footeasily. H_2 flood hazard (depth 0.5–1 m) also known as low hazard zone where people may get exposed to hazard especially children's, cattle's and animals, in this, evacuation on foot for adults become difficult. H_3 flood hazard (depth 1–2 m) people may get drowned in this zone but they are safe in their homes where plinth level is 1–1.2 m above ground level. H_4 Flood hazard (depth 2–5 m) is a high flood hazard where people are not safe even inside their house so in this zone people should make their way towards roof for safety purpose. H_5 extreme flood hazard is the zone where single storied house may drowned and people are not at all safe in this scenario even if they make their way towards the roof. Sensitivity analysis is carried out for study area for three different roughness coefficients for flood plains by using GIS tools.

5 Results and Discussion

HEC-RAS simulated results are in the form of inundation extent with depth, water surface elevation and velocity with respect to time. Simulated raster results are stored in two decimal floating point numbers in tiff file format. Simulated results can be generated for desired date and time from simulated period. For present study, results for specific time 23rd September 2008 at 0800 h as shown in Fig. 5 was selected to validate with RADARSAT satellite microwave data acquired on the same date and time and delineated flood from RADARSAT satellite can be observed with one in Fig. 4. The F1 and F2 measures of fit have been evaluated for all the simulation using GIS tools shown in Table 3.

The maximum simulated depth of inundation was considered for generating the flood hazard map. The depth is classified into five categories H_1 to H_5 as shown in Fig. 6. Many villages on the north side and south side of river have extreme and high hazard zone. Villages lying on the north side floodplain such as Kokulpur, Megha, Dhurukuda, Ostla and Chaasnara and villages lying on the south side flood plains such as Similia, Singabilli, Nilkantapur are in extreme hazard zone. The villages on the north side flood plain such as Kandarpur, Ostia, Fulabadi, some part of Chaasnara, khandahata, Kantatahara, Bishnupur, Kanthipur, Gaudapadapatna, Dhurkudia, Patenigam and south side of flood plain such as Gayalbank,

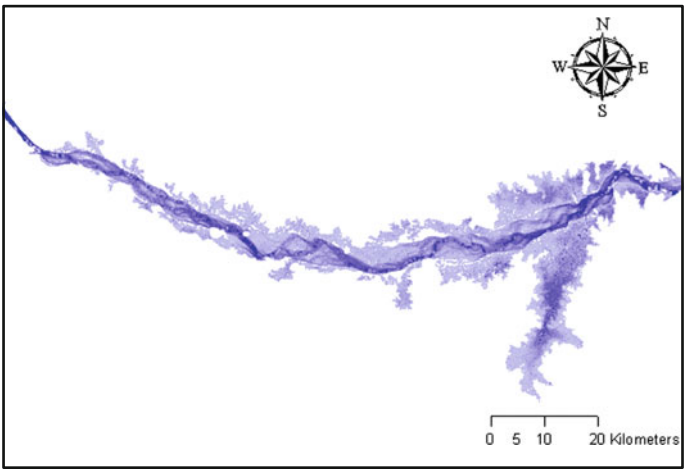

Fig. 5 Simulated flood by HEC-RAS at 23/09/2008 at 0800 h

Table 3 (a) Model performance with respect to different roughness coefficient, n_c is roughness coefficient for channel, n_p is roughness coefficients for floodplains and F1, F2 are measures of fit. (b) Flood inundation area observed and simulated

(a)

Sr. no	Roughness coefficient		Correctly predicted flood cells 'A'	Over predicted flood cell 'B'	Under predicted flood cell 'C'	F1	F2
	n_c	n_p					
1	0.032	0.020	1,553,668	206,750	52,092	0.85	0.74
2	0.032	0.030	1,554,075	519,470	51,685	0.73	0.50
3	0.032	0.040	1,554,381	745,570	48,379	0.67	0.35

(b)

Sr. no	Roughness coefficient		Flood observed (FO) hectares	Flood simulated (FS) hectares	F0/FS		
	n_c	n_p					
1	0.032	0.020	17,057.6	18,125.10	0.94		
2	0.032	0.030	17,057.6	21,252.30	0.80		
3	0.032	0.040	17,057.6	23,483.30	0.72		

PathapurKusupangi, Ghasiput, Harirajpur, Banki, Bilipada, Manipur, Barapadanapur, Nistipur, Ambajit are in high hazard zone. From flood report, flood depth of 2.43 m was observed at Bilipada and Pathapur villages [9]. All theses villages were affected by flood [5]. The velocity map shown in Fig. 7 was generated for extreme inundation extent. Velocity variation can be observed in velocity map. Velocity for river channel is in the range of 1.4–2.85 m/s, where as in flood plains velocity ranges from 0 to 1.4 m/s.

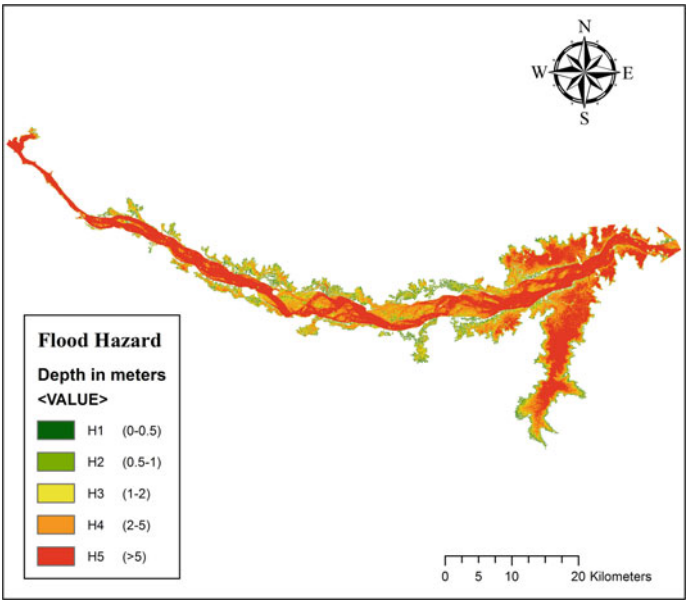

Fig. 6 Flood hazard map

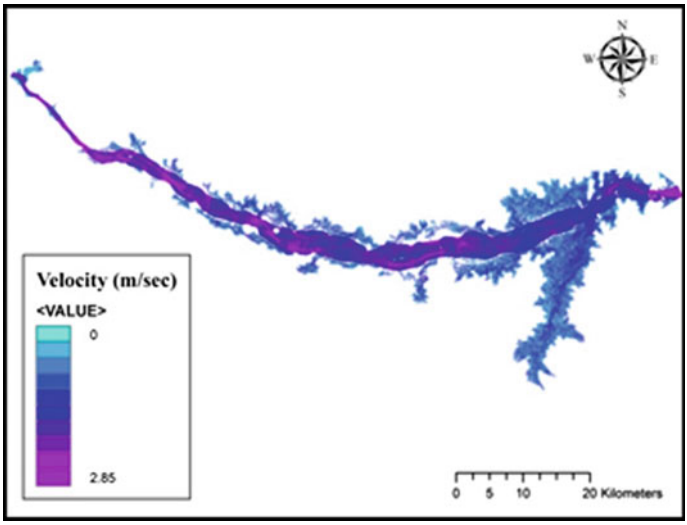

Fig. 7 Velocity map

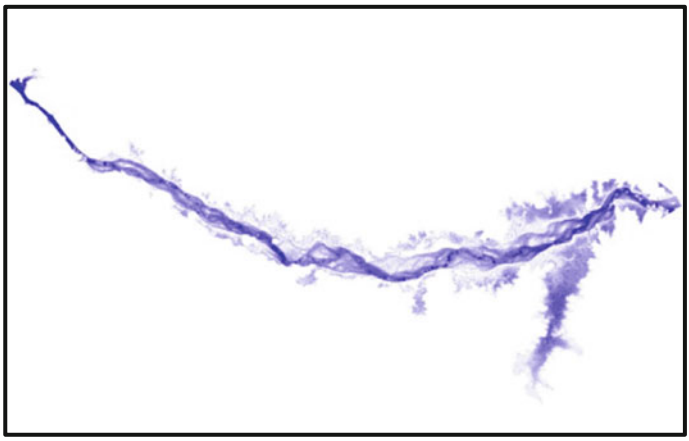

Fig. 8 Results for roughness coefficient 0.020

6 Sensitivity Analysis

Sensitivity analysis has been carried out for three different roughness coefficients for floodplains. The simulated inundation results for three roughness coefficients (0.020, 0.030 and 0.040) for flood plain is shown in Figs. 8, 9 and 10 respectively. More inundation can be observed for 0.040 followed by 0.030 comparatively to 0.020 roughness coefficient. The inundated area statistics for different roughness coefficient is shown in Table 3. Inundation is increasing on floodplains with increase in roughness coefficient for floodplains.

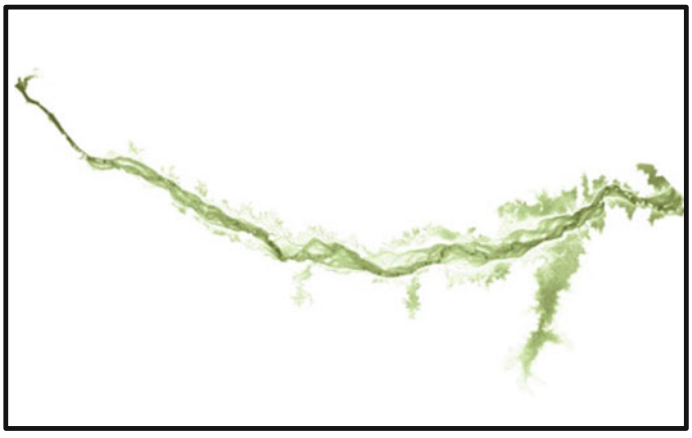

Fig. 9 Results for roughness coefficient 0.030

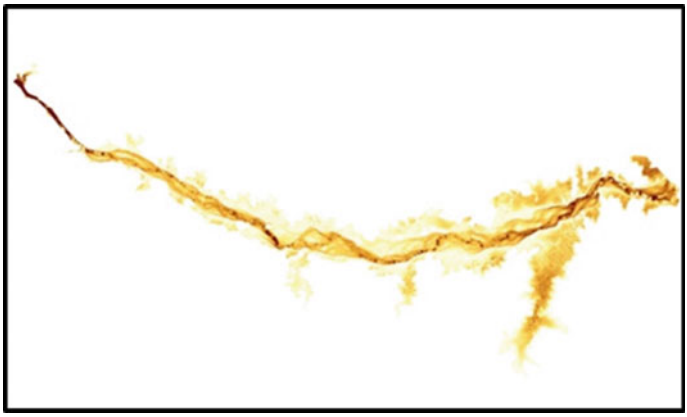

Fig. 10 Results for roughness coefficient 0.04

7 Conclusion

The simulated result of flood inundation extent shows best performance when compared with Radarsat satellite image. The model performance is best in case of roughness coefficient 0.032 for channel and 0.020 for floodplains. The villages Kokulpur, Megha, Dhurukuda, Ostla Chaasnara Similia, Singabilli, Nilkantapur are most vulnerable as simulated flood depths in some part of these villages are greater than 5 m. The villages Kandarpur, Ostia, Fulabadi, some part of Chaasnara, khandahata, Kantatahara, Bishnupur, Kanthipur, Gaudapadapatna, Dhurkudia, Patenigam, Gayalbank, PathapurKusupangi, Ghasiput, Harirajpur, Banki, Bilipada, Manipur, Barapadanapur, Nistipur, Ambajit are having flood depths ranging from 2 to 5 m falls in high hazard zone, In this zone people can not be safe at homes, so in such scenario they are suggested to make their way towards roof in case of houses constructed in Reinforced cement concrete or load bearing structures. The HEC-RAS model is sensitive to manning's roughness coefficient, for study area the simulated area of inundation is increasing with increase in manning's roughness coefficient values.

Acknowledgements Authors are grateful to U.S Army Corps of Engineers for developing and providing HEC-RAS software freely available. Authors are also grateful to ISRO NRSC (National Remote Sensing Center) for providing geographic as well as hydrologic data without which study could not have been carried out.

References

1. Beura D.: Floods in Mahanadi River, Odisha, India: its causes and management. Int. J. Eng. Appl. Sci. (IJEAS) **2**(2); ISSN: 2394-3661
2. Di Baldasarre, G., Schumann, G., Bates, P.: A technique for the calibration of hydraulic models using uncertain satellite observations of flood extent. J. Hydrol. **367**, 276–282 (2009)
3. Horrit, M., Di Baldasarre, G., Bates, P., Brath, A.: Comparing the performance of a 2-Dfinite element and a 2-D finite volume model of floodplain inundation using airborne SAR imagery. Hydrol. Process. **21**, 2745–2759 (2007). February 2015
4. http://www.osdma.org/ViewDetails.aspx?vchglinkid=GL047&vchplinkid=PL060
5. http://www.undp.org/content/dam/india/docs/cr-se-ed-drm-29100801.pdf
6. MLIT: Flood Hazard Mapping Manual in Japan. In: Ministry of Land Infrastructure and Transportation, p. 87 (2005)
7. MoyaQuiroga, V., Kure, S., Udo, K., Mano, A.: Application of 2D Numerical Simulation for the Analysis of the February 2014 Bolivian Amazonia Flood: Application of the New HEC-RAS Version 5. RIBAGUA Elsevier, pp. 25–33 (2016)
8. Parhi, P.K., Sankhua, R.N., Roy, G.P.: Calibration of channel roughness for Mahanadi River, (India) using HEC-RAS Model. J Water Resour. Prot. **4**, 847–850 (2012)
9. reliefweb.int/report/india/india-orissa-flood-update-vol1-19-sep-2008
10. Vinod, K.: Sharma Natural Disaster Management in India Environment and Development View Point

Chapter 78
Distribution of Seasonal Snow Cover Mapping Using Satellite Data in Sutlej Basin

E. Srinivas, T. Nagaraju, E. Sivasanker, K. Sreedhar and K. Ramesh Reddy

Abstract Snow is an essential resource present in the Himalayas. Snow cover is important for both climatological studies as well as hydrological applications. Snow cover area measured for snow melt runoff for planning hydropower projects. In this study, ablation pattern of cloud cover on Snow cover area (SCA) carried out to evaluate elevation zone wise and seasonal snow cover area for Sutlej basin. This technique can be used for estimation of snow melt run of in Sutlej basin using multispectral satellite data. The maximum SCA observed from satellite data were 88% February month while 20% of basin area by the end of May in the study area. The snow cover in lower elevation zones is generally disappearing in April and May months whereas the snow melt runoff in June is primarily from higher elevation zones. The results are acceptable and can be employed. Such result study of snow cover monitoring can provide vital inputs for planning the hydro-electric power projects as well as irrigation and drinking water supplies.

Keywords Remote sensing · DEM · Snow cover map

E. Srinivas (✉)
Department of Applied Geo Chemistry, Osmania University,
Hyderabad 500007, India
e-mail: srinivase4@gmail.com

T. Nagaraju
Department of Geology, Osmania University, Hyderabad 500007, India
e-mail: tnr.2020@gmail.com

E. Sivasanker
Water Resource Division, Department of Space, NRSC, ISRO,
Government of India, Hyderabad 500625, India
e-mail: sivasankar_e@nrsc.gov.in

K. Sreedhar
Department of Applied Geochemistry, Osmania University,
Hyderabad 500007, India
e-mail: sreedhar.kuntamalla@gmail.com

K. Ramesh Reddy
Nabocns Consultancy services, Masab Tank, Hyderabad, Hyderabad, India
e-mail: kothamidde6@yahoo.com

P. J. Rao et al. (eds.), *Proceedings of International Conference on Remote Sensing for Disaster Management*, Springer Series in Geomechanics and Geoengineering,
https://doi.org/10.1007/978-3-319-77276-9_78

1 Introduction

The Himalayas is the youngest mountain which is formed by continent collision between the northward moving Indian plate and the Eurasian plate during 50–60 million years ago [1]. The Himalayas is 2500 km long mountain ranges from west to east comprised of 30 mountains rising more than 7300 m and includes the highest mountain peak (8848 m) of the Everest. Sutlej River in Western Himalayas contributes a major extent of inflows into Bhakra reservoir in Himachal Pradesh, India [2]. The snow cover accumulated in winter months melts in lean summer months which are vital during the period of high demand for water and power [3]. The snow cover varies year to year [4]. The snow that melts during summer months provides substantial runoff during lean period for hydro-electric power generations as well as irrigation and drinking water supplies. The terrain being hazardous and inaccessible across high altitudes and across international borders. The remote sensed satellite data provides the most appropriate and valuable information during winter season and melts in subsequent summer months. In North India, availability of snow melt runoff is very critical. The classification of satellite image is an information extraction process that involves pattern recognition of spatial properties of various surfaces features and categorizing the similar features. The objectives of the present study are snow cover map in Sutlej basin and to estimate elevation zone wise snow cover area using Boolean algebra model.

2 Study Area and Data Used

Sutlej river basin in Western Himalayas is the study area. The river Sutlej is one of the main tributaries of Indus and has its origin near Manasarovar and Rakas lakes in Tibetan plateau at an elevation of about 4500 m (approx.) [3]. Its length is 47,000 km^2 in the area. The Sutlej basin is geographically located between 30° 00′N, 76° 00′E and 33° 00′, 82° 00′E. Characteristics of the basin and inaccessibility of the major part of it make remote sensing application ideal for hydrologists to monitor the snow cover information of the region and assess the resulting water resource [5]. Geographically, the mountain ranges extend throughout the basin with altitudes ranging from about 2200 to 7000 m above mean sea level [1]. The most important factors controlling the climate and weather types in the Himalayas are altitude and aspect. Snow is the least during August. Fresh snowfall starts at the end of September and continues till the end of March [6]. During summer months namely, April–May–June, vast amount of snow melt results in heavy runoffs in snow field rivers such as Sutlej [4]. For the snow cover mapping, the satellite data from AVHRR sensor onboard NOAA satellite resolution is 1.1 km NOAA/AVHRR Images imaging at about 13:30 h local are used in this study.

3 Methodology

Snow cover in Sutlej basin was mapped using ERDAS/Imagine digital image processing software. The digital analysis steps can be classified into (I) Pre-processing, (II) Classification (III) Post (statistic)-classification processing (VI) Estimation of snow cover area elevation wise from NOAA/AVHRR data. The data processing steps were done with digital image processing techniques using Erdas Imagine s/w. The bands 1 (0.58–0.68 μm) and 2 (0.725–1.1 μm) of the AVHRR give maximum differentiation between non-snow [7] and snow covered areas and with cloud. The middle Infra Red band 3 (3.55–3.95 μm) assist in separating clouds from snow. It has been observed that in the band 3, clouds on the Himalayas usually occurring near the snowline appear to have quite a low reflectance compared to snow [8]. This phenomenon helps to separate such clouds from the surrounding snow. In the thermal band, high clouds have definite high range of digital values compared to snow, assisting in the identification of such clouds. To have a better control over classification parallel-o-piped algorithm has been adopted. Before classification, the first step is to create a signature file. The signature file is used to store the definition of classes to be classified in the form of thresholds in different bands of the satellite data.

In the present study, snow is taken as one class or object. In this if we select some pixels of snow then the similar DN value of pixels in the image will be selected and grouped as one object. This process is completed until all the pixels covered with snow are selected. There fore if any little amount of snow is not selected then by increasing the threshold values we can select the unselected snow. The fine tuning must be done by slightly increasing or decreasing the threshold values by repeated iterations with marginal increase or decrease so that snow is not over classified or under classified. This process is to be complete until all the snow pixels are selected. The overall objective of image classification procedures is to automatically categorize all pixels into image into specific land cover classes or themes. The set of radiance measurements obtained in various discrete wavelength bands for each land cover represent the spatial response pattern. The variability in spectral response pattern of land features from the basis for their discrimination on the satellite data. The satellite data may contain some amount of cloud cover in some parts of the region of interest. To ascertain whether snow is present under the cloud or not, it is necessary to compare with a reference image of that region approximately of the same time period such that no major error is made in editing the image. To minimize such editing errors, a snow cover mask of the region was generated which contains maximum likelihood snow cover in that region using a series of past images of that area during that period. This image is generated using union algorithm as specified below Table 1 for each month namely March, April, May and June months.

The classified snow image is edited using maximum snow mask to eliminate cloud cover. The cloud pixels are replaced with the corresponding pixels of maximum snow mask image. The Boolean algebra used for editing the cloud pixels with

Table 1 Truth table of editing cloud pixels

Condition	Input value	Mask	Output value
Cloud-snow	Cloud	Snow	Snow
Cloud-non snow	Cloud	Non snow	Non snow
Snow-non snow	Snow	Non snow	Non snow
Snow-snow	Snow	Snow	Snow

the help of snow cover mask of the study area. The classified image is used to extract the snow cover portion of Sutlej basin using the Sutlej basin mask image. The classified images are shown in the Fig. 1. Snow cover area Statistics in the Sutlej basin are computed by generating a matrix using classified image and reference basin mask. The snow cover area within the basin is expressed as percentage of total basin area denoting snow cover area available in the basin as on that date. Thus, the snow cover area values have been computed for all the images. The classified snow image is compared with basin mask image to compute the snow cover area within the basin.

The elevation of the terrain has a dominant role in snow accumulation. High elevation in general terms witness lesser, which in terms leads to higher snow accumulation temperature [1]. The digital elevation model of Sutlej basin at 30 m resolution has been taken from ASTER data available freely from http://glcfapp.umiacs.umd.edu:8080/esdi/index.jsp. Digital terrain model is defined as the digital representation of spatial distribution of terrain characteristics. Sutlej basin elevation map as shown in the Fig. 2.

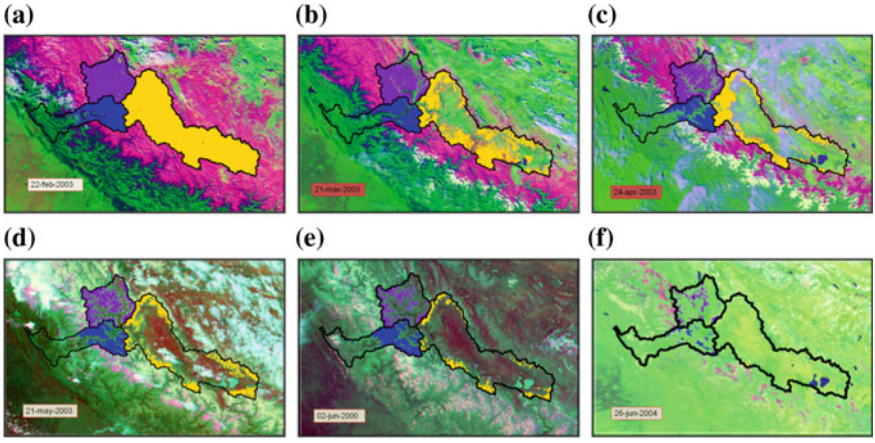

Fig. 1 Snow cover area decreased monthly wise of Sutlej basin on **a** 22 Feb, **b** 21st Mar, **c** 24th Apr, **d** 21st May, **e** 02 Jun and **f** 26th Jun in 2003 year

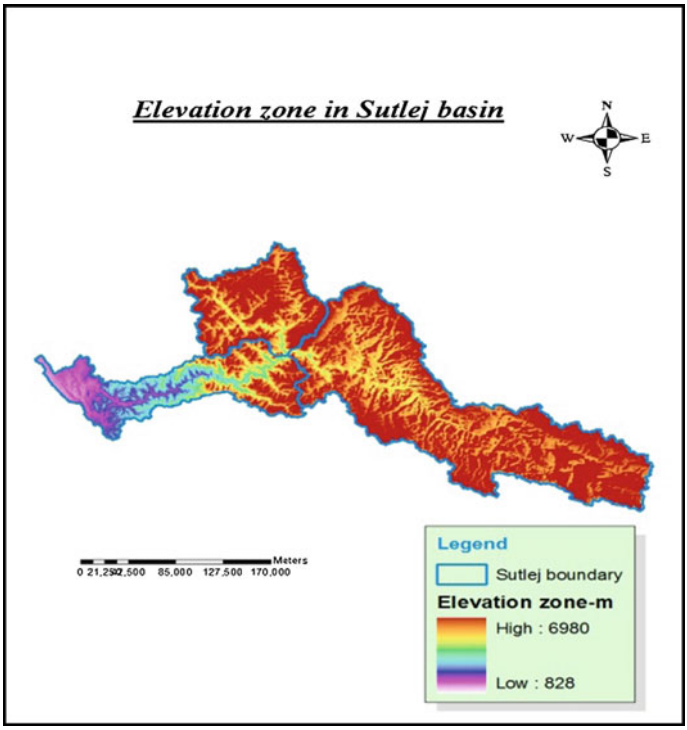

Fig. 2 DEM satellite image for the Sutlej

4 Analysis and Results

The NOAA/AVHRR satellite data during the period February to June months of the years 2000, 2001, 2002, 2003 and 2004 have been used in this study since the snow cover depletion and the resultant snow melt runoff is predominant in this period considering the data availability and suitability. Snow cover mapping was done using digital image processing techniques for Sutlej basin. The Sub basin wise snow cover area statistics were computed. The snow cover area existing on different dates in Sutlej basin is shown in Table 2. The Tibet portion of Sutlej basin is approximately 60% of the total basin area. The snow cover in Tibet region depletes early in summer months whereas the snow cover in Spiti, Lower Sutlej regions deplete slowly and continue till the end of June month. The snow cover area approaches maximum possible value in the month of February and the depletion starts in the month of March depending on the prevailing temperature conditions. The maximum SCA (within the dataset used in this study) observed from satellite data is 88% recorded on 22 Feb 2003. The SCA is approximately 20% of basin area by the end of May in general. The year to year variation in SCA is very significant.

Table 2 Snow covers area in Sutlej basin

S. no	Date	Snow cover area in Sutlej basin (Area in km^2)				
		Spiti (10,087)	Tibet (29,970)	Lower-sutlej (11,418)	Total area (51,475)	Total SCA (% of total basin area)
1	22-Feb-03	9834	29,949	5361	45,144	88
2	22-Feb-04	9446	17,693	4388	31,527	61
3	11-Mar-03	8735	22,236	4746	35,717	69
4	21-Mar-03	7133	13,962	4113	25,209	49
5	31-Mar-03	9428	21,448	5052	35,928	70
6	15-Mar-04	7030	6837	3450	17,317	34
7	01-Mar-04	9084	13,707	4247	27,039	53
8	07-Apr-03	8678	13,091	3992	25,761	50
9	24-Apr-03	6921	9325	4108	20,354	40
10	04-Apr-01	6347	25,283	3275	34,906	68
11	06-Apr-01	8601	18,123	4574	31,298	61
12	05-Apr-02	5367	18,392	3202	26,961	52
13	14-May-03	6648	11,642	4677	22,966	45
14	16-May-03	5877	9262	3041	18,180	35
15	21-May-03	5514	7232	3788	16,534	32
16	10-May-04	4290	2996	2829	10,115	20
17	23-May-01	3902	8452	3650	16,004	31
18	24-May-01	4151	7184	3837	15,172	29
19	06-May-04	6158	7159	3696	17,013	33
20	29-May-04	4016	3684	2175	9874	19
21	02-Jun-00	3423	4062	3926	11,411	22

The Sutlej basin has been divided into 5 elevation zones as shown in Table 3 using DEM of Sutlej basin considering the frequency distribution of the area and elevation. The elevation zone mask image has been developed as shown in the Fig. 3. Elevation zone wise snow cover area identified as shown in the Fig. 4.

The snow cover area in each elevation zone has been computed using the snow cover map. The minimum elevation in the Sutlej basin is about 500 m and maximum elevation is about 7400 m. It is observed that about 65% of the basin area is above 4500 m. Elevation about 10.75, 8.53 and about 15% of the basin area is in zone 1, zone 2 and zone 3 respectively as shown following Table 4.

It is observed that zone 1 contains snow cover generally up to March and Zones 3, 4, 5 contain the snow cover predominantly till June end. The snow in zone 1 and zone 2 generally disappeared by the middle of May month. The snow melt in later part of May and June months is predominantly from zone 3, zone 4 and zone 5. This implies snow cover above 4500 m elevation is contributing to the snow melt runoff in later part of summer months. The snow melt process is controlled by snow water equivalent and the energy input the snow pack. As the melting period

Table 3 Elevation zone wise snow cover area

S. no	Date	Zone 1	Zone 2	Zone 3	Zone 4	Zone 5	Total km^2 (51,472 km^2)
1	01-Mar-04	0	1190	2792	9105	13,955	27,042
2	11-Mar-03	32	1934	5033	14,560	14,159	35,718
3	15-Mar-04	0	532	1543	4588	10,657	17,320
4	21-Mar-03	0	896	2352	9832	12,130	25,210
5	04-Apr-01	37	1367	4897	15,777	12,830	34,908
6	05-Apr-02	19	1014	2673	11,365	11,139	26,210
7	06-Apr-01	88	1483	3096	12,171	14,457	31,296
8	07-Apr-03	0	807	2580	9429	12,945	25,762
9	24-Apr-03	50	944	1885	5908	11,568	20,355
10	10-May-04	3	281	626	1774	7431	10,114
11	14-May-03	34	1280	1832	6600	12,922	22,668
12	29-May-04	0	134	366	1410	7963	9873
13	06-May-04	0	456	1182	3783	11,593	17,015
14	22-Feb-03	248	3594	7617	18,026	15,661	45,145
15	16-May-03	4	253	775	4698	12,452	18,181
16	21-Mar-03	0	896	2352	9832	12,130	25,210
17	31-Mar-03	36	2085	3797	14,382	15,627	35,928
18	15-Apr-04	4	339	782	4380	10,580	16,084

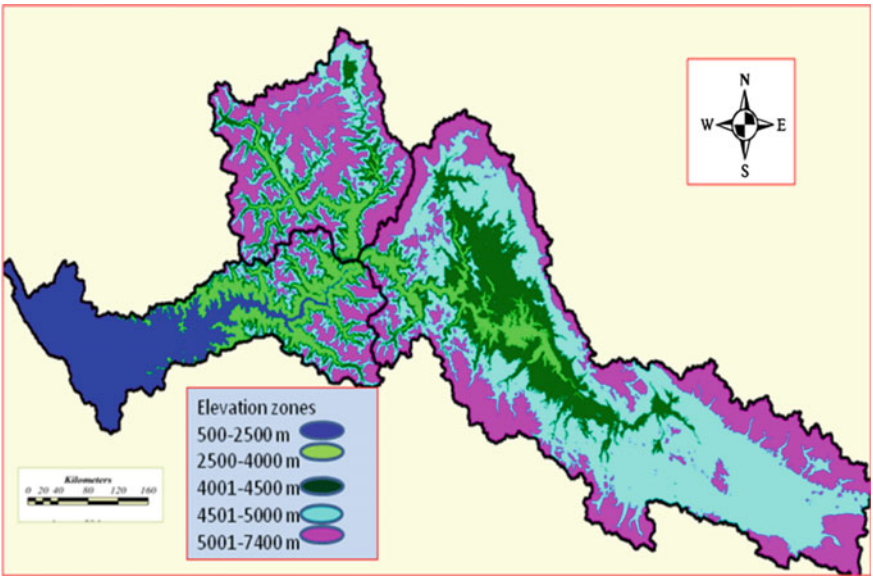

Fig. 3 Elevation zones in Sutlej basin

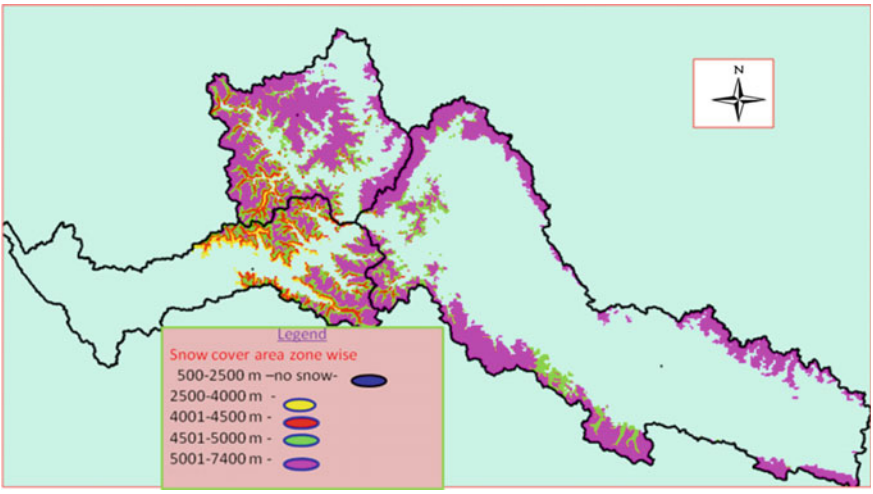

Fig. 4 Elevation zone wise Snow cover area in Sutlej

Table 4 Elevation zones in Sutlej basin

Zone	Elevation Range	Area (Km^2)	% of Basin
Zone 1	0–2500 m	5533	10.75
Zone 2	2501–4000 m	4393	8.53
Zone 3	4001–4500 m	7713	14.98
Zone 4	4501–5000 m	18,124	35.21
Zone 5	5001–7500 m	15,709	30.52
	Total	51,472	

advances, the temperature keeps rising accelerating the snow melt runoff. Initially, lower elevation zones contribute to the runoff and slowly the higher elevation zones start contributing. For the purpose snow melt runoff modeling, elevation zone wise contributions are modeled during the summer months.

5 Conclusions

In snow cover map studies, energy input to the snowpack is an important component. The conclusions of the present study are summarized hereunder. In this study, the NOAA/AVHRR data have been used to compute snow cover in Sutlej basin in Western Himalayas. The ASTER Digital Elevation Model has been used to identify 5 elevation zones within the Sutlej basin. The snow cover in each elevation zone has been computed. It is observed that about 65% of the basin area is above 4500 m elevation in Sutlej basin. The snow cover in lower elevation zones is generally disappearing in April and May months whereas the snow melt runoff in

June is primarily from higher elevation zones. Generally below 4000 m in Sutlej basin, do not explain the variability in the vertical plane as the snow melt is predominantly from elevations above 4500 m. This experiment with larger data set can improve the accuracy of estimation.

References

1. Majumdar, T.J.: Areal snow cover estimation over the Himalayan terrain using INSAT-1D VHRR data. Geocarto International **17**(3) (2002)
2. Paul, P.R., Ramana Rao, C.L.V., Siva Sankar, E.: A new approach in operational long-term snow melt runoff forecasting in Satluj basin using snow cover depletion patterns. In: Proceedings of international symposium on snow and its manifestations (Extended abstracts) (26–28 Sept 1994), pp. 340–342. Snow and avalanche study establishment, Manali, India. Sineh, P., Kumar, N.: Effect of orography on precipitation in the western Himalayan region. J. Hvdrol. **199**, 183–206 (1997)
3. Reuben Paul P., Ramana Rao, Ch., Siva Sankar, E.: A new approach in operational long—term snowmelt runoff modeling in Sutlej basin using snow cover depletion patterns. In: International Symposium on snow and related manifestation "SNOWSYMP-94", Manali, India (1994)
4. Siva Sankar, E. Operational digital snowcover mapping, workshop on remote sensing applications in snow hydrology, 11–12 May 1993, NRSA, India
5. Rama Moorthi, A.S, Paul. P.R., Ramana Rao, Ch.L.V.: Snow studies in Himalaya—snowmelt runoff modeling, Asia and Oceania—environmental change monitoring. Murai, (ed.) (1991)
6. Hall, D.K., Martinec J.: Remote sensing of ice and snow. Chapman and Hall, London (1985)
7. Muzylev, E.L., Uspensky, A.B., Startseva, Z.P., Volkova, E.V., Kukharsky, A.V.: Using AVHRR/NOAA and MODIS/Terra information on land surface characteristics for modeling vertical water and heat fluxes from river basin (2007)
8. Siva Sankar, E., Reuben Paul, P., Ramana Rao, Ch.: Applications of remote sensing information on snow in hydrological modeling, workshop on remote sensing application in snow hydrology, 11–12 May 1993, NRSA, India